MendelNet

Editors:

Radim Cerkal

Natálie Březinová Belcredi

Lenka Prokešová

Proceedings of 25th International PhD Students Conference

7-8 November 2018, Brno, Czech Republic

Mendel University in Brno
Faculty of AgriSciences

MendelNet 2018

Proceedings of 25th International PhD Students Conference
7–8 November 2018, Brno, Czech Republic

Editors: Radim Cerkal, Natálie Březinová Belcredi, Lenka Prokešová

The MendelNet 2018 conference would not have been possible without the generous support of The Special Fund for a Specific University Research according to the Act on the Support of Research, Experimental Development and Innovations and the **support of**:

BIOMIN Czech s.r.o.

DYNEX TECHNOLOGIES, spol. s r.o.

PELERO CZ o.s.

Profi Press s.r.o.

Research Institute of Brewing and Malting, Plc.

Romer Labs Diagnostic GmbH

All contributions of the present volume were peer-reviewed by two independent reviewers. Acceptance was granted when both reviewers' recommendations were positive.

ISBN 978-80-7509-597-8

Committee Members:

Section Plant Production

Prof. Ing. Radovan Pokorný, Ph.D. (Chairman)

Assoc. Prof. Ing. Stanislav Hejduk, Ph.D.

Assoc. Prof. Ing. Vladimír Smutný, Ph.D.

Ing. Jan Winkler, Ph.D.

Section Animal Production

Prof. Ing. Gustav Chládek, CSc. (Chairman)

Prof. MVDr. Leoš Pavlata, Ph.D.

Ing. Zdeněk Hadaš, Ph.D.

Ing. Milan Večeřa, Ph.D.

Section Fisheries and Hydrobiology

Assoc. Prof. Ing. Radovan Kopp, Ph.D. (Chairman)

Assoc. Prof. MVDr. Miroslava Palíková, Ph.D.

Ing. Jan Grmela, Ph.D.

RNDr. Michal Šorf, Ph.D.

Wildlife Research

Assoc. Prof. Ing. Josef Suchomel, Ph.D. (Chairman)

Ing. Vladimír Hula, Ph.D.

Ing. Ondřej Košulič, Ph.D.

Mgr. Jan Šipoš, Ph.D.

Section Agroecology and Rural Development

Prof. Dr. Ing. Milada Šťastná (Chairman)

Assoc. Prof. RNDr. Antonín Vaishar, CSc.

Assoc. Prof. Ing. Hana Středová, Ph.D.

Ing. Bohdan Stejskal, Ph.D.

Section Food Technology

Assoc. Prof. Ing. Jan Pospíchal, CSc. (Chairman)

Prof. MVDr. Ing. Tomáš Komprda, CSc.

Assoc. Prof. Ing. Libor Kalhotka, Ph.D.

Assoc. Prof. Ing. Šárka Nedomová, Ph.D.

Ing. Miroslav Jůzl, Ph.D.

Section Plant Biology

Ing. Pavel Hanáček, Ph.D. (Chairman)

Assoc. Prof. Ing. Tomáš Vyhnánek, Ph.D.

RNDr. Ludmila Holková, Ph.D.

Mgr. Jan Zouhar, Ph.D.

Section Animal Biology

Prof. MVDr. Zbyšek Sládek, Ph.D. (Chairman)

Prof. RNDr. Aleš Knoll, Ph.D.

Prof. Ing. Tomáš Urban, Ph.D.

Ing. Aleš Pavlík, Ph.D.

Section Techniques and Technology

Assoc. Prof. Ing. Vojtěch Kumbár, Ph.D. (Chairman)

Assoc. Prof. Ing. Jiří Fryč, CSc.

Ing. Adam Polcar, Ph.D.

Ing. Petr Trávníček, Ph.D.

Section Applied Chemistry and Biochemistry

Prof. RNDr. Vojtěch Adam, Ph.D. (Chairman)

Assoc. Prof. RNDr. Jiří Urban, Ph.D.

Assoc. Prof. Mgr. Markéta Vaculovičová, Ph.D.

Ing. Simona Dostálová, Ph.D.

Mgr. Tomáš Vaculovič, Ph.D.

PREFACE

The 25th International PhD Students Conference for undergraduate and postgraduate students was hosted by the Faculty of AgriSciences, Mendel University in Brno, the Czech Republic, on November 7–8, 2018. It provided a relevant platform to discuss new trends in plant and animal production, fisheries and hydrobiology, wildlife research, agroecology and rural development, food technology, plant and animal biology, techniques and technology, applied chemistry and biochemistry, and beyond with participants arriving both from the Czech and European educational and research institutions.

The success of the event is reflected in the papers received, with participants coming from diverse backgrounds – stimulating a substantial international and multicultural exchange and mutual share of experience and ideas. The accepted papers are published in full in these proceedings after being admitted to Conference Proceedings Citation Index (Clarivate Analytics).

The conference of this calibre can succeed only as a team effort, so the editors express their thanks and gratitude to all committees and reviewers both for their outstanding work and invaluable comments and advice.

The Editors

TABLE OF CONTENTS

SECTION PLANT PRODUCTION

SECTION ANIMAL PRODUCTION

SECTION FISHERIES AND HYDROBIOLOGY

SECTION WILDLIFE RESEARCH

SECTION AGROECOLOGY AND RURAL DEVELOPMENT

SECTION FOOD TECHNOLOGY

SECTION PLANT BIOLOGY

SECTION ANIMAL BIOLOGY

SECTION TECHNIQUES AND TECHNOLOGY

SECTION APPLIED CHEMISTRY AND BIOCHEMISTRY

PLANT PRODUCTION

The fertilization of fenugreek (*Trigonella foenum-graecum* L.) with sulphur and boron

Jiri Antosovsky, Petr Skarpa
Department of Agrochemistry, Soil Science, Microbiology and Plant Nutrition
Mendel University in Brno
Zemedelska 1, 613 00 Brno
CZECH REPUBLIC

jiri.antosovsky@mendelu.cz

Abstract: The foliar application of different sulphur fertilizers and their effect on biomass yield of fenugreek was examined in small plot field experiment in the experimental station Vatín. The effect of foliar application of boron was also examined. Variants of fertilization included in the experiment were: 1. Unfertilized, 2. Thiosulphate sulphur, 3. Elemental sulphur, 4. Polysulphide sulphur and 5. Boron. The highest yield of fenugreek, 22.1 t/ha, was obtained after fertilization with polysulphide sulphur. The yield on this variant was higher by 8.7% compared to the unfertilized control. Foliar application of boron had provided second highest yield, 21.4 t/ha, which was an increase by 5.1% in comparison with unfertilized variant. The content of sulphur in plants was statistically significantly higher after application of each form of sulphur in comparison with the unfertilized control. The highest content of sulphur in plants was measured after thiosulphate application. Foliar fertilization by boron resulted in significantly increased content of boron in plants compared to the control variant.

Key Words: fenugreek, sulphur, boron, yield

INTRODUCTION

Genetically modified materials for industrial processing or food and feed preparation have been increasingly discussed in recent years (Evanson and Santiello 2004, Kolodinsky 2008). For example, the farmers in Switzerland or Germany can only produce GMO-free milk from dairy farms (Bickel et al. 2009, Mann and Venus 2015). Therefore, cattle on such dairy farms have to be fed only with feed without addition of GMO products. One of the most frequently used sources of protein for animal husbandry is extracted grit from soybean. The amount of soybean produced in European Union is negligible compared to the import of soybean from the world (COCERAL 2015). Unfortunately, majority of this soybean is genetically modified. The long-term effect of GMO on human and animal organism is yet to be discovered, but a considerable part of our society is pushing for GMO-free product. Therefore, it is necessary to find a possible solution. One of the possibilities is to examine an alternative source of protein for animal husbandry, for example fenugreek (*Trigonella foenum-graecum* L.).

This work is a segment of a two-year experiment with various interconnected partial goals. The aim of the experiment is to secure the production of feed (especially protein) for animal husbandry. The partial goals are examining the soil quality and nutrition of plants, microbiological purity of plants or digestibility of nutrients, especially nitrogenous substances from individual feeds. Two possible sources of protein are examined in the experiment - buckwheat (*Fagopyrum esculentum*) and fenugreek (*Trigonella foenum-graecum* L.). The aim of this part of the experiment is to examine fenugreek as a possible alternative source of protein for production of feed. Fertilization with sulphur may improve the yield and quality of fenugreek. Fenugreek belongs to the legume plants and it is characterized as an environmentally friendly plant. The high yield of fenugreek is influenced by environmental and agricultural factors, such as fertilization or irrigation. Fenugreek contains biologically active substances (protein, amino acids, lipids, etc.) and high content of biogenic elements, such as phosphorus, sulphur or magnesium (Zuk-Golaszewska and Wierzbowska 2017). Therefore, the obtained biomass from this experiment is going to be used as a feed for animals in another part of the work.

MATERIAL AND METHODS

The experiment was established as a small plot field experiment in the experimental station Vatín (49°31'07.2"N 15°58'09.7"E). The different sources of sulphur (thiosulphate, elemental and polysulphide) and fertilization with boron and their effect on yield of fenugreek biomass are examined in the experiment. The variants of fertilization and their doses are described in Table 1. Each variant had three repetitions.

Table 1 Foliar fertilization of fenugreek (Vatín, 2017)

Variants of fertilization	Fertilizer	Dose of fertilizer
1. Control variant	-	0
2. Thiosulphate sulphur	FOLIT®ThioSulf	3 l/ha
3. Elemental sulphur	FERTI MK - S 800 SC	5 l/ha
4. Polysulphide sulphur	SULKA - K	3 l/ha
5. Boron	BOROSSAN FORTE	2 l/ha

The forecrop for fenugreek was a clover harvested for seeds. The harrowing of soil was performed before sowing. Fenugreek (variety Hanka) was sown on 26th May 2017 by sowing machine Oyord. The rate of sowing was 100 kg/ha. The size of one plot was 10 m^2. The basic fertilization of fenugreek with NPK (16-16-16) fertilizer was performed on 3rd June 2017. The dose of fertilizer was 500 kg/hectare. The foliar application of examined fertilizers was performed one month later (4th July 2017). The fenugreek was harvested on 29th August 2017. The harvest was performed by a feed grass cutter machine. The yield of biomass was found, and fenugreek was left to dry for hay. A plant samples of green biomass from each variant was taken and prepared for chemical analysis (content of nitrogen, sulphur and boron). Figure 1 is comparing the course of weather during the experimental year 2017 with the long-term normal 1961–1990 (both for Vysočina region). The average annual temperature in the experimental year 2017 was 8.3 °C, which is an increase by 1.1 °C in comparison with the average annual temperature in the long-term normal 1961–1990 (7.2 °C).

The content of nitrogen in plants was determined by Kjeldahl method, content of boron and sulphur was determined by ICP-OES method. The obtained results were evaluated by single factor analysis of variance (ANOVA) followed by testing at a 95% ($P < 0.05$) level of significance using the Tukey test. The data were processed using the STATISTICA CZ 12. Results are expressed as a mean ± standard deviation (SD).

Figure 1 Course of weather during the long-term normal 1961–1990 in comparison with the experimental year 2017 for region Vysočina (CHMI)

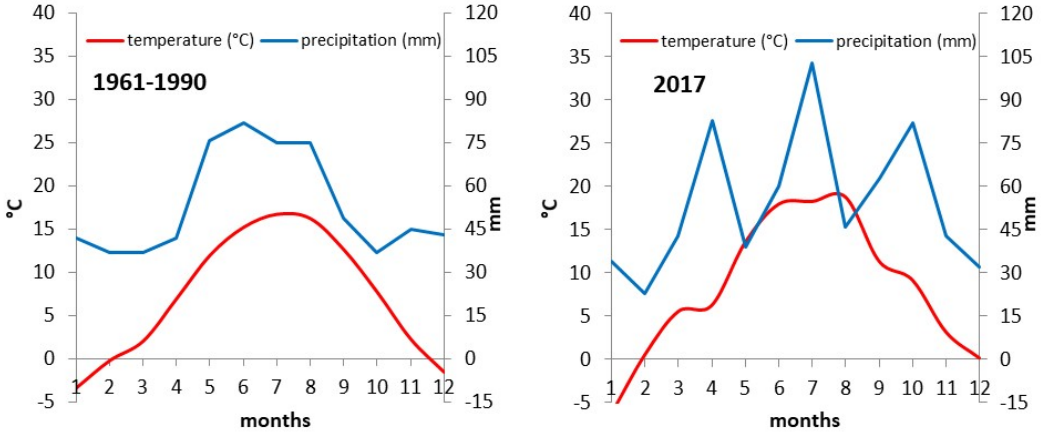

RESULTS AND DISCUSSION

The average yields of green fenugreek biomass and fenugreek hay and their statistical differences among observed variants are described in Figure 2. There were no statistical differences between fertilizers applied in this experiment.

The highest yield of biomass was achieved on variant with polysulphide sulphur application. The average yield of plant biomass in this variant reached 22.1 t/ha, which represents an increase by 8.7% compared to the unfertilized control (20.4 t/ha). The fertilizer with polysulphide sulphur used in the experiment is one of the most concentrated sulphur sources in clear solution form. Another advantage of polysulphide sulphur is the possibility to use this form also as a plant protection against diseases and insects (mostly as fungicide). The elemental and thiosulphate sulphur both provided by ca 4% lower yield in comparison with control variant. This could be the result of irregular precipitation and drought during the year (Figure 1). Therefore, the irrigation of forage crops is an important part for achieving a higher yield, especially in recent years (Ramkishor and Kumawat 2015, Piri et al. 2012, Al-Solaimani et al. 2009). The effectiveness of elemental sulphur depends on several factors including particle size, dose and method of application or environmental conditions. Thiosulphate sulphur contains ca ½ of S as SO_4^- and ca ½ as elemental S, therefore the effectiveness of thiosulphate is partially similar to the elemental sulphur form. The result from this experiment is similar to the experiment performed by Šenkyříková and Ryant (2007). There was also no statistical increase in meadow forage yield after various sulphur form application.

Figure 2 Average yield of fenugreek green biomass and fenugreek hay (2017)

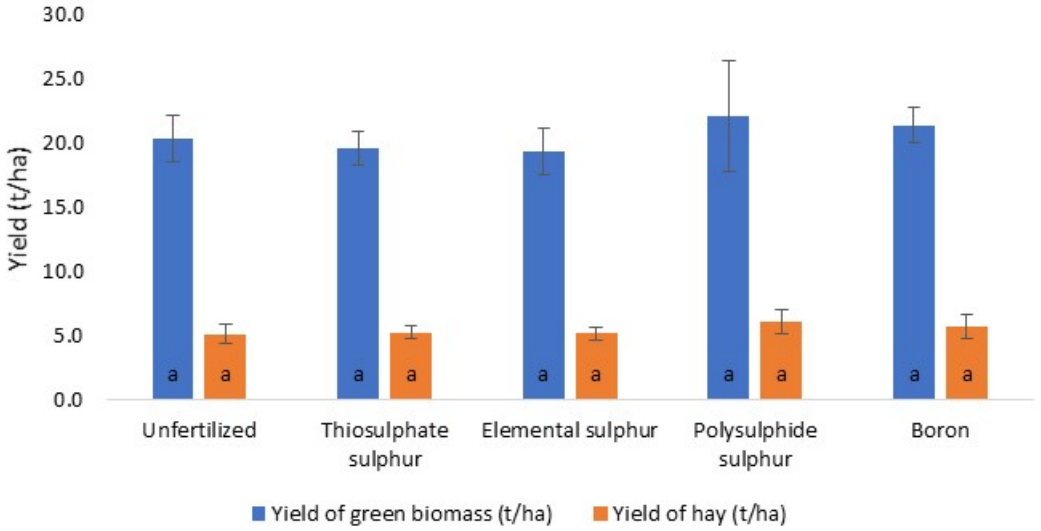

Legend: Means with same letter are not significantly different (P<0.05); Results are expressed as a mean ± standard deviation

The average yield of fenugreek after foliar application of boron reached 21.4 t/ha, which is an increase by 5.1% in comparison with the unfertilized variant. The deficiency of boron in fenugreek leads to failure off flowering, decreased apical growth and small crisped yellowing leaves (Mølgaard and Hardman 2009). The increase in fenugreek yield after foliar application of boron were also observed in experiments performed by Yousif and Abid (2012), Kumar et al. (2010) and Pariari et al. (2009). Their results also recommend the application of boron in combination with zinc for achieving a higher yield.

The highest yield of fenugreek hay is also described in Figure 2. The highest yields were again observed on variant fertilized with polysulphide sulphur (6.1 t/ha) and variant with boron (5.7 t/ha). There was an increase in yield by 18.2% and 11% on these variants in comparison with unfertilized control (5.1 t/ha). However, Tukey test did not reveal any statistical differences. Increased yield of green biomass and dry forage was also found out by Sheta et al. (2010) in the experiment with pearl millet (*Pennisetum glaucum*). An interesting result was obtained on variants with thiosulphate and elemental sulphur in comparison with yield of green biomass. The yield of hay on these variants is higher by ca 1% in comparison with unfertilized control.

The average contents of sulphur and boron in dry matter of fenugreek in examined variants of fertilization are described in Figures 3 and 4. It is evident from Figure 3, that the foliar application of sulphur had positive effect on content of sulphur in plants. The statistically significant difference

was found between the unfertilized control and each variant with sulphur fertilization. The foliar application of thiosulphate sulphur provided the highest content of sulphur, 0.26%.

Statistically significant difference was found out also between unfertilized control variant and variant with foliar application of boron, as it is evident from Figure 4. The content of boron in plants increased from 14.0 mg/kg (unfertilized) to 18.0 mg/kg (Borosan forte). This is an increase by 28.3%.

Figure 3 Average content of sulphur in dry matter of fenugreek (2017)

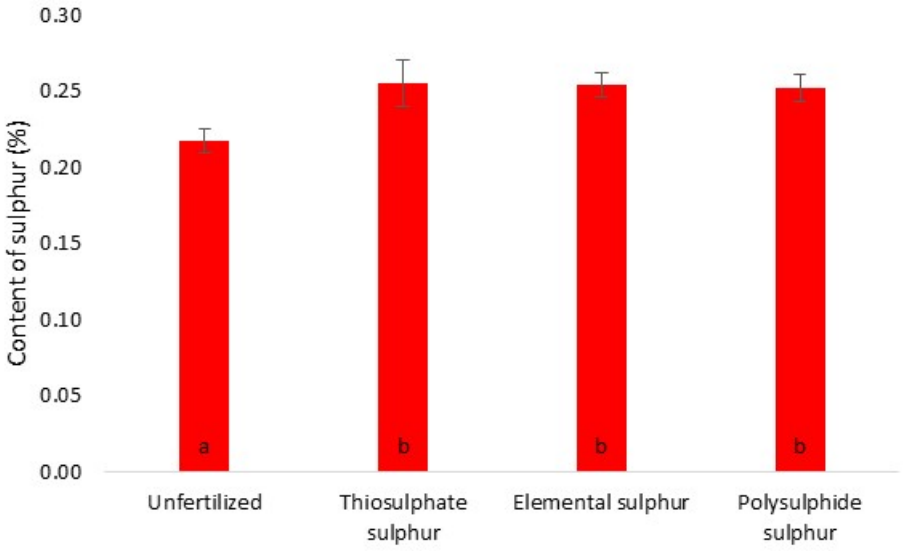

Legend: Means with same letter are not significantly different (P<0.05); Results are expressed as a mean ± standard deviation

Figure 4 Average content of boron in dry matter of fenugreek (2017)

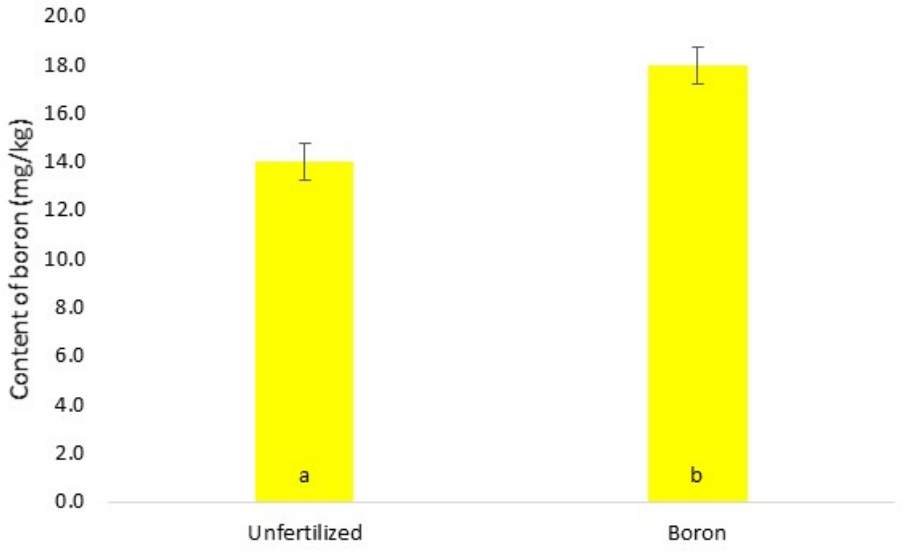

Legend: Means with same letter are not significantly different (P<0.05); Results are expressed as a mean ± standard deviation

CONCLUSION

Foliar application of boron increased the yield of fenugreek in comparison with unfertilized control. The difference was not statistically significant, even though the application of boron is important for the quality. The content of boron in plants was significantly higher than unfertilized

control. Foliar application of sulphur had no statistical effect on yield of fenugreek, although the application of polysulphide form increased the yield of fenugreek by 8.7% compared to the control variant. The content of sulphur in plants was significantly higher on each variant of sulphur form in comparison with unfertilized variant.

ACKNOWLEDGEMENTS
The research was financially supported by grant IGA no. TP 4/2017.

REFERENCES

Al-Solaimani, S.G. et al. 2009. Effect of irrigation water salinity, irrigation interval and sulphur fertilizers rates on forage yield, yield components and quality of blue panic grass (*Panicum antidotale* L.). Journal of King Abdulaziz University – Meteorology, Environment and Arid Land Agriculture, 20(2): 113–115.

Bickel, M. et al. 2009. Kaufmotive und Zahlungsbereitschaften für Erzeuger-FairMilch-Produkte der Upländer Bauernmolkerei. [Online], Available at: https://core.ac.uk/download/pdf/10927566.pdf. [2017-08-07].

COCERAL. 2015. Facts and figures relative to the import of GM products. [Online], Available at: http://www.coceral.com/data/1429715168Factsheet_GMreview_22April2015.pdf. [2017-08-08].

Evanson, R.E., Santiello, V. 2004. Consumer Acceptance of Genetically Modified Food. Wallingford: CAB.

Kolodinsky, J. 2008. Affect or information? Labeling policy and consumer valuation of rBST free and organic characteristics of milk. Food Policy, 33(6): 616–623.

Kumar, J.N.U. et al. 2010. Effect of boron and zinc on growth, yield and quality of fenugreek (*Trigonella foenum-graecum* L.). Indian Agriculturist, 54(1/2): 71–75.

Mann, S., Venus, T. 2015. GMO free milk: A system comparison of Germany and Switzerland. Agroscope Science, 21: 1–11.

Mølgaard, P., Hardman, R. 2009. Boron requirement and deficiency symptoms of fenugreek (*Trigonella foenum-graecum* L.) as shown in water culture experiment with inoculation of *Rhizobium*. The Journal of Agricultural Science, 94(2): 455–460.

Pariari, A. et al. 2009. Influence of boron and zinc on increasing productivity of fenugreek (*Trigonella foenum-graecum* L.). Journal of Crop and Weed, 5(2): 57–58.

Piri, I. et al. 2012. Effect of sulphur fertilizer on sulphur uptake and forage yield of *Brassica juncea* in condition of different regimes of irrigation. African Journal of Agricultural Research, 7(6): 958–963.

Ramkishor, V.H.P., Kumawat, B.L. 2015. Effect of clay mixing, irrigation and sulphur on growth and yield of fenugreek on loamy sand soil. Asian Journal of Soil Science, 10(1): 29–33.

Šenkyříková, A., Ryant, P. 2007. Impact after application of various sulphur on yield and quality of meadow forage. [Online], Available at: https://mnet.mendelu.cz/mendelnet07agro/articles/fyto/senkyrikova.pdf. [2017-08-08].

Sheta, B.T. et al. 2010. Influence of nitrogen, potassium and sulphur levels on growth, yield attributes and yield of forage pearlmillet (*Pennisetum glaucum* L.). Asian Journal of Soil Science, 5(1): 21–25.

Yousif, A.Y., Abid, A.H. 2012. The effect of magnetic seeds and foliar fertilization of Bo and Ca on growth characteristics and yield of Fenugreek plants. Diyala Agricultural Sciences Journal, 4(2): 154–165.

Zuk-Golaszewska, K., Wierzbowska, J. 2017. Fenugreek: productivity, nutritional value and uses. Journal of Elementology, 22(3): 1067–1080.

Sensitivity of different genotypes of *Calonectria pseudonaviculata* isolates to active fungicidal ingredients

Marie Bartikova, Ivana Safrankova
Department of Crop Science, Breeding and Plant Medicine
Mendel University in Brno
Zemedelska 1, 613 00 Brno
CZECH REPUBLIC

marie.bartikova@mendelu.cz

Abstract: Pathogen *Calonectria pseudonaviculata* is a causal agent of boxwood blight disease on *Buxus* spp. Since its first occurrence in 2010 in the Czech Republic on young plants in the production nursery it can be nowadays find also on older plantings of boxwood in chateau gardens and parks. At present the existence of two genotypes of *Calonectria pseudonaviculata* is known: G1 (*Calonectria pseudonaviculata*) and G2 (*Calonectria henricotiae*). Preventive measures are often not sufficient enough to control this pathogen, therefore chemical management needs to be included. Active ingredients of common fungicides registered in the Czech Republic were tested on four isolates, obtained from infected plants from chateau gardens. Fungicide efficacy on mycelia growth of each pathogen culture was evaluated *in vitro*. Comparison of active ingredients cyprodinil+fludioxonil, tebuconazole+fluopyram, prochloraz and thiophanate-methyl shows significantly the best results in mycelia growth inhibition. Fungicides containing active ingredient prochloraz and thiophanate-methyl are registered in the Czech Republic only for field crops use. Statistically significant difference of reduced mycelia growth inhibition of G2 by kresoxim-methyl was proved only for one of three isolates at 0.03% concentration of active ingredient. At 3% concentration of kresoxim-methyl the reduced inhibition of mycelia growth of G2 genotypes was proved.

Key Words: Calonectria henricotiae, Cylindrocladium buxicola, Cylindrocladium pseudonaviculatum, boxwood blight, fungicides

INTRODUCTION

Pathogen *Calonectria pseudonaviculata* (*Cps*) (Crous et al. 2002) Lombard et al. 2010 (syn = *Cylindrocladium buxicola* Henricot and Culham 2002; *Cy. pseudonaviculatum* Crous et al. 2002) causes the blight of the boxwood (*Buxus* L.). Similar symptoms on boxwood were for the first time described in New Zealand and identified caused by pathogen *Calonectria spathulata* (Ridley 1998). In the same year, the occurrence of the pathogen *C. pseudonaviculata* was recorded in Europe for the first time (Henricot et al. 2000). Subsequently, it had gradually spread to other European countries – Germany, Croatia, Belgium, France, Spain, etc. and to Western Asia. It has been present in the Czech Republic (CZ) since 2010 (Šafránková et al. 2013). Since then, it has spread out not only within production nurseries, but also to older plantings of boxwood in chateau gardens and parks. At present, two phylogenetic genotypes of *Cps* are known. Genotype G1 (*C. pseudonaviculata – Cps*), the name *C. psedonaviculata* remained and genotype G2 was classified as *Calonectria henricotiae – Che* (Gehesquière et al. 2016). Both genotypes can be find in Europe (Gehesquière et al. 2016). To this date only *Cps* is present in the United States of America (Crouch 2018, personal communication). DNA sequencing is necessary to identify the genotype, because symptoms expression on boxwood plants between both genotypes is unrecognizable with the naked eye. At first, dark brown spots with lighter center are formed on leaves, size and number of the spots gradually increase with higher infection pressure, followed by leaf–fall and defoliation. Thin dark brown to black lesions often occur on the branches and can lead to the dieback of the shoots.

Control measures to eliminate the spread of *Cps* are primarily focused on prevention, i.e. adherence to hygienic principles, removal of infected parts of plants including the fallen leaves, prevention or reduction of the foliage moisture period and selection of suitable cultivars (Brand 2006, Henricot et al. 2008, Henricot and Wedgwood 2013, LaMondia 2014, 2015). The chemical control is

derived from the results of laboratory and field tests of active fungicidal ingredients efficacy. In the past the efficiency of commercial fungicides (active ingredients) was tested *in vitro* on conidia germination and on mycelium growth. The genotype *Cps* has been tested, mainly. A positive effect on conidia germination was reached by active ingredients tolylfluanid, mancozeb, chlorothalonil and fludioxonil+cyprodinil (Brand 2006) and azoxystrobin, kresoxim-methyl, mancozeb (Henricot et al. 2008, Šafránková et al. 2013). Active ingredients prochloraz, propiconazole, thiophanate-methyl, mancozeb (Brand 2006) and kresoxim-methyl and penconazole (Henricot et al. 2008, Šafránková et al. 2013), have showed inhibitory activity on mycelial growth. Henricot and Wedgwood (2013) report, that effective treatment of diseases *in vivo* was achieved with fungicides with the active ingredients prochloraz and boscalid+pyraclostrobin applied in two treatments at 14-day intervals. Laboratory test results demonstrated the difference in sensitivity of *Cps* and *Che* to fungicide active agents. Genotype *Che* is in comparison to *Cps* less sensitive to the active ingredients tetraconazole and kresoxim-methyl (Gehesquière et al. 2016).

No fungicides directly against *Cps* are registered in the Czech Republic, only fungicides against pathogens causing leaf spots on ornamental plants may be used. Active fungicidal ingredients from different FRAC groups (Fungicide Resistance Action Committee) with different mechanisms of effect, registered in the Czech Republic for ornamental plants, have been selected for fungicides efficacy tests. In addition, the efficacy of the active ingredients prochloraz and thiophanate-methyl, registered against pathogens on field crops, was also tested.

The objectives of the experiment were to verify and compare the efficacy of active fungicidal ingredients *in vitro* on mycelia growth of *Cps* pathogen isolates of two genotypes, obtained from the infected boxwood plants in CZ, further to compare the sensitivity of individual isolates to the active ingredients at the recommended concentration level. And finally, to determine the phylogenetic genotype of the *Cps* isolates based on their reaction to the increased concentration of the active ingredient kresoxim-methyl.

MATERIAL AND METHODS

Fungal isolates

Samples of plant material of symptomatic plants from four locations in the Czech Republic (chateau gardens: Libochovice Chateau – LIB02, Flower Garden Kroměříž Chateau – KPK1–401, Chateau Dobříš – DS01 and Chateau Nové Město nad Metují – NMM01) were placed in a humid chamber (at 21–23 °C, 12/12 light cycle) in order to induce sporulation of the *Cps* pathogens and to obtain pure cultures.

Efficacy of active fungal ingredient(s) and sensitivity of isolates

The recommended amount of active ingredient according to their etiquette (Table 1) was added to previously cooled down (50 °C) media MEA (Malt Extract Agar, HiMedia, Laboratories Pvt. Ltd.). The amended media were poured into a 9 cm diameter Petri dishes. Pure MEA was used as a control variant. Agar plugs (5×10^{-3} m diameter) from the periphery of 14 day-old cultures were transferred to the center of prepared petri dishes. Each active ingredient or combination of two active ingredients in the fungicide and pathogen isolate (4) was tested in three replicates. Cultures were left for three weeks at 23 °C in the dark. Growth of mycelia was monitored and the efficacy of the active ingredient on mycelial growth was assessed after 7, 11 and 21 days. The diameter of the colonies was measured in two directions.

Measurement results after 21 days were statistically evaluated by Analysis of variance (ANOVA) with standard error (SE). The differences among the fungicide active ingredients and the sensitivity of pathogen isolates were subsequently compared between each other using Fisher LSD test at a 95% ($P < 0.05$) level of significance, Statistica (StatSoft CZ s.r.o.). The Abbott formula (1925) was used to evaluate the effectiveness of applied fungicides in relation to the control (in %). In addition, the efficacy of the active ingredient kresoxim-methyl, at 3×10^{-5} kg/l concentration was tested in order to determine the genotypes according to their different response to this active ingredient. The obtained data were evaluated by Abbott formula (1925).

$$\% = 1 - \frac{n\,T}{n\,Co} \times 100$$

Legend: n – Area of mycelium, T – Treated, Co - Control

Table 1 Overview of used fungicides, their active ingredient(s), classification within the FRAC system and used concentration according to the etiquette

Fungicide	Company	Active Ingredient(s)	FRAC Code(s)	Concentration (%)
Control	-	-	-	-
Merpan 80 WG	ADAMA CZ s.r.o.	captan (0.8 kg/kg)	M04	0.2
Switch	AgroBio Opava, s.r.o.	cyprodinil (0.375 kg/kg) + fludioxonil (0.25 kg/kg)	9/12	0.1
Ortiva	Syngenta Limited	azoxystrobin (0.25 kg/l)	11	0.1
Luna Experience SC 400	Bayer S.A.S.	tebuconazole (0.2 kg/l) + fluopyram (0.2 kg/l)	3/7	0.025
Discus	BASF SE	kresoxim-methyl (0.5 kg/kg)	11	0.03
Mirage 450 EC	ADAMA CZ s.r.o.	prochloraz (0.45 kg/l)	3	0.1
Topsin	Nisso Chemical Europe GmBH	thiophanate-methyl (0.5 kg/l)	1	0.1

RESULTS AND DISCUSSION

Fungal isolates

One isolate of genotype G1 – *C. pseudonaviculata* (NMM01) and three G2 isolates – *C. henricotiae* (LIB02, KPK1-401, DS01) were obtained. Data on the molecular identification of the genetic subtype of the pathogen has not been published yet.

Efficacy of active fungal ingredient(s) and sensitivity of isolates

The mycelium growth was significantly inhibited by cyprodinil+fludioxonil, tebuconazole+fluopyram, prochloraz (Figure 1) and thiophanate-methyl cyprodinil+fludioxonil, among which no statistically significant difference was found ($P < 0.05$). Also azoxystrobin had on isolate KPK1-401, a statistically significant inhibitive effect.

Table 2 The length (cm) of mycelia diameter measured after 21 days

Active Ingredient(s)	LIB02	KPK1–401	DS01	NMM01	LIB/KPK/DS/NMM
captan	$2.07^{b} \pm 0.05$	$3.07^{b} \pm 0.07$	$2.97^{b} \pm 0.03$	$3.02^{c} \pm 0.08$	a/b/b/b
cyprodinil+ fludioxonil	$0.50^{a} \pm 0.00$	$1.12^{a} \pm 0.19$	$0.72^{a} \pm 0.14$	$0.5^{a} \pm 0.00$	a/b/a/a
azoxystrobin	$4.77^{d} \pm 0.07$	$0.5^{a} \pm 0.00$	$4.90^{d} \pm 0.31$	$3.55^{d} \pm 0.08$	c/a/c/b
tebuconazol+ fluopyram	$0.5^{a} \pm 0.00$	$0.67^{a} \pm 0.11$	$0.5^{a} \pm 0.00$	$0.5^{a} \pm 0.00$	a/b/a/a
kresoxim-methyl	$3.03^{c} \pm 0.05$	$2.42^{b} \pm 0.59$	$4.03^{c} \pm 0.16$	$2.60^{b} \pm 0.19$	a/a/b/a
prochloraz	$0.5^{a} \pm 0.00$	$0.5^{a} \pm 0.00$	$0.5^{a} \pm 0.00$	$0.5^{a} \pm 0.00$	a/a/a/a
thiophanate-methyl	$0.5^{a} \pm 0.00$	$0.5^{a} \pm 0.00$	$0.5^{a} \pm 0.00$	$0.5^{a} \pm 0.00$	a/a/a/a

Legend: No significant differences between each isolates ($P < 0.05$) are expressed by the same letters. For active ingredients the superscript letters can be compared only within the parameter (column); differences between isolates are shown in last column.

Henricot et al. (2008) and LaMondia (2014) demonstrated an inhibitory effect on mycelia growth using the active ingredient kresoxim-methyl. Gehesquière et al. (2016) describe the possibility of determining genotypes G1 – *Gps* and G2 – *Che* based on their sensitivity to the active ingredients kresoxim-methyl (10^{-5} kg/l) and tetraconazole (2×10^{-6} kg/l). Mycelial growth of G1 is completely inhibited at these concentrations. The lower efficacy of the active ingredient kresoxim-methyl in inhibiting the mycelium growth of the G1 genotype, as described by Gehesquière et al. (2016) was statistically significant only for DS01 isolate. A significant difference of the DS01 isolate is visible in Figure 2. Among the remaining three isolates, there was no statistically significant difference in inhibition of mycelial growth at level of significance ($P < 0.05$). Lower concentration (3×10^{-7} kg/l) of kresoxim-methyl used at this test may be the reason for insufficient inhibitory activity compared to the multiple concentrations used in previous experiments 2×10^{-5} kg/l (Henricot et al. 2008), 4×10^{-5} kg/l – 24×10^{-5} kg/l (LaMondia 2014) and 10^{-5} kg/l (Gehesquière et al. 2016).

Although there was no statistically significant difference of mycelial growth inhibition by kresoxim-methyl between NMM01 and LIBO2 and KPK1-401 isolates, mycelial growth inhibition of NMM01 isolate is optically apparent in the Figure 2.

Figure 1 Mycelia growth 100% inhibited by active ingredient prochloraz

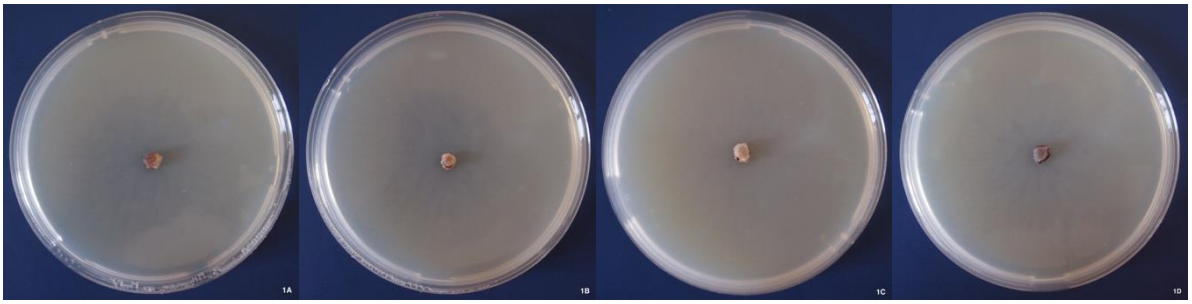

Legend: 1A – LIB02; 1B – KPK1–401; 1C – DS01; 1D – NMM01

Figure 2 Mycelia growth inhibition by active ingredient kresoxim-methyl at 3×10^{-5} kg/l concentration

Legend: 2A – LIB02; 2B – KPK1–401; 2C – DS01; 2D – NMM01

Compared to the control, the best inhibitory effect on the mycelial growth of all four isolates was shown by the active ingredients cyprodinil+fludioxonil, tebuconazole+flupyram, prochloraz and thiophanate-methyl (Figure 3). The active ingredients prochloraz (Figure 1) and thiophanate-methyl achieved 98–99% inhibitory effect across all isolates compared to the control. The results of the strong inhibitory effect of the active ingredient prochloraz are consistent with previously published results (Brand 2006, Henricot et al. 2008). The active ingredient azoxystrobin showed a 99% inhibitory effect on the KPK1-401 isolate. This result does not match the previous tests results showing, that azoxystrobin has a very good inhibitory effect on conidia germination, but insufficiently inhibits mycelia growth (Brand 2006, Henricot et al. 2008). The active ingredient captan with contact mechanism of action had 61–73% efficacy in inhibiting mycelial growth across all isolates after 21 days versus control.

In comparison to control, kresoxim-methyl (3×10^{-5} kg/l) up to 93% inhibitory effect on mycelia growth was achieved on NMM01 isolate (Figure 4). At this concentration, the inhibitory effect of kresoxim-methyl compare to control was -3% (LIBO2), 11% (KPK1-401) and 14% (DS01). These results are comparable to those of Gehesquière et al. (2016). The mycelium growth of all four isolates effected by kresoxim-methyl after 21 days is shown in Figure 5.

Figure 3 Results of the efficacy of active fungal ingredients at recommended concentrations according to Abbott formula (in %)

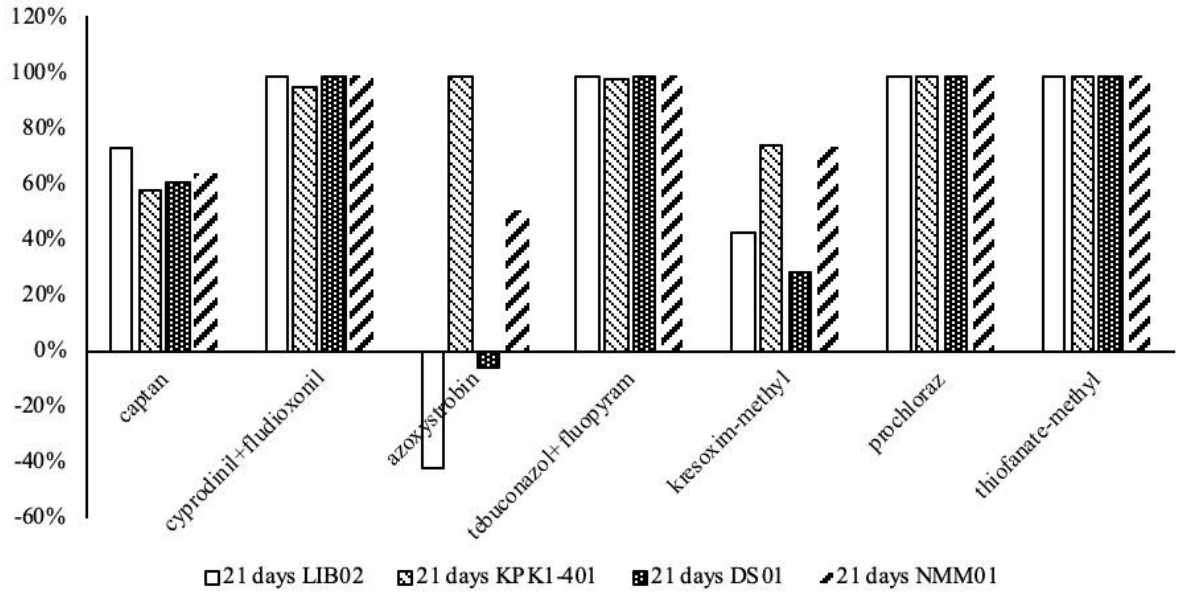

Legend: axis x shows used active ingredients on each isolate, axis y expresses efficacy of active ingredients against control in %, measured after 21 days

Figure 4 Results of the efficacy of kresoxim-methyl at 3 × 10^{-5} kg/l according to Abbott formula (in %)

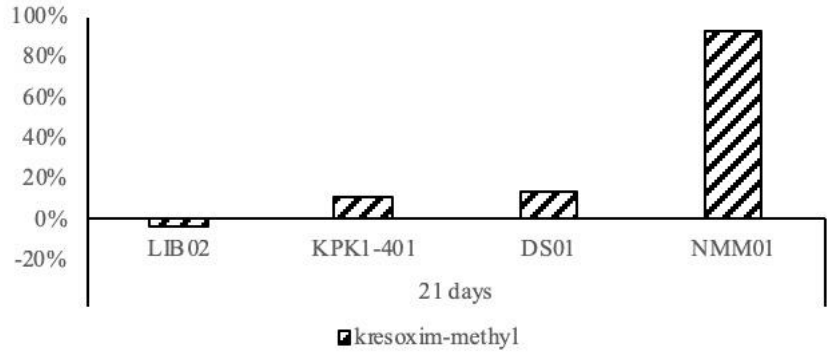

Legend: axis x shows used active ingredient on each isolate, axis y expresses efficacy of kresoxim–methyl against control in %, measured after 21 days

Figure 5 Mycelia growth inhibition by active ingredient kresoxim-methyl at 3 × 10^{-5} kg/l concentration

Legend: 5A – LIB02; 5B – KPK1–401; 5C – DS01; 5D – NMM01

CONCLUSION

Field trials should follow laboratory experiments to verify the effectiveness of fungicides and their combinations on already infected boxwood plants in order to give the best demonstration of effectiveness in field conditions. The remains question is how to proceed with the use of the active

ingredients prochloraz and thiophanate-methyl, which are not registered for ornamental plants in the Czech Republic but prove to be the most effective.

ACKNOWLEDGEMENTS
This research was financially supported by IGA grant no. AF-IGA-IP-2018/033.

REFERENCES

Abbott, W.S. 1925. A Method of Computing the Effectiveness of an Insecticide. Journal of Economic Entomology, 18: 265–267.

Brand, T. 2006. In vitro-Wirkung fungizider Wirkstoffe auf Konidienkeimung und Myzelwachstum von *Cylindrocladium buxicola*. Nachrichtenblatt des Deutschen Pflanzenschutzdienstes, 58: 117–121.

Crous, P.W. et al. 2002. *Cylindrocladium pseudonaviculatum* sp. nov. from New Zealand, and new *Cylindrocladium* records from Vietnam. Sydowia, 54(1): 23–34.

Gehesquière, B. et al. 2016. Characterization and taxonomic reassessment of the box blight pathogen *Calonectria pseudonaviculata*, introducing *Calonectria henricotiae* sp. nov. Plant Pathology, 65: 37–52.

Henricot, B., Culham, A. 2002. *Cylindrocladium buxicola*, a new species affecting *Buxus* spp., and its phylogenetic status. Mycologia, 94(6): 980–997.

Henricot, B. et al. 2008. Studies on the Control of *Cylindrocladium buxicola* Using Fungicides and Host Resistance. Plant Disease, 92: 1273–1279.

Henricot, B. et al. 2000. A new blight disease on *Buxus* in the UK caused by the fungus *Cylindrocladium*. Plant Pathology, 49: 805.

Henricot, B., Wedgwood, E. 2013. Evaluation of Foliar Fungicide Sprays for the Control of Boxwood Blight, Caused by the Fungus *Cylindrocladium buxicola*. Plant Health Progress [Online], Available at: http://www.plantmanagementnetwork.org/pub/php/research/2013/boxwood/. [2018-09-10].

LaMondia, J.A. 2014. Fungicide efficacy against *Calonectria pseudonaviculata*, causal agent of boxwood blight. Plant Disease, 98: 99–102.

LaMondia, J.A. 2015. Management of *Calonectria pseudonaviculata* in boxwood with fungicides and less susceptible host species and varieties. Plant Disease, 99: 363–369.

Lombard, L. et al. 2010. Phylogeny and systematics of the genus *Calonectria*. Studies in Mycology, 66: 31–69.

Ridley, G. 1998. New plant fungus found in Auckland box hedges (*Buxus*). Forest Health News, 77: 1–2.

Šafránková, I. et al. 2013. Leaf spot and dieback of *Buxus* caused by *Cylindrocladium buxicola*. Plant Protection Science, 49: 165–168.

Plant species composition of vineyards in two Moravian wine villages, Mělčany and Rajhrad

Helena Hanusova[1], Jiri Stastny[1], Jiri Sochor[2], Tomas Kopta[2,3], Jan Winkler[1,2]
[1]Department of Plant Biology
[2]Department of Viticulture and Enology
[3]Department of Vegetable Growing and Floriculture
Mendel University in Brno
Zemedelska 1, 613 00 Brno
CZECH REPUBLIC

helcahanusova@gmail.com

Abstract: The purpose of this work is to compile a list of species growing in vineyards of wine villages Mělčany and Rajhrad. The Mělčany and Rajhrad villages are governed by the wine law as wine villages belonging to the wine region of Moravia and subregion of Znojmo. Floristic survey was carried out in two vine lines within the Mělčany wine village cadastre: "Veselá hora, Seslice".and one vine line "Hájiska" within the Rajhrad wine village. A total of 62 vascular plant species were found during the botanical monitoring of vegetation. The most frequent species were *Chenopodium album*, *Festuca rubra*, *Achillea millefolium* agg., *Convolvulus arvensis*, *Avena fatua*, *Amaranthus retroflexus* and *Plantago lanceolata.*

Key Words: flora, *Chenopodium album*, viticulture, weed

INTRODUCTION

Vineyards create a very interesting ecosystem with very specific conditions. As a consequence, they are creating a place for a variety of plant species. Species-rich plant communities are the basis for the animal species richness and stability of the entire ecosystem. The basic of viticulture in the 21st century is especially the maintenance and the increase of the soil fertility. Soil fertility is determined by the positive interaction of bedrock weathering and chemistry, environmental conditions, activity of soil organisms and human influence. The complete exclusion or minimal application of pesticides that are toxic to individual components of soil edaphon and the greening of vineyard are very important for long-term sustainable soil management (Pavloušek 2007).

Thanks to greening and usage biological plant protection, the potential cost of plant protection is reduced (Landis et al. 2000). The species composition of vegetation can support natural enemies of harmful organisms of crops (Gurr et al. 2004). For example, plants providing nectar can increase the activity of predators and parasitoids (Winkler et al. 2006). Novák et al. (2014) say that abandoned vineyards in area Tokaju Nagy-Hill form a habitat for many rare and endangered plant species. Organic vineyard management contributes significantly to the conservation of critical habitats and native plant species (Von Hase et al. 2010).

The purpose of this work is to compile a list of species growing in vineyards in wine villages Mělčany and Rajhrad. Further, to evaluate species diversity and importance of occurring plant species.

MATERIAL AND METHODS

Characterization of the study site Mělčany

Cadastral area of Mělčany is located in the South Moravian Region, about 20 km south of Brno. The altitude is about 230 m a. s. l. The area falls into a very warm and dry climatic region within Czechia.

The total area of the Mělčany cadastral area is 742.3 ha, of which the agricultural land is 665.3 ha. Within agricultural land, arable land takes up 617.3 ha, meadows and pastures 1.7 ha, gardens 9.6 ha and vineyards 36.7 ha.

The Mělčany village is governed by the wine law as a wine village belonging to the wine region of Moravia and subregion of Znojmo. Within the Mělčany wine village, 2 vine lines were floristically surveyed: Veselá hora and Seslice. Two other vine lines are Nad Humny and Jezuity, which were not planted with vineyards and therefore not evaluated.

Characterization of study site Rajhrad

Cadastral area of Rajhrad is in the neighbourhood of Mělčany. The altitude is about 190 m a. s. l. The area falls into a very warm and dry climatic region within Czechia.

The total area of the Rajhrad cadastral area is 949.1 ha, of which the agricultural land is 727.8 ha. Within agricultural land, arable land takes up 579.1 ha, meadows and pastures 0.8 ha, orchards 45.8 ha, gardens 57.0 ha and vineyards 45.1 ha.

The village Rajhrad is governed by the wine law as a wine village belonging to the wine region of Moravia and subregion of Znojmo. Within the wine village of Rajhrad, there is only one vine line called Hájiska.

Methodology of evaluation of vegetation species composition

Evaluation of vegetation was made using a floristic list of the found species. Evaluation was made in July 2017. Scientific names of individual plant species were used according to Kubát et al. (2002). The found species were registered during the monitoring. Occurrence of each recorded species was evaluated using a simple three-point scale after completion of the inspections.

Scale of species frequency:

3 – very frequent (dominant) species

2 – scattered species or frequent species on some parts of the vineyard

1 – species with rare occurrence

RESULTS AND DISCUSSION

The first evaluation area was the vine line Veselá hora (wine village Mělčany). Alternating grassed and cultivated inter-rows are applied as a cultivation method in the entire vineyard. A total of 29 plant species was found during the floristic survey.

The following taxa belong to frequently occurring species (scale evaluating 3) on this vine line: *Achillea millefolium* agg., *Avena fatua*, *Convolvulus arvensis*, *Dactylis glomerata*, *Festuca rubra*, *Chenopodium album* agg., *Medicago lupulina* and *Potentilla argentea.*

Common species with frequent occurrence were (scale evaluating 2): *Amaranthus retroflexus*, *Artemisia vulgaris*, *Bromus hordeaceus*, *Capsella bursa-pastoris*, *Elytrigia repens*, *Erigeron annuus*, *Hordeum murinum*, *Lolium perenne*, *Lotus corniculatus*, *Phacelia tanacetifolia*, *Plantago lanceolata*, *Raphanus raphanistrum*, *Rosa canina* and *Taraxacum* sect. *Ruderalia.*

Species with rare and sporadic occurrence on this vine line were (scale evaluating 1): *Carduus acanthoides*, *Conyza canadensis*, *Eryngium campestre*, *Falcaria vulgaris, Medicago minima*, *Robinia pseudacacia* and *Setaria viridis.*

The second evaluation area was vine line Seslice (wine village Mělčany). During the monitoring were found on this vine line 30 plant species.

Among the very frequently occurring species on this vine line belong (scale evaluating 3): *Achillea millefolium* agg., *Amaranthus retroflexus*, *Avena fatua*, *Convolvulus arvensis*, *Festuca rubra*, *Chenopodium album*, *Plantago lanceolata*, *Trifolium repens* and *Vicia sativa.*

Common species with frequent occurrence were (scale evaluating 2): *Carduus acanthoides*, *Consolida regalis*, *Conyza canadensis*, *Elytrigia repens*, *Holcus lanatus*, *Hordeum murinum*, *Lotus corniculatus*, *Potentilla reptans*, *Sanguisorba officinalis* and *Taraxacum* sect. *Ruderalia.*

Species with rare and sporadic occurrence on this vine line were (scale evaluating 1): *Anthemis arvensis*, *Artemisia vulgaris*, *Echinochloa crus-galli*, *Festuca ovina*, *Festuca pratensis*, *Filago arvensis*, *Lactuca serriola*, *Phacelia tanacetifolia*, *Poa pratensis*, *Silene latifolia* and *Tragopogon dubius.*

The third evaluation area was vine line Hájiska (wine village Rajhrad). Altogether, 36 plant species were found on this vine line.

Among the very frequently occurring species on this vine line belong (scale evaluating 3): *Achillea millefolium* agg., *Amaranthus retroflexus*, *Festuca rubra*, *Chenopodium album* agg. and *Setaria pumila.*

Common species with frequent occurrence were (scale evaluating 2): *Artemisia vulgaris*, *Avena fatua*, *Carduus acanthoides*, *Convolvulus arvensis*, *Conyza canadensis*, *Dactylis glomerata*, *Descurainia sophia*, *Erigeron annuus*, *Euphorbia esula*, *Fagopyrum esculentum*, *Geranium pusillum*, *Phacelia tanacetifolia*, *Rosa canina*, *Thlaspi arvense*, *Trifolium incarnatum* and *Vicia sativa.*

Species with rare and sporadic occurrence on this vine line were (scale evaluating 1): *Aethusa cynapium*, *Elytrigia repens*, *Erodium cicutarium*, *Euphorbia cyparissias*, *Galium album*, *Geranium pratense*, *Lolium perenne*, *Plantago lanceolata*, *Salvia pratensis*, *Saponaria officinalis*, *Sonchus arvensis*, *Sonchus asper*, *Sonchus oleraceus*, *Tragopogon dubius* and *Viola arvensis.*

Among the most occurring plant species in evaluated vineyards were especially annual species *Chenopodium album* agg., *Amaranthus retroflexus* and *Avena fatua.* From perennial plant species, *Achillea millefolium* agg., *Festuca rubra* and *Convolvulus arvensis* dominated here. According to Lososová et al. (2010), *Amaranthus retroflexus*, *Convolvulus arvensis*, *Chenopodium album* agg. and *Taraxacum* sect. *Ruderalia* belong among the most significant weeds species in vineyards.

From the plant species that are classified as invasive, the following were found: *Amaranthus retroflexus*, *Conyza canadensis* and *Erigeron annuus*. Among the found plant species, we can also name those that are able to compete directly with the grape-vine, such as *Artemisia vulgaris, Convolvulus arvensis, Rosa canina* and *Robinia pseudacacia.* In addition, two rare species of plants were found (*Medicago minima* (C3) and *Filago arvensis* (C3).

In vine lines of village Mělčany, altogether 43 plant species were found. In vineyards of village Rajhrad, 36 plant species were found altogether. If we compare our data with data form other vineyards, we can say that number of species found during our monitoring is lower. According to Maxianova et al. (2016), 104 plant species were found in wine village Popice. During the research of vineyards of wine village Pouzdřany,102 plant species were found (Liskova et al. 2016), in vineyards of wine village Syrovice, 40 plant species were found according to Stastny et al. (2017). In vineyards of wine village Žabčice, Bartosova et al. (2017) has found 97 plant species. The lower number of species is mainly due to the smaller area of the vineyards and also due to an isolation from main area of South Moravian vineyards.

CONCLUSION

Altogether, 62 plant species were found during the botanical monitoring of vegetation. The most occurring species were *Chenopodium album* agg., *Festuca rubra*, *Achillea millefolium*, *Convolvulus arvensis*, *Avena fatua*, *Amaranthus retroflexus* and *Plantago lanceolata.*

ACKNOWLEDGEMENTS

This work was supported by a Programme of applied research and development of national and cultural identity, project DG16P02R017 “Viticulture and winery for preservation and restoration of cultural identity of winery regions in Moravia “.

REFERENCES

Bartoskova, V. et al. 2017. Species composition of vegetation in wine villages Žabčice and Unkovice. In Proceedings of International PhD Students Conference MendelNet 2017 [Online]. Brno, Czech Republic, 8–9 November, Brno: Mendel University in Brno, Faculty of AgriSciences, pp. 33–38. Available at: https://mnet.mendelu.cz/mendelnet2017/mnet_2017_full.pdf. [2018-08-08].

Gurr, G. et al. 2004. Ecological Engineering for Pest Management: Advances in Habitat Manipulation for Arthropods. 1st ed., Canberra, Australia: CSIRO publishing.

Kubát, K. et al. 2002. Klíč ke květeně České republiky. 2st ed., Praha: Academia.

Landis, D.A. et al. 2000. Habitat management to conserve natural enemies of arthropod pests in agriculture. Annual Review of Entomology, 45: 175–201.

Liskova, M. et al. 2016. Species Composition of Vegetation in Vineyards of the Winery Village Pouzdřany. In Proceedings of International PhD Students Conference MendelNet 2016 [Online]. Brno, Czech Republic, 9–10 November, Brno: Mendel University in Brno, Faculty of AgriSciences, pp. 106–110. Available at: https://mnet.mendelu.cz/mendelnet2016/mnet_2016_full.pdf. [2018-08-08].

Lososová, Z. et al. 2010. Monitoring biologické rozmanitosti vinic na jižní Moravě. Zahradnictví, 10: 22–23.

Maxianova, A. et al. 2016. Species Composition of Vegetation in Vineyards of the Winery Village Popice. In Proceedings of International PhD Students Conference MendelNet 2016 [Online]. Brno, Czech Republic, 9–10 November, Brno: Mendel University in Brno, Faculty of AgriSciences, pp. 111–116. Available at: https://mnet.mendelu.cz/mendelnet2016/mnet_2016_full.pdf. [2018-08-08].

Novák, T.J. et al. 2014. Soil and vegetation transformation in abandoned vineyards of the Tokaj Nagy-Hill, Hungary. Catena, 123: 88–98.

Pavloušek, P. 2007: Encyklopedie révy vinné. 1st ed., Brno: ComputerPress.

Stastny, J. et al. 2017 Species composition of vegetation in wine village Bratčice and Syrovice. In Proceedings of International PhD Students Conference MendelNet 2017 [Online]. Brno, Czech Republic, 8–9 November, Brno: Mendel University in Brno, Faculty of AgriSciences, pp. 137–140. Available at: https://mnet.mendelu.cz/mendelnet2016/mnet_2016_full.pdf. [2018-08-08].

Von Hase, A. et al. 2010. Evaluating private land conservation in the Cape Lowlands, South Africa. Conservation Biology, 24: 1182–1189.

Winkler, K. et al. 2006. Nectar resources are vital for Diadegma semiclausum fecundity under field conditions. Basic and Applied Ecology, 7: 133–140.

Plant species composition of vegetation in vineyards of the wine village Velké Bílovice

Pavel Jagos[1], Pavel Dovolil[1], Jiri Sochor[2], Tomas Kopta[2,3], Jan Winkler[1,2]
[1]Department of Plant Biology
[2]Department of Viticulture and Enology
[3]Department of Vegetable Growing and Floriculture
Mendel University in Brno
Zemedelska 1, 613 00 Brno
CZECH REPUBLIC

winkler@mendelu.cz

Abstract: The purpose of the work is to compile a list of plant species growing in vineyards of the wine village Velké Bílovice. Nine vine lines were surveyed and all plant species were recorded. Numbers of species found in individual vine lines are as follows: *Nová hora* (83 species), Zadní hora (86), Přední hora (90), *Dlouhá hora* (56), *Široká hora* (65), *Pod Belegrady* (49), *Vinohrádky* (41), *Obory* (29), *Obecní* (22). The most frequent plant species represented in most vine lines were: *Chenopodium album, Convolvulus arvensis, Lolium perenne, Amaranthus retroflexus, Taraxacum* sect. *Ruderalia* and others. The number of species in the monitored vineyards of Velké Bílovice is relatively high – 156 species. Compared to the numbers of plant species in vineyards of other surveyed wine-growing villages, it is the highest number of species ever found in the vineyards of Morava region

Key Words: vegetation, vineyards, plant species, Velké Bílovice

INTRODUCTION

According to the rules of integrated viticulture takes place in our vineyards establishing and maintaining targeted greening in interrows by the rich herb mixtures (Pavloušek 2017). The diversity of species is related to securing and preserving landscape segmentation and it´s diversity. It has been demonstrated a direct relationship between the distance of vineyards to groups of trees and the presence of natural predators and parasites of grapevine pests (Thomson and Hoffmann 2009, 2013).

Selecting a method for targeted greening in vineyards must first be considered from several aspects. A vineyards are typically set up in steep terrain with perfect exposure to sunlight, which affects the evaporation of water and thus may give rise to stressful situations for vines (Pavloušek 2011).

Experiments with different mixtures of perennial species-rich herbs in the Tokaj region of Hungary to the east in the years 2012–2013 showed that the inter-row weed control during the first year after planting mix is best characterized by herb species with rapid initial growth. During the second year, weeds with the highest coverage and abundances were: *Lotus corniculatus, Medicago lupulina, Plantago lanceolata, Trifolium repens* and *Trifolium pratense*. The obvious is the need for diversity of species in the long term mixtures, in terms of creating a plant cover in different abiotic conditions and also longer-term time horizon result in greater flexibility of use. From a practical point of view, the herb mixtures should be compiled from species with similar seed sizes for easier seeding application (Miglécz et al. 2015).

The purpose of the work is to compile a list of species growing in vineyards of the wine village Velké Bílovice. Furthermore, to evaluate the importance of plant species in terms of vine cultivation and ecosystem services. Vineyards today are perceived as a community of plants where grapevine grows together with other plant species. Occurrence of many species of plants prevent erosion, provide food for the insect and vertebrates, enriches the soil with nitrogen. However, the vineyards also

contain invasive species, which pose a danger not only for the vegetation of the vineyards but also for the surrounding ecosystems.

MATERIAL AND METHODS

Characterization of growing locality Velké Bílovice

The cadastral area of Velké Bílovice is located in the South Moravian Region, about 45 km south-east of Brno or about 10 km north of Břeclav. The altitude is in the range of 176–262 m.

The area falls into a very warm and dry climatic region. The bedrock is composed of Paleogene claystone and sandstone flysch zone, overlaid incoherently loess and loess loams. The total area of the Velké Bílovice cadastral area is 2573 ha, where agricultural land covers 2226.3 ha. Vineyards occupy a respectable area of 681 ha within the agricultural land.

The Velké Bílovice village is governed by the wine law (Decree no. 254/2010) as a wine village belonging to the wine region of Moravia and the Velké Pavlovice wine subregion. There are nine vine lines (Nová hora, Zadní hora, Přední hora, Dlouhá hora, Široká hora, Pod Belegrady, Vinohrádky, Obory, Obecní) within the wine village cadastral area.

Methodology of evaluation of vegetation species composition

Evaluation of vegetation was made using a floristic list of the found species. Evaluation was made in the course of July 2016. Scientific names of individual plant species were used according to Kubát et al. (2002). Plant species were recorded during inspection surveys out for each wine line separately. Occurrence of each recorded species was evaluated using a simple three-point scale after completion of the inspections.

Scale for evaluating of species occurrence:

3 – very frequently occurring species (dominant species)

2 – common species with frequent occurrence at least on some parts on the vineyard (sub-dominant species)

1 – species with rare and sporadic occurrence

RESULTS AND DISCUSSION

Altogether 156 plant species were recorded by floristic survey in the monitored vine lines. Frequency of occurrence of each species were evaluated by a three-point scale. The results are shown at the Table 1. Within the *Nová hora* vine lines, 83 species of plants were found. There are 86 species of plants found in the *Zadní hora* vine lines. There are 90 species of plants found in the *Přední hora* vine lines. There are 56 species of plants found in the *Dlouhá hora* vine lines. There are 65 species of plants found in the *Široká hora* vine lines. There are 49 species of plants found in the *Pod Belegrady* vine lines. There are 41 species of plants found in the *Vinohrádky* vine lines. There are 29 species of plants found in the *Obory* vine lines. There are 22 species of plants found in the *Obecní* vine lines.

The most frequency plant species represented in most vine lines were: *Chenopodium album, Convolvulus arvensis, Lolium perenne, Amaranthus retroflexus, Taraxacum sect. Ruderalia, Echinochloa crus-galli, Setaria pumila, Trifolium repens, Polygonum aviculare, Hordeum murinum, Amaranthus powellii, Plantago major, Cirsium arvense, Achillea millefolium, Portulaca oleracea, Chenopodium hybridum, Erigeron annuus*.

Subdominant species (scale evaluating 2) with sporadic presence in relation to a specific vine lines, were: *Tripleurospermum inodorum, Senecio vulgaris, Conyza canadensis, Mercurialis annua, Capsella bursa-pastoris, Calamagrostis epigejos*.

In other cases, it is a sporadic occurrence or rare species or species used in species-rich greening mixtures in vineyards.

According to Lososová et al. (2010) among the most important weeds of our vineyards are: *Amaranthus retroflexus, Convolvulus arvensis, Chenopodium album, Taraxacum* sect. *Ruderalia* and *Cirsium arvense*. These weeds were very dominant in vineyard in Velké Bílovice. One of these

weeds was *Lolium perenne*. Lososová et al. (2010) draw attention to the fact that ocurrence of *Lolium perenne* in vineyards decreases numbers of weeds, which must be attributed to its ability to successfully compete with other species.

Table 1 Occurrence of species in vine lines of the wine village of Velké Bílovice

	Vine lines								
Species	Nová hora	Zadní hora	Přední hora	Dlouhá hora	Široká hora	Pod Belegrady	Vinohrádky	Obory	Obecní
Acer negundo	-	-	1	-	-	-	-	-	-
Agrimonia eupatoria	-	-	-	1	-	-	-	-	-
Achillea millefolium	2	1	2	1	1	2	2	2	2
Ailanthus altissima	-	1	1	-	-	-	-	-	-
Amaranthus albus	-	-	-	-	-	1	-	-	-
Amaranthus blitoides	-	-	-	-	2	-	-	-	-
Amaranthus powellii	2	2	2	2	2	2	2	2	-
Amaranthus retroflexus	3	3	2	2	2	2	2	2	3
Anthyllis vulneraria	-	1	-	-	-	-	-	-	-
Arctium lapa	2	1	-	-	-	-	-	-	-
Arctium tomentosum	2	1	1	-	2	-	-	-	-
Arenaria serpyllifolia	1	2	-	1	-	-	1	-	-
Armoracia rusticana	1	-	1	-	-	-	-	-	-
Arrhenatherum elatius	1	1	2	-	-	1	2	-	-
Artemisia absinthium	-	1	1	1	-	-	-	-	-
Artemisia vulgaris	2	1	2	-	-	1	-	-	-
Asclepias syriaca	1	1	-	-	-	-	-	-	-
Asparagus officinalis	1	-	-	-	-	-	-	-	-
Astragalus cicer	-	1	-	-	-	-	-	-	-
Astragalus glycyphyllos	-	-	1	-	-	-	-	-	-
Atriplex oblongifolia	-	1	-	-	-	-	-	-	-
Atriplex patula	1	2	1	-	1	1	2	-	-
Atriplex sagittata	1	-	1	-	-	1	2	-	-
Ballota nigra	-	1	1	-	-	1	-	-	-
Bromus hordeaceus	-	2	-	1	1	1	-	-	-
Bromus inermis	1	-	1	-	-	-	-	-	-
Bromus sterilis	2	2	-	-	2	-	-	2	-
Bromus tectorum	2	1	1	-	-	-	-	-	-
Calamagrostis epigejos	2	2	2	2	2	-	-	-	-
Camelina sativa	-	1	-	-	-	-	-	-	-
Capsella bursa-pastoris	1	1	1	1	2	1	2	1	-
Carduus acanthoides	2	1	2	1	1	-	-	-	-
Caucalis platycarpos	-	-	2	-	-	-	-	-	-
Cerastium arvenxe	-	-	1	-	-	-	-	-	-
Cichorium intybus	-	1	1	1	-	-	-	-	-
Cirsium arvense	1	2	2	2	2	2	2	1	1
Conium maculatum	1	-	-	-	1	-	-	-	-
Consolida regalis	1	-	-	-	-	-	-	-	-
Convolvulus arvensis	3	2	3	3	3	3	3	2	3
Conyza canadensis	1	2	2	2	2	-	-	2	1
Crepis biennis	2	1	1	1	-	1	-	-	-
Crepis tectorum	1	2	2	1	1	-	-	-	-
Cynodon dactylon	1	1	-	-	1	-	-	-	-
Cynoglossum montanum	-	-	-	-	1	-	-	1	-
Dactylis glomerata	1	1	-	1	1	1	-	1	-
Datura stramonium	1	-	-	1	2	-	1	1	-
Daucus carota	1	2	1	1	-	1	2	-	-
Descurainia sophia	1	-	-	-	-	-	-	-	-
Digitaria sanguinalis	-	-	-	-	-	-	-	-	2

Table 2 Occurrence of species in vine lines of the wine village of Velké Bílovice - continue

Species	Vine lines								
	Nová hora	Zadní hora	Přední hora	Dlouhá hora	Široká hora	Pod Belegrady	Vinohrádky	Obory	Obecní
Echinochloa crus-galli	2	2	1	2	2	1	3	3	2
Echium vulgare	1	-	-	-	-	-	-	-	-
Elytrigia repens	1	1	1	2	-	-	-	-	1
Epilobium ciliatum	1	-	-	-	-	-	2	1	-
Epilobium montanum	-	-	-	-	-	1	1	-	-
Erigeron annuus	2	2	2	2	1	2	1	2	-
Erodium cicutarium	-	1	1	-	-	-	-	-	-
Euphorbia helioscopia	-	-	1	-	1	-	-	-	-
Fagopyrum esculentum	-	-	-	1	-	-	-	-	1
Falcaria vulgaris	-	2	2	-	-	-	-	-	-
Fallopia convolvulus	-	-	1	-	1	-	-	-	-
Festuca ovina	-	1	-	-	-	1	-	-	-
Festuca rubra	-	-	-	-	2	1	-	2	-
Festuca valesiaca	-	-	-	-	2	-	-	-	-
Galinsoga parviflora	-	-	1	-	-	-	-	-	1
Galium album	-	-	1	-	-	-	-	-	-
Galium mollugo	1	-	-	-	-	-	-	-	-
Galium verum	-	-	1	-	-	-	-	-	-
Geum urbanum	-	-	-	-	1	-	-	-	-
Hieracium pilosella	-	1	-	1	-	-	-	-	-
Hordeum murinum	2	2	2	2	2	2	3	1	-
Hypericum perforatum	-	1	1	-	-	-	-	-	-
Chamomilla recutita	-	-	1	-	-	-	-	-	-
Chenopodium album	3	3	3	3	3	3	3	2	3
Chenopodium hybridum	2	3	1	2	2	1	3	-	-
Chenopodium strictum	2	-	-	-	-	-	-	-	-
Inula salicina	-	-	1	-	1	-	-	-	-
Juglans regia	1	1	-	-	-	1	-	-	-
Lactuca serriola	1	1	1	1	1	1	1	1	-
Lamium album	-	1	-	-	1	-	-	-	-
Lamium amplexicaule	2	1	-	-	-	-	-	-	-
Lapsana communis	1	-	-	-	-	-	-	-	-
Lathyrus pratensis	-	-	-	1	-	-	-	-	-
Lathyrus tuberosus	1	-	1	2	2	-	1	-	-
Lavatera thuringiaca	-	1	1	-	-	-	-	-	-
Leucosinapis alba	1	1	-	-	-	-	-	-	1
Linaria vulgaris	1	-	1	-	-	-	-	1	-
Lolium perenne	3	3	3	3	3	3	3	3	-
Lotus corniculatus	-	1	1	-	2	2	2	-	-
Lycium barbarum	-	-	1	-	-	-	-	1	-
Malva neglecta	1	-	2	1	1	1	2	-	-
Malva pusilla	-	-	-	-	-	-	1	-	-
Malva sylvestris	-	-	1	-	-	-	-	-	-
Medicago lupulina	1	3	2	1	1	1	-	-	-
Melica transsilvanica	1	1	-	-	-	-	-	-	-
Melilotus officinalis	-	-	1	-	-	-	-	-	-
Mercurialis annua	2	2	2	2	2	-	-	-	-
Onobrychis viciifolia	1	1	1	1	1	1	1	-	1
Origanum vulgare	1	-	-	-	-	-	-	-	-
Panicum miliaceum	1	-	-	1	1	-	-	-	-
Papaver rhoeas	-	1	1	-	-	-	-	-	-
Pastinaca sativa	2	1	2	-	-	1	1	-	-
Peucedanum alsaticum	1	1	1	-	-	-	-	-	-

Table 3 Occurrence of species in vine lines of the wine village of Velké Bílovice - continue

Species	Vine lines								
	Nová hora	Zadní hora	Přední hora	Dlouhá hora	Široká hora	Pod Belegrady	Vinohrádky	Obory	Obecní
Phacelia tanacetifolia	1	2	-	-	-	-	-	-	1
Phragmites australis	-	-	1	-	-	-	-	-	-
Picris hieracioides	1	1	-	-	-	1	-	-	-
Plantago lanceolata	1	1	-	1	1	-	1	-	-
Plantago major	2	3	3	2	2	2	-	1	-
Poa annua	-	-	1	3	-	-	-	-	-
Poa bulbosa	-	-		1	-	-	-	-	-
Polygonum aviculare	3	2	2	2	2	2	-	2	2
Portulaca oleracea	1	-	2	-	3	3	3	-	3
Potentilla argentea	-	1		-	-	-	1	-	-
Prunus avium	-	-	1	-	-	-	-	-	-
Quercus robur	-	-	-	-	1	-	-	-	-
Ranunculus repens	-	-	-	1	-	-	-	-	-
Raphanus raphanistrum	-	1	-	-	-	-	-	-	-
Reseda lutea	1	2	2	-	1	-	-	-	-
Rosa canina	1	1	1	1	1	1	-	-	-
Rubus sp.	1	-	1	-	1	-	-	-	-
Rumex crispus	-	-	-	-	-	1	-	-	-
Salvia pratensis	-	-	1	-	-	-	-	-	-
Salvia verticillata	1	-	-	-	-	-	-	-	-
Sambucus nigra	-	-	1	-	1	-	1	-	-
Securigera varia	-	1	1	-	-	2	-	-	-
Senecio vulgaris	2	2	2	3	1	-	2	-	-
Setaria pumila	2	2	2	2	3	2	-	2	2
Setaria verticillata	2	-	1	-	-	-	-	-	-
Setaria viridis	-	-	1	2	-	-	-	-	-
Silene latifolia	1	1	1	1	-	-	1	-	-
Silene vulgaris	-	-	-	-	-	-	-	-	1
Silybum marianum	-	1	-	-	-	-	-	-	-
Sisymbrium altissimum	-	-	1	-	-	-	-	-	-
Solanum nigrum	1	1	1	2	-	-	-	-	-
Solidago canadensis	-	-	-	1	1	1	2	-	-
Sonchus asper	1	1	-	1	-	-	-	-	-
Sonchus oleraceus	-	-	-	-	1	1	-	-	1
Stachys annua	1	1	1	-	-	1	-	-	-
Stellaria media	2	1	1	1	-	2	1	-	-
Symphytum officinale	1	-	1	-	-	-	-	-	-
Tanacetum vulgare	-	-	-	-	-	-	1	-	-
Taraxacum sect. *Ruderalia*	3	2	2	3	2	3	3	2	1
Thlaspi arvense	1	1	-	-	1	1	-	-	-
Thlaspi perfoliatum	-	1	-	-	-	-	-	-	-
Tragopogon dubius	1	-	1	-	1	-	-	-	-
Tragopogon orientalis	-	1	-	-	1	-	-	-	-
Trifolium incarnatum	-	1	-	1	2	1	-	2	-
Trifolium pratense	-	1	1		2	-	-	2	1
Trifolium repens	2	2	2	2	2	2	2	2	1
Tripleurospermum inodorum	1	2	1	2	2	2	2	1	
Urtica dioica	1	1	-	2	1	-	-	-	-
Urtica urens	-	-	1	-	-	-	-	-	-
Verbena officinalis	-	1	-	-	1	-	-	-	-
Veronica persica	-	-	1	-	2	-	-	-	-
Viola arvensis	-	-	-	-	-	-	1	-	-
Xanthium strumarium	-	-	-	-	-	-	1	-	-

The number of species in the monitored vineyards of Velké Bílovice is relatively high – 156 species. In the vineyards of the Popice wine village, Maxianova et al. (2016) found 104 species, in the vineyards of the Pouzdřany wine village Liskova et al. (2016) found 102 species, in the vineyards of the Syrovice wine village Stastny et al. (2017) found 40 species and in the vineyards of the Žabčice wine village Bartoskova et al. (2017) found 97 species. Compared to the numbers of plant species in vineyards of other surveyed wine-growing villages, it is the highest number of species ever found in the vineyards of Morava region.

CONCLUSION

During the vegetation monitoring of vineyards in the wine-growing village of Velké Bílovice, 154 plant species were found. The most occurrence plant species were: *Chenopodium album, Convolvulus arvensis, Lolium perenne, Amaranthus retroflexus, Taraxacum* sect. *Ruderalia, Echinochloa crus-galli, Setaria pumila, Trifolium repens, Polygonum aviculare, Hordeum murinum, Amaranthus powellii, Plantago major, Cirsium arvense, Achillea millefolium, Portulaca oleracea, Chenopodium hybridum, Erigeron annuus.*

ACKNOWLEDGEMENTS

This work was supported by a Programme of applied research and development of national and cultural identity, project DG16P02R017 "Viticulture and winery for preservation and restoration of cultural identity of winery regions in Moravia ".

REFERENCES

Bartoskova, V. et al. 2017. Species composition of vegetation in wine villages Žabčice and Unkovice. In Proceedings of International PhD Students Conference MendelNet 2017 [Online]. Brno, Czech Republic, 8–9 November, Brno: Mendel University in Brno, Faculty of AgriSciences, pp. 137–140. Available at: https://mnet.mendelu.cz/mendelnet2017/mnet_2017_full.pdf. [2018-20-08].

Kubát, K. et al. 2002: Klíč ke květeně České republiky. 2 vyd., Praha, CZ: Academia.

Liskova, M. et al. 2016. Species Composition of Vegetation in Vineyards of the Winery Village Pouzdřany. In Proceedings of International PhD Students Conference MendelNet 2016 [Online]. Brno, Czech Republic, 9–10. November, Brno: Mendel University in Brno, Faculty of AgriSciences, pp. 106–110. Available at: https://mnet.mendelu.cz/mendelnet2016/mnet_2016_full.pdf. [2018-08-08].

Lososová, Z. et al. 2010. Monitoring biologické rozmanitosti vinic na jižni Moravě. Zahradnictví, 20(10): 22–23.

Maxianova, A. et al. 2016. Species Composition of Vegetation in Vineyards of the Winery Village Popice. In Proceedings of International PhD Students Conference MendelNet 2016 [Online]. Brno, Czech Republic, 9–10. November, Brno: Mendel University in Brno, Faculty of AgriSciences, pp. 111–116. Available at: https://mnet.mendelu.cz/mendelnet2016/mnet_2016_full.pdf. [2018-08-08].

Miglez, T. et al. 2015. Establishment of three cover crop mixtures in vineyards. Scientia Horticulturae, 197(2): 117–123.

Pavloušek, P. 2017. Praktické poznatky k zakládání a udržovaní ozelenění ve vinicích. Vinařský obzor, 110(2): 67–69.

Pavloušek, P. 2011. Pěstováni révy vinné – moderní vinohradnictví.1. vyd., Praha: Grada.

Stastny, J. et al. 2017. Species composition of vegetation in wine village Bratčice and Syrovice. In Proceedings of International PhD Students Conference MendelNet 2017 [Online]. Brno, Czech Republic, 8–9. November, Brno: Mendel University in Brno, Faculty of AgriSciences, pp. 137–140. Available at: https://mnet.mendelu.cz/mendelnet2016/mnet_2016_full.pdf. [2018-08-08].

Thomson, L.J., Hoffmann, A.A. 2009. Vegetation increases the abundance of natural enemies in vineyards. Biological Control, 49(3): 259–269.

Thomson, L.J., Hoffmann, A.A. 2013. Spatial scale of benefits from adjacent woody vegetation on natural enemies within vineyards. Biological Control, 64(1): 57–65.

Species spectrum of weeds on field with sorghum (*Sorghum bicolor*)

Pavel Jagos[1], Leos Kadlcek[1], Pavel Horky[2], Jan Winkler[1]
[1]Department of Plant Biology
[2]Department of Animal Nutrition and Forage Production
Mendel University in Brno
Zemedelska 1, 613 00 Brno
CZECH REPUBLIC

winkler@mendelu.cz

Abstract: The aim of the work was to record the weed species on a field with sorghum cultivated for silage. Further, we determined the weed species, which could decrease the quality of silage or endanger the state of cattle health. The experimental land is located in the cadastral area of Žabčice (South Moravia, Czech Republic). The field survey was conducted in July 2018. Vegetation evaluation was carried out using phytosociological plots. Multivariate analyzes of ecological data were used to determine the impact of crop cover on weeds. Several poisonous species (*Consolida regalis, Datura stramonium, Euphorbia esula, Euphorbia helioscopia, Lactuca serriola* and *Solanum nigrum*) have been found and considered that with high proportion in silage could cause a cattle poisoning and health problems.

Key Words: vegetation, redundancy analysis, plant survey, *Sorghum bicolor*, fodder

INTRODUCTION

Sorghum [*Sorghum bicolor (L.) Moench*] is the fifth most cultivated grain in the world (Ottman 2009). Worldwide, it is considered to be the most important food for over 500 million people in 30 countries, and it is also the main animal feed (Kumar et al. 2012). Compared to other cereals, sorghum grows fast and produces high-quality grains, so it can replace other cereals in feeding dairy cattle and poultry (Ghani et al. 2015). In areas with high rainfall, sorghum is used for silage (Gholami et al. 2013).

Sorghum silage has a similar feed value to corn silage, has a similar nutrient content and higher yields under conditions of lower moisture. Sorghum and sorghum silage have proved to be an alternative feed for dairy cows (Miron et al. 2007). Furthermore, it is not attacked by maize pests and can be grown as a pre-crop, which can reduce the pests pressure on maize (Branson et al. 1969). Sorghum yields are usually lower than corn, but yields may be higher especially under stress conditions (Aydin et al. 1999, Abdelhadia and Santini 2006).

However, despite the large agronomic potential, the total area of sorghum has declined due to limited weed control (Kumar et al. 2012). Sorghum is a poor competitor against weeds due to slow growth in the first 20 days of 25 days (Rizzardi et al. 2004). Even a low level in the initial stage of weed may reduce the yield of grain sorghum. Incorporating monocotyledonous weeds in the first two weeks can reduce the yield of sorghum by up to 20% (Smith and Scott 2010). Magani (2008) reports that uncontrolled weed growth results in 40–60% loss of yields in sorghum. Losses in yields in sorghum can range from 15 to 97%, depending on the variety of sorghum, weed species, weed pollution time and environmental conditions (Mishra 1997, Tamado et al. 2002).

The aim of the work was to evaluate the species spectrum of weeds on a field with sorghum (cultivated for silage) and to determine the weed species, which could decrease the quality of silage or endanger the state of cattle health.

MATERIAL AND METHODS

Characterization of growing locality

The experimental plot (land block 3002/1) is located in the cadastral area of Žabčice (South Moravia, Czech Republic). The total land area is 30.43 ha. The Žabčice village is situated less than 25 km south of Brno. It belongs to the geomorphological area of Dyje-Svratka Valley. Žabčice is located in a maize production area, in flat terrain of 184 meters above sea level. The region of Žabčice can be considered as very dry and warm. The annual rainfall is 483.3 mm and the average annual temperature is 9.2 °C (the time period from 1961 to 1990).

Evaluation of weed species composition on the selected field with sorghum

The field survey was conducted in July 2018. Vegetation evaluation was carried out using phytosociological plots. The area of the plots was 12 square meters. Altogether 20 phytosociological plots were recorded on the field. The total coverage of sorghum and coverage of individual recorded weeds were estimated in percentages. The scientific names of each plant species were used according to Kubát et al. (2002).

Multivariate analyzes of ecological data were used to determine the impact of weed cover on weeds. The choice of optimal analysis was governed by the length of the gradient determined by Detrended Correspondence Analysis (DCA), determined by segments. Based on this procedure, a gradient length of 2.59, redundancy analysis (RDA) was obtained and decisive for ordination diagram. Significance of the crop cover on weed species was tested by Monte Carlo permutation test (999 permutations). The data was processed using the Canoco 5.0 computer program.

RESULTS AND DISCUSSION

A total of 39 species of weeds were found. The average coverage of each species is shown in Table 1. The most frequent were grasses (*Digitaria sanguinalis*, *Elytrigia repens*, *Setaria pumila* and others) and amaranths (mainly *Amaranthus retroflexus*). Also according to Grichar (2006) and Fromme et al. (2012), weeds of the Poaceae family are the most harmful on sorghum fields. Traore et al. (2003) found *Abutilon theophrasti* or Moore et al. (2004) reported an *Amaranthus palmeri* as very problematic weeds in sorghum. Both of these species are fortunately rare in the Czech Republic. On the other hand, other invasive species from *Amaranthus* genus can be dangerous instead of *A. palmeri*.

The results of Monte Carlo test in RDA analysis are insignificant ($\alpha = 0.067$). Graphic result is nevertheless presented in the form of ordination diagram (Figure 1). It is clear from the results that sorghum by its coverage is not able to statistically affect the weeds coverage. However, it should be noted that this is only one-year results and the growth of weeds was very low. The very low growth of weeds could be affected by the very warm and dry weather in vegetation season of 2018.

The sorghum has been grown for the production of silage and it is therefore necessary to evaluate the weeds found from the point of view of the quality of the feed. Several poisonous species (*Consolida regalis, Datura stramonium, Euphorbia esula, Euphorbia helioscopia, Lactuca serriola* and *Solanum nigrum*) have been found and considered that with high proportion in silage could cause a cattle poisoning and health problems. In addition, there have been found species of plants with various spines, hooks or trichomes, structures difficult to feed, and potentially cause digestive problems for cattle (*Amaranthus powellii, Amaranthus retroflexus, Bromus hordeaceus, Bromus tectorum, Lappula squarrosa, Lycopsis arvensis, Setaria pumila* and *Setaria viridis*).

Our results show that weeds can significantly affect the quality of sorghum silage and thus affect the performance and health of breeding cattle. Care must be taken to evaluate the species composition of weeds and to determine the proportion of harmful weed species in harvested forage.

Table 1 Average coverage of weed species in the selected sorghum field

Plant species	Shortcut	Average coverage (%)
Achillea millefolium	*Ach mill*	0.10
Amaranthus powelli	*Ama powe*	0.10
Amaranthus retroflexus	*Ama retr*	1.65
Arenaria serpyllifolia	*Are serp*	0.30
Bromus hordeaceus	*Bro hord*	0.25
Bromus tectorum	*Bro tect*	0.40
Capsella bursa-pastoris	*Cap burs*	0.25
Consolida regalis	*Con rega*	0.10
Convolvulus arvensis	*Con arve*	1.10
Conyza canadensis	*Con cana*	0.15
Datura stramonium	*Dat stra*	0.55
Descurainia sophia	*Des soph*	0.05
Digitaria sanguinalis	*Dig sang*	1.50
Echinochloa crus-galli	*Ech crus*	0.90
Elytrigia repens	*Ely repe*	1.00
Erodium cicutarium	*Ero cicu*	0.45
Euphorbia esula	*Eup esul*	0.75
Euphorbia helioscopia	*Eup heli*	0.10
Falcaria vulgaris	*Fal vulg*	0.05
Fallopia convolvulus	*Fal conv*	0.10
Geranium pusillum	*Ger pusi*	0.10
Chenopodium album	*Che albu*	0.60
Lactuca serriola	*Lac serr*	0.05
Lappula squarrosa	*Lap squa*	0.20
Lepidium ruderale	*Lep rude*	0.05
Linaria vulgaris	*Lin vulg*	0.25
Lolium perenne	*Lol pere*	0.25
Lycopsis arvensis	*Lyc arve*	0.10
Matricaria discoides	*Mat disc*	0.05
Polygonum aviculare	*Pol avic*	0.55
Portulaca oleracea	*Por oler*	0.50
Setaria pumila	*Set pumi*	3.00
Setaria viridis	*Set viri*	0.55
Solanum nigrum	*Sol nigr*	0.05
Taraxacum sect. *Ruderalia*	*Tar Rude*	0.05
Thlaspi arvense	*Thl arve*	0.10
Trifolium arvense	*Tri arve*	0.15
Tripleurospermum inodorum	*Tri inod*	0.25
Viola arvensis	*Vio arve*	0.05
Total coverage		65.60
Sorghum coverage		56.65

Figure 1 Ordination diagram showing the relationship of found weed species and sorghum cover

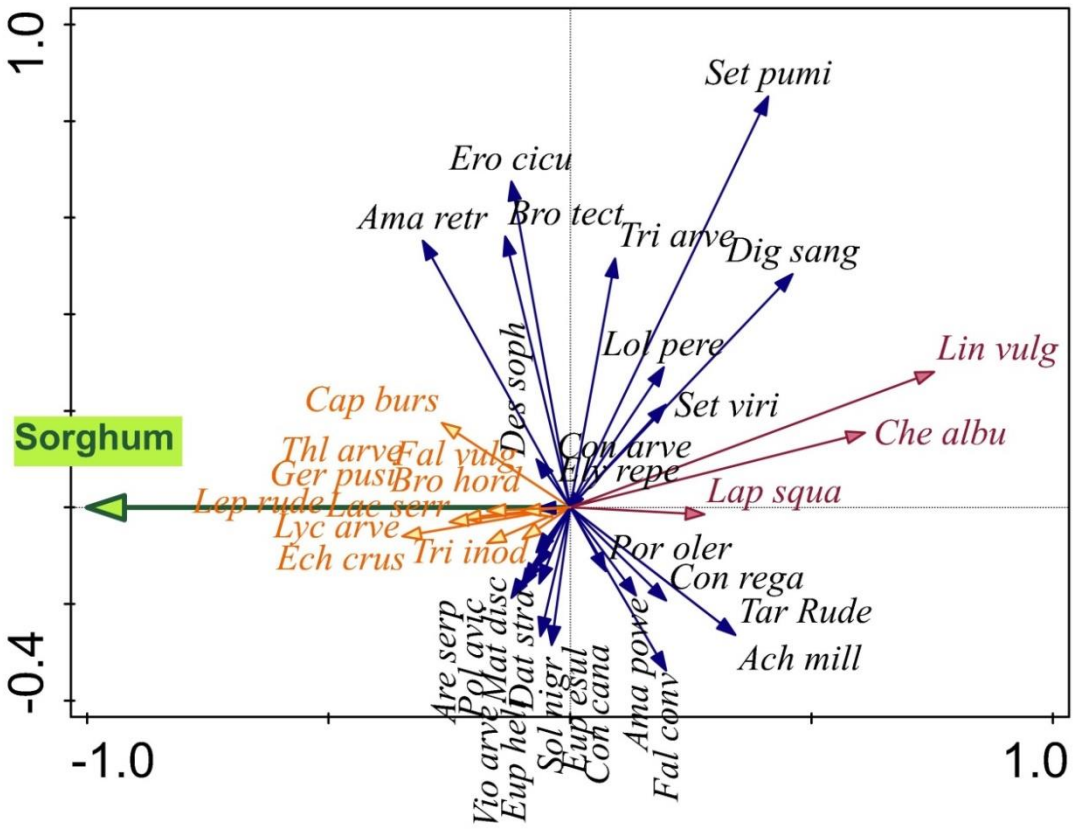

CONCLUSION

In crops of sorghum, a total of 39 species of weeds found. Among the species found, poisonous weeds and weeds were difficult to digest. These species may reduce the quality of sorghum silage and also endanger the health of cattle. Furthermore, the results suggest that sorghum can not suppress weed by its competitive ability. However, the results are only one-year and also affected by the weather in 2018, which was very warm and dry. Multi-year observation is needed to formulate more accurate conclusions.

ACKNOWLEDGEMENTS

The work was created as an output of the project: AF-IGA-2018-tym001: Comparison of the impact of climate change on photosynthesis C3 and C4 plants cycles which are used in livestock feed.

REFERENCES

Abdelhadia, L., Santini, F.J. 2006. Corn silage versus grain sorghum silage as a supplement to growing steers grazing high quality pastures: Effects on performance and ruminal fermentation. Animal Feed Science Technology, 127(1–2): 33–43.

Aydin, G. et al. 1999. Brown midrib sorghum in diets for lactating dairy cows. Journal of Dairy Science, 82(10): 2127–2135.

Branson, T.F. et al. 1969. Toxicity of sorghum roots to larvae of the western corn rootworm. Journal of Economic Entomology, 62(6): 1375–1378.

Fromme, D.D. et al. 2012. Weed control and grain sorghum (*Sorghum bicolor*) tolerance to pyrasulfotole plus bromoxynil. International Journal of Agronomy and Plant Production, 24: 59–69.

Ghani, A. et al. 2015. Evaluation of different sorghum (*Sorghum bicolor* L. Moench) varieties for grain yield and related characteristics. Science Letters Journal, 3(2): 72–74.

Gholami, S. et al. 2013. Non-chemical management of weeds effects on forage sorghum production. International Journal of Advanced Biological and Biomedical Research, 1: 614–623.

Grichar, W.J. 2006. Weed control and grain sorghum tolerance to flumioxazin. Crop Protection, 25(2): 174–177.

Kubát, K. et al. 2002: Klíč ke květeně České republiky. 1. vyd., Praha: Academia.

Kumar, U. et al. 2012. *Sorghum*. In Impacts of Climate Change on the Agricultural and Aquatic Systems and Natural Resources within the CGIAR's Mandate. Montpellier: Consultative Group on International Agricultural Research, pp. 136–144.

Magani, I.E. 2008. Weed control in sorghum-groundnut mixture in the simultaneous farming system of Southern Guinea Savanna zone of Nigeria. The Journal of Animal and Plant Sciences, 1: 3–8.

Miron, J. et al. 2007. Comparison of two forage sorghum varieties with corn and the effect of feeding their silages on eating behavior and lactation performance of dairy cows. Animal Feed Science Technology, 139(1–2): 23–39

Mishra, J.S. 1997. Critical period of weed competition and losses due to weeds in major field crops. Farm Journal Issues Listing, 33: 19–20.

Moore, J.W. et al. 2004. Palmer amaranth (*Amaranthus palmeri*) effects on the harvest and yield of grain sorghum (*Sorghum bicolor* L.). Weed Technology, 18(1): 23–29.

Ottman, M. 2009. Growing Grain Sorghum in Arizona. Arizona Cooperative Extension. [Online], 1(1): 141–144. Available at: https://extension.arizona.edu/pubs/growing-grain-sorghum-arizona. [2018-08-11].

Rizzardi, M.A. et al. 2004. Manejo e controle de plantas daninhas em milho e sorgo. In Manual de Manejo e Controle de Plantas Daninhas. Embrapa Uva e Vinho: Bento Gonçalves, pp. 571–594.

Smith, K., Scott, B. 2010. Weed control in grain sorghum. In Grain Sorghum Production Handbook. Little Rock, AR, USA: Cooperative Extension Service, University of Arkansas, pp. 47–49.

Tamado, T. et al. 2002. Interference by the weed *Parthenium hysterophorus* L. with grain sorghum: influence of weed density and duration of competition. International Journal of Pest Management, 48(3): 183–188.

Traore, S. et al. 2003. Velvetleaf interference effects on yield and growth of grain sorghum. Agronomy Journal, 95(5): 1602–1607.

Potato virus Y transmission by *Sitobion avenae* and *Myzus persicae*

Katerina Jegrova[1], Brian Fenton[2], Hana Sefrova[1]
[1]Department of Crop Science, Breeding and Plant Medicine
Mendel University in Brno
Zemedelska 1, 613 00 Brno
CZECH REPUBLIC
[2]Crop & Soils Systems
Scotland's Rural College (SRUC)
Ferguson Building, Craibstone Estate Bucksburn AB21 9YA
UNITED KINGDOM

xjegrova@mendelu.cz

Abstract: The control of aphid PVY vectors is necessary in potato seed crops. *Potato virus* Y is one of the most damaging potato viruses. In this study relative efficiency factor (REF) of *Sitobion avenae* (Fabricius, 1775) in comparison to *Myzus persicae* (Sulzer 1776) was evaluated. One thousand plants of *Physalis floridana* were used as indicator plants for transmission by 1360 aphids in total. *S. avenae* did not transmit PVY once while *M. persicae* transmitted PVY in 26.6% cases.

Key Words: PVY, grain aphid, *Sitobion avenae*, relative efficiency factor, virus transmission, crop protection

INTRODUCTION

Potato crops have an important role in agriculture as well as cereals and oilseeds in United Kingdom (UK). The potato planted area has been up to 145.000 ha in 2017. There are large production areas of seed potatoes in Scotland, it is over 40% of potato planted area in Scotland with the remainder being for consumable potatoes (Department for Environment, Food & Rural Affairs 2017).

Aphid control is necessary on seed potato crops in order to prevent the spread of *Potato leafroll virus* (PLRV) and viruses which cause mild and severe mosaic (Evans 2010). *Potato virus* Y (PVY) is the most important virus in Mediterranean countries. The second important virus is PLRV, though in recent years its importance seems to be decreasing (Loebenstein and Gaba 2012). The same situation is observed in UK: PLRV was once the most common virus in seed stocks and traditionally caused the greatest yield loss in ware crops. PLRV has been reduced to very low levels in seed potato growing areas in recent years. Nowadays larger losses are caused by other viruses such as PVY. Combined quality and yield losses make PVY the most damaging of the potato viruses (AHDB Potatoes 2015).

PVY is a nonpersistent virus which is transmitted by many aphid species colonising potatoes but also by species of non-potato-colonizing aphids (Edwards 1963). The second group of aphids are probing the potato leaves in search of suitable hosts, only few seconds are sufficient for the acquisition of PVY (USDA 2018).

There is a pest monitoring website available for the growers in UK maintained by Fera Science Ltd where recent information of aphid distribution and abundance in fields are provided. The data for this software is collected from yellow water traps (YWTs) and it is used to produce traffic light type warning system. There is also up-to-date news (Bulletin Weeks) on the distribution and abundance of aphids at a regional scale based on data from a network of sixteen Rothamsted/SASA air suction traps. This monitoring is important for decision making: if and when there is a need to use insecticide treatments against vectors.

The study of Verbeek et al. (2009) states that PVY control systems rely on measuring virus pressure and vector pressure in the field. Calculation of the vector pressure is based on the relative efficiency factors (REF) of aphid species. REF express the transmission efficiency of aphid species in relation to the transmission efficiency of *Myzus persicae* (Sulzer 1776), the most efficient vector

of PVY. According to AHDB webpage it was given a value 0.01 to *S. avenae* and but later it was changed to 0.60. REF is mentioned at this webpage as relative transmission efficiency (RTE).

The AHDB funded project (Fenton et al. 2013) had used different clones of *S. avenae*, but this was prior to genotyping and therefore it is not known which clones were used. Two clones of *S. avenae* were used for the purposes of this study, a susceptible clone and resistant clone to pyrethroids. In cereal crop production pyrethroids are extensively used to control *S. avenae* which exerts a strong selection pressure for resistance. In 2011 the first control failures on cereal crops in England were detected. Gaynor Malloch in her work identifies *S. avenae* clones in Scotland. Pyrethroid resistance was found particularly in a single genotype – SA3 (Malloch et al. 2013). This raised a question what was the PVY REF of different *S. avenae* genotypes and in particular SA3?

MATERIAL AND METHODS

Aphids and plant hosts

Two aphid species were used for this study: *Myzus persicae* (MP) type J as a control and *Sitobion avenae*, resistant clone (SA3) and susceptible clone (SS). Aphid colonies of *M. persicae* were reared on healthy potato plants and colonies of *S. avenae* on barley plants. Apterous adults or 3rd or 4th instar nymphs were taken for the transmission. Potato plants were used for PVY acquisition by aphids: nontreated control plants and plants treated with the pyrethroid Hallmark Zeon. Seedlings of *Physalis floridana* were used as PVY indicator plants.

Transmission experiment

Modified methods originally published in research article by Fenton, B. et. al. (2014) were used for the transmission experiment. The transmissions were carried out from 15 August to 14 September 2017. On 15 and 16 August only nontreated potato leaves were used for testing of 4 replicates per day to compare PVY efficiency transmission between *Myzus persicae* and *Sitobion avenae*. On 17 August, 4, 5 and 6 September 6 batches per day were tested and in these cases pyrethroid treated and untreated potato leaves were used to see also differences in PVY transmission between SS and SA3 (pyrethroid sensitive and resistant). On 12, 13 and 14 September triple the number of individuals SS and SA3 were used to increase vector pressure.

For the transmission which included untreated leaves for PVY acquisition the following methods were used. Leaves of a treated potato plant and nontreated control plant were cut from the plant and used for PVY acquisition by aphids. These two variants were supposed to show differences in PVY transmission between the susceptible and resistant clones of *S. avenae*. The fresh green leaves without any signs of senescence were used and placed into a plastic cup container. Two cups were used, the lower one had a small amount of water, so the leaves were able to reach the water through the hole in the upper one.

The aphids were moved by brush from colonies into a glass vial for 2 hours to starve them and to ensure probing on the new host leaf. 20 aphids were taken for every batch: 10 MP and 10 SA3 or 10 MP and 10 SS. The aphids were then transmitted on PVY-infected potato leaf for acquisition which took 7 minutes. One potato leaf was used for the acquisition of PVY virus for two batches: a variant of MP and SA3 and another variant MP and SS to make sure that the same conditions for acquisition were provided. After that aphids were moved individually onto a *P. floridana* seedling: 1 aphid per 1 plant and every seedling was covered by a small cap including gauze lid to prevent escape of aphids.

The trays with *P. floridana* seedling were moved to a glass house the next day. Every seedling was checked to see if the aphid is still present on the *P. floridana* plants. This fact was marked in a form: present/not. Then plants were sprayed by Hallmark Zeon (lambda-cyhalothrin). On the second day they were sprayed by Provado (thiacloprid). These two insecticides were used to make sure that both susceptible and resistant clone were killed after the transmission. The plants were evaluated after 3 weeks for PVY symptoms. The symptomatic plants were smaller than asymptomatic plants and they had wrinkled leaves (Figure 1).

Figure 1 The reaction of Physalis floridana to PVY infection, the symptomatic plants are highlighted in red

RESULTS AND DISCUSSION

Sitobion avenae results

S. avenae had tendency to probe potato and then migrate to find more suitable host. Therefore *P. floridana* plants were evaluated the day after the transmission to see if *S. avenae* individuals stayed on the plants: 84 individuals were observed. Despite this fact and the fact that same conditions for the PVY acquisition from the same potato leaf were provided for both species, *M. persicae* and *S. avenae*, there were no PVY infected *P. floridana* plants after *S. avenae*. Three hundred and twenty plants were used for initial transmission and the ratio was 1 MP: 1 SA3 or 1 SS. Then the vector pressure was increased by changing ratio to 1 MP to 3 SA3 or 3 SS: there were further 540 transmission on 180 plants and there was also no infected *P. floridana*.

The differences of PVY transmission efficiency between the clones SA3 and SS could not be evaluated, because there was no infected *P. floridana* plant.

Myzus persicae results

There were 500 *P. floridana* plants used for transmission of 500 *M. persicae* in total. One hundred and thirty-three plants were infected by PVY virus which was 26.6% (see Figure 2). We observed 372 *M. persicae* individuals on the leaves of *P. floridana* the next day after the transmission.

Figure 2 PVY positive P. floridana plants by date of transmission

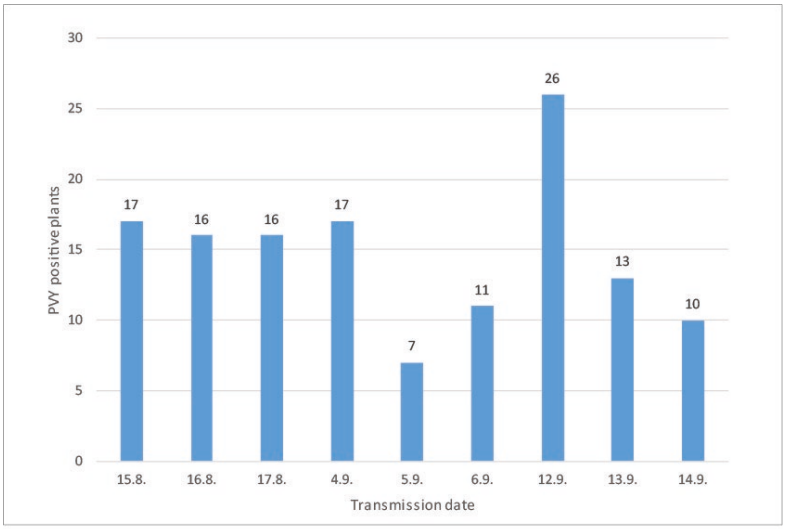

Overall results

There were 50 batches in this study which means 1000 plants of *P. floridana* which were used as indicator plants and 1360 aphids were used for transmission in total.

The results suggest that the REF score of 0.6 for *S. avenae* is not representative of the current clone in the UK and could be resulting in increased use of insecticides. The results of this study are similar to results of research conducted by Verbeek et al. (2009) where it was given REF 0.00 to *S. avenae*.

CONCLUSION

S. avenae did not transmit PVY while *M. persicae* transmitted PVY in 26.6% cases under same conditions. This corresponds to a very low transmission rate for *S. avenae*, consistent with previous REF studies.

ACKNOWLEDGEMENTS

This study was arranged as a doctoral traineeship in cooperation with Crop & Soils Systems department (SRUC). Thanks to Dr Gaynor Malloch for providing genotyped aphids of each species. Thanks also to Dr Andy Evans for placing Katerina Jegrova in Aberdeen.

REFERENCES

AHDB Potatoes. ©2015. Potato Leafroll Virus. [Online] Available at: https://potatoes.ahdb.org.uk/gallery/potato-diseases (PLRV). [2018-09-10].

Department for Environment, Food & Rural Affairs. 2017. Farming statistics – final crop areas, yields, livestock populations and agricultural workforce at 1 June 2017-UK [Online]. Available at: https://assets.publishing.service.gov.uk/government/uploads/system/uploads/attachment_data/file/670004/structure-jun2017final-uk-21dec17.pdf. [2018-09-10].

Edwards, A.R. 1963. A Non-colonizing Aphid Vector of Potato Virus Diseases. Nature, 200: 1233–1234.

Evans, A. 2010. Aphids and Aphid-borne virus disease in potatoes [Online]. 1st ed., Edinburgh: The Scottish Agricultural College. Available at: https://www.sruc.ac.uk/download/downloads/id/1343/tn492_aphids_and_aphiod-borne_virus_disease_in_potatoes.pdf. [2018-09-10].

Fenton, B. et al. 2013. Final Report. Aphids & Virus Transmission in Seed Crops. Ref: R428 [Online]. 1st ed., United Kingdom Potato Council: Agriculture and Horticulture Development Board. Available at: https://potatoes.ahdb.org.uk/sites/default/files/publication.../R428_Final%20Report.pdf. [2018-09-10].

Fenton, B. et al. 2014. Stopped in its tracks: how λ-cyhalothrin can break the aphid transmission of a potato potyvirus. Wiley Online Library [Online], 71(12): 1611–1616. Available at: https://onlinelibrary.wiley.com/doi/abs/10.1002/ps.3967. [2018-09-10].

Loebenstein, G., Gaba, V. 2012. Advances in Virus Research, Chapter 6 – Viruses of Potato. [Online] 1st ed., Department of Virology, Agricultural Research Organization, Bet Dagan, Israel: Academic Press. Available at: https://doi.org/10.1016/B978-0-12-394314-9.00006-3. [2018-09-10].

Malloch, G. et al. 2013. Research Report Analysis of Grain Aphid (Sitobion avenae) Populations-genetic composition and the frequency of pyrethroid resistance [Online]. 1st ed., United Kingdom: Agriculture and Horticulture Development Board. Available at: https://cereals.ahdb.org.uk/media/525211/214-0004-fpr.pdf. [2018-09-10].

USDA. ©2018. Managing Potato Virus Y in Seed Potato Production. Information on PVY [Online]. Available at: http://www.potatovirus.com/index.cfm/page/PVYinfo.htm. [2018-09-10].

Verbeek, M. et al. 2009. Determination of aphid transmission efficiencies for N, NTN and Wilga strains of Potato virus Y. Annals of Applied Biology [Online], 156(1): 39–49. Available at: https://onlinelibrary.wiley.com/doi/abs/10.1111/j.1744-7348.2009.00359.x. [2018-09-10].

Weed infestation of fields with Westerwolds annual ryegrass (*Lolium multiflorum* var. *Westerwoldicum*)

Leos Kadlcek[1], Pavel Horky[2], Jan Winkler[1]
[1]Department of Plant Biology
[2]Department of Animal Nutrition and Forage Production
Mendel University in Brno
Zemedelska 1, 613 00 Brno
CZECH REPUBLIC

leos.kadlcek@mendelu.cz

Abstract: Westerwolds annual ryegrass (*Lolium multiflorum* var. *Westerwoldicum*) is cultivated in various parts of the world as a fodder crop for beef cattle, generally mixed with soya or maize. Efforts to improve the annual production of high-quality fodder has increased the importance of cultivation of Westerwolds annual ryegrass. The objective of the paper is to assess weed infestation on fields with Westerwolds annual ryegrass, i.e. to record weed species occurrence and to evaluate the relationship between crop coverage and weed species presences and abundances. The assessed lands were located in the cadastral area of Rebešovice (South Moravia, Czech Republic). The vegetation recording was made using phytosociological plost in June 2018. A total of 36 weed species were identified in the plots, where annual weeds *Anagallis arvensis* and *Oxalis fontana* were found as most abundant. *Datura stramonium* or *Echinochloa crus-galli*, for example, were found more frequently on plots covered by sparse crop, pointing to low crop ability to suppress several weeds. Weed species composition changed very little according to the crop coverage. The most problematic weeds in fodder crops are poisonous species, we found *Aethusa cynapium, Datura stramonium, Equisetum palustre, Euphorbia helioscopia, Fumaria officinalis* and *Solanum nigrum*, which can cause health problems after cattle feeding.

Key Words: weed, plant protection, Rebešovice, herbology, fodder crop

INTRODUCTION

Westerwold annual ryegrass (*Lolium multiflorum* var. *Westerwoldicum*) is cultivated in various parts of the world together with soya or maize as a fodder crop for cattle (Carvalho et al. 2010). It is sometimes used as a cover crop, particularly in situations where rapid stabilisation of the soil surface is the main priority. The main advantage of ryegrass is economical reliability and speed of establishment (Evers and Nelson 1994).

Westerwold ryegrass is often described as an annual ryegrass, but in practice it may persist in swards for 1–3 years. Poor soils, diligent cutting to prevent seeding, and hard winters all help eliminate it over time. Efforts to improve the annual production of this high-quality cattle fodder has increased the importance of cultivation of annual grass species (Hoveland et al. 1981).

The aim of the paper was to assess the weed species frequency land with Westerwolds annual ryegrass and evaluate influence of crop cover on weed species coverages. Weeds with negative influence on fodder quality are discussed.

MATERIAL AND METHODS

Characterization of growing locality

The assessed fields (soil block 6003/1; soil block 6903) are located in the cadastral area of Rebešovice (South Moravian Region, Czech Republic). The area is 11.18 ha and is situated in the maize production area, in a flat area of an elevation about 200 m a.s.l. The land is farmed by Zemědělské družstvo Rajhradice.

Assessment of weed infestation in selected fields

The field assessment was made in course of June 2018. In total, 7 phytosociological plots of an area 12 m^2 were made on the land. Percentage scale was applied to take into account the weed coverages. Cover of Westerwolds annual ryegrass was estimated in percentages directly in the field. Mean of weed species coverages per plots were counted. The scientific names of each plant species were unified according to Kubát et al. (2002).

Multidimensional analyses of ecological data were used to determine the relationship between Westerwolds annual ryegrass coverage and recorded weed species. The selection of the optimal analysis was governed by the length of gradient determined in Detrended Correspondence Analysis (DCA). Therefore, we applied redundancy analysis (RDA) for further data processing after we found a short gradient of 2.17 standard deviation units in DCA. Monte-Carlo test (999 permutations) was used for determination of significance of the result. The data were processed using Canoco 5.0 computer software (Ter Braak and Šmilauer 2012).

RESULTS AND DISCUSSION

In total, we identified 36 weed species on the land. The list cover of species identified on the study plots is shown in Table 1. The results of the Monte-Carlo test in RDA, which assessed the relationship of weed species to coverage of crop at the significance level $\alpha = 0.775$ and therefore statistically not conclusive. The graphic outcome is an ordination diagram (Figure 1).

Figure 1 Ordination diagram illustrating the relationship of weed species and cover of Westerwolds annual ryegrass. For abbreviations see Table 1.

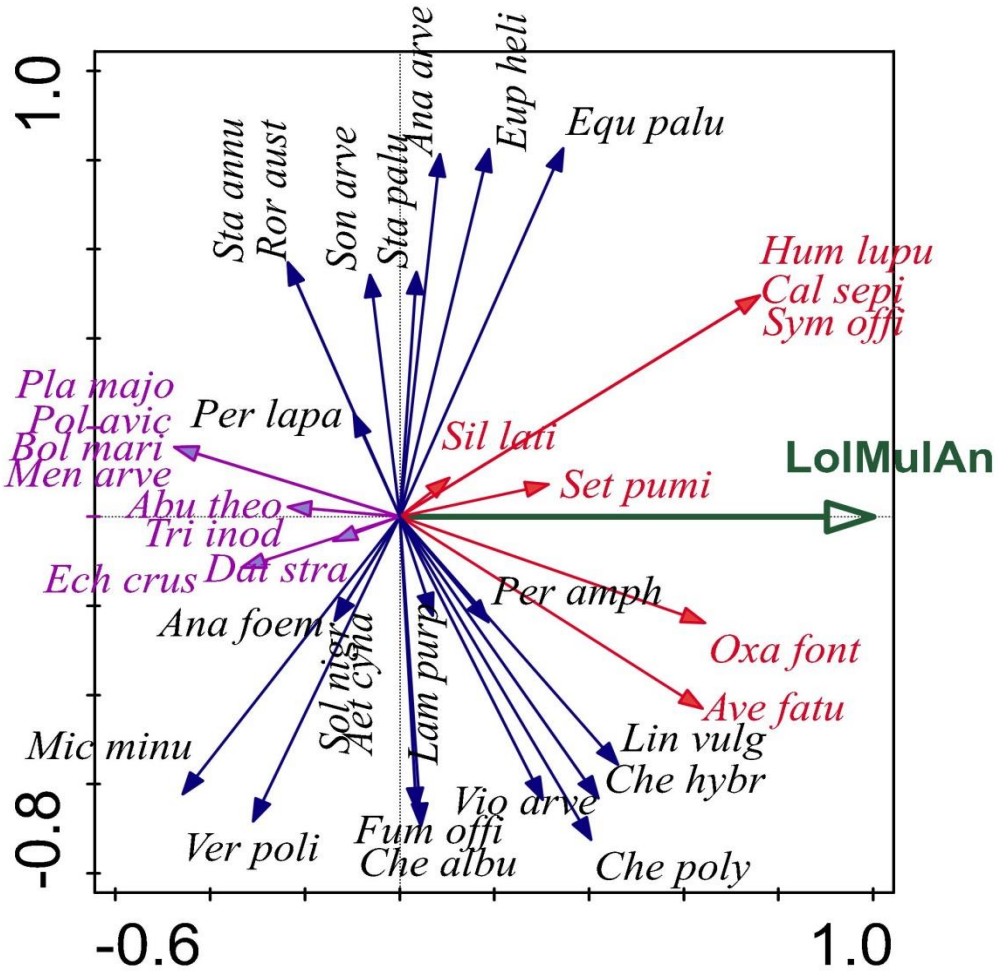

Table 1 List of recorded weed species, abbreviations used in Figure 1 and mean values of species covers in phytosociological plots (n= 7).

Plant species	Abbreviations	Average cover (%)
Abutilon theophrasti	*Abu theo*	0.14
Aethusa cynapium	*Aet cyna*	0.14
Anagallis arvensis	***Ana arve***	**13.57**
Anagallis foemina	*Ana foem*	0.14
Avena fatua	*Ave fatu*	0.86
Bolboschoenus maritimus	*Bol mari*	0.14
Calystegia sepium	*Cal sepi*	0.29
Datura stramonium	*Dat stra*	5.71
Echinochloa crus-galli	*Ech crus*	0.86
Equisetum palustre	*Equ palu*	2.86
Euphorbia helioscopia	*Eup heli*	2.00
Fumaria officinalis	*Fum offi*	2.86
Humulus lupulus	*Hum lupu*	0.14
Chenopodium album	***Che albu***	**4.71**
Chenopodium hybridum	*Che hybr*	1.29
Chenopodium polyspermum	*Che poly*	0.86
Lamium purpureum	*Lam purp*	2.14
Linaria vulgaris	*Lin vulg*	0.43
Mentha arvensis	*Men arve*	0.14
Microrrhinum minus	*Mic minu*	1.57
Oxalis fontana	***Oxa font***	**10.00**
Persicaria amphibia	*Per amph*	0.71
Persicaria lapathifolia	***Per lapa***	**5.43**
Plantago major	*Pla majo*	0.14
Polygonum aviculare	*Pol avic*	0.14
Rorippa austriaca	*Ror aust*	0.14
Setaria pumila	*Set pumi*	0.43
Silene latifolia	***Sil lati***	**6.71**
Solanum nigrum	*Sol nigr*	0.14
Sonchus arvensis	*Son arve*	1.14
Stachys annua	*Sta annu*	0.14
Stachys palustris	*Sta palu*	1.71
Symphytum officinale	*Sym offi*	0.29
Tripleurospermum inodorum	*Tri inod*	0.14
Veronica polita	*Ver poli*	3.00
Viola arvensis	*Vio arve*	0.71
Total cover of weeds		60.00
Lolium multiflorum var. *Westerwoldicum*	LolMulAn	36.86

The results indicate that the ryegrass cover was not significant for weed species heterogeneity. The ryegrass growth was disconnected and fragmentary due to the warm and dry weather during whole vegetation season 2018. This could have affected the low competitive ability of the ryegrass and the increased weed infestation level.

Ryegrass crop is used mainly as fodder for cattle, therefore higher attention have to be done on frequency of poisonous weeds. *Aethusa cynapium, Fumaria officinalis, Datura stramonium, Equisetum palustre, Euphorbia helioscopia* and *Solanum nigrum* were found during the monitoring. With a high rate of presence in the fodder, these species might cause poisoning and health problems for cattle. In addition, we found plant species that reduce the digestibility of fodder or reduce fodder intake due to their awns, hooks and trichomes. There are: *Avena fatua, Bolboschoenus maritimus, Humulus lupulus* and *Symphytum officinale*. High frequency of *Oxalis fontana* was surprising to us, because this species does not belong among typical weeds of conventionally managed arable land, was quite extraordinary.

CONCLUSION

A total of 36 weed species were identified in the fields with Westerwolds annual ryegrass. The results indicate that the ryegrass is not able to suppress weeds, at least during drier and warmer climatic conditions observed in a year 2018. Disconnected and fragment crop cover influenced to the increased weed infestation level. The recorded weeds included species that are poisonous or reduce the fodder digestibility. We are presenting here only results after one-year monitoring which can be moreover affected by the specific climatic conditions in 2018. Long-term monitoring here for necessary for formulation of more accurate conclusions.

ACKNOWLEDGEMENTS

The paper is an outcome of the project: AF-IGA-2018-tym001: Comparison of the impact of climate change on photosynthesis C3 and C4 plants cycles which are used in livestock feed.

REFERENCES

Carvalho, P.C.F. et al. 2010. Managing grazing animals to achieve nutrient cycling and soil improvement in no-till integrated systems. Nutrient Cycling in Agroecosystems [Online], 88(2): 259–273. Available at: http://dx.doi.org/10.1007/s10705-010-9360-x. [2018-07-07].

Evers, G.W., Nelson, L.R. 1994. Overseeding bermudagrass with annual ryegrass. In Proceedings of American Forage and Grassland Conference. Lancaster, Pennsylvania, 6–10 March. Georgetown, Texas: American Forage and Grassland Council, pp. 190–193.

Hoveland, C.S. et al. 1981. Seeding legumes into tall fescue sod [Online]. 1st ed., Alabama: Auburn University. Available at: http://aurora.auburn.edu/bitstream/handle/11200/2454/1710BULLpdf?sequence=1.

Kubát, K. et al. 2002. Klíč ke květeně České republiky. 1st ed., Praha: Academia.

Ter Braak, C.J.F., Šmilauer, P. 2012: Canoco reference manual and users guide: software for ordination (version 5.0). Microcomputer Power, Ithaca.

Distribution of weed species on land with combined crops of spring triticale (*xTriticosecale*) and field pea (*Pisum sativum* var. *arvense*)

Barbora Kotlanova[1], Leos Kadlcek[1], Pavel Horky[2], Jan Winkler[1]
[1]Department of Plant Biology
[2]Department of Animal Nutrition and Forage Production
Mendel University in Brno
Zemedelska 1, 613 00 Brno
CZECH REPUBLIC

b.stromska@email.cz

Abstract: Growing crops with dense canopy help regulate weeds, especially those resistant to herbicides. The aim of the study is to determine the relationship between the mixed crop (x *Triticosecale* and *Pisum sativum* var. *arvense*) and individual weed species. The main use of the crops is to produce silage for cattle feeding. From this perspective, the presence of some species is undesirable. The experimental land is located in cadastral territory of the village of Mladějovice (Olomouc District). The evaluation of weed infestation in mixed crop of (x *Triticosecale* and *Pisum sativum* var. *arvense*) was carried out using phytosociological plots. The evaluation was conducted in July 2018.There were 41 weed species found in total. Several poisonous weeds were found as *Euphorbia helioscopia or Solanum nigrum*. Another weed species have their negative effects due to decreasing digestibility (*Avena fatua, Bromus sterilis, Cirsium arvense, Equisetum arvense, Galium aparine, Rumex obtusifolius, Setaria pumila, Setaria viridis*) and are considered as unsuitable for beef cattle. The grown herb mixtures have the potential to suppress some weed species (e.g. *Apera spica-venti, Setaria* spp.). However, the reaction of all weed species was not the same. Some weed species were able to successfully resist the competition of the sown mixture.

Key Words: crop production, vegetation, survey, plant diversity, Mladějovice

INTRODUCTION

Competitiveness of cultivated crops is the primary mechanism of indirect weed control (Mhlanga et al. 2016). The direct damage caused by weeds depend on environmental conditions, biological properties of the crops and intensity of the cultivation technique (Boguzas et al. 2010, Swanton et al. 2015).

Cultivation of crops with densely connected stands aids suppress the weeds through the competition for light water space and nutrients (Bezuidenhout et al. 2012). It is important particularly for weeds resistant to herbicides (Webster et al. 2013).

Combination of crop species may be one of the important factors in weed suppression. Uchino et al. (2012) state that rye (*Secale cereale*) was the most suitable candidate for a mixture with hairy vetch (*Vicia villosa*) and for effective weed suppression.

There are two agroecological approaches at present: (i) intercropping, i.e., combined growth of two or more crops in the same space (Malézieux et al. 2009); and (ii) the use of cover crops, i.e., combined sowing of two crops with different harvest times on the same plot (Hartwig and Ammon 2002). Weed suppression by intercropping or cover crops is based on key ecological principles, such as growing competition between the sown crops and weeds for light, nutrients and water and for underground and aboveground space (Liebman and Dyck 1993).

The objective of the paper is to determine the relationship between the sown mixture of crops (triticale and field pea) and annual weed species.

MATERIAL AND METHODS

Locality characteristics

The experimental land is located in the cadastral area of Mladějovice (soil block 6302/11) in (district of Olomouc). It belongs to the geomorphological area of Upper Moravian Graben. The area is situated in a sugar beet production area, in a flat area with elevation of 250 m a.s.l. The total land size is 20.42 ha and is farmed by Paseka zemědělská a.s.

Assessment of weed infestation in mixed triticale and field pea

The field assessment was made in the course of July 2018. In total, 20 phytosociological plots were made on the land. The area of each plot was 12 m^2 and percentage scale was applied to take into account the coverage. Means of weed species coverages were counted. The scientific names of vascular plant species were used according to Kubát et al. (2002).

Multidimensional analyses of ecological data were used to determine the joined effect of triticale and field pea coverage on the weed species. All of 20 original phytosociological plots were analysed. The selection of the optimum analysis was governed by the length of gradient, determined by Detrended Correspondence Analysis (DCA). We selected redundancy analysis (RDA) for further data processing after we found a short gradient of 2.39 standard deviation units in DCA Monte-Carlo test (999 permutations) was used for determination of significance of the result. The data were processed using Canoco 5.0 computer software (Ter Braak and Šmilauer 2012).

RESULTS AND DISCUSSION

In total, we identified 41 weed species on the land. The list of species and mean coverage of species identified on study plots is shown in Table 1. Several poisonous weeds were found as *Euphorbia helioscopia* or *Solanum nigrum*. Another weed species have their negative effect due to decreasing digestibility and are considered as unsuitable for beef cattle (*Avena fatua, Bromus sterilis, Cirsium arvense, Equisetum arvense, Galium aparine, Rumex obtusifolius, Setaria pumila, Setaria viridis*).

The results of the RDA, which assessed the relationship of weeds species with a separate coverage of crops are significant at the significance level $\alpha = 0.007$ for both the canonic axes and are therefore statistically conclusive. The graphic outcome is an ordination diagram (Figure 1).

Based on the visual distribution of species arrows in the diagram (Figure 1), the weed species can be divided into three categories. The first category are weed species that are well suppressed by the cover of the mixed crop (triticale + field pea), namely: *Apera spica-venti*, *Rumex obtusifolius*, *Setaria pumila*, *Setaria viridis*, *Sisymbrium loeselii* and *Tripleurospermum inodorum*. The well-connected growth of triticale and field pea has the potential to suppress these species successfully.

The second category of weed species includes those that are able to compete with the crop and grow under the higher crop cover, namely: *Avena fatua*, *Brassica napus* subsp. *napus Capsella bursa-pastoris*, *Chenopodium hybridum*, *Solanum nigrum*, *Stellaria media*, *Veronica persica* and *Viola arvensis*. These species have the potential to assert themselves in well-connected stands and are therefore strongly harmful in combined stands of triticale and field pea.

The third species category was affected by other factors more than the crop cover ability. The identified species from this category include: *Amaranthus* sp., *Bromus sterilis*, *Cirsium arvense*, *Convolvulus arvensis*, *Echinochloa crus-galli*, *Equisetum arvense*, *Euphorbia helioscopia*, *Fallopia convolvulus*, *Galium aparine*, *Geranium dissectum*, *Chenopodium album*, *Chenopodium pedunculare*, *Chenopodium strictum*, *Lamium purpureum*, *Linaria vulgaris*, *Medicago sativa*, *Myosotis arvensis*, *Oxalis fontana*, *Plantago major*, *Poa annua*, *Polygonum aviculare*, *Sinapis arvensis*, *Stachys palustris*, *Symphytum officinale*, *Thlaspi arvense* and *Valerianella locusta*. The response of the weed species found in our study can be also a consequence of the one-year results and may be different over multiple-year observation.

Table 1 List of recorded weed species, abbreviations used in Figure 1 and mean values of species covers in phytosociological plots (n=20).

Plant species	Abbreviations	Mean cover (%)
Amaranthus sp.	*Ama*	1.30
Apera spica-venti	*ApeSpica*	0.95
Avena fatua	*AveFatu*	0.80
Brassica napus subsp. napus	*BraNapu*	0.75
Bromus sp. (*Bromus* cf. *arvensis*)	*BroArve*	0.70
Bromus sterilis	*BroSter*	0.25
Capsella bursa-pastoris	*CapBurs*	0.60
Cirsium arvense	*CirArve*	1.75
Convolvulus arvensis	*ConArve*	1.60
Echinochloa crus-galli	***EchCrus***	**6.55**
Equisetum arvense	*EquArve*	0.65
Euphorbia helioscopia	*EupHeli*	0.95
Fallopia convolvulus	*FalConv*	0.40
Galium aparine	*GalApar*	1.70
Geranium dissectum	*GerDiss*	0.30
Chenopodium album	***CheAlbu***	**4.75**
Chenopodium hybridum	*CheHybr*	0.05
Chenopodium pedunculare	*ChePedu*	0.25
Chenopodium strictum	*CheStri*	1.55
Lamium purpureum	*LamPurp*	0.45
Linaria vulgaris	*LinVulg*	0.05
Medicago sativa	*MedSati*	0.10
Myosotis arvensis	*MyoArve*	0.15
Oxalis fontana	*OxaFont*	0.05
Plantago major	*PlaMajo*	0.05
Poa annua	***PoaAnnu***	**4.00**
Polygonum aviculare	*PolAvic*	1.05
Rumex obtusifolius	*RumObtu*	0.40
Setaria pumila	***SetPumi***	**10.65**
Setaria viridis	*SetViri*	1.75
Sinapis arvensis	*SinArve*	0.05
Sisymbrium loeselii	*SisLoes*	0.05
Solanum nigrum	*SolNigr*	0.40
Stachys palustris	*StaPalu*	0.25
Stellaria media	*SteMedi*	1.85
Symphytum officinale	*SymOffi*	0.25
Thlaspi arvense	*ThlArve*	0.50
Tripleurospermum inodorum	*TriInod*	0.20
Valerianella locusta	*ValLocu*	0.10
Veronica persica	*VerPers*	1.50
Viola arvensis	***VioArve***	**2.05**
Total cover of weeds		92.35
x *Triticosecale*	Tritical	58.15
Pisum sativum var. *arvense*	Pisum	22.80

Figure 1 Ordination diagram illustrating the relationship of weed species (small arrows) and cover of crops, triticale and field pea (large arrows), separately. For abbreviations see Table 1.

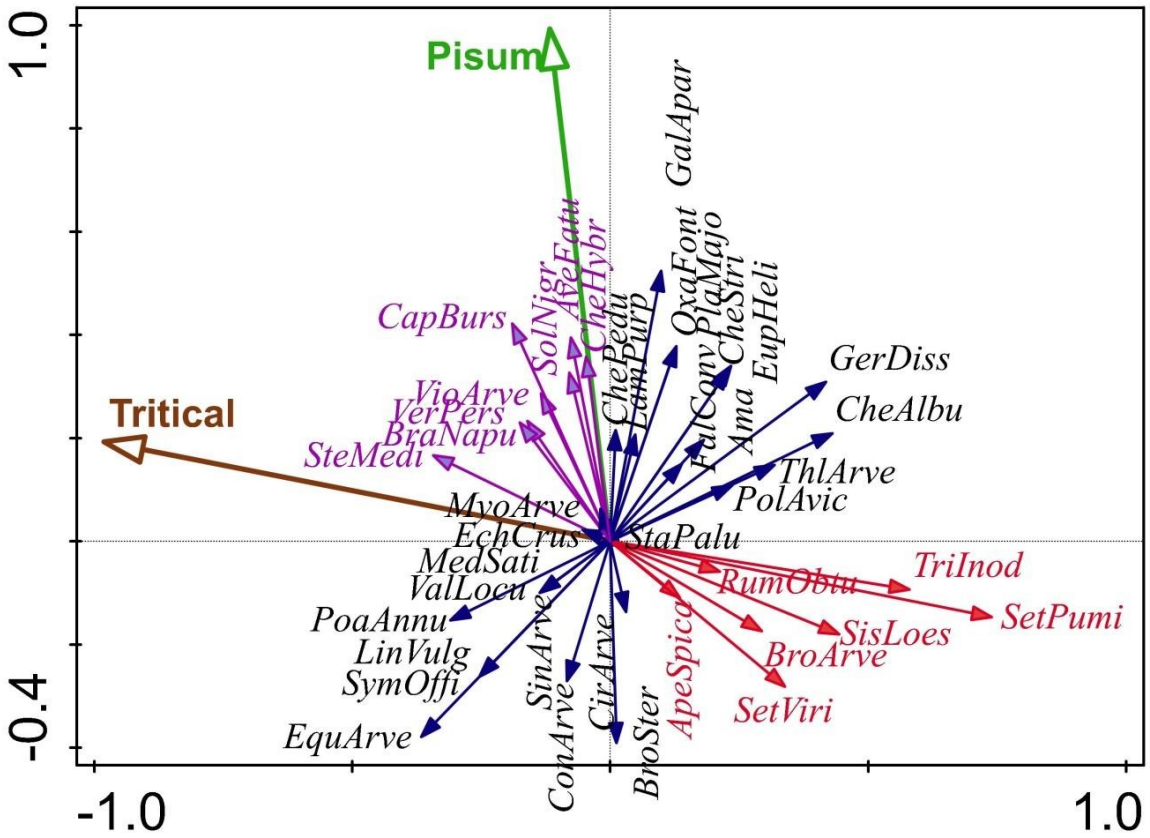

CONCLUSION

A total of 41 weed species were identified in the mixed stand of triticale and field pea. The cultivated mixture has the potential to suppress some weed species contrary to single crops. However, the response of all the species was not identical. Some of the species were capable of successfully withstanding the competition of the sown mixture. We are presenting here only one-year results, which can be moreover affected by the very warm and dry weather in 2018. Observation over more years is necessary for formulation of more accurate conclusions.

The primary use of the triticale and field pea mixture is for production of silage for cattle fodder. From this perspective, the presence of some of the species is undesirable. This refers primarily to the poisonous weed species *Euphorbia helioscopia*, *Solanum nigrum*. In addition, there are species that reduce digestibility and are poorly accepted by cattle (*Avena fatua, Bromus sterilis, Cirsium arvense, Equisetum arvense, Galium aparine, Rumex obtusifolius, Setaria pumila, Setaria viridis*).

ACKNOWLEDGEMENTS

The paper is an outcome of the project: AF-IGA-2018-tym001: Comparison of the impact of climate change on photosynthesis C3 and C4 plants cycles which are used in livestock feed.

REFERENCES

Bezuidenhout, S.R. et al. 2012. Cover crops of oats, stooling rye and three annual ryegrass cultivars influence maize and *Cyperus esculentus* growth. Weed Research [Online], 52(2): 153–160. Available at: http://dx.doi.org/10.1111/j.1365- 3180.2011.00900.x. [2018-07-08].

Boguzas, V. et al. 2010. Weed response to soil tillage, catch crops and farmyard manure in sustainable and organic agriculture. Zemdirbyste, 97(3): 43–50.

Hartwig, N.L., Ammon, H.U. 2002. Cover crops and living mulches. Weed Science, 50(1): 688–699.

Kubát, K. et al. 2002. Klíč ke květeně České republiky. 1st ed., Praha: Academia.

Liebman, M., Dyck, E. 1993. Crop rotation and intercropping strategies for weed management. Ecological Application, 3: 92.

Malézieux, E. et al. 2009. Mixing plant species in cropping systems: concepts, tools and models. A review. Agronomy for Sustainable Development, 29: 43–62.

Mhlanga, B. et al. 2016. Weed management in maize using crop competition: a review. Crop Protection [Online], 88: 28–36. Available at: http://dx.doi.org/10.1016/j. cropro.2016.05.008. [2018-7-8].

Swanton, C.J. et al. 2015. Experimental methods for crop-weed competition studies. Weed Science [Online], 63(1): 2–11. Available at: http://dx.doi.org/10.1614/WS-D13-00062.1. [2018-07-08].

Ter Braak, C.J.F., Šmilauer, P. 2012: Canoco reference manual and user's guide: software for ordination (version 5.0). Microcomputer Power, Ithaca.

Uchino, H. et al. 2012. Effect of interseeding cover crops and fertilization on weed suppression under an organic and rotational cropping system. 1. Stability of weed suppression over years and main crops of potato, maize and soybean. Field Crops Research [Online], 127(2): 9–16. Available at: http://dx.doi.org/10.1016/j.fcr.2011.10.007. [2018-07-08].

Webster, T.M. et al. 2013. Winter cover crops influence *Amaranthus palmeri* establishment. Crop Protection [Online], 52(1): 130–135. Available at: http://dx. doi.org/10.1016/j.cropro.2013.05.015. [2018-07-08].

Influence of sulfur fertilization on soybean microbiota

Petr Kouril, Libor Kalhotka, Eva Burdova, Marie Skolnikova, Jiri Antosovsky, Petr Skarpa
Department of Agrochemistry, Soil Science, Microbiology and Plant Nutrition
Mendel University in Brno
Zemedelska 1, 613 00 Brno
CZECH REPUBLIC

petr.kouril@mendelu.cz

Abstract: The aim of our work was to investigate the effect of various forms of fertilization with sulfur on the soybean microbiota. The following forms of sulfur were used in the experiment: 1. no application; 2. thiosulfan sulfur; 3. elemental sulfur and 4. polysulfide sulfur. The most significant effect on the number of microorganisms present in a first year of the experiment in thiosulfate sulfur which most affected *Enterobacteriaceae* that have been detected $1.9x10^3$ CFU/g in comparison with control variant, where the counts were $3.6x10^3$ CFU/g. In the second year of the experiment was changed because the biggest influence began to show a form of elemental sulfur, which most affected the yeast counts. The treated sample was detected $1.4x10^3$ CFU/g in comparison with the control sample which was detected $6.6x10^4$ CFU/g. Other applied forms of sulfur did not significantly affect the numbers of microorganisms.

Key Words: soybean, fertilization, microorganisms, sulfur

INTRODUCTION

Soy is one of the perspective of nutrition of farm animals among the most valuable protein feed. It can be grown either as forage or grain. As forage is mostly used on farms in the USA and Canada, where it is grown in a mixture with corn for silage production. Grain contains 30% digestible nitrogenous substances and 17% of fat (Horký et al. 2015).

Sulfur in plant nutrition plays a very important role in the primary and secondary metabolites of plants that are closely related to nutritional values. In vegetables is affects protein synthesis and the formation of secondary metabolites (essential oils, glucosinolates etc.). In legumes is necessary for symbiotic nitrogen fixation, thus positively affects the nutritive value of proteins comprising sulfur-containing amino acids (Hlušek et al. 2002).

On green plants there is an epiphytic microbiota whose amount and species composition is very variable and is influenced by weather conditions, habitats, agrotechnology levels and many other factors. Epiphytic microbiota is very important in the process of silage on which contribute most lactic acid bacteria. Their amount ranges from 10^2 to 10^5 CFU/g. Other agents are enterobacteria, which can cause considerable loss in silage. Unwanted microorganisms are clostridia, which is the agent of buttering fermentation. Very problematic is the presence of yeast and mold that can produce mycotoxins, which represent one of the most serious contamination of feed (Havlíček et al. 2014).

The aim of the contribution was to determine the microbial settlement of the above-ground parts of plants with respect to the groups of microorganisms that may be of importance in the feed industry and to assess the possibility of influencing the epiphytic microbiota by different forms of sulfur applied on the leaf.

MATERIALS AND METHODS

Soybean – *Glycine max* (variety Bohemians) was sown in the pot contains 10 kg of soil to a depth of 2–3 cm. Ten seeds were sown in each pot. After emergence was left in the tank 5 plants. Foliar application of sulfur fertilizers was performed in stage of 10^{th} leaf. Each pot contained 5 selected soybean plants in the vegetative stage. Fertilizers had the recommended dose specified by the manufacturer. This recommended dose per hectare was recalculated for use in a quantitative experiment (calculated

with 550,000 plants per hectare). Fertilizer variants are described in Table 1. Each variant had 4 replicates. The experiment was conducted in two years. At the end of the experiment (plants in the stage suitable for harvest as green feed), a 10 g average sample was taken from each pot (16 pieces).

Table 1 Variants of fertilization and dose of sulfur per pot in individual variants

Variants of fertilization	Fertilizers	Dose of sulfur per pot
1. Control	-	
2. Thiosulfate sulfur	FOLIT®ThioSulf	8.3 mg
3. Elemental sulfur	FERTI MK - S 800 SC	36.4 mg
4. Polysulfide sulfur	SULKA - K	6.7 mg

The sample weight (10 g) of the original green mass was shaken for 1 minute with 90 ml of sterile saline in a sterile PE bag on a STOMACHER homogenizer (Interscience, France) to release the microorganisms from the surface of the plant material. From the solution was then prepared by decimal dilution series. The following groups of microorganisms were determined in the samples:

- Total plate count (TPC) on the PCA agar (Biokar Diagnostics, France) at 30 °C for 72 h.
- Bacteria of the *Enterobacteriaceae* family on VRBG agar (Biokar Diagnostics, France) at 37 °C for 24 hours.
- Thermosensitive aerobic and sporulating microorganisms on PCA agar (Biokar Diagnostics, France) at 30 °C in 48 hours after a previous 10 min heating at 85 °C.
- Micromycetes (yeast and mold) on Cloramphenicol glucose agar (Biokar Diagnostics, France) at 25 °C in 120 hours.

After a period of cultivation in petri dishes were grown colonies characteristic subtracted and the result after the conversion expressed as colony forming units – CFU/g.

RESULTS AND DISCUSSION

From the results in the first year of the experiment, it is clear that none of the tested forms of sulfur had a significant effect on soybean microorganism settlement. When comparing the individual variants, we find that there were only slight differences in the number of microorganisms. The largest difference was found in the number of *Enterobacteriaceae* using thiosulphate sulfur when their amount was detected in the values of $1.9x10^3$ CFU/g than without application sulfur, wherein their amount was $3.6x10^3$ CFU/g. A further significant difference was detected in the same form of sulfur in yeast counts where $2.1x10^2$ CFU/g was detected compared to $5.7x10^2$ CFU/g in the sulfur-free variant. Detailed results are given in Table 2.

Table 2 Mean values and standard deviation of significant microorganisms in CFU/ g in the first year of the experiment

Variant	TPC	*Enterobacteri-aceae*	TMR ae	Micromycetes		
				Total	Yeast	Molds
1	$9.4x10^4±1.1 x10^5$	$3.6x10^3±4.3 x10^3$	$2.0x10^2±1.4 x10^2$	$6.7x10^3±8.6 x10^2$	$5.7x10^2±1.7 x10^2$	$6.1x10^3±9.3 x10^2$
2	$2.1x10^5±2.8 x10^5$	$1.9x10^3±1.3 x10^3$	$4.3x10^2±2.7 x10^2$	$7.7x10^3±3.8 x10^3$	$2.1x10^2±8.0 x10^1$	$7.5x10^3±3.8 x10^3$
3	$2.1x10^5±2.0 x10^5$	$1.1x10^4±1.4 x10^4$	$3.6x10^2±8.6 x10^1$	$8.9x10^3±2.2 x10^3$	$6.2x10^2±3.6 x10^2$	$8.3x10^3±2.6 x10^3$
4	$2.0x10^5±2.0 x10^5$	$2.0x10^4±2.9 x10^4$	$1.5x10^2±5.7 x10^1$	$6.2x10^3±1.5 x10^3$	$5.0x10^2±4.1 x10^2$	$5.7x10^3±1.3 x10^3$

Legend: TPC – total plate count, TMR ae – aerobic thermosensitive microorganisms

In the second year of the experiment, the effect of sulfur application was more pronounced. The largest differences were observed in TPC, where $7.1x10^4$ CFU/g was detected in the sulfur-free variant, while thiosulfate sulfur was detected at $3.3x10^4$ CFU/g and polysulfide sulfur $3.7x10^4$ CFU/g.

Even more significant influence was the application of sulfur to the number of yeasts. There were $6.6x10^4$ CFU/g in the sulfur-free variant, whereas all the applied forms of sulfur reduced the number of yeasts by one order. The largest decrease was observed in the elemental sulfur variant, when their amount was $1.4x10^3$ CFU/g versus $6.6x10^4$ CFU/g in the sulfur-free variant. Detailed results are given in Table 3.

Table 3 Mean values and standard deviation of significant microorganisms in CFU / g in the second year of the experiment

Variant	TPC	*Enterobacteri-aceae*	TMR ae	Micromycetes		
				Total	Yeast	Molds
1	$7.1x10^4$±$6.1x10^4$	$1.2x10^3$±$1.3x10^3$	$1.8x10^2$±$5.5x10^1$	$7.0x10^4$±$1,1x10^5$	$6.6x10^4$±$1.1x10^5$	$3.9x10^3$±$5.3x10^2$
2	$3.3x10^4$±$1.2x10^4$	$3.6x10^3$±$3.6x10^3$	$3.0x10^2$±$1.6x10^2$	$1.3x10^4$±$2.5x10^3$	$3.5x10^3$±$1.6x10^3$	$9.1x10^3$±$2.7x10^3$
3	$5.8x10^4$±$2.7x10^4$	$6.8x10^2$±$9.3x10^2$	$1.6x10^2$±$4.0x10^1$	$1.1x10^4$±$2.4x10^3$	$1.4x10^3$±$6.5x10^2$	$9.1x10^3$±$2.7x10^3$
4	$3.7x10^4$±$5.5x10^3$	$7.1x10^2$±$6.2x10^2$	$1.8x10^2$±$4.0x10^1$	$1.2x10^4$±$4.8x10^3$	$1.6x10^3$±$8.6x10^2$	$1.0x10^4$±$4.6x10^3$

Legend: TPC – total plate count, TMR ae – aerobic thermosensitive microorganisms

Kalhotka (2017) in his work dealt with the microorganisms in the green stuff. It states that the CPM in the legume plants is in the range 10^6 to 10^{10} CFU/g. In the samples we analyzed, the CPM ranged between 10^4 and 10^5 CFU/g. In our opinion, this difference is caused by the application of sulfur, but the origin of the samples. Furthermore, in its work, the amount of bacteria of the *Enterobacteriaceae* family ranged from 10^2–10^5 CFU/g. The values we have found correspond to these figures. Last tracked a group of microorganisms that his work was micromycets states, which include yeasts and molds. Their amount is in the range of 10^4 to 10^6 CFU/g for legume plants. Compared with our results, these are higher values. Our values ranged from 10^3 to 10^4 CFU/g. Doležal et al. (2012) reports that enterobacteria are a significant epiphytic microflora on green plants, where they occur in the range 10^6–10^8 CFU/g. Compared with our results, we ranged between 10^3–10^4 CFU/g in the first year and 10^2–10^3 CFU/g in second year. In our opinion, the difference in sulfur effect on the number of microorganisms between the first and second year of the experiment could be partly due to higher average temperature and lower relative air humidity during the second year of the experiment. In addition to our groups of microorganisms, lactic acid bacteria are also present on green plants, which are especially important for the production of silage. Their amount ranges from 10^2 to 10^5 CFU/g (Havlíček et al. 2014).

CONCLUSION

The results obtained during the first year of the experiment indicate that thiosulfan sulfur has the greatest impact on the number of microorganisms. In this form, enterobacteria and yeasts were the most affected compared to untreated samples. In the second year, the situation has changed. Thiosulfan form of sulfur affected only CPM counts. In this year, the elemental form of sulfur most affected by enterobacteria and yeasts was most affected by microorganisms. Other applied forms of sulfur did not have a negative effect on the number of microorganisms.

ACKNOWLEDGEMENTS

The research was financially supported by IGA grant, no. TP_4/2017.

REFERENCES

Doležal, P. et al. 2012. Konzervace krmiv a jejich využití ve výživě zvířat. Olomouc: Petr Baštan.
Havlíček, Z. et al. 2014. Zdravotní bezpečnost krmiv, stájové prostředí a výskyt mastitid. Brno: Mendelova univerzita v Brně.
Hlušek, J. et al. 2002. Výživa a hnojení zahradních plodin. 1.vyd., Praha: Martin Sedláček.

Horký, P. et al. 2015. Krmné suroviny [Online]. Available at: https://web2.mendelu.cz/af_291_projekty2/vseo/stranka.php?prez=271. [2018-08-29].

Kalhotka, L. 2017. Problematické mikroorganismy a jejich metabolity v krmivech – zelená píce. In Proceedings of Farmářská výroba sýrů a kysaných mléčných výrobků XIV. Brno, Czech Republic, 18 May, Brno: Mendelova univerzita v Brně, pp. 30–33.

Spatial analysis of crop yields maps in precision agriculture

Jiri Mezera[1], Vojtech Lukas[1], Jakub Elbl[1,2], Vladimir Smutny[1]
[1]Department of Agrosystems and Bioclimatology
Mendel University in Brno
Zemedelska 1, 613 00 Brno
[2]Spearhead Czech s.r.o.
Revolucni 130/30, 751 17 Horni Mostenice
CZECH REPUBLIC

jmezera@seznam.cz

Abstract: Information about yield distribution within the fields is crucial for evaluation and planning of site specific crop management practices. This paper presents methodology of the processing of data from yield mapping to produce reliable yield maps. The study was conducted on the yield data of winter wheat recorded during the harvest in 2016 on the fields with total area 248 ha at the farm company SALIX MORAVA a.s. (locality Zdounky, Kroměříž, Czech Republic). Analysis of outliers and re-calibration of sensor values was identified as the most important part of data pre-processing. Some of these procedures are discussed in the paper to ensure high quality output dataset for next processing – spatial interpolation. In this step, Empirical Bayesian Kriging proved its ability for full automatization of yield maps creation in GIS environment. Last part of the study is focused on the creation of relative yield maps as the main information for identification of under- and over-average yield areas, which can support the agronomist decisions on the crop treatment intensity in the form of variable rate application (fertilizers, crop protection, etc.).

Key Words: site specific crop management, spatial variability, GIS, yield mapping

INTRODUCTION

For site specific crop management treatments, such as variable rate application of fertilizers or crop protection, main information about field variability is required. Main source of the information is based on the sensor mapping techniques, soil sampling, crop sensing or yield mapping. Differences of crop yield levels are often used as the indicator of field heterogeneity, if yield maps are available.

Recent studies shown that there are many factors influencing the spatial variability of crop yields, such as evapotranspiration (Johnen et al. 2014), topographic attributes (Kumhálová et al. 2014) or combined effects of soil fertility and weed control (Mallarino et al. 1999). Yield is the integrator of landscape and climatic variability and therefore provide useful information for identifying management zones (Kleinjan et al. 2007). Management zones represent in the context of precision agriculture areas possessing homogenous attributes in landscape and soil condition. These areas should lead to the same results in crop yield potential, input use efficiency and environmental impact (Schepers et al. 2004). Delineation of management zones for site specific crop management, is usually based on yield maps over the past few years. Similar to the evaluation of yield variation from multiple yield data described by Blackmore et al. (2003), the aim is to identify high yielding (above the mean) and low yielding areas related as the percentage to the mean value of the field. Also the inter-year spatial variance of yield data is important for agronomists to distinguish between areas with stable or unstable yields. However, classification of management zones from time-series of yield maps appears limited because of the high frequency of erroneous data sets, systematic errors in the recorded data and their restricted yield predictive ability (Joernsgaard and Halmoe 2003).

Aim of the study was to describe a methodology of yield data processing, spatial analysis and to indicate its interpretation for the decision support of agronomists.

MATERIAL AND METHODS

Study area

Input data of winter wheat were acquired during the year 2016 by mapping of fields with total area 248 ha at farm company SALIX MORAVA a.s. (part of Spearhead Czech s.r.o. holding). Zdounky area is located in the sugar beet production area (Křen et al. 2015) in district Kroměříž (49.2978514N, 17.3931164E). According to Quitt climate classification is the climatic condition of the region slightly warm to warm and slightly damp (T3, MT2). The long-term average annual temperature during 1961–1990 is 8.1 °C and the average precipitation is 550–700 mm. The fields are located at an altitude of 205–320 m a.s.l. The soil types are Chernozem, Haplic Luvisol, Cambisol and Fluvisol with medium to deep soil depth. The humus content is moderately high, equal to 2–3%. Soil pH value ranges between 6.6–7.2. Fields are flat to moderately sloped.

Yield data recording

Yield data were recorded during harvest of 248 ha of winter wheat in 2016 at farm company SALIX MORAVA a.s. in Zdounky (part of Spearhead Czech s.r.o. holding). The climatic condition of the region is slightly warm to warm and slightly damp. The long-term average annual temperature is 8.1 °C and the average precipitation is 550–700 mm.

Data were acquired by grain harvesters Claas Lexion 670 with swath width 7.5 m and equipped by sensor system for estimation of grain flow, grain moisture and DGPS receiver. The output of monitoring are point data with the values of coordinates, altitude, actual crop yield, grain moisture, harvester speed, swath width, heading and other. Claas Lexion uses board computer software CEBIS for recording of data on the memory card and later download of files to the PC for next data processing.

Data processing

Recorded data as *.aft files were transformed in SMS software (AgLeader, USA) into shapefile format and later processed, analyzed and visualized in Geographic Information System ArcMap 10.3.1 (ESRI, Redlands, USA) in coordinate system WGS 1984. Statistical evaluation was carried out by Statistica 10 (Tibco, USA).

RESULTS AND DISCUSSION

Point data filtering

First step in pre-processing was filtering of yield data and identification of outliers as necessary procedure before spatial interpolation. Raw yield data contain large number of erroneous values which are recorded during harvest. Such errors may include, for example, extremely high or low yield values that arise in the event of a rapid change in travel speed, or if the operator does not adjust the working width correctly according to the real swath of harvester. More detailed description of the errors elimination in yield data is given by Lyle et al. (2014) and Simbahan et al. (2004).

Because the algorithm for automatically identification of above-mentioned errors in yield records is under development and traditional statistic approach doesn't consider spatial distribution of data, correction for data outliers was done manually for each field separately. Main task was to determine minimal and maximal yield values, corresponding to the biological crop yield feasible at the site-specific conditions. In the case of field 8202/1 with winter wheat, the yield value of 3 t/ha and maximum 14 t/ha was set as the limits of crop yields. These values correspond to the yield ranges reached by winter wheat for this site and farm in recent years. Also deleting values acquired by non-full swath was part of pre-processing. All point values with swath width lower than 7.5 m were deleted from dataset. Last part of filtering was focused on the short segments of point data with rapidly changes of values in relation to their neighborhoods.

Figure 1 An example of pre-processing of yield data from two harvesters – recalibration of data and spatial interpolation (OK – ordinary kriging, EBK – empirical bayesian kriging)

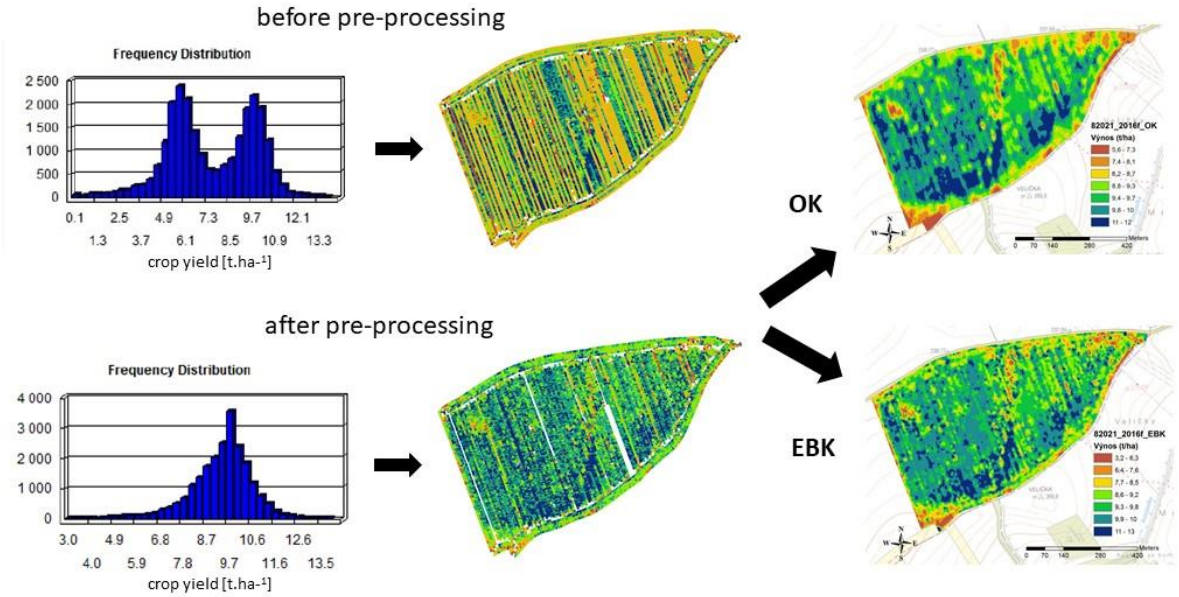

Initial investigation of data showed that many fields were harvested by two machines, but their data do not correspond with the real average yield per fields and also such as pair of datasets is not corresponding to each other, there is a shift in their mean value. This is well documented by non-overlapping histograms, as shown on example of 8202/1 (44 ha) in Figure 1. This systematic error is probably caused by inaccurate calibration of grain flow sensor on the start of the field harvest. However post-hoc calibration is possible by correction coefficient of both datasets to reach the mean value of real average yield of the field. Correction values were estimated for both harvester datasets separately as the deviation of average yield to the real average yield value for whole field obtained from the weighting of trailers before grain storage. This approach is possible in the situation that both harvesters were driving next to each other and are covering the similar yielded parts of the field. For example, the average yield at field 8202/1 (44 ha) was for the dataset from first combine harvester 5.86 t/ha, from second harvester 9.37 t/ha, while the real average crop yield was 9.16 t/ha. Shift of histogram values between both datasets occurred in high visible stripes in final maps with lower and higher values, which was not related to the real changes in crop yield and also not interpretable (Figure 1). Table 1 shows correction coefficients for all processed yield datasets.

Table 1 Calibration coefficients and basic statistics of the yield data

Field ID	Area [ha]	Calibration coefficients		Crop yield [t/ha]						
		Harvester #1	Harvester #2	Min	Max	Range	Average	Std. dev.	Sum [t]	CV [%]
0402/1	41.23	0.95	1.41	3.94	10.50	6.56	7.58	0.82	312.59	10.80
4002/1	20.01	1.12	0.70	6.65	12.20	5.55	10.47	0.96	209.47	9.15
4003/1	6.47	0.75	0.94	4.84	12.39	7.55	9.44	1.15	61.11	12.15
4107/1	7.12	0.75	1.00	4.35	11.41	7.05	9.33	1.13	66.45	12.12
8101/2	21.61	1.00	1.50	5.86	10.92	5.06	9.21	0.78	199.13	8.49
8102/1	8.07	0.96	1.62	4.63	11.85	7.22	9.06	1.22	73.20	13.41
8201/1	4.8	0.96	1.40	4.57	9.56	4.98	7.22	0.98	34.68	13.59
8202/1	44.02	1.00	1.56	5.55	11.53	5.98	9.43	0.78	415.20	8.32
9301/3a	57.44	1.50	0.96	3.65	10.68	7.03	7.67	0.80	58.30	10.43
9302/16	7.73	0.96	1.53	3.81	10.14	6.32	7.54	1.05	440.60	13.98

Legend: Std. dev. – standard deviation; CV – coefficient of variation

Spatial interpolation of point data

Spatial interpolation allows estimation of the value at the non-mapped location by neighboring measured values. The output is continuous map where all parts of the area of interest are covered by estimated values. The image of final maps depends on the interpolation methods and its parametrization. For this study, two types of kriging methods were used: Ordinary Kriging (OK) and Empirical Bayesian Kriging (EBK). Both Kriging methods are a reliable but computationally more demanding method characterized by smoothing local extremes by underestimating high values and evaluating the low (Kumhálová 2010). Implementation of EBK in ESRI ArcGIS allows the automatization of interpolation process by setting of kriging parameters individually for each field, thus allows processing of all fields in one batch. Final output product is a raster map with spatial resolution of 5 m per pixel, an example for OK and EBK is shown in Figure 2. Map computed by EBK technique showed lower smoothing effect proved by higher occurrence of local extreme values, thus high reliability of input data coming from filtering process is required.

Interpretation of yield maps

Absolute values of crop yield in maps are appropriate for economic analysis of the crop production and also for nutrient balance calculation. For support of agronomic decision more usable is relative expression of the crop yield by normalization of yield maps. This includes an analysis of yield levels within the fields by comparison of actual yield on the specific area (represented by pixel) to the field-average value of yield map. Classification of relative yield levels for field 8202/1 proved that almost half of the area (46.8%) is in the average yield class (96–105%), under-average yield classes (60–95%) at the 29.2% of area (mostly near to the headlands) and over-average (106–120%) at 23.9% of area, located in the low-sloped part of the field. Information about the distribution of the yield level could be considered by crop management practices, at least where the treatment intensity is related to the expected crop yield, such as plant nutrition.

Figure 2 Yield map expressed as the relative yield to the field average value (left) and area percentage of yield classes (right), both for field 8202/1.

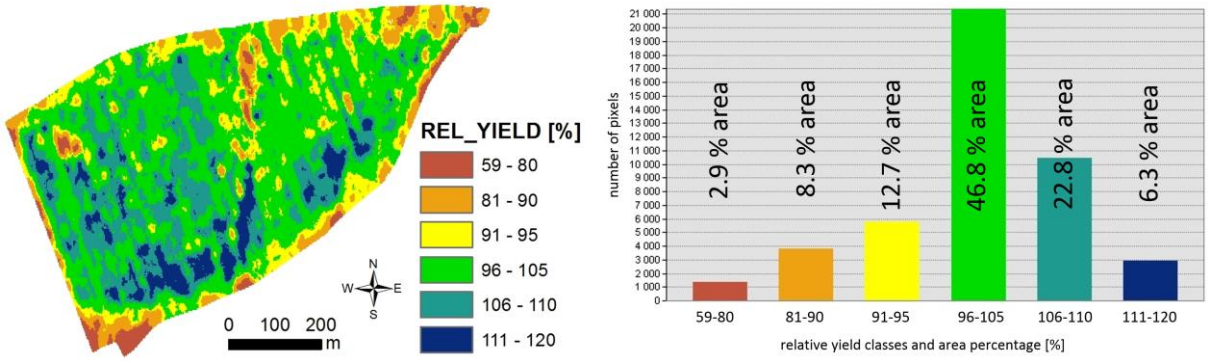

Combination of relative expression of the yield for multiple years allows an estimation of site specific potential yield, which can be used for comparison between different crops and different environments and also for estimation of plausible future limits to crop yields (Evans and Fischer 1999). Blackmore and Larscheid (1997) proposed a procedure for delineation of management zones based on the relative yield maps. They set three yield zones: a) high yielded and stable, b) low yielded and stable and c) unstable. On areas with a high stable yield, it should be managed so that inputs (fertilizers, crop protection) do not limit yields. On areas with low stable yields, more detailed analysis of yield-limiting factors needs to be done and growers may be able to reduce inputs without reducing yield. In the case of unstable areas, precise identification of yield-determining factors may be usually very difficult (Blackmore 2000). According to the study of Joernsgaard and Halmoe (2003) trend (multitemporal) maps will account for much more than 1/3 of the annual intra-field variation on average.

However, the presence of complete series of yield maps for all fields is rare, thus remote sensed data are analyzed to determine in field variability of crops thru vegetation indices as an alternative to the yield maps. Response of crop yield via remotely sensed spectral measurement of plant variables is well known Bauer (1975) and remote sensing may be an indicators of yields. As the study of Batchelor

et al. (2002) show, also implementation of crop models can lead to predict crop yield based on the weather data.

CONCLUSIONS

Yield mapping by grain flow sensors in harvesters provides crucial information for precision agriculture about the crop yield distribution within the fields. However, for reliable interpretation of the yield correct pre-processing of data must be carried out to correct a number of errors, such as outliers and spatial inconsistent values. As it was shown in the study, big challenge is the combination of datasets from two harvesters, especially in the case that both sensors were non-calibrated. Correction of these effect enhance quality of final maps in the next step of data processing – spatial interpolation. In this study, geostatistical method Empirical Bayesian Kriging proved its ability for full automatization of yield maps creation in GIS environment.

Besides absolute values of crop yield also calculation of relative yield as the percentage to the field average value can be recommended. Identification of under- and over-average yield areas support the agronomist decisions on the crop treatment intensity in the form of variable rate application (fertilizers, crop protection, etc.). Recent studies show that aggregation of relative yield maps from multiple years is valuable information for further planning of site specific crop management.

ACKNOWLEDGEMENTS

This study was supported by research projects NAZV QJ1610289 "Efficient use of soil productivity by site specific crop management" and TACR ALFA TA04021389 "Development of the system for variable rate application of pesticides and fertilizers using crop monitoring". Data from field experiments were provided by SALIX MORAVA a.s. and Spearhead Czech s.r.o.

REFERENCES

Batchelor, W.D. et al. 2002. Examples of strategies to analyze spatial and temporal yield variability using crop models. European Journal of Agronomy, 18(1–2): 141–158.

Bauer, M.E. 1975. The Role of Remote Sensing In Determining The Distribution and Yield of Crops, In Advances in Agronomy. Academic Press, pp. 271–304.

Blackmore, S. 2000. The interpretation of trends from multiple yield maps. Computers and Electronics in Agriculture, 26(1): 37–51.

Blackmore, S., Larscheid, G. 1997. Strategies for Managing Variability. In First European Conference on Precision Agriculture. UK: BIOS Scientific Publishers, pp. 851–859.

Blackmore, S. et al. 2003. The Analysis of Spatial and Temporal Trends in Yield Map Data over Six Years. Biosystems Engineering, 84(4): 455–466.

Evans, L.T., Fischer, R.A. 1999. Yield Potential: Its Definition, Measurement, and Significance. Crop Science, 39(6): 1544–1551.

Joernsgaard, B., Halmoe, S. 2003. Intra-field yield variation over crops and years. European Journal of Agronomy, 19(1): 23–33.

Johnen, T. et al. 2014. An analysis of factors determining spatial variable grain yield of winter wheat. European Journal of Agronomy, 52(Part B): 297–306.

Kleinjan, J. et al. 2007. Productivity zones from multiple years of yield monitor data. In GIS applications in agriculture. Boca Raton: CRC Press, pp. 65–80.

Křen, J. et al. 2015. Obecná produkce rostlinná. Brno: Mendel University in Brno.

Kumhálová, J. 2010. Využití GIS v precizním zemědělství. PhD thesis, Brno: Masaryk University.

Kumhálová, J. et al. 2014. Use of landsat images for yield evaluation within a small plot. Plant, Soil and Environment, 60(11): 501–506.

Lyle, G. et al. 2014. Post-processing methods to eliminate erroneous grain yield measurements: review and directions for future development. Precision Agriculture, 15(4): 377–402.

Mallarino, A.P. et al. 1999. Interpreting Within-Field Relationships between Crop Yields and Soil and Plant Variables Using Factor Analysis. Precision Agriculture, 1(1): 15–25.

Schepers, A.R. et al. 2004. Appropriateness of Management Zones for Characterizing Spatial Variability of Soil Properties and Irrigated Corn Yields across Years. Agronomy Journal, 96(1): 195–203.

Simbahan, G.C. et al. 2004. Screening yield monitor data improves grain yield maps. Agronomy Journal, 96: 1091–1102.

Assessment of yields of 20 varieties of sorghum at two different locations

Katerina Mrvova[1], Barbora Umlaskova[1], Ivana Kolackova[1], Vladimir Smutny[2], Petr Elzner[3], Leos Pavlata[1]
[1]Department of Animal Nutrition and Forage Production
[2]Department of Agrosystems and Bioclimatology
[3]Department of Crop Science, Breeding and Plant Medicine
Mendel University in Brno
Zemedelska 1, 613 00 Brno
CZECH REPUBLIC

kacka.mrvova@seznam.cz

Abstract: Sorghum is one of the most cultivated crops in the world, especially in countries with warm climate and dry areas. The aim of this study was to compare fresh matter and dry matter yield of 20 sorghum varieties at locations with different fertility in two sowing dates (in late May and in late June). The highest yield of fresh matter of all had KWS Merlin (*Sorghum sudanense*) at less fertile location – 1st sowing date (135.41 t/ha). This variety had also the highest value of dry matter yield at the same location (53.58 t/ha). The lowest value of fresh matter yield had KHS5G07 (grain form of sorghum) – 19.13 t/ha, also at less fertile location - 2nd sowing date. And the lowest yield of dry matter had Arsenio, as well the grain sorghum type (4.17 t/ha). Based on the data found it was concluded that it depends more on sorghum variety and its form (grain or non-grain), than on a soil types. From the results is clear that the better time for sorghum sowing is late May and it is also evident that some varieties of sorghum can be grown at different locations with different soil fertility, but with similar yields.

Key Words: sorghum, C4-plants, yield, fresh matter, dry matter, silage sorghum

INTRODUCTION

Due to the climate change, the production of feedingstuffs, mainly roughages, in the southern regions of Moravia is often limited. The main problem is long-therm period of high temperatures and minimum amount of rainfall. These climate changes cause mitigation of vegetation and reduce yield (Rajčáková et al. 2006).

But we have some possibilities to solve this problem. We can´t affect these changes, but we can start cultivate dry-cured crops like a sorghum. Sorghum (*Sorghum bicolor*) is the fifth most important cereal crop in the world and it is grown over 42 million ha (Reddy et al. 2004), but in our country is still less used.

Sorghum has several economically important potential uses such as feed (grain and biomass), food (grain), fuel (ethanol production), fibre (paper), fermentation (methane production) and fertilizer (Tari et al. 2012).

The quality of sorghum produce and yield is affected by a wide range of biotic (diseases and insect pests) and abiotic (drought and problematic soils) factors (Reddy et al. 2004). And also it depends on varieties or hybrids of sorghum. Even if it´s undemanding crop, it´s clear that higher yield of fresh matter and dry matter will be achieved in ideal conditions such as suitable medium loam soil adequately supplied with nutrients (Hermuth et al. 2012). The aim of this study is to compare yields of fresh and dry matter of different varieties of sorghum at two locations with different fertility.

MATERIAL AND METHODS

Characteristic of field experimental station in Žabčice

Experimental part was processed on Field experimental station in Žabčice, which is located 49°00'50.3"N and 16°36'03.6"E in maize production area in the South Moravian region. This territory belongs among the warmest and also driest regions in the Czech Republic

Sorghum was sown at two different locations. The first location - Obora has clay loam soil and the soil type is fluvisol. Obora has good availability of groundwater (Svratka River), which fluctuates 0.8–2.5 m below the soil surface during the year. The second location named Písky has light sandy soil and it is drier than Obora. The average annual temperature is 9.2 °C, the warmest month in the year is July with an average daily air temperature of 19.3 °C. The coldest month is January and average temperature is -2.0 °C.

Characteristic of varieties

Part of the seeds was furnished by KWS company and SEED SERVICE company. Some varieties are grain-sorghum type: Express, Arsenio, KHS5G07, Sweet Susana, Sweet Carolina, Buffalo Grain BMR and Ruzrok. Some are hybrids with Sudanese grass (*Sorghum sudanense*) – Latte, KWS Sole. And the third variants are clean *Sorghum bicolor* (KWS Zerberus) or hybrid *Sorghum bicolour x bicolour* (KWS Kalisto) and hybrid of *Sorghum saccharatum* and *Sorghum sudanense* (Big Kahuna BMR).

*BMR is shortcut of Brown Mid Rib – form with a reduced lignin content of 40−60%, which cause higher digestibility. The outer mark of this form of sorghum is the brown central (mid) rib (Hermuth et al. 2012).

Characteristic of experiment

Table 1 Overview of harvest dates of 20 sorghum varieties at two different locations and both dates of sowing

Varieties	OBORA		PÍSKY	
	Harvest dates 1st sowing	Harvest dates 2nd sowing	Harvest dates 1st sowing	Harvest dates 2nd sowing
Ruzrok	11. 8. 2017		18. 8. 2017	19. 10. 2017
DSM 45-480	25. 8. 2017		25. 8. 2017	19. 10. 2017
Express	18. 8. 2017		18. 8. 2017	
Sweet Susana	25. 8. 2017	12. 10. 2017	25. 8. 2017	12. 10. 2017
Sweet Caroline	13. 9. 2017		30. 8. 2017	
PSE CE BMR	30. 8. 2017	23. 10. 2017	30. 8. 2017	19. 10. 2017
Buffalo Grain BMR	13. 9. 2017		29. 9. 2017	
Big Kahuna BMR	29. 9. 2017		29. 9. 2017	
Nutri Honey BMR	30. 8. 2017	23. 10. 2017	13. 9. 2017	19. 10. 2017
Nutri Honey	25. 8. 2017	12. 10. 2017	25. 8. 2017	12. 10. 2017
Triumfo BMR	30. 8. 2017		30. 8. 2017	
Latte	30. 8. 2017		13. 9. 2017	
KWS Freya	18. 8. 2017	12. 10. 2017	30. 8. 2017	19. 10. 2017
KWS Sole	25. 8. 2017	12. 10. 2017	25. 8. 2017	19. 10. 2017
KWS Merlin	30. 8. 2017	23. 10. 2017	29. 9. 2017	19. 10. 2017
KWS Tarzan	30. 8. 2017	23. 10. 2017	29. 9. 2017	19. 10. 2017
KWS Zerberus	30. 8. 2017	23. 10. 2017	29. 9. 2017	19. 10. 2017
KWS Kallisto	30. 8. 2017	12. 10. 2017	30. 8. 2017	12. 10. 2017
Arsenio	18. 8. 2017	12. 10. 2017	18. 8. 2017	12. 10. 2017
KHS5G07	18. 8. 2017	12. 10. 2017	18. 8. 2017	12. 10. 2017

Twenty varieties of sorghum were sown in late May (May 24th) and only 14 of them were sown also in late June (June 26th), at two different locations in the amount of 278 thousand seeds per hectare. Fertilization was done only at Obora and contained phosphorus (Superphosphate 45% at 90 kg/ha), potassium (potassium salt at 120 kg/ha) and nitrogen (urea at 120 kg/ha) fertilization. And the preceding crop was maize.

The mass of sorghum was harvested form 3 rows and depending on the content of dry matter, because the important indicator of sorghum quality is dry matter, which should be between 28% and 35% in silage harvest period. The harvest dates of every variety of sorghum are shown in Table 1.

The yields of fresh matter were statistically compared in the first and second sowing. Data has been processed by Microsoft Excel (USA) and Statistica version 12.0 (CZ). We used one-way analysis (ANOVA). To ensure evidential differences Scheffe´s test was applied and $P < 0.05$ was regarded as statistically significant difference.

RESULTS AND DISCUSSION

From values in Table 2 is clear that the better time for sorghum sowing is late May, because the dry matter in late June is very low for most varieties and it may cause problems in the silage production, in particular a higher risk of greater outflow of silage juices. But this problem can be solved by an intensive withering that can increase the dry matter to the required value.

Table 2 Overview of average values of dry matter yields and fresh matter yields of sorghum at both locations and both dates of sowing

	Obora 1st sowing		**Obora 2nd sowing**		**Písky 1st sowing**		**Písky 2nd sowing**	
Varieties	Average yield [t/ha]		Average yield [t/ha]		Average yield [t/ha]		Average yield [t/ha]	
	Fresh matter	Dry matter	Fresh matter	Dry matter	Fresh matter	Dry matter	Fresh matter	Dry matter
Ruzrok	37.21 a	12.55			29.21 a	8.45	25.48	5.26
DSM 45-480	46.87 a	13.41			34.46 b	10.04	28.89	6.50
Express	43.44 a	10.81			49.02 a	12.33		
Sweet Susana	47.26 a	12.97	42.22 a	8.79	30.87 b	8.39	50.07 a	12.15
Sweet Caroline	66.96 a	19.51			50.81 b	14.44		
PSE CE BMR	58.67 a	15.82	44.44 a	9.09	52.59 a	13.96	20.30 b	4.47
Buffalo Grain BMR	63.11 a	18.07			55.41 a	15.18		
Big Kahuna BMR	117.63 a	31.09			73.33 b	15.13		
Nutri Honey BMR	45.93 a	12.51	44.89 a	9.27	53.78 a	15.26	31.53 a	5.79
Nutri Honey	59.35 a	16.05	43.70 a	8.82	49.24 a	13.48	61.78 a	12.51
Triumfo BMR	44.00 a	12.28			37.48 a	9.98		
Latte	75.85 a	19.96			98.52 a	26.83		
KWS Freya	59.85 a	16.90	42.67 a	11.36	51.41 a	14.35	45.78 a	8.56
KWS Sole	48.33 a	15.18	44.74 a	10.63	53.51 a	17.16	35.47 a	5.95
KWS Merlin	71.85 a	19.97	64.44 a	12.26	135.41 b	53.58	90.37 a	17.46
KWS Tarzan	60.30 a	17.26	56.59 a	12.52	65.93 a	24.17	90.22 b	16.26
KWS Zerberus	63.41 a	17.77	58.96 a	12.11	93.93 a	31.17	100.89 b	20.05
KWS Kallisto	50.22 a	15.36	52.74 a	14.95	72.30 a	22.31	46.67 a	9.56
Arsenio	54.43 a	13.58	30.07 a	7.37	40.28 a	10.90	19.56 a	4.17
KHS5G07	42.01 a	10.99	25.63 a	6.81	30.09 a	8.51	19.13 a	4.68
Average values	**57.83**	**16.10**	**45.92**	**10.33**	**57.88**	**17.28**	**47.58**	**9.53**

According to the results presented in Table 2, yields of all varieties are very different. Green boxes content the highest average values and grey boxes content the lowest average values. As can be seen the highest yield of fresh matter of all has KWS Merlin (*Sorghum sudanense*) at Písky location – 1st sowing (135.41 t/ha). This variety has also the highest value of yield of dry matter of all at the same location (53.58 t/ha). The height of the stand was 2.90 meters in the time of harvest. The dry matter content at this variety was 39.57% at the time of harvest, which is very high value. According to the Rajčáková (2005), the values above 35% can be probably risky. These values cause an increased risk of aerobic instability of the feed. So it would be better to harvest this variety a week earlier. But KWS Company represented this variety of sorghum as a new dimension of stability and yield, so maybe they have right and in future it would be the best choice in animal nutrition. Such high yields have reached at less fertile location, which is another interesting fact.

Contrariwise, the lowest value of yield of fresh matter has KHS5G07 (grain form of sorghum) at Písky location - 2nd sowing (19.13 t/ha). And the lowest yield of dry matter has Arsenio, also the grain - sorghum type (4.17 t/ha) and also at Písky location - 2nd sowing. The results in Table 2 show that the grain - sorghum types has lower yields of fresh matter and also of dry matter than any other varieties of sorghum. So it can be caused by lower vegetation, because grain varieties of sorghum generally have lower height of the stand. But grain types have higher levels of nutritionally valuable albumins and globulins, than in non-grain varieties (Prugar 2008). So it is important to set priorities.

The last row in the Table 2 shows average values of each variety. And it can be seen the different between both locations is very low. Average values of fresh matter yields are almost similar in the case of the 1st sowing. Maximal different is in the case of the 2nd sowing in column of fresh matter yield and that is only 1.66 t/ha.

Table 2 presents also the differences between both locations at fresh matter yield in case of 1st sowing are statistically significant at DSM 45-480, Sweet Susana, Sweet Caroline, Big Kahuna BMR and KWS Merlin. Values of varieties: PSE CE BMR, KWS Tarzan, KWS Zerberus are statistically significant in the yields of fresh matter in case of 2nd sowing.

Povolný and Hampl (2015) tested sorghum varieties (for use on silage), where they also ranked varieties: KWS Tarzan, KWS Freya, Sweet Caroline and Sweet Susana. They compare varieties at six different locations and the dates of sowing were done since mid-May. The following Table 3 describes the differences between their and our experiment.

From Table 3 can be read, that the differences are not too big, just only at Sweet Susana is a difference of 14.83 t/ha. In this case is evident that these varieties can be grown at different locations with similar yields.

Table 3 Comparison of two experiments - Averages of total fresh matter yields of 4 selected sorghum varieties

Varieties	Povolný and Hampl 2015	Our results
KWS Tarzan	66.00 t/ha	63.12 t/ha
KWS Freya	51.70 t/ha	55.63 t/ha
Sweet Caroline	64.00 t/ha	58.89 t/ha
Sweet Susana	53.90 t/ha	39.07 t/ha

This year, the experiment was repeated and we are now putting together results that will make it possible to compare both years and so to satisfy our prerequisites. And then we will be able to tell which varieties of sorghum are ideal in certain habitats.

CONCLUSION

This experiment shown, that the differences of fresh matter and dry matter yields at different locations are not too high. There are certain differences between the varieties within the habitats, but that could be supposed. It can be said that both locations are appropriate for sorghum growth - dried and less fertile Písky as well as more fertile Obora. Some varieties achieved higher yield at less fertile location, for example: KWS Merlin, which had the highest yield of all varieties. Another

was KWS Sole, KWS Zerberus, KWS Kallisto, Latte and Nutri Honey BMR. So it depends more on the variety than on the site conditions.

We can say that dry conditions of South Moravia region are not problem for sorghum growing. Even from the results of this experiment is evident that some varieties of sorghum can be grown at different locations with different soil fertility, but with similar yields. And this is our vision.

ACKNOWLEDGEMENTS

The research was financially supported by the AF-IGA-2018-tym001: Comparison of the impact of climate change on photosynthesis C3 and C4 plants cycles which are used in livestock feed.

REFERENCES

Hermuth, J. et al. 2012. Čirok obecný Sorghum bicolor (L.) Moench, možnosti využití v podmínkách České republiky: Metodika pro praxi [Online]. Praha-Ruzyně: Výzkumný ústav rostlinné výroby, v.v.i. Available at: https://www.vurv.cz/sites/File/Publications/ISBN978-80-7427-093-2.pdf. [2018-09-12].

Povolný, M., Hampl, B. 2015. Výsledky zkoušek užitné hodnoty ze sklizně 2014: Čirok- registrované odrůdy + odrůdy ve zkouškách [Online]. Brno: Ústřední kontrolní a zkušební ústav zemědělský. Available at: http://eagri.cz/public/web/file/399243/ZUH_Cirok_2014.pdf. [2018-09-12].

Prugar, J. 2008. Čirok. In Kvalita rostlinných produktů na prahu 3. tisíciletí. Praha: Výzkumný ústav pivovarský a sladařský ve spolupráci s komisí jakosti rostlinných produktů ČAZV, pp. 156–157.

Rajčáková, L. 2005. Pestovanie ciroku sudásnkeho v suchom postihovaných oblastiach. Krmivářství, 38(4): 36–37.

Rajčáková, L., Mlynář, R. 2006. Cirok sudánsky: alternatívna silážna plodina pre suchom postihované oblasti Slovenska. Slovenský Chov [Online], 1: 20–21. Available at: http://www.cvzv.sk/pdf/Konzervacia-a-silazovanie-krmiv/Cirok%20sudansky%20-%20alternativna%20silazna%20plo.pdf. [2018-09-12].

Reddy, B. et al. 2004. Sorghum Research Reports: Genetic Enhancement and Breeding - Sorghum Breeding Research at ICRISAT – Goals, Strategies, Methods and Accomplishments [Online]. Andhra Pradesh, India: ICRISAT. Available at: http://oar.icrisat.org/1292/1/ISMN-45_5-12__2004.pdf. [2018-09-12].

Tari, I. et al. 2012. Salinity Stress: Response of Sorghum to Abiotic Stresses: A Review. Journal of Agronomy and Crop Science [Online], 11: 264–274. Available at: http://eds.b.ebscohost.com/eds/pdfviewer/pdfviewer?vid=1&sid=d019f79b-afe8-4718-9e33-9dc7649c65db%40sessionmgr101. [2018-09-12].

Occurrence of pests of sorghum and ryegrass in weather extreme year 2018

Aneta Necasova, Eva Hrudova
Department of Crop Science, Breeding and Plant Medicine
Mendel University in Brno
Zemedelska 1, 613 00 Brno
CZECH REPUBLIC

aneta.necasova@mendelu.cz

Abstract: Sorghum (*Sorghum vulgare* var. *sudanense*) and ryegrass (*Lolium multiflorum*) are crops unpretentious for growing conditions and can provide high yields of green matter. Sorghum is characterized by high tolerance to drought. In this monitoring, attention was paid to the occurrence of the pests of these crops and the intensity of the attack under the field conditions of South Moravia. Due to the extreme weather conditions in the 2018 growing season, the occurrence of pests was low, and the plants were not significantly damaged. The presence of the key pest, which is the European corn borer (*Ostrinia nubilalis*) was monitored using a light trap. The adults appeared in the vegetation, but the damage typical for this pest was not recorded.

Key Words: Sorghum vulgare var. *sudanense*, *Lolium multiflorum*, monitoring, pest, *Ostrinia nubilalis*

INTRODUCTION

Good quality feed is the basis for proper nutrition of farm animals. In recent years, the main problem has been the lack of precipitation. The result is a reduction in production and quality of crops, which have been traditional for the Czech Republic. That is why other plant species, more adapted to stress caused by changing climatic conditions, are being sought.

Sorghum (*Sorghum vulgare* var. *sudanense*) is one of the longest cultivated crops, in world production it is ranked among the five most cultivated cereals. All forms of sorghum have a wide range of uses – in food, feed, for technical and energy purposes. Cultivated area of sorghum are constantly expanding, it is currently being cultivated in the Czech Republic, in particular, for using as an alternative to maize in biogas stations (Venclová 2014). Sorghum is also used as a quality feed for livestock, for its low starch content, very good digestibility and a high yield of green silage (Venclová 2014). The spread of its cultivation is related to the more frequent occurrence of pathogens and pests. Young plants contain hydrogen cyanide, thanks to which is not attacked by insect pests, birds or animals, like maize is (Chobotová and Prokeš 2013).

Sorghum is a cultural thermophilic crop, its properties and the appearance are the most similar to corn (Venclová 2014). The advantage is natural adaptability to different environmental conditions (temperature, length of the day, light, soil), Currently, it is becoming more perspective for its high tolerance to drought and heat. This is due, in particular, to the construction of a root system which is fine and dense and penetrates to depths of more than 150 cm (Chobotová and Prokeš 2013). A thin wax layer is present on leaves and stem (Sharma 1993). In the case of drought, the plants slow down their development and regenerate very quickly after the precipitation arrives (Chobotová and Prokeš 2013). The most common diseases of sorghum are smut (*Sphacelotheca sorghi, Sphacelotheca cruenta*) and leaf spot *(Colletotrichum sublineolum; Ascochyta sorghi; Ramulispora sorghi; Cercospora sorghi* etc.), or mold (*Sclerospora sorghi*) and rust (*Puccinia purpurea*) (Hýsek et al. 2010). Sorghum is attacked mainly by insects or higher animals. Young plants can be attacked by wireworm - click beetle larvae (*Agriotes* spp.), or cockchafer larvae (*Melolontha melolontha*) that damage the root system. In the Czech Republic, common pest is the European corn borer (*Ostrinia nubilalis*). On sorghum, the symptoms are the same as for maize (Hermuth 2012). Birds are locally causing considerable damage on inflorescence. In the USA, midge *Contarinia* (*Diplosis*) *sorghicola*, which has a short generation interval, is a dangerous pest of sorghum. In Europe this midge is found in France, Greece, Spain and Russia (EPPO 2018). An ant *Linepithema humilis* is also found there (Hermuth 2012).

The ryegrass (*Lolium multiflorum*) is the most important annual grass species, which provides high yields of fodder and dry matter. It is used in intensive short-term mixtures on arable land or as a cover crop for permanent grasslands. It has also been used as an intercrop for green fertilization (Macháč 2013). Fungal pathogens negatively affect the quality of fodder. These are mainly powdery mildew of cereals (*Erysiphe graminis*), or rust (*Puccinia coronata* var. *coronata*, *P. graminis* var. *graminicola*, *P. hordeii*) and smut (*Ustilago lolii, Tilletia contraversa, T. lolii*), eventually leaf spot (*Rhynchosporium morthosporum, R. secalis, Spermospora lolii, Ascochyta avenae, Septoria tritici* var. *lolicola, Stagonospora nodorum*) (Kulovaná 2002, Brandenburger 1985). The field vole (*Microtus arvalis*) is pest causing the main damage on ryegrass (Mytyska 2015).

We supposed, the pests mentioned above are present at monitored localities Žabčice and Rebešovice. The level of their harmfulness was monitored too.

MATERIAL AND METHODS

Selected locations

For the field experiment, two locations were selected, each for one crop. An experimental field in Žabčice, at the School farm of Mendel University in Brno, was used for growing a sorghum. The experimental area of ryegrass was located south of Brno in the village of Rebešovice, on the field of the agricultural cooperative Rajhradice. Monitoring was carried out in these locations. The description of both locations is given in Table 1.

Table 1 Description of individual locations

Locality	Žabčice	Rebešovice
Coordinates	49°1'18.658"N, 16°36'56.003"E	49°06'23.9"N, 16°38'21.2"E
Altitude	185 m a. s. l.	204 m a. s. l.
Average annual temperature	10.07 °C	9.5°C
Average annual precipitation	550 mm	500 mm
Average temperature 2018	12.5 °C	11.2 °C
Average precipitation 2018	-	-

Sorghum monitoring in field conditions

The experimental area of sorghum was established on 29. 5. 2018. The chosen variety was 'KWS Tarzan'. The experimental site was the former vineyard. The size of sown parcels was 30 m^2. In addition to monitoring pests, this experiment mainly served to assess the different fertilization options. The variant was 7 and were always in 4 reps. In total, there were 28 parcels there.

During the 2018 growing season (June–July), the presence of pests was monitored. The last assessment was made on 31. 7., as well as the harvest. The occurrence of pests, signs and intensity of attack according to the scale given in Table 2 were evaluated. The presence of European corn borer (*Ostrinia nubilalis*) was regularly monitored using a light trap placed in the growth and by visual inspections of the plants, during which the laying eggs on the leaves was observed. In addition, the occurrence of Lema black cereal beetle (*Oulema melanopus*), Lema blue cereal beetle (*O. cyanea*) and damage by Western corn rootworm (*Diabrotica virgifera*) was monitored, as possible pests of sorghum.

Table 2 Scale for evaluation of plant damage

Degree of damage	Percentage of the destroyed leaf /root area
0	Without damage
1	5–20
2	21–40
3	41–60
4	61–80
5	80–100

Ryegrass monitoring in field conditions

On 5. 3. 2018 the ryegrass was sawn on the experimental field of the total area of 12 ha. The variety 'Diplomat' with a sowing rate of 20 kg/ha was selected. The pre-crop was corn for grain. Treatment by fungicides or insecticides was unnecessary during the vegetation (April–July), only herbicides were applied. Lema black cereal beetle (*Oulema melanopus*), Lema blue cereal beetle (*O. cyanea*) were observed. Visual inspections of the plants were performed regularly. These took place in five terms – 10. 4., 11. 5., 13. 6., 3. 7. and 19. 7.

RESULTS AND DISCUSSION

The elapsed vegetation season was unfavorable both for the plants themselves and for the occurrence of pests. The reason was, above all, the extreme course of weather with very high temperatures, as confirmed by Říha (2018), and lack of precipitation. As Buntin (2012) states, sorghum is, moreover, itself a tolerant crop for insect attack, which may be another reason why no more damage was visible.

Sorghum (*Sorghum vulgare* var. *sudanense*)

The presence of adult European corn borer into the light trap was observed from 2. 5. to 20. 7. 2018 in the locality Žabčice as is evident from Figure 1. The presence of European corn borer eggs on the leaves was monitored, but not detected in monitoring terms, although in the control of maize (outside of this experiment) the eggs were recorded. On the contrary, Hermuth and Kosová (2018) recorded presence of European corn borer and signs of damage on sorghum. The occurrence and the damage caused by Lema black cereal beetle (*Oulema melanopus*), Lema blue cereal beetle (*O. cyanea*) and Western corn rootworm (*Diabrotica virgifera*) was monitored at the same time and there was also no evidence of damage caused by Lema black and blue cereal beetles or the presence of their larvae, although adults appeared in this field. Their lesser harmfulness can also be caused by weather. Kher et al. (2012) state that climate change can change both their spread and their abundance. Imagoes of Western corn rootworm were present in the crop, but the damage caused by them was not evident. Sharma (1993) reports *Rhopalosiphum maidis* as a pest of sorghum, but it does not cause significant damage. The aphids and the damage caused by them were not detected during the monitoring.

Figure 1 Dates and numbers of specimens Ostrinia nubilalis in the light trap

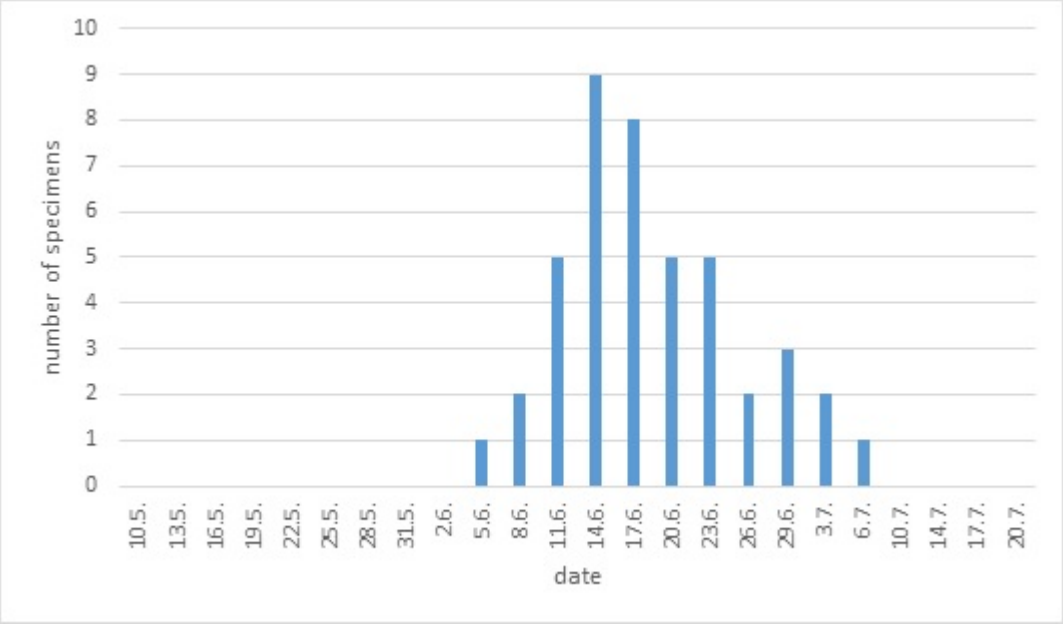

Ryegrass (*Lolium multiflorum*)

During pest monitoring on ryegrass in the 2018 growing season, no pests were observed to visibly damage the plant. A number of species of pollinator were observed during inspection visits of the field.

CONCLUSION

During the first year of monitoring of the health status of sorghum and ryegrass, no pest infestation and damage to crops was found. Sorghum is a crop that is relatively resistant to pests in our local environment. The zero-infestation by the pests could be partly influenced by the weather, with a lack of precipitation and extremely high temperatures. Also ryegrass was not damaged this year. Since monitoring was carried out just for one year so far, it is the initial results and the acquired data is not to be considered entirely conclusive.

ACKNOWLEDGEMENTS

The research was financially supported by grant no. AF-IGA-2018-tym001.

REFERENCES

Brandenburger, W. 1985. Parasitische Pilze an Gefässpflanzen in Europa. 1st ed., Stuttgart: Fischer.

Buntin, G.D. 2012. Grain Sorghum Insect Pests and Their Management. UGA Cooperative Extension Bulletin 1283 [Online]. Available at: http://extension.uga.edu/publications/detail.html?number=B1283&title=Sorghum%20Insect%20Pests%20and%20Their%20Management. [2018-08-28].

Chobotová, M., Prokeš, K. 2013. Čirok, plodina s budoucností. Farmář, 2: 24–26.

EPPO Global Database. 2018. Stenodiplosis sorghicola (CONTSO). [Online]. Available at: https://gd.eppo.int/taxon/CONTSO/distribution. [2018-08-27].

Hermuth, J. 2012. Čirok obecný – Sorghum bicolor (L.) MOENCH: možnosti využití v podmínkách České republiky. Metodika pro praxi. Praha: Výzkumný ústav rostlinné výroby, v.v.i.

Hermuth, J., Kosová, K. 2018. Pěstební technologie zrnového čiroku odrůdy Ruzrok. 1. vyd., Praha: Výzkumný ústav rostlinné výroby, v.v.i.

Hýsek, J. et al. 2010. Choroby a škůdci čiroku pěstovaného v podmínkách České republiky. In Hodnotenie genetických zdrojov rastlín pre výživu a poľnohospodárstvo. Piešťany, Slovak Republic, 26–27 May, Piešťany: Centrum výskumu rastlinnej výroby Piešťany, pp. 137–138.

Kher, S. et al. 2012. Sustainable management of cereal leaf beetle. Top Crop Manager [Online]. Available at: https://www.topcropmanager.com/insect-pests/sustainable-management-of-cereal-leaf-beetle-10916?jjj=1535459090867. [2018-08-28].

Kulovaná, E. 2002. Kvalita obilnin. Úroda [Online], 8(5): 58–60. Available at: https://uroda.cz/kvalita-obilnin. [2018-08-21].

Macháč, R. 2013. Pěstování jílku mnohokvětého jednoletého na semeno v ekologickém zemědělství. Uplatněná certifikovaná metodika. OSEVA vývoj a výzkum s.r.o.

Mytyska, V. 2015. Přínosy pěstování travních osiv pro zemědělský podnik. Bachelor thesis, Mendel University in Brno.

Říha, K. 2018. Úvaha o změnách počasí a pěstování. Agromanual.cz [Online]. Available at: https://www.agromanual.cz/cz/clanky/technologie/uvaha-o-zmenach-pocasi-a-pestovani. [2018-08-27].

Sharma, H.C. 1993. Host-plant resistence to insects in Sorghum and its role in integrated pest management. Crop Protection, 12(2): 11–34.

Venclová, B. 2014. Má čirok budoucnost jako energetická plodina – ano, nebo ne? Úroda [Online], 11: 8. Available at: https://uroda.cz/ma-cirok-budoucnost-jako-energeticka-plodina-ano-nebo-ne/. [2018-08-21].

The fungal pathogens of *Sorghum vulgare* and *Lolium multiflorum* with focus on feed quality

Eliska Novakova, Ivana Safrankova
Department of Crop Science, Breeding and Plant Medicine
Mendel University in Brno
Zemedelska 1, 613 00 Brno
CZECH REPUBLIC

eliska.novakova@mendelu.cz

Abstract: In 2018 an occurrence of fungal pathogens of *Sorghum vulgare* var. *sudanense* and *Lolium multiflorum* was evaluated in laboratory and field condition. The lab experiment was done on sorghum variety ´KWS Tarzan´ seeds and on ryegrass variety ´Diamant´ seeds. Pathogens from genus *Alternaria*, *Aspergillus* and *Cladosporium* were identified and from the overall quantity of seeds infection has been detected on 91.5% of seeds (method of "wet cell") and 87% of seeds tested on agar medium. Pathogens of genus *Alternaria*, *Fusarium* and *Aspergillus* were identified on ryegrass seeds and from the overall quantity of seeds, 75.5% tested by "wet cell" method were infected. The sorghum plants in the field conditions were slightly infected by *Colletotrichum sublineola* pathogens and slight infection of pathogens of *Blumeria graminis*, *Puccinia graminis* var. *graminicola* and *P. coronata* var. *coronata* was identified on the ryegrass plants. It is possible that very dry and hot summer is responsible for the low infection of sorghum and ryegrass in the field conditions. Farmers should choose the right variety and location for use in the Czech Republic conditions.

Key Words: disease, forage crops, monitoring, seeds

INTRODUCTION

Forage crops are farm animals feed component. Hot and dry weather during vegetation has negative influence on the biomass production. It is a reason for changing the type of forage crops which are being cultivated, in particular maize. The kind of suitable forage crops seems to be sorghum (*Sorghum vulgare* var. *sudanense*). It is the most important crop of arid areas (Moudrý and Strašil 1999). In the Czech Republic, sorghum has been cultivated since the mid-20th century. Nowadays sorghum is grown for biogass station, only.

The area for sorghum cultivations is increasing. This fact increases the risk for the occurrence of fungal pathogens. The most important fungal pathogens of sorghum rank leaf spots diseases caused by pathogen as *Colletotrichum sublineola*, (Baroncelli et al. 2014), *Ascochyta sorghi, Bipolaris sorghicola* (Jonar et al. 2011), *Cercospora sorghi*, *Helminthosporium turcicum*, *Ramulispora sorghi*. Other diseases are rust *Puccinia purpurea* (Kuthan 2012), smut *Sphacelotheca sorghi* a *S. cruenta* and mold *Sclerospora sorghi*.

The next important species of forage crops is ryegrass (*Lolium* spp.) which has a good fodder quality. This kind of forage crop has a good influence on soil fertility and function of soil protection. Currently the ryegrass areas are decreasing or stagnate (Cagaš 2016). Its demands on sufficient moisture, higher temperature and sensitivity on fungal pathogens and dryness are the reason why ryegrass is less cultivated than before (Hejduk 2014).

Among the most important ryegrass pathogens are: powdery-mildew *Blumeria graminis* (Cagaš and Macháč 2001), rusts *Puccinia graminis* var. *graminicola*, *P. coronata* var. *coronata*. *P. hordeii*, blackening of the base of stalks *Gaeumannomyces graminis* (Kazda et al. 2010) and smuts (*Ustilago lolii*, *Tilletia contraversa*, *T. lolii*).

The aim of this study was to identify sorghum and ryegrass growing possibilities in south Moravian conditions, and to determine the spectrum of fungal pathogen, which occurred during the vegetation and seeds pathogens, also.

MATERIAL AND METHODS

Field experiments were set up in 2018 in Žabčice (49°1'18.658"N, 16°36'56.003"E) and Rebešovice (49°06'23.9"N, 16°38'21.2"E) locations (Table 1). The course of weather on both localities in year 2018 is given in Figure 1 and 2. Sorghum seeds were sown in Žabčice, on a former vineyard, on 29. 5. 2018 (40 kg/ha), without pre-crop. The sorghum has been sown on 28 parcels of 12×1,6 m.

Ryegrass seeds have been sown in Rebešovice on 5. 3. 2018 (20 kg/ha) with grain maize being used as pre-crop. The ryegrass has been sown on 2 fields (9.34 ha a 1.85 ha) with 4 experimental parcels of 2×2 m.

Table 1 Locality characteristics (source: http://www.obecrebesovice.cz/; http://szp.mendelu.cz/o-nas/26430-poloha)

Locality	Crop	Altitude	Average precipitation	Average temperature
Žabčice	*Sorghum*	182 m a. s. l.	480 mm	9.5 °C
Rebešovice	*Lolium*	204 m a. s. l.	450–500 mm	9–10 °C

Figure 1 Development of precipitation and temperature, Žabčice

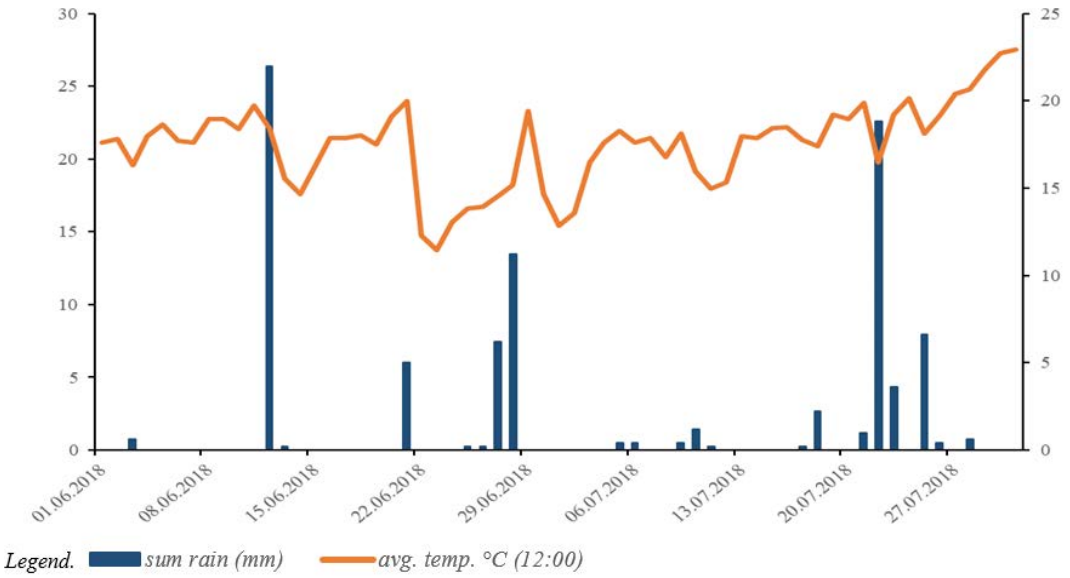

Figure 2 Development of precipitation and temperature, Rebešovice

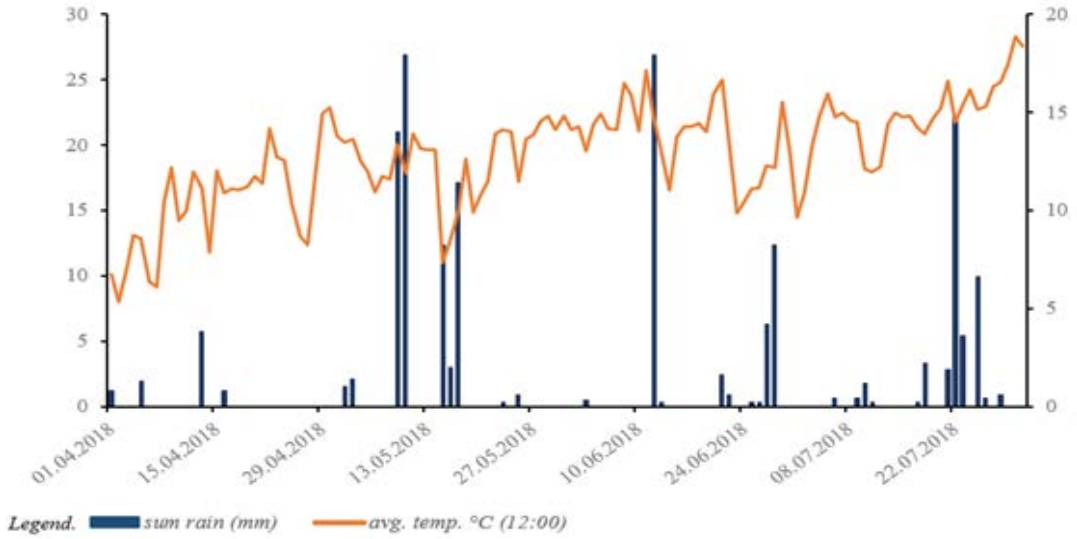

Evaluation of the occurrence of pathogens during vegetation

Total health condition of growth and occurrence of sorghum pathogens were evaluated in June–July of 2018 (2. 6., 27. 6., 16. 7. and 31. 7.; Figure 3) and total health condition of growth and occurrence of ryegrass pathogens were evaluated in April–July of 2018 (10. 4., 11. 5., 13. 6., 3. 7. and 19. 7.; Figure 4). Leaves with symptoms of the disease were photographed and collected for microscopic identification of the pathogen according to morphological characteristic.

Figure 3 Growth of Sorghum vulgare var. sudanense, Žabčice 16. 7. 2018 (https://www.google.com/maps)

Figure 4 Growth of Lolium multiflorum Rebešovice 3. 7. 2018 (https://www.google.com/maps)

Detection of sorghum and ryegrass seed pathogens

The occurrence of pathogens of sorghum seeds (*Sorghum vulgare* var. *sudanense*) variety 'KWS Tarzan' and ryegrass seeds (*Lolium multiflorum*) variety 'Diamant' were determined by the standard methods of wet cell and on agar medium. Two variants have been determined: without surface disinfection and with surface disinfection. First variant contained 200 seeds (10 seeds/ 1 Petri dish in 20 reps) and the second variant contained 150 seeds (10 seeds/ 1 Petri dish in 5 reps) for each of the three kinds of surface disinfection. The cultivation was carried out under standard laboratory conditions (temperature 20/25 °C, light mode 14/10 hour) for 7 days. The frequency of pathogen occurrence has been evaluated. Pathogens were isolated and identified under microscope by their morphological characteristics. If it was not possible to identify the pathogen directly from seeds, cultivation of the pathogen had to be done in cultured dirt of Potato Dextrose Agar (PDA), Sabouraud agar (SA), Malt extract agar (MEA).

To identify the microflora of seeds on agar medium in Petri dish (Ø 9 cm), 50 seeds were disinfected with a solution of 70% ethanol (soaking the seeds for 5 minutes), 50 seeds were treated with sodium hypochlorite solution at 1: 9 ratios with distilled water (5 minutes of soaking) and 50 seeds were treated with undiluted sodium chromate (60 sec seeding). Then the seeds were being washed by distilled water for 3 minutes. After washing the seeds were dried in sterile conditions (flow-box, 5 minutes) and placed on Petri dish with agar (PDA, SA). Cultivation lasted 7–10 days, (23/20 °C, 14/10-hour light mode). Pathogens were identified based on specific morphological characteristics and proportional infestation of the seeds by fungal pathogens has been evaluated.

RESULTS AND DISCUSSION

Monitoring and detection of sorghum and ryegrass pathogens in field conditions

Due to extreme weather conditions (high temperatures and lack of precipitation; Figure 1 and 2), which were unfavourable for the pathogen development, rare occurrence of fungal pathogens on sorghum and ryegrass was observed during 2018 vegetation season. Only an isolated occurrence of the pathogens was documented, and it did not reach the values required for determining its intensity.

Colletotrichum sublineola and *Ramuliospora sorghi* were identified on the sorghum leaves. These pathogens were described by Hýsek et al. (2010) and Tesso et al. (2012).

A low occurrence of powdery mildew (*Blumeria graminis*) was recorded on the leaves of ryegrass on 10. 4. 2018, but the very dry weather was not favourable for pathogen spreading. *Puccinia graminis* var. *graminis* and *P. coronata* var. *coronata* uredospore were documented on several plants on 13. 6. 2018. These pathogens were identified after the occurrence of teliospores. The occurrence of these pathogens is described, for example Kulovaná (2002). The minimal occurrence of pathogens did not affect the quality of the fodder.

Frequency of seed pathogens of sorghum and ryegrass

The occurrence of microflora was determined for the seeds of sorghum and ryegrass without surface disinfection (Figure 5 and 8). From the total quantity of sorghum (*Sorghum vulgare* var. *sudanense*) 91.5% (183 seeds) was infected and only 8.5% (17 seeds) was without infection. The *A. alternata* (Figure 7), *A. tenuissima* (Figure 6), *Aspergillus flavus and Cladosporium herbarum* fungus were identified.

Figure 5 Cultivation of sorghum

Figure 6 Sporulation of A. tenuissima

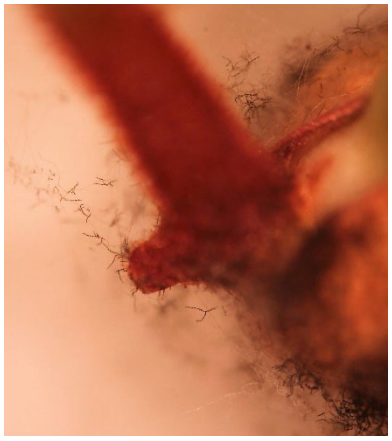

Figure 7 Conidia Alternaria alternata

From the total quantity of ryegrass seeds which were evaluated (200 seeds), 75.5% of them were infected *A. tenuissima* (Figure 9) and *Aspergillus flavus* (Figure 10), *Fusarium* sp. And *Bipolaris* sp. were present.

Figure 8 Cultivation of ryegrass

Figure 9 Sporulation A. tenuissima

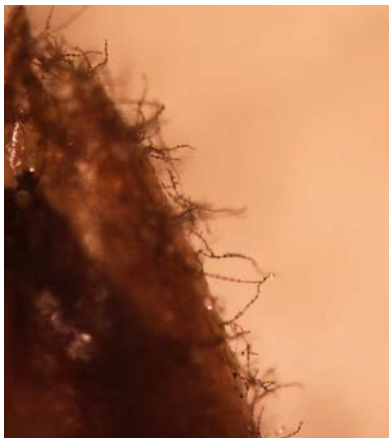

Figure 10 Sporulation Aspergillus flavus

Detection of sorghum and ryegrass pathogens in agar medium

There were no major differences of contamination among seeds of different surface disinfectants, which reached up to 82% (ethanol; Table 2). The lowest contamination was revealed by the treatment by sodium chlorate (78%), so the disinfection was insufficient. *Alternaria tenuissima*, *Cladosporium herbarum*, *Aspergillus flavus* and *Penicillium* sp. pathogens were identified. The occurrence of pathogens is identical with other authors' data, for example Hýsek et al. (2010), Jonar et al. (2011), who also describe other pathogens as *Trichoderma*, *Ascochyta* and *Fusicladium sorghum*, which were not found in our tests.

Table 2 The number of infected and healthy seeds of sorghum with surface disinfection

Sorghum seeds (10 seeds/Petri dish)						
Desinfectans	Ethanol 70%		NaClO and destilled water (1:9)		NaClO	
	Numb. of infected s.	Numb. of healthy s.	Numb. of infected s.	Numb. of healthy s.	Numb. of infected s.	Numb. of healthy s.
	41	9	40	10	39	11

Pathogens of ryegrass seeds on agar medium could not be evaluated, because there was a strong infestation of *Rhizopus* sp., which occurs especially when seeds are stored under unsuitable conditions.

CONCLUSION

The hot summer with tropical temperatures and low precipitations during vegetation season has a negative influence on the currently cultivated fodder, especially maize. Sorghum can be used as a suitable replacement, because it has higher resistance to fungal pathogens and resistance to drought but with the risk of soil erosion. A possible suitable substitute is ryegrass, even though it is more demanding for water conditions, but it contributes to soil remediation and protects it against erosion. For the implementation of these crops into crop rotation, it is necessary to choose a suitable soil location and treatment, to take into account the pre-crop and, last but not least, a suitable variety that is resistant to the most important pathogens. Multiple observations are necessary to determine the spectrum and importance of pathogens.

ACKNOWLEDGEMENTS

The research was financially supported by grant no. AF-IGA-2018-tym001.

REFERENCES

Baroncelli, R. et al. 2014 Draft genome sequence of Colletotrichum sublineola, a destructive pathogen of cultivated sorghum. Genome Announcements, 2(3): e00540-14.

Cagaš, B. 2016. Současný stav českého travního a jetelového semenářství. Zubří: Sdružení pěstitelů trav a jetelovin [Online], Available at: http://www.sptjs.cz/seminar/Cagas_2016.pdf. [2018-08-20].

Cagaš, B., Macháč, J. 2001. Ochrana trávosemenných kultur proti plevelům, chorobám a škůdcům. Ústav zemědělských potravinářských informací: Praha.

Hejduk, S. 2014. Obilniny. In Pícninářství. Brno: Mendelova univerzita v Brně, pp. 19–37.

Hýsek, J. et al. 2010. Choroby a škůdci čiroku pěstovaného v podmínkách České republiky. In Hodnotenie genetických zdrojov rastlín pre výživu a poľnohospodárstvo. Piešťany: Centrum výskumu rastlinnej výroby Piešťany, pp. 137–138.

Jonar, I. et al. 2011. The Effect of Seed-borne Mycoflora from Sorghum and Foxtail Millet Seeds on Germination and Disease Transmission. Mycobiology, 39(3): 206–218.

Kazda, J. et al. 2010. Encyklopedie ochrany rostlin: polní plodiny. 1. vyd., Praha: Profi Press.

Kulovaná, E. 2002. Kvalita obilnin. Úroda [Online], Available at: https://uroda.cz/kvalita-obilnin/. [2018-08-22].

Kuthan, A. 2010. Ochrana čiroku proti škodlivým činitelům: plevele choroby a ochrana. Kukuřičné listy. [Online], Available at: http://www.crs-marketing.cz/files/crs-kukuricne-listy-c.4-2010-155.pdf. [2018-08-22].

Moudrý, J., Strašil, Z. 1999. Pěstování alternativních plodin. České Budějovice: JČU ZF.

Moudrý, J. et al. 2005. Pohanka a proso. Praha: Ústav zemědělských a potravinářských informací.

Tesso, T. et al. 2012. Sorghum pathology and biotechnology-a fungal disease perspective: Part II. Anthracnose, stalk rot, and downy mildew. European Journal of Plant Science and Biotechnology, 6(1): 31–44.

Response of sorghum on nitrogen and sulphur fertilization

Marie Skolnikova, Petr Skarpa
Department of Agrochemistry, Soil Science, Microbiology and Plant Nutrition
Mendel University in Brno
Zemedelska 1, 613 00 Brno
CZECH REPUBLIC

mar.skolnikova@seznam.cz

Abstract: Sorghum is suitable crop for semi-arid regions with limited irrigation capacity or dry land with unpredictable rainfall. The combination of rising temperature and change of rainfall distribution during the year makes some localities of Czech Republic right place for sorghum cultivation. Sufficient nitrogen and sulphur nutrition is important for sorghum growth and yield. The aim of this study was to compare the effect of common fertilizers and fertilizers with nitrification and urease inhibitors on sorghum biomass yield in condition of Žabčice. In precise small-plot experiment was used these fertilizers: Urea and DASA which represented common fertilizers, Alzon neo–N, Urea^{stabil} and Ensin which represented fertilizers with inhibitors. Variant with DASA and Ensin, which contain nitrogen and sulphur, had higher biomass yield than variant fertilized by Urea and Urea^{stabil}. The highest biomass yield was found on variant Alzon neo–N (28.47 t/ha). Nevertheless, all variants with fertilizers with inhibitors had slightly higher biomass yield than variants with common used fertilizers without inhibitors.

Key Words: sorghum biomass yield, nitrogen and sulphur nutrition, fertilizers with inhibitors

INTRODUCTION

Sorghum (*Sorghum vulgare* var. *sudanense*) belongs to the five most cultivated cereals for human nutrition in the world. Africa and Asia are the biggest producers of sorghum for food industry, sorghum cultivated in Europa, USA and Australia are mostly used for feeding animals. The estimated area of this crop is several hundred hectares in the Czech Republic (Hermuth et al. 2012) and we cultivate sorghum mainly for silage as a source of forage for livestock production systems or for biogas production (Podrábský 2008).

Sorghum has large root system which is useful for obtain water and nutrition from greater soil depth. This crop is more resistant to temperature changes during the vegetation than maize (Hermuth et al. 2012) and it is also more resistant to drought than maize, especially for better water management in plant (Assefa et al. 2010). The other advantages of cultivating sorghum are easy and cheap herbicide protection, no problems with occurrence of pests *Diabrotica* (Podrábský 2008), toleration of wide range of soil conditions, from heavy clay soils to light sand (Smith and Frederiksen 2000). For these reasons sorghum could be good alternative for maize in dry and warm conditions which start to be typical for some localities in the Czech Republic during several last years (Kuthan 2012).

Sorghum uptakes nutrients very slowly in the beginning of vegetation and higher demanding on N starts after the first 20 days (Espinoza 2004), so using fertilizers with inhibitors, which could provide nutrients for longer time, seems very suitable. Hermuth et al. (2012) stated that nitrogen fertilization increases the yield of biomass and the content of protein which enhanced the quality of sorghum forage. Sulphur fertilization also has influence on increase the yield and the quality of forages crops (Hallmark and Brown 1994) and moreover, it could improve nitrogen utilization efficiency by the crops (Fismes et al. 2000). The aim of this experiment was the determination of the effect of common nitrogen and sulphur fertilizers and nitrogen and sulphur fertilizers with inhibitors on sorghum biomass yield.

MATERIAL AND METHODS

The precise small-plot experiment was established in very warm and dry climatic region at the Field Trial Station in Žabčice in Southern Moravia. As model crop was used sorghum variety KWS Tarzan which was seed on May 29, 2018. The soil of experiment field was light sand and size of one parcel was 30 m^2. The effect of nitrogen and sulphur fertilization was observed, the fertilizers were applied in single doses before sowing according to the scheme in Table 1. All variants were conducted in four repetitions.

Table 1 Diagram of small-plot experiment

Variant	Fertilizer	Dose of nitrogen (kg/ha)	Dose of sulphur (kg/ha)
1	Urea	115	0
2	Urea^{stabil}	115	0
3	Alzon neo–N	115	0
4	DASA	117	58.5
5	Ensin	117	58.5

Legend: Alzon neo–N – urea with nitrification and urease inhibitors, Urea^{stabil} – urea with urease inhibitor, DASA – ammonium sulphate nitrate, Ensin – ammonium sulphate nitrate with nitrification inhibitors.

The content of nitrogen and sulphur in fertilizers was: Urea – 46% N, Urea^{stabil} – 46% N, Alzon neo–N – 46.3% N, DASA – 26% N and 13% S and Ensin – 26% N and 13% S. On June 6, 2018 three plants from each variant were taken for the determination of the contents of macronutrients in above-ground parts. The samples of plant mass were prepared for analyses, they were dried at temperature of 60 °C and then crushed in a grinder and homogenized. According to Zbíral et al. (2005) the resultant of crushed plant mass was mineralized using a mixture of H_2SO_4 and H_2O_2 in microwave system (Milestone Ethos 1, Bergamo, Italy). For determination of nitrogen content was used method of Kjeldahl, phosphorus was determined colorimetrically using Unicam 8625 UV/Vis spectrometer (ATI Unicam, Cambridge, UK). Atomic Absorption Spectrophotometry (AAS) was used for determination of potassium, magnesium and calcium using ContrAA 700 instrument (Analytik Jena AG, Jena, Germany). The harvest was performed on July 31, 2018. The samples for determination of dry matter content of biomass at harvest were prepared from chaff of 10 plants which were dried to constant weight at the temperature of 105 °C. For statistical evaluation of the yield was used Statistica 12 CZ programme, ANOVA analysis of variance and follow-up tests according to Fisher (LSD test) at 95% ($P<0.05$) level of significance. Results are expressed as a mean ± standard error (SE).

RESULTS AND DISCUSSION

According to the results in Table 2, the highest content of nitrogen was found in variant with Urea^{stabil} (4.86%). The content of N in all the other variants with fertilizers with inhibitors was not increased in comparison of variant with Urea and DASA (without inhibitors). The content of phosphorus and calcium in dry matter in above–ground parts were enhanced in variants with DASA and Ensin in comparison of variants without sulphur fertilization. The lowest content of calcium was found on variant with Urea, in other variants was Ca content higher than on this variant, so sulphur fertilization and fertilizers with inhibitors had positive effect on Ca content in dry matter of sorghum.

Table 2 Content of macroelements in above-ground parts of sorghum

Variant	% content in dry matter				
	N	P	K	Ca	Mg
Urea	4.71	0.45	6.05	2.19	0.38
Urea^{stabil}	4.86	0.47	5.72	2.32	0.38
Alzon neo–N	4.65	0.44	4.85	2.34	0.39
DASA	4.71	0.59	5.96	2.89	0.49
Ensin	4.67	0.50	5.44	2.48	0.39

Hermuth et al. (2012) presented that the dry matter content of biomass at harvest for silage should be 28−35 %. The harvest with lower dry matter content is not impossible but it is not recommended because of low economical efficiency. In our experiment, the range of dry matter content was from 20.3% to 21.6% without any significant differences (Table 3).

Table 3 Dry matter content of biomass at harvest. Means with same letter are not significantly different (P<0.05).

Variant	Dry matter content (%) ± SE
Urea	$21.5^{a} \pm 1.11$
Urea^{stabil}	$21.5^{a} \pm 0.03$
Alzon neo–N	$20.3^{a} \pm 1.13$
DASA	$21.0^{a} \pm 0.41$
Ensin	$21.6^{a} \pm 0.59$

The precipitation during year 2018 was lower than normal precipitation in locality of experimental field in Žabčice (Figure 1), the temperature was also different than normal temperature. Low precipitation in combination with high temperature was not favorable to growth of most cultivated crops in our country, sorghum yield is also reduced under dry conditions (Assefa et al. 2010). Although different water requirements of sorghum cultivars are reported by Giles et al. (1976), Venuto and Kindiger (2008) mentioned that total precipitation should be at least 40 cm for right sorghum growth.

Figure 1 Climograph of Žabčice.

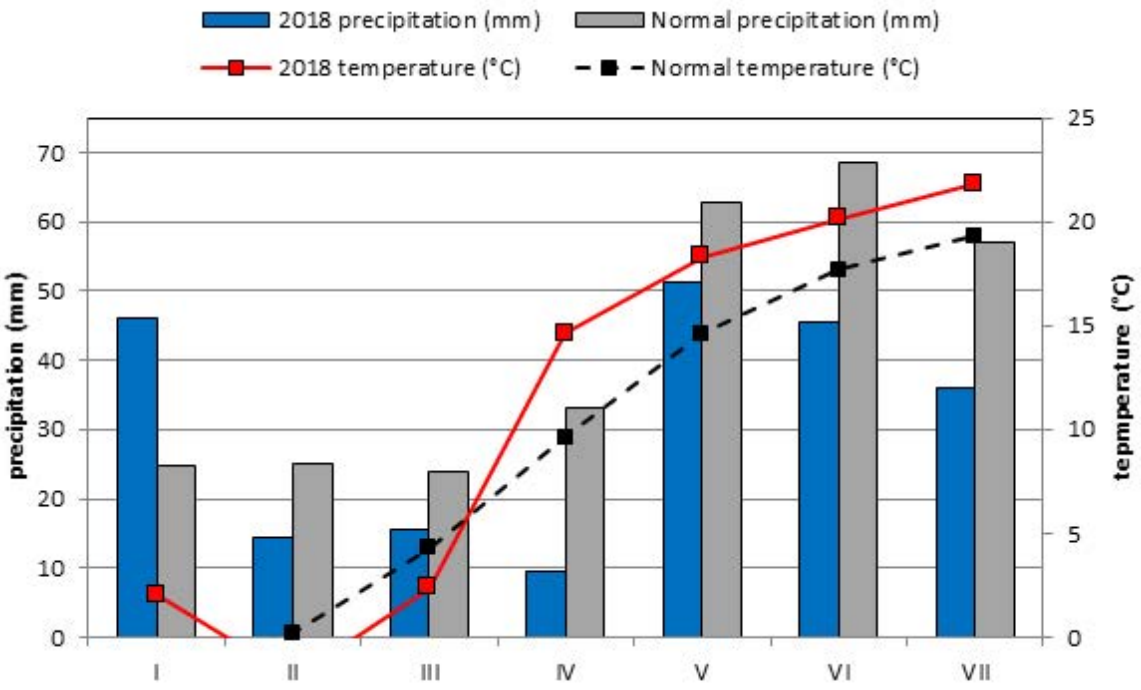

In study of Haankuku et al. (2014) was found that nitrogen fertilization had almost none effect on sorghum biomass yield if the sorghum was cultivated in the drought condition caused by precipitation under the long-term average during period of April to September. The amount of precipitation during vegetation in our experiment field was not favorable for sorghum. The differences between variants were not very considerable, nevertheless we found slight increase in variants with fertilizers with inhibitors. In comparison of Urea fertilizer and urea with inhibitors (Urea^{stabil}, Alzon neo–N), fertilization with urea with inhibitors enhanced sorghum biomass yield. Using of fertilizers with nitrification inhibitors helps to maintain N availability to crops (Grant et al. 1996) and improve the nutritional quality of fodder plants (Montemurro et al. 1998). According to Figure 2, fertilizers

with nitrogen and sulphur (DASA, Ensin) had positive effect on biomass yield which is higher than in variant with Urea and Urea^{stabil} (without sulphur). Unfortunately, these increased yields were not significantly different. The highest biomass yield (28.47 t/ha) was found on variant without Alzon neo–N (without sulphur), it was about 6.6% higher than on variant with Urea.

Figure 2 The yield of sorghum biomass (t/ha). Means with same letter are not significantly different (P<0.05).

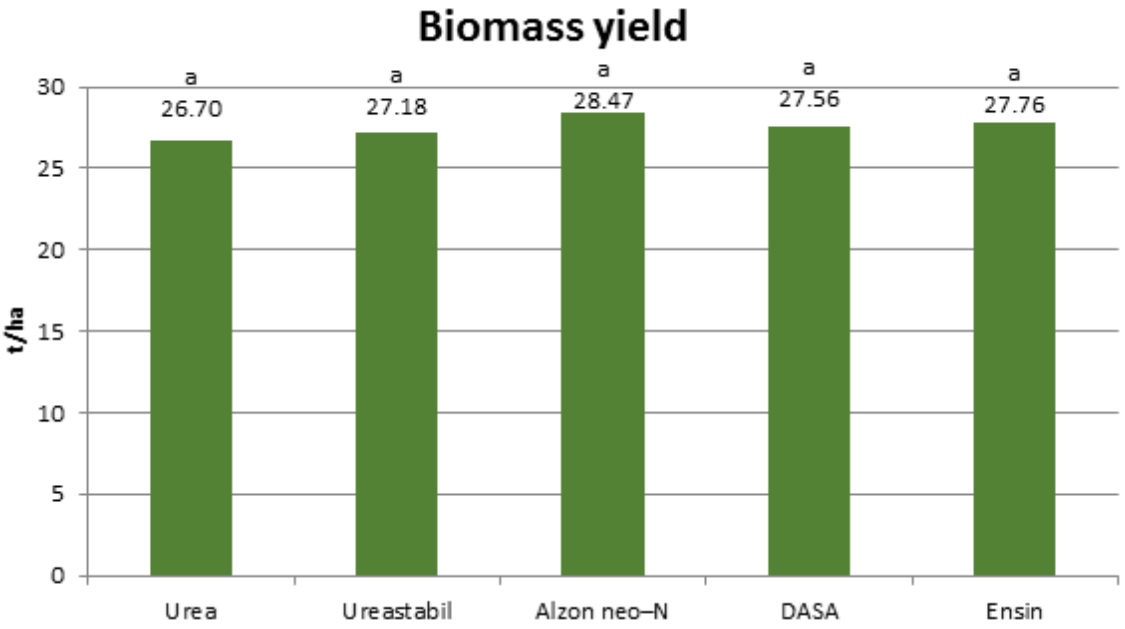

CONCLUSION

Sorghum seems to be very suitable crop for semi-arid regions with limited irrigation capacity or dry land with unpredictable rainfall. Harmonic nitrogen and sulphur nutrition is important for sorghum biomass yield and quality of forage. Using fertilizers with nitrification and urease inhibitors contributes to maintaining nitrogen availability to crops which helps to better fertilization efficiency. In our experiment, all variants with fertilizers with inhibitors had slightly higher biomass yield than variants with common used fertilizers without inhibitors. Variants with sulphur (DASA, Ensin) had more positive effect on biomass yield than variant with Urea and Urea^{stabil}, but the highest biomass yield was found on variant with fertilizer Alzon neo–N (28.47 t/ha) which contains nitrification and urease inhibitors.

ACKNOWLEDGEMENTS

The research was supported by grant no. AF-IGA-2018-tym001.

REFERENCES

Assefa, Y. et al. 2010. Grain sorghum water requirement and responses to drought stress: A review. Crop Management [Online], 9(1). Available at: https://www.mssoy.org/uploads/files/crop-mgmt-nov-2010.pdf. [2018-09-12].

Espinoza, L. 2004. Fertilization and liming. In Arkansas Grain Sorghum Production Handbook - MP297. [Online]. Little Rock: University of Arkansas, pp. 21–24. Available at: https://www.uaex.edu/publications/pdf/mp297/4_fertilization_lime.pdf. [2018-09-08].

Fismes, J. et al. 2000. Influence of sulfur on apparent N-use efficiency, yield and quality of oilseed rape (Brassica napus L.) grown on a calcareous soil. European Journal of Agronomy [Online], 12(1): 127–141. Available at: https://pdfs.semanticscholar.org/2675/3f77825f653f0c590f037d0264441b4f2a2e.pdf. [2018-09-02].

Giles, K.L. et al. 1976. Effect of water stress on the ultrastructure of leaf cells of sorghum bicolor. Plant Physiology [Online], 57(1): 11–14. Available at: https://www.ncbi.nlm.nih.gov/pmc/articles/PMC541954/pdf/plntphys00155-0019.pdf. [2018-09-12].

Grant, C.A. et al. 1996. Volatile losses of NH3 from surface-applied urea and urea ammonium nitrate with and without the urease inhibitors NBPT or ammonium thiosulphate. Canadian Journal of Soil Science [Online], 76(3): 417–419. Available at: http://www.nrcresearchpress.com/doi/10.4141/cjss96-050#.W5vMgM4zbIU. [2018-09-08].

Haankuku, Ch. et al. 2014. Forage Sorghum Response to Nitrogen Fertilization and Estimation of Production Cost. Agronomy Journal [Online], 106(5): 1659–1666. Available at: http://agecon.okstate.edu/faculty/publications/4982.pdf. [2018-09-05].

Hallmark, W.B., Brown, L.P. 1994. Interactive effects of sulphur and potassium fertilization on Bermudagrass hay yields. Sulphur Agriculture, 18: 41–44.

Hermuth, J. et al. 2012. Čirok obecný – Sorghum bicolor (L.) MOENCH: možnosti využití v podmínkách České republiky. Metodika pro praxi. Praha: Výzkumný ústav rostlinné výroby.

Kuthan, A. 2012. Choroby čiroku v podmínkách České republiky. Farmář, 18: 38–39.

Montemurro, F. et al. 1998. Effects of rease and Nitrification Inhibitors Application on Urea Fate in Soil and Nitrate Accumulation in Lettuce. Journal of Plant Nutrition [Online], 21(2): 245–252. Available at: https://www.tandfonline.com/doi/abs/10.1080/01904169809365399. [2018-09-12].

Podrábský, M. 2008. Nový hybrid čiroku se súdánskou trávou. Agromanuál, 2: 66–67.

Smith, C.W., Frederiksen, R.A. 2000. Sorghum: Origin, history, technology, and production. 1st ed., New York: John Wiley and Sons.

Venuto, B., Kindiger, B. 2008. Forage and biomass feedstock production from hybrid forage sorghum and sorghum–sudangrass hybrids. Grassland Science [Online], 54(4): 189–196. Available at: https://onlinelibrary.wiley.com/doi/pdf/10.1111/j.1744-697X.2008.00123.x. [2018-09-05].

Zbíral, J. et. al. 2005. Analýza rostlinného materiálu: Jednotné pracovní postupy. 2nd ed., Brno: Ústřední kontrolní a zkušební ústav zemědělský.

The effect of nitrogen and sulphur fertilizers with inhibitors on poppy seed yield

Marie Skolnikova, Petr Skarpa
Department of Agrochemistry, Soil Science, Microbiology and Plant Nutrition
Mendel University in Brno
Zemedelska 1, 613 00 Brno
CZECH REPUBLIC

mar.skolnikova@seznam.cz

Abstract: The aim of this study was the determination of the effect of nitrogen and sulphur fertilizers with inhibitors on poppy seed yield. The Czech Republic is one of dominant producer of poppy for food industry and sufficient nutrition plays important role in poppy growth, especially nitrogen and sulphur have huge effect on poppy growing and seeds production. The nitrogen fertilizers with nitrification and urease inhibitors were used in this small-plot experiment and their effect on poppy seed yield was observed. Urea fertilizer and DASA (ammonium sulphate nitrate) represented common fertilizers, Alzon neo–N, Urea^{stabil} and Ensin were used like fertilizers with inhibitors. We found only slight enhancing of seed yield on variant with inhibited urea (variant with Alzon neo–N and Urea^{stabil}), the higher seed yield was found on variant with DASA (185 kg/ha) and Ensin (188 kg/ha). Fertilizers DASA and Ensin include sulphur which has important effect on poppy seed production, so the seed yield in these variants was enhanced in compare with variants without sulphur fertilization.

Key Words: poppy seed yield, fertilizers with inhibitors, nitrogen and sulphur fertilization

INTRODUCTION

Poppy (*Papaver somniferum* L.) is traditionally cultivated crop in the Czech Republic which also belongs to dominant group of poppy growers for food industry (Liška 2017). Sufficient nutrient supply is essential for right growth and seed yield of poppy. Especially nitrogen plays important role in nutrition of poppy. The demands on the nitrogen nutrition start early after germination and they last until formation of generative organs (Bechyně et al. 2001). Not only nitrogen but also sulphur has important effect on poppy yield. Vašák (2010) stated that 1 ton of poppy seed need 18 kg of sulphur. It is also reported that sulphur nutrition has positive effect on seed yield and also on oil production (Páleníček 2009).

Nitrogen fertilization is necessary for plant cultivation and the consumption of nitrogen fertilizers has been rising. Using nitrogen fertilization is also connected with N losses like volatilization or N leaching which have negative effects on life environment. These losses have important impacts on groundwater quality and greenhouse gas emissions and they are also decrease economic efficiency of fertilization (Edmeades 2004). N losses are not always limited by using common nitrogen fertilizers (reduction of N losses depends on agrotechnological factors like type of fertilizers application, doses of fertilizers etc.) and using fertilizers with inhibitors of N transformation help to bigger reduction of N losses and increase N-use efficiency (Nielsen 2006). The most using fertilizer with inhibitors is urea due to high content of nitrogen (46%) and relatively low-cost production (Trenkel 1997). According to rising intensification of agriculture, the fertilizers with inhibitors represent the way how to make the agriculture more eco-friendly. The aim of this study was the determination of the effect of nitrogen and sulphur fertilizers and nitrogen and sulphur fertilizers with inhibitors on poppy yield in the condition of the Czech Republic.

MATERIAL AND METHODS

The effect of nitrogen and sulphur fertilizers on poppy yield was observed in the precise small-plot experiment at the Field Trial Station in Žabčice. This station is located in Southern Moravia in very warm and dry climatic region. The precrop was winter wheat. As model crop was used poppy variety

Major (sowing rate 1.5 kg/ha) which was sown on 17 April 2018. The size of one parcel was 20.4 m^2. Fertilizers were applied in single doses before sowing according to the scheme in Table 1. All variants were conducted in four repetitions.

Table 1 Diagram of small-plot experiment

Variant	Fertilizer	Dose of nitrogen (kg/ha)	Dose of sulphur (kg/ha)
1	Urea	101	0
2	Alzon neo–N	101	0
3	Urea^{stabil}	101	0
4	DASA	104	52
5	Ensin	104	52

Legend: Alzon neo–N – urea with nitrification and urease inhibitors, Urea^{stabil} *– urea with urease inhibitor, DASA – ammonium sulphate nitrate, Ensin – ammonium sulphate nitrate with nitrification inhibitors.*

Urea (46% N), Alzon neo–N (46.3% N), Urea^{stabil} (46% N), DASA (26% N and 13% S) and Ensin (26% N and 13% S) were used as nitrogen and sulphur fertilizers. In stage of 6–8 true leaves, the samples of 10 poppy plants from each variant were taken for the determination of the contents of macronutrients in above-ground parts. First, the samples of plant mass were dried at temperature of 60 °C and then they were crushed in a grinder and homogenized. After that the resultant crushed plant mass was mineralized using a mixture of H_2SO_4 and H_2O_2 in microwave system (MILESTONE ETHOS 1, Bergamo, Italy) according to Zbíral et al. (2005). Nitrogen content was determined by method of Kjeldahl, phosphorus was determined colorimetrically using Unicam 8625 UV/Vis spectrometer (ATI Unicam, Cambridge, UK). The determination of potassium, magnesium and calcium was performed by Atomic Absorption Spectrophotometry (AAS) in the mineralized samples with the ContrAA 700 instrument (Analytik Jena AG, Jena, Germany). For determination of sulphur the samples of plant mass were also dried, crushed and homogenized and after that the samples were mineralized using a mixture of H_2O_2 and HNO_3 in microwave system (MILESTONE MLS 1200 MEGA, Bergamo, Italy). The determination was performed by Inductively coupled plasma optical emission spectroscopy (ICP-OES) using JY-24 instrument (JOBIN-YVON, France) according to Zbíral et al. (2005). The harvest was performed on 31 July 2018 and the seed yield of every variant was determined.

The effect of the fertilization was evaluated by ANOVA analysis of variance followed by testing at a 95% ($p < 0.05$) level of significance using Fischer's LSD test (Statistica CZ 12 programme).

RESULTS AND DISCUSSION

In comparison of variant with common fertilizers (Urea, DASA) and variant with fertilizers with inhibitors (Alzon neo–N, Urea^{stabil}, Ensin), the content of nitrogen in dry matter in above-ground parts of poppy was increased only in variant with Alzon neo–N (Table 2). The content of calcium was supported on variants fertilized by urea with inhibitors (Alzon neo–N, Urea^{stabil}). The content of Ca and Mg was also enhanced in these variants in contrast to variants without sulphur fertilization (DASA, Ensin), for example variant with DASA contained about 29% more magnesium and about 32% more calcium than variant with Urea. It is obvious that sulphur content was increased in variants with DASA and Ensin in contrast to variants without sulphur fertilization. According to results in Table 2, sulphur fertilization had impact on macroelements composition of poppy plants.

Table 2 Content of macroelements in above-ground parts of poppy

Variant	% content in dry matter					
	N	**P**	**K**	**Ca**	**Mg**	**S**
Urea	4.71	0.45	6.05	2.19	0.38	0.50
Alzon neo–N	4.86	0.47	5.72	2.32	0.38	0.52
Urea^{stabil}	4.65	0.44	4.85	2.34	0.39	0.54
DASA	4.71	0.59	5.96	2.89	0.49	0.66
Ensin	4.67	0.50	5.44	2.48	0.39	0.65

The yield of poppy seed is very depended on the weather condition in specific year (Fábry et al. 1992). One of limiting factor is sufficient amount of moisture during the vegetation, especially from elongation stage to flowering. The lack of moisture in this period could cause huge decreasing of poppy seed yield (Roubal 2003). The weather condition during vegetation in year 2018 was not favourable to growth, development and seed yield of poppy, high temperatures with combination of insufficient precipitation had negative effect on seed yield (Figure 1).

Figure 1 Climograph of Žabčice

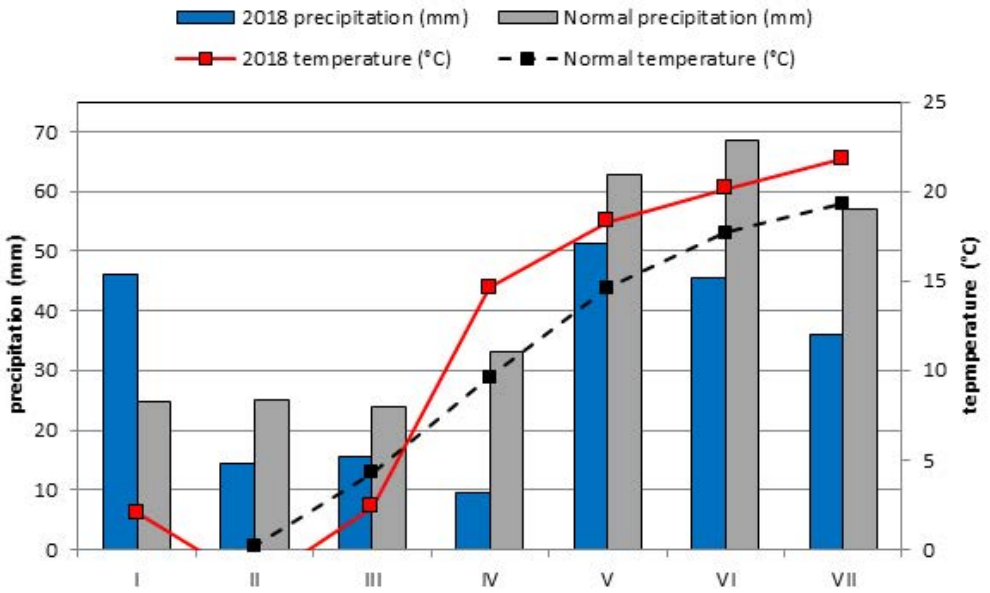

According to results in Figure 2, variants with urea fertilizers with inhibitors (Alzon neo–N, Urea^{stabil}) showed only slight enhancing in seed yield in contrast to variant fertilized by Urea. Edmeades (2004) stated that is difficult to predict the effects of nitrification inhibitors, there are many factors which have impact on effect of nitrification inhibitors. Harrison and Webb (2001) present that some of these factors are soil factors (texture, temperature, moisture content etc.) or climate factors (rainfall intensity and frequency). Hendrickson (1992) mentioned the benefits of urea application with urease inhibitors could be also variable and the reduction in ammonium volatilization could not lead to increase in crop yield.

Figure 2 The yield of poppy seed (kg/ha). Means with same letter are not significantly different (P<0.05)

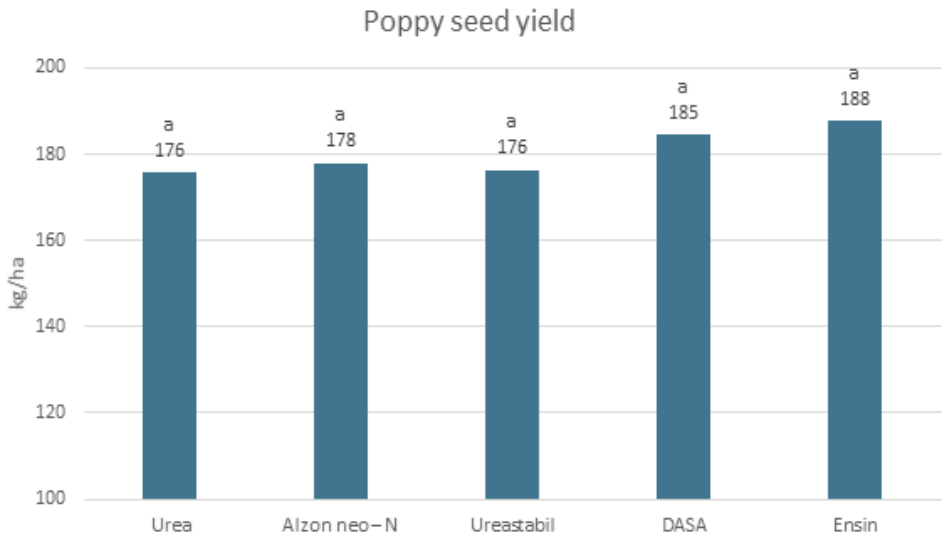

Legend: Means with same letter are not significantly different (P<0.05)

Slightly higher seed yield (but not significant) was found on variant with Ensin (DASA with nitrification inhibitor) application in comparison with DASA fertilization. Variant with Ensin had the highest seed yield of all variants (188 kg/ha). Fertilizers with sulphur had positive effect on seed yield which was higher in variant with DASA and Ensin. Seed yield of variant with DASA was about 5% higher than the lowest seed yield of variant with Urea (without sulphur). Variant with Ensin had about 6.8% higher seed yield that variant with Urea. In study of Páleníček et al. (2005) and Subrahmanyam et al. (1992) it is also reported increased poppy seed yield after sulphur application.

CONCLUSION

The poppy seed yield is influenced not only by nutrients, weather condition has also important effect on it. Unfortunately, the weather condition during year 2018 was very unfavorable for poppy growing and it had also negative effect on seed yield which was lower than average seed yield. In comparison of variants with common fertilizers and variants with fertilizers with nitrification and urease inhibitors we found slightly enhancing on poppy seed yield in variants with inhibitors. The bigger difference in seed yield was detected between variants with nitrogen fertilization and variants with nitrogen and sulphur fertilization (DASA, Ensin). Seed yield was higher in variants with DASA and Ensin, so according to these results, the sulphur had positive effect on seed yield. The highest seed yield (188 kg/ha) was determinated in variant with Ensin (ammonium sulphate nitrate with nitrification inhibitor).

ACKNOWLEDGEMENTS

The research was supported by grant no. AF-IGA-IP-2018/015.

REFERENCES

Bechyně, M. et al. 2001. Mák. Praha: Agrospoj.

Edmeades, D.F. 2004. Nitrification and urease inhibitors: A review of the national and international literature on their effects on nitrate leaching, greenhouse gas emissions and ammonia volatilisation from temperate legume-based systems [Online]. Hamilton East: Environment Waikato. Available at: https://www.waikatoregion.govt.nz/services/publications/technical-reports/tr/tr200422. [2018-08-28].

Fábry, A. et al. 1992. Olejniny. Praha: Ministerstvo zemědělství ČR.

Harrison, R., Webb, J. 2001. A review of the effect of N fertiliser type on gaseous emissions. Advances in Agronomy [Online], 73: 65–108. Available at: https://www.researchgate.net/publication/222263358_A_review_of_the_effect_of_N_fertilizer_type_on_gaseous_emissions. [2018-09-08].

Hendrickson, L.L. 1992. Corn yield response to the urease inhibitor NBPT: five year summary. Journal of production agriculture [Online], 5(1): 131–137. Available at: https://eurekamag.com/research/007/162/007162015.php. [2018-08-30].

Liška, M. 2017. Situační a výhledová zpráva olejniny [Online]. Praha: Ministerstvo zemědělství. Available at: http://eagri.cz/public/web/mze/zemedelstvi/rostlinna-vyroba/rostlinne-komodity/obiloviny/situacni-a-vyhledove-zpravy-olejniny/. [2018-08-28].

Nielsen, R.L. 2006. N Loss Mechanism and Nitrogen Use Efficiency. Purdue Nitrogen Management Workshops [Online]. West Lafayette: Purdue University. Available at: https://www.agry.purdue.edu/ext/pubs/2006NLossMechanisms.pdf. [2018-09-10].

Páleníček, L. 2009. Optimalizace výživy máku jarního (*Papaver Somniferum* L.) dusíkem a sírou. PhD dissertation, Mendel University in Brno.

Páleníček, L. et al. 2005. Nitrogen and sulphur in the nutrition of poppy (*Papaver somniferum*, L.). In Proceedings of International PhD Students Conference MendelNet´05 Agro [Online]. Brno, Czech Republic, 29 November. Brno: Mendel University in Brno, Faculty of Agronomy, pp. 37. Available at: https://mnet.mendelu.cz/archiv/book/mendelnet_05.pdf. [2018-08-28].

Roubal, T. 2003. Regulace tvorby výnosu a poléhání jarního máku. In Sborník řepka, mák, hořčice. Praha, 19 February. Praha: AF ČZU v Praze, pp. 142–149.

Subrahmanyam, K. et al. 1992. The effect of forms of sulphur on yield and quality of seed, oil and alkaloids of opium poppy (Papaver somniferum, L.). Acta – Horticulturae [Online], 306(1): 431–435. Available at: https://www.actahort.org/books/306/306_57.htm. [2018-09-02].

Trenkel, M.E. 1997. Controlled-Release and Stabilized Fertilizers in Agriculture [Online]. Paris: International Fertilizer Industry Association. Available at: http://www.wnkgroup.com/Controlled-Release%20fertilizer%20in%20Agriculture.pdf. [2018-08-30].

Vašák, J. 2010. Mák. Praha: Powerprint.

Zbíral, J. et. al. 2005. Analýza rostlinného materiálu JPP. ÚKZÚZ.

Improved root system for better wheat drought tolerance

Marie Smardova, Jana Klimesova, Tomas Streda
Department of Crop Science, Breeding and Plant Medicine
Mendel University in Brno
Zemedelska 1, 613 00 Brno
CZECH REPUBLIC

xsmardo1@mendelu.cz

Abstract: Larger root system allows better use of water and nutrients from the soil as has been already proven several times. Deep-rooting varieties can be successful on soils with higher levels of groundwater in dry years. It is necessary to precisely identify suitable phenotypes for deliberate plant breeding e.g. for tolerance to drought. The aim of the research was to analyze the measured data on the size of the root system in three phenological stages in the years 2015–2017, to evaluate the relationship between the root system size (RSS) and the yield of the grain. The root system size and winter wheat grain yield were evaluated in the field experiment at a dry locality in Branišovice (South Moravia, Czech Republic). The properties of the root system of various genotypes in years with different meteorological conditions were identified. The correlation analysis of the relationships between RSS and grain yield was significant particularly in 2015. Early genotypes created a larger root system at the time of RSS measurement which was subsequently reflected by an increase in grain yield.

Key Words: root system size, grain yield, electrical capacitance, soil moisture

INTRODUCTION

Moisture certainty analyses in the Czech Republic proved an increase of the driest areas and drought event probability increased in the 1961–2010 period (Středová et al. 2011). At locations with a regular drought occurrence, the strategies that help the field crops to overcome this stress are recommended. Breeding of varieties on tolerance to drought is highly desirable but is very demanding due to the polygenic founding of this genetic feature and its low heritability (Cattivelli et al. 2008). It is generally known that plants under water stress regulate the ratio of the aboveground and underground biomass to the root system prosperity (Gregory 2006). Early varieties with rapid initial development, growth, premature flowering, and overall shorter growing season are able to complete their development and to mature at a time before drought produces a significant negative impact on yield (Blum and Naveh 1976). A larger root system allows better use of water, nutrients or heavy metals from the soil as well (Bodner et al. 2010, Kovárník and Cerkal 2011, Nemcova and Gersl 2017). The size of the root system, resp. root depth and root density in the soil profile layers, is critical for the availability of water usable by plants. Creating a large and an efficient root system can be the basis for achieving high yields of field crops (Středa et al. 2013, Wu et al. 2017). It was observed that wheat and barley varieties with a larger root system achieved higher yields (Svačina et al. 2014, Robinson et al. 2018). However, the size of the root system is not always a great advantage. If drought does not occur, the development of a larger root system is an unnecessary investment of the plant at the expense of other photosynthesis products.

The aim of the research was to analyze the measured data on the root system size in three phenological phases in selected winter wheat genotypes for years 2015–2017, to evaluate the impact of factors influencing the size of the root system and to determine the relation between the root system size and the grain yield.

MATERIAL AND METODS

The root system size (RSS) and grain yield of winter wheat were evaluated in a three-year field experiment at the locality in Branišovice (South Moravia, Czech Republic, approximate GPS 48.9530581N, 16.4304708E). The long-term climatic conditions of the region are stated by Středa

et al. (2013). The soil moisture content [volume %] was measured at 10-min intervals using VIRRIB automatic electromagnetic sensors (AMET Velké Bílovice, CZ).

In 2015, 2016 and 2017, 37 breeding lines of winter wheat were monitored, respectively, 14 and 6. Analysis of variance was carried out on 6 genotypes of winter wheat 501, 509, 517, 527, 531, 533. The experiment on a small plot (area: 1.8 m^2) was based on 5 repetition. The rate of seeding was 4 million seeds per hectare. Standard doses of fertilizers and plant protection products according to valid recommendations have been used to treat plants. Plants were planted in rows with an inter-line spacing of 20 cm. Six randomly selected plants were used for measurement of the root system electrical capacitance in nanofarads (Chloupek 1972, Cseresnyés et al. 2014, Kormanek et al. 2016) using LCR meter Extech 380193 (Extech instruments, NH, USA) at a frequency of 1 kHz in the stage of stem elongation BBCH 30–40 (Meier 1997), flowering stage (BBCH 61–70) and grain filling stage (BBCH 71–85) in each repetition. Grain harvesting took place in full maturity of the plants (BBCH 90).

Statistical data processing by the analysis of variance at a significance level of $p \leq 0.05$ with subsequent Tukey HSD test and correlation analysis was carried out using STATISTICA 10 (Statsoft, Tulsa, OK).

RESULTS AND DISCUSSION

The analysis of influence of the experimental factors is shown in Table 1. Influence of the year (soil moisture in Figure 1; the driest year was 2017, the most humid was 2016) on the root system size was statistically significant at all stages of plant development. The year influences the RSS from 55.6% and different plant genotype from 25.4% in the stage of stem elongation. Statistically significant difference of the year influence on the RSS increases to 67.9% in the heading stage. Data variability of RSS is represented by genotype only 15.4% in this stage. The year influence on the RSS represents 66.9% in the grain filling. The greatest genotype influence is at the beginning of the stem elongation, and in the next stages of development it becomes not so marked.

Table 1 Influence of experimental factors in % on the wheat root system size in individual growth stages

Factor	Stem elongation	Heading stage	Grain filling stage
Year (Y)	55.6*	67.9*	66.9*
Genotype (G)	25.4*	15.4*	14.0
Interaction Y×G	11.3*	9.0	8.8
Error	7.7	7.7	10.3

*Legend: * Statistically significant difference level of $p \leq 0.05$*

Figure 1 Soil humidity at a depth of 30 cm (Branišovice, 2015–2017)

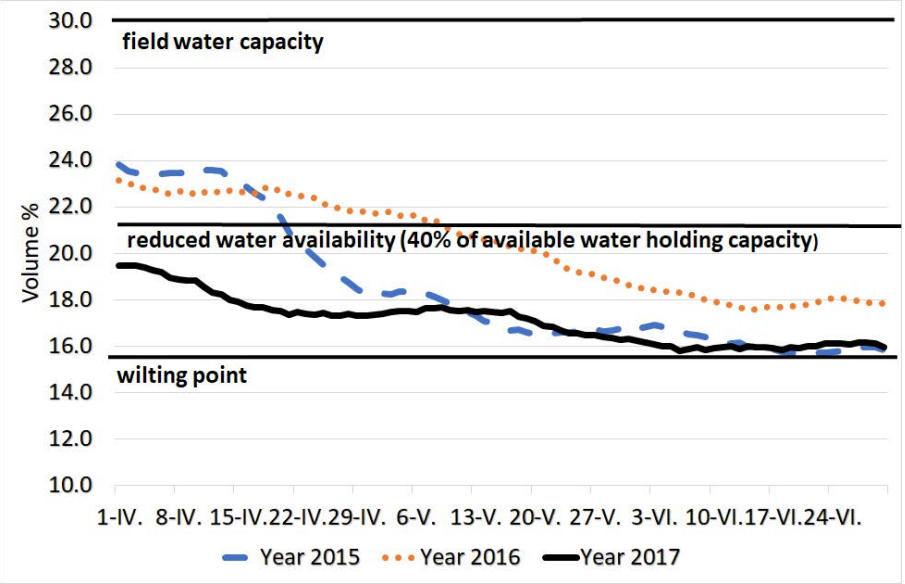

Figure 2 Wheat RSS in the stem elongation (Branišovice, 2015–2017)

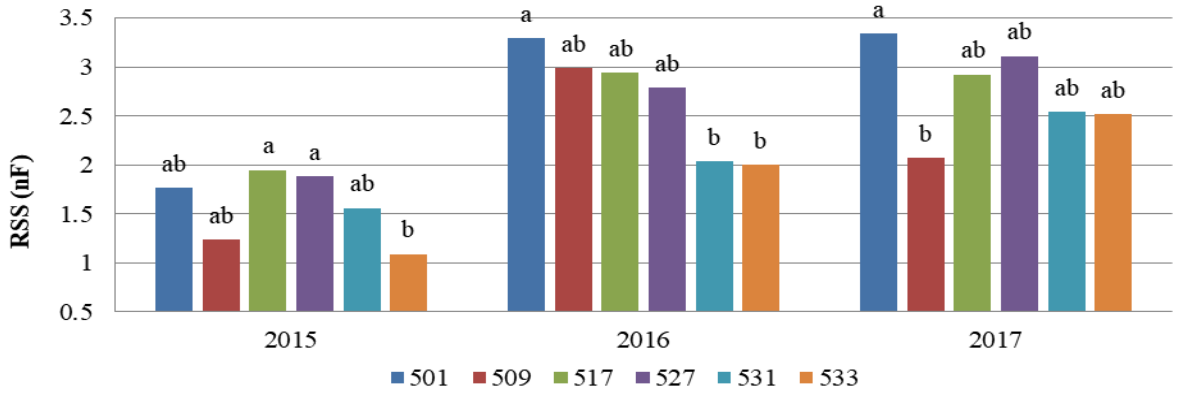

Legend: RSS – root system size, Different letters (a, ab, b) indicate a statistically significant difference between genotypes in the years 2015–2017

Figure 2 shows a significant statistical difference between individual genotypes in the stage of stem elongation between 2015 and 2017.

Figure 3 Wheat RSS in the heading stage (Branišovice, 2015–2017)

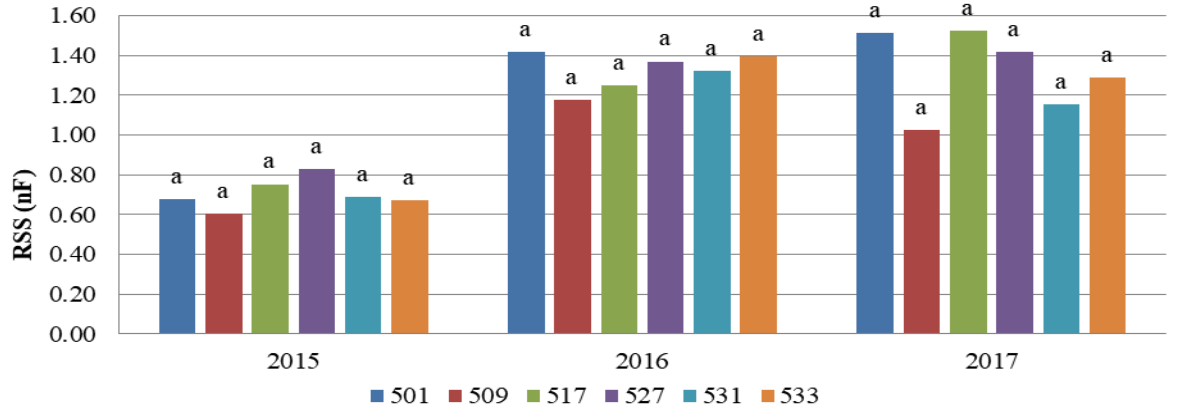

Legend: RSS – root system size, Same letter (a) indicates a statistically inconclusive difference between genotypes in the years 2015–2017

There was no statistically significant difference for the RSS in the stages of heading (Figure 3) and grain filling (Figure 4) for the years 2015–2017. Genotype 509 is ranked between the genotype with the smallest measured RSS in both developmental stages.

Figure 4 Wheat RSS in the grain filling stage (Branišovice, 2015–2017)

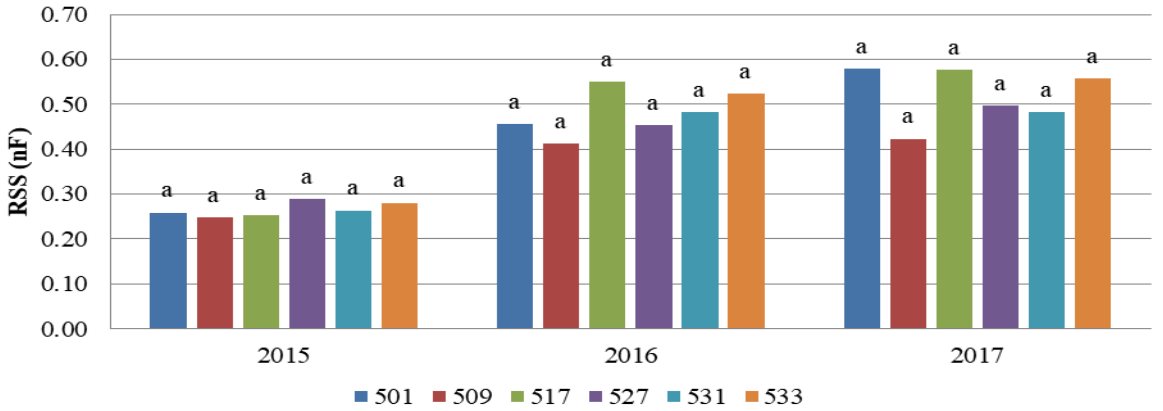

Legend: RSS – root system size, Same letter (a) indicates a statistically inconclusive difference between genotypes in the years 2015–2017

Table 2 Relationship between RSS and grain yield of winter wheat expressed by correlation coefficient

Year/Years	Number of genotypes (n)	Stem elongation	Heading stage	Grain filling stage	Average
2015	All (n=39)	0.414**	0.161	0.159	0.394*
	Late (n=11)	0.350	0.362	0.029	0.454
	Early (n=26)	0.494*	0.028	0.109	0.417*
2016	All (n=14)	0.378	0.513	-0.052	0.487
	Late (n=5)	-0.622	0.181	-0.581	-0.555
	Early (n=9)	0.452	0.579	0.066	0.661
2015+2016	All (n=14)	0.472	0.603*	0.362	0.581*
	Late (n=5)	-0.801	0.747	0.047	-0.685
	Early (n=9)	0.663	0.439	0.413	0.784*
2017	All (n=6)	-0.293	-0.516	-0.283	-0.367

Legend: All – early and late genotypes, Late – late genotypes, Early – early genotypes, statistically significant values of correlation coefficient level of $p \leq 0.05$, ** statistically significant values of correlation coefficient level of $p \leq 0.01$.*

Statistically significant correlation between the RSS in the stage of stem elongation and the grain yield of all 39 genotypes (r = 0.414) was detected in 2015. In the next stages of plant development, the dependence was positive, the larger root system contributed to the higher grain yield, but it was not statistically significant. Positive significant correlation on grain yield in 2015 in the stage of shoot growth was represented by the root system of early genotypes (r = 0.494). The mean values of the year 2015 point to statistically significant effect between RSS and grain yield (r = 0.394) and higher grain yields of early genotypes with higher RSS (r = 0.417). There is not statistical significance between values of grain yield and RSS in 2016. Positive correlations and hence higher grain yields were achieved in early genotypes, which also had a larger root system (r = 0.661). From the above mentioned correlation coefficients, it is not always possible to consider the positive relationship between the root system size and the grain yield. In particular, in 2017, the root system did not affect the grain yield; on the contrary, the larger root system had a negative impact on grain yield. In extraordinary dry year 2017 the bigger roots probably could not have given plants an advantage, since there was no water available in the soil. Quite the opposite it was rather an useless waste of assimilates.

CONCLUSION

The RSS was significantly affected by the genotype of winter wheat (501, 509, 517, 527, 531, 533) in the stem elongation and heading stage during the three-year experiment. The significant impact on RSS has been traced between genotype and year interaction but only in the stage of shoot growth. The correlation analysis of the relationships between RSS and grain yield was particularly significant in 2015. Early genotypes of winter wheat created a larger root system when the water is available, which was subsequently reflected by an increase in grain yield.

ACKNOWLEDGEMENTS

The research was financially supported by the project QJ1510098 of the National Agency for Agricultural Research.

REFERENCES

Blum, A., Naveh, M. 1976. Improved water-use efficiency by promoted plant competition in dryland sorghum. Agronomy Journal, 68: 111–116.

Bodner, G. et al. 2010. Improved evaluation of cover crop species by growth and root factors. Agronomy for Sustainable Development, 30: 455–464.

Cativelli, L. et al. 2008. Drought tolerance improvement in crop plants: an integrated view from breeding to genomics. Field Crops Research, 105: 1–14.

Chloupek, O. 1972. The relationship between electric capacitance and some other parameters of plant roots. Biologia Plantarum, 14: 227–230.

Cseresnyés, I. et al. 2014. Simultaneous monitoring of electrical capacitance and water uptake activity of plant root system. International Agrophysics, 28(4): 537–541.

Gregory, P.J. 2006. Plant Roots: Growth, Activity and Interaction with Soils. 1st ed., Oxford, UK: Blackwell Publishing Ltd.

Kormanek, M. et al. 2016. Modification of the tree root electrical capacitance method under laboratory conditions. Tree Physiology, 36(1): 121–127.

Kovárník, J., Cerkal, R. 2011. Comparison of the Leaf Area Index and the Root System Size in Selected Varieties of Spring Barley. In Proceedings of International PhD Students Conference MendelNet 2011. Brno, Czech Republic, 23 November, Brno: Mendel University in Brno, Faculty of Agronomy, pp. 65–70.

Meier, U. 1997. BBCH-Monograph. Growth stages of plants – Entwicklungsstadien von Pflanzen – Estadios de las plantas – Développement des Plantes. Berlin and Wien: Blackwell Wissenschaftsverlag.

Nemcova, M., Gersl, M. 2017. Screening analysis of toxic metals on specific allotment garden areas in the City of Brno and its surroundings. In Proceedings of 24th International PhD Students Conference (MendelNet 2017), 8–9 November, Brno, Mendel University in Brno, pp. 419–423.

Robinson, H. et al. 2018. Root architectural traits and yield: exploring the relationship in barley breeding trials. Euphytica, 214: 151.

Středová, H. et al. 2011: Climatic factors of soil estimated system. In International Scientific Conference on Bioclimate – Source and Limit of Social Development. Topolcianky, Slovakia. Nitra: SPU v Nitre, pp. 137–138.

Středa, T. et al. 2013. Prediction of adult western corn rootworm (Diabrotica virgifera virgifera LeConte) emergence. Plant Protection Science, 49: 89–97.

Svačina, P. et al. 2014. Uncommon selection by root system size increases barley yield. Agronomy for Sustainable Development, 34(2): 545–551.

Wu, W. et al. 2017. Quantification of canola root morphological traits under heat and drought stresses with electrical measurements. Plant and Soil, 415: 229–244.

ANIMAL PRODUCTION

The effect of chicken genotypes on cutted pasture intake

Vojtech Anderle, Lucie Kupcikova, Martina Lichovnikova, Vladimir Zmrhal
Department of Animal Breeding
Mendel University in Brno
Zemedelska 1, 613 00 Brno
CZECH REPUBLIC

lucie.kupcikova@mendelu.cz

Abstract: The aim of the study was to estimate intake of cutted pasture in different chicken genotypes. The experiment involved of 150 day-old chickens of three genotypes (3 x 50); medium-growing JA 757 hybrid, fast-growing ROSS 308 and the slow-growing males of meat-laying type ISA Dual. Two different feeders were used in each box, one with diets and second one with cutted pasture. Both feeds were available for chickens ad libitum. Pasture was weighted and supplied fresh daily in the morning and the rest was weighted in the evening. Average daily pasture consumption increased for all hybrids as a function of age. The experiment was stopped when daily pasture intake had no increased any more. The maximum average daily pasture intake was the highest ($P < 0.05$) for ISA Dual hybrid 25.8 g/day at the age 13 weeks, whereas for the JA 757 hybrid, this was only 16.1 g/day at the age 9 weeks. ROSS 308 hybrid had maximum daily pasture intake only 13.1 g/day at the age 7 weeks.

Key Words: JA 757, ROSS 308, ISA Dual

INTRODUCTION

Animal welfare considerations currently tend to favour systems of outside-reared animals in European agriculture. Consumers also demand food from outside-reared poultry, especially broilers, as in the case of small individual holders or organic farming. Access to an outdoor area would allow to the birds to express their natural exploring behavior, but also to ingest plants, invertebrates or soil. In general, it is expected that birds have a distinct feed intake in free range which contributes to their supply with nutrients. Horsted et al. (2007a, b) assumed that the ingestion of plant particles of high quality reduces the intake of compound feed without affecting laying performance, by this reducing feed costs. Thus, this intake of plant particles can be regarded as a valuable feed supplement (Fölsch et al. 1999). Intake of pasture can be influenced by a number of factors, such as genotype, age, breeding technology, but also species composition of pasture, vegetation period or soil conditions (Hörning et al. 2002, Horsted et al. 2007a, Dal Bosco et al. 2014). In most studies feed intake in the pasture was determined by estimation from changes in vegetation cover (Horsted et al. 2007b, Jondreville et al. 2010, Trei et al. 2013) and by analysis of crop contents (Antell and Ciszuk 2006). The disadvantage of these methods is that feed intake is calculated either on the basis of rather defective estimations or by the contents of a very small section of the GIT of the birds. Therefore, it seems more promising to determine the amount on the basis of exact pasture intake in indoor system.

The aim of the study was to estimate maximum possible intake of cutted pasture in different chicken genotypes with different growth rates in indoor system depending on the chicken age.

MATERIAL AND METHODS

The experiment was carried out in the experimental equipment of pavilion M of the Faculty of AgriSciences Mendel University in Brno. The experiment included 150 day-old chickens of three genotypes; medium-growing JA 757 hybrid as a representative of the most fed alternative chickens, classic fast-growing broilers ROSS 308 and a slow-growing males of dual purpose hybrid ISA Dual.

The chickens were placed in 12 boxes, four boxes of each of the genotypes (12–13 chickens per box). Chickens were housed in room with controlled environmental conditions. Water in nipple drinkers was available ad libitum. Two different feeders were used in each box, one with diets and second one with cutted pasture. Both feeds were available for chickens *ad libitum*. The complete diets were fed

according to the recommendations for the individual hybrids in pellets. Composition of the diets and nutrients content are given in Table 1 and Table 2.

Table 1 Composition of the diets

Feed [%]	Starter	Grower	Finisher
Wheat	36.9	48.4	48.7
Maize	20.0	20.0	20.0
Soybean meal	29.4	15.9	12.6
Soybeans	5.0	4.0	4.0
Rapeseed meal	1.5	1.5	2.0
DDGS	0	2.5	4.0
Soybean oil	1.3	0	0
Calcium carbonate	1.3	1.0	0.9
Monocalcium phosphate	1.0	0.7	0.6
Fish meal	1.0	0	0
Animal fat	0.9	4.1	1.0
Lysine	0.4	0.6	0.4
Methionine	0.3	0.3	1.0
Natural rock salt	0.3	0.3	0.3

Pasture was weighted and supplied fresh daily in the morning and the rest was weighted in the evening (after 12 hours). The experiment was stopped when daily pasture intake had no increased any more. Pasture came from a park-like lawn with a rich presence of legumes (60% of the legumes -*Trifolium repens* L., *Lotus corniculatus* L., *Medicago lupulina* L., 30% grasses - *Lolium perenne* L., *Poa pratensis* L., *Festuca pratensis* Huds., *Festuca rubra* L., 10% herbs - *Ajuga reptans* L., *Plantago major* L., *Bellis perennis* L.) from the Mendel University Arboretum in Brno. Lawn was harvested at a height of approximately 10 cm by a rotary drum garden mower with a collecting bin. Pasture was cut to a length of ± 1 cm. Content of nutrients was as follow; 29.4% of CP and 16.7% of crude fibre. Starter was fed before grower. ISA Dual fed grower diet from 35 days of age, followed by finisher from age 70 days. Genotype JA 757 fed grower from day 23 of chickens' age and finisher was fed from 50 days of age.

Table 2 Content of nutrients in the diets

Content nutrients [g/kg]	Starter	Grower	Finisher
Crude protein	228.0	180.0	171.7
ME_N [MJ]	11.98	12.89	13.13
Fat	55.0	72.2	80.7
Fiber	35.8	34.9	36.2
Lysine	13.70	11.10	9.51
Methionine	6.10	5.20	4.33
Ca	8.3	6.4	6.0
Na	1.7	1.6	1.6
P	6.58	5.20	5.00

ROSS 308 fed grower from 10 days of age and finisher from 25 days of age. Habitual period for cutted pasture intake was from 10 days of chicken age to third week of age, when pasture intake was estimated on daily basis for each box. Statistical analysis was performed using the UNISTAT 5.1 (Unistat Ltd., England), Scheffe test was used for estimation effect of age and genotypes on cutted pasture intake.

RESULTS AND DISCUSSION

Average daily cutted pasture intake increased for all hybrids as a function of age (Table 3).

Table 3 Average daily cutted pasture intake per chicken depending on age

Weeks of age	Average daily fodder consumption per chicken [g]		
	ROSS 308	JA 757	ISA Dual
3rd	6.21[a]	7.61[a]	---
4th	9.37[b]	8.14[a]	---
5th	10.53[bc]	9.07[ab]	10.34[a]
6th	12.08[cd]	9.22[ab]	12.66[ab]
7th	13.13[d]	11.25[b]	14.57[ab]
8th	---	13.98[c]	15.63[abc]
9th	---	16.11[c]	18.19[abc]
10th	---	---	18.74[abc]
11th	---	---	19.41[abc]
12th	---	---	21.00[bc]
13th	---	---	25.84[c]
Average*	**9.99[a]**	**10.16[a]**	**16.61[b]**
SE	0.297	0.284	0.393
Sum	**359.2**	**527.7**	**1094.7**

Legend: SE– standard error; a, b, c– means of the same order designated by different letters are significantly different between hybrids (P<0.05); a, b, c, d– means of the same order designated by different letters are significantly different between weeks of age for hybrid (P<0.05).*

Pasture intake significantly increased in ROSS 308 till seventh week of age ($P < 0.05$), with maximum daily consumption 13.13 g/chicken. Experiment for this hybrid in this age was also stopped because of live weight of chickens. There is no interest in too heavy chickens in the market.

Maximum pasture intake in JA 757 was observed in week nine (16.11 g/chicken), however the intake did not significantly increased from eight week of age. In ISA Dual fattening period was prolonged and the maximum cutted pasture intake was observed at 13th week of age, 25.84 g/chicken. Calculating average daily pasture intake during fattening period, significantly highest consumption was observed in ISA Dual in comparison with ROSS 308 and JA 757 ($P < 0.05$). These data can be taken in consideration at balancing diets for different genotypes in free range system. Almeida et al. (2012) reported average daily intake of pasture 5g in female and 8g in male of slow growing chickens genotype (Bresse gauloise breed) from 80th to the 113th days and 9g in female and 20 g in male in the medium-growing genotype chickens (hybrid Kosmos 8 Red). Lorenz et al. (2013) estimated that pasture consumption represents from 10 to 15% of the total feed intake in broilers. Ponte et al. (2008) indicated for fast-growing broilers the intake of pasture from 2.5 to 4.5% of the total amount of feed consumption, which is 10–18g of pasture at the end of fattening. These results confirmed our expectations as well as recommendations of Skřivan and Englmaierová (2015) that for pasture intake slow-to-medium-growing hybrids are the most suitable.

CONCLUSION

The maximum average daily intake of cutted pasture was the highest ($P < 0.05$) for ISA Dual hybrid at the age 13 weeks 25.8 g/day, whereas for the JA 757 hybrid, this intake was 16.1 g/day at age 9 weeks. ROSS 308 had the highest pasture intake 13.1 g/day at the age 7 weeks. It seems, that cutted pasture is the most suitable for slow-to-medium-growing chickens in alternative systems of poultry meat production.

ACKNOWLEDGEMENT

The research was financially supported by grand no. AF-IGA-IP 2017/003.

REFERENCES

Almeida, G.F. et al. 2012. Feed intake and activity level of two broiler genotypes foraging different types of vegetation in the finishing period. Poultry Science, 91(9): 2105–13.

Antell, S., Ciszuk, P. 2006. Forage consumption of laying hens - The crop content as an indicator of feed intake and AME content of ingested forage. Archiv für Geflügelkunde, 70: 154–160.

Dal Bosco, A. et al. 2012. Fatty acid composition of meat and astimated indices of lipid metabolism in different poultry genotypes reared under organic system. Poultry Science, 91(8): 2039–2045.

Dal Bosco, A. et al. 2014. Effect of range enrichment on performance, behavior and forage intake of free-range chickens. The Journal of Applied Poultry Research, 23(2): 137–145.

Fölsch, D.W. et al. 1999. Artgemäße Hühnerhaltung-Grundlagen und Beispiele aus der Praxis. Unveränderte Auflage, Stiftung Ökologie und Landbau, Bad Dürkheim, 4: 59.

Hörning, B. et al. 2004. Auslaufhaltung von Legehennen. KTBL Arbeitspapier, no. 279, KTBL, Darmstadt. pp. 67.

Horsted, K. et al. 2007a. Botanical composition of herbage intake of free-range laying hens determined by microhistological analysis of faeces. Archiv für Geflügelkunde, 71: 145–151.

Horsted, K. et al. 2007b. Crop content in nutrient-restricted versus non-restricted organic laying hens with access to different forage vegetations. British Poultry Science, 48(2): 177–84.

Jondreville, C. et al. 2010. Organic chemical contaminants in hens egg: regulatory context, modes and risk of transfer. INRA Productions Animals, 23(2): 205–213.

Lorenz, C. et al. 2013: Method to estimate feed intake from pasture in broilers and laying hens. Archiv für Geflügelkunde, 77(3): 160–165.

Petherick, J.C., Duncan, I.J.H. 1989. Behaviour of young domestic fowl directed towards different substrates. British Poultry Science, 30: 229–238.

Ponte, P.L.P. et al. 2008. Pasture intake improves the performance and meat sensory attributes of free-range broilers. Poultry Science, 87: 71–79.

Skřivan, M., Englmaierová, M. 2015. Metodika: Chov slepic na pastvě zvyšuje obsah vitamínu a karotenoidů ve vejcích. Praha Uhříněves: VÚŽV v.v.i.

Tong, H.B. et al. 2014. Effect of free-range days on a local chicken breed: growth performance, carcass yield, meat quality, and lymphoid organ index. Poultry Science, 93(8): 1883–9.

Trei, G. et al. 2013. Auslaufnutzung von Legehennen und Nahrungsangebot im Grünauslauf bei mobiler Haltung im Sommerhalbjahr. 12. Wissenschaftstagung Ökologischer Landbau. Bonn, Deutschland, 5–8 März. Berlin: Verlag Dr. Köster, pp. 630–633.

Comparison of nutrient composition of sorghum varieties depending on different soil types

Daria Baholet, Katerina Mrvova, Pavel Horky, Leos Pavlata
Department of Animal Nutrition and Forage Production
Mendel University in Brno
Zemedelska 1, 613 00 Brno
CZECH REPUBLIC

dariabaholet@gmail.com

Abstract: The aim of this study was made to compare the nutrient composition of 7 selected varieties of sorghum. The comparison was done two different localities, with different soil types (clay loam soil – fluvial soil and light sandy soil) in the region of South Moravia. The sampling of sorghum varieties were at two different locations and was realized 12 weeks after sowing, followed by analysis of nutrient composition as dry matter, N-substances, fibre, ADF - Acid Detergent Fibre and NDF – Neutral Detergent Fibre. Based on the data found it was concluded that it depends more on sorghum variety and its form than on the soil type.

Key Words: sorghum, silage sorghum, nutrition, C4-plants, chemical composition

INTRODUCTION

Origins of wild predecessors of *Sorghum bicolor* (L.) Moench extend to year 8000 BC in African countries such as Sudan and Ethiopia, but later it spread further to the world and it is heavily used as a multifunctional crop nowadays (Gamar et al. 2018, Venkateswaran et al. 2018). Main producers are U.S.A., Nigeria and India, with world annual production of almost 64 million tonnes (Tayyib et al. 2016). It is known for its high drought resistance, with capacity to extract soil water from up to 114 cm from the plant's position (Nielsen et al. 2018).

Primarily is sorghum used as a cereal in human diet comparable to other grains. Nutritional value is high due to 4.4–21.1% protein, 2.1–7.6% fat, 1.0–3.4% crude fibre, 57.0–80.6% total carbohydrates, 55.6–75.2% starch, 1.3–3.3% total ash, total minerals 179–1360 mg per 100 g and unique phytochemicals (Ratnavathi 2019). Some authors compare its feeding value to corn, it has potential to be used in forage and silage for ruminants or added into dry food formulations for pets (Alvarenga et al. 2018, Ronda et al. 2018, Vermerris et al. 2013).

Other uses of this C4 crop include fibre and biofuel crop with growth period of only 3–5 months (Barcelos et al. 2016, Sathya et al. 2016). However the ethanol yield per hectare of sorghum is estimated to 13 600 l (Barcelos et al. 2016). Sorghum is also being tested for its phytoremediation use thanks to its ability to absorb heavy metals from soil, unfortunately insufficiently in field conditions (Sathya et al. 2016, Soudek et al. 2014).

The aim of this study was compare the nutrient composition of selected varieties of sorghum at two different locations, resp. different soil types in South Moravia region.

MATERIAL AND METHODS

Characteristic of field experimental station in Žabčice

The field experiment was realised in Žabčice, GPS location Obora (49°011596.7N 16°602572.2E), and Písky (49°0041.8N 16°3609.3E). 179 meter above sea level, located in maize production area of the region of South Moravian. This territory belongs among the warmest regions in the Czech Republic. The drought is increased by the winds that cause a large evaporation of soil moisture.

There were two locations where the sorghum was sown. First location named Obora has clay loam soil and the soil type is fluvial soil. Obora has good availability of groundwater (Svratka River), which fluctuates 0.8–2.5 m below the soil surface during the year. The second location named Písky has light sandy soil and it is drier than the first. Part of the seeds was furnished by KWS Company and SEED SERVICE Company. The soil was prepared on the 24th April 2018 with harrows, than the first sowing was done on the 24th May 2018, in 3cm depth. Harvesting has taken place on the 21th August 2018, 12 weeks after sowing. Parcels size is 18.1 m².

Characteristic of selected varieties

Seven varieties were chosen: DSM 45-480, Sweet Susana, Buffalo Grain BMR, Big Kahuna BMR, Nutri Honey BMR, Nutri Honey and KWS Freya.

Sampling of sorghums varieties (7 on Obora and the same 7 varieties on Písky location) was realized on the 28th July 2018 (12 weeks after sowing). From each variety was sampled about 2 kg of fresh matter, then the samples were chopped and processed.

Data has been processed by Microsoft Excel (USA) and Statistica version 12.0 (CZ). We used one-way analysis (ANOVA). To ensure evidential differences, Schaeffer's test was applied and $P < 0.05$ was regarded as statistically significant difference.

RESULTS AND DISCUSSION

The important indicator of sorghum quality by silage preparation is dry matter, which should be between 28% and 35% in silage harvest period. From Table 1 can be seen that dry matter values of sorghums are very different – they range from 17% to 29%. Big Kahuna BMR has lower dry matter value; conversely the highest value was apparent in DSM 45-480 variety on both locations and variety KWS Freya at Obora location. Dry matter value correlated with earliness of varieties. From Table 1 is apparent that some varieties mature earlier than others.

Přikryl et al. (2010) compared changes in nutritive value of sorghum depending on the date of sampling. He decided the optimal time for the preservation of sorghum was determined when the dry matter was about 16%. He said for the preservation of sorghum is necessary to choose a two-phase harvest with respect to the low content of dry matter. By intensive withering is necessary to adjust the dry matter content to at least 28%. So he decided to choose phase with low dry matter, and his experiment was based on other parameters, especially N-substances. At this time was N-substances value 17.1% which is optimal.

Rajčáková (2005) compared sorghum at four different locations in south Slovakia. She determined N-substances in range 13.1–18.6% also in optimum values.

N-substances are the highest quality indicator of sorghum. Range of N-substances contain in sorghum is from 13% to 18% (Doležal 2014). The results in table 1 show that N-substances are relatively low, especially at Obora locations, even though urea fertilization. Second habitat Písky, which should be less productive, was not fertilized by nitrogen and had highest contain of N-substances. This may correspond with the fact that the soil is well supplied by nitrogen. However, low values do not mean problem, because we can increase N-substances in crop by higher fertilization.

Another important parameter is NDF. Professional literature states that if the NDF content is too high, it cause increase of feed volume and reduce the potential intake of dry matter by animals. The range of NDF values by Rajčáková (2005) was from 54% to 55.2%. In our research were the values of this parameter from 41.72% to 54.12%, this is very large dispersion which related to the content of fibre. These results demonstrate large divergence among selected varieties. Differences between habitats are not too high, but it depends on variety.

The dry matter is more or less the same on both location, the more fertile Obora and less fertile Písky, it depends mainly on the variety of sorghum. Only N-substances and ash are heavily influenced by habitat conditions, but these parameters can be affected mainly by fertilization.

Table 1 Nutritional characteristics of different sorghum varieties collected on 21th august 2018

1.	DSM 45-480	Dry matter	N-compounds	Fat	Fibre	ADF	NDF
Obora		29	8.50	2.61	19.48	22.17	41.72
Písky		29	8.38	2.58	29.66	32.08	54.04
2.	Sweet Susana	Dry matter	N-compounds	Fat	Fibre	ADF	NDF
Obora		27	8.08	2.03	28.66	37.54	54.58
Písky		27	12.62	2.53	22.07	25.24	50.4
3.	Buffalo Grain BMR	Dry matter	N-compounds	Fat	Fibre	ADF	NDF
Obora		23	7.89	2.53	24.28	27.32	47.30
Písky		22	14.05	2.92	21.66	23.77	48.00
4.	Big Kahuna BMR	Dry matter	N-compounds	Fat	Fibre	ADF	NDF
Obora		19	9.10	2.66	25.58	29.26	48.06
Písky		17	14.2	2.72	23.28	24.64	47.05
5.	Nutri Honey BMR	Dry matter	N-compounds	Fat	Fibre	ADF	NDF
Obora		23	7.94	2.3	24.94	28.04	47.58
Písky		21	10.99	2.8	26.14	30.14	50.83
6.	Nutri Honey	Dry matter	N-compounds	Fat	Fibre	ADF	NDF
Obora		27	7.11	2.21	23.46	30.01	44.92
Písky		27	9.08	2.7	21.98	26.41	45.46
7.	KWS Freya	Dry matter	N-compounds	Fat	Fibre	ADF	NDF
Obora		29	6.59	2.06	30.51	34.73	54.12
Písky		26	10.02	2.12	25.86	29.05	49.63

Legend: ADF – Acid Detergent Fiber, NDF – Neutral Detergent Fiber

CONCLUSION

The results of this research testify that differences of selected nutrition parameters between comparing locations are not too high. And this is very interesting detection, because we can state that both locations are appropriate for sorghum growth – dried and less fertile Písky as well as more fertile Obora. The results show that dry conditions of South Moravia region are not problem for sorghum growing. In some cases can be desirable because of differences in specific parameters.

It cannot be state that the dry matter is demonstrably higher at one or at the other habitat; it depends mainly on the variety of sorghum. Only N-substances and ash are heavily influenced by habitat conditions, but these parameters can be affected mainly by fertilization.

But if we talk about differences between grain and non-grain forms of sorghum regardless of habitat, we can state that these divergent are very big. So the form of sorghum is also very important if we have to choose the ideal sorghum variety for animal nutrition.

ACKNOWLEDGEMENTS

The research was financially supported by the AF-IGA-2018-tym001: Comparison of the impact of climate change on photosynthesis C3 and C4 plants cycles which are used in livestock feed.

REFERENCES

Alvarenga, I.C. et al. 2018. Effects of milling sorghum into fractions on yield, nutrient composition, and their performance in extrusion of dog food. Journal of Cereal Science [Online], 82: 121–128. Available at: https://www.sciencedirect.com/science/article/pii/S0733521018301541. [2018-10-05].

Barcelos, C.A. et al. 2016. Sweet sorghum as a whole-crop feedstock for ethanol production. Biomass and Bioenergy [Online], 94: 46–56. Available at: http://iopscience.iop.org/article/10.1088/1755-1315/141/1/012032. [2018-10-15].

Doležal, P. 2014. Má čirok budoucnost jako energetická plodina – ano, nebo ne? Úroda [Online]. Available at: http://uroda.cz/ma-cirok-budoucnost-jako-energeticka-plodina-ano-nebo-ne. [2018-10-23].

Gamar, Y.A. et al. 2018. Analysis of genetic difference within and between of wild relatives of sorghum in sudan, using SSRs Pakistan Journal of Botany [Online], 50: 2231–2236. Available at: https://cgspace.cgiar.org/handle/10568/97589. [2018-10-15].

Nielsen, D.C. et al. 2018. Skip row planting configuration shifts grain sorghum water use under dry conditions. Field Crops Research [Online], 223: 66–74. Available at:

http://digitalcommons.unl.edu/cgi/viewcontent.cgi?article=1872. [2018-10-15].

Přikryl, J. et al. 2010: Nutriční hodnota jednosečných čiroků. Syninfo: měsíčník společnosti Syntegra. [Online]. Available at:
http://www3.syngenta.com/country/cz/cz/syngenta/kestazeni/syninfo/Documents/Syninfo-10-09-web.pdf. [2018-10-15].

Rajčáková, L. 2005. Pestovanie ciroku sudásnkeho v suchom postihovaných oblastiach. Krmivářství, 9(4): 36–37.

Ratnavathi, C.V. 2019. Grain Structure, Quality, and Nutrition. In Breeding Sorghum for Diverse End Uses. Duxford, United Kingdom: Woodhead Publishing, pp. 193–207.

Ronda, V. et al. 2019. Sorghum for Animal Feed, In Breeding Sorghum for Diverse End Uses. Woodhead Publishing, pp. 229–238. [Online]. Available at https://doi.org/10.1016/B978-0-08-101879-8.00014-0. [2018-10-25].

Sathya, A. et al. 2016. Cultivation of Sweet Sorghum on Heavy Metal-Contaminated Soils by Phytoremediation Approach for Production of bioethanol. In Bioremediation and Bio Economy. Elsevier, pp. 271–292. [Online]. Available at: https://doi.org/10.1016/B978-0-12-802830-8.00012. [2018-10-25].

Soudek, P. et al. 2014. Accumulation of heavy metals using Sorghum sp. Chemosphere 104: [Online], 15–24. Available at: https://doi.org/10.1016/j.chemosphere.2013.09.079. [2018-10-15].

Tayyib, S. et. al. 2016. URL Food and Agriculture Organization of the United Nations (FAO) [Online]. Available at: http://www.fao.org/faostat/en/?#data/QC/visualize. [2018-10-25].

Venkateswaran, K. et al. 2018. Domestication and Diffusion of Sorghum bicolor. In Breeding Sorghum for Diverse End Uses. Woodhead Publishing, pp. 15–31.

Comparison of the performance between the best jumping horses in Czech Republic and the world

Michaela Brudnakova, Eva Sobotkova
Department of Animal Breeding
Mendel University in Brno
Zemedelska 1, 613 00 Brno
Czech Republic

michaela.brudakova@mendelu.cz

Abstract: The article deals with the performance ratings of show jumping horses participating in competitions held in Czech Republic and also in the world, taking into consideration factors such as breed, sex, age and year of start. Data used in the research has been gathered from the official website of the Czech Equestrian Federation (CJF), covering years 2010 and 2016 and from The Federation Equestre Internationale (FEI) covering also the same years. Program STATISTICA 2012 was used and in the case that the factor was highly significant, the SCHEFFE´S test. The analysis of horse performance ratings shows that breed, age, sex and year of start have statistically high significant impact on performance in both years in Czech Republic. The best performance results in the Czech Republic has horses in the age category 13–16 years with 7.42 auxiliary points (AAP), the most successful sex is group of stallions with 7.44 AAP and breed with the highest amount of auxiliary points is Zangersheide with 7.73 AAP. In the world ratings the analysis shows that only the year of start has highly significant impact on the performance. Therefore, it is possible to claim that average values
of the performance of this particular breed have increased. In the analysis of the factor year of start there was statistically high significance that in the year 2016 are the better results in performance in Czech Republic and also in the world.

Key Words: show jumping, sports breeds of horses, performance, riding, factors, impact

INTRODUCTION

All great jumpers have two qualities. The first one is the physical ability to get their bodies up into the air. The second one is the mental combination of courage and a great desire to be careful-reluctant to touch, let alone wallop, a rail (Marks 2015). The duration of competitive life for warmblood horses has been found to be shorter in the jumping discipline compared to dressage (Ducro et al. 2009). The main aim of this research is to provide how important the impact of these factors is: breed, sex, age and the year of start on the performance in jumping competitions. We want to compare and find out some differences between the jumping horses in the Czech Republic and whole world.

MATERIAL AND METHODS

Data used in this article has been taken from the Survey of Sport Horses from the year 2010 and 2016 (www.cjf.cz) with the analysis of overall 1000 horses and also from the World Survey. Of Sport Horses from the year 2010 and 2016 (www.FEI.com) with the same number of horses. The performance has been evaluated according to the number of points from particular competitions within the given year (season). Formula for calculating of auxiliary points (AAP) is officially provided in accordance to CJF performance ratings (CJF 2018) and the FEI world performance rating (FEI 2018). The auxiliary points are a positive transformation of the penalty points obtained by the animal during the competition. Data related to individual years have been processed by the statistic program STATISTICA 2012 by means of descriptive characteristics and using the multi-factor Analysis of Variance (ANOVA). Influencing factors that have been analyzed were breed, age, sex and the year

of start. If a particular effect has been proved statistically, Scheffe's method has been used for comparison.

RESULTS AND DISCUSSION

In 2010, 3873 horses participated in show jumping disciplines, what made 83% of overall amount of horses participating in competitions in the Czech Republic. In 2016, it was 4136 horses competing in show jumping, 80% of overall amount of horses competing in the Czech Republic that year. Based on the above results, show jumping disciplines belong to the most popular ones with representation of significant number of riders and horses. One research finds out that the big influence on the competitive life of jumping horses have also their mood, temperament and emotional reaction (Mills 2012).

Table 1 Descriptive results of data in 2016 and 2010 in the Czech Republic

Descriptive statistics				
	Average	Median	Minimum	Maximum
2010	6.73	5.50	5.13	14.31
2016	7.42	6.65	5.50	16.89

Table 2 Descriptive results of data in 2016 and 2010 in FEI

Descriptive statistics				
	Average	Modus	Minimum	Maximum
2010	446.79	235	205	2110
2016	602.18	355	340	2095

Data from Table 1 and Table 2 provided that averages in the year 2016 are higher in Czech Republic and also in the world like data from the year 2010. Performance of horses is better and increases every year. Also minimum of the points is higher in every case but really great improvement can be seen in the world database in which is the difference between minimal auxiliary point (AAP) in year 2010 and between the year 2016 is 121 points. In Czech Republic it can be seen that maximum of the points is higher at the year 2016, but in the world evaluation we can see points decrease at the year 2016. Variation coefficient proved that the population of the horses in the Czech Republic and the world is more settled.

Table 3 Statistic analysis ANOVA in the Czech Republic and world

Factors	CJF	FEI
AGE	**	-
SEX	**	-
BREED	**	-
YEAR OF START	**	**

Legend: Significance: $P \leq 0.01$ (**) statistically highly significant, $P \leq 0.05$ (*) statistically significant

The analysis ANOVA provided that in the Czech Republic has each factor (age, sex, breed and the year of start) statistically higher significance, so we use Scheffes test on the each of these factors.

Unfortunately, the analysis ANOVA in the database from the world shows that only factor "the year of start" has a statistically higher significance, so in the rest of the factor the focus is just on the average values. The factor year of start has been analyzed also in the Scheffes test.

For the following tests was used Scheffe's test.

Factor age

In the factor age the Scheffes test shows that there are statistically highly significant differences between the categories with the youngest horses and horses in the ages between 7–12 years

and 13–16 The biggest number of auxiliary points has a group of horses in the age between 13–16 with AAP 7.42, following the group of horses between 6–12 years old with 7.18 AAP and the group of the oldest horses on the third place with 6.69 AAP. The lowest amount of points has a group of the youngest horses with 5.87 AAP. In the situation in the world reached the group of 6–12 years old horses the most auxiliary points 590.83, following the group of 13–16 years old horses with 540.45 AAP, the group of the oldest horses on the third place with 519.3. The group of the youngest horses is missing in the world database. Unfortunately, in case of the factor age and the world we were just working with average values because there was no statistically significance. Another research shows that the most successful horses are in the age group between 12–13 years of age and older horses have lower performance results (Maršálek et al. 2005).

Factor sex

In the Czech Republic there is the most successful sex the group of stallions with 7.44 AAP, which is statistically higher significant different from the group of geldings (7.06 AAP) and mares (6.89 AAP). Another research says that stallions reach the lower number of penalty points than geldings and mares. In the case of mares there is higher percentage of refusing jumps. This research considers that the factor sex has significant impact on performance of horses (Maršálek et al. 2005). In the situation in the world only average values have been analyzed and the biggest amount of the points has a group of mares with 529.03 AAP, stallions with 525.23 AAP and geldings on the third place with 521.60 AAP. But there are no big differences between each category. But another research says that in the dressage competitions stallions are preferred too, because of their temperament (Soušková 2018). In the Eventing more geldings are being used, because they are easier to control (Fikesová 2017).

Factor breed

From the perspective of show jumping performance, the most successful breeds in 2010 and 2016: Zangersheide with the highest performance rating (7.73 AAP), Westphalian horse (7.49 AAP) and the horses with unknown pedigree (7.64) on the third place. The breeds with the lowest amount of points are Slovak Warmblood in Czech Republic (6.56 AAP), English Thoroughbred (5.47 AAP) and the lowest amount of point have Other non-sporting breeds (5.41 AAP). Worldwide there was no statistical significance so the focus was only on the average values. In research (Popovici et al. 2015) was also no statistical significance in European sport breeds. These results are not surprising at all, because in case of all warmblood sport horses are used breeding schemes that share the same objectives even if the procedure for selection varies in different European countries. The most successful breed in the world is Zangersheide with 570.32, followed by Holsteiner horse with 565.93 AAP and the Other European sport breeds with 524.95. The lowest amount of the points in the database of the best 500 jumping horses in the world have horses with unknown pedigree (416.29 AAP). The CJF database and the worldwide database cannot be compared as they use different evaluation system.

Factor year of start

There is statistically high significance that the year 2016 is successful than year 2010. In the CR is the performance of horses better 0.68 AAP up in the year 2016 and in the world the progress can be seen of evaluation of horses about 155.23 AAP up.

CONCLUSION

The aim of this research was the analysis of data and particular factors which may influence the performance of jumping horses around the world. The most important factors such as age, sex, breed and the year of start have been chosen and the analysis has been provided on which horse category has the greatest extend. In the Czech Republic has been proved that the all of the factors have a statistically high significance and influence on the performance of horses. It has been proved that the most
successful breed was Zangersheide with 7.73 AAP in the case of the both years 2010 and 2016. From the perspective of the age, it has been statistically proved that horses aged 13–16 years were the most successful in a both of years with 7.42 AAP. Statistically proven the most successful sex

in both years are stallions with 7.44 AAP. In the comparison of the performances from the database of CJF from the years 2010 and 2016 there is statistically proven that the year 2016 with 7.41 average value of AAP is more successful than the year 2010 with 6.73 average value of AAP. In the world database we proved only the factor year of start like statistically high significant. Other factors have been proceeded only by using of average values. It is a database of the best jumping horses in the world, so there are no big differences among horses. The most successful breed in the world is also Zangersheide with 570.32 AAP. In average values the most successful age group is the category of 6–12 years old horses with 590.83 AAP. The sex group with the highest performance result are mares with 529.03 AAP. Unfortunately, CJF and FEI use different evaluation system, so particular results cannot be compared. Generally, it is possible to confirm that the sport performance in the region of research is overall increasing not only from the perspective of imported breeds but also from the perspective of the Czech Warmblood which has proven a visible increase in its performance. There is a same trend in the Czech Republic as worldwide there are increasing numbers of imported horses.

REFERENCES

CJF (Česká jezdecká federace). 2010. Přehled o sportovních koních CR. [Online]. Available at: http://www.cjf.cz/files/stranky/dokumenty/prehledy-o-sportovnich-konich/roc-2010-web.pdf. [2010-09-01].

CJF (Česká jezdecká federace). 2016. Přehled o sportovních koních CR. [Online]. Available at: http://www.cjf.cz/files/stranky/dokumenty/prehledy-o-sportovnich-konich/rocenka2016.pdf. [2010-09-01].

CJF (Česká jezdecká federace). 2018. Skoková pravidla. [Online]. Available at: http://www.cjf.cz/files/stranky/dokumenty/pravidla/2018/Skoky/2018_pravidla_skokova_0403.pdf. [2010-09-01].

Ducro, B. et. al. 2009. Influence of foot conformation on duration of competitive life in a Dutch Warmblood horse population. Equine Veterinary Journal, 41(41): 144–148.

Evans, M. 2013. The psychology of performance horses. Canadian Horse Journal [Online], 1(1): 2–3. Available at: https://www.horsejournals.com/riding-training/english/hunter-jumper/psychology-performance-horses. [2010-09-01].

FEI (Federation Equestre Internationale). 2018. Jumping rules. [Online]. Available at: https://inside.fei.org/sites/default/files/JumpRules_26thEd_2018_clean_0.pdf. [2010-09-01].

FEI (Federation Equestre Internationale). 2010. Rankings/ Standing research. [Online]. Available at: https://data.fei.org/Ranking/Search.aspx?rankingCode=S_WR. [2010-09-01].

FEI (Federation Equestre Internationale). 2016. Rankings/ Standing research. [Online]. Available at: https://data.fei.org/Ranking/Search.aspx?rankingCode=S_WR. [2010-09-01].

FEI (Federation Equestre Internationale). 2018. Rules and point system Federation Equestre Internationale. [Online]. Available at: https://inside.fei.org/fei/events/fei-nations-cup-series/jumping/points-rules. [2010-09-01].

Fikesová, V. 2017. Analysis of breeding and performance of horses in the Czech Republic based on eventing competitions. Diploma thesis, Mendel University in Brno.

Marks, D. 2015. How your horse jumps: Understanding your horse's jumping mechanics can make you a better rider and trainer-and help him stay sounder. Practical Horseman [Online], 12(12): 1–4. Available at: https://practicalhorsemanmag.com/health-archive/horse-jumps-30014. [2010-09-01].

Maršálek, M. et. al. 2005. The influence of the age, sex and performance level of horses on their success in the show jumping competition. Journal of Central European Agriculture, 6(4): 547–553.

Popovici, A. et. al. 2015. Competition jumping horses: effects of age, sex and breed on the FEI, WBFSH world ranking. Bulletin UASVM Animal Science and Biotechnologies, 72(1): 22–28.

Soušková, K. 2018. Analýza výkonnosti koní v Českej republike z hľadiska drezúrnych súťaží. Diploma thesis, Mendel University in Brno.

Evaluating the descendants of stallions from the Cor de la Bryère line in Czech Warmblood breeding

Zuzana Kubikova, Iva Jiskrova, Barbora Kubistova
Department of Animal Breeding
Mendel University in Brno
Zemedelska 1, 613 00 Brno
CZECH REPUBLIC

x.kubiko6@mendelu.cz

Abstract: The main aim of this study was to evaluate the influence of the stallion Cor de la Bryère's line in Czech Warmblood breeding. The significance of this breeding line was evaluated by performing a comparison of the body measurements of descendants by the most important stallions permitted to act as stud horses within Czech Warmblood breeding. The specific observed attributes for evaluating the quality of the stallions were the values of descendants' basic body measurements, i.e. stick height at withers, tape height at withers, chest circumference and cannon bone circumference. A total of seven breeding stallions were compared, three of which were Holsteiners, three Hanoverians and one a Czech Warmblood. The comparison group consisted of 347 descendants of the Czech Warmblood breed by the sires Calanthano, Carlos, Carol, Cartouche, Catango Z, Comero and Chazar. A high statistically conclusive influence of the sire was only established for cannon bone circumference. With the other body measurements, the influence of the sire was not proven. When evaluating individual years according to cannon bone circumference, the best group was judged to be descendants born in the year 1994. Furthermore, it was determined that on average both sexes of the descendants of this line meet the breed standard for the Czech Warmblood in terms of cannon bone circumference. Another factor evaluated was stick height at withers, which, like cannon bone circumference, is subject to the breed standard for the Czech Warmblood. In this case it was not possible to statistically demonstrate the effect of the observed factors. In view of the importance of this body measurement, the maximum, minimum and average values were evaluated, and on this basis it can be said that for stallions from the Cor de la Bryère line, breeders should select mares with a smaller body frame but a thick cannon bone.

Key Words: stallion, offspring, Czech Warmblood, Holsteiner, Hanoverian

INTRODUCTION

History of the stallion Cor de la Bryère

Cor de la Bryère was the son of the Thoroughbred stallion Rantzau, who played an active role in French sport horse breeding. Rantzau was the leading stud horse for dressage, showjumping and event horses in France between 1971 and 1973. His bloodline produced countless outstanding sport and stud horses (Muller 2018).

Štěrba (2018) writes that in 1971 it was necessary to find a stud horse for Holsteiner breeding that would positively influence the jumping technique and rideability of his offspring, as these had been adversely affected by the massive use of the Thoroughbred. At that time the French stud was enjoying great successes, and so the board of the Holsteiner stud decided to lease a stallion of French breeding and thereby discovered the three-year-old stallion - rather immature but exuding quality - by the Thoroughbred Rantzau out of Quenotte by Lurioso. The French were not keen on him, did not include him in the breeding programme and advised his breeder to have him gelded.

The main asset Cor de la Bryère brought to sport horse breeding was an unprecedented jumping style and action of the front legs. Each year he produced first-class horses for all equestrian disciplines. Some of the greatest include Contrast, followed by Corlandus (silver medal in dressage at the 1988 Olympic Games) and numerous showjumping champions such as Caletto I, Colando I, Corrado I, Cheyenne, Cera, Cordalmé Z, Cor d´Almé Z, Corland, Cash and many more.

His grandchildren have also been very successful, such as the Olympic champion Classic Touch, the world champion Fein Cera, Coriano, Calvaro Z, Careful, Operette la Silla, Cayon, Cabrio and Clinton (Muller 2018).

Verband der Züchter des Holsteiner Pferdes (2016) writes that Cor de la Bryère became another pillar of Holsteiner breeding after the stud horse Langraf. Along with the line of Ladykiller XX, the "Corde" line has therefore been one of the strongest lines in establishing modern sport horse breeding.

According to Kirsan (2017), at the time of Cor de la Bryère's transfer to Holstein, including the Selle Français breed in Thoroughbred breeding was quite unprecedented. The Selle Français breed as a whole was not viewed positively at that time – not even in its homeland, much less abroad. However, this opinion was transformed by the legendary stallion Cor de la Bryère.

The "Corde" line has also had an influence on Czech Warmblood breeding, where according to Dušek et al. (2011) the relatively short period of improvement and the number of breeds used has affected the variability of the conformation. Consequently, breeders' efforts are now directed towards the greatest possible homogenization of conformation and consolidation of the breed.

MATERIAL AND METHODS

The underlying database was created on the basis of data obtained from the website of the Association of Czech Warmblood Breeders. Seven stud horses from the Cor de la Bryère line were selected and the relevant data on the stud horses and their offspring were collected. The database contains a total of 347 descendants, and the following data were recorded for each of them: name, year of birth, body measurements stick height at withers (SWH), tape height at withers (TWH), chest circumference (ChC) and cannon bone circumference (CBC) and information about the sire.

Table 1 Distribution of descendants into groups according to the year of birth

Number	Year of birth
1	1994
2	1995
3	1996
4	1997
5	1999
6	2000
7	2001
8	2002
9	2003
10	2004
11	2005
12	2006
13	2007
14	2008
15	2009
16	2010
17	2011
18	2012
19	Other

Table 2 Distribution of stud horses into groups

Number	Stallion
1	2772 Calanthano
2	2800 Carlos
3	410 Carol
4	2726 Cartouche
5	814 Catango Z
6	411 Comero

Table 3 Distribution of horses into groups by sex

Number	Sex
1	Mare
2	Stallion
3	Gelding

Model equation:

$y_{ijk} = \mu + p_i + q_j + r_k + e_{ijk}$

where:

y_{ijk} is the observed effect (KVP, KVH, OH, Ohol)

μ is the total average of the set

p_i is the fixed effect of the i-th group of sires ($i = 1,\ldots, 7$)

q_j is the fixed effect of the j-th year of birth ($j = 1,\ldots, 22$)

r_k is the fixed effect of the k-th sex ($k = 1,2,3$)

e_{ijk} is the random effect

Based on the results from the general linear model, the differences between values were established by subsequent testing according to Tukey-B. The test was conducted at a significance level of $P \leq 0.05$.

The database of descendants was created in the programme Microsoft Office Excel 2010. The data acquired were then statistically processed using a GLM linear model in the statistical programme UNISTAT 6.5. The underlying database for evaluating the general linear model contains seven stud horses and their 347 descendants. Each stud horse was assigned an internal identification number from 1 to 7 solely for our purposes. The influence of the sire, year of birth and sex on the values of the basic body measurements was observed. The descendants' years of birth were also given a number, with item number 19 (other) encapsulating descendants born in the years 1993, 1998, 2013 and 2016, which had to be amalgamated because of their low numbers. Likewise, it was necessary to number sex distribution, this time from 1 to 3.

RESULTS AND DISCUSSION

Evaluation by the GLM model revealed statistical conclusiveness of the observed influences for only one basic body measurement – cannon bone circumference. This confirmed that the transfer of sires' phenotypic traits to offspring exhibits a degree of heritability, but according to these results it is primarily bone mass.

The influence of the year of birth emerged as statistically inconclusive for the attributes SWH, TWH and ChC. In the case of CBC, however, this influence exhibited high statistical conclusiveness. This result can be explained by the fact that in one of the years more descendants with an above-average cannon bone circumference were born.

Cannon bone circumference is an important breed attribute subject to the standards for the Czech Warmblood. That is why the values of this measurement are extremely important, since

they indicate the strength of the skeleton, which is highly desirable. Especially at present, it is essential that stud horses with the ability to pass on a strong skeleton to their descendants are included in breeding, because the influence of a large variety of different breeds in Czech Warmblood breeding has resulted in it becoming lighter, which is highly undesirable for breeding.

The evaluation of sex within CBC again revealed a highly statistically conclusive influence. It can therefore be stated that the importance of monitoring this attribute was confirmed and statistically proven. The breed standard for Czech Warmblood breeding gives the threshold for cannon bone circumference as 19.5−22 for mares and 21−22.5 for stallions.

Table 4 Comparison of results of the stud horses according to CBC of descendants by Tukey-B testing

Stud horse	No. of descendants	Average CBC
2772 Calanthano	31	20.35
2667 Chazar	9	20.48
410 Carol	91	20.57
411 Comero	59	20.77
814 Catango Z	118	20.78
2726 Cartouche	36	20.96
2800 Carlos	3	21.17

This table shows that the highest average values for the cannon bone circumference measurement are achieved by descendants of the stud horse 2800 Carlos. Although this group of descendants contains only three mares, all of them achieve the upper threshold of the breed standard. According to Hanušová (2002), the stud horse 2800 Carlos is the great-grandson of the excellent stallion Calypso II, one of the most important sons of the founder of the line. As far as the other groups of descendants are concerned, it is positive that on average all of them achieve values of 20.3 and above. However, each stud horse has mares among its offspring which do not achieve even the lower threshold of the standard for cannon bone circumference. Mares with a lighter skeleton of this type are not beneficial for further breeding.

Table 5 Results of multiple comparison according to Tukey-B for individual years

Year	No. of descendants	Group average	1997
1997	9	19.96 cm	
1995	7	20.03 cm	
Other	8	20.13 cm	
1999	13	20.22 cm	
2009	14	20.46 cm	
1996	7	20.50 cm	
2005	39	20.61 cm	
2003	33	20.62 cm	
2002	34	20.69 cm	
2010	13	20.74 cm	
2006	32	20.75 cm	
2001	16	20.76 cm	
2011	8	20.79 cm	
2000	11	20.82 cm	
2007	17	20.85 cm	
2008	43	20.91 cm	
2004	27	20.95 cm	
2012	11	21.07 cm	
1994	5	21.82 cm	**

*The results marked by **are statistically significant on P<0.05.*

Based on the results obtained by multiple comparison according to the Tukey-B method, it can be said that a statistically highly conclusively greater cannon bone circumference is achieved by descendants born in 1994 compared with the year 1997.

Upon closer examination of the initial database, it can be said that descendants from the year 1997 were considerably influenced by dams. It was found that in five out of nine cases the dams were registered in the stud book for the English Thoroughbred. In contrast, in the year 1994 two descendants had pedigrees which were entirely free of the English Thoroughbred to the fifth generation; in another two cases the Thoroughbred did not appear in the pedigree until the fourth and fifth generation, and only one descendant had a Thoroughbred dam. This finding confirms the fact that the influence of the English Thoroughbred in lightening the skeleton of the Czech Warmblood is very marked. Štencl (1977) stated in his publication that the imprudent choice of an unsuitable stud horse results in undesirable traits being introduced into the breeding of half-breds, particularly lightening of the skeleton.

It is therefore obvious that this has been an issue in breeding for more than 40 years. For this reason, breeders should be careful in the selection of mating pairs and should not include mares that do not even fulfil the minimum values of the breed standard in Czech Warmblood breeding.

Table 6 Comparison of the results of sex according to CBC by Tukey-B method

Sex	Number	Average CBC	Mares
Mares	322	20.64 cm	
Stallions	14	21.25 cm	**
Geldings	11	21.64 cm	**

*The results marked by **are statistically significant on P<0.05.*

This table shows that stallions and geldings have a statistically highly conclusively greater cannon bone circumference than mares. This result can be considered very positive, since stallions and geldings should have a stronger skeleton than mares through the influence of sexual dimorphism. Bílek et al. (1957) claim that horses for breeding should have clearly expressed dimorphic traits, because horses with poorly expressed sexual dimorphism do not generally produce good results in breeding.

The average values of all the groups thus meet the breed standard for the Czech Warmblood. What is clearly disadvantageous for breeding, however, is the fact that stallions have a smaller cannon bone circumference in the group average than geldings, which cannot be used for subsequent breeding.

Table 7 Comparison of the results of maximum, minimum and average values of SWH between sexes

Sex	Maximum	Minimum	Group average
Mares	186 cm	158 cm	173.47 cm
Stallions	186 cm	153 cm	174.29 cm

The statistical evaluation of stick height at withers failed to demonstrate statistical conclusiveness of the influence of the sire, year of birth or sex. However, it is possible to determine the minimum, maximum and average values and then compare these with the breed standard. For mares this is in the range 161−167 cm and for stallions 162−170 cm. According to the table, it can be stated that the maximum for both mares and stallions greatly exceeds the standard, while the mimimum falls significantly below it. Even the average values of both sex groups exceed the breed standard, by 6.47 cm for mares and 4.29 cm for stallions. This finding suggests that for stallions from the Cor de la Bryère line, breeders should select mares with a smaller body frame but a thick cannon bone. This is confirmed by the Association of Czech Warmblood Breeders (2016), which in its yearbook places emphasis on the conformation of the modern Czech Warmblood horse, which can only be achieved by the careful selection of horses for breeding.

CONCLUSIONS

A highly statistically conclusive influence of the sire was established only with cannon bone circumference. With the other body measurements, the influence of the sire was not proven. When evaluating the individual years, it was found that the best group according to cannon bone circumference consisted of descendants born in 1994. Furthermore, it was established that on average both sexes of descendants from this line meet the breed standard for the Czech Warmblood in terms of cannon bone circumference, which is considered very positive. Another factor which it was necessary to evaluate was stick height at withers, which like cannon bone circumference is subject to the breed standard for the Czech Warmblood. In this case it was not possible to statistically prove the influence of sires, year of birth or sex. Due to the importance of this body measurement, evaluation of the maximum, minimum and average values was at least performed. According to the values obtained, it can be said that for stallions from the Cor de la Bryère line, breeders should select mares with a smaller body frame but a thick cannon bone, since the breed standard was greatly exceeded in the average values for both stallions and mares. It should be noted that all the stallions from the evaluated line are beneficial for Czech Warmblood breeding. Because of this, breeders should continue to include descendants of this line in breeding, thereby anchoring the traits passed on by the founder of the line.

ACKNOWLEDGEMENTS

This work was funded by the Internal Grant Agency at the Mendel University in Brno, Faculty of AgriSciences, under Grant TP 7/2017: Analysis of performance and behaviour of farm animals in relation to ambient temperature variability and possibilities of elimination of its impact.

REFERENCES

Bílek, F. et al. 1957. Speciální zootechnika chov koní II. díl. 1.vyd., Praha: Státní zemědělské nakladatelství.

Dušek, J. et al. 2011. Chov koní. 3. vyd., Praha: Nakladatelství Brázda.

Hanušová, K. 2002. Vybrané linie chovu německého teplokrevníka – Cor de la Bryere. Jezdectví, 50(9): 31–32

Kirsan, K. 2017. Cor de la Bryere Corde - a classic Improvement Sire. Sport Horse Breeder. [Online]. Available at: https://www.sport-horse-breeder.com/cor-de-la-bryere.html. [2018-06-20].

Müller, J. 2018. Corrado II. Equinní reprodukční centrum Pardubice-Mnětice. [Online]. Available at: http://www.muller-equine.cz/reprodukce-koni-1/galerie-hrebcu/corrado-ii.htm. [2018-06-20].

SCHČT, 2016. Ročenka 2016 [online]. 1. vyd., Písek: AP tiskárna. Available at: http://www.schct.cz/cz/uvod/rocenky-schct/rocenka-2016.html. [vid. 2018-07-10].

Štencl, F. et al. 1977. Vývoj chovu koní u nás II. Díl. 1. vyd., Pardubice: Ústav veterinární osvěty.

Štěrba, V. 2018. Nejznámější světové linie v původech sportovních koní – Cor de la Bryére. Česká společnost hipologická. [Online]. Available at: http://www.cshipo.estranky.cz/clanky/pro-zacinajici-chovatele/chov-a-slechteni-koni/nejznamejsi-svetove-linie-v-puvodech-sportovnich-koni---cor-de-la-bryere.html. [2018-06-20].

Verband der Züchter des Holsteiner Pferdes. ©2016. Ein zuchtkonzept setzt sich durch. Holsteiner Verband. [Online]. Available at: https://www.holsteiner-verband.de/der-verband/holsteiner-pferde/zuchtkonzept. [2018-06-20].

Pregnancy duration in mares

Martina Malinska, Eva Koru, Petr Rezac
Department of Animal Morphology, Physiology and Genetics
Mendel University in Brno
Zemedelska 1, 613 00 Brno
CZECH REPUBLIC

martina.malinska@seznam.cz

Abstract: Accurate prediction of pregnancy duration is an important aspect in managing mares' reproduction. Pregnancy duration was affected by the month of mating ($P < 0.01$) and the year of conception ($P < 0.01$). The age of mares at the time of mating did not influence pregnancy duration. Similarly, stillborn foals did not significantly affect pregnancy duration. In conclusion, pregnancy duration was influenced by the month of mating and the year of conception. The knowledge of these factors is very important for the most accurate determination of parturition date.

Key Words: mare, reproduction, foal, season

INTRODUCTION

In horse reproduction, there is still a wide range of unanswered questions about pregnancy and timing of birth (Cilek 2009). This research area is very important, for example, for sport horse breeders whose aim is often to get foaling at the beginning of the year because of a greater maturity of foals compared to those born later. Simultaneously, more accurate prediction of birth date is very important for the preparation of the mare on parturition and early detection of any problems during or after parturition (Rezac et al. 2013). The physiological duration of pregnancy is relatively broad, ranging from 320 to 365 days, and is affected by several different factors.

Pregnancy duration is affected by environmental, fetal and maternal factors (Satué et al. 2011). The key environmental factors are the breeding season, photoperiod, and treatment with artificial light. Within the fetal factors, the sex of the foal is cited. The most important maternal factors are age, breed, and number of births.

The objective of the study was to examine the variability of pregnancy duration in mares. Simultaneously, the influence of the year, month of mating, age of mare and occurrence of stillborn foals on pregnancy duration were assessed.

MATERIAL AND METHODS

Animal characteristics

The assessment of pregnancy duration in mares was carried out on a total of 86 Old Kladruber mares. Mares had an average age of 9 years, ranging from 4 to 18 years. A total of 190 completed pregnancies were evaluated. Pregnancy duration was determined as the interval from the date of the last mating to the date of delivery. Both primiparous and multiparous mares were included in the experiment. The number of foalings ranged from 1 to 7. Three months before delivery, mares were fed 12 kg hay/day, 1.5 kg oats/day and 0.5 kg barley/day.

Statistical analysis

Statistical analysis was conducted using SAS (SAS Institute Inc., Cary, NC, USA). The normality of distribution of pregnancy duration in mares was verified using the Kolmogorov-Smirnov test. The effects on pregnancy duration in mares were analyzed by the mixed model procedure.

RESULTS AND DISCUSSION

The effect of the year of mating on pregnancy duration in mares is shown in Figure 1. Pregnancy duration in mares mated in 2015 was shorter than other years ($P < 0.05$). The influence of the month of

mating on pregnancy duration in mares is shown in Figure 2. Pregnancy was longest in mares mated in March, thereafter pregnancy gradually shortened, and the shortest pregnancy was in mares mated in July ($P < 0.01$). The age of mares at the time of mating (Figure 3) and the occurrence of stillborn foals (Figure 4) did not significantly affect pregnancy duration.

Figure 1 Mean pregnancy duration ± SEM in mares mated in different years

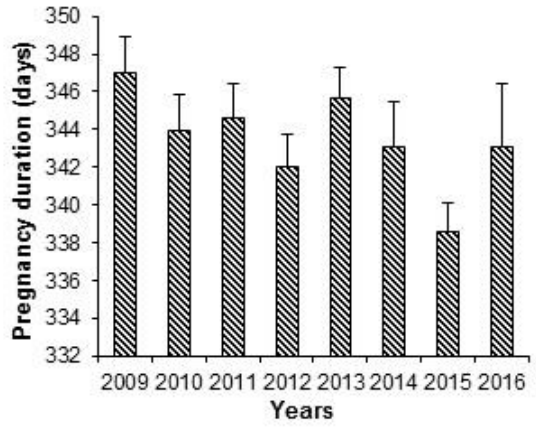

Figure 2 Mean pregnancy duration ± SEM in mares mated in different months

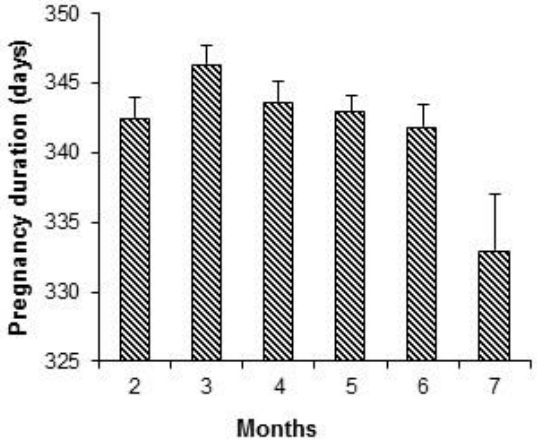

Figure 3 Mean pregnancy duration ± SEM in mares of different ages

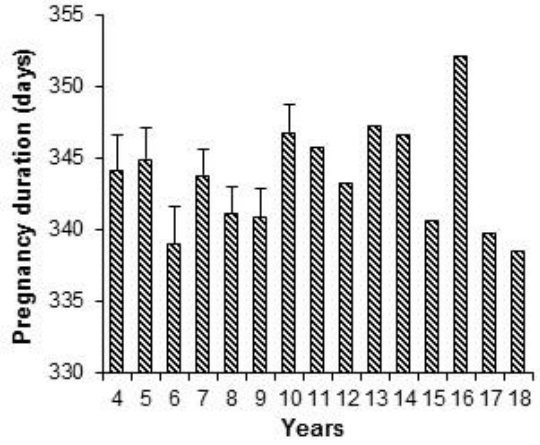

Figure 4 Mean pregnancy duration ± SEM in mares that delivered alive or dead foals

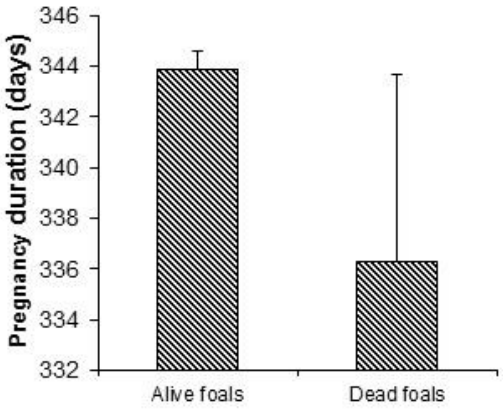

Although not all authors agree, some of them state that the year of mating affects pregnancy duration (Valera et al. 2006, Cilek 2009). The main cause could be the varying nutritional quality of feed in different years. The influence of the month of mating on pregnancy duration was described in several studies (Perez et al. 2003, Rezac et al. 2013). They documented the phenomenon that mares mated at the beginning of the year had significantly longer pregnancies than those mated at the end of breeding season. Winter et al. (2007) did not find any effect of mares' age on pregnancy duration in mares. The incidence of stillborn foals did not influence pregnancy duration. Satué et al. 2011 report that neither fetal complications were observed in pregnancies exceeding 400 days.

CONCLUSION

Pregnancy duration was influenced by the month of mating and the year of conception. Further research will be necessary to better understand the causes of variability of pregnancy duration in horses.

ACKNOWLEDGEMENTS

The research was financially supported by a grant AF-IGA-IP 2018/045.

REFERENCES

Cilek, S. 2009. The survey of reproductive success in Arabian horse breeding from 1976–2007 at Anadolu State farm in Turkey. Journal of Animal and Veterinary Advances, 8(2): 389–396.

Perez, C.C. et al. 2003. Gestation length in Carthusian Spanishbred mares. Livestock Production Science, 82(2–3): 181–187.

Rezac, P. et al. 2013. Different effects of month of conception and birth on gestation length in mares. Journal of Animal and Veterinary Advances, 12(6): 731–735.

Satué, K. et al. 2011. Factors influencing gestational length in mares: A review. Livestock Science 136(2–3): 287–294.

Valera, M. et al. 2006. Genetic study of gestation length in Andalusian and Arabian mares. Animal Reproduction Science, 95(1–2): 75–96.

Winter, G.H.Z. et al. 2007. Gestational length and first postpartum ovulation of Criollo mares on a stud farm in Southern Brazil. Journal of Equine Veterinary Science, 27(12): 531–534.

Influence of the yeast based feed mix supplementation on the quantity and quality of holstein cows milk during the summer season

Stanislav Navratil, Daniel Falta
Department of Animal Breeding
Mendel University in Brno
Zemedelska 1, 613 00 Brno
CZECH REPUBLIC

stanislav.navratil@mendelu.cz

Abstract: This paper is targeted on the influence of the yeast – based feed mix supplementation on quantity and quality of the Holstein cows milk during the summer season. The experiment for this work took place on the University farm in Žabčice. To this experiment, 64 cows of Holstein cattle were included. Cows were divided into two groups with the same yield, same feed and same condition. Cows were monitored for three 92 days: pre-experimental period (31 days), experimental period (31 days) and post-experimental period (30 days). Milk yield, milk composition and temperature were under evaluation for whole experiment. Data for environmental temperature were collected every 30 minutes by HOBO data logger placed in height of animal withers. Data concerning the milk yield and composition were collected from Milk Recording Scheme. The supplementation of yeast increased the yield of 1.67 kg during the experimental period. When comparing experimental group and control group, the yield of experimental group was elevated of 1.44 kg. When it comes to temperature, this was higher in August in comparing to both July and September. The addition of the yeast of this type to the feed ration can alleviate the effects of the heat stress. Farmers could profit from this supplementation, but further experiments are required.

Key Words: cattle, heat stress, yeast mix, supplementation, milk yield

INTRODUCTION

High temperatures can be a large problem in modern agriculture. Not only dry seasons in the plant production, but also the heat stress in animal production is altering the composition and the amount of animal products. Milk production is one of the finest examples of this influence. A large number of the authors are agree, that during the heat stress, cattle also alters its feeding behavior (West 2003, De Rensis and Scaramuzzi 2003).

Also, amount of consumed water rises. In contrary, dry matter and time of feeding is decreases (West 2003, Rhoads et al., 2009). Restriction of dry matter intake is one of the most common manifestation of heat stress of cattle. Problem also is, that the heat stress does not manifest itself immediately. According to Spiers et al. (2004) the heat stress manifested as a decrease of dry matter intake after 24 hours from exceeding the limit temperature.

There is a number of ways how to manage a heat stress of a cattle. According to Armstrong (1994) and West (2003) a lot of farmers increase a percentage of concentrated feed in a feeding ratio as a reaction to heat stress. This can lead to the increase of non-protein nitrogen. Hassan and Roussel (1975) claim, that these substances have influence on the increase of rectal temperature.

Other complications on physiological level are also present, when heat stress in imminent. Rhoads at al. (2013) claim, that ruminants have increased sensitivity of insuline to glucose test. This can be caused by elevated excrecion of pankreas. With heat stress, body uses more energy for cooling down and therefore, better use of glucose is required (Rhoads et al. 2009). Shwartz et al. (2009) claim, that this problem is similar to negative energy balance. In contrary to the negative energy balance, the heat-stressed cows have lower level of glucose mobilisation.

Another issue is loss of certain elements and substances thanks to the heat stress. Hyeok Joong Kang et al. (2017) in their work say, that cholesterol LDL, HDL, glucose, albumin, calcium and phosphorus levels are decreases with rising temperature.

A large number of animal nutrition companies offer substances to alleviate heat stress impact. Zimbelman et al. (2013) tested the effect of by-pass niacin. Results of this study shows, that supplementation of this vitamin helps to stabilise the yield and lowers vaginal temperature when the heat stress is imminent. Not only vitamins, but also antioxidants are important for reduction of heat stress impact. Shekh et al. (2017) used zinc to achieve aforementioned. Results show, that zinc supplementation decreases effect of HSP (heat-shock protein).

MATERIALS AND METHODS

The experiment for this paper was executed on the university farm in Žabčice in period from July to September 2017. In total 64 cows of Holstein breed (H 100) were included to the experiment. Cows were divided in to the two groups. Group A (1 – experimental group) and group B (9 – control group). Both groups were given the same feed ration, with the exception of addition of yeast to the experimental group during the August. The feeding ratio consisted of maize and alfalfa silage and alfalfa hay. From the mineral feed grinded limestone was presented. Concerning the stage of lactation, in both groups were equally represented cows of all stages.

The experimental period was divided into the three parts: pre experimental period (July), experimental period (August), and post-experimental period (September). This partition was made because of endeavour to fully describe the effects of yeast supplementation on the yield.

During the experimental period, the yeast was added to the feeding ration of the group A on daily bases in the amount recommended by manufacturer. The yeast was presented to the group A once per day. Dose of the yeast – based feed mix was 10 grams per day and cow.

Temperature data were collected automatically by HOBO (Onset) data logger. Data were collected every 30 minutes.

The data about milk yield and composition were collected from the milk recording scheme. All the data were processed and evaluated in Statistica 12 program.

RESULTS AND DISSCUSION

In the Table 1, the yield and composition of milk of group A (experimental group) can be observed. The higher yield in the experimental period (August) can be caused by the supplementation of yeast – based feed mix to the feed ration. The yield was elevated of 1.26 kg with comparison to pre – experimental period. Also, when comparing to the control group, the yield of experimental group was elevated of 0.23 kg. Salvati et al. (2014) executed experiment with supplementation of yeast *Saccharomyces cerevisiae* to the feed ration. The results show increase of the yield after first five days of the application. In our experiment, the effect of this yeast is apparent as well. Between July and August, 1.68 kg of milk is gained in August.

Table 1 Yield and milk composition of group A

Yield (kg)	Fat (%)	Protein (%)	Temperature °C
37.54	3.46	3.36	16.26^{A}
38.80	2.78	2.73	21.66^{B}
37.13	3.29	3.24	21.52^{B}

Legend: Values in the same column marked with different symbols (A to B) are different (P < 0.01)

In Table 2, the yield and milk composition of group B (control group) is displayed. As can be observed, the difference between July and other months is apparent. There is a large drop in yield during experimental and post – experimental period. This could be caused by a higher temperature in the August (experimental period).

The fact, that lower yield continued to the post – experimental period could be caused by persistence of heat stress symptoms. The temperature in September is lower, than in other months These can last a few months after the excessive heat stress is imminent (Toufar and Dolejš 1996, Černý et al. 2016). Also, there is an increase of yield (0.69 kg) between July and August. This increase is much smaller in comparing to experimental group increase.

Table 2 Yield and milk composition of group B

Month	Yield (kg)	Fat (%)	Protein (%)	Temperature (°C)
9	29.78	3.40	3.42	16.26^{A}
8	38.57	3.29	3.24	21.66^{B}
7	35.07	3.29	3.18	21.52^{B}

Legend: Values in the same column marked with different symbols (A to B) are different (P < 0.01)

In the table 3 can be observed the difference between the two groups. There is an apparent difference especially between July and August (Pre-experimental and experimental period) in yield (1.26 kg). The drop in yield during the hotter August is drastic for group B. Group A did not suffer such drop, the yield is even higher than in pre-experimental period. This can be, again, caused by the yeast supplementation to the feeding ratio. Lyons (1993) claim, that the supplementation of same yeast – based mix as we used elevates the yield of 7.3%. Also a huge drop in yield can be observed in control group from August to September. This drop is almost 9 kg of milk. Experimental group shows smaller decrease (1.26 kg) This can be caused by yeast supplementation.

Table 3 Comparison of group A and B during whole experimental period

	July			August			September		
	Yield (kg)	Fat (%)	Protein (%)	Yield (kg)	Fat (%)	Protein (%)	Yield (kg)	Fat (%)	Protein (%)
A	37.13	3.29	3.24	38.80	2.78	2.73	37.54	3.46	3.36
B	35.07	3.29	3.18	38.57	3.18	3.07	29.78	3.40	3.42

CONCLUSION

This paper is targeted on the influence of the yeast – based feed mix supplementation on quantity and quality of the Holstein cows milk during the summer season. The experiment for this work was conducted on the university farm in Žabčice, in total 64 cows of Holstein cattle was included to this experiment. Cows were divided into two groups with the same yield and same feeding ration. Only during Experimental period, the experimental group was fed with yeast. Cows were monitored for three months: pre-experimental period (July), experimental period (August) and post-experimental period (September). Milk yield, milk composition and temperature were all part of evaluation. It was concluded, that the supplementation of yeast elevated the yield of 1.67 kg during the experimental period. When comparing experimental group and control group, the yield of experimental group was elevated of 1.44 kg. The temperature in August was higher than both in September and July.

AKNOWLEDGEMENT

This study was supported by grant of IGA no. TP 7/2017.

REFFERENCES

Armstrong, D.V. 1994. Heat stress interaction with shade and cooling. Journal of Dairy Science, 77: 2044–2050.

Černý, T. et al. 2016. The effect of the season on the behavior and milk yield of the czech fleckvieh cows. Acta Universitatis Agriculturae et Silviculturae Mendelianae Brunensis [Online], 64(4): 1125–1130. Available at: https://acta.mendelu.cz/media/pdf/actaun_2016064041125.pdf. [2018-08-15].

Hassan, A., Roussel, J.D. 1975. Effect of protein concentration in the diet on blood composition and productivity of lactating Holstein cows under thermal stress. Journal of Agricultural Science, 85: 409–415.

Kang, H.J. et al. 2017. Effects of ambient temperature and dietary glycerol addition on growth performance, blood parameters and immune cell populations of Korean cattle steers. Asian-Australasian Journal of Animal Sciences, 30(4): 505.

Lyons, T.P. 1993. Požadavky současnosti na vývoj biotechnologických metod v oblasti výživy a krmení zvířat. In Sborník z Biotechnologie ve výživě zvířat. VII. Evropské přednáškové turné, Brno, pp. 11–24.

Rensis, F., Scaramuzzi, R.J. 2003. Heat stress and seasonal effects on reproduction in the dairy cow - A review. Theriogenology, 60(6): 1139–1151.

Rhoads, M.L. et al. 2009. Effects of heat stress and plane of nutrition on lactating Holstein cows: I. Production, metabolism, and aspects of circulating somatotropin. Journal of Dairy Science, 92: 1986–1997.

Rhoads, R.P. 2013. Nutritional interventions to alleviate the negative consequences of heat stress. Advances in Nutrition, 4(3): 267–276.

Sheikh, A.A. et al. 2017. Inorganic zinc supplementation modulates heat shock and immune response in heat stressed peripheral blood mononuclear cells of periparturient dairy cows. Theriogenology, 95: 75–82.

Shwartz, G. et al. 2009. Effects of a supplemental yeast culture on heat stressed lactating Holstein cows. Journal of Dairy Science, 92: 935–942.

Spiers, D.E. et al. 2004. Use of physiological parameters to predict milk yield and feed intake in heat-stressed dairy cows. Journal of Thermal Biology, 29: 759–764.

Toufar, O., Dolejš, J. 1996. Odraz vlivu extrémních stájových teplot na užitkovosti dojnic chovaných v uzavřené stáji. In Sborník příspěvků z 11. ročníku odborného semináře s mezinárodní účastí Aktuální otázky bioklimatologie zvířat. Brno, ČR, 11. prosince. Brno: NOEL, pp. 60–62.

West, J.W. 2003. Effects of heat-stress on production in dairy cattle. Journal of Dairy Science, 86: 2131–2144.

Zimbelman, R.B. et al. 2013. Effects of utilizing rumen protected niacin on core body temperature as well as milk production and composition in lactating dairy cows during heat stress. Animal Feed Science and Technology, 180(1–4): 26–33.

The effect of hoof trimming on locomotion score and milk production of dairy cows

Ivana Novotna, Zdenek Havlicek
Department of Morphology, Physiology and Animal Genetics
Mendel University in Brno
Zemedelska 1, 613 00 Brno
CZECH REPUBLIC

novotna.ivca@post.cz

Abstract: The study is focused on the assessment of locomotion score in Holstein cattle. The evaluation was carried out on a farm where 414 dairy cows are kept. The ratio of lame and non-lame cows was determined by visual motion analysis during 5 months from April 2018 to August 2018. The lameness was evaluated on a five-point scale. Score 1 corresponding to a non-lame cow and a score 5 to a severely lame cow. Furthermore, the effect of lameness on milk production (kg/day) was monitored, as a assumption that dairy cows with a higher locomotion score would have lower milk production than non-lame cows was not confirmed.

Key Words: Locomotion score, dairy cow, lameness

INTRODUCTION

Hoof lesions and lameness in cattle is currently a serious problem in the dairy industry and significantly affects the health and welfare of animals (Westin et al. 2016). The prevalence of these diseases positively correlates with the increasing milk production (Potterton et al. 2012, Bicalho and Oikonomou 2013). Lameness has a negative impact on longevity, reproduction and dairy production (Blowey 2012, Solano et al. 2016).

Early identification, immediate treatment of clinical signs, and the specific prevention for the farm must be provided to decreasing the number of lame cows (García-Munoz et al. 2017). Important is to find out the cause of the disease early and to distinguish whether it is an infectious disease, lesions caused by excessive grinding, trauma or laminitis (Nordlund et al. 2004). A low percentage of lameness is reflection of farm management, which should include regular footbaths, routine hoof trimming, convenient boxes and clean housing (García-Munoz et al. 2017).

Visual motion analysis of dairy cows is one of the most common methods for detection of lameness (Nordlund et al. 2004, Rodríguez et al. 2015). This method can be used for individual cows as well as for the herd (Hulsen 2007). It is a non-invasive, easy to apply and cheap method. On the other hand, it is a subjective, time-consuming method, and the exact standard of how animals can be evaluated is not given. Standing and walking deviations are observed in the evaluation of the locomotion score (Schlageter-Tello et al. 2014).

MATERIAL AND METHODS

Locomotion score was evaluated in a production stable where 414 Holstein dairy cows were kept in free-stall barns. Dairy cows were divided into two stables with a total capacity of more than 500 cows. Hoof trimming was irregular, mostly when lameness was detected. Preventive hoof trimming of all cows was carried out in June in the middle of our monitoring. Regular disinfecting footbaths were made in formalin once a month.

The monitoring was done before cows entering the milking parlor and after leaving milking parlor, where the locomotion score was determined on the five-point scale and the abnormalities were recorded. During evaluation cows moved on a flat, hard and non-slip floor. The five-point scale determined the degree of lameness. According by Hulsen (2007) in score 1, the back was straight when cow was standing and walking. In score 2, the ridge was arched while walking, but it was still straight when standing. For score 3, the back was arched while standing and walking and the cow made shorter

gait with one or more limbs. When the score 4, the cow was severely lame and attempted to carry weight with healthy limbs. In score 5 the cow did not stand on the affected limb, preferred to lie and unwillingly got up.

So far, 5 monitoring were made. First observation was on 6.4.2018, second on 11.5.2018, third on 19.6.2018, fourth on 24.7.2018 and last monitoring on 20.8.2018. On each day of observation milk production (kg) was recorded. The collected data was evaluated by the number of lame cows identified during the monitoring, development of a lameness during all measurements, repeatability of lameness and effect of hoof trimming on lameness in dairy cows. Furthermore, the effect of lameness on dairy production was evaluated.

RESULTS AND DISCUSSION

Figures 1, 2, 3, 4 and 5 indicate the percentage of dairy cows with locomotion score 1, 2, 3, 4 and 5 that were found for each measurement. When first measurement 73.4% of dairy cows did not lame. The most of lame cows 15.0% were captured with a locomotion score 3. When second observation 66.4% of dairy cows had locomotion score 1 and the most of lame cows, 16.5% had a locomotion score 3. In third measurement 65.0% of cows were non-lame and 19.3% had locomotion score 3. At fourth monitoring 80.0% cows were non-lame and 9.4% had locomotion score 2. At the last observation, 85.5% cows did not lame and 7.7% had a locomotion score 3. From the available data, it was found that 66.0% of cows were lame during at least one measurement, and in 29.0% of cows, the lameness was repeated for more measurements.

Figure 1 Percentage of dairy cows with locomotion score 1

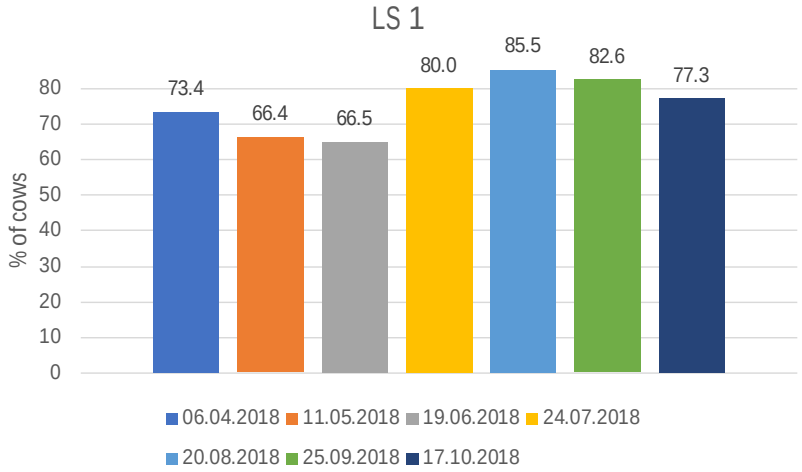

Figure 2 Percentage of dairy cows with locomotion score 2

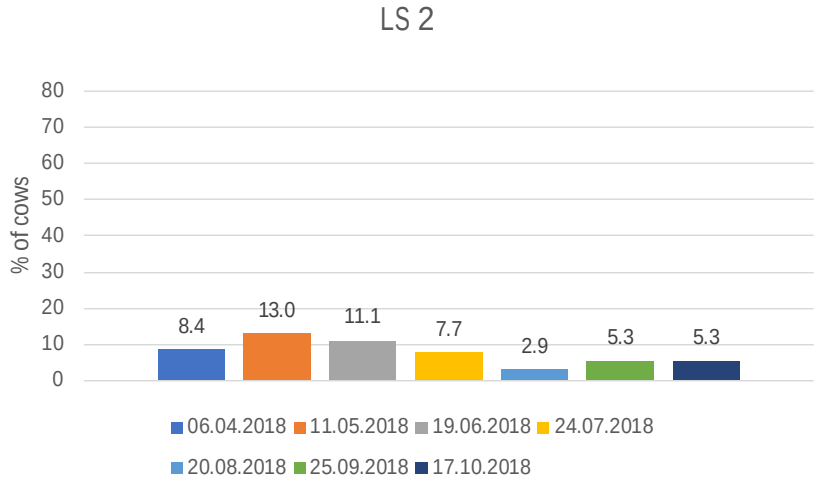

Figure 3 Percentage of dairy cows with locomotion score 3

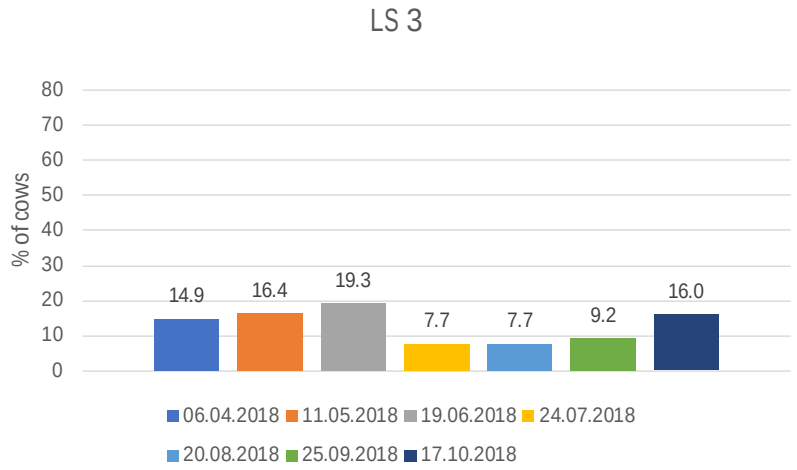

Figure 4 Percentage of dairy cows with locomotion score 4

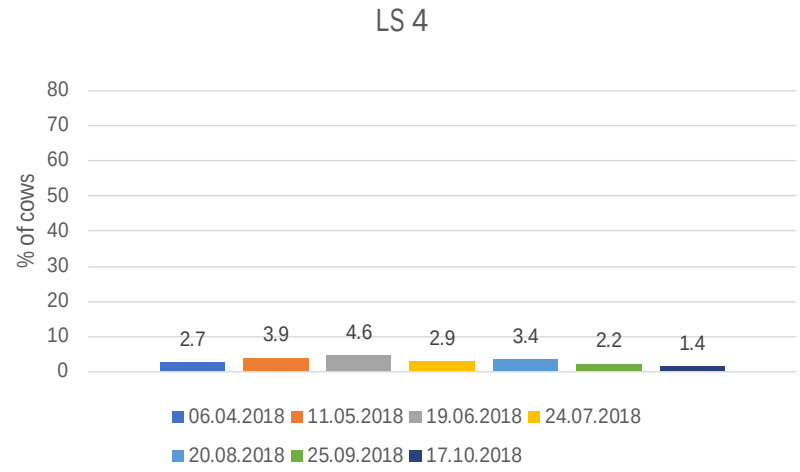

Figure 5 Percentage of dairy cows with locomotion score 5

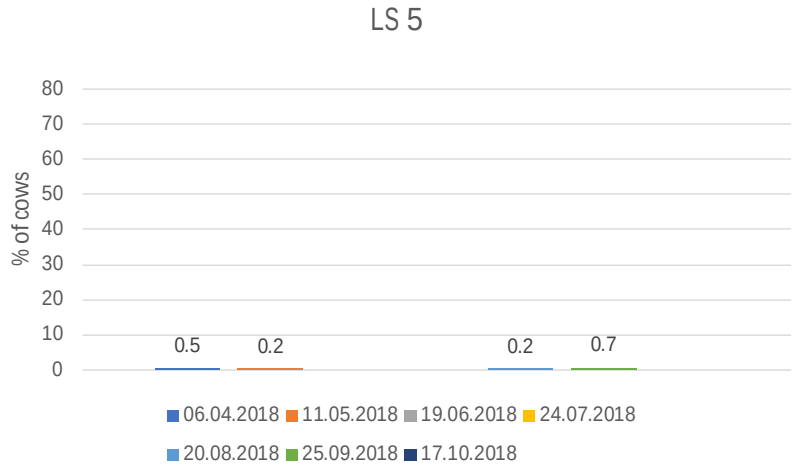

During the first three evaluations, from April to June, the number of non-lame cows decreased slightly, and the number of lame cows increased. On further measurements after preventive hoof trimming the number of cows with locomotion score 1 started to rise and the number of cows with locomotion score 2, 3, 4 and 5 began to decline. During hoof trimming, it was found that most cows had only overgrowth horn. Dry and hot summer weather may have contributed to lower problems with hooves. In contrast, Van Hertem et al. (2014) in their study found an increase in locomotion score

after hoof trimming. This explains that the hoof trimming caused discomfort and pain, which led to a change of walking.

In table 1 is average daily milk yield of dairy cows (kg) with locomotion score 1, 2, 3, 4 and 5. First observation shows, that cows with locomotion score 1 had average daily milk yield 33.4 kg, the highest milk production had cows with locomotion score 3 (37.0 kg) and lowest cows with locomotion score 5 (24.2 kg). During second measurement was found, that non-lame cows had average milk production 34.0 kg and highest milk production had cows with locomotion score 4 (39.8 kg) and lowest cows with locomotion score 5 (37.5 kg). At the third monitoring cows with locomotion score 1 had average milk production 35.0 kg, higher milk production had cows with locomotion score 3 (35.1 kg) and lower cows with locomotion score 4 (34.8 kg). Fourth observation shows, that non-lame cows had lowest average milk production 35.1 kg and highest milk production had cows with locomotion score 3 (36.9 kg). At third and fourth observation there were no cows with locomotion score 5. During last monitoring cows with locomotion score 1 had highest milk production (35.4 kg) and lowest milk production had cows with locomotion score 5 (18.4 kg).

Table 1 Average daily milk yield of dairy cows (kg) with locomotion score 1, 2, 3, 4 and 5

	LS 1	LS 2	LS 3	LS 4	LS 5
06.04.2018	33.4	36.7	37.0	36.5	24.2
11.05.2018	34.0	39.0	39.3	39.8	37.5
19.06.2018	35.0	35.0	35.1	34.8	
24.07.2018	35.1	36.3	36.9	36.5	
20.08.2018	35.4	32.3	32.3	32.3	18.4

Figure 6 shows the average daily milk yield of dairy cows (kg) with locomotion score 1, 2, 3, 4 and 5. For the first measurement, milk production of cows with locomotion score 2, 3 and 4 were higher than milk production of cows with locomotion score 1. Drop in milk production associated with lameness was observed at locomotion score 5. Second and fourth measurement showed a higher milk production at locomotion score 2, 3, 4 and 5 than cows with locomotion score 1. Only at the last observation confirmed the assumption, that cows with higher locomotion score will have lower milk production than non-lame cows.

Average milk production (kg) in cows with locomotion score 1 was 34.6 kg, in cows with locomotion score 2 was 35.9 kg, in cows with locomotion score 3 was 36.1 kg, in cows with locomotion score 4 was 36.0 kg and in cows with locomotion score 5 was average milk production 26.7 kg. The variance from the assumption could be due to the fact, that the average milk yield was calculated independently of the parity and lactation phase, where the higher milk production is expected at the higher parity and the lactation peak. While a higher locomotion score usually also appears at a higher parity. Therefore, further research will take into consideration these factors.

The research results were confirmed by the study by Archer et al. (2010), who also did not notice a reduction in daily milk production during lameness, but up to 10 months later. They found out that dairy cows, sometimes lame, had a higher milk production than cows that never lame, just like Bicalho et al. (2008). This finding confirms the theory that lameness is a production disease associated with higher milk production.

On the contrary, our assumptions have been confirmed by Charfeddine and Pérez-Cabal (2017), who found that the disease of hooves and increased locomotion score had a negative effect on dairy production. In some cases, milk losses have been detected prior lameness.

Figure 6 Average milk yield of dairy cows

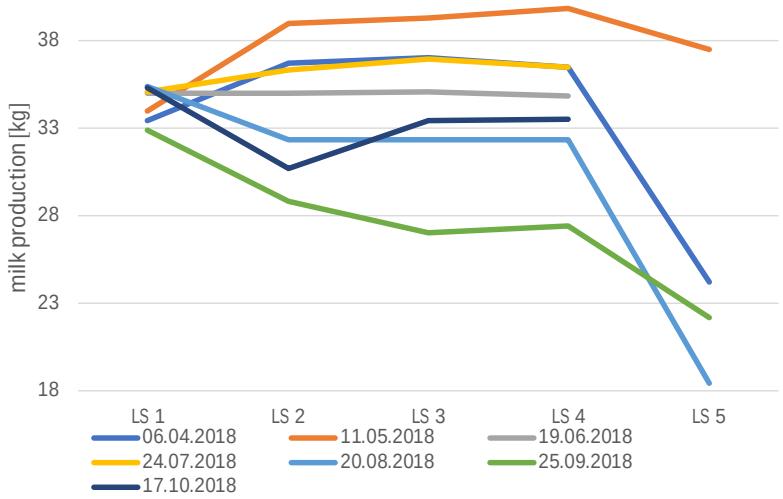

CONCLUSION

After processing the data, it was found that hoof condition was good on the farm and get improved during last two observations. The percentage of non-lame cows was at first observation 73.4%, at second 66.4%, at third 65.0%, at fourth 80.0% and at last measurement 85.5%. The most of lame cows have locomotion scores 3 and 2, never predominate the number of cows with locomotion score 4 or 5.

After preventive hoof trimming of all cows in June there was hoof condition significantly improved and the number of dairy cows with locomotion score 1 increased.

Assessment of the effect of lameness on milk production has not confirmed the assumption that cows with locomotion score higher than 1 would have lower milk production than non-lame cows. Cows with locomotion score 1 had average milk production 34.6 kg. On the other hand, higher milk production was found in dairy cows with locomotion score 2 (35.9 kg), 3 (36.1 kg), and 4 (36.0 kg) and a significant decrease was found in locomotion score 5 (26.7 kg).

ACKNOWLEDGEMENTS

Research reported in this publication was supported by grant no. AF-IGA-IP-2018/067.

REFERENCES

Archer, S.C. et al. 2010. Association between milk yield and serial locomotion score assessments in UK dairy cows. Journal of Dairy Science, 93(9): 4045–4053.

Bicalho, R.C., Oikonomou, G. 2013. Control and prevention of lameness associated with claw lesions in dairy cows. Livestock Science, 156(1–3): 96–105.

Bicalho, R.C. et al. 2008. Strategies to analyze milk losses caused by diseases with potential incidence throughout the lactation: A lameness example. Journal of Dairy Science, 91(7): 2653–2661.

Blowey, R. 2012. Cattle Lameness and Hoofcare. Ipswich, Old Pond Publishing Ltd.

Charfeddine, N., Pérez-Cabal, M.A. 2017. Effect of claw disorders on milk production, fertility, and longevity, and their economic impact in Spanish Holstein cows. American Dairy Science Association, 100(1): 653–665.

García-Munoz, A. et al. 2017. Effect of hoof trimer intervention in moderately lame cows on lameness progression and milk yield. Journal of Dairy Science, 100: 9205–9214.

Hulsen, J. 2007. Cow signals. Praha, Profi Press.

Nordlund, K.V. et al. 2004. Investigation Strategies for Laminitis Problem Herds. American Dairy Science Association, 87: (E. Suppl.): E27–E35.

Potterton, S.L. et al. 2012. A descriptive review of the peer and non-peer reviewed literature on the treatment and prevention of foot lameness in cattle published between 2000 and 2011. The Veterinary Journal, 193(3): 612–616.

Rodríguez, A.R. et al. 2015. Thermographic assessment of hoof temperature in dairy cows with different mobility scores. Livestock Science, 184: 92–96.

Schlageter-Tello, A. et al. 2014. Manual and automatic locomotion scoring systems in dairy cows: A review. Preventive Veterinary Medicine, 116(1–2): 12–25.

Solano, L. et al. 2016. Prevalence and distribution of foot lesions in dairy cattle in Alberta, Canada. American Dairy Science Association, 99(8): 6828–6841.

Van Hertem, T. et al. 2014. The effect of routine hoof trimming on locomotion score, ruminating time, activity, and milk yield of dairy cows. American Dairy Science Association, 97(8): 4852–4863.

Westin, R. et al. 2016. Cow- and farm-level risk factors for lameness on dairy farms with automated milking systems. American Dairy Science Association, 99(5): 3732–3743.

The antioxidant enrichment of Duroc boar diet and its effect on quality of ejaculate during the summer season

Magdalena Pribilova[1], Pavel Horky[1], Lenka Urbankova[1], Milan Vecera[2]
[1]Department of Animal Nutrition and Forage Production
[2]Department of Animal Breeding
Mendel University in Brno
Zemedelska 1, 613 00 Brno
CZECH REPUBLIC

magdalena.pribilova@mendelu.cz

Abstract: Good quality of ejaculate is very important for the amount of produced insemination doses (ID). Main monitored parameters are volume of ejaculate, concentration of sperm, sperm motility and morphologically abnormal sperm. During the oxidative stress of organism sperm cells are damaged by the free radicals, especially by reactive oxygen species (ROS). Oxidative stress is considered as one of the main causes of male infertility.
In this study we monitored qualitative and quantitative parameters of boars ejaculate during summer season, when we have assumed the heat stress. Two groups of Duroc boars were monitored. First was the control group (n = 6) without any antioxidant supplements in their diet. Second group was the experimental group (n = 6) with supplementation of antioxidant complex (selenium, zinc, vitamin E and C) in their diet. The results have been compared after four months of experimental period. In motility, there was statistically significant difference between groups after two months by 8.06% ($P < 0.05$). In experimental group, motility did not decreased below required level (70%) unlike the control group. In morphologically abnormal sperm, there was observed statistically significant increase ($P < 0.05$) in control group, even above the required level (20%) for ID preparation.

Key Words: antioxidant, infertility, boar, stress

INTRODUCTION

Oxidative stress is considered as one of the main causes of male infertility, approximately 30–80% (Ahmadi et al. 2016). When ROS exceeds organism natural antioxidant defence, it can be considered as oxidative stress (Tremellen 2008). Reason why ROS are increased in higher level can be temperature, electromagnetic waves, bad air condition, insecticides, alcohol consumption, obesity and poor nutrition (Aitken and De Iuliis 2007). ROS causes the cascade of lipid peroxidation of plasma membranes of cells, which consists high level of polyunsaturated fatty acids (Eskenazi et al. 2005). The main pathological results are DNA damages associated with mitochondrial membrane disruption (Hosen et al. 2015). Among the most frequently occurring defects of sperm belongs low sperm concentration (oligozoospermia), reduced sperm motility (asthenospermia), morphologicaly abnormal sperm (teratozoospermia) and their combination (oligoasthenoteratozoospermia) (WHO 2010).

Antioxidants are natural, biological or chemical, compounds that limiting or neutralising of free radicals and halting the chain reaction leading to oxidative stress in organism (Singh et al. 2015). Seminal plasma includes vitamin E, vitamin C, superoxiddismutase, gluthatione and thioredoxin. These antioxidants neutralize free radicals and protecting sperm cells from ROS damage (Tremellen 2008). Selenium is component of glutathione peroxidase, which neutralised peroxide radicalsand protect body tissues before ti damages body tissues (Horký et al. 2012). Moreover, selenium is important for physiological sperm development and maturation (Blair 2007). Zinc is a part of enzyme superoxide dismutase, essential in antioxidant chain. Zinc is also important in development of sexual organs and their activity (Jelínek et al. 2003). Vitamin E, especially α-tocopherol, has anti-sterility effect, what is important in cell protection during the oxidative stress. Tocopherols inhibit formation of very toxic lipoperoxides (Racek 2003). Vitamin C, the L-ascorbic acid, together with tocopherol, protecting sperm cell membranes form peroxidation (Horký et al. 2016), thus decreasing the amount of pathological sperm in ejaculate (Svoboda 2011).

MATERIAL AND METHODS

The experiment had been running at insemination station in Velké Meziříčí (AgroMeřín, Czech Republic) during the summer season (June–September). Monitored were two equal groups of Duroc boars (± 275 kg, ± 2.5 years). First group, the control group (n = 6), was fed only by basic feed mixture (see Table 1, Table 2). Second group, the experimental group (n = 6), was fed by basic diet with addition of vitamin-mineral premix in dose of: 0.5 mg Se, 70 mg Zn, 70 mg vit. E and 350 mg vit. C per kilogram of basic feed mixture. Doses of antioxidant were calculated on base of Zeman et al. (2006).

Table 1 Composition of basic feed mixture (MEp 12.6 MJ/kg)

Component	% of feed mixture
Barley grain	36.00
Wheat grain	20.36
Oat grain	20.00
Soybean meal (SBM)	14.50
EKPO T (biscuit meal)	3.00
BergaFat (palm oil)	2.10
Calcium carbonate	1.50
Monocalciumphosphate	1.20
Mineral vitamin premix for boars 0.5%	0.50
Sodium chloride	0.40
Magnesium oxide	0.15
L-Lysine HCl	0.14
L- Threonine	0.09
Methionine DL	0.06

Table 2 Composition of premix (0.5%)

Parameter	Unit	Quantity
Vit.A	U.I.	3 000 000
Vit.D3	U.I.	400 000
Vit.B1	mg	500
Vit.B2	mg	1 200
Vit.B6	mg	800
Vit.B12	mg	6
Vit.K3	mg	600
Biotine	mg	70
Folic acid	mg	200
Niacinamide	mg	8 000
Calcium pantothenate	mg	4 000
Choline chloride	mg	55 200
Betaine	mg	26 500
Lysine in the form of L-Lysine monohydrochloride	g	225.79
Butylhydroxi-toluene	mg	400
Ethoxyquin	mg	179.82
Mn - form of manganese oxide	mg	19 759.89
Fe - form of iron carbonate	mg	23 624.51
Co - form of cobalt sulphate heptahydrate	mg	91.35
I - form of potassium iodide (KI)	mg	229.20
Carrier ad. - wheat meal and calcium carbonate	kg	1

After analysis of basic feed mixture there was measured antioxidants per kg is dose: 0.02 mg selenium, 21.5 mg zinc, 9.9 mg vit. E and 16.0 mg vit. C.

During the monitored period there was installed temperature and relative humidity (RH) measuring device datalogger (Voltcraft DL-121TH, Germany), placed in animal living zone. Temperature and RH was measured in hour interval and the results of measuring are shown in Figure 1 Figure 2.

Figure 1 Maximum and average temperature in the stable

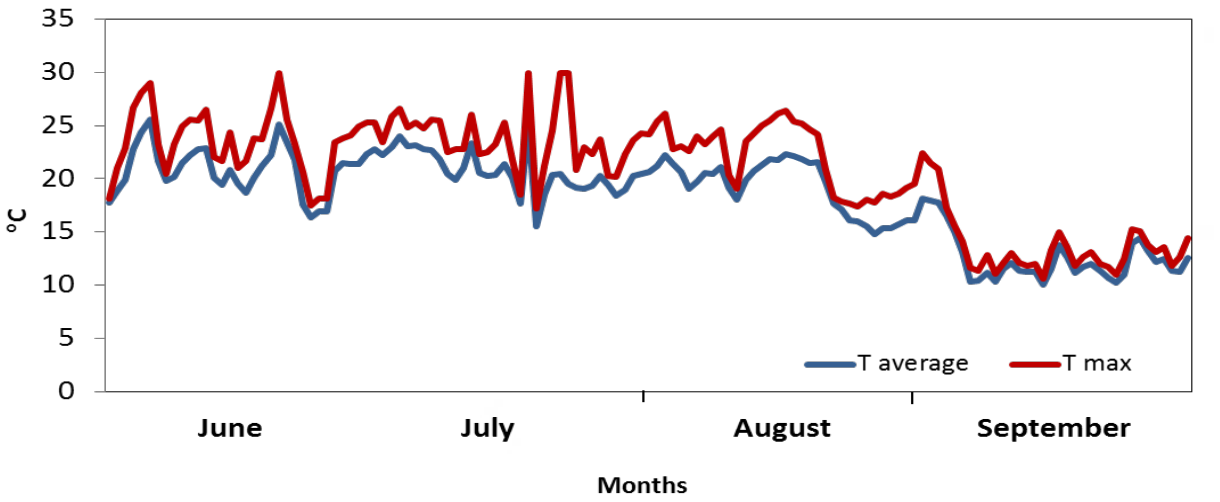

Figure 2 Maximum and average relative humidity in the stable

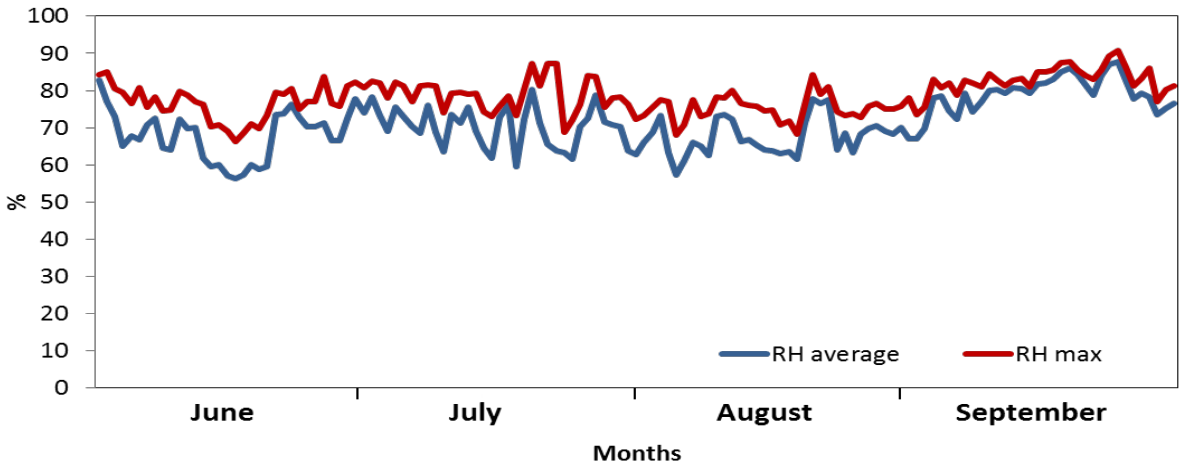

Boars ejaculate was taken by hand-gloved technique once a week. Analysis of ejaculate was performed by Lovercamp et al. (2013).

Volume of ejaculate was measured by weighing with 1 g to 1 ml conversion. Concentration of sperm was determined by using self-calibrating spectrophotometer Spekol 11 (SpermaCueTM, Minitube of America, Verona, WI) at wavelength 340–850 nm. The sample for spectrophotometer measuring was prepared by mixing 9 ml of 1M HCl and 0.25 ml of ejaculate. Total sperm account was calculated by: volume of ejaculate x concentration of sperm. For sperm motility determination the ejaculate sample (500 µl) was diluted with 500 µl of Androhep diluent and incubated in 37 °C for 30 min. After incubation the sample was monitored in contrast microscope with digital camera (Olympus microscope IX 71 S8F-3; Tokio, Japan) and Sperm Vision™ software (Minitube of America, Verona, WI). For morphology determination was 50 µl of each ejaculate fixed by 5 µl 10% buffered formalin, than 5 µl of this sample was dropped on slide incubated for 30 min (in 25 °C and 100% humidity to immobilize the sperms. Coloration of samples was saturated in water solution of congo-red and then in 0.5% aqueous solution of crystal violet. Sperm morphology

was evaluated by using a phase contrast microscope (Zeiss, Germany) with an oil immersion lens at a magnification of 1500×. Subjective assessment was performed by a single qualified person.

The statistical analysis was done by using STATISTICA.CZ version 10.0 (Czech Republic). The results were stated as the mean ± standard variance. Statistical significance was observed between the groups (the first sampling was taken as a control one) using ANOVA and Scheffe's test – the two-factor analysis (the first factor was the animal group, the second one – the sampling factor) for parameters of ejaculate volume, sperm concentration, motility and percentage of morphologically abnormal sperm. The difference ($P < 0.05$) was considered as significant.

RESULTS AND DISCUSSION

In Figure 3 are shown measured results of volume of ejaculate from both groups. The curve trend is very similar in both groups during the experiment, so it can be said that supplementation of vitamin-mineral premix has no statistically significant effect on ejaculate volume in boars. But in both groups there was over-limit dose of ejaculate volume (requirements for Duroc boars is at least 80 ml for preparation of ID). In control group there was average volume 186.95 ml and in experimental group 236.50 ml.

In Figure 4 it can be seen, that there are no statistically significant results as well. Even in control group was measured higher concentration of sperm than the experimental group. It can be caused by lower volume of ejaculate in control group. As Knecht et al. (2014) states that sperm concentration decreases with higher level of ejaculate volume, and conversely. But both concentrations are suitable for ID preparation (requirement is 300 x 10^6/ml).

Figure 3 Volume of ejaculate

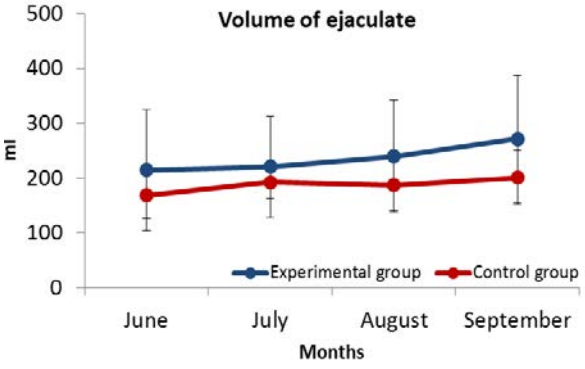

Figure 4 Concentration of sperm

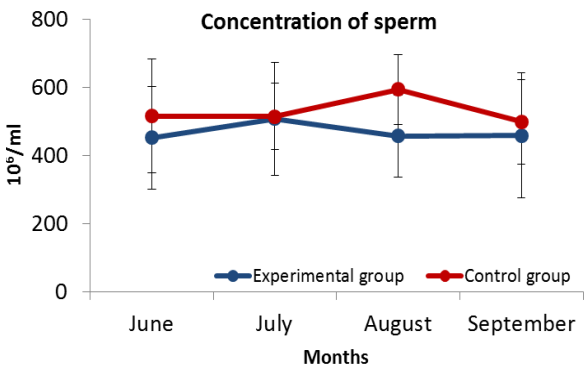

Figure 5 shows total rate of spermatozoa in ejaculate. As the results above, there is no statistically significant difference between monitored groups. Average values of total sperm account were in control group 94.05 x 10^9 and in experimental group 99.66 x 10^9 Marin-Guzman et al. (2000) in their experiment show higher amount of sperm cells in group of boars with supplementation of selenium compared to group without supplementation. We did not confirm this hypothesis.

In Figure 6 there are results of motility measurement of monitored groups. As it can be seen, there is big difference between groups, in August even statistically significant difference by 8.057% ($P < 0.05$). For ID preparation is required 70% motility. Form the diagram is evident, that control group did not reached the required motility, so their ejaculate could not be used for ID. Motility of experimental group fulfilled motility requirement, their average motility value was 73.87%.

In monitoring of morphologically abnormal sperm, shown in Figure 7, there is no statistically significant difference between groups. But it is visible, that in control group is statistically significant increase of abnormal sperm between July and August (by 8.61%) ($P < 0.05$). In comparison with Table 2, in June and July the daily maximum temperatures reached a peak up to 30 °C, which can cause an oxidative stress in boars. Whereas the maximum percentage of morphologically abnormal sperm for ID preparation is 20%, the control group did not fullfiled the requirement. On the contrary, it can be said that supplementation of antioxidants alleviated the increase of morphologically abnormal sperm in experimental group.

Figure 5 Total rate of sperm

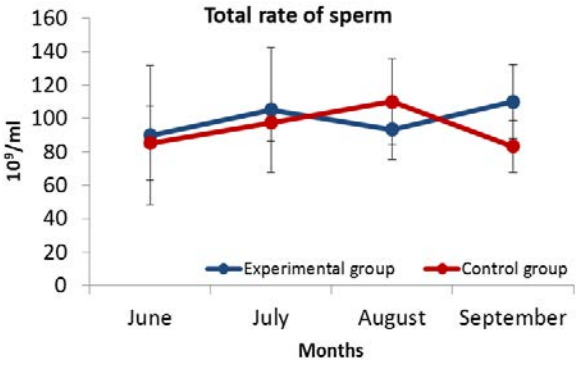

Figure 6 Motility of sperm

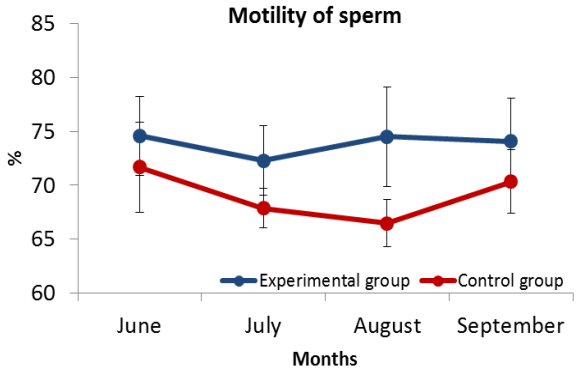

Figure 7 Morphologically abnormal sperm

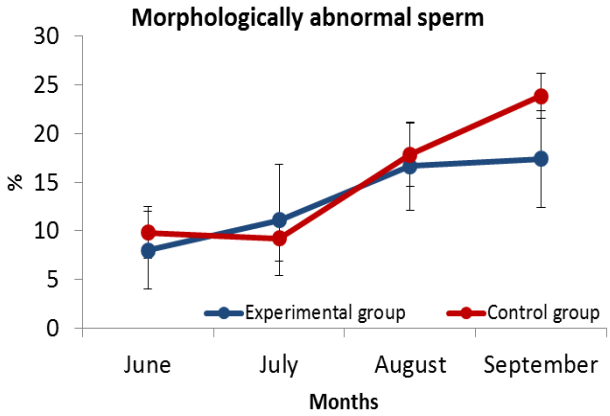

Abad et al. (2013) showed that supplementation of combination of L-carnitine, Vitamin C and E, coenzyme Q10, zinc and vitamin B12 improves parameters of ejaculate in human. On the contrary, Galatioto et al. (2008) recorded improvement only in total sperm account after antioxidant therapy of N-acetylcysteine, vitamins E, C and A, copper, zinc etc. Barranco et al. (2013) state that in summer months motility significantly decreases compared to the rest of the year. Addition of zinc in diet can improve sperm motility and morphology (Hadwan et al. 2014, Elgazar et al. 2005). Sperm concentration could be improved by supplementation of combination L-carnitine, CoQ10, vitamin E and vitamin C for at least three months (Gvozdjáková et al. 2015).

Values of qualitative assessment of the ejaculate for the production of insemination doses taken from the standard ČSN 46 7114 ‘’Boars sperm’’.

CONCLUSION

Although we have not achieved the desire results, we can state that supplementation of antioxidant complex can improve, or at least can stabilize the quality of ejaculate. From the results we can confirm, that addition of vitamin-mineral premix stabilizes the value of sperm motility in comparison with control group of boars without supplementation. In motility, the difference between groups was statistically significant in August, after approximately 60 days of supplementation.

ACKNOWLEDGEMENTS

This project was funded from grants and IGA TP 7/2017: Analysis of performance and behaviour of farm animals in relation to ambient temperature variability and possibilities of elimination of its impact.

REFERENCES

Abad, C. et al. 2013. Effects of oral antioxidanttreatment upon the dycamics of humansperm DNA fragmentation and subpopulations of spermwith highly degraded DNA. Andrologia, 45: 211–216.

Ahmadi, S. et al. 2016. Antioxidant supplements and semen parameters: An evidence based review. International Journal of Reproductive BioMedicine, 14(12): 729–736.

Aitken, R.J., De Iuliis, G.N. 2007. Origins and consequences of DNA damage in male germ cells. Reproductive BioMedicine Online, 14: 727–733.

Barranco, I. et al. 2013. Season of Ejaculate Collection Influences the Freezability of Boar Spermatozoa. Cryobiology, 67(3): 299–304.

Blair, R. 2007. Nutrition and feeding and organic pigs. 2st ed., Cambridge, MA: CABI.

Elgazar, V. et al. 2005. Zinc-regulating proteins, ZnT-1, and metallothionein I/II are present in different cell populations in the mouse testis. Journal of Histochemistry and Cytochemistry, 53: 905–912.

Eskenazi, B. et al. 2005. Antioxidant intake is associated with semen quality in healthy men. Human Reproduction, 20: 1006–1012.

Galatioto, G.P. et al. 2008. May antioxidant therapy improve sperm parameters of men with persistent oligospermia after retrograde embolization for variococele? World Journal of Urology, 26: 97–102.

Gvozdjáková, A. et al. 2015. Coenzyme Q10, α-Tocopherol, and Oxidative Stress Could Be Important Metabolic Biomarkers of Male Infertility. Disease Markers, 2015: 1–6.

Hadwan, M.H. et al. 2014. Study of the effects of oral zinc supplementation on peroxynitrite levels, arginase activity and NO synthase activity in seminal plasma of Iraqi asthenospermatic patients. Reproductive Biology and Endocrinology, 12: 1–8.

Horký, P. et al. 2012. Effect of organic and inorganic form of selenium on antioxidant status of breeding boars ejaculate revealed by electrochemistry. International Journal of Electrochemical Science, 7(10): 9643–9657.

Horký, P. et al. 2016. Effect of Diet Supplemented with Antioxidants (Selenium, Copper, vitamins E and C) on Antioxidant Status and Ejaculate Quality of Breeding Boars. Annals of Animal Science, 16(2): 521–532.

Hosen, M.B. et al. 2015. Oxidative stress induced sperm DNA damage, a possible reason for male inferitlity. Iranian Journal of Reproductive Medicine, 13: 525–532.

Jelínek, P. et al. 2003. Fyziologie hospodářských zvířat. 1. vyd., Brno: Mendelova zemědělská a lesnická univerzita.

Knecht, D. et al. 2014. The Influence of Boar Breed and Season on Semen Parameters. South African Journal of Animal Science, 2014(44): 1–9.

Lovercamp, K.W. et al. 2013. Effect of dietary selenium on boar sperm quality. Animal Reproduction Science, 138: 268–275.

Marin-Guzman, J. et al. 2000. Effect of dietary selenium and vitamin E on spermatogenic development in boars. Journal of Animal Science, 78: 1537–1543.

Racek, J.N. 2003. Oxidační stres a možnosti jeho ovlivnění. Praha: Galén.

Singh, F. et al. 2015. Reductive stress impairs myoblasts mitochondrial function and triggers mitochondrial hormesis. BBA, 1853: 1574–85.

Svoboda, M. 2011. Význam selenu a vitamínu E pro zdraví prasat. Náš chov, 7: 31–33.

Tremellen, K. 2008. Oxidative stress and male infertility - a clinical perspective. Human Reproduction Update, 14(3):243–258.

World Health Organization. 2010. WHO laboratory manual for the examination and processing of human semen. 5th ed., Geneva, Switzerland: World Health Organization.

Zeman, L. et al. 2006. Výživa a krmení hospodářských zvířat. 1. vyd. Praha: Profi Press.

Comparison of two *in vitro* direct contact methods for testing acaricidal effect of essential oils in poultry red mites (*Dermanyssus Gallinae*)

Iva Radsetoulalova, Martina Lichovnikova
Department of Animal Breeding
Mendel University in Brno
Zemedelska 1, 613 00 Brno
CZECH REPUBLIC

iva.radsetoulalova@mendelu.cz

Abstract: The aim of this study was to test the effectiveness of selected essential oils against the poultry red mite (*Dermanyssus gallinae*) by two different methods - glass vial bioassay and Petri-dishes. Both methods are in vitro direct contact methods. In both methods the same concentration of essential oils, lavender, cinnamon, clove bud, were used: 0.5; 0.25; 0.12; 0.06; 0.03; 0.015 µL/cm^2. The average mortality in the negative control was 2%. There was no significant effect of in vitro methods on poultry red mite mortality in essential oils with high acaricidal effect, cinnamon and clove bud, up to concentration 0.03 µL/cm^2. In vitro methods had significant effect on poultry red mite mortality using lavender essential oil, with lover acaricidal effect, at concentrations 0.5; 0.25; 0.12 and 0.06 µL/cm^2. It is necessary to pay more attention in vitro methods testing lower concentration of essential oils or essential oils with lower acaricidal effect.

Key Words: natural botanical acaricides, clove bud, cinnamon, lavender, red mite

INTRODUCTION

The poultry red mite (PRM, *Dermanyssus Gallinae*) is obligatory hematophagous pseudoparasite of birds. This ectoparasite feeds blood of its host, but it lives and develops out of host's body. All development stages feed blood except larva stage and adult males feeds only sometimes (Kim et al. 2004, Sparagano et al. 2014).

High incidence of PRM is one of an economic problem in egg production. Poultry red mites are found up to 95% flocks in Europe, USA, Japan and China. The cost expends on fight with this parasite and production losses are calculated on 360 million EUR per year (Teuling 2017). Infestation by this parasite can lead to decrease in egg production and its quality, aggressive feather-pecking hens or cannibalistic behavior. Poultry red mite may be a vector of a variety of poultry pathogens including zoonosis. Its faeces and small hairs on his cuticle are strong allergens. Workers in poultry houses can have eczema and even dermatitis in strong infestations (Dohnal 2009, Sparagano et al. 2014).

PRM has very fast life cycle and some of them are resistant against commercial acaricides against this mite. Adult PRM can survive from 6 to 8 months without feed. It may be one of the origin of the infestation in new flock in poultry house (Dohnal 2009, Nordenfors et al. 1999, Sparagano et al. 2014). These problems have highlighted the need for the development of alternative PRM control. It seems essential oils with its acaricidal effect could be an alternative to commercial pesticides.

Plant essential oils are biological active substances of aromatic plants – aromatic hydrocarbons. Essential oil is chemical complex mixture of 20–80 monoterpenes, which are contained in different concentrations. Main substances in essential oil, from 1 to 5, are characteristic for given plant species (eugenol (65%) is typical for clove bud) (George et al. 2009, Kim et al. 2004, 2007, Pavela 2011).

There is a lot of studies testing acaricidal effect of essential oils with very different results using different in vitro methods. The aim of this study was to test the effectiveness of selected essential oils against the poultry red mite (*Dermanyssus gallinae*) by two different methods - glass vial bioassay and Petri-dishes.

MATERIAL AND METHODS

The acaricidal effectiveness of selected plant essential oils against poultry red mites was tested via in vitro direct contact methods - by glass vial bioassay and Petri-dishes. All chemicals were of reagent grade. Three essential oils derived from clove bud, lavender and cinnamon were examined. Oils were diluted in Tween 20 (essential oil : Tween 1:1), than it was diluted with water to final concentrations: 0.5; 0.25; 0.12; 0.06; 0.03; 0.015 µL/cm^2.

Colonies of poultry red mites (*Dermanyssus gallinae*) used in these tests were collected in poultry houses in the Czech Republic in 2018. There were used plastic containers filled with rolled cardboard attached to the constructions. After 3–5 days the containers with poultry red mites were closed by lids and transferred to the laboratory. Female PRM were tested within three days after collection (Sparagano et al. 2013).

In the first method each of the essential oils was applied on two circles of filter paper (Whatman No. 1; 25 mm diameter) at the bottom of the glass vial at tested concentration in amount of 50 µL solution. The solvent of solution was then evaporated (within 50 minutes) at glass vial bioassay method. Ten movable female mites were placed on the impregnated filter paper at the bottom of the glass vials. Each glass vial was then closed with lid (Hubert et al. 2015).

In the second method at Petri-dishes each of the essential oils was applied on a circle of filter paper (Whatman No. 2; 42.5 mm diameter) in glass Petri-dish at tested concentration in amount of 150 µL solution. Filter papers were allowed to air-dry for 7 minutes before adding approximately 20 adult female of PRM. Each Petri-dish was then covered with lid and sealed with parafilm. All Petri-dishes were stored at laboratory temperature (George et al. 2010).

Always six repetition per each concentration and oil and negative control were used for each method. Negative control contained no essential oil on filter paper (Tween : water 1:1). The mortality of the poultry red mites was measured 24h after the treatment. Poultry red mites were considered dead if they did not move after they were prodded with an entomological tweezer. Mite mortality was assessed under magnification (× 2.5 illuminated bench magnifier).

The percentage mortality of mites under each treatment was calculated (100 x dead mites/total mites). The effect of in vitro methods in each essential oils on PRM mortality was statistically analyzed using t-test software Unistat 5.1 (Unistat Ltd, England).

RESULTS AND DISCUSSION

Comparison of the acaricidal activity of three plant essential oils at a dose of 0.5; 0.25; 0.12; 0.06; 0.03; 0.015 µL/cm^2 with solvents of Tween 20 with water, against female poultry red mites by two in vitro methods is shown in Table 1. All used essential oils gave more than 95% mortality against PRMs at concentration 0.5 µL/cm^2. The most effective essential oils were clove bud and cinnamon, lavender was generally less effective. The average mortality in controls was 2%.

Clove bud essential oil caused 100% mortality at all concentrations at glass vial bioassay method. At Petri-dishes method clove bud caused more than 80% mortality at all concentrations. Between these two methods was no significant difference in this essential oil.

Cinnamon essential oil caused 100% mortality at all concentrations at glass vial bioassay method. At Petri-dishes method cinnamon caused more than 75% mortality at all concentrations except 0.015 µL/cm^2, where was 39% mortality. Between these two methods was no significant difference, except concentration 0.015 µL/cm^2, where was significant difference. Cinnamon at glass vial method was significantly more effective considering to the efficiency of cinnamon at Petri-dishes method at concentration 0.015 µL/cm^2.

In lavender essential oil there were significant differences ($P<0.05$) in PRM mortality between these two in vitro methods at concentration 0.5, 0.25, 0.12 and 0.06 µL/cm^2. In concentration 0.03 and 0.015 µL/cm^2 there were no significant differences between the methods, however the mortality was very low. Lavender at glass vial method was significantly more effective considering to the efficiency of lavender at Petri-dishes method at concentration 0.5 µL/cm^2.

Lavender at Petri-dishes method was significantly more effective considering to the efficiency of lavender at glass vial method at concentrations 0.25; 0.12 and 0.06 µL/cm^2.

Based on previous results (Rádsetoulalová et al. 2017), at concentration 0.5 µL/cm² there was no significant difference between the efficiency of lavender, cinnamon and clove bud at glass vial bioassay method. Clove bud and cinnamon were significantly more effective considering to the efficiency of lavender. At concentration 0.15 µL/cm² there was significant difference between the efficiency of clove bud and lavender, however both caused less than 10% mortality.

Strong acaricidal effects of clove bud and cinnamon cause high rate of mortality of poultry red mites independently on method used. At testing lavender essential oil with lower acaricidal effect (except 0.5 concentration µL/cm²) influence of method may show up. Despite significant difference between methods at concentration 0.5 µL/cm² the mortality rate was very high in both methods.

Table 1 Influence of essential oils to mortality poultry red mites – comparison glass vial bioassay method and Petri-dishes method

Essential oil	Average mortality poultry red mites ± SE (%)					
	Dose (µL/cm²)					
	0.5	0.25	0.12	0.06	0.03	0.015
Clove bud glass vials	100.0 ± 0.0^{a}	100.0 ± 0.0^{a}	100.0 ± 0.0^{a}	100.0 ± 0.0^{a}	100.0 ± 0.0^{a}	100.0 ± 0.0^{a}
Clove bud Petri-dishes	98.3 ± 1.7^{a}	100.0 ± 0.0^{a}	93.3 ± 4.4^{a}	89.2 ± 8.2^{a}	100.0 ± 0.0^{a}	82.5 ± 11.1^{a}
Cinnamon glass vials	100.0 ± 0.0^{a}	100.0 ± 0.0^{a}	100.0 ± 0.0^{a}	100.0 ± 0.0^{a}	100.0 ± 0.0^{a}	100.0 ± 0.0^{b}
Cinnamon Petri-dishes	100.0 ± 0.0^{a}	93.8 ± 6.3^{a}	100.0 ± 0.0^{a}	99.2 ± 0.8^{a}	76.3 ± 8.2^{a}	39.2 ± 8.3^{a}
Lavender glass vials	100.0 ± 0.0^{b}	67.5 ± 13.5^{a}	18.3 ± 7.0^{a}	10.0 ± 3.7^{a}	3.3 ± 2.1^{a}	1.7 ± 1.7^{a}
Lavender Petri-dishes	97.5 ± 1.1^{a}	100.0 ± 0.0^{b}	80.8 ± 7.8^{b}	25.8 ± 5.4^{b}	25.0 ± 9.7^{a}	4.2 ± 2.4^{a}

Legend: a, b – the values marked with different letters make statistically significant difference between the methods in individual essential oil at specific concentration; SE – standard error of mean

CONCLUSION

The results of these experiments suggest that used essential oils derived from clove bud, cinnamon and lavender may make effective natural botanical pesticides against poultry red mites (*Dermanyssus Gallinae*). The most effective essential oils were oils derived from clove bud and cinnamon, lavender was generally less effective.

There was no significant effect of in vitro methods on poultry red mite mortality in essential oils with high acaricidal effect, cinnamon and clove bud, up to concentration 0.03 µL/cm². In vitro methods had significant effect on poultry red mite mortality using lavender essential oil, with lover acaricidal effect, at concentrations 0.5, 0.25, 0.12 and 0.06 µL/cm².

It is necessary to pay more attention in vitro methods testing lower concentration of essential oils or essential oils with lower acaricidal effect.

ACKNOWLEDGEMENTS

The research was financially supported by the grant no. AF-IGA-IP-2018/003.

REFERENCES

Dohnal, K. 2009. Nezvaný host Dermanyssus gallinae alias čmelík kuří. Drůbežář, 9: 9–13.

George, D.R. et al. 2009. Mode of action and variability in efficacy of plant essential oils showing toxicity against the poultry red mite, *Dermanyssus gallinae*. Veterinary Parasitology, 161: 276–282.

George, D.R. et al. 2010. Environmental interactions with the toxicity of plant essential oils to the poultry red mite *Dermanyssus gallinae*. Medical and Veterinary Entomology 24: 1–8.

Hubert, J. et al. 2015. Certifikovaná metodika pro hodnocení účinnosti akaricidních látek na skladištní roztoče a pro identifikaci rezistence. Praha: Výzkumný ústav rostlinné výroby, v.v.i.

Kim, S.-I. et al. 2004. Acaricidal activity of plant essential oils against *Dermanyssus gallinae* (*Acari: Dermanyssidae*). Veterinary Parasitology, 120: 297–304.

Kim, S.I. et al. 2007: Contact and fumigant toxicity of Oriental medicinal plant extracts against *Dermanyssus gallinae* (*Acari: Dermanyssidae*). Veterinary Parasitology, 145: 377–382.

Nordenfors, H. et al. 1999. Effects of temperature and humidity on oviposition, molting and longevity of *Dermanyssus gallinae* (*Acari: Dermanyssidae*). Journal of Medical Entomology, 36: 68–72.

Pavela, R. 2011. Botanické pesticidy. České Budějovice: Kurent, pp. 36–37.

Rádsetoulalová, I. et al. 2017. Acaricidal aktivity of plant essential oils against poultry red mite (*Dermanyssus Gallinae*). In Proceedings of International PhD Students Conference MendelNet 2017 [Online]. Brno, Czech Republic, 8 and 9 November, Brno: Mendel University in Brno, Faculty of AgriSciences, pp. 260–265. Available at: https://mnet.mendelu.cz/mendelnet2017/mnet_2017_full.pdf.

Sparagano, O.A.E. et al. 2013. Comparing Terpenes from Plant Essential Oils as Pesticides for the Poultry Red Mite (*Dermanyssus gallinae*). Transboundary and Emerging Diseases 60: 150–153.

Sparagano, O.A.E. et al. 2014. Significance and Control of the Poultry Red Mite, *Dermanyssus gallinae.* Annual Review of Entomology, 59: 447–66.

Teuling, M. 2017. The battle against red mites. Poultry World [Online]. Available at: http://www.poultryworld.net. [2018-08-15].

Analysis of performance of horses in the Czech Republic and in the world based on dressage competitions

Katarina Souskova, Eva Sobotkova
Department of Animal Breeding
Mendel University in Brno
Zemedelska 1, 61300 Brno
CZECH REPUBLIC

souskovakatarina@gmail.com

Abstract: This work is focused on horses participating in dressage competitions in Czech Republic and in the whole world. We tested statistical evaluation of the effect of the age, breed, sex and year of start on performance in dressage competitions. The data were taken from rankings of the best dressage horses that are issued by the Czech Equestrian Federation and from world dressage rankings that are issued by Fédération Équestre Internationale. We focused on the year 2010 and 2016. The dressage performance has been evaluated on the basis of reached auxiliary points (AAP) in Czech rankings and points in world rankings. We have processed and evaluated the data using programmes STATISTICA 2012 and UNISTAT 6.5. Factor of the age, sex and breed have a statistically highly evaluated influence on dressage performance of the best dressage horses in Czech Republic. The highest performance have the horses at the age of 17 and higher (5.59 AAP), stallions (6.08 AAP) and breed KWPN (6.15 AAP). Factor of age, breed and year of start have a statistically highly evaluated influence on dressage performance of the best dressage horses in the world. Horses at age from 7 to 12 years (1340.21 points) and group of Scandinavian Warmblood Breeds (1448 points) have the highest dressage performance in the world rankings. Performance of the horses included in dressage rankings increased from the 2010 to year 2016 in Czech Republic and also in the world.

Key Words: dressage, performance, competition

INTRODUCTION

Dressage, the highest expression of horse training, is considered to be the most artistic of the equestrian sports and can be traced back to the ancient Greece. The horse has to perform at a walk, trot and canter, and all tests are ridden from memory and follow a prescribed pattern of movements. The only exception is the Freestyle which is specially choreographed for each horse and is performed to music. The popularity of Dressage has increased rapidly in recent years and the sport now regularly attracts huge crowds. Dressage is undoubtedly the most aesthetically pleasing of the disciplines in the FEI stable (FEI 2016).

The object of dressage is the harmonious development of the physique and ability of the horse. As a result, it makes the horse calm, supple, loose and flexible, but also confident, attentive and keen, thus achieving perfect understanding with his rider (Loch 1990).

These qualities are demonstrated by the freedom and regularity of the paces, the harmony, lightness and ease of the movements, the lightness of the forehand and the engagement of the hindquarters, originating from a lively impulsion, the acceptance of the bit, with submissiveness, thoroughness without any tension or resistance (FEI 2018).

Equestrian sports have become more popular over the last decades. Success at the highest level of competition requires an intensive preparation. Horses therefore are competing more and more in only one of the disciplines to maximize the chance of winning. Breeders increasingly focus on one specific discipline in their breeding and mating decisions. (Rovere et al. 2017)

Rating dressage performance is a current worldwide theme that is debated from the point of genetics (Steward et al. 2009), veterinary (Jongersen 1996) and breeding (Popovici et al 2014, Koenen and Aldridge 2002).

MATERIAL AND METHODS

For the determination of a comparative base we used Ranking of the Best Dressage Horses of 2010 and 2016 that is issued by the Czech Equestrian Federation. Horses included in this rankings started in dressage competitions at least 6 times during evaluated years in Czech republic. The horses in the rankings are arranged according to the average auxiliary points (AAP). Auxiliary points are obtained by a conversion of the actual result of the horse in dressage competitions converted by means. We also used Dressage World Ranking of 2010 and 2016 that is issued by Fédération Équestre Internationale. The horses in the rankings are arranged according to points. Matrices for calculation of auxiliary points and points are different so we cannot compare them between each other. From each ranking we eliminated a pony.

For statistical analysis we used the programme STATISTICA 2012 and UNISTAT 6.5. In descriptive statistic we evaluated arithmetical mean, modus, median, maximum, minimum and standard deviation. For statistical analysis we used the method (Analysis of Variance) ANOVA and following tests by Scheffe´s multiple comparisons. We used the multi-factorial analysis.

RESULTS AND DISCUSSION

We can see from the Table 1 and Table 2 that average dressage performance is growing in Czech Republic (from 3.97 to 5.22 AAP) and in the world (from 1103.15 to 1565.9 points). Median, minimum and maximum values was higher in 2016 than in 2010. Increasing values show improved dressage performance among best dressage horses in both, Czech Republic and the world.

Table 1 Descriptive statistic of evaluations of the performance (according to auxiliary points) of best dressage horses in Czech Republic in 2010 and 2016

AAP variable	Mean	Median	Minimum	Maximum	Standard deviation	Variable coefficient
2010	3.97	3.06	1.25	14.78	2.96	74.51
2016	5.22	4.25	1.88	21.11	3.61	69.2

Table 2 Descriptive statistic of evaluations of the performance (according to points) of best dressage horses in the world in 2010 and 2016

Points variable	Mean	Median	Minimum	Maximum	Standard deviation	Variable coefficient
2010	1103.15	1082	542	2771	383.35	0.35
2016	1565.9	1499	1105	2928	332.26	0.21

Thanks to the statistic method ANOVA we found out that factor of the age, sex and breed had statistically higher significance effect on the performance of best dressage horses in Czech Republic. In the world factor of the age, breed and year of start was statistically highly significant. We did not prove effect of the sex.

Table 3 Effect of the respective factors on the performance of best dressage horses in Czech Republic

Performance	Age	Sex	Breed	Year of start
AAP	**	**	**	-

$P \leq 0.01$ (**) statistically highly significant, $P \leq 0.05$ (*) statistically significant

Table Effect of the respective factors on the performance of best dressage horses in the world

Performance	Age	Sex	Breed	Year of start
Points	**	-	**	**

$P \leq 0.01$ (**) statistically highly significant, $P \leq 0.05$ (*) statistically significant

Factor of the age had statistically highly significant effect on dressage performance in Czech Republic and in the world. Stewart et al. (2009) also state that age of the horse was significantly associated with performance.

Figure 1 Average values of points of the respective age groups

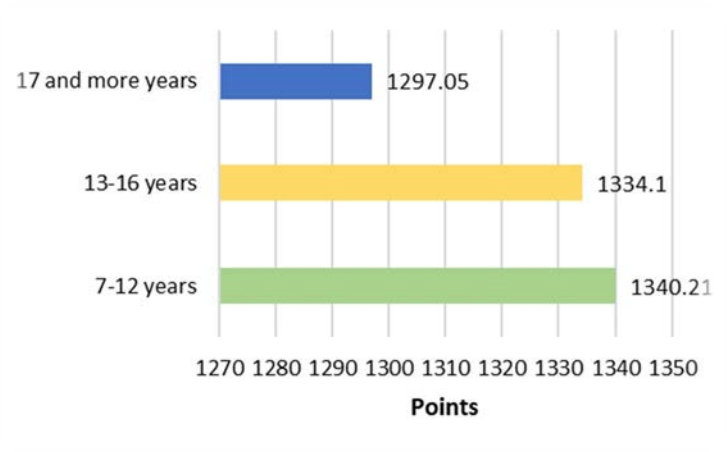

Figure 2 Average values of auxiliary points of the respective age groups

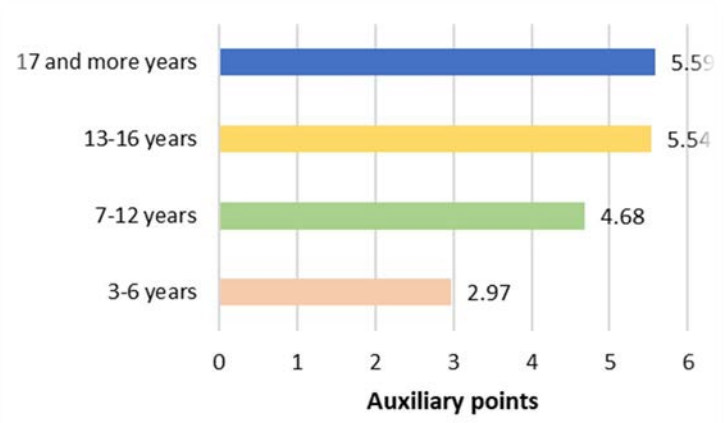

In world dressage ranking, there are only horses which are older than seven years due to the highest level of the competitions. Compare to this in Czech Republic there is also a younger group from 3 to 6 years and these horses compete in lower level competitions. In the world the highest performance is reached by the group from 7 to 12 years (1340.21 points). In Czech Republic the oldest group had the highest performance (5.59 AAP). Due to higher level and requirement in world rankings more successful are horses in most productive age. The highest performance of the oldest group in Czech Republic is mostly caused by few individuals with really good results. Stewart et al. (2009) state that it is unusual for horses to compete at advanced ages and only the most consistent horses will continue to compete. We can state that in dressage sport the experience is very important but on the Grand Prix level the horses from 7 to 12 years are the most successful.

We statistically proved the effect of sex on performance of best dressage horses in Czech Republic but not in the world. This can be caused by the fact that all horses in world rankings compete in the highest level. Contrary to this, there are also some horses among the best dressage horses in Czech Republic that compete in lower level competitions. In the world rankings higher standards are required and there are stallions, geldings and mares with similar dressage performance. In Czech Republic group of stallions had highest performance (6.08 AAP), than it was in group of geldings (4.5 AAP), and group of mares (3.81 AAP) had lowest dressage performance. This can be caused by problematical behaviour of mares. Jongersen (1996) states that trainers who are involved in various components of equine industry frequently report variations in the performance of a mare apparently related to the estrus cycle. Pryor and Tibary (2005) state that estrus has long been considered an important factor in reduced athletic performance. Budzynska et al. (2014) state that sex has an effect on behavioural reactivity of horses an it is important to consider this factor during selection for a particular type of riding. Brudňaková (2018) stated that group of stallions had the highest performance in show jumping competitions.

Figure 3 Average values of auxiliary points of the respective sexes

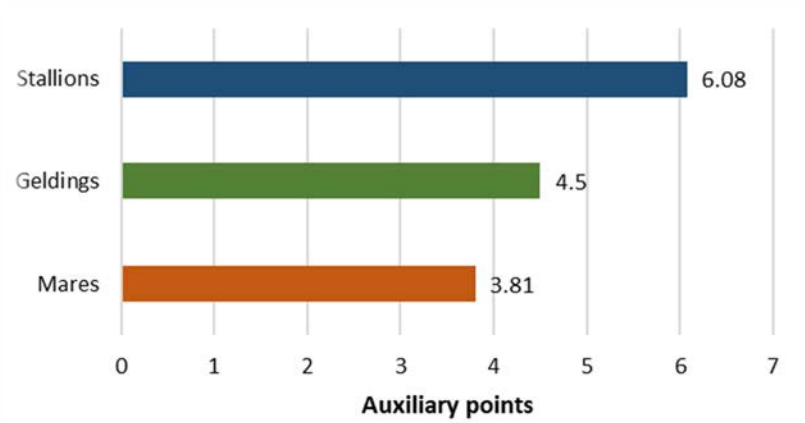

Factor of the breed was proved as statistically highly significant in both rankings. Stewart et al. (2009) state that breed significantly affects dressage competition performance.

Figure 4 Average values of points of respective breed

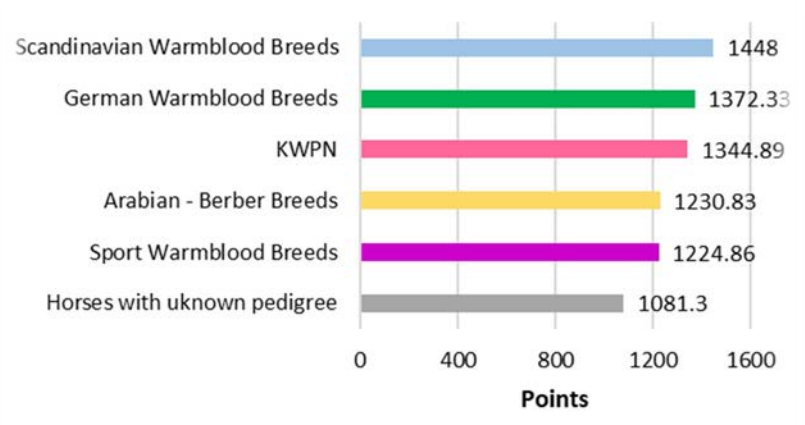

Figure 5 Average values of auxiliary points of respective breeds

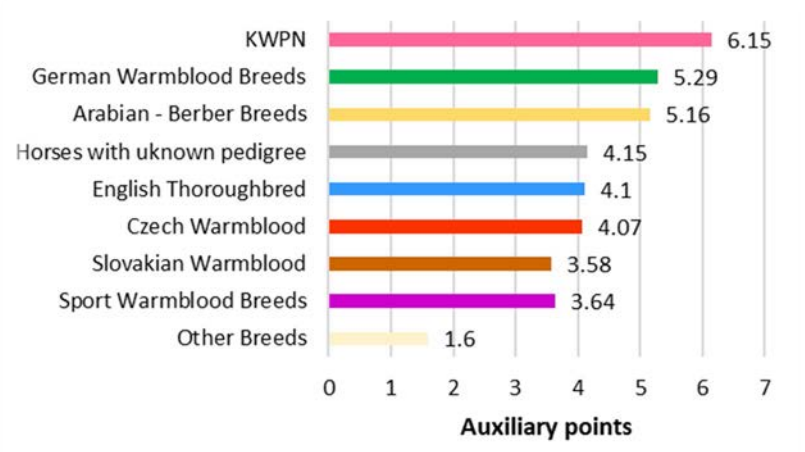

As we can see from Figure 4, the highest dressage performance in the world was reached by group of Scandinavian Warmblood Breeds (1448 points) such as Danish Warmblood, Finnish Warmblood, Estonian Sport Horse and Swedish Warmblood. German Warmblood Breeds and KWPN had high performance in both, world and Czech rankings. Rovere et al. (2015) state that most warmblood horse stud books aim to improve the performance in sport and that the Dutch Royal Warmblood Studbook (KWPN) includes the highest score achieved in competition by a horse to evaluate its genetic ability

of performance. Arabian - Berber Breeds are still on a higher position in dressage sport but due to extended paces that are very important in modern dressage these breeds have lower performance. In Ranking of the Best Dressage Horses of Czech Republic there are also other breeds represented, mostly English Thoroughbred and Czech Warmblood horses. In Czech Republic group of other breeds (1.6 AAP) had the smallest number of reached points. Stewart et al. (2009) found out in their study that breeds that are not breeding for dressage had lower performance in this discipline.

CONCLUSIONS

In the present study we evaluated the effects of the individual factors on the dressage performance of horses included in Czech and world rankings. Evaluation of the sport performance was based on the auxiliary points in Czech ranking and points in world ranking. We tested statistical evaluation of the factor of the age, breed, sex and year of start on dressage performance of the horses. We used data from year 2010 and 2016.

When we compare year 2010 and 2016, we can see increasing values that show improved dressage performance among the best dressage horses in both, Czech Republic and the world.

We found out that factor of the age, sex and breed had statistically highly significant effect on the performance of the best dressage horses in Czech Republic. In the world factor of the age, breed and year of start was statistically highly significant.

Our results show that group from 7 to 12 years had the highest dressage performance in world ranking. In Czech ranking it was the oldest group. We can conclude that because of the higher level and requirement in world rankings horses in the most productive age are more successful. The youngest group is not represented in the world ranking because of the Grand Prix level of competitions and in Czech ranking this group had the lowest performance. This can be caused by the fact that this horses compete in lower level competitions and are not experienced enough. We can state that dressage sport experiences are very important but on the top level competitions horses from 7 to 12 year are the most successful.

We statistically proved the effect of the sex on dressage performance just in Czech ranking. In Czech Republic group of stallions had the highest performance, than it was group of geldings and group of mares had the lowest dressage performance. Such a good results of stallions can be caused by the fact that dressage is subjectively marked discipline so temperament and presentation of stallions can have an effect on its rating. There can be also some problems with mares such as problematical behaviour and back pain related to their estrous cycle.

Our statistical analysis showed that group of Scandinavian breeds had the highest dressage performance in world ranking. German Warmblood Breeds and KWPN had high performance in both, world and Czech rankings. In Czech ranking there are also other breeds represented, mostly Czech Warmblood, Slovakian Warmblood and English Thoroughbred. These breeds are successful in lower level competitions but only a few individual horses compete in Grand Prix level.

Our results show some differences in Czech and world dressage sport caused by different standards that are set for its rankings. In world ranking, there are higher requirements than in Czech Republic so the results are different.

In conclusion I want to recommend to riders, who want to compete in the top level dressage competitions, to choose one of the foreign breeds that are selected for sport performance such as Scandinavian Warmblood Breeds, German Warmblood Breeds and KWPN and horses from 7 to 12 years.

REFERENCES

Budzynska, M. et al. 2014. Behavioural and physiological reactivity of mares and stallions evaluated in performance tests. Acta Veterinaria-Beograd, 64(3): 327-337. [Online]. Available at: https://content.sciendo.com/view/journals/acve/64/3/article-p327.xml. [2018-10-25].

Brudňaková, M. 2018. Analysis of Performance of Horses in Czech Republic Based on Show Jumping Competitions. In Animal Breeding 2018 [Online]. Mendelova univerzita v Brně, pp. 11-19. Available at: https://is.mendelu.cz/auth/lide/clovek.pl?id=69038;zalozka=5;podrobnosti=266409. [2018-08-09].

ČJF. 2010. Přehled o sportovních koních ČR 2010 [Online]. Available at: http://www.cjf.cz/files/stranky/dokumenty/prehledy-o-sportovnich-konich/roc-2010-web.pdf. [2018-08-08].

ČJF. 2016. Přehled o sportovních koních ČR 2016 [Online]. Available at: http://www.cjf.cz/files/stranky/dokumenty/prehledy-o-sportovnich-konich/rocenka2016-05-zebricky.pdf. [2018-08-11].

FEI 2016. About Dressage. [Online]. Available at: https://inside.fei.org/fei/disc/dressage/about-dressage. [2018-08-12].

FEI Dressage World Ranking. [Online]. Available at: https://data.fei.org/Ranking/Search.aspx?rankingCode=D_WR. [2018-08-23]

FEI 2018. Dressage Rules [Online]. Available at: https://inside.fei.org/sites/default/files/DRE-Rules_2018_Clean_Version_0.pdf. [2018-08-04].

Jongersen, J.S. 1996. Effect of the estrous cycle on performance in athletic mares. Compendium on Continuing Education for the Practicing Veterinarian [Online], 18: 692–698. Available at: https://www.researchgate.net/publication/281595909_Effect_of_the_estrous_cycle_on_performance_in_athletic_mares. [2018-08-10].

Koenen, E.P.C., Aldridge, L.I. 2002. Testing and Genetic Evaluation of Sport Horses in an International Perspective. In Conference at the 7th World Congress Genetic Applied to Livestock Production [Online]. Montpellier, France, 19–23 August, pp. 1–5. Available at: https://www.biw.kuleuven.be/genlog/livgen/research/interstallion/publications/wcgalp-paper.pdf. [2018-08-10].

Loch, S. 1990. Dressage: The Art of Classical Riding. Hampshire: The Sportsman´s Press.

Popovici, A.R. et al. 2014. Competition dressage horses: Effect of age, sex and breed on the FEI/WBFSH world ranking. Journal of Biotechnology. 185: 39. [Online]. Available at: https://www.sciencedirect.com/science/article/pii/S0168165614004763. [2018-08-16].

Pryor, P., Tibary, A. 2005. Management of Estrus in the Performance Mare. Clinical Techniques in Equine Practise [Online], 4: 197-209. Available at: https://www.sciencedirect.com/science/article/pii/S153475160500065X. [2018-10-25].

Rovere, G. et al. 2015. Analysis of competition performance in dressage and show jumping of Dutch Warmblood horses. 2015. Journal of Animal Breeding and Genetics [Online], 133: 503-512. Available at: https://www.ncbi.nlm.nih.gov/pubmed/27237865. [2018-10-25].

Rovere, G. et al. 2017. Genetic correlations between dressage, show jumping and studbook-entry traits in a process of specialization in Dutch Warmblood horses. Journal of Animal Breeding and Genetics [Online], 134: 162–171. Available at: https://www.ncbi.nlm.nih.gov/pubmed/27678258. [2018-10-25].

Steward, I.D. et al. 2009. Genetic evaluation of horses for performance in dressage competitions in Great Britain. Livestock Science [Online], 128: 36–45. Available at: https://www.sciencedirect.com/science/article/pii/S1871141309003424. [2018-08-16].

The influence of postpartum metabolic disease on the milk composition in the first hundred days of lactation in dairy cows

Barbora Umlaskova, Katerina Mrvova, Leos Pavlata
Department of Animal Nutrition and Forage Production
Mendel University in Brno
Zemedelska 1, 613 00 Brno
CZECH REPUBLIC

xumlasko@mendelu.cz

Abstract: The goal of the study is to monitor the parameters of milk in dairy cows during the first 100 days of lactation. The cows, breed of Czech Pied (n = 1918) were included in the trial. Data gained during the regular control of performance were gathered during two years and analysed and processed in program Milk Profit Data. According to the results, the health of the herd was evaluated. The correlation between the individual parameters and the occurrence of metabolic disease was observed. Data of Milk Profit Data were divided into three groups (According to the stage of lactation – first 21 days, a period from 22 to 60 days, and the rest of it). In the milk samples selected parameters were analysed (milk fat, milk protein, fat/protein, lactose, somatic cell count (SCC), milk urea, citric acid, β-hydroxybutyrate, acetone, free fatty acids). The number of lactation, the day of ongoing lactation and the yield are also known from the control of performance. Based on the results, the correlation between negative energy balance and increased values of ketone bodies as β-hydroxybutyrate and acetone were observed. There is a statistically significant difference in the amount of fat in milk between the first 21 days of lactation (4.10 ± 0.70%) and the rest of the observed period (3.83 ± 0.62% and 3.87 ± 0.60%). That is related to the lipolysis at the beginning of lactation. The older cows on the higher number of lactation are much more predisposed for ketosis development. That is confirmed by the positive correlation between the amounts of BHB and number of lactation.

Key Words: ketosis, negative energy balance, postpartum period, milk, control of performance

INTRODUCTION

The transition period in dairy cows is the closest period to the parturition. It takes 3 weeks before and 3 weeks after the birth (Drackley 1999). This time is decisive for the next lactation. The cows suffer from the negative energy balance (NEB) that is connected with the parturition. There are a lot of physiological changes for the individual cow. Because of that, the disease incidence in early lactation is high (Smith et al. 2017). In case of developing NEB ketogenesis occurs. Increasing values of β-hydroxybutyrate (BHB) are associated with the risk of developing the other diseases like displaced abomasa, clinical ketosis, retained placenta or metritis (Ospina et al. 2010). All these metabolic disorders or infectious diseases are reflected in the composition of the milk. The metabolic diseases belong to the risk factors for the development of mastitis and may influence milk composition and its quality. During the mastitis, the increased number of somatic cells is noticed, especially polymorphonuclears (Lukášová 1999). Control of performance includes cow specification, milk yield, and data gained from laboratory analysis. These include determination of milk fat, milk protein, fat/protein, lactose, somatic cell count (SCC) and milk urea (ČMSCH 2016). There are also the milk minor constituents like ketones (acetone, BHB), citric acid and free fatty acids (Pavlata 2018). The results of control performance pride money. This is important for the farmers. Not only of the cost of treatment during the mastitis and other diseases but also the high financial penalties in case of antibiotic residues that can be identified in bulk milk (Blowey and Edmondson 2010). Moreover, these data show the state of health of the herd. The observation of ketone bodies in milk and blood is the easiest way for the prevention or the diagnosis of ketosis. There exists the correlation between their values in blood and milk. The concentration of acetone, acetoacetate, and BHB is analysed. High correlation coefficients were found between acetone and acetoacetate in blood, and between milk and blood acetone. As the best

way for detection of subclinical ketosis with the most sensitivity and specificity combination, the acetoacetate in blood and milk was obtained, with the thresholds 125 and 50 µmol/l, respectively (Enjalbert et al. 2001).

MATERIAL AND METHODS

The target of this article was to process data obtained from the control of performance (CP). The observed animals were Czech Pied breed in their first 100 days of lactation. They were stalled at one farm. The data were gathered during two years. All the animals included in the trial were fed with the same feed ration determined to the cows at the peak of lactation. Feed ration was consisted of maize silage (24 kg), hay (1 kg) and concentrate mixture (10 kg). The concentrate mixture contained cereals, protein concentrate (soybean and rape meal solvent extract) and vitamins (0.25 kg).

Between determined components of milk belong milk fat, milk protein, fat/protein, lactose, somatic cell count (SCC), milk urea, nitrogenous substances, energy, citric acid, acetone, BHB, and free fatty acids (FFA). The other data that are known from CP is milk yield in the testing day, a day of ongoing lactation, and the number of lactation. All these data were gathered and divided into three groups according to the stage of lactation. Cows in the first 21 days of lactation were in the group one, the second group includes cows between 22 and 60 days of lactation, and the rest of the trial herd makes the group 3 (61 to 100 days of lactation).

Data has been processed by Microsoft Excel (USA) and Statistica version 12.0 (CZ). We used one-way analysis (ANOVA). To ensure evidential differences Scheffe´s test was applied and $P < 0.05$ was regarded as the statistically significant difference. The relationship of the set parameters was tested by correlation analysis. For the relationship of values, the correlation coefficient (r) was calculated.

RESULTS AND DISCUSSION

The results of the milk data are presented in Tables 1 and 2. The relationship between individual milk parameters is presented in Table 3.

Table 1 Milk constituents (mean ± standard deviation) in dairy cows divided into three groups first 21 days of lactation (21), second group till 60 days (60) and the last till 100 days of lactation (100). Fat [%], protein [%], fat/protein (F/P), lactose [%], somatic cell count (SCC)[thousand/ml], urea [mg/100ml].

	Fat	Protein	F/P	Lactose	SCC	Urea
21	4.10 ± 0.70^{b}	3.44 ± 0.33^{a}	1.20 ± 0.21^{c}	5.03 ± 0.21^{a}	328.38 ± 969.69^{b}	28.44 ± 4.80^{ab}
60	3.83 ± 0.62^{a}	3.30 ± 0.27^{b}	1.16 ± 0.21^{b}	5.07 ± 0.19^{b}	190.10 ± 515.03^{a}	28.16 ± 4.41^{a}
100	3.87 ± 0.60^{a}	3.46 ± 0.28^{a}	1.12 ± 0.17^{a}	5.01 ± 0.19^{a}	200.21 ± 517.48^{a}	29.05 ± 4.54^{b}

Legend: $^{a, b, c}$ – different letter in column means statistically significant difference $P > 0.05$

Milk fat is the indicator of metabolic disease. It is produced in the mammary gland from acetic acid. The milk fat threshold is 3.5–4.5%. The average value in whole testing group (n = 1918) is 3.88 ± 0.63%. The values in the individuals' groups divided according to the stage of lactation can be seen in Table 1. The statistically significant difference was proved in the first 21 days of lactation and the rest. There can be observed the increased fat level in milk at the beginning of ketogenesis, due to lipolysis. On the other hand, lack of fibre in food causes decreased values of fat in milk (Pavlata 2018). Schulz et al. (2014) described that cows fed with high energy food had statistically higher levels of milk fat compared to normally fed cows. The values of milk fat were 6.04 ± 0.31% and 4.33 ± 0.31% respectively in the first two weeks postpartum and 4.33± 0.24% and 4.03 ± 0.24% in the next period in two months.

Level of protein in milk is influenced by the amount of energy in food. The nutrition and level of rumen fermentation, metabolic diseases, breed, number and stage of lactation are the factors that influence the synthesis of milk protein (Doubek 2007). There were observed a statistically significant difference between the period 1 and 2 (3.44 ± 0.33 and 3.30 ± 0.27) and between the period

2 and 3 (3.30 ± 0.27 and 3.46 ± 0.28). All the values were in the reference range (3.1–3.8%). The values are comparable to the study from 2014 (Schulz 2014). The ratio of fat to protein (F/P) is the indicator of energy balance and acidogenic stress. It is supposed to be between 1.05 and 1.18 for Holstein. The increased level shows the energy deficit and so ketosis (Pavlata 2018). There was proved the positive correlation between F/P and the number of lactation. Prevalence of ketosis increases from a low prevalence in the first lactation and the follow-up lactations. The age prevalence was highest (40.8%) at the age of 5.5–6.5 years (Sangram et al. 2016). The negative correlation between F/P and the lactation stage proves negative energy balance caused by the excessive energy load at the beginning of lactation.

Table 2 milk minor constituents (mean ± standard deviation) in dairy cows divided into 3 groups – first 21 days of lactation (21), second group till 60 days (60) and the last one till 100 days of lactation

	Yield [kg]	Energy	Citric acid [%]	Acetone [mmol/l]	BHB [mmol/l]	FFA [mmol/100g of fat]
21	29.93 ± 6.90^{a}	-0.13 ± 2.03^{a}	0.18 ± 0.04^{b}	0.05 ± 0.05^{a}	0.03 ± 0.03^{a}	0.65 ± 0.36^{a}
60	31.05 ± 6.87^{a}	-0.96 ± 1.90^{b}	0.17 ± 0.03^{a}	0.05 ± 0.04^{a}	0.03 ± 0.03^{a}	0.68 ± 0.35^{a}
100	28.58 ± 6.46^{b}	0.15 ± 1.99^{a}	0.17 ± 0.03^{a}	0.05 ± 0.04^{a}	0.03 ± 0.03^{a}	0.75 ± 0.37^{b}

Legend: $^{a, b, c}$ – different letter in column means statistically significant difference P > 0.05
FFA – free fatty acids

The urea is the indicator of nitrogen intake and metabolism. The level above 33 mg/100 ml points at lack of energy or increased intake of nitrogenous substances. Another reason for increased values the mastitis case is. On the contrary, the amounts lower than 15 mg/100 ml can be seen in the case of the dietetic fault, liver insufficiency or long-term anorexia (Doubek 2007). The reference interval ranges from 20 to 30 mg/100 ml. The all average values were observed as physiological (28.44 ± 4.80 mg/100 ml, 28.16 ± 4.41 mg/100 ml, 29.05 ± 4.54 mg/100 ml). Epithelium and leucocytes belong to somatic cells. The increased number of these attests to mastitis, deficiency of selenium and zink, metabolic disease, a method of milking etc. The limit of somatic cell count (SCC) done by the norm must not exceed 400 000 in 1 ml of milk. None of the average values of SCC transcends the limit, but there was the statistically significant difference between the first period and the following periods (328.38 ± 969.69, 190.10 ± 515.03, 200.21 ± 517.48). Retrospective studies indicate the increased number of somatic cells in cows in which the dry period was reduced. However, the other experimental studies did not prove the influence on SCC and the length or even absence of dry period (Čermáková et al. 2014).

Subclinical ketosis is a metabolic disorder that often goes undiagnosed and causes economical loses in farms. It is characterized by increased levels of ketone bodies in blood, milk, and urine. The ketone bodies in milk correlate with the increased amount of ketone bodies in the blood. The monitoring of these is important especially in dairy cows in their first third of lactation when the highest prevalence of ketosis is supposed to be. Ketones that are analysed from the milk sample are acetone and BHB. Neither acetone nor BHB were observed risen in their average values during the first 100 days of lactation (0.05 ± 0.05 mmol/l, 0.05 ± 0.04 mmol/l, 0.05 ± 0.04 mmol/l for acetone, and 0.03 ± 0.03 mmol/l for BHB). Nevertheless, only individual samples have the diagnostic significant importance. As a table of correlation (Table 3) shows, there is a negative correlation between ketones (both acetone and BHB) and milk protein, nitrogenous substances, and energy.

All these parameters are decreased in the energy deficit. The positive correlation between BHB and somatic cell count can be seen. That confirms increase mastitis incidence in ketosis.

Higher amounts of free fatty acids (FFA) in the individual milk samples show the presence of metabolic disorder as negative energy balance, lipomobilisation syndrome, ketosis, mastitis. The highest limit for FFA in milk is supposed to be under 1.3 mmol/100 g of fat (ČMSCH 2016). The average value of FFA in the first 100 days of lactation was 0.70 ± 0.36 mmol/100 g of fat. According to the results of the correlation with the lack of energy the amount of FFA rises.

Table 3 Correlation (r) in all milk samples (n =1918) – lactation number (L No), day of lactation (D of L), yield, fat, protein, Fat/protein (F/P), lactose, somatic cell count (SCC), urea, nitrogenous substances (NS), energy, citric acid (CA), acetone, β-hydroxybutyrate (BHB), free fatty acids (FFA).

	L No	D of L	Yield	Fat	Protein	F/P	Lactose	SCC	Urea	NS	Energy	CA	Acetone	BHB	FFA
L No															
D of L	-0.02														
Yield	0.38**	-0.15**													
Fat	0.10**	-0.09**	0.03												
Protein	-0.06	0.14**	-0.29**	0.22**											
F/P	0.13**	-0.16**	0.18**	0.85**	-0.31**										
Lactose	-0.29**	-0.09**	-0.01	-0.10**	-0.15**	-0.02									
SCC	0.14**	-0.04	-0.11**	0.07*	0.10**	0.01	-0.35**								
Urea	-0.03	0.09**	-0.06	0.16**	-0.08*	0.19**	0.10**	-0.08**							
NS	-0.14**	0.13**	-0.35**	0.15**	0.05	0.12**	0.07	-0.03	0.78**						
Energy	-0.12**	0.18**	-0.44**	0.19**	0.91**	-0.29**	-0.10**	0.10**	0.10**	0.10**					
CA	0.03	-0.13**	0.08*	0.30**	-0.16**	0.38**	-0.01	-0.04	-0.04	0.05	-0.15**				
Acetone	0.04	-0.05	0.08**	0.01	-0.10**	0.06	-0.09**	0.06	0.06	-0.11**	-0.09**	0.38**			
BHB	0.11**	-0.04	0.04	0.15**	-0.21**	0.26**	-0.29**	0.15**	0.15**	-0.07*	-0.19**	0.41**	0.58**		
FFA	-0.11**	0.13**	-0.06*	-0.01	-0.18**	0.09**	0.09**	-0.02	-0.02	0.16**	-0.15**	-0.01	-0.03	-0.03	

*Legend: *p < 0.05; **p < 0.01*

CONCLUSION

The results of the research show the correlation between the individual parameters characterising energy supply and development of the metabolic disease, especially lipomobilisation syndrome and ketosis. There was also confirmed the connection between the age of the cow (lactation number) and incidence of ketosis. Development of ketosis manifests itself with increased values of BHB influence somatic cell count. However, the average values of milk samples do not have the corresponding value. The individual values are necessary for the prevention and diagnosing the ketosis.

ACKNOWLEDGEMENTS

The research was financially supported by the project of IGA FA MENDELU No. AF-IGA-2018-tym002 and the authors wish to express their thanks.

REFERENCES

Blowey, R., Edmondson, P. 2010. Mastitis Control in Dairy Herds [Online]. 2nd ed., Wallingford: CABI. Available at: https://lactoscan.com/editor/ufo/manuals/SCC/Mastitis_Control_in_Dairy_Herds_2nd (veterinary-student.blogfa.com).pdf. [2018-08-08].

Čermáková, J. et al. 2014. Zkrácená doba stání na sucho a její vliv na zdraví mléčné žlázy a telat. Veterinářství, 64: 29–33.

ČMSCH. 2016. Zásady provádění kontroly mléčné užitkovosti. [Online]. Available at: https://www.cmsch.cz/getattachment/Ke-stazeni/Kontroly-uzitkovosti/Metodika-Zasady-provadeni-kontroly-mlecne-uzitko/2018_zasady_provadeni_kontroly_mlecne_uzitkovosti.pdf.aspx/?lang=cs-CZ. [2018-09-12].

Doubek, J. 2007. Interpretace základních biochemických a hematologických nálezů u zvířat. 1st ed., Brno: Noviko.

Drackley, J.K. 1999. Biology of Dairy Cows During the Transition Period: The Final Frontier? Journal of Dairy Science [Online], 82(11). Available at: http://search.ebscohost.com/login.aspx?direct=true&db=edsagr&an=edsagr.US201302956343&scope=site. [2018-09-13].

Enjalbert, F. et al. 2001. Ketone Bodies in Milk and Blood of Dairy Cows: Relationship between Concentrations and Utilization for Detection of Subclinical Ketosis. Journal of Dairy Science - Champaign Illinois [Online], 84(3): 583–589. Available at: http://search.ebscohost.com/login.aspx?direct=true&db=edsbl&an=RN093148137&scope=site. [2018-09-13].

Hofírek, B. 2009. Poruchy metabolismu. In Nemoci skotu. Brno: Noviko, pp. 668–673.

Lukášová, J. 1999. Hygiena a technologie produkce mléka. Brno: Veterinární a farmaceutická univerzita Brno.

Ospina, P.A. et al. 2010. Evaluation of Nonesterified Fatty Acids and β-hydroxybutyrate in Transition Dairy Cattle in the Northeastern United States: Critical Thresholds for Prediction of Clinical Diseases. Journal of Dairy Science [Online], 93(2): 546–554. Available at: http://eds.b.ebscohost.com/eds/detail/detail?vid=6&sid=d64b32ec-c73d-4fde-908c-30eeb897697e%40sessionmgr120&bdata=Jmxhbmc9Y3Mmc2l0ZT1lZHMtbGl2ZQ%3d%3d#AN=48177489&db=bsu. [2018-09-13].

Pavlata, L. 2018. Inovace v chovu hospodářských zvířat – přežvýkavci. In Proceedings of Společnost mladých agrárníků. Kruh u Jilemnice, 15.–16. 1. 2018. Brno: Mendelova Univerzita v Brně.

Sangram, B. et al. 2016. Prevalence of Ketosis in Dairy Cows in Milk Shed Areas of Odisha state, India. Veterinary World [Online], 9(11): 1242–1247. Available at: http://eds.b.ebscohost.com/eds/detail/detail?vid=8&sid=d64b32ec-c73d-4fde-908c-30eeb897697e%40sessionmgr120&bdata=Jmxhbmc9Y3Mmc2l0ZT1lZHMtbGl2ZQ%3d%3d#AN=edsdoj.32f76916bfca4b88b50b1776e0fa7aa3&db=edsdoj. [2018-09-13].

Schulz, K. et al. 2014. Effects of Prepartal Body Condition Score and Peripartal Energy Supply of Dairy Cows on Postpartal Lipolysis, Energy Balance and Ketogenesis: An Animal Model to Investigate

Subclinical Ketosis. Journal of Dairy Research [Online], 81(3): 257–266. Available at: http://search.ebscohost.com/login.aspx?direct=true&db=edswsc&an=000340274300001&scope=sit. [2018-09-13].

Smith, G. et al. 2017. Association between Body Energy Content in the Dry Period and Post-calving Production Disease Status in Dairy Cattle. Animal [Online], 11(9): 1590–1598. Available at: http://search.ebscohost.com/login.aspx?direct=true&db=edswsc&an=000408019500021&scope=site. [2018-09-13].

The influence of sodium selenite and selenium nanoparticles on the antioxidant status of laboratory rats

Lenka Urbankova[1], Magdalena Pribilova[1], Pavel Horky[1], Jiri Skladanka[1], Pavel Kopel[2]
[1]Department of Animal Nutrition and Forage Production
[2]Department of Chemistry and Biochemistry
Mendel University in Brno
Zemedelska 1, 613 00 Brno
CZECH REPUBLIC

lenka.urbankova@mendelu.cz

Abstract: The aim of the experiment was to compare the influence of different forms of selenium (sodium selenite, selenium nanoparticles) on the organism of laboratory rats. The males of Wistar albino rat strain were sorted into 3 groups. The first group (n = 5) served as control with no selenium (Se) addition. The second group was fed with mixture containing 1.2 mg/kg of diet of sodium selenite (Na_2SeO_3). The third group (n = 5) was fed with mixture containing selenium nanoparticles (1.2 mg Se/kg of diet). After 30 days of experiment, the rats were slaughtered and antioxidant activity by TEAC and DPPH method were measured in liver, blood and kidney. Oxidative stress of organism was evaluated by levels of superoxide dismutase (SOD) and malonyldialdehyde (MDA) concentration. Statistically significant differences were measured in liver samples by the TEAC method (decrease in Na_2SeO_3 group by 47%, $p < 0.05$) and DPPH (decrease in both selenium groups, Na_2SeO_3 by 43% and SeNPs by 41%, $p < 0.05$). The addition of selenium almost did not affect the concentration of SOD in the organism. There was a small decrease in the level of MDA in the liver and kidney compared to the control group. Results showed selenium nanoparticles may be a potential candidate for further evaluation as selenium supplement with antioxidant properties and be used against selenium deficiency in organism.

Key Words: rats, nanoparticles, TEAC, DPPH, superoxide dismutase, malonyldialdehyde

INTRODUCTION

Selenium is a component of several major metabolic pathways, including antioxidant defense system, reproduction, thyroid hormone metabolism, immune function, and protecting the cells from the harmful effects of free radicals, and viral inhibition (Brown and Arthur 2001, El-Demerdash and Nasr 2014, Hoffmann and Berry 2008). Selenium is important for biosynthesis of selenoenzymes and selenoproteins (Dogan et al. 2016). Selenium concentration in plants is dependent from its content in the soil. In European Union the Se content is relatively low, therefore it is necessary to supplement it into the diet of farm animal (Horky et al. 2016). Nowadays, many researches try to develop new forms of selenium serving as an alternative source for selenium supplement for the animal body. Selenium deficiency leads to a higher rate of lipid peroxidation, damage of membrane structures, impaired reproduction, rapid aging of the organism (Horky et al. 2016). Therefore, the selenium supplement is recommended to the diet not only for humans but also for livestock. However, these Se supplements, especially the inorganic ones, are usually toxic when taken above their nutritional dosage (Zhang and Spallholz 2009).

Recent studies have shown that selenium nanoparticles exhibit lower toxicity by increasing the activity of seleno-enzymes compared to other selenium compounds (selenium, 3,5-selenomethionine, Se-yeast and methylselenocysteine) (Zhang et al. 2007). Moreover, they are able to inhibit the growth of microorganisms and exhibit anticancer activity (Tran and Webster 2011). Nanoparticles can be variously modified and becoming active and thus be the ideal medium for the targeted drug delivery as well as for nutrients in the body (Bai et al. 2017).

MATERIAL AND METHODS

Animals

The feeding experiment was carried out in the experimental facility of Department of Animal Nutrition and Forage Production of Mendel University in Brno. Throughout the whole experiment, microclimatic conditions were observed and controlled at temperature of 23 ± 1 °C and constant humidity of 60%. The photoperiod was maintained at 12 hours of light and 12 hours of darkness with a maximum illumination of 200 lx. As a model animals for this experiment males of the Wistar albino rat were selected and divided into 3 groups of 5 pieces. The average weight of rats at the beginning of the experiment was 139 grams. The first group served as a control with no addition of selenium in their feed. The second group was supplemented with selenium in the form of Na_2SeO_3 at a dose of 1.2 mg/kg of diet. The third group was fed with selenium in form of nanoparticles at a dose of 1.2 mg/kg of diet. All groups were fed with monodiet containing 0.03 mg Se/kg of diet. The experiment duration was 30 days. The animals had access to feed and drinking water ad libitum. At the end of the experiment, the animals were slaughtered (in accordance with the act on the protection of animals against cruelty No. 246/1992 Coll.) and samples of blood, liver and kidney tissue were collected and subjected to biochemical analyses.

Preparation of samples

Liver, kidney: 2 grams of samples from each variant were homogenized with the addition of liquid nitrogen and 1.5 mL of MilliQ water. After homogenization, each sample was sonicated using an ultrasound needle for 2 minutes, shaken for 10 minutes, and centrifuged for 20 minutes at 16 400 rpm and at 4 °C. 100 µL of supernatant was taken from each sample and mixed with 100 µL of 10% trifluoroacetic acid and centrifuged again for 20 minutes at 16 400 rpm and 4 °C. After the centrifugation, the supernatant was taken and analysed.

Blood: 200 µL of sample from each variant were placed into liquid nitrogen for 2 minutes and 500 µL of water was added. Each sample was sonicated with an ultrasound needle for 2 minutes, shaken for 1 minute, and centrifuged for 20 minutes at 16 400 rpm and at 4 °C. 200 µL of supernatant was taken from each sample and mixed with 200 µL of 10% trifluoroacetic acid. The samples were again centrifuged for 20 minutes at 16 400 rpm and 4 °C. After centrifugation, the supernatant was analysed.

Preparation of selenium nanoparticles modified by glucose and reduced by cysteine

250 mg of glucose was dissolved in Milli Q water (40 mL) with constant stirring. Subsequently, 5 mL of Na_2SeO_3. $5H_2O$ (0.263 g/50 mL) were added and the pH adjusted to 6.3 with 1 M HCl dropwise. Subsequently, 1 mL of cysteine (1.21/50 mL) was added. The mixture was decolorized to orange and the pH increased to 7.3.

Oxidative status determination

For determination of antioxidant activity, a BS-400 automated spectrophotometer (Mindray, China) was used. It was composed of cuvette space tempered to 37 ± 1 °C, reagent space with a carousel for reagents (tempered to 4 ± 1 °C), sample space with a carousel for preparation of samples and an optical detector. Transfer of samples and reagents is provided by robotic arm equipped with a dosing needle (error of dosage up to 5% of volume). Cuvette contents were mixed by an automatic mixer including a stirrer immediately after addition of reagents or samples. Contamination was reduced due to its rinsing system, including rinsing of the dosing needle as well as the stirrer by MilliQ water.

TEAC

Briefly, ABTS• (54.9 mg) was dissolved in 20 mL of phosphate buffer (pH 7.0; 5 mM) and activated to cation of ABTS+ radical by addition of MnO_2 (1 g) under occasional stirring for 30 min. Subsequently, volume of 15 µL of sample was added. Solution was subsequently diluted by phosphate buffer to absorbance (t0) 0.500 ± 0.01. Absorbance of solution was measured at $\lambda = 734$ nm.

DPPH

150 µL of R1 reagent (0.095 mM 2,2-diphenyl-1-picrylhydrazyl - DPPH) was pipetted into plastic cuvette. Subsequently, volume of 15 µL of sample was added. This method is based on the ability of stable free radical of 2,2-diphenyl-1-picrylhydrazyle to react with donors of hydrogen. DPPH has

strong absorption in UV-VIS spectrum, absorbance was measured for 12 min at λ = 505 nm. To assess the production of free radicals absorbance difference of the reagent without sample and reagent with sample after ten-minute incubation was taken.

Photometric determination of malondialdehyde according to Hong (2000)

The principle of malondialdehyde determination is reaction between malondialdehyde (MDA) with thiobarbituric acid (TBA) under formation of TBA-MDA-TBA adduct that absorbs strongly at 535 nm. Trichloroacetic acid (TCA) is added to the sample because of its ability to precipitate proteins, bilirubin, unsaturated fatty acids and lipoproteins. A 300 µL sample of blood plasma was mixed with 10 µL 0.5 M solution of butylated hydroxytoluene (BHT) in 96% ethanol (*v*/v) and 310 µL 20% TCA (*v*/*v*) prepared in 0.6 M HCl. After 20 min incubation on ice mixture was centrifuged at 11.000 rpm. for 15 min. Subsequently, 400 µL of supernatant was mixed with 800 µL of 30 mM TBA and mixture was incubated in a thermomixer Comfort (Eppendorf, Germany) at 90 °C for 30 min. After cooling in ice MDA absorbance was measured using a spectrophotometer at 535 nm and the concentration was subtracted from the calibration curve.

Determination of superoxide dismutase (SOD)

Kit 19160 SOD (Sigma Aldrich, USA) was used for assay of superoxide dismutase (SOD, EC 1.15.1.1.). A 200 µL volume of reagent R1 (WTS solution diluted 20 times with buffer) was pipetted into a plastic cuvette and agent was incubated at 37 °C for 108 s (1 min, 48 s). Afterwards, a 20 µL volume of sample was pipetted and in 378 s (6 min, 18 s), the reaction was started by adding a 20 µL volume of reagent R2 (enzyme solution 167 times diluted with buffer). Mixture was incubated for 72 s (1 min, 12 s) and then absorbance was measured at λ = 450 nm. Kinetic reaction was measured for 108 s (3 min) and absorbance was read every 9 s.

Statistics

The data were processed statistically using STATISTICA.CZ, version 12.0 (the Czech Republic). The results were expressed as mean ± standard deviation (SD). Statistical significance was determined using ANOVA and Scheffé's test (one-way analysis).

RESULTS AND DISCUSSION

The aim of the experiment was to determine whether new form of selenium, based on nanotechnology, can influenced the antioxidant status of rats. For this purpose, TEAC and DPPH method was applied to determination of antioxidant activity. Further, activity of SOD was determined because it is an important endogenous antioxidant enzyme that acts as a component of the first line of defence system against reactive oxygen species (ROS) (Ighodaro and Akinloye 2017). And as marker of lipid peroxidation and oxidative stress concentration of MDA was used.

Antioxidant activity was determined using TEAC and DPPH assays. Trolox was used as the standard. From the results is obvious that antioxidant activity of blood reached the similar levels in selenium treated groups (Na_2SeO_3, SeNPs) and control group (Figure 1). This effect could be explained by the ability of blood to quickly cope with oxidative stress (Horký 2014). Similar results have been confirmed by other authors (Urbankova et al. 2018, Horky et al. 2016). In the case of antioxidant status of liver, the significant difference was estimated between Na_2SeO_3 (decrease by 47%, $p < 0.05$) treated rats and control measured by TEAC method (Figure 1A). And also between Na_2SeO_3 (by 43%) and SeNPs (by 41%) group compared with control measured by DPPH method (Figure 1B). But not between groups fed by Na_2SeO_3 and SeNPs. The TEAC and DPPH method showed reduced antioxidant status of the experimental group in comparison to the control groups. In kidney samples in selenium groups decrease was measured but with no significant difference

Selenium supplementation (both Na_2SeO_3 and selenium nanoparticles) did not influence the enzymatic activity of SOD in blood, kidney and liver compared to the control sample (Figure 2A). It is obvious that Se supplementation (both of Na_2SeO_3 and SeNPs) did not reduce the activity of the important antioxidant defense against oxygen radicals in rats.

The disfunctions of the antioxidant system may be expressed by an increased degree of lipid peroxidation. In this study the lipid peroxidation level measured by (MDA) content was not significantly

different in experimental groups compared with control in all samples (liver, blood, kidney). Slight decrease was in blood, liver and kidney samples in SeNPs group (Figure 2B). Also López et al. (2010) observed lower levels of MDA when selenium (0.4 mg of Se/kg of diet) was added to the diet.

Figure 1 Influence of sodium selenite and selenium nanoparticles on antioxidant activity measured by TEAC (A) and DPPH (B) method

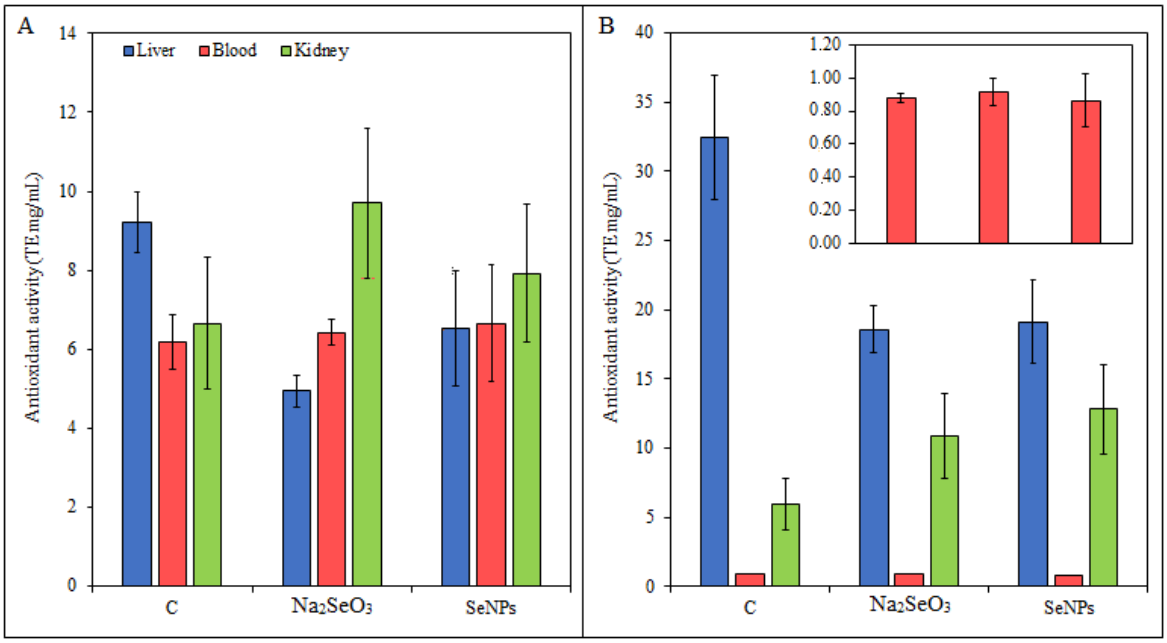

Figure 2 Influence of sodium selenite and selenium nanoparticles on SOD activity (A) and MDA concentration (B)

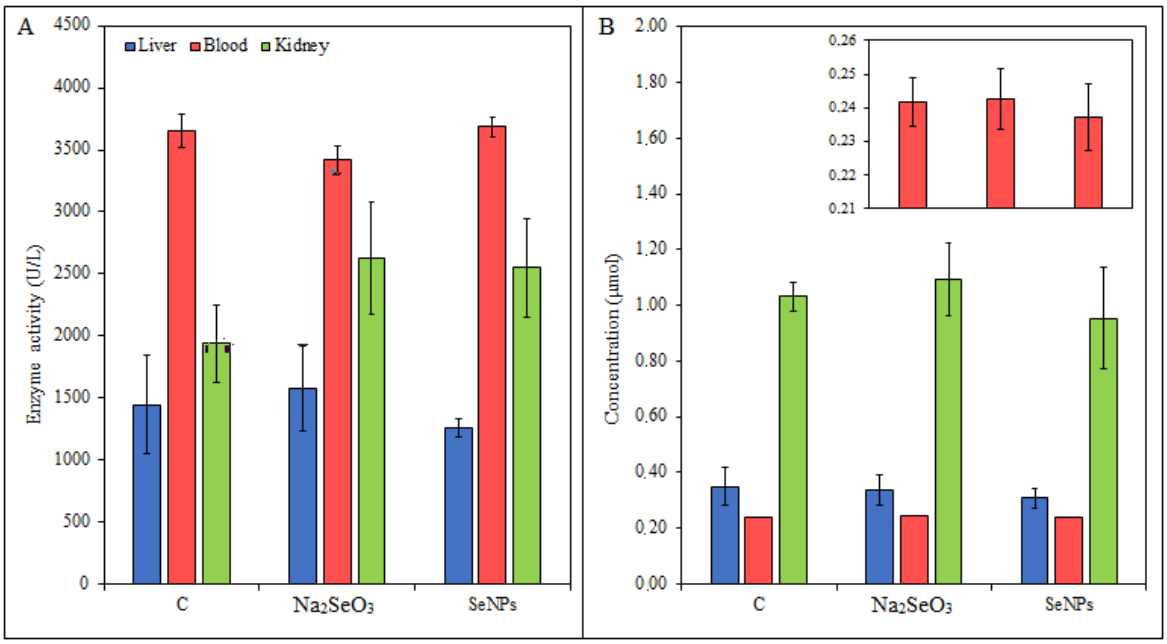

CONCLUSION

The Na_2SeO_3 and SeNPs supplementation of rats did not cause the damage the antioxidant system. The levels of the main indicators of oxidative stress were in the standard. Research suggests that

selenium nanoparticles can be used in nutrition of monogastric animals. For further investigation the selenium nanoparticles are perspective option in solving the issue of selenium supplementation.

ACKNOWLEDGEMENTS
The research was financially supported by the IGA MENDELU TP 1/2016.

REFERENCES

Bai, K. et al. 2017. Preparation and antioxidant properties of selenium nanoparticles-loaded chitosan microspheres. International Journal of Nanomedicine, 12: 4527

Brown, K.M., Arthur, J.R. 2001. Selenium, selenoproteins and human health: a review. Public Health Nutrition, 4(2b), 593–599.

Dogan, H. et al. 2016. Determination of glutathione, selenium, and malondialdehyde in different edible mushroom species. Biological Trace Element Research, 174(2): 459–463.

El-Demerdash, F.M., Nasr, H.M. 2014. Antioxidant effect of selenium on lipid peroxidation, hyperlipidemia and biochemical parameters in rats exposed to diazinon. Journal of Trace Elements in Medicine and Biology, 28(1): 89–93.

Hoffmann, P.R., Berry, M.J. 2008. The influence of selenium on immune responses. Molecular Nutrition & Food Research, 52(11), 1273–1280.

Hong, Y.L. et al. 2000. Total plasma malondialdehyde levels in 16 Taiwanese college students determined by various thiobarbituric acid tests and an improved high-performance liquid chromatography-based method. Clinical Biochemistry, 33(8): 619–625.

Horký, P. 2014. Influence of increased dietary selenium on glutathione peroxidase activity and glutathione concentration in erythrocytes of lactating sows. Annals of Animal Science, 14(4): 869–882.

Horky, P. et al. 2016. Electrochemical Methods for Study of Influence of Selenium Nanoparticles on Antioxidant Status of Rats. International Journal of Electrochemical Science, 11(4): 2799–2824.

Ighodaro, O.M., Akinloye, O.A. 2017. First line defence antioxidants-superoxide dismutase (SOD), catalase (CAT) and glutathione peroxidase (GPX): Their fundamental role in the entire antioxidant defence grid. Alexandria Journal of Medicine. In Press.

Lopez, A. et al. 2010. Effect of organic selenium in the diet on sperm quality of boars. Reproduction in Domestic Animals, 45(6): e297–305.

Sochor, J. et al. 2010. Content of phenolic compounds and antioxidant capacity in fruits of apricot genotypes. Molecules, 15(9): 6285–6305.

Tran, P.A., Webster, T.J. 2011. Selenium nanoparticles inhibit Staphylococcus aureus growth. International Journal of Nanomedicine, 6: 1553–1558.

Urbankova, L. et al. 2018. Antioxidant status of rats' blood and liver affected by sodium selenite and selenium nanoparticles. Peer Journal, 6: e4862.

Zhang, J., Spallholz, J.E. 2009. Toxicity of Selenium Compounds and Nano-Selenium Particles. In General, Applied and Systems Toxicology. John Wiley & Sons.

Zhang, J. et al. 2007. Elemental selenium at nano size (Nano-Se) as a potential chemopreventive agent with reduced risk of selenium toxicity: comparison with se-methylselenocysteine in mice. Toxicological Sciences, 101(1): 22–31.

FISHERIES AND HYDROBIOLOGY

Effect of the addition of zeolite to the rainbow trout diet

Veronika Brumovska, Eva Postulkova, Michal Sorf, Jan Mares
Department of Zoology, Fisheries, Hydrobiology and Apiculture
Mendel University in Brno
Zemedelska 1, 613 00 Brno
CZECH REPUBLIC

brumovska.veronika@seznam.cz

Abstract: The aim of the project was to verify the positive effect of the addition of clinoptilolite to feed mixtures for rainbow trout on the production parameters and the condition of the fish, including economic evaluation. The fish were fed with industrially produced granular feed Biomar EFICO Enviro 920 Advance 4.5 mm. The experimental diet was supplemented with the addition of clinoptilolite at 0%, 1%, 2% and 4%. The experiment was performed on 120 individuals of rainbow trout. The fish were placed into 8 tanks, each tank contained 15 individuals of fish. The experiment lasted 51 days. At the end of the experiment, the samples of muscles for chemical analysis of the structure of body tissue were taken, namely: dry matter content, nitrogenous substances, fat and ash. The production efficiency of the addition of clinoptilolite to feed mixtures was assessed using basic indicators: specific growth rate (SGR), feed factor (FCR), their relative ratio (FCR/SGR) and yield. The results showed that the use of clinoptilolite in the tested doses in fish nutrition does not lead to statistically significant changes in the chemical structure of fish muscles. The improvement of the production parameters happened while using experimental mixtures with 1% and 2% addition of clinoptilolite. Feed mixtures which were applied did not have any conclusive impact on the yield of fish that ranged in 82.9−84.7%. The lowest cost on fish gain had the 1% option, which also achieved the highest financial impact and overall profit. Moreover, the 2% option was also better than the control group in all monitored parameters. The 4% option achieved the worst economic results from all studied groups.

Key Words: rainbow trout, *Oncorhynchus mykiss*, clinoptilolite, feed additives, zeolite

INTRODUCTION

Natural zeolites (e.g. clinoptilolite) are a microporous crystalic hydrated aluminosilicates (Querol et al. 2002). They are unique thanks to their specific physico-chemical features such as ion exchange and adsorption-desorption properties. Zeolites are used in various industrial sectors including agriculture, aquaculture, waste water treatment and air purification. They are widely used in animal nutrition since the half of the sixties. Zeolite supplements are well tolerated by animals. They support biomass production and even improve animal health (Martin-Kleiner et al. 2001). Many studies show higher daily increment and food conversion in pigs, calves, sheep and broilers (Feithiere et al. 1994) when zeolites were added to the animal diet. There is a great potential in the application of zeolite materials for water quality improvement of fish farms and fish transportation tanks by selective capturing of ammonia and toxic heavy metals (Ghasemi et al. 2018).

Fish are a valuable source of animal protein and fat in human diet. They are rich in essential amino acids, mainly n-3 fatty acids. The content of these compounds in fish can be changed by altering the feed mixture (Paritova et al. 2013). The addition of clinoptilolite into the feed mixture for fish breeding is relatively new and can have many positive effects. Better nutrient utilization, fish growth support, positive effect on body composition and excretion were reported (Kanyilmaz et al. 2015).

Paritova et al. (2013) focused on the effect of zeolites as the additive on chemical, biochemical and histological profile of fish. The experiment was done with rainbow trout and feed dose was enriched by the addition of 1%, 2%, 3% and 4% of the natural zeolite. The results showed the positive effect of zeolite on muscles, amino acid and fatty acid composition. Moreover, the addition of natural zeolites did not cause any pathological alteration in the liver, muscles nor in other internal organs of fish. No further negative effect were find out.

The aim of the presented study was to verify the positive effect of clinoptilolite addition to the feed mixture for rainbow trout. For practical use, it was necessary to verify the optimal amount of allowance for production parameters and fish status, including economic appreciation.

MATERIAL AND METHODS

Description of the experimental diets

The fish were fed with the industrially produced granular feed Biomar EFICO Enviro 920 Advance 4.5 mm provided by Danish firm BioMar. Clinoptilolite produced by Slovak company ZEOCEM, a.s. was chosen as the addition to the fish diet. The composition of clinoptilolite is hydrated sodium-calcium aluminosilicate of sedimentary origin ≥ 80% and clay materials ≤ 20% (without fibers and quartz). The additive grain size is 0−50 μm. The experimental diet was supplemented with the addition of clinoptilolite at 0%, 1%, 2% and 4% (Table 1).

Table 1 Composition of experimental diets

	Control	**1%**	**2%**	**4%**
Biomar EFICO Enviro 920 Advance	100%	99%	98%	96%
Clinoptilolite	0%	1%	2%	4%

Description of the equipment

The experiment took place in the aquarium room at the Department of Fisheries and Hydrobiology of Mendel University in Brno. The recirculation system with its own bio filter Nexus 210 was used in order to ensure stable conditions during the whole testing. Altogether, eight tanks of approximately 160 litres were used; two tanks for each option.

Description of the experiment

A total of 120 individuals of rainbow trout with an initial weight of 151 ± 2.63 g were use during the experiment. The fish were placed in eight tanks, each tank contained of 15 individuals of fish. The fish had been put into tanks three weeks before the test started due to acclimatization. During that time, the fish were fed ad libitum with Biomar EFICO Enviro 920 Advance. The experiment lasted 51 days in total.

Trout feeding was done manually, in three doses (at 8:00, 13:00 and 18:00 hours). The feed dose was determined based on the initial weight of each group of fish at 2.73% of the weight of the stock. The control weighting was performed every 14 days in order to modify the feed dose.

The sample of water was taken every morning before feeding in order to check the concentration of ammonia ions, nitrites and chlorides. This sample was analysed by spectrophotometer WTW photoLab 6600 UV.VIS, Germany (Horáková 2007). The basic physicochemical parameters of water were measured twice a day using multimeter HachLange HQ40d, Germany (water temperature, oxygen content (mg/l), oxygen saturation (%) and pH).

Sampling and analysis

Before the experiment started, the length parameters of each fish were determined (TL – total length, SD – standard length, W – weight). Furthermore, each fish was weighted and measured at the end of the experiment. The samples of muscles for the chemical analysis of the structure of body tissue were taken: dry matter content, nitrogenous substances, fat and ash. Dry matter content was determined by the drying the sample to a constant weight at 105 °C. Fat content was determined using the Soxhlet method, by extraction with diethyl ether for ten hours. The content of ash was determined gravimetrically after ignition of the sample in an electric furnace at a temperature of 550 °C to a constant weight. The nitrogen content was determined according to the Kjeldahl as nitrogen content and the nitrogen content was calculated using a coefficient of 6.25 based on a relatively constant 16% nitrogen content in proteins (Mareš et al. 2015).

Furthermore, the productive efficiency of the addition of clinoptilolite to the feed mixtures was assessed with the use of basic indicators: specific growth rate (SGR), feed factor (FCR), their relative

ratio (FCR/SGR) and yield (Mareš et al. 2015). Besides, the assessment of the economic effect was included into the final evaluation of the addition of clinoptilolite to feed mixtures.

Potential impacts of different diet on all studied characteristics were evaluated by a one-way ANOVA procedure using statistical software Statistica 13.3 (TIBCO Software 2017).

RESULTS AND DISCUSSION

Production parameters

The FCR between the individual options ranged in 0.86−1.00 (Figure 1). The highest values (0.86) belonged to the option with the addition of clinoptilolite at 1%. Similar values (0.88) were achieved for the 2% option. The lowest values were recorded for the 4% option (1.00), which achieved higher feed factor than the control group (0.92). However, described differences were not significant ($F = 0.82$, $df = 3$, $p = 0.50$). The SGR ranged in 1.75−1.89%/d. In comparison with the control group (1.75%/d), the growth rate increased for all options with clinoptilolite added, but not significantly ($F = 2.36$, $df = 3$, $p = 0.21$). The highest increase was obtained in the 1% option (1.86%/d), then the 2% option (1.84%/d), the lowest in the 4% option (1.78%/d).

Lower values of the mutual ratio between FCR and SGR are more favourable as the ratio expresses the need for feed to achieve 1% growth. The lowest values (0.45) were recorded in the 1% option, followed by the 2% option (0.48) and the highest values (0.56) were measured in the 4% option which was worse than the control group (0.52).

Figure 1 Production parameters

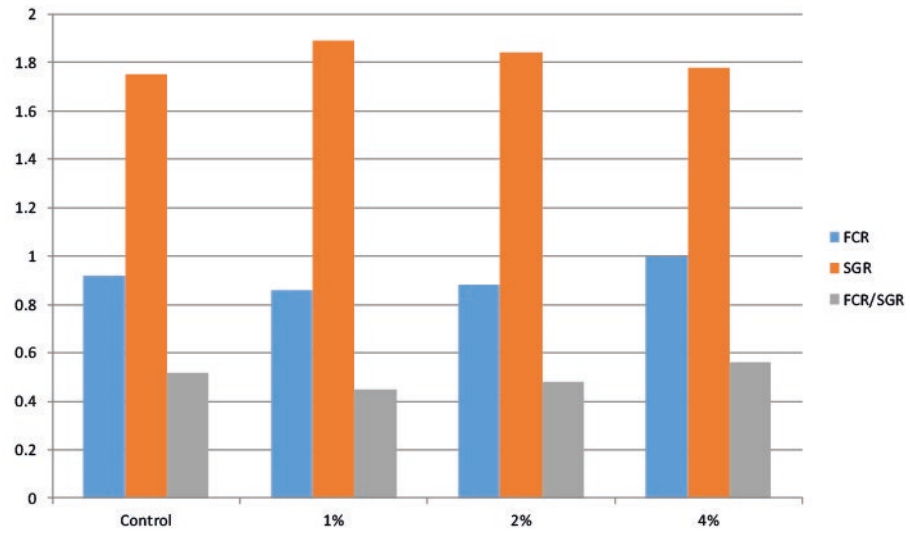

Legend: Specific growth rate (SGR), feed factor (FCR), their relative ratio (FCR/SGR)

Alsted et al. (1995), based on the monitoring of 23 Danish farms using high-energy feeds, shows that FCR averaged at 0.92 (0.68−1.31) and the SGR was observed at 0.75%/d (0.48−1.28%/d). In comparison with mentioned authors, our results demonstrated average values of the FCR and higher values of SGR.

The yield was determined as a percentage of the weight of fish without guts from the total weight of the fish (Table 2). The average values were always calculated of the group of ten fish.

Table 2 Yield

	Control	1%	2%	4%
Yield	83.7±1.7	82.9±2.1	84.6±1.5	84.7±1.2

Legend: Values are given as the average value ± standard deviation

Compared to the control group, a lower yield was recorded in only 1% of the addition. The change was caused by increased values of fat in guts. The yield of fish did not reach a statistically significant difference ($F = 2.64$, $df = 3$, $p = 0.19$) and its values ranged between 82.9−84.7%. Other studies show that the values of yield may range in 79.15−81.6% (Gebauer 2004) and 80.8−85.8% (Pavlík 2011). The

requirement of ČSN 46 6802 which sets a minimum yield of 78% was fulfilled in all experimental groups.

Composition of body tissues

The analysis of muscle samples was performed individually from three fish in each group. The average values were always calculated from three samples. The addition of clinoptilolite to the feed mixtures did not have statistically significant effect on the composition of the muscles of the fish from individual variants (Table 3).

Table 3 Composition of muscles

	Dry matter (%)	Protein content in pure matter (%)	Fat content in pure matter (%)	Ash content in pure matter (%)
Control	28.45±4.20	20.26±2.96	7.60±1.67	1.67±0.13
1%	26.84±1.29	20.38±1.38	6.27±0.44	1.55±0.08
2%	26.97±1.15	18.89±0.71	7.60±1.81	1.55±0.12
4%	27.99±0.91	19.41±1.04	8.51±0.64	1.49±0.07

Legend: Values are given as the average value ± standard deviation

The result of the study showed that the use of clinoptilolite in the experimental doses in the fish feed does not lead to the significant changes of chemical composition of fish muscles. The values stated are favourably comparable with the study of Testi et al. (2006) on rainbow trout. The similar values were measured by Paritova et al. (2013) in the study with the addition of zeolite to the rainbow trout diet. In contrast to our study, when using experimental mixtures, it recorded an increase of the values in all monitored parameters. In our study, the values of ash and dry matter had slightly declining trend. In case of the proteins, the 1% option slightly increased. The values of fat were, compared with the control group, lower in the 1% option, comparable in the 2% option and lower in the 4% option.

Economic evaluation

After 51 days of observation, the FCR ranged in 0.86−1.00 between individual options. Having set the feed price, we earned the cost of 1 kg of fish. The price of Biomar EFICO Enviro 920 Advance varies depending on the quantity of purchased product in 34−42 CZK/kg VAT excluded. The price of clinoptilolite ranges in 200−250 EUR/ton. The exchange rate of ČNB on 3rd August 2018 was 25.66 CZK/EUR. The price of the experimental mixtures was calculated from the averages of quoted prices, i.e. Biomar feed 43.70 CZK/kg VAT included and clinoptilolite – 5.77 CZK/kg.

Fish increments of 1kg of feed varied between 1.00−1.16 for each variant. After the fish price is set, the financial effect of the feed application is expressed.

Table 4 Cost of fish increment, financial effect and total profit

	Price of experimental mixture (CZK/kg)	FCR	Costs per 1 kg of fish increment (CZK)	FCE	Price of fish (CZK/kg)	Financial effect
Control	43.7	0.92	40.2	1.09	120	130.4
1%	43.3	0.86	37.3	1.16	120	139.5
2%	42.9	0.88	37.8	1.14	120	136.4
4%	42.2	1.00	42.2	1.00	120	120.0

The lowest cost on the fish increment was the 1% option which also achieved the highest financial effect and overall profit. The first option was followed by the 2% option which was also significantly better in all monitored parameters than the control group. The 4% option achieved the worst economic results from all experimental groups.

CONCLUSION

The improvement of the production parameters occurred while using the experimental mixtures with 1% and 2% addition of clinoptilolite. The effect of the value of the addition on quality and chemical composition of produced fish meat was not detected. Furthermore, applied feed mixtures did not have statistically significant effect on the fish yield which ranged between 82.9−84.7%. The ČSN

requirements, which sets minimal yield on 78%, were fulfilled with all option. The evaluation of potential benefits of the clinoptilolite addition could be done by setting of a prime level at which we can claim its overall added value.

Moreover, the economic expression of the production effect belongs to the final assessment of the effect of the application of experimental mixtures. The lowest cost on the fish increment achieved the 1% option which also achieved the highest financial effect and overall profit. The results of the 2% option were better in all monitored parameters than the control group. The worst economic results were detected in the 4% option.

ACKNOWLEDGEMENTS

This study was financially supported by the grant no. AF-IGA-IP-2018/052. The research was financially supported by IGA MENDELU grant, no. AF-IGA-2018-tym004. The results and outputs were processed using the equipment financed by the project OP VaVpI CZ.1.05/4.1.00/04.0135 Teaching and research capacities for biotechnology disciplines and infrastructure expansion. The study was processed with the support of the project NAZV QJ1510077 Increasing and improving salmonid fish production in the Czech Republic using their genetic identification.

REFERENCES

Aldted, N. et al. 1995. Practical experience with high energy diets, FCR, growth and quality. Journal of Applied Ichtyology, 11(3–4): 329–335.

ČSN (466802) 1989. Sladkovodní tržní ryby. Praha, ÚVN.

Feithiere, R. et al. 1994. The Utilization of Sodium in Sodium Zeolite A by Broilers. Poultry Science, 73(1): 118–121.

Gebauer, D. 2004. Zhodnocení efektu aplikace krmných směsí s různým obsahem energie v chovu pstruha duhového (Oncorhynchus mykiss) v zimním období. Diplomová práce, MZLU v Brně.

Ghasemi, Z. et al. 2018. Aplication of zeolites in aquaculture industry: a review. Reviews in Aquaculture, 10(1): 75–95.

Horáková, M. 2007. Analytika vody. 2nd ed., Praha: VŠCHT Praha.

Kanyilmaz, M. et al. 2015. Effects of dietary zeolite (clinoptilolite) levels on growth performance, feed utilization and waste excretions by gilthead sea bream juveniles (*Sparus aurata*). Animal Feed Science and Technology, 200(1): 66–75.

Mareš, J. et al. 2015. Akvakultura – základy výživy a krmení ryb. 1st ed., Brno: Mendelova univerzita v Brně.

Martin-Kleiner, I. et al. 2001. The Effect of the Zeolite Clinoptilolite on Serum Chemistry and Haematopoiesis in Mice. Food and Chemical Toxicology, 39(7): 717–727.

Papaioannou, D. et al. 2005. The role of natural and synthetic zeolites as feed additives on the prevention and/or the treatment of certain farm animal diseases. A review. Microporous and Mesoporous Materials, 84(1–3): 161–170.

Paritova, A. et al. 2013. The Influence of Chankanay Zeolites as Feed Additives on the Chemical, Biochemical and Histological Profile of the Rainbow Trout (*Oncorhynchus mykiss*). Journal of Aquaculture Research and Development, 5(1): 205.

Pavlík, M. 2011. Vliv podmínek chovu pstruha duhového (*Oncorhynchus mykiss*) na jeho nutriční hodnotu. Diplomová práce, Mendelova univerzita v Brně.

Querol, X. et al. 2002. Application of zeolitic material synthesised from fly ash to the decontamination of waste water and flue gas. Journal of Chemical Technology and Biotechnology, 77(3): 292–298.

Testi, S. et al. 2006. Nutritional traits of dorsal and central fillets from three farmed fish species. Food Chemistry, 98(1): 104–111.

TIBCO Software Inc. 2017. Statistica (data analysis software system), version 13. http://statistica.io.

The effect of antidepressants in surface water on *Danio rerio* organism

Nikola Hodkovicova[1,3], Monika Urbanova[2], Pavla Sehonova[1,2], Petr Chloupek[2]
[1]Department of Animal Protection, Welfare and Behaviour
[2]Department of Veterinary Public Health and Forensic Medicine
University of Veterinary and Pharmaceutical Sciences Brno
Palackeho tr. 1946/1, 612 42 Brno
[3]Department of Immunology
Veterinary Research Institute, Brno
Hudcova 296/70, 621 00 Brno
CZECH REPUBLIC

h16015@vfu.cz

Abstract: The concentration of antidepressants occurring in surface water is rising worldwide because of their ineffective removal at wastewater treatment plants. However, the knowledge of their impact on aquatic organisms is limited. For our assay, three different antidepressants with different mechanisms of action were chosen to assess the impact on the *Danio rerio* body formation mechanism. The antidepressants were tested in two concentrations – environmentally-relevant (according to literature sources) and 100x higher. The method used was relative gene expression and genes were selected as representatives of the heart, brain, spine, eye and mesoderm formation. The results showed that the gene expression mechanism and welfare status are disrupted already in environmentally-relevant concentrations.

Key Words: fish, amphibian, embryo, qRT-PCR, gene expression

INTRODUCTION

The worldwide increasing use of pharmaceuticals acting together with their incomplete and ineffective removal at wastewater treatment plants (WWTP) cause surface water pollution. For example, in the case of venlafaxine, the removal rate in a WWTP is only 40% (Metcalfe et al. 2010). The amount of drug residues in water and aquatic organisms is rising to the range from ng to µg per Litre. This seems to be an important issue due to their possible adverse effects on aquatic organisms (Santos et al. 2010, Baker and Kasprzyk-Hordern 2013).

In our study, we tested three different antidepressants with diverse mechanisms of action. We tested them in environmentally-relevant concentrations and the 100x higher concentration for evaluation of the dose-dependent effect. The venlafaxine antidepressant is part of serotonin and norepinephrine reuptake inhibitors class (SNRI) and the concentration reported in surface water is approximately 300 ng/l (Baker and Kasprzyk-Hordern 2013). The second tested amitriptyline is a tricyclic antidepressant and its concentration in surface water is also about 300 ng/l (Baker and Kasprzyk-Hordern 2013). The last one tested was sertraline belonging to the selective serotonin reuptake inhibitor class (SSRI). Conners et al. (2009) reported its concentration as approximately 100 ng/l.

Danio rerio (zebrafish) was chosen as a representative of the non-target organisms because it serves as a commonly used ecotoxicological model for *Cyprinidae* (Scholz et al. 2008). The aim of this study was to assess the potential impact of three different antidepressants on the function of gene expression mechanism and to help to clarify the mechanism of toxic effect. One gene was chosen for diverse body systems: for mesoderm induction, the bone morphogenetic protein 4 (*bmp4*) gene (Marques et al. 2016); for the heart development, the NK2 homeobox 5 (*nkx2.5*) gene (Harrington et al. 2017); for brain and spine formation, the orthodenticle homeobox 2 (*otx2*) gene (Albuixech-Crespo et al. 2017) and for eye development, the paired box 6b (*pax6b*) gene (Williams et al. 2017). According to the mentioned literature sources, primer sequences were also selected.

MATERIAL AND METHODS

A total of 1050 zebrafish embryos was observed under a stereomicroscope for selection of embryos between 4 and 16-cell stages and for removal of unfertilized ones. After that, the embryos were randomly distributed to Petri dishes – 150 eggs in each dish.

The tested concentrations of amitriptyline and venlafaxine were set up as 0.3 and 30 µg/l; the concentrations used for sertraline were 0.1 and 10 µg/l. – A total of 150 eggs were exposed to each tested concentration. One group of 150 eggs was used as a control and was exposed to dilution water only. Petri dishes were kept at a temperature of 26 °C and a photoperiod of 12:12 hours until 144 hours post fertilization.

After exposure, the amount of 10 mg of embryos was weighed in 2 mL Eppendorf vials. Thus eight repetitions for every tested concentration were created; to sum it up, seven diverse concentration groups in eight repetitions were tested. Afterwards, the samples were fixed in RNAlater (Thermo Fisher Scientific, Czech Republic), left at 4 °C overnight and then stored at -80 °C until RNA extraction.

After homogenisation, RNA extraction using the RNeasy Mini kit (Qiagen, Germany) was performed according to the manufacturer's protocol. As a negative control of contamination, DNAse/RNAse free water with master mix was used.

Total RNA was reverse-transcribed using Moloney Murine Leukemia Virus Reverse Transcriptase (Invitrogen, United Kingdom) and oligo-dT primer at 37 °C for 50 min and at 70 °C for 15 min. As house-keeping reference gene, the elongation factor 1 alpha 1 (*ef1a1*) was used. Relative gene expression was calculated for *bmp4*, *nkx2.5*, *otx2* and *pax6b*. As master mix for quantitative real-time PCR analysis, SYBR Green Master (Qiagen, Germany) was used; the analysis was performed using the LightCycler® 480 (Roche, Germany). Statistical analysis was performed with Unistat 5.6 programme for Excel, using the Shapiro-Wilk normality testing. The multiple comparison of concentrations was used and the difference between groups was assessed as significant at $p < 0.05$.

RESULTS AND DISCUSSION

The results of relative gene expression for amitriptyline antidepressant showed significance for the *bmp4* and *pax6* gene, both of these significant changes revealed down-regulation in the higher concentration. Data are shown in Figure 1.

Figure 1 The results of relative gene expression of amitriptyline for individual genes (nkx2.5, otx2, bmp4, pax6) in relation to the reference gene ef1a1 expressed as n ± SEM (n=8).

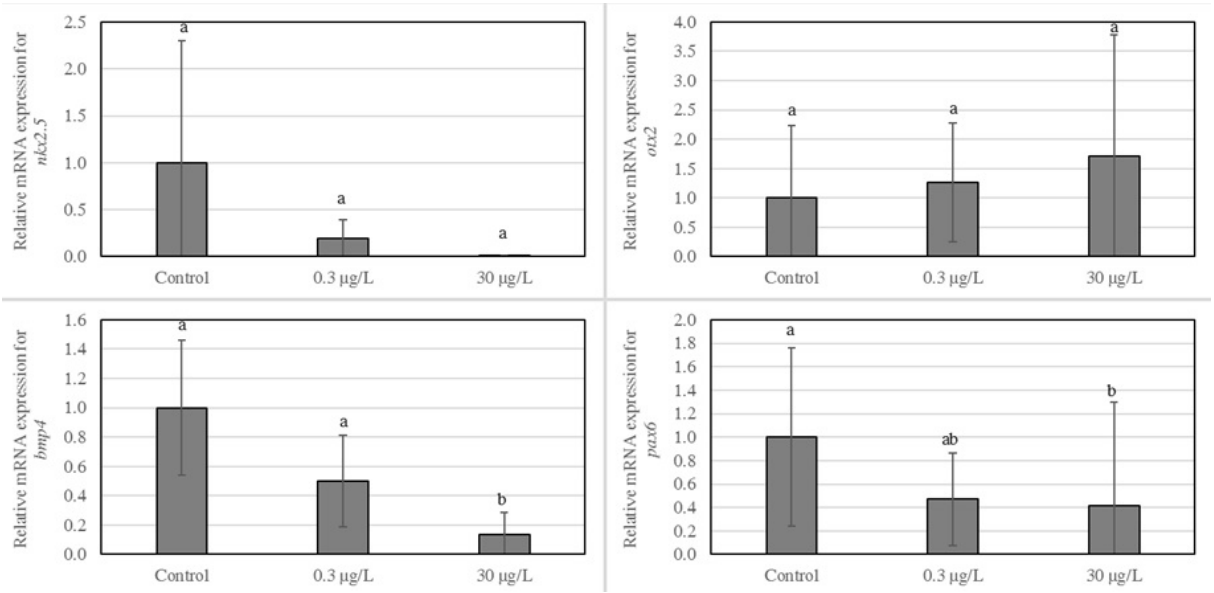

Legend: SEM – standard error of mean; a,b – significance between groups ($p < 0.05$)

The results of gene expression for venlafaxine revealed significance for all genes, except *nkx2.5*. A similar trend was observed for other genes – the gene expression was down-regulated in the lower

concentration when compared to control and even more down-regulated in the higher concentration. The results are presented in Figure 2.

Figure 2 The results of relative gene expression of venlafaxine for individual genes (nkx2.5, otx2, bmp4, pax6) in relation to the reference gene ef1a1 expressed as n ± SEM (n=8).

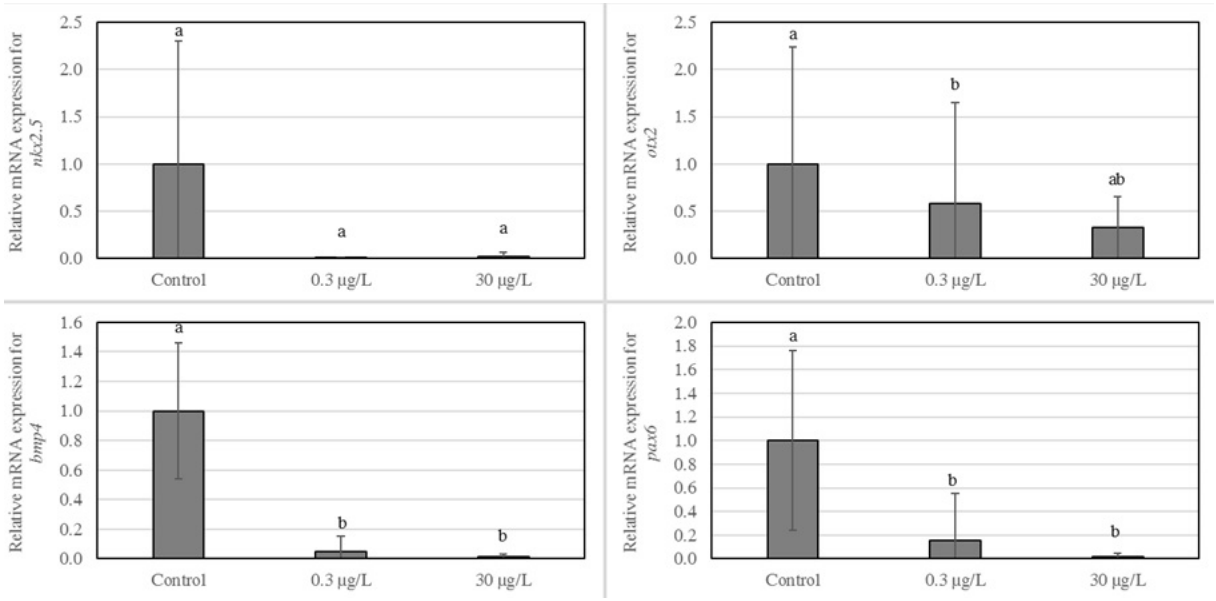

Legend: SEM – standard error of mean; a,b – significance between groups (p < 0.05)

A significant down-regulation was observed for *otx2* and *bmp4* when the embryos were exposed to sertraline. In addition, the down-regulation of gene expression in both tested concentrations was observed for the *pax6* gene. The results are showed in Figure 3.

Figure 3 The results of relative gene expression of sertraline for individual genes (nkx2.5, otx2, bmp4, pax6) in relation to the reference gene ef1a1 expressed as n ± SEM (n=8).

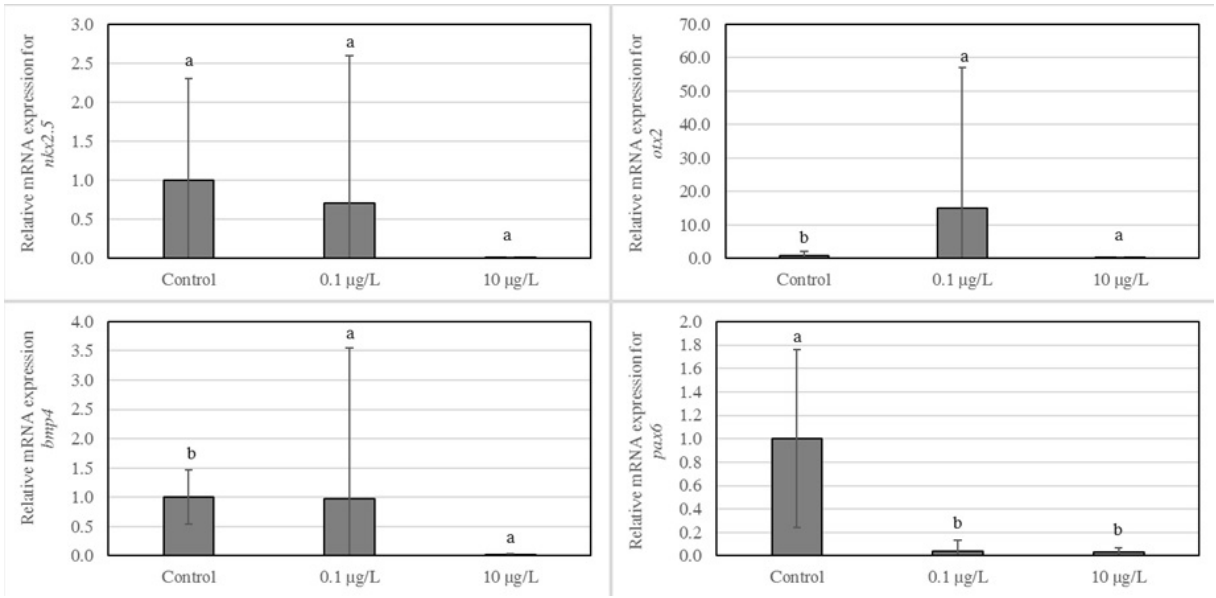

Legend: SEM – standard error of mean; a,b – significance between groups (p < 0.05)

Amitriptyline is known to cause cardiotoxicity (Vohra et al. 1975); however, there was no significant impact in case of any tested antidepressant on the *nkx2.5* gene, which is involved in heart development. The impact on brain and spine development, namely effect on *otx2* gene expression, was revealed for sertraline and venlafaxine and, according to Andreazzoli et al. (1997), this could lead to defects in embryo gastrulation. For all tested antidepressants, the impact on *bmp4* and *pax6* gene was observed. The *bmp4* is responsible for bone development and this gene was also identified to have a positive effect on increased growth (Albertson et al. 2005). However, the down-regulation of *bmp4*

could possibly lead to negative impact on bone formation. The *pax6* was also down-regulated in case of all tested antidepressants. According it is responsible for the appropriate eye and neural formation (Nornes et al. 1998), the down-regulation of this gene could lead to the negative effect on the embryos correct evolution.

To sum up, a similar trend was observed for most of the results of gene expression. The down-regulation of gene expression of most of the genes was observed in the environmentally-relevant concentration and, moreover, the down-regulation was even higher in the 100x higher concentration. Thus, even in environmentally-relevant concentrations, we can observe the impact of these drugs, which commonly contaminate the surface water, on gene expression. We can suspect that even these small amounts of pharmaceuticals in surface water can disrupt the body formation mechanism on the basic level. It follows that the body systems, i.e. brain, eye and heart development, spine formation and even mesoderm induction, can be disturbed during the embryo phase which, as a result, can interfere with the fish organism development.

CONCLUSIONS

The aim of this study was to assess the impact of antidepressants residues contaminating the surface water on non-target *Danio rerio* organism development by monitoring gene expression. The results showed that the gene mechanism can be disrupted already in environmentally-relevant concentrations of antidepressants in water.

ACKNOWLEDGEMENTS

Research reported in this publication was supported by the Internal Grant Agency of the University of Veterinary and Pharmaceutical Sciences Brno [no. 207/2018/FVHE], ERDF/ESF "Profish" [no. CZ.02.1.01/0.0/0.0/16_019/0000869] and by the Ministry of Education, Youth and Sport of the Czech Republic [no. LO1218].

REFERENCES

Albertson, R.C. et al. 2005. Integration and evolution of the cichlid mandible: the molecular basis of alternate feeding strategies. Proceedings of the National Academy of Sciences of the United States of America, 102(45): 16287–16292.

Albuixech-Crespo, B. et al. 2017. Molecular regionalization of the developing amphioxus neural tube challenges major partitions of the vertebrate brain. PLoS Biology, 15(4): e2001573.

Andreazzoli, M. et al. 1997. Activating and repressing signals in head development: the role of Xotx1 and Xotx2. Development, 124(9): 1733–1743.

Baker, D.R., Kasprzyk-Hordern, B. 2013. Spatial and temporal occurrence of pharmaceuticals and illicit drugs in the aqueous environment and during wastewater treatment: New developments. Science of the Total Environment, 454−455: 442–456.

Conners, D.E. et al. 2009. Growth and development of tadpoles (*Xenopus laevis*) exposed to selective serotonin inhibitors, fluoxetine and sertraline, throughout metamorphosis. Environmental Toxicology and Chemistry, 28(12): 2671−2676.

Harrington, J.K. et al. 2017. Nkx2.5 is essential to establish normal heart rate variability in the zebrafish embryo. American Journal of Physiology. Regulatory, Investigative and Comparative Physiology, 313(3): ajpregu.00223.2016.

Marques, C.L. et al. 2016. Comparative analysis of zebrafish bone morphogenic proteins 2, 4 and 16: molecular and evolutionary perspectives. Cellular and Molecular Life Sciences, 73(4): 841–857.

Metcalfe, C.D. et al. 2010. Antidepressants and their metabolites in municipal wastewater, and downstream exposure in an urban watershed. Environmental Toxicology and Chemistry, 29(1): 79–89.

Nornes, S. et al. 1998. Zebrafish contains two pax 6 genes involved in eye development. Mechanisms of Development, 77(2): 185–196.

Santos, L.H.M.L.M. et al. 2010. Ecotoxicological aspects related to the presence of pharmaceuticals in the aquatic environment. Journal of Hazardous Materials, 175(1-3): 45–95.

Scholz, S. et al. 2008. The zebrafish embryo model in environmental risk assessment – applications beyond acute toxicity testing. Environmental Science and Pollution Research, 15(5): 394–404.

Vohra, J. et al. 1975. The effect of toxic and therapeutic doses of tricyclic antidepressant drugs on intracardiac conduction. European Journal of Cardiology, 3(3): 219–227.

Williams, A.L. et al. 2017. Cyp1b1 regulates ocular fissure closure through a retinoic acid-independent pathway. Investigative Ophthalmology and Visual Science, 58(2): 1084–1097.

Use of by-products from hemp processing in the nutrition of common carp (*Cyprinus carpio* L.)

Ondrej Maly[1], Jan Mares[1], Ondrej Palisek[1, 2], Michal Sorf[1], Eva Postulkova[1]
[1]Department of Zoology, Fisheries, Hydrobiology and Apiculture
Mendel University in Brno
Zemedelska 1, 613 00 Brno
[2]Research Institute of Fish Culture and Hydrobiology
University of South Bohemia in Ceske Budejovice
Zatisi 728/II, 389 25 Vodnany
CZECH REPUBLIC

ondra.malous@gmail.com

Abstract: The aim of this study was to find out the effect of addition of by-products from hempseed processing into feeding mixtures used in the farming of common carp. The feed KP1 (control diet A) was supplemented with hempseed cakes in two batches, at the amounts of 5% (B), 10% (C), and 15% of batch I (D), and 15% of batch II (E). Ten tanks of a volume of 180 l were stocked with 20 pcs of common carp fingerlings of the L15 breed and a mean weight of 35.37 g. During the 64-day experimental period, production indicators (FCR, SGR, and their ratio), basic haematological indicators (RBC, Hb, MCHC, MCV, PCV, MCH), and the fatty acid (FA) spectrum were monitored. For production indicators, the best results were obtained with the mixture containing 10% hempseed cake (FCR–3.29, SGR–0.8). A significant increase of the haematocrit value was achieved in groups C and E compared to the control diet A. Regarding the mean corpuscular haemoglobin concentration (MCHC) and glucose content, the values were decreased in groups D and E compared to the control group A. Regarding FA, γ-linolenic acid was significantly increased in group E compared to the control group A. In this study, we did not observe the positive effect of the addition of hempseed cake on the change of the FA content in favour of n-3.

Key Words: hempseed cake, fatty acid FA, production indicators, haematology

INTRODUCTION

Common carp is the most frequently farmed fish in the Czech Republic. Its annual production ranges around 18 thousand tonnes, with over a half of the production being exported to the surrounding countries. Fish consumption in the Czech Republic ranges around 5.5 kg, of which approximately 1.4 kg are freshwater fish (SVZ Ryby 2017). Dietetically, fish meat is important food rich in proteins and FA. Fish fat is a valuable source of FA. Fish cannot synthesize essential FA, namely, linoleic acid of the n-6 family, and α-linolenic acid of the n-3 family, therefore, these acids need to be supplemented into the carp feed. Another source of these acids can be plant oils of selected crops (Palíšek 2017). Generally, plant oils are relatively poor in acids of the n-3 family; however, with the exception of linseed, hempseed, sage or milk thistle oils (Hasan 2002). Fish cannot change the position of the first multiple bond, i.e. change the acid group, however, due to the process of elongation and desaturation, they can change the length of the carbonaceous chain of the FA (Mareš et al. 2015). Unsaturated FA are very important in human diet. They decrease the cholesterol level in blood plasma, lower the blood pressure, and improve kidney function. They also have a positive effect in the treatment of cardiovascular diseases (Chloupek et al. 2005). Furthermore, Chloupek et al. (2005) report that humans should take linoleic and alpha-linolenic acids at a ratio of approximately 1 : 1.5. However, due to the inappropriate diet, the ratio of these acids is 1 : 20–40. Due to the favourable fat composition, easy digestibility of meat, and low content of connective tissue protein, fish meat consumption 2–3 per week is recommended by the World Health Organisation (Palíšek 2017).

Various alternative crops or by-products from the processing of such crops have been increasingly used in fish feeds. Reasons for this are e.g. decreasing the financial cost of the feed production (substitution for fish meal), the possibility of affecting the health condition of the fish,

utilizing secondary products from the processing or the possibility to influence the fish meat quality. For instance, Kukačka (2012) report that administering a feed containing linseed oil can effectively influence the FA spectrum in fish meat. This was confirmed by Zajíc et al. (2012) who showed a lowering of cholesterol in a group of people who had consumed the meat of fish fed a linseed supplemented feed. Apart from linseed, distillers' grains (Vetešník 2001), oilcakes from oil pressing such as sunflower or soybean (Jirásek 1989) or rapeseed (Kukačka 2012) are utilized in this manner. Furthermore, molasses, yeast, green algae or blue-green algae are among the supplements used in the feeding practice (Mareš et al. 2015).

The prospective plant feeds studied in the fish farming in our country include the traditionally produced hemp (*Cannabis sativa*). In the Czech Republic, hemp is grown on approximately 200 ha. Hemp cultivation is subsidized in which case hemp varieties with a THC content of up to 0.2% can be legally grown (Holubář et al. 2014). In fish farming, the alternative sources are mainly hempseed cake, hempseed meal, and other hemp residues collected from oil processing. The whole hemp seed contains approximately 25% proteins which makes it a potentially very good protein source. Furthermore, it contains 34% saccharides, mostly fibre, and around 35% oil. Hemp oil contains more than 80% polyunsaturated FA of which a high percentage, approximately 18%, is α-linolenic acid (Wang et al. 2007). A number of studies have focused on hemp in fish nutrition. For example, Lunger et al. (2006) studied the effects of substituting fish meal with hempseed cake. They showed that fish meal can be substituted by up to 40% of alternative components. The study also confirmed the fact that the used diet has a major effect on the fish meat quality. Similar results were found in a study by Webster et al. (2000) who reported no negative effect of the use of a hemp-containing feed mixture without fish meal on the production indicators in the farming of European sea bass fingerlings.

Secondary products from alternative crop processing have become an interesting fraction in feed production. Press cakes from oil production have been recognized as a rich source of proteins and especially of FA. Therefore, we studied the addition of hempseed processing by-products to the diet of common carp. The addition of hempseed cake to the carp feed can possibly affect the composition and spectrum of FA or change the ratio of n-6 to n-3 acids in the muscle of common carp. Moreover, the health condition of the consumers can be positively affected by consumption of this feedstock.

MATERIAL AND METHODS

Characterization of feeding mixtures

The feed KP1 from VKS Stříbrné Hory was used to produce five experimental diets. The control feed (A) was the KP1 mixture; the others were mixtures enriched with the hempseed cake of the Finola variety originated in Česká Metuje, at the proportions of 5% (B), 10% (C), 15%^{I} (D), 15%^{II} (E). The mixtures were supplemented with rapeseed oil to contain the same energy level.

Experimental design

Ten tanks of the volume of 180 l connected to the recirculation system (Figure 1) were stocked each with 20 pcs of common carp of the breed L15, originated in Rybníkářství Pohořelice a.s. (South Moravia), of a mean weight of 35.37 g. The mean water temperature during the experiment was 23.2 °C and more than 85% on average oxygen saturation of water was maintained. The fish were fed with the five diets for a period of 64 days, in two repetitions. Before the start of the testing, the fish were acclimated for 14 days and introduced to the new feed. The daily feeding ration corresponded to 2% of the tank stock weight and was divided into three partial rations. Basic hydrochemical characteristics of water were monitored individually in regular intervals. At the beginning and at the end of the experiment, the fish were weighed and measured both individually and as a group. The stocks were re-weighed at two-week intervals for the purpose of adjusting the feeding ration.

Monitored parameters

Basic production parameters such as the FCR (feed conversion ratio) and the SGR (specific growth ratio) and their mutual ratio (FCR/SGR) were monitored (Mareš et al. 2015).

Others included basic haematological parameters such as red blood cells (RBC), haemoglobin (Hb), haematocrit (PCV – packed cell volume), mean cell volume (MCV), mean corpuscular

haemoglobin concentration (MCHC) and mean cell haemoglobin (MCH). Further, glucose concentration (Gl) from blood plasma was determined (Svobodová and Pravda 1986).

Furthermore, the FA content was monitored using the method of capillary gas chromatography with nitrogen used as the carrier gas (Palíšek 2017); FA extraction was done following the method of Folch et al. (1957).

Figure 1 The design of the experiment

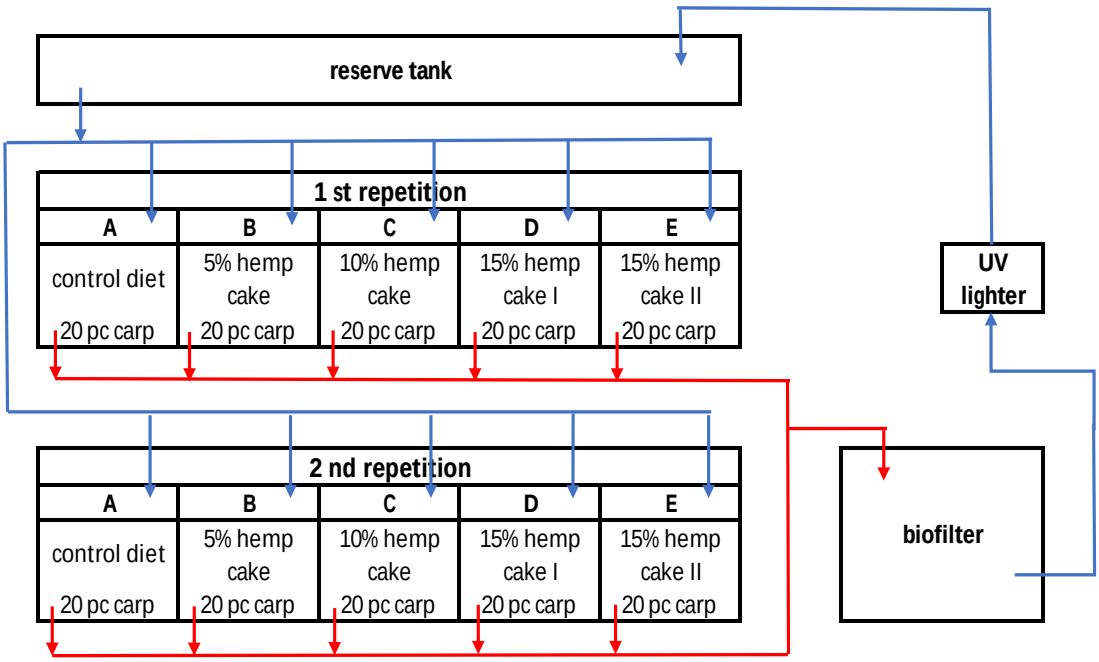

Statistical analyses

All the parameters studied were evaluated by the one-way ANOVA using statistical software Statistica 13 (TIBCO, 2017). The Tukey HSD post-hoc test was used to distinguished among experimental diets.

RESULTS AND DISCUSSION

Production parameters

The best production parameters were obtained for the diet C, i.e. the diet with a supplement of 10% hemp cake. For this diet, the obtained results were 3.14 for FCR and 0.83%/d for SGR. Thus, there was a decrease in the FCR values and an increase in the SGR values compared to the control diet which is commonly used in the aquaculture practice for fingerling breeding. High FCR values and low SGR values of the basic feeding ration are mainly due to the low protein content (14.64%), compared to the study by Zugárková (2017) which achieved 2.44 FCR and 0.99 SGR at a protein content of 22.9%. Saoud et al. (2018) report that the addition of hemp oil to the tilapia diet negatively influences FCR by significantly increasing the fish metabolism which was confirmed by a higher oxygen consumption by the fish.

Table 1 Production parameters

Diet	Growth (g)	Feed consumption (g)	FCR	SGR (%/d)	FCR/SGR
A	812.15	2823.35	3.69	0.75	4.92
B	879.95	2899.51	3.29	0.80	4.11
C	**900.35**	**2816.49**	**3.14**	**0.83**	**3.78**
D	878.00	2842.65	3.25	0.82	3.96
E	863.00	2859.41	3.34	0.79	4.22

Haematological and biochemical parameters

Table 2 Haematological parameters and glucose concentration in studied fish. Significant differences between particular diets are in bold and distinguished by superscripts (e.g. ^{C,E} *means significant difference of the diet indicated in the column from diets C and E).*

	A A ± SD	B A ± SD	C A ± SD	D A ± SD	E A ± SD
RBC [T/l]	1.56 ± 0.32	1.70 ± 0.35	1.76 ± 0.28	1.55 ± 0.19	1.65 ± 0.29
Hb [g/l]	81.44 ± 6.02	78.36 ± 7.75	83.33 ± 6.21	78.50 ± 5.67	85.55 ± 9.42
PCV [l/l]	**0.27 ± 0.01**^{C,E}	**0.27 ± 0.01**^{C,E}	**0.30 ± 0.02**^{A,B}	**0.28 ± 0.01**	**0.30 ± 0.02**^{A,B}
MCV [fl]	18.29 ±3.22	16.98 ± 3.78	17.63 ± 2.29	18.44 ± 2.32	19.31 ± 2.42
MCHC [l/l]	**0.30 ± 0.02**^{C,D}	**0.29 ± 0.02**	**0.27 ± 0.01**^{A}	**0.28 ± 0.02**^{A}	**0.28 ± 0.02**
MCH [pg]	53.82 ± 9.36	49.39 ± 12.31	48.22 ± 7.21	50.65 ± 6.44	55.41 ± 7.84
Gl [mmol/l]	**4.46 ± 0.78**^{D,E}	**4.42 ± 0.84**	**3.69 ± 0.85**	**3.23 ± 0.85**^{A,B}	**3.09 ± 0.62**^{A,B}

In haematological indicators, several blood components were significantly affected. The PCV level was significantly increased in diets C and E ($F = 6.15$, $df = 4$, $p < 0.001$) compared to the control diet A. In contrast, MCHC was significantly decreased in diets D and E ($F = 3.25$, $df = 4$, $p = 0.02$) compared to the control diet A. Gl was significantly decreased in diets D and E ($F = 7.28$, $df = 4$, $p < 0.001$) compared to the control diet A. All the determined haematological parameters and biochemical indicators are within the physiological range for common carp (Svobodová and Pravda 1986). Nevertheless, we can assume that with the increasing percentage of hempseed cake, the MCHC values and glucose content in the carp blood are decreased. Saoud et al. (2018) report that using hemp oil in the diet of Nile tilapia did not influence any of the above mentioned parameters. The addition of hemp oil had no positive effect on the immune system of the fish.

Content of n-3 and n-6 fatty acid

Table 3 Content of fatty acid. Significant results are in bold and distinguished by superscripts (e.g. ^{C,E} *means significant difference of the diet indicated in the column from diets C and E).*

	A	B	C	D	E
C18:2 n-6	10.77	12.23	12.25	14.31	14.05
C18:3 n-6	**0.32**	**0.46**^{D}	**0.37**^{E}	**0.68**^{B,E}	**0.71**^{C,D}
C18:3 n-3	1.38	1.54	1.50	1.70	1.80
C18:4 n-3	0.13	0.14	0.12	0.18	0.19
C20:4 n-6	3.10	2.76	1.99	3.98	3.93
C20:4 n-3	0.03	0.04	0.05	0.13	0.04
C20:5 n-3	0.87	0.79	0.77	0.95	1.02
C22:4 n-6	0.30	0.24	0.15	0.36	0.35
C22:5 n-6	0.03	0.03	0.03	0.13	0.05
C22:5 n-3	0.54	0.50	0.34	0.69	0.71
C22:6 n-3	2.64	2.32	1.77	3.83	3.39
Σ n-3	5.59	5.34	4.55	7.48	7.15
Σn-6	14.52	15.72	14.78	19.45	19.10
n-3/n-6 ratio	0.39	0.34	0.30	0.37	0.36

Regarding the FA composition, only the γ-linolenic acid content in the diet E was significantly higher ($F = 6.4$, $df = 4$, $p < 0.01$) compared to the control diet A. Diets D and E achieved the best values for both FA n-6 and n-3, however, the increase was not statistically significant. No significant effect of the addition of hempseed cake on the content of FA of the n-3 and n-6 families was found in this study. De Souza et al. (2007) proved the effect of linseed oil on the n-3 to n-6 FA ratio in Nile tilapia. The total fat content was not affected; only the proportion of n-3 was higher compare to n-6.

CONCLUSION

The presented study focused on the addition of hempseed cake to common carp diet. The addition of hemp cake to the feeding mixture at the proportion of 10% had a positive effect on decreasing the feed conversion and increasing the growth rate. The addition of hempseed cake altered some haematological and biochemical indicators such as the haematocrit value, mean corpuscular haemoglobin concentration or the glucose content. Based on the obtained results we assumed that the addition of hempseed cake can affect the haematological parameters. The mean corpuscular haemoglobin concentration and glucose content in the blood of fish were decreasing with the increasing percentage of hempseed cake. In terms of FA, no significant effect on the FA spectrum was found. The presumed improvement of the n-6 to n-3 ratio in favour of n-3 acids was not observed as well.

To conclude, we cannot confirm that the addition of hempseed cake can influence the FA spectrum and thus the overall quality of the final product, fish meat.

ACKNOWLEDGEMENTS

The research was financially supported by the NAZV QK1810296 "The use of alternative components and innovative techniques in fish nutrition", and the Project OP VaVpI CZ.1.05/4.1.00/04.0135 "Výukové a výzkumné kapacity pro biotechnologické obory a rozšíření infrastruktury" ("Teaching and research capacities for biotechnological fields and expansion of infrastructure").

REFERENCES

de Souza, N.E. et al. 2007. Manipulation of fatty acid composition of Nile tilapia (*Oreochromis niloticus*) fillets with flaxseed oil. Journal of the Science of Food and Agriculture, 87(9):1677–1681.

Folch, J. et al. 1957. A simple method for the isolation and purification of total lipides from animal tissues. The Journal of Biological Chemistry, 226(1):497–509.

Hasan, M.R. 2002. Nutrition and Feeding for Sustainable Aquaculture Development in the Third Millennium. In: Aquaculture in the Third Millennium [Online]. Bangkok, Department of Aquaculture, Thailand. 20–25 February 2000, pp. 193–219. Available at: http://www.fao.org/docrep/003/ab412e/ab412e10.htm. [2018-07-10].

Holubář, J. et al. 2014. Len a konopí 2014. [Online]. Available at: http://eagri.cz/public/web/file/299559/Len_konopi_2014.pdf. [2018-07-10].

Chloupek, O. et al. 2005. Pěstování a kvalita rostlin. 1st ed., Brno: Mendelova zemědělská a lesnická univerzita v Brně.

Jirásek, J. 1989. Biologické a technologické aspekty intenzivního chovu kapřího plůdku. Doktorská dizertační práce, Vysoká škola zemědělská Brno.

Kukačka, V. 2012. Použití netradičních komponentů v krmných směsích pro plůdek kapra obecného (*Cyprinus carpio* L.). Diplomová práce, Mendelova univerzita v Brně.

Lunger, A.N. et al. 2006. Replacement of fish meal in cobia (*Rachycentron canadum*) diets using an organically certified protein. Aquaculture, 257(1–4):393–399.

Mareš, J. et al. 2015. Akvakultura – základy výživy a krmení ryb. 1st ed., Brno, Mendelova univerzita v Brně.

Palíšek, O. 2017. Vliv produktů ze zpracování konopí ve výživě kapra obecného (*Cyprinus carpio* L.). Diplomová práce, Mendelova univerzita v Brně.

Saoud, P. et al. 2018. Effect of cannabis oil on growth performance, haematology and metabolism of Nile tilapia (*Oreochromis niloticus*). Aquaculture Research, 49:809–815.

Situační výhledová zpráva – Ryby. 2017. Praha: Ministerstvo zemědělství ČR.

Svobodová, Z., Pravda, D. 1986. Jednotné metody hematologického vyšetření ryb. 022. Výzkumný ústav rybářský a hydrobiologický Vodňany: Jihočeské tiskárny.

TIBCO Software Inc. (2017). Statistica (data analysis software system), version 13. http://statistica.io.

Vetešník, L. 2001. Využití suchých výpalků v krmných směsích pro kapří plůdek. Diplomová práce, Mendelova lesnická a zemědělská univerzita v Brně.

Wang, X. et al. 2007. Characterization, amino acid composition and in vitro digestibility of hemp (*Cannabis sativa* L.) proteins. Food Chemistry, 107(1):11–18.

Webster, C.D. et al. 2000. Use of hempseed meal, poultry by-product meal, and canola meal in practical diets without fish meal for sunshine bass (*Morone chrysops*×*Morone saxatilis*). Aquaculture, 188(3–4):299–309.

Zajíc, T. et al. 2012. Maso kapra obecného (*Cyprinus carpio* L.) se zvýšeným obsahem omega 3 mastných kyselin jako nástroj prevence a rehabilitace kardiovaskulárních onemocnění. Interní medicína pro praxi, 14(11):437–440.

Zugárková, I. 2017. Využití krmiv se sníženým zatížením vodního prostředí fosforem v chovu kapra. obecného (*Cyprinus carpio* L.). Diplomová práce, Mendelova univerzita v Brně.

Effect of terbutryn on aquatic organisms

Eva Postulkova[1], Michal Sorf[1,2], Jan Grmela[1], Radovan Kopp[1]
[1]Department of Zoology, Fisheries, Hydrobiology and Apiculture
Mendel University in Brno
Zemedelska 1, 613 00 Brno
[2]Department of Ecosystem Biology
University of South Bohemia in Ceske Budejovice
Branisovska 1760, 370 05 Ceske Budejovice
CZECH REPUBLIC

eva.postulkova@mendelu.cz

Abstract: The aim of the study was to determine the growth inhibition effect of terbutryn on freshwater algae *Desmodesmus communis*, *Chlorella kessleri* and cyanobacteria *Anabaena* sp. The experimental inhibition concentrations ranged from 0.004 to 1.250 mg/L. IC50 values analysed by the non-linear regression were as follows: 0.012 mg/L for *Desmodesmus communis*, 0.188 mg/L for *Chlorella kessleri* and 0.666 mg/L for *Anabaena* sp.

Key Words: algae, cyanobacteria, inhibition, microtiter plate, toxicology

INTRODUCTION

Terbutryn (2-(terc-butylamino)-4-(ethylamino)-6-(methylthio)-s-triazine) belongs to a group of substituted symmetric triazines (s-triazines). There are two groups of triazine herbicides: asymmetric triazines or triazinones on one hand and symmetric triazines on the other hand (Plhalová et al. 2010). Symmetric triazines are substances similar to herbicides used in agriculture for inhibiting a broad-leaved weed and grasses (Arufe et al. 2004). The main commercial symmetric triazines are ametryn, prometryn and terbutryn (Breckenridge et al. 2010). Terbutryn was used worldwide to weed control in crops such as cereals, legumes, potatoes, corn, sugar cane and under fruit trees. Terbutryn is selective and systemic herbicide inhibiting photosynthesis. It is used also against submerged and floating macrophytes, algae and cyanobacteria in watercourses, lakes and ponds (Moretti et al. 2002, Daho 2006). Terbutryn does not affect soil microorganisms and has low toxicity for birds. On the other hand, terbutryn is highly toxic for algae (even in low concentrations, Rioboo et al. 2007), toxic for fish and moderately toxic for cladocerans (Daho 2006). The substance is moderately soluble in water (22 mg/L) and is potentially bioaccumulative in aquatic organisms. It is a lipophilic substance biologically available for monocellular algae and hence could be a part of the food chain (Rioboo et al. 2007). Although the terbutryn application is forbidden in many countries, it can still be found in the water systems (Daho 2006, Rioboo et al. 2007). Preparations containing terbutryn have not been registered in the Czech Republic since 2005 (Plhalová et al. 2010).

Figure 1 The structural formula of terbutryn (Royal Society of Chemistry 2015).

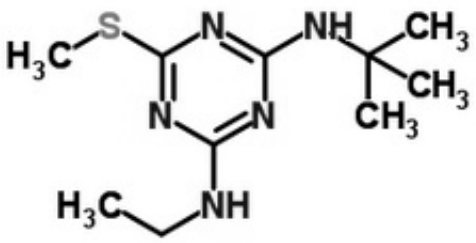

The application of chemical substances to the environment caused by human activities can be of high risk for both the nature and human's health. Legislation of Europeans and other industrial countries needs appropriate data to evaluate the risks of the registration of new chemical preparations

such as pesticides, biocides and medicines. This data contains information about toxicity on various trophic levels (Scholz et al. 2008). Acute toxicity assays together with the growth inhibition assay serves as a basic tool for the evaluation of the potential toxic effect of the particular substance on live organisms (Kočí 2006). Growth inhibition assays are the basic ecotoxicological practise for a risk assessment of industrial chemical substances and pesticides (Brust et al. 2001). Algae are common test organisms sensitive to many toxic preparations and therefore are widely used in toxicity assays (Zhang et al. 2012). Algae, as primary producers, are key functional organisms in aquatic food chains (Machado and Soares 2012). Planktonic algae and cyanobacteria such as *Desmodesmus communis, Chlorella kessleri*, *Pseudokirchneriella subcapitata*, and *Anabaena* sp. can be used in growth inhibition assays (ÚNMZ 2012). The first part of the organism which is in contact with the chemical substance is the cell membrane. The cell membrane integrity is crucial for the functioning and viability of the cell itself. Cells with the damaged membrane are usually classified as dead cells. The cell membrane integrity evaluation is based on fluorescence methods (Machado and Soares 2012). Fluorescence shows a photosynthetic pigment of algae and cyanobacteria in living cells (Gregor and Maršálek 2006).

Even though terbutryn has been banned in many countries including the Czech Republic, the substance is still detected in the water. Terbutryn can leach from soil to the aquatic ecosystems. Its metabolites can be found in the drinking water long time after its last application. In this study, we aimed at the toxic effect of terbutryn determined by the comparable standardize method on various aquatic organisms, namely algae *D. communis*, *C. kessleri* and cyanobacteria *Anabaena* sp.

MATERIAL AND METHODS

Inoculum preparation

The assay was performed on a green algae *D. communis, C. kessleri* and cyanobacteria *Anabaena* sp. The algae inoculum was taken during the exponential growth of the inoculum culture and put to the assay two days before the cultivation. The inoculum was added to the nutrient solution (Z medium) in a density of 10^4 cells.ml/L to allow growth throughout the assay without the risk of nutrient depletion. Erlenmeyer flasks of 150 ml were used for the pre cultivation which took place in a constant temperature of 26±1°C and a constant light intensity of 7000 lx.

Preparation of concentration series

Terbutryn was dissolved in distilled water. Two concentration series with the dilution factor of two were prepared: 0.004883; 0.009766; 0.019531; 0.039063; 0.078125; 0.15625; 0.3125; 0.625; 1.25 mg/L and 0.003906; 0.007813; 0.015625; 0.03125; 0.0625; 0.125; 0.25; 0.5; 1 mg/L. Altogether 18 different stock solutions were prepared.

Figure 2 Microtiter plate – pipetting scheme.

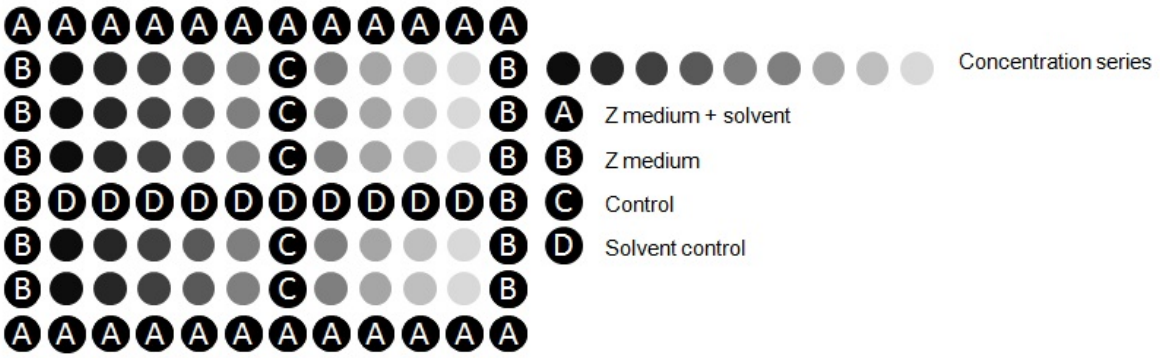

Legend: See the text for the details.

The inoculum samples were pipetted to a microtiter plates (Figure 2). The microtiter plate has nine tested concentrations in five replicates and the control group. Tested series were prepared by mixing

each stock solution with the inoculum (190 µl of the inoculum + 10 µl of the stock solution). The control group with Z medium (190 µl of the inoculum + 10 µl of Z medium) and the control with solvent only (190 µl of the inoculum + 10 µl of distilled water).

Incubation

Microtiter plates were closed by a cap during the incubation to prevent air contamination and to reduce evaporation. Incubation was carried out in the same conditions as the inoculum preparation (temperature: 26±1°C; light intensity: 7000 lx).

Fluorescence measurement

Measurement of fluorescence was made every 24 hours using the spectrophotometer (TECAN Infinite M1000 PRO) with the excitation wave length of 590 nm and the emission of 680 nm. The content of microtiter plates was re-mixed before each measurement. The assay lasted for 72 hours.

The IC50 estimation

The results were evaluated in software MS Excel (Microsoft) to figure the percentage of inhibition. Then, a dose-response curve based on a nonlinear regression was constructed in GraphPad Prism 7.04 (GraphPad Software, La Jolla California USA, www.graphpad.com). The inhibition concentration in which 50% of tested organisms died (IC50) was estimated as the fitted midpoint of the curve.

RESULTS AND DISCUSSION

The inhibition concentration of terbutryn in 72 hours (72hIC50) for *D. communis* was **0.012 mg/L** (log concentration 1.915, R^2 = 0.977), for *C. kessleri* **0.188 mg/L** (log concentration 0.7255, R^2 = 0.976) and for cyanobacteria *Anabaena* sp. **0.666 mg/L** (log concentration = 0.164 (R^2 = 0.887). The most sensitive taxon was *D. communis*, the most resistant cyanobacteria *Anabaena* sp. (Figure 3).

There are plenty of published data about the content of terbutryn in surface waters. Concentration of 0.02 µg/L of terbutryn was found in samples from river Elbe (Saxony, Germany). Concentrations in surface waters in Bavaria ranged from 0.6 to 1.2 µg/L (Brust et al. 2001). The highest concentration found in surface waters of the Czech Republic is 0.02 µg/L (Velíšek et al. 2009).

Arufe et al. (2004) presented the 72hLC50 of 1.41 mg/L for *Sparus aurata* yolk sac fry exposed to the commercial herbicide with terbutryn (59.4%). The same author presented results of toxicity assays with various time exposition: 24hLC50 – 3.66 mg/L, 48hLC50 – 2.18 mg/L. As a conclusion, the toxicity increases with increasing exposition time. The results show different sensitivity between *S. aurata* and *Vibrio fisheri* to commercial herbicide containing terbutryn (59.4%). Herbicide toxicity was more than one order lower in *V. fisheri* (15 min EC50 – 15.94 mg/L) than for *S. aurata* yolk sac fry (72hLC50 – 1.41 mg/L) (Arufe et al. 2004). Terbutryn is moderately toxic for fish. Bathe et al. (1973) presented LC50 being 4 mg/L for *Cyprinus carpio*, Arufe et al. (2004), Kidd and James (1991) presented 96hLC50 for *Oncorhynchus mykiss* 3 mg/L. Arufe et al. (2004) and Daho (2006) mentioned the results of acute toxicity assays and growth inhibition assays of other aquatic organisms, e.g. *Skeletonema costatum* 9dEC50 – 0.91 µg/L, *Dolichospermum flos-aquae* 7dEC50 – 3.4 µg/L, *Daphnia magna* 48hEC50 – 7.1 mg/L and *Lepomis macrochirus* 96hLC50 – 4 mg/L. Those results showed high toxicity of terbutryn for *S. costatum* and *D. flos-aquae*.

Plhalová et al. (2010) compared the acute toxicity of terbutryn using *Danio rerio* and *Poecilia reticulata.* The average value of terbutryn toxicity for embryonic stage of *D. rerio* was 8.04 mg/L, for juvenile *D. rerio* was the average value 96hLC50 5.71 mg/L. The results shows higher sensitivity of juvenile stages compared to the embryonic stage of *D. rerio*. The average value of terbutryn 96hLC50 for juvenile stage of *P. reticulata* was 2.85 mg/L. Comparison of the average LC50 of terbutryn for *D. rerio* and *P. reticulata* showed significantly higher sensitivity of *P. reticulata*.

Figure 3 Dose-Response curve of tested organisms.

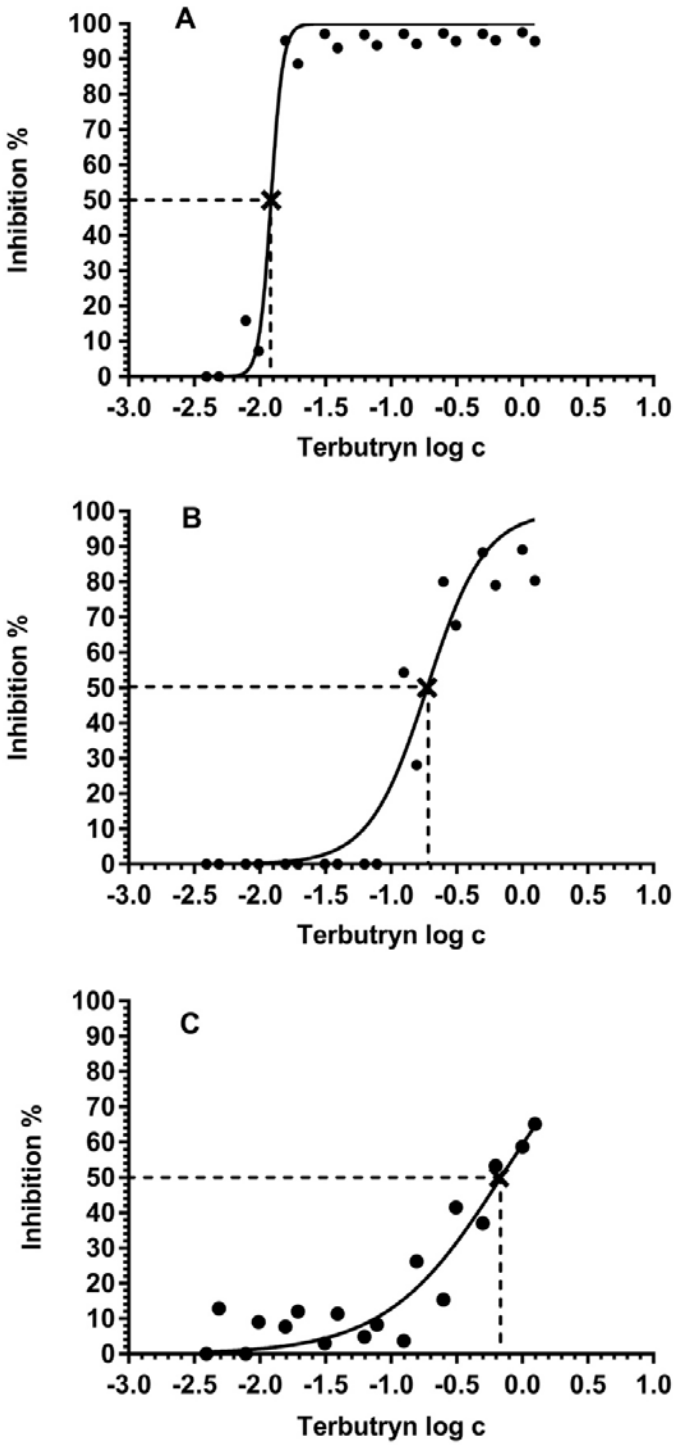

Legend: A – Desmodesmus communis, B – Chlorella kessleri, C – Anabaena sp. Crosses shows IC50.

CONCLUSION

In conclusion, the terbutryn is highly toxic to green algae and cyanobacteria according to the calculated inhibitory concentrations (72hIC50). The most sensitive species was the green algae *D. communis* (72hIC50 was 0.012 mg/L) followed by *C. kessleri* (72hIC50 was 0.188 mg/L), the most

resistant cyanobacteria *Anabaena* sp (72hIC50 was 0.666 mg/L). The results are confirmed by other authors who show that the acute toxicity of terbutryn is also high to other aquatic organisms. Based on our results, the natural concentrations causing the acute toxicity of the most sensitive green algae should be 600 times higher than the highest concentration found in surface waters in the Czech Republic (0.02 µg/L). The potential environmental risk is bioaccumulation which can be important even in relatively low natural concentration of terbutryn.

ACKNOWLEDGEMENTS

The research was financially supported by the project OP VaVpI CZ.1.05/4.1.00/04.0135, IGA MENDELU grant, no. AF-IGA-2018-tym004 and NAZV QJ1620240.

REFERENCES

Arufe, M.I. et al. 2004. Toxicity of a commercial herbicide containing terbutryn and triasulfuron the seabream (*Sparus aurata* L.) larvae: comparsion with the Microtox test. Ecotoxicology and Environmental Safety, 59(2): 209–216.

Bathe, R. et al. 1973. Determination of pesticide toxicity to fish. Schriftenr. Ver. Wasses-Boden-Lufthxg. Berlin-Dahlem 37, 241–256.

Breckenridge, Ch.B. et al. 2010. Symmetrical Triazine Herbicides: A Review of Regulatory Toxicity Endpoints. In Hayes´ Handbook of Pesticide Toxicology. University of California: Robert Krieger, pp. 1711–1723.

Brust, K. et al. 2001. Effects of terbutryn on aufwuchs and *Lumbriculus variegates* in artificial indoor streams. Environmental Toxicology and Chemistry, 20(9): 2000–2007.

Daho, M.B. 2006. Ecotoxicological evaluation of the herbicide terbutryn. Master´s thesis, University of Uppsala.

Gregor, J., Maršálek, B. 2006. Fluorescenční metody kvantifikaci planktonních cyanobakterií. In Cyanobakteria 2006. Brno, Czech Republic, 24–25 May. Botanický ústav AV ČR Průhonice, pp. 91–95.

Kidd, H., James, D.R. 1991. The Agrochemicals Handbook third ed. Royal Society of Chemistry Information Services, Cambridge, UK.

Kočí, V. 2006. Význam testů toxicity pro hodnocení vlivu látek na životní prostředí. Chemické listy, 100(10): 882–888.

Machado, M.D., Soares, E.V. 2012. Development of short-term assay based on the evaluation of the plasma membrane integrity of the alga *Pseudokirchneriella subcapitata*. Applied Microbiology and Biotechnology, 95(4):1035–1042.

Moretti, M. et al. 2002. In vitro testing for genotoxicity of the herbicide terbutryn: cytogenetic and primary DNA damage. Toxicology in Vitro, 16(1): 81–88.

Plhalová, L. et al. 2010. Comparison of Terbutryn Acute Toxicity to *Danio rerio* and *Poecilia reticulata*. Acta Veterinaria Brno, 79(4): 593–598.

Rioboo, R. et al. 2007. Population growth study of the rotifer *Brachionus* sp. fed with triazine-exposed microalgae. Aquatic Toxicology, 83(4): 247–253.

Royal Society of Chemistry. 2015. ChemSpider Search and share chemistry. [Online]. Available at: http://www.chemspider.com/Chemical-Structure.12874.html. [2018-07-2].

Scholz, S. et al. 2008. The zebrafish embryo model in environmental risk assessment-applications beyond acute toxicity testing. Environmental Science and Pollution Research, 15(5): 394–404.

ÚNMZ. 2012. Kvalita vod – Zkouška inhibice růstu sladkovodních zelených řas. ČSN EN ISO 8692 (75 7740). Praha: Úřad pro technickou normalizaci, metrologii a státní zkušebnictví.

Velíšek, J. et al. 2009. Effects of sup-chronic exposure to terbutryn in common carp (*Cyprinus carpio* L.). Ecotoxicology and Environmental Safety, 73(3): 384–390.

Zhang, L.J. et al. 2012. Development and application of whole sediment toxicity est using immobilized freshwater microalgae *Pseudokirchneriella subcapitata*. Environmental Toxicology and Chemistry, 13(2): 377–386.

Quantitative analyses of phytoplankton in Zámecký pond – three years research

Marija Radojicic, Jiri Hetesa, Barbora Musilova, Radovan Kopp
Department of Zoology, Fisheries, Hydrobiology and Apiculture
Mendel University in Brno
Zemedelska 1, 613 00 Brno
CZECH REPUBLIC

radojicic.marija88@gmail.com

Abstract: Quantitative analyses of phytoplankton in Zámecký pond were conducted during the period from April to October in years 2014, 2016 and 2017. Abundance was determined by counting cells in Bűrker chamber. The lowest abundance during the vegetative season was in the year 2014, and highest in 2017. Centric diatoms were the most dominant in April 2014. Genera of Chlorophyta (*Scenedesmus*, *Desmodesmus, Oocystis*, *Monoraphidium*, *Coelastrum*) common for fishponds were recorded in all months in different number, but with the highest density in June 2014 and April 2016. During the rest of the study period Cyanobacteria, which were mainly represented by the genera *Dolichospermum, Microcystis*, *Aphanizomenon* and species *Cuspidothrix issatschenkoi, Pseudanabaena limnetica* and *Planktothrix agardhii* was the most dominant division. Algal bloom occurred every year, with highest peaks in August 2014, September 2016 and July 2017. However, the big difference in abundance among study years was noticed. The highest phytoplankton density was recorded in July 2017, when 7.98 million cells per ml of water were registered, of which 55% was *Dolichospermum flos-aquae* and 44% species of genus *Microcystis*. The obtained abundance values from 2016 and 2017 are higher than any recorded before.

Key Words: cyanobacterial bloom, season, *Microcystis*, abundance

INTRODUCTION

Zámecký fishpond is situated close to the village Lednice in the District Břeclav (South Moravian Region, Czech Republic). The area of fishpond is 27 ha, mean depth is 1.15 m and it is supplemented with water from the river Stará Dyje. The owner and the user of the fishpond is The National Heritage Institute. Zámecký fishpond, together with four others (Nesyt, Hlohovecký, Prostřední and Mlýnský fishponds), has been a part of the National Nature Reserve Lednické rybniky since 1953. This Reserve is one of the most important bird areas in the Czech Republic. These fishponds are also (since 1990) recognized as Wetlands of International Interest under the Ramsar Convention. Lednické rybníky, with the surrounding landscape, are a part of the Lednice-Valtice area, which was inscribed on the UNESCO World Cultural and Natural Heritage List in 1996.

First phytoplankton research of Zámecký fishpond dated from 1920. Interestingly, even in this period, when fish breeding was extensive, fishpond was characterized as eutrophic (Bayer and Bajkov, 1929). After the Second World Word intensification of fishpond management increased (including feeding, fertilization and larger quantity of stocked fish), leading to increment of phytoplankton abundance. To restore the species diversity of aquatic organisms, a maintenance plan for Lednické rybníky was prepared (Lázničková 1993). According to the plan, fishery in Zamecký fishpond was regulated by declines in fish stocking and lower introduction of herbivorous fish. However, despite the regulation of stock, phytoplankton abundance was still high. Decreases in the number of stocked fish (since 1998) were accompanied by increases in fish numbers from the Dyje river. During the 2000–2003 period, cyanobacteria-forming water bloom was observed in a great amount (Kopp 2006).

Zámecký fishpond has been left without stocking since 2004 (AOPK 2012). This led to a short-term decrease in phytoplankton abundance and chlorophyll a values, and increase in water transparency (Kopp 2006). Low fish stocks enabled the growth of submerged aquatic macrophytes and filamentous algae, which were later replaced by the free-floating aquatic plants influencing the chemical and light regime of water column. At first, reduction of stocking had a positive influence on water quality,

however an increase in chlorophyll a values and abundance of phytoplankton have been recorded again since 2008 (Kopp et al. 2016). According to the newest management plan for The National Nature Reserve Lednické rybniky for the period 2012–2021 (AOPK 2012), Zámecký pond should be harvested at least once in a three-year interval. However, harvesting has not been done even once since year 2007.

In water bodies, such as Zámecký pond, which are important bird areas, research of phytoplankton development and its effects on water transparency is of great importance. Under conditions of low water transparency, bird brood cannot find suitable food. According to Musil (2006) fishponds with conditions suitable for breeding water bird species are those having a water transparency of more than 50 cm.

Aim of the study was to compare the phytoplankton community of Zámecký fishpond during the vegetative season over a three-year period.

MATERIAL AND METHODS

Water temperature, pH and conductivity were measured immediately on site using mobile instruments (Hach Lange and Hanna instruments), always at the outflow at the same time (in the morning).

Phytoplankton research was conducted during 2014, 2016 and 2017. Samples were taken in 2014 once a week and in 2016 and 2017 once a month during the vegetation season from April to October. Samples for the determination of the phytoplankton species and genera were collected using the 20 µm mesh planktonic net and live material was analysed under a light microscope Olympus BX51 using standard keys. Determined taxa were classified into eight divisions: Cyanobacteria, Dinophyta, Cryptophyta, Chrysophyta, Xantophyta, Bacillariophyta, Euglenophyta and Chlorophyta (Reynolds 2006).

Quantitative phytoplankton samples, were taken with tube water sampler (Andělova tyč) from the surface water layer (0–30 cm), put in 50 ml plastic bottles and preserved in Lugol's solution. Samples were concentrated using filtration equipment by Marvan (1957), after which the abundance of algae and cyanobacteria was calculated by counting cells in a Bűrker chamber. Colonies of genera *Microcystis* were disintegrated using ultrasound. Approximately 25 ml of the samples were exposed to ultrasound SONOPULS HD 2070 (Bandelin electronic, Germany) for 3 minutes with 20% strength. The data are expressed as a number of cells per millilitre. Average values of week samples are used to present monthly values of phytoplankton abundance in 2014.

RESULTS AND DISCUSSION

Values of *in situ* measured parameters are presented in Table 1.

Table 1 Values of the measured abiotic parameters in Zámecký pond

Zámecký fishpond	Water temperature (°C)			pH			Conductivity (µS/cm)		
	2014	2016	2017	2014	2016	2017	2014	2016	2017
April	13.5	17.0	15.1	8.96	7.80	8.69	626	565	621
May	17.0	17.8	14.4	8.18	8.88	8.15	696	517	453
June	21.6	23.9	21.3	8.21	9.24	8.17	725	538	703
July	22.5	23.2	22.3	8.59	9.40	8.25	656	509	618
August	20.4	23.7	25.0	9.23	9.02	9.61	569	534	549
September	19.9	21.2	23.1	8.67	8.91	9.19	640	541	590
October	12.5	-	12.5	8.76		7.91	570		905

The highest phytoplankton abundance in Zámecký pond was observed in July 2017, and the lowest in April 2016. The maximal peak of abundance in every year was in a different month (Figure 1).

Throughout the study period cyanobacteria was the most dominant division. Only in April 2014 and 2016, and June 2014 this group was not the most abundant one (Figure 2).

Figure 1 Change in phytoplankton abundance in studied fishpond

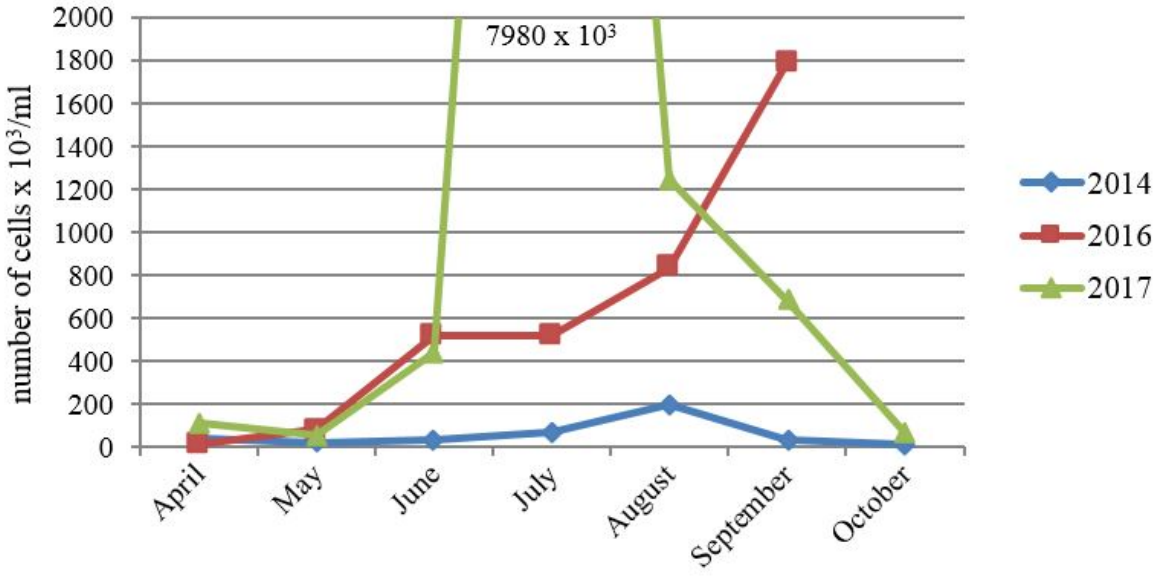

The lowest abundance during the entire season was recorded in 2014, when compared to 2016 and 2017. Centric diatoms represented mainly by *Cyclostephanos invisitatus* and genus *Stephanodiscus* were the most numerous in April 2014. Colonial cyanobacteria *Eucapsis densa* was the most dominant species in May, while small Chlorophyta *Monoraphidium minutum* was the most numerous one in June 2014. From July to September, the most abundant representatives belonged to the group of cyanobacteria, with the dominance of *Dolichospermum flos-aquae* and *D. perturbatum,* which were the most numerous species from July to September, followed by *Cuspidothrix issatschenkoi* in July, and *Planktothrix agardhii* in August. In October 2014, genus *Aphanizomenon* was the most abundant. Genera of Chlorophyta (*Scenedesmus, Desmodesmus*, *Oocystis, Pediastrum, Aktinastrum, Coelastrum*) were recorded in all months in different numbers.

Figure 2 Abundance of cyanobacteria and algae divisions documented in Zámecký pond

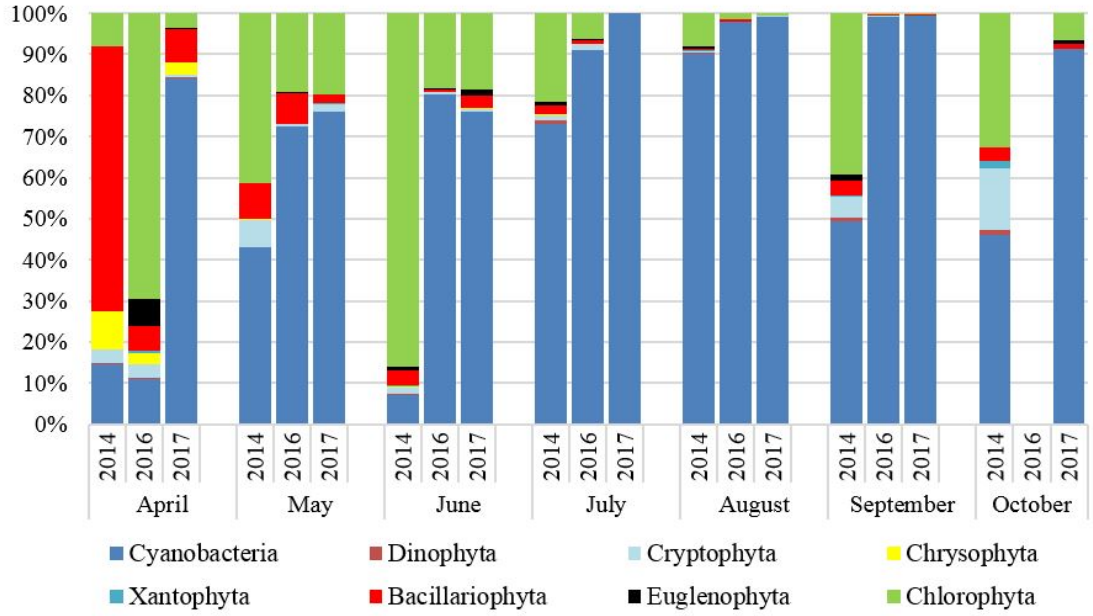

Green algae *Pseudopediastrum boryanum* was the most abundant at the beginning of the season 2016, after which the dominance of Cyanobacteria was recorded (Figure 2). *Aphanizomenon* was the most numerous in May 2016, *Planktothrix agardhii* and *Pseudanabaena limnetica* in June, when *Cuspidothrix issatschenkoi* was also registered in a noticeable quantity. *Dolichospermum flos-aquae*

was the most dominant species in July; representatives of genus *Microcystis* in August, and these two taxa were equally represented in September.

Cyanobacteria were the most dominant group over the entire 2017 (Figure 2). *Microcystis* was registered in high numbers in every month, with its dominance in April, May and October. *Planktothrix agardhii* was the most numerous in June, while *Dolichospermum flos-aquae* together with representatives of genus *Microcystis* was dominant from July to September.

Algal blooms were recorded in every year of the study period, but with high variance in the cell number. The main algal species responsible for bloom in Zámecký fishpond are the *Dolichospermum flos-aquae*, *Microcystis aeruginosa*, *M. ichtyoblabe*, and *M. wesenbergii* and this was confirmed in different studies (Sukop and Kopp 2001, Sukop and Kopp 2002, Ramezanpoor et al. 2004, Kopp 2006, Heteša 2018).

The highest value of abundance was in July 2017 when *Dolichospermum flos-aquae* was the most dominant with 4.42 million cells per ml, followed by genus *Microcystis* with 3.55 million cells per ml. Previous research of phytoplankton in Zámecký fishpond has also shown a high abundance of cyanobacteria in summer months, but not as high as in this study. Kopp (2006) and Ramezanpoor et al. (2004) state that in the summer months of 2000–2003, a significant growth of cyanobacteria forming water bloom was observed. Density of cyanobacterial blooms often exceeded 1 million cells per 1 ml of water. The increase of phytoplankton abundance during the 2000–2003 period was probably caused by diverse factors, such as a higher input of cyanobacteria from the river Stará Dyje and the Reservoir Novomlýnské, and changes in the zooplankton structure affected by changes in the fish species composition (Kopp 2006, Kopp et al. 2016). The amount of fish stock is one of the main key factors that affects the development of zooplankton and indirectly phytoplankton. However, due to the cessation of stocking and input of fish from Stara Dyje river the current state of fish population can only be estimated. Considering the fact that the draining of the pond was last carried out in 2007 and water level was lowered to about one-half of the original pond volume in 2016, the estimations are that the fish population is very dense and has a negative effect on zooplankton and phytoplankton community.

CONCLUSION

Zámecký pond is part of a National Nature Reserve, important bird area; and fishery management is highly limited by the purpose of nature conservation. Since 2004 it has been left without stocking, with the idea to improve the water quality and environment for waterfowl. However, the research of phytoplankton conducted in vegetative season 2014, 2016 and 2017 has shown that the current way of managing does not achieve positive effects. One of the suggested solutions for suppressing cyanobacterial blooms is removing the high layer of sediment, which is a source of nutrients in addition to suitable fishery management.

ACKNOWLEDGEMENTS

The research was financially supported by IGA MENDELU grant, no. AF-IGA-2018-tym004.

REFERENCES

AOPK (Agentura ochrany přírody a krajiny České republiky). 2012. Plán péče o Národní přírodní rezervaci Lednické rybníky na období 2012–2021 [Online]. Available at: http://palava.ochranaprirody.cz/res/archive/081/012027.pdf?seek=1371224232. [2018-05-10].

Bayer, E., Bajkov, A. 1929. Hydrobiologická studia rybníků Lednických, I. Výzkum heleoplanktonu a jeho poměrů quantitativních. Sborník Vysoké školy zemědělské v Brně. Brno, p. 165.

Heteša, J. 2018. Vývoj fytoplanktonu zámeckých rybníků v Lednici. In Sborník Regionálního muzea v Mikulově. Mikulov: RegioM, pp. 21–34.

Kopp, R. 2006. Phytoplankton of the Zámecký Pond. Czech Phycology, 6: 111–125.

Kopp, R. et al. 2016. Zámecký rybník v Lednici – změny kvality vody v závislosti na intenzitě rybářského hospodaření. In Proceedings of Rybníky 2016. Praha, Česká republika, 23–24 June, Praha: Česká společnost krajinných inženýrů, České vysoké učení technické v Praze, Univerzita

Palackého v Olomouci, Výzkumný ústav vodohospodářský T. G. Masaryka, Česká zemědělská univerzita v Praze, pp. 115–123.

Lázničková, S. 1993. Plán péče na období 1994–1999. Lednické rybníky, Brno.

Marvan, P. 1957. K metodice kvantitativního stanovení nanoplanktonu pomocí membránových filtrů. Preslia, 29: 76–83.

Musil, P. 2006. A review of the effects of intensive fish production on waterbird breeding populations. In Waterbirds around the world. Edinburgh: TSO Scotland Ltd., pp. 520–521.

Ramezanpoor, Z. et al. 2004. Phytoplankton diversity and their succession in water bodies of the Lednice park during 2002 season. Acta Universitatis Agriculturae et Silviculturae Mendelianae Brunensis, 2: 83–96.

Reynolds, C. 2006. Ecology of phytoplankton. 1st ed., Cambridge, UK: Cambridge University Press.

Sukop, I., Kopp, R. 2001. Monitoring planktonních společenstev a sledování hydrochemických parametrů na Lednických rybnících v roce 2001. Závěrečná zpráva RŽP Brno.

Sukop, I., Kopp, R. 2002. Monitoring planktonních společenstev a sledování hydrochemických parametrů na Lednických rybnících v roce 2002. Závěrečná zpráva RŽP Břeclav.

Proliferative kidney disease in farmed and wild salmonids - risk of spreading and transmission

Eva Syrova, Veronika Kovacova, Ivana Papezikova, Hana Minarova, Miroslava Palikova
Department of Ecology and Diseases of Game, Fish and Bees
University of Veterinary and Pharmaceutical Sciences Brno
Palackeho tr. 1946/1, 612 42 Brno
CZECH REPUBLIC

syrovae@vfu.cz

Abstract: Proliferative kidney disease is a serious disease of salmonid fish. It causes economic losses in intensive salmonid fish farming and has been an increasing threat to wild salmonid populations in open waters. This prompts the question as to what are the risks of spreading and transmission of its causative agent *Tetracapsuloides bryosalmonae* from intensive breeding farms to open waters. The aim of this study was to examine samples of salmonid fish from the open waters of the Czech Republic using molecular biological methods in order to find the incidence of *T. bryosalmonae.* A total of 212 salmonid fish were obtained from seven localities in the years 2016 and 2017. Obtained samples of kidney tissue were examined using PCR and real-time PCR. The presence of the parasite was confirmed using the molecular method in all the monitored locations. This is the first study focused on the presence of *T. bryosalmonae* in the open waters of the Czech Republic.

Key Words: Tetracapsuloides bryosalmonae, parasite, PCR, salmonid fish, temperature

INTRODUCTION

Proliferative kidney disease (PKD) is an increasingly often mentioned and discussed disease related not only to intensive salmonid fish farming but to open waters as well. The causative agent of the disease is *Tetracapsuloides bryosalmonae* (Myxozoa: Malacosporea). It is a two-host endoparasite which uses freshwater bryozoans (Bryozoa) and salmonid fish in its development cycle. The agent invades predominantly one-year-old fish, with kidney being the main affected organ (Feist et al. 2001, Okamura et al. 2001, Okamura et al. 2011).

In terms of pathological findings in the affected fish, most frequent are observations of enlarged body cavity, exophthalmus, kidney swelling, spleen swelling, ascites, pale liver and gills, dark skin colouration and small knot-like formations in organs (Hedrick et al. 1993, Palikova et al. 2017). In intensive farming, PKD can cause considerable economic losses. Mortality here ranges around 30% and if other negative factors set in during the course of the disease such as stress, higher water temperature or secondary infection, mortality may reach up to 95% (Okamura et al. 2011, Schmidt-Posthaus et al. 2012, Palikova et al. 2017). In intensive fish farming, the greatest losses caused by the disease occur in younger categories of rainbow trout (*Oncorhynchus mykiss*) (Okamura et al. 2011).

Efforts are made to monitor PKD occurrence in salt waters (predominantly in the states of Northern Europe). The presence of *T. bryosalmonae* including the clinical symptoms in fish has been determined in some salmonid species (*Salmo trutta*, *Salmo salar, Oncorhynchus mykiss*) there but considering the demands of the monitoring procedure, the results are not as explicit as in fish farming, and their quantity is insufficient (Wahli et al. 2002, Okamura et al. 2011, Skovgaard and Buchmann 2012). Some studies have discussed the suspicion that PKD along with the acting of other negative factors may be involved in the massive decrease of wild salmonid populations (Wahli et al. 2002, Streud et al. 2007). In the future, the situation may grow even more serious in consequence of the global water temperature rise, as the water temperature is a conditioning factor for the release of spores from the bryozoans (Strepparava et al. 2018).

Considering the alarming decrease in salmonid populations in open waters, the question arises as to what are the risks of spreading and transmission of *T. bryosalmonae* from breeding farms into open

waters. Grabner and El-Matbouli (2008) have proved a reverse bryozoan infection from brown trout (*Salmo trutta*) and brook trout (*Salvelinus fontinalis*) through the outflow water from tanks with infected fish.

In the Czech Republic, the causative agent of PKD has so far been detected only in intensive fish farming. Its presence in open waters has not been monitored systematically so far, as it has been e.g. in Switzerland (Wahli et al. 2002). The aim of this study was to quantitatively and qualitatively assess the obtained samples from salmonids of the open waters of the Czech Republic in order to determine the occurrence of *T. bryosalmonae* in the open waters and confirm the presence of this causative agent by using molecular biological methods; and furthermore, to provide a brief reflection on the risks of the spreading and transmission of the causative agent of PKD including the ways of minimizing the said risks.

MATERIAL AND METHODS

Samples of salmonids

A total of nine catches of salmonids were performed on seven rivers in the Czech Republic during the years 2016 and 2017. A total of 212 fish were caught. The fish were humanely killed and subjected to pathological examination during which a sample of the kidneys was taken from each fish and fixed in 10% formaldehyde for further examinations. The experiment was conducted in accordance with the EU Directive 2010/63/EU on animal experiments.

DNA extraction from paraffin-embedded tissue sections

DNA was purified with a QIAamp DNA FFPE Tissue Kit (QIAGEN) according to the manufacturer's instructions. DNA concentrations were measured by spectrophotometry using NanoDrop spectrophotometer (ThermoFisher Scientific, Vienna, Austria) and then stored at -20 °C until use.

PCR and real-time PCR for detection of parasite DNA

Extracted DNA was used for qualitative parasite examination to detect the presence of *T. bryosalmonae* in samples by PCR. The PCR amplification was performed as described by Kent et al. (1998) using the PKX specific primers 5F and 6R. Gel electrophoresis was used to visualize the products.

To assess the individual relative parasite load, the parasite DNA was quantified using the qRT-PCR (Bettge et al. 2009).

Sequencing analysis

DNA from PCR was purified using the SureClean Plus solution (Bioline Reagents Ltd., UK) according the manufacturer's instructions and was sequenced in both directions (Biogen, Czech Republic) using the amplification primers 5F and 6R.

RESULTS AND DISCUSSION

During the nine catches at seven open water localities (at two localities, catches were performed both in 2016 and 2017) in the Czech Republic, a total of 212 salmonid fish were caught. The numbers of fish from the respective localities and the results of the molecular biological examination of kidney tissue are summarized in Table 1, where the parasite's DNA was confirmed in the positive samples by the molecular method. The sequencing method confirmed *T. bryosalmonae* as the actual causative agent.

In 78% (n = 165), the results of PCR and real-time PCR were fully compatible. In 22% (n = 47) of cases, PCR failed to confirm the presence of *T. bryosalmonae* DNA in kidney tissue; in contrast, real-time PCR detected the causative agent in these samples. Real-time PCR is a method characterized by high sensitivity and reliability, and can be evaluated as a more accurate method compared to the classical PCR (Logan et al. 2009).

The resulting data cannot be deemed positive for the future of salmonids in open waters; the parasite's DNA was confirmed by both molecular methods in all of the monitored locations. Since the outbreak of PKD is dependent on a higher water temperature, aggravation of the situation as regards this

disease is to be expected in the open waters of the Czech Republic, considering the climate change (Strepparava et al. 2018).

Table 1 Summary of characteristics of 212 samples of wild salmonid fish

Examination date	Location No.	PCR (+/n)	qRT-PCR (+/n)
2016	1	18/19	19/19
	2	9/30	29/30
	3	22/29	27/29
	4	14/25	25/25
	5	10/16	12/16
2017	6	24/29	27/29
	3	13/16	16/16
	2	13/17	16/17
	7	22/31	23/31

In intensive salmonid fish farming the situation is more serious in terms of prevalence and mortality of PKD (Palikova et al. 2017). There is a major risk of spreading and transmission of the causative agent through fish, or even through water, to the open waters. It needs to be noted, however, that in most cases, the causative agent is introduced to the intensive farming with the water flowing in from locations with the occurrence of infected bryozoans. In intensive farming, efforts are made to find a suitable species for the farming, i.e. a salmonid line with a higher resistance to PKD, and thus to minimize the losses in fish farming as well as the risk of the spread to the open waters (Grabner and El-Matbouli 2009). Fish from intensive farming with the occurrence of PKD should not be stocked into open waters; especially those species in which the release of spores and reverse infection of bryozoans has been shown. The occurrence of PKD and the spread of its causative agent in intensive fish farming as well as in open waters should be closely monitored.

CONCLUSIONS

In conclusion, this is the first study monitoring the presence of the causative agent of PKD, *T. bryosalmonae* in the open waters of the Czech Republic using molecular biological methods. The parasite's DNA was confirmed in all the monitored open water localities. A number of strategies can be used to minimize the spreading and transmission of the disease from breeding farms to the open waters. However, there are still many unclear areas regarding the spread of the parasite, the resistance of its hosts or the effect of the environmental conditions on the spread of the disease. This topic warrants further research, as PKD is at present one of the most serious diseases of salmonid fish.

ACKNOWLEDGEMENTS

This study was funded by the Internal Grant Agency of the University of Veterinary and Pharmaceutical Sciences Brno (project no. 219/2017/FVHE) and by NAZV QJ KUS QJ1510077. We thank Vojtech Balaz of the Department of Biology and Wildlife Diseases for help with laboratory experiments and data analysis and Karin Hermanska for the translation.

REFERENCES

Bettge, K. et al. 2009. Proliferative kidney disease (PKD) of rainbow trout: temperature- and time-related changes of *Tetracapsuloides bryosalmonae* DNA in the kidney. Parasitology, 136: 615–625.

Feist, S.W. et al. 2001. Induction of proliferative kidney disease (PKD) in rainbow trout *Oncorhynchus mykiss* via the bryozoan *Fredericella sultana* infected with *Tetracapsula bryosalmonae*. Diseases of Aquatic Organisms, 45: 61–68.

Grabner, D.S., El-Matbouli, M. 2008. Transmission of *Tetracapsuloides bryosalmonae* (Myxozoa: Malacosporea) to *Fredericella sultana* (Bryozoa: Phylactolaemata) by various fish species. Diseases of Aquatic Organisms, 79: 133–139.

Grabner, D. S., El-Matbouli, M. 2009. Comparison of the susceptibility of brown trout (*Salmo trutta*) and four rainbow trout (*Oncorhynchus mykiss*) strains to the myxozoan *Tetracapsuloides bryosalmonae*, the causative agent of proliferative kidney disease (PKD). Veterinary Parasitology, 165: 200–206.

Hedrick, R.P. et al. 1993. Proliferative kidney disease of salmonid fish. Annual Review of Fish Diseases, 3: 277–290.

Kent, M.L. et al. 1998. Ribosomal DNA Sequence Analysis of Isolates of the PKX Myxosporean and Their Relationship to Members of the Genus *Sphaerospora*. Journal of Aquatic Animal Health, 10: 12–21.

Logan, J. et al. 2009. Real-time PCR. In Current Technology and Application. Norfolk: Caister Academic Press.

Okamura, B. et al. 2001. Patterns of occurrence and 18S rDNA sequence variation of PKX (*Tetracapsula bryosalmonae*), the causative agent of salmonid proliferative kidney disease. Journal of Parasitology, 87(2): 379–385.

Okamura, B., et al. 2011. Lifecycle complexity, environmental chase and the emerging status of salmonid proliferative kidney disease. Freshwater Biology, 56(4): 735–753.

Palikova, M. et al. 2017. Proliferative kidney disease in rainbow trout (*Oncorhynchus mykiss*) under intensive breeding conditions: Pathogenesis and haematological and immune parameters. Veterinary Parasitology, 238: 5–16.

Schmidt-Posthaus H. et al. 2012. Kidney pathology and parasite intensity in rainbow trout *Oncorhynchus mykiss* surviving proliferative kidney disease: time course and influence of temperature. Diseases of Aquatic Organisms, 97: 207–218.

Skovgaard, A., Buchmann, K. 2012. *Tetracapsuloides bryosalmonae* and PKD in juvenile wild salmonids in Denmark. Diseases of Aquatic Organisms, 101(1): 33–42.

Strepparava, N. et al. 2018. Temperature-related parasite infection dynamics: the case of proliferative kidney disease of brown trout. Parasitology, 145: 281–291.

Streud, E. et al. 2007. Severe mortality in wild Atlantic salmon *Salmo salar* due to proliferative kidney disease (PKD) caused by *Tetracapsuloides bryosalmonae* (Myxozoa). Diseases of Aquatic Organisms, 77(3), 191–198.

Wahli T., et al. 2002. Proliferative kidney disease in Switzerland: current state of knowledge. Journal of Fish Diseases, 25: 491–500.

Effect of phytase addition and citric acid on the production parameters of feed for Common Carp (*Cyprinus carpio* L.)

Iveta Zugarkova, Jan Mares, Ondrej Maly, Jan Grmela
Department of Zoology, Fisheries, Hydrobiology and Apiculture
Mendel University in Brno
Zemedelska 1, 613 00 Brno
CZECH REPUBLIC

xzugark1@mendelu.cz

Abstract: The aim of the experiment was to evaluate the effect of addition phytase enzyme together with citric acid to Feed conversion ratio (FCR) and a Specific growth rate (SGR) in feed for common carp. The phytase addition increases the digestibility of phytate phosphorus from plant components in feed mixtures. The addition of citric acid (CA) optimize a pH level in guts for the phytase enzyme. For the experiment was prepared five types of feed. The basic component was a commercial mixture for carp (KP1) with 10% share of soybean meal. This mixture was fed to the control group. Next 4 experimental mixtures were prepared by addition of 500 FTU, 1000 FTU, 500 FTU + 3% of CA and 1000 FTU + 3% of CA. The test was made in 10 tanks (5 groups with one replication) with 15 specimens in each group. The test lasted 72 days. Results show statistically insignificant differences of production parameters in groups 500 FTU and 1000 FTU, but differences of FCR and SGR were statistically significant in groups 500 FTU+CA and 1000 FTU + CA. FCR of these groups decreased by 20% over the control group (one–way ANOVA: F=24, df=4, P=0.002). SGR increased by 11% over the control group (one–way ANOVA: F=17.93, d.f.=4, P=0.004).

Key Word: common carp, phosphorus, fish nutrition, Feed conversion ratio

INTRODUCTION

More frequent use of plant components in fish nutrition leads to higher content of phosphorus in feed. The phosphorus in plants is deposited in the form of phytic acid (Lundová 2014). Phytic acid in plants is poorly digestible for monogastric animals and fish. It can also limit some minerals in the body bounded to phosphoric acid residues (Kalač and Míka 1997). Singh (2008) reports the highest content of phytic acid in seeds, especially in packs and bran. The most available phytic acid is stored in the seed germ.

According to Simons et al. (1990), the phytase can be found in rumens micro flora of ruminants, plants and external microorganisms. The microflora of monogastric animals and fish is poor and a digestibility of the phytic acid is low. To increase the digestibility in monogastric animals and fish are used exogenous industrial phytases. This phytases are produced by genetically modified micro–organisms and extracted. The main benefit of increased phosphorus digestibility is lower phosphorus in excrements and consequent lower load on the aquatic environment (Brož 2002).

The use of phytase in feeds is complicated by its sensitivity to pH level and ambient temperature. Shah et al. (2015) states the highest phytase activity in the range of pH from 2.5 to 5.5. Fish without a stomach has neutral pH in guts and the phytase activity cannot be optimal. For the pH level optimization are added organic acids to the feed mixtures for example a citric acid. The acids decrease the pH level in the digestive tract and they slows the secretion. According to Cao et al. (2007) is the maximum tolerated temperature for phytases about 40–60 °C. During the feed processing (granulation or pelleting) is the temperature up to 100 °C, at this point phytase proteins denature and the digestibility of the phosphorus cannot be influenced.

The aim of the experiment was to evaluate the effect of phytase and citric acid in the standard feed mixture on the production parameters.

MATERIAL AND METHODS

Characteristic of experimental feeds

Basic mixture

For the basic mixture was used KP1 (Výroba krmiv spol. s.r.o., Stříbrné Hory, Czech Republic). The main component of the feed is crushed wheat, corn, wheat flour, wheat bran, extracted soybean meal, rapeseed expector and soybean oil. The mixture is enriched with a mineral–vitamin premix. Due to the low crude protein content (17.89%) was the experimental mixture enriched by addition of 10% soybean extract.

Phytase enzyme

For the experiment was selected Phyzyme XP 10.000 TPT (Danisco Animal Nutrition, Denmark) suitable for use on plant–based feeds. Phytase in this preparation is produced by bacteria *E.coli*. It contains 10.000 FTU per gram in bulk or liquid form. The preparation has increased resistance to proteolytic enzymes and higher relative activity over a wide range of pH. The thermo stability of the enzyme is increased by TPT technology (Thermo Protective Technology) up to 95 °C and thus is suitable for granulation.

Experimental feed

The basic mixture was made by mixing the KP1 with soybean meal and binder (Pellet-Dur, Röthel GmbH, Gudensberg, Germany). To the basic mixture were added 500 FTU (FyThase Unit) or 1000 FTU phytase enzymes. Dry feed was homogenized for 2 hours using a kitchen robot (Kitchen Aid Heavy Duty 5kpm5, United States). The mixture was moistened after homogenization by 40 °C water and processed to dough. The citric acid for acidified feed was dissolved in the water. The dough was adjusted to pellets by meat grinder (Kitchen Aid Heavy Duty 5kpm5, United States) and dried at 40 °C in a hot air sterilizer (STERICELL 11, BTM Medical Technology s.r.o.). After cooling, the granules were stored in dry plastic boxes.

Table 1 Composition of compound feeds

	Control	F500	F1000	F500C3	F1000C3
KP1	90%	90%	90%	87%	87%
Soybean meal	10%				
binder	0.5%				
phytase		500 FTU	1 000 FTU	500 FTU	1 000 FTU
Citric acid				3%	3%

Test characteristics

The experiment was made in ten glass tanks (160 l) in a recirculating system (RAS) at the Department of Fisheries and Hydrobiology MENDELU in Brno (Czech Republic). The RAS included a mechanical and biological filter, a UV lamp and the water was vigorously aerated. The test was conducted for 72 days. To each tank was stocked 15 specimens of a common carp (*Cyprinus carpio* L.) on an average weight of 134.4 g (W) and average total length of 199.5 mm (TL). The fish were adapted to environmental conditions and feeds prior to the start of the experiment for 14 days. Each group had one repeating.

The fish were individually measured (TL) and weighed (W) at the beginning of the test. Fish was fed daily at 8:00, 13:00 and 18:00. The feed dose was 3% of total weight of each group. Control weighting and measurements were performed every 14 days and then were adjusted the feed rates. Final measurements and weighting was performed in the end of the test. Total amount of used feed was determined. The total increment and individual increment (g and %), FCR (feed consumption / total increment), SGR ($[(\ln w_t - \ln w_0) / t] * 100$) and their relative ratio were calculated for the production parameters.

The water temperature (°C), dissolved oxygen (mg/l), oxygen saturation (%) and pH were measured optically (HQ40D, HACH, LANGR GmbH, Germany) twice a day. Chlorides (Cl^-), ammoniacal nitrogen ($N–NH^{4+}$) and nitrites ($N–NO^{2-}$) were monitored daily using a spectrophotometer (PhotoLab 6600 UV–VIS).

Potential impacts of different diet on all studied characteristics were evaluated by a One-Way ANOVA procedure using statistical software Statistica 13.3 (TIBCO Software, 2017).

RESULTS AND DISCUSSION

Production parameters

There were no water chemistry fluctuations that could affect feeding take during the feed test. The observed parameters varied in values suitable for carp according to Svobodová et al. (2007).

Table 2 Increment from collections

	W_{total}	$\bar{x}$	W_{total}	$\bar{x}$	Increment	
	g	g	g	g	g	%
	Start		End			
Control	2 000	67	4 015	134	2 015	101
F500	2 008	67	3 815	127	1 807	90
F1000	1 992	66	3 795	127	1 803	91
F500C3	2 013	67	4 348	145	2 335	116
F1000C3	2 036	68	4 493	150	2 457	121

Legend: W_{total} – total weight of group, number – number of specimens, x – average weight of specimen. Number of carps both at the beginning and at the end was 30.

Table 2 shows the fish growth (g and %) based on the weight of the groups (W_{total}) at the beginning and at the end of the test. The lowest growth was achieved in groups with 500 FTU and 1000 FTU phytase enzymes. The decrease over the control group was 10%. The citric acid addition groups showed an increase of approximately 16% respectively 21% over the control group. According to Nwanna and Schwarz (2007), the use of inorganic phosphorus in feed mixtures increases the average daily weight of common carp unlike the feed with the addition of the Ronozyme P phytase enzyme at 1000, 2000 and 4000 FTU.

The most favourable values of FCR and SGR were obtained in groups F500C3 and F1000C3 regardless of the phytase level in the feed. The FCR of both feeds with citric acid was decreased by 20% over the control group (one–way ANOVA: F = 24.09, df = 4, P = 0.002), as shown in the table 3. The worst results were reported by F500 which increased by 3% over the control group. Čítek et al. (1998) states the FCR between 45 for plant glycid feeds, especially wheat and barley.

The SGR increase of 11% over control group in groups F500C3 and F1000C3 (one–way ANOVA: F = 17.93, df = 4, P = 0.004). The citric acid–free groups showed worse results than the control group, as can be seen in the table 3. The differences did not reach a statistically significant level.

Danwitz (2016), in his study with *Psetta maxima* L., used feed based on fishmeal and rapeseed oil. An increase in FCR and a decrease in SGR was achieved using 1000 FTU and 2000 FTU enzymes Natuphos® 5000 G. In contrast, Khajehpour et al. (2012) reported decrease in FCR and increase in SGR of the common carp fed by plant–based feed with 500 FTU enzyme Natuphos® 5000 G.

Figure 1 FCR

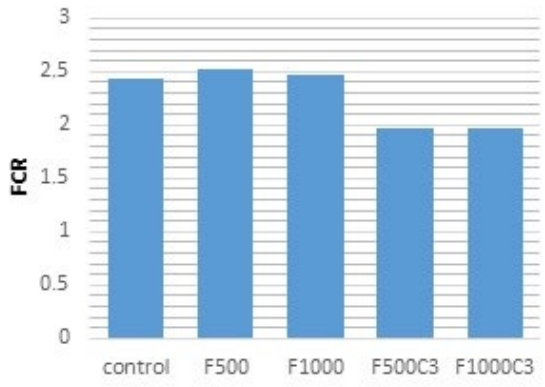

Figure 2 SGR

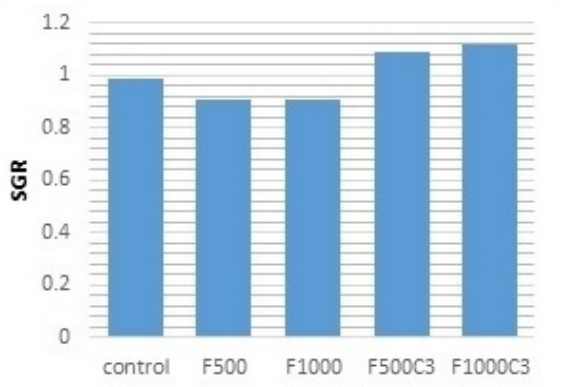

Table 3 Production parameters – statistically significant differences are red

	Control	F500	F1000	F500C3	F1000C3
FCR	2.44	2.52	2.46	1.97	1.97
SGR	0.99	0.91	0.91	1.09	1.12
FCR / SGR	2.46	2.77	2.70	1.81	1.76

CONCLUSION

The aim of this experiment was to find out whether the addition of phytase enzyme and citric acid in feed mixtures had an impact on fish production parameters. The best increment was achieved in fish fed by feed with phytase and 3% citric acid. The growth of F1000C3 group increased by 21% over control group. The groups with CA were also significantly better in FCR by 20% and SGR by 11% over the control group. Feed mixtures with the addition of phytase and without the citric acid showed worse results than the control group. Questionable is the use of minerals bounded to the residues of the phosphoric acid. The addition of phytase to the fish feed is an appropriate choice due to the increasing use of plant components for fish nutrition and not only for the reduction of the negative impact to the environment.

ACKNOWLEDGEMENTS

The research was financially supported by the IGA grant, no IP_12/2017. The results and outputs were processed using the equipment financed by the project OP VaVpI CZ.1.05/4.1.00/04.0135 Teaching and research capacities for biotechnology disciplines and infrastructure expansion. The study was processed with the support of the project NAZV QK1810296.

REFERENCES

Brož, J. 2002. Krmné enzymy ve výživě drůbeže. Veterinářství [Online], 52: 111–113. Available at: http://vetweb.cz/krmne-enzymy-ve-vyziv-drubeze/. [2018-08-27].

Cao, L. et al. 2007. Application of microbial phytase in fish feed. Enzyme and Microbial Technology, 40: 497–500.

Čítek, J. et al. 1998. Rybníkářství. 3rd ed., Praha: Informatorium.

Danwitz, A. et al. 2016. Dietary phytase supplementation in rapeseed protein based diets influences growth performance, digestibility and nutrient utilization in turbot (*Psetta maxima* L.). Aquaculture, 450: 405–411.

Kalač, P., Míka, V. 1997. Přirozené škodlivé látky v rostlinných krmivech. 1st ed., Praha: Ústav zemědělských a potravinářských informací.

Khajehpour, G. et al. 2012. Dietary Crude Protein, Citric Acid and Microbial Phytase and Hematocrite of Common Carp, *Cyprinus carpio* L., Juveniles. World Journal of Zoology, 7(2): 118–122.

Lundová, Z. 2014. Vliv exogenní fytázy na stravitelnost fytátového fosforu u slepic. Diplomová práce, Mendelova univerzita v Brně.

Nwanna, L.C., Schwarz, F.J. 2007. Effect of supplemental phytase on growth, phosphorus digestibility and bone mineralization of common carp (*Cyprinus carpio* L.). Aquaculture Research, 38: 1037–1044.

Shah, S.Z.H. et al. 2015. Supplementation of phytase and citric acid to soybean meal based diet enhance muscle mineralization of rohu, *Labeo rohita*, juveniles. Journal Science, 5(9): 796–800.

Simons, P.C.M. et al. 1990. Improvement of phosphorus availability by microbial phytase in broilers and pigs. British Journal of Nutrition, 64: 525–540.

Singh, P.K. 2008. Phytic acid and phytase in chicken nutrition. World´s Poultry Line, 4(10): 23–26.

Svobodová, Z. et al. 2007. Nemoci sladkovodních a akvarijních ryb. 4th ed., Praha: Informatorium.

TIBCO Software Inc. 2017. Statistica (data analysis software system), version 13. http://statistica.io.

WILDLIFE RESEARCH

Contribution to the knowledge on the dragonfly fauna (Insecta: Odonata) of Islamic Republic of Iran

Attila Balazs[1,2], Otakar Holusa[2]
[1]Department of Zoology, Fisheries, Hydrobiology and Apiculture
[2]Department of Forest Protection and Wildlife Management
Mendel University in Brno
Zemedelska 1, 613 00 Brno
CZECH REPUBLIC

balazsaeko@gmail.com

Abstract: Intensive fieldworks were undertaken in northern parts of Islamic Republic of Iran during midsummer seasons in 2017 and 2018. Overall species richness reached 35 species at 21 visited localities. Thirteen species from 5 families from the suborder Zygoptera and 22 species from 4 families from the Anisoptera suborders were recorded in our study. The most valuable species caught were e. g., *Epallage fatime*, *Coenagrion pulchellum*, *C. lunulatum*, *Aeshna vercanica*, *Caliaeshna microstigma*, *Cordulegaster vanbrinkae*, *C. nobilis*, *Sympetrum flaveolum*, *S. vulgatum decoloratum* or *Selysiothemis nigra*. First time *Aeshna vercanica* is documented from Gilan Province and *Cordulegaster nobilis* for Ardabil Province. Its habitat in this province is discussed.

Key Words: *Aeshna vercanica*, *Cordulegaster nobilis*, macroinvertebrate sampling, wetland ecosystems

INTRODUCTION

The Middle East was always charming for European biologist including odonatologists, despite of political instabilities, scarce water habitats or relatively low odonate diversity. The very first contributor from the territory of Islamic Republic of Iran in terms of dragonflies was Selys in the 19th century. Thence several authors dealt with dragonflies both residents and foreigners. For the first comprehensive work in this topic we had to wait until Heidari and Dumont (2002) published the "An annotated check-list of the Odonata of Iran". The paper enlightened the extent of the knowledge about the odonates of Iran. Many taxonomic and zoogeographic problems were sold but naturally, many of them remains unanswered by the lack of knowledge.

A new era has begun with the exhaustive research conducted in the last few years. Several species disappeared from the latter national check-list due to misidentifications, whilst many species appeared as a new country records (e.g., *Platycnemis kervillei*, *Sympecma gobica*, *Libellula fulva pontica*), or some of them were rediscovered (such as *Coenagrion persicum*, *Cordulegaster vanbrinkae*), or even a species was described as a new (and distinct) species for science – *Aeshna vercanica* (Jeziorski 2013, Sadeghi and Dumont 2004, Schneider et al. 2014, Schneider et al 2015, Schneider and Ikemeyer 2016, Schneider et al. 2016). Recently a new check list was published with the species list counting 100 autochthonous species (Schneider et al. 2018). The species list seems to be more or less complete, but we can still expect additional new records for the country or taxonomic riddle could be solved in the future (*Coenagrion vanbrinkae* recently synonymised as *Coenagrion ornatum*, see Kosterin and Ahmadi 2018).

Hereby, we present additional information on the occurrence of dragonflies recorded in the Islamic Republic of Iran during summers of 2017 and 2018. The survey had been conducted on East-Azerbaijan and Ardabil Provinces (Irano-Turanian region) in the Northwestern part of the country and in Gilan, Zanjan, Mazandaran, Golestan and North Khorasan Provinces (Caspian region) in the North and Northeastern part of Iran (Figure 1). We visited various types of habitats in the Caspian Hyrcanian mixed forests, Elburz Range forest steppe and at the transition zone of Central Persian desert basins ecoregions at the Caspian "horseshoe". Our paper does not bring any new country record, but for the first time is *Aeshna vercanica* reported from Gilan Province and *Cordulegaster nobilis* for Ardabil Province. There is an additional site for the rare *Coenagrion lunulatum* in Ardabil Province.

MATERIAL AND METHODS

Study area

The Elburz Mountains often reaches over 5000 m a. s. l., it act as natural barrier between the Caspian Sea and the Iranian Plateau. Therefore, it causes 1850 mm precipitation in Gilan Province (Ghorbani 2013). Over the caspian shoreline, the mean annual temperature is 15 °C, with maximum 44 °C on the eastern coast and (the mean annual temperature here is 18 °C), where the total precipitation is < 200 mm. The lowlands of the Caspian region had been completely altered into intensive and diversified agricultural land with patchy settlements and towns. *Quercus castaneifolia*, *Parrotia persica*, *Zelkova carpinifolia* and *Olea capensis* with shurbs such as *Buxus hyrcana* and *Ruscus hyrcanus* are found in the lower part of the mountains. *Fagus orientalis* replaces these species at the middle zone, whilst the uppermost part is occupied by steppes and xeric dwarf semi-shrubs i.e., *Quercus macranthera* which is also characteristic for the Elburz Mountains. The main tree species of Elburz Range forest steppes are *Juniperus foetidissima, Quercus macranthera, Carpinus orientalis* and *Acer hyrcanum* with dominant shrubs as *Pistacia atlantica*, *Cotoneaster racemiflora* and *Acer turcomanicum* (Sagheb–Talebi et al. 2014).

Figure 1 Map of studied localities in Islamic Republic of Iran during years 2017–2018

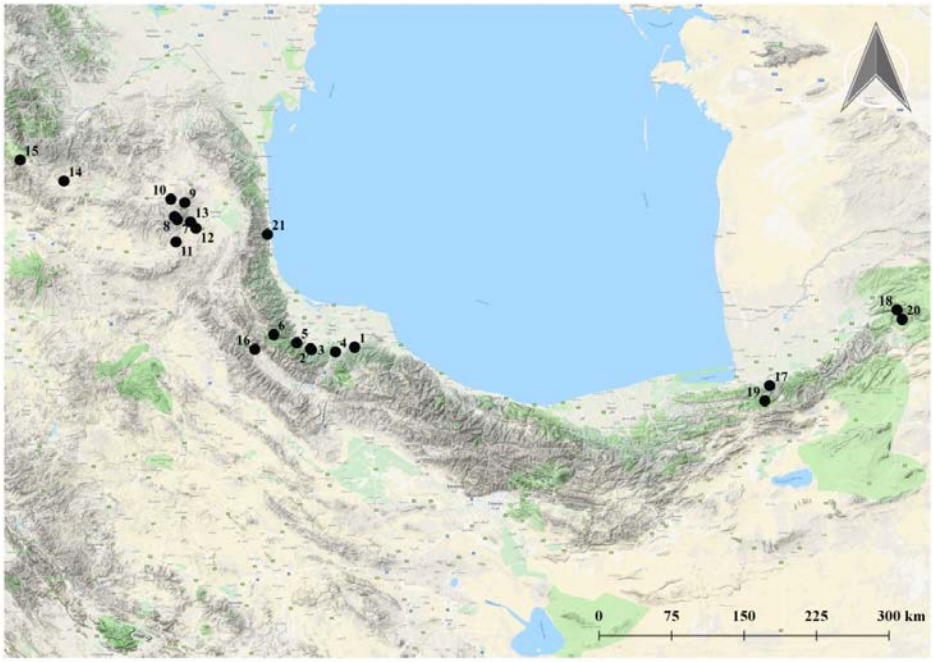

Sampling

The expedition consisted of two fieldworks, the first lasted from 9th till 21st July of 2017, the second one from 15th July to 15th August of 2018. Our taxonomic classification is following Schneider et al. (2018). Observed and captured adult specimens were identified using Dijsktra and Lewington (2014), Ambrus et al. (2018) and Galliani et al. (2017), exuviae via Brochard et al. 2012, whilst larvae of *Gomphus schneiderii* by the help of Schneider et al. (2017). Specimen densities were categorised according to Smallshire and Beynon (2010). All specimens were captured and identified by A. Balázs and they are deposited in his private collection. The map was generated by QGIS version 2.18. Parameters of water quality were measured by HI98129 tester.

List of localities

Loc. 1. *Siab Bijar* (سیاه بیجار, 37°2'21.160"N, 49°53'56.923"E, 300 m a. s. l., Gilan Province, 23 °C, 7.85 pH, 425µS, 200 TDS, 11. 8. 2018). Slowly flowing water hided in the forest. Deepest point approximately, at 50 cm, average about 30 cm. The muddy bottom is rich in organic materials.

Loc. 2. *Visrud lower* (ویسرود, 37°1'32.460"N, 49°24'19.128"E, 195 m a. s. l., Gilan Province, 25 °C, 8.17 pH, 365 µS, 183 TDS, 9. 8. 2018). Wide, deep and overshadowed stream in agricultural land surrounded by the Hyrcanian forest. Larvae of Gomphidae are hiding on the roots of trees.

Loc. 3. *Visrud upper* (ویسرود, 37°1'3.226"N, 49°24'52.229"E, 287 m a. s. l., Gilan Province, 21 °C, 8.45 pH, 391 µS, 195 TDS, 9. 8. 2018). Shallower but stronger current of water in this spring decorated with huge balvans.

Loc. 4. *Emamzadeh Hashem* (امام زاده هاشم, 36°59'49.299"N, 49°41'5.049"E, 193 m a. s. l., Gilan Province, 23 °C, 7.88 pH, 410 µS, 205 TDS, 8. 8. 2018). Shallow forest stream where the sediment is composed by mud and rocks (Figure 2). A cattle grazing reduces the vegetation in the surroundings.

Loc. 5. *Qale Rudkhan* (قلعه رودخان, 37°4'42.86"N, 49°14'57.48"E, 330 m a. s. l., Gilan Province, 19 °C, 7.64 pH, 172 µS, 86 TDS, 12–13. 8. 2018). Smaller but wild river with bigger rocks and sandy bottom in the Hyrcanian mixed forest steppe ecoregion. During rainy periods, the water current reaches even 70 cm/s.

Loc. 6. *Masuleh* (ماسوله, 37°9'10.302"N, 48°59'27.095" E, 955 m a. s. l., Gilan Province, 12. 8. 2018). Forest clearings on the northern side of the hill in front of the stunning Masuleh village.

Loc. 7. *Alvars, at Gurgur waterfall* (آبشار گورگور، الوارس, 38°10'20.38"N, 47°54'32.66"E, 2471 m a. s. l., Ardabil Province, 21 °C, 7.03 pH, 141 µS, 69 TDS, 18–19. 7. 2018). Smaller (178 m^2) and shallow lake, in the northern part ended in peat bog that is grazed by cows (Figure 2). No fishes.

Loc. 8. *Meimand* (میمند, 38°11'47.65"N, 47°52'39.40"E, 2958 m a. s. l., Ardabil Province, 23 °C, 7.38 pH, 90 µS, 46 TDS, 21–30. 7. 2018). Mountain lake (5000 m^2) with muddy sediments, almost fully overgrowned by natant vegetation. Without fishes. Intensive sheep grazing are present here.

Loc. 9. *Bane Kharmandali* (بنه خرمندلی, 38°19'24.565"N, 47°59'54.846"E, 2300 m a. s. l., Ardabil Province, 22 °C, 7.3 pH, 282 µS, 141 TDS, 23. 7. 2018). Mountain 55854 m^2 big and eutrophic lake (Figure 2).

Loc. 10. *Golden lake* (آتگلی, 38°21'5.804"N, 47°50'6.906"E, 2800 m a. s. l., Ardabil Province, 18 °C, 8.61 pH, 415 µS, 207 TDS, 27. 7. 2018). Beautiful clear and small lake (424 m^2) with water depth over 50 cm. Fishes are not present.

Loc. 11. *Sari Qayeh* (قیه ساری, 37°58'30.603"N, 47°53'33.051"E, 1840 m a. s. l., East Azerbaijan Province, 31 °C, 9.02 pH, 303 µS, 149 TDS, 3. 8. 2018). Big (21853 m^2) eutrophic lake with diverse floristic elements.

Figure 2 Photographies of visited localities (2 – Loc. 7; 3 – Loc. 4; 4 – Loc. 9; 5 – Loc. 21)

Loc. 12. *Rowshanaq* (روشنق, 38°5'43.538"N, 48°7'1.199"E, 1475 m a. s. l., Ardabil Province, 28.1 °C, 8.28 pH, 2059 µS, 1075 TDS, 4. 8. 2018). Bigger but shallow stream with current of 10 cm/s, with gravel and mud sediments. Algae are present in the water.

Loc. 13. *Sareyn* (سرعین, 38°9'3.610"N, 48°3'23.200"E, 1718 m a. s. l., Ardabil Province, 26. 7. 2018). Small and shallow muddy pond beside town Sareyn.

Loc. 14. *Varzeghan* (ورزقان, 38°30'38.83"N, 46°38'2.06"E, 1683 m a. s. l., East Azerbaijan Province, 18. 7. 2017). Big (304323 m^2) and shallow lake with muddy sediment. Not overvegetated.

Loc. 15. *Molk-e-Qozzāt* (قضات ملک, 38°41'44.27"N, 46° 8'34.41"E, 1252 m a. s. l., East Azerbaijan Province, 19. 7. 2017). Rocky, smaller but strong stream with water depth of 20 cm in temperate conifer forest area.

Loc. 16. *Darram* (درام, 37°1'17.64"N, 48°46'41.95"E, 479 m. a. s. l., Zanjan Province, 18 °C, 8.03 pH, 204 µS, 102 TDS, 12. 7. 2017). Three meters wide and strong (30 cm/s) stream with big rocks. Surroundings are olive groves.

Loc. 17. *Chahar Bagh* (چهارباغ, 36°41'42.745"N, 54°33'45.420"E, 2030 m a. s. l., Golestan Province, 15. 7. 2017). Stream in Hyrcanian forest with water depth 15 cm (average) and current of 10 cm/s.

Loc. 18. *Dasht* (دشت, 37°22'21.11"N, 55°59'37.40"E, 933 m a. s. l., Golestan Province, 19 °C, 8.2 pH, 290 µS, 124 TDS, 14. 7. 2017). Dragonflies found at very small pond.

Loc. 19. *Shahkou Olia* (شاهکو هعلیا, 36°33'29.72"N, 54°30'28.86"E, 2360 m a. s. l., Golestan Province, 18 °C, 8.46 pH, 854 µS, 427 TDS, 15. 7. 2017). Small rivulet with maximum water depth to 30 cm and current of 20 cm/s.

Loc. 20. *Cheshmeh Khan* (خان چشمه, 37°17'15.37"N, 56°3'4.68"E, 1025 m a. s. l., North Khorasan Province, 14. 7. 2017). Very dry, but agriculturally active area in xeric shrublands. A huge dam is under construction here.

Loc. 21. *Keshli* (کشلی, 38°2'31.29"N, 48°55'12.90"E, -29 m a. s. l., Gilan Province, 29 °C, 7.6 pH, 628 µS, 316 TDS, 6. 8. 2018). Sandy beach at the Caspian Sea. Dense emerging vegetation covers the shoreline where river enters to Caspian Sea (Figure 2).

RESULTS AND DISCUSSION

Altogether 35 dragonfly species were recorded during two field trips in 2017 and 2018 respectively (which is 35% of the overall species richness of odonates in Iran). (Abbreviations used: obs. – observed, ex. – exuviae, L. – larva).

Species list

1) *Calopteryx splendens orientalis* (Selys, 1887) Loc. 1: 2–5♂, 1 ♀ obs; Loc. 2: 11–20♂, 6–10♀; Loc. 3: 6–10♂, 2–5♀; Loc. 4: 11–20♂, 6–10♀; Loc. 5: 6–10♂, 2–5♀; Loc. 12: 2–5♂, 1♀; Loc. 15: 2–5♂, 1♀; Loc. 18: 1♂;
2) *Calopteryx splendens intermedia* (Selys, 1887) Loc. 16: 1♂;
3) *Epallage fatime* (Charpentier, 1840) Loc. 16: 1♂;
4) *Lestes barbarus* (Fabricius, 1798) Loc. 8: 1♂; Loc. 9: 1♂;
5) *Lestes dryas* (Kirby, 1890) Loc. 8: 1♂; Loc. 13: 1♂;
6) *Lestes sponsa* (Hansemann, 1823) Loc. 7: 1♀; Loc. 10: 1♂;
7) *Sympecma fusca* (Vander Linden, 1820) Loc. 6: 1♂; Loc. 15: 2–5♂, 1♀;
8) *Ischnura pumilio* (Charpentier, 1825) Loc. 7: 2♂; Loc. 8: 1♂; Loc. 12: 1♂; Loc. 13: 2–5♂, 1♀;
9) *Ischnura elegans* (Vander Linden, 1820) Loc 11: 1♀; Loc. 14: 1♂; Loc. 20: 1♂;
10) *Enallagma cyathigerum* (Charpentier, 1840) Loc. 7: 11–20♂, 2–5♀; Loc. 9: 2–5♂, 1♀; Loc. 14: 1♂;
11) *Coenagrion puella* (Linnaeus, 1758) Loc. 7: 1♂; Loc. 9: 2♂; Loc. 13: 1♂;
12) *Coenagrion lunulatum* (Charpentier, 1840) Loc. 7: 2♂;
13) *Platycnemis dealbata* (Selys in Selys & Hagen, 1850) Loc. 2: 2–5♂; Loc. 11: 2–5♂; Loc. 20: 1♂;

14) *Aeshna mixta* (Latreille, 1805) Loc. 17: 11–20♂;
15) *Aeshna vercanica* Schneider et al., 2015 Loc. 2: 1♂; Loc. 5: 5♂;
16) *Anax imperator* (Leach, 1815) Loc. 11: 1♂ obs.;
17) *Anax parthenope* (Selys, 1839) Loc. 11: 1♂ obs.; Loc. 14: 1♂;
18) *Caliaeschna microstigma* (Schneider, 1845) Loc. 18: 4 ex.;
19) *Gomphus schneiderii* (Selys, 1850) Loc. 2: 2 L.;
20) *Onychogomphus lefebvrii* (Rambur, 1842) Loc. 16: 1♂;
21) *Cordulegaster vanbrinkae* (Lohmann, 1993) Loc. 1: 2 L.; Loc. 3: 1 ex.; Loc. 4: 8 L; Loc. 5: 2 L.;
22) *Cordulegaster nobilis* (Morton, 1916) Loc. 7: 1 ♂ obs.; Loc. 19: 2–5♂, 2–5♀;
23) *Libellula depressa* (Linnaeus, 1758) Loc. 7: 2–5♂, 2 ex.;
24) *Orthetrum albistylum* (Selys, 1848) Loc. 3: 2–5♂;
25) *Orthetrum coerulescens anceps* (Schneider, 1845) Loc. 16: 1♂; Loc. 20: 1♂;
26) *Orthetrum brunneum* (Fonscolombe, 1837) Loc. 12: 1♂; Loc. 20: 1♂;
27) *Orthetrum sabina* (Drury, 1773) Loc. 1: 11–20 ♂, 1♀, 4 L., 1 ex.; Loc. 4: 6–10♂; Loc. 5: 6–10♂;
28) *Sympetrum sanguineum* (Müller, 1764) Loc. 12: 1♂, 2–5♀ (very small specimens)
29) *Sympetrum flaveolum* (Linnaeus, 1758) Loc. 7: 1♂; Loc. 8: 1♂; Loc. 9: 1♂;
30) *Sympetrum fonscolombii* (Selys, 1840) Loc. 7: 1♂; Loc. 11: 2–5♂; Loc. 14: 1♂;
31) *Sympetrum striolatum* (Charpentier, 1840) Loc. 15: 1♂; Loc. 18: 1♂;
32) *Sympetrum vulgatum decoloratum* (Selys, 1884) Loc. 8: 1♂,1♀;
33) *Crocothemis erythraea* (Brullé, 1832) Loc. 4: 1♂; Loc. 20: 1♂;
34) *Selysiothemis nigra* (Vander Linden, 1825) Loc. 21: 2–♂, 2–5♀;
35) *Pantala flavescens* (Fabricius, 1798) Loc. 6: 11–20♂; Loc. 7: 1♂; Loc. 8: 1♂; Loc. 16: 11–20♂; Loc. 20: 1♂.

Notes to some species

We found males of the uncommon *Sympetrum flaveolum* at three sites in high altitudes in Ardabil Province. Eslami et al. (2014) first time caught the species in 2014. Our specimens have not extensive yellow area to the nodus, but they were reduced to the arculus in the forewings and to the triangle, and the posterior parts of cubital crossveins in the hindwings.

We are adding two additional localities for *Aeshna vercanica* in Gilan Province, filling the gap between Mazandaran Province in Iran and Lankaran Province in Azerbaijan. During our fieldwork, we found them at the foothills of lower hills. There the species were found at stream with very strong current (not rivulets as in Mazandaran province). However, we found many adult specimens but no females of *Aeshna vercanica*.

In relatively high densities were found also specimens of *Cordulegaster nobilis* at village Shahkou Olia (Golestan Province). Here they seems to be doing very well, since many larvae and copulation wheels of pairs were found as well (Figure 3).

Figure 3 Copulation of Cordulegaster nobilis at Shahkou Olia (Photo: A. B.)

CONCLUSION

Iran has remarkable species richness in many orders of insects. This is also true for dragonflies, but they are under serious threat due to many aspects of negative human activities. The most urgent problems are dam constructions, over extraction and pollution of water resources. Further monitoring is needed to tracking trends of odonates population dynamics for better understanding of the impacts of alterations their (in many cases) untouched biotopes to artificial not appropriate habitats.

ACKNOWLEDGEMENTS

This research was financially supported by the International Relations Office of Mendel University in Brno, via Traineeships for Ph.D. students. Many thanks go to Ali Salehi and Javid Imanpour–Namin (University of Gilan, Sowme´eh Sara) for their exceptional support and to Elyas Ahmadi (University of Gilan, Rasht) for the help with the Persian transcription.

REFERENCES

Ambrus, A. et al. 2018. Magyarország szitakötőinek kézikönyve. 1st ed. Budapest: Magyar Természettudományi Múzeum, Herman Ottó Intézet Nonprofit Kft.

Brochard, Ch. et al. 2012. Fotogids Larvenhuidjes van Libellen. 1st ed. Zeist: KNNV Uitgeverij.

Dijsktra, K.D., Lewington, R. 2014. Field Guide to the Dragonflies of Britain and Europe including western Turkey and north-western Africa. Gillingham: British Wildlife Publishing.

Eslami, Z. et al. 2014. *Sympetrum flaveolum* (Odonata: Libellulidae) a new species record for Iran. Journal of Entomological Society of Iran, 34: 71–73.

Galianni, C. et al. 2017. Dragonflies and Damselflies of Europe. A scientific approach to the identification of European Odonata without capture. 1st ed. Verona: WBA Handbooks 7.

Ghorbani, M. 2013. The Economic Geology of Iran. Mineral Deposits and Natural Resources [Online]. 1st ed., Dordrecht: Springer Science+Business Media Dordrecht 2013. Available at: https://www.springer.com/gp/book/9789400756243. [2017-11-28].

Heidari, H., Dumont, H.J. 2002. An annotated check-list of the Odonata of Iran. Zoology in the Middle East, 26(1): 133–150.

Jeziorski, P. 2013. First record of *Sympecma gobica* (Odonata: Lestidae) from Iran. Klapalekiana, 49: 39–42.

Kosterin, O.E., Ahmadi, A. 2018. Odonata observed in Central Zagros, Iran in late May 2017. International Dragonfly Fund [Online], 117: 1–65. Available at: https://www.researchgate.net/publication/324594641_Odonata_observed_in_Central_Zagros_Iran_in_late_May_2017 [2018-08-21].

Sadeghi, S., Dumont, H.J. 2004. First record of *Libellula fulva pontica* Selys, 1887 (Odonata, Anisoptera) from Iran. Zoology in the Middle East, 32(1): 116–117.

Schneider, T. Ikemeyer, D. 2016. Notes on Odonata species in South-West Iran including *Plactycnemis kervillei* (Martin, 1909) as a new species for Iran. Entomologische Zeitschrift, 126, 3–8.

Schneider, T. et al. 2014. Rediscovery of *Cordulegaster vanbrinkae* in Iran (Odonata: Cordulegastridae). Odonatologica, 43: 25–34.

Schneider, T. et al. 2015. *Aeshna vercanica* spec. nov. from Iran (Anisoptera: Aeshnidae) and a new insight into the Aeshna cyanea-group. Odonatologica, 44: 81–106.

Schneider, T. et al. 2016. Rediscovery and redescription of *Coenagrion persicum* (Lohmann 1993) with description of the female, and some notes on habitat selection (Odonata: Coenagrionidae). Zootaxa [Online], 4103(6): 561– 573. Available at: https://biotaxa.org/Zootaxa/article/view/zootaxa. 4103.6.6. [2017-01-30].

Schneider, T. et al. 2017. Description of last instar larva of *Gomphus kinzelbachi* Schneider, 1984 and new aspects on distribution and habitats in Iran (Odonata: Gomphinae). Zootaxa [Online], 4365(6): 455–466. Available at: https://doi.org/10.11646/zootaxa.4365.4.5. [2018-08-22].

Schneider, T. et al. 2018. Checklist of the dragonflies (Odonata) of Iran with new records and notes on distribution and taxonomy. Zootaxa [Online], 4394 (1): 001–040. Available at: https://www.researchgate.net/publication/323728036_Checklist_of_the_dragonflies_Odonata_of_Iran with_new_records_and_notes_on_distribution_and_taxonomy. [2018-04-10].

Smallshire, D., Beynon, T. 2010. Dragonfly Monitoring Scheme Manual. British Dragonfly Society.

Talebi, K.S. et al. 2014. Forests of Iran. A Treasure from the Past, a Hope for the Future. Plant and Vegetation 10. 1st ed., Dordrecht: Springer Science+Business Media Dordrecht 2014. Available at: https://www.springer.com/gp/book/9789400773707. [2017-11-28].

Quantification of greenhouse gas emissions from forest fire in the area of the Slovak Paradise National Park

Katarina Koristekova, Michal Miklos, Martin Janco, Miriam Valkova
Department of Natural Environment
Technical University in Zvolen
T.G. Masaryka 24, 960 53 Zvolen
SLOVAK REPUBLIC

katarina.koristekova@gmail.com

Abstract: Forests play a significant role in the protection of biodiversity and ecological functions. In the areas exposed to fire risks, forests are important carbon reservoirs, which represent a source of emissions during fires. Fire regime is not a characteristic feature of the Central European area. As global warming and climate change continues, fires threaten central European countries more frequently. In the past, fire risk was relatively low, and fires threatened Central Europe only under extreme weather fluctuations, but in the last years these anomalies have occurred more frequently, and it is assumed that their course and intensity will gradually increase. In the presented paper we deal with the quantification of greenhouse gas emissions from forest fires. We base our work on the inventory methodology of the Intergovernmental Panel on Climate Change. We tried to apply its individual conceptions (TIER 1–3) in the conditions of Slovakia, and presented the problems of their applications. The results indicate that the conceptions differ in the quantification of biomass available for burning, which was underestimated in the case of TIER 1 conception in comparison to TIER 2 and TIER 3, and also in the quantification of emissions. The emissions produced during the flameless burning phase were underestimated, while the CO_2 emissions were slightly overestimated when comparing TIER 2 and TIER 3 approaches. The final assessment of the whole process points out at the problematic issues in the calculations of GHG emissions. To determine the overall accuracy of this calculation it will be necessary to pay more attention to the mentioned problematic issues.

Key Words: greenhouse gas emissions, forest fires, FCCS model, IPCC methodology

INTRODUCTION

To assess the atmospheric impact of biomass burning, and especially to represent it quantitatively in models of atmospheric transport and chemistry, accurate data on the emission of trace gases and aerosols from biomass fires are required. Emissions must typically be represented in the form of spatiotemporally resolved fields, where the emission per unit area and time is provided at a specified spatial and temporal resolution. These fields are obtained by multiplying an exposure term, for example, the amount of biomass burned within a grid cell during a time interval, with an emission factor, that is, the amount of the chemical species released per mass of biomass burned (Andreae and Metlet 2001).

The greenhouse gas emissions from the forest fire at Krompľa site in the Slovak Paradise National Park have been quantified for several reasons. The main reason was to point out at the different results obtained by applying individual conceptions of the inventory methodology of the Intergovernmental Panel on Climate Change from the year 2006. Another reason was the fact that the Slovak Paradise National Park belongs to the EECONET European network and NECONET national network, and is a bio-centre of the supra-regional significance. Slovak paradise national park is a region situated SW from the city of Spišská Nová Ves. It is one of the nine National Parks in Slovakia, and enjoys legal protection since 1964. The climate of the territory is mild warm, mild dry, with cold winter and average temperatures ranging from 6 to 7 °C. The territory of the Slovak Paradise is characterized by the low precipitation totals (570–650 mm per year) due to the rain shadow of the Tatra Mts, in which is the whole area situated (Škvarenina et al. 2003, Škvarenina et al. 2009a, Vido et al. 2015, Vido et al. 2016). The geological ground of wild-land area mainly consists of limestone and partly of dolomite. The karst relief together with the mentioned subterranean caves and rifts act as a good drainage of the whole terrain and serve as the excellent air-conditions promoting the propagation of fire, if it occurs. Rendzinas

which have developed as the main types of soil here, are rocky and very shallow. These types of soil are not able to keep larger amounts of water (Šály 1985). Due to its properties, soil here quickly gets rid of any water and dries soon after rain (Gömöryová et al. 2013). During a dangerous summer or drought periods, this soil contains very small amount of water (Střelcová et al. 2006). The continual cover of dense grass is represented by plant communities consisting of rather higher and very combustible species. Natural forests growing on steep slopes and rocky ridges consist of the "relict" pine and pine – larch stands with the spruce and the beech at bottoms of numerous rifts and valleys. Due to the lack of soil water, the coniferous litter here is very difficult to disintegrate and so represents the highly flammable stock of fuel. Extraordinary dangerous from the fire propagation point of view are young pine and spruce stands (up to 20 years of age). They contain a lot of dry branches that are growing very closely to the land surface that is often covered by grass (Škvarenina et al. 2009a, Škvarenina et al. 2009b).

MATERIAL AND METHODS

1 Approach according to TIER 1

We selected the methodology of the presented research aimed at the quantification of the greenhouse gas emissions on the base of PPCC methodology.

The methodology TIER 1 approach uses general data on the amount of biomass in the country and its characteristics, while these data are obtained from the tables in the guidelines, and some input parameters are neglected.

We used the following relationship (equation 1 according to the 2006 IPCC Guidelines) to calculate the emissions of CO_2, CO, CH_4, N_2O and NO_x:

$$L_{fire} = A \bullet M_B \bullet C_f \bullet G_{ef} \bullet 10^{-3} \quad (1)$$

where:

L_{fire} = the amount of emissions of a particular greenhouse gas from the fire in tonnes,

A = burnt area in hectares,

M_B = the amount of the fuel available for burning in tonnes per hectare,

C_f = a combustion factor,

G_{ef} = an emission factor in grams per kilogram of the dry burnt fuel.

2 Approach according to TIER 2

According to TIER 2 methodology approach, we focused mainly on the quantification of the amount of biomass occurring on the fire ground during the combustion period. The goal was to quantify the biomass of living and dead trees, standing and lying trees, non-woody vegetation, and the above-ground humus layer. We tried to model these data (tree biomass) or to gather them from the available literature sources.

- **Quantification of tree biomass**

We determined the tree biomass using Sibyla growth simulator (GS). GS is a system, which attempts to mimic the behaviour of a forest using the principles of ecosystem and cybernetic modelling based on the individual tree growth modelling. It uses a set of mathematical models and algorithms (Fabrika 2012). We used the data representing the Krompľa – Tri kopce site of the forest unit State forests Hrabušice as input data.

Subsequently, we used Sibyla GS to calculate the amount of dry biomass of the whole trees. This is calculated using the allometric relationships for the different tree parts of the individual tree species (Riccardi et al. 2007). The final values of the dry mass are divided into the following categories: roots and stump, stem wood, stem bark, branches, foliage, and the whole tree. For further calculations we used only the results of the crown dry mass (branches and foliage) (Fabrika 2012).

- **Quantification of biomass in standing dead trees**

The quantification of the amount and the stock, as well as the dry mass of standing dead trees followed the same approach as for the biomass of trees. In GS, the number of the standing dead trees is generated using the tree mortality model (Fabrika 2012) The emissions were calculated using the whole

dry mass (excluding root biomass), because the characteristics of standing dead trees (mainly moisture) differ from the qualities of living trees, and all their above-ground biomass can be used during fire (Fabrika 2012).

- **Quantification of other forest biomass**

We summarised other forest biomass, such as deadwood of different dimensions, non-woody vegetation, and above-ground humus from the available literature sources and subsequently used them in the calculations of GHG emissions.

- **Combustion and emission factors**

Similarly to TIER 1 approach, the values of the combustion and emission factors of individual gases were taken from the 2006 IPCC methodology.

3 Approach according to TIER 3

The 2006 IPCC – TIER 3 methodology for the quantification of the emissions from combustion assumes their calculation using sophisticated models, which account for the rules of the whole process, and emissions are calculated from detailed input data (IPCC 2006).

In our case, we applied the input data obtained using the above-mentioned approach (according to TIER 2) in modelling combustion processes and biomass available for the combustion using the models of FCCS (Ottmar et al. 2003) FARSITE (Finney 1998) and CONSUME (Ottmar 2014) and the whole process of emission calculation is in a simplified manner presented in the following process diagram (Fig. 1).

Figure 1 Process diagram of our proposal of the approach for calculating greenhouse gas emissions using TIER 3 conception

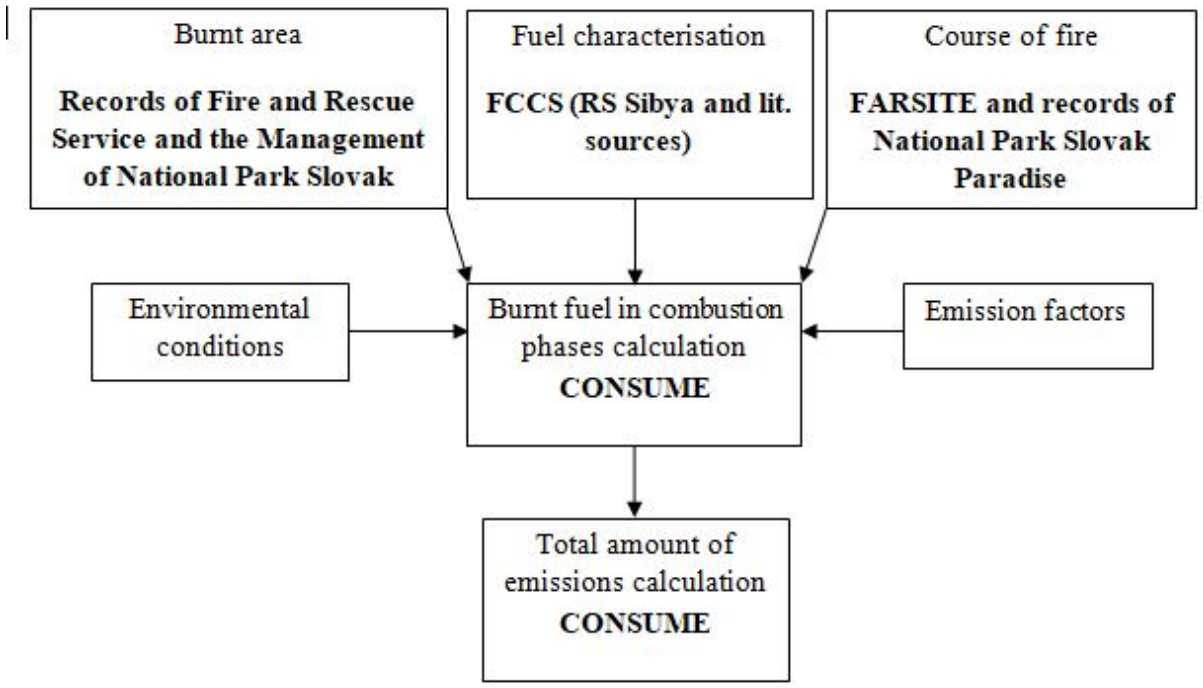

Correction of results

The borders of the fire after its extinction enclosed an area of 79.42 ha. Some parts within this area were not attacked by fire. Their total area was approximately 15.5 ha. The location of these parts was unknown. Due to this, we calculated the emissions from the area of 79.42 ha. Hence, for the realistic representation of the amount of the produced emissions from this fire we need to account for the correction equal to -20%.

RESULTS AND DISCUSSION

The resulting emissions calculated using three conceptions of the 2006 IPCC methodology are presented together with the amount of burnt biomass in Table 1.

Table 1 Resulting emissions of greenhouse gases in tonnes calculated following TIER 1–3 conceptions without correction and with correction by -20% that accounts for the unburnt part of the fire ground

Emissions	TIER 1 [t]	TIER 2 [t]	TIER 3 [t]	TIER 1 after correction [t]	TIER 2 after correction [t]	TIER 3 after correction [t]
PM_{10}	-	-	21.35	-	-	17.08
$PM_{2.5}$	-	-	19.36	-	-	15.49
CO	168.26	237.47	242.21	134.61	189.98	193.79
CO_2	2467.28	3482.10	3046.42	1973.82	2785.68	2437.14
CH_4	7.39	10.43	12.30	5.91	8.34	9.84
NMHCs	-	-	9.24	-	-	7.392
N_2O	0.41	0.58	-	0.33	0.46	-
NO_x	4.72	6.66	-	3.78	5.33	-
Burnt biomass	1572.52	2219.31	1986.78	1258.02	1775.45	1589.42

The higher results for TIER 2 in comparison to TIER 1 resulted from the higher values of burnt biomass. The difference is approximately 30 per cent. In the case of TIER 2 and TIER 3 conceptions we can compare only the emissions of CO, CO_2 and CH_4.

We recorded higher emissions of CO and CH_4 for TIER 3 although the total burnt biomass calculated on the base of TIER 3 conception was lower (by 10.5%) than the burnt biomass calculated using TIER 2 conception. This difference mainly results from the proportions of biomass that burnt during the flaming and Smoldering phases. Their final ratio for the whole fire event was calculated as 2:3 (flaming: smoldering phase). Since the emissions of CO and CH_4 are produced mainly during the smoldering phase of combustion, its greater proportion on biomass combustion resulted in the increase of these emissions (by 2.8% in the case of CO, and 22.5% in the case of CH_4) calculated using TIER 3 conception in comparison to TIER 2 conception, which is based on the calculation of emissions using a single emission factor for the whole burnt biomass.

In the case of CO_2 emissions we found their amount for TIER 3 lower by 11.9% than for TIER 2. It is not possible to make general conclusions for fires in Slovakia from the revealed differences in the amount of the produced emissions in the modelled fire. This is mainly due to the period, when the fire occurred, i.e. at the end of October. Although the air humidity of that period was very low and hence, it promoted the rate of fire spread as well as its intensity, the fuel was moister than during summer months, and during night hours the fire did not progress. Therefore, the fire intensity in both the flaming and smoldering phases of combustion was lower than that of the fires that would occur during drier summer months.

CONCLUSION

Greenhouse gas emissions can be quantified using several approaches. On the base of the previous chapters it is clear that nowadays, modelling of greenhouse gas emissions from forest fires in the conditions of Slovakia has its restrictions. They can be divided into two main groups. One includes precise recording of data about forest fires, and the second one includes input data about stand biomass for calculation and modelling.

The input data on stand biomass, which burnt during the fire, are essential for the calculation of the produced emissions. However, in nature this information substantially varies, mainly in the countries like Slovakia. The heterogeneity of ecosystems driven by orographic, edaphic, and climatic conditions complicates the acquisition of the data on biomass at different sites of Slovakia. In addition to the variability, the demand for this information is a significant obstacle to their precise determination. Since the biomass usually burnt during fires is economically only a little usable (although this is currently

changing because of the demand for biomass for energy purposes), its mapping has been emphasized mainly due to its heterogeneity.

ACKNOWLEDGEMENTS

This work was accomplished as a part of VEGA projects No.: 1/0589/15, 1/0570/16, 1/0111/18 of the Ministry of Education, Science, Research and Sport of the Slovak Republic and the Slovak Academy of Science; and the projects of the Slovak Research and Development Agency No.: APVV-15-0425 and APVV-15-0497. The authors thank the agencies for the support.

REFERENCES

Andreae, M.O., Metlet, P. 2001. Emission of trace gases and aerosols from biomass burning. Global Biogeochemical Cycles, 15(4): 955–966.

Fabrika, M. 2012. What is the simulator of forest biodynamics SIBYLA. [Online]. Available at: http://etools.tuzvo.sk/sibyla/english/. [2018-09-12].

Finney, M.A. 1998. FARSITE: Fire Area Simulator – Model Development and Evaluation. Res. Pap. RMRS–RP–4, USDA Forest Service, Rocky Mountain Research Station.

Gömöryová, E. et al. 2013. Responses of soil microorganisms and water content in forest floor horizons to environmental factors. European Journal of Soil Biology, 55: 71–76.

IPCC. 2006. Guidelines for National Greenhouse Gas Inventories. Institute for Global Environmental Strategies, Japan. [Online]. Available at: http://www.ipcc-nggip.iges.or.jp/public/2006gl/index.html. [2018-09-20].

Ottmar, R.D. 2014. Wildland fire emissions, carbon, and climate: Modeling fuel consumption. Forest Ecology and Management, 317: 41–50.

Ottmar, R.D. et al. 2007. An overview of the Fuel Characteristic Classification System – Quantifying, classifying, and creating fuelbeds for resource planning. Canadian Journal of Forest Research, 37(12): 2383–2393.

Riccardi, C.L. et al. 2007. Quantifying physical characteristics of wildland fuels using the Fuel Characteristic Classification System Canadian. Journal of Forest Research, 37(12): 2413–2420.

Střelcová, K. et al. 2006. Influence of tree transpiration on mass water balance of mixed mountain forests of the West Carpathians. Biologia, 61(19): 305–310.

Šály, R. 1985. Soil conditions. In Slovenský raj – Chránená krajinná oblasť. Príroda: Bratislava, pp. 59–68.

Škvarenina, J. et al. 2003. Analysis of the natural and meteorological conditions during two largest forest fire events in the Slovak Paradise National Park. In Proceedings of the International Scientific Workshop on Forest Fires in the Wildland–Urban Interface and Rural Areas in Europe: an integral planning and management challenge. Athens, Greece, 15–16 May. Chania: Mediterranean Agronomic Institute of Chania, pp. 29–36.

Škvarenina, J. et al. 2009a. Progress in dryness and wetness parameters in altitudinal vegetation stages of West Carpathians: time–series analysis 1951–2007. Idojárás, 113(1–2): 47–54.

Škvarenina, J. et al. 2009b. Occurrence of Dry and Wet Periods in Altitudinal Vegetation Stages of West Carpathians in Slovakia: Time-Series Analysis 1951–2005. In Bioclimatology and Natural Hazards. Netherlands: Springer, pp. 97–106.

Vido, J. et al. 2015. Drought Occurrence in Central European Mountainous Region (Tatra National Park, Slovakia) within the Period 1961–2010. Advances in Meteorology, 248728: 8.

Vido, J. et al. 2016. Identifying the relationships of climate and physiological responses of a beech forest using the Standardised Precipitation Index: a case study for Slovakia. Journal of Hydrology and Hydromechanics, 64(3): 246–251.

Vegetation of the selected Slovakian ski pistes

Michal Miklos, Katarina Koristekova, Martin Janco, Miriam Valkova
Department of Natural Environment
Technical University in Zvolen
T. G. Masaryk street 24, 960 53 Zvolen
SLOVAK REPUBLIC

miklosmiso@gmail.com

Abstract: In this study, the floristic composition of ski piste grasslands was compared between the plots treated and untreated by the artificial snow. Research was accomplished in the four ski centers of Central Slovakia (Inner Western Carpathians; temperate zone) located under 1000 m a.s.l. To identify floristic diversity, the Shannon-Wiener's diversity index and Pielou's evenness index was calculated from the vegetation relevés. Results showed occurrence of the varied vegetation mosaic (comprising four to five vegetation units - alliances), both on the treated and untreated plots. Floristic composition of studied plots contained species typical for: i.) mesic hay meadows, ii.) mesic pastures and disturbed perennial grasslands, iii.) mesic montane meadows, iv.) grasslands of deforested sites of montane belts, and v.) oligotrophic grasslands. Species diversity between treated and untreated plots was significantly different in one of four ski centers, while species evenness was significantly different in two of four assessed ski centers. Mixture of species is result of the past and present management activities. Studied ski pistes were based on the mesic hay meadows, pastures and perennial grasslands that were originally natural mesic forests. Operation of the ski pistes on the existing grasslands and meadows can finally save these plant communities against the succession and degradation as in the studied sites. Fundamental differences in the species composition between the plots treated and untreated by the artificial snow was not observed.

Key Words: floristic composition, meadow, grassland, ski resort, artificial snow, piste

INTRODUCTION

Growing popularity of winter tourism leads to development of European mountainous regions (Rixen et al. 2011, Mikloš et al. 2018). More and more popular winter sports increase public demand for the smooth ski pistes with perfect snow conditions. Regardless of climate change, new ski pistes are created and snowed by the artificial snow even at the higher elevations of Alps and Carpathians. Creation of new ski pistes usually includes deforestation, removal of topsoil and vegetation layer and building infrastructure (roads, ski lifts, engineering networks) (Freppaz et al. 2013). In the fragile mountainous ecosystems these activities may lead to geo-hazards such as massive soil erosion or landslides with consequences of the ecosystem´s degradation. Many studies identified decline in biodiversity and changes of plant communities (Burt and Rice 2009, Roux-Fouillet et al. 2011). Mentioned studies were conducted in the higher elevations of Alps, mostly above the 1000 m a.s.l., in the Alpine habitats or in the deforested areas.

Compared to previous studies, in the presented work ski pistes under 1000 m a.s.l., based on the existing grasslands and meadows, were analyzed. The vegetation of four ski pistes in four ski centers was studied to achieve the following aims:

- to identify and compare floristic composition and diversity on the representative parts of ski pistes where the snowmaking is used and not used.

- to identify plant species of the disturbed parts of ski piste where the topsoil and vegetation layer was damaged.

MATERIAL AND METHODS

The investigations were carried out in the four ski centers of Central Slovakia (Inner Western Carpathians). Study sites are described in the Table 1.

In the summer 2016, 8 relevés (quadrant size 1 m^2) and 2 relevés (quadrant size 25 m^2) in each of four ski centers were made according to methods of Zurich-Montpellier school (Braun-Blanquet 1964) using the new Braun-Blanquet 9-membered ordinal cover abundance scale (Westhoff et van der Maarel 1978). Each pair of 4 relevés (1 m^2) was made according to the GLORIA field manual (2015) on the geomorphologically most similar sites with same soil, humidity and management conditions. 4 relevés were under the influence of the artificial snow, while remaining 4 relevés were not. Each 4 relevés were located within the 25 m^2 relevé where the list of species was made. For phytosociological survey were selected most representative parts of ski pistes. Vegetation types were defined on the basis of locally characteristic species. Identified vegetation alliances are briefly described in Hegedüšová et Škodová (2014). Calculation of the Shannon-Wiener's diversity index (H') and Pielou's evenness index (J) was done in the JUICE software.

*Table 1 Description of the study sites. * according to Miklós (2002), Gömöryová et al. (2013), Hrvoľ et al. (2009), Mikloš et al. (2017), Minďáš and Škvarenina (1994), Šatala et al. (2017), Střelcová et al. (2006), Vilček et al. (2016)*

Ski center	Krahule	Malinô	Košútka	Jasenská
Region	Pohronie	Liptov	Podpoľanie	Turiec
Mountain	Kremnické vrchy	Veľká Fatra	Veporské vrchy	Veľká Fatra
Ski piste elevation (m a.s.l.)	895 – 1 060	545 – 1 209	510 – 720	540 – 640
Relevé elevation (m a.s.l.)	990	950	670	590
Grassland management	Mowing Grazing	Mowing	Mowing Grazing	Mowing
Aspect (°)	225	45	360	360
Slope (°)	10	20	10	10
Longitude	185650.90	191535.39	193216.33	190036.73
Latitude	484343.52	490307.98	483323.99	490031.63
Climatic region *	Cool	Cool	Moderately warm	Cool
Annual precipitation totals (mm) *	1000 – 1200	900 – 1000	800 – 900	700 – 800
Mean January air temperature (°C) *	-5 – -6	-5 – -6	-5 – -6	-4 – -5
Mean July air temperature (°C) *	12 – 14	14 – 16	16 – 18	14 – 16
Geological base *	Andesites	Limestones	Tonalites	Sandstones
Soil type *	Cambisols	Cambisols	Cambisols	Rendzic Leptosols
Potential natural vegetation (forest) *	Beech/Fir-beech	Spruce-pine	Beech/Fir-beech	Beech/Fir-beech

RESULTS

In all four study sites, the vegetation was mosaic (comprising of four to five vegetation units - alliances), both on the treated and untreated plots, were identified. Floristic composition of relevés contained species typical for: i.) mesic hay meadows (*Arrhenatherion elatioris* Luquet 1926), ii.) mesic pastures and disturbed perennial grasslands (*Cynosurion cristati* Tüxen 1947), iii.) mesic montane meadows (*Polygono bistortae-Trisetion flavescentis* Br.-Bl. et Tüxen ex Marschall 1947), iv.) grasslands of deforested sites of montane belts (*Nardo strictae-Agrostion tenuis* Sillinger 1933), and v.) oligotrophic grasslands distributed from the lowland areas to the montane belt in Central Europe (*Violion caninae* Schwickerath 1944). On the parts of ski pistes where the vegetation and soil was disturbed because of deforestation, infrastructure creation or machine grading, the high occurrence of the ruderal plant species (*Sambucus ebulus*, *Calamagrostis epigejos*, *Cirsium arvense*, *Solidago Canadensis*, *Tanacetum vulgare* etc.) or pioneer tree species (*Betula pendula*, *Salix caprea*, *Populus tremula*) was identified. On the snowed parts of studied ski pistes the higher occurrence of the dry hay meadow species was detected (*Leontodon hispidus*, *Euphrasia rostkoviana*, *Thymus pulegioides*, *Cruciata glabra* etc.). In the Košútka ski center, every season mulched seedlings of *Betula pendula* on the graded part of ski piste (sandy-skeletal soil) resulted in the high frequency of occurrence and coverage. The parts of ski piste with natural snow had optimal conditions and higher frequency of occurrence tall broadleaf grasses (*Dactylis glomerata*, *Phleum pratense*, *Alopecurus pratensis*) and herbs (*Taraxacum* sect. *Ruderalia*, *Aegopodium podagraria*, *Anthriscus sylvestris* etc.).

Species diversity between treated and untreated plots (by the artificial snow) was significantly different in Košútka ski center (p-value: 9.7 x 10^{-3}), while species evenness was significantly different in Košútka (p-value: 0.031) and Malinô ski center (p-value: 0.024).

*Figure 1 Mean species evenness and species diversity on the plots treated by the artificial snow and on the untreated plots with natural snow. * indicate significant difference between treated and untreated plots at the 95.0% confidence level (unpaired t test).*

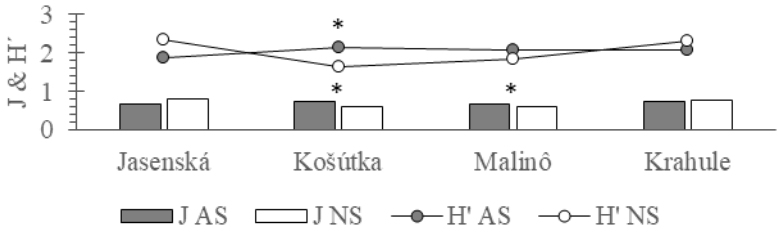

Legend: J – Pielou's evenness index, H' – Shannon-Wiener's index, AS – artificial snow, NS – natural snow

DISCUSSION

In the presented study, the substantial changes in species composition on the plots treated by the artificial snow were not observed, except for disturbed parts of slope (Rixen et al. 2003), probably because the ski pistes were based on the existing grasslands and meadows (vegetation management remained unchanged – mowing, grazing). Snowed parts of studied ski pistes are in operation every season, while parts with natural snow are open for skiers irregularly (shortage of natural snow). Occurrence of tall and broadleaf grasses and herbs on the edge or adjacent parts of ski pistes with natural snow is probably a result of lower intensity of the ski slope operation. Lower intensity can protect the vegetation (defoliation) and soil layer (protect the nutrient-rich topsoil layer against erosion) against damage (Rixen et al. 2003). On the contrary, higher intensity of winter management (grooming, skiing) on the snowed parts of ski slopes can favor species of nutrient-poor, dry meadows (Pohl et al. 2009). On the studied ski pistes, the species of dry hay meadows were more frequent on the snowed, disturbed parts. Higher occurrence of woody plants (seedlings) on the snowed ski pistes was not observed by the other studies. On Swiss ski pistes, the woody plants are reduced because of mechanical damage (Rixen et al. 2003). The significant changes in species diversity were not observed compared to other authors (Rixen et al. 2003, Allegrezza et al. 2017), probably because the original vegetation was saved during the ski center construction and because the milder environmental condition (Allegrezza et al. 2017).

CONCLUSION

On the ski pistes where vegetation and soil layer is not disturbed during its creation, the mosaic of original plant communities occurs. High frequency of occurrence on these slopes has grass and herbs species of mesic meadows and grasslands. Floristic composition and species diversity on the snowed parts and parts of ski slopes with natural snow is not particularly different. Floristic composition differs mainly on the disturbed parts of slopes where the trees and shrubs were removed, the piste was graded or the ski center infrastructure was built. The disturbed sites are colonized by the ruderal and pioneer species. The pioneer tree species can occupy ski slopes where the vegetation and topsoil layer was removed (ski piste grading) and bare sandy-skeletal soil occurs. Mulching the seedlings only stimulate theirs spreading. Grasslands and meadows of ski pistes must be moved or grazed because the high vegetation is unacceptable for the ski piste operation. In general, the original and species-rich plant communities are damaged on some parts of studied ski pistes but on the other parts are maintained by the proper management and thus, saved against the succession.

ACKNOWLEDGEMENTS

This work was accomplished as a part of VEGA projects No.: 1/0589/15, 1/0111/18. of the Ministry of Education, Science, Research and Sport of the Slovak Republic and the Slovak Academy of Science; and the projects of the Slovak Research and Development Agency No.: APVV-15-0425 and APVV-15-0497. The authors thank the agencies for the support.

REFERENCES

Allegrezza, M. et al. 2017. Effect of snowpack management on grassland biodiversity and soil properties at a ski resort in the Mediterranean basin (central Italy). Plant Biosystems, 151(6): 1101–1110.

Burt, J.W., Rice, K.J. 2009. Not all ski slopes are created equal: disturbance intensity affects ecosystem properties. Ecological Applications, 19(8): 2242–2253.

Freppaz, M. et al. 2013. Soil Properties on Ski-Runs. In The Impacts of Skiing and Related Winter Recreational Activities on Mountain Environments. Bussum, Netherlands: Bentham Science Publisher, pp. 45–64.

Gömöryová, E. et al. 2013. Responses of soil microorganisms and water content in forest floor horizons to environmental factors. European Journal of Soil Biology, 55: 71–76.

Hrvol', J. et al. 2009. Long-term results of evaporation rate in xerothermic Oak altitudinal vegetation stage in Southern Slovakia. Biologia, 64: 605–609.

Mikloš, M. et al. 2017. Effect of forest ecosystems on the snow water equivalent in relation to aspect and elevation in the Hučava river watershed, Poľana Biosphere Reserve (Slovakia). Ekológia, 36(3): 268–280.

Mikloš, M. et al. 2018. The Suitability of Snow and Meteorological Conditions of South-Central Slovakia for Ski Slope Operation at Low Elevation—A Case Study of the Košútka Ski Centre. Water, 10(7): 907.

Miklós, L. 2002. Landscape Atlas of the Slovak Republic. 1st ed., Bratislava, Banská Bystrica, Slovakia: Ministry of Environment of the Slovak Republic, Slovak Environmental Agency.

Minďáš, J., Škvarenina, J. 1995. Chemical composition of fog cloud and rain snow water in Biosphere Reserve Pol'ana. Ekologia-Bratislava, 14(2): 125–137.

Pohl, M. et al. 2009. Higher plant diversity enhances soil stability in disturbed alpine ecosystems. Plant and Soil, 324(1-2): 91–102.

Rixen, C. et al. 2003. Does artificial snow production affect soil and vegetation of ski pistes? A review. Perspectives in Plant Ecology, Evolution Systematics, 5(4): 219–230.

Rixen, C. et al. 2011. Winter tourism and climate change in the Alps: An assessment of resource consumption, snow reliability, and future snowmaking potential. Mountain Research and Development, 31(3): 229–236.

Roux-Fouillet, P. et al. 2011. Long-term impacts of ski piste management on alpine vegetation and soils. Journal of Applied Ecology, 48(4): 906–915.

Střelcová, K. et al. 2006. Influence of tree transpiration on mass water balance of mixed mountain forests of the West Carpathians. Biologia. 61(19): 305–310.

Šatala, T. et al. 2017. Influence of beech and spruce sub-montane forests on snow cover in Poľana Biosphere Reserve. Biologia, 72(8): 854-861.

Vilček, J. et al. 2016. Minimal change of thermal continentality in Slovakia within the period 1961–2013. Earth System Dynamics, 7(3): 735–744.

Local extinctions of threatened species of *Pedicularis* L. in agriculture landscape of southeastern Bohemian-Moravian Highlands

Jan Oulehla[1], Martin Jirousek[1,2], Filip Lysak[3]
[1]Department of Plant Biology
Mendel University in Brno
Zemedelska 1, 613 00 Brno
[2]Department of Botany and Zoology
Masaryk University
Kotlarska 2, 611 37 Brno
[3]Cyrilov 6, 594 61 Bory
CZECH REPUBLIC

xoulehla@mendelu.cz

Abstract: The general extinction of organisms belongs to significant environmental problems through the world. In addition to the rare species which long-term occurred only on several localities, we face today the problem of a massive retreat of number of species that perhaps seven decades ago were considered to be relatively common. Primarily competitive weak species retreat or local extinct in behalf of the stronger competitive ones, the better adapted to human-modified eutrophic agriculture landscape. Using very detailed local floristic data of *Pedicularis palustris* and *P. sylvatica* north of Velké Meziříčí (southeastern Bohemian-Moravian Highlands), we demonstrate continual retreat of species abundances in two-time periods, recent situation with state approximately twenty years ago. *Pedicularis palustris* was historically known from two localities in the region, both of them disappeared and the species has not been found for more than ten years. *Pedicularis sylvatica* survives only on a third of the sites known from 1990s, with a large decrease in abundances. Multiple factors, eutrophication, abandonment of land, warmer and drier climate periods, unsuitable local-management practices in some cases, speed up significantly the process of local species extinction, within a relatively short time period of twenty years. Similar fate has met also other species of plants or animals in different regions.

Key Words: biodiversity, botanical survey, eutrophication, nature protection, wet grasslands

INTRODUCTION

There are in total four species of *Pedicularis* (*Orobanchaceae* family) in the recent Czech flora, leaving aside *Pedicularis sceptrum-carolinum* which has occurred in the Czech Republic until 1966 (Hrouda 2000, Danihelka et al. 2012). *Pedicularis* species are root hemiparasites that requires light and wet conditions, with low competitive ability. *Pedicularis exaltata* is critically endangered species which survives within the Czech Republic only on one locality in White Carpathians (NPR Porážky). *Pedicularis sudetica* subsp. *sudetica* is endemic subspecies to the Krkonoše Mts (there are other subspecies of *P. sudetica* with arctic circumboreal distribution; Krahulec 2006). Only occurrence of two species, *Pedicularis palustris* and *P. sylvatica*, is documented from more regions of the Czech Republic including southeastern Bohemian-Moravian Highlands (Figure 1).

Both studied species, *Pedicularis palustris* and *P. sylvatica*, are monocarpic perennial non-clonal herbs. Both studied species are classified as endangered species due to the large continuous retreat during last decades. *Pedicularis palustris* is classified as critically threatened species (C1t) according to traditional national criteria used in Red Lists of vascular plants (Grulich and Chobot 2017), whereas as an endangered species (EN) according to international criteria (IUCN 2012; Grulich and Chobot 2017). *Pedicularis sylvatica* still remains as the most numerous species of the genus within the Czech Republic and is classified as endangered species (C2t), and according to IUCN concept as vulnerable species (VU; Grulich and Chobot 2017). All species of *Pedicularis* are on the list of the vascular plants nationally protected by law (Conservation Act no. 114/1992 and Decree no. 395/1992).

Figure 1 Distribution of Pedicularis palustris *(left map) and* P. sylvatica *(right map) in the Czech Republic based on floristic records (maps taken from ISOP AOPK ČR, 2018). The blue rectangles define the studied area.*

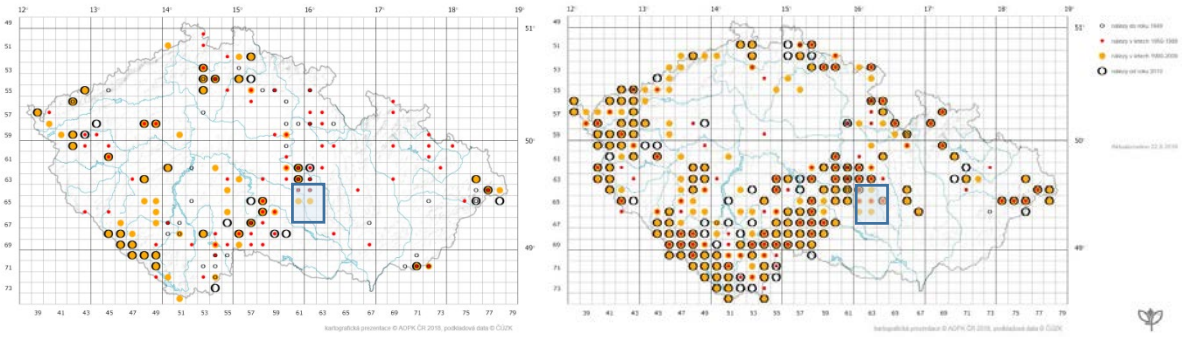

Low productive wet habitats as fens, sedge wetlands, wet meadows and submontane acidophilous grasslands are most typical for the occurrence of the studied species (Hrouda 2000, Chytrý 2007). In the region of southeastern Bohemian-Moravian Highlands were these habitats common in the past and also occurrence of both studied species was higher than nowadays (Figure 1). Wetland and grassland habitats were historically used as pastures. After the World War Two, wetlands were mainly drained and transformed into agriculture land as highly productive meadows during the Socialist Czechoslovakia. Recently, they are partly managed and partly abandoned. Eutrophication, drainage and lack of management have resulted in vegetation change, biodiversity decrease and disappearance of both, natural habitats and competitive-weak threatened species in them. Besides *Pedicularis* species also other co-occurring vascular plants (e.g. *Dactylorhiza majalis*, *Parnassia palustris*) or bryophytes (e.g. *Helodium blandowii*, *Paludella squarrosa*) were reported to decrease their populations or totally lost (Lysák 2000, Lysák 2010, Oulehla 2017). More distinct declines of suitable habitat and species occurrences were in lower altitudes (Pelhřimov Region, Velké Meziříčí Region), whereas relatively more pristine species-rich fen localities remained more preserved in higher altitudes of Žďárské Vrchy Hills (Peterka et al. 2014).

Given that the data on frequency of wetland plants were available from the studied region of Velké Meziříčí (Lysák 2000), we are able to demonstrate changes in population sizes of particular threatened plant species after 20 years in great detail. Field notes, knowledge about history of localities and ecology of studied plant species can help us to understand the causes of species population decreases and comment possibilities of their restoration.

MATERIAL AND METHODS

Study area

The studied area is located in the southeastern part of the Bohemian-Moravian Highlands, north of the town of Velké Meziříčí (Figures 2–3). The altitude is around 500–600 meters above sea level. The long-term mean annual temperature is 7–8 °C and long-term average precipitation 600–700 mm (average data for the period 1981–2010 taken from the Czech Hydrometeorological Institute Web Sites: http://portal.chmi.cz).

Mires with active peat formation are rare within the region and physiognomically resemble rather slightly acidic fen meadows (*Caricion canescenti-nigrae* alliance). Wet meadows (*Calthion palustris* alliance), formed after drainage of fens, are recently abandoned or inappropriately managed with continuous decreasing of threatened wetland plants including *Pedicularis* species (Oulehla 2017).

Floristic survey

All of the known historical localities of *P. sylvatica* with abundance data were revisited repeatedly at least twice in a year (15 localities; Lysák 2000). Nine of these localities were monitored for four years (2015–2018). Other historical localities of *P. sylvatica* and also *P. palustris* with potential distribution, i.e. with suitable wet conditions and management, were visited only once or rather unsystematically. Only few localities remain recently unseen. The individuals of *P. sylvatica* were counted, together

with vegetation description, recording of co-occuring species, moisture evaluating and management characterisation.

Data presentation

Floristic data regarding to the *Pedicularis palustris* and *P. sylvatica* distribution from field monitoring, literature excerption and web floristic database excerption (PLADIAS 2018) has been mapped (ESRI ArcGIS Desktop; Figures 2–3). Map with historical data contains occurrences of *Pedicularis palustris* and *P. sudetica* recorded by Lysák (2000) and map of current data contains recent occurrences between 2015–2018. The individual localities where the monitoring of *Pedicularis sylvatica* populations took place is commented in detail, discussed and the comparison to the situation 20 years ago is stated.

The nomenclature of vascular plants follows Danihelka et al. (2012) and nomenclature of syntaxa follows Chytrý (2007).

RESULTS AND DISCUSSION

Occurence of *Pedicularis sylvatica*

Twenty years ago, *P. sylvatica* was known only from 16 localities and other four localities were known as extinct (Lysák 2000).

Population of *P. sylvatica* disappeared from Ústecký pond and Mrázkova meadow (close to Bory village) due to successional change after eutrophication after 1996 and 1980s, respectively (Lysák 2000). The locality of *P. sylvatica* near Kříže (close to Černá village) disappeared due to spruce afforestation after 1994 and in Oudoly (close to Kadolec village) as a result of *Calamagrostis epigeios* and *Scirpus sylvatica* expansion after abandonment of mowing after 1993. The recovery of the species is irreversible on these four localities.

Recently, only seven of the localities of *P. sylvatica* were found as still existing. No new locality was found neither on historical localities nor new localities within the region (Figure 2, Figure 3). The biggest population of *P. sylvatica* in the region was known from Ochoz pond (close to Olší nad Oslavou village), where hundreds of individuals were counted here under the pond dam in 1990s. The population here almost disappeared due to improperly chosen management of mowing. The meadow is partly overgrown by tall grasses (*Calamagrostis canescens*) and partly regularly mulched. The mulch left on the ground cover small plant species and especially it returns the nutrients back to the ecosystem during the decomposition of biomass. Eutrophication led to expansion of competitively strong species (*Rumex obtusifolius*, *Alopecurus pratensis*) at the expense of the original vegetation. The species is no longer present here, but smaller population occurs in a short-grass vegetation northeast of the pond. The latter population is continuously weakened by grass mowing in the inappropriate term of flowering. Only minimum of plants still left and can produce the seeds for next generations. The germination is strongly limited by a dense grass carpet. There is no surface disturbance for attaching the seedlings.

Vegetation succession after abandonment of management led to *P. sylvatica* disappearing in nearby Zátoky locality. Similarly, the occurrence of *P. sylvatica* is no longer known for localities in the vicinity of Chroustov and Sklené nad Oslavou village (at the municipal wells, Vosecký pond and Sklenský pond). Three localities were known in 2002 close to Bohdalov village, where one of them extinct due to expansion of *Calamagrostis* spp., two others (Brychzovský pond and Rendlíčkový stream) were not revisited.

The occurrence of *P. sylvatica* close to Bobrůvka village. The species was historically only sparsely distributed on the land under the municipal wells in the past. It seemed to disappear here as a result of lack of the mowing. This management was later restored and the occurrence of this species was confirmed in 2017, but only one individual was recorded and no individual was found one year later. The loss of the whole population is probably caused due to the inappropriately chosen term of cutting at the time of flowering and absence of grass-carpet disturbances. New seedlings probably appeared from the seed bank from previous years until it was exhausted. In recent years, the drought climate further deteriorates the original wet soil conditions. Historically, there was a stable population of about 50 individuals at Čechův pond margin. This population continuously extinct as a result of the liming, and partly due to depositions left after pond sediments removing. Changes in the ecosystem

biogeochemistry led into eutrophication following by the vegetation succession. There were only 2 individuals found in years 2016 and 2017.

Figure 2 Historical distribution of Pedicularis palustris *(blue circles) and* P. sylvatica *(red circles) in the studied region.*

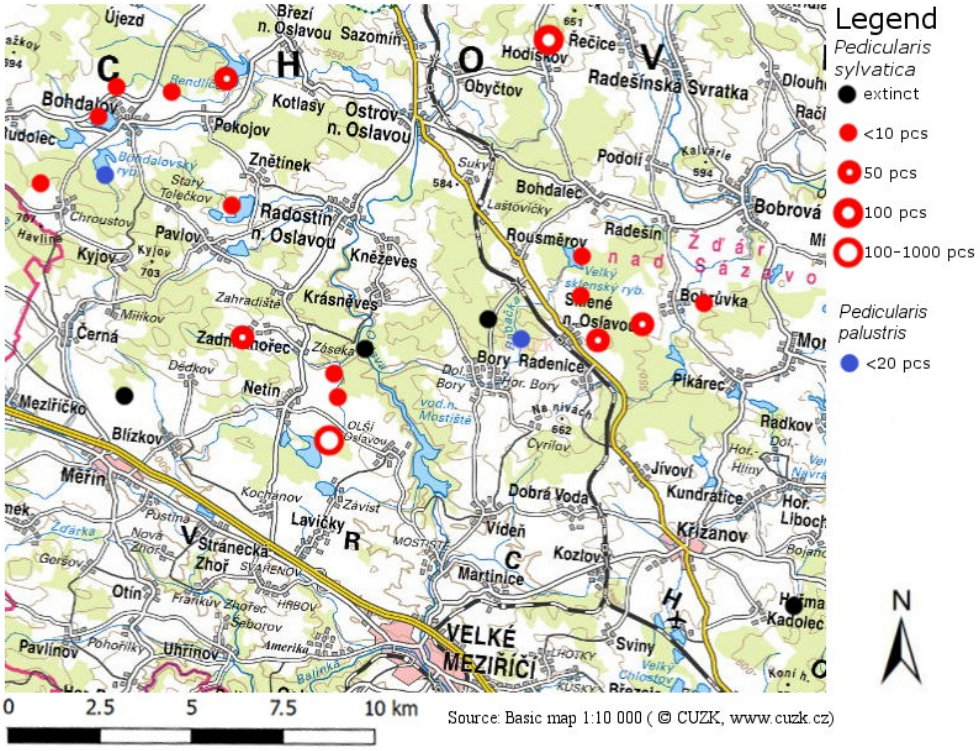

Figure 3 Current distribution of Pedicularis palustris *(blue symbols) and* P. sylvatica *(red circles) in the studied region*

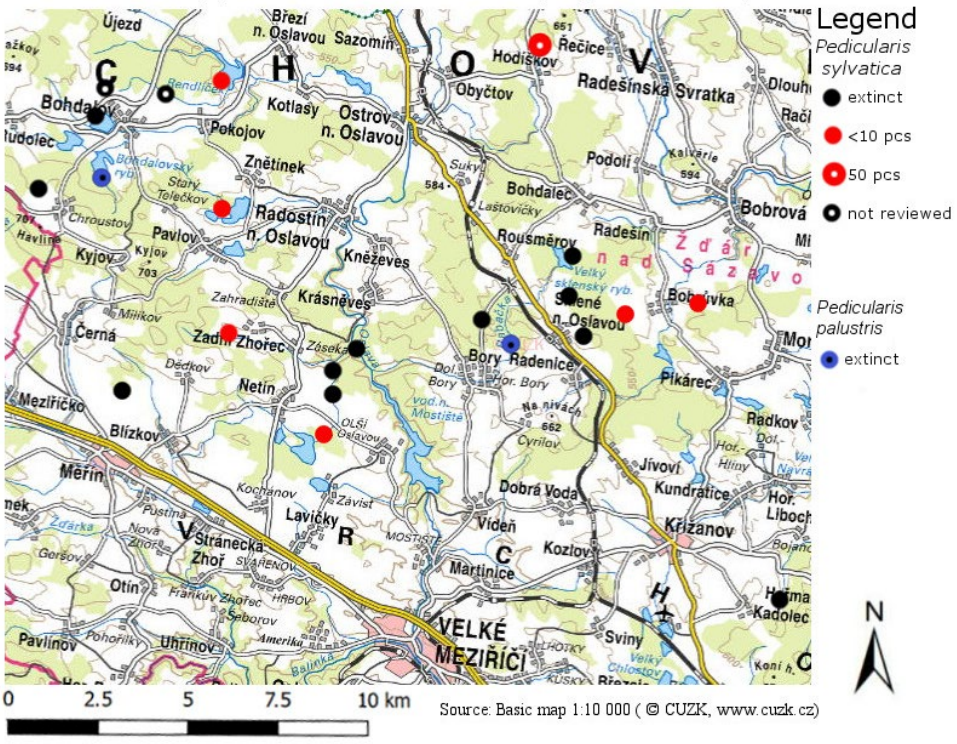

One of the few preserving populations can be found close to Znětínský pond (close to Znětínek village) with several individuals, contrary to dozens individuals known 20 years ago. There is also the biggest occurrence of *Taraxacum nordstedtii* in the region north from Velké Meziříčí.

Approximately 100 individuals of *P. sylvatica* were counted by Lysák (2000) close to Hodíškovský pond. Nowadays, twenty years ago, the locality is a protected area and is regularly mowed. The population partly decreased, but active management has led to preservation of the population, which remain probably as most numerous in the whole region with approximately 50 pieces counted recently on the locality. Similarly, about 50 individuals were counted at the Rendlíčkový pond (close to Březí nad Oslavou) in 2002 (F. Lysák, personal observation). The revision of the occurrence was carried out later by A. Rešlová in 2012 (PLADIAS 2018). Close to Nový pond to the west (close to village Zadní Zhořec), new finding was recorded in 2004 (F. Lysák, personal observation). There were about 50 individuals counted in 2004. Later revision of the occurrence made by L. Čech did not mention the numbers of individuals (PLADIAS 2018).

Occurrence of *Pedicularis palustris*

Rarer of both studied species was documented from the region from two localities - Bohdalovský pond and Těšíkův pond (PLADIAS 2018). Twenty individuals were counted in 2001 on the latter locality (F. Lysák, personal observation). Both of the population extinct due to the successional vegetation changes after management abandonment. At the Těšíkův pond, the last mowing was observed in 2001 and the species continuously disappeared in subsequent years. In 2016, mowing has been restored to recover the population, unfortunately without success. The species did not appear anymore through optimal environmental conditions and management, probably because of absence of viable seeds in the soil.

Causes of *Pedicularis* populations decline

The main cause of declining and disappearing populations of *Pedicularis sylvatica* is the eutrophication caused by nutrient input from fertilizing agriculture land in the surrounding and absence of suitable mowing management. Higher nutrient availability prefers expansion of strongly competitive nitrophilous species at the expanse of more and more endangered poorly competitive species of native wetland habitats. The survey showed that even in mowed meadows the numbers of individuals decreased. Dense vegetation dominating by grasses prevents germination and rooting of seedlings in patches with absence of disturbations. The other reason can be connected with climate changes, which are now more unfavourable for species dependent on regular precipitation and water saturation. Paradoxically, period of drought during summer has partly also a positive effect at Znětínský pond, by cracking the surface of the dense grassland. Regular mowing is not enough, we need also to set up a management that would include needs with respect to phenology of the target species, with combination of surface disruptions. A good example could be grazing. This problem also applies to other plants in the region (*Dactylorhiza majalis*, *Parnassia palustris*, *Taraxacum nordstedti*). For *Pedicularis palustris*, it is hard to find recommendations. It looks that the seed bank of the species is exhausted, and historical findingss were only residual of the dying populations. The species has disappeared and suitable habitats are no longer there.

CONCLUSION

Despite the huge effort put into nature conservation in the Czech Republic, financial covering and/or qualifying practice of the nature conservation management is still insufficient and we still see a continuous biodiversity decline and degradation of natural habitats. Monitoring of populations of two threatened species, *Pedicularis palustris* and *P. sylvatica*, in study region confirms the need for more effective local nature conservation. One of the studied species, *P. sylvatica*, declined in number of populations to a third during twenty years with decreasing in population sizes in the persistent localities. The second species, *P. palustris*, extinct completely in the whole region. Reducing population abundances also in case of well-managed localities indicates a change in abiotic factors due to climate change. Whereas the human-made negative influences on natural habitats, are possible to reduce by suitable management. Preventive measures in the form of restricting direct fertilization and liming of wet meadows are crucial. Whereas, unfortunately, the main source of eutrophication, nutrients leaching from the surrounding agricultural landscape, are difficult to simple limit. Continual long-term pasture

and mowing in terms corresponding to species phenology with small disturbations important for germination of the seedlings, remain as the most suitable management possibilities.

ACKNOWLEDGEMENTS

The research was taken during the bachelor and diploma study of the first author and the long-term continuous vegetation monitoring and practical restoration activities of the third author.

REFERENCES

Chytrý, M. 2007. Vegetace České republiky 1. Travinná a keříčková vegetace. 1. vyd., Praha: Academia.

Danihelka, J. et al. 2012. Checklist of vascular plants of the Czech Republic. Preslia, 84: 647–811.

Grulich, V., Chobot, K. 2017. Červený seznam ohrožených druhů ČR: Cévnaté rostliny. Příroda, 35: 1–178.

Hrouda, L. 2000. Pedicularis L. – všivec. In Květena České republiky. Praha: Academia, pp. 455–461.

International Union for Conservation of Nature (IUCN). 2012. Guidelines for Application of IUCN Red List Criteria at Regional and National. Levels. Version 4.0. [Online]. Available at: http://s3.amazonaws.com/iucnredlist-newcms/staging/public/attachments/3101/reg_guidelines_en.pdf. [2018-10-01].

Krahulec, F. 2006. Species of vascular plants endemic to the Krkonoše Mts (Western Sudetes). Preslia, 78(4): 503–516.

Lysák, F. 2000. Ohrožená mokřadní květena Velkomeziříčska a její ochrana. Diplomová práce, Univerzita Palackého v Olomouci.

Lysák, F. 2010. Ohrožené mechorosty rašelinišť na Vysočině. Závěrečná zpráva projektu podpořeného z Fondu Vysočiny. [Online]. Available at: https://www.kr-vysocina.cz/assets/File.ashx?id_org=450008&id_dokumenty=4033298. [2018-08-21].

Oulehla, J. 2017. Současný stav vybraných mokřadů na Velkomeziříčsku a změny v druhovém složení rostlin po 20 letech. Bakalářská práce, Mendelova univerzita v Brně.

Peterka, T. et al. 2014. Testing floristic and environmental differentiation of rich fens on the Bohemian Massif. Preslia, 86(4): 337–366.

PLADIAS. 2018. Database of the Czech flora and vegetation. [Online]. Available at: http://www.pladias.cz. [2018-10-01].

Pollination and pollinators of haskap (*Lonicera caerulea*)

Ales Vladek, Marian Hybl, Antonin Pridal
Department of Zoology, Fisheries, Hydrobiology and Apidology
Mendel University in Brno
Zemedelska 1, 613 00 Brno
CZECH REPUBLIC

apridal@mendelu.cz

Abstract: The study was focused on pollination in haskap (varieties Viola and Gerda). The aim was to verify impact of free pollination on fruit harvest and to observe bee haskap pollinators. The percent fruit set was compared among four treatments: free pollination, hand-self/cross-pollination and no manipulation. The significantly highest production was found under free pollination in the both varieties. The fruit production under isolation was without statistically significant differences with except of Viola in the hand-cross-pollinated treatment. Similarly, in case of the fruit weight, the differences were highly significant in the both varieties Gerda and Viola. The significantly heaviest fruits were under free pollination in both varieties. The average fruit weight in Viola under isolation was significantly higher only in hand-cross-pollinated treatment. In Gerda, only treatment without manipulation was significantly different from hand-cross pollination. The free pollination resulted in earlier and shorter harvesting in the both varieties. Entomophilous character of haskap is proven exactly. The hand-cross-pollination was not able to maximize the fruit set. This proves that there is any unspecified impact of pollinators on effectivity of pollination in haskap. Preliminary results on haskap bee pollinator diversity suggest preference by long-tongued bees especially bumblebees. Other experiments have to be carried out to more clarify the reasons for low haskap productivity under isolation with hand-cross-pollination.

Key Words: Lonicera caerulea, haskap, hand pollination, fruit set, pollinator

INTRODUCTION

There are concerns about how to meet the growing food demand while protecting ecosystems and biodiversity (Brussaard et al. 2010). One factor how to increase the crop production in line with sustainable development is to provide crops with optimal pollination to maximize the quantity and quality of the yield (Garratt et al. 2013).

Lonicera caerulea var. *kamtschatica*, also known as haskap (Figure 1), honeysuckle or honeyberry, is fruit shrub producing edible fruits ripening extremely early – even before strawberry. Haskap is resistant to very low temperatures, plant up to -40 °C and flowers up to -8 °C (Řezníček and Salaš 2015). The recent original distribution of haskap is circumpolar (Frier et al. 2016) and becomes to be popular fruit for similar flavour as blue berries and potential health benefits (Svarcova et al. 2007).

Haskap has double-flower inflorescence forming a compact fruit with two berries (Frier et al. 2016). The fruit shape and harvest time depend on the cultivar features. Fruits ripen from the end of May till June in temperate zone (Bożek 2012).

Hascap is highly rewarding bee forage plant with attractive nectar (Bożek and Wieniarska 2006) and pollen (Bożek 2007). These features indicate demands of haskap on entomophily, therefore, cross-pollination and self-incompatibility. There were performed experiments on pollination under free and isolated conditions (Bożek 2012) confirming self-incompatibility and by different pollinators (Frier et al. 2016) confirming impact of pollinator specificity. Self-incompatibility in different haskap varieties was proved also cyto-embryologically (Boyarskikh 2017).

For comprehensively experimental examine pollination requirements it needs to be designed pollinated positive controls under isolation (Corber et al. 1991). The impact of hand-self/cross-pollination in haskap under isolation has not yet been verified, thereby, impact of free pollination/pollinators is not sufficiently assessed.

Therefore, the aim of this study was to compare percent fruit set and average weight of fruit in dependence of different pollination method also under isolation. Diversity of bee pollinators (Hymenoptera: Apiformes) was observed during blooming period of haskap.

MATERIAL AND METHODS

Experiment was carried out in spring 2018 in Žabčice (southern Moravia, Czech Republic), on the experiment farm of Mendel University where are black soils. The flat surface with average altitude 185 m and average precipitation 380–550 mm and average year temperature over 10 °C dominate in this area. Two varieties (Viola and Gerda) were selected for this experiment. Hand pollination was made by very soft painting brush. Isolation of flowers against free flying insects was achieved by special textile around branches – organdy and fruits against birds by plastic net covering whole shrubs. Rainproof marker was used to marking of flowers. The pollen from variety Tomichka and cultivar Průhonický semenáč (wild seedling) were used for pollination of varieties Viola and Gerda due to their compatibility (Boyarskikh 2017). Entomological hand-catching net was used for sampling bees pollinating haskap.

The experimental design was created according to principles by Corbet et al. (1991). Therefore, four treatments were founded: a) unlimited access of pollinators – free pollination, and three isolated treatments without pollinators b) hand-pollination by own pollen – self-pollination, c) hand-pollination by foreign pollen from compatible pollenizers – cross-pollination and d) without any manipulation.

Each variety (shrubs) and each treatment (branches) consist from three repetitions – triplets (n=3). On every branch up to one hundred flowers were included in experiments in following blooming dates: 9. 4., 11. 4., 13. 4., 15. 4., 17. 4., 19. 4. and 22. 4. 2018. Harvest of fruits was performed in these dates: 8. 5., 11. 5., 14. 5., 16. 5., 18. 5. and 21. 5. 2018. The percent fruit set was counted as proportion the number of fruit to the number of inflorescences. For every partial harvest were found number of fruits and total weight of harvested fruits. The proportion of these parameters was used to determine average weight of fruit.

Bees pollinating haskap were sampled in appropriate sunny weather and form 10 to 16 hours at site in Žabčice, Brno and Příbram na Moravě. The 20 honeybee colonies were placed in close proximity of hascap plantation in Příbram n. M.

The results were statistically analysed with a one-way ANOVA analysis and a post-hoc Tukey's test ($\alpha = 0.05$). The percent fruit set were transformed by arcsin (x) to improve normality.

Figure 1 Haskap – Lonicera caerulea:

a) hand-made pollination *b) small garden bumblebee Bombus hypnorum* *c) haskap fruits*

RESULTS

Differences in the percent fruit set in dependence of the pollination method are depicted in Figure 2. The differences were highly significant in the both varieties Gerda ($F_{0.95\ (3,8)} = 41.99$; $P < 0.001$) and Viola ($F_{0.95\ (3,8)} = 34.53$; $P < 0.001$). The significantly highest production (Tukey test,

α = 0.05) was found under free pollination in the both varieties. The fruit production under isolation was without statistically significant differences (α > 0.05) with except of Viola in the hand-cross-pollinated treatment.

Figure 2 Percent fruit set according to variety and pollination method (ANOVA, Tukey test, α = 0.05)

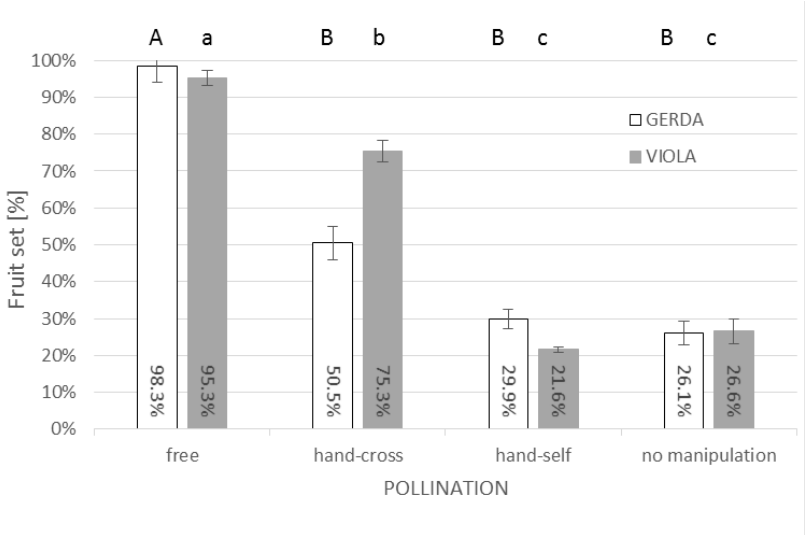

Similar but not the same results were in case of the fruit weight (Figure 3). The differences were highly significant in the both varieties Gerda ($F_{0.95\ (3,8)} = 22.12$; $P < 0.001$) and Viola ($F_{0.95\ (3,8)} = 56.39$; $P < 0.001$). The significantly heaviest fruits (Tukey test, α = 0.05) were recorded under free pollination in both varieties. The average fruit weight in Viola under isolation was significantly higher (α > 0.05) only in hand-cross-pollinated treatment. In Gerda, only treatment without manipulation was significantly different from hand-cross pollination.

Figure 3 Average weight of fruit according to variety and pollination method (ANOVA, Tukey test, α = 0.05)

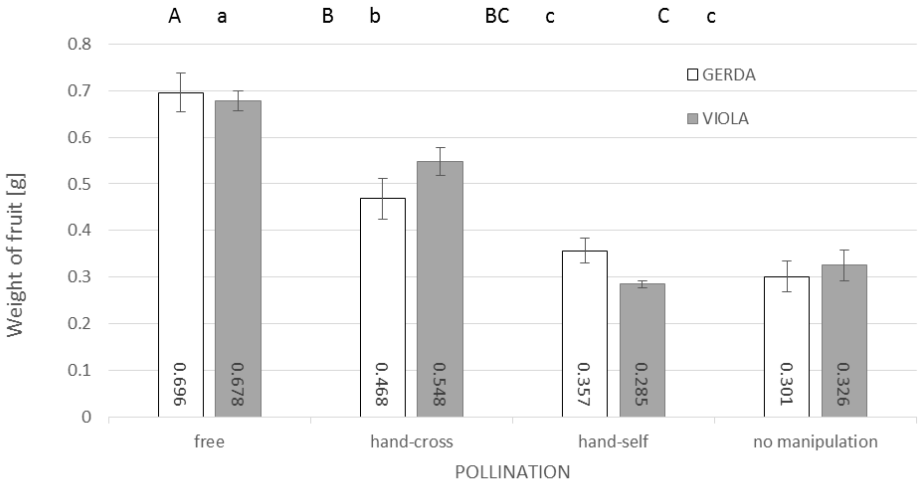

The free pollination resulted in earlier harvesting in the both varieties (Figure 4). The top of harvesting intensity (i.e. the highest fruit set per harvest day) was achieved clearly at first under the free pollination treatment. The harvest tops came later (about one harvest day) under isolation compared with the free pollination and at the same time compared with these three treatments. Duration of harvesting was longer about 2–3 days under isolated treatments of the pollination methods.

Figure 4 Percent fruit set in time order of harvest

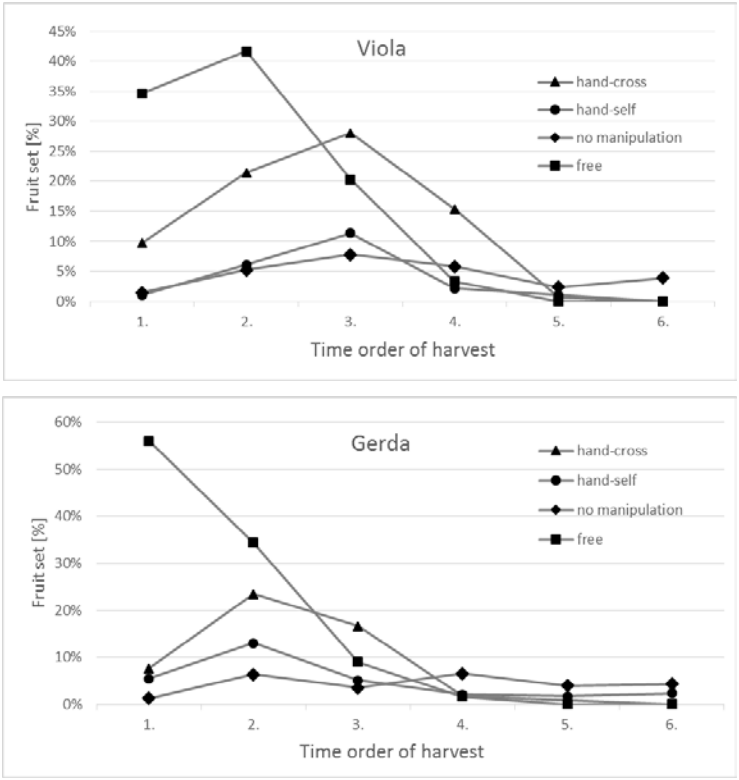

There were preliminarily observed several species of bee pollinators (Table 1). Extremely high density of bumble bees was recorded just in Příbram n. M. and contrary in Žabčice and Brno where the solitary bees or honeybees were more numerous. Higher density was typical of the long-tongued bees; in bumblebees *Bombus hortorum* and in solitary bees *Anthophora plumipes*.

Table 1 Preliminary results on diversity and dominance of bee pollinators in Lonicera caerulea

Location →	**Žabčice**	**Brno**	**Příbram n. Moravě**
Bumblebees ***Bombus* spp.**	*Bombus* - *hortorum* - *pratorum* - *sylvarum* - *lapidarius* - *terrestris* [13%]	*Bombus* - *hortorum* - *pratorum* - *pascuorum* - *hypnorum* - *lapidarius* - *terrestris* - *lucorum* [9%]	*Bombus* - *hortorum* - *hypnorum* - *pratorum* - *pascuorum* [94%]
Solitary bees	*Anthophora plumipes* *Evyleus pauxillus* *Evylaeus morio* *Osmia bicornis* *Andrena bicolor* *Xylocopa* (*Xylocopa*) sp. *Eucera nigrescens* [42%]	*Anthophora plumipes* *Evylaeus morio* *Osmia cornuta* *Andrena flavipes* *Xylocopa* (*Xylocopa*) sp. [59%]	*Anthophora plumipes* *Nomada succincta* [4%]
Western honeybee ***Apis mellifera***	[45 %]	[32%]	[2%]

Legend: Names of species are listed in order of decreasing dominance. Underlined names represent eudominant species. Percentages in square brackets represent group dominance.

DISCUSSION

The significantly highest percent fruit set under free pollination and three-time lower one under isolation without manipulation confirm results by Bożek (2012). Entomophilous character of haskap is undisputable also with respect to the delayed harvesting of fruits in the treatments under isolation. The shorter harvest period due to optimal pollination conditions was described also in other crops (Williams

1985, Racys and Montviliene 2005). It is remarkable that the hand-cross-pollination was not able to maximize the fruit set in comparison with free pollination. This result indicates that there was any "pollinator" factor(s) in the free pollination maximizing fruit productivity (both fruit set and weight). Possible explanations are as follow: haskap flower needs a) higher number of visits to be thoroughly fertilized with aim to place higher amount of pollen grains on stigma (Rader et al. 2009, Frier et al. 2016) and/or b) specific pollenizer to achieve compatibility (Boyarskikh 2017). Due to these possible factors the differences in the fruit productivity between hand-cross- and hand-self-pollination treatments were statistically significant (in Viola) or insignificant (in Gerda). The minimal insignificant differences between treatments hand-self-pollinated and without manipulation could be caused by low limited level of self-compatibility. Flowers without manipulation were pollinated by an assumed internal process of self-transfer of own pollen grains inside of the same flower from anther to stigma (Frier et al. 2016). Likely, this self-fertilization process was able to maximise fruit productivity by itself, therefore, the hand-transferred pollen grains inside of the same flower by brush was redundant. It was not so in the case of hand-cross-pollination compared with hand-self-pollination where the transfer of foreign pollen increased the fruit productivity as it is discussed above. Other experiments have to be carried out to more clarify the reasons for low haskap productivity under isolation with hand-cross-pollination.

Honeybees are able to gain nectar and pollen as it was apparent from higher density at Žabčice. However, in spite of 20 colonies in close proximity haskap, extremely low honeybee dominance was recorded. These results indicate high competitive effect of long-tongued bees due to deep corolla in haskap flowers. Habitats in vicinity of Příbram n. M. are more appropriate for nesting of bumblebees. Haskap is circumpolar species. In this region the best adapted bee pollinators are just bumblebees (Kevan et al. 1993). It is possible that there is any ecological relationship "plant-pollinator". Therefore, it is probable the bumblebee populations were somewhat disadvantaged beside other bees at the sites with lower altitude and warmer and dryer conditions (i.e. Brno and Žabčice). The "*Lonicera-Bombus*" relationship can be also somewhat special as it was confirmed in the case of *Lonicera periclymenum* (Ottosen 1987). How complicated and heterogeneous relationships are between plants and pollinators is currently being discovered (Brittain et al. 2013).

CONCLUSIONS

1. Haskap harvest parameters (percent fruit set, fruit weight and term and duration of harvest) were not optimized even by hand-cross-pollination treatment in compare with free pollination. This proves that there is any unspecified impact of pollinators on effectivity of pollination process in haskap.

2. Preliminary results on haskap bee pollinator diversity suggest preference by long-tongued bees especially bumblebees.

ACKNOWLEDGEMENTS

We are indebted to Libor Dokoupil, Magdalena Tvrznikova (Department of Breeding and Propagation of Horticultural Plants, Mendel University in Brno) for sharing of haskap plantation in university farm and Vojtech Reznicek (from the same department) for pomological consultations. We thank for technical assistance in laboratory Lucie Havlova (Department of Zoology, Fisheries, Hydrobiology and Apidology, Mendel University in Brno).

REFERENCES

Boyarskikh, I.G. 2017. Features of Lonicera caerulea L. reproductive biology. Agricultural Biology, 52(1): 200–210. (in Russian with English abstract).

Bożek, M., Wieniarska, J. 2006. Blooming biology and sugar efficiency of two cultivars of *Lonicera kamtschatica* (Sevast.) Pojark. Acta Agrobotanica, 59(1): 177–182.

Bożek, M. 2007. Pollen productivity and morphology of pollen grains in two cultivars of honeyberry (*Lonicera kamtschatica* (Sevast.) Pojark.). Acta Agrobotanica, 60(1): 73–77.

Bożek, M. 2012. The Effect of Pollinating Insects on Fruiting of Two Cultivars of *Lonicera caerulea* L. Journal of Apicultural Science, 56(2): 5–11.

Brittain, C. et al. 2013. Synergistic effects of non-Apis bees and honey bees for pollination services. Proceedings of the Royal Society B: Biological Sciences, 280(1754): 20122767.

Brussaard, L. et al. 2010. Reconciling biodiversity conservation and food security: scientific challenges for a new agriculture. Current Opinion in Environmental Sustainability, 2(1): 34–42.

Corbet, S.A. et al. 1991. Bess and the pollination of crops and wild flowers in the European community. Bee World, 72: 47–59.

Frier, S.D., et al. 2016. Comparing the performance of native and managed pollinators of Haskap (*Lonicera caerulea*: Caprifoliaceae), an emerging fruit crop. Agriculture, Ecosystems & Environment, 219: 42–48.

Garratt, M.P.D. et al. 2013. Avoiding a bad apple: insect pollination enhances fruit quality and economic value. Agriculture, Ecosystem and Environment, 184: 4–40.

Kevan, P.G. et al. 1993. Insects and plants in the pollination ecology of the boreal zone. Ecological Research, 8(3): 247–267.

Ottosen, C.-O. 1987. Male bumblebees (*Bombus hortorum* L.) as pollinators of *Lonicera periclyneum* L. in N.E.-Zealand, Denmark. Flora, 179: 155–161.

Racys, J., Montviliene, R. 2005. Effect of bees-pollinators in buckwheat (*Fagopyrum esculentum* M Moench) crops. Journal of Apicultural Science, 49(1): 47–51.

Rader, R. et al. 2009. Alternative pollinator taxa are equally efficient but not as effective as the honeybee in a mass flowering crop. Journal of Applied Ecology, 46(5):1080–1087.

Řezníček, V., Salaš, P. 2015. Gene pool of less widely spread fruit tree species. Acta Universitatis Agriculturae et Silviculturae Mendelianae Brunensis, 52(4): 159–168.

Svarcova, I. et al. 2007. Berry fruits as a source of biologically active compounds: the case of *Lonicera caerulea*. Biomedical Papers, 151(2): 163–174.

Williams, I.H. 1985. The pollination of swede rape (*Brassica napus* L.). Bee World, 66(1): 16–22.

AGROECOLOGY AND RURAL DEVELOPMENT

Observing the soil erosion on sloping vineyards when different soil cover applied

Alice Cizkova[1], Patrik Burg[1], Vladimir Masan[1], Jana Burgova[2], Vladimir Visacki[3]
[1]Department of Horticultural Machinery
[2]Department of Breeding and Propagation of Horticultural Plants
Mendel University in Brno
Zemedelska 1, 613 00 Brno
CZECH REPUBLIC
[3]Department of Agricultural Engineering
University of Novi Sad
Dr Zorana Đinđića 1, 21000 Novi Sad
SERBIA

alice.cizkova@mendelu.cz

Abstract: This paper work discusses and evaluates the results of the impact of several types of cover materials on the soil erosion in the vineyards in the Czech Republic. The experiment was based on four variants where three types of cover materials were selected for the protection against soil erosion: cereal straw (var. A, the consumption of covering material was 1200 g/m^2), wood chips (var. B, the consumption of cover material was 4000 g/m^2) and compost (var. D, the consumption of cover material was 2000 g/m^2). The fourth control variant (var. C) consisted of a cultivated interlayer without cover material. During the measurements in years 2017–2018, the soil was picked up by the tools very similar to "catch pockets". The conclusive results of the evaluation indicate the positive effect of the cover materials on the protection of soil erosion even when affecting the soil moisture. Out of all evaluated variants, the washout was not recorded in Variant A, in which the mulching material was in form of cereal straw. For other cover materials, a small amount of washout was recorded in the range between 0.02–15.00 g/m^2, which was directly related to the total rainfall precipitation. The results showed that the highest number of soil washout (15 g/m^2) occurred, when the control variant without the use of cover material was applied. The results also show the positive effect of mulching materials on the values of soil moisture. The highest average soil moisture was in two-years period measured in the soil covered by the cereal straw (26.54–32.43% vol.), on the other hand, the lowest soil humidity was measured in the fourth control variant (20.45–22.74% vol.).

Key Words: vineyard, water erosion, soil erosion, covering materials, soil slip

INTRODUCTION

Water erosion is considered one of the major threats to soil resources directly connected to the climatic, edaphic and geomorphologic conditions (Novara et al. 2015). The main reason is the frequent absence of systematic protection of eroded endangered plots, which would limit the loss of soil to an acceptable level. In the Czech Republic, the water erosion threatens more than 50% of agriculturally farmed soil (Javůrek and Vach 2010). The attention is also paid to the growing trend of endangered soils by erosion in vineyards, particularly those sloping vineyards that suffer from the greatest loss of land. The main reason for their high erodibility are practices that keep the soil between the vines bare during the entire year and these bare surfaces are affected by intense storms that induce severe water erosion and runoff processes (Arnáez et al. 2007). Moreover, vineyards are often planted on steep-sloping soils (Arnáez et al. 2007) with poor nutrient and organic matter content (Novara et al. 2015).

According to Anderson and Norman (2011), vineyards represent one of the most important crops in terms of income and employment in global scale. For these reasons, adequate soil management practices are needed to contribute to a more sustainable viticulture, which includes evaluation to determine whether they are acceptable to the farmers who will have to utilize them (Galati et al. 2015). While the issue of soil erosion on land used for crop production is subject to a great deal of attention

and a number of papers are published with regards to this topic, there is insufficient information on the issue of erosive soil endangerments in vineyards.

In the world, various methods of protection against soil erosion have been verified, including mulching foils, underground stones, various plant cover variants and, last but not least, various mulching materials (Blavet et al. 2009). Among the soil conservation practices that are lately in vineyard praxis verified, the mulching seems to be the most perspective and effective method in reducing water and soil loss and improving soil condition (Cerdà et al. 2015).

The aim of this paper is to determine the amount of soil erosion from the interconnection of vineyards covered by different types of mulch materials.

MATERIALS AND METHODS

Experimental area

For experimental measurements, a test site was selected. This site is located in the "Velke Pavlovice" wine-growing sub-region, in the area of small town "Rakvice" and on the track called "Kozí Horky" (Latitude: 48°51′29″N, Longitude: 16°48′48″E). This site is in a corn production area, with a very warm and dry climate, with an altitude of 164 metres above sea level. The slope of the land is up to 10%. The soils are classified as a pelic chernozem on very heavy substrates (clays, marshes, carpathian flys and tertiary sediments), on a scale from heavy to very heavy with a lighter horizon, rarely gravely, with a tendency of moisture on the surface in the profile. Skimmer is classified from none up to 10%.

Character of mulching materials and experiment variants

The experiment was based on 4 variants, for which 3 kinds of cover material were chosen for the soil protection – crushed cereal straw (variant A, consumption of covering material 1200 g/m^2, volume weight 100 kg/m^3), wood chips (variant B, consumption of cover material 4000 g/m^2, volume weight 400 kg/m^3) and compost made from grape pomace, grass, wood chips and vegetable waste (variant D, consumption of covering material 2000 g/m^2, volume weight 560 kg/m^3). The fourth control variant (C) consisted of a cultivated interlayer without covering material.

Measuring of meteorological data and soil moisture

A weather station was installed in the experimental vineyard, which recorded data on air temperature, soil temperature, rainfall and soil moisture at a depth in between 0.1 and 0.3 m. In all experimental variants, the soil moisture values were measured by "VIRRIB" humidity meters, located at a depth in between 0.1 and 0.3 m. The soil humidity was recorded during the vegetation every day at regular fifteen-minute intervals using the "VIRRIBLOGGER" recording unit.

Evaluation of soil erosion

The erosion of soil was detected by special pockets created for retaining loose soil with free flow of water. The width of each pocket was 1 m and its length was 0.5 m, the back part of the pocket was 0.3 meter-high with sloping sides. The length of the monitored slope was approximately 100-meter and 1-meter width. Each pocket was made of polyethylene with flow holes in the back of the pocket. Inside of the pocket, a nonwoven, dense cloth was inserted, which captures the soil slides and the leachate water flows through holes in the rear. The captured content of sediments is collected, dried, weighed and re-calculated to the amount of uneven soil of 1 ha. When removing the loose soil, a soil moisture sample is taken before drying the sludge itself. The weight of the fabric is deducted from the weight of the soil. The content of the soil is determined by the content of the nutrients, the pH and the humus content.

Analytical methods

The experiment has started on April 1, 2017 and continued throughout the year 2018. Since this date, the soil was continually monitored. The initial physical state of the soil was determined, by using "Kopecky physical cylinders", soil humidity gravimetrically humus content by Novák methodology and soil reaction (Mehlich III method). The soil was analysed for the content of basic nutrients, humus and

soil reaction according to the "Methodology of the Central Institute for Surveying and Testing in Agriculture" and compared with the soil analyses carried out at the beginning of the growing season.

"Kopecky physical cylinders" are made of stainless steel, usually of a volume of 100 cm^3 and a maximum height of 5 cm. They are used to determine the physical properties of soils in their intact state (Jandák et al. 2003).

Statistical analysis

A statistical analysis was performed using the software package "Statistics 12.0" (StatSoft Inc., Tulsa, Oklahoma, USA). Analysis of variance was conducted, and the results were compared using Tukey's multiple range assay at a significance level $\alpha = 0.05$.

RESULTS AND DISCUSSION

At the experimental level, there have always been, at the beginning of vegetation, evaluated the moisture of soil. The value was different in each depth of soil (0.1–0.3 m), and was in between 18.78–24.21% weigh in the year 2017, and in the year 2018 in between 17.08–18.54% volume. The average value was then 21.35% volume. In Table 1 you can find two-years results of physical characters withdrawn samples of soil. The content of nutrients in soil at the beginning of vegetation is stated in Table 2.

Table 1 Physical character of soil

Depth (m)	Density (g/cm^3)		Porosity (%)		Volume				Maximum capillary capacity		Minimal air capacity	
					Water		Air					
					(% volume)				(% volume)			
Year	2017	2018	2017	2018	2017	2018	2017	2018	2017	2018	2017	2018
0–0.1	1.05	1.39	59.95	47.11	25.40	23.66	34.55	23.45	45.91	35.83	14.04	11.28
0.1–0.2	1.23	1.36	53.23	48.14	26.47	24.01	26.76	24.13	37.48	36.09	15.75	12.06
0.2–0.3	1.29	1.42	50.95	45.64	24.13	26.40	26.83	19.24	36.99	35.41	13.96	10.23
Average	1.19	1.39	54.71	46.96	25.33	24.69	29.38	22.27	40.13	35.78	14.58	11.19

Table 2 The results of soil chemical analysis in respective variants

Depth (m)	(mg/kg)				N_c (%)	Humus (%)	pH_{KCl}	HA/FA
	K – p	Mg – p	P – p	Ca – p				
Year 2017								
0–0.1	410	448	44	4569	0.23	3.51	7.4	0.93
0.1–0.2	476	469	38	4890	0.24	3.50	7.4	0.97
0.2–0.3	501	490	46	5111	0.21	3.47	7.4	0.96
Average	462.33	469.00	42.67	4856.67	0.23	3.49	7.4	0.95
Year 2018								
0–0.1	423	440	40	4499	0.22	3.50	7.3	0.95
0.1–0.2	485	452	47	4476	0.21	3.49	7.4	0.97
0.2–0.3	507	488	49	5096	0.21	3.46	7.4	0.97
Average	471.67	460.00	45.33	4690.33	0.21	3.48	7.4	0.97

Legend: HA – humic acids; FA – fulvic acids

From the values shown in the Figure 1 and Figure 2, we can see that the highest soil moisture was found, during the two-year period, in the soil covered by straw. In 2017, the average value in this variant was 26.57% vol. and in 2018 32.43% vol. In the control variant, average soil moisture values were 22.74% vol. (2017) and 20.45% vol. (2018), for wood chip variant the values were 21.96% vol. (2017) and 23.99 (2018), and for compost variant the values were 21.66% (2017) and 21.86% (2018). Sarkar and Singh (2007) report the positive effect of mulching on retention of soil moisture after the rainfalls. They also found that mulching soil is able to maintain 19 to 21 mm more of soil moisture in the profile up to 1.2 m than the soil without being covered by mulching material. Badalíková and Bartlová (2007) states that mulching organic stuff can be a mean of improving soil moisture ratios that can favorably affect the quantity and quality of yield. Straw mulching then refers to a favorable agro-environmental measure as it can, to a certain extent, reduce soil erosion.

Dvořák (2013) claims that the application of straw as a mulching material brings its negatives as well, which are reflected by the reduction of nitrogen content in the soil, which is manifested even on the worse nutritional status of the stands. The application of a mulching material in warmer conditions has proved to be a mean of influencing soil temperature (higher minimal temperature and lowering of daily maximum as well as the average temperature for vegetation). Paul et al. (2004) states that differently colored cover materials in various ways absorb radiation and reduce heat losses due to convection and radiation. This is reflected in the modification of the temperature amplitude on the surface and consequently also in the soil profile with a direct impact on humidity ratios.

Figure 1 The value of soil moisture and rainfalls in the year 2017

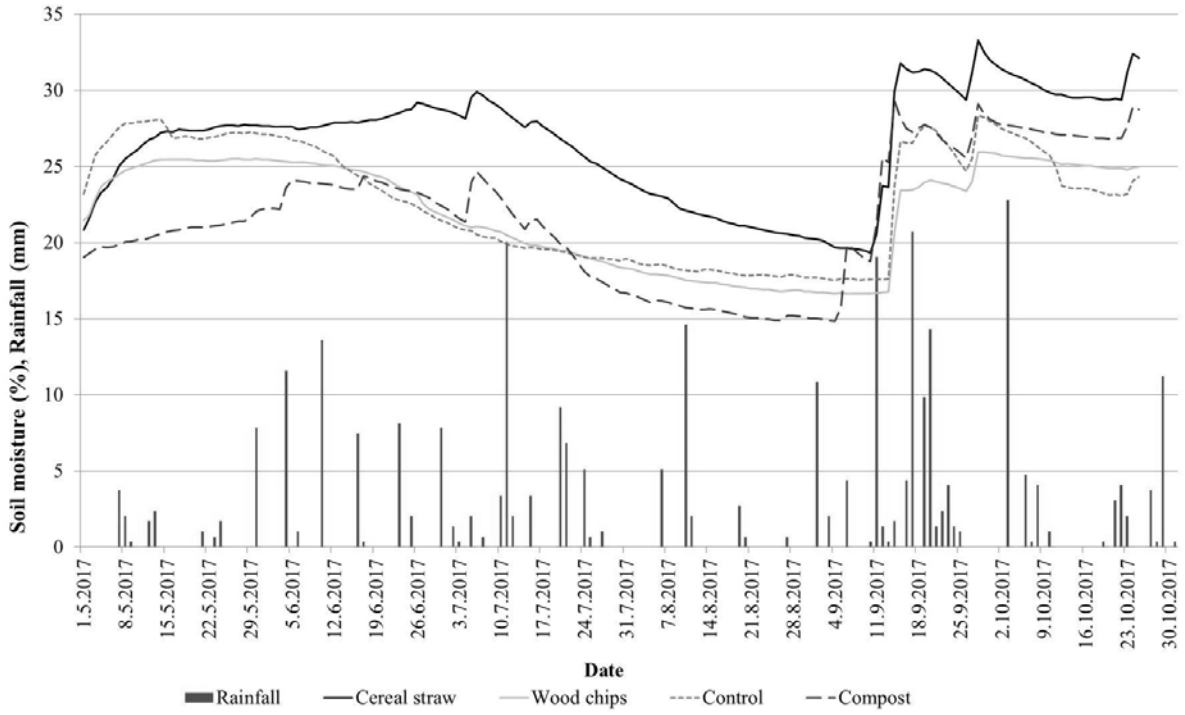

Figure 2 The values of soil moisture and rainfalls in the year 2018

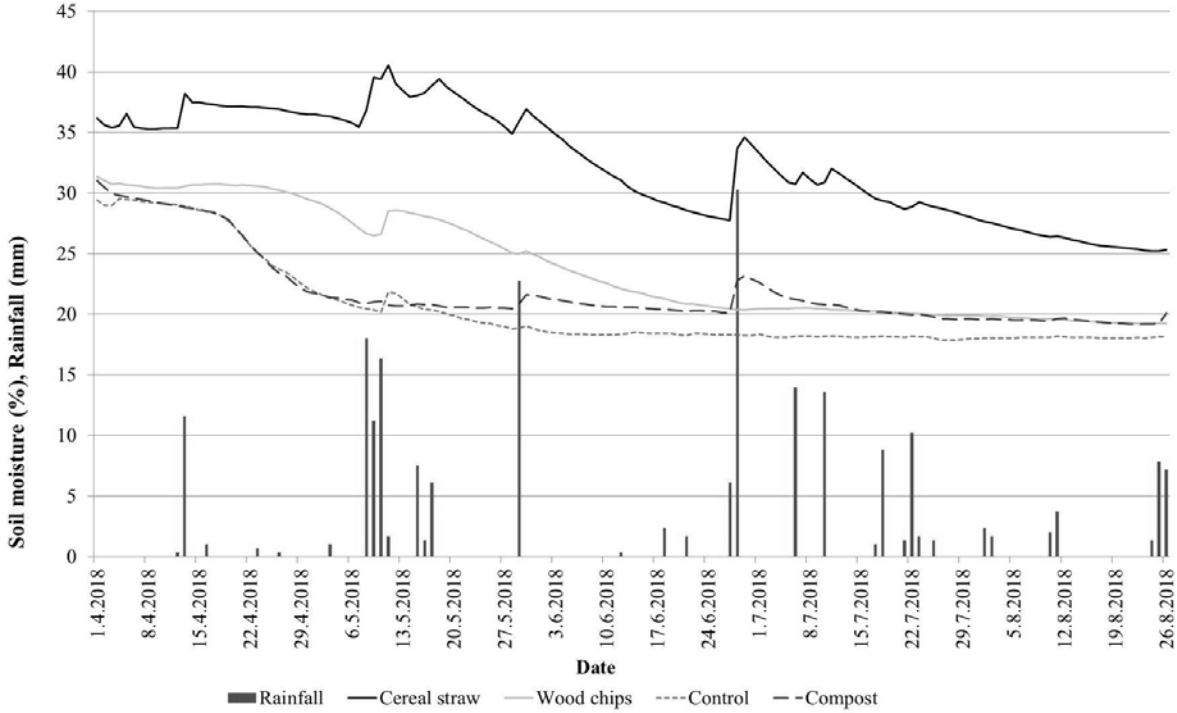

In overall, during the two vegetation periods, a low amount of rainfall was recorded – 160 mm in 2017 and 205 mm in 2018. In 2017, soil erosion was recorded only in three terms as shown in Table 3, and in 2018 only in two terms as seen in Table 4. The results of the experimental measurements indicate that from all the evaluated variants no soil washout was recorded for variant A. For other cover materials, a small amount of washout was recorded in the range of 0.02–15.00 g/m^2, which was directly related to the total rainfall precipitation. The measurements show that erosion effects occur only when the rainfalls are over 20 mm per day. The highest values of washout were recorded for control variant C (control), in which the soil loss in the year 2017 was 15 g/m^2. The obtained values were statistically evaluated by variance analysis and Tukey's multiple range test at a significance level $\alpha = 0.05$, as shown in Table 3 and Table 4.

Table 3 The soil erosion – evaluation of variants (2017)

Experiment variants	Date and amount of the erosion (g/m^2)			The scale of erosion (g/m^2)	
	10.06.2017	11.07.2017	10.08.2017	**Average**	**Amount**
A (cereal straw)	0.01 ± 0.00^a	0.01 ± 0.00^a	0.01 ± 0.00^a	0.01 ± 0.00^a	0.03
B (wood chips)	0.01 ± 0.00^a	1.00 ± 0.15^a	0.01 ± 0.00^a	0.34 ± 0.51^a	1.02
C (control)	2.01 ± 0.06^b	6.99 ± 1.41^b	6.00 ± 0.40^b	5.01 ± 2.45^b	15.00
D (compost)	0.01 ± 0.00^a	4.98 ± 0.87^b	3.02 ± 0.24^b	2.67 ± 2.27^{ab}	8.01

Legend: Data are expressed as means ± standard deviation, different letters in the same columns represent significant difference ($P < 0.05$).

Table 4 The soil erosion – evaluation of variants (2018)

Experiment variants	Date and amount of the erosion (g/m^2)		The scale of erosion (g/m^2)	
	29.05.2018	28.06.2018	**Average**	**Amount**
A (cereal straw)	0.01 ± 0.00^a	0.01 ± 0.00^a	0.01 ± 0.00^a	0.02
B (wood chips)	0.01 ± 0.00^a	0.01 ± 0.00^a	0.01 ± 0.00^a	0.02
C (control)	0.36 ± 0.03^b	1.93 ± 0.19^b	1.15 ± 0.65^b	3.29
D (compost)	0.01 ± 0.00^a	0.01 ± 0.00^a	0.01 ± 0.00^a	0.02

Legend: Data are expressed as means ± standard deviation, different letters in the same columns represent significant difference ($P < 0.05$).

The values given in Table 3 and Tab. 4 prove the positive influence of grain strain, wood chips and compost on reducing of soil degradation in comparison to the control variant without covering material. This condition has been confirmed for all terms in which washout was measured. Prosdocimi et al. (2016) states that straw, already in small doses of 75 g/m^2, has a positive effect on the water conditions in the soil profile and at the same time, it limits the water erosion on sloping land. On average, it reduces water loss by 14%, this effect occurs immediately after application of straw. Jordan et al. (2010) claim that a dense straw cover protects the soil from the direct impact of raindrops and contributes to increased surface roughness which, in turn, increases time to ponding and reduces sheet flux, enhancing infiltration. García Moreno et al. (2013) states, that straw is very efficient at reducing water losses under low frequency - high magnitude rainfall events, and we contribute to increased knowledge with the finding that straw cover can be a key factor in reducing the amount of runoff generated. According to what Lieskovsky and Kenderessy (2014) have been examining, the mulch materials have a positive effect on soil quality as it improves soil organic matter, soil biological activity and infiltration rates.

The results obtained in the wine-growing conditions in the Czech Republic show, that straw, together with other types of cover materials, has a positive effect on the surface of the interlayer in terms of erosion reduction. Moreover, there will be further experiments carried out in the forthcoming period that will be directed to determining the amount of mulch used in relation to economic aspects.

CONCLUSIONS

This experimental evaluation focused on the issue of soil erosion in the interconnection of vineyards in two-year period from 2017 until 2018, in the conditions of the Czech Republic, in the area of small town called Rakvice. The experiment was carried out in four variants using different types of cover. Resulting statistical analyzes of measured data, related to the soil erosion, confirm the positive effect of cover materials in their counter-erosion protection. Out of evaluated variants, minimal washout was measured when using a layer of cereal straw.

The use of cover materials can be considered as a promising way of protecting the soil from erosion and at the same time as a measure for increasing the soil moisture.

ACKNOWLEDGEMENTS
This paper was finalized and supported by the project TH02030467 "Development and verification of machine for in-depth installation of organic stuff to soil in vineyards and orchards (2017-2020)".

REFERENCES

Anderson, K., Norman, D. 2011. Global wine markets, 1961 to 2009: a statistical compendium. Adelaide: University of Adelaide Press.

Arnáez, J. et al. 2007. Factors affecting runoff and erosion under simulated rainfall in Mediterranean vineyards. Soil and Tillage Research [Online], 93(2): 324–334. Available at: https://www.sciencedirect.com/science/article/pii/S0167198706001358. [2018-08-28].

Badalíková, B., Bartlová, J. 2012: Influence of incorporated organic matter on soil and infiltration. In Soil – School. Gödöllö: Szent Istvan University Press, pp. 293–298.

Blavet, D. et al. 2009. Effect of land use and management on the early stages of soil water erosion in French Mediterranean vineyards. Soil and Tillage Research, 106: 124–136.

Cerdà, A. et al. 2015. The use of barley straw residues to avoid high erosion and runoff rates on persimmon plantations in Eastern Spain under low frequency – high magnitude simulated rainfall events. Soil Research, 54 (2): 154–165.

Dvořák, P. 2013. Povrchové mulčování u brambor. Zemědělec, 13: 28.

Galati, A. et al. 2015. Towards more efficient incentives for agri-environment measures in degraded and eroded vineyards. Land Degradation & Development, 26: 557–564.

García-Moreno, J. et al. 2013. Mulch application in fruit orchards increases the persistence of soil water repellency during a 15-years period. Soil Tillage Research, 130: 62–68.

Jandák, J. et al. 2003. Cvičení z půdoznalství. 1 vyd. Brno: Mendelova zemědělská a lesnická univerzita v Brně.

Javůrek, M., Vach, M. 2010. Effect of cover crops in conservation soil tillage systems. Proceedings of Agro the XIth ESA Congress. Montpellier, France, pp. 241–242.

Jordán, A. et al. 2010. Effects of mulching on soil physical properties and runoff under semi-arid conditions in southern Spain. Catena, 81: 77–85.

Lieskovský J., Kenderessy, P. 2014. Modelling the effect of vegetation cover and different tillage. Practices on soil erosion in vineyards: A case study in Vráble (Slovakia) using watem/sedem. Land Degradation & Development, 25: 288–296.

Novara, A. et al. 2015. Effectiveness of carbon isotopic signature for estimating soil erosion and deposition rates in Sicilian vineyards. Soil Tillage Research, 152: 1–7.

Paul, K. I. et al. 2004. Soil temperature under forests: A simple model for predicting soil temperature under a range of forest types. Agricultural and Forest Meteorology, 121(3–4): 167–182.

Prosdocimi, M. et al. 2016. The immediate effectiveness of barley straw mulch in reducing soil erodibility and surface runoff generation in Mediterranean vineyards. Science of The Total Environment [Online], 547: 323–330. Available at: https://www.sciencedirect.com/science/article/pii/S016819230300203X. [2018-08-29].

Sarkar, S., Singh, S. 2007. Interactive effect of tillage depth and mulch on soil temperature, productivity and water use pattern of rainfed barley (Hordeum vulgare L.). Soil and Tillage Research, 92(1–2): 79–86.

The concept of landscaping of municipal waste landfill

Julita Dworak[1], Eugeniusz Koda[1], Magdalena Daria Vaverkova[1,2]
[1]Faculty of Civil and Environmental Engineering
Warsaw University of Life Sciences
Nowoursynowska 159, 02 776 Warsaw
POLAND
[2]Department of Applied and Landscape Ecology
Mendel University in Brno
Zemedelska 1, 613 00 Brno
CZECH REPUBLIC

julita.dworak@gmail.com

Abstract: Municipal solid waste (MSW) landfill Łubna was the last place where non-sorted MSW from Warsaw were directed. The paper presents the evaluation of reclamation works on the MSW landfill of Łubna. The remediation works conducted since 1996 include: installation of bentonite barrier, leachate drainage system, shaping and stabilization berms or mineral and biological cover. The aim of reclamation works in the landfill was to improve the condition of the natural environment. Moreover, the paper presents the concept of landscaping of the MSW landfill Łubna. It is proposed to use the area of approximately 22 ha as a recreation area with thematic zones.

Key Words: landfill, leachate, landscaping, reclamation works

INTRODUCTION

The landfilling is the one of the methods to store the municipal solid waste (Koda et al. 2016). Worldwide on landfills the MSW storage is ca. 95% in total. In 2016 in Poland there were 320 places of waste storage. The area of those landfills is about 1860 ha (GUS 2017). Many of the landfills have been closing because the legal and technical requirements have not been filled. The land degradation due to waste storage concerns degradation of soil, water and vegetation resources

MSW landfill Łubna is located in the north-east part of Poland, near Góra Kalwaria district. Storing of municipal waste at MSW landfill Łubna started in 1978, on the place where environmental standards are not fulfilled. Łubna landfill was the only sanitary landfill where MSW from Warsaw and neighboring district was stored (700–1000 Mg/day). The exploitation permission of the landfill was valid until the end of year 2002. The reclamation works on the landfill have been carried out since 1996 and started by shaping and stabilizing the slopes of the landfill, and applying waste products for berms construction. The construction of the bentonite cut – off wall and system of leachate drainage (1997–1998) was the most important technical part of reclamation works to minimize the negative impact of pollutants into the surrounding groundwater environment (Koda and Paprocki 2000). The vegetation and the mineral cover has been designed since 2012 and guaranteed the stability of the slopes. Moreover, the reclamation works included drilled tens of degassing wells. The objective of the present investigation was to present technical solutions carried out as part of the reclamation of landfills, which were necessary for its further development. An experimental investigation was conducted to explore whether these solutions will be able to effectively protect the environment in the area surrounding of the landfill.

MATERIAL AND METHODS

MSW landfill Łubna is an embankment type structure, covering the area of ca. 22 ha and it is approximately 60 m high. The landfill was closed in 2011. The stability of landfill slopes was assured by filling the berms with waste, what was the first step of reclamation works. High and considerable inclination of landfills slopes was reinforcement by berms filled with cohesive soil and compost (Figure 1). Construction of the berms seems to be the most effective method of stability improvement of old landfills for further remediation works. The berm construction needs the extension of landfill in

the close vicinity. It is important to ensure appropriate slopes inclinations for geotechnical safety reasons (Platis et al. 2017).

Figure 1 Reinforcement scheme of the slopes of Łubna landfill

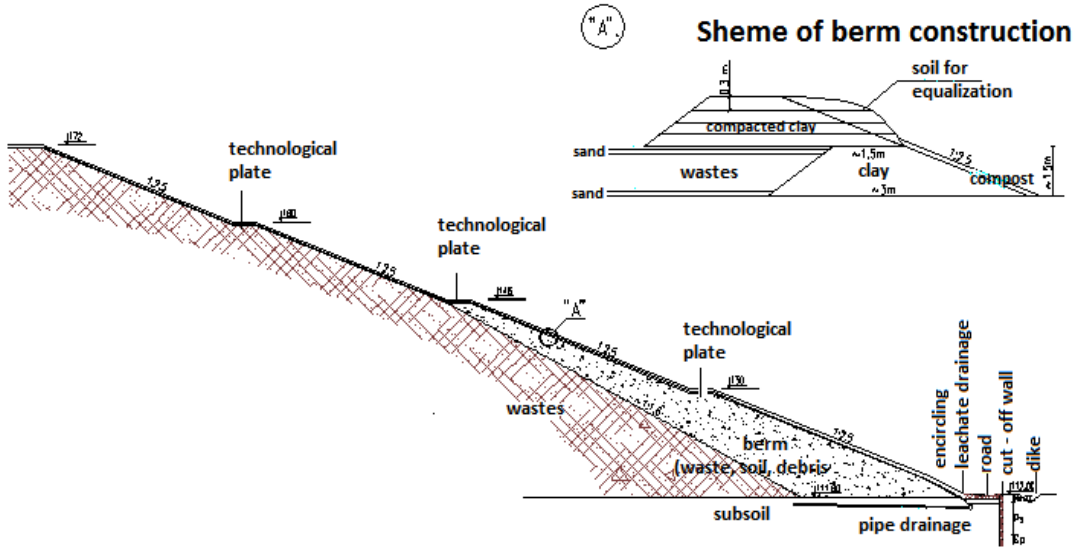

Leachate generated on the landfill has unfavorable impact on environment. The amount of the leachate depends on precipitation, biological and chemical activities of landfill, age of waste or hydrogeological condition of the area (Adamcová et al. 2017). The migration of the pollutants depends on hydro-geological structure. MSW landfill Łubna is located on easy penetrable layer by pollutants. Permeable sands layer is present on 2–4 m depth. Below practically impermeable layers of boulder clays are situated, and occurs also on other impermeable clay layers.

One of the engineering reclamation solutions introduced on the MSW landfill Łubna was the groundwater protection by bentonite barrier of 0,6 m thickness and peripheral drainage for leachate collection. A bentonite cut – off wall was constructed to protect the first aquifer against the transport of pollutants. Because of hydro-geological conditions the barrier wall was constructed on 5.5–17 m depth. The permeability coefficient for the barrier is below 10^{-9} m/s (Solidur 274S). During the reclamation works on the landfill body the drilled tens of wells were performed, and used as a biogas source. The scheme of the old landfill before and after remedial works is presented in Figure 2.

Figure 2 The old landfills schemes before and after remedial works (Koda and Paprocki 2000)

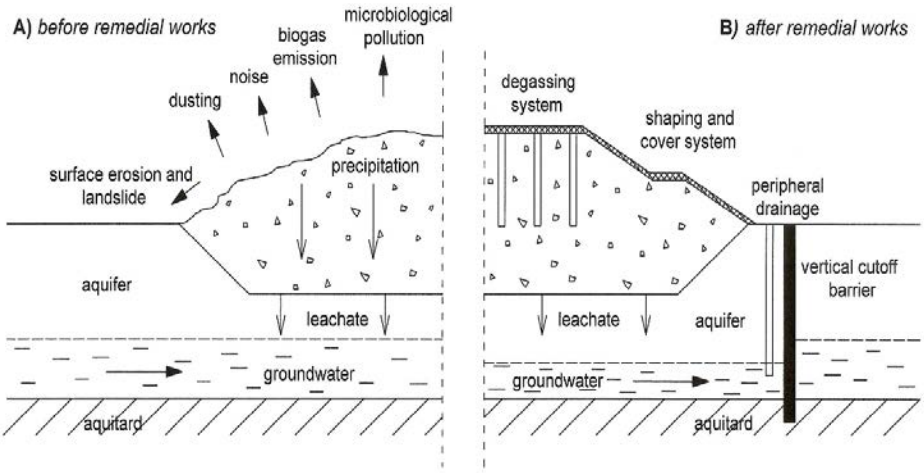

At the beginning of waste storage, the MSW landfill Łubna did not have any drainage system. The leachate was penetrating the permeable layers and polluting the first layer of natural groundwater. The peripherial pipe drainage was designed around perimeter. At the same time to simplify the collection of leachate "finger" pipe drainage has been designed (Koda and Paprocki 2000). Constructed in 1998 the

bentonite cut–off wall mainly focused to prevent the first groundwater layer (Figure 3). Significant improvement of soil-water environment is visible in analysis of water quality results. The development plan of reclamation works solution is presented in Figure 4.

Figure 3 Scheme of remediation solutions around Lubna landfill (Koda and Paprocki 2000)

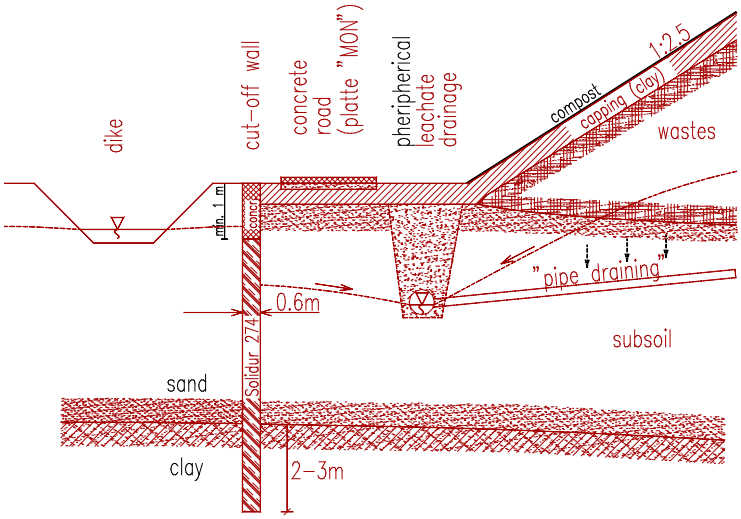

Figure 4 Development of reclamation plan and local water monitoring system of Łubna landfill (Koda and Paprocki 2000)

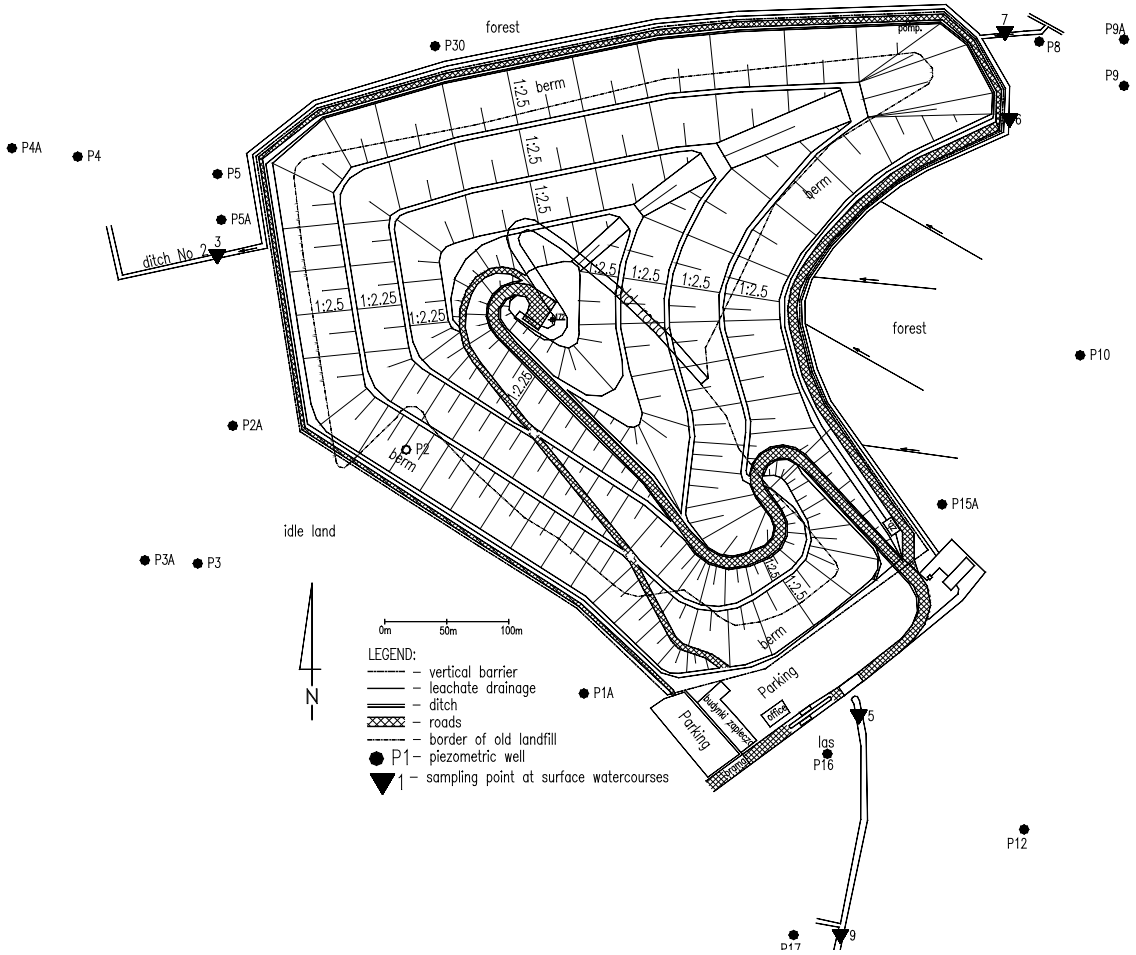

The restoration of degraded area is essential to ensure safety in further use and limit negative impact on the environmental (Chen et al. 2017). The mineral system for covering the slopes and shaping the body waste, allows moisture and oxygen penetration thought the waste necessary to oxygen fermentation. The permeability coefficient for the mineral cover is lower than 10^{-9} m/s. The vegetation cover of landfill slopes was designed by using appropriate plant species, e.g. trees, shrubs or perennials (Koda et al. 2013, Vaverkova et al. 2018). The landfill area restoration was based on natural process. Changes on degraded area including biological cover, depend on weather season, natural flow of organic matter and energy, temporary condition of ecosystem (Keesstra et al. 2018) and landfill slope inclination (Figure 5). The compost layer produced by mixed waste was used as subsoil for planting.

Figure 5 Concept of the biological reclamation of landfill slope.

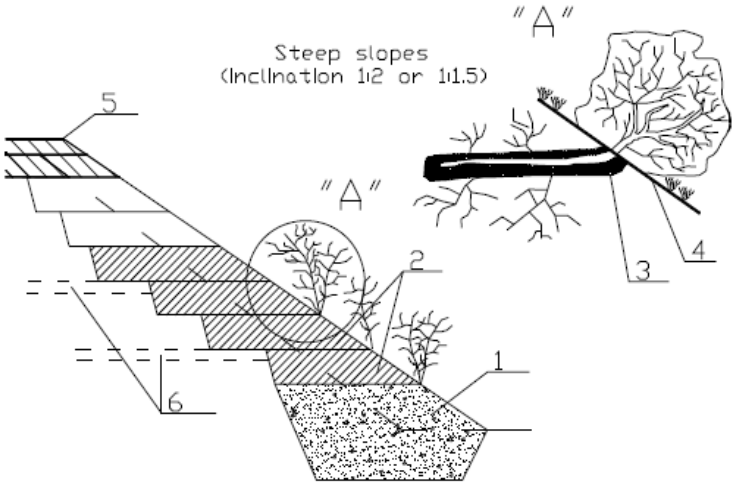

Legend: 1 – petrifiedash, 2 – condensed ashes, 3 – bundles of fascine introduced in the layer of dewatered sewage sludge, 4 –hydroseeding layer, 5 – protective layers seeded by the mixtures of grasses, 6 – adjusted sanitary layers

RESULTS AND DISCUSSION

Figure 6 shows the landfill before the realization and technical reclamation in 1993 and 2002 (1, 2) subsequently the condition of realized landfill in 2008 (3, 4).

Figure 6 Northern slopes of Łubna landfill in 1993 (1), 2002 (2) and 2008 (3, 4)

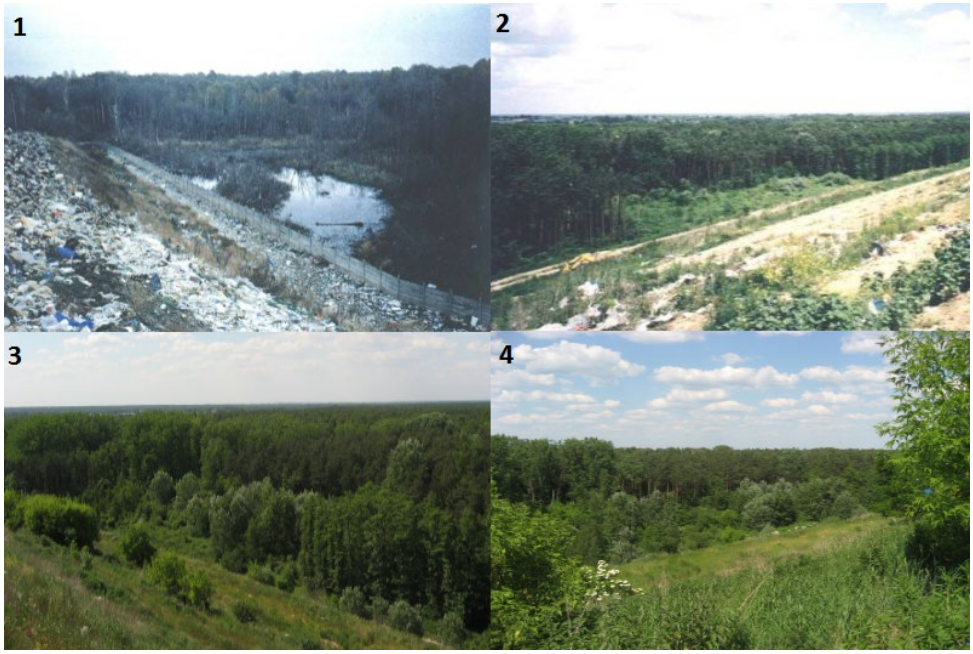

Directions of the reclamation works lead the place of waste storage to improved environmental conditions. Taking into account the local conditions: local law and strategic documents of the commune, it is proposed to use landfill as recreation area (Figure 7).

It is proposed to create recreation area such as:

- Family rest zone – covered all landfill. The zone is includes bicycle and walking paths located around and on the slopes of the landfill, connected on the top of berm.
- Educational zone – running along main road on the top of the berm. Zone for education regarding the waste management and how to use the renewable energy sources.
- Renewable energy sources zone – created on southern slope. The energy produced by photovoltaic panels will be used as energy for the street lights.
- Aircraft modeling zone – created on western and north-west part of the landfill.

Figure 7 The concept of landscaping of Łubna municipal waste landfill

CONCLUSION

The right direction of the remedial works carried out on the MSW landfill Łubna is improved by environmental changes observed over the years. Closing of the cut – off bentonite wall and drainage system for leachate, were the main engineering activities. Moreover, the remedial works ensured the stability of the slopes, such solutions as new technological roads and active degassing system was also performed at the site. During the remediation works the mineral cover and biological reclamation have been accomplished. Actually the landfill is covered by trees, shrubs and perennials. The slopes of the landfill are reinforced and it can be stated that they are safe. MSW landfill Łubna covers the area of

approximately 22 ha. It is proposed to use the area of landfill as a recreational park and as a part of tourist trials in Góra Kalwaria district.

REFERENCES

Adamcová, D. et al. 2017. Environmental assessment of the effects of a municipal landfill on the content and distribution of heavy metals in Tanacetum vulgare L. Chemosphere, 185:1011–1018.

Chen, X.W. et al. 2016. Ecological performance of the restored south east new territories (SENT) landfill in Hong Kong (2000–2012). Land Degradation & Development, 27: 1664–1676.

GUS (Główny Urząd Statystyczny), 2017. Gospodarka odpadami. In Informacje i opracowanie statystyczne GUS 2017 r. Warszawa: Główny Urząd Statystyczny, pp. 320–343.

Keesstra, S. et al. 2018. The superior effects of nature based solution in land management for enhancing ecosystem services. Science on the Total Environment, 610–611: 997–1009.

Koda, E., Paprocki, P. 2000. Durability of leachate drainage systems of old sanitary landfills. In Proceeding of the 3rd International Conference on Filters and Drainages in Geotechnical and Environmental Engineering. Warsaw, 5–7 June, pp. 215–222.

Koda E. et al. 2013. Potential of plants application in the initial stage of landfill reclamation process. Polish Journal of Environmental Studies, 22(6): 1731–1739.

Koda, E. et al. 2016. Ammonium concentration and migration in groundwater in the vicinity of waste management site located in the neighborhood of protected areas of Warsaw, Poland. Sustainability, 8(12): 1253.

Platis, A. et al. 2017. Reinforced Earth Used in Uncontrolled Landfill Final Closures-The Case of Syros Landfill. International Journal of Geoengineering Case Histories, 4(1): 1–13.

Vaverková, M.D. et al. 2018. The use of vegetation as a natural strategy for landfill restoration. Land Degradation & Development [Online]. 1–7. Available at: https://doi.org/10.1002/ldr.3119. [2018-09-11].

Wysokiński, L. et al. 2003. Badania gruntów do budowy przesłon izolacyjnych na składowiska odpadów. Warszawa:Instytut Techniki Budowlanej. Dział Wydawniczy.

Problems of very small municipalities in the South Moravian Region perceived by their mayors

Andrea Leskova, Antonin Vaishar
Department of Applied and Landscape Ecology
Mendel University in Brno
Zemedelska 1, 613 00 Brno
CZECH REPUBLIC

yleskova@mendelu.cz

Abstract: The Czech Republic is characterized by high fragmentation of settlements and high number of very small municipalities. The high fragmentation of municipalities in the Czech Republic has long been discussed. The debaters indicate a number of problems arising from management and sustainability of a very small municipality as well as a lack of willingness to merge the municipalities. This research deals with the problems of very small municipalities of up to 200 inhabitants in the South Moravian Region perceived by their own mayors. The mayors of selected very small municipalities are contacted and in a semi-structured interview they are asked about the problems they register in the municipality. The most interviewed mayors perceive as a problem a high unnecessary increasing administration. Problems associated with municipal management generally occur in interviews very often. Other common problems are social problems such as population decline or moving socially weak and troubled people, which occur mainly in districts distant from Brno (Hodonín and Znojmo districts).

Key Words: small municipalities, unnecessary increasing administration, municipal management, social problems, population decline

INTRODUCTION

The Czech Republic with its relatively high number of municipalities (6 258 municipalities, 2017) is characterized by a high fragmentation of the municipalities and has a different settlement structure compared to other European countries. Swianiewicz (2002) indicates that the Czech Republic has 80% of municipalities with less than 1000 inhabitants, France 77%, Slovakia 68%, Spain 61%, Hungary 54%, Latvia 32%, Italy 24%, whereas 16 countries of the EU do not have such municipalities. An optimal municipal size and efficiency is the subject of several researchers (Martins 1995, Holzer et al. 2009, Zafra-Gómez and Pérez Muñiz 2010). An average population per municipality in the Czech Republic is about 1 700 inhabitants. A very small municipality in this work is defined as a municipality with less than 200 permanent residents. There are almost 1 500 municipalities (24%) of this size category in the Czech Republic (CSO 2017).

Kadeřábková and Jetmar (2010) state that the small municipalities have limited ability to ensure their further development (or to maintain their attractiveness for their inhabitants) under the current rules for the distribution of public funds. Hampl and Müller (1998) see the high fragmentation of municipalities in the Czech Republic as unsustainable, they see problem mainly in the sphere of municipal management and excessive fragmentation of financial resources. However, despite the rational arguments against fragmentation, they do not expect changes in the functioning of the municipalities in that time, they assume resistance of the municipalities themselves, even those well-functioning and wealthy. Further they add that radical reforms of the municipal systems in developed European countries have been carried out in a period of prosperity, in which they believe that the general public is more open for administrative changes.

The Ministry of Agriculture of the Czech Republic (2015) reports that for the long-term problems of small municipalities with up to 500 inhabitants there is a lack of civic amenities (school, library, post office, medical ordination, grocery and other services), almost 20% of the population of municipalities is not connected to sewerage and 10% of them are not supplied by public water supply, a lot of municipalities do not have a sewage treatment plant yet. Other problems include poor transport

infrastructure availability, lack of high-speed internet services in certain areas, or lack of job opportunities (80% of inhabitants of municipalities commute) and the threat of restrictions on business in municipalities. Žlábková (2013) also states that any development activity of small municipalities is dependent on subsidies and often the administration associated with the project in the grant application is an invincible problem for very small municipalities.

The importance of the problem of the small municipalities is also emphasized by Hampl and Müller (1998), who point to the fact that although their share in the population and thus in the economy of the state is insignificant, their share in the area of the administered territory is already quite significant. Even though only 2% of all Czechs live in the very small municipalities, they take care of 10% of the territory of the Czech Republic. These are areas that represent the natural potential of the state, therefore they emphasize the need to ensure good management of this potential.

This research focuses on these very small municipalities with less than 200 inhabitants and aims to examine their problems in terms of how their own mayors see them. The geographic focus of the research is the South Moravian Region, where very small municipalities, appear to have the highest negative demographic development according to statistical indicators such as population growth, ageing index and unemployment rate. There are a total of 107 very small municipalities with less than 200 inhabitants in this region, which are predominantly located in the districts of Blansko, Brno-Country and Znojmo (CSO 2017).

MATERIAL AND METHODS

In the preparatory phase of research, statistical data of these very small municipalities were evaluated, both within the whole Czech Republic and within the South Moravian Region. Statistical indicators were, in particular, population growth, ageing index and unemployment rate. These very small municipalities are located in 5 districts: Blansko (31 municipalities), Brno-Country (29 municipalities), Hodonín (4 municipalities), Vyškov (5 municipalities) and Znojmo (38 municipalities). Map of these municipalities was created (Figure 1). From these municipalities, a sample of municipalities was selected for subsequent semi-structured interviews with the mayors of these municipalities. In the districts of Hodonín and Vyškov, all municipalities were selected, due to their small number. In the districts of Blansko, Brno-Country and Znojmo, in each of them there were selected municipalities of three size categories: 1–70 inhabitants, 71–140 inhabitants, 140–200 inhabitants, so that from each size category one municipality was selected in which the statistical data appears to be “prosperous” (high population growth, low ageing index, low unemployment rate) and one municipality that appears to be a “lagging behind” (high population decline, high ageing index, high unemployment rate).

These communes were subsequently contacted by mail. There are 9% of mayors of the municipalities responded to the mail. Those mayors who did not respond to the mail were then contacted by phone. 70% of the respondents responded positively to the telephone offer of interview. Then, the meeting with the mayors followed and a semi-structured interview about the problems that they record as the mayors. The conversations were recorded on the dictaphone, in case of a disagreement with the recording, the responses were written. Six mayors were visited directly in the municipality during office hours at a municipal office without a pre-arranged meeting. In the case of a dissatisfaction with the mayor's interview or impossibility of contacting the mayor (the telephone is not welcome – 10%, he is not present at the municipal office during office hours), another representative municipality with similar statistical data was subsequently selected in the districts of Blansko, Brno-Country and Znojmo. So far, 17 municipalities have been visited, another 4 mayors answered about the problems by telephone and one responded about the problems in mail. The project is still ongoing.

Research is focused on the qualitative detection of the problems of the very small municipalities, but the answers of the mayors have often been aggregated, so a chart of the most frequent answers was created based on the geographical location (district), where the very small municipality is situated.

Figure 1 Very small municipalities with less than 200 inhabitants in the South Moravian Region as of 1st January 2016. Source: © ArcČR ARCDATA PRAHA, ZÚ, ČSÚ, 2016, own processing

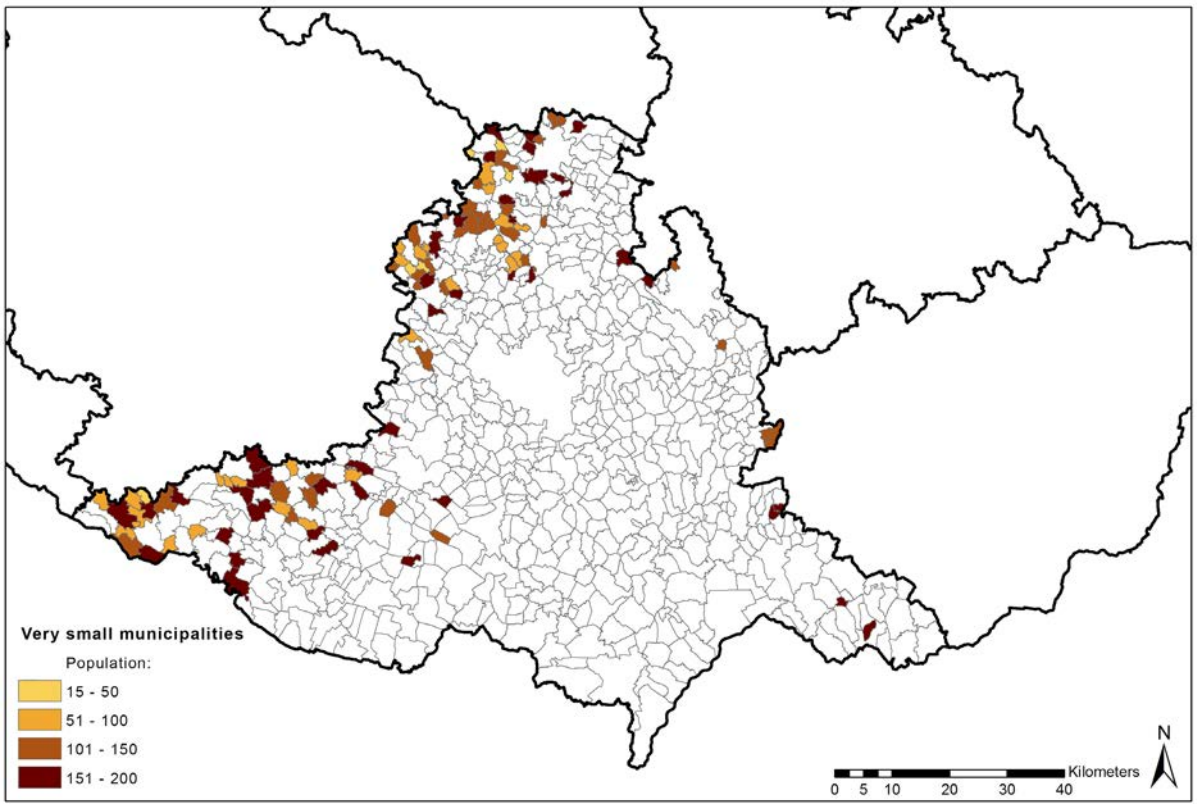

RESULTS AND DISCUSSION

The most common problem perceived by the mayors of the very small municipalities is unnecessary increasing administration, in which 10 out of 22 interviewed mayors agreed (see Figure 2). This problem occurs almost in all districts. In the district of Znojmo, none of the mayor of very small municipality mentioned increasing administration as a problem. When they were asked about this, some said they were already accustomed to increasing administration habits, and did not see this as a potential improvement. However, this problem is not likely to be seen only by the mayors of the very small municipalities, but it is quite possible that even the mayors of larger municipalities can perceive this as a problem. It is also important to point out that mayors who see the increasing administration as a problem agree (without asking the interviewer) that this administration is often unnecessary, irrational or illogical. The number of questionnaires that the mayors has been approached in recent years is, according to them, often irrelevant, and does not have any other practical significance, as well as the unnecessary administration often waste precious time of mayors of these very small municipalities who perform their duties outside their employment.

The most recurring problems were imminent repair of road communication as an economic burden on the municipality's budget, inability to get capable people into the municipality leadership as a problem in the very small municipalities of various districts of the South Moravian Region and permanent decrease of the population perceived as a problem mainly by mayors of the very small municipalities in the district of Hodonín. The problem of recurring elections to municipal councils, especially in small municipalities, is already dealt with by Hampl and Müller (1998).

These individual problems, described by the mayors of the very small municipalities, are then grouped into five main domains: operational, municipal management, natural, social and building problems (see Figure 3). The most represented are the management problems, mainly due to the frequency of the answer of unnecessary increasing administration as a problem. Another major problem domain is the social area of the very small municipalities, the mayors are facing problems such as population decline, socially weak and problematic people, disputes between residents, aging,

few children under 15, unemployment, non-adaptive immigrants or people who are not engaged in cultural events.

Figure 2 Problems of very small municipalities in South Moravian Region perceived by their mayors. Source: own research

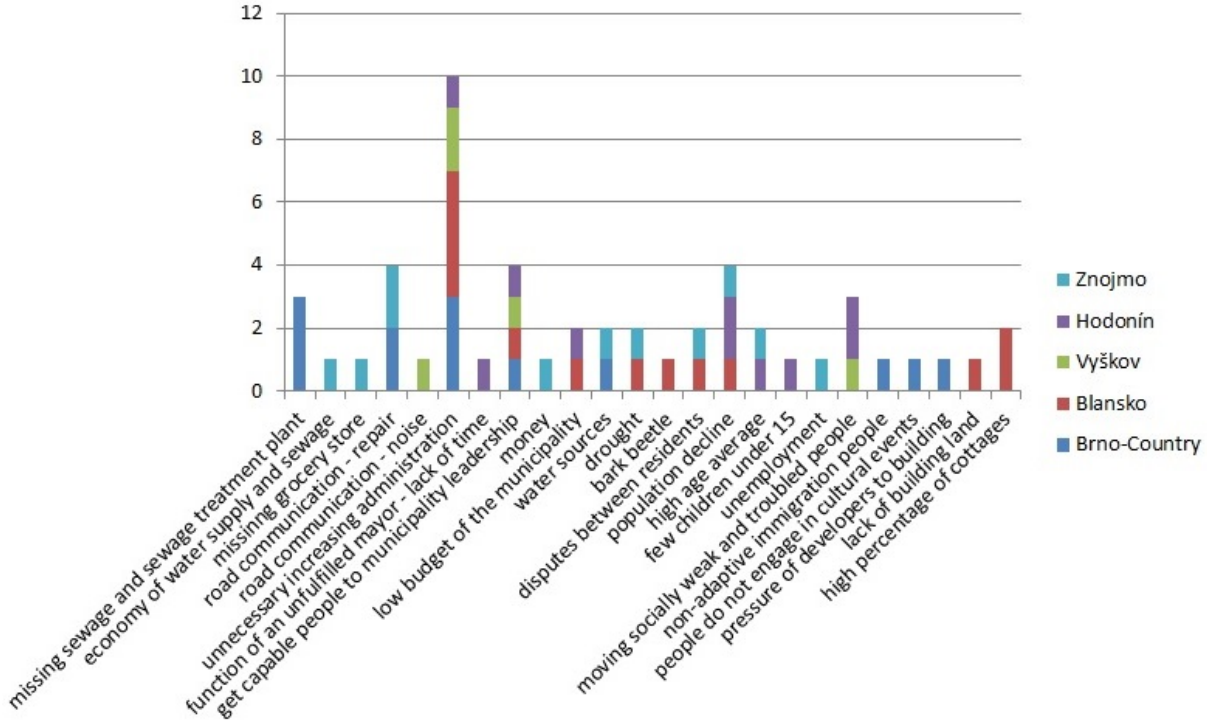

Another major problem domains are operational problems such as missing sewage and sewage treatment plant, economy of water supply and sewage, missing grocery store or problems with the transport - the duty of maintenance of roads or problems from noise from frequented roads.

Figure 3 Domains of problems of very small municipalities in South Moravian Region perceived by their mayors. Source: own research

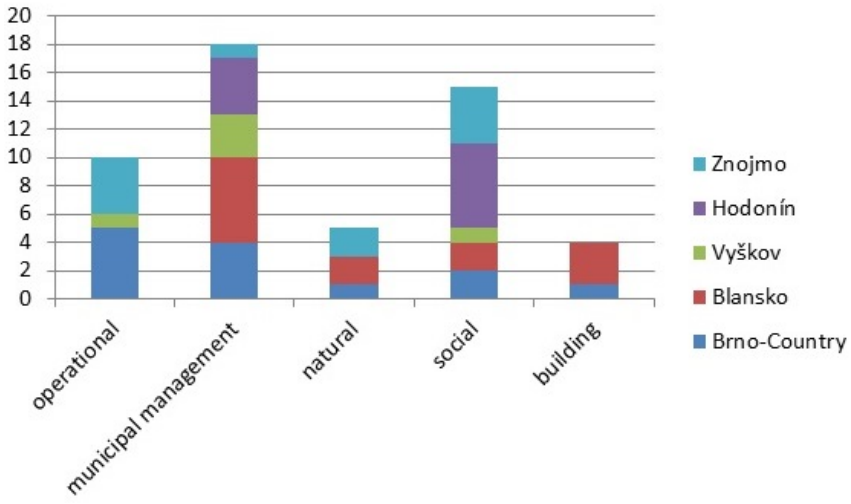

From the geographical point of view, it is possible to notice the differences in the problems seen by the mayors of the very small municipalities between the districts in the vicinity of Brno (districts Blansko and Brno-Country) and districts distant from Brno (districts Hodonín and Znojmo). While building problems, such as the pressure of developers to building or lack of building land, are rather the domains of the suburbanization areas of Brno, while social problems such as population decline, socially weak and troubled people, disputes between residents, high age average, few children under 15, unemployment, are rather the domains of areas more distant from the city of Brno, although the

social problems associated with the problematic inclusion of the population of suburban areas such as non-adaptive immigrants and people not involved in cultural events also occur in areas in the vicinity of Brno. The results confirm the overall persistence of peripheral areas (Musil and Müller 2008, Novotná 2005) and the problem of suburbanization, as perceived by more mayors of municipalities (Vaishar 2013).

Although in most of these very small municipalities there is almost no civic amenities (school, library, post office, medical practice, grocery store), only one mayor perceives missing of the grocery store as a problem. Similarly, although in many of the visited municipalities there is no sewage and sewage treatment plant, only 3 mayors see missing sewage as a problem. However, problems with water supply, when they occur, are often much more serious than missing sewage.

Although Žlábková (2013) states that the administration linked to the project in the grant application is an invincible problem for the very small municipalities, none of the interviewed mayors identified this as a problem.

CONCLUSION

The high fragmentation of the municipalities in the Czech Republic has been discussed since its inception in 1990. Experts indicate a number of problems arising from management and sustainability of a very small municipality as well as a lack of willingness to merge municipalities (Hampl and Müller 1998, Matějová et al. 2016, Schnaubert 2016). The aim of this research was to find out what problems of the very small municipalities in the South Moravian Region are perceived by their own mayors. The most interviewed mayors perceive as a problem a high unnecessary increasing administration. Problems associated with municipal management generally occur in interviews very often. Other common problems are social problems such as population decline or moving socially weak and troubled people, which occur mainly in districts distant from Brno (Hodonín and Znojmo districts), which confirms the overall persistent problem of peripheral areas.

It would be interesting to select problems perceived by mayors, which depend on the size of the settlement from those which are connected with the independence of the small municipality. If the village is not independent, the most frequent problems (an overwhelming administration, difficult municipal management, limited number of people able to work in the municipal council) will not exist for it. Problems with missing social infrastructure (shops, schools etc.), or social problems depend on the settlement size regardless the administrative dependency or independency and they would exist in any case. On the other side, problems of technical infrastructure like maintenance of roads or sewage systems would be solved easier within the larger administrative unit.

However, although it may seem that the disadvantages of independence predominate, the mayors of the very small municipalities are not willing to merge municipalities. In the overwhelming cases, they like to make their own decisions about what will happen in the village and leave no decision to anyone in another municipality. The advantage of the independence of the very small municipalities is seen also in the fact that these municipalities create quasi small social group, where the people are familiar with each other and communicate directly. Often the representatives of most families of the very small municipality regularly meet at a municipal council meeting and are arguing about the situation in the village, so the own council is an element of social sustainability of the very small municipality. Also bigger social control can play its role there.

ACKNOWLEDGEMENTS

The research was financially supported by grant no. AF-IGA-IP-2018/010 „Problems and sustainability of very small villages in South Moravian Region“.

REFERENCES

Czech Statistical Office (CSO). 2017. Veřejná databáze. Počet a věkové složení obyvatel k 31. 12. podle obcí [Online]. Available at: https://vdb.czso.cz/vdbvo2/faces/cs/index.jsf?page=vystup-objekt-parametry&pvo=DEM03&z=T&f=TABULKA&sp=A&skupId=526&katalog=30845&pvo=DEM03&pvokc=101&pvoch=40762&c=v3~2__RP2016MP12DP31. [2018-08-08].

Hampl, M., Müller, J. 1998. Jsou obce v České republice příliš malé? Geografie – Sborník České geografické společnosti, 103(1): 1–12.

Holzer, M. et al. 2009. Literarure review and analysis related to optimal municipal size and efficiency [research report]. Camden: Ruttgers University.

Kadeřábková, J., Jetmar, M. 2010. Selected issues of the development of small municipalities in the Czech Republic, financing of municipalities. European Countryside, 2(2): 102–117.

Martins, M.R. 1995. Size of Municipalities, Efficiency, and Citizen Participation: A Cross-European Perspective. Environment and Planning C: Politics and Space, 13(4), 441–458.

Matějová, L. et al. 2016. "Small is beautiful". Pros and Cons of territorial fragmentation on the example of the Czech Republic. In Comparative Studies and Regionally Focussed Cases Examining Local Governments. Hershey, PA: IGI Global, pp. 113–134.

Ministry of Agriculture of the Czech Republic. 2015. Program rozvoje venkova ČR na období 2014 – 2020 [Online]. Available at: http://rskuk.cz/files/PRV/PRV_1._modifikace_schvalena_verze_EK.pdf. [2018-08-08].

Musil, J., Müller, J. 2008. Vnitřní periférie v České republice jako mechanismus sociální exkluze. Czech Sociological Review, 44(2): 321–348.

Novotná, M. 2005. Problémy periferních oblastí. 1st ed., Praha: Univerzita Karlova v Praze.

Schnaubert, J. 2016. Možnosti řešení velkého počtu malých obcí v ČR. Diplomová práce, Masarykova univerzita.

Swianiewicz, P. 2002. Consolidation or Fragmentation? The Size of Local Governments in Central and Eastern Europe. 1st ed., Budapest: Open Society Institute.

Vaishar, A. 2013. Změny krajiny na okraji velkých měst. Je suburbanizovaný venkov ještě venkovem? 1st ed., Brno: Mendelova univerzita v Brně.

Zafra-Gómez, J.L., Pérez Muñiz, M.A. 2010. Overcoming Cost-Inefficiencies within Small Municipalities: Improve Financial Condition or Reduce the Quality of Public Services? Environment and Planning C: Politics and Space, 28(4), 609–629.

Žlábková, J. 2013. Komparace velikostní struktury obcí v Jihočeském kraji a Dolním Bavorsku. In INPROFORUM 2013. Sborník z mezinárodní vědecké konference „Zdroje a limity ekonomického růstu a předpoklady vývoje české ekonomiky". České Budějovice, Czech Republic, 7 and 8 November, České Budějovice: Jihočeská univerzita v Českých Budějovicích, pp. 391–396.

Determination of phytotoxicity of compost from biodegradable waste from canteen

Alzbeta Maxianova, Dana Adamcova, Magdalena Daria Vaverkova
Department of Applied and Landscape Ecology
Mendel University in Brno
Zemedelska 1, 613 00 Brno
CZECH REPUBLIC

xmaxiano@mendelu.cz

Abstract: This research was aimed at determining the compost phytotoxicity that was based on waste from catering, restaurants and similar facilities. Research has shown whether gastro waste compost can be used to enrich the soil as an organic fertilizer. For composting were selected raw materials like rice, potatoes and vegetables, which were composted in an electric composter for 4 weeks. After this time the compost was tested for the Phytotoxkit test. The compost was tested at various concentrations of 25%, 50% and 100% and mixed with the OECD reference soil. For research were used seeds *Sinapis Alba* for their rapid germination and growth of the roots. Results from phytotoxicity test demonstrated compost is toxic for plant because no seed germinated.

Key Words: phytotoxicity, gastro waste, composting, phytotoxkit, electric composter

INTRODUCTION

Every year is wasted about 88 million tonnes of food in the European Union (Scherhaufer et al. 2018). Gastro waste is defined as biodegradable waste generated in restaurants, canteens, food and other similar establishments. It is food waste from production, manufacturing and also food products that do not comply with quality or unconsumed residues of eatables and food (www.fcc-group.eu). In the Czech Republic, these wastes are marked in the waste catalogue in regulation no. 93/2016 collection as biodegradable kitchen and canteen waste with the number 20 01 08 (Hřebíček et al. 2011). However, is easy defining this waste its removal is not. There are several methods of disposal of food in European countries. It is dependent on whether food is derived from or contains ingredients of animal origin, but if it is safe, unsold food products can be donated (Moult et al. 2018). In some regions, these products are also used to feed livestock. In the Czech Republic, the feeding of livestock by animal by-products was prohibited, one of the reasons being protection against the spread of BSE- Bovine Spongiform Encephalopathy and other transmitted diseases (Hřebíček et al. 2011).

One of the methods of food disposal is aerobic composting and anaerobic digestion, co-generation or landfilling (Scherhaufer et al. 2018). But at a landfill which contains high food waste has the characteristics of large leachate production rate and fast gas generation (Zhan et al. 2017). Landfill gas represents a potential health risk mainly because of gas emissions such as methane, carbon dioxide, water vapor and non-methane organic compounds. Also odor nuisances can occur. Long exposure can generate bad reactions for humans (Wu et al. 2018). But for anaerobic digestion, food waste has a great potential because of methane. Anaerobic digestion is a pollution free technology for corventing organic mater into bioenergy (Ma et al. 2018). The composting is one of the economic and environmental biological process degradation of wastes. It is aerobic thermophilic microbial disposal when organic waste is converted into humic substances (Zhao et al. 2017).

The advantages of composting are soil quality improvement, which gives is source for microorganisms and soil animals. Compost is important source that affects physical, chemical and biological attributes of soil (Plíva et al. 2016). Composting can be carried out in several types – home composting, community composting, municipal composting and industrial composting in boxes or reactors. For every type of composters, it is important to ensure the correct conditions for microorganisms like supply of raw materials, ensuring adequate air access and moisture management (Hřebíček et al. 2011).

MATERIAL AND METHODS

Characteristics of composting

This research made use of ingredients from the local canteen of the Mendel University in Brno. For the composting, ingredients (Figure 1) such as rice, potatoes and vegetable salads of various processing were used. These ingredients were supplied in a 2 : 2 : 1 ratio of rice (2 kg), potatoes (2 kg), vegetables (1 kg). The total weight of the ingredients was 5 kg. After weighing the right amount, the ingredients were homogenized and blended in the composter where they were composted for 4 weeks on the recommendation of the manufacturer of the electric composting plant. On a daily basis, composting was humidified with water to prevent compost drying as it could result in slowing down or stopping the composting process (www.menejodpadu.shop). On the contrary, in excess moisture, steam and moisture were drained away by pipeline placed behind the sink.

In our laboratory, we used for gastro waste an electric composter GreenGood 02 (GG02), which is a specialized for composting leftovers and waste from the kitchen. According to the user manual the compost is adapted to waste composting such as cooked foods, expired food, fruits and vegetables as well as fish bones, pasta, rice, meat and meat products, egg shells, compostable bioplastics and bio-packagings. The GG02 compost operates on the principle of biodegradation with the Acidulo™ microorganisms. The Acidulo™ microorganisms belong to the Firmicute strains, which, thanks to the high temperature of up to 70 °C, salinity and acidity of the environment are able to multiply rapidly and thus biowaste within 24 hours (www.menejodpadu.shop).

After 4 weeks, the gastro waste composting process was ended. The necessary amount was taken for the phytotoxicity test and the remainder was placed in an open vessel where the compost maturing process was still under way.

Figure 1 Gastro waste and final compost (Maxianová 2018)

Phytotoxicity test

The phytotoxkit microbiotest by MicroBioTests Inc. was used for the phytotoxicity test. The Phytotoxic microbiotest measures the decline of seed germination and long root after 3 days, seeds which indicate the presence of toxicant or contaminations in soil. For this test, several seeds like *Sorghum saccharatum*, *Lepidium sativum* and *Sinapis alba* were used. All of them have been selected for their rapid germination and growth of the roots. We were using seeds of *Sinapis alba*. OECD reference, a special reference soil for the Phytotoxkit microbiotest, was used for control. For Phytotoxic we needed incubator or temperature controlled room at 25 °C (MicroBiotest Inc. 2015). The test set also contained test plates made of transparent polyvinyl chloride. Each test plate also had a top part that prevented the material from spilling. Compost samples were at various concentrations where the samples were mixed with OECD soil in a percentage of 25%, 50%, 100% and each sample had 3 replications.

We took the compost and weighed the appropriate amount when 100% of the concentrations were 90 cm^3 and we found out how many grams of compost it is. After the calculation, we found out how many grams of sample is needed at 50% and 25% concentration. After we drove the appropriate amount of a given concentration, we added the appropriate amount of water to the sample. Up to 90 cm^3, i.e. the full capacity, we can provide with 35 ml of distilled water. The quantity of the weighed sample was poured into the test plate where it was then moistened with the appropriate amount of

distilled water. Subsequently, using the spatula, we mixed the sample to moisten it evenly. In this way prepared sample, we have attached a filter paper that has been soaked in water and we put the plant seeds on top of it. We took approximately 10 seeds and applied uniformly on the filter paper at the same height of about 1 cm from the edge of the filter paper and about 1 cm apart. Upon completion, we closed the test table and placed it in a vertical position in the direction of growth. The prepared test table was placed in an incubator with a set temperature of 25 °C for 3 days. The test plates must be kept at constant temperature and in the dark. After 3 days we selected and documented the test plates. After opening the test plate, we measured the root length and recorded in the Result Sheet and after this we calculated the seed germination.

The seed germination calculation is based on the formula:

(A-B)/A x 100 = %

A is for reference soil and B is for test soil. Based on the formula, we have received results. Positive values indicate inhibition over OECD soil. If they inhibit it means that a soil or substrate sample suppresses the growth and germination of the plants, moreover, may contain some component that is toxic. On the contrary, negative values show the stimulation when the substrate encourages plant seed growth.

RESULTS AND DISCUSSION

On the basis of the Plíva criteria (2016), it was clear that gastro waste compost did not show signs of mature, stable compost. The finished compost should have a pleasant smell of forest land and in no case should stink. The compost from the gastro-wasting smelled souric and showed a slightly light brown colour than the black colour. In addition, compost also contained non-decomposable particles. That it is an immature compost was also showed on results from Phytotoxicity. Figure 2 clearly shows that the compost samples strongly inhibited the growth of roots by up to 100% compared to OECD soil, since the average length of seed roots was 0 mm, meaning that none of the sample concentrations (25%, 50% and 100%) showed possibility of roots.

Figure 2 The phytotoxkit results OECD soil and samples 25%, 50%, 100% after 3 days (Maxianová 2018)

One of the solutions why the compost results showed inhibited growth is that the pH value of the sample was 4 pH, with an optimal pH value of compost being between 6.5 and 8.5, close to neutral (Plíva et al. 2016). Jiang et al. (2011) claim that the pH decrease is caused by organic acids produced in the early composting phase.

Since the composting is dependent on microorganisms, it is necessary to create a favourable environment. One option is to add additives that can alter the physical and chemical properties of compost such as moisture, airiness, nutrition, and pH regulation (Sanchez-Monedero et al. 2018). The most commonly used additives include sawdust, sugar cane and wood residues (Chang et al. 2010), but good additives are also cartridges and newspapers due to their rapid degradability (Eftoda et al. 2004).

A good solution for using this compost would be to let it mature longer or use additives.

CONCLUSION

Gastro waste is a waste from canteens, restaurants, but also from stores where food is thrown into a dustbin after the expiration date. This waste is defined in the law of the Czech Republic, but its removal is more complicated. This is a large amount of organic material that cannot be used to feed livestock nor can be stored in the landfill to a greater extent. A suitable but costly alternative is combustion or co-incineration. A cheaper alternative is composting, which is currently rarely used. Unfortunately, this alternative is not easy because gastro waste forms a variety of components which release organic acids that degrade the compost. The finished compost cannot be used directly on the soil. According to the results of the research, compost can not be used like organic fertilizer without improving its quality.

ACKNOWLEDGEMENTS

This research was financially supported by grant IGA no. TP 3/2018.

REFERENCES

Chang, J.I. et al. 2010. Effects of bulking agents on food waste composting. Bioresource Technology, 101(15): 5917–5924.

Eftoda, G. et al. 2004. Determining the critical bulking agent requirement for municipal biosolids composting. Compost Science & Utilization, 12(3): 208–218.

FCC Environment. ©2009-2018. Co je gastroodpad. [Online]. Available at: https://www.fcc-group.eu/cs/ceska-republika/sluzby/svoz-gastroodpadu/co-je-to-gastroodpad.html. [2018-08-13].

Hřebíček, J. 2011. Projektování nakládání a s bioodpady v obcích. 2nd ed., Praha: Nakladatelství MŽP.

Jiang, T. et al. 2011. Effect of C/N ratio, aeration rate and moisture content on ammonia and greenhouse gas emission during the composting. Journal of Environmental Sciences, 23(10): 1754–1760.

Ma, C. et al. 2018. Towards utmost bioenergy conversion efficiency of food waste: Pretreatment, co-digestion, and reactor type. Renewable and Sustainable Energy Reviews, 90: 700–709.

Menej odpadu. ©2018. Elektrický kompostér GG02 [Online]. Available at: https://www.menejodpadu.shop/elektricke-kompostery/elektricky-komposter-gg02/. [2018-08-10].

MicroBiotest Inc. ©2015. Phytotestkit complete test [Online]. Available at: http://www.microbiotests.be/SOPs/Phytotestkit%20(complete%20test)%20SOP%20-%20A5.pdf. [2018-08-20].

Moult, J.A. et al. 2018. Greenhouse gas emissions of food waste disposal options for UK retailers. Food Policy, 77: 50–58.

Plíva, P. et al. 2016. Kompostování a kompostárny. 1st ed., Praha: vydavatelství Profi Press s.r.o.

Sanchez-Monedero, M.A. 2018. Role of biochar as an additive in organic waste composting. Bioresource Technology, 247: 1155–1164.

Scherhaufer, S. et al. 2018. Environmental impacts of food waste in Europe. Waste Management, 77: 98–113.

Wu, C. 2018. Assessment of the health risks and odor concentration of volatile compounds from a municipal solid waste landfill in China. Chemosphere, 202: 1–8.

Zhan, L.T. 2017. Biochemical, hydrological and mechanical behaviors of high food waste content MSW landfill: Liquid-gas interaction observed from a large-scale experiment. Waste Management, 68: 307–318.

Zhao, Y. et al. 2017. Roles of composts in soil based on the assessment of humification degree of fluvic acids. Ecological Indicators, 72: 473–480.

Ecological stability at the time of the Stable Cadastre and today

Pavla Pokorna
Department of Applied and Landscape Ecology
Mendel University in Brno
Zemedelska 1, 613 00 Brno
CZECH REPUBLIC

pavla.pokorna@mendelu.cz

Abstract: At the present time of droughts, flash floods and diminishing biological diversity, ecological stability is one of the most important landscape indicators. A solution can be seen in the carefully worked-out plan of the Territorial System of Ecological Stability, which is –unlike other solutions- supported by the Czech legislation. The objective of this study is to assess the difference in ecological stability at the time of the Stable Cadastre and today in order to identify possibilities for designing stabilization elements in the landscape based on historic structures recorded in the Stable Cadastre. Ecological stability is calculated by using the ratio of relatively stable and unstable plots. Four cadastral areas used in the assessment (Terezín, Ratíškovice, Hodonín and Nový Poddvorov) fall under the Hodonín municipality with extended powers. In all monitored territories, since 1845, the ecological stability index has decreased. Therefore, studying a stable cadastre can help us to make positive changes in the landscape.

Key Words: ecological stability, stable cadastre, Hodonín

INTRODUCTION

Ecological stability is ecosystem capacity to counterbalance changes caused by external agents and to sustain its natural properties and functions (§ 4 of Act no. 17/1992 Sb.). It features in fact the indicative and regulative role of biota because the existence of biota provides for the ability to cope with unfavourable fluctuations of the abiotic environment (Kolejka 2013). For a possibility to determine roughly the ecological stability of a certain area (e.g. cadastral area, watershed), a so-called coefficient of ecological stability (CES) was constructed as a ratio of relatively ecologically stable and relatively ecologically unstable plots. The coefficient of ecological stability (Lipský 1998) was used in the maps of ecological stability published for the Atlas of the Environment and Population Health in 1992.

The nowadays landscape has to face various problems of which the most serious ones are lack of water and soil erosion. Returning to landscape ecological stability could help stop the further development of these problems. A basis for the ecological stability is a sufficient amount of ecologically important segments in the landscape. A good landscape structure helps to provide sufficient biodiversity to maintain a large number of plant and animal species (Walz 2011). Their minimum area is 1 ha (Maier 2012). Nevertheless, the sufficient amount of ecologically important segments by itself will not guarantee ecological stability of the area; significant is also their interconnection and recurrence of the species of individual segments (forest, wetland, steppe …). The interconnection will function by means of line communities whose breath has to be at least 15 m (Bínová et al. 2017). An important role of these elements consists in a so-called edge effect, i.e. increased biodiversity on the borderline of ecosystems. Such ecologically important segments interconnected by line elements constitute a skeleton of ecological stability, which is established in the Czech legislation as a Territorial System of Ecological Stability (ÚSES) (§ 3 of Act no. 114/1992 Sb.). The idea of ÚSES emerged at the beginning of the 1980s as a possibility to return relative stability to the landscape even at its intensive use. The main goal is to separate unstable parts of the landscape by a system of relatively stable ecosystems (Míchal 1994).

The current looks of the landscape started to form with the arrival of industrialization at the beginning of the 19th century. The landscape structure with its individual elements is best documented by the Stable Cadastre – a comprehensive work published in 1824–1843. Thanks to the obligatory

Imperial prints, we can imagine how the landscape looked like in those times. Thanks to the knowledge of historic structures and current findings about ecological stability, we can create harmonic and stable landscape now. For that, we may use for example the above-mentioned Territorial System of Ecological Stability (ÚSES).

In this paper, I would like to answer the question whether the landscape in the first half of the 19th century was stable in terms of our today's perceptions and thus whether the Stable Cadastre maps are useful for land use planning.

MATERIAL AND METHODS

Coefficient of ecological stability (CES) can be calculated by using several methodologically well-proven methods of which the simplest one is according to Míchal (1994) comparing the relatively ecologically stable and unstable plots:

$$C_{es} = \frac{Forest\ soil + Meadows + Pastures + Gardens + Fruit\ orchards + Vineyards + Water\ surfaces}{Built\text{-}up\ areas + Arable\ land + Hop\ fields}$$

Another methodology employs a numerical coefficient to differentiate ecological significance of individual types of plots. The third method of calculation according to Agroprojekt dwells on the condition of individual plots in the territory and cannot be used for the assessment of historic plots only based on the information from the maps (Lipský 1998).

The calculation method chosen to fulfil the project objective was that of the ratio of stable and unstable plots. Data for calculating ecological stability of the territory in 1845 was acquired from the Report on the comparison of plots in 1845 and 1948, included in the annex to the Stable Cadastre and available on www.archivnimapy.cuzk.cz. Data for calculating the current state was originating from the CORINE Land Cover 2012 satellite photographs.

The CES values can be interpreted according to the scale created by Löw and Míchal (2003):

- CES < 0.3 excessively used cultural land with a clear disturbance of natural structures;
- CES 0.4–0.8 intensively used cultural land with a considerable employment of (agro)industrial elements;
- CES 0.9–2.9 common cultural landscape with technical objects in relative accord with the character of relatively natural elements;
- CES > 2.9 technical objects dispersed on small plots with the dominance of relatively natural elements;
- CES > 6.2 relatively natural area.

CES was calculated for entire cadastral areas within the borders from 1845. Since the results will lay foundations for a further research in the Hodonín municipality with extended powers, cadastral areas falling under that municipality were selected. Because the partial survey was only to verify a possibility of using the Stable Cadastre to return ecological stability to the territory, only four cadastral areas were chosen for the verification – two with the lowest current coefficient of ecological stability (Terezín and Nový Poddvorov) and two with the highest current coefficient of ecological stability (Hodonín and Ratíškovice).

RESULTS AND DISCUSSION

The area in which the analysed cadastral area is located has been used for agriculture since the Middle Ages. From the second half of the 19th century even to the industry, especially mining and processing of minerals. The area lies close to the Czech-Slovak border.

Figure 1 Map of analysed area

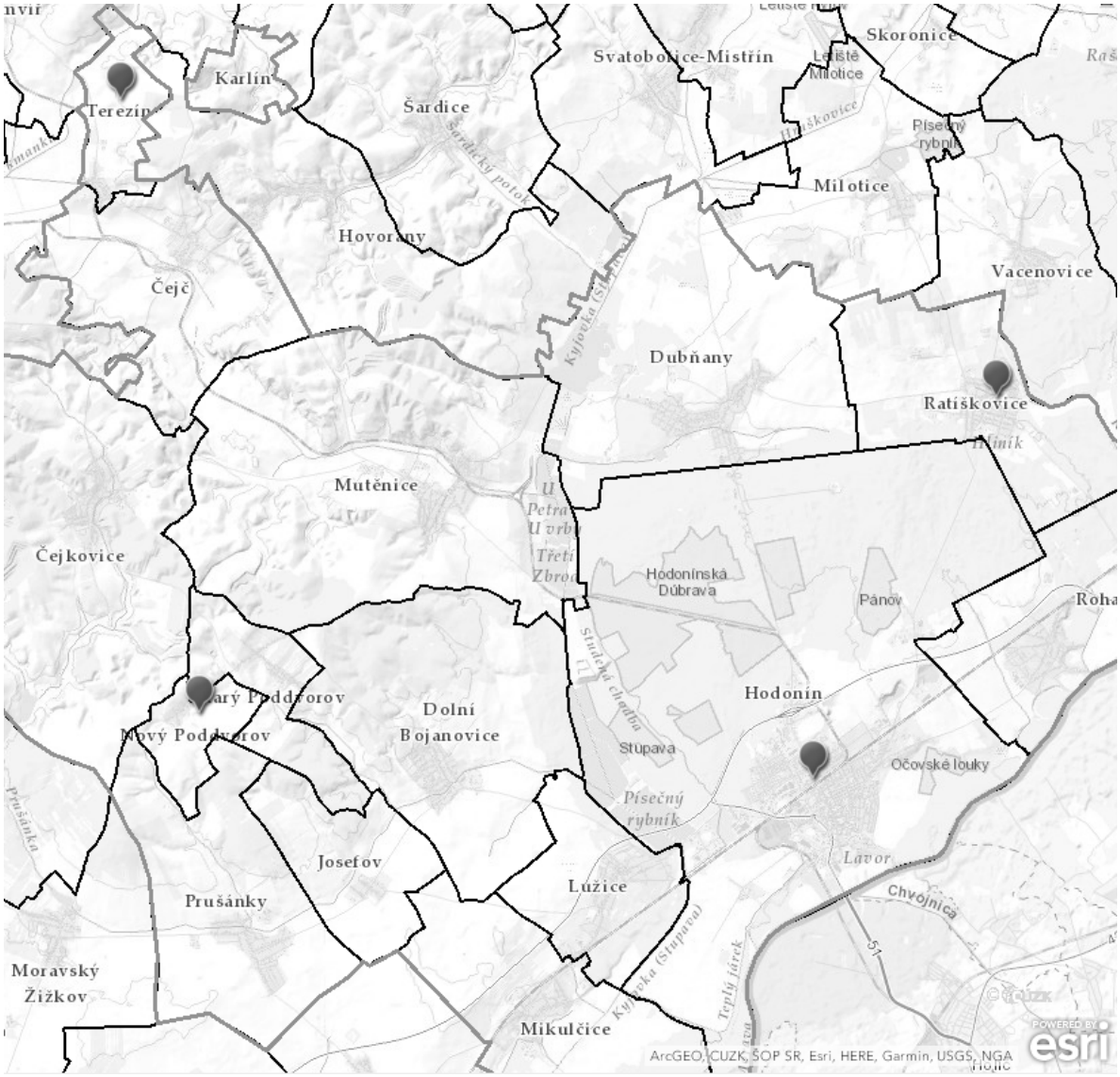

We calculated the coefficient of ecological stability for all four cadastral areas in 1845 and 2012 (Table 1).

Table 1 Result values CES

Cadastral area	*CES 1845*	*CES 2012*	*Difference*
Hodonín	5.23	2.15	3.09
Nový Poddvorov	0.25	0.09	0.16
Ratíškovice	2.06	1.37	0.70
Terezín	1.01	0.05	0.97

As compared with 2012, CES was higher in 1845 in all four cadastral areas. The greatest difference can be seen in the Hodonín cadastral area where the nearly relatively natural landscape became the common settled landscape – namely due to the loss of permanent grasslands and sprawling built-up areas (Figure 1). The least difference was recorded in the cadastral area of Nový Poddvorov where a modest loss of forests and permanent grasslands was compensated for by the increased area of orchards. The difference in this cadastral area is low even if compared with the low CES in 1845, where fields occupied nearly 80 % of the cadastre and their acreage further grew later. In Terezín, the level of ecological stability dropped nearly to zero. This territory is completely missing ecologically significant segments that would prevent the system from collapsing. Nearly 90% of the area is occupied by fields

and as compared with the past, permanent grasslands are missing that increased the coefficient of ecological stability, which however still corresponded to the intensively used cultivated landscape. The Ratíškovice cadastral area recorded the greatest loss of permanent grasslands; on the other hand, the forest area increased by 200 ha and the cadastre was classified as common cultural landscape in both periods.

Figure 2 Land types in the cadastral area Hodonín of the year 2012 and 1845

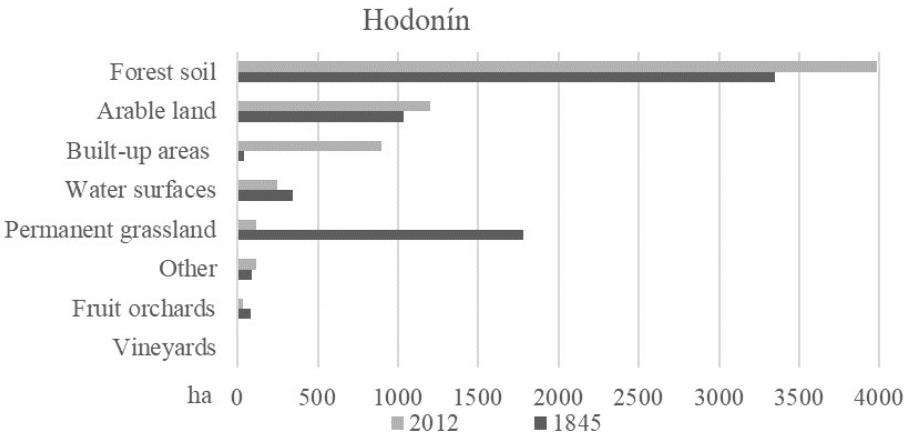

Figure 3 Land types in the cadastral area Nový Poddvorov of the year 2012 and 1845

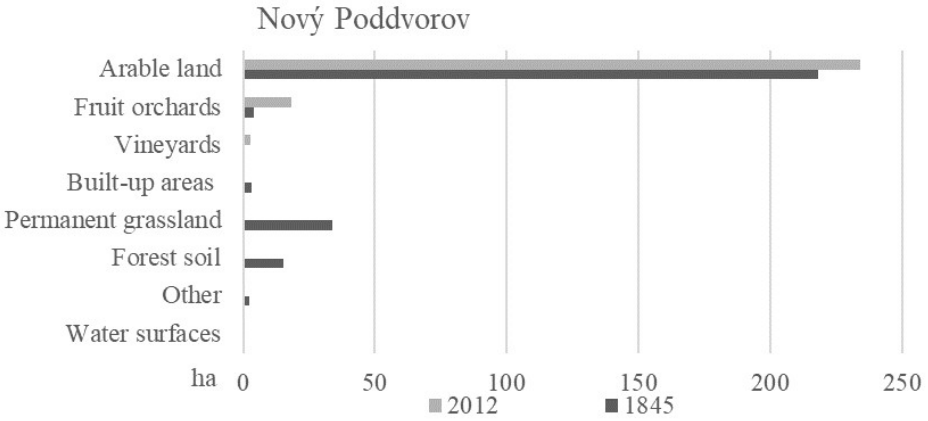

Figure 4 Land types in the cadastral area Ratíškovice of the year 2012 and 1845

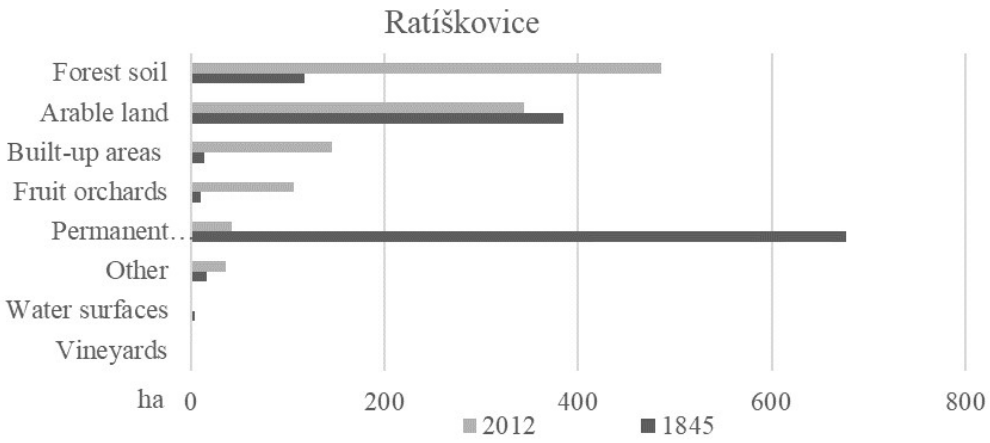

Figure 5 Land types in the cadastral area Terezín of the year 2012 and 1845

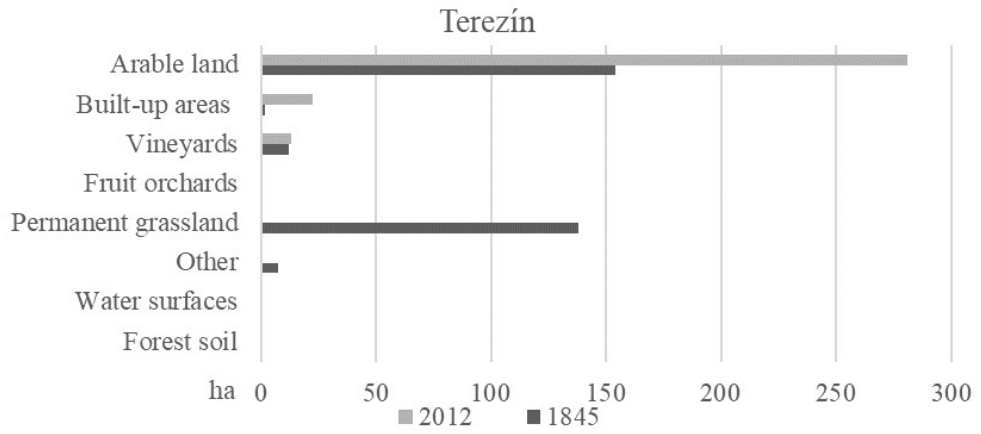

It is also important for ecological stability that ecosystems occur over a long term in the landscape. Therefore, it is useful to make use of the historic location of individual plots in designing measures for better ecological stability. In this, we can use maps from the military mapping (1764–1768, 1836–1852, 1876–1880) and aerial photographs from the 20th century in addition to the maps of the Stable Cadastre. Microstructure in the landscape is important for ecological stability, but it is hard to read from a stable cadastre due to its non-taxation. That is why other map works are important for further exploration of historical structures.

The greatest difference in the land use of all surveyed plots was the absence of permanent grasslands, nowadays pastures in particular, which would be able to fulfil not only the stabilization but also production function if restored as pastures or meadows again. Important is, however, that the meadows are established amidst large field areas to refine landscape texture and to bring a so-called edge effect into the landscape.

CONCLUSION

The above-data indicate that some of surveyed cadastral areas were intensively used for agricultural production already in 1845. The values show that no great changes occurred in land use types, most often the permanent grasslands disintegrated amongst the other categories. The most important information captured in the maps of Stable Cadastre is the historic landscape structure, which should become a starting point for land use planning so that frequent alternation of ecosystems could help the stabilization function and development of biological diversity. The ecologically most stable landscape is a landscape without human interventions with a coefficient of ecological stability higher than 6.2. In the conditions of our country, such a landscape occurs in borderland mountains and national parks. Landscapes managed by humans should feature the coefficient of ecological stability ranging between 9.9 and 2.9 – the higher the better so that the landscapes can cope with both climatic extremes and occasional management mistakes of the man.

ACKNOWLEDGEMENTS

The research was financially supported by the grant AF-IGA-2018-tym004 which is funded by Internal Grant Agency of Faculty of AgriSciences, Mendel University in Brno.

REFERENCES

Bínová, L. et al. 2017. Metodika vymezování územního systému ekologické stability. Metodický podklad pro zpracování plánů územního systému ekologické stability v rámci PO4 OPŽP 2014-2020 [Online]. Věstník Ministerstva životného prostředí, květen 2017. Praha: MŽP. Available at: https://www.mzp.cz/cz/uzemni_system_ekologicke_stability. [2018-08-02].

Česká Republika. 1992. Zákon č. 17/1992 Sb., o životním prostředí. In: Sbírka zákonů České republiky. 4: 81–89. Also available at: http://aplikace.mvcr.cz/sbirka-zakonu/SearchResult.aspx?q=1992&typeLaw=zakon&What=Rok&stranka=13. [2018-08-18].

Česká Republika. 1992. Zákon č. 114/1992 Sb., o ochraně přírody a krajiny. In: Sbírka zákonů České republiky. 28: 666–692. Also available at: http://aplikace.mvcr.cz/sbirka-zakonu/SearchResult.aspx?q=1992&typeLaw=zakon&What=Rok&stranka=11. [2018-08-18].

Kolejka, J. 2013. Nauka o krajině: geografický pohled a východiska. 1. vyd., Praha: Academia. Živá příroda.

Lipský, Z. 1998. Krajinná ekologie pro studenty geografických oborů. 1. vyd., Praha: Karolinum.

Lipský, Z. 2000. Sledování změn v kulturní krajině: učební text pro cvičení z předmětu Krajinná ekologie. 1. vyd., Kostelec nad Černými lesy: Lesnická práce.

Löw, J., Míchal, I. 2003. Krajinný ráz. 1. vyd., Kostelec nad Černými lesy: Lesnická práce.

Maier, K. 2012. Udržitelný rozvoj území. 1. vyd., Praha: Grada.

Míchal, I. 1994. Ekologická stabilita. 2. vyd., Brno: Veronica.

Walz, U. 2011. Landscape Structure, Landscape Metrics and Biodiversity. Living Reviews in Landscape Research [Online], 5(3). Available at: http://www.livingreviews.org/lrlr-2011-3. [2018-10-04]

Denitrifying woodchip bioreactor shutdown during dry periods

Katerina Schrimpelova, Jitka Mala, Zuzana Bilkova, Karel Hrich
Institute of Chemistry
Faculty of Civil Engineering
Brno University of Technology
Veveri 331/95, 602 00 Brno
CZECH REPUBLIC

schrimpelova.k@fce.vutbr.cz

Abstract: There is a growing acceptance of denitrifying bioreactors, an innovative *in-situ* treatment technology, as an effective tool for the removal of nitrates from agricultural outflows. Denitrifying bioreactors are containers or trenches filled with various types of organic material that releases bioavailable organic carbon over a long period. Wood-particle materials, such as sawdust and woodchips, are used most frequently as fill media. The presented research focuses on wet bioreactor shutdown during dry weather periods and its impact on nitrate removal rate and fill media leaching under various inflow NO_3^--N concentrations and hydraulic retention times (HRTs). The experiment was conducted in laboratory bioreactors filled with poplar woodchips at an average temperature of 19 °C, at inflow NO_3^--N concentrations of 20 mg/L and 40 mg/L, and at HRTs ranging from 1.6–2.1 d. Three shutdowns were performed, lasting two, two and three weeks, during which the fill media were kept flooded. The steady outflow NO_3^--N concentrations of all bioreactors were below 3 mg/L. Outflow COD (chemical oxygen demand) and BOD (biochemical oxygen demand) stabilised below 400 and 200 mg/L, respectively, while TKN (total Kjeldahl nitrogen) stabilised at 1 to 2 mg/L. The shutdowns did not significantly affect either the NO_3^--N removal process or the release of organic compounds from the denitrifying bioreactor fill media. Outflow TKN concentrations after recommissioning increased to 2–3.5 mg/L, subsequently decreasing to steady values within three weeks. The water stagnating in the bioreactors during their shutdowns contained elevated concentrations of NO_3^--N, COD, BOD and TKN (4–6 mg/L, 1,200–1,600 mg/L, 600–900 mg/L and 2.5–5 mg/L, respectively), but the volume of water was small. Thus, the long-term benefits brought to the aquatic environment by denitrifying bioreactors highly exceed the occasional negative impact of discharged stagnant water.

Key Words: denitrifying woodchip bioreactor, wet shutdown, dry period, nitrates, organic matter release

INTRODUCTION

The excessive application of fertilizers and animal manure in agriculture and subsequent nitrogen losses from agricultural areas are responsible for nitrate contamination of the aquatic environment worldwide, which results in eutrophication, toxic algal blooms, hypoxia, and habitat deterioration (Galloway et al. 2003). The prevention of the nitrate pollution of water bodies is covered by the European Directive (Council of the European Communities 1991).

There is a growing acceptance of denitrifying bioreactors, an innovative *in-situ* treatment technology, as an effective tool for the removal of nitrates from agricultural outflows (Christianson and Shipper 2016). Denitrifying bioreactors are containers or trenches filled with various types of organic material that releases bioavailable organic carbon over a long period. Organic carbon has three important functions in heterotrophic denitrification, which converts nitrates to nitrogen gas. It provides an anoxic environment, acts as an electron donor, and serves as a substrate for the growth of denitrifying microorganisms (Schipper et al. 2010).

The organic fill medium is one of the most important factors controlling the denitrification process. Wood-particle materials, such as woodchips and sawdust, are used most frequently (Schipper et al. 2010). They have many advantages. They provide constant nitrate removal rates over decades (Robertson 2010), exhibit a high C:N ratio (Robertson and Anderson 1999) (which is preferred due to the need to avoid excessive nitrogen leaching), maintain high hydraulic conductivity (van Driel et al. 2006), and require minimum maintenance (Robertson 2010).

Operating conditions, including inflow nitrate concentration, HRT, and temperature, are other important factors affecting processes in denitrifying bioreactors. Their influence on nitrate removal rate was analysed by Addy et al. (2016), who applied meta-analysis approaches to data from 26 published studies dealing with 57 separate bioreactor units. They concluded that nitrate removal rate rises with increasing inflow nitrate concentration, and that furthermore this effect is fostered by a sufficient HRT (at least 6 h) and a temperature greater than 6 °C. Denitrification requires a pH ranging from 6 to 8. Denitrification rate decreases with falling pH (Paul and Clark 1996).

A sufficiently long HRT and an adequately high temperature do not only promote nitrate removal, but unfortunately also the leaching of bioreactor fill media. Cameron and Schipper (2010) assume that a longer HRT enables greater dissolution of organic carbon, and that a higher temperature supports faster microbial decomposition of fill media, releasing NH_4–N, organic nitrogen and carbon.

The operating conditions of a denitrifying bioreactor, including its shutdown during dry periods, highly depend on natural conditions (the amount of precipitation and irrigation in particular). In general, fluctuating flow rates may result in lower removal efficiency even at high HRTs (Christianson et al. 2011). During conditions of no flow or very low flow, denitrifying bioreactors can be left dry, partially flooded, or wet.

The effect of wet/dry shutdown on bioreactor function and its impact on the environment is complex. In the case that desiccation occurs, the imported dissolved oxygen may reduce denitrification to the benefit of aerobic mineralization. On the other hand, mineralization leads to oxygen consumption, and the organic carbon released after the dry period may support rapid denitrification for a limited time period after rewetting (Woli et al. 2010, Weigelhofer and Hein 2015). Consistently saturated woodchips degrade more slowly than periodically desiccated chips (Christianson et al. 2012).

The goal of the presented research was to determine how wet bioreactor shutdown during dry weather periods affects nitrate removal rate and fill media leaching under various inflow NO_3^--N concentrations and HRTs.

MATERIAL AND METHODS

The experiment was conducted in 0.3 m^3 vertical cylindrical bioreactors filled with poplar woodchips of a particle size ranging from 2 mm to 20 mm. The bioreactors were loaded with tap water enriched with potassium nitrate. A water-saturated environment was maintained in the bioreactors by a flexible pipe. The average outflow water temperature was 19 °C.

The bioreactors were operated at inflow NO_3^--N concentrations of 20 mg/L and 40 mg/L. The experiment was conducted with two replicates. After achieving steady operation, the bioreactors were shut down for various periods of time. Three shutdowns were performed, lasting two, two and three weeks. The fill media were kept flooded. At the end of the shutdowns, the bioreactors were discharged and the stagnant liquid was analyzed. Afterwards, they were filled with inflow water and operated till a new steady state was achieved. Some of these operational phases differed in HRTs, as discussed below.

Sampling was carried out on a weekly basis. The pH was measured via a Hach HQ40d multi-parameter meter (Loveland, Colorado, USA). NO_3^--N was measured by the UV absorption method with a Hach optical Nitratax plus sc Sensor (Loveland, Colorado, USA). The COD, BOD, and TKN were analysed by the following methods: COD – semi-micro method with potassium dichromate and photometric evaluation; BOD – dilution and seeding method with allylthiourea addition and five-day incubation time; TKN – acid digestion using concentrated sulphuric acid together with catalyst tablets (KJELTABS ST – Thompson & Capper Ltd) and photometric determination of the released ammonia via the photometric indophenol method. A paired *t*-test (significance level of 0.05) was used to verify the similarity of the parallel bioreactors outlet parameters.

NO_3^--N removal rates were calculated as $[\Delta c(NO_3^-\text{-N}) \cdot Q] / V$, where $\Delta c(NO_3^-\text{-N})$ was the difference between the inflow and outflow NO_3^--N concentrations (mg/L), Q was the water flow rate (L/d) and V was the bioreactor filling volume (L). Removal efficiency was calculated from the inflow and outflow NO_3^--N concentrations.

RESULTS AND DISCUSSION

Statistical analysis did not show any difference between all outlet parameters of bioreactors fed with 20 mg/L NO_3^--N and also TKN and pH of those fed with 40 mg/L NO_3^--N. The outlet NO_3^--N, COD, and BOD concentrations of the latter bioreactors differed. However, the differences were not big, as can be seen from Figures 1, 5, and 6.

Nitrate removal

The outflow NO_3^--N concentrations (Figure 1) of bioreactors with both 20 and 40 mg/L inflow NO_3^--N concentrations were below 3 mg/L during the whole experimental period. NO_3^--N removal efficiency (Figure 2) corresponded with these low values – it was 92% and 97% in average for the 20 and 40 mg/L inflow NO_3^--N concentrations, respectively. NO_3^--N removal rates (Figure 3) were high for both cases – about 5 and more than 10 mg/(L·d) for the 20 and 40 mg/L inflow NO_3^--N concentrations, respectively. The difference in the NO_3^--N removal rates was caused by the amount of NO_3^--N available for denitrification. Despite bioreactors shutdowns the rates were in the range of 2–22 mg/L/d, which was published by Schipper et al. (2010) for various wood-based materials in continuous operated bioreactors. The high NO_3^--N removal efficiencies clearly show that the rates could be even higher.

During the shutdowns, decay of organic fill media caused the outflow pH to drop from 6–7 to approx. 5 (Figure 4). Denitrifying bacteria require pH between 6 and 9. (Paul and Clark 1996) After recommissioning, pH rapidly increased. Bioreactors with higher inflow NO_3^--N concentrations recovered faster with regard to pH, probably because greater amounts of OH^- ions are produced during denitrification. Under these conditions, NO_3^--N removal rate was restored and outflow NO_3^--N concentration stabilised at its former values.

In the 17th week, HRTs of all columns were increased from 1.6 and 1.9 d in case of 20 and 40 mg/L inflow NO_3^--N concentrations, respectively, to 2.1 d for both concentrations. Longer HRT is favourable for NO_3^--N removal efficiency, but can cause deterioration in bioreactor outlet water quality in released compounds concentrations, such as COD, BOD, and TKN. (Schipper et al. 2010) The increase in HRTs in the 17th week did not affect NO_3^--N removal efficiency (Figure 2). The HRTs of 1.6 to 2.1 d were relatively long in comparison with some published papers, describing bioreactors successfully operating at HRTs of about 8 h. (Christianson et al. 2012) It can be assumed that the bioreactor operation is less stable at shorter HRTs, and thus any change in operation parameters like shutdown could probably cause longer recovery period.

Figure 1 Outflow NO_3^--N concentration

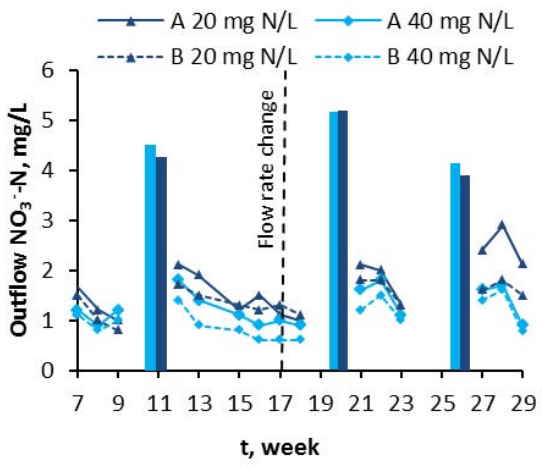

Figure 2 NO_3^--N removal efficiency

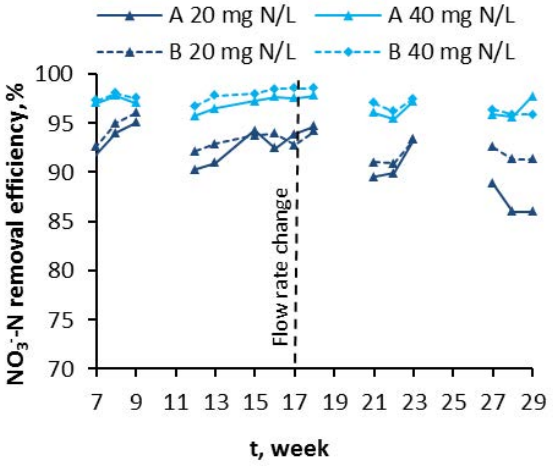

Figure 3 NO_3^--N removal rate

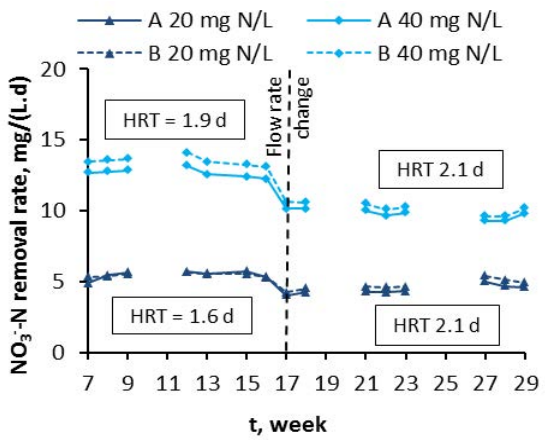

Figure 4 Outflow pH values

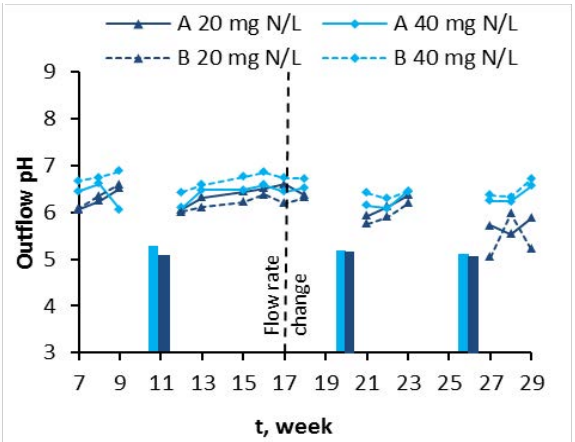

Release of organic substances and TKN

The presence of organic substances and TKN in outflow was caused by their release from the fill media. Outflow COD and BOD (Figure 5 and 6) stabilised below 400 and 200 mg/L, respectively, which was sufficient for denitrification. Steady outflow TKN (Figure 7) was below 2 mg/L.

The release of both COD and BOD followed a similar pattern, and after recommissioning their concentrations rapidly dropped to their former values. Shutdown caused a relatively high increase in outflow TKN. Its concentration decreased more slowly. It is evident from Figures 5–7 that there were no significant differences between shutdowns. Thus, it can be stated that the lengths of shutdowns and HRTs did not significantly affect fill media leaching after bioreactor recommissioning.

Figure 5 Outflow COD

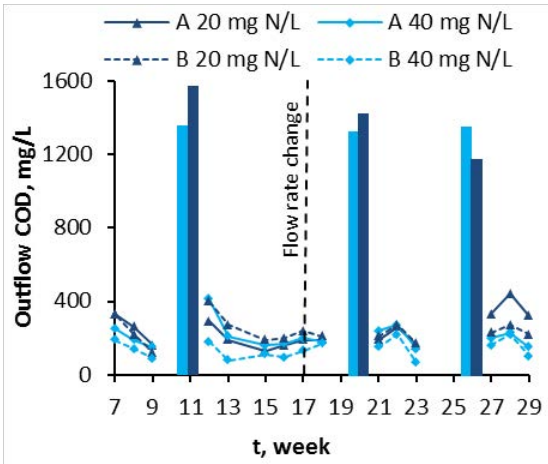

Figure 6 Outflow BOD

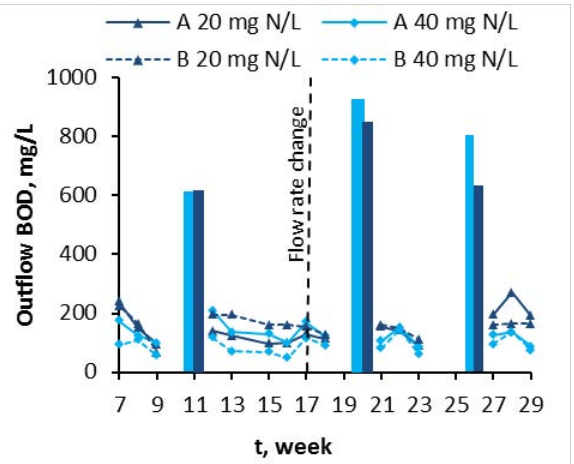

Figure 7 Outflow TKN concentrations

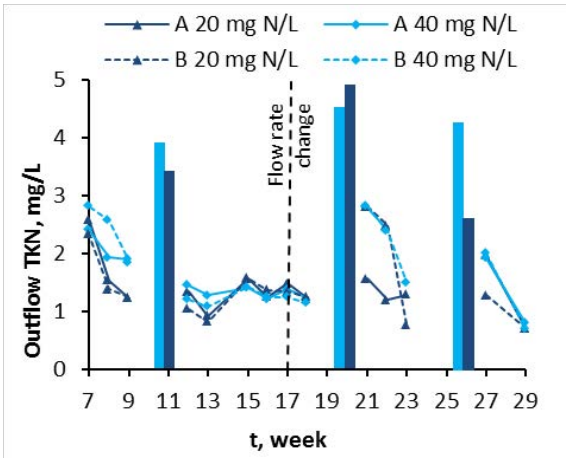

Stagnant water

The quality of stagnant water in the shutdown bioreactors is presented in the form of columns in Figures 1 and 4–7 (average values). The stagnant water contained elevated residual NO_3^--N concentrations (4–6 mg/L), which were probably caused by the conditions prevailing during stagnation. Denitrification was hampered by several of the assessed parameters, and by the insufficiently high pH of 5 in particular. NO_3^--N removal could also have been influenced by other factors, such as the leaching of compounds adversely affecting denitrification bacteria. The release of potentially harmful substances from wood materials has been described by several authors, such as Svensson et al. (2014). The organic matter contents and TKN in the stagnant water were relatively high: 1,200–1,600 mg/L, 600–900 mg/L, and 2.5–5 mg/L for COD, BOD, and TKN, respectively. The duration of the shutdowns (two and three weeks) did not significantly affect the release of organic compounds and TKN from the fill media. However, 29 weeks of bioreactor operation is a short time period compared with its duration in real use. The bioreactor can last for a minimum of 15 years (Schipper et al. 2010). Thus, its behaviour during shutdowns can differ after a longer period of operation. It was described at field bioreactors that concentrations of compounds leached from bioreactor fill media decrease in time. (Robertson 2010)

Besides the quality of stagnant water, its quantity is also important for the evaluation of its impact on the aquatic environment. Although the stagnant water quality was poor, its volume was quite small. At a woodchip porosity of approx. 50% and an HRT of approx. 2 d, the stagnant water volume would be equivalent to the two-day flow rate.

CONCLUSION

Wet shutdowns with a duration of 2–3 weeks under 20 and 40 mg/L inflow NO_3^--N concentrations and HRTs from 1.6 to 2.1 d did not significantly affect the NO_3^--N removal process or the release of organic compounds from denitrifying bioreactor fill media. The bioreactors returned to fully functional operation within one week of recommissioning. The release of TKN after recommissioning was higher, though its outflow concentrations decreased to steady values within three weeks.

The quality of the water stagnating in the bioreactors during their shutdowns was poor, but its volume was quite small. Thus, it can be concluded that the long-term benefits brought to the aquatic environment by denitrifying bioreactors highly exceed the negative impact of occasionally discharged stagnant water.

The tested shutdown durations were relatively short. Longer shutdowns would probably affect bioreactor operation to a larger extent. Also behaviour of the bioreactor under shorter HRT can differ. We plan to investigate both these subjects in our future research.

ACKNOWLEDGEMENTS

This research and paper was funded by the Ministry of Agriculture of the Czech Republic, Project No. QJ1520280.

REFERENCES

Addy, K. et al. 2016. Denitrifying bioreactors for nitrate removal: A meta-analysis. Journal of Environmental Quality, 45(3): 873–881.

Cameron, S.G., Schipper, L.A. 2010. Nitrate removal and hydraulic performance of organic carbon for use in denitrification beds. Ecological Engineering, 36(11): 1588–1595.

Christianson, L.E., Schipper, L.A. 2016. Moving denitrifying bioreactors beyond proof of concept: Introduction to the special section. Journal of Environmental Quality, 45(3): 757–761.

Christianson, L.E. et al. 2011. Optimized denitrification bioreactor treatment through simulated drainage containment. Agricultural Water Management, 99(1): 85–92.

Christianson, L.E. et al. 2012. A practice-oriented review of woodchip bioreactors for subsurface agricultural drainage. Applied Engineering in Agriculture, 28(6): 861–874.

Council of the European Communities. 1991. Council Directive of 12 December 1991 concerning the protection of waters against pollution caused by nitrates from agricultural sources (91/676/EEC). In:

Official Journal of the European Communities L375, 0001–0008. Also available at: https://www.eea.europa.eu/policy-documents/council-directive-91-676-eec. [2018-08-15]

Galloway, J.N. et al. 2003. The nitrogen cascade. BioScience, 53(4): 341–356.

Paul, E.D., Clark, F.E. 1996. Soil Microbiology and Biochemistry. 2nd ed., San Diego, USA: Academic Press.

Robertson, W.D. 2010. Nitrate removal rates in woodchip media of varying age. Ecological Engineering, 36(11): 1581–1587.

Robertson, W.D., Anderson, M.R. 1999. Nitrogen removal from landfill leachate using an infiltration bed coupled with a denitrification barrier. Groundwater Monitoring and Remediation, 19(4): 73–80.

Schipper, L.A. et al. 2010. Denitrifying bioreactors – An approach for reducing nitrate loads to receiving waters. Ecological Engineering, 36(11): 1532–1543.

Svensson, H. et al. 2014. Leaching patterns from wood of different tree species and environmental implications related to wood storage areas. Water and Environment Journal, 28(2): 277–284.

van Driel, P.W. et al. 2006. Denitrification of agricultural drainage using wood-based reactors. Transactions of the American Society of Agricultural and Biological Engineers, 49(2): 565–573.

Weigelhofer, G., Hein, T. 2015. Efficiency and detrimental side effects of denitrifying bioreactors for nitrate reduction in drainage water. Environmental Science and Pollution Research, 22(17): 13534–13545.

Woli, K. P. et al. 2010. Nitrogen balance in and export from agricultural fields associated with controlled drainage systems and denitrifying bioreactors. Ecological Engineering, 36(11): 1558–1566.

Possibilities of application of phenological observations

Eva Stehnova[1], Hana Stredova[1], Ivan Novotny[2]
[1]Department of Applied and Landscape Ecology
Mendel University in Brno
Zemedelska 1, 613 00 Brno
[2]Research Institute for Soil and Water Conservation
Zabovreska 250, 156 27 Praha 5 – Zbraslav
CZECH REPUBLIC

eva.stehnova@mendelu.cz

Abstract: This paper deals with the practical application of phenological data. Ways of using phenological data are presented in case studies (from the area – applied and landscape ecology – occurrence of allergens and soil erosion, agriculture and climatology) for the Czech Republic (Central Europe). Phenological data were obtained from direct observations of the Czech hydrometeorological institute. Data were evaluated for different long-term periods (from 1931 to 2012). Period of pollen occurrence for common hazel, goat willow, white birch and small-leaved lime is defined in this article. Pollen of analysed trees can appear in landscape as follows: common hazel from the 33rd day to the 118th day of the year, goat willow from the 61st day to the 125th of the year, white birch from the 96th day to the 138th day of the year and small-leaved lime from the 163rd day to the 215th day of the year. Spring barley, maize and sugar beet were evaluated in this paper. Analysed phenological data show great variability in individual year. The prolongation of growing season was found out for spring barley in locality Branišovice (South Moravia, the Czech Republic). Prolongation of the growing season can be caused climate change, varietal specifics, sowing and harvest dates, sowing density, more powerful and modern agricultural machinery etc. Length of the growing season is one of the main factors influencing the value of protective effect of vegetation (so called factor C). It has been found that the longer the crop on the plot is the lower the value of factor C.

Key Words: growing season, spring barley, pollen allergens, C factor, Czech Republic

INTRODUCTION

Term of the onset of phenological phases (for example emergence, heading, tillering, beginning of flowering etc.) and operations sowing and harvest are recorded in phenological observations. The phenological phase is an annual recurring, externally well recognizable, repeatedly occurring development of plant organs every year.

Data from phenological observations can be used in a number of disciplines but also in practice. We can mention three basic areas in which phenological data possible to use: a) Applied and landscape ecology, b) Agriculture and c) Climatology (on the basis case studies).

MATERIAL AND METHODS

The article is composed of case studies addressing the different areas of phenological data utilization. Different localities, crops and time periods were evaluated in individual case scales. The summarizing table is shown in Table 1.

These phenological phases were evaluated for field crops in this paper: emergence (EM), tillering (TI), the beginning of leaf sheath elongation (BLSE), first node (FN), second node (SN), swelling of the sheath of the last leaf (SSLL), heading (HE), milky ripeness (MR), yellow ripeness (YR) and full ripeness (FR). Phenological phases: beginning of flowering 10%, 50%, 100% (BF 10, 50, 100) and end of flowering (EF) were evaluated for tree species in pollen analysis.

Sowing (SD) and harvest (HA) were also evaluated which are monitored in phenological observation for field crops. Closer specification of individual phenological phases and term of sowing

and harvest are given in Methodological prescription No. 2 – Instruction for the activity of phenological stations for field crops (Valter 1982).

Most of the territory of the Czech Republic falls according Köppen climate classification into the damp continental climate (Dfb). The average annual temperature is between 5.5 °C and 9 °C in the Czech Republic. The average annual rainfall is 686 mm (Tolasz 2007).

Calculation of the protective effect of vegetation (so called factor C) was performed on the grounds of Methodology – Protection of agricultural land from erosion (Janeček et al. 2012). The calculation of C factor was made on the basis of the formula %R × C and this value divided by 100 (Wischmeier and Smith 1978).

Table 1 Summarizing table of evaluated locality, period and crops

Area of use	Subcategories	Locality	Altitude (m a.s.l)	Analysed periods	Kind of plant
Applied and landscape ecology	Pollen allergens	Český Rudolec, Březina, Lednice,	540 450 165	1991–2012	common hazel, white birch, small-leaved lime, goat willow
	Soil erosion control	Tupesy,	240	1961–2012	sugar beet, maize, spring barley
		Sokolnice	255		
		Strážnice	177		
		Ivanovice na Hané	220		
		Luhačovice	329		
		Tečovice	260		
Agriculture	-	Strážnice	177	1991–2010	spring barley
Climatology	-	Branišovice	180	1931–2012	spring barley

RESULTS AND DISCUSSION

a) Applied and landscape ecology

The first possible use of phenological data within applied and landscape ecology is the **monitoring of pollen allergens** in the landscape.

Figure 1 lists the average terms for the occurrence of white birch, common hazel, small-leaved lime and goat willow. The average time of flowering is evaluated in these trees also. Pollen of common hazel is one of the earliest allergens scattering in the air. Common hazel flowering on average thus: at locality Lednice from the 60th day to the 81rd day of the year, at locality Březina from the 80th day to the 95th day of the year and at locality Český Rudolec from the 67th day to the 93rd day of the year. Pollen of goat willow is another allergen occurring in the landscape which appears at locality Březina from the 88th day to the 111th day of the year and at locality Český Rudolec from the 84th day to the 103rd day of the year. Pollen grains of white birch are other allergen that appears in air. Pollens of white birch are among the most aggressive allergens. White birch has on average the shortest flowering time from analysed tree species (from 9 days to 14 days). White birch flowering at the analysed localities on average thus: from the 102nd day to the 116th day of the year in Lednice, from the 120th day to the 129th day of the year in Březina and from the 115th day to the 125th day of the year in Český Rudolec. Pollen of small-leaved lime appears at the latest of the analysed the trees species. It flowering from the 178th day to the 198th day of the year at locality Březina and from the 186th day to the 200th day of the year at locality Český Rudolec.

The occurrence of allergens was determined on the basis of measured phenological data for individual years. Figure 2 was created from the terms of the earliest date of flowering and the latest date of end of flowering. Pollen grains of common hazel appear in nature first from the 33rd day to the 118th day of the year. Pollen of goat willow is the second in line of analysed allergens. Goat willow

blooms in term from the 61st day to the 125th of the year. Pollen of white birch may occur from the 96th day to the 138th day of the year. Small-leaved lime flowering as the last of the analysed plants. It was flowering from the 163rd day to the 215th day of the year (Figure 2).

Anti-erosion protection of soil is the second possibility of using phenological data in applied and landscape ecology. Protective effect of vegetation (so called C factor) enters into calculation of value of long-term soil loss from a given plot (Wischmeier and Smith 1978). The C factor depends on vegetation cover and agronomic management. Soil cover plays an important role for soil protection from the erosion (Boardman and Poesen 2006).

Figure 1 Average values of occurrence of pollen allergens from selected tree species

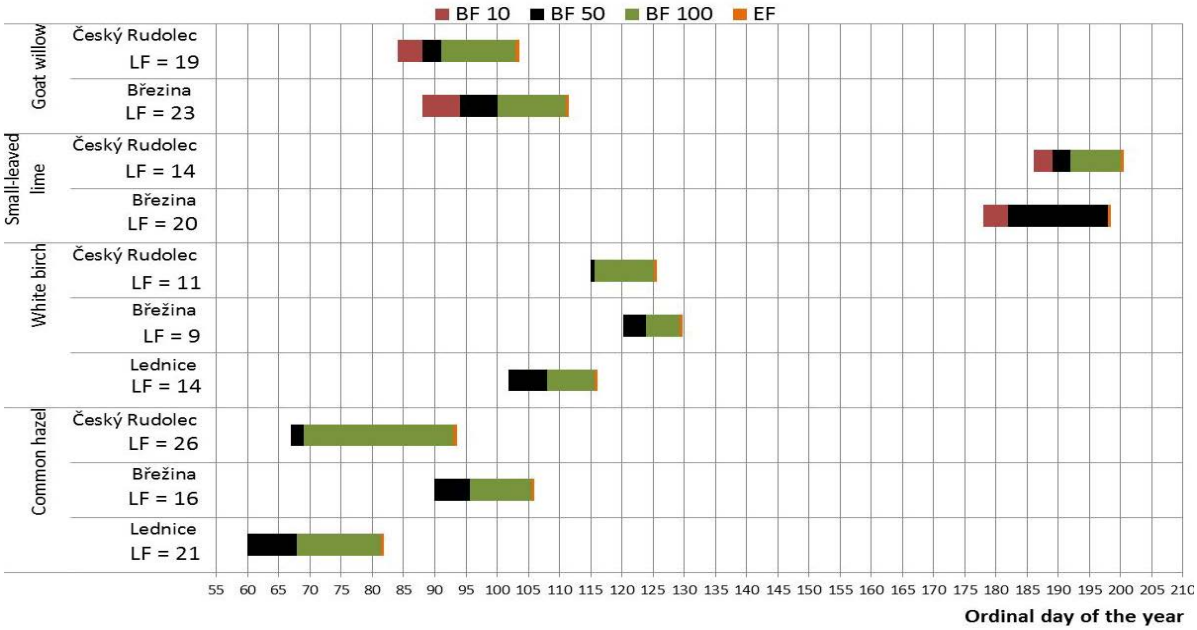

Figure 2 Demarcation of the occurrence of allergens of common hazel, goat willow, white birch and small-leaved lime

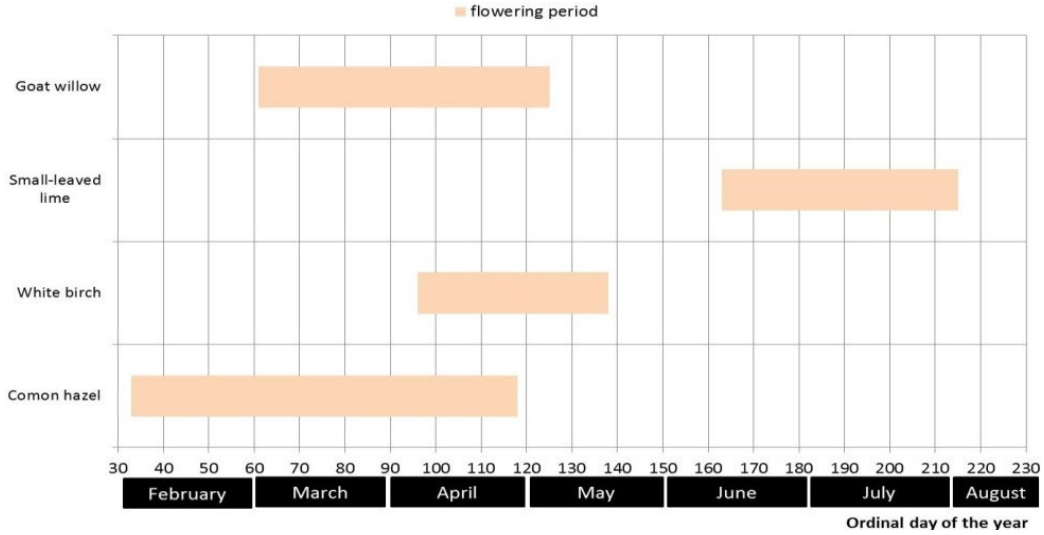

Dates of sowing and harvest (data from phenological observations) were used for calculation values of C factor. The largest percentage difference between values of C factors was found out in the spring barley at locality Luhačovice (Table 2). Lower value of C factor was found out for a long growing season. The main reason for the lower value of C factor in long growing season is that the crop protects the surface of the soil longer. The same result was found out in other contributions (Stehnova and Stredova 2016).

Date of sowing is another important factor that affects the value of C factor. The sooner the spring barley is sowed, the value of C factor is lower. The sowing and emergency of plants are characterized as a crisis period due to soil erosion. In this period the soil is insufficiently protected by vegetation and could happen the big loss of soil. Erosion dangerous period of plants (sowing, emergence) had to occur in period when erosion dangerous rains don´t occur. Erosion dangerous rains appear from April to October (with different probability).

Table 2 Values of C factor for extreme years at selected locality

Crop	Phenological station	Length of the growing season	Year	Data from phenological observations		Value of C factor	Percentage difference
				Sowing	Harvest		
Sugar beet	Tupesy	192	1970	21 March	28 September	0.3408	28.9%
		134	1974	5 May	15 September	0.4793	
	Sokolnice	199	1974	14 March	28 September	0.3317	24.6%
		157	1981	30 April	3 October	0.4397	
Maize	Strážnice	193	2010	23 April	1 November	0.4679	12.5%
		113	1992	16 April	7 August	0.4714	
	Ivanovice na Hané	154	2007	2 April	3 September	0.4294	32.1%
		97	1994	2 June	7 September	0.6315	
Spring barley	Luhačovice	154	1983	18 April	25 July	0.2535	43.5%
		98	1974	5. March	6 August	0.1433	
	Tečovice	154	1974	22 February	25 July	0.1930	24.1%
		95	1964	14 April	18 August	0.2126	

b) Agriculture

A detailed analysis of phenological data is also useful in agricultural practice for example in the application of plant protection products, in yield and growth models, in optimizing irrigation, pathogen prediction, agrometeorological modelling etc. It is clear from graph (Figure 3) that individually years show great variability. Roetzer et al. (2000) states that phenological manifestations of plants are closely related to seasonal weather conditions. This may be a reason for the large variability of phenological data at the analysed localities. Variability of phenological phases and climatic conditions can have a significant effect also on seed quality.

Earliest sowing was performed in year 2007 (the 54th day of the year) and in year 1997 (the 66th day of the year). In these years the longest growing season was found out (144 days). The shortest growing season was found out in years 1996 (115 days) and 2008 (114 days).

c) Climatology

However, phenology is most commonly associated with climate change. Phenology is often referred to as the auxiliary science of climatology. Above all due to the close relationship between phenological data and climatic conditions of the external environment (Sobíšek 1993). We need long-term phenological observations for a climatic analysis that can be used to study climate change.

The average values of phenological phases and average term of sowing and harvest were rated for three long periods (Figure 4). It was found out that the growing season (GS) was prolonged (GS is understood as an interval between sowing and harvest). Šiška and Takáč (2008) state that GS will be extended about 21 days by 2020 and about one month by year 2050. However, long-term changes in field crop phenology may not be due to only climatic changes but may also be influenced by varietal

specifics, better farming techniques, sowing density, sowing and harvest timing, microclimate conditions etc.

A positive relationship between plant development and temperature has been demonstrated in Germany i.e. increasing air temperature causes a shortening in the phenological phase (Estrella et al. 2007). This trend was also found at locality Branišovice. Trend of shortening the interval between the phenological phases was detected at the phenophasis emergence and heading. Phenological analysis with use linear trend analysis for apricot (Velkopavlovická variety) shows that phenological phases beginning of flowering occurs earlier about 2 days in every decades (Chuchma et al. 2016). The earlier date of sowing was found out also in this locality. Prolongation of interval between sowing and emergence was found. The earlier sowing affects the following phenological stages. This "measure" is sometimes considered adaptive measures to adapt to climate change (Rezaei et al. 2017).

Figure 3 Detailed analysis of phenological data for spring barley at locality Strážnice

Figure 4 Analysis of long-term values of average terms onset of phenological phases and sowing and harvest of spring barley at Branišovice locality

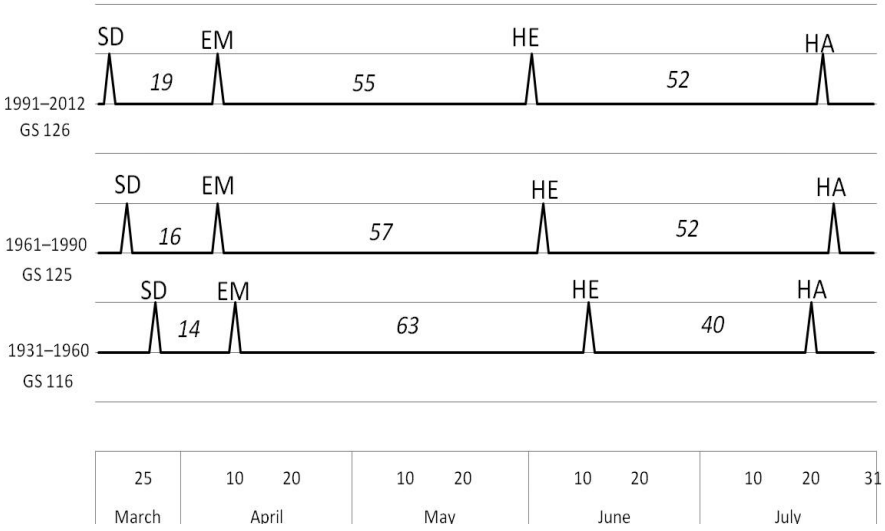

CONCLUSION

Phenological data are a valuable data source. Their use is possible within many scientific disciplines but also in agricultural practice. The article provides examples of the use of these data in several case studies.

Analysed phenological data show great variability in individual year. The Prolongation of growing season was found for spring barley also. The shortening of interval between phenological phases (emergence and heading) was found out in spring barley. Climate change can cause cased the prolongation of the growing season but it is important to consider other possible factors that may affect the length of the growing season for example varietal specifics, sowing and harvest dates, sowing density, more powerful and modern agricultural machinery etc.

Dates of sowing and harvest were used in calculating the protective effect of vegetation (C factor) also. Length of the growing season is one of the main factors influencing the value of factor C. It has been found out that the longer the crop on the plot is the lower the value of factor C. Phenological data were also used for monitoring pollen allergens. It was found out that allergens appear in the following order common hazel, goat willow, white birch and small-leaved lime.

ACKNOWLEDGEMENTS

The research was financially supported by the project No. QK1720285 “New methods for adjustment of altered crop water requirements in irrigation systems across Czechia as affected by soil and climate changes”.

REFERENCES

Boardman, J., Poesen, J. 2006. Soil erosion in Europe. Chichester: Wiley.

Chuchma, F. et al. 2016. Bioindication of climate development on the basis of long-term phonological observation. In Proceedings of International PhD Students Conference MendelNet 2016 [Online]. Brno, Czech Republic, 9 November, Brno: Mendel University in Brno, Faculty of AgriSciences, pp. 380–383. Available at: https://mnet.mendelu.cz/mendelnet2016/mnet_2016_full.pdf. [2018-08-26].

Estrella, N. et al. 2007. Trends and temperature response in the phenology of crops in Germany. Global changes biology, 13(8): 1737–1747.

Janeček, M. et al. 2012. Metodika – Ochrana zemědělské půdy před erozí. Praha: Česká zemědělská univerzita.

Rezaei, E.E. et al. 2017. Climate and management interaction cause diverse crop phenology trends. Agricultural and Forest Meteorology, 233: 55–70.

Roetzer, T. et al. 2000. Phenology in central Europe-differences and trends of spring phenophases in urban and rural areas. International Journal of Biometeorology [Online], 44(2):60–66. Available at: https://www.researchgate.net/publication/237201703_Phenology_in_central_Europe_-_Differences_and_trends_of_spring_phenophases_in_urban_and_rural_areas. [2018-08-24].

Sobíšek, B. 1993. Meteorologický slovník výkladový terminologický. 1st ed., Praha: Academia.

Stehnova, E., Stredova, H. 2016. Phenology of sugar beet in the context of the water erosion risk. Listy cukrovarnicke a reparske, 132(12): 380–386.

Šiška, B., Takáč, J. 2008. Klimatická změna a polnohospodárstvo Slovenskej republiky: dosledky, adaptačné opatreni a možné riešenia. Bratislava: Slovenská bioklimatologická spoločnosť.

Tolasz, R. 2007. Atlas podnebí Česka. Praha: Český hydrometeorologický ústav.

Valter, J. 1982. Metodický předpis č. 2 – Návod pro činnost fenologických stanic. Polní plodiny. 1st ed., Praha: Český hydrometeorologický ústav.

Wischmeier, W.H., Smith, D.D. 1978. Predicting rainfall erosion losses – a guide book to conservation planning. Washington: U.S. Department of agriculture.

Phthalates concentration in leachate from operating and closed municipal landfills of central Poland

Pawel Wowkonowicz[1], Marta Kijenska[1], Eugeniusz Koda[2]
[1]Department of Environmental Chemistry and Risk Assessment
Institute of Environmental Protection – National Research Institute, Warsaw
Krucza St. 5/11d, 00-548 Warsaw
[2]Department of Geotechnical Engineering
Warsaw University of Life Sciences – SGGW, Warsaw
Nowoursynowska St. 159, 02-776 Warsaw
POLAND

pawel.wowkonowicz@ios.edu.pl

Abstract: Phthalates (PAEs) are organic esters of phthalic acid used mainly as plasticizers in the production of PVC products, but also as additives in the production of paints and varnishes. The content of plasticizers in soft PVC products may reach up to 40–60%. With the global yearly production of phthalates estimated at approx. 5–8 million tons, large amounts of PAEs had to end up on the landfills and therefore can be found in high concentrations in the municipal landfills leachate. The landfills without proper environmental protection systems may pose a threat to the environment and human health. In this research two landfills with different "history and parameters" were studied. First landfill was closed in 2011 and a remediation process started in 1996, while the second one is currently under a closing process but is still in use. Those landfills were compared in terms of phthalates concentration in raw leachate. It was found that most of the PAEs concentrations were below LOQ, with an exception of DEHP, DBP and DIBP. The highest DEHP concentrations were detected on landfill 1 in 2015, in summer, ranging from 32.2 to 38.6 µg/l, autumn <LOQ to 20.2 µg/l and winter 16.5 to 19.6 µg/l. Also in summer 2015 the highest DEHP concentrations were detected on landfill 2 (ranging from <LOQ to 19.3 µg/l). During the study no correlation between the sampling seasons and PAEs concentrations were observed. Moreover, the landfill 1 releases more DEHP than landfill 2 because it contains more than fivefold amount of waste. Interesting fact is that landfill 1 underwent remediation in 1996 and has been closed for many years (since 2011) but DEHP emissions are still present in the leachate. In 83% of studied all samples DEHP concentrations exceeded (from 2.5 to 18.7 times) the acceptable EU limits for surface water (1.3 µg/l).

Key Words: DEHP, DBP, PAE, PVC, contamination

INTRODUCTION

Phthalates (PAEs), which are organic esters of phthalic acid, are used mainly as plasticizers in the production of polyvinyl chloride (PVC) products, but they are also used as additives in the production of cellulosics, polyvinyl acetates and polyurethane resins (Sailas et al. 2015). One-third of the mass of phthalates produced is used for the production of soft PVC products (cable insulation, floor coverings, footwear, wallpaper, furniture, etc.), while the remaining two-thirds are used to manufacture the products from hard PVC (Europe Commission DGXI.E.3). Most commonly used PAEs in the production of PVC were di(2-ethylhexyl) phthalate (DEHP) and di-n-butyl phthalate (DBP) (Gao et al. 2016). The content of plasticizers in soft PVC products may reach up to 40–60% (Erythropel et al. 2014, Gao et al. 2016).

PAEs are not chemically but only physically bond to a polymer matrix, which allows them to migrate to the product surface and leach to the environment (Erythropel. et al. 2014, Sailas et al. 2015). The global production of phthalates is estimated at approx. 5-8 million tons a year (Gao and Wen 2016, Przybylińska and Wyszkowski 2016, Vaverkova and Adamcova 2018) and since the landfilling has been the most popular techniques of municipal waste disposal (Gworek et al. 2015, Koda et al. 2017), large amounts of PAEs had to end up on the landfills. Precipitated water which penetrates through the landfill body can carry many chemicals including PAEs, which can be found in high concentrations in the

municipal landfills leachate (Asakura et al. 2004, Gao and Wen 2016). The leachate migrating to ground or surface water may cause water contamination making it unfit for drinking (Koda 2012). Therefore, the landfills without proper environmental protection systems, such as leachate collection systems, may pose a threat to the environment and human health (Przybylińska and Wyszkowski 2016).

PAEs are consider as toxic (Grynkiewicz-Bylina 2011) and widespread environmental pollutants (Przybylińska and Wyszkowski 2016). PAEs are endocrine disruptors which may result in health problems including hepatomegaly, osteoporosis, feminization of boys, weight loss, and skin and breast cancer (Sailas et al. 2015). They might also have negative effects on reproduction, fertility and carcinogenicity (Net et al. 2015). For the human population, the main concern is related to bioaccumulation of PAEs over long term exposure to contaminated food or drinking water (Gao et al. 2016).

This paper presents the results of the first exhaustive study conducted on the concentration of phthalates in raw municipal leachates in Poland.

MATERIAL AND METHODS

Characterization of landfills, location and technical data

Two large municipal waste landfills in a radius of up to 70 km from Warsaw were selected for the study (figure 1). During the selection of the landfills their age, size and operational status were taken into account. The first landfill was closed in 2011, and a remediation process started in 1996, while the second one is currently under a closing process but is still in use. Both landfills have vertical barriers for controlling the flow and leachates collection systems in place.

The following landfills were selected:

1. Location 1 – year of launch 1978, 5.5 million m^3 of waste and area of 21.7 ha.
2. Location 2 – year of launch 1970, 0.9 million m^3 of waste and area of 8.7 ha.

Figure 1 Landfills location map.

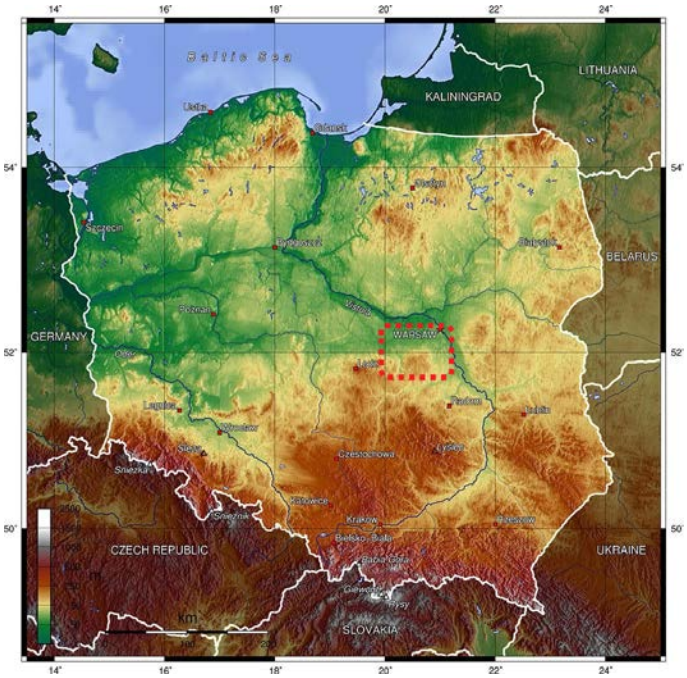

Characterization of analytical procedure

The research material consisted of samples of raw leachate collected from the leachate tanks. All the samples were collected according to the EPA Ireland Landfill manual. Each sample was taken in triplicate, using only phthalate-free objects (metal buckets, Teflon pump tubes, etc.). After collection, the samples were kept in glass containers and insulated with a phthalate-free layer (aluminium foil with

plastic or rubber caps). Samples were collected from two municipal waste landfills in summer, autumn, winter 2015 and spring, summer, autumn 2016.

Phthalates concentrations were determined with the W-PTHGMS01 method, based on US EPA 8061A, 3500, 3510 in the accredited laboratory (The Certificates of Accreditation no. 819/2015 and 319/2016). This method is suitable for groundwater and potable water, leachate and sewage analysis.

The following PAEs were analysed in this study: dimethyl phthalate (DMP), diethyl phthalate (DEP), di-n-propyl phtalate, di-n-butyl phthalate (DBP), di-isobutyl phthalate (DIBP), di-pentyl phthalate (DPP), dutyl benzyl phthalate (BBP), di-cyclohexyl phthalate (DCP), di(2-ethylhexyl) phthalate (DEHP) and di-n-octyl phthalate (DOP).

RESULTS AND DISCUSSION

The results of PAEs concentrations are presented in Table 1. Most of the PAEs concentrations were below LOQ (DMP, DEP, DPP, BBP, DCP, DNOP and di-n-propyl phthalate), with an exception of DEHP, DBP and DIBP, whereas the concentration of the last two were much lower (ranging from <LOQ to 1.64 µg/l and from <LOQ to 2.83 µg/l accordingly). DEHP was the most prevalent and in the concentrations many times higher than the other PAEs, ranging from <LOQ to 38.6 µg/l. High concentrations for DEHP were expected as historically PAE was the most commonly used plasticizer and represented around half of all PAEs used in Europe in the past (Jonsson et al. 2003). Similar DEHP concentrations in the landfills leachate were reported in Japan [9.6-49 µg/l], China [n.d.-46 µg/l], Sweden [<1-9 µg/l] or Denmark [<1-3 µg/l]. The resultant DEHP concentrations were lower than those reported in Sweden (Göteborg) [97-346 µg/l], Germany [up to 240 µg/l] and Italy [88-460 µg/l] (Wowkonowicz and Kijeńska 2017). The reason for those differances could be other composition of waste in Western and Eastern Europe, but also a fact that those studies were conducted more more then 15 years ago, when DEHP was much more frequently used plastisizer then now.

The highest DEHP concentrations were detected on landfill 1 in 2015 in summer, ranging from 32.2 to 38.6 µg/l, autumn <LOQ to 20.2 µg/l and winter 16.5 to 19.6 µg/l. Also in summer 2015 the highest DEHP concentrations were detected on landfill 2 (ranging from <LOQ to 19.3 µg/l). It should be also noted that year 2015 was much drier when 2016 and summer 2015 was the driest among all the seasons with an average precipitation of 32.6 mm for this region (see Table 2).

Table 1 PAEs concentrations in municipal solid waste landfill raw leachate – summer, autumn, winter 2015 and spring, summer, autumn 2016.

PAE name	Loca-tion	Content range of phthalates (n=3) in leachate in different seasons of 2015 and 2016 [µg/l]					
		2015			2016		
		Summer	Autumn	Winter	Spring	Summer	Autumn
Di-n-butyl phthalate (DBP)	Landfill 1	<LOQ	<LOQ	<LOQ	<LOQ	<LOQ	<LOQ
	Landfill 2	<LOQ	<LOQ	<LOQ	<LOQ	<LOQ-1.64	<LOQ
Di-isobutyl phthalate (DIBP)	Landfill 1	<LOQ	<LOQ	<LOQ	<LOQ	<LOQ	<LOQ
	Landfill 2	<LOQ	<LOQ	<LOQ	<LOQ-1.13	<LOQ-2.83	<LOQ
Di(2-ethylhexyl) phthalate (DEHP)	Landfill 1	<LOQ-38.6	<LOQ-20.2	16.5-19.6	2.7-4.7	11.3-12.8	<LOQ
	Landfill 2	<LOQ-19.3	<LOQ	<LOQ	<LOQ-2.3	<LOQ	<LOQ

Legend: LOQ for all PAEs (except DEHP) was 0.6 µg/l, LOQ for DEHP was 1.3 µg/l. For some samples LOQ was raised due to matrix interference. Measurement uncertainty was (+/-35%).

Table 2 Average precipitation in the region during sampling seasons.

Year	Season	Average precipitation in the region* [mm]
2015	Summer	32.65
	Autumn	47.65
	Winter	37.81
2016	Spring	37.20
	Summer	66.68
	Autumn	58.07

*Legend:*based on the data from meteorological stations provided by the Institute of Meteorology and Water Management—National Research Institute (IMGW-PIB).*

DEHP was the only PAE determined in the majority of samples analysed. It was observed, that mean concentrations of DEHP in leachate from landfill 1 were much higher than those determined in leachate from landfill 2 (see Figure 2).

Figure 2 Mean DEHP concentrations in municipal solid waste landfill raw leachate.

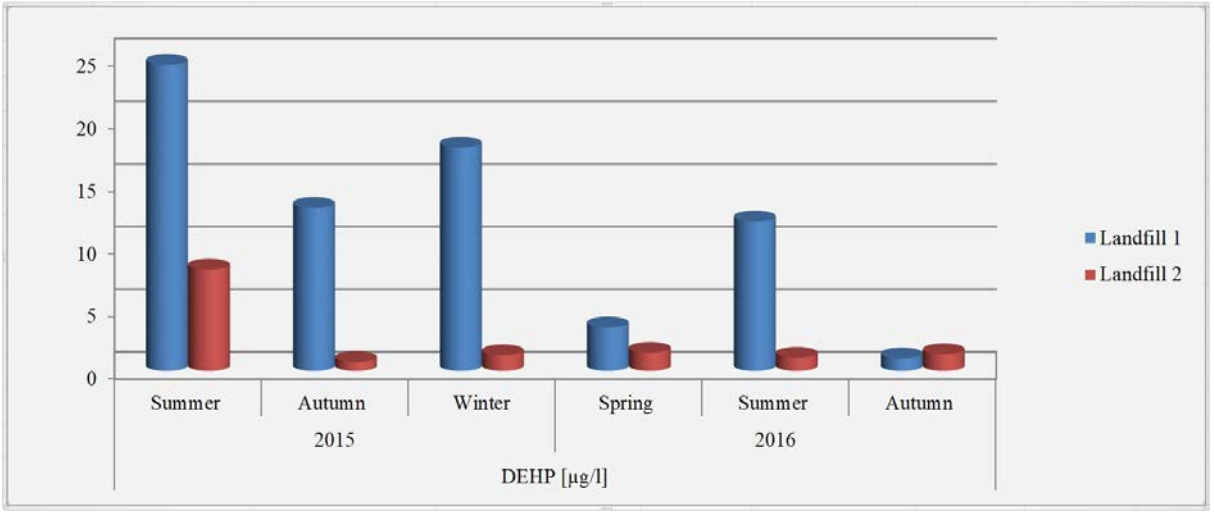

Legend: The concentrations presented on Figure 2 are average concentrations (n=3). In case a single sample concentration was <LOQ, the value 0.5LOQ was taken into average, in accordance with Commission Directive 2009/90/EC.

CONCLUSION

The research material, which consisted of the samples of raw landfills leachate, shows presence of the following PAEs in at least one sample: DEHP, DBP and DIBP. Out of all 10 analysed PAEs, DEHP was the most prevalent ranging from <LOQ to 38.6 µg/l.

There is a relationship between the landfill size and the PAE concentrations with comparable precipitations in the region. The landfill 1 releases more DEHP than landfill 2 as it contains more than fivefold amount of waste. Interesting fact is that landfill 1 underwent remediation in 1996 and has been closed for many years (since 2011) but DEHP emissions are still present in the leachate.

In 83% of samples mean DEHP concentrations exceeded (from 2.5 to 18.7 times) the acceptable EU limits for surface water (1.3 µg/l).

During the study no correlation between the sampling seasons and PAEs concentrations have been observed, which was also concluded by Asakura et al. (2004). The highest DEHP concentrations were detected on both landfills in summer 2015 (the driest of all investigated seasons).

ACKNOWLEDGEMENTS

The research was financially supported by the Polish Ministry of Science and Higher Education, grants numbers 10-OZ -BI-1492/15 and 10-OZ -BI-1516/16.

REFERENCES

Asakura, H. et al. 2004. Behavior of endocrine-disrupting chemicals in leachate from MSW landfill sites in Japan. Waste Management [Online], 24: 613–622. Available at: https://doi.org/10.1016/j.wasman.2004.02.004. [2018-08-20].

Erythropel, H.C. et al. 2014. Leaching of the plasticizer di(2-ethylhexyl)phthalate (DEHP) from plastic containers and the question of human exposure. Applied Microbiology and Biotechnology [Online], 98: 9967–9981. Available at: https://doi.org/10.1007/s00253-014-6183-8. [2018-08-20].

Europe Commission DGXI.E.3. 2000. ARGUS in association with University Rostock. The behaviour of PVC in landfill. Final Report. Available at: http://ec.europa.eu/environment/waste/studies/pvc/landfill.pdf. [2018-08-20].

Gao, D.W., Wen, Z.D. 2016. Phthalate esters in the environment: A critical review of their occurrence, biodegradation, and removal during wastewater treatment processes. Science of the Total Environment [Online], 541: 986–1001. Available at: https://doi.org/10.1016/j.scitotenv.2015.09.148. [2018-08-20].

Gao, M. et al. 2016. Effects of di-n-butyl phthalate and di (2-ethylhexyl) phthalate on the growth, photosynthesis, and chlorophyll fluorescence of wheat seedlings. Chemosphere [Online], 151: 76–83. Available at: https://doi.org/10.1016/j.chemosphere.2016.02.061. [2018-08-20].

Grynkiewicz-Bylina, B. 2011. Dangerous phthalates in children's environment. Ecological Chemistry and Engineering. S[Online], 18(4): 455–463. Available at: http://tchie.uni.opole.pl/ece_s/S18_4/S4_2011.pdf. [2018-08-20].

Gworek, B. et al. 2015. Influence of a Municipal Waste Landfill on the Spatial Distribution of Mercury in the Environment. PLoS ONE [Online], 10(7): e0133130. Available at: https://doi.org/10.1371/journal.pone.0133130. [2018-08-20].

Jonsson, S. et al. 2003. Mono- and diesters from ophthalic acid in leachates from different European landfills. Water Research [Online], 37: 609–617. Available at: https://doi.org/10.1016/S0043-1354(02)00304-4. [2018-08-20].

Koda, E. 2012. Influence of vertical barrier surrounding old sanitary landfill on eliminating transport of pollutants on the basis of numerical modelling and monitoring results. Polish Journal of Environmental Studies, [Online], 21(4): 929-935. Available at: http://www.pjoes.com/pdf-88824-22683?filename=Influence%20of%20Vertical.pdf. [2018-08-20].

Koda, E. et al. 2017. Levels of Organic Pollution Indicators in Groundwater at the Old Landfill and Waste Management Site. Applied Sciences [Online], 7(6): 638, Available at: https://doi:10.3390/app7060638. [2018-08-20].

Net, S. et al. 2015. Reliable quantification of phthalates in environmental matrices (air, water, sludge, sediment and soil): A review. Science of the Total Environment [Online], 515–516: 162–180. Available at: https://doi.org/10.1016/j.scitotenv.2015.02.013. [2018-08-20].

Przybylińska, P.A., Wyszkowski, M. 2016. Environmental contamination with phthalates and its impact on living organisms. Ecological Chemistry and Engineering. S, 23(2): 347–356.

Sailas, B. et al. 2015. A monograph on the remediation of hazardous phthalates. Journal of Hazardous Materials [Online], 298: 58–72. Available at: https://doi.org/10.1016/j.jhazmat.2015.05.004. [2018-08-20].

Vaverkova, M.D., Adamcova, D. 2018. Case study of landfill reclamation at Czech landfill site. Environmental Engineering and Management Journal, 17(3), 641–648. Available at: http://eemj.eu/index.php/EEMJ/article/view/3529. [2018-08-20].

Wowkonowicz, P., Kijeńska, M. 2017. Phthalate release in leachate from municipal landfills of central Poland. PLoS ONE [Online], 12(3): e0174986. Available at: https://doi.org/10.1371/journal.pone.0174986. [2018-08-20].

Assessment of the effect of landfill leachate irrigation of different doses on selected plants

Jan Zloch[1,2], Dana Adamcova[1], Tomas Vyhnanek[3], Vaclav Trojan[3], Jan Winkler[3], Biljana Dordevic[3], Marie Bjelkova[4], Maja Radziemska[5], Martin Brtnicky[2], Magdalena Daria Vaverkova[1]

[1]Department of Applied and Landscape Ecology
[2]Department of Geology and Pedology
[3]Department of Plant Biology
Mendel University in Brno
Zemedelska 1, 613 00 Brno
[4]Agritec, Research, Breeding and Services, Ltd.
Zemedelska 2550/16, 787 01 Sumperk
CZECH REPUBLIC
[5] Faculty of Civil and Environmental Engineering
Warsaw University of Life Sciences
Nowoursynowska 159
02-776 Warsaw
POLAND

jan.zloch@mendelu.cz

Abstract: Landfilling is one of the most common methods of waste management (WM). Landfilling of municipal solid waste (MSW) can pose a risk to the environment. During the disposal of waste, many physical, chemical and biological reactions occur in the landfill body, and pollutants (e.g. heavy metals) are generated that pose contamination of water present. Those contaminated waters are called leachate. Leachate water is drained into a leakage drainage pond which is isolated from the surrounding environment by a HDPE foil. However, there is a risk of contamination of the surrounding environment and therefore the quality of leachate water must be monitored. This study focuses on the assessment of leachate effects on plant material (*Cannabis sativa* L. and *Sinapis alba* L.). The phytotoxic effect of landfill leachate was provided according to the modified semichronic test to *Cannabis sativa* L. and *Sinapis alba* L. The methodology consists of establishing a phytotoxicity test using vital *Cannabis sativa* L. and *Sinapis alba* L. seeds and leachate samples in laboratory conditions. Seeds of hemp and mustard are cultivated in Petri dishes on a leachate solution of varying concentrations. From the comparison of the results (root lengths) and the reference samples, the inhibition or stimulation of leachate on plant growth is calculated. The conducted tests clearly show that the susceptibility of *Sinapis alba* L. to noxious agents is higher than in the other surveyed plant. Inhibition in mustard seeds at concentrations 50%, 75% and 100% was high. At the concentration of 20%, mustard exhibited a certain resistance and did not respond to harmful substances so sensitively as at the other concentrations. Both in mustard and in cannabis, the growth of roots was in some cases stimulated at the concentration of 20%.

Key words: waste, toxicity, root length, inhibition, concentration

INTRODUCTION

Common practice for the disposal of MSW is landfilling; however, landfills can become serious sources of soil and water pollution if technical measures and landfill facilities are. Landfills usually produce leachate water, i.e. leachates resulting from the surplus of precipitation and organic waste degradation within the landfill. Mixed with rainwater, leachates can pollute soil and groundwater, which has a potential impact on water ecosystems and human health (Romero et al. 2013). Leachates usually consist of diverse organic and inorganic compounds dissolved or suspended in wastewater (Mendoza et al. 2017). To prevent the pollution of the surrounding environment, the leachates have

to be drained and accumulated in the leachate pond. They can be also recycled directly on the landfill through waste biodegradation (Sonawane et al. 2017).

Understanding the possible impact on the environment and characteristics of leachates is important in choosing the most feasible methods of landfill water management. The objective of the present investigation was to deduce the effect of different doses of leachate application on the growth of selected plants. Our experiment was conducted to explore leachate effects on the growth of the seedlings of *Cannabis sativa* L. and *Sinapis alba* L. and to determine the tolerance of these plants to the contamination by leachates. Mustard is sensitive to the range of chemicals and hemp has a phytoremediation potential. This is reason why these plants are ideal for this study of toxicity. The study is a part of the long-term research of the Zdounky-Kuchyňky landfill.

MATERIALS AND METHODS

Site description

The Zdounky-Kuchyňky landfill (49.2490778N, 17.3121181E) has been in operation as disposal facility permitted to receive commercial and MSW since 1996 (Figure 1). The landfill is situated in a pronounced morphological depression and the existing roads III/428 17 Zdounky-Nětčice and III/432 15 Nětčice-Troubky demarcate its premises. Altitudes ranging from 240–396 m a.s.l. document the rugged topography. The landfill itself is situated at altitude of 251–280 m a.s.l. (Voběrková et al. 2017, Vaverková et al. 2018).

Figure 1 Location of Zdounky-Kuchyňky landfill

Natural conditions

The area on which the landfill is situated was formerly used for agriculture (plant production). Terrain is formed by a wide valley with an elevation of up to 30 m whose bottom descends iapproximately west direction. The area hydrographic axis is the surface watercourse of Lipinka, which opens into the Olšinka on the western limit of Zdounky. After ca 500 m, the Olšinka opens intthe Kotojedka surface stream. All these watercourses are little important for water management in the area. Climatically, the area belongs in the T2 warm zone with warm up to mildly warm springs, long warm and dry summers, very short transitional periods of autumn, and mildly warm, dry up to very dry winters with a very short period of snow cover (Voběrková et al. 2017, Vaverková et al. 2018).

Basic characteristic of the facility

Landfill is a facility for the disposal of waste, at the terrain level or beneath (Code D1, Annex no. 23, Decree no. 383/2001 Sb. on waste management details). The landfill is classified as falling in the S-OO group (other waste), subgroup S-OO3. It is intended for the storage of waste from the category of other waste including waste materials with a substantial content of organic, biologically decomposable substances, which cannot be assessed based on their aqueous leachates. A part of the landfill body was sealed and reclaimed in two phases. Biogas pumped from the landfill is burnt in the motor-generator unit producing electric energy. A part of the landfill body crown

is operated as a composting plant. In 2013, a new part of the landfill (so-called 4th phase) was put into operation, linked with the hitherto used landfill bottom (Voběrková et al. 2017, Vaverková et al. 2018).

Leachate sampling

Landfill leachate samples (Figure 2) were collected from February through December of 2017. The samples were not collected in January (2017) because the ponds were frozen. The frequency of collecting the samples was once a month. Samples (0.5 L/sample) of leachate were collected in sterile collection containers. The sample were stored in airtight polyethylene bottles and transported to the laboratory for chemical analysis. Parameters of pH, electrical conductivity (EC), dissolved oxygen (DO) were estimated on site (in situ) at the time of sampling with a Multi-Parameter Meter HQ30d Portable. Preliminary analyses of the leachate were conducted in 2017. Seasonal changes and toxic potency of leachate were determined by Zloch et al. 2018 using *Sinapis alba* L. (mustard). Remaining samples were kept for further analysis in freezer at -18 °C in the dark in order to keep its characteristics constant.

Figure 2 Landfill leachate samples collection and in situ analyses

Phytotoxicity test

Cannabis sativa L. and *Sinapis alba* L., were used as a test organism to assess toxicity of the samples. The treatments consisted of various concentrations of 20%, 50%, 75% and 100%. Each dilution series concentration was tested using three replicate samples. *Cannabis sativa* L. and *Sinapis alba* L., were exposed to the solutions for a total of 72 h. The seeds were germinated in petri dishes on filter paper on the bottom. The distilled water with tested liquid (leachate) was added into each dish, and 15 healthy looking seeds of similar size were evenly spread onto the surface of the filter paper. The petri dishes were covered by a glass cap to prevent loss due to evaporation and were located in the dark thermostat (t = 24 °C, air humidity 80%). Root length were recorded at the end of the 3 day.

Figure 3 Root length test

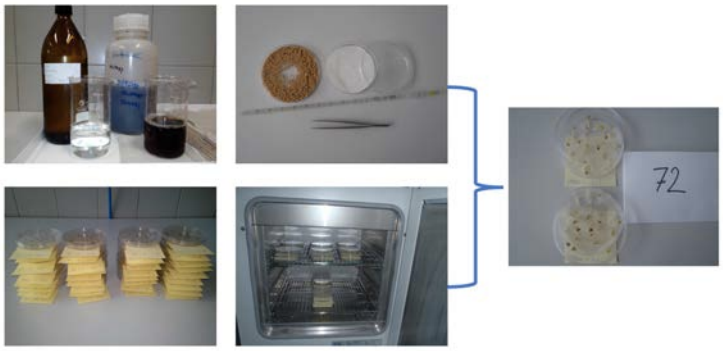

Calculations and Data analysis

The analyses and the length measurements were performed using the Image Tool 3.0 for Windows (UTHSCSA, San Antonio, USA). The bioassays were performed in three replicates. The root growth inhibition (RI) were calculated with the formula (Eq. 1):

$$RI = A - B/A \times 100 \qquad (1)$$

Where: A means root length in the control; B means root length in the test; RI means root growth inhibition.

RESULTS AND DISCUSSION

Table 1 shows results of analysed parameters of leachate collected from the Kuchyňky landfill of MSW.

Table 1 Chemical parameters of leachate (wastewater)

Source of water	Parametr	Month										
		2	3	4	5	6	7	8	9	10	11	12
Landfill leachate - leachate pond	DO [mg/l]	6.61	4.45	1.93	0.63	1.21	3.66	2.17	4.58	1.46	1.13	2.08
	pH	6.48	7.5	8.05	8.05	7.8	8.17	8.17	7.66	7.66	7.36	8.7
	CONDUCTIVITY [µS/cm]	2069	5260	12020	10400	10540	9240	9950	10750	12900	6650	12930

The leachate pH was mainly alkaline (average 7.8). Furthermore, low values of dissolved oxygen (DO) in the leachate (0.6–6.6 mg/dm^3, average 2.7 mg/dm^3) indicated high organic pollution of this water. Leachate conductivity was 2069–12930 µS/cm.

Leachate toxicity – *Cannabis sativa* L.

Our results showed that the root length of *Cannabis sativa* L. cultivated in the leachate originating from the Kuchyňky landfill of MSW Kuchyňky was inhibited in a majority of samples (Figure 4).

Figure 4 Inhibition of Cannabis sativa L. root length cultivated with leachate

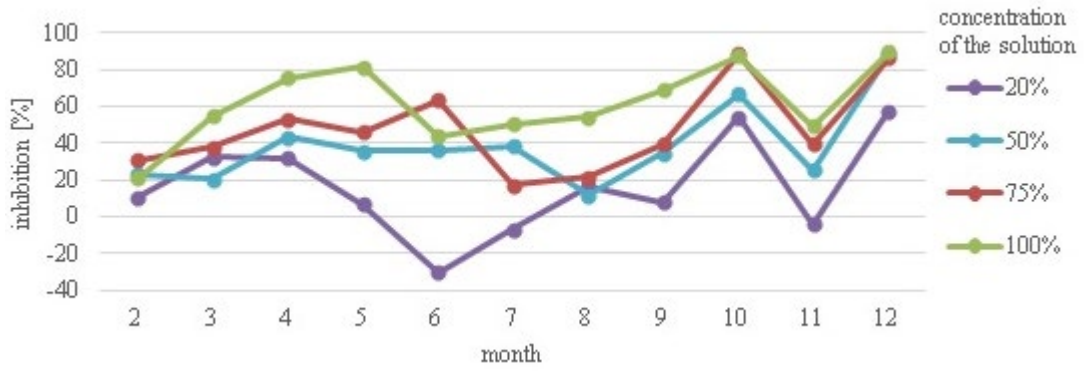

The greatest inhibition occurred in October samples with the leachate concentration of 75% and in December samples with the remaining leachate concentrations (20%, 50%, and 100%). In the case of the full leachate concentration, the inhibition ranged between 21.1% in February and 87.8% in October up to 89.8% in December. The root length of *Cannabis sativa* L. was higher when the leachate for cultivation was diluted with distilled water, mainly in samples collected in February and during the vegetation season between May and August. The inhibition of roots growth at the 75% concentration of leachate ranged from 17.4% in July to 88.8% in October; at the 50% concentration, it ranged from 12.0% in August to 88.9% in December, whereas at the 20% concentration it was from 6.8% in May to 57.4% in December. Only in 3 samples cultivated with the leachate at the concentration of 20%, root length surpassed the control test by 30.1%, 6.7% and 4.2% in June, July and November, respectively. Growth stimulation in these months for concentration of 20% was due to lower concentrations of pollutants in leachates.

Leachate toxicity – *Sinapis alba* L.

A comparable pattern was observed for the inhibition of *Sinapis alba* L. root length cultivated with the same leachate and shown in Figure 5. Likewise, the root length was higher in the case of diluted leachate and in samples collected in February and March, and during the summer months, too. However, *Sinapis alba* L. was more responsive and sensitive to toxic components found in the leachate sample.

Figure 5 Inhibition of Sinapis alba L. root length cultivated with leachate

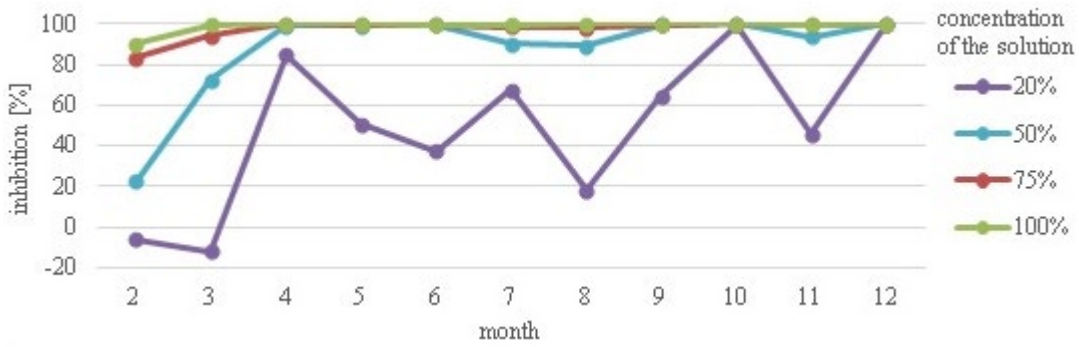

All samples with the 75% leachate concentration and a majority of samples with the leachate concentrations of 50% and 20% exhibited the inhibition higher than 80%, while in the case of the full leachate concentration, all samples showed the inhibition even higher than 90%. The inhibition of samples collected in October and December was equal (approximately 100%) at all concentrations. The lowest inhibition at the 50% leachate concentration was equal to 22.6% and observed in samples from February, and the lowest inhibition at the 20% leachate concentration was 17.9% and observed in samples from August. Moreover, samples cultivated at the 20% leachate concentration surpassed the control test by 5.9% and 11.9% in February and March, respectively. The quantity and quality of leachate is influenced by the amount, composition and moisture content of the solid waste, as well as by local factors such as hydrogeological conditions, climate, and height and type of landfill. Moreover, high annual precipitation can be the reason for relatively low leachate toxicity. In our case, root growth stimulation for the concentration of 20% was due to lower concentrations of pollutants in leachates.

Phyto-toxicity of landfill wastewaters has been subject to many studies of which one explores a potential relationship between the physical and chemical properties of leachates and their toxicity (Pablos et al. 2011, Budi et al. 2016). With respect to the fact that leachates represent mixtures of toxic substances released from the stored waste, risks should be realized connected with their possible leakages into the surrounding environment. The results of our research indicate that although *Cannabis sativa* L. exhibits certain inhibition to the action of toxic substances, it is still more resistant than *Sinapis alba* L. the plant resistance being given by its remediation capacity (Davison et al. 2006). *Cannabis sativa* L. has a potential to deposit toxic pollutants in its biomass in the form of heavy metals (Sinha et al. 2006), which results in its higher resistance to the action of harmful substances as compared with other plants – in our study represented by *Sinapis alba* L.

CONCLUSION

Our experiment was to characterize properties of leachate waters from the landfill. Leachates represent a mixture of harmful substances released from the stored waste and precipitation water, the properties of which change during the year. The phytotoxicity tests confirmed the negative influence of leachates on higher plants, resp. on their growth of roots. The experiment demonstrated that the seeds of *Sinapis alba* L. are more susceptible to leachates (especially at higher concentrations) than the seeds of *Cannabis sativa* L. Thanks to its adaptability and phytoremediation capacity, *Cannabis sativa* L. represents a potential for being used in the decontamination of the environment and the species is a subject of numerous studies. The detected values bring important information about a possible impact of leachates on the vegetation in landfill surroundings and can be used for landfill management. Data from the long-term monitoring of landfill leachates are necessary

to understand how the properties may change after the landfill closure (in case that the landfill is covered with a sealing layer to prevent penetration of precipitation water).

ACKNOWLEDGMENTS

The research was financially supported by grant IGA No. TP 5/2017.

We would like to express our great appreciation to the management of the landfill DEPOZ, Ltd. Namely, we are very grateful to Ing. Ivan Mohler and his colleagues for their assistance and their willingness to provide their time so generously. We would like to express our appreciation to Dr. Anna Adamska (Poznań University of Life Sciences, Faculty of Environmental Engineering and Spatial Management) for her assistance in sample preparation and analysis.

REFERENCES

Budi, S. et al. 2016. Toxicity identification evaluation of landfill leachate using fish, prawn and seed plant. Waste Management, 55: 231–237.

Davison, L. et al. 2006. Dealing with nitrogen in subtropical Australia: seven case studies in the diffusion of ecotechnological innovation. Ecological Engineering, 28: 213–223.

Mendoza, M.B. et al. 2017. Groundwater and leachate quality assessment in balaoan sanitary landfill in la union, northern Philippines. Chemical Engineering Transaction, 56: 247–252.

Pablos, M.V. et al. 2011. Correlation between physicochemical and ecotoxicological approaches to estimate landfill leachates toxicity. Waste Management, 31: 1841–1847.

Romero, P. et al. 2013. Raw and digested municipal waste compost leachate as potential fertilizer: comparison with a commercial fertilizer. Journal of Cleaner Production, 59: 73–78.

Sinha, S. et al. 2006. Distribution of metals in the edible plants grown at Jajmau, Kanpur (India) receiving treated tannery wastewater: relation with physico-chemical properties of the soil. Environmental Monitoring and Assessment, 115: 1–22.

Sonawane, J.M. et al. 2017. Landfill leachate: A promising substrate for microbial fuel cells. International Journal of Hydrogen Energy, 42(37): 23794–23798.

Vaverková, M.D. et al. 2018. Assessment and evaluation of heavy metals removal from landfill leachate by *Pleurotus ostreatus*. Waste and Biomass Valorization, 9(3): 503–511.

Voběrková, S. et al. 2017. Effect of inoculation with white-rot fungi and fungal consortium on the composting efficiency of municipal solid waste. Waste Management, 61: 157–164.

Zloch, J. et al. 2018. Seasonal Changes and Toxic Potency of Landfill Leachate for White Mustard (Sinapis alba L.). Acta Universitatis Agriculturae et Silviculturae Mendelianae Brunensis, 66(1): 235–242.

FOOD TECHNOLOGY

The use of saturated medium-chain fatty acids in wine production technology

Klara Chvalinova, Mojmir Baron, Jiri Sochor
Department of Viticulture and Viniculture
Mendel University in Brno
Valticka 337, 69144 Lednice
CZECH REPUBLIC

klarachvalinova@seznam.cz

Abstract: The use of sulphur dioxide has a long history in viniculture. Due to its negative effect on human health, it is necessary to search for substances that could reduce, or even exclude, the need for sulphur dioxide in wine making. One option is use of saturated medium-chain fatty acids (MCFA) that can inhibit yeast activity. In this study, the effect of mixing octanoic acid (C_8), decanoic acid (C_{10}) and dodecanoic acid (C_{12}) in the ratio 2:7:1, respectively, on their residuals and sensory properties is examined. After application of six different concentrations in combination with two doses of SO_2, the MCFA content was measured and sensory analysis was performed. The results show that the higher the dose of MCFA is, the more of them were bound to the yeast bodies and the lower the content is in the wine. Sensory analysis shows a dose of 20 mg/l as a limit, below which consumers are unable to perceive differences among MCFA doses, and the odour of MCFA declines with the duration of wine ageing.

Key Words: saturated medium-chain fatty acids, octanoic acid, decanoic acid, sulphur dioxide, yeast

INTRODUCTION

Sulphur dioxide (SO_2) is a very important additive in wine production. It inhibits reproduction of yeasts, which causes deceleration or stopping of alcoholic fermentation. It also kills bacteria that can bring about the incidence of wine diseases. Concurrently, it deactivates oxidation enzymes and bonds oxidation products and also oxygen. Thanks to these effects, it has been used for many centuries. Although the addition of SO_2 to wine was temporarily prohibited in 15th century, its use, although still legally limited, has been preserved until today.

Most winemakers would agree that it is impossible to dispense with sulphur dioxide in wine production, it is only possible to limit its quantity. However, the fundamental problem remains that SO_2 is a major allergen (notification of its content at a concentration above 10 mg/l must be given) and consumption at higher doses causes health issues (headache, stomach ache, asthmatic problems) (Lester 2013); therefore, restriction of its application, due to the ever–increasing consumption of wine in the Czech Republic, is highly desirable.

This problem could be solved by the introduction of new substances (as a supplement to SO_2) that have the same effects on microorganisms as sulphur dioxide while not harming human health and not influencing the sensory properties of the wine. In this case, an interesting group is saturated medium-chain fatty acids. These compounds occur in wine naturally – they can be produced by yeasts themselves as intermediates of lipid synthesis during fermentation (Tehlivets et al. 2007). Some of them support alcoholic fermentation, such as palmitic acid (C_{16}) and stearic acid (C_{18}) but acids with shorter chains, octanoic acid (C_8), decanoic acid (C_{10}) and dodecanoic acid (C_{12}) cause its deceleration, particularly in late-fermentation phases (Viegas and Sa-Correia 1997). There are changes in the lipid build-up in the cytoplasmic membranes of yeast, the pH of the cell decreases and the proton gradient is disturbed (Alexandre et al. 1996), and cells then lose their viability.

The advantage of MCFA, unlike sulphur dioxide, is their harmlessness to health. They occur naturally in animal milk fats and coconut oil. However, their disadvantage is that they lack antioxidant effects. They can also influence the aromatic expression of the wine – their aroma resembles coconut, soap, dull fat, wax (Li et al. 2008). Due to low effective doses applied to wine, the risk is negligible.

The aim of this study is to monitor the effects of saturated medium-chain fatty acids used in wine technology, especially their behaviour after application to wine and their influence on the sensory properties of wine.

MATERIAL AND METHODS

Design of experiment

After the grapes were processed, the must was transferred to a stainless-steel tank, where alcoholic fermentation started after 48 hours. During the fermentation of the must to a residual sugar content of 17.6 g/l, 36 l of wine was taken and subsequently divided into 12 carboys with a volume of 3 l then further divided into two rows. Immediately after distribution, a mixture of saturated fatty acids was applied in quantities of 5, 10, 20, 30, 40 and 60 mg/l to each row. After 24 hours of application of the saturated fatty acids, a sample was taken from each carboy into a glass vial with a volume of 187 ml. All 12 samples were stored in the freezer. Subsequently, sulphur dioxide in the form of liquid sulphur (ammonium bisulphite) was applied at doses of 20 mg/l to one row and 40 mg/l to the second row. After 48 hours application of a mixture of saturated fatty acids, samples from each carboy were taken again. Sampling was again carried out after 168 hours and 672 hours (one month) of the application of sulphur dioxide.

Material

In this experiment the must of variety 'Hibernal' was used. Sulphur dioxide was used in liquid form as 40% ammonium hydrogen sulphite, namely Supersolfosol (BS Vinarske potreby, Czech Republic).

Saturated fatty acids were applied in the form of a mixture of octanoic acid (C_8), decanoic (C_{10}) and dodecanoic (C_{12}) with ratio 2:7:1, respectively. A hundred mg of the mixture was dissolved in 1 l of aqueous potassium hydroxide solution. This solution was applied to the wine in combination with sulphur dioxide, and these combinations are shown in the Table 1.

Table 1 MCFA and SO_2 application variants

Amount of SO_2 (mg/l)	Amount of MCFA (mg/l)					
20	5	10	20	30	40	60
40	5	10	20	30	40	60

Methods

In basic analysis of the must, the sugar content was determined refractometrically (Altago, Japan), titratable acid content and assimilable nitrogen content were determined using a TitroLine Easy automatic titrator (manufacturer SI Analytics GmbH, Germany) and the pH of the must was determined with a pH meter (WTW pH 526 and SenTix 21 pH electrode WTW, Germany). Residual sugar was determined with an ALPHA analyser (Bruker, USA) operating on the principle of Fourier transform infrared spectrometry using the Attenuated Total Reflection (ATR) sampling technique. To determine the content of saturated fatty acids before and after the mixture application, a gas chromatography mass spectrometer (GC-MS, Shimadzu, Japan) was used. The results were statistically processed (Statistics, StatSoft, USA).

RESULTS

Using the gas chromatograph, the content of the saturated fatty acid residues in the wine was analysed. Two variants of sulphur dioxide dosing, 20 mg/l and 40 mg/l, were used during the experiment. However, the results show that the sulphur dioxide content does not have a significant effect ($\alpha = 0.05$) on the content of saturated MCFAs in the wine, and the residue is generally higher (not shown) at 40 mg/l; however, this difference is negligible. Also, the results of dodecanoic acid are not significant, therefore they are not shown.

MCFA content before the MCFA mixture application:

C_8 – 6.76 mg/l

C_{10} – 2.18 mg/l

MCFA content

Results of statistical analysis at a significance level of $\alpha = 0.05$ (Figure 1) show the differences between the individual resultant octanoic or decanoic acid values are not as significant as the differences between the original doses, while at a dose of 5 mg/l, approximately 40% of the MCFA content has been attached (final C_8 content 7.31–7.67 mg/l, C_{10} 2.68–3.09 mg/l), and more than 85% MCFA was attached at a dose of 60 mg/l (final C_8 content 12.05–14.025, C_{10} 7.17–9.72 mg/l). These results indicate an increasing ability of yeast to receive and bind saturated fatty acids with increasing dose of MCFA. Analyses were performed on samples 24 hours, 168 hours and 672 hours after SO_2 application. The resulting MCFA content remains almost unchanged over 672 hours.

Figure 1 Octanoic and decanoic acid content depending on MCFA dose

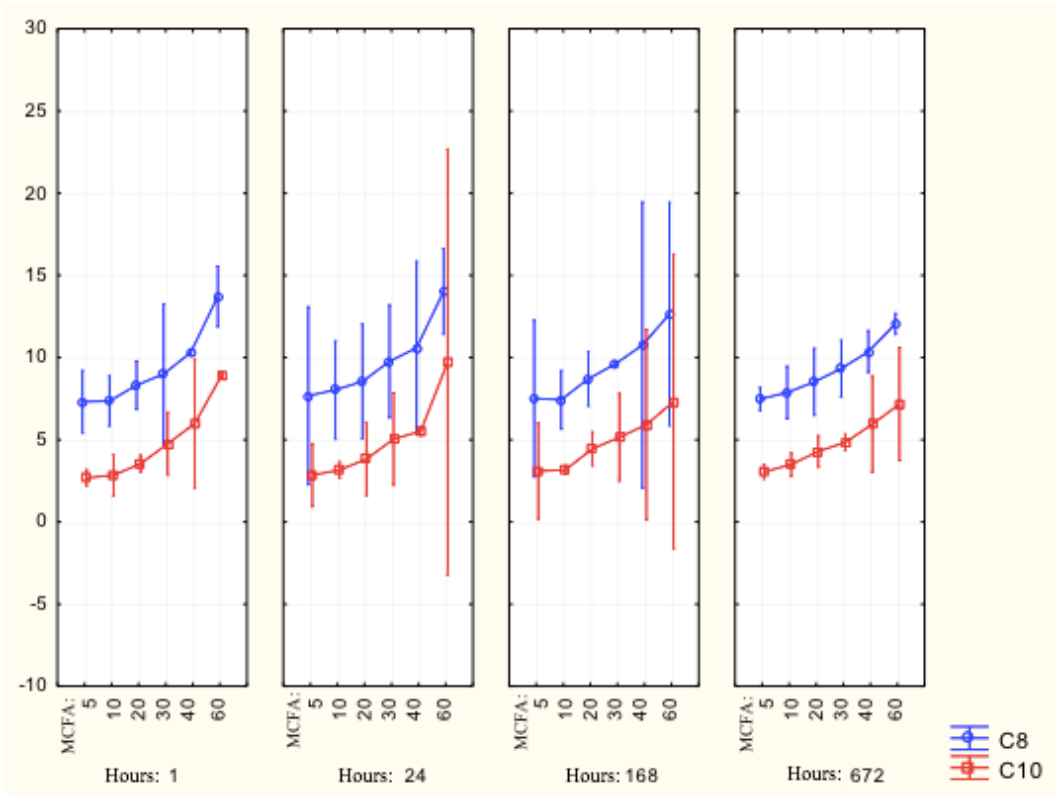

Sensory analysis

Sensory analysis of the wine was carried out 24 hours after SO_2 application, one month (672 hours) after SO_2 application and 3 months (1800 hours) after SO_2 application, for all 12 variants. Sensory expression of saturated MFCA, usually described as 'coconut, soap, ductile fat, wax', was evaluated. Each of twelve glasses contained one sample according to the variants listed in Table 1. The expression was scored points, ranging from 1 to10 points, with 10 being the best (the highest intensity of expression). The significance level of the statistical analysis was $\alpha = 0.05$.

An important limit in this study is 20 mg/l MCFA. At doses of 20 mg/l MCFA and less, the evaluator is not able to perceive differences between doses. At doses higher than 20 mg/l, the expression of MCFA increases and becomes more evident to the evaluator. However, at doses of 30, 40 and 60 mg/l the differences of perception are eliminated again, and the differences between the assigned points is minimal (Figure 2).

Figure 2 shows the MCFA sensory-expression evaluation. The most striking sensory response occurs 24 hours after the application of SO_2, and the lowest occurrence 1,800 hours after the application

of SO_2. As the number of hours increases, the sensory effect of saturated fatty acids reduces. After application, the MCFAs are bound to the yeast bodies and the sludge particles are gradually deposited on the bottom of the vessel.

The amount of SO_2 applied does not have a pronounced effect on the expression of saturated middle-chain fatty acids.

Figure 2 Sensory response depending on time and dose of MCFA applied

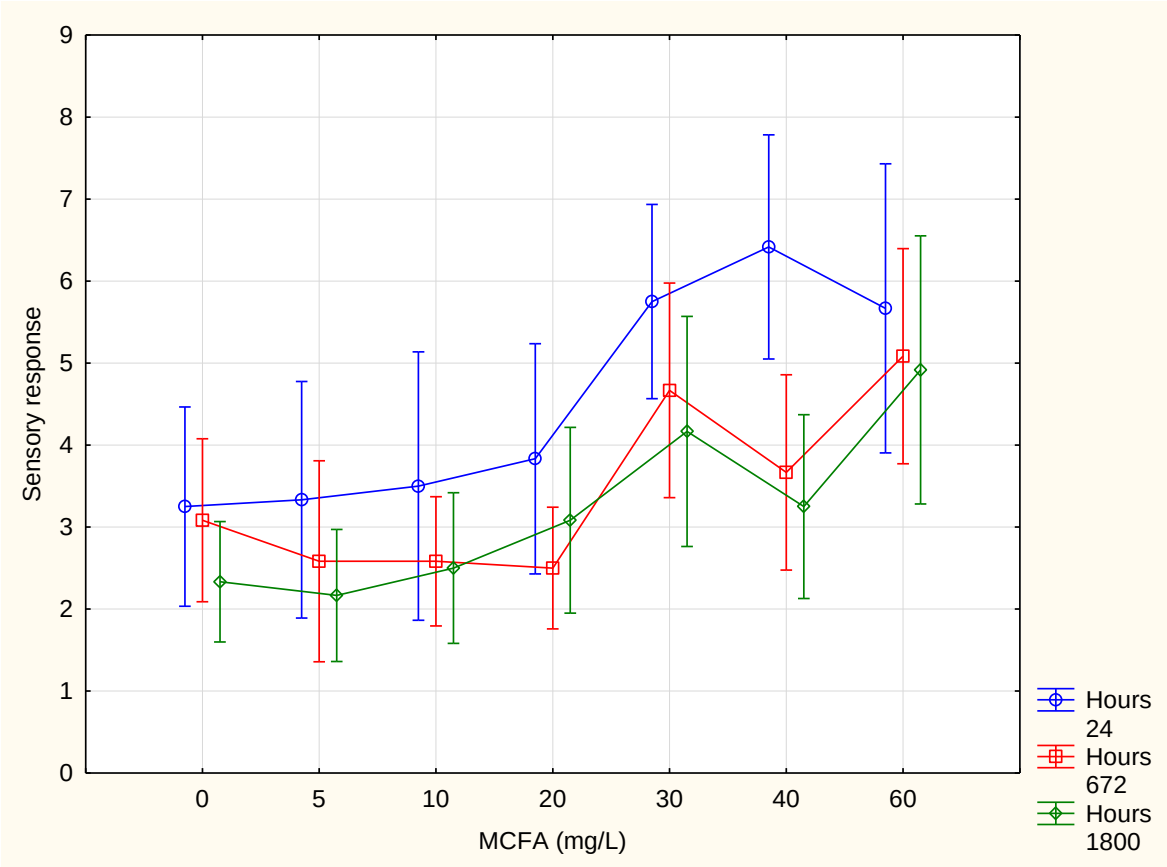

DISCUSSION

It is important to detect substitutes or supplements of sulphur dioxide, due to their harmful effects on health. In several scientific papers (Baron 2013, Babikova et al. 2012), although still not quite enough the effect of MCFA added to wine on yeast during fermentation was investigated, although the effects of fatty acids have been a subject of research for a relatively long time (Viegas et al. 1989). The results of this study show that the more MCFA added, the more of them were received by the yeasts. Although the resulting residues were logically higher with higher dose added, the ratios of bound MCFA were different. This phenomenon could be explained by the fact that the more MCFA contained, the higher is the activity of cell carriers and the greater is the amount of MCFA the yeast receives. Given the ratio of MCFA in the mixture, there was a significantly higher intake of decanoic acid, which coincides with the results achieved by a team of French scientists (Lafon-Lafourcade et al. 1984). At the end of the fermentation due to increased membrane permeability, decreased ATP concentration and inhibition of ATPase may incur yeast-cell disruption and pouring out of their contents into the surroundings (Viegas et al. 1989).

The sensory properties of MCFAs have been studied exclusively in ethanol and water solutions (Ferreira et al. 2000, Gomez-Miguez et al. 2007). The results of the studies point to the fact that evaluation of the sensory expression of saturated fatty acids shows an even lower number of points with an increasing number of hours (weeks). Over time, sludge particles, including dead yeast with MCFAs bound, are deposited on the bottom of the vessel, and thus the typical sensory expression of these acids is fades away. This fact is very positive for wine-making practice, due to the low dosages added which should not exceed 10 mg/l (Babikova et al. 2012, Baron et al. 2017). An important limit

in this experiment appears to be the 20 mg/l MCFA dose. At doses of 5, 10 and 20 mg/l, evaluators were unable to recognise a difference between these doses, while at doses of 30, 40 and 60 mg/l there was a significant increase in typical expression. In Babikova's work (Babikova et al. 2012), the negative effect of saturated MFCAs is perceived by all evaluators only at a dose of 30 mg/l or higher. Differences between the values of this study and the work of the Babikova can be caused, for example, by different varieties, the temperature of the wine and the glasses, as well the subjective response of the evaluator playing an important role.

CONCLUSION

The aim of the study is to observe the MCFA's behaviour after being added to wine and their influence on the sensory properties of the wine. The results of this experiment (MCFA residues) show that approximately 40% of MCFA content is bound at a dose of 5 mg/l, but more than 85% of MCFA is bound at a dose of 60 mg/l, therefore increasing the dose of MCFA also increases the rate of MCFA absorption by yeasts. This applies to both octanoic acid and decanoic acid. Sensory analysis was an important part of the experiment. This shows an MCFA dose of 20 mg/l as the limit above which we are able to recognise the differences in MCFA doses. At a dose of 20 mg/l the expression of saturated fatty acids is minimal. There is also the influence of sludge particles. During maturation, sludge particles with MCFA–bound yeast cells are deposited, and thus their sensory effect is reduced. Due to the low doses of MCFA used, this is positive for wine makers.

REFERENCES

Alexandre, H. et al. 1996. Alteration in membrane fluidity and lipid composition, and modulation of H(+)–ATPase activity in Saccharomyces cerevisiae caused by decanoic acid. Microbiology, 142(3): 469–475.

Babikova, P. et al. 2012. Increasing the efficiency of sulphur dioxide in wine by using of saturated higher fatty acids. Acta Universitatis Agriculutrae et Silviculturae Mendelianae Brunensis, 60(1): 17–22.

Baron, M. 2013. Možnosti snížení obsahu oxidu siřičitého v technologii révových vín: původní vědecká práce. 1 vyd. Brno: Mendelova univerzita v Brně: Folia Universitatis Agriculturae et Silviculturae Mendelianae Brunensis.

Baron, M. et al. 2017. The inhibition of Saccharomyces cerevisiae population during alcoholic fermentation of grape must by octanoic, decanoic and dodecanoic acid mixture. In Proceedings of 40th World Congress of Vine and Wine 2017 [Online]. Lednice. BIO Web of Conferences, pp. 1–6. Available at: https://www.bio-conferences.org/articles/bioconf/abs/2017/02/bioconf-oiv2017_02025/ bioconf-oiv2017_02025.html. [2018-09-10].

Ferreira, V. et al. 2000. Quantitative determination of the odorants of young red wines from different grape varieties. Journal of the Science of Food and Agriculture, 80(11): 1659–1667.

Gomez–Miguez, M.J. et al. 2007. Volatile components of Zalema white wines. Food Chemistry, 100(4): 1464–1473.

Lafon–Lafourcade, F. et al. 1984. Inhibition of Alcoholic Fermentation of Grape Must by Fatty Acids Produced by Yeasts and Their Elimination by Yeast Ghosts. Applied and Environmental Microbiology, 47(6): 1246–1249.

Lester, M.R. 2013. Sulfite sensitivity: significance in human health. Journal of the American College of Nutrition, 14(3): 229–232.

Li, H. et al. 2008. Impact odorants of Chardonnay dry white wine from Changli County (China). European Food Research and Technology, 227(1): 287–292.

Tehlivets et al. 2007. Fatty acid synthesis and elongation in yeast. Biochimica et Biophysica Acta (BBA) – Molecular and Cell Biology of Lipids, 1771(3): 255–270.

Viegas, C.A., Sa–Correia, I. 1997. Effects of low temperatures (9–33°C) and pH (3.3–5.7) in the loss of Saccharomyces cerevisiae viability by combining lethal concentrations of ethanol with octanoic and decanoic acids. International Journal of Food Microbiology, 34(3): 267–277.

Viegas, C.A. et al. 1989. Inhibition of Yeast Growth by Octanoic and Decanoic Acids Produced during Ethanolic Fermentation. Applied and Environmental Microbiology, 55(1): 21–28.

Use of dry ice in wine technology

Radim Holesinsky[1], Mojmir Baron[1], Jiri Mlcek[2], Tunde Jurikova[3], Jiri Sochor[1]

[1]Department of Viticulture and Enology
Mendel University in Brno
Valticka 337, 691 44 Lednice

[2]Department of Food Analysis and Chemistry
Tomas Bata University in Zlín
Vavreckova 275, 760 01 Zlín
CZECH REPUBLIC

[3]Institute for Teacher Training
Constantine the Philosopher University in Nitra
Drazovska 4, 949 74 Nitra
SLOVAK REPUBLIC

holes.radim@gmail.com

Abstract: This experiment focuses on the use of dry ice for maceration in rosé wine. Wines produced using two different methods, a short maceration and a cold maceration for 14 days, are compared in this paper. The wines were made from the Blaufränkisch variety. We focused on analysing total polyphenolic compounds, total anthocyanins, and total flavanols. Antioxidant activity was determined using the DPPH test. Each method was determined spectrophotometrically by a biochemical analyser. We confirmed a higher content of all these measured values in rosés in the cold maceration. Polyphenolic compounds were increased by 17% and antioxidant activity by almost 80%. Flavanol content was increased by 170% and anthocyanin content by 50%. Sensory analysis results were interesting as wine produced by cold maceration proved to be more intense and richer in aroma and taste.

Key Words: cryomaceration, rosé, dry ice, antioxidants, antioxidant activity

INTRODUCTION

Cryomaceration is a widely used technology today. This is a maceration of must with a quick subcooling of crushed and stem-free grapes below 5 °C. The must is left cool for several hours or days at this temperature. The basis is extracting a large number of substances contained in the skin. This process takes place without alcohol and the substances are soluble in an aqueous solution (Ortega-Heras et al. 2012).

The purpose of cryomaceration is the intense extraction of flavour compounds, phenols, and monoterpenes caused by longer contact times between skin and must (Moreno-Arribas and Polo 2009).

Wines produced by cold maceration show a higher amount of aromatic compounds compared to wines produced by the conventional method without subcooling. Such wines also show a higher stability to oxidation and better variety properties in terms of both aroma and taste.

The cold maceration method is used to improve the overall character of the wine and increase varieties. Complex, full-bodied wines are created. Thanks to this, we can produce higher quality wine with better properties than when we use the conventional method (Parenti et al. 2004).

Álvarez et al. (2006) has the same opinion that varietal wines are produced during maceration. The taste of wines is full, extractive, and harmonious and the aroma is more aromatic than in wines pressed immediately.

MATERIAL AND METHODS

Material

Blaufränkisch grapes were harvested manually. The harvesting took place in the Moravia wine-growing zone, Mikulov subregion, Lednice wine village, Na Valtické vineyard site.

Grape harvesting took place on 1 November 2016. The measured sugar content at harvest was 20.3 °NM. The pH was 3.32, the titratable acid content 6.9 g/l and the assimilable nitrogen content was 214.5 mg/l. The initial pomace temperature was 11 °C.

Technology of Preparation

The harvested grapes were crushed using a grape crusher (Enoitalia, Italy) and the must was divided into two plastic containers with vessel 1 for conventional maceration and vessel 2 for cryomaceration. There was approximately 100 kg of must in each vessel. The temperature for control maceration was 11 °C. Control maceration was for 1 day. For cryomaceration was the temperature between 3–4 °C. Cold maceration with ice was for 14 days.

Sample Preparation

The wines were centrifuged (3000 x g; 6 min.) before determining individual parameters. Each spectrophotometric determination was performed using a Miura One automated biochemical analyser (I.S.E. S.r.l.; Guidonia (RM) – Italy), where the incubation takes place at 37 °C and incubation times need to be adjusted to the operating cycles of the device.

Estimation of Contents of Total Phenols

The Folin-Ciocalteu method, based on the reduction of a phosphotungsten-phosphomolybdate complex by phenols to blue reaction products, was used for determination of phenolic compounds. The sample (0.5 mL) was pipetted into cuvette and diluted with ACS water (1.5 mL). Subsequently, Folin-Ciocalteu reagent (50 µL) was added and the solution was incubated at 22 °C for 30 min. The absorbance was measured using a HELIOS Gama spectrometer at a wavelength $\lambda = 670$ nm against blank. Results were expressed as equivalents of gallic acid in mg/100 g.

Estimation of Total Contents of Anthocyanins

These measurements were performed using well-established spectrophotometric methods (Somers and Evans 1977, Zoecklein et al. 1990). The wine sample was placed into a 0.2-cm path-length quartz cuvette, 200 µL of the sample and 1.8 mL of 1.1 M HCL were added and the resulting solution was thoroughly mixed and kept for a period of 180 min at the room temperature. A 0.22 M solution of $K_2S_2O_5$ was used as a blank. The absorbance was read at 520 nm (A_{520}^{HCl}) for anthocyanins. Concentrations of total anthocyanins (mg L^{-1}) were calculated as follows:

Total content of anthocyanins (mg/L) = 4 × dilution × [A_{520}^{HCl} – (5/3) × A_{520}^{SO2}]

Estimation of Total Flavanols

Total flavanols were estimated using the *p*-dimethylaminocinnamaldehyde (DMACA) method (Vivas et al. 1994). As compared with the widely used vanillin method, a great advantage of this method is that there is no interference from anthocyanins. Wine (20 µL) was poured into a 1.5-mL Eppendorf tube and 980 µL of DMACA solution (0.1% in 1 M HCl in MeOH) was added. The mixture was vortexed and allowed to react at the room temperature for 12 min. The absorbance at 640 nm was then read against a blank sample prepared in a similar way but without DMACA. Results were expressed as mg/L of catechin equivalents.

Estimation of Antioxidant Activity by the DPPH Method

The determination procedure was described earlier (Sochor et al. 2010). When doing this, a 150 µL volume of the reagent (0.095 mM 2.2-diphenyl-1-picrylhydrazyl – DPPH) was incubated with 15 µL of wine sample. The absorbance was measured at 505 nm for 10 min and the output ratio was calculated as a difference between absorbance values measured at the 10th minute and the 2nd minute of the assay procedure.

Sensory Analysis

The sensory analysis took place on 21 March 2017. The wines were evaluated by 12 tasters all certified according to CSN ISO 8586-1 or CSN ISO 8586-2. All varieties were rated using a 100-point scale according to OIV.

RESULTS AND DISCUSSION

Secondary metabolites are mostly contained in the grape skin; these are mainly phenolic and aromatic compounds. There are different options for breaking the skin and releasing the substances. Maceration of grapes is one of the first technological steps in winemaking and, at the same time, one of the most important. The basis of future wines is formed at this stage. High levels of pigments and other substances are released during maceration, which is due to the disturbance of grape skins when crushed. Enzymes (pectinases and glycosidases) are also present in the must, which promote the extraction of colour and aromatic and phenolic compounds.

Determination of the Content of Polyphenolic Compounds

Polyphenols play an important role in winemaking. They are responsible for the differences between white and red wines, especially for the colour and taste of red wines. They affect the appearance, aroma, taste, fullness, and antimicrobial and antioxidant properties of wine.

Figure 1 Values of the content of polyphenolic compounds during maceration in wine

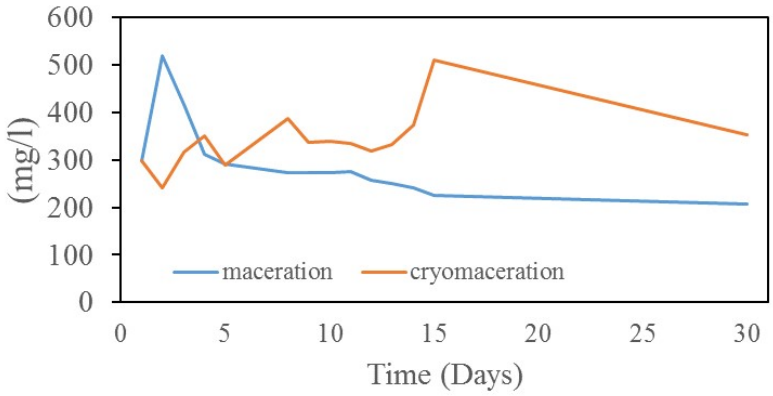

Polyphenolic compounds have antioxidant and antimicrobial properties and their higher content can serve as a possible substitute for SO_2. Diagram 1 shows a distinct increase in polyphenol compounds after pressing (control – day 2; cryomaceration – day 15). Both options had over 500 mg/l after pressing. However, the control had a significantly lower content of polyphenol compounds than the cold option after fermentation (day 30). With longer maceration, polyphenolic compounds are more stable and their content remains higher in the finished wine after fermentation. Longer maceration can, therefore, reduce the SO_2 content in wines (Figure 1). The increase in polyphenolic compounds during cold maceration was confirmed by Gil-Muñoz et al. (2009), who macerated the Cabernet Sauvignon and Shiraz varieties at 10 °C for seven days.

Determination of Antioxidant Activity

Antioxidant activity deactivates free radicals. Its purpose is to protect the wine from oxidation or loss of colour. It is especially associated with polyphenolic compounds in grape seeds and skins. Antioxidant activity should protect the composition and function of different molecules.

The increase in antioxidant activity in cryomaceration was 0.5 times higher than that of the control option. The antioxidant activity was increased after pressing the grapes (control – day 2; cryomaceration – day 15). This value was stable in the cold option during fermentation (days 1–15). On the contrary, the control sample decreased by half. The value in the wine is 88 mg/l in cryomaceration and 42.3 mg/l in the control. Obviously, we can increase the antioxidant capacity and extract more antioxidants from the skins with longer maceration. Therefore, we can achieve lower sulphuration in the resulting wine and the wine has a greater ageing potential (Figure 2).

Figure 2 Values of antioxidant activity during maceration in wine

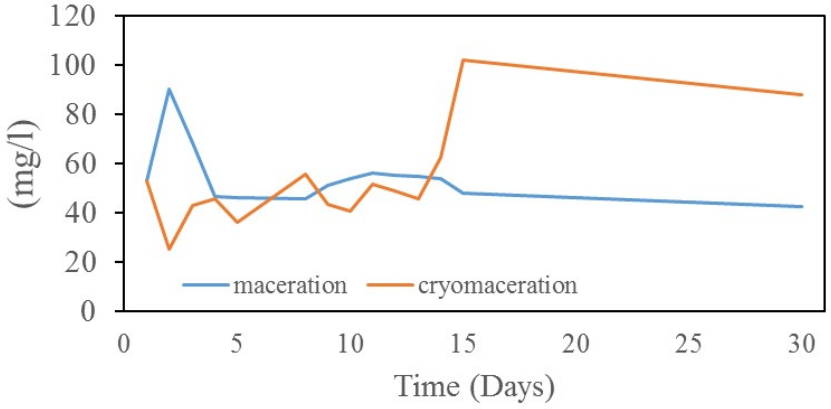

Determination of Reducing Power

Reducing power means reducing ferric ions in gallium acid. Longer maceration increases the ability of the wine to reduce these ions. We can also use the term antioxidant power. Thanks to maceration, we increase the amount of antioxidant substances in must and hence the reducing power. We protect the wine from possible oxidation.

Determination of Flavanol Content

Flavanols are mostly part of the condensed tannins and are important for the taste and structure of wine. They occur as monomers but the majority is in the form of polymers. Their monomers are colourless and do not exhibit the properties of polyphenols and tannins. They have the properties of tannins as polymers.

Figure 3 Values of the content of flavanol in wine

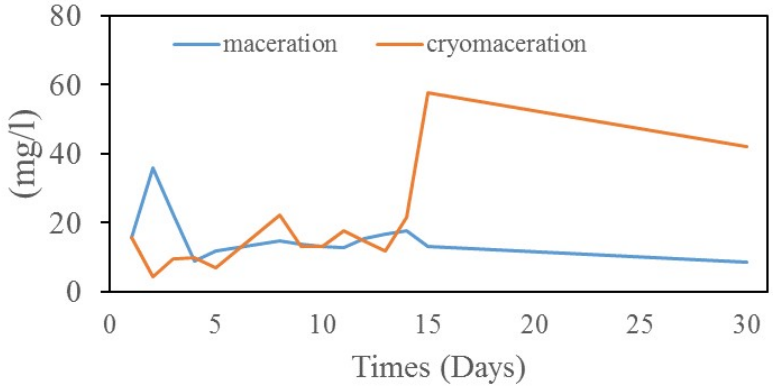

Flavanol content increased after grape pressing (control – day 2; cryomaceration – day 15). In the control variant, the amount of flavanols was 35 mg/l before fermentation. The amount of flavanols before fermentation was 58 mg/l in cryomaceration. The value of the control variant in the resulting wines is four times lower than the cold variant. Cryomaceration allows us to stabilise flavanols during fermentation and to increase their content in wine. Longer maceration can thus positively affect the taste and fullness of wine (Figure3).

Vázquez et al. (2010) confirmed the increase of flavanols in their experiment. We achieved the same results in our experiment when the flavanol content was four times higher in cryomaceration.

Determination of Anthocyanin Content in Rosés

Anthocyanins form the basis of the colour in rosés and maceration has a great effect on their extraction. It is, therefore, necessary to pay attention to these substances. Colour intensity and shade vary both in terms of the quantitative and qualitative composition of anthocyanins and their response to environmental components.

As assumed, the content of anthocyanins increased after pressing (control – day 2; cryomaceration – day 15) and decreased after fermentation (day 30). However, it decreased by one third in the cold variant and by almost sevenfold in the control variant. The cold variant had four times higher content of anthocyanins than the control variant. Colour stability was achieved during fermentation in the cold variant, resulting in a more intense colour of the finished wine (Figure 4).

Figure 4 Values of the content of anthocyanin in wine

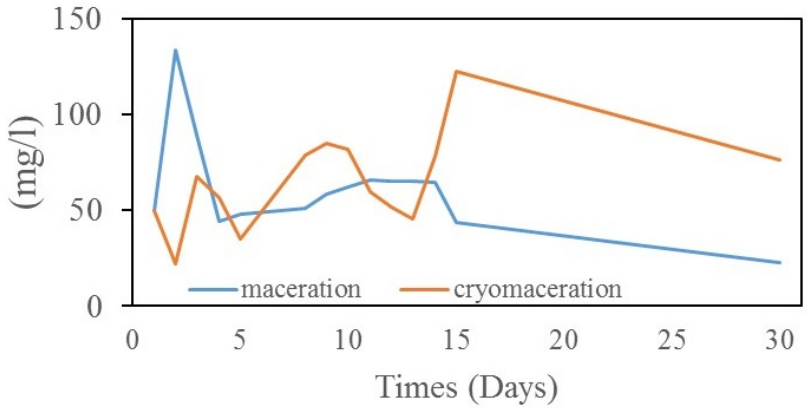

The content of anthocyanins increased by 50% and of polyphenolic compounds by 17% in cold maceration. Álvarez et al. (2006) agrees with this, confirming the higher content of polyphenolic compounds and anthocyanins in cold maceration in his work. The experiment was carried out using the Monastrell variety. The experiment was carried out in two options (cold maceration at 6–8 °C and cold maceration at 0–2 °C using dry ice) with the maceration duration of four and eight days. The dry ice option proved more significant where the content of anthocyanins and polyphenols was higher. We also cooled the pomace using dry ice in our experiment.

The increase in anthocyanins and polyphenolic compounds in cold maceration was also confirmed by Gil-Muñoz et al. (2009), who macerated the Cabernet Sauvignon and Shiraz varieties at 10 °C for seven days.

Sensory Analysis Results

From the sensory point of view, the cold maceration had better results – an average score of 85 points compared to the option produced using the conventional maceration (average of 80 points). The wine was more intense in aroma and taste. It excelled in completeness, fullness, and longer ageing potential. This wine was stronger in the aroma with a touch of dried fruit and green tones.

CONCLUSION

This paper dealt with different methods of maceration in rosés. The measured values show that the test samples reached the expected results. Cryomaceration results in the wines assessed were significantly higher than expected. Different temperatures and durations of maceration proved to be crucial. Thanks to cryomaceration, polyphenolic compounds in the wine increased. The increase in polyphenolic compounds positively affected the aroma, taste, and organoleptic properties of the wine. There was an increase in antioxidant activity, giving the wine greater potential to avoid oxidation. The content of flavanols and anthocyanins also increased. Cryomaceration had a positive effect on the wine sensory analysis. However, the maceration temperature generally appears to be more important for increasing the content of anthocyanins and polyphenol compounds than length of maceration.

The results obtained from this experiment showed the effect of cryomaceration on the measured values and organoleptic properties of the wine.

ACKNOWLEDGEMENT

The financial support received for the project DG16P02R017 “Viticulture and Enology for Maintaining and Restoring Cultural Identity Wine Regions in Moravia” is gratefully acknowledged.

REFERENCES

Álvarez, I. et al. 2006. Impact of prefermentative maceration on the phenolic and volatile compounds in Monastrell red wines. Analytica Chimica Acta, 563(1–2): 109–115.

Gil-Muñoz, R. et al. 2009. Influence of low temperature prefermentative techniques on chromatic and phenolic characteristics of Syrah and Cabernet Sauvignon wines. European Food Research and Technology, 228(5): 777–788.

Moreno-Arribas, M., Polo, M. 2009. Wine chemistry and biochemistry. 1st ed., New York, USA: Springer-Verlag.

Ortega-Heras, M. et al. 2012. Comparative study of the use of maceration enzymes and cold pre-fermentative maceration on phenolic and anthocyanic composition and colour of a Mencía red wine. LWT–Food Science and Technology, 48(1): 1–8.

Parenti, A. et al. 2004. Effects of cold maceration on red wine quality from Tuscan Sangiovese grape. European Food Research and Technology, 218(4): 360–366.

Pulido, R. et al. 2000. Antioxidant activity of dietary polyphenols as determined by a modified ferric reducing/antioxidant power assay. Journal of Agricultural and Food Chemistry, 48(8): 3396–3402.

Sochor, J. et al. 2010. Fully automated spectrometric protocols for determination of antioxidant activity: advantages and disadvantages. Molecules, 15: 8618–8640. doi:10.3390/molecules15128618

Somers, T.C., Evans, M.E. 1977. Spectral evaluation of young red wines – anthocyanin equilibria, total phenolics, free and molecular SO_2, chemical age. Journal of the Science of Food and Agriculture, 28: 279–287.

Vázquez, E.S. et al. 2010. Effect of the winemaking technique on phenolic composition and chromatic characteristics in young red wines. European Food Research and Technology, 231(5): 789–802.

Vivas, N.G.Y. et al. 1994. Estimation du degree de polymerization des procyanidins du raisin et du vin par la méthode au p-dimethylaminocinnamaldéhyde. Journal International des Sciences de la Vigne et du Vin, 28: 319–336.

Zoecklein, B.W.F. et al. 1990. Production wine analysis. 1st ed., New York, USA: Van Nostrand Reinhold, pp. 129–168.

Esters of phthalic acid in sous-vide meat products made at 70 °C

Marcela Jandlova[1], Alzbeta Jarosova[1], Josef Kamenik[2]
[1]Department of Food Technology
Mendel University in Brno
Zemedelska 1, 613 00 Brno
[2]Department of Gastronomy
University of Veterinary and Pharmaceutical Sciences Brno
Palackeho tr. 1946/1, 612 42 Brno
CZECH REPUBLIC

marcela.jandlova@mendelu.cz

Abstract: Phthalic acid esters are plasticizers that are used in plastics. They are also used in plastics that come into contact with food. Our study investigated the effect of temperature and time on the concentration of phthalates. They were studied meat products wrapped in vacuum plastic packaging heat-treated in a water bath at 70 °C for 4 hours and for 8 hours, when part of the samples were exposed to reheating at 70 °C for 1 hour. All samples were in three repeats. Two esters, dibutyl phthalate (DBP) and di-(2-ethylhexyl) phthalate (DEHP), were determined both in the corresponding plastic packaging and in the meat products. And it was found that the concentrations of the two phthalic acid esters were decreased with the longer time of the heat treatment in the plastic packages, but the re-heating for 1 hour caused the concentrations increase. The average concentration in the heat-treated meat products, at a concentration of 1 gram of fat, was both DBP and DEHP higher with a longer heat treatment time (70 °C /4 hours and 70 °C /8 hours). After reheating for one hour, the DBP concentrations were higher than without reheating, and the DEHP concentrations were increased at 70 °C/4 hours + 1 hour than without reheating and decrease at 70 °C/8 hours + 1 hour than without reheating.

Key Words: meat, packaging, DBP, DEHP, contaminants

INTRODUCTION

Phthalic acid esters are currently ubiquitous contaminants, especially dibutyl phthalate (DBP) and di-(2-ethylhexyl) phthalate (DEHP). They are used in plastics, as plasticizers, where they can be up to 40% (Velíšek and Hajšlová 2009). However, plastics, whether additives such as plasticizers, antioxidants, stabilizers, or monomers and oligomers, can migrate from plastics because they are not chemically bonded (Piotrowska 2005). Higher temperatures lead to the decomposition of both additives and polymer chains of plastics, which can accelerate the release of plastic additives (plasticizers) (Nerin et al. 2002). Migration of the packaging components into the packaged product is typical for polymeric materials. The ingredients migrate without visible destruction of the packaging. It depends on the amount and substances migrating from the packaging, which determine the suitability of use. The materials being in contact with food have set the migration limits by the legislation (Dobiáš 2012). The Commission Regulation (EU) No 10/2011, dealing with plastic articles and materials intended for contact with food, sets specific migration limits for DBP of 0.3 mg/kg of food and DEHP of 1.5 mg/kg of food (EU. 2011). Phthalic acid esters are potentially carcinogenic. Exposure to phthalates causes problems with the respiratory system, the genital system especially by male animals, problems with the endocrine system and the digestive system (Pilka et al. 2012). Sous-vide cooking is the heat treatment of food vacuum-packed in plastic thermostable bags. This technology guarantees the temperature of the heating is well controlled, thus improving the controllability, reproducibility and microbial safety of food even at lower temperatures of the heat treatment. It also allows to maintain food nutritional value, sensory and textural qualities (Baldwin 2012).

MATERIAL AND METHODS

The meat was bought in the market of the Czech Republic. The meat was divided into pieces of approximate weight of 150 g. They were vacuum packed at the Department of Gastronomy at the University of Veterinary and Pharmaceutical Sciences in Brno, where they were also heat-treated in water bath. The heat treatment of the six samples was carried out at 70 °C for 4 hours with a further six samples at 70 °C for 8 hours. The half of the samples from each variation was immediately processed on the samples for analysis. The other half of the samples from each variant were stored in a refrigerator for 24 hours and then heated in a water bath at 70 °C for 1 hour and then processed to the samples for analysis. Samples processing and analysis took place at the Department of Food Technology MENDELU. Two esters of phthalic acid, DBP and DEHP, were determined both in meat products and in their packaging. The packages were washed in distilled water before being analyzed and allowed to dry. Determination of phthalic acid esters in plastics was carried out according to the method of Gajdůšková et al. (1996) and the meat according to Jarošová et al. (1999). Measurement was performed on HPLC with UV detection at 224 nm, with Zorbax Eclipse C8 column, and acetonitrile was used as the mobile phase. The evaluation was done using software Data Analysis of Agilent Technology. The results were further elaborated using Microsoft Excel.

RESULTS AND DISCUSSION

Table 1 shows a decrease of concentrations both phthalic acid esters determined in plastic packaging with longer heat treatment time (70 °C/4 h and 70 °C/8 h). Comparing the average concentrations of phthalic acid esters thermally treated at 70 °C /4 h + 1 h and 70 °C/8 h + 1 h, the two phthalic acid esters also showed a decrease of the concentrations in plastic packages. However, if it compared heat treating with the same reheating time (70 °C/4 h at 70 °C/4 h + 1 h, as well as for an 8 hour variation) the average concentration DEHP and DBP had always increased.

Table 1 Average concentrations of dibutyl phthalate (DBP) and di-(2-ethylhexyl) phthalate (DEHP) in plastics

Heat treatment	DBP [μg/dm^2]	DEHP [μg/dm^2]	DBP [μg/g of plastic]	DEHP [μg/g of plastic]
70 °C/4 h	4.01	3.40	4.75	4.03
70 °C/4 h + 70 °C/1 h	4.35	5.81	4.87	6.50
70 °C/8 h	2.18	1.70	2.43	1.91
70 °C/8 h + 70 °C/1 h	2.42	4.51	2.65	4.95

Figure 1 Average concentrations of dibutyl phthalate (DBP) and di-(2-ethylhexyl) phthalate (DEHP) in meat products [μg/g of fat]

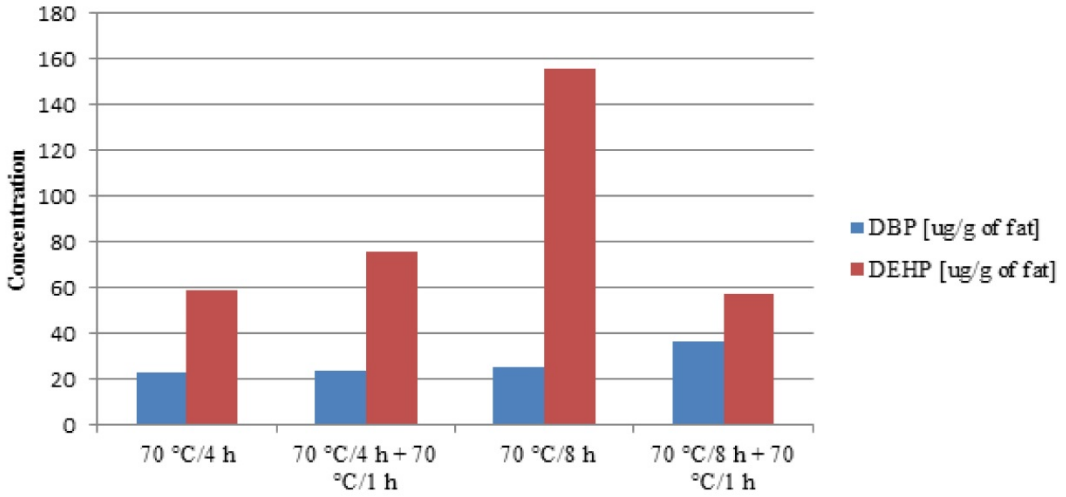

Table 2 Concentrations of dibutyl phthalate (DBP) and di-(2-ethylhexyl) phthalate (DEHP) in heat treated meat products

Heat treatment	DBP [µg/g of fat]	DEHP [µg/g of fat]	DBP [µg/g of dry matter]	DEHP [µg/g of dry matter]	DBP [µg/g of original matter]	DEHP [µg/g of original matter]
70 °C/4 h	15.63	68.69	5.35	23.51	1.76	7.75
	19.93	23.12	5.94	6.89	1.80	2.09
	32.50	84.74	10.58	27.60	3.33	8.68
70 °C/4 h + 70 °C/1 h	7.15	92.18	1.34	17.25	0.37	4.76
	34.07	31.93	14.56	13.65	5.10	4.78
	29.43	104.51	10.47	37.18	3.19	11.32
70 °C/8 h	25.23	140.98	3.08	17.22	0.81	4.54
	24.42	155.79	5.79	36.93	1.74	11.11
	27.06	171.45	12.90	81.72	4.53	28.69
70 °C/8 h + 70 °C/1 h	44.71	52.13	11.97	13.95	3.45	4.02
	27.73	43.91	6.55	10.37	1.92	3.04
	37.97	75.67	12.94	25.78	4.05	8.07

Concentration results for heat treated meat are shown in Table 2 and the average concentration per gram of fat in Figure 1. It can be seen from the graph that the average DEHP concentration, when compared 70 °C/4 h with 70 °C/8 h, was with longer time heat treatment higher, as well as at 70 °C/4 h, and reheating for 1 hour also increased compared to the without reheating. Mean concentrations of DBP have always increased with a longer period of time, with results per gram of fat.

The logical relationship can be seen with higher DEHP concentration by reheating samples (70 °C/8 h compare with 70 °C/8 h + 1 h) in plastic packaging, which is associated with a decrease in DEHP concentration in reheat meat products. An important component to which phthalic acid esters could pass is theoretically water. However, in Jandlová et al. (2018) was stated that the concentration of phthalic acid esters, both DBP and DEHP, in water from a water bath, which was heated with vacuum plastic packaged meat products, dropped compared to the original distilled water (the distilled water without heating).

In the study Jandlová et al. (2017) dealing with the sous-vide heat treatment meat products was detected the loss of both DBP and DEHP concentrations in µg/g of fat compared to the original raw meat. Similarly, a greater decrease in DBP and DEHP concentrations with a higher heat treatment temperature was also observed. The thermal variants were used in the study 53 °C, 18 hours and 70 °C, 2 hours. And in the plastic wraps, the sum of the DBP and the DEHP concentrations, were again decreased in both thermal treatments compared to the without heat treatment and compared to the higher temperature of heat treatment.

In the study Clausen et al. (2011), where was examined the amount of emitted DEHP from PVC in the emission cell at different temperatures, it was found that the amount of DEHP emitted with increasing temperature grew.

In the study Rastkari et al. (2017) was researched the concentration of DEHP in acidic fluids in HDPE and PET bottles, which was increased with increasing temperature (4 °C, 20 °C, 50 °C), whereas in DBP, the concentration was increased with higher temperature in acidic fluids to 25 °C, and decreased at 50 °C. It was mentioned, that the DBP was probably hydrolyzed at 50 °C, because the hydrolysis is faster with higher temperature and in the more acid environment.

CONCLUSION

The average concentrations in plastic wraps of the two phthalic acid esters determined at 70 °C/4 h and 70 °C/8 h with longer heat treatment times decreased. However, with the use of reheating, they

always had a higher concentration than those without reheating. The average concentration of DEHP in the meat products treated by the sous-vide technology in a water bath at 70 °C/4 h and at 70 °C/8 h was higher with a longer heat treatment time, as well as at 70 °C/4 h with 1 hour reheating also increased compared to no reheating. The average DBP concentrations always increased with a longer warming time, with results per gram of fat. Esters of phthalic acid can migrate from the packaging to food, as well as from food to packaging. Mutual migration probably occurred in the case of DEHP concentration 70 °C/8 h and 70 °C/8 h + 1 h, which increased in plastic packagings and simultaneously decreased in heat treated meat products.

ACKNOWLEDGEMENTS
This research was supported by grant no. AF-IGA-IP-2018/059.

REFERENCES

Baldwin, D.E. 2012. Sous vide cooking: A review. International Journal of Gastronomy and Food Science [Online], 1(1): 15–30. Available at: http://linkinghub.elsevier.com/retrieve/pii/S1878450X11000035. [2017-08-18].

Dobiáš, J. 2012. Balení. In Procesy a zařízení potravinářských a biotechnologických výrob: Technologie potravin. Ostrava: KEY Publishing s.r.o., pp. 443–450.

Clausen, P.A. et al. 2011. Influence of Temperature on the Emission of Di-(2-ethylhexyl) phthalate (DEHP) from PVC Flooring in the Emission Cell FLEC. Environmental Science & Technology [Online], 46(2): 909–915. Available at: http://pubs.acs.org/doi/10.1021/es2035625. [2018-09-13].

EU. 2011. Commission Regulation (EU) No 10/2011 of 14 January 2011 on plastic materials and articles intended to come into contact with food. In OJ L 12: 1-89. Also available at: https://www.fsai.ie/uploadedFiles/Reg10_2011.pdf**.** [2017-08-19].

Gajdůšková, V. et al. 1996. Occurrence of phthalic acid esters in food packaging materials. Potravinářské Vědy, 14: 99–108.

Jandlová, M. et al. 2018. Uvolňování esterů kyseliny ftalové do vodní lázně při tepelném opracování mas technologií sous-vide. In Sborník XLIV. konference o jakosti potravin a potravinových surovin, Brno, 28 February. Brno: Mendelova univerzita v Brně, pp. 139–145.

Jandlová, M. et al. 2017. Estery kyseliny ftalové ve vzorcích masa připravených technologií sous-vide. In Hygiena a technologie potravin XLVII. Lenfeldovy a Höklovy dny: Sborník přednášek a posterů. Brno, 18–19 October. Brno: Veterinární a farmaceutická univerzita Brno, pp. 156–159.

Jarošová, A. et al. 1999. Di-2-ethylhexyl phthalate and di-n-butyl phthalate in the tissues of pigs and broiler chicks after their oral administration. Veterinary Medicine, 44(3): 61–70.

Nerin, C. et al. 2002. Potential migration release of volatile compounds from plastic containers destined for food use in microwave ovens. Food Additives and Contaminants [Online], 19(6): 594–601. Available at: http://www.tandfonline.com/doi/abs/10.1080/02652030210123887. [2017-08-19].

Pilka, T. et al. 2012. Antropopatogénny vplyv ftalátov na ľudské zdravie. Slov. Antropol. [Online], 15(1): 45–52. Available at: http://www.eaup.fpv.ukf.sk/dokumenty/pub/a21_clanok03.pdf. [2017-08-20].

Piotrowska, B. 2005. Toxic Components of Food Packaging Materials. In Toxins in Food. Boca Raton, FL: CRC Press, pp. 313–333.

Rastkari, N. et al. 2017. The Effect of Storage Time, Temperature and Type of Packaging on Release of Phthalate Ester into Packed Acidic Juice. Food Technology and Biotechnology [Online], 55(4): 562–569. Available at: http://www.ftb.com.hr/images/pdfarticles/2017/October-December/FTB-55-562.pdf. [2018-09-13].

Velíšek, J., Hajšlová, J. 2009. Chemie potravin II. 3rd ed., Tábor: OSSIS.

Sensory evaluation of yoghurt with addition of baobab powder, milk thistle flour, cricket flour, chia flour

Marcela Jandlova[1], Vojtech Kumbar[2], Alzbeta Jarosova[1], Roman Pytel[1], Sarka Nedomova[1], Sylvie Ondrusikova[1]
[1]Department of Food Technology
[2]Department of Technology and Automobile Transport
Mendel University in Brno
Zemedelska 1, 613 00 Brno
CZECH REPUBLIC

marcela.jandlova@mendelu.cz

Abstract: In our study, yoghurts with 1% and 3% baobab powder, milk thistle flour, cricket flour, chia flour were sensory evaluated. The basic raw material was used natural yogurt with a fat content of 1.5% and 3.5%. The worste valuated yogurts were with cricket flour, the best in the total impression was natural yoghurt with the fat content of 3.5%, the yoghurt with 3% of baobab powder (fat yogurt 1.5%), the yoghurt with 1% milk thistle flour (1.5% fat yoghurt), the yoghurts with chia flour (1.5% fat yoghurt) and the natural 1.5% fat yoghurt.

Key Words: yoghurt, fibre, health, sensory, baobab

INTRODUCTION

Yoghurt is one of the most widely fermented products that contains thermophilic lactic acid bacteria, which produces lactic acid from the lactose, reducing the pH of the product and increasing the shelf life of the product. At the same time, other sensory and nutritionally important substances are produced by fermentation (Plocková 2009).

Yoghurts must contain according to Czech Decree No. 397/2016 Coll. in the current version, a protosymbiotic mixture of *Streptococcus salivarius* subsp. *thermophilus* and *Lactobacillus delbrueckii* subsp. *Bulgaricus* in 1 gram of 10^7 microorganisms (Česká republika 2016). Numbers of yoghurts are produced that contain other probiotic cultures, especially from the genus *Lactobacillus*. Probiotics are called live microorganisms that have a positive effect on the health of the consumer if they are supplied in sufficient quantity. Better health effects have probiotics, which are taken together with prebiotics. Prebiotics also have a positive influence on the health of the consumer, they support the activity and growth of the intestinal microflora, it is an indigestible part of the food (Čurda and Štětina 2014). Both probiotics and prebiotics reduce the risk of colon cancer, support the immune system and improve the digestive system function. Probiotic microorganisms of the genus *Bifidobacterium* are also used, and also some others as *Bacillus* spp., *Escherichia faecium*, *Escherichia fecalis*, and other (Plocková and Horáčková 2010).

The dairy industry has been developing functional dairy foods in recent years, with the addition of prebiotics, probiotics, peptides, non-dairy and dairy ingredients. When a functional food is referred to as a food that is consumed in normal human meals, it brings, in addition to the basic nutritional function, a health benefit to the consumer, whether it can be by adding vitamins, minerals, fiber, or reducing the fat content, etc. (Plocková and Horáčková 2010).

MATERIAL AND METHODS

Two kinds of natural yoghurt were purchased in the Czech Republic's market, yoghurt with 1.5% of fat and 3.5% of fat, Yoghurts were mixed with 1% and 3% baobab powder (South African origin), milk thistle flour (country of origin Czech Republic), cricket flour (the country of origin Great Britain), chia flour (the country of origin Czech Republic), and filled into cups. The second day was the sensory evaluation of these products. Sensory were evaluated by 6 experienced sensor assessors (five women and one man). The descriptors were amount of freed whey, acceptability of color (10 = acceptable,

0 = unacceptable), sour aroma (10 = very intensive, 0 = unintensive), acceptability of total aroma (10 = acceptable, 0 = unacceptable), viscosity (10 = dense, 0 = sparse), texture (10 = smooth, 0 = grainy), stickiness (10 = extreme, 0 = without stickiness), sandiness (10 = very sandiness, 0 = without sandiness), acceptability of texture (10 = acceptable, 0 = unacceptable), taste of sour intensity (10 = very sour, 0 = without sour), acceptability of taste (10 = excellent, 0 = unacceptable,), total impression.

The production of yogurt mixes and sensory evaluation took place in Pavilion M at the Institute of Food Technology Mendel University in Brno. This research was carried out in Biotechnology Pavilion M, financed by the OP VaVpI CZ.1.05/4.1.00/04.0135 project at the Department of Food Technology at Mendel University in Brno.

RESULTS AND DISCUSSION

The sensory results from the evaluation of the freed whey are shown in Figure 1. The least freed whey, 3 times marked "without whey", had yoghurt with 3% chia flour (3.5% fat yoghurt). Very much freed whey, 2 times marked "very much" had with 3% milk thistle flour (1.5% fat yoghurt), and with 1% cricket flour (1.5% fat yoghurt).

Figure 1 Frequency of amount of freed whey

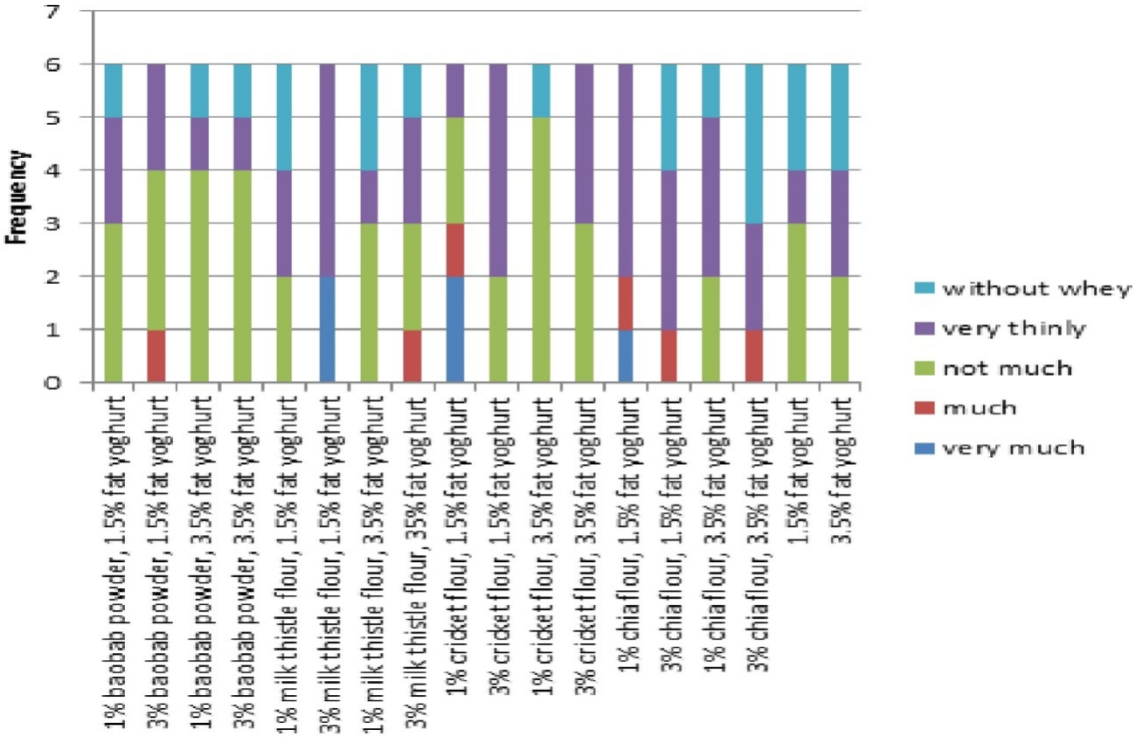

Figure 2 shows most of the descriptors. The best color acceptability has natural yoghurt, and yoghurt with 1% baobab powder. The worst color acceptability was rated 1.5% yoghurt with 3% cricket flour. The most acidic yogurt was rated 3.5% fat yoghurt with 1% baobab powder, the least acidic yoghurt with 1% cricket flour. The most acceptable of the total flavor was 1.5% fat yoghurt with 1% baobab powder, the least acceptable of the total flavor was yogurts with 3% cricket flour. The thickest yogurt was labeled 1.5% fat yoghurt with 3% chia flour and 3.5% fat yoghurt with 3% chia flour. Natural 3.5% fat yoghurt was determined as the sparsest. The smoothest texture was found at 3.5% fat yoghurt, the grainiest at 3.5% fat yoghurt with 3% milk thistle flour and at 1.5% fat yoghurt with 3% milk thistle flour.

The most extreme stickiness was detected by yoghurt with 3% chia flour. The least intensive stickiness was detected by natural yogurts with baobab powder. The most extreme sandiness with 3% milk thistle flour, the least intensive sandiness were natural yoghurts. Acceptability of the texture – the most acceptable texture was detected by natural yogurts and yogurts with baobab powder. The worst acceptance of the texture was found by yoghurt with 3% milk thistle flour and 3% chia flour.

The most acidic yogurt detected in the mouth was yoghurt with 3% baobab powder and the least acidic yoghurt was determined with 1% cricket flour (1.5% fat), 3% cricket flour (3.5% fat) and with 3% chia flour. The best acceptable taste was found by 1% baobab (1.5% fat), 1% chia flour (1.5% fat), natural yoghurt with 3.5% fat and 1% chia flour (3.5% fat). The worst ratings were determined by yogurts with cricket flour.

Figure 2 Sensory evaluation of yoghurts divided into groups with the same added raw ingredients

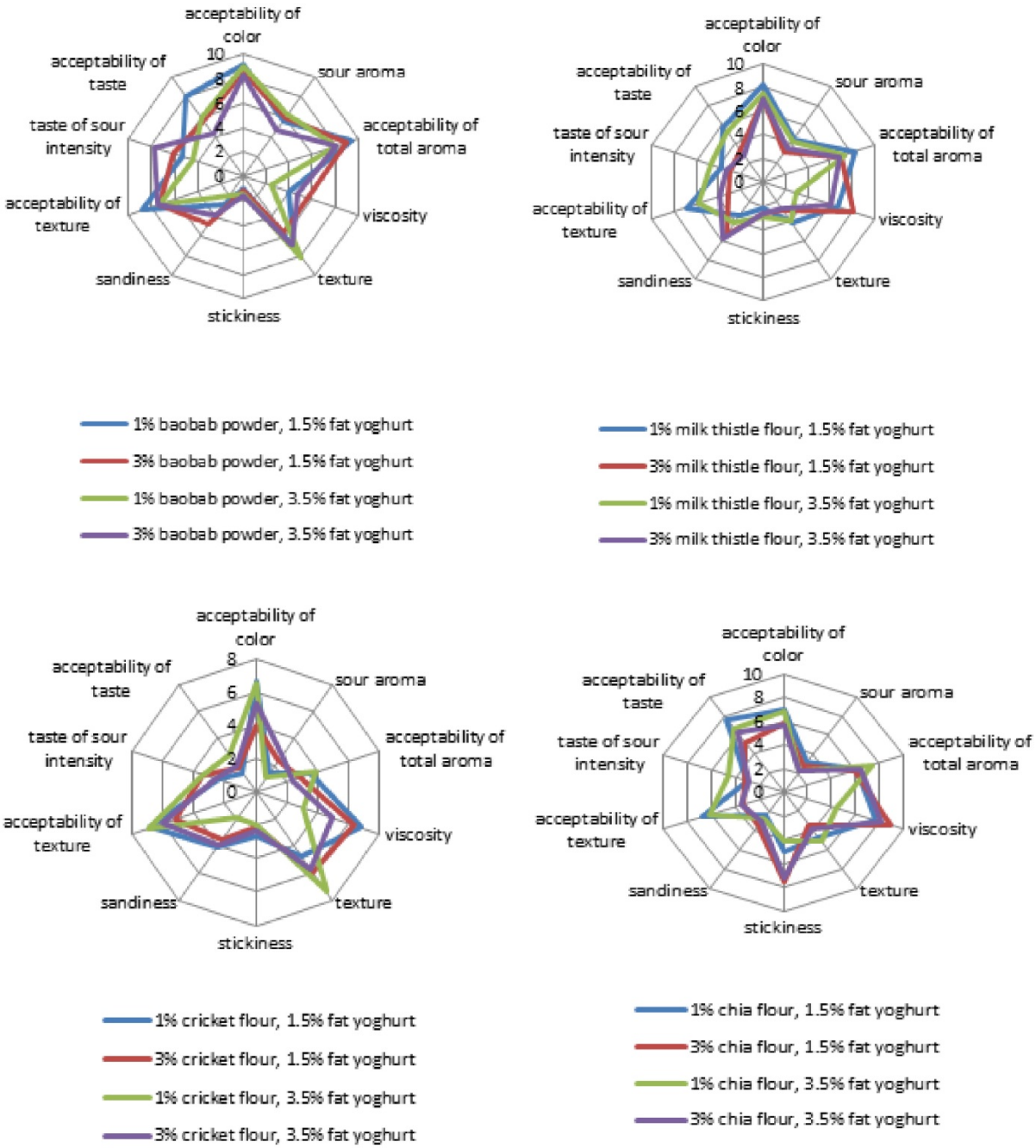

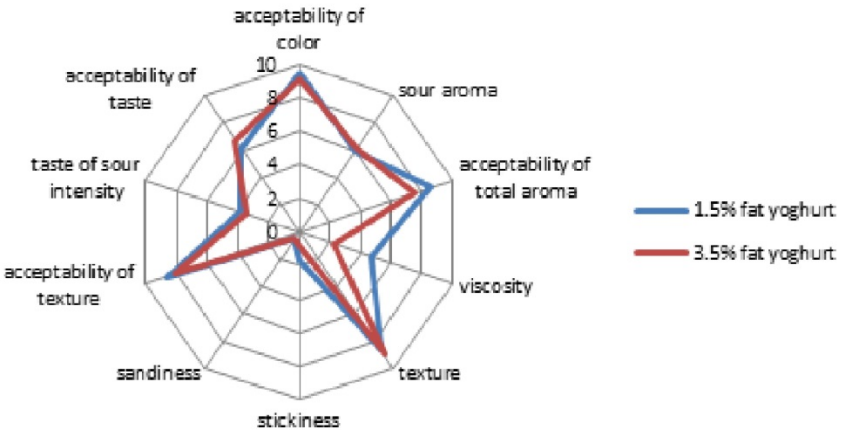

The total impression of the sensory evaluation is shown in Figure 3. The best total impression, 2 times evaluated "excellent", was determined by natural yoghurt 3.5% fat, 1 times evaluated "excellent", was detected by 1.5% fat yoghurt with 3% baobab powder, also by 1.5% fat yoghurt with 1% milk thistle flour, then by 1.5% fat yoghurt with chia flour and by natural yoghurt with 1.5% fat. The worst overall impression, 5 times labeled "unacceptable", was found by 1.5% fat yoghurt with 1% cricket flour, 4 times detected "unacceptable", was determined by 1.5% fat yoghurt with 3% cricket flour, then 2 times marked "unacceptable" was detected by 3.5% fat yoghurt with 1% and 3% cricket flour and 1.5% fat yoghurt with 3% chia flour.

Figure 3 Frequency of total impression

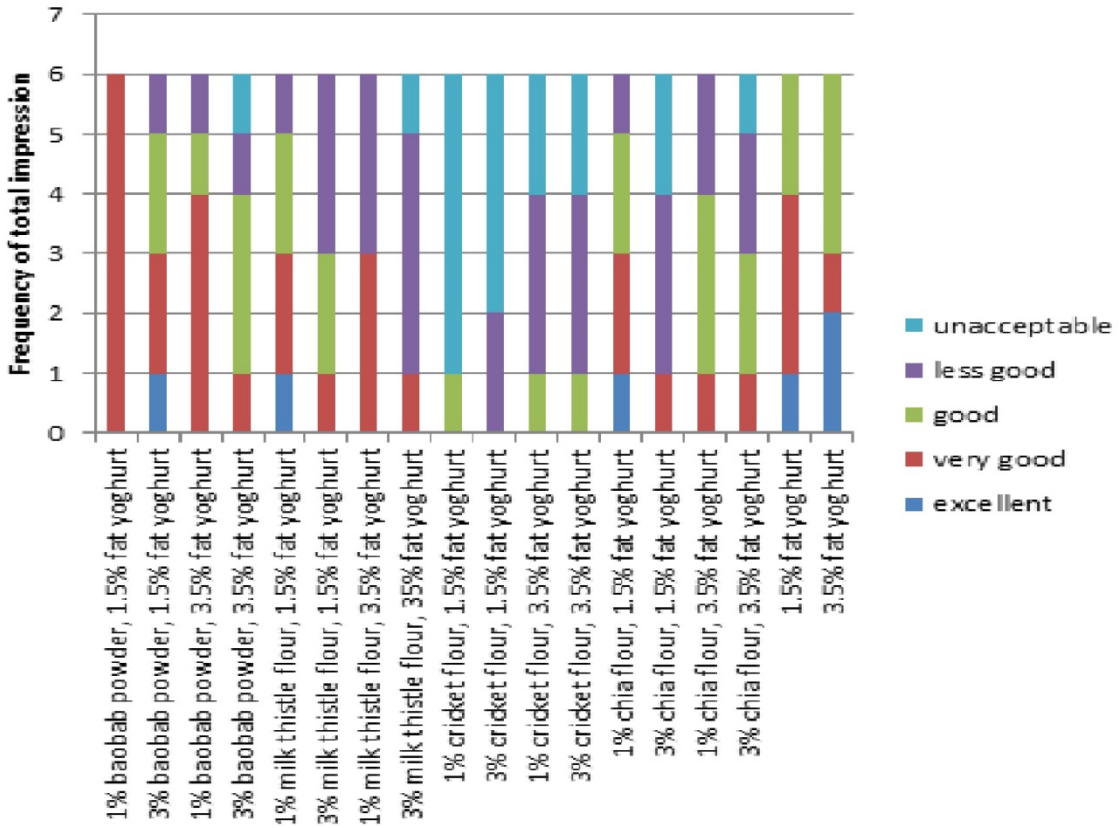

In the study by Jandlova et al. (2017), where was the sensory evaluation of yoghurts with the addition of various raw materials: apple fiber, chia flour, nopal powder, quinoa flour, and bamboo fiber. The best evaluated was yoghurt with 1% of bamboo fiber and the worst evaluated yoghurt was with 5 % of quinoa flour.

CONCLUSION

Overall, yogurts with cricket flour were evaluated as the worst. Whether the acceptability of taste or the total impression, but also the least sour, which is associated with worse product shelf life. The best evaluation of acceptability of taste was determined by yogurts with baobab powder and chia flour. The best total impression was detected by natural yoghurt with 3.5% fat, by 1.5% fat yoghurt with 3% baobab powder, then by 1.5% fat yoghurt 1% milk thistle flour, by 1.5% fat yoghurt with chia flour and by natural 1.5% fat yoghurt. It is seemed appropriate to add healthy foods to yoghurts, but from our research is not seemed appropriate to add cricket flour, because the cricket flour has a specific unusual taste that consumers would have to become accustomed to or would have to season the products with something tasty.

ACKNOWLEGEMENTS

This research was financed by the grant: IGA FA MENDELU No. TP 2/2017 "Effect of additives on the rheological behaviour of food stuffs and raw materials for their production".

REFERENCES

Česká republika. 2016. Vyhláška č. 397/2016 Sb. vyhláška o požadavcích na mléko a mléčné výrobky, mražené krémy a jedlé tuky a oleje. In: Sbírka zákonů České Republiky.

Čurda, L., Štětina, J. 2014. Mléko a mléčné výrobky. In Potravinářské zbožíznalství: technologie potravin. Ostrava: KeyPublishing s.r.o., pp. 118-150.

Jandlova, M. et al. 2017. The sensory evaluation of yoghurts with chia flour, quinoa flour, nopal powder, apple fiber and bamboo fiber. In Proceedings of International PhD Students Conference MendelNet 2017 [Online]. Brno, Czech Republic, 8–9 November, Brno: Mendel University in Brno, Faculty of AgriSciences, pp. 547–552. Available at: https://mnet.mendelu.cz/mendelnet2017/mnet_2017_full.pdf. [2018-09-12].

Plocková, M. 2009. Fermentovaná mléka, probiotika, prebiotika. In Co byste měli vědět o výrobě potravin: Technologie potravin. Ostrava: KeyPublishing s.r.o., pp. 263–273.

Plocková, M., Horáčková, Š. 2010. Funkční potraviny a probiotika. In Sborník Svět potravin a kouzlo biotechnologií – 24. letní škola pro středoškolské profesory chemie, biologie a biochemie a nadané studenty středních škol. Vysoká škola chemicko-technologická v Praze, 24.–26. srpna, Ostrava: KeyPublishing s.r.o., pp. 58–62.

Assessment of possibilities of food grade gelatines preparation from chicken skin

Petr Mrazek[1], Pavel Mokrejs[1], Robert Gal[2]
[1]Department of Polymer Engineering
[2]Department of Food Technology
Tomas Bata University in Zlin
Vavreckova 275, 760 01 Zlin
CZECH REPUBLIC

p_mrazek@ft.utb.cz

Abstract: Chicken skin is a product obtained from the poultry meat processing. This tissue contains mainly fat and proteins, especially collagen. Collagen could be gained from a purification process in which undesirable components, such as fats, pigments and globular proteins, are extracted from the skin. Purified collagen might be used as a starting material for the preparation of high gel strength gelatines applied in food, pharmaceutical and cosmetic industry. Chicken skins are also suitable for processing into collagen hydrolysates of various molecular weights with different purposes as food and cosmetic additives. The aim of this study was to prepare gelatines from chicken skins. Prior to the extraction, non-collagen parts from chicken skin were removed with 1M NaCl, 0.5% NaOH; fats were removed with mixture of Petroleum Ether and Ethanol (1:1). 5 samples of gelatines were prepared by extraction with hot water after pre-treatment with proteolytic enzyme. Effect of extraction conditions, different extraction temperatures (40–80 °C) and fixed extraction time (60 min), on gelatine gel strength and yield of the process, were examined. Yields of extracted gelatines ranged between 42–72%. Gel strengths of prepared gelatine samples were between 252–354 Bloom. What is more, prepared chicken skin gelatines were compared with commercial pork and beef gelatines. Results displayed that prepared chicken skin gelatines have comparable gel strength with commercial gelatines.

Key Words: chicken skin, collagen, collagen hydrolysate, extraction, food grade gelatine, protease

INTRODUCTION

Chicken meat is currently one of the most often consumed types of meat and its consumption has been increasing steadily respecting the global population growth. The global chicken meat consumption was 66 million tonnes in 2000, 91 million tonnes in 2009 and 94 million tonnes in 2013 (Seong et al. 2015). Naturally, enormous amounts of by-products, such as viscera, feet, heads, bones, blood, feathers and skins, are produced as well. In general, these by-products are composted or used in the livestock feed production. Poultry by-products contain significant amounts of proteins, enzymes and lipids possible to be processed further into valuable products with a wide range of applications in medicine, pharmacy, food and cosmetic industry (Bueno-Solano et al. 2009).

Gelatine is an exceptional food hydrocolloid with diverse possibilities of usage. This polypeptide is obtained by partial hydrolysis of collagen, a protein found in animal tissues. In gelatine production, prior to the extraction of collagen in hot water, tissue is treated by acid (type A gelatine) or alkali (type B gelatine). Treatment with acid or alkali causes collagen breakage to produce collagen soluble in warm water (gelatine). There are three key factors during the gelatine production influencing its properties: time, temperature and pH. The process can be accelerated if higher temperatures and longer time period are applied. Traditional sources of collagen are skins, connective tissues and bones of beef or pork origin. However, alternative sources, such as fish bones, skins and scales have become more important as well. Also, poultry by-products including chicken, turkey or duck skin are considered as another alternative (Schrieber and Gareis 2007).

Several studies have been devoted to preparation and properties of gelatines obtained from chicken skin. Sarbon et al. (2013) characterized chicken skin gelatines as a possible alternative to mammalian gelatine. Rasli and Sarbon (2015) studied effects of different drying methods on rheological, functional and structural properties of these gelatines compared to beef gelatine.

Sarbon et al. (2015) examined the effect of interactions between gelatine and whey protein on rheological and thermal properties. Wan Omar and Sarbon (2016) analysed the effect of drying methods on functional properties and antioxidant activity of chicken skin gelatine hydrolysate. Nor et al. (2017) investigated the influence of plasticizers concentration on chicken skin gelatine films.

Gelatine shows excellent emulsifying, foaming, film-forming and stabilizing properties which determine it to many different applications, particularly in food industry. Gelatine also performs a unique ability to bind large amounts of water and form a thermo-reversible gel with a melting point close to the temperature of the human body (Schrieber and Gareis 2007). Nevertheless, the origin of gelatine may be problematic for many consumers because of the risk of BSE (Bovine Spongiform Encephalopathy) or religious aspects as both Judaism and Islam do not accept the consumption of pork skin (Badii and Howell 2003). Thus, gelatine prepared from alternative sources has been gaining more significance and attention.

The aim of the work is to assess possibilities of processing chicken skin into gelatines and investigate effects of proposed technological conditions on the yield of gelatine and gelatine gel strength.

MATERIALS AND METHODS

Chicken skins, by-products of chicken breast cuttings processing, were purchased from Raciola ltd., Uherský Brod, Czech Republic. Prior to experiments, they were stored at -20 °C. They were analysed and results can be seen in Table 1. Dry matter content was determined by drying the sample at 105 ± 2 °C and is defined as the percentage of sample weight after and before drying. Kjeldahl method was applied to analyse protein content (ISO 937:1978) and lipid content was determined using Soxhlet method (Cruz-Fernández et al. 2017). Hydroxyproline content was established to calculate the amount of collagen (ISO 3496:1978). Samples were annealed to determine their mineral content (Gelatin Manufacturers Institute of America 2013). Each test was repeated three times. Results were reported as arithmetic mean with standard deviation.

Regarding commercial gelatine, beef (type B) and pork (type A) gelatines of the grain size of 2 mm were supplied by IPL (Uherský Brod, Czech Republic).

Table 1 Composition of the chicken skin

	Dry matter (% ± SD)	Proteins (% ± SD)[a]	Collagen[b] (% ± SD)[a]	Fat (% ± SD)[a]	Minerals (% ± SD)[a]
Chicken skin	53.6 ± 1.5	16.5 ± 1.3	92.6 ± 0.1	85.0 ± 2.4	0.9 ± 0.3

Legend: [a] based on dry weight of the raw material; [b] from total protein content

Appliances, tools and chemicals

These appliances were employed in the experiment: Stevens LFRA Texture Analyser for measuring the strength of gel (Leonard Farnell and Co ltd., England), SPAR Mixer SP-100AD-B meat cutter (TH Industry RD, Taiwan), Memmert ULP 400 drying device (Memmert GmbH + Co. KG, Germany), LT 43 shaker (Nedform, Czech Republic), Kern 440 – 47 electronic scale and Kern 770 electronic analytical balance (both Kern, Germany), A 10 labortechnik analytical mill (IKA-Werke, Germany), Nabertherm muffle furnace (Nabertherm GmbH, Germany), Samsung refrigerator and Parnas-Wagner distillation apparatus.

Chemicals used in analyses were: NaCl, NaOH, petroleum ether, ethanol and chloroform (Verkon, Czech Republic); all of analytical grade. Polarzyme 6.0 T – serine endoprotease manufactured by fermentation of microorganisms that are not present in the final product (Novozymes, Denmark) with declared enzyme activity of 6 KPPU/g (kilo protease unit/g).

Processing of chicken skins into gelatine

Processing of chicken skins (flow chart in Figure 1) into gelatine involved 6 steps as follows:

1. First, chicken skins were obtained from chicken processing company. Then they were immediately washed with tap water, cleaned and cooled to 0–5 °C to avoid bacterial contamination.

They were ground and homogenized. Temperature of the material should not exceed 12 °C. Afterwards, the material was frozen to the temperature of about -3 °C.

2. Next step of grinding involved two phases, pre-grinding and pulping. It was performed in an industrial meat cutter using a 20–30-mm kidney-shaped cutter head and 3-mm cutter head. Afterwards, raw material was packed into PE bags and frozen to -36 °C. Chicken skins were stored at -20 °C and thawed at 10 °C in a refrigerator for 12 h (overnight) before further processing.

3. Then, separation of undesirable non-collagen components followed. Firstly, raw material was treated by shaking in 1M NaCl at a ratio of 1:10 (w/v) for 3 h at room temperature, then filtered through PA fabric and rinsed with water. The process was repeated two times. In the next step, raw material was shaken in 0.5% NaOH at the ratio of 1:10 (w/v) for 18 h at room temperature and then filtered and rinsed with water again.

4. Separation of fat was next, very important step as chicken skins contain a high amount of fat (Table 1). Raw material was dried at 35 °C in a forced circulation oven and afterwards defatted with a solvent mixture of Petroleum Ether + Ethanol (1:1) at the ratio of 1:10 (w/v). The mixture was shaken for 96 h at room temperature, filtered and a new solvent mixture was used. This was repeated four times. Defatted chicken skin was air dried overnight. Then it was ground using A 10 labortechnik analytical grinder with a grain size set to 1–2 mm.

5. Pre-treatment with proteolytic enzyme (Polarzyme 6.0 T) followed. Material was mixed with distilled water at the ratio of 1:20 (w/v) in a 2-litre Erlenmayer flask, pH was adjusted to 7.5 ± 0.3 and 0.5% (based on dry matter of starting material) of enzyme was added into the mixture. It was shaken for 20 h, filtered and rinsed with water properly.

6. Five experiments with different extraction temperatures of 40, 50, 60, 70 and 80 °C were performed. Conditions were set based on preliminary experiments. Pre-treated material (25.0 ± 0.5 g) was mixed with distilled water at the ratio of 1:20 (w/v) in a 2-litre glass vessel, heated to the extraction temperature and stirred continuously by magnetic stirrer at a speed of 350 rpm for 60 min. Then, the mixture was heated to 100 °C for 5 min to inactivate residual content of enzyme (added in step 5). It was filtered through G3 filtering crucible and gelatine solution was dried on an anti-adhesive plate, 500 mL on a square of 22 mm x 32 mm at 45 °C for approximately 48 hours. Resulting gelatine film was ground using A 10 Labortechnik analytical grinder with a grain size of 1–2 mm and weighed.

Yield of gelatine and gelatine gel strength

The yield of extraction (η) was calculated using the formula:

$$\eta = \frac{m_1}{m_0} \cdot 100\ (\%),$$

where m_1 is weight of dried gelatine (g) and m_0 is weight of air dried of chicken skin (g) after step 4.

Gelatine gel strength was determined according to the Gelatin Manufacturers Institute of America (2013). Gelatine gel strength (Bloom value) was measured by rigidity of gel of 6.67% gelatine solution prepared as follows. 7.5 g of gelatine was weighed and placed into a bloom jar with a volume of 150 mL and dimensions as follows: overall height of 85 mm, inside diameter of 59 mm, outside diameter of 66 mm, neck inside diameter of 41 mm and shoulder height of 65 mm. Then 105 mL distilled water were added. Resulting 6.67% gelatine solution was allowed to swell at room temperature for 3 h. The bloom jar was heated in water bath at 65 °C and magnetic stirrer was used in order to dissolve all pieces of gelatine. After that, the bloom jar was cooled at room temperature and kept in a refrigerator for 16–18 h (overnight) to form gelatine gel. Then the bloom jar was placed into Stevens LFRA Texture Analyser. Gel strength was expressed as a force (weight in g or Bloom) required to depress a plunger of 0.5" diameter (sharp edge) by penetration speed of 1 mm/s to a prescribed area of the surface of the gelatine sample to a distance of 4 mm. The analysis was repeated three times.

Statistical analysis

One-way ANOVA was applied to all results using Minitab 18 statistical software for Windows (Minitab 213 Inc., USA).

Figure 1 Flow chart of processing of chicken skin into gelatine

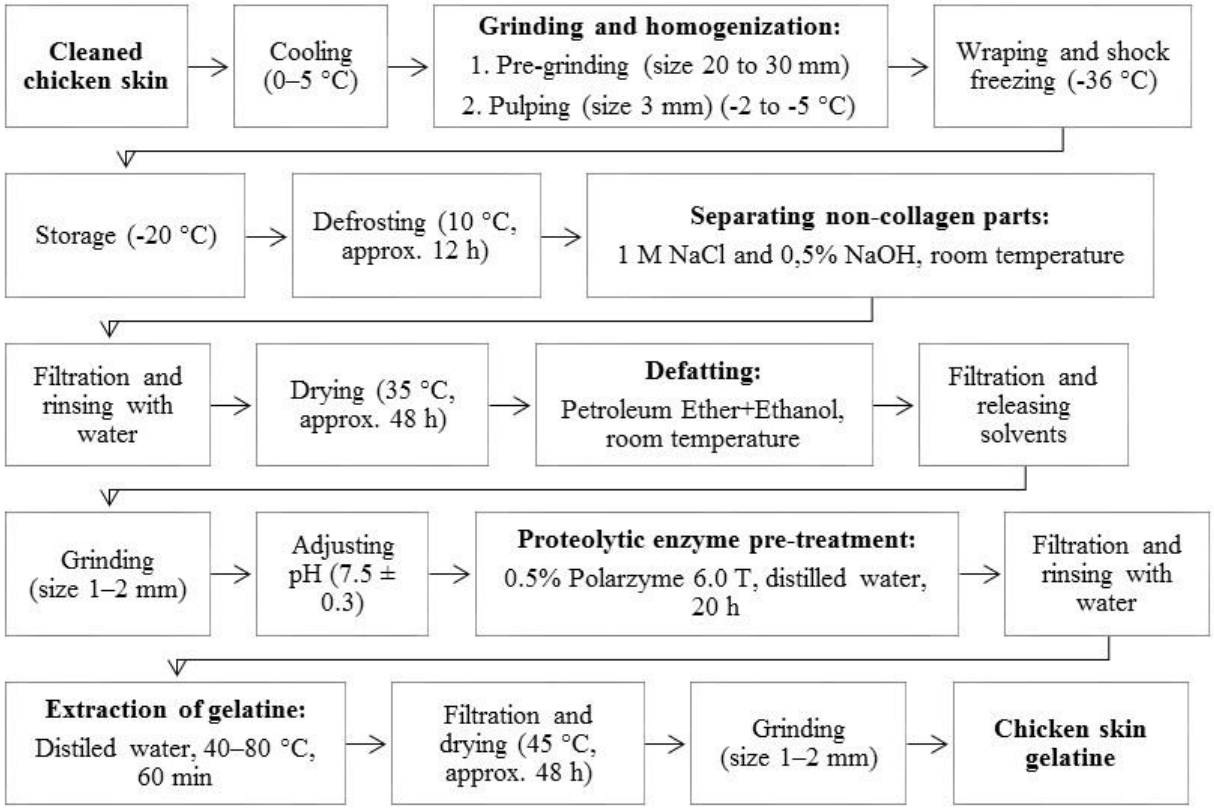

RESULTS AND DISCUSSION

Results of all experiments are shown in Table 2.

Table 2 Results of experiments

Exp. No.	Extraction temperature (°C)	Yield of extraction (%)	Gel strength (Bloom ± SD)
1	40	41.9	354 ± 2.49
2	50	47.1	352 ± 0.94
3	60	72.4	252 ± 3.85
4	70	53.8	312 ± 1.25
5	80	49.8	306 ± 1.69

Yield of extraction

The yield of gelatine obtained from extraction is generally dependent on particular species, age of animals, collagen type (amino-acid composition), degree of intermolecular collagen cross-linking and method of extraction (Widyasari and Rawdkuen 2014). The yield of gelatine extracted from chicken skin initially grew with an increasing extraction temperature. This might be due to the fact that higher temperature causes higher degree of collagen hydrolysis. Dramatic increase in the yield was observed between the temperatures of 50 °C and 60 °C. However, at 70 °C the yield of extraction significantly decreased to almost the same level as at 50 °C. This decline could be caused by partial collagen denaturation. A further increase of temperature to 80 °C caused a small decline in a yield. Nevertheless, the yield of extraction was considerably high (over 40%) at all extraction temperatures which was probably due to the fact that chicken skin collagen was very young and thus cross-linked weakly. The highest yield of extraction of 72% was achieved at 60 °C. This may be considered as the optimal extraction temperature for this type of collagen as can be seen in Figure 2. Sarbon et al. (2013) reported the yield of extraction of chicken skin gelatine of only 16% in contrast to these results. Sompie and Triasih (2018) determined the yield of extraction of chicken legskin gelatine as very low

with the values ranging from 12 to 14%. Similar results were reached by Widyasari and Rawdkuen (2014) in their study of chicken feet gelatine (13%).

Figure 2 Yield of extraction of chicken skin gelatines at different extraction temperatures

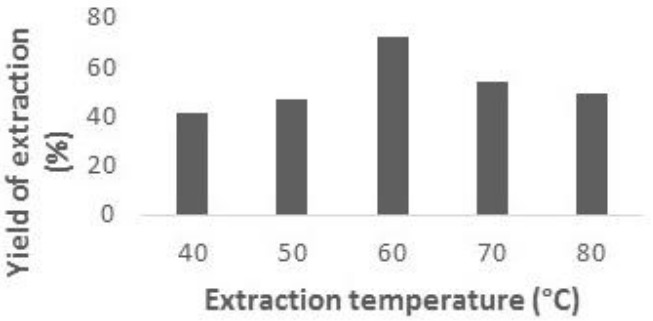

Gelatine gel strength

Gelatine gel strength (Bloom value) is one of the most crucial properties of gelatine and is a decisive indicator of its quality. Commercial gelatine from mammalian sources performs its gel strength typically within a range of 50–300 Bloom (Schrieber and Gareis 2007). Results of gel strength of chicken skin gelatines are shown in Figure 3A. Significantly high values of gel strength were recorded during all experiments. Gel strength declined with an increasing extraction temperature with the only exception of the temperature of 60 °C when a sudden drop of gel strength was registered. This may be caused by higher extraction temperature shortening the length of collagen chains of gelatine (a lower molecular weight of gelatine). The drop at 60 °C can be related to a very high extraction yield. Nevertheless, connection between gel strength and yield of extraction has been observed: the higher yield of extraction, the worse gel strength. Higher extraction yield is caused by higher level of hydrolysis, thus resulting in a decline of gelatine gel strength. The highest gel strength of 352 Bloom was recorded at the temperature of 40 °C. The values of gel strength of commercial beef and pork gelatines were 275 Bloom and 300 Bloom, respectively. Figure 3B shows a comparison of these gelatines with prepared gelatine extracted at 40 °C. Even though prepared chicken skin gelatines and commercial gelatines have fairly similar gel strengths, gelatine extracted at 40 °C showed gel strength by 17% higher. Sarbon et al. (2013) reported gel strength of chicken skin gelatine of 355 Bloom, which is almost the same value as in this study. Sompie and Triasih (2018) examined gel strength of chicken leg skin gelatine with the values of only around 78 Bloom. And Widyasari and Rawdkuen (2014) determined gel strength of chicken feet gelatine ranging between 79 and 185 Bloom.

Figure 3 Gel strength of chicken skin gelatines (A) and comparison with beef and pork gelatines (B)

3A) *3B)*

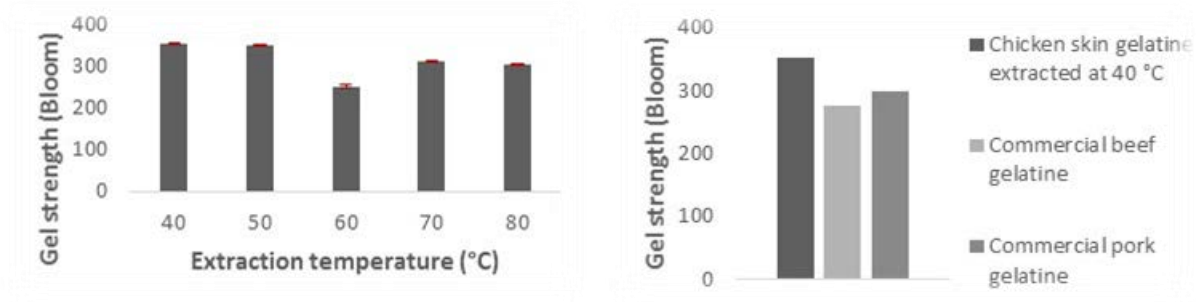

CONCLUSION

Composition of chicken skins, by-products of chicken breasts processing, were analysed. What is more, gelatine was prepared. Undesirable components, such as non-collagen proteins and fat, were eliminated. Gelatine extractions were performed in water at 5 different temperatures at constant time. Also, the influence of extraction temperature on gelatine yield and gelatine gel strength (the most

important parameter of gelatine quality) was examined. The highest yield of 72% was achieved at 60 °C and the highest gel strength of 352 Bloom was obtained at 40 °C. Generally, gel strength of all prepared gelatines reached considerably high values of over 250 Bloom. Further quality characteristics important for food industry including water holding and fat binding capacity, emulsifying and foaming properties will be the subject of further analyses.

Results of these experiments have proved that high quality chicken skin gelatine with comparable gel strength to commercially available gelatines from pork and beef should be considered as an important, accessible alternative for mammalian gelatine.

ACKNOWLEDGEMENTS

This research was financially supported by the Internal Grant Agency of the Faculty of Technology, Tomas Bata University in Zlín, ref. IGA/FT/2018/008 and IGA/FT/2018/003.

REFERENCES

Badii, F., Howell, N.K. 2003. Elucidation of the Effect of Formaldehyde and Lipids on Frozen Stored Cod Collagen by Ft-Raman Spectroscopy and Differential Scanning Calorimetry. Journal of Agricultural and Food Chemistry, 51(5): 1440–1446.

Bueno-Solano, C. et al. 2009. Chemical and Biological Characteristics of Protein Hydrolysates from Fermented Shrimp By-Products. Food Chemistry, 112(3): 671–675.

Cruz-Fernández, M. et al. 2017. Smartphone Determination of Fat in Cured Meat Products. Microchemical Journal, 13: 8–14.

GMIA Standard Testing Methods for Edible Gelatin. 2013. [Online]. Available at: http://www.gelatin-gmia.com/images/GMIA_Official_Methods_of_Gelatin_Revised_2013.pdf. [2018-05-03].

ISO Standard 3496-1978: Meat and Meat Products: Determination of L Hydroxyproline Content.

ISO Standard 937-1978: Meat and Meat Products: Determination of Nitrogen Content.

Nor, M. et al. 2017. Effects of Plasticizer Concentrations on Functional Properties of Chicken Skin Gelatin Films. International Food Research Journal, 24(5): 1910–1918.

Rasli, H.I., Sarbon, N.M. 2015. Effects of Different Drying Methods on The Rheological, Functional and Structural Properties of Chicken Skin Gelatin Compared to Bovine Gelatin. International Food Research Journal, 22(2): 584–592.

Sarbon, N.M. et al. 2013. Preparation and Characterisation of Chicken Skin Gelatin as an Alternative to Mammalian Gelatin. Food Hydrocolloids, 30(1): 143–151.

Sarbon, N.M. et al. 2015. Effect of Chicken Skin Gelatin and Whey Protein Interactions on Rheological and Thermal Properties. Food Hydrocolloids, 45: 83–92.

Schrieber, R., Gareis, H. 2007. Gelatine Handbook: Theory and Industrial Practice. Weinheim: Wiley-VCH-Verl, pp. 348.

Seong, P.N. et al. 2015. Characterization of Chicken By-Products by Mean of Proximate and Nutritional Compositions. Korean Journal for Food Science of Animal Resources, 35(2): 179–188.

Sompie, M., Triasih, A. 2018. Effect of Extraction Temperature on Characteristics of Chicken Legskin. In Proceedings of IOP Conference Series: Earth and Environmental Science 2017 [Online] Semarang, Indonesia, 26–27 September, pp. 12089. Available at: http://iopscience.iop.org/article/10.1088/1755-1315/102/1/012089/meta. [2018-08-10].

Wan Omar, W., Sarbon, N. 2016. Effect of Drying Method on Functional Properties and Antioxidant Activities of Chicken Skin Gelatin Hydrolysate. Journal of Food Science and Technology, 53(11): 3928–3938.

Widyasari, R., Rawdkuen, S. 2014. Extraction and Characterization of Gelatin from Chicken Feet by Acid and Ultrasound Assisted Extraction. Food Applied Bioscience Journal, 2(1): 85–97.

Effect of additives on the rheological properties of quail liquid egg products

Sylvie Ondrusikova[1], Lubomir Lampir[2], Sarka Nedomova[1], Roman Pytel[1], Vojtech Kumbar[3]
[1]Department of Food Technology
[3]Department of Technology and Automobile Transport
Mendel University in Brno
Zemedelska 1, 613 00 Brno
[2]Department of Horticulture
Czech University of Life Sciences Prague
Kamycka 129, 165 00 Prague
CZECH REPUBLIC

ondrusikova.sylva@seznam.cz

Abstract: The aim of this work was to monitor changes of rheological properties of liquid quail egg products depending on the types and concentration of additive substances (sugar, salt, citric acid, triethyl citrate, soya lecithin and protein). Viscosity values were determined at the temperature of 21 °C using a rotating viscometer with a standard spindle at the shear strain rates of 0.279/s, 2.79/s, and 27.9/s. The rheological behaviour of liquid quail egg products (egg yolk, egg albumen and whole egg) was carried out using a concentric cylinder system. Experimental results were modelled using power-law (also known as Ostwald-de Waele) model. Flow curves of all liquid egg products exhibited non-Newtonian behaviour.

Key Words: quail eggs, rheological properties, shear strain rate, liquid egg products, power-law model, additives

INTRODUCTION

Traditionally, eggs for the small-scale market are labeled as shell, but due to changes in lifestyle and technology, the demand for industrially processed egg masses is increasing. These products can be classified as chilled, dried or frozen products and are most commonly used in the food industry, especially bakery or confectionery industry (Atilgan and Unluturk 2008). Liquid egg albumen is most commonly used in the bakery and confectionery industry, thanks to its foam-forming ability and its stability, which is not only used for loosening. Egg melange, which is obtained by mixing egg yolk and albumen, is used as an ingredient mainly in the bakery and confectionery industry, but also in the catering industry for the preparation of omelets or mixed eggs (Atilgan and Unluturk 2008). Liquid egg masses are further used to make mayonnaise, dressings, sauces, pasta (Alvarez et al. 2006). Liquid egg products are additive for several reasons, one of the most important and extensively used in the food industry are foam stabilization and preservation. The use of these products in the food industry requires knowledge of their rheological properties (Cabral et al. 2011). Each liquid egg product that is marketed must be pasteurized. This process is carried out using a continuous flow in stainless steel pipes with defined conditions, a constant flow velocity, and temperature, especially (Guilmineau and Kulozik 2007). The rheological properties of food are important in terms of design and determination of flow processes, quality control, sensory evaluation, as well as food storage. The basic variable that characterizes the behaviour in the flow is the viscosity that determines the degree of internal resistance, i.e. resistance to flow (Kokini and Dogan 2006). The viscosity of liquid egg products depends on a number of factors – egg age, temperature, pH, specific gravity, water content and stress (shear forces). The rheological parameters have great meaning in many problems of industry. For example, the design of piping and pumping systems requires knowledge of the pressure drop due to the flow in straight pipe segments and through valves and fittings (Kumbár et al. 2015a). Friction losses caused by the presence of valves and fittings usually result from disturbances of the flow, which is forced to change direction abruptly to overcome path obstructions and to adapt itself to sudden

or gradual changes in the cross section or shape of the duct (Kumbár et al. 2015b). Principle the flow of fluids is directly proportional to the force that is applied is used to describe the class of liquids known as Newtonian fluids. Water is the best-known Newtonian fluid. A large number of fluid foods had a non-Newtonian behaviour – what means to say that they do not exhibit a direct proportionality between shear stress and shear rate – and different flow models can be used to describe their flow behaviour. One of the most extensively used is the Ostwald-de Waele model, given as the power-law model (Telis-Romero et al. 2006).

MATERIAL AND METHODS

To determine the rheological behaviour of liquid egg products with supplements were used Japanese quail eggs (*Coturnix coturnix japonica*) the breed Pharaon in 20th week of age from cages in South Moravia. Quails were fed a complete feed mixture throughout the laying season. For the preparation of liquid quail egg products, the egg was manually broken properly, the individual liquid egg masses separated (albumen, yolk and melange) and further homogenized. All liquids were filtered in order to separate impurities (chaladza, membranes). The thus prepared liquid eggs products were added suplements at various concentrations and was measured viscosity depend on shear strain rate. The 40 ml of samples for each liquid egg product were prepared and stored at 4°C before measurement. The following additives were added to the liquid quail egg products: salt (enriched with potassium iodide, Kaufland Czech Republic v.o., produced in Austria), powdered sugar (containing antifoulants, Tesco Stores ČR a.s., produced in Slovakia), citric acid (anhydrous, manufacturer Lach-Ner, s.r.o., based in Neratovice, Czech Republic), triethyl citrate (manufacturer FICHEMA s.r.o., based in Brno), soy lecithin (supplier of SOYA INTERNATIONAL, United Kingdom), corn syrup (Country Life Producer, Ltd., Slovakia), soy protein (manufactured by Azelis Czech Republic s.r.o., based in Prague). The viscosity of each sample was carried out using a rotary viscometer DV-3P (Anton Paar, Austria) equipped with a coaxial cylinder sensor system and measuring the torque of the standard spindle (TR8) immersed in the sample at constant temperature of 21 °C. For the measurement were used a shear strain rates of 0.279/s, 2.790/s, and 27.90/s. The values of viscosity was measured ten times and resulting in an average dynamic viscosity value. Ostwald-de Waele model is also known as power-law model. This widely used equation takes the form

$$\tau = K \cdot \dot{\gamma}^{n}$$

where τ is the shear stress, K is a consistency index, $\dot{\gamma}$ is the shear strain rate, and n is a flow index that indicates the type of liquid. For a Newtonian liquid $n = 1$; for a dilatant fluid $n > 1$ and for pseudoplastic fluid $n < 1$. The most non-Newtonian foods are shear thinning in < 1 (Bourne 2002). Statistical analysis of the differences was based on Statistica12 (TIBCO, CA, USA), namely single-factor ANOVA – Duncan's test. Software MATLAB with toolbox Curve fitting (MathWorks, MA, USA) was used to modelling of the experimental results. The statistically inconclusive difference was considered to be a result whose probability value reached $p > 0.05$.

RESULTS AND DISCUSSION

The viscosity was determined in relation to the three different shear strain rate. The viscosities of tested liquid egg products are displayed in Table 1. The highest viscosity values reached the liquid egg yolk at a shear strain rate of the 0.279/s, which is consistent with the study by Alitgan et al. (2008). The viscosity of liquid egg white and whole liquid eggs is significantly lower than that for liquid egg yolk. With a lower viscosity value of liquid quail egg whites and whole egg correspond the study Kumbár et al. 2015c. Simeonovová et al. (2013) shows the viscosity values of the liquid egg white 2500 mPa·s, which also corresponds to our viscosity results at a shear rate of the 0.279/s. The flow curves of the liquid quail egg products are shown in Figure 1. The liquid egg yolk exhibits the value of n closed to 1 i.e. its behaviour is close of the Newtonian liquid. For liquid quail egg yolk, the flow index is closer to 1 with the addition of 10% corn syrup (Table 2). The flow index for liquid egg yolk ranged from 0.68 (without additives) to 0.94 (10% corn syrup), indicating that egg yolk is pseudo-plastic in nature (Figure 2). The consistency index ranged from 0.21 (10% corn syrup) to 5.03 $Pa \cdot s^{n}$ (6% sugar and 6% salt). Telis-Romero et al. (2006) reports the values of the 0.84 to 0.88 flow index for a fresh

liquid egg yolk such as a higher value than our index. The more significant non-Newtonian behaviour exhibits liquid quail egg albumen and liquid whole quail egg, with the same result describing of Kumbár et al. (2015c). With values of the quail egg yolk flow index is also the same as Atilgan and Unluturk (2008), which gives the same values for fresh liquid egg yolks. The increasing of viscosity of the egg yolk can improve the quality of processing foods such as baked cakes. In which, the increasing of apparent viscosity is associated with a bigger cake size. Also, increasing the hardness of mayonnaise, because the higher the viscosity of the liquid quail egg products, the faster and more stable it occurs and the formation of a stable foam or sauce (Gouda et al. 2017).

Table 1 Result of viscosity depending on shear strain rate.

Liquid quail egg product	Shear strain rate [/s]	Viscosity [mPa·s]	Shear stress [Pa]
Yolk	0.279	11841.90[a]	3003.89
	2.79	2149.04[a]	5995.82
	27.9	932.13[a]	26006.43
Albumen	0.279	2059.80[b]	574.68
	2.79	250.68[a]	699.40
	27.9	29.61[a]	826.12
Whole egg	0.279	1944.08[b]	542.40
	2.79	268.06[a]	747.89
	27.9	53.74[a]	1499.35

Legend: [a, b] – different superscripts in a line indicate a statistically significant difference at $p < 0.05$.

Figure 1 Experimental records of the flow curves (shear stress vs. shear rate) for all liquid quail egg products – Ostwald-de Waele model.

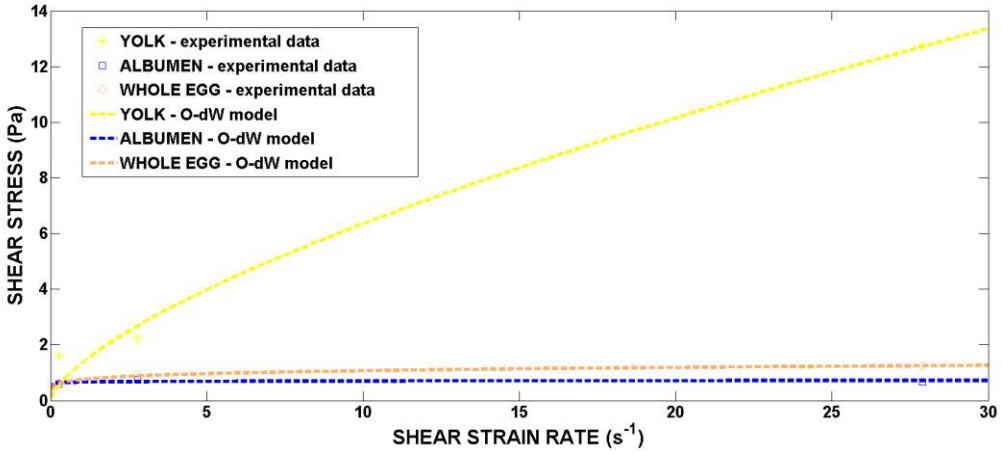

Table 2 Coefficients of the Ostwald-de Waele rheological model for liquid quail eggs yolk.

Quail liquid egg product	Additives	K [Pa·s^n]	n [-]	R^2
Yolk	without	1.34	0.68	0.98
	10% sugar	0.97	0.69	0.99
	10% salt	*	*	*
	6% sugar and 6% salt	5.03	0.80	1.00
	6% sugar and 12% salt	*	*	*
	12% sugar and 6% salt	3.03	0.82	1.00
	10% corn syrup	0.21	0.94	1.00
	0.4% soy lecithin	0.60	0.88	1.00
	1% soy protein	1.33	0.90	1.00

*Legend: * – denotes out of range, could not be modelled.*

Figure 2 Experimental records of the flow curves (shear stress vs. shear rate) for liquid quail egg yolk – Ostwald-de Waele model.

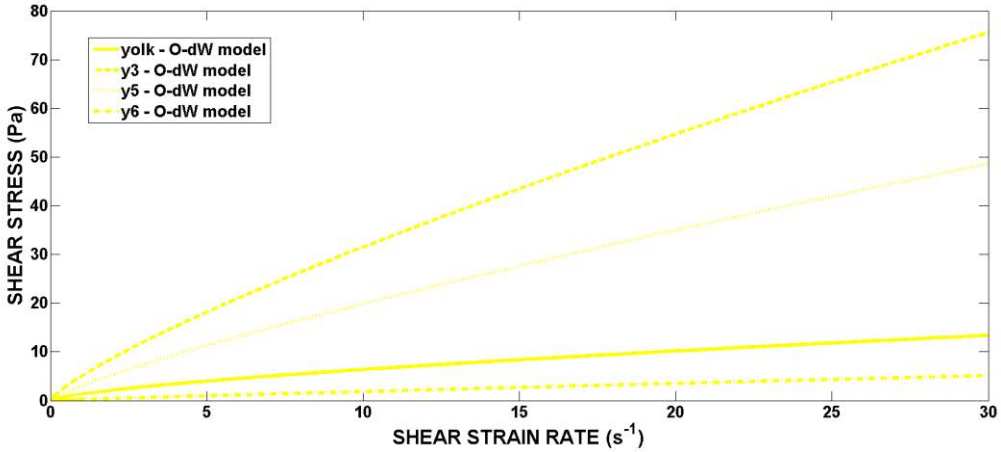

Coefficients of the Ostwald-de Waele rheological model for liquid quail eggs albumen are shown in the Table 3. The flow index of liquid egg albumen ranged from 0.03 (without addition and with 2% ethyl citrate) up to 0.17 (12% sugar and 6% salt). Egg albumen foaming properties can be improved by the addition of sucrose (effect on foam stability) or salt (effect of foaming capacity) before pasteurisation (Bourne 2002). However, sucrose reduces foaming capacity while salt reduce foam stability. A protective effect on foam stability against damage from heat treatment was also obtained by adding cations such as cooper in egg albumen (Nys et al. 2011). The viscosity of the liquid egg albumen exhibits some decrease with increasing shear rate. The consistency index ranged from 0.28 (0.4% soy lecithin) up to 1.09 $Pa \cdot s^n$ (0.03 % triethyl citrate). The shear thinning behaviour of liquid egg albumen is shown in Figure 3. Egg albumen is shown typical non-Newtonian behaviour.

Coefficients of the Ostwald-de Waele rheological model for liquid quail whole eggs are shown in the Table 4. The flow index of liquid egg albumen ranged from 0.12 (10% sugar) to 0.49 (10% porn syrup). The consistency index ranged from 0.14 (0.4% soy lecithin) to 0.99 $Pa \cdot s^n$ (2% triethyl citrate). Li et al. (2018) indicates the influence of additives on liquid quail egg products of the whole egg with 0.15% sodium diphosphate significantly affects the rheology of liquid egg products which can be used in the production and stabilization of egg gels.

Table 3 Coefficients of the Ostwald-de Waele rheological model for liquid quail eggs albumen

Quail liquid egg product	Additives	K [$Pa \cdot s^n$]	n [-]	R^2
Albumen	without	0.66	0.03	0.22
	10% sugar	0.59	0.09	1.00
	10% salt	0.72	0.09	0.65
	6% sugar and 6% salt	0.60	0.15	0.99
	6% sugar and 12% salt	0.67	0.04	0.15
	12% sugar and 6% salt	0.70	0.17	1.00
	1% citric acid	0.87	0.06	0.69
	0.03% triethyl citrate	1.09	0.05	1.00
	2% triethyl citrate	0.81	0.03	0.47
	10% corn syrup	0.31	0.12	0.91
	0.4% soy lecithin	0.28	0.06	0.99
	1% soy protein	0.36	0.10	0.84

Figure 3 Experimental records of the flow curves (shear stress vs. shear rate) for liquid quail egg albumen – Ostwald-de Waele model.

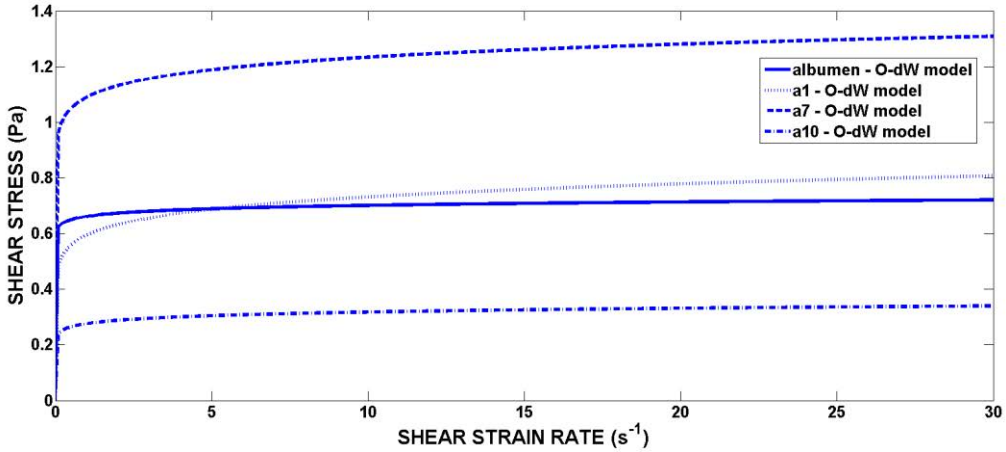

Table 4 Coefficients of the Ostwald-de Waele rheological model for liquid quail whole eggs

Quail liquid egg product	Additives	K [Pa·s^n]	n [-]	R^2
Whole egg	without	0.76	0.15	0.99
	10% sugar	0.90	0.12	1.00
	50% sugar	0.88	0.47	0.95
	2% salt	0.88	0.27	0.94
	1% citric acid	0.63	0.21	1.00
	0.03% triethyl citrate	0.65	0.21	0.97
	2% triethyl citrate	0.99	0.06	1.00
	10% corn syrup	0.16	0.49	0.99
	0.4% soy lecithin	0.14	0.47	0.99
	1% soy protein	0.25	0.26	0.87

Figure 4 Experimental records of the flow curves (shear stress vs. shear rate) for liquid quail whole egg – Ostwald-de Waele model.

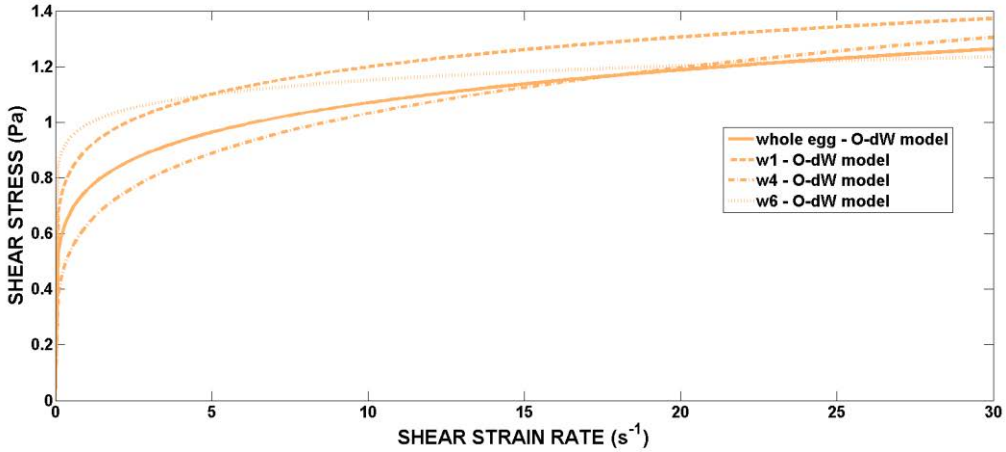

CONCLUSION

The practical importance of knowledge of rheological parameters was outlined. These parameters can be used in various software applications dealing with a numerical simulation of flow problems. Experimental data were successfully fitted to the Ostwald-de Waele model. The quail egg liquids exhibit shear thinning behaviour.

Supplements were added to liquid quail egg products to track influence of rheological behaviour. The viscosity of liquid egg albumen increased after addition of triethyl citrate, while the lowest levels are achieved by the addition of soy lecithin. These findings can be used not only in the design of industrial equipment and pipelines in the manufacturing industry, but mainly in the food industry, especially in bakeries and confectionery industries, where higher viscosities can be used to stabilize the product, not only in terms of technology but also in canning, where most of the additives used as a food preservative.

ACKNOWLEDGEMENTS

This research was supported and financed by project TP 2/2017 "Effect of additives on the rheological behaviour of foodstuffs and raw materials for their production" of Internal Grant Agency FA MENDELU.

REFERENCES

Alvarez, E. et al. 2006. Comparison of rheological behaviour of salad sauces. International Journal of Food Properties, 9: 907–915.

Atilgan, M.R., Unluturk, S. 2008. Rheological properties of liquid egg products (LEPS). International Journal of Food Properties, 11(2): 296–309.

Bourne, M. 2002. Food texture and viscosity: concept and measurement. Elsevier.

Cabral, R.A.F. et al. 2011. Friction losses in valves and fittings for liquid food products. Food and Bioproducts Processing, 89(4): 375–382.

Gouda, M. et al. 2017. Effects of four natural antioxidant phenyl terpenes on emulsifying and rheological properties of egg yolk. LWT-Food Science and Technology, 83: 59–67.

Guilmineau, F., Kulozik, U. 2007. Influence of a thermal treatment on the functionality of hen's egg yolk in mayonnaise. Journal of Food Engineering, 78(2): 648–654.

Kokini, J.L., Dogan, H. 2006. Rheological properties of foods. In Handbook of Food Engineering. CRC Press, pp. 13–136.

Kumbár, V. et al. 2015a. Effect of egg storage duration on the rheology of liquid egg products. Journal of Food Engineering, 156: 45–54.

Kumbár, V. et al. 2015b. Fluid dynamics of liquid egg products. Journal of Biological Physics, 41(3): 303–311.

Kumbár, V. et al. 2015c. On the influence of storage duration on rheological properties of liquid egg products and response of eggs to impact loading–Japanese quail eggs. Journal of Food Engineering, 166: 86–94.

Li, J. et al. 2018. Effects of selected phosphate salts on gelling properties and water state of whole egg gel. Food Hydrocolloids, 77: 1–7.

Nys, Y. et al. 2011. Improving the Safety and Quality of Eggs and Egg Products: Volume 1: Egg Chemistry, Production and Consumption. Elsevier.

Simeonovová, J. et al. 2013. Technologie drůbeže, vajec a minoritních živočišných produktů. 2. vyd. Mendelova univerzita v Brně.

Telis-Romero, J. et al. 2006. Rheological properties and fluid dynamics of egg yolk. Journal of Food Engineering, 74(2): 191–197.

Study of the influence of brewing water on selected quantitative beer indicators and on content of B vitamins

Lenka Puncocharova[1], Jaromir Porizka[1, 2], Pavel Divis[1, 2]
[1]Department of Food Chemistry and Biotechnologies
[2]Materials Research Centre
Brno University of Technology
Purkynova 118, 612 00 Brno
CZECH REPUBLIC

xcpuncocharoval@fch.vut.cz

Abstract: Brewing water is one of the basic raw materials for beer production and knowledge of its composition and pH is essential for the proper conduct of the entire brewing process. In this work it was observed how the composition of water influences OG, ABV and content of B vitamins. This paper is dedicated to synthetic water production by adding chemicals to deionized water. These models of hard and soft water were used for brewing pale bottom-fermented beer. Samples of wort, hopped wort, young beer and beer were taken during different phases of beer production. Then they were modified according to the chosen method and analysed. For B vitamins HPLC-DAD was used for quantification. According to the results water pH affects analytes content during the beer production and in the final product. Hard water seemed to be a better extraction buffer and its composition (pH) positively affected some processes during brewing technology. One of them was obtaining higher OG compared to soft water. The beer made from hard water also contained more B vitamins.

Key Words: brewing water, water pH, OG, ABV, B vitamins, HPLC

INTRODUCTION

Beer is globally popular alcoholic beverage prepared from a grain malt, water, hops and yeasts. Brewing technology is constantly evolving, and this opens the possibility of exploring the brewing processes more deeply. Beer is composed of about 94% of water, so water becomes an essential but often neglected ingredient in beer production (Comrie 1967). Therefore, composition of brewing water should be one of the studied properties. Each beer style calls for a different composition of brewing water. Some breweries even have their own sources of water. This makes their products original. Water also has a significant effect on the chemical and sensory characteristics of beer.

Calcium and magnesium salts are predominant elements in water. Term of water hardness is used for the description of the content of calcium and magnesium salts (Kadlec 2002). It represents the sum of calcium, magnesium and barium ions, or is the content of all cations with a charge greater than one. Carbonate water hardness corresponds to the content of calcium and magnesium bicarbonates. When the wort is boiled, bicarbonates are decomposed by removing carbon dioxide to create more or less soluble carbonates. Non-bicarbonate water hardness (stable) consists of calcium and magnesium salts of sulfuric acid, hydrochloric acid, nitric acid and others. These components are not affected by the wort boiling (Kadlec 2002, Basařová et al. 2010).

Water hardness is important in assessing the quality of water used in brewing. As a result, several types of brewing water were allocated based on the type of a produced beer. One of them is Pilsner water. It is a soft water with small proportion of inorganic compounds and is suitable for strongly hopped bottom-fermented beers. To produce strongly hopped top-fermented ales, Burton on Trend is used. This type of water is very hard and contents high concentration of sulphate. Other well-known brewing waters types are Munich, Dortmund and Vienna. Other important parameters which correlates with water hardness are pH and ionic strength (Basařová et al. 2010).

The dissolved salts are present in water at low concentrations, but significantly affect the sensory qualities of beer, enzymatic activity during mashing and regulate processes during boiling, cooling and fermentation of the wort (Comrie 1967). For example, calcium ions may be present in high amounts

in water (up to 200 mg/l) (Basařová et al. 2010). Calcium is essential because it reduces the pH of mash by interactions with phosphates and malt proteins. Decreasing the pH is beneficial for optimal function of some malt enzymes – it promotes stability of α-amylase against thermal denaturation (Comrie 1967, Basařová et al. 2010). Calcium silicate also causes a beer gushing. Magnesium ions stimulate yeast enzyme activity during fermentation and is a cofactor for some enzymes. Alkaline metals are found in water at lower concentrations, higher concentrations are in barley malt. It shows inhibitory effect on some malt enzymes, but it has positive physiological significance during fermentation. Metals are also present at various concentrations in water. It is enzymes cofactor and influences proteolytic degradation of malt. High content of metals causes dark colour of mash and beer foam and the mashing slows down. This reduces the fullness of flavour and the bitterness of the beer (Basařová et al. 2010).

Another parameter of the beer, which can be affected by the composition of brewing water is content of vitamins of the B group. Main sources of the vitamins of B group are malt and yeast activity. Biologically active forms are associated with enzyme complexes involved in various metabolic processes such as Citric cycle, β-oxidation, electron transport and other biochemical reactions (Hucker et al. 2011, Hucker et al. 2016). Damaged or dead cells may release the vitamin into the solution, so it can easily end up in the final product during beer production (Hucker et al. 2011).

The aim of this paper is to assess the impact of the composition of the brewing water on selected analytes in the technology of beer. For experiments, Pilsner type beers of soft and hard synthetic water were brewed, and samples of wort, hopped wort, young beer and beer were taken during production. Subsequently, the samples were analysed. HPLC was used for the assay. OG values were determined by refractometer and pH values were determined by pH meter. The assessment of differences between soft and hard water was provided by the statistical method of analysis of variance (ANOVA).

MATERIAL AND METHODS

Synthetic water preparation and beer production

Synthetic water was prepared according to Smith et al. (2002) by adding selected compounds to distilled water. By this way soft and hard model water was created.

For study of the influence of brewing water on selected analytes, beer was brewed from soft and hard synthetic water in three replicates. These were the pale bottom-fermented beers also called lagers. The raw materials were pale Pilsner barley malt (Malt house Bernard, Rajhrad), Sládek hop pellets (alpha acid content of 8.08%) and Saflager S-23 yeasts. Milled barley malt was mixed with brewing water of 38 °C and then mashing process was done in an infusion method. Evaporated water was compensated with distilled water. The values of OG and pH were measured in wort after lautering. Then it was continued with wort boiling for 90 min. After this process whirlpooling of wort was done. Also, the values of original gravity (OG) and pH were measured. The wort was cooled down to 14 °C and then it was inoculated and aerated. The worked in a fridge and the temperature was set to 14 °C. The end of fermentation was indicated steady or slowly decreased OG value. The OG value was in range of 7.3–7.0% during beer bottling. OG and pH values were measured in the samples of young beer. Then bottled beer was put in a fridge and the temperature was set to 7 °C. The secondary fermentation and maturing were done for three weeks.

Measurement of basic quantitative parameters of tested beers

The OG values were measured refractometrically. The pH of synthetic water was measured by the pH meter.

Determination of B group vitamins by HPLC analysis

The samples of wort, hopped wort, young beer and beer were degassed by ultrasound and then diluted with distilled water. All samples were analysed by HPLC with a DAD (diode array detector) to determine the quantity of B vitamins. Specifically, it was aimed at riboflavin, niacin, pyridoxine and cobalamin. B vitamins were separated on Polar C18 column (150 mm x 3.0 mm; particle size 2.6 µm) with set temperature to 40 °C. The mobile phase consisted of 10mM ammonium formate and 0.1% solution of formic acid (solvent A) and acetonitrile and 0.1% solution of formic acid (solvent B). Gradient elution was used for the analysis. The gradient was as follows: 0 min, 100% A;

12 min, 40% A; 15.10 min, 100% A and then held for another 7 min. The data were collected by the Agilent 1260 Infinity chromatographic data system.

Statistical analysis

Data analysis and statistical evaluation was carried out by Microsoft Excel and XLSTAT. Influence of the brewing water on the selected parameters of beer was evaluated by analysis of variance ANOVA (Analysis of variance). ANOVA was set to a confidence interval of 95%.

RESULTS AND DISCUSSION

Selected quantitative beer indicators

First, the pH of prepared synthetic water models was measured. The average pH value of soft water was 7.68 ± 0.23, the average pH value of hard water was 8.47 ± 0.08. Compared to theoretical pH, the measured values were lower. The theoretical model of soft water pH was 7.83 and 8.49 hard water (Smith et al. 2002).

Figure 1 shows difference between pH of soft and hard water during mashing. During mashing, the pH decreases due to malt enzymes activity, which releases phosphates from nucleic acids. In the process of wort boiling, the wort acidity is increased by precipitation of phosphates in the presence of calcium and magnesium ions. Hop bitter acids and Maillard reaction products further contribute to pH reduction. When fermenting, the pH decreases by the activity of yeasts that consume amino acids and produce organic acids. The pH also changes because of presence of the carbon dioxide, which dissolves in the solution (Basařová et al. 2010).

Figure 1 Changes of synthetic water pH during beer production

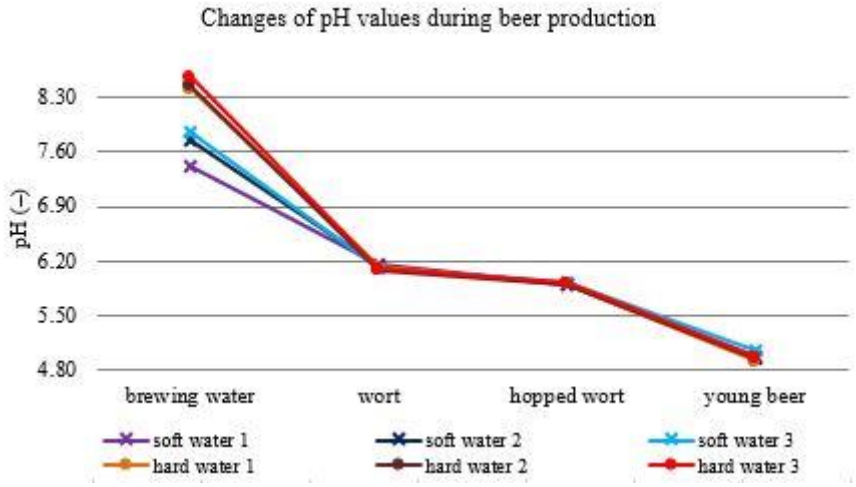

OG (original wort extract) and ABV (Alcohol by Volume) were selected as the basic quantitative indicators for beer brewing. The extract of the original wort was used to express the total carbohydrate content presented in the medium. Differences in beers prepared from different kind of synthetic water were observed. Both, original gravity and concentration of alcohol were statistically different. The mean value of wort OG prepared by using soft water was 12.6 ± 0.1%, while wort OG of hard water was 13.05 ± 0.05% (see Figure 2). Higher yields in hard water are probably due to higher amounts of Mg^{2+} and Ca^{2+} ions, which stabilize α-amylases and increase its activity (Karbassi and Saboury 2000, Saboury et al. 2005). After wort boiling, the OG slightly increased, probably due to the extraction of chemical compounds in hop. A large decline occurred during fermentation when yeasts utilized carbohydrates. A small drop occurred during secondary fermentation and maturing in bottles because yeasts largely depleted the substrate and was no longer as vital as at the beginning. The process of fermentation of all samples is shown in Figure 3. As the yeast assimilated the substrate, the OG also declined and the ethanol concentration in the medium grew as expected. Complete fermentation of experimental beers took 70 hours.

Figure 2 Changes of OG in individual phases of beer production

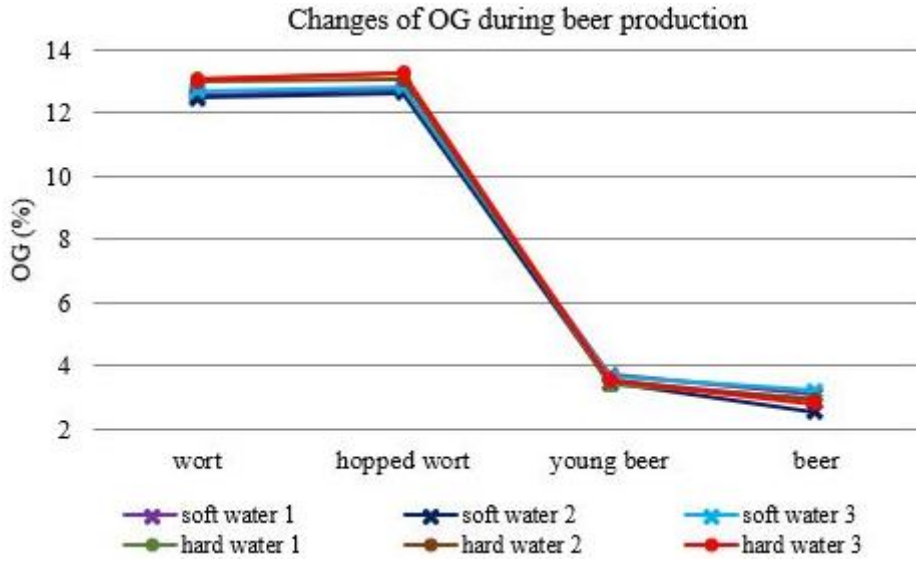

Figure 3 OG and ABV changes during primary fermentation

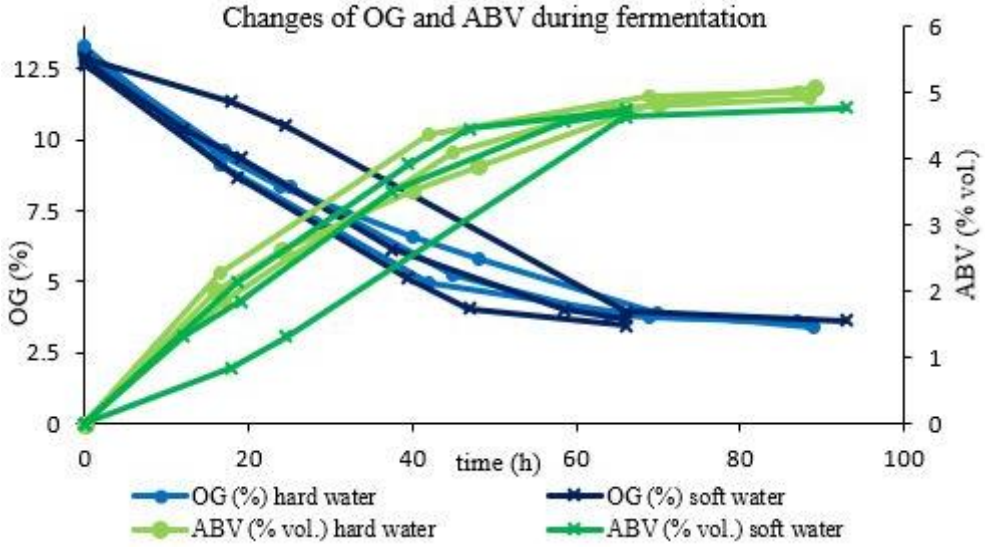

Quantification of selected B vitamins

Determination of B2 (riboflavin), B3 (niacin), B6 (pyridoxine), B12 (cyanocobalamin) vitamins were done to assess the influence of the two different kind of experimental brewing waters on content of B vitamins. The concentration of the last two mentioned vitamins was below the detection limit in all samples. The results of the analysis of the determined B vitamins are shown in Tables 1 and 2.

Table 1 Quantification of B3 vitamin (F_{krit} = 7.71)

Type of sample	Type of water	Mean	Min	Max	P	F
Wort	soft	31.68	30.07	33.18	0.0007	92.2144
	hard	40.85	40.25	41.36		
Hopped wort	soft	36.13	32.92	41.56	0.0674	6.2091
	hard	43.05	42.14	43.97		
Young beer	soft	8.97	6.70	10.59	0.7838	0.0861
	hard	9.34	8.54	10.11		
Beer	soft	8.99	7.97	10.02	0.0448	8.3243
	hard	10.97	10.47	11.63		

Statistically significant differences between hard and soft water were found in wort (P = 0.0007, F = 92.214). Hard water seemed to work as a better extraction agent due to different pH and ionic strength. Content of vitamin B changed during the brewing. In the presence of yeast, the level of B3 vitamin declined rapidly as yeast used vitamin in the wort in biochemical processes and nicotinic acid synthesis does not occur (Basařová et al. 2010). Relatively small, but significant difference in concentration of vitamin B was found in final product. A slightly higher average concentration of vitamin B was determined in beer from hard water. This phenomenon is probably caused by releasing cell content during yeast autolysis.

Usual content of niacin in beer is around 5 mg/l (Basařová et al. 2010). The measured values are higher in comparison with the literature, approximately 8–12 mg/l. High vitamin content can be caused by no further treatment after beer bottling, unlike commercial beers, which are filtered and often pasteurized.

Table 2 Quantification of B2 vitamin (F_{krit} = 7.71)

Type of sample	Type of water	Mean	Min	Max	P	F
Wort	soft	0.90	0.84	0.93	0.0385	9.2210
	hard	1.00	0.96	1.01		
Hopped wort	soft	1.09	0.97	1.18	0.5513	0.4221
	hard	1.14	1.11	1.16		
Young beer	soft	0.29	0.27	0.33	0.0008	83.2461
	hard	0.57	0.53	0.62		
Beer	soft	0.77	0.70	0.90	0.3008	1.4099
	hard	1.02	0.62	1.25		

Very similar trend was observed for B3 vitamin. Statistically significant differences were found in wort and young beer (shown in Table 2). Riboflavin was better extracted from barley malt during mashing in hard brewing water than in soft. This could be due to different pH of the water. Riboflavin is a thermostable vitamin, there were observed no loss of the vitamin in the process of wort boiling. During fermentation there was a certain decrease in vitamin content, the greatest difference was observed in soft water. In hard water, to thereby prevent high losses probably because riboflavin form stable complexes with Zn^{2+}, Ni^{2+}, Co^{2+}, Cu^{2+}, Ca^{2+}, Mg^{2+} (Sheraz et al. 2014). In beer, the vitamin concentration was probably increased by the release of yeast autolysis.

Usual content of riboflavin in beer is approximately 0.25 mg/l (Olšovská et al. 2012). When comparing the values and literature the B2 vitamin concentration is several times higher – 0.6 to 1.2 mg/l. Again, it is probably the reason for omitting post fermentation adjustments.

CONCLUSION

The brewing water is one of raw materials used for beer production in a brewery and knowledge of its composition and pH is necessary for correct run of the whole process.

Evaluation of the influence of two synthetically prepared water types on basic quantitative parameters was done. In addition, effect on content of B group vitamins were assessed. In conditions of laboratory six samples of pale bottom-fermented pilsner type beer were brewed in synthetic soft and hard water. The pH value of soft water was approximately 0.8 pH lower than pH of hard carbonate water. During beer production the samples of wort, hopped wort, young beer and beer was taken and the pH and OG and ABV values were measured.

The composition of brewing water had influence on extraction during mashing. Wort prepared from hard synthetic water had OG higher than 13%, while wort prepared from soft synthetic water had OG equal to 12.6%. Composition of hard synthetic water had positive effect on amylase activity during mashing. It means that a more concentrated product can be obtained from the same amount of malt. This is interesting for the producer in terms of technology and investment.

Other part of this study was focused on exploration of effects of different brewing water on content of B vitamins. B2, B3 vitamins were determined. B vitamins are present in barley malt, but the biggest

changes of concentration are observed during primary fermentation. Composition of brewing water had an influence on B2 vitamin content in wort and young beer. Hard synthetic water was better extraction agent and bivalent ions, which were present in hard water and created stable complex with B2 vitamin. Analysis of variance did not demonstrate statistically significant differences in beer due to big range of data. Another research may show the contrary. Statistically significant differences in content of B3 vitamin were also found, specifically in wort and beer. Higher concentrations were determined in samples prepared by using hard synthetic water.

The research shown that brewing water influences selected basic parameters. In the final product – beer – it was found out that hard brewing water is better for higher yields of OG. Brewing water also affects the content of riboflavin and niacin.

ACKNOWLEDGEMENTS

This work was financially supported by the project: Materials Research Centre at FCH BUT Sustainability and Development, REG LO1211, with financial support from the National Programme for Sustainability I and FCH-S-18-5334 (Ministry of Education, Youth and Sports).

REFERENCES

Basařová, G. et al. 2010. Pivovarství: teorie a praxe výroby piva. Praha: Vydavatelství VŠCHT.

Comrie, A.A.D. 1967. Brewing liquor. Journal of the Institute of Brewing, 73(4): 335–346. Available at: https://onlinelibrary.wiley.com/doi/abs/10.1002/j.2050-0416.1967.tb03050.x [2018-04-19].

Hucker, B. et al. 2011. The Quantitative Analysis of Thiamin and Riboflavin and Their Respective Vitamers in Fermented Alcoholic Beverages. Journal of Agricultural and Food Chemistry, 59(23): 12278–12285. Available at: http://pubs.acs.org/doi/abs/10.1021/jf202647x [2018-05-07].

Hucker, et al. 2016. Vitamins in brewing: presence and influence of thiamine and riboflavin on wort fermentation. Journal of the Institute of Brewing, 122(1): 126-137. Available at: http://doi.wiley.com/10.1002/jib.293 [2018-05-07].

Kadlec, P. 2002. Technologie potravin II. Praha: Vysoká škola chemicko-technologická.

Karbassi, F., Saboury, A.A. 2000. Thermodynamic studies on the interaction of calcium ions with alpha-amylase. Thermochimica Acta [Online], 362(1–2): 121–129. Available at:

http://linkinghub.elsevier.com/retrieve/pii/S0040603100005797 [Accessed May 06, 2018].

Olšovská, J. et al. 2012. Nové trendy v kapalinové chromatografii a jejich využití v analýze piva a pivovarských surovin: Část 2. Stanovení cis/trans- izomerů iso-α-hořkých kyselin v pivu metodou ultraúčinné kapalinové chromatografie. Kvasný průmysl [Online], 58(4): 94–99. Available at: https://kvasnyprumysl.cz/pdfs/kpr/2012/04/01.pdf [2018-06-03]

Saboury, A.A. et al. 2005. Thermodynamic study of magnesium ion binding to alpha amylase. Indian Journal of Biochemistry & Biophysics, 42(5): 326–329. Available at:

http://nopr.niscair.res.in/bitstream/123456789/3533/1/IJBB%2042(5)%20326-329.pdf [2018-05-06].

Sheraz, M.A. et al. 2014. Photo, thermal and chemical degradation of riboflavin. Beilstein Journal of Organic Chemistry, 10(4): 1999–2012. Available at:

http://www.beilstein-journals.org/bjoc/content/10/1/208 [2018-05-05].

Smith, E.J. et al. 2002. Methods for preparing synthetic freshwaters. Water Research, 36(5): 1286–1296. Available at: https://www.ncbi.nlm.nih.gov/pubmed/11902783 [2018-04-29].

Selected qualitative parameters of oils from *Hippophae rhamnoides* L. and *Rosa canina* L.

Michaela Vaidova[1], Vladimir Masan[1], Alice Cizkova[1], Patrik Burg[1], Miroslav Macak[2]
[1]Department of Horticultural Machinery
Mendel University in Brno
Zemedelska 1, 613 00 Brno
CZECH REPUBLIC
[2]Department of Machines and Production Biosystems
Slovak University of Agriculture in Nitra
Tr. A. Hlinku 2, 949 76 Nitra
SLOVAKIA

vladimir.masan@mendelu.cz

Abstract: Considering the increasing demand of new sources of high quality foods, this study evaluates the antioxidant capacity, total phenolic compounds and fatty acids composition in sea buckthorn and rose hip oil produced by screw cold pressing. The highest yields when producing the sea buckthorn oil were reached by the 6 mm of nozzle diameter at 50 rpm speed (0.0767 kg of oil per 1 kg of seeds) and when producing the rose hip oil, it was by the 6 mm of nozzle diameter at 30 rpm speed (0.0116 kg of oil per 1 kg of seeds). The results show the high level of PUFA values 51.39% in sea buckthorn oil and 76.23% in rose hip oil. The predominant fatty acid was linoleic, 31.76% in sea buckthorn oil and 54.10% in rose hip oil. The antioxidant capacity of the sea buckthorn oil was 54.67 mg (TEA)/g and of the rose hip oil were 64.45 mg (TEA)/g. The total phenolic compounds of the sea buckthorn oil were 43.71 mg (GAE)/g and of the rose hip oil was 46.77 mg (GAE)/g. The values of both parameters (DPPH and TPC) are in both oils very similar.

Key Words: antioxidant capacity, total phenolic compounds, fatty acids, oil, screw press

INTRODUCTION

In recent years, a number of cold-pressed oils from different kinds of seeds and fruits have appeared on the market and got the attention of customers. These oils have specific characteristics and flavours, and often contain valuable bioactive substances with plenty of health benefits. As the example of those less-known oils are oils from either sea buckthorn or rose hip. The rose hip and sea buckthorn seed oils, according to many studies, have very similar quality as grape-seed oil and pomegranate-seed oil, which have been very popular on the market recently.

Sea buckthorn oil produced form this fruit varies and its content depends on the fact, if the oil is extracted from either the seeds or the pulp of the fruit. Regularly, the both methods are used for oil production. The seeds content is up to 10% of fruit weigh and store up to 12% of oil, that has thick consistency, specific taste, smell and light yellow colour (Krejcarová et al. 2015, Nogala-Kalucka et al. 2010).

Sea buckthorn oil is a unique natural substance with high amount of biologically active components. The clinical tests and science research (Zheng et al. 2017, Michel et al. 2012) carried out during the 20th century prove its healing and nutritious benefits. It has being used for inside of the body as well as outside treatments. It serves as a biogenic stimulator with ability to reduce the pain in a same way as analgesics do (Krejcarová et al. 2015, Yang and Kallio 2002).

The seeds of rose hip (*Rosa canina* L.) are a waste product from the manufacture of rose hip juice or syrup, and contain from 4.9% to 17.82% of oil. The health benefits of rose hip are attributed to the presence of bioactive compounds such as ascorbic acid, carotenoids, and phenolic compounds. Apart from improving lipid metabolism and a possible anticancerogenic effect, the rose hip oil showed a positive influence on dermatoses, ulcers and other skin diseases too and became quite popular in beauty industry as well (Özcan 2002).

Oil extracted from rose hip seeds has been revealed as a substantial source of unsaturated fatty acids, the most abundant being linoleic (35.9–54.8%), followed by α-linolenic (16.6–26.5%) and oleic (14.7–22.1%) acids (Özcan 2002, Szentmihályi et al. 2002).

When it comes to technological part of the pressing the sea buckthorn seeds in order to produce the oil, the continuous screw presses are being used. Cakes produced contain 15–20% of oil. These cakes are being extracted in continuously working extractors (Velíšek 2002). The oil from rose hip is produced directly from the continuous screw presses.

The benefit of screw pressing is to produce high-quality oil containing bioactive compounds, without using organic solvent. Screw pressed method has low investment costs for equipment in comparison to the supercritical fluid extraction method. Another benefit of screw pressing is to provide a simple and reliable method of processing small batches of seeds. The quality of oils is the factor that decides on the further use of oil in food industry (Prescha et al. 2014).

Considering the increasing demand of new sources of high quality vegetable proteins, this study evaluates the antioxidant capacity, total phenolic compounds and fatty acids composition in sea buckthorn and rose hip oil produced by screw pressing.

The aim of this study is to verify the oil production from the local sources of seeds and to compare its qualitative parameters.

MATERIAL AND METHODS

Material

The fruits of sea buckthorn (*Hippophae rhamnoides* L.) were harvested during February 2017 on the lands of Faculty of Horticulture, Mendel University in Lednice, Czech Republic in order to gain the juice. Harvesting of sea buckthorn berries was started after the temperature fell significantly below the freezing point. The fruits were harvested manually by shaking of the twigs directly in the orchard and gathered on the outspread tarps. A mixed sample was set in by picking up the berries of various varieties together. After pressing, the drying of the marc was done in the shadow on the sieves in room on the fresh air for about a week. A prototype of vibratory separator was used to separate the seeds from marc. The seeds collected by this method were further pressed.

The fruits of *Rosa canina* L. "Pollmeriana" were harvested during January 2017 on the lands of the fruit company called Ovosad based in Myjava, Slovakia. The harvest was realized by tractor trailed harvester SP-07 (Elektronik, Serbia). After the harvest, the drying process took place in room on the fresh air, in the shadow on the sieves for about a month. Dry fruits were cut into pieces and their seeds were separated by the prototype of vibratory separator. The seeds collected this way were further pressed as well.

Screw press

The screw press type UNO FM 3F made by the Farmet Company in Czech Republic was used for experimental measurements. This model is suitable for pressing of all kinds of oilseeds. The drive is configured for three-phase voltage with variable speed of the main drive using a frequency converter, which enables better optimization of pressing parameters. The press components are: an electric motor (1.5 kW power), transmission, pressing device, motor starter and frequency converter (this allows precise adjustment of rpm from 0 to 200). The pressing device components are: a matrix, 220 mm screw, head, heating mantle, nozzle holder and nozzles of different in diameter (6, 8 and 10 mm).

Determination of density of oils

Density of oils was determined pycnometrically according to the standard ČSN EN ISO 6883. This international standard specifies a method for the determination of the conventional mass per volume ("litre weight in air") of vegetable fats and oils. Determination of density was performed in triplicate.

Analysis of fatty acids

The preparation for fatty acids analysis was performed by transesterification. The oil samples from pressed oil was dissolved in 2 ml of isooctane and homogenized in ultrasound. After adding 2 ml of methanol sodium, the mixture was heated under condensator for 5 minutes. Subsequently, 2 ml BF3

(boron trifluoride) was added (through the cooler) and the mixture was heated again under the same condensator for another 5 minutes. After that, 2 ml of isooctane was added to the mixture, shaked and left for 1 minute to settle down. At the very end, 5 ml of saturated sodium chloride solution was added. The analysis of fatty acids was performed on the gas chromatograph HP 4890D (Hewlett Packard, USA) with a flame ionizing detector (GC-FID). The separation was performed on column DB-23 (60 m x 0.25 mm x 0.25 µm). Every sample was measured in triplicates.

Antioxidant capacity (DPPH radical scavenging) and total phenolic compounds (TPC)

The preparation to determine the antioxidant capacity and total phenolic compounds in pressed oil was as follows: 0.5 g of sample was weighed while and extracted into 7.5 ml of 50% methanol, sonicated for 60 min at the room temperature and then centrifuged at 16 100 g for 20 min at 4 °C temperature. After centrifugation, the methanol phase was removed.

The analysis of antioxidant capacity was determined using 1,1-diphenyl-2-picrylhydrazyl (DPPH) and the test was performed on the spectrophotometer Boeco S-200 (Boeco, Germany) where the absorbance at the wavelength of 534 nm was measured. The result was calculated to mg of Trolox equivalent activity (TEA) per gram of sample. Every sample was measured in triplicates.

The analysis of total phenol content was performed on the spectrophotometer Boeco S-200 (Boeco, Germany) where the absorbance at the wavelength of 660 nm was measured. The result was calculated to mg of gallic acid equivalent (GAE) per gram of sample. Every sample was measured in triplicates.

Statistical analysis

As determinations were done in triplicate the data were reported as means ± standard deviation. Statistical analyses were performed by the software "Statistica 12.0" (StatSoft Inc., USA).

RESULTS AND DISCUSSION

The oil yield

The oil yield depends on the pressing speed, attained pressure, length of pressure action, conditions of oil outflow at a maximum pressure, viscosity, and oil temperature. During oil production, it was found out that the nozzle of size 8 and 10 mm sketchily press the material and does not produce appropriate amount of oil. Moreover, the speeds stated above in the Table 1, made the extracting not possible as the press was becoming blocked. In overall, especially when it comes to sea buckthorn, the problematic was for the presser to start and to set ideal working process for the oil production.

Table 1 Values of pressing time (h), yield of oil (kg) and press capacity (kg/h), at the optimal settings of presser (diameter of the nozzle and speed)

Parameters	Sample of oil	
	Sea buckthorn	Rose hip
Mean of nozzle (mm)	6	6
Speed (rpm)	50	30
Pressing time of 1 kg of seeds (h)	0.2839 ± 0.0125	0.4256 ± 0.0340
Yield of oil from 1 kg of seeds (kg)	0.0767 ± 0.0306	0.0116 ± 0.0031
Press capacity (kg/h)	0.2724 ± 0.1185	0.0272 ± 0.0064

The highest yields when producing the sea buckthorn oil were reached by the 6 mm of nozzle diameter at 50 rpm speed (0.0767 kg of oil per 1 kg of seeds) and when producing the rose hip oil, it was by the 6 mm of nozzle diameter at 30 rpm speed (0.0116 kg of oil per 1 kg of seeds). The regular yield of the sea buckthorn oil is approximately 5–15% (Krejcarová et al. 2015, Yang and Kallio 2002) and of the rose hip oil it is 3.3–6.7% (Szentmihályi et al. 2002, Del Valle et al. 2000).

The sea buckthorn oil density was 911.5 ± 9.3 kg/m^3 and the rose hip oil density was 923.5 ± 8.1 kg/m^3, that is similar to those values that other authors declare (Del Valle et al. 2000).

Fatty acids composition

Linoleic, vaccenic, alfa-linolenic, palmitic acids were the predominant fatty acids in the sea buckthorn oil (Table 2), which confirms the results of Zheng et al. (2017), Yang and Kallio (2002).

The highest content of pressed oils was represented by poly-unsaturated fatty acids (PUFA) which 51.39%, respectively, whereas the mono-unsaturated fatty acids (MUFA) content in oil extracted from seeds represented 29.03%, showing twice as high value than of the PUFA in pressed oils.

Saturated fatty acids (SFA) content was 18.82% in pressed oil, which is slightly higher content in comparison with what Zheng et al. (2017) declares.

Table 2 Fatty acid composition, antioxidant capacity and total phenolic content of pressed oil

Parameters		Sample of oil	
		Sea buckthorn	Rose hip
Fatty acid composition (%) (v/w)	C14:0/myristic	0.11 ± 0.00	0.05 ± 0.01
	C16:0/palmitic	16.23 ± 0.80	4.01 ± 0.01
	C16:1n7/palmitoleic	5.42 ± 0.16	0.09 ± 0.01
	C18:0/stearic	2.48 ± 0.06	2.48 ± 0.05
	C18:1n7/vaccenic	19.73 ± 0.25	16.36 ± 0.12
	C18:1n9C/oleic	3.66 ± 0.09	0.46 ± 0.02
	C18:2n6C/linoleic	31.76 ± 0.11	54.10 ± 0.44
	C18:3n6/gamma-linolenic	0.15 ± 0.00	0.08 ± 0.00
	C18:3n3/alfa-linolenic	18.58 ± 0.07	20.66 ± 0.34
	C18:4n3/stearidonic	0.35 ± 0.00	0.95 ± 0.04
	C20:1/eicosaenoic	0.22 ± 0.01	0.31 ± 0.02
	C20:4n3/eicosatetraenoic	0.15 ± 0.00	0.12 ± 0.01
	C20:5n3/eicosapentaenoic	0.04 ± 0.00	0.09 ± 0.00
	C22:4n6/adrenic	0.09 ± 0.00	0.09 ± 0.01
	C22:5n6/docosapentaenoic	0.15 ± 0.01	0.12 ± 0.01
	C22:5n3/clupanodonic	0.08 ± 0.00	0.02 ± 0.01
	C22:6n3/docosahexaenoic	0.03 ± 0.00	0.00 ± 0.00
	SFA (%)	18.82 ± 0.74	6.53 ± 0.05
	MUFA (%)	29.03 ± 0.19	17.21 ± 0.13
	PUFA (%)	51.39 ± 0.18	76.23 ± 0.59
	Antioxidant Capacity (DPPH) (mg TEA/g)	54.67 ± 0.62	64.45 ± 1.20
	Total Phenolic Content (mg GAE/g)	43.71± 0.83	46.77 ± 0.89

Legend: Values are means ± standard deviations of a triplicate measurements; SFA: saturated fatty acids; MUFA: mono-unsaturated fatty acids; PUFA: poly-unsaturated fatty acids; TEA: trolox equivalent activity; GAE: gallic acid equivalent.

In the rose hip oil, the dominant were compositions like, once again, linoleic, vaccenic, alfa-linolenic acids, but, on the other hand, the rose hip oil had significantly lower content of SFA because of low content of palmitic acid compared to the sea buckthorn oil. The PUFA values were much higher than expected, 76.23%, and the ration between the PUFA and MUFA values was significantly higher. The values of each acids reflect the results of other authors (Ilyasoğlu 2014, Prescha et al. 2014).

Two fatty acids – stearic and adrenic acid, were the fatty acids, with no differences in both oils. Moreover, the concentration of other acids had only minimal differences in their values, and content wise were both oils very similar to each other.

To increase the PUFA values and to lower SFA values in diet of a person is a favourable step to do to reduce the risk of cardiovascular disease. This statement is supported by the results of Kang et al. (2005) which indicates that the PUFA and SFA values ratio is ideal when it is between 1.0–1.5. Our own produced sea buckthorn oil and rose hip oil significantly exceed this ratio and therefore are suitable as a supplement to the diet. The high level of PUFA values restrains them to be used for frying, but on the other hand, the PUFA values are a benefit for the stability of cold-pressed oils (Prescha et al. 2014).

Antioxidant capacity (DPPH radical scavenging) and total phenolic compounds (TPC)

The antioxidant capacity of the sea buckthorn oil was 54.67 mg Trolox equivalent activity (TEA)/g (Table 2). This value is similar to what Kagliwal et al. (2012) states, a bit lower then what Nogala-Kalucka et al. (2010) declares, but still lower in comparison with Zheng et al. (2017). Buřičová and Réblová (2008) state the value 24 mg/g.

The antioxidant capacity of the rose hip oil was 64.45 mg Trolox equivalent activity (TEA)/g, which is same as authors Nogala-Kalucka et al. (2010), and Buřičová and Réblová (2008) state.

The TPC of the sea buckthorn oil was 43.71 mg of gallic acid equivalent (GAE)/g. Michel et al. (2012) claims the value 120 mg (GAE)/g and Nogala-Kalucka et al. (2010) 115 mg (GAE)/g – but both of them claim this value in seeds.

The TPC value of the rose hip oil was 46.77 mg of gallic acid equivalent (GAE)/g. Ercisli (2007) states the value 96 mg (GAE)/g, Javanmard et al. (2017) state the value in average 93 mg (GAE)/g, while all of them claim this value as it was in fruits. Only Nogala-Kalucka et al. (2010) states the value 40 mg (GAE)/g in seeds. The values of both parameters (DPPH and TPC) are in both oils very similar.

CONCLUSION

The study verified the possibilities of sea buckthorn and rose hip oil production on a screw press. The highest yields when producing the sea buckthorn oil were 0.0767 kg of oil per 1 kg of seeds and when producing the rose hip oil, it was 0.0116 kg of oil per 1 kg of seeds. The values of DPPH and TPC was in both oils very similar and very high. The ration between the PUFA and MUFA values was significantly higher (51:29 and 76:17) and is the factor that decides on the further use of oil in food industry.

ACKNOWLEDGEMENTS

This research was financially supported by the project IGA - ZF/2017 - AP004 – "Possibilities of pressing oil from seeds of fruit crops".

REFERENCES

Buřičová, L., Réblová, Z. 2008. Czech medicinal plants as possible sources of antioxidants. Czech Journal of Food Sciences, 26(2): 132–138.

Del Valle, J.M. et al. 2000. Comparision of conventional and supercritical CO_2-extracted rosehip oil. Brazilian Journal of Chemical Engineering, 17(3): 335–348.

Ercisli, S. 2007. Chemical composition of fruits in some rose (Rosa spp.) species. Food Chemistry, 104(4): 1379–1384.

Ilyasoğlu, H. 2014. Characterization of rosehip (*Rosa canina* L.) seed and seed oil. International Journal of Food Properties, 17(7): 1591–1598.

Javanmard, M. et al. 2017. Characterization of biochemical traits of dog rose (*Rosa canina* L.) ecotypes in the central part of Iran. Natural Product Research, 32(14): 1738–1743.

Kagliwal, L.D. et al. 2012. Antioxidant-rich extract from dehydrated seabuckthorn berries by supercritical carbon dioxide extraction. Food and Bioprocess Technology, 5(7): 2768–2776.

Kang, M.J. et al. 2005. The effects of polyunsaturated: saturated fatty acids ratios and peroxidisability index values of dietary fats on serum lipid profiles and hepatic enzyme activities in rats. British Journal of Nutrition, 94(4): 526–532.

Krejcarová, J. et al. 2015. Sea buckthorn (*Hippophae rhamnoides* L.) as a potential source of nutraceutics and its therapeutic possibilities - a review. Acta Veterinaria Brno, 84(3): 257–268.

Michel, T. et al. 2012. Antimicrobial, antioxidant and phytochemical investigations of sea buckthorn (*Hippophaë rhamnoides* L.) leaf, stem, root and seed. Food Chemistry, 131(3): 754–760.

Nogala-Kalucka, M. et al. 2010. Phytochemical content and antioxidant properties of seeds of unconventional oil plants. Journal of the American Oil Chemists' Society, 87(12): 1481–1487.

Özcan, M. 2002. Nutrient Composition of Rose (Rosa canina L.) Seed and Oils. Journal of Medicinal Food, 5(3): 137–140.

Prescha, A. et al. 2014. The antioxidant activity and oxidative stability of cold-pressed oils. Journal of the American Oil Chemists' Society, 91(8): 1291–1301.

Szentmihályi, K. et al. 2002. Rose hip (*Rosa canina* L.) oil obtained from waste hip seeds by different extraction methods. Bioresource Technology, 82(2): 195–201.

Velíšek, J. 2002. Chemie potravin 1. 2. vyd., Tábor: OSSIS.

Yang, B., Kallio, H. 2002. Composition and physiological effects of sea buckthorn (*Hippophaë*) lipids. Trends in Food Science & Technology, 13(5): 160–167.

Zheng, L. et al. 2017. Fatty acid, phytochemical, oxidative stability and in vitro antioxidant property of sea buckthorn (*Hippophaë rhamnoides* L.) oils extracted by supercritical and subcritical technologies. LWT - Food Science and Technology, 86: 507–513.

Živočišné a rostlinné tuky a oleje - Stanovení konvenční objemové hmotnosti (ve vzduchu). ČSN EN ISO 6883 (588827). Praha: Úřad pro technickou normalizaci, metrologii a státní zkušebnictví.

Changes of fatty acids content in rat liver after different diet

Veronika Zigmundova, Tomas Komprda, Veronika Rozikova
Department of Food Technology
Mendel University in Brno
Zemedelska 1, 613 00 Brno
CZECH REPUBLIC

xzigmund@mendelu.cz

Abstract: The aim of this research was to observe changes of fatty acids content in liver tissues of model animals after different diet. Within the experiment the male rats of the laboratory strain Wistar Albino were used and divided into five groups. Model animals were fed daily *ad libidum* with basic feed mixture (control group) and feed mixture enriched of 8% of selected oils for 10 weeks. *Schizochytrium alga* oil – DHA oil and fish oil (test groups), safflower oil and palm oil (negative control groups) were used. At the end of the experiment the liver tissue of rats was removed and analyzed. Fatty acids content was determined with usage of gas chromatography based on the combination of lipid extraction and derivatization. It was concluded that fatty acids content in liver tissue of rats is influenced by addition of tested oils in the diet. Dietary changes, particularly replacement of some dietary components, could reduce the risk of inflammatory diseases.

Key Words: fatty acid, gas chromatography, oil, rat liver

INTRODUCTION

Fatty acids represent the main constituent of lipids and play very important role in human nutrition and health. They are considered as energy resources for the whole body, structural components, precursors for signal molecules, they are essential for development of central nervous system etc. (Grofová 2010). It is known that fatty acid composition of the diet influences the fatty acid composition of stored and structural lipids in different body compartments. The results obtained in many previous studies indicate that not only total fat intake but also dietary fatty acid composition have an important effect in the development of obesity, type 2 diabetes and cardiovascular diseases (Andersson et al. 2002).

From the point of view of nutrition physiology fatty acids are distinguished into groups according to number of double bonds in a molecule to saturated fatty acids (SFA), monounsaturated fatty acids (MUFA) and polyunsaturated fatty acids (PUFA). PUFA group includes series of n-3 and n-6 characterized by different physiological effects (Grofová 2010, Erdman et al. 2012).

SFA are positively associated with concentrations of inflammation markers in plasma. The replacement of SFA-rich diet with a MUFA–rich diet can cause a decrease in plasma inflammatory molecules and could result in an improvement in insulin sensitivity and LDL-cholesterol levels (Dijk et al. 2009). The representative compounds of PUFA n-3 and n-6 series are essential α-linolenic acid (18:3n-3) and linoleic acid (18:2n-6) and their important metabolites eicosapentaenoic acid (20:5n-3), docosahexaenoic acid (22:6n-3) and arachidonic acid (20:4n-6) (Grofová 2010). The final metabolites of these fatty acids are eicosanoids, influencing the regulation of inflammatory response (Noolen et al. 2014). Increased intake of fatty acids of n−3 serie is a possible dietary strategy to reduce the incidence of coronary artery disease and a high proportion of fatty acids of n−3 serie in red blood cell membranes is associated with a reducing of primary cardiac arrest (Andersson et al. 2002).

This experiment was focused on observing of changes in fatty acids content in rat liver after different diet enriched by selected oils. The aim of the experiment was to find out whether the fatty acid composition of rat liver can be influenced by the diet composition and apply received knowledge in human nutrition.

MATERIAL AND METHODS

Model animal and diet intervention description

Fifty adult male rats of the laboratory strain Wistar Albino (Faculty of Medicine, Masaryk University, Brno, Czech Republic) were used and housed in the plastic boxes (53.5 x 32.5 x 30.5 cm) at room conditions of 23 ± 1 °C, humidity 60% and 12/12 h light/dark cycle. Model animals were randomly divided into five groups composed of ten animals and were fed daily *ad libidum* with free access to drinking water at the same time. Feed mixture (Biokron, Blučina, Czech Republic) was composed of wheat, oat, wheat sprouts, soybean meal, extruded soybean, maize, dried milk, dried whey, dried yeast, grounded limestone, monocalcium phosphate, salt, L-lysine hydrochloride, premix of vitamins and minerals. Animals were fed with basic feed mixture - granules (control group) and feed mixture enriched of 8% of selected oils for 10 weeks. The effect of dietary *Schizochytrium alga* oil – DHA oil and fish oil (test groups), safflower oil and palm oil (negative control groups) was tested. Composition of used feed mixtures is presented in Table 1. Feed consumption was measured daily and animals were weighed in weekly intervals. At the end of the experiment liver tissue of each animal was removed under anesthesia and analyzed.

The experiment was performed in compliance with the Czech National Council Act No. 246/1992 Coll. to protect animals against cruelty, the Amended Act No. 162/1993 Coll., and was approved by the "Commission to protect animals against cruelty" of the Mendel University in Brno and of the Ministry of Agriculture of the Czech Republic.

Table 1 Composition of used feed mixtures for rats

Fatty acid (in % of total fatty acids)	Granules	DHA oil	Fish oil	Safflower oil	Palm oil
Myristic	0.3	2.9	3.5	1.8	1.2
Palmitic	0.1	19.2	19.1	30.2	33.6
Palmitoleic	0.4	2.8	7.1	4.3	2.4
Heptadecanoic	0.2	0.3	0.7	0.5	0.3
Stearic	3.5	4.8	5.9	6.2	6.15
Oleic	30.2	35.5	37.9	42.7	44.9
Linoleic	53.7	2.3	1.6	11.7	2
Linolenic	0.4	0.5	1	0.6	0.4
Gamma-Linolenic	10.4	1.7	3.2	2.3	2.4
Eicosadienoic	0.2	0.5	0.6	0.5	0.5
Homo-Gamma-Linolenic	0.2	0.5	1.1	0.9	0.2
Arachidonic	0.2	0.6	1.6	1.1	0.4
EPA	0.2	1.1	4.8	0.8	0.6
DTA	0.1	6.1	0.8	21.6	0.9
DPA	0.3	1	1.9	4.2	0.8
DHA	0	20	9.1	2	3
Total lipids (in %)	5.5	8.4	6.7	8.5	5.7

Fatty acids determination and statistical evaluation

Liver tissue of rats was analyzed according to the protocol described in the paper of Komprda et al. (2013) with usage of gas chromatography based on the combination of lipid extraction and derivatization.

Methyl esters of fatty acids were separated and identified by gas chromatography with nitrogen as a carrier gas. Gas chromatograph Fisons GC 8000 series equipped with capillary column DB-23.60 m x 0.25 mm x 0.25 µm (Agilent Technologies, USA), flame ionization detector and autosampler HT300A were used. Determined separation conditions were 1.5 ml/min for flow rate, pressure of 200 kPa, split ratio of 20 : 1. The temperature program was set up at 140 ˚C/1 min., gradient 5 ˚C/ min. to 200 ˚C/1 min, gradient 3 ˚C/min. to 240 ˚C held for 15 min., injector was heated at temperature of 250 °C, detector

at temperature of 260 °C. Fatty acids content in analysed samples was expressed in mg/100 g of the analysed tissue.

The measured data were statistically evaluated by one-way analysis of the variance ratio test, including Tukey's post-hoc test ($p < 0.05$) in Statistica 12 (StatSoft, USA) and in Microsoft Excel 2010 programmes.

RESULTS AND DISCUSSION

The experiment was focused on observing of differential effect of selected dietary oils on fatty acids content in the liver tissue of rats. The influence of palm oil (source of PUFA n-6 serie), safflower oil (source of PUFA n-6 serie), fish oil (source of PUFA n-3 serie) and *Schizochytrium microalga* oil - DHA oil (source of PUFA n-3 serie) was tested.

Diet rich in SFA affects expression of genes involved in inflammation processes, whereas consumption of MUFA-rich diet leads to anti-inflammatory profile contributing to health improvements, which is accompanied by LDL-cholesterol decrease. Thereby the replacement of dietary SFA with MUFA can reduce the risk of inflammation-related diseases such as metabolic syndrome. The increased PUFA intake could be accompanied by the decreasing of proinflammatory genes (Dijk et al. 2009). According to Komprda (2003) and Grofová (2010) the total recommended daily intake of fats is regarded at 30% of which PUFA group should be represented by 7%. The optimal ratio of PUFA to SFA is regarded the ratio of 3: 1. PUFA n-6 serie should be represented by 5%, PUFA n-3 serie should create 1%, of which eicosapentoenoic fatty acid (EPA, 20:5n-3) and docosahexaenoic fatty acid (DHA, 22:6n-3) only 0.5%. Total content of SFA, MUFA and PUFA groups detected in the liver tissue of rats is shown in Figure 1.

Figure 1 Content of SFA, MUFA and PUFA groups in the liver tissue of rats

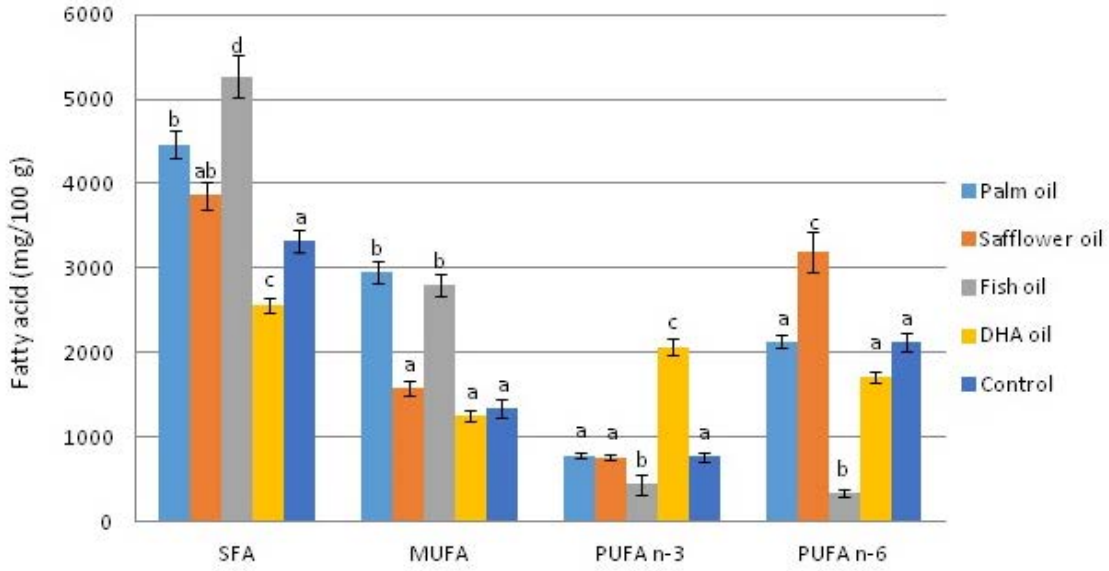

Legend: [A-D] means with different letters within a given trait differ at P < 0.05

High content of palmitic (16:0) and stearic (18:0) acids of SFA serie and oleic (18:1n-9) acid of MUFA serie was detected in all tested groups. The increased quantity of PUFA n-6 serie (linoleic acid, 18:2n-6; arachidonic acid, 20:4n-6) was expected in a group with diet enriched of safflower oil compared with other groups. High content of EPA was measured in fish oil, therefore Grofová (2010) states that fish should be consumed at least twice per week. High quantity of DHA was found out in DHA oil. Dietary EPA and DHA are important constitutions of cell membranes from the point of view of their fluidity and behavior of the integral membrane proteins (Schitz and Ecker 2008), they show anti-inflammatory (Calder 2013), antiplatelet and antiarrhythmic properties (Wiktorowska-Owczarek et al. 2015). Consumption of PUFA n-3 serie and restriction of SFA, trans-fatty acids and PUFA n-6 food intake appear as an appropriate diet (Grofová 2010). Representation of individual fatty acids of SFA, MUFA and PUFA groups in rat liver is shown in Table 2 and 3.

Table 2 SFA and MUFA content in the liver tissue (mg/100g)

Group	14:0	16:0	17:0	18:0	16:1n-7	18:1n-9
PO	60.0	2949.9	9.6	1442.3	60.8	2885.4
SO	57.2	2295.6	44.2	1463.4	46.8	1539.4
FO	145.0	3525.8	85.7	1513.7	322.7	2483.1
DHAO	52.4	1663.6	39.5	813.3	57.2	1197.2
Control	53.0	1914.2	50.8	1300.2	81.0	1262.4

Legend: PO- Palm Oil, SO – Safflower Oil, FO – Fish Oil, DHAO – DHA Oil

Table 3 PUFA content in the liver tissue (mg/100g)

Group	PUFA n-3				PUFA n-6					
	18:3	20:5	22:5	22:6	18:2	18:3	20:2	20:3	20:4	22:4
PO	4.1	5.3	129.7	644.8	232.8	79.3	68.5	49.3	1657.8	44.2
SO	66	25.1	92.8	576.9	524.3	83	271.7	79	2078.6	159.6
FO	16.5	77.8	70.5	276.1	124.9	62.6	22	18.4	95.9	19.6
DHAO	8.5	192.9	123.9	1747.1	108.1	51.5	20.1	52.3	1216.2	258.9
Control	0	38.4	117.7	612.1	219.8	109.4	30.3	25.5	1710.8	32.1

Legend: PO- Palm Oil, SO – Safflower Oil, FO – Fish Oil, DHAO – DHA Oil

The highest value of the PUFA n-6/n-3 ratio was measured in the safflower oil (negative control group) in comparison to the other test and control groups. The diet enriched by fish oil and DHA oil (test groups) caused significant reduction of the PUFA n-6/n-3 ratio in liver tissue (Figure 2).

Figure 2 The ratio of PUFA n-6 : n-3 series in the liver tissue of rats

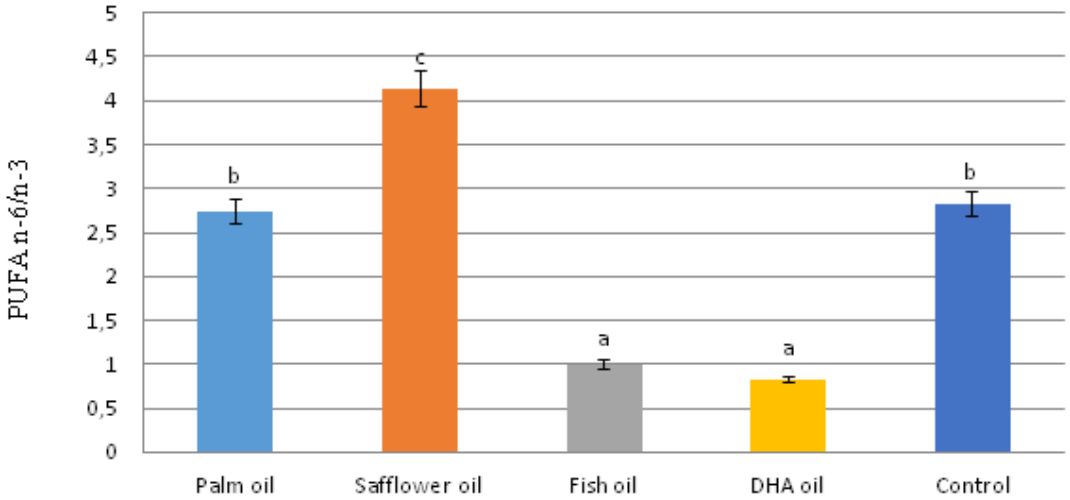

Legend: [A-D] means with different letters within a given trait differ at P < 0.05

PUFA n-6/n-3 ratio approaches almost to an optimum due to increased amounts of PUFA n-3 serie in the diet. The ratio 1 : 1 of PUFA n-6/n-3 is considered ideal, but it is significantly higher (15-16,7 : 1) in economically developed countries (Simopoulos 2008). Therefore, the World Health Organization recommends 5 : 1–2 : 1 ratio. PUFA double bonds are susceptible to oxidation, therefore the higher consumption of the lipophilic antioxidant vitamin E (recommended daily dose of 10 mg/day) is suggested for prevention of undesirable oxidation in molecules (Picková 2010, Svačina 2012).

CONCLUSION

It can be concluded based on our results that fatty acids composition in the diet correlates with their deposition in liver tissues of rats. The qualitative and quantitative representation of fatty acids

depends not only on the diet, but on the nutrient conversion as well, which is affected by a number of factors (Rozíková et al. 2012). Therefore, access to nutrition could have significant preventive or therapeutic effects. It is necessary to mention the results of this experiment carried out on rats as model animals should be interpreted cautiously concerning dietary recommendations for humans.

ACKNOWLEDGEMENTS

The research was financially supported by the Internal Grant Agency of the Mendel University in Brno (project No. TP 3/2017). The results and outcomes were prepared using instrumentation funded from the Research and Development for Innovations Operational Programme, project CZ.1.05/4.1.00/04.0135 Teaching and Research Facilities for Biotechnological Disciplines and Extension of Infrastructure.

REFERENCES

Andersson, A. et al. 2002. Fatty acid composition of skeletal muscle reflects dietary fat composition in humans. The American Journal of Clinical Nutrition [Online], 76(6): 1222–1229. Available at: https://academic.oup.com/ajcn/article/76/6/1222/4689554. [2018-09-01].

Calder, P.C. 2013. N-3 Fatty acids inflammation and immunity: new mechanisms to explain old actions. Proceedings of the Nutritional Society [Online], 72(3): 326–336. Available at: https://www.ncbi.nlm.nih.gov/pubmed/23668691. [2018-09-12].

Dijk, S.J. et al. 2009. A saturated fatty acid–rich diet induces an obesity-linked proinflammatory gene expression profile in adipose tissue of subjects at risk of metabolic syndrome. The American Journal of Clinical Nutrition [Online], 90(6): 1656–1664. Available at: https://academic.oup.com/ajcn/article/90/6/1656/4598127. [2018-09-10].

Erdman, J.W. et al. 2012. Present Knowledge in Nutrition. 10th ed., Ames: International Life Sciences Institute.

Grofová, Z. 2010. Mastné kyseliny. Medicína pro praxi: časopis praktických lékařů [Online], 7(10): 388–390. Available at: https://www.medicinapropraxi.cz/artkey/med-201008-0010_Mastne_kyseliny.php. [2018-9-02].

Komprda, T. 2003. Základy výživy člověka. Brno: MZLU.

Komprda, T. et al. 2013. The effect of dietary *Salvia hispanica* seed on the content of n-3 long-chain polyunsaturated fatty acids in tissues of selected animal species, including edible insects. Journal of Food Composition and Analysis, 32: 36–43.

Noolen, L.V. et al. 2014. Docosahexaenoic acid supplementation modifies fatty acid incorporation in tissues and prevents hypoxia induced-atherosclerosis progression in apolipoprotein-E deficient mice. Prostaglandin, Leukotrienes and Essential Fatty Acids [Online], 91(4): 111–117. Available at: http://www.sciencedirect.com/science/article/pii/S0952327814001252. [2018-09-09].

Picková, I. 2010. Svět potravin a kouzlo biotechnologií. Ostrava: Key Publishing,

Rozíková, V. et al. 2012. Effect of palm oil and salmon oil fatty acids composition in the tissues of rats. In Proceedings of International PhD Students Conference MendelNet 2012 [Online]. Brno, Czech Republic, November, Brno: Mendel University in Brno, Faculty of Agronomy. Available at: https://mnet.mendelu.cz/mendelnet2012/articles/35_rozikova_644.pdf. [2018-09-03].

Schmitz, G. et al. 2008. The opposing effects of n-3 and n-6 fatty acids. Progress in Lipid Research [Online], 47(2): 147–155. Available at: https://www.ncbi.nlm.nih.gov/pubmed/18198131. [2018-09-11].

Simopoulos, A.P. 2008. The importance of the omega-6/omega-3 fatty acid ratio in cardiovascular disease and other chronic diseases. Experimental Biology and Medicine [Online], 233(6): 674–688. Available at: http://journals.sagepub.com/doi/abs/10.3181/0711-MR-311?url_ver=Z39.88-2003&rfr_id=ori%3Arid%3Acrossref.org&rfr_dat=cr_pub%3Dpubmed&. [2018-9-7].

Svačina, Š. 2012. Dietologie pro lékaře, farmaceuty, zdravotní sestry a nutriční terapeuty. Praha: Triton.

Wiktorowska-Owczarek, A. et al. 2015. PUFAs: Structures, Metabolism and Functions. Advances in Clinical and Experimental Medicine [Online], 24(6): 931–941. Available at: https://www.ncbi.nlm.nih.gov/pubmed/26771963. [2018-09-08].

PLANT BIOLOGY

Effective pollen management during production of hybrid seeds of *Petunia hybrida*

Marketa Cerna, Josef Cerny, Petr Salas
Department of Breeding and Propagation of Horticultural Plants
Mendel University in Brno
Valticka 337, 691 44 Lednice
CZECH REPUBLIC

marketa.c@email.cz

Abstract: Basic principle of production F1 seeds of *Petunia hybrida* is pollination of maternal component with pollen collected from paternal plants. The aim of production companies is to make this process most effective in terms of costs and one way how to achieve it is to eliminate the waste. The aim of this experiment was to determine if pollen diluted with microcrystalline cellulose can be used for successful pollination. This would represent significant reduction of pollen and paternal plants needed for F1 seeds production. Maternal plants were pollinated by: 100% pollen, pollen diluted with 50% of microcrystalline cellulose and pollen diluted with microcrystalline cellulose in 1:1 ratio and number of formed seeds per seed capsule was examined. Based on the results from 4 hybrid combinations, there was no statistically significant difference. Maternal plants can be pollinated with the pollen diluted with microcrystalline cellulose in 1:1 ratio, which represents 50% less paternal plants needed.

Key Words: Petunia hybrida, pollen, microcrystalline cellulose

INTRODUCTION

Production of hybrid seeds of *Petunia hybrida* is very expensive, so production companies are aiming to decrease the costs (Anderson 2007). One possibility, relocating the production to countries with low minimal wages in problematic in many ways, and many companies are searching for new options, like increasing effectivity of the whole production process (Gerats and Strommer 2009).

Better pollen management is a promising way how to decrease costs. Basic principal of the F1 seeds production is pollinating maternal plants with a pollen collected from paternal plants. This can be done manually flower by flower, or significantly faster, when pollen is collected with a vacuum collector and then applied on the flowers of maternal plants with a brush.

Amount of pollen applied with a brush is several times higher than amount of pollen grains needed for perfect pollination of maternal flower. Increasing volume of pollen by adding inert material represents savings of pollen and thereby less paternal plants are needed.

Multiple inert materials were tested for this reason (Franke and Galun 1977). Pollen has to stay loose and remain the germination after addition of this material. Milled polyester was tested for Petunias and had no negative effect on pollen quality (Weiguang et al. 2003). Next step in optimalization of pollen management is to determine the amount of inert material that can be added without decreasing of number developed seeds in the seed capsule. First step to do so, is to test the germination of pollen collected from paternal plants. There are many methods for testing pollen germination. Very exact is germination testing on medium with boron and sacharosis content (Brewbaker and Kwack 1963). Pollen disperged in the drop of this medium germinates in 4-6 hours. This method imitates the best the natural conditions after putting pollen to stigma. Drawback of this method is very long time needed for the obtaining the results.

For fast determination of pollen germination is better fluorescein diacetate (FDA) method. This substance penetrates through pollen cytoplastmic membrane, where is transfomed by the metabolism of vital cell to fluorescein. Fluorescein has absorb maximum 494 nm and emites green signal when 512 nm. So in the fluorescent microscope metabolically active pollen grains shine green, dead are without fluorescence. This method is widely accepted as reliable for testing pollen germination (Pinillos and Cuevas 2008). Advantage is also the speed of this method, results are available within minutes.

MATERIAL AND METHODS

Characterization of experimental design and methods

The aim of this research was to determine if it is possible to successfully pollinate maternal plants of *Petunia hybrida* with pollen diluted with inert material. Usually are maternal plants pollinated with pollen collected from paternal plants, but in this case is surplus of pollen grains applied on stigma.

Based on pre-research experiments focusing on testing pollen germination after dilution with: (1) milled silica, (2) vermiculite and (3) microcrystalline cellulose, the pollen germination was not influenced only by microcrystalline cellulose, so only this material was used in this experiment.

Maternal and paternal components for production of 4 hybrid varieties *Petunia hybrida*, provided by Czech biotechnological company Černý-BioPro, Prague were sown in January 2018 planted in the plug trays under supplemental light and transplanted to 6 cm and later to 12 cm pots. Standard cultivation guidelines were followed.

5 maternal and 5 paternal plants for each of the 4 tested hybrid varieties were planted. Pollen from paternal plants was collected with a special pollen collector that was developed (Cerna et al. 2018). The vacuum created by vacuum pump makes pollen collection more efficient. Pollen germination was tested using fluorescent dye (Pinillos and Cuevas 2008) and only pollen with germination more than 85% was further used for pollinating maternal plants. Collected pollen was divided into 3 thirds: (1) control, (2) pollen diluted with addition on 50% of microcrystalline cellulose LK (produced by Lachema, Czech Republic), and (3) pollen diluted with microcrystalline cellulose in 1:1 ratio.

From the beginning of June for 4 weeks, the maternal plants were pollinated twice a week. On every maternal plant 15 flowers suitable for pollination (fully flowering, wet stigma) were selected, the rest of flowers were removed from the plant. 5 flowers were pollinated with pollen (1) and flower was wrapped with red cotton. 5 flowers were pollinated with pollen (2) and wrapped with blue cotton and 5 flowers were pollinated with pollen (3) and wrapped with orange cotton.

This was done for 4 consecutive weeks, twice per week, so the aim was to get 200 seed capsules per one hybrid combination, 5 maternal plants x 5 flowers x 4 weeks x 2 pollination per week = 200 seed capsules.

Seed capsules were harvested from the plants about 3 weeks after pollination, when capsule did not crack yet. Seed capsules were dried and stored separately for every hybrid combination and every pollen type.

100 seed capsules from the group were randomly selected and amount of seeds per capsule was counted.

T-test was used to determine if there is a statistically significant difference when the maternal plants are pollinated only with pollen (control) and with pollen diluted with microcrystalline cellulose (50 or 100 weight %). Program STATISTICA 12 was used.

RESULTS AND DISCUSSION

Average amount of seeds per 1 seed capsule for 4 tested hybrid varieties – Lavina White F1, Lavina Salmon F1, Marika F1 and Lucie F1 are listed in Figure 1.

For all four tested varieties, there was not statistically significant difference in amount of developed seeds per 1 seed capsule when the maternal plants were pollinated with pollen from paternal plants and with pollen diluted with 50 and 100% of microcrystalline cellulose. T-test results are listed in tables 1–4.

The germination of pollen used in this experiment was more than 85%. This was tested using fluorescein diacetate (FDA) method. Metabolically active pollen grains were shining green (Figure 2A). Method (Figure 2B) using germination on medium with boron and sacharosis content (Brewbaker and Kwack 1963) was not used in this experiment, since this method is very lenghty.

Figure 1 Average amount of seeds per seed capsule

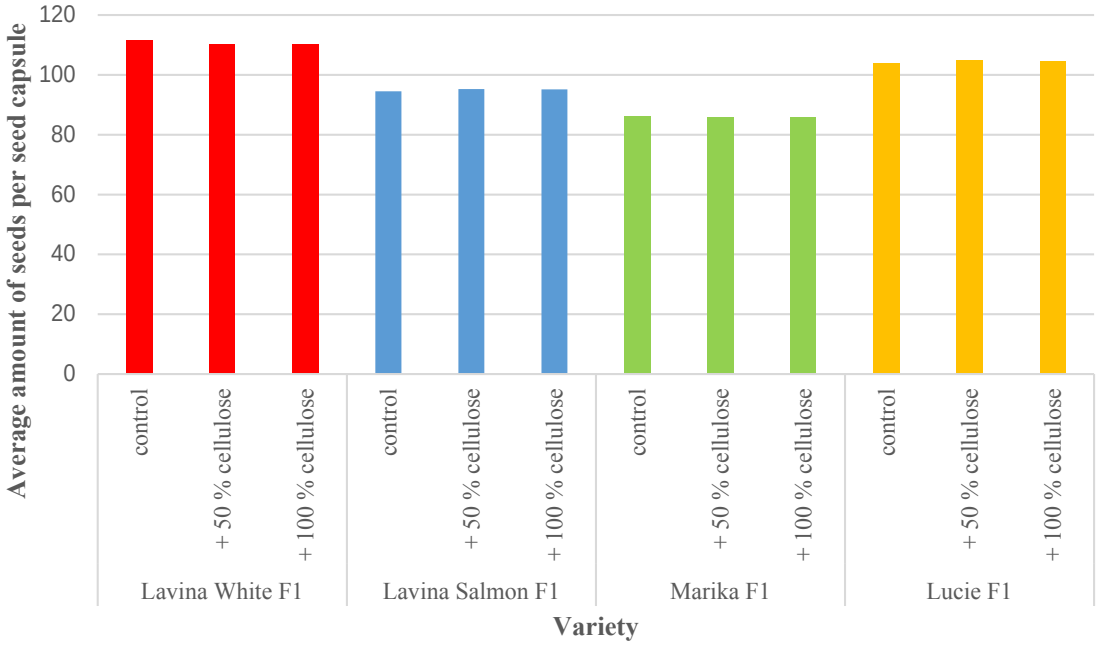

Table 1 T-test for Lavina White F1

	Mean Group 1	Mean Group 2	t-stat.	sv	p	Units per group 1	Units per group 2	Stand. deviation 1	Stand. deviation 2	F-stat.	p Variances
Control vs. 50% cellulose	111.440	110.030	0.842	198	0.40	100	100	12.028	11.665	1.063	0.761
Control vs. 100% cellulose	111.440	110.160	0.859	198	0.39	100	100	12.028	8.780	1.869	0.002

Note: T-test for independent samples; p statistics p = 0.05; measures in pieces of seeds per 1 seed capsule; computed in STATISTICS 12

Table 2 T-test for Lavina Salmon F1

	Mean Group 1	Mean Group 2	t-stat.	sv	p	Units per group 1	Units per group 2	Stand. deviation 1	Stand. deviation 2	F-stat.	p Variances
Control vs. 50% cellulose	94.550	95.300	-1.053	198	0.29	100	100	5.381	4.668	1.329	0.159
Control vs. 100% cellulose	94.550	95.160	-0.905	198	0.37	100	100	5.381	4.054	1.762	0.005

Note: T-test for independent samples; p statistics p = 0.05; measures in pieces of seeds per 1 seed capsule; computed in STATISTICS 12

Table 3 T-test for Lucie F1

	Mean Group 1	Mean Group 2	t-stat.	sv	p	Units per group 1	Units per group 2	Stand. deviation 1	Stand. deviation 2	F-stat.	p Variances
Control vs. 50% cellulose	103.730	104.680	-1.234	198	0.22	100	100	5.757	5.107	1.271	0.234
Control vs. 100% cellulose	103.730	104.490	-1.133	198	0.26	100	100	5.757	3.445	2.793	0.000

Note: T-test for independent samples; p statistics p = 0.05; measures in pieces of seeds per 1 seed capsule; computed in STATISTICS 12

Table 4 T-test for Marika F1

	Mean Group 1	Mean Group 2	t-stat.	sv	p	Units per group 1	Units per group 2	Stand. deviation 1	Stand. deviation 2	F-stat.	p Variances
Control vs. 50% cellulose	86.080	85.910	0.306	198	0.76	100	100	3.997	3.872	1.066	0.753
Control vs. 100% cellulose	86.080	85.670	0.779	198	0.44	100	100	3.997	3.423	1.363	0.125

Note: T-test for independent samples; p statistics p = 0.05; measures in pieces of seeds per 1 seed capsule; computed in STATISTICS 12

Figure 2 Testing of pollen germination

A) Fluorescein diacetate (FDA) method

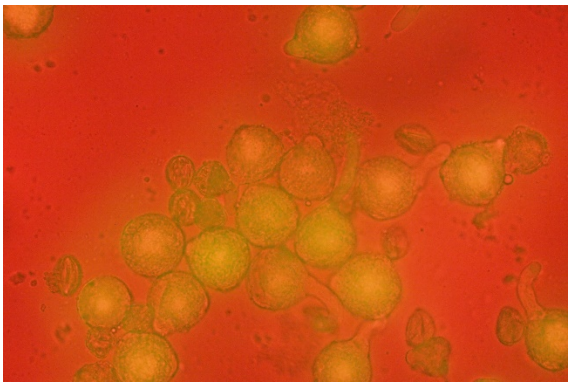

B) Medium with boron and sacharosis content

Based on the results of conducted experiments, there is no statistical difference between amounts of developed seeds per 1 seed capsule when the maternal plant was pollinated with pure pollen collected from paternal plant or if it was pollinated with pollen diluted with 50 or 100 weight percent of microcrystalline cellulose. This means that addition of inert material (in this experiment microcrystalline cellulose) to increase the pollen volume does not have negative impact on pollination quality and number of developed seeds.

In the pre-phase of the experiment 3 inert materials were tested – milled silica, vermiculite and microcrystalline cellulose. Based on that, the best results were obtained while using microcrystalline cellulose LK, this material homogenizes easily with pollen after multiple shaking. Pollen grain is also partially compounded of cellulose (Sink 1984), so the diluted material has similar chemical and physical characteristics. For the similar purpose was, according to Weiguang et al. (2003), used milled nylon that had no negative impact on pollen germination also after multiple days of storing. Authors of this experiment were evaluating vitality of pollen with a test of pollen tube growth in the style. According to us, counting number of develped seeds in the seed capsule is more precise. It is well kvantificated process that involves process from pollination to seed formation. This closely represents the conditions of comercial seed production. Milled nylon was not avaliable for us, so we were not able to include it into our experiment.

Results of pre-phase of experiment also show, that dilution of pollen in higher ratio than 1:1 leads to rapid decreasement of number of formed seeds. Based on that, the only dilution with 50 and 100 weight percent was tested.

Using diluted pollen represent significant savings. According to Sink 1984, 15% of all production costs of hybrid seeds are allocated for pollen collection. Based on our findings (Cerna et al. 2017), the costs for pollen collection were 17% of total for hybrid combination with fertile maternal component and 30% for combination with sterile maternal component. Price of 1 gram of pollen of component 5 is 3 EUR. For Petunias of grandiflora type, the price of 1 gram of pollen is between 3 and 8 EUR. These costs would reduce by half, if using diluted pollen in ratio 1:1 with inert material. Additional savings would be due to less paternal parents need to be planted to obtain pollen for pollination of the same number of maternal plants.

The cost of inert material used of increasing weight of the pollen is low. 1 gram of microcrystalline cellulose costs 0.08 EUR, 1 gram of milled silica costs 0.03 EUR, 1 gram of vermiculite costs 0.04 EUR and 1 gram of milled nylon costs 0.75 EUR.

CONCLUSION

Modern biotechnologies enable production companies to secure the competitiveness in the market and reduce the production costs not by relocation the production to countries with lower labor costs, but by making the process more effective. Pollen management is a curtail part of hybrid production. Pollen collecting is very labor intensive process that can be simplified by using pollen collector with vacuum pump. During the pollination, more pollen grains than necessary are applied to the stigma. Thanks to

dilution of pollen with the inert material that does not influence the number of formed seeds, it is possible to reduce the waste of pollen and less paternal plants are needed. Based on the conducted experiment the dilution of pollen with microcrystalline cellulose in ratio 1:1 has no negative effect on pollen, quality of pollination and number of formed seeds.

ACKNOWLEDGEMENTS
The research was financially supported by IGA Inovativní technologie opylování u Petunia hybrida (IGA - ZF/2018 - AP004).

REFERENCES

Anderson, N.O. 2007. Flower Breeding and Genetics: Issues, Challenges and Opportunities for the 21st Century. 1st ed., Dordrecht, Netherlands: Springer.

Brewbaker, J.L., Kwack, B.H. 1963. The essential role of calcium ion in pollen germination and pollen tube growth. American Journal of Botany, 50(9): 859–865.

Cerna, M. et al. 2017. Influence of CMS on seeds production of Petunia hybrida [Online]. Available at: http://scieconf.com/archive/?vid=1&aid=2&kid=90501-429 [2018-10-08].

Cerna, M. et al. 2018. Pollen production of paternal components of Petunia hybrida [Online]. Available at: https://scieconf.com/actual-conferences-and-papers/?pa=504&cmd=det [2018-08-08].

Franke, R., Galun, E. 1977. Pollination Mechanisms, Reproduction and Plant Breeding. 1st ed., Berlin, GE: Springer-Verlag.

Gerats, T., Strommer, J. 2009. Petunia: Evolutionary, Developmental and Physiological Genetics. 1st ed., New York, USA: Springer.

Pinillos, V., Cuevas, J. 2008. Standardization of the fluorochromatic reaction test to assess pollen viability. Biotechnic & Histochemistry [Online], 83(1): 15–21. Available at: https://doi/full/10.1080/10520290801987204. [2018-08-01].

Sink, K.C. 1984. Petunia. 1st ed., Berlin, Germany: Springer-Verlag.

Weiguang, Y. et al. 2003. Polyester and nylon powders used as pollen diluents preserve pollen germination and tube growth in controlled pollinations. Sexual Plant Reproduction [Online], 15: 265–269. Available at: https://link.springer.com/article/10.1007/s00497-002-0160-6. [2018-08-01].

The role of ubiquitin-conjugating enzymes during seed germination

Hana Habanova, Anna Hyskova
Department of Molecular Biology and Radiobiology
Mendel University in Brno
Zemedelska 1, 613 00 Brno
CZECH REPUBLIC

habanova.ha@gmail.com

Abstract: Regulated protein turn-over is one of the key determining factors of successful plant growth and development. Not only protein synthesis but also targeted protein degradation was widely reported to be involved in multiple metabolic or regulatory processes in cells (e.g. removing of negative regulators in different signalling pathways, mobilization of storage compounds or degradation of misfolded proteins). Seed germination is a crucial phase of plants life which is characterized with highly intensive proteome dynamics, caused by degradation of stored proteins and *de novo* proteosynthesis. Here, we focused on the effect of proteasome degradation on seed germination and seedling establishment, using *Arabidopsis thaliana ubc* mutant lines. Further, we employed an LC-MS profiling to study this effect at proteome level. Our results indicate a significant overlap of candidate proteins between all tested *ubc* lines, even though the reported expression patterns of chosen UBCs are significantly different.

Key Words: seed, protein degradation, proteomics, mass spectrometry

INTRODUCTION

Seed germination is a highly complex phase of plant's life which ensures generative propagation and plant's survival under unfavourable environmental conditions. After maturing, the so-called orthodox seeds (typical for temperate climate zone), undergo a period of intensive desiccation and enter the dormant state. At this state, dry seeds wait for favourable conditions. Seed germination starts with intensive water intake followed by metabolism reactivation. Shortly after metabolism reactivation, nucleic acids and proteins are newly synthetized to cover requirements of rapidly developing tissues, and at the same time, degradation of storage and unneeded compounds takes place (Rajjou et al. 2012). The targeted protein degradation does not only remove storage or unwanted proteins, but it has been widely reported that targeted protein degradation is employed in multiple signalling pathways, including those of phytohormones (Černý et al. 2016). In such cases, the negative regulators have to be removed to enable signal transduction. For example, the signalling of gibberellin (the key phytohormone promoting seed germination) requires the removal of its negative regulators called DELLA proteins.

Proteins in plant cells are degraded by multiple ways, with ubiquitin-26S-proteasome system (UPS) apparently being the most frequent. Proteins are determined for this degradation system by attaching a small protein ubiquitin, a process catalysed by three enzymes in sequential reactions: ubiquitin-activating enzyme (E1), ubiquitin-conjugating enzyme (E2, UBC) and ubiquitin-ligating enzyme (E3). In *Arabidopsis thaliana* genome, E3s are encoded by more than 1,500 genes and are responsible for substrate specificity (Mazzucotelli et al. 2006). In contrast, UBCs encompass less than 40 genes in *Arabidopsis* genome (Kraft et al. 2005).

MATERIAL AND METHODS

Plant material and experimental set up

Arabidopsis thaliana T-DNA insertion mutant lines were purchased from Nottingham Arabidopsis Stock Centre (NASC; www.arabidopsis.info), namely SALK_043014C (N656419; *ubc4* – AT5G41340), SALK_123573C (N686744; *ubc20* – AT1G50490) and SAIL_284_G06

(N862354; *ubc27* – AT5G50870). Lines were propagated together with Columbia wild type line (Col-0). Each line was genotyped and only homozygote plants were harvested.

For plate assay, 10 seeds of each line were sown on a half-strength Murashige & Skoog (Ducheva Biochemie) plant agar medium and cultivated under long-day conditions (21 °C, 100 µmol/m^2/s light intensity; 19 °C, no illumination). 6-days-old seedlings were photodocumented, and the cotyledon area was calculated using ImageJ.

For proteomics analysis, 20–30 mg of dry seeds (Col, *ubc4*, *ubc20*, *ubc27*) were placed on plate with filter paper (Whatman) and 4 ml of water. Seeds were cultivated for 48 hours under long-day conditions and then harvested and stored at -80 °C.

Sample preparation and proteomic analysis

Samples were homogenized (RetschMill MM400) and total protein was extracted using TCA/acetone/phenol extraction (Cerna et al. 2017). 100 µg aliquot of protein sample was digested with trypsin (Promega) and desalted. Samples were eluted with 150 µl 50% and 200 µl 100% acetonitrile (ACN) and then evaporated to reach 10–20 µl of the samples in water. The samples were analyzed by gel-free shotgun profiling, using nanoflow C18 reverse-phase liquid chromatography with a 15cm column (Zorbax, Agilent), a Dionex Ultimate 3000 RSLC nano-UPLC system (Thermo) and an UHR maXis impact q-TOF mass spectrometer (Bruker). The samples were analyzed in at least two technical replicates by nanoflow C18 reverse-phase liquid chromatography using a 15cm column (Zorbax, Agilent), a Dionex Ultimate 3000 RSLC nano-UPLC system (Thermo) and an UHR maXis impact q-TOF mass spectrometer (Bruker). The spectra were processed by Data Analysis 4.1and recalibrated in Preview program. Resulting MGF files were searched against Arabidopsis (TAIR 10) protein database via Proteome Discoverer 2.1, using Sequest and Mascot searching algorithms with following parameters: Enzyme - trypsin, max two missed cleavage sites; Mass tolerance - 35 ppm (MS) and 0.1 Da (MS/MS); Modifications - up to three dynamic modifications including Met oxidation, Asn/Gln deamidation, Lys methylation, N-terminal acetylation, Ser/Thr/Tyr phosphorylation.

Data evaluation

The arithmetic average and standard deviations were calculated from each dataset of cotyledon area. The variance between the datasets was analyzed by a one-way ANOVA and Tukey post-hoc test in OriginPro 2016 software.

The proteome profiling data acquired by Proteome Discoverer 2.1 were normalized to eliminate the variability in samples concentrations. The protein quantification was based on the number of peptide spectral matches (PSMs). Only the proteins with an absolute fold-change of at least 2.0 between abundance in control (Col-0 seedlings) and mutant proteome were included in the list of *ubc* mutation-responsive candidates.

RESULTS AND DISCUSSION

In this study, we chose three *UBC* with different expression patterns (the expression data were acquired from freely available online databases: www.araport.org, www.arabidopsis.org). Gene *UBC27* is expressed more or less ubiquitously, but *UBC20* is expressed only after germination during seedling establishment and its highest expression rate is also reached in shoot meristems. On the other hand, *UBC4* is predominantly found to be expressed in anthers and seeds, its protein product is highly accumulated during seed development/desiccation, and its degradation takes place during seed germination.

Proteasome inhibition via *ubc* mutation affects seedling growth

Generally, germination of seeds (including *Arabidopsis*) is not evenly distributed, but exhibits several populations with a different level of dormancy. Osmotic agents, an exposure to low/high temperature, and growth regulators can all be used to synchronize the germination rate. We hypothesized that the synchronization of seeds with an impaired UBC system could be more affected than that of the wild type, and thus we compared germination and growth of *ubc* mutant lines with and without stratification (cold-induced synchronization). We found that seed stratification significantly affected the seedling growth (Figure 1). The seedlings grown from stratified seeds were characterized by larger

cotyledons and there was no visible difference between Col-0 and *ubc* lines. On the other hand, in the absence of stratification the *ubc4* line showed significantly larger cotyledon area than Col-0. The expression pattern of ubc4 indicates that it has a role in seed maturation and our results indicate that its mutation could have a negative effect on seed dormancy or a positive effect on seed germination. The BLAST search revealed that its orthologue in *S. cerevisiae* (ScUBC8, identity >60%; www.yeastgenome.org) is involved in negative regulation of gluconeogenesis by mediating glucose-induced ubiquitination of fructose-1,6-bisphosphatase. This indicates that the second possibility is more likely, and UBC4 is likely a negative regulator of seed germination and its absence increases the germination rate.

Figure 1 UBC mutation affects seed germination and seedling establishment. The relative cotyledon area calculated by ImageJ (100% - Col-0 without stratification) and the error bars mean standard deviations. The variance between the datasets was analyzed by ANOVA.

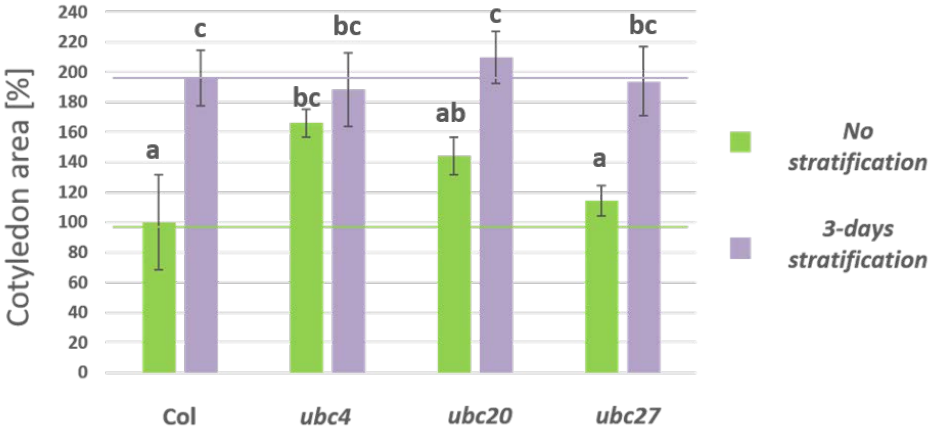

Mutation of different *UBC* genes affects mostly the same proteins

The effect of proteasome inhibition was further studied employing an LC-MS analysis using seeds without stratification. The seeds of Col-0 and *ubc* lines were imbibed in water for 48 hours, then proteins were extracted and analyzed be gel-free shotgun proteome profiling approach. At the same time, we analyzed proteomes of dry seeds of all lines. The proteomics data were pre-processed using principal component analysis (PCA) to determine the variation between the *Arabidopsis* lines at protein level (Habánová and Luklová 2017), and it was found that *ubc* lines are separated from Col-0 seeds mainly in the PC2 (Figure 2).

Figure 2 PCA showing clustering of ubc mutant lines at the level of dry seeds and after 48 hours of imbibition

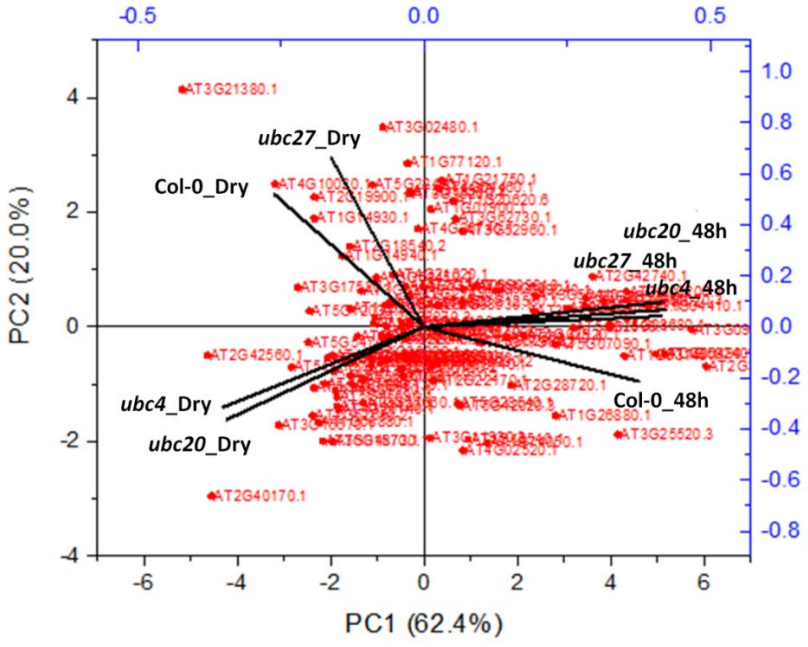

The further data processing and quantification revealed lists of candidate proteins which were mostly increased in *ubc* lines. Interestingly, most of the candidate proteins (45) were shared in all three mutants (Figure 3a) and had the same direction of regulation based on at least 10 PSMs. We clustered these shared candidates (Figure 3b) according to their protein-protein interactions using STRING database (www.string-db.org). The candidate protein groups encompass a wide range of cellular processes, including primary metabolism, stress-induced responses and regulatory pathways. As we expected, there are also proteins involved in seed development and germination which could directly corresponds with altered seedling establishment compared to Col-0.

Figure 3 The candidate proteins probably involved in response to ubc4, ubc20 and ubc27 mutation. a) Venn diagrams showing the overlap between all candidate proteins from each mutant line. b) Protein-protein interaction-based map of 45 candidate proteins shared in all mutant lines.

a)

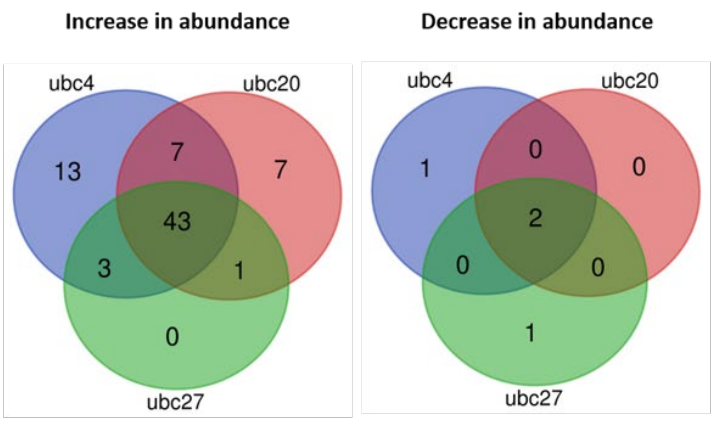

b)

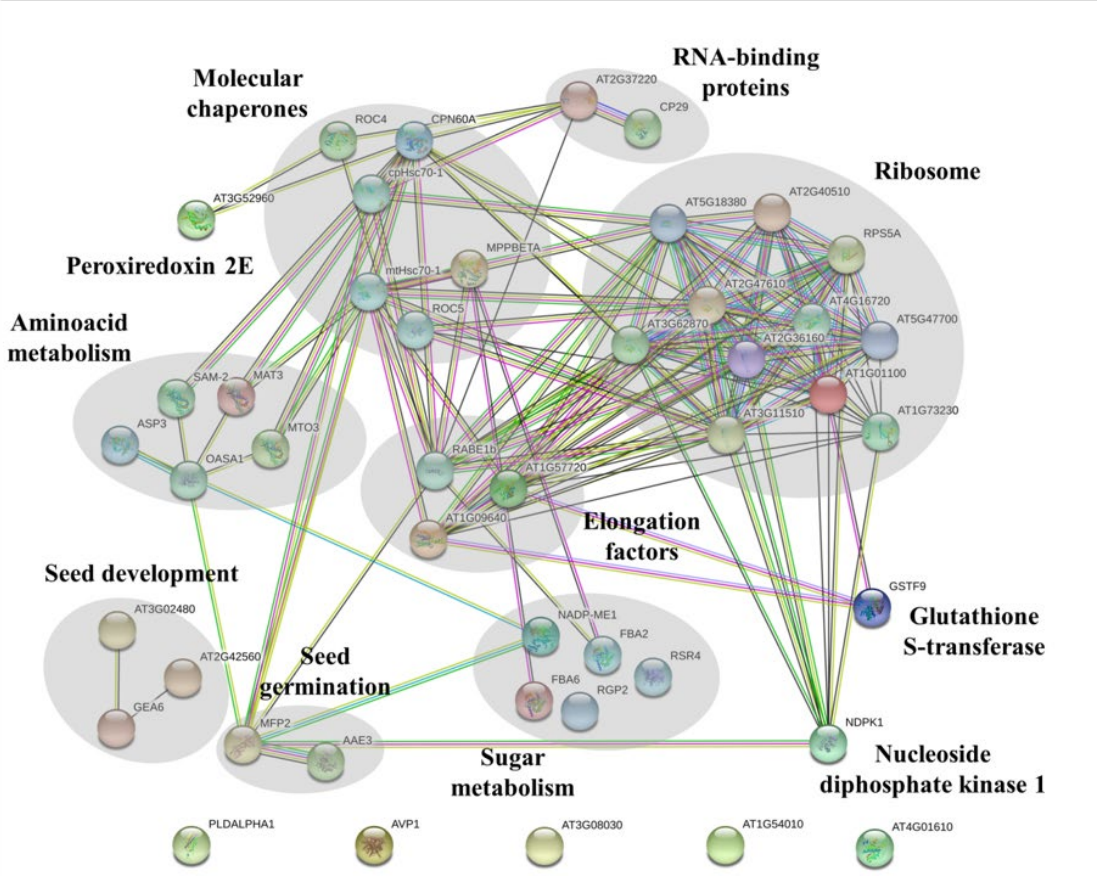

Based on present state of knowledge, we would expect different sets of differentially abundant proteins for each of the *ubc* mutants. The analyzed *UBC*s have contrasting expression patterns and

belong to a different protein classes within the UBC family. However, the biological functions of individual UBCs are far from being resolved. Moreover, a single loss-of-function mutation does not necessarily provide sufficient power to elucidate complex relations in UPS-mediated regulations, and the observed similarity in mutant's proteome could reflect only the enhanced germination rate.

CONCLUSION

Targeted protein degradation is a highly complex and regulated set of multiple enzymatic and non-enzymatic processes. In ubiquitin-26S-proteasome system, the most frequent way of protein removal in plants, UBC proteins play a key role in protein ubiquitination and their targeting for degradation. To get a deeper insight into the effect of proteasome inhibition during *Arabidopsis* seed germination we employed three *ubc* mutant lines (*ubc4, ubc20, ubc27*). Since these *UBC*s differ in their expression-specificity, we wanted to elucidate if the mutant lines will show a different phenotype and proteome dynamics in comparison to Col-0 (wild type) and between each other. Our plate assay results showed that in the absence of priming, the mutant lines have an enhanced growth rate. Further, we analyzed the effect of *UBC* mutation at proteome level. We found that proteins with significant changes in abundance were mutually similar among all three *ubc* lines, including the level of regulation. Our results are a first step to elucidate complex mechanisms of UBC in seed germination, and more efforts will have to be made to get a deeper insight into the role of proteasome-dependent protein degradation.

ACKNOWLEDGEMENT

The research was financially supported by grant AF-IGA-IP-2018/014 (Internal Grant Agency of Faculty of AgriSciences, Mendel University in Brno) and grant 7AMB17AT027 (Czech-Austrian Mobility Program, co-funded by MEYS (CZ) and OeAD (AT)). Hana Habánová – Brno Ph.D. Talent Scholarship Holder – Funded by the Brno City Municipality.

REFERENCES

Cerna, H. et al. 2017. Proteomics offers insight to the mechanism behind Pisum sativum L. response to pea seed-borne mosaic virus (PSbMV). Journal of Proteomics, 153: 78–88.

Černý, M. et al. 2016. The role of proteome in phytohormonal signalling. Biochimica et Biophysica Acta (BBA)-Proteins and Proteomics, 1864(8): 1003–1015.

Habánová, H., Luklová, M. 2017. Objective evaluation of seed germination by proteomics and principal component analysis. In MendelNet 2017 Proceedings of International PhD Students Conference [Online]. Brno, Czech Republic, 8 and 9 November, Brno: Mendel University in Brno, Faculty of AgriSciences, pp. 630–634. Available at: https://mnet.mendelu.cz/mendelnet2017/mnet_2017_full.pdf.

Kraft, E. et al. 2005. Genome analysis and functional characterization of the E2 and RING-type E3 ligase ubiquitination enzymes of Arabidopsis. Plant Physiology, 139(4): 1597–1611.

Mazzucotelli, E. et al. 2006. The E3 ubiquitin ligase gene family in plants: regulation by degradation. Current Genomics, 7(8), 509–522.

Rajjou, L. et al. 2012. Seed germination and vigor. Annual Review of Plant Biology, 63: 507–533.

Effect of lycorine on the green algae *Chlamydomonas reinhardtii* under UV-C irradiation

Martina Kolackova[1,2], Marek Dvorak[1], Borivoj Klejdus[1], Dalibor Huska[1,2]
[1]Department of Chemistry and Biochemistry
Mendel University in Brno
Zemedelska 1, 613 00 Brno
[2]Central Institute of Technology (CEITEC)
Brno University of Technology
Purkynova 123, 612 00 Brno
CZECH REPUBLIC

martina.kolackova@mendelu.cz

Abstract: Lycorin (LYC) is an inhibitor of the growth in higher plants through the inhibition of the last step of ascorbic acid biosynthesis. Ascorbates are mainly involved in regulation of intracellular levels reactive oxygen species. There is still limit information about its green microalgal toxicity and specificity. Therefore, present experiment was focused on the LYC toxicity on the green microalgae, *Chlamydomonas reinhardtii,* moreover the cells of microalgae were exposed to UV-C irradiation to increase ROS. The attention was primary given to the antioxidant response. The higher concentrations than 25 µM LYC with 30 min UV-C (250 nm) exposure absolutely inhibited the growth. 10 µM LYC and 25 µM LYC treatment together with UV-C irradiation suppress the growth caused oxidation stress and enhances antioxidant response.

Key Words: Chlamydomonas reinhardtii, UV irradiation, lycorine

INTRODUCTION

Lycorine (LYC) is Amaryllidaceae alkaloid which suppress the growth in the higher plants (Deleo et al. 1973). It is considered to inhibit the last step in ascorbic acid (AA) biosynthesis (Onofri et al. 2003). AA is important plants and algal substance. Among it's the most important roles are antioxidant substance, enzyme cofactor and a precursor for oxalate and tartrate synthesis. Later, it was discovered that it also participates in growth and resistance to environmental stress. AA is pivotal antioxidant in scavenging reactive oxygen species (ROS), its synthesis increases during oxidative stress. (Lin et al. 2016; Smirnoff and Wheeler 2000). LYC use in microalgae research has been poorly studied. Some studies using LYC reported that AA participates in cooper stress tolerance in *Ulva compressa* or cadmium in *Scenedesmus quadricauda* (Kovacik et al. 2017; Mellado et al. 2012). However, the results of LYC treatments are controversial, some investigation showed only its toxic effect (Loewus 2000).

Algae are photosynthetic organisms. Apart from photosynthetically active radiation (400–700 nm), algae are also exposed to UV light (Tao et al. 2010). Because UV-A and UV-B are passed though atmosphere, their toxicity is widely observed in the different living organisms (Holzinger and Lutz 2006, Tao et al. 2010). UV-C is electromagnetic radiation that includes wavelengths shorter than 280 nm. It has the highest energy from UV radiation. It is efficiently filtered by the ozone layer in the stratosphere. Therefore, its toxicity insufficiently studied (Muller-Xing et al. 2014). Owing to the ozone depletion, there is a risk of UV-C radiation penetration on Earth. Accordingly, it is important to understand how plants respond to UV-C in terms of stress resistance, growth and development. The protective mechanisms of plants to UV-C stress could include the formation of antioxidant compounds (Castronuovo et al. 2014).

Because there is limit information related to LYC and UV-C irradiation toxicity, green algae, *Chlamydomonas reinhardtii,* was exposed to LYC treatment and 10 or 30 min UV-C (250 nm) irradiation. UV is generally to be toxic because it triggers oxidative stress and enhance the accumulation of ROS (Castronuovo et al. 2014, Holzinger and Lutz 2006, Tao et al. 2010). Therefore, the attention of present experiment was given to growth and antioxidant response.

MATERIAL AND METHODS

Cultivation of algae

LYC and UV irradiation toxicity was tested by cultivating *Chlamydomonas reinhardtii* in the presence of 10, 25, 50 and 100 µM LYC and 10 and 30 min/day UV-C exposure. *Chlamydomonas reinhardtii* was cultivated under sterile conditions in Tris-Acetate-Phosphate medium (TAP medium) at 21 ± 1 °C and illuminated at 130 µmol/m/s with a 12 h light/12 h dark photoperiod. Then, algae (700 mg of fresh biomass) were inoculated into the Erlenmayer flasks containing 150 ml of liquid TAP medium supplemented with the corresponding LYC concentration. Thereafter, the selected samples were exposed to UV-C (250 nm) for 10 and 30 min per day. After 5 days, *Chlamydomonas reinhardtii* were harvested and lyophilized.

Optical density

Optical density was measured every day. 200 µl of fresh sample was added into the wells of UV transparent spectrophotometric desk and left to stand for 20 min at room temperature. Thereafter, the absorbance of sample was measured at 750 nm against a blank. The result was expressed as optical density value (OD750); (Chioccioli et al. 2014).

Growth rate

Biomass increase was evaluated in zero and harvesting day. The samples were rinsed 3 times to remove residual medium. Thereafter, samples were lyophilized and weighed. Growth rate was calculated as $\mu = \ln (x1/x0)/t1\text{-}t0$ where x1 and x0 are weight of algae (g/L) and the culture time t1 and t0 days (Krzeminska et al. 2014).

Extraction methodology

Three replicates were performed for each sample. The weighing of lyophilized sample was homogenized by the homogenizer in 1 ml of extraction solvents which were 80% methanol, 96% ethanol and acetone. Incubation was followed for 2 hours at 55 °C (Hynstova et al. 2018).

Estimation of total antioxidant capacity

The total antioxidant capacity of extracts was investigated by phosphomolybdenum assay (Alam et al. 2013). Trolox was used as the standard.

Determination of polyphenols

The total phenolic content was detected by FC assay (Folin-Ciocalteu assay), based on the reduction of a phosphowolframate – phosphomolybdate complex by phenolic compounds (Kosar et al. 2005). Gallic acid was used as the standard. The result was expressed as an equivalent in mg gallic acid on 1 g dry weight.

Determination of flavonoids

The flavonoids were determined by colorimetric method (Jia et al. 1999). Rutin was used as the standard. The result was expressed as an equivalent in mg rutin on 1 g dry weight.

DPPH assay

α, α-diphenyl-β-picrylhydrazyl (DPPH) free radical scavenging assay was used to determinate antioxidant activity (Brandwilliams et al. 1995). The result was expressed as a value EC50 in mg/ml. EC50 is extract's concentrations to obtain 50% antioxidant effect.

Determination of chlorophylls (a and b), total carotenoids and pheophytins

Spectrophotometric determination of chlorophylls (a and b) and total carotenoids were measured at 665, 649 and 479 nm. Weighing of lyophilized sample was extracted in 96% ethanol. Extract was pipetted into the holes of UV transparent spectrophotometric plate. Thereafter, the chlorophyll a (Ca), chlorophyll *b* (Cb), and total carotenoids (Cx + c) were calculated as: $C_a = 13.95 * A665 – 6.88 * A649$ (µg/ml), $C_b = 24.96 * A649 – 7.32 * A665$ (µg/ml), $C_{x+c} = (1000 * A479 – 2.05 * C_a – 114.8 * C_b) / 245$ (µg/ml); (Hynstova et al. 2018).

Statistical analysis

Each sample had 3 biological and 2 technical repetitions. All data was expressed as a mean of standard deviation. The data were determined by one-way ANOVA variance test followed by T-test at $p < 0.05$.

RESULTS AND DISCUSSION

Effect of toxicant on the growth

Preliminary screening for potential concentrations was done by growth study based on daily spectrophotometric reading of absorbance at 750 nm. Different concentrations of LYC (10 µM, 25µM, 50 µM and 100 µM) and time of UV-C irradiation (10 and 30 min) were used for pre-experiment.

Growth was inhibited by an increasing concentration of the toxicant. 50 and 100 µM LYC inhibited the growth. But their combination with UV-C irradiation was too toxic for *C. reinhardtii* (Figure 1A). Other treatment also suppressed the growth compared to control, combination of LYC and UV had synergistic effect (Figure 1B, C). Therefor, 10 µM LYC, 25 µM LYC, 10 min of UV-C irradiation, 30 of UV-C irradiation and their different combination were chosen for sequential analysis. There was no change between control and 10 µM LYC.

Previous study reported that 100 µM decreased the growth and at very low concentration 10^{-6} suppressed the cell division in higher plant, red algae and yeast (Arrigoni et al. 1975). Beyond, *Ulva compressa* was treated up to 100 µM concentrations, despite there was no mention about growth inhibition (Mellado et al. 2012). Most of yeasts strains haven't showed sensitivity to LYC (Onofri et al. 2003). Different organisms, even within order, are differently sensitive to LYC (Arrigoni et al. 1975, Onofri et al. 2003).

Figure 1 Influence of Lycorine treatments and UV-C irradiation on the growth of Chlamydomonas reinhardtii. Error bars correspond to standard error of mean. A, B, C) Optical density in value OD 750 during 96 hours.

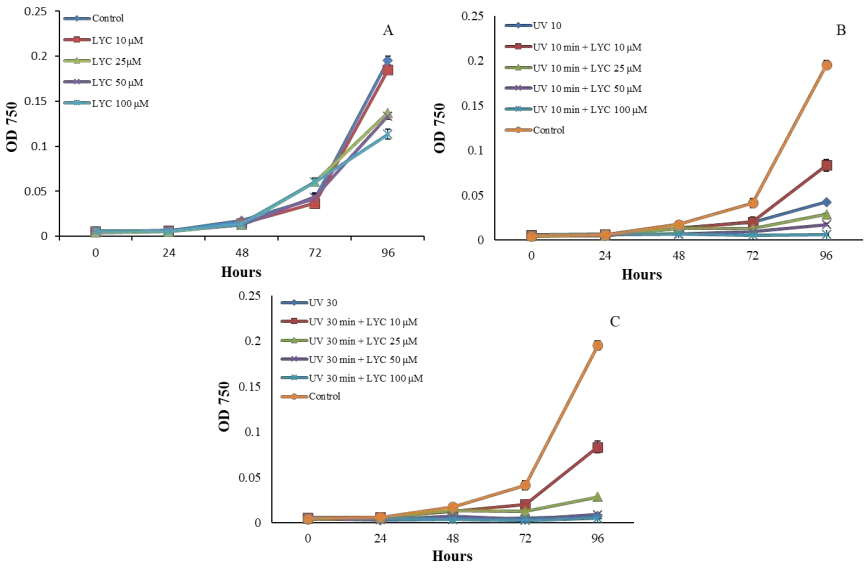

Polyphenols and flavonoids are secondary metabolites with antioxidant properties, their syntheses often increase during stress. Due to the structure, flavonoids are consider for protective compounds during UV irradiation (Holzinger and Lutz 2006). In our case, significant increase of flavonoids was observed only in 10 µM LYC, 25µM LYC and 25µM LYC + 30 min UV irradiation. No shift was monitored in UV-C exposure (Figure 2). Carotenoids can be overproduction in response to light stress in *Duneliella salina* (Fu et al. 2013). In our experiment, there was no enhancement. Reduced chlorophyll and carotenoids level was also observed in *Bellerochea yucatanensis, Biddulphia sinensis, Ditylum brightwellii, Lauderia annulata* and *Thalassiosira rotula* under UV-B irradiation (Dohler 1985).

Figure 2 A) Polyphenols contain expressed as mg GAE g DW, Flavonoids contain expressed as mg RE g DW (dry weight). B) Amount of chlorophyll a, chlorophyll b and carotenoids expressed as mg/ml. Error bars correspond to standard error of mean. (*) indicate significant differences compared to the control ($p < 0.05$, $n = 6$) according to T-test.

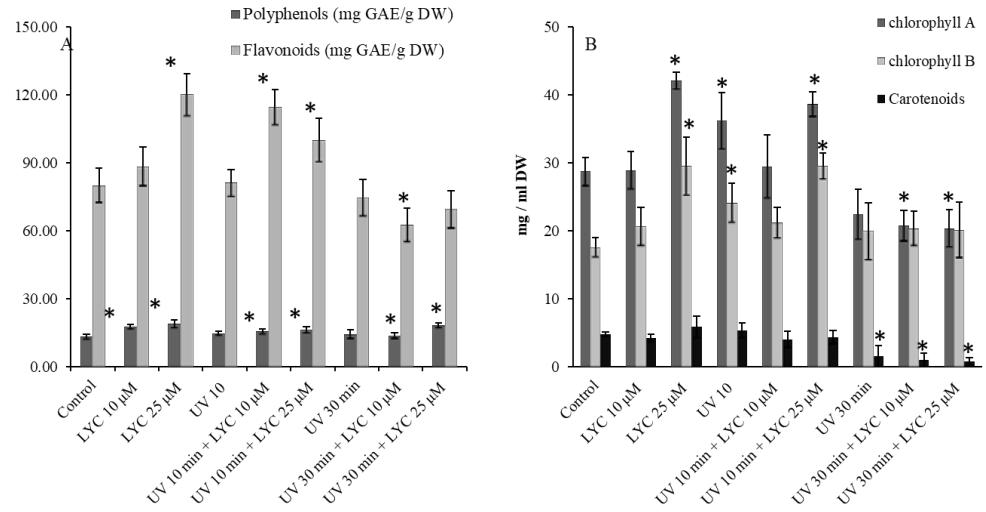

Antioxidant testing was completed by total antioxidant capacity and DPPH assay. Total antioxidant capacity was significant increased in all treatment except 10 µM LYC (Figure 3 A). DPPH assay was expressed as value EC 50. It means what concentration you need to reduce 50 % of DPPH solution. The control samples achieved the highest values. All treatments samples responded to stress increased antioxidant response (Figure 3).

Figure 3 A) Total antioxidant capacity expressed as mmol/l Trolox g DW (dry weight). B) DDPH assay expressed as a value EC 50. Error bars correspond to standard error of mean. (*) indicate significant differences compared to the control ($p < 0.05$, $n = 6$) according to T-test.

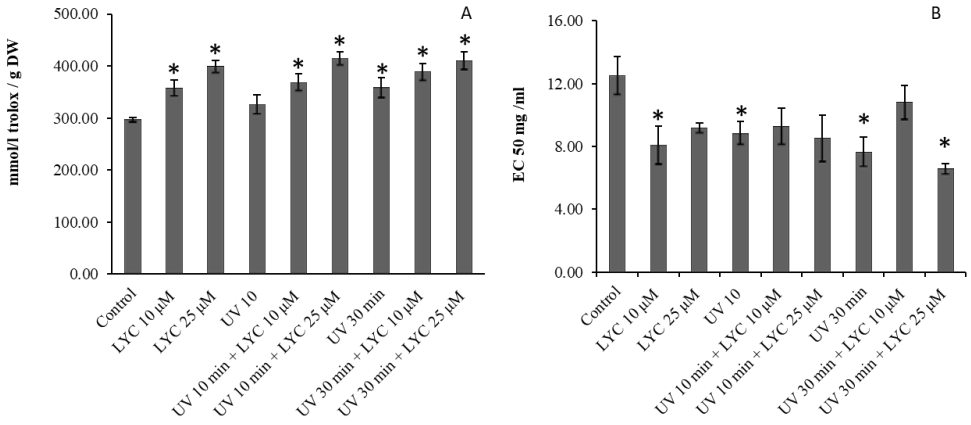

CONCLUSION

Strategies for UV experiment and substance toxicity are complicated. Their toxicity depends on many circumstances as a concentration, time of exposure, wavelength, distance from radiation etc. In our conditions, 30 min UV-C (250 nm) irradiation exposure with higher than 25 µM LYC treatment were highly toxic and absolutely inhibited the growth. All treatment, apart from 10 µM LYC, had negative impact on the growth and redox state. They suppressed the growth caused oxidation stress and enhanced antioxidant response. Next step is going to target on molecular level of toxicity focused mainly on enzymatic and non-enzymatic antioxidant substances. Moreover, it could be interesting to find optimal doses and use hormesis to increase beneficial compounds.

ACKNOWLEDGEMENTS
The research was financially supported by the Internal Grand Agency of Mendel University in Brno IP 55/2018 and CEITEC 2020 (LQ1601) with financial support from the Ministry of Education, Youth and Sports of the Czech Republic under the National Sustainability Programme II.

REFERENCE

Alam, M. et al. 2013. Review on in vivo and in vitro methods evaluation of antioxidant activity. Saudi Pharmaceutical Journal, 21(2):143–152.
Arrigoni, O. et al. 1975. Lycorine as an Inhibitor of Ascorbic-Acid Biosynthesis. Nature, 256(5517): 513–514.
Brandwilliams, W. et al. 1995. Use of a Free-Radical Method to Evaluate Antioxidant Activity. Food Science and Technology-Lebensmittel-Wissenschaft & Technologie 28(1):25-30.
Castronuovo, D. et al. 2014. Uv-C Irradiation Effects on Young Tomato Plants: Preliminary Results. Pakistan Journal of Botany, 46(3): 945–949.
Chioccioli, M. et al. 2014. Flow Cytometry Pulse Width Data Enables Rapid and Sensitive Estimation of Biomass Dry Weight in the Microalgae Chlamydomonas reinhardtii and Chlorella vulgaris. Plos One, 9(5): e97269.
Deleo, P. et al. 1973. Metabolic Responses to Lycorine in Plants. Plant and Cell Physiology, 14(3): 487–496.
Dohler, G. 1985. Effect of Uv-B Radiation (290–320nm) on the Nitrogen-Metabolism of Several Marine Diatoms. Journal of Plant Physiology, 118(5): 391–400.
Fu, W.Q. et al. 2013. Enhancement of carotenoid biosynthesis in the green microalga Dunaliella salina with light-emitting diodes and adaptive laboratory evolution. Applied Microbiology and Biotechnology, 97(6): 2395–2403.
Holzinger, A. et al. 2006. Algae and UV irradiation: Effects on ultrastructure and related metabolic functions. Micron, 37(3): 190–207.
Hynstova, V. et al. 2018. Separation, identification and quantification of carotenoids and chlorophylls in dietary supplements containing Chlorella vulgaris and Spirulina platensis using High Performance Thin Layer Chromatography. Journal of Pharmaceutical and Biomedical Analysis, 148: 108–118.
Jia, Z.M. et al. 1999. The determination of flavonoid contents in mulberry and their scavenging effects on superoxide radicals. Food Chemistry, 64(4): 555–559.
Kosar, M. et al. 2005. Effect of an acid treatment on the phytochemical and antioxidant characteristics of extracts from selected Lamiaceae species. Food Chemistry, 91(3): 525–533.
Kovacik, J. et al. 2017. Ascorbic acid affects short-term response of Scenedesmus quadricauda to cadmium excess. Algal Research-Biomass Biofuels and Bioproducts, 24: 354–359.
Krzeminska, I. et al. 2014. Influence of photoperiods on the growth rate and biomass productivity of green microalgae. Bioprocess and Biosystems Engineering, 37(10): 2137–2137.
Lin, S.T. et al. 2016. Enhanced Ascorbate Regeneration Via Dehydroascorbate Reductase Confers Tolerance to Photo-Oxidative Stress in Chlamydomonas reinhardtii. Plant and Cell Physiology, 57(10): 2104–2121.
Loewus, F.A. 2000. Biosynthesis and metabolism of ascorbic acid in plants and of analogs of ascorbic acid in fungi. Phytochemistry, 52(1999): 193–210.
Mellado, M. et al. 2012. Copper-induced synthesis of ascorbate, glutathione and phytochelatins in the marine alga Ulva compressa (Chlorophyta). Plant Physiology and Biochemistry, 51:102–108.
Muller-Xing, R. et al. 2014. Footprints of the sun: memory of UV and light stress in plants. Frontiers in Plant Science, 2014(5): 474.
Onofri, S. et al. 2003. Effects of lycorine on growth and effects of L-galactonic acid-gamma-lactone on ascorbic acid biosynthesis in strains of Cryptococcus laurentii isolated from Narcissus pseudonarcissus roots and bulbs. Antonie Van Leeuwenhoek International Journal of General and Molecular Microbiology, 83(1): 57–61.
Smirnoff, N. et al. 2000. Ascorbic acid in plants: Biosynthesis and function. Critical Reviews in Plant Sciences, 19(4): 267–290.
Tao, Y. et al. 2010. The effects of sub-lethal UV-C irradiation on growth and cell integrity of cyanobacteria and green algae. Chemosphere, 78(5): 541–547.

Light applied during cold acclimation modulates recovery of the petiole growth after the freezing stress

Vladena Koukalova, Adela Horakova
Department of Molecular Biology and Radiobiology
Mendel University in Brno
Zemedelska 1, 613 00 Brno
CZECH REPUBLIC

vladena19@seznam.cz

Abstract: Temperature is a key environmental factor in plant production and its extremes cause high annual losses in agriculture. In this work, we have focused on the role of light conditions during cold acclimation process on the recovery of the growth after the freezing stress in *Arabidopsis thaliana*. Some mechanisms inducing cold tolerance were already been found but the role of light in these processes is still far from being resolved. Here we monitored the effect of the light during cold acclimation period on the recovery of the growth after the freezing stress. Our results show that the growth after the freezing stress represented by petiole elongation was attenuated in plants acclimated under standard light conditions and red light promoted faster recovery of the petiole growth. Our data demonstrate that light quality plays important role in recovery of the growth after the freezing stress.

Key Words: Arabidopsis thaliana, light, cold acclimation, cold stress, freezing stress

INTRODUCTION

Plants as sessile organisms have developed a great ability to adapt to adverse environmental conditions. Ambient temperature is a major factor affecting all aspects of plant life. Every plant species require specific temperature range for its proper growth and development and temperature also delimits plants geographical distribution (Pavlů et al. 2018). However, the temperature may exceed the optimal range and cause damage or death of the plants (Lyons 1973, Levitt 1980). The plants exposed to low nonfreezing temperature have developed adaptive mechanisms inducing higher tolerance to freezing stress (Thomashow 1999). These mechanisms involve many biochemical and physiological changes including inhibition of the growth, changes in gene expression, induction of antifreeze proteins, accumulation of osmoprotectants, changes in membrane composition or changes in the redox status in the plants (Janda et al. 2014).

It was shown that light plays an important role during the cold acclimation process. Light induces the expression of genes related to the low temperature (Wang et al. 2016) and higher light intensity induces some cold protective mechanisms (Gray et al. 1997). *In Arabidopsis thaliana* higher tolerance to freezing stress was also achieved by application of a lower ratio of red/far-red light (R/FR); (Franklin and Whitelam 2007).

In this work, we have studied the effect of the light spectrum during the acclimation period on the recovery of the petiole growth after the freezing stress.

MATERIAL AND METHODS

Plant material (*Arabidopsis thaliana*; accession Col-0) was cultivated according to Skalák et al. (2016) in hydroponics containing half-strength Murashige and Skoog medium at 20 °C under 8 h day/16 h night regime for 5 weeks (Figure 1). Plants with 13-14 rosette leaves were then acclimated at 5 °C under different light conditions (cool white light = 100 µmol/m^2/s; red light (660 nm) = 20 µmol/m^2/s). After acclimation period plants were exposed for 8 hours to freezing temperature under the dark and then regenerated at 20 °C under standard light conditions (100 µmol/m^2/s; white light; short day). Length of the 10 longest petioles of each plant was manually measured from images (Top-view; Canon camera) in ImageJ software (Koukalova and Medvedova 2016). Statistical analysis was performed in Statistica12 software. Sample size n > 20 plants was used in all treatments.

Figure 1 Hydroponic cultivation of Arabidopsis thaliana.

RESULTS AND DISCUSSION

Previous studies have shown that light applied during cold acclimation period plays an important role in cold tolerance (Gray et al. 1997). To study the effect of light on the recovery of the growth after the freezing stress we grew set of *Arabidopsis* plants (n > 50) in hydroponics under 100 µmol/m^2/s for 5 weeks. In this stage, plants rosette was formed by 13–14 leaves. Plants in hydroponics were then transferred into the growing chamber with a temperature set to 5 °C. In this chamber, plants were cultivated for another 7 days for acclimation in two light regimes – standard white light intensity (100 µmol/m^2/s) and low red light intensity (20 µmol/m^2/s; 660 nm). Freezing stress was applied by cultivation of acclimated plants under -5 °C for 8 h in dark. After the stress plants were cultivated under standard light intensity and 20 °C for the next 18 days. The recovery of the growth was determined by measuring the growth of the petioles. Analysis showed that during the acclimation period the growth of the plant petioles was inhibited and there was no difference between plants cultivated under different light regimes. Interestingly, recovery of the growth after the freezing stress was significantly affected by light applied during the acclimation period (Figure 2).

Figure 2 The petiole length before freezing stress and after the recovery period. Bars represent arithmetic mean and error bars represent 95 % confidence intervals (n > 150) . Labelling: Control no stress = plants cultivated under 100 µmol/m^2/s of white light without cold acclimation, 100 WHITE = plants acclimated under 100 µmol/m^2/s of white light, 20 RED = plants acclimated under 20 µmol/m^2/s (660 nm). Statistical significance was evaluated by Kruskal-Wallis test (p < 0,05).

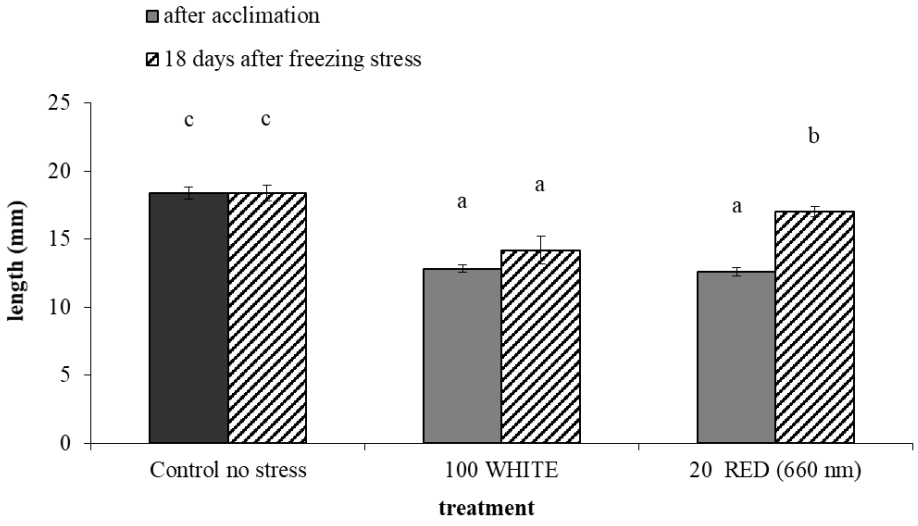

Our results demonstrate that plants cultivated under the red light show higher recovery of the petiole growth after the freezing stress (Figure 2). Previous studies showed that a lower ratio of R/FR light improves tolerance to freezing stress (Franklin and Whitelam 2007). Here we show that red light could improve also the recovery of the growth after the freezing stress. It is not clear whether the tolerance to the freezing stress induced by red light is related with faster recovery described in this work. In plants, it has been proven that tolerance to stress and recovery after the stress period are two distinct

features. For example, it was demonstrated that plants with decreased level of active cytokinin show improved tolerance to water deficit, but this effect was followed by a slower recovery phase (Prerostova et al. 2018) thus mechanism of red light action in tolerance and recovery could be distinct. Red light activates phytochrome signalling and drives photosynthesis very efficiently and both these processes could contribute to improvement of the plant recovery after the stress. Photosynthesis is connected with generation of reactive oxygen species which modulates and orchestrates response to stress and level of these species could affect the growth after the stress. On the other hand, the faster recovery could be also directly caused by expression of the specific genes regulated by light signalling cascade. To answer the role of the light signalling or photosynthesis in recovery process requires additional experiments to be conducted.

CONCLUSION

It is a long time known, that light plays important role in cold tolerance and survival. We have demonstrated that also the regeneration of the growth after the freezing stress is influenced by light conditions during the acclimation period.

ACKNOWLEDGEMENT

The research was financially supported by the internal grant of Mendel University in Brno AF-IGA-IP-2018/030.

REFERENCES

Franklin, K.A., Whitelam, G.C. 2007. Light-quality regulation of freezing tolerance in *Arabidopsis thaliana*. Nature Genetics, 39(11): 1410–1413.

Gray, G.R. et al. 1997. Cold Acclimation and Freezing Tolerance (A Complex Interaction of Light and Temperature). Plant Physiology, 114(2): 467–474.

Janda, T. et al. 2014. Interaction of Temperature and Light in the Development of Freezing Tolerance in Plants. Journal of Plant Growth Regulation, 33(2): 460–469.

Koukalova, V., Medvedova, Z. 2016. ImageJ Software as a Tool for Determining Morphometric Parameters. In Proceedings of International PhD Students Conference MendelNet 2016 [Online]. Brno Czech Republic, 9 November, Brno: Mendel University in Brno, Faculty of AgriSciences, pp. 722–725. Available at: https://mnet.mendelu.cz/mendelnet2016/mnet_2016_full.pdf.

Levitt, T. 1980. Chilling, Freezing, and High Temperature Stresses. 2nd ed., New York, USA: Academic Press.

Lyons, J. M. 1973. Chilling injury in plants. Annual Review of Plant Physiology, 24: 445–466.

Pavlů, J. et al. 2018. Cytokinin at the Crossroads of Abiotic Stress Signalling Pathways. International Journal of Molecular Sciences, 19(8): 2450.

Prerostova, S. et al. 2018. Cytokinins: Their Impact on Molecular and Growth Responses to Drought Stress and Recovery in *Arabidopsis*. Frontiers in Plant Science, 9: 655.

Skalák, J. et al. 2016. Stimulation of ipt overexpression as a tool to elucidate the role of cytokinins in high temperature responses of *Arabidopsis thaliana*. Journal of Experimental Botany, 67(9): 2861–2873.

Thomashow, M.F. 1999. Plant cold acclimation: freezing tolerance genes and regulatory mechanisms. Annual Review of Plant Physiology and Plant Molecular Biology, 50: 571–599.

Wang, F. et al. 2016. Phytochrome A and B Function Antagonistically to Regulate Cold Tolerance via Abscisic Acid-Dependent Jasmonate Signaling. Plant Physiology, 170(1): 459–471.

Plant-pathogen interactions: *Plasmodiophora brassicae* proteins in the root gall of Arabidopsis

Veronika Malych, Miroslav Berka
Department of Molecular Biology and Radiobiology
Mendel University in Brno
Zemedelska 1, 613 00 Brno
CZECH REPUBLIC

veronikamalych@gmail.com

Abstract: Plasmodiophora brassicae is an obligate, biotrophic pathogen causing a clubroot disease in *Brassicaceae* species. Here we employed an LC-MS proteomics analysis to identify major *P. brassicae* proteins within the infected roots of *Arabidopsis thaliana*. We identified over 300 proteins and employed bioinformatics to assign putative functions to the top-ranking proteins. The identified proteins include for example salicylic acid methyltransferase or an orthologue of *Phytophthora infestans* HSP 70 protein.

Key Words: proteome, club root, *Arabidopsis thaliana*

INTRODUCTION

Plasmodiophora brassicae Wor. is a soil-borne, obligate pathogen that causes clubroot disease of plants of the *Brassicaceae* family (Hwang et al. 2012). *P. brassicae* belongs to the class Plasmodiophorida, a pathogenic group of protists in the Phytomyxea within the supergroup Rhizaria (Bass et al. 2009). This plant pathogen has a negative impact on the production of cruciferous crops worldwide (Dixon, 2014), causes significant yield losses and reduces the seed quality in economically important crops, including Chinese cabbage, cauliflower, kohlrabi, turnip, oilseed rape or radish (Dixon, 2009). The clubroot disease is a serious threat to the agriculture production in the Czech Republic because the rapeseed production is one of the largest in the sector, representing around 10% of the total agricultural area (FAOSTAT). Moreover, the incidence of the clubroot disease has significantly increased in 2018 thanks to the disease-favourable conditions in the previous year (Konradyová and Kazda 2018).

Here, we analysed infected Arabidopsis roots, identified key proteins of *P. brassicae*, and evaluated their function(s).

MATERIAL AND METHODS

Material

Plants of *Arabidopsis thaliana* (L.) Heyhn. ecotype Columbia (Col-0) were cultivated on the soil substrate in a greenhouse under long day and temperature of 25 °C. The *P. brassicae* isolate 'e3' used in this study was described by (Fähling et al. 2003) and was produced in the susceptible Chinese cabbage (*Brassica rapa* ssp. *pekinensis* cv. Granaat) and had been propagated ever since in the same cabbage variety. Two weeks old seedlings were inoculated according to Ludwig-Müller et al., 2017. Briefly, each plant was inoculated with 1 ml of resting spores of *P. brassicae* (10^7 spores/ml in potassium buffer; 50 mM KH_2PO_4, pH adjusted to 5.5 with 1 M K_2HPO_4) by slowly injecting the spore suspension around the hypocotyl. The same amount of potassium buffer was applied to a group of control plants. Infected and control roots were harvested after 28 dai (days after inoculation), flash frozen in liquid nitrogen, then homogenized (Retsch Mill MM400) and stored at -80 °C.

Protein extraction and LC-MS analysis

Proteomic analyses were performed using a gel-free shotgun protocol as described previously (Novák et al. 2015, Černý et al. 2019). Briefly, proteins were extracted with trichloroacetic acid (TCA)/acetone precipitation followed by phenol extraction from app. 50 mg of ground tissue. The resulting protein pellets were solubilized and then digested in solution with Trypsin Gold, Mass

Spectrometry Grade (Promega) overnight. The tryptic digests were then desalted by C18 SPE (Agilent), dried (Speed-vac system, Thermo), dissolved in 0.5% (v/v) formic acid in 2% (v/v) acetonitrile and analysed as described earlier (Baldrianová et al. 2015). The samples were analysed by nanoflow C18 reverse-phase liquid chromatography using a 15 cm column (Zorbax, Agilent), a Dionex Ultimate 3000 RSLC nano-UPLC system (Thermo) and an UHR maXis impact q-TOF mass spectrometer (Bruker). Peptides were eluted with a 120-min, 4% to 40% acetonitrile gradient and spectra were acquired at 2 Hz (MS) and 10 to 20 Hz (MS/MS) using an intensity-dependent mode with a total cycle time of 7 s.

Protein identification

The measured spectra were extracted by Bruker's Data Analysis 4.1 and processed as described previously (e.g. Cerna et al. 2017) with minor modifications. In brief, spectra were recalibrated by Preview (www.proteinmetrics.com) and were searched against *P. brassicae* (6/2015) and *Arabidopsis thaliana* (Araport) protein sequence databases by Sequest HT with the following parameters: Enzyme - trypsin, max one missed cleavage sites; Mass tolerance - 35 ppm (MS) and 0.1 Da (MS/MS); Dynamic modifications - Met oxidation, Asn/Gln deamidation; Dynamic modifications (peptide terminus) - N-terminal acetylation; Dynamic modifications (protein terminus) - N-terminal Met-loss, N-terminal Met-loss/acetylation, N-terminal dimethylation. Data were processed and visualized by ProteomeDiscoverer 2.2 (Thermo). Only proteins identified based on at least three peptides were used for the analysis.

Data analysis

The protein abundance was estimated by the so-called peptide spectral matches (PSMs). The orthology search via Basic Local Alignment Search Tool (BLASTP 2.7.1+) from UniProt (https://www.uniprot.org/blast/) was used to identify putative function(s) with the following parameters: Target database - UniProtKB; E-Threshold - 10; Matrix - auto; Filtering - none; Gapped - yes; Hits - 250.

RESULTS AND DISCUSSION

Detection and quantitation of *P. brassicae* proteins

To identify *P. brassicae* proteins, Arabidopsis roots were infected, and the developed root galls were used for proteomics analysis as described in Material and Methods. In total, we identified 1,036 peptides assigned to *P. brassicae*, representing more than 300 proteins. However, as illustrated in the Figure 1, 47 of these peptides are shared between *P. brassicae* and *A. thaliana*, and are likely false positives. Shared peptides represent only 7% of the identified *P. brassicae* PSMs but can form a substantial part of PSMs in several genetically conserved proteins. For example, it represents 32, 38 and 38% for the actin family, RNA helicase and ATP synthase, respectively. Though the protein sequence coverage and possibility of multiple post-translational modifications somewhat limit our conclusions, it can be assumed that these peptides originate from the host plant genome and not from the pathogen. For this reason, only non-shared peptides were selected for the following functional analysis.

Figure 1 Number of peptides identified in infected and control samples

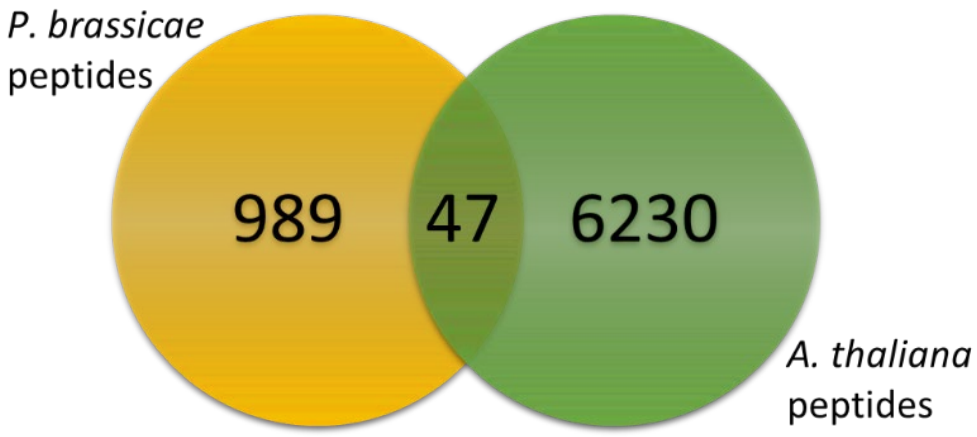

Functions of major *P. brassicae* proteins identified in root galls

The genome of *P. brassicae* was sequenced, assembled and analyzed in 2015 (Schwelm et al. 2015) but the level of protein annotation is not optimal. For this reason, we employed orthology search in BLAST to elucidate the role of uncharacterized proteins. It is interesting to note that the top 44 proteins represent nearly 75% of the total *P. brassicae* proteome (Figure 2). The heat shock family proteins (HSPs) are the most abundant proteins, and the protein from the Hsp70 family represents 7% of all PSMs. The major *P. brassicae* proteins contain also three transmembrane proteins. However, the BLAST search did not reveal any similar ortholog with available functional annotation. It is interesting to note that all these three proteins share a close sequence similarity (>70%) and it is tempting to speculate that they have a role in *P. brassicae*-mediated infection. The 12th most abundant protein which contributes by 2.5% to *P. brassicae* proteome composition is salicylic acid methyltransferase. Reports indicate that this enzyme suppresses plant defense by methylation and inactivation of salicylic acid (Ludwig-Müller et al. 2014).

Figure 2 Annotation of the most abundant P. brassicae *proteins based on their orthologs*

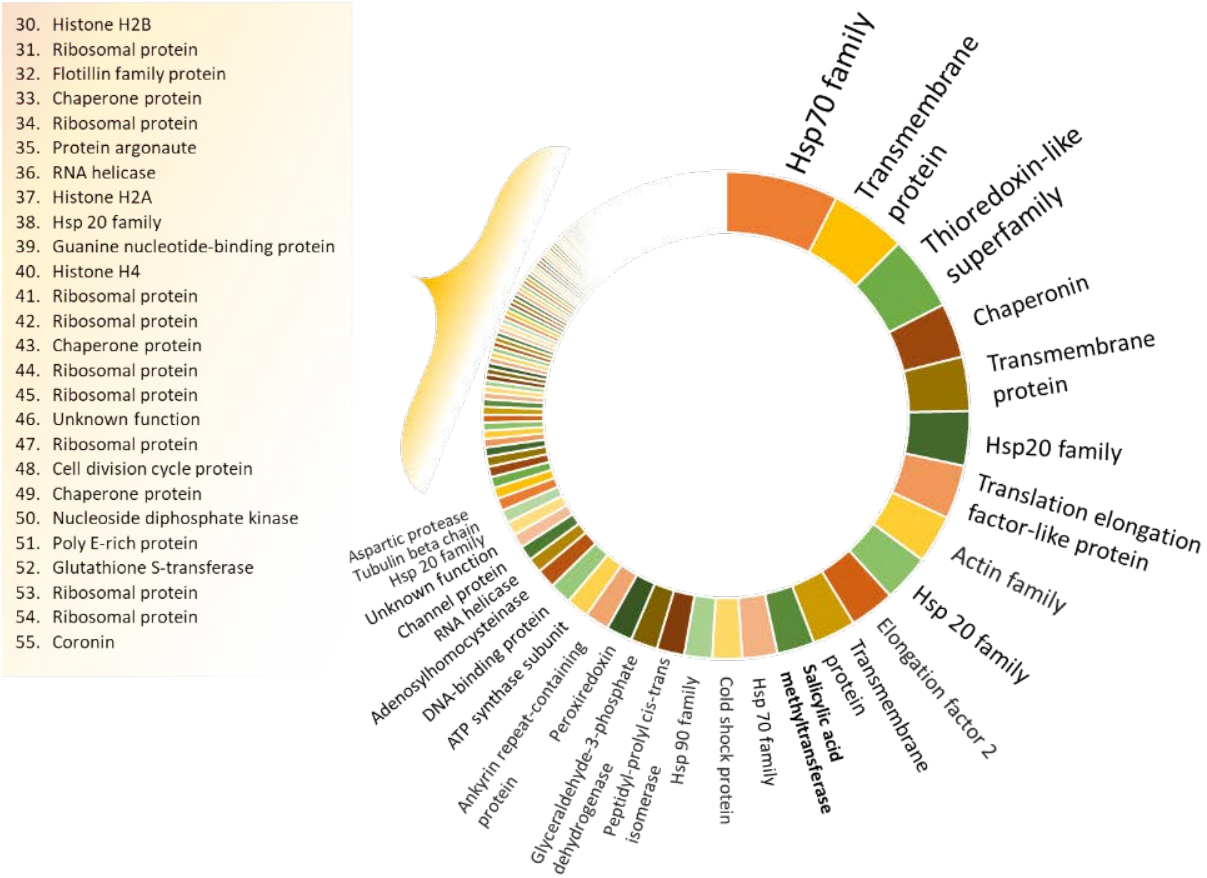

The most abundant *P. brassicae* proteins can be categorized into eight groups based on their function (Figure 3). HSPs and chaperons represent the largest category with ca 32% of all PSMs. Expression of these HSPs has been detected in earlier publications e.g. (Sundelin et al. 2011), and a large representation of HSPs was also found in the proteome of the biotrophic cereal-infecting rust *Puccinia triticina* (Song et al. 2010). Thus, it can be assumed that the HSPs group are important for plant-pathogen interactions. Other highly abundant functional groups are translation and redox homeostasis, including peroxiredoxin that plays a role in hydrogen peroxide-mediated signalling (Černý et al. 2018). The primary energetic metabolism is significantly underrepresented in the dataset which correlates with the fact that *P. brassicae* is a biotrophic pathogen and fully dependable on its host.

Figure 3 Function groups of the most abundant protein depend on PSMs

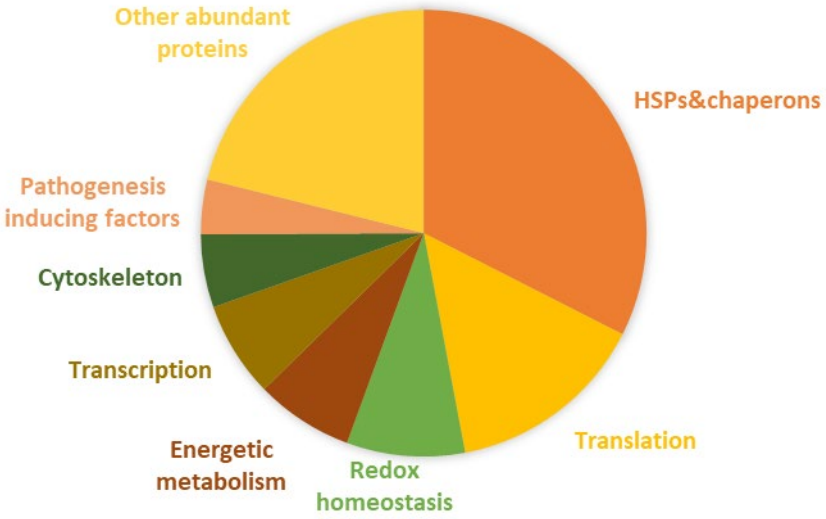

CONCLUSION

Our analysis identified 300 proteins of *P. brassicae* based on 989 pathogen-specific peptides. We found that 75% of the total pathogen proteome is represented only by 44 proteins and we employed bioinformatics to elucidate their (putative) function. Our results revealed an important role of HSPs proteins that represent 32% of *P. brassicae* proteome. Further, the BLAST search revealed that nine of the most abundant *P. brassicae* proteins have close orthologues in *Phytophthora* species, indicating shared mechanisms of pathogenicity.

ACKNOWLEDGEMENTS

The research was financially supported by AF-IGA-IP-2018/014 (Internal Grant Agency of Faculty of AgriSciences, Mendel University in Brno) and by the Ministry of Education, Youths and Sports of the Czech Republic from MOBILITY project 8J18DE015 (Multilevel analysis of the clubroot disease and its biological control by an endophytic fungus).

REFERENCES

Baldrianová, J. et al. 2015. *Arabidopsis* proteome responses to the smoke-derived growth regulator karrikin. Journal of Proteomics, 120: 7–20.

Bass, D. et al. 2009. Phylogeny of novel naked filose and reticulose Cercozoa: Granofilosea cl. n. and Proteomyxidea revised. Protist, 160(1): 75–109.

Cerna, H. et al. 2017. Proteomics offers insight to the mechanism behind *Pisum sativum* L. response to Pea seed-borne mosaicvirus (PSbMV). Journal of Proteomics, 153: 78–88.

Černý, M. et al. 2018. Hydrogen Peroxide: Its Role in Plant Biology and Crosstalk with Signalling Networks. International Journal of Molecular Sciences, 9(8): 2812.

Černý, M. et al. 2019. Fractionation Techniques to Increase Plant Proteome Coverage: A Combined Parallel Separation on Protein and Peptide Level. In Functional Proteomics: Methods and Protocols. New York: Humana Press, pp. 80–94.

Dixon, G.R. 2009. The occurrence and economic impact of *Plasmodiophora brassicae* and clubroot disease. Journal of Plant Growth Regulation, 28(3): 194–202.

Dixon, G.R. 2014. Clubroot (*Plasmodiophora brassicae* Woronin)–an agricultural and biological challenge worldwide. Canadian Journal of Plant Pathology, 36(sup1): 5–18.

Fähling, M. et al. 2003. Pathotype separation of *Plasmodiophora brassicae* by the host plant. Journal of Phytopathology, 151(7–8): 425-430.

Food and Agriculture Organization of the United Nations. 2017. Data [Online]. Available at: http://www.fao.org/faostat/en/#data. [2018-08-21].

Hwang, S.F. et al. 2012. *Plasmodiophora brassicae*: a review of an emerging pathogen of the Canadian canola (*Brassica napus*) crop. Molecular Plant Pathology, 13(2): 105–113.

Konradyová, V., Kazda, J. 2018. Ozimá řepka na pozemcích s *Plasmodiophora brassicae*. Úroda, 66(6): 94–98.

Ludwig-Müller, J. et al. 2014. A novel methyltransferase from the intracellular pathogen *Plasmodiophora brassicae* methylates salicylic acid. Molecular Plant Pathology, 16(4): 349–364.

Ludwig-Müller, J. et al. 2017. Manipulation of auxin and cytokinin balance during the *Plasmodiophora brassicae–Arabidopsis thaliana* interaction. In Auxins and Cytokinins in Plant Biology. New York: Humana Press, pp. 41–60.

Novák, J. et al. 2015. Roles of proteome dynamics and cytokinin signaling in root-to-hypocotyl ratio changes induced by shading roots of *Arabidopsis* seedlings. Plant Cell Physiology, 56(5): 1006–1018.

Schwelm, A. et al. 2015. The *Plasmodiophora brassicae* genome reveals insights in its life cycle and ancestry of chitin synthases. Scientific Reports, 5: 11153.

Song, X. et al. 2011. Proteome analysis of wheat leaf rust fungus, *Puccinia triticina*, infection structures enriched for haustoria. Proteomics, 11(5): 944–963.

Sundelin, T. et al. 2011. Identification of expressed genes during infection of Chinese cabbage (*Brassica rapa* subsp. *pekinensis*) by *Plasmodiophora brassicae*. Journal of Eukaryotic Microbiology, 58(4): 310–314.

Isolation and detail characterization of *aba1* T-DNA insertion mutant line of *Arabidopsis thaliana*

Yuliia Malysheva[1], Valeriia Kopytko[1], Jan Zouhar[2], Jan Skalak[1]
[1]Department of Molecular Biology and Radiobiology
Mendel University in Brno
Zemedelska 1, 613 00 Brno
[2]Central European Institute of Technology (CEITEC)
Mendel University in Brno
Zemedelska 1, 613 00 Brno
CZECH REPUBLIC

x.malyshe@mendelu.com

Abstract: Abscisic acid is a plant hormone that affects many biological processes during plant lifespan including stomatal movement, seed and bud dormancy and organ size. Nevertheless, the role of abscisic acid in photomorphogenesis remains rudimentary. To study the role of abscisic acid in different light conditions, the characterization of homozygous mutant lines in biosynthetic gene encoding zeaxanthin epoxidase (ABA1) is essential for genetic studies. Here, we present isolation and characterization of one of the T-DNA insertion mutant lines of *Arabidopsis thaliana* ecotype Colombia-0, where the insertion is located in 5´ UTR region (SALK_027326). We identified the homozygous plants from a segregating parental line by PCR. The corresponding PCR products were identical to those of a confirmed homozygous line (SALK_027326C). However, the *ABA1* transcript abundance in isolated homozygous line was almost identical to the *ABA1* transcript abundance in the wild-type plants, as was revealed by RT-qPCR analysis. Because the phenotype of the selected homozygous line was also similar to wild-type plants in response to a low light, we conclude that the 5´ UTR mutation in the *ABA1* gene does not affect the gene function and thus this line is not an eligible candidate for further genetic studies.

Key Words: Arabidopsis thaliana, abscisic acid, zeaxanthin epoxidase, photomorphogenesis

INTRODUCTION

Plant growth and development is regulated by many internal and external stimuli, such as the plant hormone abscisic acid (ABA). The role of ABA is well documented in plant processes including the seed development (maturation, desiccation, germination) and response to various abiotic factors (Tuteja 2007, Kermode 2005), ABA is also known to regulate water evaporation through the regulation of development and function of guard cells (Leung and Giraudat 1998).

ABA is synthesized via the methyl-D-erythritol-4-phosphate pathway. Zeaxanthin epoxidase (ABA1) converts zeaxanthin into antheraxanthin, a very first precursor of ABA (Zaharia et al. 2005). Previous reports have shown the important role of ABA1 in seed development and modulation of stress-related gene expression as well as its role in late skotomorphogenic growth (Barrero et al. 2008). However the role of ABA in developmental processes under different light conditions stays unclear.

The expanding field of plant hormonal research identified an extensive spectrum of effects on plant growth and development in several decades of intense research. In spite of modern omics approaches and genome-wide analysis of gene expression that identify thousands of candidate genes to be involved in this process, the classical genetic approaches are still necessary to validate those data and moreover to build a models of upstream/downstream regulations (Fukushima et al. 2009, Koornneef et al. 1997). This so-called reverse genetic method is used to assess the function of a gene by analyzing the phenotypic changes of the plants. However, the generation of mutant lines frequently produces a high number of lines that even containing the mutation they do not affect the function of a gene. Thus the proper isolation and characterization of selected mutant lines is essential to identify a null allele (Koornneef 1991).

To shed a light on the function of ABA1 in photomorphogenic growth, we have collected a broad list of ABA1 mutant lines. In this study, we focus on a characterization of a T-DNA insertion mutant line that showed a wild-type phenotype, while having the T-DNA insertion in homozygosity.

MATERIAL AND METHODS

Growth conditions of plants and isolation of T-DNA line

Arabidopsis plants were cultivated in growing chambers (Percival Scientific) at 21 °C with 60–70% relative humidity with 16-h day period at a light intensity of 20 µmol/m^2/s. Two T-DNA insertion lines in ABA1 (At5g67030), SALK_027326, SALK_027326C, and SAIL_310_B03 were obtained from the Nottingham Arabidopsis Stock Centre (NASC). Genotyping was performed using T-DNA- and gene-specific primers designed using the T-DNA Primer Design tool from the Salk Institute Genomic Analysis Laboratory (http://signal.salk.edu/tdnaprimers.2.html). ABA1 gene-specific primers were LP = CCACCACCAACATCCGAAGA and RP = ACTTGGTGAGTTTCCCTGAGA. Electrophoresis of the PCR products was performed in the agarose gel matrix.

DNA extraction

Leaves of 21-day-old Arabidopsis plants were frozen in liquid nitrogen and ground in the homogenization mill. The total DNA was extracted using standard DNA extraction protocol (Edwards et al. 1991).

RNA extraction and RT-qPCR

Leaves of 21-day-old Arabidopsis plants were frozen in liquid nitrogen and ground in the homogenization mill. The total RNA was extracted using RNeasy Plant Mini Kit (Qiagen) with DNase treatment as previously described (Novák et al. 2015). 1 µg of RNA have been used for cDNA synthesis by RevertAid Reverse Transcriptase (ThermoFisher). ABA1 transcript abundance was analysed by using intron-spanning primers LB = ATGAAGTGTGTTGCGTTGCT and RB = GAAGGAGGCAAATGATGGAG designed in the Universal ProbeLibrary Assay Design Center (probe nu. 94, Roche Life Science), and UBQ10 (At4g05320) was used as a reference gene.

Hypocotyl elongation assay

Seedlings of T-DNA insertion lines and corresponding wild-type were cultivated in the growing chamber (Percival Scientific) at 21 °C with 60–70% relative humidity with 16–h day period at a light intensity of 20 µmol/m^2/s for 7 days. Seedlings ($n \geq 10$ in 3 biological repeats) were photographed and hypocotyl length was measured using ImageJ (http://rsb.info.niv.gov/ij/).

RESULTS AND DISCUSSION

Isolation of homozygous T-DNA insertion mutant in ABA1

The ABA1 gene includes 16 exons and 15 introns where the T-DNA insertion of SALK_027326 takes place in the 5´ UTR region (Figure 1A). Currently, several *aba1* alleles have been isolated and sequenced to obtain an overview of possible mutations within the *ABA1* gene except SALK_027326 line (Barrero et al. 2005). To extend the list of *aba1* mutants, we decided to screen this particular line. The presence of T-DNA was confirmed by PCR in 12 segregating plants (SALK_027326) and 5 homozygous plants (SALK_027326C), while the wild-type contains no T-DNA allele (Figure 1B). One SALK_027326 also did not contain T-DNA allele that classified this particular plant as wild-type. One SALK_027326 plant contained both alleles that classified this particular plant as heterozygous.

T-DNA insertion of SALK_027326 line does not affect the function of ABA1

The analysis of several SALK_027326 plants identified those that are homogenous and thus the transcription of ABA1 might be negatively affected. To test this hypothesis, we performed a RT–qPCR analysis of the *ABA1* transcript levels in wild-type and homozygous SALK_027326 plants (Figure 2 A). The levels of the *ABA1* transcripts were found to be increased in SALK_027326 line, but this change did not reach statistical significance (two-sample *t*-test; $p < 0.05$), suggesting no change in the *ABA1* transcription after T-DNA insertion.

Figure 1 Isolation of homozygous SALK_027326 mutants of Arabidopsis. (A) Gene model of ABA1 showing T-DNA insertion site for SALK_027326 line. (B) Genotype analysis by PCR using target specific primers. The primer combination is highlighted above each gel segment.

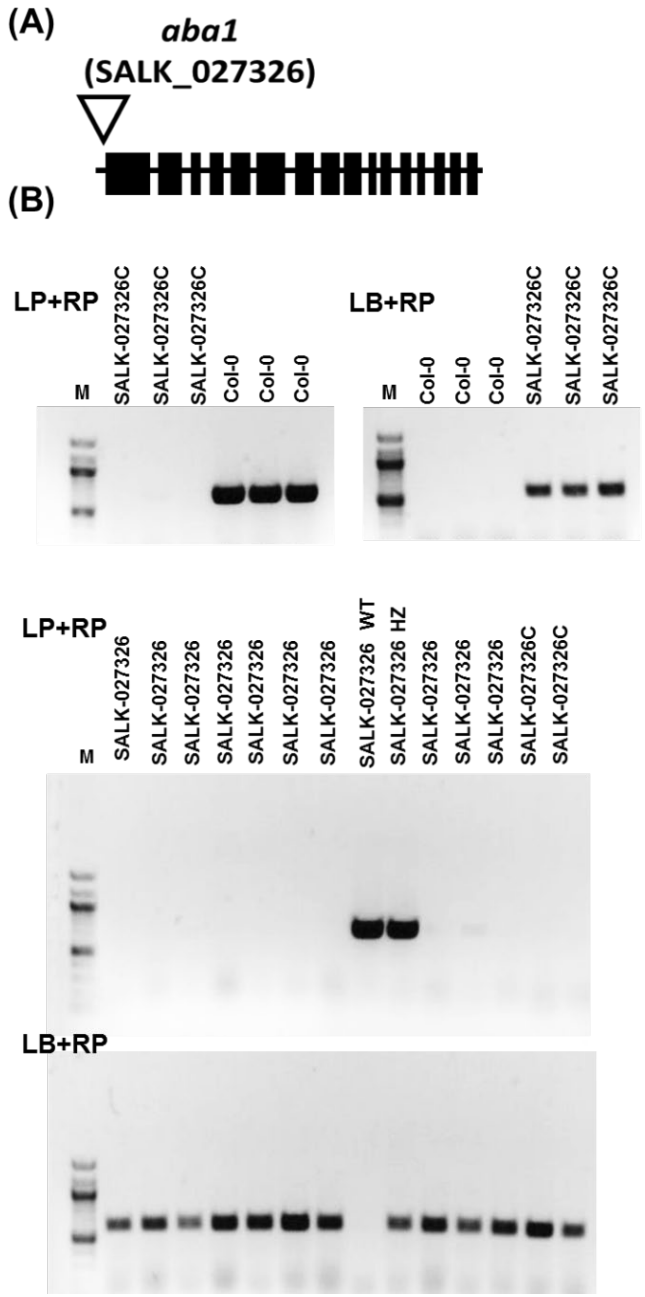

Legend: LP + RP = gene-specific primers, LB + RP = T-DNA-specific primers, WT– wild-type line, HZ – heterozygous line, M – DNA marker. Exons are indicated by black boxes, and introns by lines between boxes.

Moreover, the growth response of both lines to low light intensity was also similar. The similar phenotype with wild-type was also observed in the case of SAIL_310_B03 line containing T-DNA insertion in an intron region of *ABA1* gene. This suggests that once the T-DNA insertion is located in a non-coding region of *ABA1* gene, the function of ABA1 seem to be not affected since the mutation in exons of *ABA1* causes severe effects on plant morphology and physiological responses (Barrero et al. 2005). Detailed characterization of the gene product in both lines by western-blot or targeted mass spectrometry analysis will be done to exclude the role of post-transcriptional processes.

Figure 2 Functional characterisation of SALK_027326 line. (A) RT-qPCR analysis of ABA1 transcript in leaves of Arabidopsis wild-type (Col-0) and T-DNA insertion (SALK_027326) plants. (B) Representative image of 7-day-old wild-type and mutant seedlings (Bar = 0.5 mm). (C) Hypocotyl elongation after 7 days of seedling growth under low light conditions. The data shown are mean ± SD.

CONCLUSION

To investigate the role of ABA biosynthetic gene *ABA1*, we obtained the SALK_027326 line from the NASC collection that was previously designated as a T-DNA insertion line in 5´ UTR region. This region is completely untranslated in many organisms, comprises sequences involved in transcription and translation regulation instead (Penalva and Sanchez 2003, Kim et al. 2014). Thus, we aimed to characterize SALK_027326 line to classify its mutation in the function of ABA1.

The phenotype similarities between wild-type and two allelic mutations SALK_027326 and SAIL_310_B03 clearly indicate that the function of ABA1 might remain unchanged. Moreover, this evidence highlights the fact that it is essential to always use more various allelic mutant lines of one particular gene in genetic studies to clarify the gene function in a particular biological process.

ACKNOWLEDGEMENTS

This work was supported by a grant 17-04607S (Czech Science Foundation) and CEITEC 2020 (LQ1601) project with the financial contribution made by the Ministry of Education, Youth, and Sports of the Czech Republic within special support paid from the National Program of Sustainability II funds.

REFERENCES

Barrero, J.M. et al. 2005. A mutational analysis of the ABA1 gene of Arabidopsis thaliana highlights the involvement of ABA in vegetative development. Journal of Experimental Botany, 56(418): 2071–2083.

Barrero, J.M. et al. 2008. The ABA1 gene and carotenoid biosynthesis are required for late skotomorphogenic growth in Arabidopsis thaliana. Plant, Cell Environment, 31(2): 227–234.

Edwards, K. et al. 1991. A simple and rapid method for the preparation of plant genomic DNA for PCR analysis. Nucleic Acids Research, 19(6): 1349.

Fukushima, A. et al. 2009. Integrated omics approaches in plant systems biology. Current Opinion in Chemical Biology, 13(5): 532–538.

Kermode, A.R. 2005. Role of abscisic acid in seed dormancy. Journal of Plant Growth Regulation, 24(4): 319–344.

Kim, Y. et al. 2014. The immediate upstream region of the 5′-UTR from the AUG start codon has a pronounced effect on the translational efficiency in Arabidopsis thaliana. Nucleic Acids Research, 42(1): 485–498.

Koornneef, M. 1991. Isolation of higher plant developmental mutants. Symposia of the Society for Experimental Biology, 45: 1–19.

Koornneef, M. et al. 1997. Genetic approaches in plant physiology. New Phytologist, 137(1): 1–8.

Leung, J., Giraudat, J. 1998. Abscisic acid signal transduction. Annual Review of Plant Physiology and Plant Molecular Biology, 49(1): 199–222.

Novák, J. et al. 2015. Roles of proteome dynamics and cytokinin signaling in root to hypocotyl ratio changes induced by shading roots of arabidopsis seedlings. Plant and Cell Physiology, 56(5): 1006–1018.

Penalva, L.O.F., Sanchez, L. 2003. RNA Binding Protein Sex-Lethal (Sxl) and Control of Drosophila Sex Determination and Dosage Compensation. Microbiology and Molecular Biology Reviews, 67(3): 343–359.

Tuteja, N. 2007. Abscisic Acid and Abiotic Stress Signaling. Plant Signaling and Behavavior, 2(3): 135–138.

Zaharia, L.I. et al. 2005. Chemistry of abscisic acid, abscisic acid catabolites and analogs. Journal of Plant Growth Regulation, 24(4): 274–284.

Morphological and photosynthetic characteristics of hemp (*Cannabis sativa* L.) grown in hydroculture with landfill leachate

Peter Mendel[1], Marie Grulichova[1], Biljana Dordevic[1], Jan Winkler[1], Vaclav Trojan[1], Magdalena Daria Vaverkova[2], Dana Adamcova[2], Marie Bjelkova[3], Tomas Vyhnanek[1]
[1]Department of Plant Biology
[2]Department of Applied and Landscape Ecology
Mendel University in Brno
Zemedelska 1, 613 00 Brno
[3]Agritec Plant Research, Ltd.
Zemedelska 16, 787 01 Sumperk
CZECH REPUBLIC

peter1mendel@gmail.com

Abstract: Effective application of phytoremediation practices requires understanding of physiological responses of various plant species to heavy metal contamination in different environments. Hemp (*Cannabis sativa* L.) as a multipurpose crop is a good model to study these processes thanks to it's economical value and sturdiness. Two cultivars of industrial hemp exposed to landfill leachate containing heavy metals were grown in hydroculture during a time period of four weeks. Morphological characteristics, photosynthesis and content of pigments were evaluated. Both hemp cultivars seem to present a suitable plant species for phytoremediation practices, at least over a short time period and as long as leachate concentration stays low.

Keywords: hemp, chlorophyll, morphology, leachate, hydroculture

INTRODUCTION

With an increasing focus on phyto-remediation options for landfill leachate, it is important to understand the responses of plant systems to landfill leachate stress. It is especially important to study the tolerant mechanisms of plant systems (Sang et al. 2010). The plants used in phytoremediation are generally annual herbs which don't have any economic value, but do have a very high extraction potential, namely hyperaccumulators (Linger et al. 2002). Selecting suitable plants tolerant to heavy metals and producing products of economic value may be a key factor in promoting the practical application of phytoremediation in polluted soils (Yang et al. 2017).

Hemp (*Cannabis sativa* L.), a multipurpose annual herbaceous plant species which has wide range of applications has the potential to serve as phytoremedial agent for removal of toxic metals from contaminated sites as well as yields high biomass (Kumar et al. 2017). The present study aimed to evaluate the response of two hemp cultivars to leachates of industrial solid waste in terms of root and shoot morphology, leaf area, photosynthetic efficiency and total content of chlorophyll and carotenoids. Plants were grown in an experimental hydroponic culture.

MATERIAL AND METHODS

Experimental setup

Two cultivars of industrial hemp (*Cannabis sativa* L.) were used in this experiment: Monoica, a Hungarian cultivar registered in 2006 and Bialobrzeskie, a Polish cultivar registered in 1968 (Bjelková 2011). Seed material was acquired from Agritec Plant Research, Ltd., Šumperk, Czech Republic. Firstly, sowing into separate plastic trays with perlite (Perlit Ltd., Czech Republic) took place, then hemp cultivars were left to germinate under standard conditions (16 hours of light per day, temperature 20–25 °C), with regular moistening of substrate included. After few days, 2–3 cm tall seedlings were uprooted from perlite and set into conically shaped plastic tubes that were placed in circular holes of a tray, which was on top of dark plastic boxes as a cover. Each box contained six

plantlets and the root system was put through the gaps on the bottom of tubes to be submerged into a nutrient solution. Four experimental groups in twenty-eight hydroponic boxes (seven boxes per group) were prepared this way for hydroponic cultivation: Bialobrzeskie and Monoica cultivars grown in Knop's nutrient solution (Hradilík 1998) in first two experimental groups as a control, then the same two cultivars grown in Knop's solution with 15% landfill leachate admixture, forming the second two, contaminated experimental groups. In addition, aeration of nutrient solution in every box was provided via system of air pumps, tubing and air stones, to ensure that the environment was aerobic enough. During experimental period of four weeks, plants were cultivated in a grow box (tent) under controlled conditions. with prolonged photoperiod (18 hours of light per day), humidity control, ventilation, air circulation and temperature regime set between 20–27 °C.

Data acquisition and evaluation

Shoot length was measured with a common millimeter scale, counting number of fully developed stem nodes was done as well. For these variables, data from three measurement points were taken: first one took place right at the beginning of an experiment as a zero state. The second measurement took place after two weeks of growth, and finally the third was done at the end of experimental period, four weeks from zero state.

Overall root length, surface area and volume of root system, average diameter, total number of root forks and leaf area was measured at the same dates as shoot length. For these variables, destructive methods were used, so there was an objective selection of four plants well representing every trial group at every measurement point. Root parameters were evaluated via scanning device Epson Perfection V700 (Epson Inc., Japan) connected to a computer with WinRHIZO software (Regent Instruments Inc., Canada). Leaf area was recorded by using a scanner UMAX Astra 4700 (UMAX Ltd., Germany), then the acquired images were evaluated by software Quick PHOTO MICRO 3.2 (PROMICRA Ltd., Czech Republic), leaf area expressed as a percentage of scanned surface.

Photosynthetic efficiency expressed as a quantum yield of electron transport in Photosystem II was measured by FlourPen FP 100 (Photon Systems Instruments Ltd., Czech Republic). This variable was measured only twice, after two weeks and at the end of the experiment.

The chlorophyll and carotenoid content in the leaves was determined only at the end of experiment. Fresh leaf samples (0.5 g) were homogenized using liquid nitrogen in a mortar and pestle, then acetone was added for extraction. The suspension was filtered using Morton filter system. The obtained filtrate was used to measure chlorophyll *a*, chlorophyll *b* and carotenoids with the spectrophotometer Spectronic 20 Genesys (Thermo Scientific). Three replicates were conducted for each variant and the level of chlorophylls and carotenoids was calculated from equations presented by Arnon (1949):

$$\text{Chl } a = 12.70\ A_{663} - 2.69\ A_{645}$$

$$\text{Chl } b = 22.90\ A_{645} - 4.68\ A_{663}$$

$$\text{Car} = 4.968\ A_{440} - 0.268\ .\ (c_a + c_b)$$

where A is absorption of the solution at 663, 645 nm and 440 nm, Chl *a* is the concentration of chlorophyll *a* (mg/l), Chl *b* of chlorophyll b (mg/l), Car is the concentration of carotenoids (mg/l) and the total content of chlorophylls was calculated as the sum of chlorophyll *a* and chlorophyll *b* (mg/l). The results were expressed as mg/g FW (fresh weight).

Data of all the parameters were statistically evaluated via software STATISTICA 12 (StatSoft Inc., USA). Significant differences were tested by one-way ANOVA and Tukey's Post-hoc test or Kruskal-Wallis test at the level of significance $\alpha = 0.05$.

Results and outputs of this research were processed in the facilities and by instrumentation financed by project OP VaVpI CZ 1.05/4.1.00/04.0135.

RESULTS AND DISCUSSION

Morphological parameters

During the measurement after two weeks, it was clear that the average leaf area in contaminated groups is significantly smaller when compared to untreated control groups for both hemp cultivars. However, during the last measurement taken after four weeks, for Bialobrzeskie cultivar there was no significant difference between control and contaminated group (Figure 1). The very same pattern was observed for root length (Figure 1) and root surface (data not shown), which is known to have a stable correlation with leaf area under stressful conditions and mostly stays unaffected by availability of resources in the environment (Sadras et al. 1989, Cheng et al. 2016).

Figure 1 Morphological parameters of hemp cultivars in control and contaminated groups

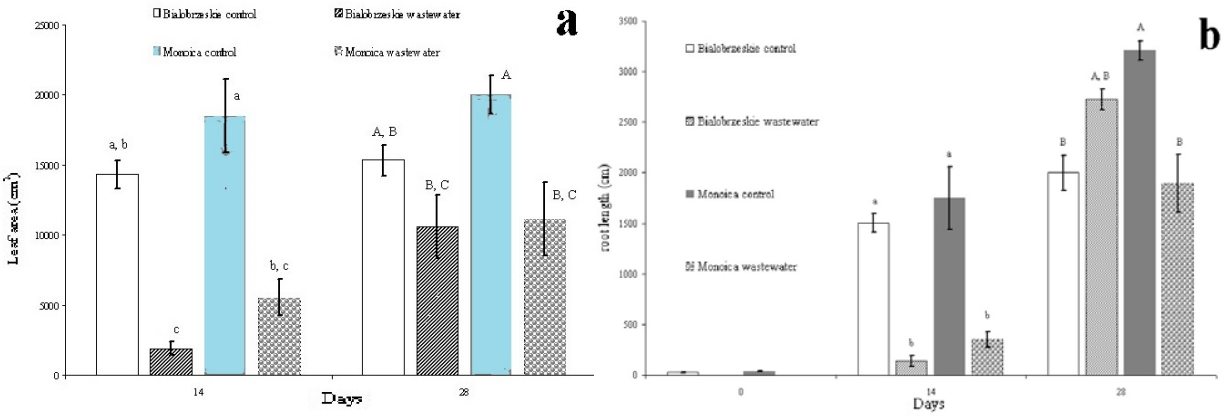

Legend: a) leaf area; b) length of the roots. Capital letters represent the statistical differences among experimental groups for both parameters at the end of experimental period, while lower case letters represent the differences after two weeks, during the first measurement

For other evaluated root variables, significant inhibition of root branching in Monoica cultivar exposed to leachate was observed at the end of experimental period. On the other hand, for contaminated group of cultivar Bialobrzeskie there was a significantly lower volume of root system compared to untreated control group (data not shown). Heavy metals contained in landfill leachate tend to primarily reduce the growth of root tip (main root), to lesser extent they reduce the lateral root zone and this may be even modified by presence and concentration of salts, as observed in an extensive study on maize (*Zea mays* L.) (Ivanov et al. 2003). Also various plant species and developmental phases respond differently to the presence of landfill leachate. Stimulation of root growth by lower concentrations of leachate, but severe inhibition by high concentration compared to control was recorded in a study on maize (*Zea mays* L.) (Sang et al. 2010) and cowpea (*Vigna unguiculata* (L.) Walp.) (Arunbabu et al. 2017).

Also in case of stem length, the general observed pattern was that shoot growth was inhibited in presence of landfill leachate. Again, in this case for cultivar Monoica, significant differences were not observed at the end of experiment anymore (data not shown). General trend is in accordance with results of Vaverková et al. (2017), where landfill leachate containing heavy metals significantly inhibited growth of hemp seedlings. Different behaviour of Monoica cultivar can be explained by better adaptation, as previous studies testing phytoremediation potential show that industrial hemp is showing really variable biological responses depending on cultivar, as well as pollutants studied (Di Candito et al. 2004, Girdhar et al. 2014).

Photosynthetic ability and content of pigments

Results for quantum yield of electron transport in Photosystem II (Φ_{PSII}) show that photosynthetic activity was mainly unaffected in the presence of leachate, with unusual observation at the end of experiment, where the Q_Y of PS II for Bialobrzeskie cultivar was actually significantly higher in contaminated group than in untreated control (Table 1).

Table 1 Quantum yield of electron transport in Photosystem II for all experimental groups of hemp

Experimental group	Φ_{PSII} ± SE	
	First measurement	Second measurement
Bialobrzeskie control	0.719 ± 0.038 a	0.646 ± 0.027 b,c
Bialobrzeskie leachate	0.639 ± 0.058 a	0.757 ± 0.014 a
Monoica control	0.758 ± 0.006 a	0.691 ± 0.023 a, b
Monoica leachate	0.671 ± 0.028 a	0.672 ± 0.026 a, b

Legend: Values are expressed as relative numbers without units, they represent a ratio of fixed CO_2 concentration to concentration of absorbed photons. Numbers are stated as the mean of the group with standard error of the mean (SE). Letters assigned to numbers stand for statistically significant differences between groups.

That represents a seemingly contradicting behaviour, as it is known that heavy metals contained in landfill leachate have a proven inhibitory effect on electron transport processes and energy transformation in Photosystem II in a lot of plant species (Paunov et al. 2018). However, concentration of pollutants is crucial, and photosynthetic efficiency of hemp can remain unaffected if exposed to heavy metals in low concentration. It was also observed that Φ_{PSII} oscillated during exposure, especially in relation with chlorophyll fluorescence (Linger et al. 2005). This can be attributed to a multitude of factors, as the leachate represents a potent mixture of chemicals (ammonia, carbon, humic acids, heavy metals, polychlorinated biphenyls), where adverse effects can be balanced by providing extra nutrition (Morozesk et al. 2017). It is especially worth noting, that control group of Bialobrzeskie cultivar exhibited signs of leaf chlorosis at the end of experiment, most likely due to nutrient deficiency, heat stress and reaching growth limits in given conditions, as on average this cultivar had significantly higher stem length than Monoica cultivar (data not shown).

The effect of leachate treatment after four weeks on pigment content of hemp plants in hydroponic culture is shown in Figure 2. The result showed an increased in the chlorophyll *a,* chlorophyll *b*, total chlorophyll and carotenoid contents, except for chlorophyll *a* of Monoica cultivar. In case of Bialobrzeskie cultivar the chlorophyll *a,* chlorophyll *b*, total chlorophyll contents are up to 2.5 times higher of leachate treated plants and carotenoid contents is up to 2 times higher.

Figure 2 Content of pigments in hemp leaves after four weeks of leachate treatment

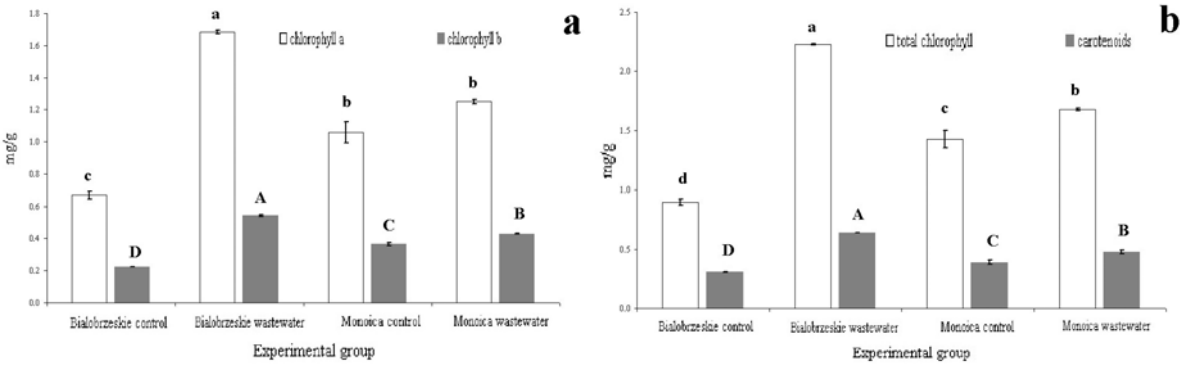

Legend: a) content of chlorophyll 'a' and chlorophyll 'b'; b) total content of chlorophyll and carotenoids. Capital letters represent the statistical differences among experimental groups for chlorophyll 'b' and carotenoids, while lower case letters represent the differences for chlorophyll 'a' and total chlorophyll

Similarly, high chlorophyll content (213 and 230%) was reported in 30–40% leachate treatment in pot experiment of bread wheat (*Triticum aestivum* L.) as compared to control (Mor et al. 2013). The increase in the level of chlorophyll and carotenoid pigments was also showed in 5–20% leachate in pot experiment of pea (*Pisum sativum* L.) (Vishnoi et al. 2013). The increase in chlorophyll content at relatively low concentration of leachate and relatively short time period may be explained by hormetic effect, manifested as an overcompensation due to disruption of homeostatsis, which was described in relation to several chemicals. This effect was recorded in studies with peppermint (Calabresci 1999) and cucumber (Cargnelutti et al. 2006). The chlorophyll content in maize (*Zea mays* L.) seedlings varied as functions of leachate concentrations and exposure time. Furthermore, chlorophyll content inhibition occurred after long exposure times or high concentrations of leachate and might result from

the damaged defence system and consequent unbalanced metabolism (Sang et al. 2010). Similarly, the tested municipal solid waste leachate in wheat seedlings showed that at lower concentration levels supports chlorophyll synthesis, but at higher levels of contaminants, it reduced the biosynthesis of chlorophyll. Thus the physiological responses of wheat seedlings to the test sample could reveal the capability of plant systems to tolerate the environmental pressure from leachate (Awasthi et al. 2017). Further the effect of different concentrations of leachate on chlorophyll *a*, *b* and carotenoid contents in cowpea (*Vigna unguiculata* (L.) Walp.) was investigated and chlorophyll *a* and *b* exhibited a similar trend, where 0.5–5% leachate was stimulation, but at 25% leachate was inhibition on the chlorophyll *a* and *b* contents. Similar to chlorophyll, the carotenoid contents showed a gradual increase from 0.5–5% leachate treatment and may be attributed to the ability of the plant to counteract the toxic effect of free radicals generated under stress (Arunbabu et al. 2017).

CONCLUSION

Morphological characteristics (stem length and leaf area, root length, root surface and volume), photosynthetic activity and content of pigments (chlorophyll and carotenoids) were evaluated during experimental period of four weeks in two cultivars of industrial hemp grown in hydroculture affected by landfill leachate. Statistically significant effects for both hemp cultivars, in almost all measured variables were observed in groups contaminated by leachate. Physiological responses, adaptability and coping mechanisms with landfill leachate show considerable variability between hemp cultivars when considering morphological parameters, although results suggest that Bialobrzeskie cultivar is less directly affected by leachate overall. In general, hemp tolerates lower concentrations of landfill leachate well without sacrificing photosynthetic efficiency or production of pigments. Current results don't provide definite answers to heavy metal tolerance and accumulation in hemp for a given experimental design, as other substances in leachate come into play. In the future, various concentrations of leachate and more hemp cultivars should be tested.

ACKNOWLEDGEMENTS

This research was financially supported by grant IGA no. TP 5/2017. All authors thank to company Agritec Plant Research, Ltd. and to Dr. Marie Bjelková for providing seed material and valuable consulting for this work.

REFERENCES

Arnon, D.I. 1949. Copper enzymes in isolated chloroplasts, polyphenoloxidase in *Beta vulgaris*. Plant Physiology, 24: 1–15.

Arunbabu, V. et al. 2017. Leachate pollution index as an effective tool in determing the phytotoxicity of municipal solid waste leachate. Waste Management, 68: 329–336.

Awasthi, A.K. et al. 2017. Municipal solid waste leachate impact on metabolic activity of wheat (*Triticum aestivum* L.) seedlings. Environmental Science and Pollution Research, 24: 17250–17254.

Bjelková, M. 2011. Use of fiber plants in phytoremediation. Doctoral thesis, Mendel University in Brno.

Calabresci, E.J. 1999. Evidence that hormesis represents an overcompensation response to a disruption in homeostasis. Ecotoxicology and Environmental Safety, 42(2): 135–137.

Cargnelutti, D. et al. 2006. Mercury toxicity induces oxidative stress in growing cucumber seedlings. Chemosphere, 65: 999–1006.

Cheng, J. et al. 2016. Functional correlations between specific leaf area and specific root length along a regional environmental gradient in Inner Mongolia grasslands. Functional Ecology, 30: 985–997.

Di Candito, M. et al. 2004. Heavy metal tolerance and uptake of Cd, Pb and Tl by hemp. Advances in Horticultural Science, 18: 138–144.

Girdhar, M. et al. 2014. Comparative assessment for hyperaccumulatory and phytoremediation capability of three wild weeds. 3 Biotech, 4(6): 579–589.

Hradilík, J. 1998. Fyziologie rostlin: Návody do cvičení. 2nd ed., Brno, Czech Republic: Mendelova zemědělská a lesnická univerzita v Brně.

Ivanov, V.B. et al. 2003. Comparative Impacts of Heavy Metals on Root Growth as Related to Their Specificity and Selectivity. Russian Journal of Plant Physiology, 50(3): 398–406.

Kumar, S. et al. 2017. *Cannabis sativa*: A Plant Suitable for Phytoremediation and Bioenergy Production. In Phytoremediation Potential of Bioenergy Plants. Singapore: Springer, pp. 269–285.

Linger, P. et al. 2002. Industrial hemp (*Cannabis sativa* L.) growing on heavy metal contaminated soil: fibre quality and phytoremediation potential. Industrial Crops and Products, 16: 33–42.

Linger, P. et al. 2005. *Cannabis sativa* L. growing on heavy metal contaminated soil: growth, cadmium uptake and photosynthesis. Biologia Plantarum, 49(4): 567–576.

Mor, S. et al. 2013. Growth behaviour studies wheat plant exposed to municipal landfill leachate. Journal of Environmental Biology, 34: 1083–1087.

Morozesk, M. et al. 2017. Effects of humic acids from landfill leachate on plants: An integrated approach using chemical, biochemical and cytogenetic analysis. Chemosphere, 184: 309–317.

Paunov, M. et al. 2018. Effects of Different Metals on Photosynthesis: Cadmium and Zinc Affect Chlorophyll Fluorescence in Durum Wheat. International Journal of Molecular Sciences, 19(3): 787.

Sadras, V.O. et al. 1989. Dynamics of Rooting and Root-Length: Leaf-Area Relationships as Affected by Plant Population in Sunflower Crops. Field Crops Research, 22: 45–47.

Sang, N. et al. 2010. Landfill leachate affects metabolic responses of *Zea mays* L. seedlings. Waste Management, 30: 856–862.

Vaverková, M.D. et al. 2017. Landfill Leachate Effects on Germination and Seedling Growth of Hemp Cultivars (*Cannabis sativa* L.). Waste and Biomass Valorization, 8: 1–8.

Vishnoi, N. et al. 2013. Phytotoxic effect of leachates of industrial solid waste on the growth of *Pisum sativum*. Journal of Environmental Biology, 34: 651–656.

Yang, Y. et al. 2017. Comparison of three types of oil crop rotation systems for effective use and remediation of heavy metal contaminated agricultural soil. Chemosphere, 188: 148–156.

Cytokinin-deficiency enhanced tolerance to chloroacetanilide herbicide metolachlor

Jaroslav Pavlu[1,2], Martina Slapakova[2]
[1]Central European Institute of Technology (CEITEC)
[2]Department of Molecular Biology and Radiobiology
Mendel University in Brno
Zemedelska 1, 613 00 Brno
CZECH REPUBLIC

pavlu@mendelu.cz

Abstract: Plant responses to synthetic organic compounds (xenobiotics) involve coordinated physiological, biochemical and signaling events. Cytokinin acts in the integration of growth control and stress response and recent works demonstrated various effects of cytokinin on glutathione content and glutathione-dependent detoxification of toxic metals/metalloids. However, the role of cytokinin in plant responses to organic xenobiotic which sequestration relies on glutathione conjugation remains to be elucidated. Here, for the first time, we probed the role of cytokinin in plant response to xenobiotics whose detoxification pathway involves formation of glutathione conjugates. We found that increased endogenous cytokinin content lowers plant resistance to triazine herbicide atrazine, chloroacetanilide herbicides, such as alachlor and metolachlor, and herbicide safeners benoxacor and fenclorim. The cytokinin-deficient plants even exhibited an enhanced tolerance to metolachlor. Altogether, we found that cytokinin modulates xenobiotic stress response, which might be of potential importance in herbicide selectivity or phytoremediation strategies.

Key Words: cytokinin, xenobiotic, herbicide, stress tolerance, glutathione

INTRODUCTION

Increasing industrialization and application of diverse chemicals causes higher incidence of organic pollutant stresses. Plants detoxify noxious pollutants via the sequential action of defense enzymes, which includes conjugation of various electrophilic xenobiotics with glutathione (GSH) by the action of glutathione-S-transferases. The GSH conjugation protects plants from the toxicity associated with exposure to herbicides of various chemical classes and might be important to determine herbicide selectivity in different plant species. Glutathione-S-transferases are also involved in the action of so called herbicide safeners, which enhance herbicide tolerance in crop plants but not in the target weeds, thus improving herbicide selectivity (DeRidder and Goldsbrough 2006, Riechers et al. 2010).

Plant responses to xenobiotics involve complex signaling pathways including phytohormone signaling (Ramel et al. 2012). Cytokinin is a plant hormone that regulates various aspects of growth and development and also certain stress responses (Pavlů et al. 2018). Although poorly elucidated, cytokinin signaling has been shown to interact with xenobiotic stress responses. *CYTOKININ RESPONSE FACTOR 6* (*CRF6*) is induced by the herbicide atrazine and *crf6* insertional mutant line exhibited lower atrazine injury than wild-type (Ramel et al. 2012). Certain cytokinin-signaling genes including *CRF6* are involved in xenobiotic stress response controlled by a phosphoregulation of RNA-polymerase II (Fukudome et al. 2014).

Moreover, there are additional lines of indirect evidence suggesting that cytokinin signaling is involved in xenobiotic response. Cytokinin regulates genes of xenobiotic metabolism, such as a glutathione-S-transferase GSTU26 that belongs to the most robustly cytokinin-responsive genes in Arabidopsis (Brenner et al. 2012). Note that the *GSTU26* is induced by the chloroacetanilide herbicides alachlor and metolachlor, and herbicide safener benoxacor (Nutricati et al. 2006) suggesting a link between cytokinin and GSH conjugation-mediated xenobiotic detoxification.

Recent reports described that cytokinin-deficient plants display a GSH-dependent arsenic (Mohan et al. 2016) and selenium (Jiang et al. 2018) resistance. In this line, we found that cytokinin triggers

GSH depletion, which is likely responsible for decreased cadmium tolerance observed in cytokinin-treated Arabidopsis (Pavlů et al., unpublished results). Interestingly, even though cytokinin has a clear effect on the GSH content and the tolerance to thiol-reactive metal(loid)s, the impact of cytokinin-GSH crosstalk on GSH conjugation of organic xenobiotics has not been studied yet. Here, we probed for the first time the effects of modulated cytokinin content on the response to triazine herbicide atrazine, chloroacetanilide herbicides alachlor and metolachlor, and herbicide safeners benoxacor and fenclorim, which are well known to form GSH-conjugates during their detoxification in plants (Brazier-Hicks et al. 2008, Cummins et al. 2011).

MATERIAL AND METHODS

Plant materials and growth conditions

Experiments were performed using Arabidopsis transgenic lines expressing bacterial isopentenyl transferase (*CaMV35S*>GR>*ipt*, line 11) (Craft et al. 2005) and barley cytokinin oxidase (*CaMV35S*>GR>*HvCKX2*, line 13) (Černý et al. 2014) and corresponding wild-type plants (*Arabidopsis thaliana* accession Col-0). 0.5 µM dexamethasone (DEX) (Sigma-Aldrich) application was utilized to induce the expression of *ipt* or *HvCKX2* to increase endogenous cytokinin biosynthesis or degradation, respectively, in the transgenic lines. Seeds were surface-sterilized with 70% ethanol and sown on 1% (w/v) agar solidified half-strength Murashige and Skoog (MS) medium (pH 5.7). Sown seeds were stratified in dark at 4 °C for 2 days and cultivated vertically in a growth chamber (AR36LX, Percival) under long-day conditions (16 h light/8 h dark) at 20 °C, 60% relative humidity, and 120 $\mu mol/m^2/s$ photon flux density. For treatments, the medium was supplemented with 0.02% (v/v) DMSO (mock) or chemicals in DMSO (0.02% (v/v) final concentration). The DEX and the herbicides and herbicide safeners (atrazine, alachlor, metolachlor, benoxacor and fenclorim) were purchased from Sigma.

Root elongation growth assay

The seedlings were germinated and grown on MS media supplemented with both 0.5 uM DEX and one of the organic xenobiotics (5 µM alachlor, 10 µM metolachlor, 20 µM benoxacor or 40 µM fenclorim) for 7 days. The 7-d-old seedlings were photographed and primary root length of at least 20 seedlings was quantified by ImageJ software (http://rsbweb.nih.gov/ij/). The statistical significance was evaluated by the Student´s *t*-test.

RESULTS AND DISCUSSION

Effects of xenobiotic on plant growth

Preliminary tests of herbicide/herbicide safener effects on plant growth were performed to identify effective concentrations of organic xenobiotics for subsequent analysis. The phytotoxic effects of the chlorinated organic compounds were observed at their micromolar concentrations. Interestingly, treatments with a specific herbicide or a herbicide safener caused well-defined phenotypes, including distinct degree of chlorosis and changes in shoot to root ratio. These particular effects of specific herbicides/herbicide safeners indicate their different mode of action.

Atrazine was found to be the most phytotoxic herbicide, triggering growth retardation at 100 nM and seedling lethality at 1 µM. At a sublethal concentration (500 nM), the atrazine-treated plantlets displayed clear intoxication symptoms, such as striking shoot retardation and visible chlorosis, which were in contrast with a moderate root growth inhibition. These detrimental atrazine effects on the shoot reflect the atrazine mechanism of toxicity. Atrazine binds to the D1 protein of the photosystem II, causing an inhibition of photosynthesis.

Treatment with chloroacetanilide herbicides alachlor and metolachlor triggered clear root shortening at 5 µM, with shoot growth inhibition being more apparent. Under the 20 µM alachlor or metolachlor treatment, plants displayed noticeable shoot growth inhibition and pale green colouring.

Benoxacor administration caused a relatively minor shoot growth inhibition, which was in a sharp contrast with a profound inhibition of root elongation at 5 µM and 20 µM. This root sensitivity leading to the intriguing phenotype of benoxacor-treated plantlets suggests that root meristem is the primary site of benoxacor injury.

Out of the tested chemicals, fenclorim administration was the least toxic. Visible inhibition of the root elongation appeared at the concentration of 20 µM. Remarkably, the fenclorim-treated plantlets displayed clear shoot growth inhibition and even visible chlorosis at 50 µM whereas root growth was inhibited to only about 40% of the control plants. Note, that roots are the primary organs of plants, which are in direct contact with xenobiotic-supplemented media, absorb the xenobiotic, and are expected to be the most sensitive to the toxic effects of xenobiotic in the media. We suggest that shoot-localized processes are the primary targets for fenclorim toxicity. This is supported by the resemblance of the fenclorim-triggered phenotype and the effect of the photosynthesis inhibitor atrazine.

For subsequent analysis, we assessed the effects of 500 nM atrazine, 5µM alachlor, 10 µM metolachlor, 20 µM benoxacor and 40 µM fenclorim which evoked the root length inhibition to 67%, 36%, 35%, 20% and 54%, respectively, in comparison to the mock-treated control (Figure 1). Note, that for cadmium which is known to be a highly toxic heavy metal, the root elongation is inhibited to 50% of control at 50 µM in Arabidopsis.

Figure 1 Representative Arabidopsis phenotypes associated with exposure to chlorinated xenobiotics

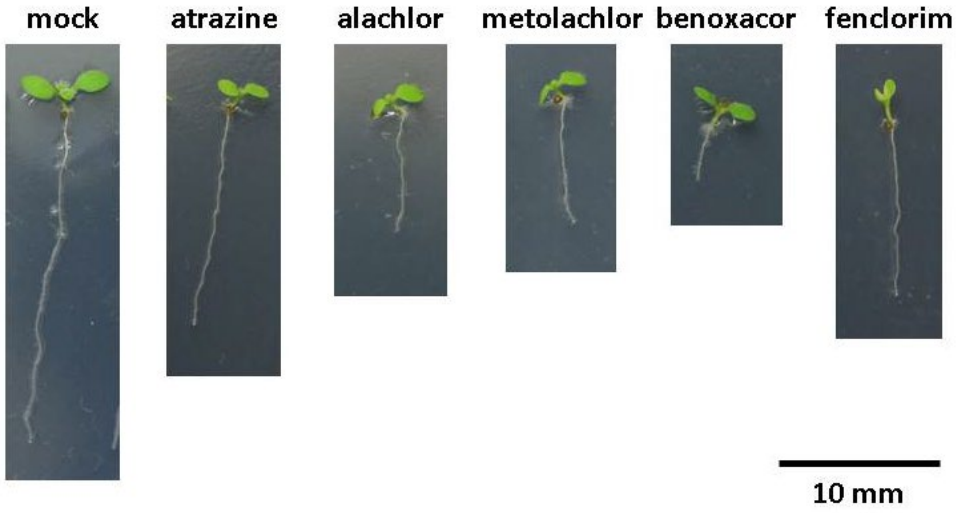

Legend: Col-0 (wild type) seedlings were germinated and grown on half-strength MS media supplemented with herbicides atrazine (500 nM), alachlor (5µM), metolachlor (10 µM), and herbicide safeners benoxacor (20 µM) and fenclorim (40 µM) for 7 days. For details see Materials and Methods.

Modulation of endogenous cytokinin content interferes with xenobiotic-associated growth response

To assess the effects of cytokinin modulation on the growth response triggered by xenobiotics treatments, the root elongation was assayed in transgenic lines with DEX-activable cytokinin biosynthesis (*CaMV35S*>GR>*ipt*) or DEX-activable cytokinin degradation (*CaMV35S*>GR>*HvCKX2*), respectively. The DEX treatment of wild-type plants did not affected the toxicity symptoms of herbicide-treated wild-type Arabidopsis (Figure 2a) excluding putative artefacts due to a crosstalk of the glucocorticoid sensing and xenobiotic response.

The increased endogenous cytokinin levels in the activated line *CaMV35S*>GR>*ipt* potentiated the root growth inhibition associated with exposure to atrazine, alachlor, metolachlor and fenclorim (Figure 2b). The negative effect of cytokinin was most remarkable in fenclorim-treated seedlings. Cytokinin did not further inhibited the root elongation in benoxacor-exposed seedlings (Figure 2b) suggesting a convergence and/or saturation of mechanisms that lead to the root growth inhibition in response to benoxacor and cytokinin.

In the activated line *CaMV35S*>GR>*HvCKX2*, the reduced cytokinin levels caused enhanced root growth as described previously (Werner et al. 2001) and similar root elongation persisted even upon xenobiotic stress in the cytokinin-deficient seedlings (Figure 2c). Interestingly, the cytokinin-deficient seedlings showed a metolachlor tolerance phenotype, as they exhibited approximately 45% root

elongation under metolachlor administration. This cytokinin depletion-provoked metolachlor tolerance was validated in two independent experimental replicas.

Figure 2 Cytokinin modulates the effect of chlorinated xenobiotics on Arabidopsis root growth

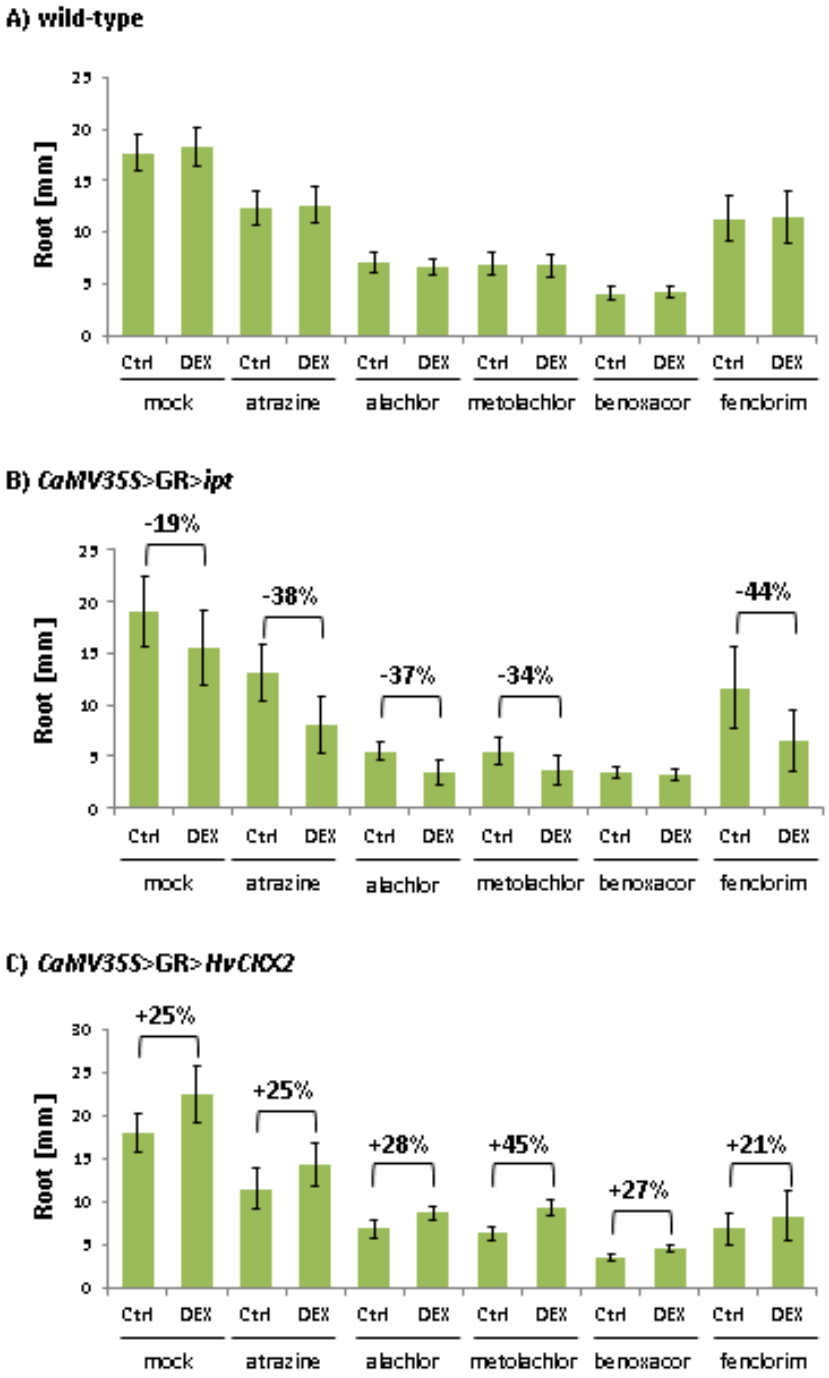

Legend: Seedlings were germinated and grown on solid half-strength MS media containing herbicides atrazine (500 nM), alachlor (5µM), metolachlor (10 µM), and herbicide safeners benoxacor (20 µM) and fenclorim (40 µM). The xenobiotic effects on root growth were followed in wild-type (A), conditionally cytokinin-overproducing transgenic line CaMV35S>*GR*>ipt *upon DEX-induced activation of the construct hosting ipt (B) and conditionally cytokinin-deficient transgenic line* CaMV35S>*GR*>HvCKX2 *upon DEX-induced activation of the construct hosting* HvCKX2 *(C). Root length of at least 25 seedlings was measured after 7 d. Error bars indicate SD. The xenobiotic-triggered root inhibition was significant at P<0.001 (t-test) in all treatments and genotypes. The relative alternations in the root length under DEX supplementation is marked if the difference was significant (P<0.01;* t-*test).*

The mode of action of cytokinin-deficiency in the mitigation of the metolachlor-triggered detrimental symptoms remains to be clarified. Noteworthy, a glutathione-dependent tolerance of arsenic and selenium in cytokinin-deficient plants has been previously reported (Mohan et al. 2016, Jiang et al.

2018). In addition, cytokinin has been suggested to participate in glutathione homeostasis, as the gene *GGCT2;1* encoding a key enzyme of glutathione degradation represents a highly cytokinin-responsive gene (Pavlů et al. 2018). We further speculate that cytokinin-regulation of *GGCT2;1* contributes to enhanced GSH level and arsenic tolerance phenotype of cytokinin-deficient plants described by Mohan et al. (2016), as both mutation and overexpression of *GGCT2;1* contributed to enhanced growth under arsenic toxicity (Paulose et al. 2013). Therefore, a future research will focus on the possible role of glutathione in the metolachlor tolerance phenotype in the cytokinin-deficient plants.

CONCLUSION

Glutathione/glutathione-S-transferase detoxification system is fundamental for xenobiotic metabolism. Recent reports showed that cytokinin modulates glutathione-dependent stress response, suggesting that cytokinin might be involved in response to xenobiotics which are detoxified via glutathione conjugation. Here, for the first time, we analysed effects of modulated endogenous cytokinin content on the response to a xenobiotic series consisting of chlorinated herbicides/herbicide safeners, which represent well recognized substrates of glutathione-S-transferase. Cytokinin potentiated xenobiotic sensitivity and cytokinin-deficiency was associated with tolerance to the metolachlor herbicide. Deciphering the role of cytokinin signaling in metolachlor injury, involvement of glutathione in the metolachlor tolerance mechanisms, and other aspects of the metolachlor tolerance phenotype provoked by severe depletion of cytokinin will constitute crucial topics for future studies.

ACKNOWLEDGEMENTS

The research was financially supported by the LQ1601 (CEITEC 2020) project (which received a financial contribution from the Ministry of Education, Youths and Sports of the CR in the form of special support through the National Programme for Sustainability II funds). The authors thank Jan Zouhar for constructive comments, manuscript proofreading and editing.

REFERENCES

Brazier-Hicks, M. et al. 2008. Catabolism of Glutathione Conjugates in Arabidopsis thaliana. Journal of Biological Chemistry [Online], 283(30): 21102–21112. Available at: http://www.ncbi.nlm.nih.gov/pubmed/18522943. [2018-09-31].

Brenner, W.G. et al. 2012. Gene Regulation by Cytokinin in Arabidopsis. Frontiers in Plant Science [Online], 31(3): 8. Available at: http://www.ncbi.nlm.nih.gov/pubmed/22639635. [2018-09-31].

Černý, M. et al. 2014. Cytokinin modulates proteomic, transcriptomic and growth responses to temperature shocks in A rabidopsis. Plant, Cell & Environment [Online], 37(7): 1641–1655. Available at: http://www.ncbi.nlm.nih.gov/pubmed/24393122. [2018-09-31].

Craft, J. et al. 2005. New pOp/LhG4 vectors for stringent glucocorticoid-dependent transgene expression in Arabidopsis. The Plant Journal [Online], 41(6): 899–918. Available at: http://www.ncbi.nlm.nih.gov/pubmed/15743453. [2018-09-31].

Cummins, I. et al. 2011. Multiple roles for plant glutathione transferases in xenobiotic detoxification. Drug Metabolism Reviews [Online], 43(2): 266–280. Available at: http://www.ncbi.nlm.nih.gov/pubmed/21425939. [2018-09-31].

DeRidder, B.P., Goldsbrough, P.B. 2006. Organ-specific expression of glutathione S-transferases and the efficacy of herbicide safeners in Arabidopsis. Plant physiology [Online], 140(1): 167–75. Available at: http://www.ncbi.nlm.nih.gov/pubmed/16361527. [2018-09-31].

Fukudome, A. et al. 2014. Arabidopsis CPL4 is an essential C-terminal domain phosphatase that suppresses xenobiotic stress responses. The Plant Journal [Online], 80(1): 27–39. Available at: http://www.ncbi.nlm.nih.gov/pubmed/25041272. [2018-9-31].

Jiang, L. et al. 2018. Cytokinin is involved in TPS22-mediated selenium tolerance in Arabidopsis thaliana. Annals of Botany [Online], 122(3): 501–512. Available at: https://academic.oup.com/aob/article/122/3/501/5032490. [2018-09-31].

Mohan, T.C. et al. 2016. Cytokinin Determines Thiol-Mediated Arsenic Tolerance and Accumulation. Plant physiology [Online], 171(2): 1418–26. Available at: https://www.ncbi.nlm.nih.gov/pubmed/27208271 [2018-09-31]

Nutricati, E. et al. 2006. Characterization of two Arabidopsis thaliana glutathione S-transferases. Plant Cell Reports [Online], 25(9): 997–1005. Available at: http://www.ncbi.nlm.nih.gov/pubmed/16538523. [2018-09-31].

Paulose, B. et al. 2013. A γ-Glutamyl Cyclotransferase Protects Arabidopsis Plants from Heavy Metal Toxicity by Recycling Glutamate to Maintain Glutathione Homeostasis. The Plant Cell [Online], 25(11): 4580–4595. Available at: http://www.ncbi.nlm.nih.gov/pubmed/24214398. [2018-09-31].

Pavlů, J. et al. 2018. Cytokinin at the Crossroads of Abiotic Stress Signalling Pathways. International Journal of Molecular Sciences [Online], 19(8): 2450. Available at: http://www.ncbi.nlm.nih.gov/pubmed/30126242. [2018-09-31].

Ramel, F. et al. 2012. Xenobiotic sensing and signalling in higher plants. Journal of Experimental Botany [Online], 63(11): 3999–4014. Available at: https://www.ncbi.nlm.nih.gov/pubmed/22493519. [2018-09-31].

Riechers, D.E., et al. 2010. Detoxification without intoxication: herbicide safeners activate plant defense gene expression. Plant physiology [Online], 153(1): 3–13. Available at: http://www.ncbi.nlm.nih.gov/pubmed/20237021. [2018-09-31].

Werner, T. et al. 2001. Regulation of plant growth by cytokinin. Proceedings of the National Academy of Sciences [Online], 98(18): 10487–10492. Available at: http://www.ncbi.nlm.nih.gov/pubmed/11504909. [2018-09-31].

ANIMAL BIOLOGY

Optimalization of cryohistological technique in rat and porcine lungs

Rea Jarosova[1], Petra Ondrackova[2], Zbysek Sladek[1]
[1]Department of Morphology, Physiology and Animal Genetics
Mendel University in Brno
Zemedelska 1, 613 00 Brno
[2]Department of Immunology
Veterinary Research Institute
Hudcova 296/70, 621 00 Brno
CZECH REPUBLIC

xjaroso3@node.mendelu.cz

Abstract: Histological freezing technique is a quick and gentle method of tissue preparation for identifying the microscopic structure. Lung tissue belongs to the less compact structures and its proper histological processing required testing of several available procedures. The optimization of freezing pulmonary tissue leads to more accurate detection of the pathological process in the lungs and better understanding pathogenesis of respiratory diseases of pigs, especially the porcine pneumonia. The aim of this work was to find a way of preserving the morphological structure of the lungs as in a physiological state. We used pulmonary tissue from 4 laboratory rats and 4 domestic pigs and freezing of samples in liquid nitrogen, iso-pentane, n-heptane and the usual process in the freezer. The results show the most appropriate procedure was after isolation of the lungs, filled part of lung over the *bronchus* by mixture of 1 : 1 Tissue Tek (O.C.T. Compound) with phosphate-buffered saline solution (PBS) and frozen in super-cooled n-heptane placed on dry ice and samples store at -80 °C.

Key Words: morphological structure, freezing technique, pulmonary tissue, porcine pneumonia

INTRODUCTION

Histological techniques allow the observation of a detailed structure of organs and tissues under a light or electron microscope. Almost any organ or tissue can be observed without prior histological modification (Zimmerman et al. 2002). The most important point of tissue histology is the fixation of tissue samples immediately after isolation so as to avoid cell decomposition – autolysis of cells. The classic paraffin histology, where the specimen fixation is performed chemically, and then the tissue sample is preserved in paraffin, leads to lipid loss and protein denaturation. There is frozen histology faster and more gentle method of tissue processing (Mescher 2018). By freezing the tissue, most of the biologically active substances, such as proteins or lipids, are preserved in the native form and it is possible to carry out the subsequent detection of antigens by immunohistochemistry (Sienko et al. 2005).

Pulmonary tissue belongs to less compact tissues and structure of lungs is very fragile. During the lifetime of the organism the lungs are filled with air which filling the lungs alveoli and preserving their morphological structure. After death there is an air leakage from the lungs and alveolar collapse (Prince and Porter 1975)

In this work, emphasis was placed on the preservation of the morphological structure of the lung, comparable to that physiological state of the organism, and the aim of the work was optimized the process of freezing, especially the isolation and fixation of lung tissue. The role of the project was to test many ways of processing the lung tissue and to find the most appropriate tissue processing technique. After testing various methods of tissue isolation and freezing, the most appropriate method has been found to maintain the alveolar structure. The outcome of this project is therefore to introduce the proven method into practice.

MATERIAL AND METHODS

Experimental material

It was used lung tissue from 4 laboratory rats (*Rattus norvegicus*) for this experiment. Rats were anesthetized with ether and sacrificed by broken a neck.

In this experiment were used 4 eight-week-old pigs (*Sus scrofa f. domestica*) from the herd without anomaly or vaccination. The pigs were kept in the accredited barrier-type animal facilities of the Veterinary Research Institute (VRI). The animal care protocol for this experiment followed the Czech guidelines for animal experimentation and was approved by the Branch Commission for Animal Welfare of the Ministry of Agriculture of the Czech Republic. The pigs were allowed to acclimatize in the animal facilities for one week, than pigs were sacrificed. The porcine experimental material was collected by trained staff from authorized and registered slaughterhouse at VRI.

Experimental design

Sampling of rat lung tissue - part of the samples was immersed in a solution of 10% sucrose for 24 hours, which increases the surface tension of the tissue and then the lungs were frozen in liquid nitrogen, isopentane (n-pentane) and n-heptane placed on dry ice, or frozen by the usual process in the freezer at -20 °C.

Some samples of rat lungs were embedded in the cryo-protective agent Tissue Tek (O.C.T. Compound, Sakura-Finetek). The others were left untreated and frozen by the various ways mentioned above. A standard fixation of 10% formalin was omitted to preserve lipids and proteins in native form.

Samples frozen by the usual process were stored at -20℃ lung samples frozen in liquid nitrogen and in super-cooled liquids (isopentane and n-heptane) were stored at -80 °C.

To preserve the morphological structure of the lung tissue, pulmonary delivery was used in two variants. First variant was filled lungs over the *bronchus* by pure embedding compound Tissue Tek and second variant was filled lungs over the *bronchus* by mixture of embedding compound Tissue Tek with PBS (Bio Whittaker, Lonza) in rate 1 : 1.

Sampling of porcine lung tissue – smaller part of the samples were tested by same procedures mentioned above and most of the samples were filled over the *bronchus* by mixture of embedding compound Tissue Tek with PBS in rate 1 : 1.

The tissue samples were cut to a thickness of 5–10μm on the cryostat (Leica Microsystems, CM 1900, GmbH, Wetzlar, Germany) at temperature -20℃. The cuts of tissue were placed on slides and fixed in pre-cooled acetone for 5 minutes and stained with Mayer hematoxylin. The total of 40 histological slides were analysed, each slide had 4 sections and evaluated in magnification 100 x. Following parameters were evaluated: nucleus visibility in cells, alveolar consistency, sharpness of the structure, the presence of artifacts.

The histological slides were evaluated by using the light microscope (Olympus BH-2, Japan) and images were taken by camera (Canon EOS 1100D, Japan) using software (Quick Photo Micro 3.0, PROMICRA, Czech Republic).

RESULTS AND DISCUSSION

Tissue fixation

Pulmonary tissue, which was immersed in 10% sucrose solution, retained the morphological structure only at the edges of the preparation or in the first row of cells, in the rest of the preparation the alveoli were collapsed and the structure was blunted.

Samples of tissue which were embedded only in the embedding compound Tissue Tek showed collapsed alveoli, poor quality of structure, poorly visible nuclei.

Samples of lung tissue filled with pure embedding compound Tissue Tek showed partial preservation of the morphological structure of the lungs, well-visible nuclei. However, the density of this reagent was not suitable for filling rat lungs which are smaller and less accessible for filling than pigs. According to (Prince and Porter 1975) is more appropriate to dilute the embedding compound Tissue Tek by PBS.

Samples of tissues filled with mixture of embedding medium Tissue Tek with PBS in ratio 1 : 1 exhibited preserved alveolar structures, well-visible nuclei, sharp structure, and from the above-mentioned variants appeared to be most suitable method (Figure 1).

Figure 1 A pulmonary tissue sample of the pig was filled over the lung bronchus by mixture of Tissue Tek with PBS 1 : 1 and frozen in n-heptane placed on dry ice. "A" preserved alveolar structure. "B" pulmonary tissue without filling with mixture of Tissue Tek with PBS, collapsed alveoli, shot structure. It does not correspond to the structure of the lungs of the physiology state. In magnification 100 ×.

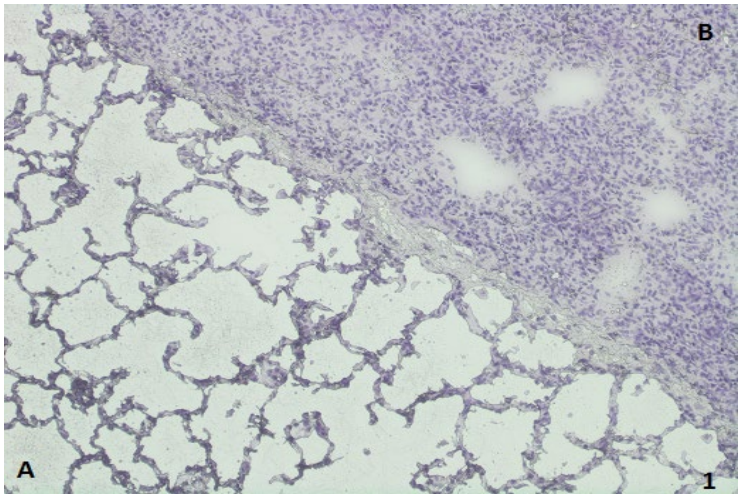

Tissue fixation

Freezing of the tissue in the freezer at -20 °C produced numerous artifacts in the form of black spots. It was suggested previously by (Stephen 2003) that slow freezing of tissue samples in the cryostat causes numerous artifacts.

Freezing of tissue by isopentane placed on dry ice proved to be a good form of freezing of the sample. The preparations were without artefacts, the tissue structure was sharp, compact (Figure 4).

Freezing of tissue in n-heptane placed on dry ice proved to be the most suitable form of freezing of samples, uniform freezing, adequate freezing rate, almost no cracks in freezing samples. The preparations were without artefacts, the structure of the tissue was sharp, compact and the alveoli were preserved. According to (Stephen and Peters 2003) faster freezing of the sample in liquid nitrogen or super-cooled liquids limits the creation of frosty artifacts but limits the precision of isolation.

Figure 2 Porcine lung tissue frozen by n-heptane placed on dry ice, tissue filled with mixture of Tissue Tek with PBS (1 : 1). In magnification 100 x. Porcine lung tissue frozen by n-heptane placed on dry ice, tissue filled with mixture of Tissue Tek with PBS (1 : 1). In magnification 100 ×.

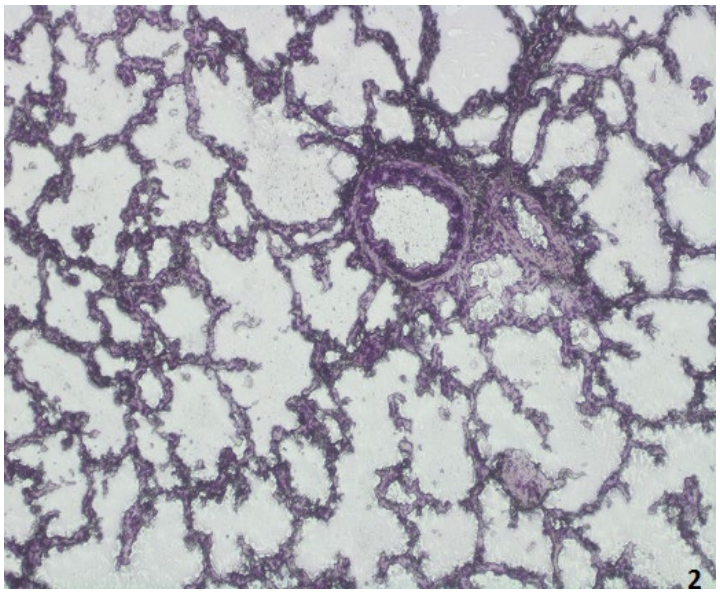

The freezing of tissues in liquid nitrogen was an aggressive form of freezing for pulmonary tissue, the samples often cracked during the freezing, the evaluated preparations had the widespread alveolar structure due to the boiling of the liquid nitrogen (Figure 3).

Figure 3 Porcine lung tissue frozen by liquid nitrogen, widespread alveolar structure due to nitrogen boiling. In magnification 100 ×.

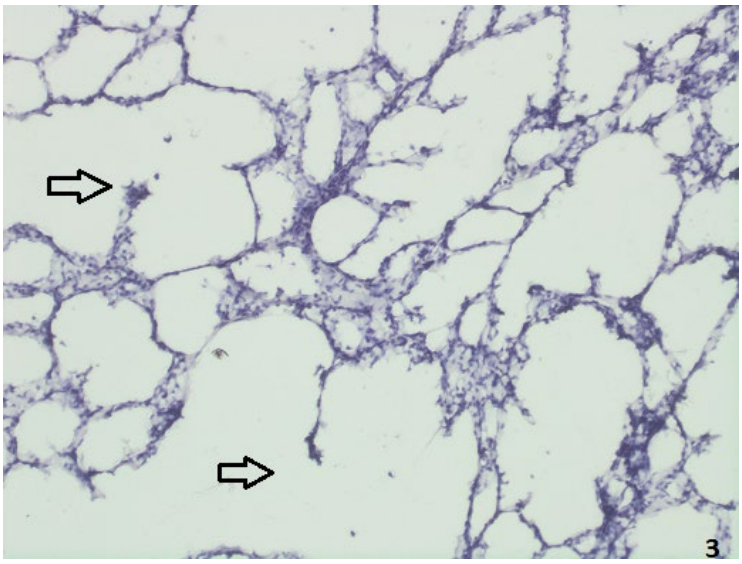

Figure 4 A sample of rat lung tissue frozen by isopentane, filled with mixture of Tissue Tek with PBS 1 : 1. In magnification 100 ×.

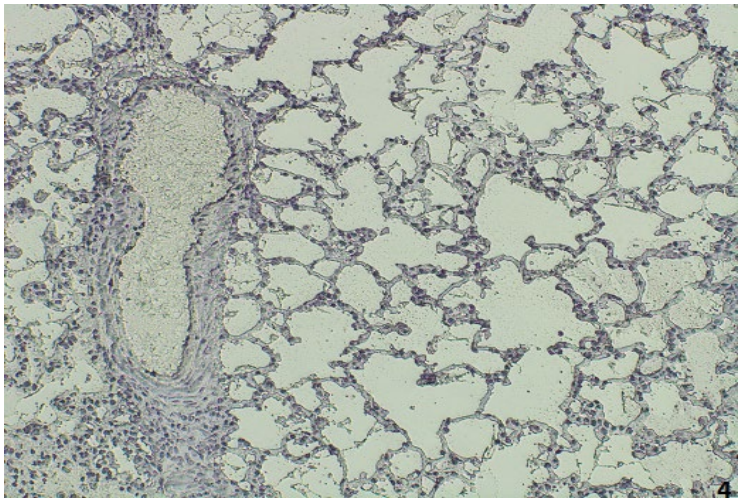

In compared to the authors (Prince and Porter 1975), whose used a 1 : 2 mixture of O.C.T. embedding compound (Tissue Tek) and phosphate-buffered saline (PBS) injected intratracheally into fresh lung tissue. The data obtained from our histological sections showed suitable method for preserving the morphological structure of the lungs is to fill lungs over the lung *bronchus* by mixture 1 : 1of embedding compound Tissue Tek with PBS and subsequent freeze in n-heptane placed on dry ice.

CONCLUSION

Optimizing the freezing of the lung tissue will lead to a better detection of the pathological process in the tissue during the study of respiratory diseases of the pigs. The preservation of the morphological structure of the lungs was important for the subsequent accurate detection of the inflammatory mediators in the lungs of pigs infected by pneumonia. The output of this project was testing of the available methods and finding the most appropriate method for preserving the proper condition of the pulmonary tissue and putting this method into practice in the study of respiratory diseases.

ACKNOWLEDGEMENTS
This research project AF-IGA-IP-2018/021 was financially supported by the Internal Grant Agency of Mendel University in Brno.

REFERENCES

Mescher, A.L. 2018. Junqueirovy základy histologie. 1st ed., Galén.

Prince, A.G, Porter, D.D. 1975. Cryostat Microtomy of Lung Tissue in an Expanded State. Stain Technology, 50(1): 43–45.

Sienko, A. et al. 2005. Frozen sections of lung specimens. Archives of Pathology & Laboratory Medicine, 129(12): 1602–1609.

Stephen R.P. 2003. The Art of Frozen Tissue Sectioning. Part I: A system for precision face down cryoembedding of tissue using feezing temeprature-embedding wells. The Journal of Histotechnology, 26(1): 11–19.

Stephen, R., Peters, M.D. 2003. Apparatus and Method for Precision Cryoembedding of Tissue Samples. Pathology Innovations, (201): 847–7600.

Zimmerman, J.J. et al. 2002. Diseases of Swine. 10th ed., Ames, Iowa: Wiley.

Transforming growth factor beta 1 production during inflammatory response of mammary gland induced by peptidoglycan

Kristina Kharkevich, Lucie Kratochvilova, Petr Slama
Department of Animal Morphology, Physiology and Genetics
Mendel University in Brno
Zemedelska 1, 613 00 Brno
CZECH REPUBLIC

xkharkev@mendelu.cz

Abstract: Intramammary infection promotes increase in production of two isoforms of transforming growth factor beta (TGF-β) which are TGF-β1 and TGF-β2. The aim of this study was to investigate the production of TGF-β1 during an inflammatory response of bovine mammary gland induced by peptidoglycan of *S. aureus*. The experiment was performed on 32 mammary glands of 8 healthy virgin crossbred heifers. Lavages of the mammary glands were analysed using sandwich ELISA technique. The results showed that stimulation with peptidoglycan led to a significant increase in the concentration of TGF-β1. We suggest that peptidoglycan of *S. aureus* stimulated immune cells to production of TGF-β1 at least in three days following stimulation of mammary glands. TGF-β1 is one of the most important cytokines in restoring the mammary gland within mastitis and stimulation with peptidoglycan helped us see the heifer's mammary gland immune response.

Key Words: mammary gland, mastitis, TGF-β, intramammary infection, peptidoglycan

INTRODUCTION

The causes of mastitis can be many, but the main ones are a because of decrease immunity and low resistance of the organism to pathogenic flora due bad conditions of housing and milking routine and the presence of pathogenic flora. One of the cattle udder reactions during inflammation is production of TGF-β1. The transforming growth factor beta (TGF-β) belongs to a family of dimeric polypeptides that are ubiquitously present in tissues and synthesized by many types of cells. There are three isoforms of the (TGF-β1, TGF-β2 and β-3) (Damstrup et al. 1993). Most of the immune cells secrete TGF-β1. Factors of TGF-β have three main biological functions: they inhibit the proliferation of most cells, but can stimulate the growth of some mesenchymal cells; they have an immunosuppressive effect and increase the formation of the extracellular matrix (Jean et al. 1993). TGF-β factors are involved in the inflammatory response process from the initial stages and at the healing stage through chemotactic attraction of cells involved in the inflammatory response and aktivity of fibroblasts. TGF-β1 plays an important role in the control of the immune system and demonstrates different types of activity in different types of cells (Duque et al. 2014).

TGF-β regulates cell growth and differentiation as well as inflammatory responses (Letterio and Roberts 1998, Bonewald 1999). TGF-β also regulates ductal growth and alveolar development in the bovine mammary gland (Daniel et al. 2001). This cytokine suppresses inflammatory responses (Letterio and Roberts 1998, Flanders and Wakefield 2009). TGF-β is associated with the presence of abundant collagen I in intralobular connective tissue in mammary glands chronically infected with *Staphylococcus aureus* mastitis during active involution. This protein's greater expression in chronic S. aureus mastitis appears to be an essential response for limiting the extent of inflammation and injury to the host (Andreotti et al. 2014). *Escherichia coli* intramammary infection induces the expression of TGF-β1 and TGF-β2 (Chockalingam et al. 2005). S. aureus is also able to induce increased production of TGF-β1 and TGF-β2 during intramammary infection (Bannerman et al. 2006). Lipopolysaccharide of *E. coli*, too, is able to induce TGF-β1 production in bovine mammary gland leukocytes in *in vitro* study (Slama et al. 2012) and in course of *in vivo* experimentally induced bovine mastitis (Slama et al. 2017).

The aim of this study was to analyse production of TGF-β1 during an inflammatory response of bovine mammary gland induced by peptidoglycan of *S. aureus*. We chose this isoform because we suggested that it is most important isoform of TGF-β in pathogenesis of mastitis.

MATERIALS AND METHODS

Animals

The experiments were carried out on 32 mammary glands of 8 virgin, clinically healthy, Holstein × Bohemian Red Pied crossbred heifers aged 16 to 18 months. The heifers were housed in an experimental tie-stall barn of Veterinary Research Institute in Brno and fed a standard ration consisting of hay and concentrates with mineral supplements. The experimental tie-stall used in this study is certified and animal care conformed to good care practice protocols. All heifers were free of intramammary infections, as demonstrated through a bacteriological examination of mammary lavages.

Experimental design

Before experimental infection, the mammary glands were treated with phosphate buffered saline (PBS) prepared with apyrogenic water. All 4 mammary gland sinuses of each heifer were rinsed stepwise with PBS to obtain a cell suspension using the following procedure. The first cell sample was obtained by lavage of the left forequarter 24 hours after administration of PBS. The remaining quarters were rinsed stepwise at two 24-h intervals and one 96-h interval in the following order: left-rear (48 h) → right-front (72 h) → right-rear (at 168 h). These PBS-treated mammary glands were set as a control for the infections, as undertaken in previous studies (for example see Slama et al. 2009). Heifers were then experimentally infected with peptidoglycan of *S. aureus* (Sigma). Subsequent lavages of the mammary gland lumens were obtained in the same manner as described. The concentration of TGF-β1 obtained from the lavages was assessed through sandwich ELISA. The following kit was used: Human/Mouse TGF beta 1 ELISA Ready-SET-Go! (eBioscience). There was used ELISA reader Sunrise (Tecan, Austria).

Experimental infection

Modified urethral catheters (AC5306CH06, Porges S.A., France) were inserted into the teat canal following thorough disinfection of the teat orifice with 70% ethanol. Through the catheter, each mammary quarter was injected with 20 ml of PBS with 50 μg and 2 ml of lavage solution was immediately collected back through the catheter directly to the syringe and subsequently used for bacteriological examination. Bacteriological examination of all lavages was performed through culture on blood agar plates (5% washed ram erythrocytes) with aerobic incubation at 37 °C for 24 hours. All lavages were pathogen-free.

Statistical analysis

Arithmetic means and standard deviations were used to describe the concentration of TGF-β1. Statistically significant differences in the concentrations of that parameter were determined using the paired t-test. The data were processed using STATISTICA 8.0 software (StatSoft CR Ltd, Prague, Czech Republic).

RESULTS AND DISCUSSION

Stimulation of mammary gland with peptidoglycan resulted in a significant increase in the concentration of TGF-β1 in comparison to the control. The concentration of TGF-β1 peaked at 48 hours following stimulation. In 72 hours, there were found decreasing of the concentration of this cytokine. No TGF-β1 was analysed in 168 hours following stimulation of mammary gland (Figure 1). Similar results were described in the article Kabourkova and Slama (2018) which was focused on the effect of muramyl dipeptide on the production of different cytokines including TGF-β1. Muramyl dipeptide is the minimal structural unit of peptidoglycan of Gram-positive bacteria. These findings could be the proof that just part of peptidoglycan of bacterial cell wall is able to induce inflammatory immune response of mammary gland.

The results suggest that peptidoglycan is able to induce immune response of bovine mammary gland with demonstrable production of TGF-β1, which is important cytokine in mammary gland

recovery in framework of mastitis (Figure 1). The similar results were found out in previous experiments with lipopolysaccharide of E. *coli* (Slama et al. 2012) and in course of in *vivo* experimentally induced bovine mastitis (Slama et al. 2017). The results of experiment are also in according to findigs in E. *coli* intramammary infection (Chockalingam et al. 2005) and S. *aureus* stimulation of intramammary infection (Bannerman et al. 2006). Up-regulation of TGF-β1 in bovine mastitic mammary glands might play an important role in bovine mammary fibrosis (Chen et al. 2017). TGF-β1 is involved in very complicated cytokine network (Jensen et al. 2013) and each new information about that cytokine is like a one small part of mosaics.

Figure 1 Change in the concentration of TGF-β1 in the mammary gland by stimulation with peptidoglycan.

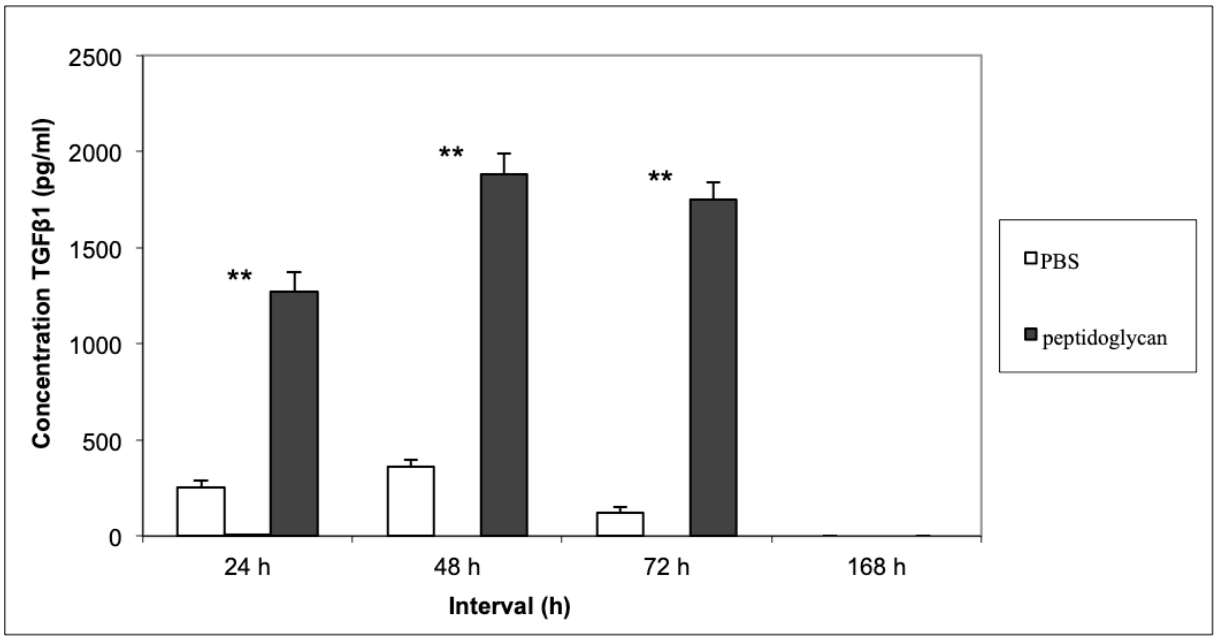

*Legend: h – hours, PBS – phosphate-buffered saline, ** – immune response by peptidoglycan stimulation.*

CONCLUSIONS

In conclusion, we suggest that peptidoglycan of *S. aureus* stimulated immune cells to production of TGF-β1 at least in three days following stimulation of mammary glands. That findings showed that this cytokine is important in the first initial phase of mastitis and also in the resolution phase of mastitis which is eminent in recovery of mammary gland tissue.

ACKNOWLEDGEMENTS

This study was supported by the projects AF-IGA-2018-tym002.

REFERENCES

Andreotti, C.A. et al. 2014. *Staphylococcus aureus* chronic intramammary infection modifies protein espression of transforming growth factor beta (TGF-β) subfamily components during active involution. Research in Veterinary Science, 96: 5–14.

Bannerman, D.D. et al. 2006. *Staphylococcus aureus* intramammary infection elicits increased production of transforming growth factor-α, β1, and β2. Veterinary Immunology and Immunopathology, 112: 309–315.

Bonewald, L.F. 1999. Regulation and regulatory activities of transforming growth factor-β. Critical Review in Eukaryotic Gene Expression, 9: 33–44.

Chen, Q. et al. 2017. TGF-β1 Induces EMT in Bovine Mammary Epithelial Cells Through the TGFβ1/Smad Signaling Pathway. Cellular Physiology and Biochemistry, 43: 82–93.

Chockalingam, A. et al. 2005. Increased milk levels of transforming growth factor-alpha, beta1, and beta2 during *Escherichia coli*-induced mastitis. Journal of Dairy Science, 88: 1986–1993.

Damstrup, L. et al. 1993. Expression of transforming growth factor β (TGFβ) receptors and expression of TGFβ1, TGFβ2 and TGFβ3 in human small cell lung cancer cell lines. British Journal of Cancer, 67(5): 1015–1021.

Daniel, C.W. et al. 2001. The transforming growth factors-β in development and functional differentiation of the mouse mammary gland. Advances in Experimental Medicine and Biology, 501: 61–70.

Duque, A. et al. 2014. Macrophage Cytokines: Involvement in Immunity and Infectious Diseases. Frontiers in Immunology, 5: 491.

Flanders, K.C., Wakefield, L.M. 2009. Transforming growth factor-βs and mammary gland involution; functional roles and implications for cancer progression. Journal of Mammary Gland Biology and Neoplasia, 14: 131–144.

Jean, E.M. et al. 1993. 14 - Cytokines in AIDS-Associated Nervous and Immune System Dysfunction. Methods in Neurosciences, 17: 243–266.

Jensen, K. et al. 2013. *Escherichia coli*- and *Staphylococcus aureus*-induced mastitis differentially modulate transcriptional responses in neighbouring uninfected bovine mammary gland quarters. BMC Genomics, 14: 36.

Kabourkova, E., Slama, P. 2018. Effect of lipopolysaccharide and muramyl dipeptide on the inflammatory cytokine production throughout inflammatory response of bovine mammary gland. Journal of Animal and Veterinary Advances, 17: 100–103

Letterio, J.J. et al. 1998. Regulation of immune responses by TGF-β. Annual Review of Immunology, 16: 137–161.

Slama, P. et al. 2009. Effect of *Staphylococcus aureus* and *Streptococcus uberis* on apoptosis of bovine mammary gland lymphocytes. Research in Veterinary Science, 87: 233–238.

Slama, P. et al. 2012. Production of bovine transforming growth factor beta 1 following stimulation with lipopolysaccharide. FEBS Journal, 279 (S1) 459.

Slama, P. et al. 2017. TGF-beta 1 production during experimentally induced mastitis caused by lipopolysaccharide. Scandinavian Journal of Immunology, 86: 286.

Effect of preparations based on algae extract on the formation of selected biochemical parameters of blood and immune response of laying hens

Damian Konkol[1], Mariusz Korczynski[1], Tomasz Brzezewski[1], Marita Swiniarska[1], Radoslaw Wilk[2], Andrzej Gawel[3], Katarzyna Chojnacka[2]
[1]Department of Environment Hygiene and Animal Welfare
Wrocław University of Environmental and Life Sciences
Chełmońskiego 38C, 51-630 Wrocław
[2]Department of Advanced Material Technologies
Wrocław University of Science and Technology
Norwida 4/6, 50-373 Wrocław
[3]Department of Epizootiology and Clinic of Birds and Exotic Animals
Wrocław University of Environmental and Life Sciences
pl. Grunwaldzki 45, 50-366 Wrocław
POLAND

damian.konkol@upwr.edu.pl

Abstract: The large-scale poultry production has led to the search for new feed materials that can be used in this sector. Such a material may be algae, which contains many biologically active compounds from its biomass. The aim of the study was to determine the effect of preparations based on extract of *Spirulina platensis* algae on selected biochemical parameters of the blood of the studied birds. The tested parameters were total cholesterol, high density lipoprotein, low density lipoprotein, triglycerides, calcium, phosphorus, aspartate aminotransferase, alanine aminotransferase and alkaline phosphatase. In addition, the effect of the extract used on the immune system of birds and the level of specific antibodies after vaccination with a combination vaccine was also checked. The obtained results showed the effect of the preparations on the activity of liver enzymes. Potential immunomodulatory properties of one of used preparations were also demonstrated.

Key Words: laying hens, algae, supercritical extraction, *Spirulina platensis*

INTRODUCTION

Poultry farming is a very important branch of the nutritional administration. Due to the high taste values, relatively low and stable prices, health-promoting properties and the lack of religious restrictions, poultry meat and eggs are products eagerly consumed by consumers. However, it should be remembered that the high genetic potential of poultry has led to intensive breeding work. Although it allowed for high production parameters of birds, it also had a negative impact on their health. This is the result of weakened bird resistance and the fact that bird's need for individual nutrients is not always covered in large-scale farming (Jankowski et al. 2012).

The solution of the problem may be feed additives, which are important component of complete nourish. Such additives may be algae and their extracts. Algae are single-cell organisms that belong to spore plants that can form colonies and multicellular thalli (Czerpak and Czeczuga 1978). They occur mainly in the aquatic environment and are photoautotrophs. These include blue-green algae, flagellates, green algae, brown algae, red algae, and borax (Czerpak and Jabłońska-Trypuć 2008). It are used both as food for humans and farm animals. The most commonly used for this purpose are brown algae, red algae and green algae, which contain in their biomass many biologically active compounds such as proteins, amino acids, lipids, carbohydrates, vitamins, minerals and unsaturated fatty acids (Hallmann 2007). In addition, algae contain in their biomass compounds such as laminarin and fucoidan with antibacterial properties. Algae can also be used to obtain polyphenols that counteract the formation of free radicals (Holdt and Kraan 2011). The use of algae in poultry nutrition may, therefore, increase the resistance of birds and protect them against metabolic diseases and fatty of internal organs.

The aim of the study was to determine the effect of preparations made on the basis of algae extract on the level of selected biochemical parameters of blood and the immune response of laying hens.

MATERIALS AND METHODS

The research was carried out at the Agricultural Experimental Station of RZD Swojec. The experimental material was blood collected from 72 hens of ISA Brown line. The birds were kept in a cage system of 3 in each cage. The cages in which the hens were kept were improved so that, in accordance with Directive 1999/74/EC, they provided birds with full welfare. The hens were maintained under standard, controlled microclimatic conditions that met the minimum requirements for this animal species. The birds were put into cages at 24 weeks of age. The animals for the experiment were chosen randomly. During the experiment, a standard light program was used.

Nutrition

Throughout the experiment, the hens were fed with a commercial complete feed mixture from Tasomix. Table 1 shows the composition of feed mixture used in the experiment. The birds had permanent access to water and received feed in the amount of 130g/hen/day.

Table 1 Composition of the feed mixture used in experiment

Feed component	Amount kg	Product code
Maize	450.99	1101
Sunflower meal	150	4046
Wheat	136	4009
Thick chalk 1.2 – 4.0 mm	66	1407
Soybean meal 45+ROV	40	4060
Dried corn decoction BIOWIN	40	4035
Guar 60	40	4139
Chalk	31.1	1406
Rapeseed oil	19	4087
Full dried blood	9	4073
Calcium-sodium posphate	4.4	1439
Lysine 50% LIQUID	2.5	2870
Bacterial Control LF2 NC	2.5	744

Layout of the experiment

The birds were divided into 4 groups of 18 hens in each (6 replicates (cages), 3 hens in a cage). Each group received a different preparation enriched with *Spirulina platensis* algae extract.

Table 2 Division into groups due to the preparations used in experiment

Group I	the control group, the hens were additionally vaccinated before the experiment with a combined IBV (infectious bronchitis virus) and NDV (Newcastle disease virus) vaccine via a *per os* route
Group II	preparation D, enriched with *Spirulina platensis* algae extract; the preparation was administered throughout the duration of the experiment in a 5 days application – 1 ml/1l water, 7 days break
Group III	preparation H, enriched with *Spirulina platensis* algae extract; the preparation was administered for the entire duration of the experiment in a 5 days application – 2 ml/1l water, 7 days break
Group IV	preparation M, enriched with *Spirulina platensis* algae extract; the preparation was administered for 6 weeks in the system of 5 days of use – 2 ml/1l water, 7 days of break, additionally hens before administration of preparation M were vaccinated with a combination vaccine IBV and NDV by the route *per os*

Table 3 presents the characteristics of the used preparations (composition in 1 kg of product).

Table 3 Characteristics of the preparations used in experiment

Materials	Preparation M	Preparation D	Preparation H
Feed materials	vegetable glycerine, sodium bicarbonate	sorbitol	magnesium sulphate, sodium chloride, monopropylene glycol, glycerine
Dietary supplements	vitamin A (1350000 IU), vitamin D_3 (200000 IU), vitamin E (50000 mg), vitamin B_1 (500 mg), vitamin B_2 (1500 mg), vitamin B_6 (700 mg), vitamin B_{12} (4000 mcg), vitamin C (25000 mg), pantothenic acid (300 mg), niacin (1000 mg), folic acid (300 mg), biotin (400000 mcg), vitamin K (400 mg), betaine (60000 mg)	vitamin D_3 (250000 UI), calcium chloride (80000 mg), magnesium (6000 mg), iron (360 mg), manganese (2000 mg), copper (150 mg), zinc (500 mg)	choline chloride (20000 mg), betaine (25220 mg), L-carnitine (10175 mg)
Sensory additives	oregano oil, dry *Echinacea purpurea* extract	-	-
Technological additives	stearyl citrate (110 g), ethoxyquina (2000 mg), potassium sorbate (5000 mg)	-	potassium sorbate (3000 mg), lemon acid (1000 mg), glycerol-polyethylene glycol (500000 mg)
Zootechnical additives	-	-	tumeric oleoresin (100000 mg), artichoke extract (12000 mg), milk thistle extract (11000 mg)

Each of the preparations contained in its composition an algae extract. The extract was produced at the Supercritical Extraction Department of the New Chemical Syntheses Institute in Puławy. The lyophilized biomass of *Spirulina platensis* algae submitted to the process of supercritical extraction using carbon dioxide as solvent, at 40 °C, under pressure 80 MPa. In the liophylisate the amount of water did not exceed 8% (Polish patent pending P. 412010).

Analysis of blood parameters

Blood for test was collected on the 30th and 120th day of the experiment in the amount of approx. 5 ml/hen. The material was obtained from the wing vein (*vena basilica*).

All necessary analysis were performed at the Biochemical Laboratory of the Department of Environment Hygiene and Animal Welfare of the Wrocław University of Environmental and Life Sciences.

In the blood serum of birds from groups I, II and III, the following parameters were determined: alanine aminotransferase (ALT) and aspartate aminotransferase (AST) – kinetic method, at 37 °C, in accordance with the recommendations of the IFCC (International Federation of Clinical Chemistry), alkaline phosphatase (ALP) – a photometric kinetic test. The content of these enzymes has been measured because ALT is an enzyme that occurs mainly in the liver, kidneys and muscles. AST is an enzyme found in all tissues of the body, especially in the cardiac muscle, skeletal muscle, liver and brain. The level of these enzymes is useful in determining the pathological states of the above-mentioned organs. The activity of both enzymes depends on the age of the hens. ALP is mainly derived from the bone, intestinal and hepatic fractions. Total cholesterol (TC) – enzymatic-photometric test, high density lipoprotein (HDL) and low density lipoprotein (LDL) with a calorimetric test – direct method and triglycerides (TG) – enzymatic tests. These parameters were measured because total cholesterol contained in the blood serum of laying hens comes from the liver and kidneys, thanks to which it is a parameter showing the state of these organs. The physiological level of cholesterol concentration is associated with the age of birds and the laying phase, a similar relationship is observed in the triglyceride concentration. In order to determine the above-mentioned parameters, ready-made reagent kits from HORIBA ABX were used.

In the blood serum, mineral compounds were also determined: phosphorus (P) – by UV method with the use of phosphomolybdate and calcium (Ca) – by photometric test using ortho-cresolphtalein complexon, using reagents from HORIBA ABX. The content of these minerals in the blood serum was measured because mineral changes occurring in laying hens organisms are one of the most important elements associated with the production of eggs. In hens used intensively, disorders in the calcium-

phosphate economy of then occur. All analysis were performed with Pentra 400 biochemistry analyzer from HORIBA ABX.

In addition, blood was collected from I group and IV group before, 5 days, and 5 weeks after vaccination. Serum levels of IBV and NDV specific antibodies were then determined by ELISA using IDEXX Laboratories, Inc. reagents.

Statistical analysis of results

The obtained results were subjected to statistical analysis using the Statistica software. The normal distribution of the obtained data was checked using the Shapiro-Wilk test. The data was then subjected to a one-way analysis of variance. Using the Duncan test, the significance of differences between groups was assessed. Differences were statistically significant when $P<0.05$.

RESULTS AND DISCUSSION

Table 4 presents results referring to the biochemical parameters of the blood of the studied birds.

Table 4 Biochemical parameters of laying hens on the 30th and 120th day of the experiment

Group	Day	TC mmol/l	ALT U/l	AST U/l	ALP U/l	HDL mmol/l	LDL mmol/l	TG mmol/l	P mmol/l	Ca mmol/l
I	30	3.70	10.1	203.1	384.92	1.09	1.08	13.07	1.94	7.31
	120	3.43	9.7	222.9	542.8[a]	0.97	0.85	11.32	1.92	7.38
II	30	3.51	9.23	196.8	361.5	1.03	0.94	11.74	1.87	7.33
	120	3.40	13.1	218.9	382.9	0.97	0.86	11.27	1.85	7.32
III	30	3.83	10.4	202.8	348.7	1.09	1.07	13.11	2.10	7.87
	120	3.40	10.5	212.5	363.6[b]	1.00	0.80	11.19	1.83	7.49

Legend: a, b – significance of differences between groups at the confidence level P<0.05. TC – total cholesterol, ALT – alanine aminotransferase, AST – aspartate aminotranserase, ALP – alkaline phosphatase, HDL – high density lipoprotein, LDL – low density lipoprotein, TG – triglycerides, P – phosphorus, Ca – calcium.

Analysis of the results showed differences only in the level of alkaline phosphatase (ALP). After 120 days of the experiment the control group showed significantly higher ($P<0.05$) level of this enzyme in comparison to group III received the preparation H. The levels of other enzymes (AST, ALT) also differed, but these were not statistically significant. In addition, the blood of hens from the group received preparation H was characterized by the smallest difference in the mean values of all the studied enzymes between 30 and 120 days of the experiment, which may mean that livers of these birds were the least heavily burdened. In the case of other analyzed parameters, differences can also be noticed, however they are not statistically significant.

The conducted research did not show any significant changes in the lipid profile of birds used in the experiment. The level of total cholesterol, its HDL and LDL fractions, and triglycerides remained were at a similar level throughout the duration of the experiment. These results do not coincide with the results obtained by Kato et al. (1984), who observed a decrease in total cholesterol and its LDL fraction and an increase in HDL fraction in blood serum of hyperlipidemic rats receiving the addition of *Spirulina platensis* algae. Different results were also obtained by Ginzberg et al. (2000), who showed a lower level of TC in the blood of White Leghorn chickens received in their diet the addition of *Porphyridium* sp.

The studies carried out did not show any influence of the applied additives on the concentration of ALT and AST in birds' blood serum. In the course of the conducted research, it was observed that the hens received the H preparation were characterized by a much lower level of the ALP in comparison with the hens from the control group. Similar results were obtained by Abdel-Daim (2014), who showed that Egyptian goats baladi, which were administered erythromycin, received simultaneously the addition of *Spirulina platensis* algae at 200 mg/kg body weight, were characterized by a lower level of ALP. The level of AST and ALT was also reduced in the tested goats, which was not confirmed by our own research. Results similar to the results obtained in the course of own research were received by Ponce-Canchihuamán et al. (2010), who did not show the effect od the addition of *Spirulina maxima* algae in the rat diet to the ALT level.

Numerous reports describe the rich mineral composition of algae, make it possible to place these plants on and equal footing with products that are essential for the health of poultry and the quality of products obtained from it. The studies carried out did not show any influence of the applied additives

on the content of calcium and phosphorus in the blood of the studied birds. Different results were obtained by Michalak et al. (2011), which showed that hens fed with the addition of macroalgae are characterized by a higher content of calcium in the blood.

Table 5 presents the results relating to the immune response of the studied birds.

Table 5 The level of IBD and NDV specific antibodies determined in the blood of birds used in the experiment

Group	I			IV		
	Start	After 5 days	After 5 weeks	Start	After 5 days	After 5 weeks
IBV mIU/ml	2336	1157	758	2708	875	798
NDV mIU/ml	1669	704[a]	665[a]	1524	1636[b]	1306[b]

Legend: a, b – significance of differences between groups at the confidence level P<0.05.

Analysis of the results, confirmed the significance of the differences in the level of specific NDV antibodies. In the case of the control group, this level decreased by more than a half, while in group IV, where the M preparation was used, there was an increase in the level of antibodies. This is probably due to the high content of antioxidants in the algae extract, which acted here as an adjuvant. In the case of IBV, the level of antibodies decreased in both group I and group IV. This may be due to the fact that the birds did not drink the recommended dose of vaccine in a timely manner. The obtained results, however, allow to indicate the potential immunomodulating properties of preparations made on the basis of algae extract.

Chu et al. (2013) reached similar conclusions by conducting a study to determine whether *S. platensis* supplementation in mice could increase the immune response to tetanus toxoid. This study showed that supplementing a diet with *S. platensis* increases the primary immune response by producing more antibodies. Rahman et al. (2006) conducted research on the immunostimulatory properties of *S. platensis* on *Litopenaeus vannamei* shrimp against white spot syndrome virus (WSSV). In this group, where the shrimp diet was enriched with *S. platensis*, the clinical symptoms of the disease were delayed by 12 hours. In contrast, in the group where antiviral cidofovir given by intramuscular injection was used, this delay was 24 hours.

CONCLUSION

The performed tests showed a significantly higher level of specific antibodies after vaccination against Newcastle disease virus (NDV) which may indicate the potential immunomodulatory properties of the M preparation. The preparation H used in group III significantly reduced the level of ALP in the blood serum of the studied birds. This may indicate an improvement in bird metabolism.

ACKNOWLEDGEMENTS

This project is finance in the framework of grant entitled: Innovative technology of seaweed extracts – components of fertilizers, feed and cosmetics (PBS/1/A1/2/2012) attributed by The National Centre for Research and Development in Poland.

REFERENCES

Abdel-Daim, M.M. 2014. Pharmacodynamic interaction of *Spirulina platensis* with erythromycin in Egyptian Baladi bucks (*Capra hircus*). Small Ruminant Research, 120(2–3): 234–241.

Chu, W.L. et al. 2013. Effect of *Spirulina (Arthrospira)* supplementation on the immune response to tetanus toxoid vaccination in a mouse model. Journal of Dietary Supplements, 10(3): 229–240.

Czerpak, R., Czeczuga, B. 1978. Occurrence, biosynthesis and biological role of carotenoids in algae. Wiadomości Botaniczne, 22(1): 47–59.

Czerpak, R., Jabłońska-Trypuć, A. 2008. Plant cosmetic raw materials. 1st ed., Wrocław: Wydawnictwo Med Pharm.

Ginzberg, A. et al. 2000. Chickens fed with biomass of the red microalga *Porphyridium* sp. have reduced blood cholesterol level and modified fatty acid composition in egg yolk. Journal of Applied Phycology, 12: 325–330.

Hallmann, A. 2007. Algal transgenics and biotechnology. Transgenic Plant Journal, 1(1): 81–98.

Holdt, S.L., Kraan, S. 2011. Bioactive compounds in seaweed: functional food applications and legislation. Journal of Applied Phycology, 23(3): 543-597.

Jankowski, J. et al. 2012. Breeding and use of poultry. 1st ed., Warszawa: Państwowe Wydawnictwo Rolnicze i Leśne.

Kato, T. et al. 1984. Effects of *Spirulina* (*Spirulina platensis*) on dietary hypercholesterolemia in rats. Journal of Japan Society of Nutrition and Food Sciences, 37: 323–332.

Michalak, I. et al. 2011. Effect of macroalgae enriched with microelements on egg quality parameters and mineral content od eggs, eggshell, blond, feathers and droppings. Journal of Animal Physiology and Animal Nutrition, 95(3): 374–387.

Ponce-Canchihuamán, J.C. et al. 2010. Protective effects of *Spirulina maxima* on hyperlipidemia and oxidative-stress induced by lead acetate in the liver and kidney. Lipids and Health and Disease, 9(1): 35.

Rahman, M.M. et al. 2006. Clinical effect of cidofovir and a diet supplemented with *Spirulina platensis* in white spot syndrome virus (WSSV) infected Pacific pathogen-free *Litopenaeus vannamei* juveniles. Aquaculture, 255(1–4): 600–605.

TNF-α and IL-10 are produced by leukocytes during the experimental inflammatory response of bovine mammary gland induced by peptidoglycan

Lucie Kratochvilova, Kristina Kharkevich, Petr Slama
Department of Animal Morphology, Physiology and Genetics
Mendel University in Brno
Zemedelska 1, 613 00 Brno
CZECH REPUBLIC

lucie.kratochvilova.umfgz@mendelu.cz

Abstract: The aim of this work was to analyse inflammatory cytokines – the tumour necrosis factor alpha (TNF-α) and the interleukin 10 (IL-10) during an inflammatory response of bovine mammary gland induced by peptidoglycan. The study was carried out on clinically healthy heifers. Obtained leukocytes were incubated for 24, 48, 72 and 168 hours with phosphate buffered saline (PBS) or with peptidoglycan under *in vivo* conditions. The concentration of TNF-α by leukocytes of the bovine mammary gland was higher [PBS: 147.82 pg/ml (±22.56), peptidoglycan: 822.43 pg/ml (±80.07)] than the production of IL-10 by bovine mammary gland leukocytes [PBS: 0 pg/ml (±0), peptidoglycan: 35.56 pg/ml (±7.88)]. Level of IL-10 was the highest in 72 hours of incubation in the mammary gland. Level of TNF-α was the highest in 24 hours of incubation in the mammary gland.

Key Words: mammary gland, immune system, cytokines, mastitis

INTRODUCTION

Cytokines are very important proteins affecting many processes in the body including the development, homeostasis, activation, differentiation, regulation, and functions of innate and adaptive immunity. Inflammation of the mammary gland (mastitis) is also affected by many cytokines. Because mastitis is the most costly disease in lactating cows and decreases the quality and quantity of produced milk, it is very important to study the pathophysiological roles of cytokines in mastitis. Their use in the diagnosis, immunotherapy, and prognosis of mastitis will grow with knowledge of the cytokine network in bovine mammary glands (Sordillo et al. 1997, Alluwaimi 2004). TNF-α is a proinflammatory cytokine with both positive and negative effects on the different tissues (Poll and Lowry 1995) and is produced also by cell types including macrophages (Korneev et al. 2017). It has been identified both in normal and infected mammary glands (Alluwaimi and Cullor 2002, Alluwaimi et al. 2003). Various cells have been found to produce this cytokine (Angelini et al. 2005). His production is caused by different pathogens including bacteria and their toxins and bacterial wall products (Bannerman 2009). Increased TNF-α levels have been detected during lactation, involution and in the periparturient period. These increased levels of TNF-α suggest its essential role in regulating the immunological function of cells and factors involved in the physiological changes within the mammary gland (Alluwaimi 2004). Bovine neutrophils play a supportive role in the innate immune response to infection by Gram-negative bacteria through their ability to produce immuno-regulating cytokines as TNF-α (Sohn et al. 2007).

IL-10 plays a crucial role in limiting inflammation and influencing the nature of the adaptive immune response to infection (Sordillo et al. 1997). IL-10 is a cytokine with multiple, pleiotropic, effects in immunoregulation and inflammation (Chan et al. 2015) and has an anti-inflammatory effect on monocytes, macrophages, and neutrophils (Moore et al. 2001). Initial and maximal production of IL-10 is detected earlier in response to Gram-negative bacteria than to Gram-positive bacteria. On the other hand, induction of IL-10 is absent or delayed in cows with the greatest persistent concentrations of bacteria in milk. This may show that earlier induction of IL-10 production is beneficial for cows' ability to limit bacteria growth and eradicate the pathogens (Bannerman 2004a, Bannerman et al. 2004b, Bannerman 2009, Kauf et al. 2007). Lipopolysaccharide of *E. coli* and muramyldipeptide (the smallest structural unit of peptidoglycan of Gram-positive bacteria) are also able to induce IL-10 production in

bovine mammary gland leukocytes (Slama et al. 2011). It was also published that TNF-α can induce lymphocyte apoptosis during experimentally induced mastitis caused by lipopolysaccharide (Slama et al. 2017). In the *in vitro* study was mentioned that production of TNF-α by mammary gland leukocytes was higher than production of IL-10 by blood leukocytes. TNF-α was produced in blood and mammary gland leukocytes in 18 hours incubation. IL-10 was produced in 2 hours from inception of incubation by leukocytes of mammary gland. Level of IL-10 was increased in 18 hours of incubation in blood leukocytes (Kratochvilova et al. 2017). The aim of this work was to analyse inflammatory cytokines (TNF-α and IL-10) during an inflammatory response of bovine mammary gland induced by peptidoglycan, because it is lack of information about this inflammatory inducer.

MATERIAL AND METHODS

The study was carried out on 8 clinically healthy heifers (Holstein x Bohemian Red Pied crossbreed) aged 16 to 18 months. Four samples were obtained by lavage of the mammary gland – 24, 48, 72 and 168 h following stimulation with peptidoglycan (Sigma, USA). Phosphate buffered saline (PBS, Sigma, USA) was used as a control. All mammary glands were rinsed with PBS to obtain cell suspensions. The first sample of cells was obtained by PBS lavage of the right-front quarter in 24 hours, the right-rear quarter in 48 hours, the left-front quarter in 72 hours, and the left-rear quarter in 168 hours following peptidoglycan challenge. The cytokine detections were determined using ELISA. The following kits were used: Bovine TNF-α Screening (Endogen, Rockford, Illinois, USA) and IL-10 (Recombinant bovine IL-10, AbD Serotec, Bio-Rad Laboratories, USA) using Sunrise reader (Tecan, Austria). Data were analysed using statistical software program STATISTICA 8.0 (StatSoft, Czech Republic). The paired t-test was used.

RESULTS AND DISCUSSION

Concentration level of TNF-α

The concentration level of TNF-α is shown in Figure 1. Production of TNF-α by leukocytes of the bovine mammary gland was the highest [PBS: 147.82 pg/ml (±22.56), peptidoglycan: 822.43 pg/ml (±80.07)] in 24 hours. The highest concentration of TNF-α produced by leukocytes of the bovine mammary gland is caused by higher neutrophil proportion. Neutrophils are major producers of TNF- α in bovine mammary gland which Sohn et al. (2007) say in their work. There is no production of TNF-α cytokines during 72 and 168 hours incubation. The concentration TNF-α was detected with 24 and 48 hours incubation. The concentration of TNF-α has dramatically decreased between 48 and 72 hours. The minimum level of TNF-α was observed 72 and 168 hours following stimulation. Bannerman et al. (2004) observed concentration of TNF-α during experimental mastitis induced by *Escherichia coli* bacteria. The highest values were measured 16 hours after infection. Riollet et al. (2000) investigated of TNF-α during experimental infection induced by *Escherichia coli* bacteria. Concentration of TNF-α has dramatically increased between 10 and 39 hours after induction of infection.

Figure 1 Concentration level of TNF-α

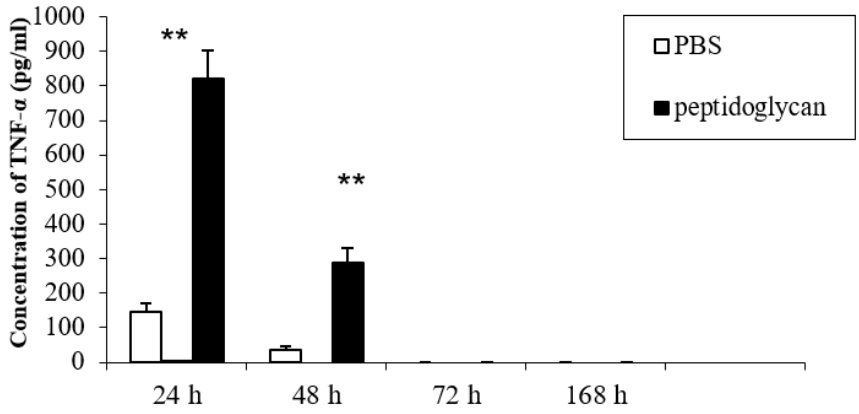

Concentration level of IL-10

The concentration level of IL-10 is shown in Figure 2. Measured levels of IL-10 of leukocytes by the bovine mammary gland was the highest [PBS: 0 pg/ml (±0), peptidoglycan: 35.56 pg/ml (±7.88)] in 72 hours. In one study, IL-10 was produced already 2 hours after beginning of the incubation of leukocytes of mammary gland with lipopolysaccharide and muramyldipeptide (Kratochvilova et al. 2017). The IL-10 concentration increases several hours after mastitis infection which can be caused by different pathogens (Bannerman et al. 2004b).

Figure 2 Concentration level of IL-10

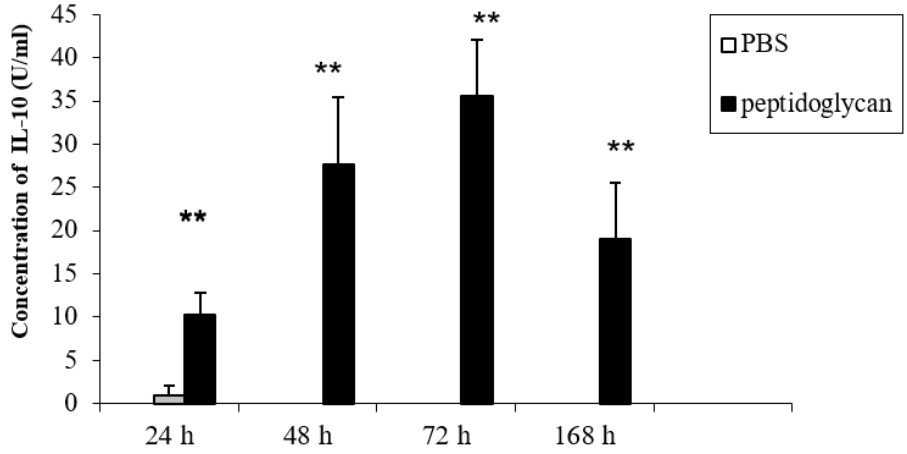

CONCLUSION

Mammary gland leukocytes production of TNF-α was higher than production of IL-10 by mammary gland leukocytes. TNF-α was produced in mammary gland leukocytes in 24 hours incubation and then gradually decreased. IL-10 was produced after 24 hours from the inception of incubation by leukocytes of the mammary gland. Level of IL-10 was the highest in 72 hours of incubation in the mammary gland. Knowledge of all net cytokines is important for effective using of cytokines during treatment of mastitis. For practical use detection of cytokines is important cheap and effective measured techniques, which can be used in the practical application for control of health condition of the mammary gland in dairy cows.

ACKNOWLEDGEMENTS

The authors wish to express their thanks to the project of IGA FA MENDELU No. AF-IGA-IP-2018/032 for the financial support.

REFERENCES

Alluwaimi, A.M. 2004. The cytokines of bovine mammary gland: prospects for diagnosis and therapy. Research in Veterinary Science, 77: 211–222.

Alluwaimi, A.M., Cullor, J.S. 2002. Cytokine gene expression of bovine milk during mid and late stages of laction. Journal of Veterinary Medicine B, 49: 105–110.

Alluwaimi, A.M. et al. 2003. The cytokines marker in the Staphylococcus aureus mastitis of bovine mammary gland. Journal of Veterinary Medicine B, 50: 105–111.

Angelini, D.J. et al. 2005. Tumor necrosis factor alpha-mediated pulmonary endothelial barrier dysfunction. Current Respiratory Medicine Reviews, 1: 233–246.

Assadullah, K. et al. 2003. Interleukin-10 therapy – review of a new approach. Pharmacology Review, 55: 241–269.

Bannerman, D.D. 2009. Pathogen-dependent induction of cytokines and other soluble inflammatory mediators during intramammary infection of dairy cows. Journal of Animal Science, 87: 10–25.

Bannerman, D.D. et al. 2004a. Escherichia coli and Staphylococcus aureus elicit differential innate immune response following intramammary infection. Clinical and Diagnostic Laboratory Immunology, 11: 463–472.

Bannerman, D.D. et. al 2004b. Innate immune response to intramammary infection with Serratia marcescens and Streptococcus uberis. Veterinary Research, 35: 681–700.

Chan, I.H. et al. 2015. The potentiation of IFN-γ and induction of cytotoxic proteins by pegylated IL-10 in human CD8 T cells. Journal of Interferon and Cytokine Research. 35: 948–955.

Kauf, A.C.W. et al. 2007. Innate immune response to intramammary Mycoplasma bovis infection. Journal of Dairy Science, 90: 3336–3348.

Korneev, K.V. et al. 2017. TLR-signalling and proinflammatory cytokines as drivers of tumorigenesis. Cytokine, 89: 127–135.

Kratochvilova, L. et al. 2017. Inflammatory cytokines produced by leukocytes of bovine mammary gland. In Proceedings of International PhD Students Conference MendelNet 2017 [Online]. Brno, Czech Republic, 8–9 November, Brno: Mendel University in Brno, Faculty of AgriSciences, pp. 708–712. Available at: https://mnet.mendelu.cz/mendelnet2017/mnet_2017_full.pdf. [2018-09-01].

Moore, W.K. et al. 2001. Interleukin-10 and the interleukin-10 receptor. Annual Review of Immunology, 19: 683–765.

Poll van Der, T., Lowry, S.F. 1995. Tumor necrosis factor in sepsis: Mediator of multiple organ failure or essential part of host defense. Shock, 3: 1–12.

Riollet, C. et al. 2000. Differential induction of complement fragment C5a and inflammatory cytokines during intramammary infections with Escherichia coli and Staphylococcus aureus. Clinical and Diagnostic Laboratory Immunology, 7: 161–167.

Slama, P. et al. 2011. Production of bovine IL-10 following stimulation with lipopolysaccharide and muramyl dipeptide. FEBS Journal, 278: 304.

Slama, P. et al. 2017. TNF-alpha can induce lymphocyte apoptosis during experimentally induced mastitis caused by lipopolysaccharide. In Proceedings of 44th Annual Meeting of the Scandinavian-Society-for-Immunology (SSI). Stockholm, Scandinavian, 17–20 October. Scandinavian Soc. Immunol, Scandinavian Journal of Immunology, pp. 286.

Sohn, E.J. et al. 2007. Shedding of sCD14 by bovine neutrophils following activation with bacterial lipopolysaccharide results in down-regulation of IL-8. Veterinary Research, 38: 95–108.

Sohn, E.J. et al. 2007. Bacterial lipopolysaccharide stimulates bovine neutrophil production of TNF alpha, IL-1 beta, IL-12 and IFN-gama. Veterinary Research, 38: 809–818.

Sordillo, L.M. et al. 1997. Immunobiology of the mammary gland. Journal of Dairy Science, 80: 1851–1865.

Cytochrome b5 gene and its association with boar taint compounds in pigs

Anna Kubesova[1], Tomas Urban[1], Kamil Stastny[2], Ales Knoll[1]
[1]Department of Animal Morphology, Physiology and Genetics
Mendel University in Brno
Zemedelska 1, 613 00 Brno
[2]Veterinary Research Institute
Hudcova 70, 621 00 Brno
CZECH REPUBLIC

anna.kubesova@mendelu.cz

Abstract: Cytochrome b5 (CYB5A) is a membrane bound protein involved in various biological processes such as being an electron transfer. In pigs, *CYB5A* is positively correlated to the level of androstenone in fat and also single nucleotide polymorphism in this gene is associated with lower androstenone in fat. We have analysed four SNPs in the promoter region of *CBY5A* gene with relative frequencies of alleles (g.165901487delG where G=0.637, g.165901767T>C where T=0.786 and C=0.214, g.165902078C>T where C=0.629 and T=0.370 and AFO16388:c.-G>T where G=0.629 and T=0.370). Same relative frequencies for alleles in g.165902078C>T and AFO16388:c.-G>T suggest their genetic linkage. Association analysis of the four SNPs and indole, skatole or androstenone have not shown any significant associations, but this might be due to the small number of animals analysed.

Key Words: boar taint, SNP, sequencing

INTRODUCTION

Boar taint is an unpleasant odour and flavour characteristic for some uncastrated male pigs. It occurs while cooking the meat and has been described as faecal-like odour. The three main substances causing boar taint are androstenone, skatole and indole. There are differences of boar taint levels in tissue among different pig breeds, also the two compounds of boar taint skatole and androstenone contribute differently to the tainted carcass (Xue et al. 1996). According to the international consumer survey in seven European countries the consumers sensitivity to boar taint differs among countries, however there was a greater degree of dislike with the increase in androstenone and skatole level (Matthews et al. 2000).

Androstenone biosynthesis is controlled by the same mechanism as other testicular steroids and during puberty androstenone levels drastically increase simultaneously with other testicular steroids (Gower 1972, Bonneau 1982). Skatole levels also increase at puberty (Babol et al. 2004), probably after an increase of testicular steroids (Zamaratskaia et al. 2004). There has been observed a relationship between metabolism of skatole and androstenone in liver which may be explained by the inhibition of enzymes metabolizing skatole by androstenone and other sex hormones (Babol et al. 1999).

To prevent this unpleasant smell of heated meat male piglets are surgically castrated shortly after birth (up to 7 days old), but due to welfare concerns there is a need for another method to prevent the unpleasant odour of meat. One of the methods is genomic selection where crucial part is to determine candidate genes with an influence on boar taint.

Enzyme CYB5A is involved in the biosynthesis of androstenone (Davis and Squires 1999) where it regulates the function of *CYP17A1* (Billen and Squires 2009). Correlation between the levels of CYB5A and the level of androstenone has been shown, with overexpression of CYB5A in pigs with high androstenone levels (Moe et al. 2007; Leung et al. 2010). Studies of genetic variation in *CYB5A* have identified four single nucleotide polymorphisms (SNP) in the promoter region - g.165901487delG, g.165901767T>C, g.165902078C>T (Bai et al. 2014) and AFO16388:c.-G>T (Lin et al. 2005).

The aim of this study was to develop a simple method for detection of SNPs mentioned above in Czech commercial hybrid boars and to determine whether the polymorphisms are associated with levels of skatole, indole and androstenone.

MATERIAL AND METHODS

Animals and tissue collection

In this study we analysed 40 boars of a commercial hybrid Large White x Landrace (sow) x Duroc. Pigs were slaughtered at 174 days of age in average and average slaughter weight of pigs was 110 kilograms. Samples for DNA extraction were collected from blood. Samples for LC-MS/MS analysis of androstenone, indole and skatole were collected from pig backfat.

DNA extraction, PCR and Sequencing

Total DNA was extracted using Tissue Genomic DNA Mini Kit (Geneaid Biotech, New Taipei City, Taiwan) according to manufacturer´s recommendation and verified by 1% agarose gel electrophoresis. DNA samples were mixed with PPP Master Mix (TopBio, Vestec, Czech Republic) and specific primers. Primers were designed using OLIGO 4.0 (Table 1) using pig genome sequence NC_010443.5 as a template. The PCR consisted of the following temperature profile: 95 ˚C for 5 min followed by 30 cycles (95 ˚C/30 s, 60 ˚C/30 s and 72 ˚C/45 s) and final elongation at 72 ˚C for 7 min. The cycler PTC-200 was used for PCR (Bio - Rad, Hercules, USA). PCR was verified by 3% agarose gel electrophoresis. For the genotyping of 4 SNP (g.165901487delG, g.165901767T>C, g.165902078C>T and AFO16388:c.-G>T), PCR products were analysed by direct Sanger sequencing using ABI PRISM 3500 genetic analyser (Thermo Fisher scientific, Waltham, USA). Levels of androstenone, indole and skatole were measured by the LC-MS/MS analysis.

Data analysis

Frequencies of alleles and genotypes were calculated as well as the Hardy – Weinberg equilibrium. The phenotypic data for all measurements and the genotypes were analysed using GLM analysis with one fixed factor (SNP) using the SAS v9.4 (SAS Institute, Cary NC, 2014).

Table 1 Primer sequences of gene CYB5A used for PCR

SNP	Sequence	Annealing temperature (˚C)	Product length (bp)
g.165901487delG g.165901767T>C	F: CGCATAGTCTGGGTCAACAGC R: CTTCGAGTCTGCGCAGAAGG	60	449
g.165902078C>T AFO16388:c.-G>T	F: CGAGTTCTGGCCAATCATCG R: GCCAGGTGCTCTTGCTGTTG	60	263

RESULTS AND DISCUSSION

The PCR amplification was not successful for some samples and primers, for final numbers of animals analysed see Table 2. Except from g.165901767T>C all SNPs were in Hardy-Weinberg equilibrium and relative frequencies of alleles were for g.165901487delG *Ins* 0.637 and *Del* 0.362, for g.165901767T>C *T*=0.786 and *C*=0.214, for g.165902078C>T *C*=0.629 and *T*=0.370 and for AFO16388:c.-G>T *G*=0.629 and *T*=0.370. According to allele frequencies polymorphisms g.165902078C>T and AFO16388:c.-G>T seem to be in a genetic linkage. Bai et al. (2014) reported European pigs to be primarily haplotype *A* (denoted as G-T-C: nt 165901487 is *G*, nt 165901767 is *T* and nt 165902078 is *C*) which might be in agreement with our findings considering the relative frequencies of alleles.

Cytochrome b5 plays role as a molecular switch and thus controls relative production of sex steroids and is likely a candidate gene for reducing boar taint without the negative effects on reproduction (Sellier et al. 2000). Another aim of our study was association analysis of analysed

genotypes and levels of indole, skatole and androstenone measured in backfat. The results are presented in Table 2. Peacock et al. (2007) found significant but modest effect of polymorphism AFO16388:c.-G>T at androstenone levels in Landrace, Yorkshire and Large White/Duroc cross and fat skatole in Duroc and Sire Line breeds. Previously, Lin et al. (2005) tested variety of breeds and found the *T* allele associated with lower CYB5A activity and with lower fat androstenone, however we have not found any association with boar taint compounds levels. To the best of our knowledge, no one have associated the three polymorphisms g.165901487delG, g.165901767T>C and g.165902078C>T with levels of indole, skatole or androstenone, but we have not found any significant associations ($P<0.05$).

It should be noticed that the low number of animals included in this study and also low levels of boar taint compounds influenced the statistical analysis and is probably the reason that we have not found any associations between *CYB5A* polymorphisms and androstenone, skatole and indole.

Table 2 Association analysis between CYB5A genotypes and indole, skatole and androstenone levels.

Polymorphism	Genotype	N	Indole		Skatole		Androstenone	
			LS Mean (ng/g)	Std.error	LS Mean (ng/g)	Std.error	LS Mean (ng/g)	Std.error
g.165901487delG	*Ins*	16	27.917	12.892	29.495	13.936	6.196	7.760
	InsDel	19	21.584	11.830	18.126	12.789	21.935	7.121
	Del	5	1.140	23.062	1.160	24.930	0.680	13.883
g.165901767T>C	*CC*	6	12.783	24.235	5.800	26.280	14.400	15.223
	TT	22	35.095	12.656	35.154	13.724	19.054	7.950
g.165902078C>T	*CC*	12	26.271	15.818	25.786	16.742	8.035	9.952
	CT	15	27.036	14.148	22.650	14.974	27.508	8.901
	TT	4	1.140	27.398	1.160	28.998	0.680	17.238
AFO16388:c.G>T	*GG*	12	26.271	15.818	25.786	16.742	8.035	9.952
	GT	15	27.036	14.148	22.650	14.974	27.508	8.901
	TT	4	1.140	27.398	1.160	28.998	0.680	17.238

CONCLUSION

Our work aimed to study the associations between selected polymorphisms of *CYB5A* gene and boar taint compounds, but no statistically significant difference between genotypes was found. We conclude this was caused by the small number of animals analysed and this result can serve as preliminary. But we have shown variability in all four SNPs in Czech commercial hybrid pigs. Further study with larger population of pigs is recommended to prove that *CYB5A* is a candidate gene for boar taint reduction.

ACKNOWLEDGEMENTS

The research was financially supported by the Ministry of Agriculture of the Czech Republic (Project No. NAZV QJ1510233).

REFERENCES

Babol, J. et al. 1999. Relationship between metabolism of skatole and androstenone in intact male pigs. Journal of Animal Science, 77: 84–92.

Babol, J. et al. 2004. The effect of age on distribution of skatole and indole levels in entire male pigs in four breeds: Yorkshire, Landrace, Hampshire and Duroc. Meat Science, 67: 351–358.

Bai, Y. et al. 2015. Differential expression of CYB5A in Chinese and European pig breeds due to genetic variations in the promoter region. Animal Genetics, 46: 16–22.

Billen, M.J., Squires, E.J. 2009. The role of porcine cytochrome b5A and cytochrome b5B in the regulation of cytochrome P45017A1. Journal of Steroid Biochemistry and Molecular Biology, 113: 98–104.

Bonneau, M. et al. 1982. Relationships between fat and plasma androstenone and plasma testosterone in fatty and lean young boars following castration. Acta Endocrinologica, (Copenhagen), 101: 129–133.

Davis, S.M., Squires, E.J. 1999. Association of cytochrome b5 with 16-androstenone steroid synthesis in the testis and accumulation in the fat of male pigs. Journal of Animal Science, 77: 1230–5.

Gower, D.B. 1972. 16-unsaturated C 19 steroids. A review of their chemistry, biochemistry and possible physiological role. Journal of Steroid Biochemistry, 3: 45–103.

Leung, M.C. et al. 2010. Examination of testicular gene expression pattern in Yorkshire pigs with the high and low levels of boar taint. Animal Biotechnology, 21: 77–87.

Lin, Z. et al. 2005. A novel polymorphism in the 5′ untranslated region of the porcine cytochrome b5 (CYB5) gene is associated with decrease fat androstenone level. Mammalian Genome, 16: 367–73.

Matthews, K.R. et al. 2000. An international study on the importance of androstenone and skatole for boar taint: III. consumer survey in seven European countrie. Meat Science, 54: 271–283.

Moe, M. et al. 2007. Gene expression profiles in testis of pigs with extreme high and low androstenone. BMC Genomics, 8: 405.

Peacock, J. et al. 2007. The effect of c.-8G>T polymorphism on the expression of cytochrome b5A and boar taint in pigs. Animal Genetics, 39: 15–21.

Sellier, P. et al. 2000. Responses to restricted index selection and genetic parameters for fat androstenone level and sexual maturity status of young boars. Livestock Production Science, 63:265–74.

Xue, J. et al. 1996. Breed differences in boar taint: relationship between tissue levels of boar taint compunds and sensory analysis of taint. Journal of Animal Science, 74: 2170–2177.

Zamaratskaia, G. et al. 2004. Plasma skatole and androstenone levels in entire male pigs and relationship between boar taint compounds, sex steroids and thyroxine at various ages. Livestock Production Science, 87: 91–98.

Decomposition of cadavers of farm animals during the wintry months by necrophagous species determined by classical and molecular genetics methods

Tamara Mifkova, Tomas Urban, Jana Horakova
Department of Morphology, Physiology and Animal Genetics
Mendel University in Brno
Zemedelska 1, 613 00 Brno
CZECH REPUBLIC

tamaramifkova@gmail.com

Abstract: The identification of insect inhabiting dead bodies is particularly relevant in forensic science, especially for post-mortem interval determination, as evidence of post-mortem manipulation of the body, evidence of the presence of toxic substances, etc. This work deals with the determination of forensically important insects occurring in cold months and extreme conditions based on molecular-genetic analyzes. For this purpose, several experimental fields were established in several locations of South Moravia. Model organisms were domestic pig (*Sus scrofa domesticus*) and chicken (*Gallus gallus domesticus*). During the experiment, 11 species of necrophagous fauna were found on cadavers, of which 6 were of the order Diptera and 5 of the order Coleoptera. In the second part of experiment these species were verified by molecular genetic methods.

Key words: necrophagous insects, decomposition, cadaver, cytochrome oxidase I, mitochondrial DNA

INTRODUCTION

Insects are a group of poikilotherm organisms, where the temperature of the body depends on the environment, for this reason the external temperature is crucial for its life. It affects all life manifestations: development, food intake, reproduction, occurrence and activity. Potential insect activity is in our climatic conditions for about 6 months, starting in the current conditions in the second decade of April and ending in the second decade of October. Seasonality is an important factor affecting the decomposition of the dead body. It is a different distribution of organisms and their basic life manifestations depending on the alternation of seasons (Hájková 2012). Dead bodies are a nutritionally rich source of food, so they are often frequented or assembled by various animals. The primary most numerous groups, colonizing the dead body, is the insect. The presence of insects on the body accelerates its decomposition through digestive juices released into the tissues, mechanical tissue disturbances and the spread of bacteria. The largest number of insects found on the carcass belongs to the order of the Diptera and Coleoptera. Their representatives have the highest proportion of tissue degradation (Gunn 2009, Rozen et al. 2008).

Forensic entomology deals with the study of insects in criminal investigations. Insects, especially necrophagous (feeding the dead body of another animal), are attracted to the decomposing body from an early stage (Joseph et al. 2011). For certain Diptera is a typical period in which the body is present. It's conditional decomposing products that attract this insect (Hirt 2015). The larvae, after a species-specific period, engage in the development on which the end is an adult person who will fly out of his puppy. The germination phase takes approximately 8–10 days from egg storage. The presence of empty pupae on the body means that, that the time necessary for the development of the fly has passed (Hirt 2015). By studying insect populations and their developmental larval stages, forensic scientists can estimate post mortem index – the term from the time of death to the body's finding (Byrd and Castner 2010), any change in the position of the corpse and cause or death (Joseph et al. 2011). For quick and accurate identification non-tropical insects contribute to modern DNA methods, mainly because of their frequent occurrence very difficult or even impossible morphological identifications (Amendt et al. 2004, Aly and Wen 2013).

The present study evaluated the decomposition of cadavers and incidence of necrophagous species during wintry months by anatomical-morphological features and variability of cytochrome oxidase I (COI) sequence of mitochondrial DNA.

MATERIAL AND METHODS

The experiment was performed from September 2016 to March 2017. Sampling was conducted at two areas of South Moravia, Czech Republic. The experimental bait of the first phase was chosen the domestic fowl (*Gallus gallus* f. *domestica*). For the second phase of the experiment was chosen cadaver of domestic swine (*Sus scrofa* f. *domestica*).

During the first period was captured a total of 209 specimens of insects in various stages of development. Samples were collected manually and identified according to anatomical-morphological features.

In the second period of our experiment we analyzed barcodes of 136 maggots. DNA for analysis was isolated from tissues using MACHEREY NAGEL Genomic DNA Kit (MACHEREY-NAGEL GmbH & Co. KG, Düren, Germany). Locus of mitochondrial cytochrome c oxidase subunit I gene (*COI*) was amplificated with two sets of primer pairs *Dip_F* + *Dip_R1* and LCO + HCO (Table 1). They were subsequently used to amplify a 658 bp fragment of the *COI* gene. Each PCR contained 5 µl of PPP MasterMix (TopBio, Ltd., Vestec, Czech Republic); 0.2 µl of each primer; 0.4 µl $MgCl_2$(TopBio, Ltd., Vestec, Czech Republic); 3.7 µl of ddH_2O (TopBio, Ltd., Vestec, Czech Republic) and 0.5 µl of DNA template. The PCR thermal regime consisted of one cycle of 3 min at 95 °C; 40 cycles of 45 s at 95 °C, 40 s at 49 °C and 1 min at 72 °C and a final cycle of 5 min at 72 °C.

The origins of the amplified sections were verified by direct PCR sequencing products. These products were purified by MinElute PCR Purification Kit from the company Qiagen GmbH (Hilden, Germany), according to the manufacturer's protocol. Verification of PCR concentration of the products were performed on a NanoDrop 2000 spectrometer from Thermo Fisher Scientific Inc. (Waltham, USA). BigDye Terminator Cycle Sequencing Kit v3.1 from Life Technologies Corp. (Carlsbad, USA) was used according to the manufacturer's instructions to prepare a sequencing reaction mixture. The resulting volume was 10 µl. Amount the DNA required for the sequencing reaction was determined by concentration and size. The final data were processed using Chromas2.6.5 and identified by bioinformatics tool BLAST and BOLD database.

Table 1 PCR primers

Primer	Sequence of primer 5´-3´	Author	Source
LCO	GGTCAACAAATCATAAAGATATTGG	Folmer et al. (1994)	BAR88098.1
HCO	TAAACTTCAGGGTGACCAAAAAATCA	Folmer et al. (1994)	BAR88098.1
Dip_F1	GTATAGTAGAAAACGGAGCTG	Horecky et al. (2015)	BAR88098.1
Dip_R1	AATCAACTAAAAATCTTAATTCC	Horecky et al. (2015)	BAR88098.1

RESULTS AND DISCUSSION

During the experiment, 11 species of necrophagous fauna were found on cadavers (Figure 1), of which 6 were of the order Diptera and 5 of the order Coleoptera – *Calliphora vicina* (Calliphoridae, Diptera), *Muscina levida* (Muscidae, Diptera), *Muscina sp*. (Muscidae, Diptera), *Neoleria sp.* (Heleomyzidae, Diptera), *Muscina prolapsa* (Muscidae, Diptera), *Thanatophilus rugosus* (Silphidae, Coleoptera), *Dermestes undulatus* (Dermestidae, Coleoptera), *Omalium rivulare* (Stapéphylinidae, Coleoptera), *Spelobia sp.* (Sphaeroceridae, Diptera), *Omosita discoidea* (Nitidulidae, Coleoptera), *Dermestes frischii* (Dermestidae, Coleoptera).

During the decomposition of the experimental cadavers the influence of the cold winter period, i.e. the late beginning of the colonization, the suppression of the Calliphoridae onset, was manifested. In two cases, only *Calliphora vicina*, who is overwintering as an adult, lagged. The family Muscidae, which is normally replaced by Calliphoridae, was again suppressed, again due to climatic conditions

(cold). Typical is the representation of the family Heleomyzidae, because this family breeds throughout the year and has spring, summer, autumn and winter species. Silphidae, Thanatophillus rugosus is a typical spring species. Dermestidae, who were found in the carnivores, fed their tissues and may have been preparing for laying. Staphylinidae are among the occasional ones who are numerous in the environment and use cadavers as an occasional source of food. *Omalium rivulare* is relatively common in buried cadavers, which is related to species bionomics, i.e., way of life, found in rake, leaves, etc. Sphaeroceridae are numerous, but only accompanying species. In cadavers, they often abstain, to a lesser extent they multiply, but are not interconnected between species and decomposition because they develop in any casting organic material. On cadavers can be found species that are commonly found in nature.

Figure 1 The number of individuals of detected species founded on cadavers

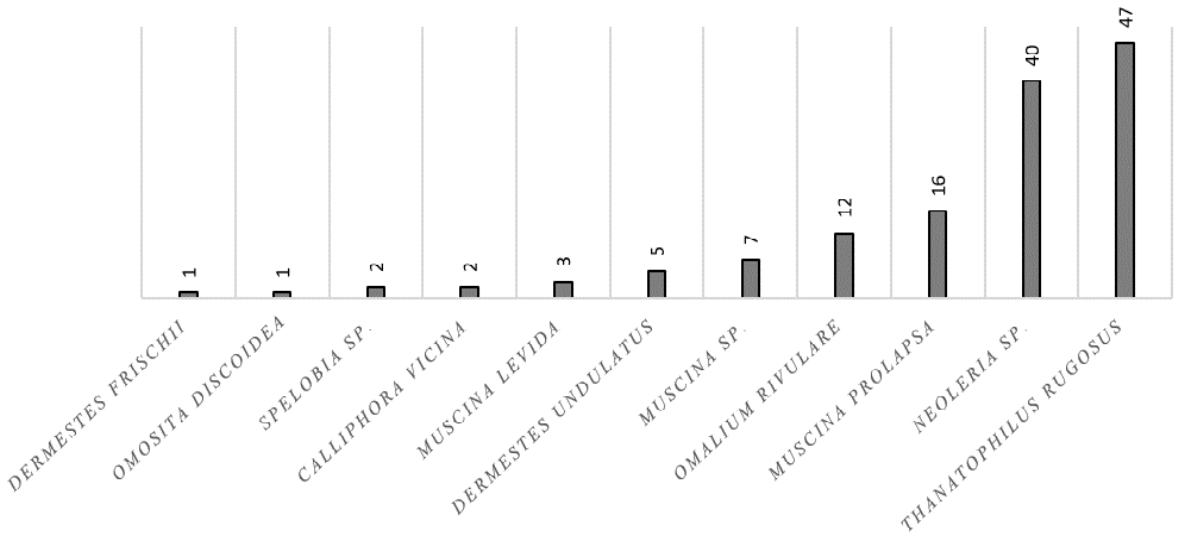

The results of our experiments prove the claim of Reed (1958) that Phoridae are rather later colonies of carcasses, like Sepsidae, Sphaeroceridae and Piophilidae. The cadavers of the representatives of these groups were found just family Sepsidae, which could have been caused by the time of collection or climatic conditions. The members of the family Staphylinidae have been found on carcasses throughout the year can be confirmed thanks to the detected individuals in this family on both cadavers (Prado e Castro et al. 2013). Madra et al. (2014) determined that the largest number of their representatives are found in the spring, which is partly confirmed by our attempt. From the experimental results, Reed (1958) and Gunn (2009) claim that low winter temperatures inhibit insect activity. However, there was observed an increase in the incidence of *Omalium rivulare* from the family Staphylinidae, whose occurrence in the winter months is reported by Anton et al. (2011), Aitchison (2001) and Jaskula and Soszyńska-Maj (2011).

Charabidze et al. (2012) reported the occurrence of *Calliphora vomitoria* or *Thyreophora cynophila* in the winter months. The occurrence of the first species was demonstrated, the occurrence of the second one was not. According to Smith (1986), the wintering of third instar larvae of some representatives of Calliphoridae in the soil was observed, according to *Calliphora vicina*, whose adults and larvae were found in the cadavers, hibernating as an adult. The research confirmed the statement by Soszyńska (2004), when the presence of representatives of the family Heleomyzidae was recorded in the Łódź Voivodeship in Poland at temperatures up to -4 °C. In the cadavers the *Neoleria* genus was also recorded, in which Ruzicka (1994) reports that its representatives are overwinning larvae and adults. This can be confirmed by the number of individuals found this year at different stages of development and in our experimental cadavers.

CONCLUSION

In study was found out species of insects participated in the decomposition of the body during the winter months. In the experiment was found a total of 11 forensic interesting species of Diptera and Coleoptera. The species were determined preliminary estimate only by anatomical-morphological analysis, in the second phase the methods of molecular genetics were used.

ACKNOWLEDGEMENTS

The research was financially supported by the internal grant agency FA IP-2018/077.

REFERENCES

Aitchison, J. 2001. Language change: progress or decay? 3rd ed., New York: Cambridge University Press.

Aly, S.M., Wen, J. 2013. Molecular identification of forensically relevant Diptera inferred from short mitochondrial genetic marker. The Libyan Journal of Medicine, 8: 20954.

Amendt, J. et al. 2004. Forensic entomology. Naturwissenschaften, 91(2): 51–65.

Anton, E. et al. 2011. Beetles and flies collected on pig carrion in an experimental setting in Thuringia and their forensic implications. Medical and Veterinary Entomology, 25: 353–364.

Byrd, J.H., Castner, J.L. 2010. Forensic entomology. The utility of arthropods in legal investigations. 2nd ed., Boca Raton: Taylor & Francis.

Charabidze, D. et al. 2012. What do flies do during the winter? Temporal variability of necrophagous Diptera at two times scales. Revue de Medecine Legale, 3(3): 120–126.

Folmer, O. et al. 1994. DNA primers for amplification of mitochondrial cytochrome c oxidase subunit I from diverse metazoan invertebrates. Molecular Marine Biology and Biotechnology, 3: 294–299.

Gunn, A. 2009. Essential forensic biology. 2nd ed., Hoboken, NJ: J. Wiley.

Hájková, L. 2012. Atlas fenologických poměrů Česka: Atlas of the phenological conditions in Czechia. 1st ed., Praha: Český hydrometeorologický ústav.

Hirt, M. 2015. Soudní lékařství. Praha: Grada.

Horecky, C. et al. 2015. Molecular genetics as a tool for forensic entomologists. In Abstract Book of 7th European Academy of Forensic Science Conference, Praha, Czech Republic, 6–11 September.

Jaskula, R., Soszyńska-Maj, A. 2011. What do we know about winter active ground beetles (Coleoptera, Carabidae) in Central and Northern Europe? ZooKeys, 100: 517–532.

Joseph, I. et al. 2011. The use of insects in forensic investigations: An overview on the scope of forensic entomology. Journal of Forensic Dental Sciences, 3(2): 89–91.

Madra, A. et al. 2014. Necrophilous Staphylininae (Coleoptera: Staphylinidae) as indicators of season of death and corpse relocation. Forensic Science International, 242: 32–37.

Prado e Castro, C. et al. 2013. Coleoptera of forensic interest: A study of seasonal community composition and succession in Lisbon, Portugal. Forensic Science International, 232(1–3): 73–83.

Reed, H.B. 1958. A Study of Dog Carcass Communities in Tennessee, with Special Reference to the Insects. American Midland Naturalist, 59: 245.

Rozen, D.E. et al. 2008. Antimicrobial strategies in burying beetles breeding on carrion. Proceedings of the National Academy of Sciences, 105 (46): 17890–17895.

Ruzicka, J. 1994. Seasonal activity and habitat associations of Silphidae and Leodidae: Cholevinae (Coleoptera) in central Bohemia. Acta Societatis Zoologicae Bohemoslovicae, 58: 67–78.

Smith, K.G.V. 1986. A manual of forensic entomology. Ithaca, N.Y.: Cornell University Press.

Soszyńska, A. 2004. The influence of environmental factors on the supranivean activity of Diptera in Central Poland. European Journal of Entomology, 101: 481–489.

The effect of peptidoglycan on production of pro-inflammatory cytokines by mammary gland leukocytes during *in vitro* study

Andrea Roztocilova[1], Lucie Kratochvilova[2], Kristina Kharkevich[2], Petr Slama[2]
[1]Department of Animal Nutrition and Forage Production
[2]Department of Animal Morphology, Physiology and Genetics
Mendel University in Brno
Zemedelska 1, 613 00 Brno
CZECH REPUBLIC

xroztoc1@node.mendelu.cz

Abstract: Cytokine network is very complicated and new knowledge about these proteins is important to develop better system of prevention, diagnosis and therapy of mastitis including decrease of antibiotic treatment. The study was implemented on eight selected healthy heifers. Leukocytes were obtained by lavage of the mammary gland 24 hours following the mammary gland stimulation by phosphate buffered saline solution (PBS). Leukocytes were cultivated for three different times. The first were cultivated for one hour, next two hours and eighteen hours. For cultivating was using peptidoglycan. Concentration of IL-1β and IFN-γ was measured by ELISA. IL-1β has the higher concentration after one hour cultivation and IFN-γ after two hours cultivation. Stimulation of mammary gland leukocytes with peptidoglycan resulted in a significant increase in the concentration of cytokines in comparison to the control. The concentration of IL-1β peaked at 1-hour incubation. In 2 and 18 hours, there were found decreasing of the concentration of this cytokine.

Key Words: mammary gland, IL-1β, IFN-γ, mastitis, cytokines

INTRODUCTION

Mastitis is an inflammation of the mammary gland caused by many kinds of bacteria such as Gram-positive bacteria like staphylococci, coagulase-negative staphylococci, streptococci, and other Gram-positive bacteria. When talking about Gram-negative bacteria, mastitis could be triggered by *Escherichia coli*, *Pasteurella*, *Proteus*, *Pseudomonas*, and *Serratia* species (Contreras and Rodríguez 2011). Peptidoglycan is a molecule naturally found in the cell wall of bacteria which is able to induce inflammatory response. Cytokines are water-soluble regulatory peptides which are produced throughout inflammation. Their concentration can be elevated during inflammation of mammary gland (Trinchieri 1997). Interleukin-1 (IL-1) plays an important role in the host defense and it is also known as one of the most effective endogenous fever inductor. This cytokine is produced by monocytes, lymphocytes, macrophages, dendritic cells, endothelial and epithelial cells, and fibroblasts (Barksby et al. 2007). Interferon gamma (IFN-γ) has multiple functions in innate and adaptive immunity (Bao et al. 2013) and regulation of early gene expression of Th2 (Torres et al. 2004).

Previously, Kabourkova et al. (2016) studied the effect of muramyl dipeptide on the production of cytokines including IL-1β. Muramyl dipeptide is the minimal structural unit of peptidoglycan of Gram-positive bacteria. We supposed the similar effect of peptidoglycan and its component muramyl dipeptide on the stimulation of mammary gland leukocytes. In the same article, there were mentioned about the effect of lipopolysaccharide on the production of cytokines by mammary gland leukocytes. Lipopolysaccharide is an endotoxin of Gram-negative bacteria. There was found the different effect of muramyl dipeptide of Gram-positive bacteria and lipopolysaccharide of Gram-negative bacteria on the response of mammary gland leukocytes.

The aim of the study was to investigate the effect of peptidoglycan of *Staphylococcus aureus* on production of pro-inflammatory cytokines (IL-1β and IFN-γ) during an *in vitro* study of bovine mammary gland leukocytes.

MATERIALS AND METHODS

Animals and experimental design

The study procedures were focused on the analysis of the pro-inflammatory cytokines IL-1β and IFN-γ. The cytokine detections were determined using sandwich ELISA. Eight clinically healthy crossbred heifers (Holstein x Czech Pied) were selected for this experiment. The heifers were group housed in a tie-stall barn and fed a total mixed diet.

The isolated leukocytes from the mammary gland were incubated with peptidoglycan of *Staphylococcus aureus* (Sigma-Aldrich, St. Louis, MO, USA) (50 µg/ml) for 1, 2, and 18 hours *in vitro* (at 37 °C in 5% CO_2). The cytokines were determined by sandwich ELISA.

Sample Collection Procedures

Samples of cell populations were obtained by lavage of the mammary gland 24 hours following the mammary gland stimulation by sterile buffered saline solution (PBS). In total, 20 ml of PBS was used. Fresh mammary gland leukocytes were adjusted (5 x 10^6/ml) in RPMI medium.

ELISA

Bovine IL-1 beta Screening Set (ThermoFisher Scientific, USA), and Bovine IFN-γ Screening Set (Thermo Scientific, USA). There was used ELISA reader Sunrise (Tecan, Austria).

Statistical Analysis

The concentration level of the cytokines was expressed as arithmetic mean (x) ± standard deviation (SD). Data were analyzed using statistical software program STATISTICA 8.0 (StatSoft ČR, s. r. o.). The paired t-test was used.

RESULTS AND DISCUSSION

Stimulation of mammary gland leukocytes with peptidoglycan resulted in a significant increase in the concentration of cytokines in comparison to the control. The concentration of IL-1β peaked at 1-hour incubation. In 2 and 18 hours, there were found decreasing of the concentration of this cytokine. Also Winter and Colditz (2002) studied the production level of IL-1β. They used *Staphylococcus epidermis* as inflammatory inductor in sheep. The IL-1β concentration level was highest 24 hours following the mammary gland stimulation. In the previous *in vitro* study (Kabourkova et al. 2016), there was found production of IL-1β two hours from the start of incubation of mammary gland leukocytes with LPS. Studies focused on IL-1β are important because this cytokine may have many functions in mastitis. Xu et al. (2018) referred about the effect of IL-1β on tight junction permeability in bovine mammary epithelial cells. IL-1β messenger RNA expression was induced by LPS and its enrichment is involved in multiple inflammatory signal pathways. Exogenous IL-1β treatment damaged the integrity of the blood-milk barrier, as indicated by the increased bovine mammary epithelial cells tight junction permeability. It is not clear whether IL-1β is also produced in stimulation by Gram-positive bacteria (Kim et al. 2011).

In contrary to the Kabourkova et al. (2016), we have found the maximal increase of IL-1β level in 1 hour following the start of co-cultivation of mammary gland leukocytes with peptidoglycan. In spite of the fact that muramyl dipeptide is the structural unit of peptidoglycan, those two agents had different effect on leukocyte response.

IFN-γ was also detected in all three time points (1, 2 and 18 hours). Highest concentration was found in the second time point (2 hours following incubation). The results suggest that peptidoglycan is able to induce immune response of bovine mammary gland with demonstrable production of pro-inflammatory cytokines by leukocytes.

Bannerman et al. (2004) confirmed higher IFN-γ level throughout initial inflammation phase and then return to the original IFN-γ values. These data correspond to the statement that IFN-γ improves the microbicidal activity of neutrophils by increasing of phagocytosis (Ellis and Beaman 2004, Schroder et al. 2004) because in the initial phase of mastitis there are highest number of neutrophils.

Figure 1 Concentration IL-β (pg/ml)

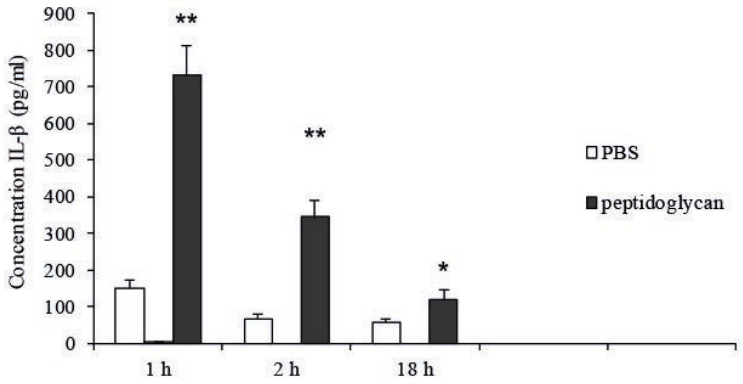

*Legend: h – hours; PBS – phosphate buffered saline; ** high statistically significant differences (p<0.01); * statistically significant differences (p<0.05)*

Figure 2 Concentration IFN-γ (pg/ml)

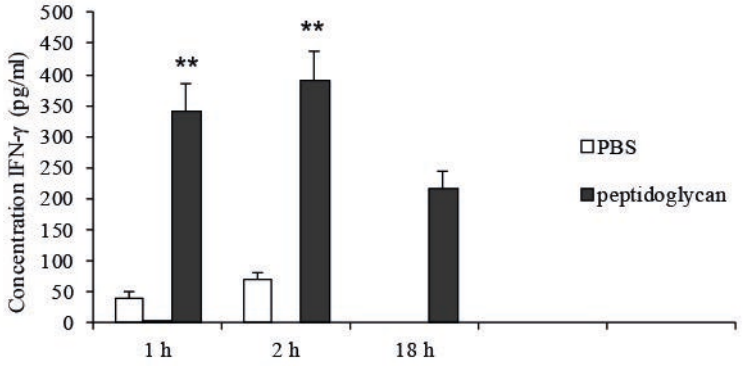

*Legend: h – hours; PBS - phosphate buffered saline; ** high statistically significant differences (p<0.01)*

The results of our experiments also suggest the potential of mammary gland leukocytes to battle with bacterial toxins as was referred in previous articles (Slama et al. 2011, Slama et al. 2012).

CONCLUSION

Peptidoglycan is able to induce production of pro-inflammatory cytokines which were represented by IL-1β and IFN-γ. It is very interesting that peptidoglycan has different effect on leukocyte inflammatory response than muramyl dipeptide. It may suggest the different way how to initiate the inflammatory response of immune cells.

ACKNOWLEDGEMENTS

The research was financially supported by the project AF-IGA-2018-tym002.

REFERENCES

Bannerman, D. et al. 2004. Escherichia coli andss Staphylococcus aureus elicit differential innate immune responses following intramammary infection. Clinical and Diagnostic Laboratory Immunology, 11: 463–472

Bao, Y. et al. 2013. Identification of IFN-γ-producing innate B cells. Cell Research 24: 161–176.

Barksby, H.E. et al. 2007. The expanding family of interleukin-1 cytokines and their role in destructive inflammatory disorders. Clinical and Experimental Immunology, 149(2): 217–225.

Contreras, G.A., Rodríguez, J.M. 2011. Mastitis: comparative etiology and epidemiology. Journal of Mammary Gland Biology and Neoplasia, 16(4): 339–356.

Ellis, T.N., Beaman, B.L. 2004. Interferon-gamma activation of polymorphonuclear neutrophil function. Immunology, 112(1), 2–12.

Schroder, K. et al. 2004. Interferon-gamma: An overview of signals, mechanisms and functions. Journal of Lekocyte Biology, 57: 163–189.

Kabourkova, E. et al. 2016. Production of cytocynes from bovine mammary gland leukocytes influenced by bacterial infection. In procedings of 12th International Scientific Conference. Boretice, Czech Republic, 13–15 June, Boretice: Animal Physiology, pp. 93–98

Kim, K.W. et al. 2011. Staphylococcus aureus induces IL-1β expression through the activation of MAP kinases and AP-1, CRE and NF-κB transcription factors in the bovine mammary gland epithelial cells. Comparative Immunology, Microbiology and Infectious Diseases, 34(4): 439–451.

Slama, P. et al. 2011. Production of bovine IL-10 following stimulation with lipolysaccharide and muramyl dipeptide. In proceedings of 36th FEBS Congress of the Biochemistry for Tomorrows Medicine. Torino, Italy, 25–30 June, FEBS Journal, 278 (1): 304–304.

Slama, P. et al. 2012. Production of bovine transforming growth factor beta 1 following stimulation with lipopolysacharide. In proceedings of 22nd IUBMB Congress/37th FEBS Congress. Sevile, Spain, 4–9 September, FEBS Journal, 279 (1): 459–459

Torres, K.C.L. et al. 2004. Endogenous IL-4 and IFN-γ are essential for expression of Th2, but not Th1 cytokine message during the early differentiation of human CD4+ T helper cells. Human Immunology, 65: 1328–1335.

Trinchieri, G. 1997. Cytokines acting on or secreted by macrophages during intracellular infection (IL-10, IL-12, IFN-γ). Current Opinion in Immunology, 9(1): 17–23.

Xu, T. et al. 2018. IL-1beta induces increased tight junction permeability in bovine mammary epithelial cells via the IL-1beta-ERK1/2-MLCK axis upon blood-milk barrier damage. Journal of Cellular Biochemistry, 119(11): 9028–9041.

Winter, P., Colditz, I.G. 2002. Immunological response of the lactating ovine udder following experimental challenge with Staphylococcus epidermis. Veterinary Immunology and Immunopathology, 89: 57–65.

Detection of ZP2 glycoprotein in bovine ovarian follicle cells and oocytes with different meiotic competence

Ivona Travnickova[1,2], Pavlina Hulinska[1], Zbysek Sladek[2], Marie Machatkova[1]
[1]Department of Genetics and Reproduction
Veterinary Research Institute
Hudcova 296/70, 621 00 Brno
[2]Department of Animal Morphology, Physiology and Genetics
Mendel University in Brno
Zemedelska 1, 613 00 Brno
CZECH REPUBLIC

xtravni2@mendelu.cz, travnickova@vri.cz

Abstract: The aim of the present study was to characterize ZP2 protein in bovine ovarian follicle cells and oocytes with different meiotic competence. A distinct band with molecular weight of about 68 kDa was demonstrated in bovine follicular cells and oocytes before and after maturation using polyclonal antibodies against ZP2 glycoprotein and the method of western blotting. Specific differences in ZP2 protein content were found among follicular cells, meiotically more and less competent bovine oocytes.

Key Words: bovine, ovarian follicle cells, oocytes, zona pellucida, ZP2 glycoprotein

INTRODUCTION

Mammalian oocytes are surrounded by a transparent envelope called the zona pellucida (ZP), which is involved in several critical aspects of fertilization. Its functions include species-selective recognition of sperm, blocking of polyspermy and protection of the oocyte and embryo until implantation (Wassarman et al. 2001, Hoodbhoy and Dean 2004, Topfer-Petersen et al. 2008).

Bovine zona pellucida consists of glycoproteins ZP2, ZP3 and ZP4 (Noguchi et al. 1994). In cattle, proteins of zona pellucida (ZP2, ZP3) are synthesised by both the follicular cells and oocytes from secondary and tertiary follicles during follicular development (Kölle et al. 1998, Hinsch et al. 2003).

The present study was designed to characterize bovine follicular cells and meiotically less and more competent oocytes at the GV and MII stages in terms of ZP2 glycoprotein abundance.

MATERIAL AND METHODS

Donors

Slaughtered Holstein dairy cows, aged 4 to 6 years, with a checked ovarian cycle stage were used as ovary donors. Only those with ovaries in the stagnation and regression phases, assessed by follicle and corpus luteum (CL) morphology, were selected for follicular cell and oocyte collection.

Follicular cell and oocyte collection

Follicular cells were collected by aspiration after medium follicle puncture (6 to 10 mm). Meiotically more competent (MMC) oocytes and meiotically less competent (MLC) oocytes were collected from medium and small follicles (2 to 5 mm) by aspiration and slicing of ovarian cortex, respectively. Only healthy cumulus-oocyte complexes with a homogenous ooplasm, surrounded by compact multiple layers of cumulus cells, were selected from each oocyte category and used in experiments.

Oocyte maturation

One half of the oocytes of each category was matured separately in TCM-199 medium, supplemented with 20 mM sodium pyruvate, 50 U/mL penicillin, 50 µg/mL streptomycin (Sigma Chemicals, Prague, Czech Republic), 5% estrus cow serum (ECS, Sevapharma, Prague, Czech Republic) and gonadotropins (P.G. 600 15 IU/mL, Intervet, Boxmeer, Holland) in four-well plates (Nunclon Intermed, Roskilde, Denmark) at 38.5 °C under 5% CO2 in air for 24 h (Knitlova et al. 2017).

Sample preparation

After aspiration of follicular cells, they were washed with PBS and centrifuged twice (200 × g, 10 min). The cumulus-oocyte complexes before (at the GV stage) and after maturation (at the MII stage) were mechanically denuded of cumulus cells using hyaluronic acid. The samples were frozen at –20 °C until examination.

SDS–PAGE analysis

The buffer containing β-mercaptoethanol was added to samples before proteins were separated by SDS-PAGE (Hoodbhoy et al. 2006). The SDS-PAGE analysis was carried out using a 12% resolving gel following the procedure described by Laemmli (1970). The electrophoresis procedures were performed for each sample, using the Mini Protean II Cell system (Bio-Rad, Prague, Czech Republic). The amount of proteins loaded was 20 µl per sample and molecular weight was estimated using Precision Plus Protein Dual Color Standards (Bio-Rad, Prague, Czech Republic).

Western blot analysis

Proteins fractionated by SDS-PAGE were transferred to PVDF membranes. The membranes were blocked overnight at 4 °C using Blotting Grade Blocker (Bio-Rad, Prague, Czech Republic) in a PBS solution. Blots were washed twice for 5 min with PBS-Tween 20 solution and incubated overnight at 4 °C with rabbit anti-ZP2 polyclonal antibody (Aviva Systems Biology, San Diego, California, USA) in dilution 1 : 150. The membranes were washed three times for 10 min with PBS-Tween 20, incubated at room temperature for 1 h with goat anti-rabbit IgG-horseradish peroxidase conjugate (Santa Cruz Biotechnology, Dallas, Texas, USA) in dilution 1 : 1000 and washed four times for 10 min with PBS-Tween 20 and twice for 10 min only with PBS solution. Finally, developing and detection of bands were performed by chemiluminescence. Briefly, the membranes were incubated with enhanced chemiluminescence detection reagents (Thermo Fisher Scientific, Waltham, Massachusetts, USA) for 2 min, and exposed to Amersham Hyperfilm ECL (GE Healthcare, Chicago, Illinois, USA) for 1 min (Zaragoza et al. 2004).

RESULTS AND DISCUSSION

The zona pellucida glycoprotein ZP2 was detected in follicular cells and MLC oocytes at the GV stage. A distinct band at a molecular weight of about 68 kDa, corresponding to molecular weight of ZP2 glycoprotein, was found as is shown in Figure 1. However, no visible ZP2 protein band was demonstrated in MLC oocytes at the MII stage.

Figure 1 Detection of ZP2 glycoprotein in follicular cells and meiotically less competent (MLC) oocytes

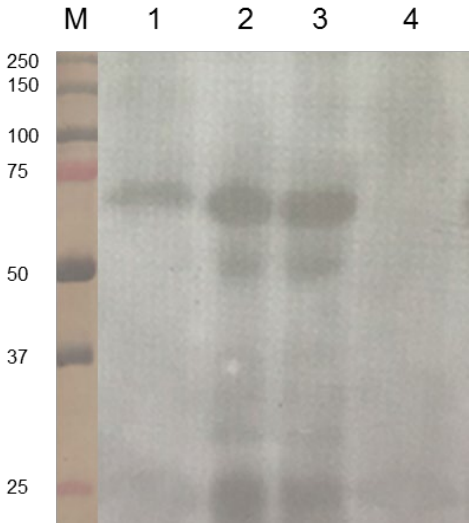

Legend: M – molecular weight standards (kDa), lane 1 – MLC oocytes at the GV stage (n=200), lane 2 – follicular cells, lane 3 – follicular cells, lane 4 – MLC oocytes at the MII stage (n=200)

Figure 2 Detection of ZP2 glycoprotein in follicular cells and meiotically more competent (MMC) oocytes

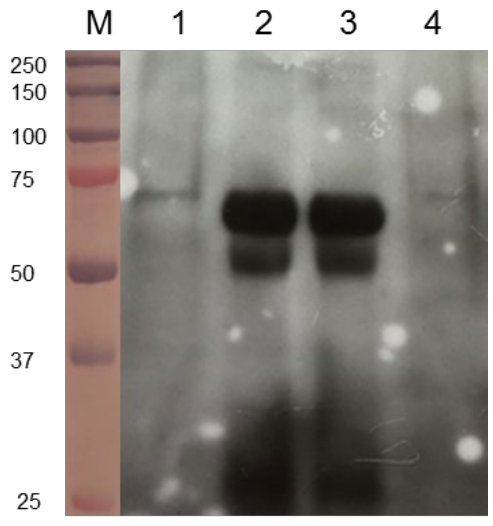

Legend: M – molecular weight standards (kDa), lane 1 – MMC oocytes at the GV stage (n=200), lane 2 – follicular cells, lane 3 – follicular cells, lane 4 – MMC oocytes at the MII stage (n=200)

The presence of ZP2 glycoprotein was also confirmed in MMC oocytes at the GV stage as is evident from Figure 2. Furthermore, a determinate ZP2 band was found in MMC oocytes at the MII stage.

Unfortunately, there is only limited data about evidence and function of ZP proteins in mammalian oocytes. In the pig, it has been described that ZP3α is the primary receptor for boar spermatozoa (Sacco et al. 1989). It is also known that both ZP2 and ZP3 proteins play an important role during sperm-oocyte binding in the mouse (Wassarman 1990). However, to the best of our knowledge, there is no study focused on ZP2 protein detection related to meiotic competence of bovine oocytes.

CONCLUSION

It was confirmed that bovine ovarian follicle cells and oocytes synthesize ZP2 glycoprotein before and after maturation.

Specific differences in ZP2 protein content were found between follicular cells and meiotically more and less competent oocytes. While meiotically more competent oocytes contained ZP2 protein at both the GV and MII stages, meiotically less competent oocytes did it only at the GV stage.

Further studies are needed to characterize ZP glycoproteins in relationship to meiotic competence of bovine oocytes.

ACKNOWLEDGEMENTS

The research was financially supported by Grants QJ1510138 and RO0518 of the Ministry of Agriculture of the Czech Republic.

REFERENCES

Hinsch, E. et al. 2003. Localization and functional importance of a conserved zona pellucida 2 protein domain in the human and bovine ovary using monoclonal anti-ZP2 peptide antibodies. Theriogenology, 60: 1331–1344.

Hoodbhoy, T., Dean, J. 2004. Insights into the molecular basis of sperm-egg recognition in mammals. Reproduction, 127: 417–422.

Hoodbhoy, T. et al. 2006. ZP2 and ZP3 traffic independently within oocytes prior to assembly into the extracellular zona pellucida. Molecular and Cellular Biology, 26(21): 7991–7998.

Knitlova, D. et al. 2017. Supplementation of L-carnitine during in vitro maturation improves embryo development from less competent bovine oocytes. Theriogenology, 102: 16–22.

Kölle, S. et al. 1998. Differential expression of ZPC in the bovine ovary, oocyte, and embryo. Molecular Reproduction and Development, 49: 435–443.

Laemmli, U.K. 1970. Cleavage of structural proteins during the assembly of the head of bacteriophage T_4. Nature, 227: 680–685.

Noguchi, S. et al. 1994. Characterization of the zona pellucida glycoproteins from bovine ovarian and fertilized eggs. Biochimica and Biophysica Acta, 1201: 7–14.

Sacco, A.G. et al. 1989. Porcine zona pellucida: Association of sperm receptor activity with the α-glycoprotein component of the M_r = 55,000 family. Biology of Reproduction, 41: 523–532.

Topfer-Petersen, E. et al. 2008. Glycobiology of fertilization in the pig. Journal of Developmental Biology, 52: 717–36.

Wassarman, P.M. 1990. Profile of a mammalian sperm receptor. Development, 108: 1–17.

Wassarman, P.M. et al. 2001. A profile of fertilization in mammals. Nature Cell Biology, 3: 59–64.

Zaragoza, C. et al. 2004. Canine pyometra: a study of the urinary proteins by SDS–PAGE and Western blot. Theriogenology, 61(7–8): 1259–1272.

New microsatellites detected in MHC I region in dromedary (*Camelus dromedarius*)

Jan Wijacki, Ales Knoll
Department of Animal Morphology, Physiology and Genetics
Mendel University in Brno
Zemedelska 1, 613 00 Brno
CZECH REPUBLIC

jan.wijacki@mendelu.cz

Abstract: The aim of this study was to find and test some microsatellites located in MHC I region and describe its variability and suitability for future testing and usability for multiplex PCR. The model organisms for this study were six dromedaries (*Camelus dromedarius*) from the Sumatra island. DNA samples were isolated from the hair of animals. Microsatellites, detected and analysed in this study, were located on major histocompatibility complex class I (MHC I) coded region. Four microsatellites were tested and verified (CAM_I_01, CAM_I_03, CAM_I_18 and CAM_I_29). Microsatellites regions were amplified by polymerase chain reaction (PCR) with specific primers. The results of fragment analysis showed that all markers have at least two or three alleles except CAM_I_18 which had only one allele. This microsatellite appeared monomorphic and unsuitable for future variability studies.

Key Words: camel, microsatellite, PCR, MHC, variability

INTRODUCTION

Microsatellite markers are high polymorphic tandem repeats using for genetic variability studies in plants and animal genetics. Microsatellite markers containing simple sequence repeats (SSR) are a valuable tool for genetic analysis (Panaud 1996). This study is focused on perfect dinucleotide polymorphic repeats located in major histocompatibility complex class I (MHC I) region.

The major histocompatibility complex (MHC) refers to the chromosomal region that is responsible for rapid (1- 3 weeks) immunologic rejection of allografts in nonimmunosuppressed animals (Snell et al. 1953).

Genes located in MHC I and II are the most polymorphic and variable genes studied in vertebrates. In these MHC classes, more than one hundred alleles occur in different animal species. This variability also occurs in humans (Bontrop et al. 1999, Robinson et al. 2013).

Class I MHC loci encode molecules that are the most polymorphic genes known. These molecules are ubiquitous in their tissue distribution and typically are recognized together with nominal antigens by cytotoxic lymphocytes (Heise et al. 1987).

The aim of this study was to find and test some microsatellites located in MHC I region and describe its variability and suitability for future testing and usability for multiplex PCR.

MATERIAL AND METHODS

Sequences, DNA samples, PCR reaction conditions, fragment analysis

For research purposes genomic sequence of *Camelus dromedarius* NW_011591121.1 (1.059 Mb) (Wu et al. 2014) was chosen (NCBI - National Center of Biotechnology Information database). The sequence was analysed by WebSat (http://www.wsmartins.net/websat/). In this sequence 58 microsatellites were detected and located. For this study were preferred perfect dinucleotide repeats with at least six motif repetitions. Four of these microsatellites were chosen for suitability verification for future analyses.

Microsatellites was analysed and verified on six samples. DNA was isolated from hair of dromedaries living on the Sumatra island. DNA was isolated using DNA, RNA and Protein purification-

NucleoSpin Tissue kit (MACHEREY-NAGEL GmbH & Co. KG, Düren, Germany) by standard protocol.

Primers for PCR amplification were designed by OLIGO Primer Analysis Software. All primers were designed according to the same parameters (T_a, T_m, nucleotides number, % GC) for future multiplex PCR suitability.

Table 1 Primers used for PCR amplification

Microsatellite	Forward primer 5' to 3'	Reverse primer 5' to 3'
CAM_I_01	GCAGCAGAGATATGCACAGAAT	CTGGCTTACTTCACTTGGAATG
CAM_I_03	AGGAAACTGGACACAGAGTGGT	CTCCTCCCTCCCCTGTATTATC
CAM_I_18	CAGGGTTCTCTGTGTGCTAGTG	CCCACAGACTGTTTGAAGTGTT
CAM_I_29	GGCTCATTCTTCCACTCAGAGA	CACATGCCACATCCCTCTAAAT

PCR master mix contains 7.9 µl PCR H_2O (Top-Bio, ltd., Prague, Czech Republic), 1.0 µl 10 × Taq Buffer (Top-Bio, ltd., Prague, Czech Republic), 0.5 µl CombiTaq polymerase (Top-Bio, ltd., Prague, Czech Republic), 0.2 µl dNTP mix (Thermo Fisher Scientific Inc., Waltham, USA), 0.1 µl forward primer. 0.1 µl reverse primer and 0.2 µl DNA sample. The total volume of PCR reaction mix was 10.0 µl.

DNA fragments were amplified according following conditions: initial denaturation at 95 °C for 3 min; 30 cycles of denaturation at 95 °C for 30 s, annealing at 58 °C for 30 s and elongation at 72 °C for 30 s; final elongation at 72 °C for 60 min and holding at 7 °C. Thermal cycler ABI Veriti 96 Well (Applied Biosystems™) was used for DNA amplification.

DNA amplification was verified by agarose electrophoresis, using 3% agarose gel, 130 V for 25 minutes. Fragments were visualised by GoodView™ (Ecoli, ltd., Bratislava, Slovak Republic) non-toxic and non-carcinogenic fluorescent stain.

For the genotyping of our samples genetic analyser ABI PRISM 3500 (Applied Biosystems™) was used. The reaction mix was composed of 11.3 µl Formamide, 0.3 µl LIZ500 size standard by Thermo Fisher Scientific Inc., Waltham, USA and 0.2 µl PCR product. Total volume of reaction mix was 11.8 µl. The reaction mixture was denaturated at 5 min/95 °C than was cooled 5 minutes on the ice. After cooling, mix was transferred to genetic analyser plate. The fragment analysis was run in POP7 polymer. To evaluate the results, the GeneMapper 5 software (Applied Biosystems™) was used.

RESULTS AND DISCUSSION

PCR amplification

The accuracy of the PCR amplification was verified by electrophoresis in 3% agarose gel (Figure 1). In this study was PCR made for each primer pair separately. This approach helped us to verify the specificity of primers. PCR amplicons were amplified without nonspecific fragments. It follows that primers were sufficiently specific.

Fragment analysis

In Figure 2 is shown the example of fragment analysis electrophoretogram. Sample in Figure 2 was homozygous in all analyzed markers.

Total amount of six samples were analysed. Three microsatellites (CAM_I_01, CAM_I_03 and CAM_I_29) were polymorphic and suitable for future analyses. Marker CAM_I_18 was monomorphic and for future analyses of diversity useless. A low number of alleles could be caused by the low number of animals in analysed group. Low variability could be also caused by locating of microsatellite in conserved or non-variable region of MHC. This study verified microsatellites usable for future analyses applied to a larger number of animals from larger area.

Table 2 Allele and genotype frequencies

CAM_I_01		CAM_I_03		CAM_I_18		CAM_I_29	
Allele (n)	Freq.	Allele (n)	Freq.	Allele (n)	Freq.	Allele (n)	Freq.
366 (2)	0.1667	196 (8)	0.6667	244 (12)	1.0000	274 (1)	0.0833
368 (7)	0.5833	206 (2)	0.1667			276 (11)	0.9167
372 (3)	0.2500	212 (2)	0.1667				

Genotype (n)	Freq.	Genotype (n)	Freq.	Genotype (n)	Freq.	Genotype (n)	Freq.
368/368 (3)	0.5000	196/196 (4)	0.6667	244/244 (6)	1.0000	274/276 (1)	0.1667
366/372 (2)	0.3333	206/206 (1)	0.1667			276/276 (5)	0.8333
368/372 (1)	0.1667	212/212 (1)	0.1667				

Figure 1 3% agarose electrophoresis of amplicons

Figure 2 Example of fragment analysis electrophoretogram

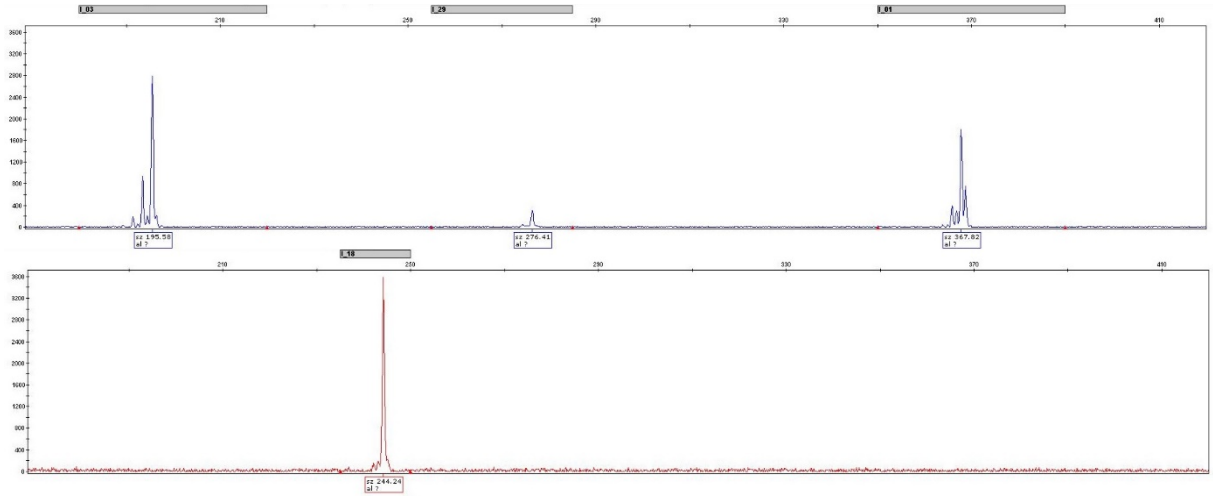

CONCLUSION

In this study, four microsatellites markers from MHC I class genome region were detected and verified. Three of these markers (CAM_I_01, CAM_I_03 and CAM_I_29) proved to be appropriate for future analyses of variability in MHC I region. In these microsatellites have been detected at least two alleles. Only one allele (224 bp) was found in marker CAM_I_18. This marker looks like unsuitable marker for variability studies because of its monomorphicity. This study may be referred to as preliminary in the field of designing markers for variability studies in MHC region. In future all known

markers will be amplified by multiplex PCR and panel will be expanded by additional markers located in class II and III region. This study has a crucial role for future genetic diversity analyses in MHC genes region in dromedaries.

ACKNOWLEDGEMENTS
The research was financially supported by the Internal Grant Agency of Mendel University in Brno, project No IP 057/2017.

REFERENCES
Bontrop, R.E. et al. 1999. Major histocompatibility complex class II polymorphisms in primates. Immunological Reviews, 167: 339–50.

Heise, E.R. et al. 1987. The major histocompatibility complex of primates. Genetica, 73(1–2): 53–68.

Panaud, O. 1996. Development of microsatellite markers and characterization of simple sequence length polymorphism (SSLP) in rice (*Oryza sativa L.*). Molecular and General Genetics MGG, 252(5): 597–607.

Robinson, J. et al. 2013. IPD—the Immuno Polymorphism Database. Nucleic Acids Research, 41: 1234–40.

Snell, G.D. et al. 1953. Analysis of the histocompatibility-2 locus in the mouse. Journal of the National Cancer Institute, 14(3): 457–480.

Wu, H. et al. 2014. Camelid genomes reveal evolution and adaptation to desert environments. Nature Communications, 5: 5188.

COL1A1 (type I collagen) gene expression in wounded skin of rats was not significantly influenced by docosahexaenoic (DHA) and eicosapentaenoic (EPA) acid enrichment of the diet

Jan Wijacki[1], Tomas Komprda[2], Veronika Rozikova[2]
[1]Department of Animal Morphology, Physiology and Genetics
[2]Department of Food Technology
Mendel University in Brno
Zemedelska 1, 613 00 Brno
CZECH REPUBLIC

jan.wijacki@mendelu.cz

Abstract: The main aim of this study was to compare expression of collagen I gene (*COL1A1*) in the healing skin of rats fed the diets enriched with docosahexaenoic (DHA) and eicosapentaenoic (EPA) fatty acid. The total of fifty Wistar Albino rats were divided into five groups (ten animals in each group). The animals were fed the basic mixture with addition of *Schizochytrium* microalga extract (D), palm oil (P), fish oil (R), and safflower oil (S), respectively. Group K served as a control fed the basic feed mixture alone. Animals were fattened eight weeks by respective diets and then excisions on their back were made by puncher in anesthesia. RNA was isolated from the samples of the healing tissue ten days post-excision and expression of the *COL1A1* and *β-actin* (reference gene) was measured by the real-time PCR. *COL1A1* gene expression in the D, P, R and S samples, did not differ significantly ($p>0.05$) from the control (K), therefore the hypothesis that EPA/DHA increase *COL1A1* expression was not proved.

Key Words: rat, RT-PCR, DHA, EPA, fatty acids

INTRODUCTION

Wound healing is generally defined as the process by which a body tissue (usually skin) repairs itself after trauma, a dynamic process aimed at restoring the structure of the injured tissue (Caetano et al. 2016). When using animal (usually rodent) models for wound healing in humans, it is important to realize that while the closure of human wounds is primarily accomplished through proliferation and migration of cells at the wound edge, contraction is the driving force behind wound closure in rodents (Pensalfini et al. 2018). The authors (Otranto et al. 2010) are cautious regarding fish oil due to the increase in collagen synthesis possibly resulting to the excessive scar tissue. According to Castilho et al. (2015), preoperative supplementation with PUFA n-3 in rats was associated with increased collagen deposition of the type I fibers in colonic anastomoses on the 5th postoperative day; no differences in the tensile strength or collagen maturation index in comparison with control were found out.

The objective of the present study was to use rats as a model organism for testing a hypothesis that rats fed with specific oils (fish oil, extract of *Schizochytrium* microalga, safflower oil and palm oil) added to the feeding mixture will have increased or decreased level of expression of *COL1A1* gene in wound tissue after excision.

MATERIAL AND METHODS

Animals, feeding, samples collecting, real-time PCR

The total of 50 rats of the laboratory strain Wistar Albino (Masaryk University, Brno, Czech Republic) were divided into 5 groups – K, D, P, R and S (10 animals for each group). The rats were housed in the plastic boxes (53.5 9 32.5 9 30.5 cm) of five animals in a room maintained at 23 ± 1 °C, humidity of 60% and 12/12 h of light/dark cycle (maximum intensity of 200 lx). The experiment was performed in compliance with the Czech National Council Act No. 246/1992 Coll. to protect animals against cruelty, the amended Act No. 162/1993 Coll., and was approved by the 'Commission to protect animals against cruelty' of the Mendel University in Brno.

Each group was fed the specific feed mixture. The animals in group D were fed by basic mixture with addition of Schizochytrium microalga extract, in group P with palm oil, in group R with fish oil, in group S with safflower oil. Group K served as a control group with no addition in feeding mixture. Feeding mixture was added by vitamin premix. Total amount of EPA, DHA and LA (linoleic acid) in mixture was 8 %.

The animals were fed daily ad libitum for eight weeks and had free access to the drinking water. After eight weeks an excision was performed in anesthesia on the back of the animals using a puncher (diameter 8 mm). Ten days later, the animals were sacrificed by isoflurane overdosing and the tissue scar from the back was removed.

One sample was collected from each animal and was immediately put into the RNAlater™ stabilization solution (Thermo Fisher Scientific) to preservation current level of RNA in tissue.

For analyses mixed samples were used (one sample mixed from three animals). Total RNA was isolated from the tissue aliquot (30 mg) using RNeasy Lipid Tissue Mini Kit (Qiagen, Valencia, CA, USA). The quality of isolation was checked on the 1.2% RNA gel visualized by ethidium bromide. The concentration of isolated RNA was measured on spectrophotometer NanoDrop 2000 (Thermo Scientific, Waltham, MA, USA). Isolated RNA was stored at -70 °C. One microgram of the isolated RNA was reverse transcribed using Omniscript RT Kit (Qiagen) and oligo-dT primers.

The obtained cDNA was used for quantitative PCR with specific primers (Zhou et al. 2017) for the rat *β-actin* (reference gene) (fw ACCAACTGGGACGACATGGAGAAA, rev TAGCACAGCCTGGATAGCAACGTA) and *COL1A1* (fw AGGGCCAAGACGAAGACATC, rev GTCGGTGGGTGACTCTGAGC). The reaction mixture was as follows: 1 µl of cDNA; 0.2 µl of AmpErase® Uracyl N-glycosylase (Applied Biosystems, Carlsbad, CA, USA); 10 µl of Power SYBR® Green PCR Master Mix (Applied Biosystems); 0.2 µl of each primer (mol/µl); and 8.4 µl of H_2O. All analyses were carried out on the 7500 Real Time PCR System (Applied Biosystems) under the following conditions: 2 min at 50 °C, 10 min at 95 °C, 40 cycles consisting of 15 s at 95 °C + 30 s at 65 °C + 30 s at 60 °C. The effectivity of each reverse transcription reaction was calculated according to the standard curve method using decimal dilution of the input cDNA. The measured CT data were analysed by considering the basal condition as the reference value for relative amount of the gene expression determined under each condition. Results were analysed using REST 2009 software (Qiagen).

RESULTS AND DISCUSSION

RNA isolation verification

RNA isolated from wound tissue was verified by 1.2% agarose gel electrophoresis in FA buffer and formaldehyde was added to the gel and buffer. RNA fragments were visualized by ethidium bromide using UV transilluminator. High Range RNA sizing standard was used for fragments sizing. Electrophoresis conditions was 110 V/30 min.

Samples concentrations measured using NanoDrop 2000 and transcription volumes

RNA concentration of all samples was measured on spectrophotometer NanoDrop 2000 (Table 1). Reverse transcription of samples was based on concentration measured data. 1 µg of RNA was transcribed to cDNA. Volume of RNA transcribed to cDNA depends on the sample concentration of RNA.

Table 1 RNA concentration and purity measured on NanoDrop 2000 and volume of RNA solution in reverse transcription mix

Sample	Concentration	260/280	Volume of 1 µg RNA for transcription (µl)	Sample	Concentration	260/280	Volume of 1 µg RNA for transcription (µl)
K1	463.5 ng/µl	2.05	2.16	**P3**	512.5 ng/µl	2.07	1.95
K2	465.2ng/µl	2.04	2.15	**R1**	370.2 ng/µl	2.07	2.70
K3	394.9 ng/µl	2.10	2.53	**R2**	392.1 ng/µl	2.04	2.55
D1	359.8 ng/µl	2.08	2.78	**R3**	652.1 ng/µl	2.02	1.53
D2	373.2 ng/µl	2.06	2.68	**S1**	509.3 ng/µl	2.06	1.96
D3	416.5 ng/µl	2.08	2.40	**S2**	528.3 ng/µl	2.04	1.89
P1	322.0 ng/µl	2.07	3.11	**S3**	360.5 ng/µl	2.06	2.77
P2	473.4 ng/µl	1.94	2.11				

The 260/280 value shown the purity of isolated RNA. Optimal range of this value is 1.8–2.0.

Comparison of expression *COL1A1*

Results of RT-PCR were analysed using REST 2009 V2.0.13 software (Qiagen). The expression for control group was adjusted to 1.000. Expressions of other groups are displayed as relative values. Comparison of results between tested and control group showed there was not differences in expression of selected markers ($p > 0.05$). There was not significant difference between D, P, R, S and control (K) group (Figure 1). K group with no additional oil in basic feeding mixture was selected as control group. In S and R group p-value was 0.088. This value is close to a significant difference. Relatively high p-values could be caused by high range of measured values of expression in each group.

Figure 1 Comparison of expression COL1A1 between tested and control group

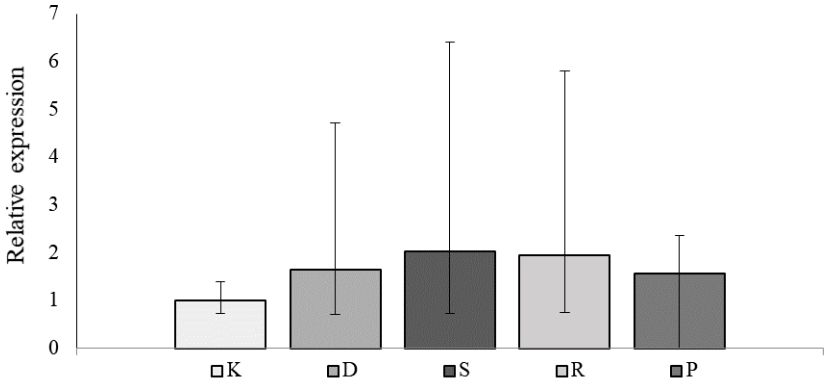

Legend: K – control group, D – DHA group, S –safflower oil group, P – palm oil group, R – fish oil group; bars at values represent 95% confidence interval

CONCLUSION

The tested hypothesis that biologically active substances present in fish oil, safflower oil and *Schizochytrium* extract, respectively, improve skin wound healing in a sense of increasing expression of *COL1A1* in the wounded tissue was not proved in the present study. The results could be influenced by the low number of samples, because in groups S and R the p-value approached the boundary of the significant difference (0.05). This was only a preliminary study to verify the methodology and to evaluate a possibility that the differences in *COL1A1*expression can be quantified in the rat model using dietary EPA/DHA. Further research will need more samples to verify our hypothesis.

ACKNOWLEDGEMENTS

The research was financially supported by the Internal Grant Agency of Mendel University in Brno, project No TP3/2017.

REFERENCES

Caetano, G.F. et al. 2016. Comparison of collagen content in skin wounds evaluated by biochemical assay and by computer-aided histomorphometric analysis. Pharmaceutical Biology, 54: 2555–2559.

Coelho de Castilho, T.J. et al. 2015. Effect of omega-3 fatty acid in the healing process of colonic anastomosis in rats. ABCD-Arquivos Brasileiros de Cirurgia Digestiva-Brazilian Archives of Digestive Surgery, 28: 258–261.

Otranto, M. et al. 2010. Effects of supplementation with different edible oils on cutaneous wound healing. Wound Repair Regen, 18: 629–636.

Pensalfini, M. et al. 2018. The mechanical fingerprint of murine excisional wounds. Acta Biomater, 65: 226–236.

Zhou, J. et al. 2017. Simultaneous silencing of TGF-β1 and COX-2 reduces human skin hypertrophic scar through activation of fibroblast apoptosis. Oncotarget, 8: 80651–80665.

TECHNIQUES AND TECHNOLOGY

Estimation of liquid deposition on corn plants sprayed from a drone

Boguslawa Berner, Aleksandra Pachuta, Jerzy Chojnacki
Department of Authomatic, Mechanics & Construction
Koszalin University of Technology
Racławicka 15–17, 75–620 Koszalin
POLAND

boguslawa.berner@tu.koszalin.pl

Abstract: Laboratory results of spraying maize plants using a multi-rotor drone are presented. The XR11001 flat fan sprayer from TeeJet was used for the tests. The liquid pressure in installation was 0.2 MPa. The height of corn plants was 1.6 m and 0.9 m above the soil surface. The drone was equipped with electric motors DJI 4114, kV – 400 and propellers with dimensions 15 x 2.2". The influence of the air stream produced by the drone rotors and the plant height on the plants sprayed from the drone spray stream was investigated. The research showed the dependence of the distribution of the deposited liquid on individual parts of plants from plant height and air flow.

Key Words: UAV, spraying plants, corn, liquid deposition, drone

INTRODUCTION

Unmanned aerial vehicles (UAVs) are used in agriculture primarily as instruments to acquire information about the rural environment (Pascuzzi et al. 2018), about the fertilization demand of plants (Mazur and Chojnacki 2017), the level of weed infestation and even about existing plant parasites (Tetila et al. 2017). Drones are currently able to perform some agrotechnical operations on crops. They can be used to spray plants with plant protection products, both chemical and biological (Berner and Chojnacki 2017a), spread fertilizers, sow seeds and plant plants. The advantage of using drones in field works is the lack of kneading soil and plants, the ability to work on hard-to-reach areas, especially due to the diversification of the terrain or the wetness of the ground. The drones enable quick movement over field crops, and enable treatments at different heights, directly above the plants (Faiçal et al. 2017).

Spraying drones can either perform autonomously, according to a previously planned flight route, or the route of their flight and treatment site can be controlled by the drone operator by means of a transmitter, in real time (Yallappa et al. 2017, Huang et al. 2009, Xue et al. 2016). The interest in using drones in plant protection is also growing due to the innovativeness of this solution, which in the future may contribute to full robotisation of field works (Mogili and Deepak 2018).

Drones – airplanes resembling airplanes can be used for spraying plants, but the most common application for field works has been drones with rotor construction, with rotating blades of propellers keeping them in the air (Berner and Chojnacki 2017b, Wei-Cai et al. 2016, Zhou and He 2016, Giles and Billing 2015). Research on the use of unmanned aerial vehicles in plant protection focuses mainly on the assessment of the quality of treatments performed with their help. To assess the treatments with drones can be used probes fixed on plants, spread over several levels of plants. They allow the assessment of the degree of liquid penetration in the plant canopy. On the basis of traces of droplets on the probes one can estimate their size and uniformity of distribution, and even the capacity of the deposited liquid (Wei-Cai et al. 2016, Berner and Chojnacki 2017b, Zhou and He 2016). The quality of the distribution of liquid plants can depend on the amount of spraying and the shape of plants as well as the accuracy of the drone moving over the plants (Tang et al. 2018, Berner and Chojnacki 2017b). In addition to the use of probes attached to the plants, a biological assessment is also carried out (Qin et al. 2018).

Spraying plants with drones can become common in the future, provided that the effectiveness of treatments performed with them will not be worse, and even better than treatments carried out with the use of ground equipment.

MATERIAL AND METHODS

The aim of the study was to assess the impact of the air stream produced by drone rotors and plant heights, on the distribution of sprayed plants from a drone.

The tests were carried out in the laboratory hall. On the high mounted treadmill was a trolley, moved by a pull rod pulled by an electric motor. The drone has been mounted to the trolley from below. It was a S900 hexacopter, manufactured by DJI. The drone was equipped with electric motors DJI 4114, kV – 400 and propellers with dimensions 15 x 2.2". Under the rotor of the drone, on the jib attached to the frame of the drone, at a distance of 0.4 m from the lower surface of the propellers, a flat stream sprayFer XR11001 from TeeJet was installed. The liquid to the sprayer was supplied from an external power source. The pressure of the liquid in the atomizer was constant and amounted to 0.2 MPa. The nozzle has been positioned so that the fan of the spray jet was directed transversely to the direction of travel of the cart with the drone. The travel speed of the trolley on the frame race was set to 1.2 m/s and did not change during the tests. The rotational speed of all drone rotors was constant and amounted to 580 rad/s, which corresponded to the power of the drone, equal to 90 N. The rotation of the drone rotor was controlled by means of an optical tachometer mounted on a drone and connected via a USB connection to a computer.

Corn plants in phase – 77 according to BBCH, bred in outdoor boxes were selected for research. All plants were shortened to an equal level – 1.6 m above the ground level in containers, which resulted in a height of 1.8 m above the floor surface in the laboratory. In the second phase of research, the plants were shortened, cutting the lower part of the plant's momentum, to 0.9 m above ground level. The boxes were set up in the laboratory under the frame with the trolley. The spacing of plants in a row transverse to the direction of travel of the trolley was 0.40 m and in a row parallel to the direction of movement of the trolley it was equal 0.70 m. The plant setting is shown in the figure 1.

Figure 1 Stand setting

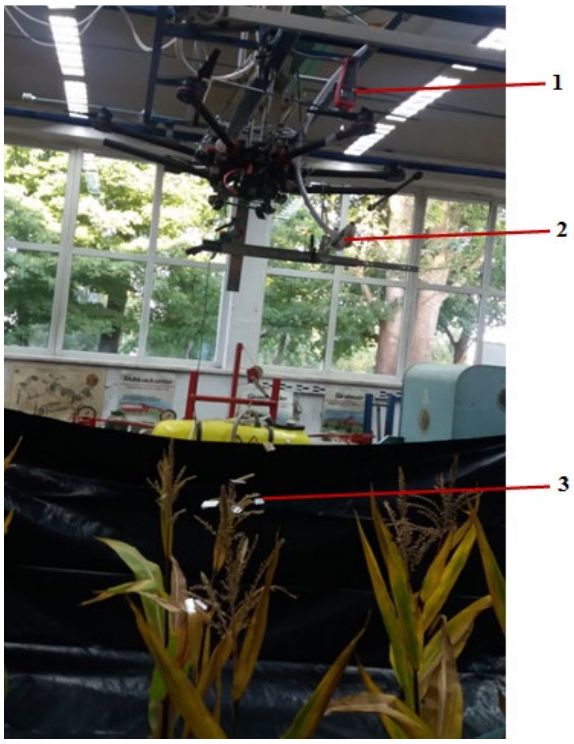

Legend: 1 – tachometer, 2 – nozzle, 3 – samplers

On three levels of plants there are placed probes with dimensions 0.02 x 0.04 m made of aluminium foil, 5 pieces on each level. Samplers were always glued on the same plant, in the same places for the same height of the plant. Samplers were placed on the top layer of the plant, on the middle layer and the lower layer 20 cm above the soil surface. In the case of tall plants, the central level was 0.9 m in the case of shortened plants – 0.55 m above the soil level.

The experiments were performed with rotating rotors and without rotating the drone's rotors, repeating each measurement three times. The probes were located on the central plant positioned exactly under the axis of the sprayer's symmetry. As the spray liquid, water stained with washable water nigrozine was used at a concentration of 0.5%. After the plants dried, the sensors were peeled off the plants and stored in sealed containers.

After completing the tests, nigrozine was washed from the probes using distilled water of indicated capacity. The concentration of the dye, which was proportional to the mass of the deposited spray liquid, was determined by means of a spectrophotometer.

RESULTS

The average results of the research of the deposited liquid on the probes are presented on figure 2 for tall plants and for low plants are on figure 3. They actually represent the concentrations of the washed dye from the surface of the probes, which are proportional to the amount of liquid deposited on them.

Figure 2 Liquid distribution on tall plants

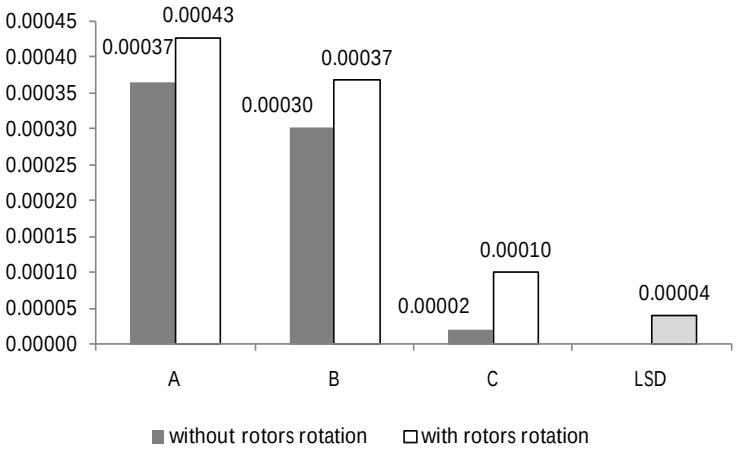

Legend: level of samplers on plant: A – top, B – middle, C – lower, LSD – Least Significant Difference

Using the analysis of variance, the significance of the influence of plant height and air blowing on the liquid deposition on selected plant levels was determined. Analysis of variance in which the factors were:

– level of samplers placement,
– plant height,
– rotors work.

Figure 3 Liquid distribution on low plants

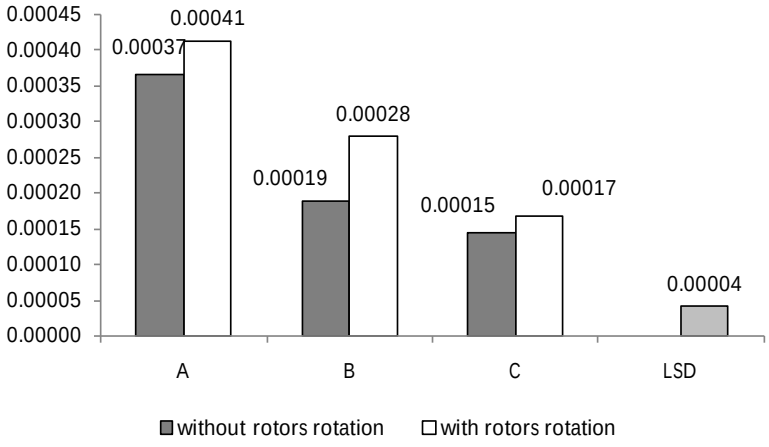

Legend: level of samplers on plant: A – top, B – middle, C – lower, LSD – Least Significant Difference

It showed the significance of the impact of plant height and rotors work for liquid deposition on corn plants with a significance level of less than 0.05. The value of the Least Significant Difference

(LSD) was also calculated. This value is shown on plots (see Figures 2 and 3). By comparing its value to the results, it can be noticed that no significant influence of the air stream on changes in the capacity of the deposited liquid on the samplers placed at the level C of low plants was found.

Based on the data obtained from the measurements, a plots of the percentage of distribution of the liquid on individual plant levels were made according to the formula described in the formula 1 (see Figures 4 and 5).

$$P_i = 100 \cdot \frac{v_i}{\sum v_i} [\%] \quad (1)$$

Where:

P_i – share of the liquid capacity deposited on the sampler on i – this level in relation to the liquid capacity deposited at all levels, %

v_i – liquid capacity deposited on the sampler at i – this level.

Figure 4 Percentage of distribution of the liquid on individual samplers levels (tall plants)

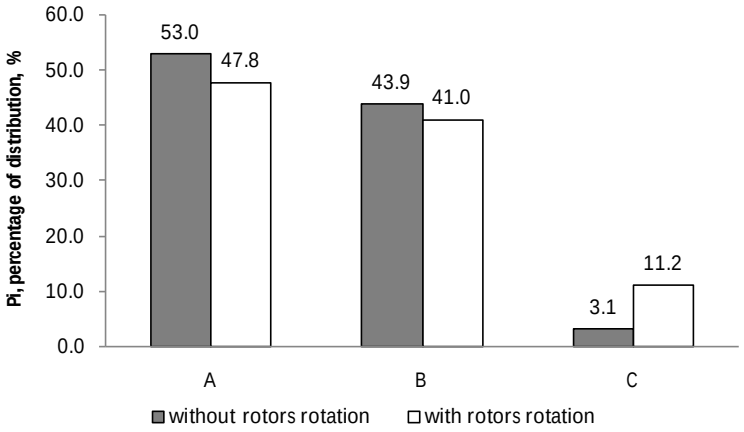

Legend: level of samplers on plant: A – top, B – middle, C – lower

Plots of the percentage distribution of liquid at individual plant levels show the relative relations between the plant height and the uniformity of liquid deposition on them.

Figure 5 Percentage of distribution of the liquid on individual samplers levels (low plants)

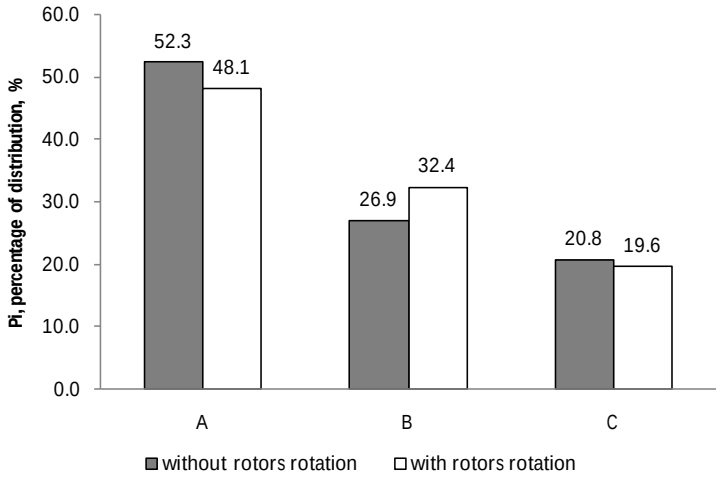

Legend: level of samplers on plant: A – top, B – middle, C – lower

CONCLUSION

The test results indicated that there is a significant effect of plant height and air flow on the distribution of liquid on corn plants. The influence of plant height is predictable and it is natural that with a free falling stream of liquid less and less it reaches the lower parts of plants. In the case of the air

stream operation, part of the liquid contained in the stream of drops was transferred to the lower parts of plants. This can be seen from the plots, both in the amount of liquid deposited and the percentage of the total deposited liquid. The air stream originating from drone rotors has positively influenced the improvement of the uniformity of settling of the liquid on the plants. It was also noticed that the air stream was part of the droplet stream outside the testing area in the laboratory.

ACKNOWLEDGEMENTS

The research was financially supported by the statutory resources of the Mechanical Faculty of the Koszalin University of Technology.

REFERENCES

Berner, B., Chojnacki, J. 2017a. Influence of the air stream produced by the drone on the sedimentation of the sprayed liquid that contains entomopathogenic nematodes. Journal of Research and Applications in Agricultural Engineering, 3(62): 26–295.

Berner, B., Chojnacki, J. 2017b. Use of drones in crop protection. In Proceedings of IX International Scientific Symposium Farm Machinery and Processes Management in Sustainable Agriculture. Lublin 2017: 46–51.

Faiçal, B.S. et al. 2017. An adaptive approach for UAV–based pesticide spraying in dynamic environments. Computers and Electronics in Agriculture, (138): 210–223.

Giles, D.K., Billing, R.C. 2015. Deployment and Performance of a UAV for Crop Spraying Chemical Engineering Transactions, 44: 307–312.

Huang, Y. et al. 2009. Development of a spray system for an unmanned aerial vehicle platform. Applied Engineering in Agriculture, 25(6): 803–809.

Mazur, P., Chojnacki, J. 2017. Comparison of two remote nitrogen uptake sensing methods to determine needs of nitrogen application. Journal of Research and Applications in Agricultural Engineering, 62(2): 76–79.

Mogili, U.M.R., Deepak, B.B.V.L. 2018. Review on Application of Drone Systems in Precision Agriculture. Procedia Computer Science, 133: 502–509.

Pascuzzi, S. et al. 2018. Unmanned aerial vehicle used for remote sensing on an apulian farm in southern Italy. In Proceedings of 17th International Scientific Conference Engineering for Rural Development. Jelgava, 23–25. 05. 2018: 149–154.

Qin, W. et al. 2018. Droplet deposition and efficiency of fungicides sprayed with small UAV against wheat powdery mildew. International Journal of Agricultural and Biological Engineering, 11(2): 27–32.

Tang, Y. et al. 2018. Effects of operation height and tree shape on droplet deposition in citrus trees using an unmanned aerial vehicle. Computers and Electronics in Agriculture, 148: 1–7.

Tetila, E.C. et al. 2017. Identification of Soybean Foliar Diseases Using Unmanned Aerial Vehicle Images. In Proceedings of IEEE Geoscience and Remote Sensing letters, 14(12): 2190–2194.

Wei-Cai, Q. et al. 2016. Droplet deposition and control effect of insecticides sprayed with an unmanned aerial vehicle against plant hoppers. Crop Protection 85: 79–88.

Xue, X. et al. 2016. Develop an unmanned aerial vehicle based automatic aerial spraying system. Computers and Electronics in Agriculture, 128: 58–66.

Yallappa, D. et al. 2017. Development and evaluation of drone mounted sprayer for pesticide applications to crops. In Proceedings of IEEE Global Humanitarian Technology Conference (GHTC): 1–7.

Zhou, L.P., He, Y. 2016. Simulation and optimization of multi spray factors in UAV. In Proceedings of ASABE Annual International Meeting, Orlando, Florida, July 17–20: 17–20.

The use of impedance testing to detect the differences between llama and alpaca wool

Paulina Cholewinska[1], Katarzyna Czyz[1], Piotr Nowakowski[1], Anna Wyrostek[1], Deta Luczycka[2], Marta Michalak[3]
[1]Institute of Animal Breeding
Chelmonskiego 38C
[2]Institute of Agricultural Engineering
Chelmonskiego 37
[3]Department of Animal Nutrition and Feed Science
Chelmonskiego 38C
Wroclaw University of Environmental and Life Sciences
51-630 Wroclaw
POLAND

paulina.cholewinska@upwr.edu.pl

Abstract: Examination of the coat is mainly based on determining the diameter of the hair, breaking strength, heat protection, etc. However, it is possible to determine the quality of the hair coat by testing the electrical characteristics, because this method is characterized by high sensitivity. It defines changes already at the molecular level, which may allow for more accurate determination of fiber quality and enable recognition of changes occurring in it. The test consists in detecting differences by means of current flow based on the dependence related to the permeability or resistance of the tested material. In the following work, the study was based on the detection of changes due to the level of impedance, i.e. complex resistance compared to the results of heat resistance of the breaking strength and the diameter of the hair. Research on electrical features showed a slightly higher level of resistance between llama and alpaca wool. There was also a significant difference ($P<0.05$) in the diameter of the hair, llama wool was characterized by a larger diameter than alpaca wool. On the other hand, the results of heat resistance and breaking strength did not show any significant differences.

Key Words: impedance, breaking strength, heat resistance, llama wool, alpaca wool

INTRODUCTION

Each material tested is characterized by a specific molecular structure, which is associated with the distribution of electric charge permanently embedded in the particle or induced on its surface. Differences in the structure of the particles cause different behavior in the electromagnetic field and determine the physical and chemical properties of the material (Cholewinska et al. 2018).

In order to determine the variability of materials, more recently the study of their electrical properties is increasingly being used, the most common are the properties associated with the behavior of the material as a dielectric or electrical conductivity. Dielectric properties of materials are the result of low conductivity or poor mobility of electric charges, as well as both factors at the same time. In the study of electrical characteristics, the use of the phenomenon of resistance, usually impedance, is also often used. Impedance means the total material resistance (passive and active), associated with the measure of resistance with which the material opposes the flow of electric current. The use of phenomena related to current flow and resistance allows the evaluation of the tested material (Cholewinska et al. 2018, Yousefi et al. 2014, Pastewski and Galla 2012).

The use of electrical features, i.e. the study of material behavior in the electromagnetic field, is a very sensitive and fast method. It offers a very attractive work tool, while not destroying the tested material, which results in lower costs and less labor than in traditional surveys. In order to determine the differences in materials or even their composition, it is possible to use the research of electrical features by thorough analysis and comparison of its behavior in the electromagnetic field and determine its properties as a dielectric. Most of the tests are carried out using an Agilent sensor, which is used to

determine the dielectric properties of solid and liquid materials. Instruments are also used to test electrical conductivity, most commonly solids, however, the equipment used depends on the material being tested and the results expected (Łuczycka 2009, Jha et al. 2011).

In addition to soils, food and agricultural products, studies on the electrical characteristics of animal hair - wool were made. They were made in the 1970s. These studies have shown that wool in the electromagnetic field exhibits dielectric properties. It owes its properties to the wax layer on the surface of the hair. Physicochemical changes under the influence of water content have also been shown, where an increase in dielectric dispersion (dependence of electric permeability on frequency) along with water content in bristles has been demonstrated (Algie and Gamble 1973).

This work was aimed at comparing with the impedance of wool lam and alpaca, and comparing the obtained results with traditional tests, i.e. tensile stress, heat protection and hair diameter.

MATERIAL AND METHODS

Animal material

The samples came from the Zoological Garden in Wroclaw. Sharing of animals took place in May at the 2 years regrowth of wool. For the measurements of electrical and heat-protection characteristics and breaking strenght, the greasy wool samples were taken from 5 animals – llama and alpaca Huacaya, weighted by weight.

Testing of electrical characteristics

The samples were tested using the Atlas Solich High Impedance Analyser Atlas 0441 at the Agricultural Engineering Laboratory of the University of Life Sciences in Wroclaw. The samples were placed between the copper electrodes in a 3.9 mm thick chamber with an inner diameter of 38 mm, made of plastic. Measurements were taken at a constant temperature of 25 ºC and 70% humidity and repeated fourth times.

Heat resistance and tensile strength testing

The examination was carried out in the Skin and Hair Cote Laboratory belong to Institute of Animal Breeding at the University of Life Sciences in Wroclaw by Matest's Apparatus for the evaluation of materials exposed to thermal radiation, heat resistance (WPC) and tensile strength (N) measurement devices. Measurements were repeated four times.

The thermal transmittance coefficient (WPC) was calculated using the formula:

$WPC = GSC_p/GSC_o$

Where:

WPC – thermal resistance

GSC_p– the density of the thermal flux passing through the test $[kW/m^2]$

GSC_0– the density of the thermal flux to be tested $[kW/m^2]$

$(GSC_p = \frac{MxC_PxR_1}{Ax\alpha})$

$(GSC_0 = \frac{M\ x\ Cp\ xR_2}{A\ x\ \alpha})$

Where:

M – mass of the aluminium calorimeter sample: 7.16g

Cp – heat specific aluminium: 900 J/kg x ºC

A – surface area of calorimeter: 0.00049m^2

α – absorption coefficient of the blackened calorimeter surface area: 0.95

R_1 – rate of increase of calorimeter temperature in the linear part of the graph (for calorimeter with sample) $[^oC/s]$

R_2 – rate of calorimeter temperature increase in the linear part of the graph (for empty calorimeter) $[^oC/s]$

The tensile strength (N) was calculated using the formula:

$N = (Fnx10^4) / (\pi x d^2 x\ 9.81)$

Where:

N – tensile strength [kg/mm^2]
Fn – breaking force [cN]
d – hair cross-sectional diameter [µm]

Elaboration of results

The results were Statistica ver. 13.1. Normality of distribution of results was evaluated by the Shapiro-Wilk test. In the case of normal distribution, differences between groups were examined using the t-student test for independent samples for results of heat resistance and breaking stress. Differences between groups were statistically significant when $P<0.05$.

RESULTS AND DISCUSSION

The study of electrical features based on impedance was characterized by significant jumps in the resistance level of the examined hair in the frequency range from 10 Hz to 160 Hz followed by a linear decrease in impedance. At a frequency of 10 Hz, wools reached extreme impedance values, the high level of resistance was characterized by alpaca wool – 1250 MΩ, where the llama wool reached a level not exceeding 997 MΩ. Differences in resistance between both animals occurred at 98 Hz, again in this case the alpaca was characterized by a higher resistance of 61.2 MΩ and llama 9.21 MΩ. In general, considering all resistance levels in the frequency range from 10 Hz to 1MHz, alpaca wool tended to have a higher level of resistance than llama wool (Figure 1).

Figure 1 Impedance of alpaca and llama wool at frequency 10-2600 Hz

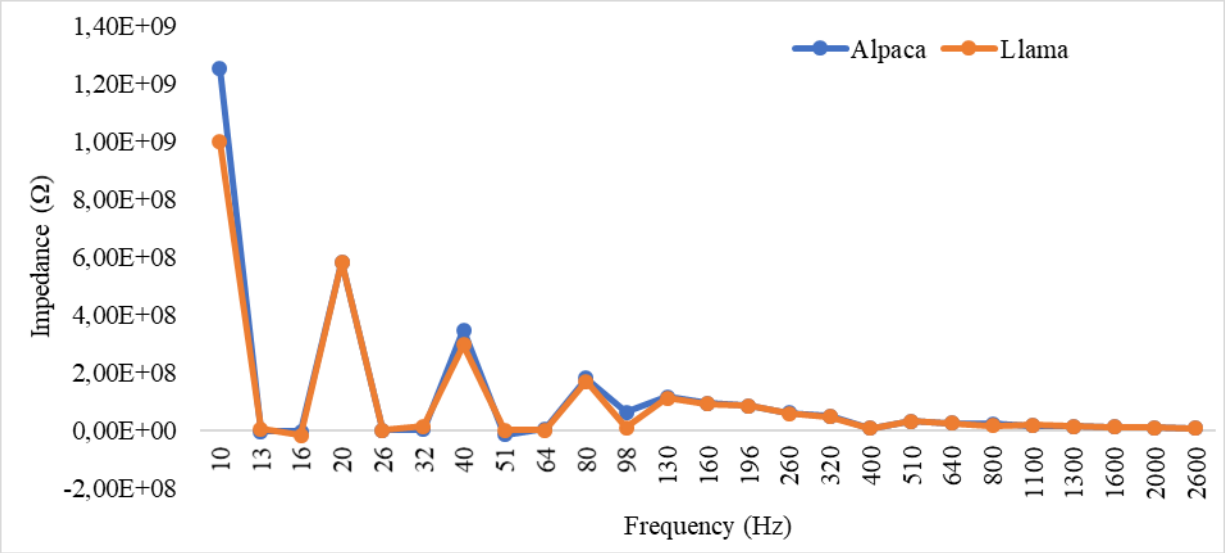

Hair diameter tests showed significant differences ($P<0.05$), where wool from llama was characterized by a higher diameter than alpaca wool. On the other hand, the examination of heat protection and breaking strength did not show any significant differences between the wool tested (Table 1).

The use of the impedance phenomenon to assess the quality of products and the changes occurring in them under the influence of various factors is becoming more and more popular. The study of the electrical properties of materials makes it possible to detect changes at the molecular level (Bancalari et al. 2016, Jha et al. 2011). It should be taken into account that impedance is influenced by external factors and its structure (Nelson 2008). Therefore, it can be suggested that in this case the obtained structure was influenced by the structure of the hair associated with the filling of keratin, because it affects the diameter of the hair. Depending on the degree of filling with keratin, the hair will differ in thickness, hygroscopicity, strength, flexibility and resistance to mechanical factors, which will vary their physical and chemical properties. Factors affecting the structure of the hair and filling with keratin are: nutrition, breed of the animal, age and environment (Cardamone et al. 2009, McKittrick et al. 2012).

Table 1 Results of diameter, breaking strength and heat protection of alpaca and llama wool

Diameter (µm)		
Alpaca	Llama	p-value
30.40	43.81	0.000005
Breaking strength (kg/mm^2)		
Alpaca	Llama	p-value
1.42	1.51	0.314
Heat protection (WPC)		
Alpaca	Llama	p-value
0.77	0.74	0.690

In addition, as the resistance increases, the material becomes a better dielectric, i.e. a material in which the current is poorly conducted, due to the higher resistance. The most important property of a pile coat as dielectric is the ability to accumulate electric charge, which causes it to act electrostatically on the human body (Cholewinska et al. 2018, Jha et al. 2011). Electrostatic interaction of fibers has a very important aspect in the creation of materials with health effects and often they are based on a cover derived from animals. In the case of both llama and alpaca wool both were characterized by dielectric properties, although alpaca wool in this case showing a tendency to achieve a generalized higher level of impedance, it can be suggested that it is more suitable for human products than wool llama. However, the lack of differences in the study of breaking stress and heat protection could be caused by too low sensitivity of the tests.

However, it should be taken into account that the research on the determination of dielectric properties and the differences between the animal's hair cover by means of the study of impedance characteristics is not fully understood. Therefore, further research is planned in the future on the application of this method, because its promising results may limit the working time in the future compared to traditional methods and its fatigue is much higher than in the case of traditional methods.

CONCLUSION

Alpaca wool is characterized by a tendency to achieve a higher level of impedance than wool llama. The studies showed differences ($P<0.05$) in the diameter of the hair, where the hair diameter from llama was 43.81µm and the alpaca 30.4 µm. There were no significant differences ($P<0.05$) between llama and alpaca wool in the study of heat protection and breaking strength.

The study of electrical properties (impedance) and the differences described between llama and alpaca wool were also confirmed in the thickness and breaking strength test. The lack of difference between llama and alpaca wool in the heat-protection test could be due to the lower sensitivity that this test shows in comparison to the testing of electrical characteristics and breaking strength.

REFERENCES

Algie, J.E., Gamble, R.A. 1973. Dielectric properties of wool and horn containing absorbed water. Kolloid-Zeitschrift und Zeitschrift für Polymere, 251(8): 554–562.

Bancalari, E. et al. 2016. Application of Impedance Microbiology for Evaluating Potential Acidifying Performances of Starter Lactic Acid Bacteria to Employ in Milk Transformation. Frontiers Microbiology, 7: 1628.

Cardamone, J.M. et al. 2009. Characterizing wool keratin. Research Letters in Materials Science, 2009: 5.

Cholewinska, P. et al. 2018. An effect of suint on sheep wool impedance and heat resistance values. Journal of Natural Fibers [Online], 1–6. Available at: https://doi.org/10.1080/15440478.2018.1494078. [2018-09-20].

Jha, S.N. et al. 2011. Measurement techniques and application of electrical properties for nondestructive quality evaluation of foods—a review. Journal of Food Science and Technology, 48(4): 387–411.

Łuczycka, D. 2009. Methodological aspects of testing electrical properties of honey. Acta Agrophysica, 14(2): 367–374.

McKittrick, J. et al. 2012. The Structure, Functions, and Mechanical Properties of Keratin. Journal of The Materials, 64(4): 449–468.

Nelson, S.O. 2008. Dielectric properties of agricultural products and some applications. Research in Agricultural Engineering, 54(2): 104–112.

Pastewski, J., Galla, S. 2012. ESD surveillance system. Scientific Letters of the Faculty of Electrical and Control Engineering–Gdansk University of Technology, 31(26): 117–122.

Yousefi, N. et al. 2014. Highly aligned graphene/polymer nanocomposites with excellent dielectric properties for high-performance electromagnetic interference shielding. Advanced Materials, 26(31): 5480–5487.

Effects of copper on operating parameters during anaerobic stabilization of sewage sludge

Tereza Dokulilova, Eliska Kobzova, Tomas Vitez
Department of Agricultural, Food and Environmental Engineering
Mendel University in Brno
Zemedelska 1, 613 00 Brno
CZECH REPUBLIC

tereza.dokulilova@mendelu.cz

Abstract: The presence of heavy metals have negative effect on sewage sludge anaerobic stabilization mainly on biogas production and quality. The objective of this study was to monitor pH, volatile acids (acetic, propionic, butyric and valeric) content in sludge and biogas production and quality during the anaerobic stabilization of sewage sludge in laboratory conditions (38 °C ± 0.2 ºC, hydraulic retention time 20 days), and to observe the effect of copper addition on the above parameters. Hypothesis which predicted the changes of monitored parameters mainly biogas quantity and quality, volatile acid content and pH after copper addition, was partly confirmed. There were no significant differences in biogas and methane production after addition of 600 and 800 mg Cu^{2+}/l. On the other hand, significant differences can be seen on pH, acetic and propionic content in sludge and hydrogen content in biogas. These parameters were significantly affected by different concentrations of copper.

Key Words: biogas production, methane yield, pH, volatile acids, inhibition

INTRODUCTION

The most frequently found heavy metals in wastewaters and then in sewage sludge from households and industry are copper (Cu), zinc (Zn), lead (Pb), mercury (Hg), chromium (Cr), cadmium (Cd), iron (Fe), nickel (Ni), cobalt (Co) and molybdenum (Mo) (Altaş 2009). Up to 50% of the heavy metals present in sludge have origin in industry, the rest comes from pipes (Cu and Pb), roofs (Cu and Zn) and detergents (Cd, Cu and Zn) (Appels et al. 2008).

The anaerobic stabilization is a complicated microbial process that involves 4 phases (hydrolysis, acidogenesis, acetogenesis and methanogenesis). Each phase is realized by the different group of microorganism. The most sensitive group to presence of toxic compounds are methanogenic *Archaea* that convert acetate, CO_2 and H_2 to methane, the energy rich part of biogas. Mainly the soluble compounds of copper and zinc can cause the 50% inhibition of methane production (Straka et al. 2010).

As is written above, the presence of heavy metals in sewage sludge can have negative effect on anaerobic stabilization mainly on biogas production and quality. The inhibition can be observed for the decrease in biogas and methane production, increase in H_2 content in biogas, decrease in pH which is caused by increase in volatile acids content.

The first objective of this study is to monitor operating parameters as pH, volatile acids (acetic, propionic, butyric and valeric acid) content in sludge and biogas production and quality during the anaerobic stabilization of sewage sludge in laboratory conditions. The second objective is to observe the effect of copper addition on the above parameters. Hypothesis predicts the changes of monitored parameters after copper addition, which indicate the inhibition of anaerobic microorganisms.

MATERIAL AND METHODS

Anaerobic sludge sample used for fermentation test was collected directly from the stabilization tank at the Wastewater treatment plant Brno – Modrice (513 000 PE), Czech Republic. The collection was realized once in April 2018 according to technical standard method ISO 5667-13. The sludge sample was transported to the Nationwide Reference Laboratory of Biogas Transformation at the Mendel University in Brno as soon as possible. The sludge temperature did not drop under 30 °C during the transport.

In laboratory, sludge sample was characterized by the analysing of parameters: total solids (TS) content, volatile solids (VS) content, pH, redox potential, conductivity. The volatile acids (acetic, propionic, butyric and valeric acid) content in sludge sample was analysed in external laboratory. The content of TS was determined according to Czech Standard Method CSN EN 15934. Fresh sample was dried at 105 ± 5 ºC to the constant weight in the laboratory oven KBC G 100 (Premeo, Poland). The content of VS was determined according to Czech Standard Method CSN EN 15169. Dry sample was determined by incinerated at 550 ± 5 ºC in the muffle furnace (LMH 11/12, LAC, Ltd., Czech Republic). The pH value was determined by using multimeter Greisinger GHM 5530 (GHM Messtechnik GmbH, Germany) with electrode GE 100. The same multimeter with electrode GR 105 was used for the determination of redox potential. The meter Greisinger GMH 5430 (GHM Messtechnik GmbH, Germany) with electrode LF 400 was used for the determination of conductivity. Sludge pH and volatile acids (acetic, propionic, butyric and valeric acid) content were analysed every third day during the fermentation test in one opened fermenter from each system.

The fermentation test was held in 3 systems, each of 8 anaerobic fermenters (volume 5 dm^3). The sludge sample of volume 3 dm^3 was filled up in each of 24 batch fermenters. Glycerine in volume 8 ml was added in all fermenters as carbon substrate for microbial growth. First system (8 fermenters) was used as blank without the addition of zinc copper. Into 8 fermenters in second system, copper chloride stock solution (concentration 150 g Cu^{2+}/l) was added, in order to achieve concentration 600 mg Cu^{2+}/l of sludge. The same stock solution was added into fermenters in third system, in order to achieve concentration 800 mg Cu^{2+}/l of sludge.

The fermentation test was held at temperature 38 °C ± 0.2 ºC. The biogas was collected in wet gas meters and measured daily over hydraulic retention time 20 days. Biogas quality (content of methane and hydrogen) was analysed during the test by gas analyser COMBIMASS® GA-s (BINDER GmbH, Germany) with the error ±3% of measured value. Biogas production was converted to standard conditions (T_0 = 273.15 K, p_0 = 101 325 Pa). The volume of biogas and methane were recalculated to biogas and methane yield, expressed as m^3 per kg of VS of the substrate. All measurements were done in triplicate. All measured values are expressed as arithmetic mean ± standard deviation. Error lines in all figures represent 5% measuring error.

Significant differences among biogas (methane) yields for blank, 600 and 800 mg Cu^{2+}/l were determined by analysis of variance (ANOVA) at $P < 0.05$ using the Tukey test. STATISTICA 12 software was used.

RESULTS AND DISCUSSION

The influence of physical and chemical condition in anaerobic stabilization tank on inhibitory potential of toxic compounds on anaerobic microorganism is significant. Thus, the characteristics of sludge at the beginning of fermentation test can be seen in Table 1.

Table 1 Characteristics of sludge at the beginning of test

	pH [-]	Redox potential [mV]	Conductivity [S/m]	TS [%]	VS [%]
Sewage sludge	7.24 ± 0.01	-63.30 ± 0.43	0.69 ± 0.01	3.24 ± 0.01	59.13 ± 0.05

The cumulative biogas production during the fermentation test is illustrated in Figure 1. In the Figure 2, the methane cumulative production can be seen. Both concentrations of copper caused significant the decrease in biogas and methane production, but there is no significant difference between biogas and methane quantity after the addition of copper in the concentration of 600 and 800 mg Cu^{2+}/l (see Table 2).

According to literature (e.g. Straka et al. 2010), the increased content of hydrogen in the biogas during the anaerobic stabilization of sewage sludge is the consequence of inhibition. The Figure 3 shows that the hydrogen content in biogas is significantly affected by inhibition level. The hydrogen content in biogas is approximately eight times higher after the addition of 600 mg Cu^{2+}/l and ten times higher after the addition of 800 mg Cu^{2+}/l, than in blank fermenters.

Figure 1 Cumulative biogas production

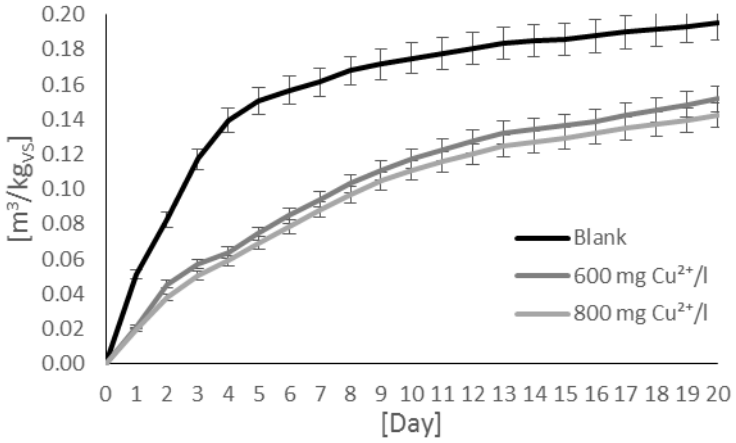

Figure 2 Cumulative methane production

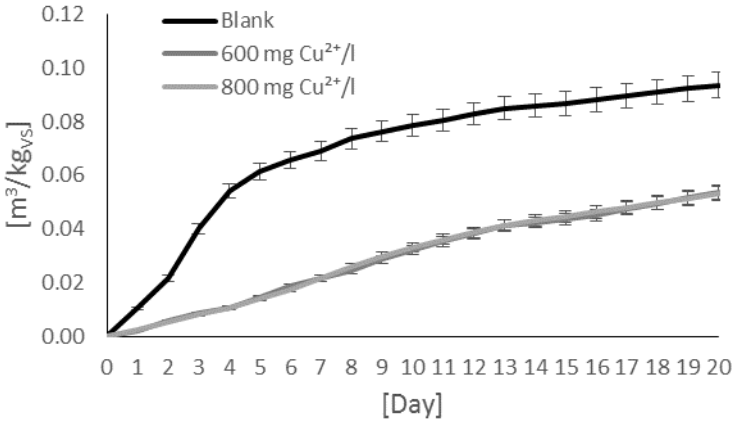

Table 2 Tukey test of the biogas and methane yields (significant differences at P < 0.05 are in bold)

		Biogas			Methane		
		1	2	3	1	2	3
Blank	1		**0.000516**	**0.000312**		**0.000516**	**0.000312**
600 mg Cu²⁺/l	2	**0.000516**		0.230176	**0.000516**		0.230176
800 mg Cu²⁺/l	3	**0.000312**	0.230176		**0.000312**	0.230176	

Figure 3 Hydrogen content in biogas

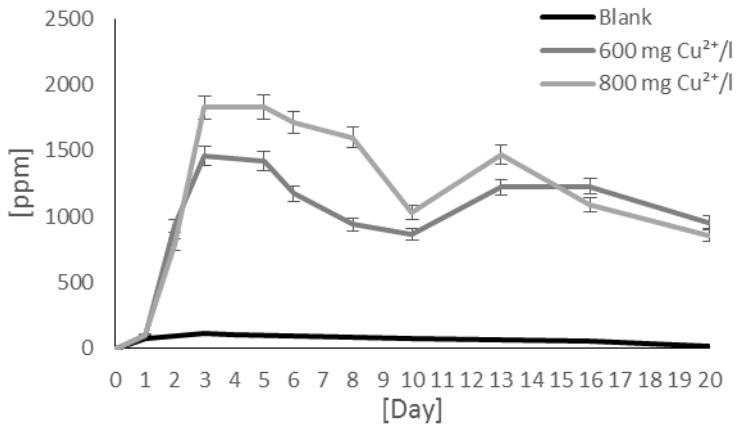

The optimal pH value in stabilization tank is between 6.8 and 7.2 (Ward et al. 2008). Due to microbial autoregulatory system, the pH value in stabilization tank stabilizes itself at the optimal level during

single stage anaerobic fermentation process (Liebetrau et al. 2012). This fact can be seen in Figure 4 after the sixth day in blank fermenters, after the ninth day in fermenters inhibited by 600 mg Cu^{2+}/l and after the eighteen day in fermenters inhibited by 800 mg Cu^{2+}/l. There can be seen that the level of inhibition significantly affected the microbial autoregulatory system.

Figure 4 Sludge pH

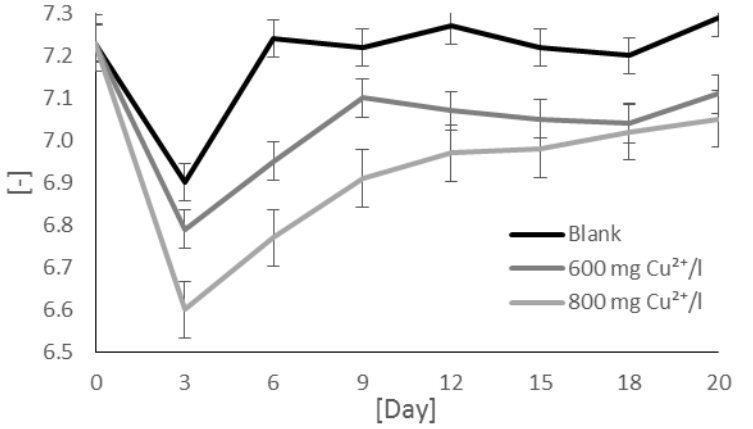

The contents of butyric and valeric acid in sludge were under the detection limit (20 mg/l) during whole test. On the other hand, the increase in acetic and propionic acid concentration after addition of 600 and 800 mg Cu^{2+}/l can be seen in Figure 5 and Figure 6, respectively. The volatile acids concentration in sludge is significantly affected by inhibition level and its course is reverse to pH value.

Figure 5 Acetic acid content in sludge

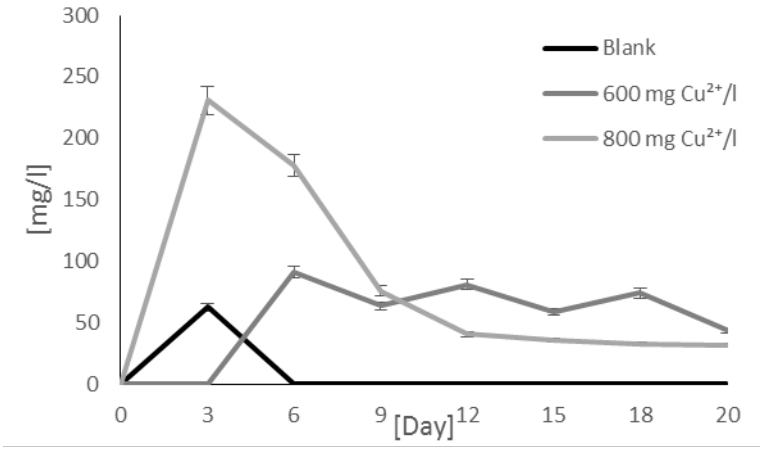

Figure 6 Propionic acid content in sludge

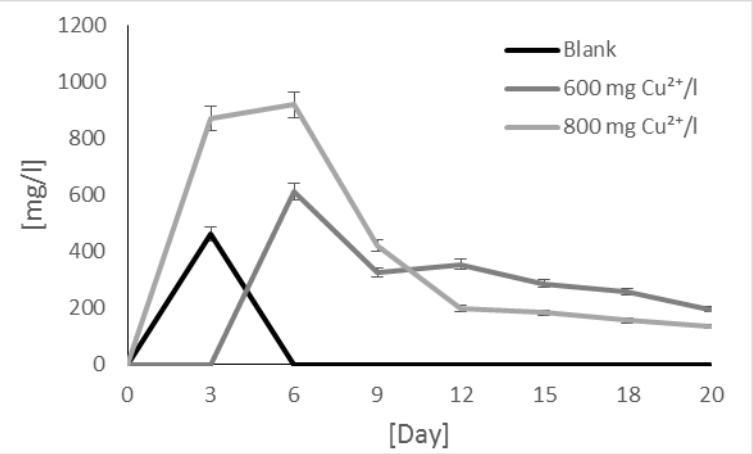

CONCLUSION

The first objective of this study was to monitor operating parameters as pH, volatile acids (acetic, propionic, butyric and valeric acid) content in sludge and biogas production and quality during the anaerobic stabilization of sewage sludge in laboratory conditions. The second objective was to observe the effect of copper addition on the above parameters. Hypothesis which predicted the changes of monitored parameters mainly biogas quantity and quality, volatile acid content and pH after copper addition, was partly confirmed. There were no significant differences in biogas and methane production after addition of 600 and 800 mg Cu^{2+}/l. On the other hand, significant differences can be seen on pH, acetic and propionic content in sludge and hydrogen content in biogas. These parameters were significantly affected by different concentrations of copper.

ACKNOWLEDGEMENTS

The research was financially supported by the project TP 6/2017: Defectoscopic quality assessment of technical and organic materials; financed by IGA FA MENDELU.

REFERENCES

Altaş, L. 2009. Inhibitory effect of heavy metals on methane-producing anaerobic granular sludge. Journal of Hazardous Materials, 162: 1551–1556.

Appels, L. et al. 2008. Principles and potential of the anaerobic digestion of waste-activated sludge. Progress in Energy and Combustion Science, 34(6): 755–781.

Czech Standards Institute. 2007. Characterization of waste - Determination of loss on ignition in waste, sludge and sediments. CSN EN ISO 15169. Praha: Czech Standards Institute.

Czech Standards Institute. 2011. Water quality – Sampling – Part 13: Guidance on sampling of sludges. CSN EN ISO 5667-13. Praha: Czech Standards Institute.

Czech Standards Institute. 2013. Sludge, treated biowaste, soil and waste – Calculation of dry matter fraction after determination of dry residue or water content. CSN EN 15934. Praha: Czech Standards Institute.

Liebetrau, J. et al. 2012. Operation of Biogas Plants. In Guide to Biogas. Gülzow: Fachagentur Nachwachsende Rohstoffe e. V., pp. 85–114.

Straka, F. et al. 2010. Bioplyn – příručka pro výuku, projekci a provoz bioplynových systémů. Praha: GAS s.r.o.

Ward, A.J. et al. 2008. Optimisation of the anaerobic digestion of agricultural resources. Bioresource Technology, 99: 7928–7940.

Laboratory equipment for testing hydrostatic transducers

Marek Halenar, Jozef Nosian
Department of Transport and Handling
Slovak University of Agriculture in Nitra
Tr. A. Hlinku 2, 949 76 Nitra
Slovak Republic

xhalenarm@is.uniag.sk

Abstract: The purpose of this article is to verify the measurement of the proposed laboratory equipment for the testing of hydrostatic transducers that serves to monitor the operation and evaluation of the components of the hydraulic circuit and the energy carrier used. The aim is to test the operation of the proposed hydraulic circuit within the range of selected operating pressures, flows and temperatures of the working fluid using the hydraulic pump of the QHD-17R tractor used in hydraulic drives of agricultural and forestry tractors. Using the verification measurement, we have proven that the proposed laboratory test equipment is suitable for testing hydraulic components as well as potential for testing and monitoring changes in the physical and chemical properties of hydraulic fluids.

Key Words: hydraulic testing transducers, verification measurement, flow characteristics

INTRODUCTION

The knowledge of physical quantities of working fluids is particularly important in the calculation of hydraulic mechanisms. It is very important to have a look at the chemical and ecological properties because all the materials used are compatible with working fluids and possible leakage of liquids can cause serious environmental problems. Currently, lubricant manufacturers are constantly seeking to improve the quality of hydraulic oils used in agricultural equipment and to reduce the impact on the environment. Hydraulic circuit and hydraulic fluid components must meet all hydraulic system requirements. The proposed device is multifunctional and serves to test the hydraulic pumps used in agricultural tractors, and by its versatility it contributes to the greening with the possibility of testing different types of ecological fluids. The advantage of laboratory tests is to shorten the time of the laboratory test. Based on the test device, we monitor the life of the hydrostatic transducers and the operating fluids themselves. By simulating load conditions such as temperature change, constant or operating pressure change, flow change, degradation of operating fluids, which can be precisely defined on the basis of the physicochemical properties of liquids, occurs. Because of this, they use accelerated hydraulic components and fluids testing in laboratory conditions to simulate operational conditions, usually specified by a standard (Tkáč et al. 2018). In this paper, we will test the functionality of this hydraulic laboratory testing device, which was designed to reduce the time required for operational testing of hydraulic fluids. Hydraulic equipment is widely used in powerful mechanisms of agricultural and forest machines as well as in many other areas. The development of modern hydraulic components is aimed at increasing the transmitted power, reducing the energy intensity, minimizing the environmental pollution and increasing the technical life and machine reliability (Asaff et al. 2014, Kosiba et al. 2016, Tóth et al. 2014). Universal tractor transmission oils (UTTO) are designed for hydraulic and transmission systems of agricultural tractors. These fluids provide lubrication functions in the gear box and transmission of energy in the hydraulic system of the tractor (Tkáč et al. 2017). The design of the hydraulic device is based uses of reducing valve which by authors (Kosiba et al. 2016, Tkáč et al. 2014).

The proposed experimental hydraulic laboratory device enables testing various types of hydraulic-transmission fluids that are being used in farming machinery and devices at various temperatures with constant or cyclical working pressure and constant or variable flow. The operational temperature of a hydraulic fluid is an important parameter that influences the fluid's physical and chemical properties. That is why the laboratory testing device also includes a cooling circuit.

MATERIALS AND METHODS

Testing device for monitoring the lifetime of hydraulic pump is increasingly important due to the efficiency, time and economical requirements of the tests. These aspects call for the development of a laboratory testing device that is able to meet such requirements. The proposed laboratory device will perform the tests by application of operating pressure, change of the hydraulic fluid's working temperature and working cycle acceleration. When establishing the testing device's requirements, we use technical parameters of the tested transducers and technical standards, which specify the requirements for reliability as follows: The technical life with rated parameters, under cyclical pressure-induced strain from zero until rated pressure with the frequency of 0.5–1.25 Hz, under pressure increase of 10–35 MPa/s, must have at least 10^6 cycles. The hydraulic pumps flow efficiency can show a maximum decrease of 20%.

Verification measurements have been performed based on the following procedure:

- during the fluid test, the hydraulic pump in the testing device was under cyclical pressure, fluctuating between 0.4 MPa and the hydraulic pumps rated pressure of 8 MPa,
- the fluid's temperature was kept at 40 °C, which prevents a mistake in the measurement and deterioration of the hydraulic fluid due to viscosity difference caused by the temperature change during measurement,
- the possibility of the hydraulic pumps change in speeds due to changing pressure was monitored with a frequency converter influenced by the increase of pressure with monitored torque curve as well.

The laboratory testing device (kinematic scheme on Figure 1) is powered by an electric motor (3) that is connected to a frequency converter (4), in order to achieve constant speeds. The hydraulic circuit is secured against overload mechanically by pressure valves (16) and electronically by pressure valves (6). To monitor operation levels, the hydraulic circuit is equipped with temperature sensors (9), (19), (20), pressure sensors (5), (10), (22) and flow sensors (2). The hydraulic circuit is also equipped with a pressure accumulator (14) to dampen pressure flushes. The accumulator is turned on by a throttle valve (12). Reaching operating temperature or simulating a higher thermal load of selected power carriers is done by an isolated reducing valve (14) that is controlled via a three way valve (7). The tank (18) is equipped with an inlet filter (20), as well as an outlet filter (16). To maintain the required operational temperature, the hydraulic circuit is equipped with a cooler (17). The hydraulic valve (11) in the hydraulic circuit cyclically applies a load on the hydraulic pump (1).

Figure 1 Scheme of the laboratory testing device for hydraulic fluids and hydraulic components testing

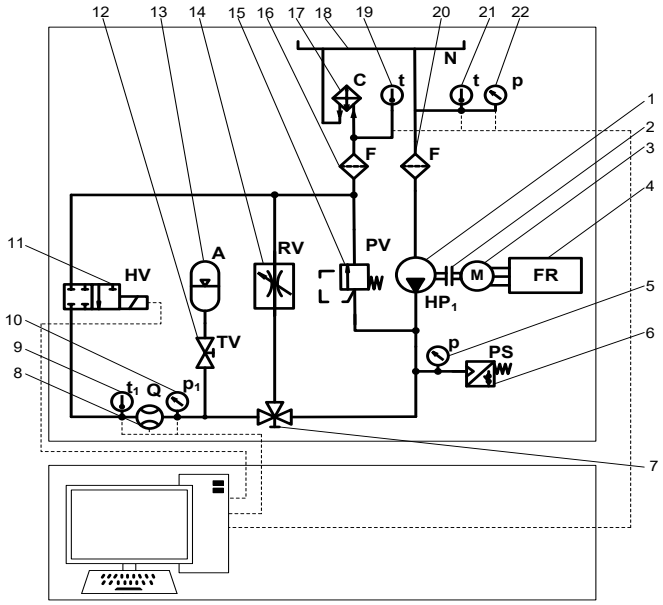

Legend: (A – Hydraulic circuit 1, B – Control and assessment circuit, 1 – HG1 hydraulic pump, 2 – coupler, 3 – electric motor, 4 – frequency converter, 5 – pressure sensor, 6 – electric pressure sensor, 7 – three way valve, 8 – flow rate sensor, 9 – temperature sensor, 10 – pressure sensor, 11 – hydraulic valve, 12 – throttle valve, 13 – pressure accumulator, 14 – reducing valve, 15 – pressure valve, 16, 20 – filter, 17 – cooler, 18 – tank, 19, 20 – temperature sensor, 22 – pressure sensor)

The laboratory testing device is equipped with a control and assessment circuit (B) to assess the measured data and control the whole system. The control and assessment circuit is interconnected with sensors in the hydraulic circuit (A).

RESULTS AND DISCUSSION

Modelling of laboratory testing device operation

The method for the verification measurement of the QHD-17R tractor hydraulic pump, which is tested by the laboratory testing device, comprises of estimating a relation between the flow of the hydraulic pump and its speeds. The measured data was compared with the manufacturer's data for the particular hydraulic pump Q_G = 23.00 dm^3.rpm, while n_G = 1,500 rpm, resulting in no significant differences between the two datasets Q_G = 23.00 dm^3.rpm. The differences were caused by the large amount of components in the hydraulic circuit, where sudden opening or closing of the distributor was causing pressure spikes.

Other usage possibilities of the laboratory testing device are derived from proposed hydraulic pump lifetime tests. This verification measured the flow of the hydraulic pump and the pressure in the hydraulic circuit in relation to opening and closing of the electro-hydraulic distributor (40) in a 5 seconds interval. The aforementioned verification measurements were made at 1,500 rpm speeds of the hydraulic pump, while the frequency converter (4) maintained constant speeds. The verification measurement results are shown in Figures 2–3.

By verification measurement of the QHD-17R hydraulic pump on the experimental laboratory device we proved that the relation between the flow and the hydraulic pumps speeds is in accordance with the manufacturer's data. We detected a difference of only 1-2%, which could have been caused by a measurement error or by measuring instruments being inaccurate within permissible limits. If we look at the relation between pressure and cycle time, the analytically set pressure values were not exceeded. Maximum pressure at speeds of 1,500 rpm was 8.19 MPa and minimum pressure was 0.3 MPa. The detected relations between the hydraulic pumps flows at speed of 1,500 rpm correspond with the pressure data during the opening or closing of the electrohydraulic distributor. Figures 2 and 3 shows that when the hydraulic pump reached speed of 1,500 rpm; the electrohydraulic distributor was in operation.

Figure 2 Verification measurement of hydraulic pumps flow (Q_G) in relation to time (t) at hydraulic pumps speeds (n_G) of 1,500 rpm

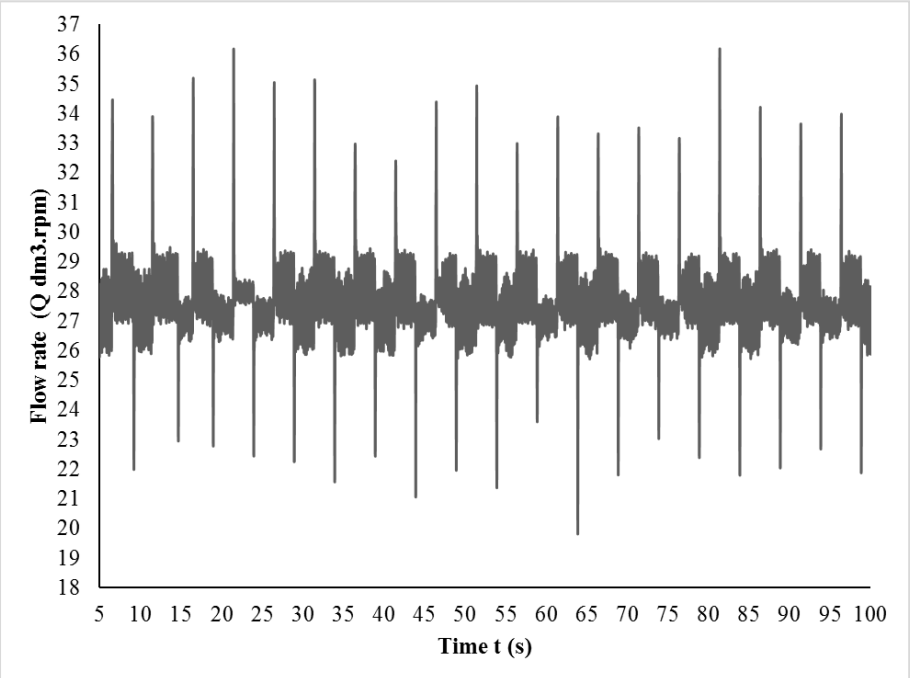

Figure 3 Verification measurement of pressure (p) in relation to time (t) at hydraulic pumps speeds (n_G) of 1,500 rpm

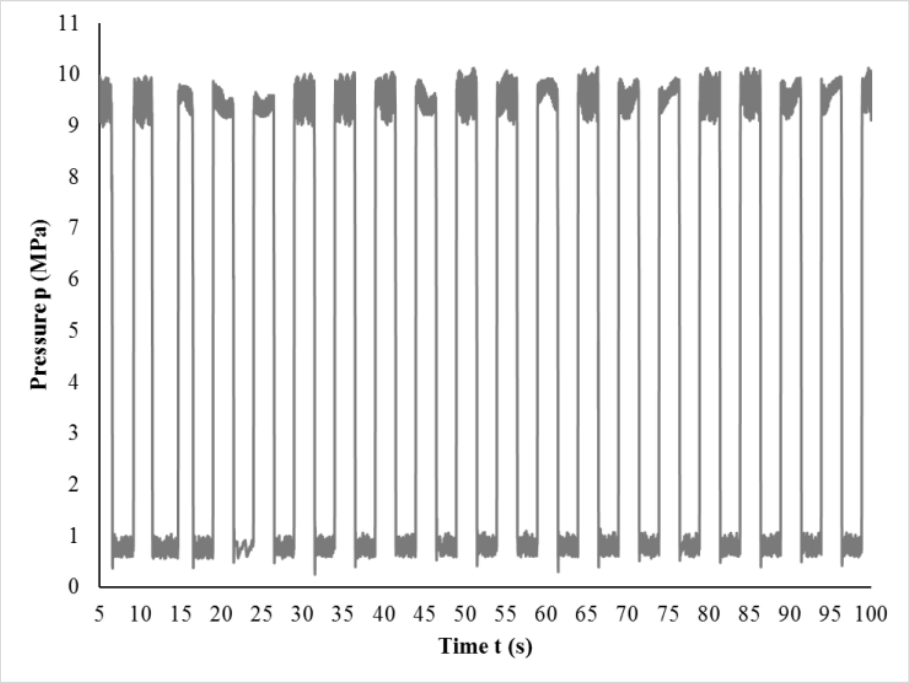

By the verification measurement, we proved that the proposed laboratory testing device is suitable for testing hydraulic circuit components, as well as, potentially, for testing and monitoring the changes in physical and chemical properties of hydraulic fluids.

Flow rate and flow efficiency of the hydraulic pump

The measurement of the flow characteristics is used to determine the impact of the hydraulic fluid on the hydraulic pump life. The flow efficiency was calculated by the formula 1. Standard deviation σ is defined as a positive square root of variance. Standard deviation is calculated if we have a complete set of possible states of the process (system). In probability theory and in statistics, standard deviation or mean square deviation is a measure of statistical dispersion. Simply said, it refers to how widely are the values distributed in a set (Kosiba et al. 2013).

When using a larger range, it is less likely that the process will run incorrectly, including the case when measured values are outside of control limits, and they are caused by random deviations. The use of a wider range makes it difficult to identify changes in the process that are non-random and must be determined. We have chosen to evaluate the data from -1σ to +1σ so that we obtain the values as close as possible to the nominal pressure of the hydraulic pump. When choosing the range of -1σ and +1σ, the credibility of results is 68.27%. The flow efficiency of the hydraulic pump was calculated from this sample of values. Figure 4 shows the flow characteristics (linear regression $Q = 0.0161 \cdot n$, $R^2 = 0.9994$.) and Figure 5 flow efficiency of the hydraulic pump after statistical processing.

Figure 4 Flow characteristics of hydraulic pump

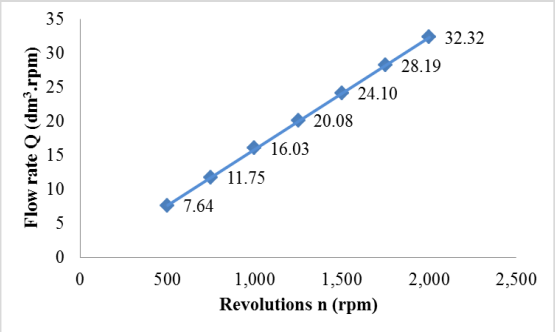

Figure 5 Flow efficiency of hydraulic pump

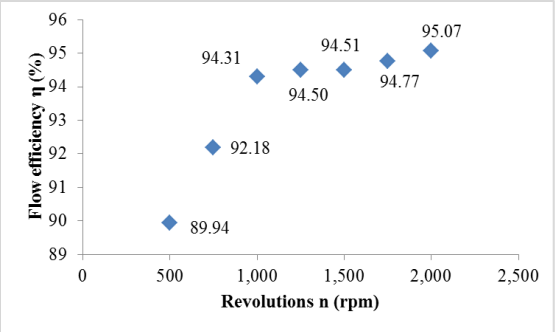

Hydraulic pump-operating conditions affect significantly the pump efficiencies, it is very important to understand how the pump efficiencies depend on the hydraulic pump-operating conditions. The measurement of the flow characteristics is used to determine the impact of the hydraulic fluid on the hydraulic pump life. Flow rate of the hydraulic pump at the speeds of 1,500 rpm (nominal speed) was n = 16.03 rpm and flow efficiency was η = 94.50%. Increased of flow rate depending on the speed is consistent by authors (Kim et al.2013, Dobrota et al. 2010) evaluated the flow efficiency of the hydraulic pump at the nominal speed η = 95.73% depending on the pressure p = 20 MPa and (Michael et al. 2012) evaluated the flow efficiency at the nominal speed η = 95.00%. These values corresponded with our results. Decrease of hydraulic pump increase flow efficiency after speed at n = 1,500 rpm corresponded with publication of the authors Li et al. (2011). Inaguma and Yoshida (2013) evaluated the flow efficiency of the hydraulic pump at the nominal speed η = 95.00 %. This value corresponded with our results.

CONCLUSION

Farm machinery manufacturers have recently tried to introduce into hydraulic systems new plant- or synthetic-based fluids and oils that are more environmentally friendly, decomposable and less damaging to water resources (Kučera et al. 2017). The main requirement of the laboratory testing device was to simulate a real hydraulic circuit of a farm tractor as closely as possible. That is why the hydraulic circuit components, cyclical load application and fluid temperature were selected based on technical and operational data of farm machinery and its real-life use. The proposed device can monitor parameters of tested hydraulic fluids and assess the changes of their properties caused by pressure and temperature.

One of the reasons for the high price of environmentally friendly hydraulic fluids is the necessity for the manufacturers of hydraulic pumps to approve the usage of the fluid in the hydraulic system and to verify its compatibility with hydraulic circuit components (Tkáč et al. 2018, Tkáč et al. 2014). The proposed laboratory testing device significantly facilitates testing and assessing the usage of various power carriers in the hydraulic systems of tractors and, optionally, provides the possibility to assess the effects power carriers have on the properties of hydraulic circuit components.

ACKNOWLEDGEMENTS

Supported by the Ministry of Education of the Slovak Republic, Project VEGA 1/0155/18.

REFERENCES

Asaff, Y. et al. 2014. Analysis of the Influence of Contaminants on the Biodegradability Characteristics and Ageing of Biodegradable Hydraulic Fluids. Strojniski Vestnik – Journal of Mechanical Engineering, 60(6): 417–424.

Dobrota, D. et al. 2010. Experimental modelling of volumetric efficiency of high-pressure external gear pump. Nase More, 57(5–6): 535–240.

Inaguma, Y., Yoshida, N. 2013. Mathematical analysis of influence of oil temperature in hydraulic pumps for automatic transmissions. SAE International Journal of Passenger Cars – Mechanical Systems, 6(2): 786–798.

Kim, J., Kim, S. 2013. The flow rate characteristics of external gear pump for EHPS. 4th International Conference on Intelligent Systems, Modelling and Simulation, Bangkok, Thailand: 346–349.

Kosiba, J. et al. 2016. Monitoring oil degradation during operating tests. Agronomy Research, 14(5): 1626–1634.

Kosiba, J. et al. 2013. Study of the impact of synthetic fluid on the lifetime of hydraulic pump. Advanced Materials Research, 801: 7–12.

Kosiba, J. et al. 2016. Effect of ecological hydraulic fluid on operation of tractor hydraulic circuit. In Trends in Agricultural Engineering 2016. Praha: Czech University of Life Sciences: 317–322.

Kučera, M., Aleš, Z. 2017. Morphology analysis of friction particles generated in tractor transmission oils. Acta Technologica Agriculturae, 20(3): 57–62.

Li, Y., et al. 2011. The Flow Pulsation Analysis of an External Gear Pump. Advanced Materials Research, 236–238, 2327–2331.

Michael, P. et al. 2012. An Investigation of external gear pump efficiency and stribeck values. SAE Technical Papers: 8.

Tkáč, Z. et al. 2017. Research of biodegradable fluid impacts on operation of tractor hydraulic system. Acta Technologica Agriculturae, 20(2): 42–45.

Tkáč, Z. et al. 2008. Testing stands for laboratory tests of hydrostatic pump of agricultural machinery. Research in Agricultural Engineering, 54(1): 183–191.

Tkáč, Z. et al. 2018. Experimental hydraulic device for the testing of hydraulic pumps and liquids. Tribology in Industry, 40(1): 149–155.

Tkáč, Z. et al. 2014. Hydraulic laboratory devices for testing of hydraulic pumps. In Materials, technologies and quality assurance II. Pfäffikon : Trans Tech Publications: 111–117.

Tóth, F. et al. 2014. Study of tribological properties of chosen types of environmentally friendly oils in combined friction conditions. Journal of Central European Agriculture, 15(1): 185–192.

Evaluation of fastening ability of cable clamp

Vaclav Kaspar, Jaroslav Zacal, Petr Dostal, Jakub Rozlivka
Department of Technology and Automobile Transport
Mendel University in Brno
Zemedelska 1, 613 00 Brno
CZECH REPUBLIC

vaclav.kaspar@mendelu.cz

Abstract: This work deals with testing the reliability of clamping of jaws with special cable clamps used in power engineering. The clamp is one of the pivotal elements of the power lines. This is where the power cable is fastened. In case of overloading and subsequent malfunction, a dangerous situation has occurred, in the extreme situation of falling down the power line lead directly to the ground. Testing the fastening capability of this element is therefore a matter that is important to deal with. A special device simulating the actual clamp load in practice was developed for test carrying cable clamps. The test system was connected to a universal blasting device, and the maximum load force was found to pull the deflected object, or to deform or destroy the clamp. The aim is to determine the specific load force for this load-bearing element, which will without fail perform its function with respect to the required safety.

Key Words: cable clamp, tensile test, deformation, maximum loading force, safety

INTRODUCTION

The development of the transmission system and its history dates back to the turn of the 18th and 19th centuries. At the time of Czechoslovakia, its length was around 1 500 km of the network, but twenty years later it was about 37 000 km of the transmission system. Today it is only 250.000 km of electricity in the Czech Republic.

The construction of the power line fastening to the columns has also undergone considerable development. First, the wires were attached directly to the ceramic insulators, pointing upwards. With increasing demands for energy transfer, the system voltage increased and the structure of insulators and clamping elements changed. The original steel clamps have been replaced by modern clamps of tempered cast iron, which are well anti-corrosion protected and have better clamping capabilities (Energetika servis).

The clamping and mechanical properties of these clamps play a major role in the reliability and safety of the entire transmission system. It is therefore appropriate to deal with them in more detail.

MATERIAL AND METHODS

Material

The material from which the test object is made is the tempered cast iron EN-GJS-350-22 (Novotný and Filípek 2004) with anticorrosive protection by galvanizing.

The object being tested is a cable clamp (Figure 1) designed to mount self-supporting cords with a supporting rope to masts. The clamp consists of a hook and its own clamp, the top of which is tilting. The clamp hook is designed to tow self-supporting cables, but is also used to secure the cables in case it is released from the jaws of the clamp. The clamps of the clamps are provided with a wavy groove and are pulled with a galvanized M10 screw. The clip clamp must be so firm that the rope does not slip (ČSN EN 50341-3:2002/Z2).

Methods

Testing was carried out on fifteen pieces of cable sockets. The test was performed on a universal tear-off device ZDM – 50 connected to the computer. The meter's software records force values every 0.02 seconds. Reliability of measuring tensile force is 0.07 N. The measurement has always been stopped when the clip stops performing its function or is broken. Universal testing device was setup for force drop 20%.

Preparing the test object

To test the cable clamp, a special clamping device (Figure 2) has been developed and constructed to simulate the load of the test object in real practice. The clamp in the product forms a circular steel wire. The product consists of three parts, a stirrup, a rod and a drawbar.

The main part of the clamping device is the rod. The rod is represented by circular steel, which is a tough, self-supporting cable in practice. The bar is firmly clamped between the jaws of the clamp. Their grip is secured by a M10 screw, tightened to a prescribed tightening torque of 50 Nm.

Another part of the preparation is a stirrup. The thimble has a wrinkled "Y" shape. It was made of structural steel ČSN 11373 (EN S235JR) by welding in a protective atmosphere by method 135, according to EN ISO 4063 (Polák and Dostál 2013). The stirrup arms are ended by massive bored steel rollers. A stick is inserted into their holes. The rollers allow easy insertion of the bar when mounting the clamp into the product, while eliminating possible parasitic side forces that could negatively affect the measurement.

The last part of the clamping device is a pull rod. This is a strip steel with a bore for screw connection. The rod is screwed to the fixed part of the test clip and serves as a mechanical connection between the clamp and the test device.

Figure 1 Tested clamp

Figure 2 Tested clamp inserted into clamping device

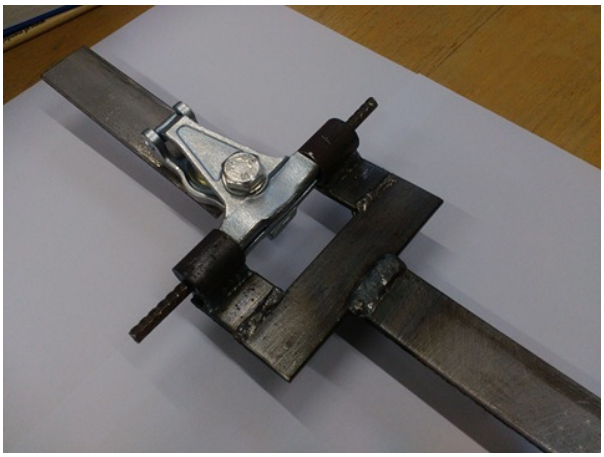

Figure 3 Clamp inserted between jaws of the blasting device

Course of the test

The test buckle clamped into the clamping device was inserted between the jaws of the universal blasting machine ZDM–50 (Figure 3). A static tensile test was then run. This stressing process was monitored and load force values N were recorded. The result of the measurement was processed into the graph as a force–load dependence on time (Začal et al. 2016).

RESULTS AND DISCUSSION

The data obtained from the measurements was processed and a graph representing the behaviour of the clamp exposed to the real load was created (Figure 4). The resulting graph shows the force acting on the buckle at time *"t"*.

In the first phase, the force gradually increases to the first break - a slight decrease. There may be slippage between the jaws and the tool, or the clearance of the screw connection. Strength continued to grow steeply, with strong jaw strain on the cable clamp tested.

Upon reaching the maximum force of 15672 N, a sharp drop in force occurred see Figure 4. With this load, the clamp is deformed and the jaws open when the clamped object is released. For this load, there is a structural problem with both parts of the clamp. The clamps are strained to bend. There was irreparable deformation and bending of the clamp arms.

The value of the maximum tensile force described here is the average maximum force. The variability of data obtained by measuring fifteen samples is described by standard deviation: 153.5 N. The confidence interval for alpha 0.05 is 77.8 N.

Figure 4 Load force depending on time

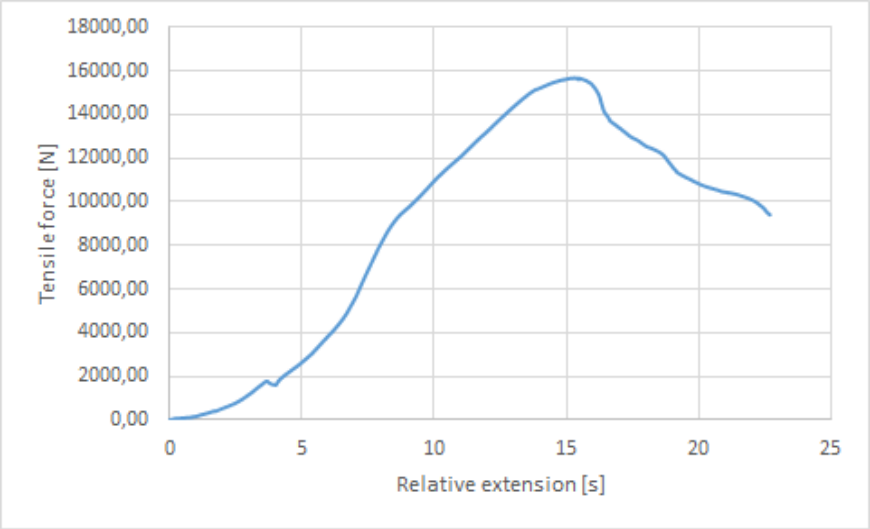

For better clarity, the measured data was recalculated and a graph plotting the dependence of the relative elongation of the sample on the voltage was generated (Figure 5). Conversion to tensile stress [MPa] was related to the projection of the area of the clamped object in the area of the entire clamping surface of the clamp jaws. The maximum stress reached 42 MPa. The object under test was extended by 22.7 mm. After that, the exam was stopped.

Subsequent photos display the clip after the test is completed. When the maximum tensile stress reached 42 MPa (load force 15672 N), the clamp was deformed and the jaw was opened (Figure 6). The snapped object slid off, the clamp stopping its function. After removing the clamp from the product, the jaws have not returned to their original state, therefore the deformation of the clamp is permanent and is not suitable for further use.

Specifically, both parts of the clamp were damaged. The fixed part of the clamp extends to the deformation in the constriction between the clamp body and the jaws. The movable (clamping) portion bent evenly over its entire length.

Figure 5 Dependence of stress on the relative extension of the test object

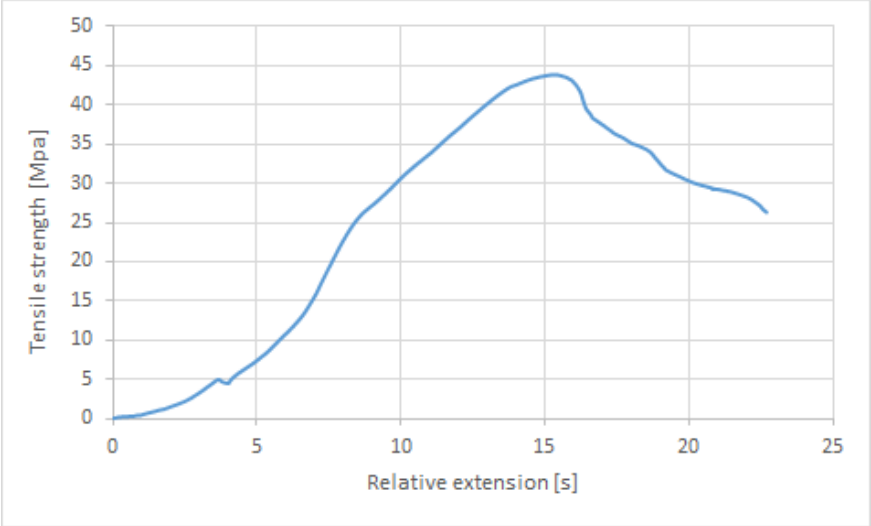

Preventing this undesirable phenomenon and thus increasing the total carrying capacity of the cable clamp would be enhanced by both emergency sites. However, this solution would have a negative impact on the overall quietness of the clamping device. Another solution could be to use better quality material (Novotný and Filípek 2004).

Figure 6 Deformation of the tested clamp

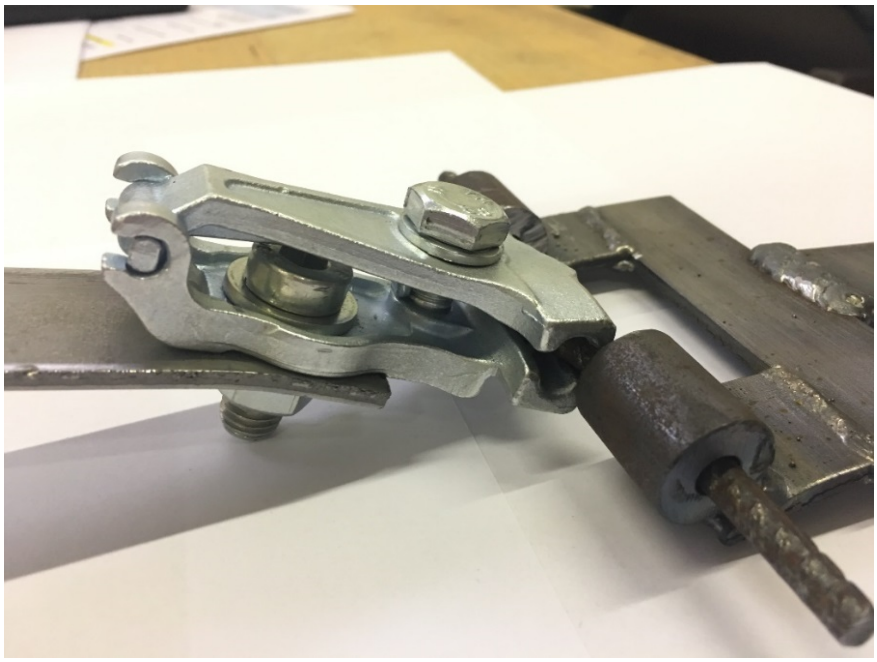

CONCLUSION

The behaviour of the clamp at its extreme load was analysed when testing the cable clamp. All jaws tested saw the jaws open and the clamped object slid off. There was a permanent deformation of both parts of the clamp. In the fixed part there was a deformation in the constriction between the body and the jaw. The clamping portion of the clamp has deformed almost uniformly over its entire length.

To overcome this limit state and increase the clamping capacity, it would be possible to amplify both critical points. This, however, would result in an increase in its total weight. The second solution would be to use a higher strength material for the clamp making.

The tested terminals were defective at an average load of 15 672 N. But this force is limiting. For practical use, a safety factor of k must be included. In the case of k = 3, therefore, the safe loading force is 5 224 N. The safety factor is chosen by the power line designer (ČSN EN 1991-1-4).

The load on individual parts of the power grid and its components is influenced by a large number of factors. This is not just a cross section of the conductor which, in a way, significantly influences the static load of the load–bearing elements, is another series of specific factors. One of them is the wind load on the system, where it is necessary to take into account the location of the building within the map of windy areas. Another example is the alternation of temperatures, the stressing of elements by thermal expansion, and, last but not least, the frost that can cause great damage and must be counted. It Had been assumed that the clamp is connected to a rigid base. However, practical situations do arise wherein the member to which the clamp does not provide a rigid base. A typical example is a clam that transfers the tensile component in steel cable that carries the load into the structure.

REFERENCES

EGÚ. 2001. Elektrická venkovní vedení s napětím nad AC 45 kV - Část 3: Soubor Národních normativních aspektů. ČSN EN 50341-3:2002/Z2. Praha: EGÚ–Laboratoř vvn a.s.

Energetika servis s.r.o. 2010. Ocelové konzoly typ IZVE–DS se svorníky na dřevěné sloupy venkovního vedení VN pro jednoduché izolované vodiče. Available at: http://www.energetika-servis.cz/tp/200603/200603.PDF. [2018-09-10].

Novotný, K., Filípek, J. 2004. Problematika fázového, strukturního a komplexního popisu mikrostruktury slitin. Kvalita a spolahlivosť strojov. Nitra: Katedra spolahlivosti strojov, pp. 219–221.

Polák, V., Dostál, P. 2013. Analysis of Modern Methods in Welding Technology of Technical materials. In Proceedings of International PhD Students Conference MendelNet 2013 [Online]. Brno, Czech Republic, 20 November, Brno: Mendel University in Brno, Faculty of Agronomy, pp. 847–851. Available at: https://mnet.mendelu.cz/mendelnet2013/articles/47_polak_925.pdf. [2018-09-10].

TNK. 2007. Zatížení konstrukcí: Obecná zatížení - Zatížení větrem. ČSN EN 1991-1-4. Praha: ČVUT v Praze, Kloknerův ústav, Technická normalizační komise: TNK 38 Spolehlivost stavebních konstrukcí.

Začal, J. et al. 2016. Compare Tensile Test of Composite and Aluminium Mateirals by Acutstic Emission. In International PhD Students Conference MendelNet 2016 [Online]. Brno, Czech Republic, 9–10 November, Brno: Mendel University in Brno, Faculty of AgriSciences, pp. 949–954.

Tensile testing of 3D printed material with digital image correlation

Vaclav Kaspar[1], Jaroslav Zacal[1], Jakub Rozlivka[1], Martin Brabec[2]
[1]Department of Technology and Automobile Transport
[2]Department of Wood Science
Mendel University in Brno
Zemedelska 1, 613 00 Brno
CZECH REPUBLIC

vaclav.kaspar@mendelu.cz

Abstract: Work is focused on Fused Deposition Modelling (FDM) in 3D printing with accented printing of samples from polyactid acid (PLA), which is a most common material used in 3D printing. The standard dog-bone shaped samples reinforced by internal ribs arranged in a grid with two different densities – 10% and 20% of internal sample volume filled by ribs, were tested for tensile strength. The development of surface strain fields during loading were analysed by a non-destructive method based on the digital image correlation (DIC) principles. It was concluded that in comparison of load curves and strain fields the support grid volume had a great effect on ultimate tensile force and deformation response of samples. From DIC pictures taken in individual loading phases it can be determined the places exhibiting the smallest surface strains, where the support ribs are located.

Key Words: 3D printing, FDM, tensile testing, Digital Image Correlation

INTRODUCTION

Most profound and commonly used method of additive manufacturing (AM) is the Fused Deposition Method (FDM). This method provides relatively low-cost and fast production of functional prototypes, which could even approach the final product within their specifications. Models manufactured using the FDM method could be formed into almost any shape, including the functional and solid-mounted systems, which are conducted with a minimal waste production, negligible in comparison with cutting or milling (Píška 2009). Principle of this method lies in heating of thermoplastic, which is rolled on the coil in form of filament, below the melting point and its feeding through rollers into the heated nozzle of a selected diameter. Here the filament is heated to a temperature above its melting point and then the material is squeezed through the nozzle into the working area, where it is deposited in thin layers onto the printing pad (Staněk et al. 2012). Used PLA material is a biodegradable plastic because it originates from natural plants such as corn, sugarcane or potatoes (Ashby and Bréchet 2003). Behaviour of polymerous materials in regard to their mechanical properties is a highly complex issue (Průša and Průša 2014). Polymers could behave as a glass, liquid, rubber, or soft and elastic solid bodies. These properties are determined by their molecular structure. Polymers, which are structured in a spatial grid pattern, show a tendency to be more fragile than polymers of other structural type (Nicholson 2006). Fundamental mechanical characteristic of material is its tensile performance. When the test sample is subjected to uniaxial tensile loading, it is possible to examine its stress-strain behaviour by means of a work diagram characterizing the relation between proportional stretching (tensile strain) and normative tension (tensile stress) in the course of loading. This curve is determined experimentally and provides an important information on material characteristics (Běhálek 2016).

Objective of experiments was the comparison of structural grid density influence on mechanical properties of materials in tension printed on FDM 3D printer. In order to evaluate the tensile mechanical behaviour of samples more complexly, their deformation response was analysed by means of optical system applying the three-dimensional Digital Image Correlation (3D-DIC) method, which is based on stereovision assessment of tested sample surface (Harper 2002).

MATERIAL AND METHODS

Polylactic acid – PLA – is the most commonly used material in 3D printing. This thermoplastic polyester is harvested from a renewable resources, e. g. corn or potato starch, and is biologically degradable in order of months (Veselka and Mikulčík 2008). This material is widely popular, mainly due to its low thermal expandability, which is so low that in most cases there is no need for a heated pad in course of printing. In comparison with acrylonitrilebutatienstyrene (ABS), the PLA is much easier to process in comparable manufacturing conditions, but final products are less stable in higher temperature environment. Printouts are usable in temperatures up to 60 °C, then the material becomes plastic. Experimental samples are shown in Figure 1.

Figure 1 Shape of testing specimen according to ČSN EN ISO 527

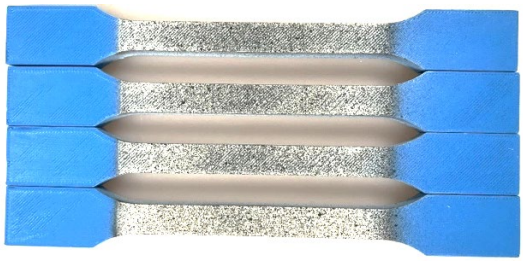

Sample preparation

FDM 3D printer forms the final printouts in a way where the filament is melted in a nozzle to a temperature above its melting point and the material is extruded into the working area, where it is deposited in thin layers onto the printing pad. All the samples were manufactured in the same conditions, where the nozzle was heated to 210 °C, printing pad was preheated to 60 °C and printing speed was set to 40 mm/s with enabled printing area cooling. Temperatures were set according to printing material manufacturer's recommendations. Bottom and top sample face consists of full 7 layers in a rectilinear pattern and sample shell by 2 layers. Layer thickness was set to 0.15 mm as a default printer setting for a majority of prints in normal quality. Difference between samples lies in support grid volume percentage. Support grid was oriented in +45° and -45° to sample major axis. Subsequently, the top and bottom layers were printed, not only for visual reasons, but also for a proper and compact coverage of a support grid. Entire sample set was printed on the FDM 3D printer Original Prusa i3 MK3. Layout and quantity of the support grid is shown on Figure 2 for individual sample groups.

Figure 2 Percentage ratio of support grid in individual samples

Testing of samples

Tested sample was clamped into the self-locking tensile jaws and subjected to uniaxial tensile load by a universal testing machine Zwick Z050/TH 3A. In course of test the basic continuously observed parameters were sample stretching (in mm) depending on applied tensile force (in N). The objective was to compare various samples; therefore, all testing procedures were conducted identically according to ČSN EN ISO 527. Tested samples were stretched in direction of its major axis in constant quasi-static loading rate of 2 mm/min, until any of end-testing criteria was reached such as force threshold or elongation threshold value.

Optical measurement was conducted with an acquisition set consisting of two CCD cameras (AVT Stingray Cooper F-504 B, Allied Vision Technologies, Osnabrück, Germany) with transversal dimensions of photosensitive cell 3.45 µm and sensor resolution 2452 × 2056 px = 5Mpx. Cameras were equipped with Pentax C2514-M lens (Pentax Precision Co., Ltd., Tokyo, Japan) with focal length 25 mm. Cameras were configured into the stereoscopic (3D) configuration (see Figure 3, left). In order to enhance the accuracy and validity of deformation measurement, the captured sample surface was coated with high-contrast black and white speckle pattern with stochastic speckles distribution (see

Figure 3, right). The speckle pattern was applied by spraying the matte thin white paint, which was after drying sprayed over with variously sized droplets of black paint. For maximum spatial resolution of tested surface the cameras were focused to sample surface that its field of view was fitted to the area of interest (AOI), which includes the area of 10×90 mm^2. Experimental data were recorded simultaneously in 0.25 s acquisition interval (4 Hz) using a synchronization device. Full-field strain data were obtained from partial derivatives of the displacement with Lagrange's notations using the Vic-3D software (Correlated Solutions, Inc.). Accuracy of measurements was determined based on the displacement and strains field detected in five pictures of unloaded test sample.

Figure 3 Tensile test setup with optical 3D-DIC system

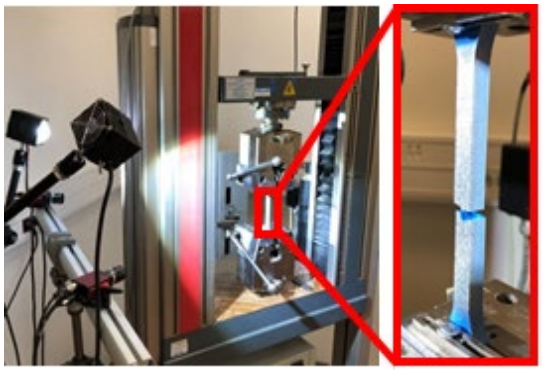

RESULTS AND DISCUSSION

Force and displacement data from individual measurements were plotted into a graph. From the graph on Figure 4 it is obvious how the support grid density influences the ultimate tensile force and overall properties of 3D printed samples for 10% grid Fmax 1424N and for 20% grid Fmax 1666N. Both sample groups demonstrate the variable maximum applied load values (Fmax), which precedes the breaking of a test sample. Vertical graph axis of load curves does not 't report a tensile stress (σ) in MPa as usual but the force value (F) in Newtons (N). The tension stress is calculated as the force divided by cross-sectional area of the sample. However, the ribbed structure of sample volume does not allow to exactly determine the cross-section area at the breakpoint. All samples are identical in their dimensions, therefore the highest average ultimate tensile force (Fmax) theoretically equals to highest tensile strength (Rm).

Figure 4 Comparison of recorded force curves of samples with 10% and 20% support grid volume

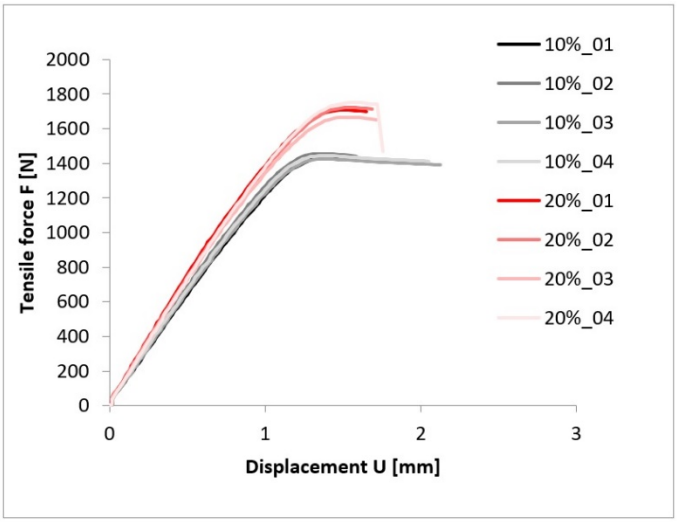

Results obtained by optical measurement (3D-DIC) in form of a strain patterns in direction of load application (ε_{yy}, *according to Lagrange*) are presented in Figure 5 and Figure 6. The deformation fields (Figure 5, 6) are located only on a sample surface and does not 't represent the 3D deformation of the internal sample structure. In Figure 5 and 6 it is obvious that deformation field in this experiment is

highly diverse in its character. These deformation fields are clearly distinguished between individual levels of applied load.

Figure 5 Strain fields in the direction of tension (ε_{yy}) at 10% grid sample (left) and 20% grid sample (right) in range of 200–1000 N

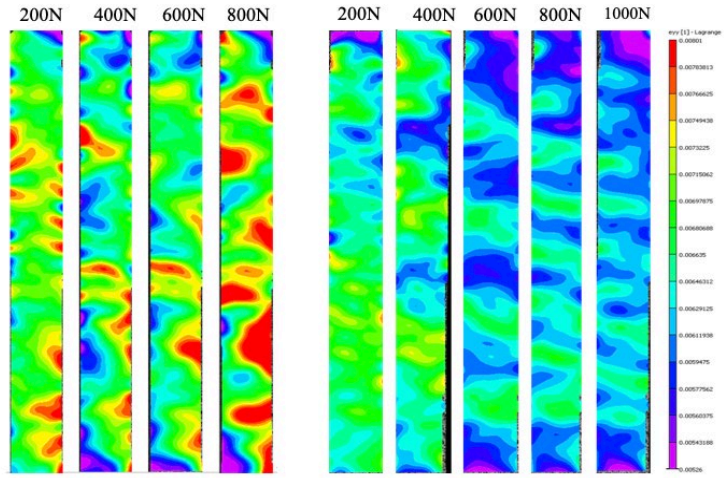

Figure 5 shows the development of tensile strains in direction of applied force at samples with 10% and 20% support grid volume due to increasing load. In red coloured areas on the sample surface the strains are the highest, therefore here occurs the highest material damage, contrary to violet colour, which determines the areas with the smallest strains. First picture from the left demonstrates the strain field in the beginning of load application at 200 N. In load levels of 400, 600 and 800 N it is obvious that areas with support grid oriented at (-45° and +45°) angle to the actual force direction show an intensification of tensile strains in areas where support grid does not 't reach the sample surface (red and orange areas). When compared the 10% and 20% support grid volume, it is apparent that denser grid support deliver higher stiffness of sample surface resulting in almost no surface strains up to 1000 N load.

Figure 6 Strain fields in the direction of tension (ε_{yy}) at 10% grid sample (left) and 20% grid sample (right) in range of 1000 N – Fmax

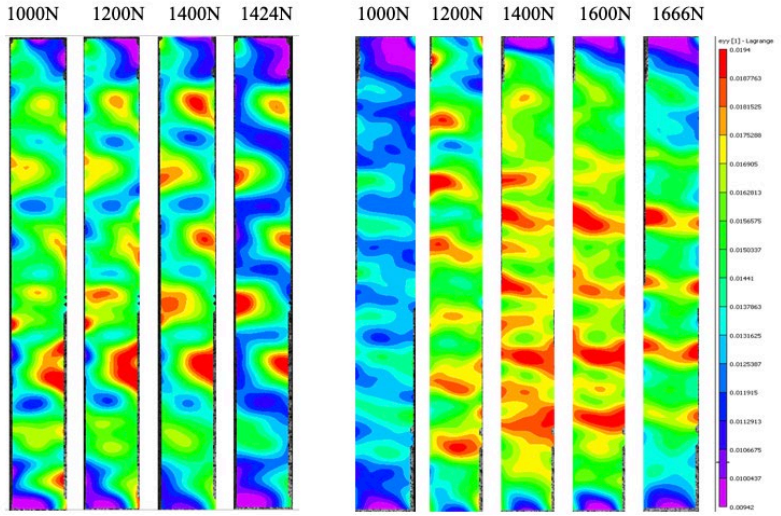

Figure 6 compares the strain field on the sample surface with 10% and 20% support grid volume at final stages of loading. At the load levels of 1000 and 1200 N the strain increases, which corresponds to more saturated colours in the deformation field of an entire sample. In final phase of loading (1424 N – 10% support grid, resp. 1666 N – 20% support grid) we can observe strain pattern that shows areas where a support ribs at ±45° orientation are located. In these areas are the smallest strains marked with blue colour. At sample edges are located red coloured hot spots, where the initial phase of micro cracks formation occurs. Strain field ε_{yy} at the final stage of loading correspond to internal sample structure.

In detailed observation of the failed samples it was concluded that samples with 10% support grid volume were broken in places where lines of support grid crossed each other Figure 7a. On the contrary, samples with 20% support grid exhibit failure between the nodes of support grid Figure 7b.

Figure 7a (left) Crack of a 10% grid sample and Figure 7b (right) Crack of a 20% grid sample

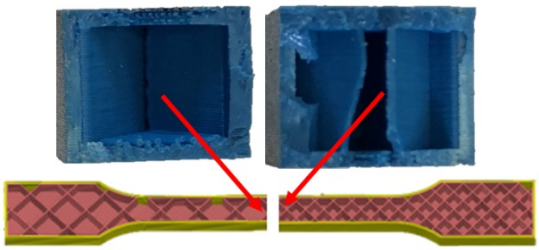

Following detailed photographs were taken with digital microscope KEYENCE VHX6000 and depict the individual layers of filament applied in course of 3D printing process, where are 7 layers of upper support and 2 layers of sample surface Figure 8. Figure also presents the internal cavities between individual adjacent layers; more details are in Figure 9.

Figure 8 Detail of crack surface of PLA material sample

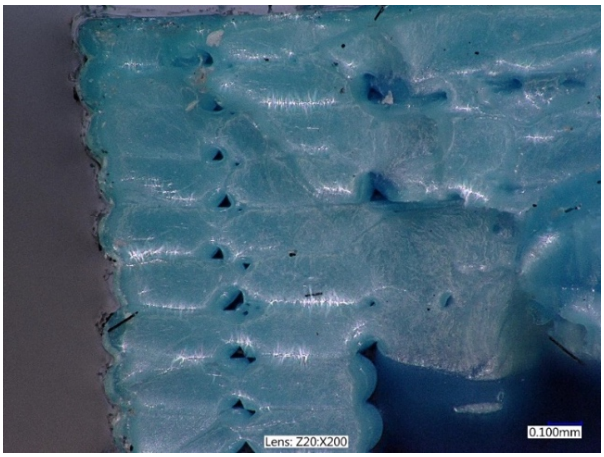

Figure 9 Detail of 2 layers of sample surface

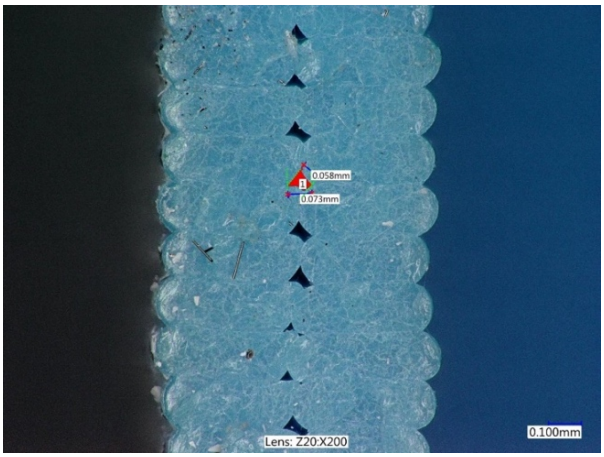

Of the common materials used in 3D printing with FDM technology the PLA material reports highly desirable mechanical properties for 3D printing in comparison with ABS material, which is highly demanding for ambient temperature in course of printing process, where in incorrect temperature occurs the undesirable shrinking of the sample. For more detailed research of gird influence it would be desirable to include other specimen of support grid shape into the experiment, namely the honeycomb grid pattern. Another important factor influencing the final sample firmness is the choice of border layers count and count of solid bottom and top surface layers. Their influence could prove more significant than support grid itself. Filament quality is a multidimensional notion which defines different parameters, from uniform spooling to biodegradability. The sample strength obtained when using a specific filament with a specific printing configuration and parameters is just one of many quality measures, and increasing the sample strength might adversely affect other parameters. The mechanical properties of a part obtained by using the FDM process depended on the filament used, and may vary between different manufacturers, colors, lots, and even spools within a single lot (Mueller 2012). However, dependencies obtained should be generalizable for all PLA-based filaments. The best combinations of printing conditions allowed for obtaining interlayer cohesion (the strength of a part loaded orthogonally to layer boundaries) close to the known parameters of bulk PLA material. This partially resolves the anisotropy problem for FDM printed parts. Bellini and Guceri (2003) printed tensile specimens and obtained an average strength of although the authors used a [0°/90°/ ± 45°] print path. In printed specimens with 90° in the XY orientation were negative air rap and the resulting tensile strength was lower due to air rap. On the other hand, the orientation as [0°/90°] direction has horizontal extruded lines. As shown in Figure 9, FDM printing method is stacking melted thread extruded filaments by applying a little pressure as nozzle between layer-by-layers (Ziemian et al. 2012). Due to the fact that

the contact area between each layer is the smallest in Figure 9 red-section, the relative adhesive force is likely to be weaker than the other sections. When a tensile force is applied to the specimen, the adhesive force is a crucial factor that determines the ability to withstand (Choren et al. 2013). These defects are either caused by the error of the printer or operator which results in the weakening of the tensile strength. Another reason why such air void are present may be due to the characteristics of the FDM printing method.

CONCLUSION

Experiment was focused on comparison of mechanical properties of materials used in 3D printing using the FDM method. Tensile testing was conducted for assessment of PLA material mechanical performance with 10% and 20% support grid volume. It was concluded that in comparison of load curves and strain fields the support grid volume had a great effect on ultimate tensile force and deformation response of samples. Experiment confirmed that objects printed of PLA material have better mechanical properties with increased support grid density. Results shows potential in printed objects with support grid could decrease the material costs while the desired mechanical properties are achieved. From a practical viewpoint the 20% grid volume represents the ideal balanced setting for achieving desired material mechanical characteristics. DIC measurements enabled the characterisation of deformation response in individual load levels in real time. From DIC pictures taken in individual loading phases it can be determined the places exhibiting the smallest surface strains, where the support ribs are located. DIC Measurements is shown as useful method for correlation between tensile testing strenght and deformation response.

ACKNOWLEDGEMENTS

The research has been supported by the project TP 6/2017: Defectoscopic quality assessment of technical and organic materials; financed by IGA FA MENDELU.

REFERENCES

Ashby, M.F., Bréchet, Y.J.M. 2003. Designing hybrid materials. Acta Materialia [Online], 51(19): 5801–5821. Available at: https://www.researchgate.net/publication/222410146_Designing_Hybrid_Materials. [2018-08-16].

Bellini, A., Guceri, S. 2003. Mechanical characterization of parts fabricated using fused deposition modeling. Rapid Prototyping Journal, 9(4), 252–264

Běhálek, L. 2016. Polymery. Verze knihy 17. [Online]. Available at: https://publi.cz/books/180/Cover.html. [2018-04-08].

Choren, J.A. et al. 2013. Young's modulus and volume porosity relationships for additive manufacturing applications. Journal of Materials Science, 48: 5103–5112.

Harper, C. 2002. Handbook of Plastics, Elastomers, and Composites. Technology New York: McGraw-Hill.

Mueller, B. 2012. Additive Manufacturing Technologies – Rapid Prototyping to Direct Digital Manufacturing. Assembly Automation, 32(2).

Nicholson, J.W. 2006. The chemistry of polymers. 3rd ed., Cambridge, UK: RSC Pub.

Píška, M. 2009. Speciální technologie obrábění. 1.vyd., Brno: Akademické nakladatelství CERM.

Průša, J., Průša, M. 2014. Základy 3D tisku [Online]. Available at: https://www.prusa3d.cz/kniha-zaklady-3d-tisku-josefa-prusi/. [2018-02-09].

Staněk, M. et al. 2012. Comparison of Different Rapid Prototyping Methods. International Journal of Mathematics and Computers in Simulation [Online], 6(6): 550–557. Available at: https://pdfs.semanticscholar.org/f99d/496ef8d0451c8735d1424dc0f644a85f0f36.pdf. [2018-08-07].

ÚNVMZ. 2012. Plasty - Stanovení tahových vlastností - Část 1: Obecné principy. ČSN EN ISO 527-1. Praha: Úřad pro technickou normalizaci, metrologii a státní zkušebnictví.

Veselka, F., Mikulčík, A. 2008. Speciální technologie. Skriptum FEKT VUT Brno: Akademické nakladatelství CERM s. r. o.

Ziemian, C. et al. 2012. Anisotropic mechanical properties of ABS parts fabricated by fused deposition modeling. In Mechanical Engineering. Intech, pp. 159–180.

Raw material used for biogas production: monitoring of its composition with XRF spectrometer

Eliska Kobzova, Tereza Dokulilova, Tomas Vitez
Department of Agricultural, Food, and Environmental Technology
Mendel University in Brno
Zemedelska 1, 613 00 Brno
CZECH REPUBLIC

xrysava6@mendelu.cz

Abstract: Quality, composition and composition ratio of raw material dosed into the biogas plant can influence a production of biogas. In raw material, a lot of unwanted components like heavy metals and other substances can be found. Their presence can lead to the inhibition of anaerobic microorganisms and thus to the decrease in biogas production. The samples of raw material (maize silage, grass silage, and GPS) were obtained from 27 biogas plants in the Czech Republic. After collection, the samples were dried, ground, hashed and the presence of heavy metals was detected by Niton^{TM} XL3t GOLDD+ XRF analyser. A universal standard material for a biological matrix (set in the measuring device) was used for comparison. The study confirms a presence of commonly occurring elements in raw materials.

Key Words: raw material, biogas plants, heavy metals, XRF screening

INTRODUCTION

In the whole world, there are a lot of ways how to reuse biomass and other organic solid wastes like physicochemical, thermochemical or biochemical conversion processes (Appels et al. 2011). Anaerobic fermentation is a natural process which leads to a production of the biogas, this process occurs naturally in wetlands, swamps and in the digestive tract of ruminants and which can also occur in a landfill (Le Mer et al. 2001). They are the microorganisms that are the most interested in transforming biodegradable organic material. The final product of its metabolism – biogas can be used as a possible source of natural renewable energy (Wilkie 2008).

In general, all types of biomass can be used as a raw material, due to the content of proteins, carbohydrates, cellulose, fats etc., but it is necessary to choose a good ratio of components and after that substrates. The content of organic substance, non-pathogenicity, nutritional value or composition of biogas are the main conditions for our selection because the type of substrate influences the amount of anaerobic fermentation products. Raw material like maize silage, grass silage or GPS ("*Ganzpflanzenschrot"* – a type of maize harvesting) can represent different ratios in the whole biogas plant station p.e. from 5 to 92 (w/w %) of fresh input substrate.

Crop treatment could be one of metal source in plants, where the metals are p.e. used as central atoms in complex compounds. Metals in plants are distributed through root tissues into plant shoots and their cell walls (Nouri et al. 2009). The digestibility of cell wall is very good in maize silage (Fontaine et al. 2003). A lot of essential elements are necessary for the correct function of enzymes and coenzymes in anaerobic fermentation and the excessive amounts of these metals can lead to the inhibition of anaerobic and mainly methanogenic microorganisms (Chen et al. 2014).

X-ray fluorescence spectrometry (XRF) is a quick and convenient method for multi-elemental and mainly non-destructive analysis. One of main advantage is a very big measurement range from a few ppm to major components, but it serves as a screening method due to the necessity of specialized standards for every type of matrix.

Various spectrometric techniques were used to determine major and minor elements in different biological matrix. These methods require sample preparation with acids and we risk the contamination.

This work is focused on the monitoring of presence of heavy metals and on determination of elements present in major compounds (K, Si, Ca, P, Al, Mg, and Ti) and in minor compounds (Cu, Mo, Zn, Fe, Cr, As, W, Cl and Pb) in raw material.

MATERIAL AND METHODS

The 44 samples of various raw material were collected from 27 biogas plant stations in the Czech Republic before dosing into the reactors. The samples were separated into three groups – maize silage, grass silage, and GPS. After collection the samples were dried, ground and the presence of heavy metals was detected by XRF Analyser.

All samples were also specified by the analysis of total solids (TS) and volatile solids (VS). To determine total solids (TS) and volatile solids (VS) content a muffle furnace (LMH 11/12, LAC Ltd., Czech Republic) was used. Raw materials were dried at 105 °C ± 5 °C to define total solids in accordance with a Czech Standard Method CSN EN 15934. Volatile solids content was defined by the incineration of the raw material at 550 °C ± 5 °C in accordance with CSN EN 15169.

For grinding of samples a cutting mill Retch SM 100 (Retsch GmbH, Germany) equipped with square holes sieve, mesh size 2.0 mm was used. During the whole experiment, we count with the identical error due to a possibility of contamination of samples from cutting mill. The exact abrasion analysis will be done. Once ground all samples were filled into special sampler with filter and prepared for measurement with XRF spectrometer Niton^{TM} XL3t GOLDD+ (Thermo Fisher Scientific, Waltham, USA). XRF analyser was fitted in portable test stand and used with four filters including voltage from 6 to 50 kV. Each filter was used for 30 seconds and all samples were measured in duplicates. Geometrically optimized large area drift detector was used without connection to helium bottle.
All measurements were done in standard laboratory conditions (t = 25° C, p= 101 kPa) and all measured values are expressed as arithmetic mean ± standard deviation. A notebook was used for machine control and data processing.

RESULTS AND DISCUSSION

Raw materials used for the XRF analysis were specified by analysing total solids, volatile solids and ash (Table 1). The obtained results were in match with results published before (Andrieu 1976, Han et al. 2014).

Table 1 Raw materials characteristics

Raw material	Total solids [%]	Volatile solids [%]	Ash [%]
Maize silage	35.25 ± 5.19	95.78 ± 1.45	1.57 ± 0.59
Grass silage	32.22 ± 5.43	88.59 ± 7.19	4.16 ± 2.00
GPS	30.23 ± 5.30	93.78 ± 4.63	2.35 ± 0.84

Maize silage contains the highest percentage of dry matter (35.25 ± 5.19%) and lowest percentage of ash (1.57 ± 0.59%). Grass silage contains lower percentage of dry matter (32.22 ± 5.43%), but higher amount of ash (4.16 ± 2.00%). It is caused by higher amount of organic compounds in maize silage.

Using the Tukey test from analysis of variance (ANOVA, $P<0.05$) in application to MS Excel XLSTAT, Addinsoft SARL shows no significant differences among total solids of maize silage, grass silage, and GPS.

Screening shows, that with sample preparation contains drying and grinding, a huge part of results are balance compounds (also called ballast), immeasurable small organic compounds elements. If all the other compounds are measured or known, the remaining compound can be determined, because the sum of all concentrations must add up to 100% (Brouwer 2010). For example, in biological compounds, carbon and oxygen are not measured, but in dried sample, there are many compounds of these elements (Table 2).

Table 2 Share of balance compounds

	Maize silage	Grass silage	GPS
Balance compounds [%]	93.44 ± 0.03	83.44 ± 0.09	85.85 ± 0.06

The highest percentage of ballast was measured in maize silage which agrees with the highest percentage of dry matter. Other values can be influence by a sample placement during measurement.

The rest of structure is composed mainly from potassium, silicon, calcium, chlorine and phosphorous (Table 3, Figure 1).

Table 3 Share of analysed elements counted without ballast - (a) maize silage, (b) grass silage, (c) GPS (n. d. – not detected)

a)	Amount	Deviation	Unit	b)	Amount	Deviation	Unit	c)	Amount	Deviation	Unit
K	37.94	0.46	%	K	34.01	0.34	%	K	38.27	0.32	%
Si	25.97	0.68	%	Si	30.38	0.51	%	Si	32.54	0.51	%
Ca	12.39	0.39	%	Ca	14.63	0.35	%	Ca	8.90	0.27	%
Cl	6.11	0.09	%	Cl	6.98	0.09	%	Cl	6.09	0.07	%
P	8.14	0.29	%	P	4.93	0.18	%	P	5.85	0.18	%
S	6.59	0.19	%	S	4.93	0.12	%	S	5.32	0.12	%
Mg	4.55	2.87	%	Mg	2.84	1.61	%		n. d.		
Al	898.71	431.38	ppm	Al	1.83	0.45	%	Al	1.47	0.45	%
Fe	274.42	19.04	ppm	Fe	1.06	0.03	%	Fe	975.51	29.29	ppm
Ti	82.31	20.98	ppm	Ti	384.72	31.45	ppm	Ti	295.12	26.87	ppm
W	98.44	25.78	ppm	W	127.54	35.17	ppm	W	165.90	31.56	ppm
	n. d.			Mn	113.73	28.64	ppm	Mn	57.30	29.61	ppm
Cr	79.51	17.41	ppm	Cr	69.20	21.66	ppm	Cr	49.85	12.30	ppm
	n. d.			Sc	65.67	20.81	ppm	Sc	23.48	11.63	ppm
Zn	42.33	4.66	ppm	Zn	60.96	6.13	ppm	Zn	46.17	5.50	ppm
Cu	18.51	6.85	ppm	Cu	21.76	8.84	ppm	Cu	30.38	8.12	ppm
Sr	14.05	0.98	ppm	Sr	45.37	1.73	ppm	Sr	21.50	1.23	ppm
Rb	6.38	0.93	ppm	Rb	25.42	1.37	ppm	Rb	11.01	1.15	ppm
Zr	10.62	1.20	ppm	Zr	19.53	1.63	ppm	Zr	18.74	1.45	ppm
Cd	14.99	3.57	ppm	Cd	14.41	4.53	ppm	Cd	15.82	4.04	ppm
Mo	11.07	1.51	ppm	Mo	10.68	1.80	ppm	Mo	12.48	1.70	ppm
Sn	9.96	6.54	ppm	Sn	10.65	7.85	ppm		n. d.		

Potassium is important in the stimulation of calcium metabolism of microorganisms in anaerobic fermentation, higher amount of this element depends on ratio of vegetative stover of the plant and grain in maize silage. For feeding low calcium levels are required, on the contrary, increasing of calcium amounts leads to stimulation and improvement of anaerobic fermentation results. (Owens et al. 1969)

Significant amounts of silicon can be increased with the inflow of gravel by rainfall (partly caused by Diatoms, major group of Algae) and on the other hand with decreasing concentrations of P origination from microorganism's excretion (Ohbuchi et al. 2008). In examined materials, it could be associated with lignin, thereby helping to maintain the physical structure of plants. (Vojtic et al. 2010)

Aluminium was detected in all samples only in small amount and with a significant deviation because of the absence of helium as an optical medium required for SDD detector. Lead non-detection confirms a barrier role of the root system in plants (Sobotik et al. 1998).

Titanium occurs in the earth in the form of titanium oxide and various minerals. Negligible quantities also occur in forage plants, this is confirmed with our results too.

Figure 1 Share of element without ballast for (a) maize silage, (b) grass silage, (c) GPS

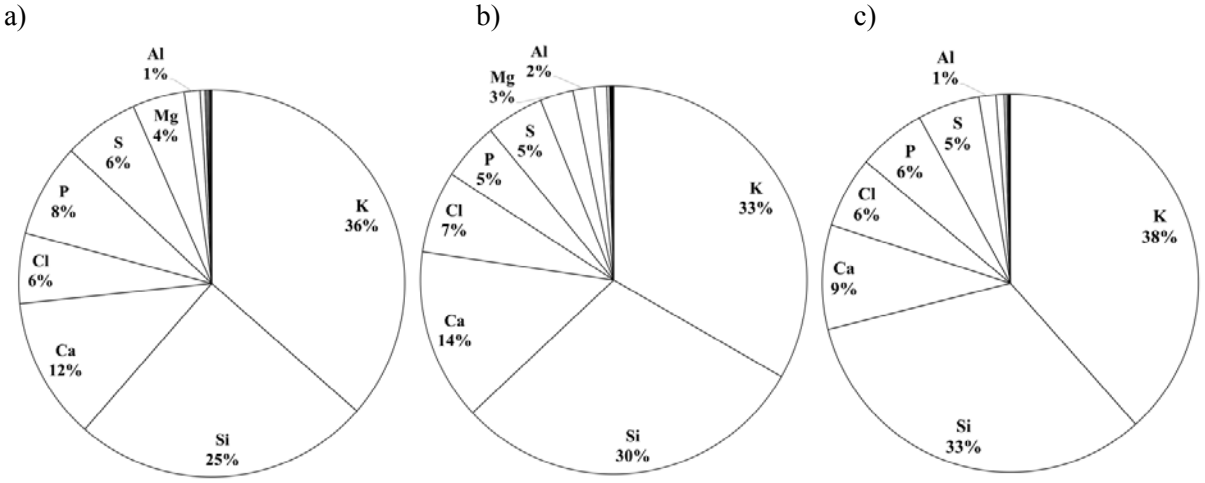

In Figure 1 we can see a dominance of potassium, silicon and calcium in all three types of raw material. Metal elements like copper, manganese or zinc are accepted by a plant from external environment and in our results, they constitute a really small amount.

CONCLUSION

The XRF method established a possibility of presence detection of 22 different elements in raw materials used for biogas production. These three types of examined raw materials were consisted mainly of ballast, potassium, silicon, calcium, phosphorus and chlorine. A lot of samples contain ppm-s of magnesium, iron and aluminium. There is lack of information available about concentrations of examined minerals in the raw material.

It was not confirmed any higher significant amount of heavy metals in our samples with a comparison with Directive 2002/32/EC of European parliament focusing on undesirable substances such as cadmium, lead, fluorine, mercury or nitrites in feed hygiene. There are not known any regulations for composition of individual raw materials only regulations for nutritional values.

XRF spectrometer can be used for easy, time-saving screening analysis. This analysis can be a good possibility to capture unwanted substances during anaerobic fermentation with a previous creation of well-described standards for this type of matrix. Our research continues with a creation of calibration XRF standards for this type of matrix.

ACKNOWLEDGEMENTS

The research was financially supported by the Internal Grant Agency of the Faculty of AgriSciences, Mendel University in Brno, no. AF-IGA-IP-2018/034.

REFERENCES

Andrieu, J. 1976. Factors Influencing the Composition and Nutritive Value of Ensiled Whole-Crop Maize. Animal Feed Science and Technology, 1(2–3): 381–92.

Appels, L. et al. 2011. Anaerobic Digestion in Global Bio-Energy Production: Potential and Research Challenges. Renewable and Sustainable Energy Reviews, 15(9): 4295–4301.

Brouwer, P. 2010. Theory of XRF - Getting Acquainted with the Principles. Almelo: PANalytical B. V.

Chen, J. L. et al. 2014. Toxicants Inhibiting Anaerobic Digestion: A Review. Biotechnology Advances, 32(8): 1523–34.

CZECH STANDARDS INSTITUTE. 2013. Sludge, treated biowaste, soil and waste – Calculation of dry matter fraction and determination of dry residue or water content. CSN EN 15934. Praha: Czech Standards Institute

CZECH STANDARDS INSTITUTE. 2007. Characterization of waste - Determination of loss on ignition in waste, sludge and sediments. CSN EN 15169. Praha: Czech Standards Institute.

Fontaine, A-S. et al. 2003. Variation in Cell Wall Composition among Forage Maize (Zea mays L.) Inbred Lines and Its Impact on Digestibility: Analysis of Neutral Detergent Fiber Composition by Pyrolysis-Gas Chromatography-Mass Spectrometry. Journal of Agricultural and Food Chemistry, 51(27): 8080–87.

Han, K. J. et al. 2014. Moisture Concentration Variation of Silages Produced on Commercial Farms in the South-Central USA. Asian-Australasian Journal of Animal Sciences, 27(10): 1436–42.

Le Mer, J. et al. 2001. Production, Oxidation, Emission and Consumption of Methane by Soils: A Review. European Journal of Soil Biology, 37(1): 25–50.

Nouri, J. et al. 2009. Accumulation of Heavy Metals in Soil and Uptake by Plant Species with Phytoremediation Potential. Environmental Earth Sciences, 59(2): 315–23.

Ohbuchi, A. et al. 2008. X-Ray Fluorescence Analysis of Sludge Ash from Sewage Disposal Plant. X-Ray Spectrometry, 37(5): 544–50.

Owens, F. N. et al. 1969. Effects of Calcium Sources and Urea on Corn Silage Fermentation. Journal of Dairy Science, 52(11): 1817–22.

Sobotik, I. et al. 1998. Barrier Role of Root System in Lead-Exposed Plants. Journal of Applies Botany-Angewandte Botanik, 72: 144–47.

Vojtic, I. et al. 2010. Content of Aluminium, Silicon and Titanium in Feed Materials of North-Eastern Slovenia. Krmiva, 49: 253–58.

Wilkie, Ac. 2008. Biomethane from Biomass, Biowaste, and Biofuels. Bioenergy, 195–205.

Evaluation of soil-geotextile filtration behaviour using the gradient ratio test

Anna Miszkowska, Zygmunt Krzywosz
Department of Geotechnical Engineering
Warsaw University of Life Sciences
Nowoursynowska 159, 02 776 Warsaw
POLAND

anna_miszkowska@sggw.pl

Abstract: Nonwoven geotextiles have been widely used in drainage systems for more than 60 years as filters to prevent the mixing of materials of varying granularity and allow for adequate water flow normal to their plane. Unfortunately, in engineering applications, nonwoven geotextiles are exposed to mechanical, biological or/and chemical clogging. Clogging is the main mechanism affecting the durability of drainage systems due to the reduction of nonwoven geotextile water permeability. For that reason, the selection of suitable nonwoven geotextiles mainly involves determining the water permeability normal to the plane and clogging potential evaluation for a soil-geotextile system. However, most of the filtration criteria based on the comparison between an indicative diameter of the soil to be filtered and geotextile characteristic opening size only. In this paper compatibility between a internally unstable soil and a geotextile filter has been evaluated using the gradient ratio test. The obtained results allowed assessing directly the compatibility of the base soil and geotextile.

Key Words: geotextile, clogging, filtration, gradient ratio

INTRODUCTION

The use of nonwoven geotextile filters is one of the oldest and most common applications in geoenvironmental and geotechnical engineering works. The main functions of that filter are to prevent the movement of fine particles from the base soil and to avoid the development of excessive pore water pressure on the interface between the geotextile filter and the base soil. Therefore, nonwoven geotextiles are the first to be in contact with saturated, soft and fine soils. It may causes physical clogging, which occurs when the particle movement of the base soil leads to the clogging of the filter pores (Figure 1). Clogging results in a decrease of drainage capacity of the geotextile filtering system and may be the cause of stability problems (Koda et al. 1989, Lejcuś et al. 2016, Miszkowska et al. 2016, Miszkowska et al. 2017, Miszkowska and Koda 2017, Palmeira and Trejo Galvis 2017). Clogging can be caused by chemical and biological processes also (Koda et al. 2016).

Figure 1 Mechanism of physical clogging

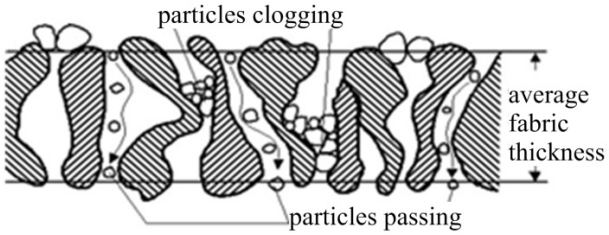

The selection criteria of nonwoven geotextile for filter application must consider three conditions: permeability, retention and anti-clogging capabilities (Giroud 1996).

Compatibility between a soil and a geotextile filter has been evaluated using the gradient ratio test (Calhoun 1972, Haliburton and Wood 1982). Using a rigid wall permeameter, a soil is placed above the geotextile filter and water is passed vertically through the soil-geotextile system under a range of hydraulic heads. In a general sense, the value of the gradient ratio, GR, can be defined as (ASTM D-5101):

$$GR = \frac{i_{LG}}{i_s}$$

where:

i_{LG} - hydraulic gradient across a soil thickness L and the geotextile, i_s - the reference gradient in the soil, measured in a region away from the geotextile (calculated for the segment of the soil specimen between 25 and 75 mm above the geotextile filter).

However, Palmeira et al. (2005) recommended to the definition of GR based on water head measurements closer to the geotextile filter interface. To avoid clogging, GR should be less than 3 (Haliburton and Wood 1982, Giroud 1996, Cazzuffi et al. 2016).

The objective of this paper is to present the laboratory tested results on internally unstable soil and nonwoven geotextile material. The obtained results will be compared with commonly used geotextile filter designed criterion.

MATERIALS AND METHODS

Characterization of nonwoven geotextile samples used in GR test

The polypropylene nonwoven geotextile sample with mass per unit area of 100 g/m^2 was analysed. The tests were performed in 5 replicates. Table 1 presents the physical, mechanical and hydraulic parameters of tested material.

Table 1 Properties of nonwoven geotextile used in GR test

Properties	Units	Values
Thickness under 2 kPa	mm	1
Tensile strength – MD	kN/m	8
Tensile strength – CMD	kN/m	8
Elongation at maximum load – MD	%	45
Elongation at maximum load – CMD	%	55
Characteristic opening size O90	µm	120
Water permeability normal to the plane	l/m^{2}s	110

Characterization of soil samples used in GR test

Tested soil is identified as silty sand (siSa). The physical and hydraulic properties are given in Table 2. Tested soil is internal unstable according to the Kenney and Lau (1985) method the assessment of internal stability soils.

Table 2 Properties of soil used in GR test

Properties	Units	Values
Silty sand fractions:		
Sand	%	80
Silt	%	17
Clay	%	3
d_{10}	mm	0.02
d_{60}	mm	0.2
d_{90}	mm	0.41
Coefficient of uniformity, C_u	-	10
Coefficient of curvature, C_c	-	3.6
Density of dry soil	t/m^3	1.75
Permeability coefficient	m/s	0.00009

Gradient Ratio test

The Gradient Ratio test were determined according to ASTM D 5101 standard using the modified apparatus shown in Figure 2 belonging to the laboratory of Department of Geotechnical Engineering at Warsaw University of Life Sciences.

To obtain additional pressure measurements in layer of soil situated close to nonwoven geotextile sample, the additional piezometers (6 and 7) were installed.

Figure 2 Schematic diagram of test apparatus (Wojtasik 2008)

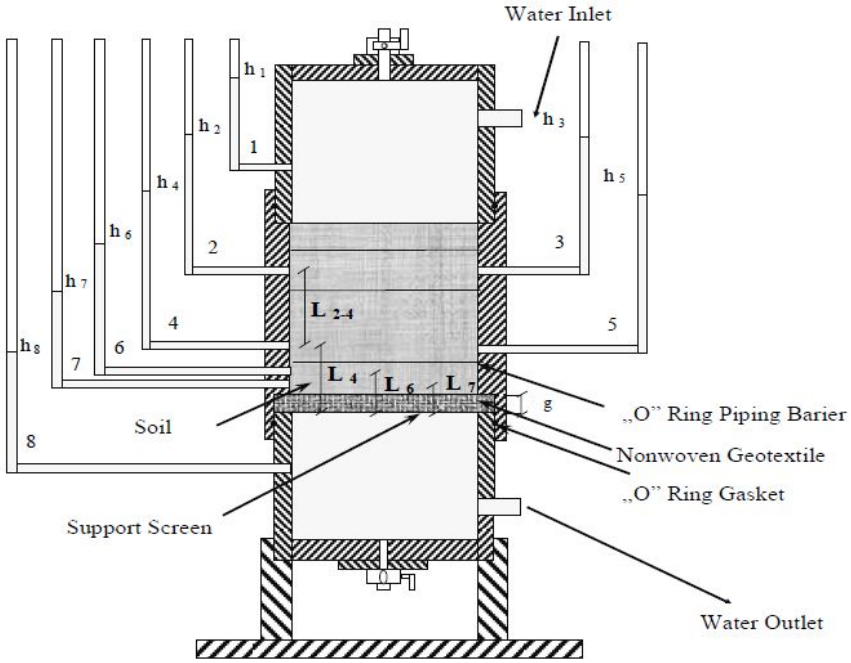

Legend: g – geotextile thickness, L_n – distance between piezometer nth and the bottom of geotextile, h_n – the piezometer reading for nth piezometer)

The tested soil were dried (under 105 °C for 24 h) and sieved with mesh 2 mm. The siSa sample was placed around the nonwoven geotextile material (see Figure 3). Then, the water was delivered into the apparatus from bottom to the top slowly in the beginning for 24 hours. After that, flow direction was changed. When the water flow reached a steady condition, the temperature of water flow (T), volume of flow (V), time of flow (t), pressure of individual piezometer (Δh) were measured for each of the hydraulic gradients at 1.0, 2.5, 5.0, 7.5 and 10.0.

Figure 3 Tested materials during the GR test

A) Nonwoven geotextile

B) Nonwoven geotextile and soil

The following piezometer readings were taken in individual zones:

- for soil:
  - zone 6–7 (4 mm layer of soil within the distance from 4 to 8 mm above nonwoven geotextile between piezometers 6 and 7),
  - zone 4.5–6 (17 mm layer of soil within the distance from 8 to 25 mm above nonwoven geotextile between piezometers 4, 5 and 6),
  - zone 2.3–4.5 (50 mm layer of soil within the distance from 25 to 75 mm above nonwoven geotextile between piezometers 2 and 3 as well as 4 and 5),
- for soil-geotextile:
  - zone 7–8 (geotextile and 4 mm layer of soil between piezometers 7 and 8),
  - zone 6–8 (geotextile and 8 mm layer of soil between piezometers 6 and 8),
  - zone 4.5–8 (geotextile and 25 mm layer of soil between piezometers 4 and 5 to 8).

RESULTS AND DISCUSSION

The gradient ratio in soil-geotextile system (GR = GR_{25}) was calculated using the following equation:

$$GR_{25} = \frac{\Delta h_{4.5-8} / L_4}{\Delta h_{2.3-4.5} / L_{2-4}}$$

where:

$\Delta h_{4.5-8}$ – the difference manometer readings between average reading of 4 and 5 piezometers and 8 piezometer [mm], $\Delta h_{2.3-4.5}$ – the distance in manometer readings between average reading of 2 and 3 piezometers and average reading of 4 and 5 piezometers [mm], L_4 – the distance between piezometer 4 and the bottom of geotextiles [mm], L_{2-4} – the distance between piezometers 2 to 4 [mm].

What is more, the relationship for the evaluation of the change gradient ratio for the soil layers 4 and 17 mm above the geotextile (SGR_4 and SGR_{17}) was calculated according to formula:

$$SGR_4 = \frac{\Delta h_{6-7} / L_{6-7}}{\Delta h_{2.3-4.5} / L_{2-4}}$$

$$SGR_{17} = \frac{\Delta h_{4.5-6} / L_{4-6}}{\Delta h_{2.3-4.5} / L_{2-4}}$$

where:

Δh_{6-7} – the distance in manometer readings between reading of 6 and 7 piezometers [mm], $\Delta h_{4.5-6}$– the difference manometer readings between average reading of 4 and 5 piezometers and 6 piezometer [mm], L_{6-7} – the distance between piezometers 6 to 7 [mm], L_{4-6} – the distance between piezometers 4 to 6 [mm].

Figure 4 presents the change of gradient ratio and soil-gradient ratio under hydraulic gradient from 1 to 10 in tested soil (at the beginning of test). The obtained results show that gradient ratio value in soil-geotextile system (GR) has increased from 0.7 to 1.32 under tested hydraulic gradient. This indicates that clogging might have occurred in the soil-geotextile layer when the system was subjected to a higher hydraulic gradient. The increase in the GR value results in a decrease in hydraulic conductivity value of the soil-geotextile layer what was presented by inter alia Hong and Wu (2011).

However, significant clogging occurred in the 17-mm soil layer situated in distance from 8 to 25 mm above nonwoven geotextile sample. At the beginning of tests, SGR_{17} was 1.4 times greater than SGR_4. Similar experimental results were reported by Wojtasik (2008). The values of SGR_4 and SGR_{17} have increased from 0.74 to 1.48 and from 1.02 to 1.6 subsequently.

Nevertheless, the GR values in the tested soil did not exceed the limit of GR = 3 and decreases with time (see Figure 5). For that reason, the tested nonwoven geotextile can be used as the filtration layer for soil with fines 20% content.

Figure 4 Relationship between hydraulic gradient and GR or SGR

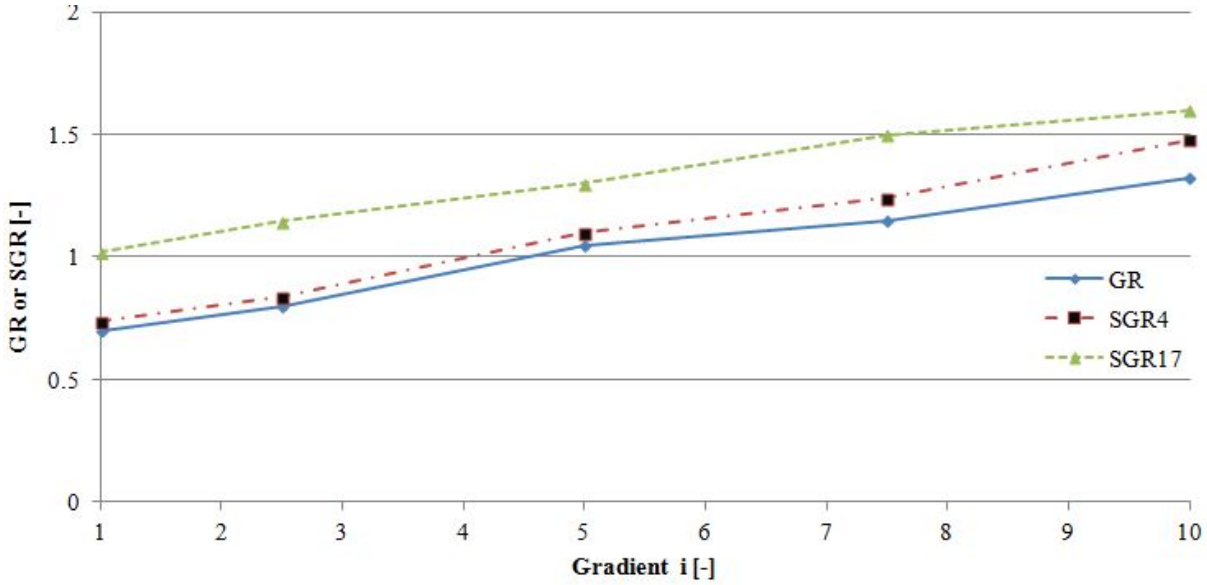

Figure 5 Gradient ratio values within the range of external hydraulic gradient i = 1 to 10 with time

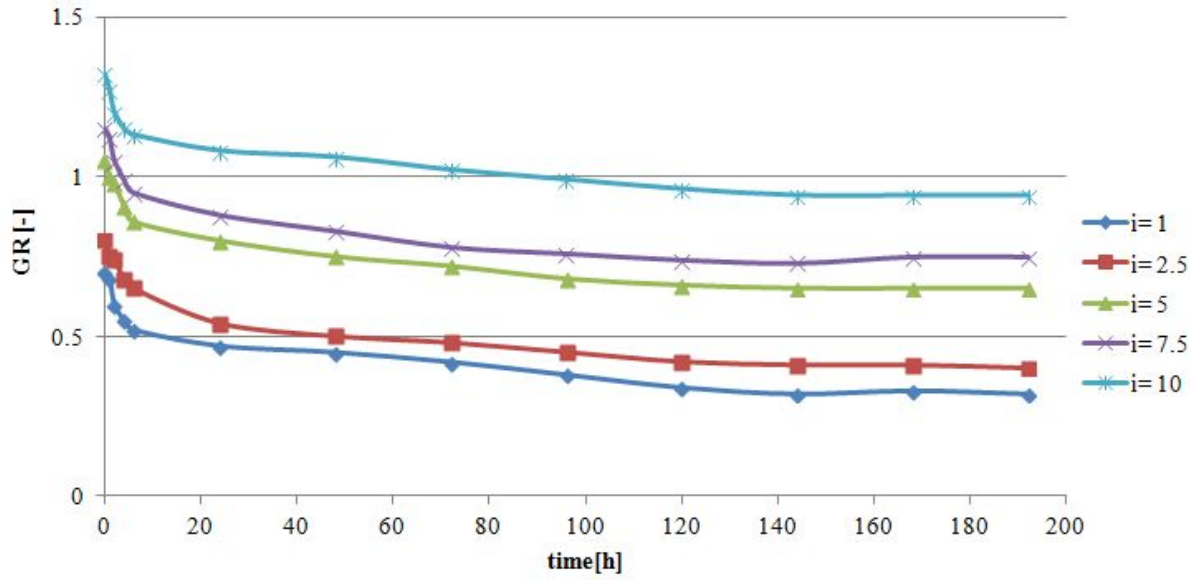

CONCLUSION

This paper studied the compatibility of the base soil (silty sand) and needle-punched nonwoven geotextile used in filtration applications. A modified experimental apparatus was used to conduct the gradient ratio tests within the range of external hydraulic gradient i = 1 to 10.

Tests carried out on a soil-geotextile combination with a relatively thin nonwoven geotextile confirmed an increase of gradient ratio values as the hydraulic gradient was increased.

However, the gradient ratio values decrease with elapsed time and reach stable values after approximately 160 hours.

The clogging process was very intense in 17 mm layer situated in distance from 8 to 25 mm above nonwoven geotextile material. But, based on commonly used anti-clogging criterion (GR< 3), the tested nonwoven geotextile can cooperate with internal unstable soil with fine content of 20%.

REFERENCES

ASTM D 5101 Standard Test Method for Measuring the Filtration Compatibility of Soil-Geotextile Systems.

Calhoun, C. 1972. Development of design criteria and acceptance specifications for plastic filter cloths. Technical report S-72-7 U.S. Army corps of engineers, waterways experiment station. Vicksburg, MS, USA, pp. 83.

Cazzuffi, D. et al. 2016. Evolution in design of geotextile filters. In Proceedings of the EuroGeo 6, Ljubljana, 25–28 September, pp. 40–63.

Giroud, J.P. 1996. Granular filters and geotextile filters. In Proceedings of the GeoFilters '96. Montreal, Canada, 29–31 May, pp. 565–680.

Haliburton, T.A., Wood, P.D. 1982. Evaluation of the U.S. Army Corps of Engineers Gradient Ratio Test for Geotextile Performance. In Proceedings of the 2nd International Conference On Geotextiles. Las Vegas, Nevada, 1–6 August, pp. 97–101.

Hong, Y.-S., Wu, Ch.-S. 2011. Filtration behaviour of soil-nonwoven geotextile combinations subjected to various loads. Geotextiles and Geomembranes, 29: 102–115.

Kenney, T.C., Lau, D. 1985. Internal stability of granular filters. Canadian Geotechnical Journal, 22(2): 215–225.

Koda, E. et al. 1989. Behavior of geodrains in organic subsoil. In Proceedings of the 12th International Conference On Soil Mechanics and Foundation Engineering. Rio de Janeiro, 13–18 August, 2, pp. 1377–1380.

Koda, E. et al. 2016. Quality Control of Non-Woven Geotextiles Used in a Drainage System in an Old Remedial Landfill. In Proceedings of the Geo-Chicago 2016, ASCE Geotechnical Special Publication, Chicago, 14–18 August, 271, pp. 254–263.

Lejcuś, K. et al. 2016. Optimisation of Operational Parameters for Nonwoven Sheaths of Water Absorbing Geocomposites in Unsaturated Soil Conditions. FIBRES & TEXTILES in Eastern Europe, 24, 3(117): 110–116.

Miszkowska, A., Koda, E. 2017. Change of water permeability of nonwoven geotextile exploited in earthfill dam. In the Proceedings of the 24th International PhD Students Conference, Brno, 8–9 November 2017, pp. 790–795.

Miszkowska, A. et al. 2016. Zmiany właściwości filtracyjnych geowłókniny po 22 latach eksploatacji w drenażu zapory ziemnej. Acta Scientiarum Polonorum Architectura, 15(3): 119–126.

Miszkowska, A. et al. 2017. Changes of Permeability of Nonwoven Geotextiles due to Clogging and Cyclic Water Flow in Laboratory Conditions. Water, 9(9): 660.

Palmeira, E.M. et al. 2005. Soil-geotextile filter interaction under high stress levels in the gradient ratio test. Geosynthetics International, 12: 162–175.

Palmeira, E.M., Trejos Galvis, H.L. 2017. Opening sizes and filtration behaviour of nonwoven geotextiles under confined and partial clogging conditions. Geosynthetics International, 24(2): 125–138.

Wojtasik, D. 2008. Evaluation of nonwoven geotextile as a filtration layer for internally unstable soils. Annals of Warsaw University of Life Sciences – SGGW, Land Reclamation, 40: 107–114.

Proposal of waste collection route with using algorithms to solve the traveling salesman problem

Jana Novotna[1], Martin Kostal[2], Stanislav Barton[3]
[1]Department of Agricultural, Food and Environmental Technology
[3]Department of Technology and Automobile Transport
Mendel University in Brno
Zemedelska 1, 613 00 Brno
[2]Department of Archaeology and Museology
Masaryk University
Arna Novaka 1, 602 00 Brno
CZECH REPUBLIC

xnovot62@node.mendelu.cz

Abstract: This thesis deals with the optimization of collection routes of separated waste in Velké Meziříčí. This waste is collected by the Technical Services VM s.r.o. The solution is designed using the well-known Traveling salesman problem method and the proposed algorithm is a combination of these methods. The algorithm is designed to work in the Maple algebraic system and the data were analysed using ArcGIS and Statistica. Gradual development and functionality of the algorithm is represented by resulting separate waste collection routes.

Key Words: ArcGIS, optimisation, collection route, algorithm, waste, separated waste, Maple

INTRODUCTION

Wastes have been associated with humanity since the beginning of its existence. Waste production is an integral part of civilization and only the quantity and composition of waste vary depending on the time and place of waste production. With the increasing number of inhabitants of the Earth's planet, the amount of waste generated by agriculture, industry and citizens' activities in the municipalities is growing, and waste management is becoming a global problem that needs to be tackled effectively. Waste contains a great deal of raw materials and energy, and it should be in everyone's interest to learn how to recover and use these raw materials and energy from waste to their advantage.

In the Czech Republic, waste management is addressed by the Waste Act, which establishes a certain hierarchy of waste management practices. This hierarchy emphasizes the prevention of waste generation, the preparation of waste for its reuse, the recycling of waste and thus the material recovery. Another successor of the hierarchy is followed by other, above all, energy recovery of waste and finally the disposal of waste by landfilling.

In addition to the above-mentioned methods of waste management, it is also necessary to focus on sub-activities with associated waste utilization and disposal. These activities include collection, collection, treatment and transport of waste. This work is primarily concerned with the transport of wastes, which is an integral part of the waste management process. All wastes must be moved from the point of collection and collected in places where they are treated, recovered or disposed of. Waste transport is often a neglected process, and it looks considerably at the economic side of this activity. But this process can be optimized and streamlined.

The thesis deals with the development and modification of the algorithm, which is able to modify each trailer's trajectory as short as possible. For this purpose, the traveler's methods and the heuristics of the proposed algorithm are used. The efficiency of the algorithm is then de-monstrous on four specific pickup routes. Part of the thesis is also the process of obtaining and processing necessary data in a suitable format.

MATERIAL AND METHODS

The area for the purpose of this work is made up of the town of Velké Meziříčí in Vysočina. Waste collection is provided by Technical Services VM s.r.o. (hereinafter TSVM) and their owner is the town of Velké Meziříčí. The TSVM for the city and other 54 municipalities in their general administration provide all public services and waste management. Waste disposal is mediated by approximately 12,000 inhabitants of the town of Velké Meziříčí and, in total, for the 25,000 inhabitants of the region.

There are 121 public collection points in the city, but not all collecting points contain collection containers for the separation of all types of waste. The plastic can be put into 182 yellow collection containers at 118 locations and its collection is in the center, the paper is weighed on Monday and can be placed in 112 places, with a total number of paper picking receptacles 150. White glass can be used in 110 white containers at 105 collection points and colored glass up to 105 collection points at 102 collection points. Their collection takes place on Friday.

At present, the TSVM is missing a permanent collection route for collecting municipal or separate waste both in the city and in municipalities. Separated waste shipments therefore take place on several irregular routes. The lengths of these routes range from about 50,000 m to 150,000 m (www.webdispecink.cz), depending on whether the pick-up truck empties the collecting tanks only in the area of the city, it adds the volume of the superstructure by the waste to the adjacent villages or leaves for the waste transshipment to another city.

Information on the status, number, spacing and accessibility of separate waste collection containers was obtained from TSVM staff from the gis.velkemezirici.cz/portal/ web portal. The site map was uploaded to ArcGis and formed the basis for subsequent vectoring of the data. As a basis of the map, a WMS orthophotomap from the geoportal.cuzk.cz website was used. Vector layers of lines, identical to road communications, come from the openstreetmap.org portal. To download, the ArcGIS Editor for Openstreetmap was used in the ArcMap environment.

The first step was to create a new project in ArcMap. The basic vector layer, which formed the map background and the source of the required area information, was downloaded from Openstreetmap using ArcMap and the directly available OpenStorm Toolbox. Using the Download, Extract and Symbolize OSM Data script, the Openstreetmap was loaded into a point-of-interest area of interest, and then all data was transferred as a vector layer to the ArcMap (Geletič 2013).

This vector layer, which only contained information on the roads in the selected area, was then moved to a pre-arranged geodatabase. All roads have received a placeholder in the form of a line. Each line is defined by a dataset. This data included the data on the type of road, the date of creation of the given line, the speed limit, the name of the street, the indication of whether it is a one way, the source of the line, the unique identification number of the given line and other information.

The Calculate Geometry function was used to calculate the distances between the intersections between the junctions (Kennedy 2009). This function can calculate the actual line length, specify its starting and ending points, and write these data into the attribute table.

The next step was the creation of points presenting collection points including the kind of waste that can be postponed. Using the Spatial Join tool in the Analysis Tools, Overlay toolkit, an attribute table for 121 collection points with 5 columns was created for these points. In these columns there is information about the line ID, which points are located, the geometry specification (point), the information about the type of collecting containers that are located at the given collection point, and the last two columns with the GPS coordinates determining the position of the points.

In some parts of the village, the situation has been simplified and some collection points and land communications have been compressed in the form of one point and one line. This resulted in a new data file that contained only 79 points in total. 76 of which featured compressed plastic pickups, 75 paper picking, 72 white glass, and 73 colored glass pickets.

These data were subsequently uploaded to Maple. An algorithm was created here, the output of which was an optimized air route for each type of waste. The following text describes the steps in the algorithm when creating trail routes.

First, the functions that are used in the main part of the algorithm when creating a partial pickup path are defined. In the first step, it is made up of four extreme coordinates located in the coordinate system most in the north, south, west, and east. These points are joined by lines to form a trapeze. The subsequent step deforms the lines and forms the wrapping polygon so that all of the points are within the polygon or form its vertices. This creates a basic partial route using basic optimization to resolve the problem of a business traveler.

The remaining points within the polygon are implemented in a partial path using the shortest insertion algorithm (http://faculty.washington.edu). This creates a trailing route using a combination of two algorithms for TSP solution.

Subsequently, adjustments are made to optimize the route to the shortest possible with regard to the computing capabilities of the computer and the time consuming to find the final solution. Path optimization is performed by the permutation of the last eight or nine points built into the trail. This number of permutations is limited to the computational difficulty of this operation, since Maple displayed an improper error message when trying to permute the last ten points. Permutation of the last few points should result in a shorter partial route between the last chosen points. If such a route was found, the original partial route was replaced by this new route.

The last part of the proposed algorithm determines whether a shorter path can be found by restarting another permutation. If this is not the case, then the whole procedure ends; if this path is to be found, all the steps from the permutation command must be repeated.

Optimal route created be using Maple were graphically displayed. These charts were uploaded to ArcGis and the resulting paths were vectorized.

RESULTS AND DISCUSSION

The aim of this work was to design an algorithm that would effectively create and subsequently optimize the collection routes for separated waste in the catchment area of Velké Meziříčí. To do this, the algebraic Maple system was used in which the algorithm originated (Bartoň 1999). The principle of the algorithm is to create a convex envelope polygon so that all the collection points represented here as points with assigned GPS coordinates are located inside or forming a polygon (Cook 2012). The subsequent step of the algorithm is to include the remaining points in the route. This integration is based on the principle of insertion algorithms, namely the shortest insertion algorithm which described Cook (2012) in his publication. With this step, all points were integrated into the continuous route where the length was measured.

The second part of the algorithm was heuristic to optimize the proposed continuous route. The principle of this optimization was to compare the lengths of a certain section of the route, with the shortest length of these sections being determined by the permutation of eight or nine consecutive collection points along the route and their relative spacing. If this shorter route between these points was found by this heuristics, this part of the route replaced the original one.

The last part of the generated algorithm was to determine whether to reuse the permutation of a route to find a shorter route than before, and then to begin this optimization. If the shorter route could not be found, the algorithm ended here. All routes so created were air routes, the distance of which was calculated by the sum of the lengths of all the lines between the points in the route. After that step were not used the other special methods. But Cook (2012) says in his publication, there can be used many modification n-opt algorithms.

All graphic processing was done in ArcMap. Maps of the city, maps showing the collection points, line network representing the roads and subsequently all the optimized routes for the collection of separated waste were recorded (www.arcdata.cz). All maple data obtained from the original raster format was converted to vectors as lines or points and created two matrices for all 121 points from the XYP_1 data set and 79 points compressed from the XYP_2 file that contained the actual distances between points. Using these matrices and a list of consecutive points in the proposed routes, the length of these routes was calculated. ArcGIS Network Analyst tool used Hemidat at al. (2017) in his thesis for organizing and analysing his geographical data. This length is calculated from point to point along the shortest possible line between them, and is therefore only a guide value for the length of the route. The length of the route for municipal waste, calculated by the Petřík and Bartoň, was determined by the

real length of the streets (Petřík and Bartoň 2016), because the collecting car has to move by along streets and not from one point to another.

Table 1 provides an overview of all route lengths resulting from the Maple optimization algorithm, calculated from the actual distance matrix according to the order of points in the optimized route, and the last route that is a real proposal which was created and measured in ArcMap.

The header of the table shows the types of separate waste for which the routes have been optimized. The first column specifies the route type and the method of route tracking. Air routes represent idealized optimal routes created by the proposed algorithm. If the permutation of the points in the algorithm have found different final path lengths, a row with these lengths is added to the table. Real lengths were calculated by the distance matrix, and the real proposed represents the route length proposed in ArcMap.

Table 1 All of optimized routes for separated waste

Route	Plastic [m]	Paper [m]	White glass [m]	Colored glass [m]
XYP_1 air	15 061	14 852	13 977	14 109
XYP_2 air	13 604	13 459	12 787	12 647
	13 590	13 375		
XYP_1 real	24 781	25 313	23 713	24 616
XYP_2 real	25 566	24 132	24 379	23 666
	25 417	24 100		
Proposed route	24 965	25 618	23 817	24 049

Using a proposed Maple algorithm, a total of 10 separate optimized air routes were created. When processing the XYP_1 file containing the coordinates of all collection points in Velké Meziříčí, only one optimized route was created for each kind of separated waste, and regardless of the number of permutated points in the algorithm, the amount of edges exchanged during permutations, and regardless of how many permutation cycles have passed. The shortest route of 13,977 m was created for collecting white glass, although this route did not contain the smallest number of collection points. The longest route was created for plastic picking. This route with the largest number of collection points was 15,061 m long. The difference between the shortest and the longest route was 1,084 m.

By contrast, when processing the second XYP_2 file with a total of 79 points, only the optimized air route was found only for white and colored glass. The algorithm has created different paths depending on the number of permutated points and optimizations of the narrow paths of plastic and paper. In both cases, the shorter route was created by using a 9-point permutation algorithm. The difference in the excavated routes was 84 m for the paper and only 14 m for the plastic, which makes less than 1% of the length of the proposed routes. The difference between the shortest and the longest route was her only 957 m.

From the results above certain assumptions in the behavior of the algorithm can be determined. Using a 9-point permutation algorithm, the same or shorter paths can be achieved than with the use of eight-point permutations. The same or better result was obtained in the first cycle of permutation of 9 points. Even with the 8-point permutation, no shorter route was created than with the first 9-point permutation.

The disadvantage of this chosen procedure is the time consuming of the calculation. The resulting route, depending on the number of collection points in this route and the computational computing used, is generated in the range of 100 to 150 minutes. Using 8-point permutation, the result was obtained within 20 minutes of the algorithm running. This option is more advantageous in time, but the solver must reconcile with the resulting routes, which may not always be the shortest. The introduced algorithm represents the creation of optimized routes regardless of the time needed. With using Petřík algorithm of Novotná et al. (2016), the calculation took several days and the results of both algorithms are comparable. There are studies, where authors compare duration of operation with using drons and try to optimize the routes so that the time needed to find the solution is as short as possible (Ha et al. 2018). However, this study focuses on optimizing routes in a particular city, and time consuming has not been taken into account.

The length of the optimized route created will not depend only on the number of collection points in the route. Since the shortest route has not been created for a file containing the smallest number of locations, it can be assumed that another factor affecting the shape and length of the route is the location of the collection points in the selected area.

The actual lengths obtained over the distance matrices range from 23,666 m for the collection of the color glass up to 25,566 m for the collection of plastic. The difference between these limits is 1,900 m. For routes from the XYP_1 file with 121 points, the difference in actual route lengths is even smaller. Just 1,600 m, the longest 25,313 m long trail was created for paper picking and the shortest track of 23,713 m for white glass. As is clear from these figures, the length of all routes created is less than 2,000 m, irrespective of the number of collection points in the route and their overall course.

When designing real routes, the shortest route of 23,817 m was created for the collection of white glass. This is only 104 m more than was calculated using Maple from the distance matrix for all 121 points. The longest 25,618 m long track was then designed to pick up paper. This route was 305 m longer than the Maple route. The 24,695 m plastic trail was designed in ArcMap and was a route that is 184 m longer than the Maple design. Only in one case was the real route created shorter than Maple's. It was a freewheel trail of color glass and the difference of 567 m between these designs was the largest. This route was determined by Maple at 24,616 m and the real design measured 24,049 m.

The difference between the shortest real and the longest real route is 1,801 m, which is 99 m less than the difference calculated for Maple routes. All real routes were created according to the design of air-optimized routes so as to respect as much as possible the order of the designated collection points as well as the local modification of the operation on the roads. Their length does not differ much from the lengths of the routes Maple has shown.

For all routes created, it is now necessary to add the length they were truncated by moving some points from the blind streets and the remote collection points. This length is 4,700 m and the shortest route for the color glass was extended to the final 28,366 m. The length of the longest paper picking route was 30,318 m long.

When comparing all routes with current routes according to the Webdispečink application, saving the proposed routes is over 20,000 m. In the case of paper picking with the longest designed route, it is 39% and the color glass with the shortest route is up to 43%. Results of Das and Bhattacharyya (2015) show that their proposed scheme is able to reduce more than 30% of the total waste collection path length with using methods of TSP. They used 100 of collection places. This algorithm optimizes routes with greater efficiency, than the algorithm which was used two year ago by Novotná et al. (2016). Here the route was optimized by from 10 to 50%. The algorithm thus offers up to 40% optimization of current trains. This can bring considerable savings on fuel costs, the operation of the harvesting technique and the workforce.

CONCLUSION

This article shows how the Salesman problem may be used in the issue of waste management. In this time there is no way to create the optimal route in a reasonable time. There is one possibility, how the proposed algorithm can be used to optimize waste collection route in specific city and how the waste management can be connected with GIS technologies for analysis and graphic output.

REFERENCES

ArcGIS – Geografické informační systémy (GIS) – ARCDATA PRAHA. Geografické informační systémy (GIS) – ARCDATA PRAHA [Online]. Available at: https://www.arcdata.cz/produkty/arcgis. [2018-02-14].

Bartoň, S. 1999. Maple V 4. 1. vyd., Bratislava: Slovenská technická univerzita.

Cook, W. 2012. Po stopách obchodního cestujícího: matematika na hranicích možností. 1. vyd., Praha: Argo.

Česká Republika. 2001. Zákon č. 185/2001 Sb., o odpadech. In: Zákony pro lidi.cz [online]. © AION CS 2010-2018. Available at: https://www.zakonyprolidi.cz/cs/2001-185. [2018-01-30].

Das, S., Bhattacharyya, B. K. 2015. Optimization of municipal solid waste collection and transportation routes. Waste Management [Online], 43: 9–18. Available at: https://www.sciencedirect.com/science/article/pii/S0956053X15004432 [2018-10-15].

Geletič, J. 2013. Úvod do ArcGIS 10. Olomouc: Univerzita Palackého v Olomouci.

Golush, T. V. 2008. Waste management research trends. New York: Nova Science Publishers.

Ha, Q.M. et al. 2018. On the min-cost Traveling Salesman Problem with Drone. Transportation Research Part C, 86: 597–621.

Hemidat, S. 2017. Evaluation of Key Indicators of Waste Collection Using GIS Techniques as a Planning and Control Tool for Route Optimization. Waste and Biomass Valorization, 8(5): 1533–1554.

Introduction to 3D data: modeling with ArcGIS 3D analyst and Google earth.[Online]. Available at: http://dx.doi.org/10.1002/9780470548776 [2018-08-29].

Kennedy, H. 2009. Introduction to 3D data: modeling with ArcGIS 3D analyst and Google earth. Hoboken, N.J.: John Wiley.

Novotná, J. 2016. Optimizing Collection Routes of Collection Places. In MendelNet 2016: Proceedings of International PhD Students Conference [Online]. Brno: Mendelova univerzita v Brně, pp. 898–903. Available at: https://mnet.mendelu.cz/mendelnet2016/mnet_2016_full.pdf. [2018-10-15].

Petřík, M., Bartoň, S. 2016. Optimization of the Municipal Waste Collection Route Based on the Method of the Minimum Pairing. Acta Universitatis Agriculturae et Silviculturae Mendelianae Brunensis, 64(3): 847–854.

Ruda, A. 2012. Základy práce s ArcGIS 10. 1. vyd. Brno: Mendelova univerzita v Brně.

TSP heuristic approximation algorithms. UW Faculty. Web Server [Online]. Available at: http://faculty.washington.edu/jtenenbg/courses/342/f08/sessions/tsp.html. [2018-07-08].

Webdispečink. © 1999-2018 HI Software Development, s.r.o., Princip a.s. [Online]. Available at: https://www.webdispecink.cz [2018-09-08].

Laboratory temperature conditions as factor influencing pore water pressure readings in unsaturated triaxial tests

Piotr Osinski
Department of Geotechnical Engineering
Warsaw University of Life Sciences
Nowoursynowska St. 159, 02-776 Warsaw
POLAND

piotr_osinski@interia.pl

Abstract: The paper aims at investigating the influence of the laboratory room temperature on sensitive of pore pressure transducers and pressure/volume controller readings. During such tests as these used in unsaturated triaxial cell, the crucial testing factor is the precise measurement of the pore air and water pressure/volume changes of the sample. For the purpose of the present study, a single wall triaxial cell equipped with digital pressure/volume controller filled with water was used to control the pore water pressure and to measure the volume change. For the water pressure change measurements the 2 and 3 MPa transducer was used. To be able to measure the respond of those devices a thermocouple and atmospheric pressure transducer were connected to the triaxial cell. The investigation revealed that due to small changes of the room temperature in laboratory the readings for pressure transducers varied +/–20 kPa, such change as of 7 °C, during 2 days lasting test, could cause obtaining the errors of pressure and volume readings exceeding the manufacturer's declared values by as much as 10 times.

Key Words: laboratory triaxial tests, temperature influence, pressure transducer readings, unsaturated soil mechanics

INTRODUCTION

Unsaturated soil mechanics is rapidly developing field of geotechnical engineering sciences. Due to 3 phases (soil, air, water) character of unsaturated soil samples the laboratory techniques applying standard approaches of soil mechanics can no longer be used. The main reason for this is the soil suction acting in not fully saturated soil that needs to be measured and analysed when determining the geotechnical parameters (Elia et al. 2017). The soil suction can be defined as the attraction that the soil exerts on free water if the two are placed in contact. This attraction can be stronger if the water inside the voids starts to evaporate. The total soil suction, has two components: matric suction and osmotic suction. The matric suction is generated by the capillarity phenomenon associated with the existence of surface tension between water and air phases within the soil voids. The matric suction is thus dependent on the soil structure as it is affected by the pore size distribution of the soil. The osmotic suction is associated with salt concentration in the pore water (Osinski et al. 2017). To be able to measure the soil suction, there are number of methods available. These are mainly: filter paper method, dew point method, high suction probes method and pressure plate method (Tang et al. 2018). One of the commonly used method for determining the soil suction plotted as so called Soil Water Retention Curves, is the pressure plate method. The pressure plate differs from other techniques since it does not measure but imposes the suction to a soil sample. The suction is imposed by controlling both, the pore air pressure and pore water pressure. The difference between the pressures defines the matric suction. The pressure plate apparatus consists of a pressure chamber, inside of which is a saturated high air entry value (HAEV) porous ceramic disc. The soil sample is placed on top of the HAEV during testing. The maximum differential pressure attainable by this kind of apparatus is dependent on the AEV of the HAEV porous ceramic disc inside the chamber. The AEV value is the maximum value of air pressure that can be applied to the chamber before air entry (or "bubbling") occurs (when air starts to flow through the HAEV porous ceramic disc) (Toll et al. 2015, Osinski et al. 2016). This approach is often used in triaxial cells for determining the mechanical parameters of soil in unsaturated conditions.

Common knowledge is that to obtain reliable laboratory data, all the factors that could influence the measurement need to be fully controlled. It is often very difficult to provide such stable conditions at every stage of the test. When it comes to standard fully saturated conditions the triaxial test is not as sensitive to the temperature changes as unsaturated one. The reason is the air pressure and volume that needs to be additionally measured during each test. The compressibility of air is much higher then water so any insignificant changes in surrounding temperature could respond as significant fluctuations in volume/pressure readings that are crucial for further determination of soil mechanical parameters, using Mohr-Coulomb models (Fredlund and Rahardjo 1993, Head and Epps 1992, Koda 2012).

MATERIAL AND METHODS

The standard traixial test is one of the most commonly used geotechnical laboratory test, widely used to determinate strength, and deformation for variety of fully saturated soils under drained and undrained conditions (Head and Epps 1992, Lipinski et al. 1997, Lipiński et al. 2017). The triaxial test involves enclosing a cylindrical soil sample in a rubber membrane and placed inside a pressure chamber and subjected to radial stresses (confining pressure). Depending on the type of the triaxial apparatus; the base pedestal can move vertically and by that movement a vertical stress is applied to the specimen from the upper end. The water pressure surrounding the sample in the pressure chamber controls confining pressure. The volume change of the sample can be measured in two ways (Fredlund and Rahardjo 1993). One technique is based on using the controller volume change: for direct volume measurement, a water pressure/volume controller is filled with de-aired water and used to control the back pressure and to measure the pore water volume change going in and out from the sample. Second technique is based on a cell volume change: the cell volume change can be measured and used to establish the total specimen volume change. This technique is not very satisfactory because the cell stiffness is not infinite and therefore specimen loading changes and cell pressure changes cause a volumetric change in the cell. In addition, the system needs excellent temperature stability. Small changes in temperature can cause large changes in the volume of the cell water. For unsaturated triaxial tests the entire procedure and the approach is rather similar. However, to be able to apply, control and measure the suction, additional elements like air pressure/volume controller and high entry value porous disc need be provided. The air entering and leaving the sample is crucial for obtaining reliable results, thus the influence of temperature could be even more influencing. The air is much more compressible comparing to water, thus the differences in readings could be much more biased if the laboratory environment is not fully controlled. The general set up for unsaturated soil triaxial rig is presented on Figure 1.

Figure 1 Bishop & Wesley triaxial cell equipped with advanced air pressure/volume controller connection for unsaturated soil sample conditions testing

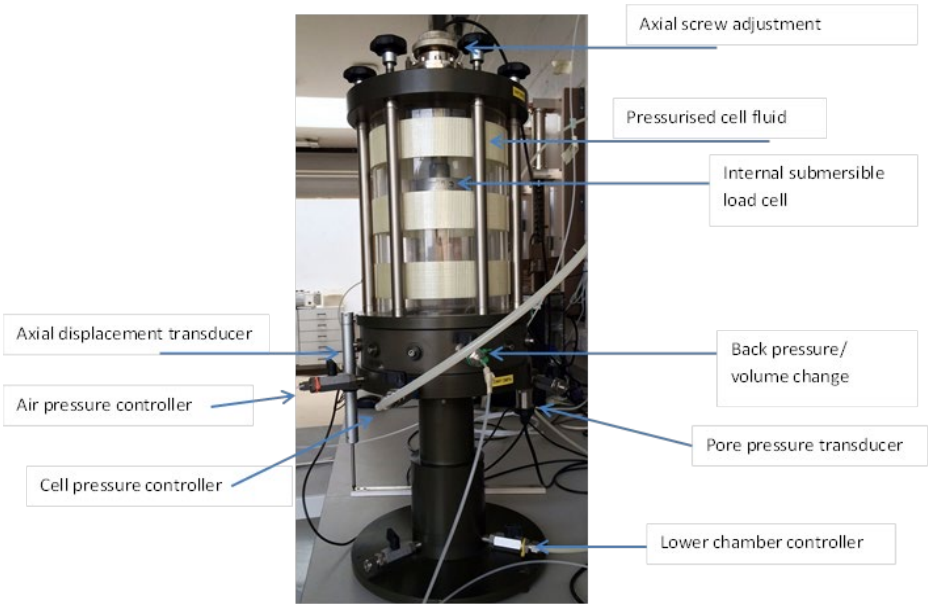

The triaxial testing system used to perform tests is an Automated Stress Path based on classic Bishop& Wesley- type stress path triaxial cell, and the air and water pressure/volume controller for unsaturated soil samples testing. It contains a number of components to enable the desired specimen stress state to be reached, and shear the specimen whilst recording the full soil response.

The crucial part of the test is a simultaneous measurement of air and water volume and pressure changes at each stage of the test. To be able to achieve it, the sample needs to be set up on the ceramic porous disc and connected to the air and water controllers to create suction. The specimen and connection set up is presented on Figure 2 (GDS 2018).

Figure 2 Soil specimen set up for applying and controlling suction during triaxial test (GDS 2018)

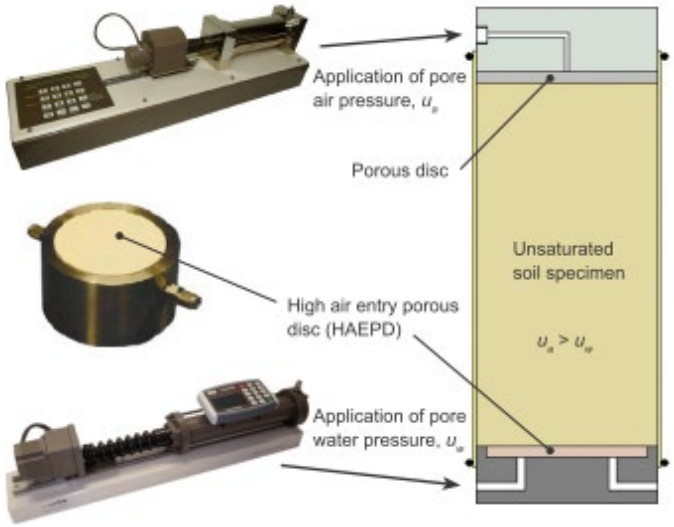

Before commencing any laboratory tests, the researcher is obliged to make sure that the results of the measurements are not biased or influenced by any external factors (Koda and Zakowicz 1998, Adamcová et al. 2016, Radziemska et al. 2017). For this reason, the author decided to perform a number of trail tests on the transducers and controllers, and their respond to changing laboratory environment conditions. The main considered factor was the laboratory room temperature.

For the trial tests there were two approaches adopted. First, having the cell fully filled with water, without a soil specimen placed on the pedestal. The second approach aimed at recording the values of the pressure when the controller connection and the transducer where left in the open water.

The investigated devices were: pore pressure transducers (2 and 3 MPa), air pressure/volume controller, back pressure/volume controller, cell pressure/volume controller. The certified accuracy of the transducers used in the study are 0.15% of declared range, thus in this case they are 3 and 4.5 kPa respectively. The technical specifications of controllers used for tests are:

- accuracy of pressure measurement: <0.1% full range;
- pressure range: 2MPa,
- volume accuracy: volume = <0.25% for 1000cc (with +/-12 mm^3 backlash up to 16MPa and +/- 5 mm^3 above 16 MPa),
- resolution of control (volume, pressure): 0.1 cm^3, 0.5 kPa,
- volume capacity: 1000cm^3

The devices used for recording the laboratory room conditions were sensitive electronic thermocouple and atmospheric pressure transducer. The entire measuring system was connected to common 8 channel serial pad and located next to each other, to give as much representative data as possible.

There were two scenarios considered while performing the trial tests investigating the influence of the temperature on the readings. The first one allowed exposure of the entire measuring system to sunlight, and the temperature in the laboratory room was not anyhow controlled. However, for the second scenario, the air conditioning (AC) was set at maintaining constant room temperature during the entire test, and the system was protected from the sunlight influence.

RESULTS AND DISCUSSION

The main reason for performing the trial tests investigating the influence of the laboratory room temperature on pressure/volume change readings for unsaturated triaxal tests, were the fluctuations observed at the shearing stage of CU reference triaxial tests. The example of plots presenting the unexpected backpressure records are provided on Figure 3. In the past there were number of researches performed on the influence of the temperature on the pore water pressures changes in soil, but there is a little knowledge of how precise and sensitive are the reading of devices used for such tests. The first research raising an awareness of the temperature influencing the pressure record for particular type of transducers were presented by Watson and Jackson in 1967. They proved the importance of having stable temperature conditions while performing the measurements, by obtaining sinusoidal fluctuations of the records. Rawlins (2012) also presented more recent investigations.

Figure 3 Fluctuations (a) and the back pressure increase (b) for CU triaxial test, shearing stage

a) *b)*

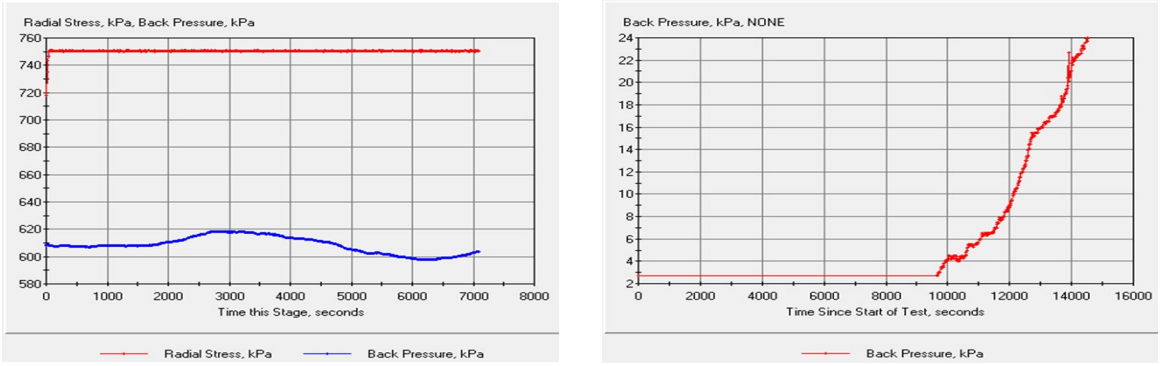

The character of the consolidated undrained triaxial test is that the backpressure during the shearing stage is disconnected from the cell, so the pressure should stay constant. Bearing in mind that the accuracy of the back pressure controller is more that 0.1% (what gives 2 kPa), the fluctuations shown on the graphs exceed 20 kPa. That is 10 time more than the acceptable level, provided by the manufacturer. For the standard triaxial tests for high effective stress, this magnitude of error could be in some cases neglected. However, speaking of unsaturated soil, there is also an air pressure/volume controller connected to the system, and both water and air pressure are used to maintained and control the suction. The Figure 4 presents the respond of the back pressure controller and 2 MPa pore pressure transducer, connected to the cell fully filled with water and left over two days, in temperature uncontrolled room.

Figure 4 Relationship between the temperature and the back pressure readings (a), and comparison between the behavior of the pore pressure transducer and the back pressure controller readings (b)

a) *b)*

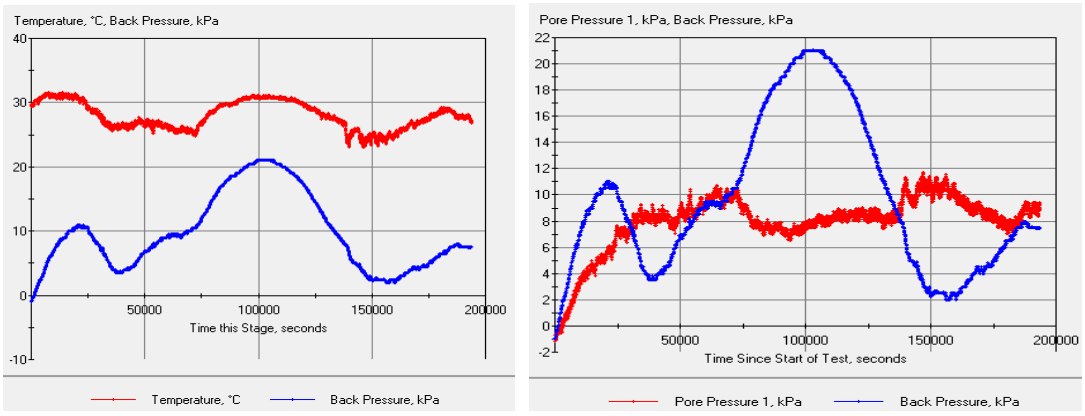

Form the Figure 4a, it is clear that the backpressure readings are highly dependent on the temperature fluctuations. The following graph (Figure 4b), revealed that the pore pressure transducer is less sensitive to the temperature changes and seems to be rather stable (falls in an error range).

The second set of tests presented on Figure 5, was performed using 3 MPa transducer, when the cell was partially filled with water, and sensors were submerged is shallow water. For these tests, the AC in the room was off, so the temperature was not controlled at all.

Figure 5 Relationship between the temperature and the back, radial and pore water pressure transducer readings, for uncontrolled room temperature

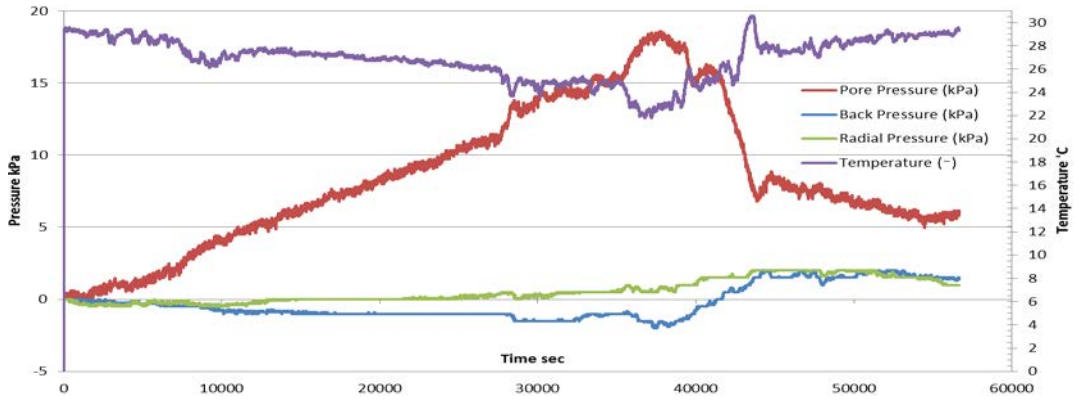

From the Figure 5 it could be seen that the change of the room temperature ranging from 22 to 30 °C (night and day time) significantly affects the pore pressure transducer records. According the manufacturer specifications the error of 3 MPa transducer should not exceed 4.5 kPa difference, but in fact it reaches almost 20 kPa starting from 0 kPa.

The final step of the tests was to investigate whether the fully controlled laboratory room temperature will result in more stable readings. For this purpose, the air condition was set to maintain the constant value (the room was isolated from air circulation). The results are presented on Figure 6.

Figure 6 Relationship between the temperature and the back, radial and pore water pressure transducer readings, at the constant laboratory room temperature

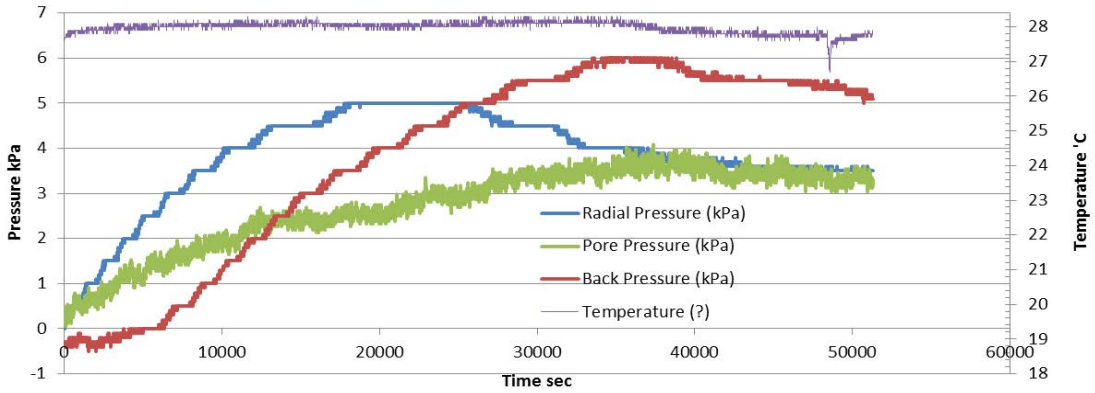

Plots on Figure 6 indicate significant improvement of the readings, and the pressure records for controllers and transducer, fall in the acceptable error range, not exceeding 6 kPa in total. The experiment proves the importance of having the laboratory conditions fully controlled and monitored.

CONCLUSIONS

The triaxial shear test, commonly used in geotechnical engineering practice is crucial for determination of mechanical parameters of soil. This type of test is complex and consists of number of sensors that gives the readings, so the further calculations of shear strength can be performed. When it comes to unsaturated soil mechanics, the triaxial rig needs to be additionally equipped with devices providing records, much more sensitive to the external sources of any potential disruption. This is why those tests need to be performed in perfectly stable laboratory environment. The present study was aiming at investigating how important for the precise measurement of parameters used for soil mechanical parameters determination, is the temperature and its changes during the testing. After performing a number of trail tests in temperature controlled room it was revealed that such change as

of 7 °C, during 2 days lasting test, could cause obtaining the errors of pressure and volume readings exceeding the manufacturer's declared values by as much as 10 times. Such biased records in case of unsaturated soil mechanics, where highly compressible medium as air is considered, are not acceptable. Thus, before performing such sophisticated geotechnical test a laboratory researcher needs to make sure that the surrounding environment is stable and fully controlled at each stage of the test.

ACKNOWLEDGEMENTS

The Authors would like to acknowledge the European Union's Seventh Framework Programme FP7/2007–2013/ under REA grant agreement no 289911. The authors also would like to acknowledge EU COST Action TU1202 "Impact of climate change on engineered slopes for infrastructure"

REFERENCES

Adamcová, D. et al. 2016. Soil contamination in landfills: a case study of a landfill in Czech Republic. Solid Earth, 7: 239–247.

Elia, G. et al. 2017. Numerical modelling of slope–vegetation–atmosphere interaction: an overview. Quarterly Journal of Engineering Geology and Hydrogeology, 50(3): 249–270.

Fredlund, D.G., Rahardjo, H. 1993. Soil mechanics for unsaturated soils. New York: Wiley.

GDS Ltd. 2018. Advanced Triaxial Testing: Part 2. [Online]. Accessible at: www.gdsinstruments.com [12.09.2018].

Head, K.H., Epps, R. 1992. Manual of soil laboratory testing. 1(2), London: Pentech Press.

Koda, E. 2012. Influence of vertical barrier surrounding old sanitary landfill on eliminating transport of pollutants on the basis of numerical modelling and monitoring results. Polish Journal of Environmental Studies, 21(4): 929.

Koda, E., Zakowicz, S. 1998. Physical and hydraulic properties of the MSW for water balance of the landfill. In Proceedings of 3rd International Congress on Environmental Geotechnics. Lisbon, Portugal, 7–11 September. Netherlands: Balkema Publishers, pp. 217–222.

Lipinski, M.J. et al. 1997. Preliminary evaluation of hazard due to liquefaction for Zelazny Most tailings pond. In Proceedings of XIV ICSMFE. Hamburg, Germany, 6–12 September. Netherlands: Balkema Publishers, pp. 1843–1846

Lipiński, M.J. et al. 2017. Influence of Fines Content on Consolidation and Compressibility Characteristics of Granular Materials. In Proceedings of WMCAUS. Prague, Czech Republic, 12–16 June. UK: IOP Publishing, pp. 032062.

Osinski, P. et al. 2016. Comparison of Soil Water Retention Curves for sandy clay, obtained using different laboratory testing methods. In Proceedings of 3rd European Conference on Unsaturated Soils [Online]. Paris, France, 12–14 September. France: EDP Sciences, pp. 11008 Available at : www.e3s-conferences.org [2018-09-15].

Osinski, P. et al. 2017. Soil water retention behaviour of granular soil–modified pore pressure transducer tests. 2017. Proceedings of 24th International PhD Students Conference (MendelNet 2017). Brno, Czech Republic, 08–09 November. Mendel University in Brno, Faculty of AgriSciences, pp. 796–801.

Radziemska, M. et al. 2017. Concept of Aided Phytostabilization of Contaminated Soils in Postindustrial Areas. International Journal of Environmental Research and Public Health, 15(1): 24.

Rawlins, S.L. 2012. Measurement Of Water Content And The State 0f Water In Soils. Soil Water Measurement, Plant Responses, and Breeding for Drought Resistance, 4: 1.

Tang, A. M. et al. 2018. Atmosphere–vegetation–soil interactions in a climate change context; impact of changing conditions on engineered transport infrastructure slopes in Europe. Quarterly Journal of Engineering Geology and Hydrogeology, 51(2): 156–168.

Toll, D.G. et al. 2015. Tensiometer techniques for determining soil water retention curves. In Proceedings of 6th Asia–Pacific Conf. on Unsaturated Soil. Guilin, China, 23–26 October. London: Taylor & Francis, pp. 15– 22.

Watson, K.K., Jackson, R.D. 1967. Temperature effects in a tensiometer-pressure transducer system. Soil Science Society of American Proceedings, Madison, 31: 156-60, 1967.

Evaluation of liquid transverse distribution under a twin spray jet installed on a drone

Aleksandra Pachuta, Berner Bogusława, Jerzy Chojnacki
Department Automatic, Mechanics & Construction
Koszalin University of Technology
Racławicka 15–17, 75–620 Koszalin
POLAND

apachuta@poczta.fm

Abstract: The article researches the influence of liquid pressure in a DGTJ60–11002 twin flat nozzle installed on a drone and the influence of air produced by moving drone rotators on changes in liquid volume transverse distribution of deposing drops stream on the patternator. The tests were conducted at liquid pressure of 0.2, 0.3, and 0.4 MPa. The significance of air stream influence on changes of transverse distribution shape of liquid volume deposed in a grooves of patternator was confirmed.

Key Words: drone, spray nozzle, patternator, liquid deposition

INTRODUCTION

Agricultural machines structures installed on unmanned flying platforms, drones, appear more and more frequently. Most frequently used are flying jets-rotor drones with installed liquid spraying device (Berner and Chojnacki 2017a). Single-rotor drones – helicopters, or multi-motor drones – multicopters, due to vertically directed thrust force produced by the rotors enable the platform to float on a specific height and moving it over objects in any direction. Spraying device installed on them consists of a liquid container, a pump, valves controlling liquid flow and jets.

A technologically advanced spraying drone can also be equipped in liquid flow registrars, as well as systems controlling and registering its flight using satellite positioning (Xue et al. 2016, Huang et al. 2009). Research indicates similar quality of results of jet spraying as compared to field boom devices spraying (Giles and Billing 2015).

Typical hydrodynamic nozzles used in field or orchard sprayers are primarily used to spray liquids. They are the most frequently nozzles with wide and narrow liquid spraying angle, but centrifugal nozzles also find use in this area (Giles and Billing 2015, Wei-Cai et al. 2016, Berner and Chojnacki 2017a, Zhou et al. 2011). Nozzles are mounted on metal beams installed on drones, or directly on drone ram, always below propellers level. During flight of the drone it causes the air stream produced by drone rotors to influence the stream of sprayed liquid and can cause its larger or smaller distortions. Air stream mass intensity and its speed result from the value of thrust force produced by drone rotors, necessary to overcome drone mass and enabling its ascend and movement.

Air stream influences liquid dispersion inside plant corona (Berner and Chojnacki 2017b). Drops stream shape changes may cause occurrence of excessive volume inconsistency of liquid disposed on plants, causing its excess or deficit (Sama et al. 2018, Smith 1992) (ISO 5682–1:2017).

Sprayed liquid stream shape changes may be evaluated through measurements of spraying angle or through changes of volume distribution of liquid disposed on patternator placed under the nozzle (Subr et al. 2017). It can also be evaluated using samples placed in a field or attached to plants. The patternator was used to assess changes of distribution of liquid containing insecticide nematodes, sprayed under the drone using XR 11002 flat spray nozzle (Berner and Chojnacki 2017c). The patternator was also use to determine change of dispersion of entomopathogenic nematodes on the sprayed cultivation area caused by air stream from drone rotors. The influence of the air stream produced by drone rotors on the change of: speed of droplets, spray angle and deposition of liquid, sprayed by the cone nozzle TR80-005C Lechler was investigated (Qing et al. 2017). It was found that range of changes of drops stream shape and spray angle, caused by the influence of air stream may also depend on position of nozzle in relations to drone rotors.

The research conducted thus far has not given a full answer regarding the factors influencing drops stream changes caused by drone rotors movement. Numerous types of nozzles used in plant spraying has never been tested.

Research objective was to assess the influence of liquid pressure in a twin flat spray nozzle installed on a drone and the influence of air stream produced by drone rotors on changes of liquid volume transverse distribution in the drops stream.

MATERIAL AND METHODS

The research utilised rotor drone–hexacopter. The drone was equipped in electric engines DJI 4114, kV – 400 and propellers of 15 x 5.2" dimensions. Power source was a Lipo12000 mA 22.2 V battery. Drone arms were raised at 8° angle to the level and turned to each other in pairs at 3° angle. Drone and its equipment was installed rigidly on a frame supported on sides. Under the drone, a patternator was put, crosswise to liquid stream width produced by the jet. Test station image presents Figure 1.

Figure 1 Test station

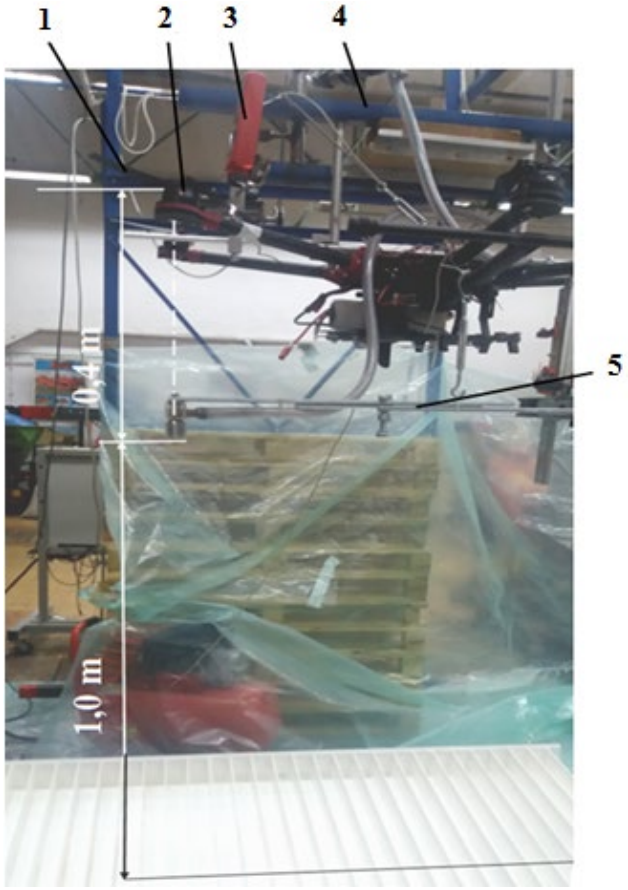

Legend: 1 – propellers, 2 – electric motor, 3 – optical tachometer, 4 – bar keeping the drone on the frame, 5 – bar with the nozzle

Nozzle was mounted under one of the drone rotors, on a long regulated blade mounted on drone frame. It was a nozzle producing double stream of drops with guard, TeeJet DGTJ60–11002. According to its manufacturing data, angle between streams equalled 60°. Jet nozzle outlet was located vertically over the drone engine central point, 0.4 m from the point of mounting of drone propellers to the engine axis. Nozzle opening was placed 1.0 m above the patternator. Grooves width of the measuring patternator equalled 0.05 m. The nozzle was supplied with liquid pumped from a stationary container by means of diaphragm pump Comet CRRC 56, driven by an electric motor. Liquid pressure was controlled through a valve installed on the pump. Liquid pressure value on the cord supplying the nozzle with the liquid was read due to the pressure sensor placed there, which transferred signal to a computer

via NI DAQCARD–6024 PCMCIA card. Data was gathered using National Instrument LabView software. Liquid pressure values accepted for the tests equalled 0.2, 0.3, and 0.4 MPa.

Drone rotors rotational speed was measured using optical tachometer connected to a computer. One value of drone rotors rotational speed was determined, which equalled 610 rad/s (5830 rot/min), which equalled drone thrust force equal 100.3 N.

The tests were conducted with operating and non-operating rotors. Each test was repeated thrice. The liquid from grooves on the patternator was gathered into measuring containers, and results were processed by calculating v_i – percentage of liquid gathered from specific grooves in relation to the total volume of liquid gathered from all grooves.

Moreover, in order to compare transverse distributions of liquid disposed on the patternator and sprayed with operating and non-operating drone rotors, liquid distribution uniformity coefficient were calculated using the following Formula (1).

$$CV = \frac{\sqrt{\frac{\sum_{i=1}^{i=n}(q_i - q_{sr})^2}{n}}}{q_{sr}} 100 \quad (1)$$

where:

CV – liquid distribution uniformity coefficient, %

q_i – volume of liquid contained in a specific container, ml

q_{sr} –average volume of liquid, ml

n – number of analysed containers

Supply water at 18 °C temperature was used for the tests. Before starting the tests, intensity of liquid dispersion from the jet at tested pressure was determined. The results presents Table 1.

Table 1 Measurement results of liquid dispersion from DGTJ60–11002–TeeJet jet

Pressure	0.2 MPa	0.3 MPa	0.4 MPa
Liquid flow	0.343 dm^3/min	0.396 dm^3/min	0.446 dm^3/min

RESULTS

On the basis of measurement results of liquid volume distribution on the patternator, percentage of liquid gathered from specific grooves in relation to the total volume of liquid gathered from all grooves, v_i was calculated. Calculation results presents graphically through charts Figure 2.

To determine the significance of the influence of liquid pressure in the nozzle and of the influence of the air stream produced by operating drone rotors on disposed liquid stream transverse distribution shape, data calculated from measurements of value v_i of specific measurements underwent bifactor variation analysis. Calculation were conducted in turn for specific grooves. On the basis of variation analysis of significance level $p < 0.05$, the significance of pressure influence was not proved, while the significance of influence of air stream on transverse distribution shape was proven. Significant changes of v_i occurred for grooves: 21, 23, 27, 29.

On the basis of achieved results of measurements of volume of liquid deposed on the groove board, distribution uniformity coefficient for each liquid pressure at non-operating drone rotors – CV and at operating rotors – CV_{blow} were calculated acc. to the Formula 1. The results presents Table 2.

Table 2 Liquid distribution uniformity coefficient values CV

Pressure	0.2 MPa	0.3 MPa	0.4 MPa
CV	59.41%	57.57%	58.31%
CV_{blow}	61.71%	60.88%	60.33%

Figure 2 Comparison of transverse distributions of liquid under the nozzle on patternator

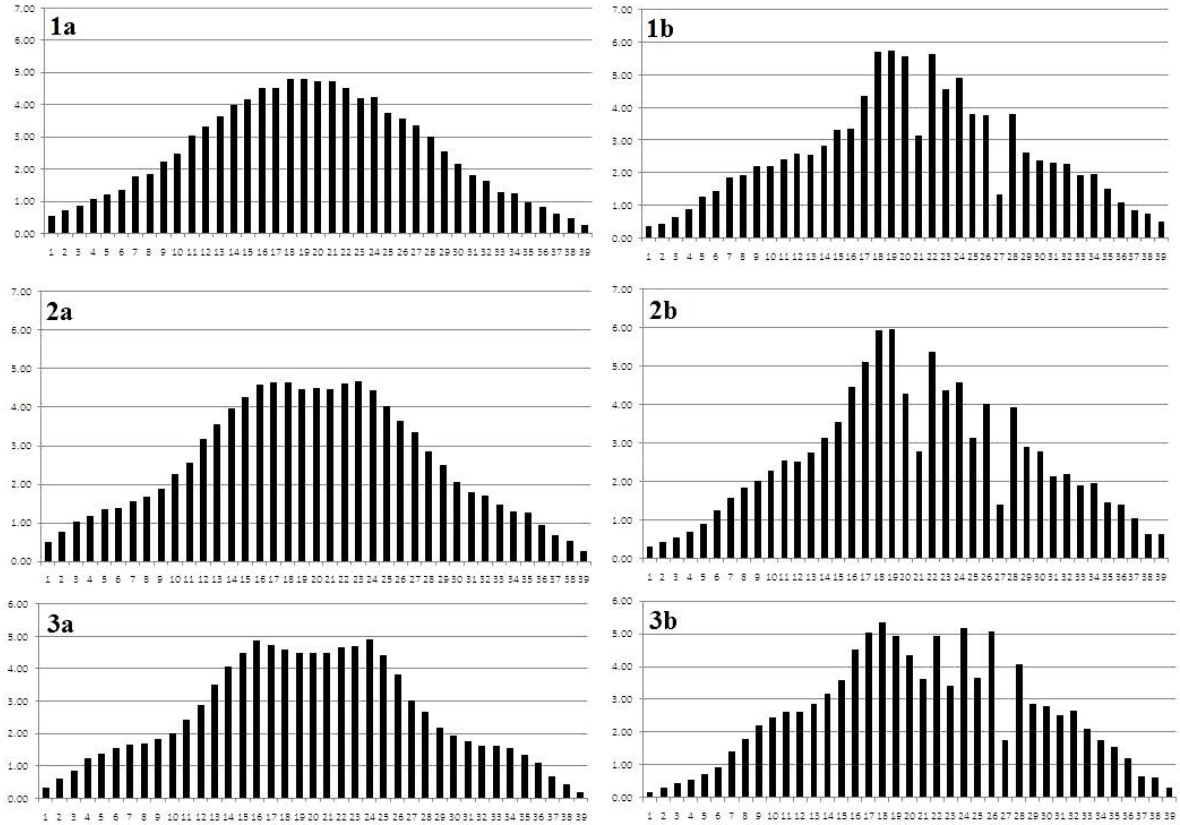

Legend: 11 – pressure 0.2 MPa, 2 – pressure 0.3 MPa, 3 – pressure 0,4 MPa, a – without operating drone rotors, b – with operating drone rotors

DISCUSSION

Calculated percentages of liquid gathered from specific grooves in relation to the total volume of liquid gathered from all grooves, v_i presented by Figure 2, indicate the possibility of distortion of sprayed liquid stream caused by a strong air stream. Distortions occurred mainly on one side of the graph. Lack of symmetry of liquid stream distortion in relation to nozzle symmetrical axis can probably result from lack of overlap of spraying nozzle position axis in relation to axis of engine rotor powering drone propeller. Lack of symmetry caused by arms tilt angle axis with rotors in relations to the level (8°) and arms bar angle in relations to the diagonal plane (3°).

Results of liquid dispersion from the jet were similar to results presented in the Table 1 of the manufacturer. According to the manufacturer's data, drops were size of medium drops at the 0.2 MPa pressure, and at remaining pressure values they remained within range of small drops. No symptoms suggesting that drops size had an influence on deposed liquid shape distribution were determined.

Air stream produced by operating drone propellers caused worsening of Liquid distribution uniformity coefficient on the groove board in each case, and significantly influenced change of transverse distribution shape of drops stream produced by the TeeJet DGTJ60–11002 twin spray jet. Drops stream distortions occurring during this jet type operation, caused by operating propellers of plant spraying drone, may decrease consistency of spraying pesticide liquid on cultivation areas.

Similarly, as in previous research works (Berner and Chojnacki 2017c, Qing et al. 2017) there was a change of the shape of liquid deposition on the patternator, due to the influence of air stream produced by the drone propellers. Although the nozzle producing double stream of drops was tested and not the cone sprayer as it was made in previous research (Qing et al. 2017), the asymmetry of the liquid distribution in relation to the jet axis was found as well. Probably, the reason of this phenomenon were also large differences in the speed of droplet streams in the parts of the spray of liquid as a result of the effect of the air stream.

CONCLUSION

The significance of influence of the air stream produced by operating drone rotors on changes of shape of transverse distribution of liquid deposed on the patternator, sprayed using DGTJ60–11002 twin spray nozzle installed on a drone, was confirmed, while the significance of pressure's influence on shape of transverse distribution of liquid sprayed with the same method was not determined.

It was found that the shape change of the transverse distribution of the settled liquid on the patternator caused by the air stream produced by the drone rotors is asymmetric with respect to the nozzle axis. There was also a significant differentiation of the volume of the deposited liquid in the subsequent grooves of the patternator.

Changing of the shape of the sprayed liquid can affect the quality of plant protection treatments using drone.

ACKNOWLEDGEMENTS

The research was financially supported by the statutory resources of the Mechanical Faculty of the Koszalin University of Technology.

REFERENCES

Berner, B., Chojnacki J. 2017a. Influence of the air stream produced by the drone on the sedimentation of the sprayed liquid that contains entomopathogenic nematodes, Journal of Research and Applications in Agricultural Engineering, 3(62): 26–29.

Berner, B., Chojnacki, J. 2017b. Use of drones in crop protection. In Proceedings of IX International Scientific Symposium Farm Machinery and Processes Management in Sustainable Agriculture. Lublin 2017: 46–51.

Berner, B., Chojnacki, J. 2017c. Zastosowanie bezzałogowych statków powietrznych do opryskiwania upraw rolniczych. Technika Rolnicza Ogrodnicza Leśna, 2: 23–25.

Giles, D.K., Billing, R.C. 2015. Deployment and Performance of a UAV for Crop Spraying Chemical Engineering Transactions, 44: 307–312.

Huang, Y.B. et al. 2009. Development of a spray system for an unmanned aerial vehicle platform. Applied Engineering in Agriculture, 25(6): 803–809.

ISO 5682–1:2017. Equipment for crop protection– Spraying equipment–Part 1: Test methods for sprayer nozzles.

Qing, T. et al. 2017. Droplets movement and deposition of an eight–rotor agricultural UAV in downwash flow field. International Journal of Agricultural & Biological Engineering, 10(3): 47–56.

Sama, M.P. et al. 2018. Validating Spray Coverage Rate Using Liquid Mass on a Spray Card. Transactions of the ASABE, 61(3): 887–896.

Smith, D.B. 1992. Uniformity and recovery of broadcast sprays using fan nozzles. Transactions of the ASAE, 35(1): 39–44.

Subr, A. et al. 2017. Testing the uniformity of spray distribution under different application parameters. In Proceedings of IX International Scientific Symposium "Farm Machinery and Processes Management in Sustainable Agriculture", Lublin 2017: 359–364.

Wei–Cai, Q. et al. 2016. Droplet deposition and control effect of insecticides sprayed with an unmanned aerial vehicle against plant hoppers. Crop Protection, 85: 79–88.

Xue, X. et al. 2016. Develop an unmanned aerial vehicle based automatic aerial spraying system. Computers and Electronics in Agriculture, 128: 58–66.

Zhou, L.X. et al. 2011. Experimental research on electrical centrifugal nozzle of aerial spray use. Chinese Agricultural Mechanization, 1: 107–111.

Mechanical and chemical resistivity of CMT welded joints

Nela Polakova, Petr Dostal, Michal Cerny
Department of Technology and Automobile Transport
Mendel University in Brno
Zemedelska 1, 613 00 Brno
CZECH REPUBLIC

nela.polakova@mendelu.cz

Abstract: The paper deals with analyzing the quality of special welded joints made by "Cold Metal Transfer" or "CMT" welding method. The aim of the experiment is to determine the impact of CMT welding on corrosion degradation of the joint. For this purpose the combination of diverse materials was used. Aluminum alloy AlMg3 and hot-dip galvanized carbon steel were welded by CMT method with AlSi5 filler material. Due to different electrode potential of welded specimen the galvanic corrosion occurred. Selecting of proper coating prevents the degradation process. For correct choice of the coating layer parameters, recognizing of corrosion process behavior of CMT joint in corrosion degradation environment with consideration of mechanical strain loading is important. This work is focused on intensity of corrosion reaction analysis in order to invent the most suitable surface layer.

Key Words: Cold Metal Transfer, corrosion, welding, degradation

INTRODUCTION

The need for joining dissimilar materials with very entails emergence of new and modification of the traditional methods of welding and brazing (Mathieu et al. 2007). Requirements for high productivity of welding or soldering and at the same time for the quality of joints cause an effort to limit the influence of the human factor (Yapp and Blackman 2004). An example of great progress in welding technology is the so-called CMT process which, in addition to other application areas, allows steel and aluminum material to be connected by an electric arc (Pickin and Young 2006).

Beginning developmental paths leading directly to the CMT falls in 1999, when he appeared requirement for controlled deposition (drip) solder on the target touch bulbs. In 2002, it was already known possibilities and advantages of CMT and began the last phase of development towards a series of usability. Now the focus is on the efficient use of this method in the industry, finding new applications and quality testing CMT welding machines for different applications (Dostál et al. 2015). Cold Metal Transfer welding is a modified MIG welding process based on short-circuiting transfer process (Talalaev et al. 2012). The wire feed rate and the cycle arcing phase are controlled to realise sufficient energy to melt both the base material and a globule of filler wire (Pickin et al. 2011). Feng et al. 2009 pointed that the CMT process is especially suitable for welding thin aluminium alloy sheets due to the low heat input and the slight deformation. From a technological point of view, the CMT method is soldering using an electric arc as a heat source for soldering the solder. For this reason, the concept of welding is used (Furukawa 2006).

Corrosion is a slow, progressive or rapid deterioration of metal body properties such as its appearance, surface aspect or mechanical properties under the influence of the surrounding environment: atmosphere, water, seawater, various solutions, organic environments, etc. (Vargel 2004).

MATERIAL AND METHODS

CMT welding method

CMT welding process currently offers interesting perspectives combination of specific properties of different materials that give the product in question required properties. Such joints were still realized only by mechanical means or adhesive. The main CMT process is the aluminum-alloy AlMg3 connection as well as the galvanized sheets. These connections, for example, offer the preconditions for unprecedented innovations in motor vehicle production (Votava et al. 2014).

CMT was developed as a result of the gradual adaptation of the MIG / MAG needs joining steel to aluminum. CMT enables controlled, almost current-free material transfer. The welding wire moves at rapid intervals in the opposite direction of its feed. The exactly defined retracted wire results in controlled release of droplets, which ensures a clean, spatter-free material transfer. These wire moves at high frequencies up to 90 Hz and require a fast-responsive wireless drive on the burner. The wire transport hose is therefore provided with a so-called buffer, i.e. a compensating member (absorber), which equalizes (absorbs) additional movements (Selvi et al. 2017).

Test sample

For measurement were prepared test samples consisting of various materials. For welding two basic materials were used: Aluminum alloy EN AW 7075 and hot-dip galvanized steel DX 51D. Samples consist of two different material parts and are welded by CMT overlapped joint. The connection has been used the most commonly used filler material for welding aluminum alloys AlSi5. Total constructed for the purposes of the experiment, 50 samples, the dimensions are evident from Figure 1.

Figure 1 The diagram of test sample

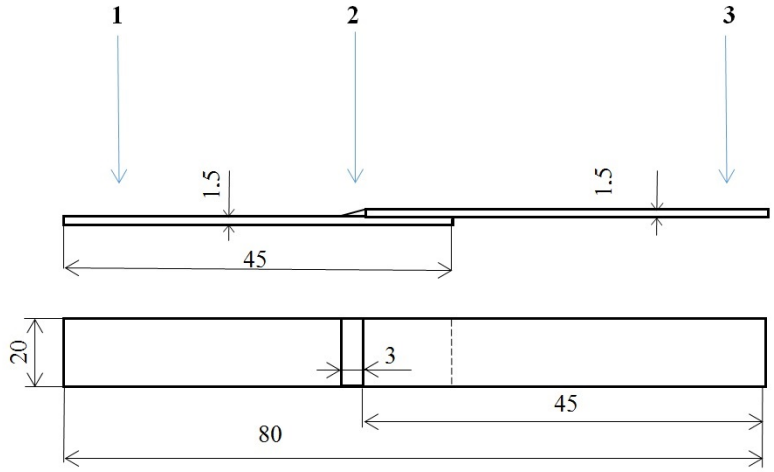

Legend: 1 – Aluminum alloy EN AW 7075, 2 – Additional material AlSi5, 3 – Hot-dip galvanized steel

Method of corrosion degradation

Corrosion tests were applied to accelerate corrosion degradation of the material and then evaluate the corrosion of the test materials. Due to the more aggressive oxidation environment, corrosion corrosion occurs several times faster than in normal conditions. The test was performed in a Liebish corrosion chamber of the S400M-TR type under the influence of salt mist. Temperature in the corrosion chamber at a test tube of 35 ° C. Concentration of sodium chloride (NaCl) 50 g ± 5 g per liter of distilled water. PH of aqueous solution 6.8. This test is suitable for testing corrosion protection for rapid detection of discontinuity, pores and defects. The controlled degradation takes place according to the standard ČSN EN ISO 9227. The samples were exposed to corrosion for 200 hours.

Tensile test method

The tensile test is the most frequently used mechanical test. The test specimens are clamped into the jaws so that the axis of the rod is parallel to the axis of the clamping jaws. The loading force is continuously increased until the sample breaks. During the tensile test process, the force applied to the test specimen and the relative elongation is measured. For the purposes of this experiment, the possibility of comparing the decrease of the maximum tensile stress of the corroded sample and the sample not loaded with corrosion environments was used. For this purpose, ZDM 5/51 was used. Control is provided by M-TEST.

RESULTS AND DISCUSSION

Visual inspection

After removing the samples from the chamber, it was visually found that the percentage of the most corrosive degradation was affected by a steel section whose surface was protected by the Aluzinc layer. The reason for this is less pronounced attack corrosion resistance of zinc to aluminum. According to literature Černý and Filípek (2014) it was found that this is galvanic corrosion. This type of corrosion is characterized by the fact that the corrosion attack concentrates on the area adjacent to the contact of the two metals (the welding area).

Tensile test

This experiment was designed to evaluate differences in mechanical properties changes in samples with different AE corrosion degradation. These were 25 samples left for 200 hours in an aggressive saline chamber and 25 samples left by environmental influences. At the same time, this experiment should evaluate the possibility of further utilization of AE in this area of measurement. It is clear from Figures 2, in the tensile test, material deformation occurs primarily in the region of the base material 3. This is primarily the area affected by the welding process (about 1.5 mm from the weld). Deformation occurs in the temperature-affected area, the sample is stretched, the joining failure is progressing slowly. The maximum tensile force was recalculated to the strength limit according to the Formula 1.

Formula 1 The maximum tensile force

$$\text{Rm } [MPa] = \frac{F_{max}[N]}{S_0[mm^2]}$$

In the corroded sample, a sudden breakage of the joint occurred when the tensile strenght exceeded about 66.7 MPa. The deformation was minimal. Sudden loss of cohesion occurred on the galvanized steel side.

Figure 2 Image of the test specimen after the tensile test

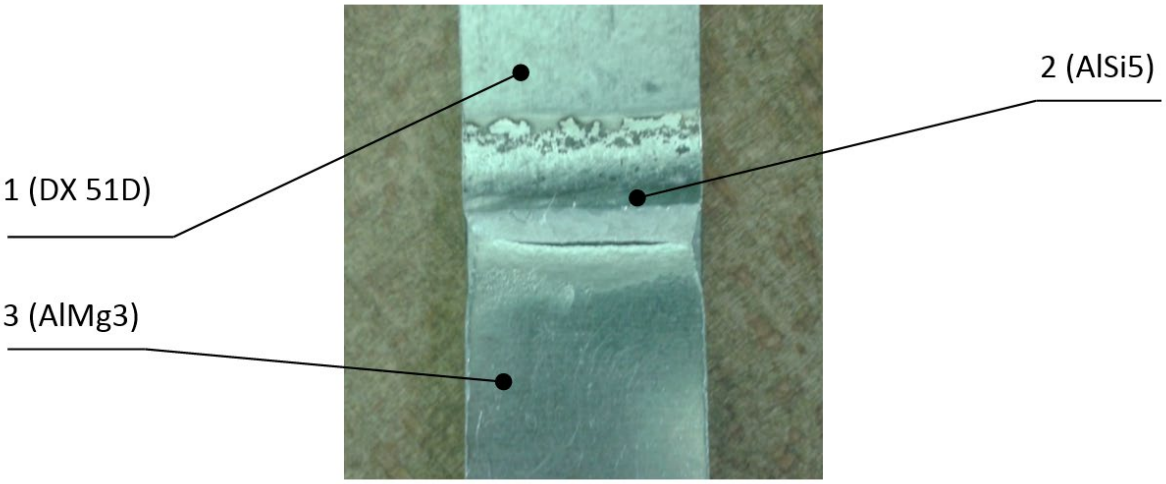

For samples that have been exposed to the aggressive environment of the salt chamber, it is clear from the Figure 3 and Figure 4 the decrease of the maximum achieved forces. From the graph it is evident that in this case, to achieve average maximum tensile strength 67.3 MPa. The maximum average tensile strength measured for original (uncorroded samples) was 79 MPa. After 200 hours of accelerated corrosion testing, the material is already degraded by galvanic corrosion at the site of the interaction of materials, with a significant reduction in cohesion. In this case, when then tensile stress is eliminated substantial formation of cracks and material discontinuity caused by stress.

Figure 3 Results tensile tests of original specimens

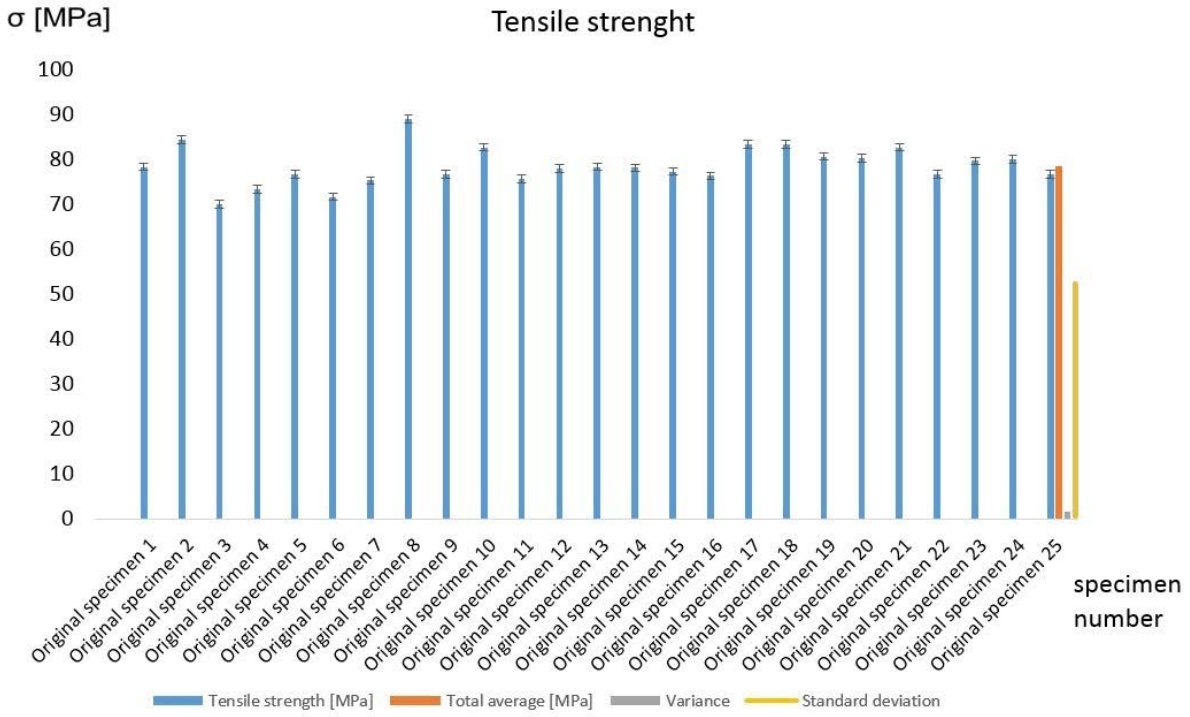

Figure 4 Results tensile tests of corroded specimens

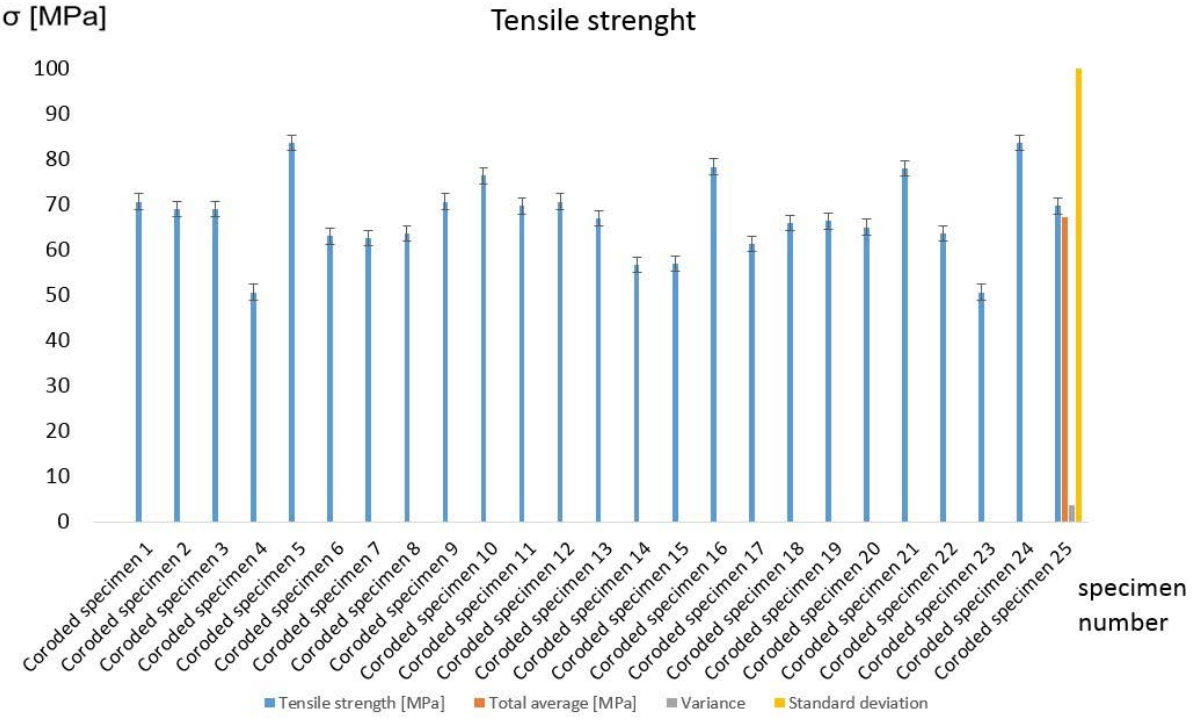

CONCLUSION

Experiment discusses CMT tensile strength weldments. We compared the mechanical resistance of corrosion-degraded samples, the samples that were not affected by corrosion degradation. Tensile test was carried out a total of 50 samples, of which 25 had been previously exposed to very aggressive environment salt fog. The results show a dramatic decrease in the tensile strength of the samples after

corrosion. This is mainly due to galvanic corrosion (Černý and Filípek 2014), which occurs with the electrochemical action of materials with different electrode potential.

Combinations of joining dissimilar materials is in terms of weight reduction structures or scaffolds important element in mechanical engineering. Considerable use of the CMT is planned in the automotive industry for bodywork. It is necessary, however, to recognize the risks described above when connecting two metals with different electrolytic potential.

The solution may be the use of a suitable surface anticorrosion layer which will reduce the influence of external factors on the base material and thereby slow down the process of electrochemical corrosion. The perspective of further research is to test these surface layers and analyze their application methodology to maximize the qualities of the CMT weld joint.

ACKNOWLEDGEMENTS

The research has been supported by the project TP 6/2017: Defectoscopic quality assessment of technical and organic materials; financed by IGA FA MENDELU.

REFERENCES

Černý, M., Filípek, J. 2014. Anodic-modified anticorrosive coatings. Acta Universitatis Agriculturae et Silviculturae Mendelianae Brunensis, 59(5): 23–30.

Dostál, P. et al. 2015. CMT Weld Resistance In Corrosive Environment. In Kvalita, technoloógie, diagnostika v technických systémoch. Nitra: SPU v Nitre, pp. 98–103.

Feng, J. et al. 2009. The CMT short–circuiting metal transfer process and its use in thin aluminium sheets welding. Materials & Design, 30(5): 1850–1852.

Furukawa, K. 2006. New CMT arc welding process–welding of steel to aluminium dissimilar metals and welding of super–thin aluminium sheets. Welding International, 20(6): 440–445.

Mathieu, A. et al. 2007. Dissimilar material joining using laser (aluminum to steel using zinc-based filler wire). Optics & Laser Technology, 39(3): 652–661.

Pickin, C.G., Young, K. 2006. Hodnocení procesu přenášení za studena (CMT) pro svařování hliníkové slitiny. Věda a technika svařování a spojování, 11(5): 583–585.

Pickin, C.G. et al. 2011. Characterisation of the cold metal transfer (CMT) process and its application for low dilution cladding. Journal of Materials Processing Technology, 211(3): 496–502.

Selvi, S. et al. 2017. Cold metal transfer (CMT) technology–An overview. Defence Technology.

UNMZ. 2007. Technické normy. CSN EN ISO 9227. Praha: Úřad pro technickou normalizaci, metrologii a statní zkušebnictví.

Talalaev, R. et al. 2012. Cold metal transfer (CMT) welding of thin sheet metal products. Estonian Journal of Engineering, 18(3): 243.

Vargel, C. 2004. Corrosion of aluminium. Elsevier.

Votava, J. et al. 2014. Degradation processes of Al-Zn welded joints. Acta Universitatis Agriculturae et Silviculturae Mendelianae Brunensis [Online], 62(3): 571–578. Available at: https://acta.mendelu.cz/media/pdf/actaun_2014062030571.pdf. [2018-09-03]

Yapp, D., Blackman, S.A. 2004. Recent developments in high productivity pipeline welding. Journal of the Brazilian Society of Mechanical Sciences and Engineering, 26(1): 89–97.

TIG welding of stainless steel and titanium with additive AG 104

Nela Polakova, Petr Dostal, Jiri Votava
Department of Technology and Automobile Transport
Mendel University in Brno
Zemedelska 1, 613 00 Brno
CZECH REPUBLIC

nela.polakova@mendelu.cz

Abstract: The article deals with welding of two basic, non-weldable materials: stainless steel X5CrNi 18-10 and titanium UNS N50400. Fusion welding of these basic materials is difficult because of the formation of brittle compounds which adversely affect the strength of the joint. Therefore, in the experiment, the interlayer was designed to weld the interlayer in the form of the AG104 additional material, which should make this heterogeneous weld successful. For arc welding, the TIG method was chosen. In order to avoid the adverse absorption of the gases of basic materials (especially titanium) and welding additive material, pure argon-protected welding was used. The quality of the resulting joint will be verified by a tensile test. Relief weld will be plotted graphically over the scanned 3D microscope. Also, the weld structure will be visualized by a 3D Keynes microscope image.

Key Words: TIG welding, argon, stainless steel, titanium, additional material AG 104

INTRODUCTION

Welding of metals is included in the joining of materials of non-disintegrable character. In all branches of industry (for example, automotive) it is desirable to combine heterogeneous materials with different melting points and other mechanical and chemical properties (Votava et al. 2014).

The heterogeneous combination of stainless steel and titanium is in the interest of many industries (e.g. the harsh industry). However, it is very difficult to combine these various materials due to their metallurgical incompatibility and the formation of intermetallic compounds (FeTi and Fe2Ti) (Pardal et al. 2016).

The main intermetallic phases formed on the interfacial regions of the titanium are α-β-Ti and Ti-Fe. Intermetallic FeTi is the phase formed in the interfacial steel region. The presence of IMC (intermetallic compounds) in intermediate areas always reduces the mechanical properties of the joint. Mechanical and physical properties are reduced in this area (Murakami et al 2003, Shiue et al. 2008).

IMC negatively affects the bonding strength in shear, and cracks in the joint. Therefore, it is desirable to have the IMC thickness as small as possible (Elrefaey and Tillmann 2007).

MATERIAL AND METHODS

The main aim of the experiment was to create a permanent joint of X5CrNi 18-10 austenitic stainless steel and UNS N50400 titanium using an additional material AG 104. 2 millimetre sheets with the length of 200 mm (4pc) were welded, after the welding they were cut by ATA Brilliant 250X circular saw (under the influence of a cooling liquid in order to avoid the damage of the welds due to the heat caused) to 20 mm strips for samples for the tensile test. The total number of the cut samples was 20. A diagram of the welded sample is in Figure 1. For welding, the TIG arc welding method was used (non-melting tungsten electrode with additive AG 104). Two types of welding parameters were selected:

A) Welding current was 110 A, welding voltage was 15 V, manual feed of the wire.
B) Welding current was 130 A, welding voltage was 14 V, manual feed of the wire.
The protecting gas was 100% argon in both cases, the flows was about 10 l/min

Figure 1 Diagram of the welded sample after the cutting

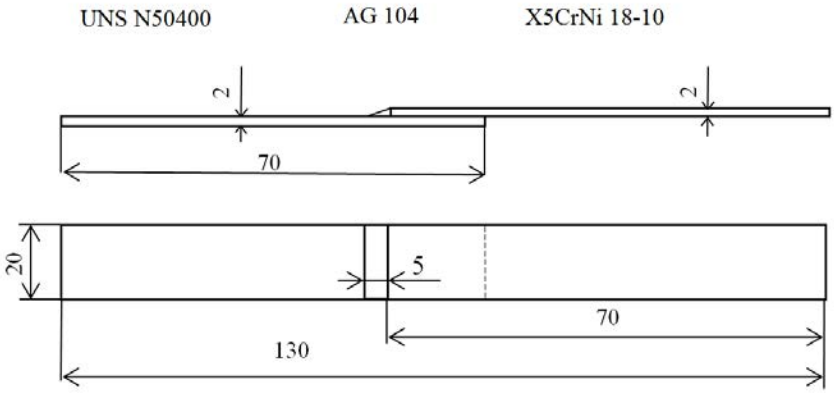

To visualize the relief of the weld surface was used 3D Keyence microscope.

To determine the internal structure of the weld, the sample was subjected to a metallographic cut. That consisted of cutting the material to the desired size (ATA Brilliant 250X Circular Saw). Further pressing into a resin and subsequent grinding on abrasive paper and polishing of diamonds. The Keyence 3D microscope was also used for optical analysis.

For the determination of tensile strength, the ZDM 5/51 test tee was used (Zacal et al 2015), which digitally records the measured values.

RESULTS AND DISCUSSION

The welding relief in Figure 2 after using the welding parameters B) (welding current was 130 A, welding voltage was 14 V, welding speed was 2 mm/s.). From relief it is seen that the welding conditions are not entirely optimal, since there is created a crack to the size of 260.16 µm. These samples also showed low tensile strength.

Figure 2 Relief of the weld

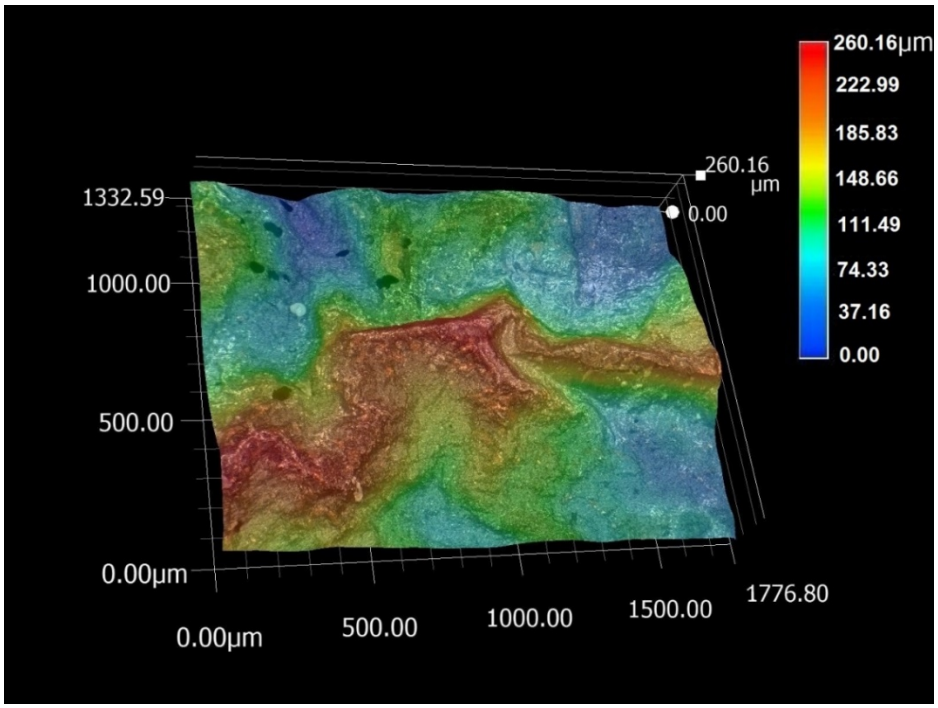

Higher values of tensile strength have resulted in welded parameter samples A) (welding current was 110 A, welding voltage was 15 V, welding speed was 2 mm/s.). Results of tensile tests on samples of welded parameters A) were similar, figure 3 shows a representative sample. The maximum tensile

force was recalculated to the strength limit according to the formula Rm $[MPa] = \frac{F_{max}[N]}{S_0[mm^2]}$. The tensile test results were 139 MPa.

Figure 3 Tensile test results

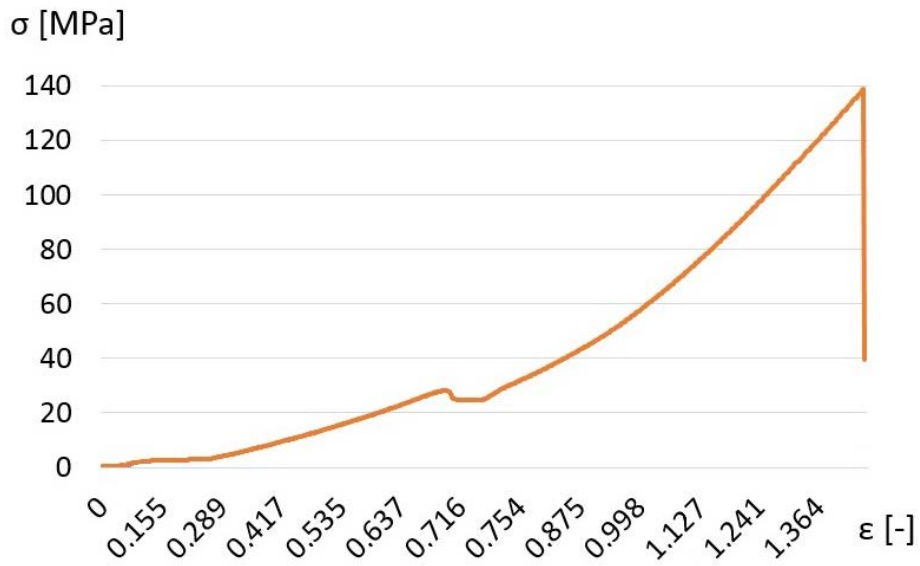

The microstructure of the successfully welded joint having the highest joint strength is shown in Figure 4.

Figure 4 Microstructure of the welded joint

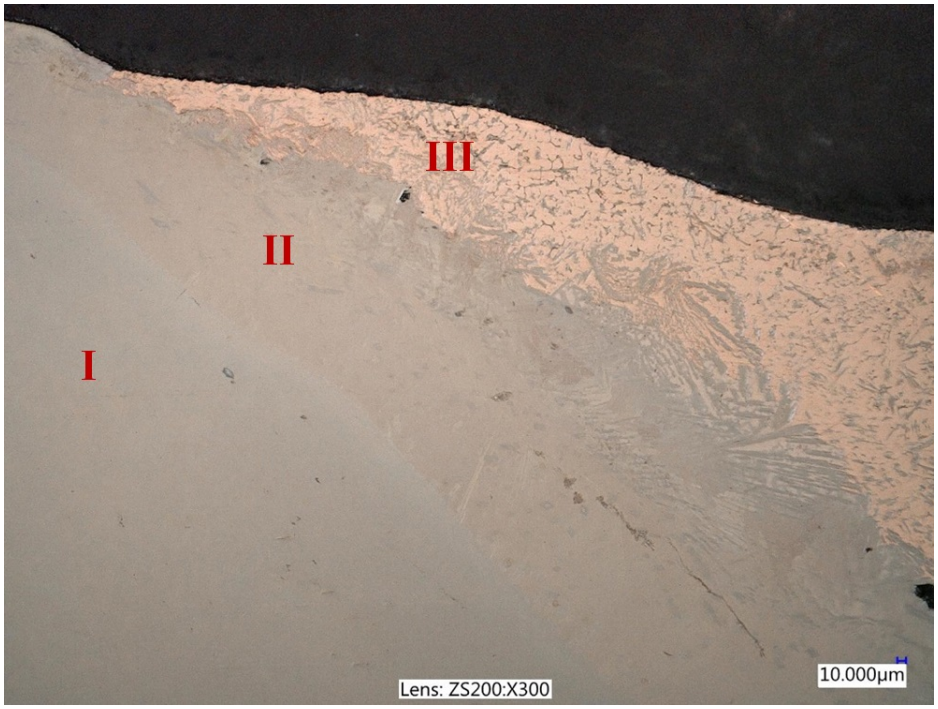

Area I is titanium base metal without molten additional material.

Area II shows titanium alloys having smaller amounts of additional material. There are Cu2Ti, Ti2Cu, TiCu alloys with Ag tracks.

Area III is the additive material (AG 104) consisting of eutectic Ag–Cu phase, silver rich solid solution phase which formed duo to the consumption of Cu by Cu–Ti phases in the main alloy, and some scattered Cu2Ti phase (Elrefaey and Tillmann 2010).

The identified microstructure is consistent with the results published in the articles Atasoy and Kahraman (2008), He et al. (2006), Shiue et al. (2003).

CONCLUSION

Arc welding method TIG (tungsten non-melting electrode) using additive AG 104 welding of two different materials - stainless steel X5CrNi 18-10 and titanium UNS N50400 was successfully realized. Ag–Cu alloys are widely used as an additional material for welding for steel joints (Kodentsov et al. 2001). The materials used successfully combined with the AgCu foil by vacuum soldering previous research (Guo et al. 2015). Instead of vacuum soldering, a protective gas consisting of pure argon was used.

Welding was performed using two welding parameters. Welding parameters with better results were: A) Welding current was 110 A, welding voltage was 15 V, welding speed was 2 mm/s.

The measured tensile strength was 139 MPa. Welder relief shown by 3D microscope Keyence visualized a crack resulting from welding under unsuitable welding conditions B) Welding current was 130 A, welding voltage was 14 V, welding speed was 2 mm/s.

The microstructure of a successful weld (which showed better results) was also acquired by the Keyence 3D microscope. The microstructure shows the three basic areas of the weld: the base material, the diffusion layer and the additive material. The strength of the welded joint of the above materials increases with decreasing the amount of energy injected into the weld.

ACKNOWLEDGEMENTS

The research has been supported by the project TP 6/2017: Defectoscopic quality assessment of technical and organic materials; financed by IGA AF MENDELU.

REFERENCES

Atasoy, E., Kahraman, N. 2008. Diffusion bonding of commercially pure titanium to low carbon steel using a silver interlayer. Materials Characterization, 59(10): 1481–1490.

Elrefaey, A., Tillmann, W. 2007. Interface characteristics and mechanical properties of the vacuum-brazed joint of titanium-steel having a silver-based brazing alloy. Metallurgical and Materials Transactions A, 38(12): 2956–2962.

Elrefaey, A., Tillmann, W. 2010. Brazing of titanium to steel with different filler metals: analysis and comparison. Journal of Materials Science, 45(16): 4332–4338.

Guo, W. et al. 2015. Microstructure and mechanical properties of C/C composite/TC4 joint with inactive AgCu filler metal. Ceramics International, 41(5): 7021–7027.

He, P. et al. 2006. Microstructure and kinetics of induction brazing TiAl-based intermetallics to steel 35CrMo using AgCuTi filler metal. Materials Science and Engineering: A, 418(1–2): 53–60.

Kodentsov, A.A. et al. 2001. The diffusion couple technique in phase diagram determination. Journal of Alloys and Compounds, 320(2): 207–217.

Murakami, T. et al. 2003. Dissimilar metal joining of aluminum to steel by MIG arc brazing using flux cored wire. ISIJ International, 43(10): 1596–1602.

Pardal, G. et al. 2016. Dissimilar metal joining of stainless steel and titanium using copper as transition metal. The International Journal of Advanced Manufacturing Technology, 86(5–8): 1139–1150.

Shiue, R.K. et al. 2003. Infrared brazing of TiAl intermetallic using BAg-8 braze alloy. Acta Materialia, 51(7): 1991–2004.

Shiue, R.K. et al. 2008. Infrared brazing of Ti–6Al–4V and 17-4 PH stainless steel with (Ni)/Cr barrier layer (s). Materials Science and Engineering: A, 488(1–2): 186–194.

Votava, J. et al. 2014. Degradation processes of Al-Zn welded joints. Acta Universitatis Agriculturae et Silviculturae Mendelianae Brunensis [Online], 62(3): 571–578. Available at: https://acta.mendelu.cz/media/pdf/actaun_2014062030571.pdf. [2018-09-03]

Zacal, J. et al. 2015. Acoustic emission during tensile testing of composite materials reinforced carbon and aramid fibers. In Proceedings of International PhD Students Conference MendelNet 2015 [Online]. Brno, Czech Republic, 12 November, Brno: Mendel University in Brno, Faculty of AgriSciences, pp. 568–572. Available at: https://mnet.mendelu.cz/mendelnet2015/mnet_2015_full.pdf. [2018-08-08].

Usage of fodder beet tuber pulp as a binder in straw pressure agglomeration

Agnieszka Zdanowicz, Jerzy Chojnacki
Department Automatic, Mechanics & Construction
Koszalin University of Technology
Racławicka 15–17, 75–620 Koszalin
POLAND

agnieszka.zdanowicz@s.tu.koszalin.pl

Abstract: Additions of binders play a crucial role in pellet quality and can improve pellet physical features. Barley chopped straw mixed with fodder beet tuber pulp was used for the palletisation process. The article examined the influence of the addition of fodder beet pulp to the substrate and of substrate moisture content on granulates hardness and gravity drop resistance. The tested relative moisture content of the raw material equaled on average between 12.3, 19.1, and 24.9%. It was determined that both pulp content increase in the mixture and relative moisture content of the raw material increased granulate hardness. The increase of pulp content in the mixture resulted in an increase of granulate gravity drop resistance.

Key Words: granulate, barley straw, fodder beet, granulate hardness

INTRODUCTION

The energise or nutritional pellet should meet requirements regarding its resistance to physical factors, which can cause it to partially or completely disintegrate. It should be resistant to, among others, crushing, breaking, and shock. To improve physical properties of the pellet, various substances which improve its resilience are mixed with biomass during its agglomeration (Obidziński 2014).

Straw excess produced by the agriculture results in using it as livestock fodder or as biofuel for fired heaters. Low contents of natural ingredients binding straw particles caused the pellet produced as a result of its agglomeration to be frail. Thus, the significance of natural, easily available, and cheap substances binding biomass particles during its pressure agglomeration in granulators keeps growing. The problem lies in the selection of natural substances as binders and determining the influence of their content in the granulated raw material on changes of mechanical properties of the received product. The smallest minimum content of the binder in the raw material used for granulate production, which makes as large as possible changes in granulate quality properties should be endeavoured to be used (Zdanowicz and Chojnacki 2017).

Flour and grain containing starch can be used as a natural binder, but the binding agent should be as cheap as possible (Chojnacki and Zdanowicz 2017). It can be a potato pulp, the by-product of the potato starch production process. It can also be fodder beet tuber pulp. It is a valuable product in fodder production (Collomba et al. 2004). Moreover, it has high energetic properties (Al-Jbawi et. al. 2016, Chakwizira et al. 2013, Shevtsov et al. 2017). It is used by farmers in a dry form, or in a mist form as fodder for farm animals. It can also be a beneficial addition to fodder for livestock (pigs, sheep, goats, horses (Pembleton et al. 2011). It is mixed with various substrates, such as hay, bran, straw, or chaff (Khogali 2011, Turki 2011). Carbohydrates in fodder beet pulp are highly digestible (in between 87 and 90%). On the other hand, its low protein content (8.7%) requires adding supplements rich in protein. Using fodder beet pulp as a binder in the production of the pellet from a straw can not only increase the energy value of the granulates used as fuel for heaters but also of straw used as the feed of farm animals.

The research objective was to assess the influence of fodder beet pulp content mixed with straw and the relative moisture content of the mixture on the hardness of the granulates made of the mixture, as well as the influence of fodder beet pulp content mixed with straw on granulate gravity drop resistance.

MATERIAL AND METHODS

The To make the granulates, barley straw with the addition of the tuber pulp of fodder beet of Syriusz variety was used. Chopped straw before granulating was refined using a universal grinding machine. Particles had size of 10–30 mm. Fodder beet tubers were refined using a mechanical grinder.

The relative moisture content of the raw materials was measured and equalled:

– for the barley chopped straw – 3.13%,

– for the fodder beet tuber pulp – 16.31%.

The planned weight percentage ratio of fodder beet pulp dry mass of the total weight of mixture dry mass equalled: 0.0; 8.0; 14.7%. For this purpose, 200.0 g of the chopped straw was measured out and mixed with, in the turns, 0.0; 20.0 and 40.0 g of fodder beet pulp. Mixture moisture content was changed through mixing an additional, measured out water volume into the prepared mixture of straw and fodder beet tuber pulp. 20; 40 and 60 ml of water, respectively, were added. Prepared samples were put in hermetically closed containers and left for 48 hours for the purpose of liquid penetrating mixture stature. Due to a different relative moisture content of the mixture ingredients and their different mass content in the mixture, adding a specific amount of water result in receiving three slightly differing relative moisture content results, which then were averaged for the same liquid additions. Values of weight content of the barley chopped straw and fodder beet tuber pulp mixture and its relative moisture content presents Table 1.

Table 1 Factors of producing a mixture of barley chopped straw and fodder beet tuber pulp

	Contant				Additional water	Moisture content	Average moisture content
	Barley chopped straw	Fodder beet tuber pulp	Barley chopped straw (d.m.)	Fodder beet tuber pulp (d.m.)			
	(g)	(g)	(%)	(%)	(ml)	(%)	(%)
1	200	0	100.0	0.0	20	11.94	
2	200	20	92.0	8.0	20	12.30	12.3
3	200	40	85.3	14.7	20	12.61	
4	200	0	100.0	0.0	40	19.28	
5	200	20	92.0	8.0	40	19.05	19.1
6	200	40	85.3	14.7	40	18.85	
7	200	0	100.0	0.0	60	25.48	
8	200	20	92.0	8.0	60	24.83	24.9
9	200	40	85.3	14.7	60	24.26	

RESULTS AND DISCUSSION

In the mixture underwent a thickening process using a pellet mill (model ZLSP 150) of 4 kW power. The thickness of the granulates double-sided matrix equalled 30 mm, and openings diameter was 6 mm.

Pellet resistance was determined on the basis of the following tests:

Pellet hardness measurement was conducted using Kahl hardness tester by crashing the pellet and determining force occurring at the moment of its structure destruction (Obidziński 2014), (Zdanowicz and Chojnacki 2017).

Gravity drop resistance was evaluated through percentage mass loss after dropping pellet portion thrice from a height of 2.0 m on a steel board of 20 mm thickness. After each drop, the samples were sifted through a sieve of 8×8 mm openings, which are the minimal admissible dimensions of utilised pellets. Pellet gravity drop resistance K was calculated using the following formula:

$$K = \frac{Mz}{M} \cdot 100 \quad (1)$$

where:

K – gravity drop resistance,

M – pellet mass before the drop, kg,

Mz – a mass of pellet remaining in the sieve, kg.

Research results of influence on granulate hardness underwent double-factor variation analysis in order to determine the significance of examined factors. The first factor was fodder beet pulp content in the mixture, the second – mixture relative moisture content. The influence of beet pulp content on average granulate hardness presents figure 1, while figure 2 presents the influence of raw material relative moisture content on average granulate hardness. As a result of variation analysis, a significant influence of both examined factors on granulate hardness was determined at significance coefficient value lower than 0.05. Increasing the amount of fodder beet tuber pulp added to the barley chopped straw caused an increase of granulate hardness. The addition of 8% pulp caused an increase of granulate hardness up to 367.78 N, while maximum (14.7%) pulp dry mass content in the mixture caused an increase of granulate hardness up to 379.18 N.

Figure 1 Influence of fodder beet tuber pulp dry mass content in relation to the total dry mass of the barley chopped straw substrate on produced pellet hardness

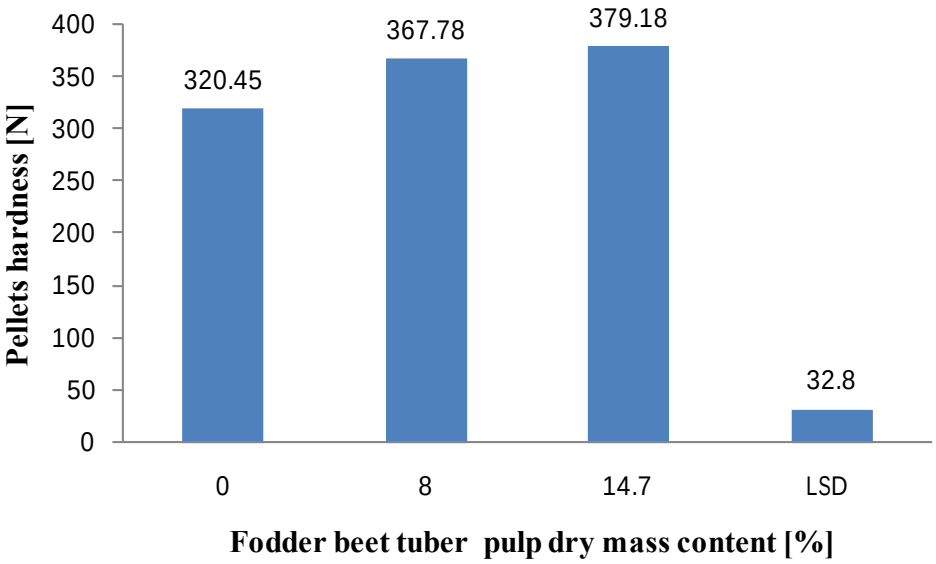

Legend: LSD – Lower Significant Difference

Granulate hardness increased also proportionally to raw material relative moisture content increase, reaching on average 416.17 N at the maximum moisture content equal 24.9%. Figure 3 presents pellet hardness changes depending on both fodder beet pulp content in the mixture and the mixture relative moisture content. The lowest pellet hardness level of 236.9 N was noted for raw material without fodder beet pulp addition and at the lowest relative moisture content – 12.3% and the highest hardness equal 436.26 N was noted at the maximum content of pulp dry mass in the mixture dry mass equal 14.7% and at the maximum relative moisture content of 24.9%.

Figure 2 Influence of relative moisture content of barley chopped straw and fodder beet tuber pulp mixture on produced pellet hardness

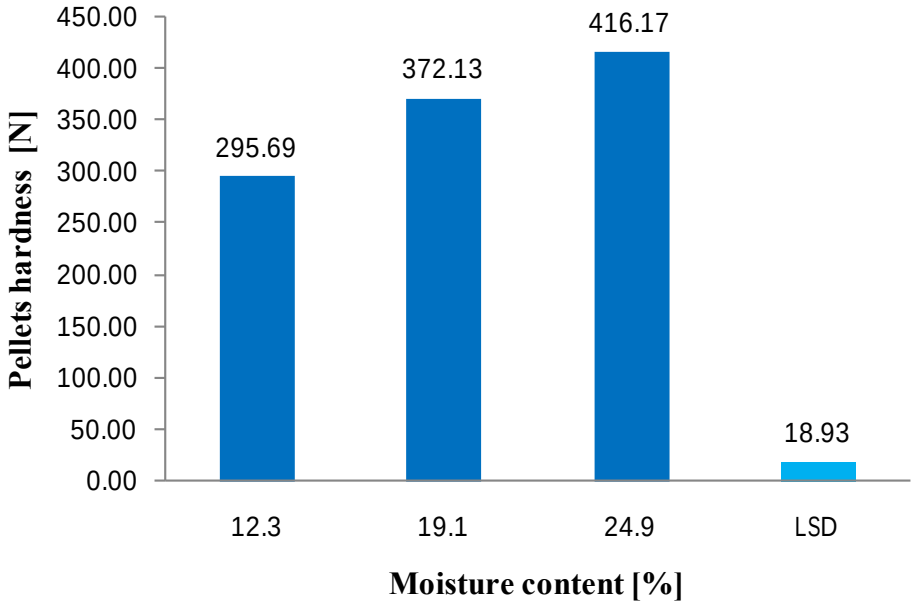

Legend: LSD – Lower Significant Difference

Figure 3 Influence of beetroot tuber pulp content and moisture content on average produced pellet hardness

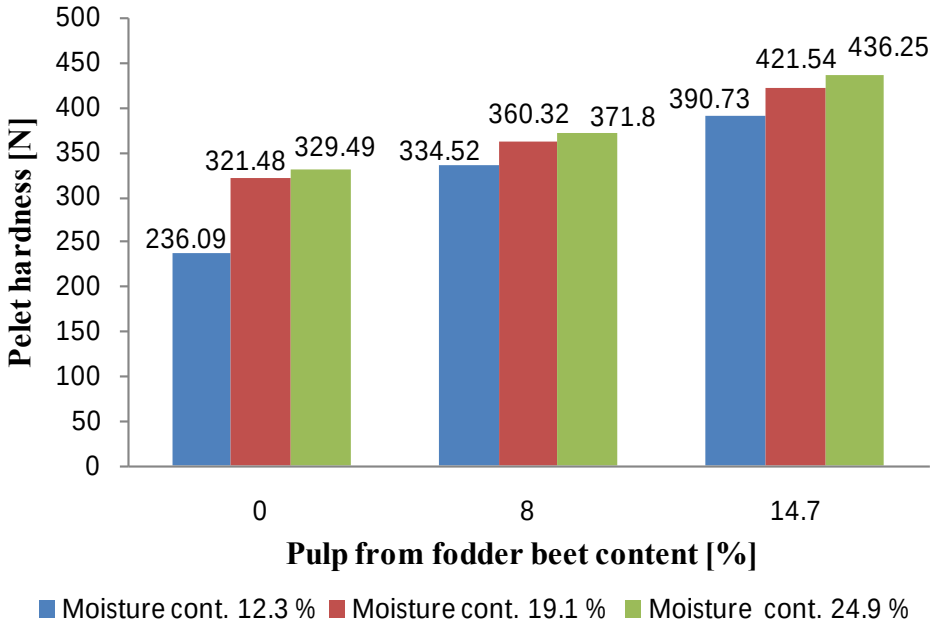

Figure 4 presents the influence of the gravity drop resistance value of the granulates produced from a mixture of barley chopped straw and fodder beet tuber pulp. The result of the conducted tests determines that increasing fodder beet pulp content in the mixture from 0 to 14.7% caused an increase of granulate gravity drop resistance value.

Figure 4 Influence of relative moisture content of barley chopped straw and fodder beet tuber pulp mixture on produced pellet hardness

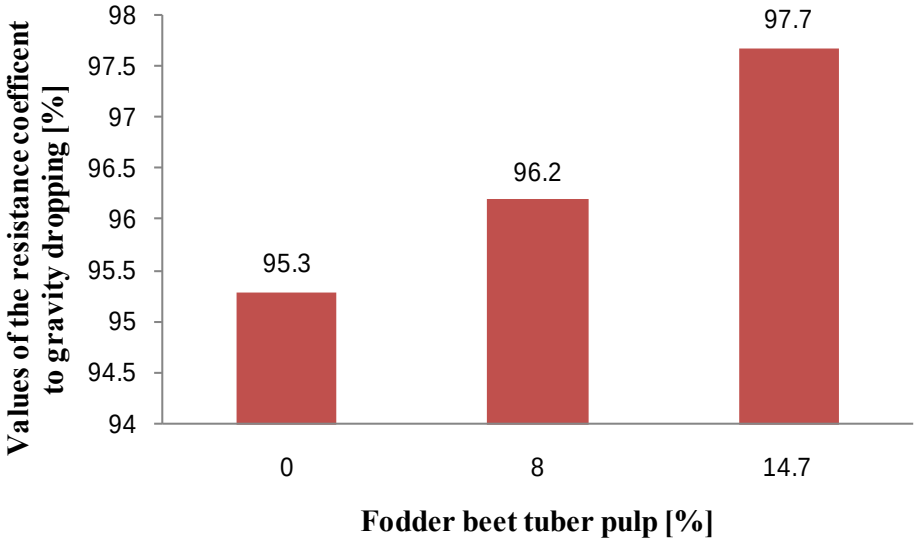

CONCLUSION

In the examined pellet made of barley chopped straw with the addition of fodder beet tuber pulp, a significant influence of fodder beet tuber pulp content and raw material moisture content on the produced granulate hardness granulate was determined.

It was determined that granulate hardness increases significantly and proportionally to increase of fodder beet tuber pulp content in the raw material and raw material relative moisture content.

It was determined that gravity drop resistance of granulate made of barley chopped straw with the addition of fodder beet tuber pulp increases proportionally to increase of fodder beet tuber pulp dry mass content.

ACKNOWLEDGEMENTS

The research was financially supported by the statutory resources of the Mechanical Faculty of the Koszalin University of Technology.

REFERENCES

Al-Jbawi, E. et al. 2016. Productivity of fodder beet (Beta vulgaris var. Crassa) cultivars as affected by plants spacing in Al Ghab Syria. Journal of Agricultural and Crop Research, 4(6): 91–99.

Chakwizira, E. et al. 2013. Effects of potassium, sodium and chloride fertiliser rates on fodder beet yield and quality in Canterbury. Proceedings of the New Zealand Grassland Association, 75: 261–270.

Chojnacki, J., Zdanowicz, A. 2017. Research into the hardness of pellet from wheat straw with an addition of ground wheat. Journal of Research and Applications in Agricultural Engineering, 62(2): 19–21.

Collomba, M. et al. 2004. Impact of a basal diet of hay and fodder beet supplemented with rapeseed, linseed and sunflowerseed on the fatty acid composition of milk fat. International Dairy Journal, 14: 549–559.

Khogali M.E. et al. 2011. Productivity of fodder beet (Beta vulgaris var. Crassa) cultivars affected by nitrogen and plant spacing. Agriculture and Biology Journal of North America, 2(5): 791–798.

Matthew C. et al. 2011. Fodder beet revisited, Proceedings of the 41st Agronomy Society of New Zealand Conference, Gisborne, New Zealand, 8–10 November 2011: 39–48.

Obidziński, S. 2014. Badania porównawcze metod oceny wytrzymałości kinetycznej granulatu. Inżynieria Przetwórstwa Spożywczego, 2/4: 26–29.

Pembleton, K., Rawnsley, R. 2011. Growing Fodder Beets on Tasmanian Dairy Farms, Tasmanian Institute of Agriculture [Online], Available at: http://www.utas.edu.au/data/assets/pdffile/0006/388113/Growing-fodder-beets-on-Tasmanian-dairy-farms.pdf. [2018-09-09].

Shevtsov, A.A. et al. 2017. Preparation and application of fodder vitamin additive choline chloride B4 on the basis of dried beet pulp in premix composition. International Journal of Pharmaceutical Research and Allied Sciences, 6(1): 217–226.

Turki, I.Y., Khogali, M.E. 2011. Effect of Feeding Fodder beet (Beta vulgaris L. var. Crassa) on Fattening Efficiency of Sudan Desert Sheep. Advances in Environmental Biology, 5(7): 1592–1596.

Zdanowicz, A., Chojnacki, J. 2017. Mechanical properties of pellet from chicken manure mixed with chopped rye straw. Journal of Research and Applications in Agricultural Engineering, 62(4): 216–218.

APPLIED CHEMISTRY AND BIOCHEMISTRY

Free amino acids pool in early response to *Plasmodiophora brassicae* infection in *Arabidopsis*

Miroslav Berka[1], Rebecca Leber[2]
[1]Department of Molecular Biology and Radiobiology
Mendel University in Brno
Zemedelska 1, 613 00 Brno
CZECH REPUBLIC
[2]Institut für Botanik
Technische Universität Dresden
Zellescher Weg 20b, 01217 Dresden
GERMANY

miroslavberka94@gmail.com

Abstract: Plasmodiophora brassicae is an important pathogen, with a worldwide impact on agriculture. Here, we analysed an early response of *Arabidopsis thalia*na to *P. brassicae* infection. We employed a GC-MS metabolomics profiling and followed the free amino acid pool. The results indicate significant alterations in nitrogen metabolism and/or anaplerotic reactions.

Key Words: metabolomics, amino acids, *Plasmodiophora brassicae*, *Arabidopsis thaliana*, clubroot

INTRODUCTION

One of the most severe damages to *Brassicaceae* can be ascribed to the clubroot disease, which is facilitated by the soil pathogen *Plasmodiophora brassicae* Wor. and has been spreading over the last few years in the Czech Republic (Voorrips 1995, Řičařová et al. 2016). Infected plants develop club-like swellings of roots and display a major reduction in the above-ground growth and biomass that lead to massive yield losses in crops, such as rapeseed, Chinese cabbage, cauliflower (Voorrips 1995, Wallenhammar 2010). The disease has been known and investigated for decades, however, the reports on metabolome changes are lacking. Here, we employed an untargeted GC-MS analysis of four-week-old *Arabidopsis thaliana* Col-0 plants, harvested 14 days post infection (dpi).

MATERIAL AND METHODS

Material

Plants of *Arabidopsis thaliana* (L.) Heyhn. ecotype Columbia (Col-0) were cultivated in the 10 ml pipette tips filled with sand and watered with the nutrient solution according to Smeets et al. 2008. Plants were grown in a greenhouse under long day and temperature of 25 °C. Two-week-old seedlings were inoculated with 200 µl of resting spores of *P. brassicae* isolate 'e3' (10^7 spores/ml in potassium buffer; 50 mM KH_2PO_4, pH adjusted to 5.5 with 1 M K_2HPO_4). Control plants were treated with the same amount of potassium buffer. Roots of control and infected plants were harvested after 14 dai (days after inoculation), flash frozen in liquid nitrogen, then homogenized (Retsch Mill MM400) and stored at -80 °C.

Metabolite extraction and GC-MS analysis

Polar metabolites were analysed as described previously (Černý et al. 2013). Briefly, metabolites were extracted with methanol/chloroform/distilled water (2.5:1:0.5), and clarified by centrifugation. The polar phase was separated by adding 0.5 ml of distilled water and 50 µl aliquots of the polar phase were concentrated on SpeedVac (Thermo). Samples were derivatized by 20 µl of methoximation solution (40 mg methoxiaminhydrochlorid in 1 ml pyridine) and incubated for 90 minutes at 30 °C with continuous shaking. After the incubation, 80 µl of silylation solution (N-methyl-N-trimethylsilyltrifluoroacetamid, MSTFA) was added and the mixture was incubated for 30 min at 37 °C with continuous shaking. GC-MS measurements were carried out on Q Exactive GC Orbitrap GC-

MS/MS (Thermo Fisher) using Trace 1300 Gas chromatograph (Thermo Fisher). Samples were injected using the split mode (1:10, total volume 1µl at 250 °C) and ionized using the electron ionization mode. For GC separation a TG-5SILMS capillary column (30 m, 0.25 mm, 0.25 µm; Thermo Fisher) was used with a 40 min temperature gradient (70 °C for 1 min followed by 9 °C per min gradient to 350 °C). The mass spectrometer operated in the full scan mode, 60,000 resolution, scan range 50-600 m/z, AGC target 1e6, maximum IT - automatic. Data were analysed by TraceFinder and CompoundDiscoverer (Thermo Fisher) using default workflow for GC-MS data. Skyline (https://skyline.ms) was used for quantification.

Data analysis

The multivariate analysis was performed using CompoundDiscoverer (Thermo Fisher). The software STATISTICA was used for evaluation of the difference between the variants. Briefly, data were tested for normal distribution using the Shapiro–Wilk test. The t-test ($p > 0.05$) was used for the dataset with normal distribution and for the other dataset, the nonparametric Mann-Whitney U test ($p > 0.05$) was used. The heatmap was created using program RStudio (https://www.rstudio.com/).

RESULTS AND DISCUSSION

Analysis of root metabolome of infected *Arabidopsis* plants

Arabidopsis thaliana is a clubroot sensitive plant presenting an ideal model for analysis of *Plasmodiophora* infection, and the first infection symptoms are visible three weeks after the infection (Ludwig-Müller et al. 1999). We employed a hydroponic culture, the system that is more convenient for the rapid harvesting of plants, which is a crucial factor for any metabolomics analysis. The initial stages of infection are the most important in the plant-pathogen interaction, as the plants' metabolism is not yet fully compromised. For this reason, plants were harvested at 14 dpi (before any visible symptoms). Root is the primary target of *P. brassicae*, and thus we focused our metabolomics analysis on roots of control and infected plants.

First, we analysed the total GC-MS metabolome profile and performed a multivariate analysis to visualise patterns and similarities within samples (Figure 1). The two first components represented more than 95% of total variance in dataset, and the PCA clearly shows the clustering between control and infected roots.

Figure 1 The GC-MS metabolomics analysis clearly separates roots of control and infected roots at 14 dpi.

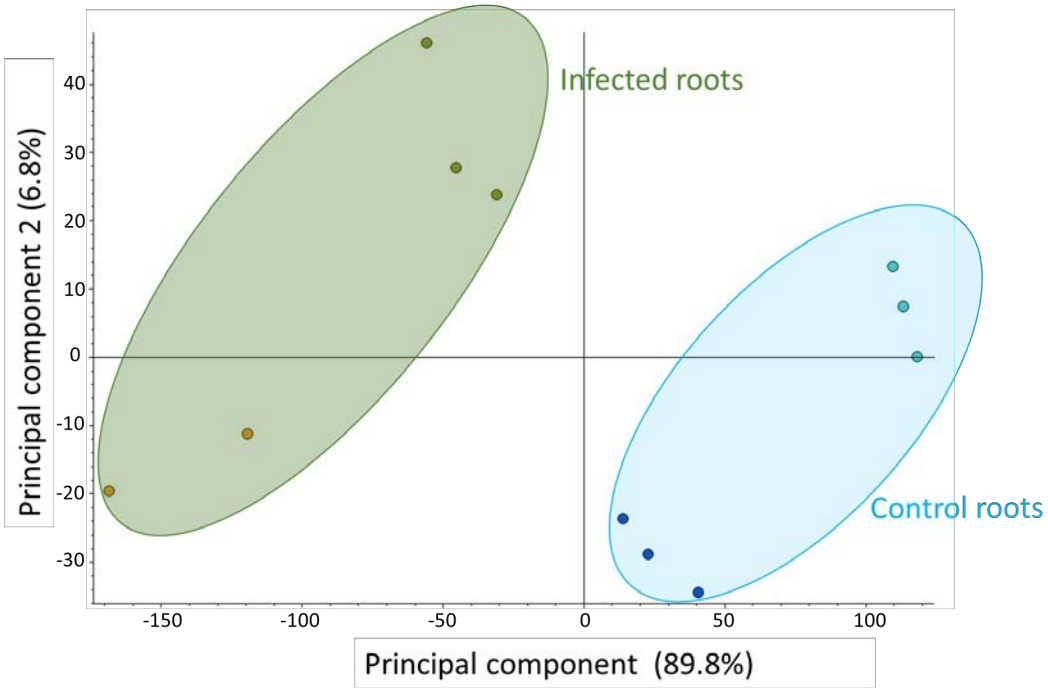

Legend: Dots represent technical and biological replicates.

Free amino acid pool in response to *P. brassicae* infection

P. brassicae is a biotrophic pathogen and like other biotrophic pathogens is reduced in several metabolic pathways. *P. brassicae* lacks genes encoding proteins involved in sulphur and nitrogen uptake, and amino acid biosynthesis of histidine, tryptophan and threonine. Arginine, lysine and thiamine synthesis is also reduced in *P. brassicae*, suggesting a dependence of their host plants for those metabolites (Schwelm et al. 2015). Therefore we have selected proteinogenic amino acids from the identified metabolites. In total, we quantified 16 proteinogenic amino acids in our samples (Figure 2). Sulphur-containing amino acids, tyrosine and tryptophan have not been identified, most likely due to their high reactivity and low amounts in plant tissues, respectively (Hildebrandt et al. 2015).

Figure 2 Extracted ion chromatograms of identified and quantified amino acids.

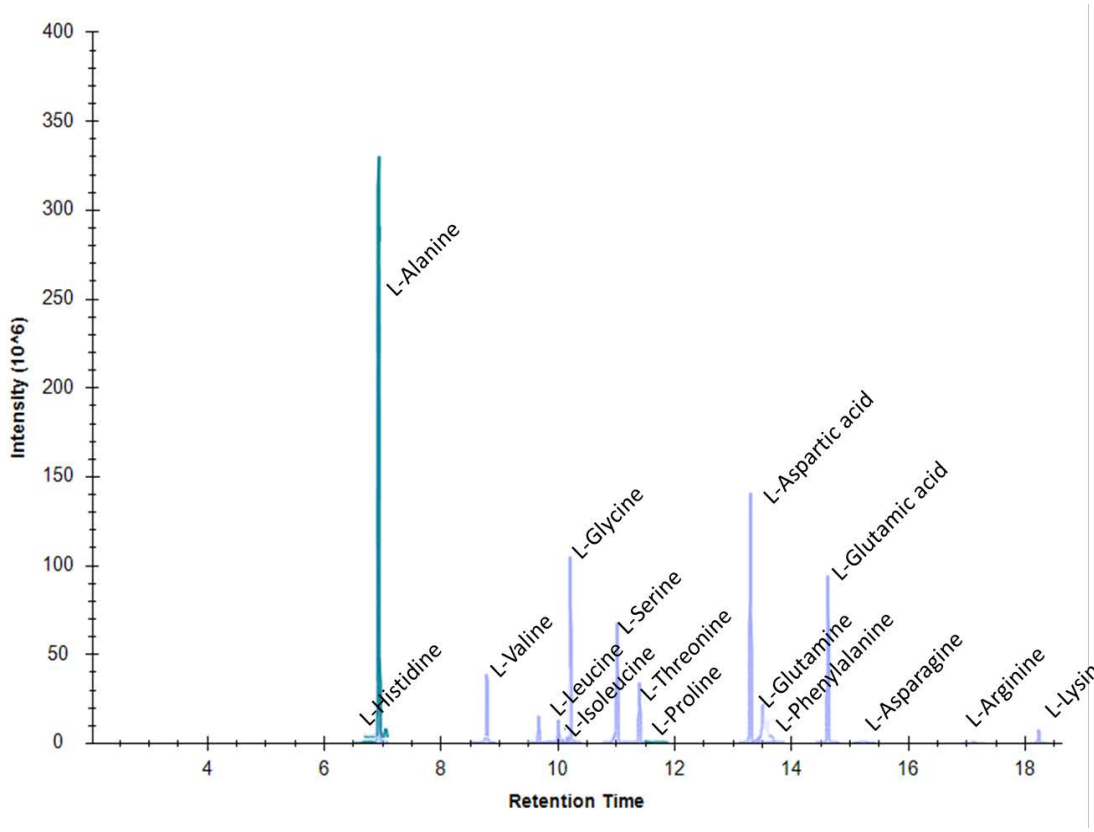

We found that the most pronounced changes are in the amino acids involved in nitrogen assimilation (Figure 3), and the observed increase in infected roots is statistically significant. This increase can be explained by two possibilities. These amino acids are fundamental in the nitrogen metabolism (Voet and Voet 2011), and their increase could coincide with the induced nitrogen mobilization in infected roots. The second plausible explanation is an increased demand on the TCA cycle, and the resulting shift in anaplerotic reactions needed for replenishing its intermediates (Voet and Voet 2011). This could supply the energy demands of the forming root gall or the demands of the plant defence mechanisms. We found a similar statistically significant increase in lysine, and the amount of other basic amino acid arginine is increasing too (though the significance is below the selected threshold of $p<0.05$). Surprisingly, we did not find any significant difference in the pool stress-related amino acid proline. Jubault et al. 2008 observed a high accumulation of proline in susceptible *Arabidopsis* plants at 21 dpi. It is thus likely that the amount of proline is increasing at later stages of the infection.

Figure 3 Free amino acid pool in early response to infection.

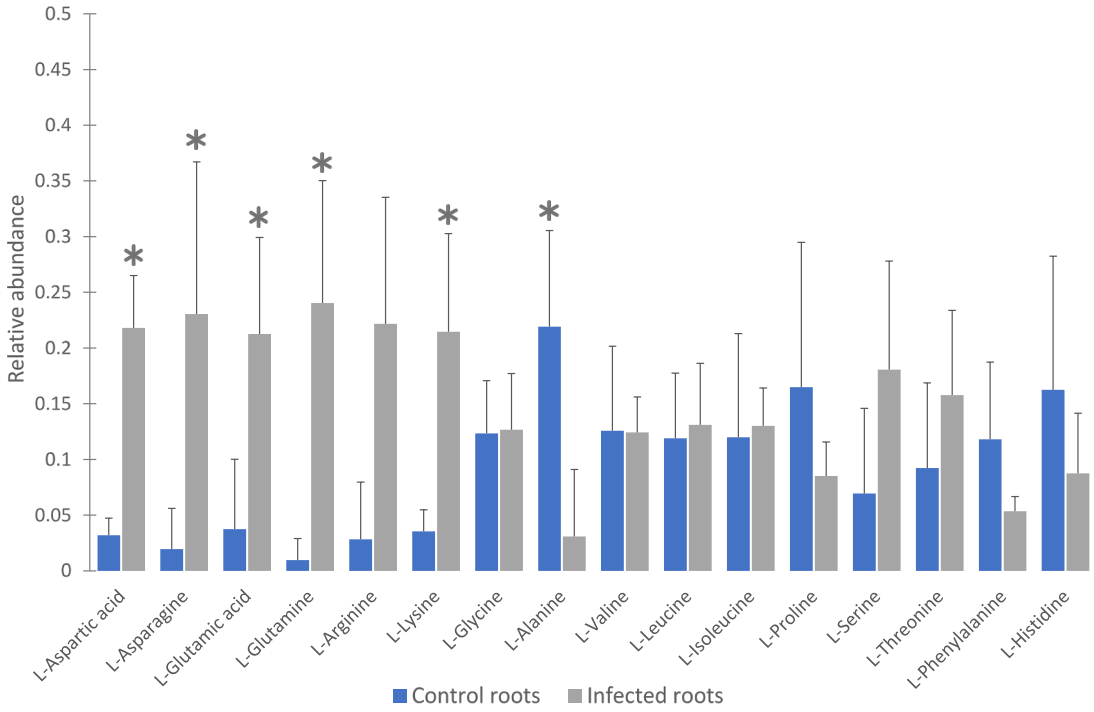

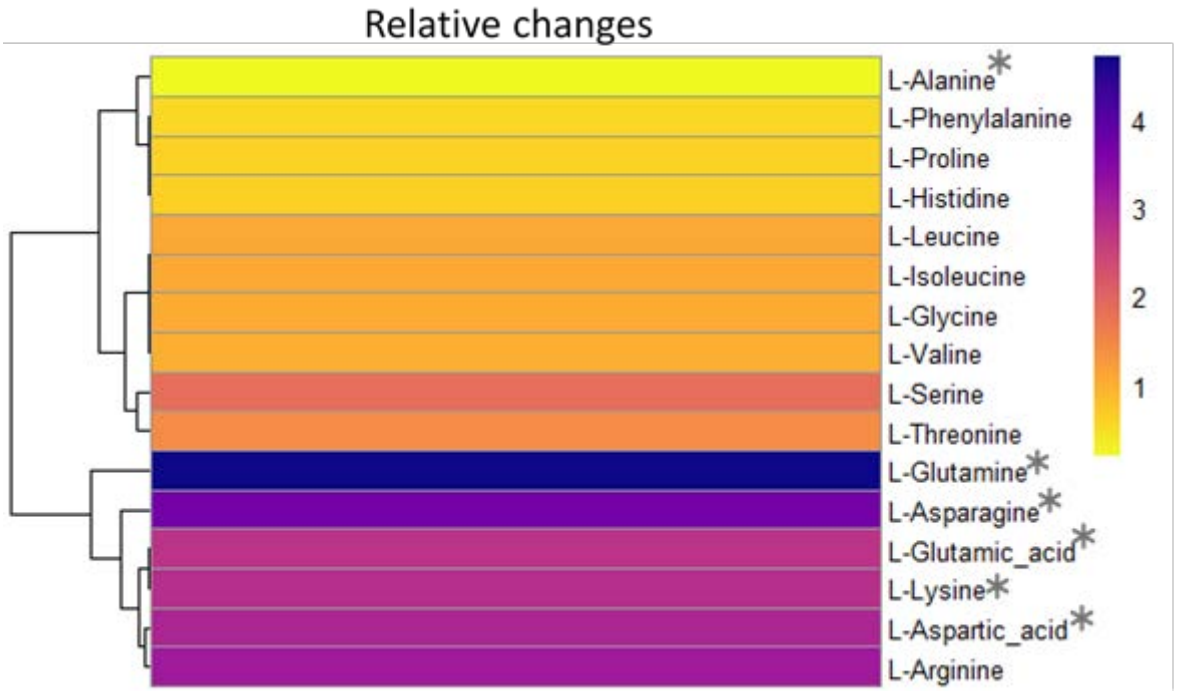

Legend: Error bars represent standard deviation, asterisks indicate statistically significant difference (t-test, p>0.05; Mann-Whitney U test, p> 0.05)

CONCLUSION

We quantified 16 free proteinogenic amino acids in our samples and found that the abundances of at least six of these are significantly changed during the early stages of *P. brassicae* infection. The observed changes indicate an alternation in the nitrogen metabolism and/or a shift in anaplerotic reactions. However, the amount of free proline, a stress-related amino acid, did not differ. Our data confirmed that in the absence of visible symptoms at 14 dpi the infection is already in progress, and we

believe that further analyses (e.g. proteome and transcriptome) at this time point will provide valuable information about plant-pathogen interaction in *P. brassicae* infection.

ACKNOWLEDGEMENTS
The research was financially supported by AF-IGA-IP-2018/014 (Internal Grant Agency of Faculty of AgriSciences, Mendel University in Brno) and by the Ministry of Education, Youths and Sports of the Czech Republic from MOBILITY project 8J18DE015 (Multilevel analysis of the clubroot disease and its biological control by an endophytic fungus).

REFERENCES

Černý, M. et al. 2013. Proteome and metabolome profiling of cytokinin action in *Arabidopsis* identifying both distinct and similar responses to cytokinin down-and up-regulation. Journal of Experimental Botany, 64(14): 4193–4206.

Hildebrandt, T.M. et al. 2015. Amino acid catabolism in plants. Molecular Plant, 8(11): 1563–1579.

Jubault, M. et al. 2008. Differential regulation of root arginine catabolism and polyamine metabolism in clubroot-susceptible and partially resistant Arabidopsis genotypes. Plant Physiology, 146(4): 2008–2019.

Ludwig-Müller, J. et al. 1999. Indole glucosinolate and auxin biosynthesis in *Arabidopsis thaliana* (L.) Heynh. glucosinolate mutants and the development of clubroot disease. Planta, 208: 409–419.

Řičařová, V. et al. 2016. Clubroot Caused by Plasmodiophora brassicae Wor.: a Review of Emerging Serious Disease of Oilseed Rape in the Czech Republic. Plant Protection Science, 52(2): 71–86.

Voet, D., Voet, J.G. 2011. Biochemistry. 4th ed. New Jersey, USA: John Wiley & Sons. John, Inc.

Schwelm, A. et al. 2015. The *Plasmodiophora brassicae* genome reveals insights in its life cycle and ancestry of chitin synthases. Scientific Reports, 5: 11153.

Voorrips, R.E. 1995. *Plasmodiophora brassicae*: aspects of pathogenesis and resistance in *Brassica oleracea*. Euphytica. 83: 139–146.

Wallenhammar, A.C. 2010. Monitoring and control of *Plasmodiophora brassicae* in spring oilseed *Brassica* crops. Acta Horticulturae, 867: 181–190.

Isolation and detection of bacteria using magnetic molecularly imprinted polymers

Jaroslava Bezdekova, Jitka Hutarova, Kristyna Tomeckova, Marketa Vaculovicova
Department of Chemistry and Biochemistry
Mendel University in Brno
Zemedelska 1, 613 00 Brno
CZECH REPUBLIC

bezdekovajar@gmail.com

Abstract: A range of biological macromolecules as antibodies, enzymes or receptors function on principles based on selective recognition. These biological macromolecules are very often used in many technical applications due to their well-defined selectivity features. Unfortunately using of biomolecules is limited by their high production costs and low stability. Therefore, an idea of creation of synthetic materials with tailor-made molecular selectivity was presented. These materials are called molecularly imprinted polymers (MIPs). MIPs use molecular imprinting of chosen molecule to creating selective binding sites in cross-linked polymer. Technique of molecular imprinting has become one of the most efficient methods that are used for preparation of selective recognition materials. MIPs are stable, robust and have low production costs. In this work, the novel sensitive method for *Staphylococcus aureus* isolation and detection based on molecular imprinting was investigated. Molecularly imprinted layer was created on a surface of magnetic particles (MPs) due to ability of MPs pre-concentrate bacteria from large sample volumes. Fluorescence microscopy was used for detection of isolated bacteria.

Key Words: molecularly imprinted polymers, magnetic particles, fluorescence, bacteria, dopamine

INTRODUCTION

Molecular imprinting is a technique which enables to create the tailor-made binding sites specific to the template (imprinted target molecule) in shape, size and functional groups in cross-linked polymer (Chen et al. 2016). MIPs have a range of advantages which includes: high chemical and physical stability, possibility of preparation the complementary binding sites for variety types of molecules (Li et al. 2012), production in large quantities and possibility of re-use (Mattiasson and Ye 2015). These features make MIPs ideal for a large number of biochemical applications.

In this work, molecular imprinting technology was used for isolation and subsequent detection of bacteria *Staphylococcus aureus* (SA). A non-covalent imprinting approach is the most commonly used due to the simplicity of preparation (Mattiasson and Ye 2015). Dopamine (DA) can be used as an effective functional monomer for creation of the polymeric layer because it undergoes an oxidative polymerization under alkaline conditions (Jiang et al. 2011). During the polymerization, the reaction occurs to create polydopamine (PDA) layer. The use of DA is beneficial due the fact that it is eco-friendly and contains a lot of functional groups (such as phenyl, amino, and hydroxyl groups) that enable reaction with imprinted molecule (Zhao et al. 2018).

Layer of molecularly imprinted polymers can be prepared on a surface of different types, material, and geometrical arrangements such as silica beads, carbon nanotubes, quantum dots and/or magnetic particles (MPs) (Zhou et al. 2010). MPs can be easily collected by an external magnetic field without necessity of centrifugation or filtration due to high magnetic sensitivity. Therefore they are enable isolate analyte from large sample volumes (Pan et al. 2011).

This work is concentrated on isolation and detection of bacteria. This topic was chosen because control and identification of the bacterial contamination is very important in many industrial branches such as food industry, environment industry or clinical diagnostic. However, current methods are time-consuming, laborious and/or expensive (Lazcka et al. 2007).

MATERIALS AND METHODS

Materials

Dopamine hydrochloride, Trizma base, Sodium dodecyl sulphate and Acetic acid were purchased from Sigma-Aldrich (St. Louis, MO, USA) in ACS purity. Dynabeads™ MyOne™ Silane and SYTO 9 were obtained from Thermo Fisher Scientific (Waltham, MA, USA).

Preparation of bacteria

The bacterial strains of *Staphylococcus aureus* NCTC 8511 and *Enterococcus faecalis* ATCC 11700 (Czech Collection of Microorganisms, Brno, Czech Republic) were cultivated in Muller-Hinton broth (MHB; Oxoid, Hampshire, UK) overnight at 37 °C and 150 rpm. The concentrations of bacterial solutions were determined by optical density at 600 nm and using the MHB the cultures were adjusted to a concentration ~1×10^6 CFU/ml. The cells were centrifuged at 8000 rpm for 10 min at ambient temperature and the supernatant was discarded. The cells were re-suspended in the same volume of 20 mM tris(hydroxymethyl)aminomethane (TRIS) of pH 8.5.

Preparation of magnetic MIPs/NIPs

The molecularly imprinted polymers prepared on the surface of magnetic particles (MPs-MIPs) were prepared according the method reported by Yang and his co-workers with slight modification (Zhou et al. 2010). Briefly, 50 µl of Fe_3O_4 nanoparticles (40 mg/ml) were three times washed by 200 µl of 20 mM TRIS (pH 8.5). Subsequently 600 µl of *Staphyloccocus aureus* (1×10^6 CFU/ml) suspended in 20 mM TRIS (pH 8.5) was added to the washed MPs. For prepare of non-imprinted polymers (NIPs), that are used as control, 600 µl of 20 mM TRIS (pH 8.5) was added to the washed MPs. The mixtures were mechanically stirred for 2 hours until the MPs were well suspended. Than 100 µl of dopamine (17.5 mg/ml) suspended in 20 mM TRIS (pH 8.5) was added, and the reaction was continued over night at room temperature. Next day, the product was collected by an external magnetic field and the template was washed out 200 µl of solution containing mixture of 5% acetic acid and 1% SDS three times and 200 µl of MilliQ water one time.

Fluorescent microscopy

An Olympus IX71 inverted fluorescence microscope was used for imaging of MIPs/NIPs. The used objective was LUCPLFLN 20 X PH. Total magnifications was 200 ×. Detector of emitted light was Hamamatsu CCD ORCA-HR (C4742-95-12HR) with pixels of 1600 × 1200, exposure time was 4 s. Filter was TX Red (λex. 545 nm, λem. 610 nm, dichroic mirror 600 nm). The images of MIPs/NIPs were evaluated using the BRUKER Molecular Imaging software.

Selectivity of adsorption

In the selectivity adsorption experiments, *Enterococcus faecalis* (EF) was chosen as a competitor. It is gram-positive bacteria and that has very similar size and shape as SA. The experiment was carried out as follows: to the MPs-MIPs were added 200 µl of EF or SA (1×10^6 CFU/ml) suspended in 20 mM TRIS (pH 8.5) and mixture was shaking for 1 hour. Then the unbound bacteria were taken away and MPs-MIPs were washed by 200 µl of MilliQ water. 18 µl of sample (MPs-MIPs with bound analyte or MPs-NIPs) was mixed with 2 µl of 50 µM SYTO 9 (dissolve in dimethylsulfoxide DMSO) and the mixture reacted for 10 minutes. Then the mixture was determined by fluorescence microscope (λex. 545 nm, λem. 610 nm, dichroic mirror 600 nm).

RESULTS AND DISCUSSION

Molecularly imprinted polymers have same function as biomolecules that are very often used for bacterial detection but are much cheaper and stable. Therefore, use of molecular imprinting technology as a promising road to overcome these problems was suggested. In this work, an approach where the molecularly imprinted layer was prepared on the surface of MPs was chosen. A scheme of MIPs preparation process is shown in Figure 1.

Figure 1 Scheme of isolation and detection of bacteria Staphylococcus aureus by magnetic molecularly imprinted polymers. A) The templates (bacteria) are mixed with magnetic nanoparticles and functional monomer (dopamine). B) Created MIPs are used for isolation of analytes (bacteria) from sample. Bounding bacteria was stained by fluorescent dye (SYTO 9) and determined by fluorescence microscopy (ex. 545 nm, em. 610 nm, dichroic mirror 600 nm)

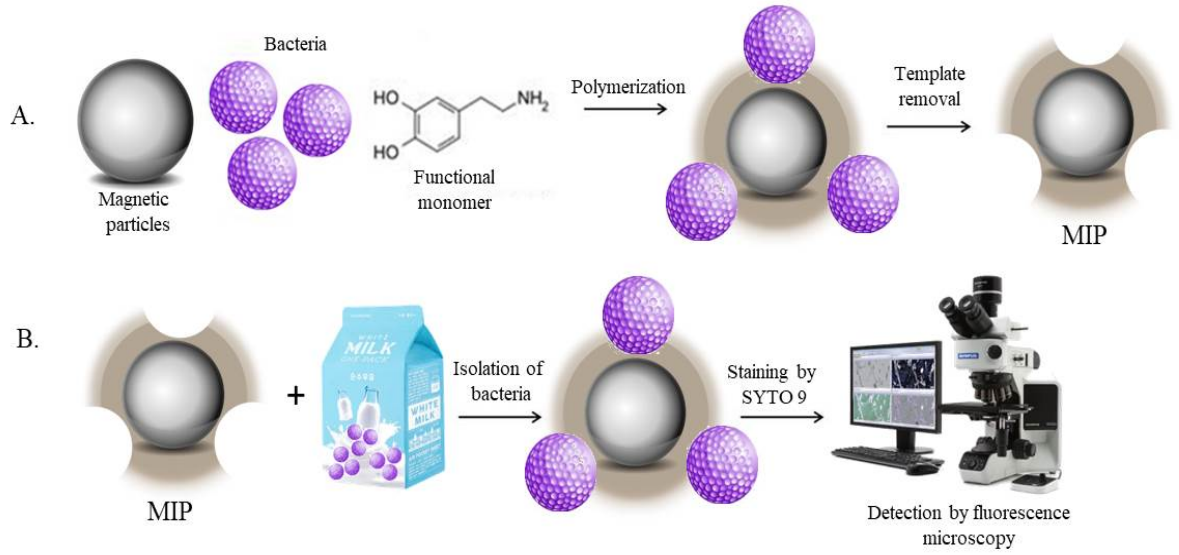

Verification of removal step

Before the prepared imprinted materials can be used in chosen application, the template molecules (bacteria) have to be removed from the polymer layer.

Prepared MIP surface has to be exhaustively washed to properly remove the template remaining within the polymerized layer to lower the background signal. Therefore, template removal is essential for method validation because this can lead to binding sites damage in terms of collapse or change in shape or size (e.g. polymer swelling).

Conditions introduced in previous work were used for template removal (Hutarova et al. 2017). Briefly, MPs-MIPs/NIPs were washed three times by 200 µl of mixture of 5% HAc and 1% SDS in ratio 1 : 1 and then once by 200 µl MilliQ water. For verification of these conditions, MPs-MIPs and MPs-NIPs before removal step and after removal step were measured. MPs-NIPs are prepared under identical conditions as MPs-MIPs. The difference is that MPs-NIPs are prepared without presence of template. MPs-NIPs are used as an indicator of nonspecific interactions with polydopamine layer. From obtained data (Figure 3 A), it can be seen that during removal step, 95% of template were washed out from MPs-MIPs surface. Therefore this approach was chosen as suitable.

Binding properties

The binding properties of prepared MPs-MIPs were investigated using 1×10^6 CFU/ml of model bacteria (SA) comparing the binding yield of MPs-MIPs and MPs-NIPs. In Figure 2, fluorescence micrographs of MIPs and NIPs prepared for SA (ex. 545 nm, em. 610 nm, dichroic mirror 600 nm) are shown. It was observed that the adsorption of bacteria on MPs-MIPs is significantly higher than in case of MPs-NIPs. The interaction of the analyte (i.e. SA) is lower with MPs-NIPs due to the unorganized and non-specific interaction between the surface and the analyte.

Data obtained using fluorescence microscopy were subsequently processed by BRUKER Molecular Imaging software. This software is able to evaluate the intensity of all fluorescenct points and summarize it. This data is more suitable for quantification of efficiency of prepared imprinted materials (Figure 3).

Figure 2 Micrographs of MPs-MIPs (A) and MPs-NIPs (B) with bacteria SA (1 × 10^6 CFU/ml) stained by fluorescent dye SYTO 9

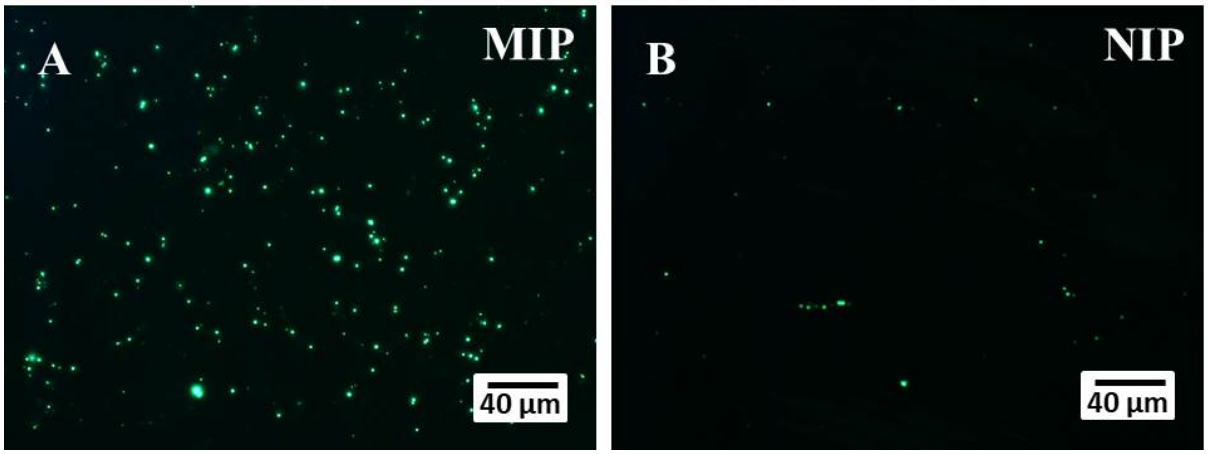

Selectivity of adsorption

For finding of selectivity it was necessary to measure the binding properties of created MPs-MIPs with a competing analyte. In this work, *Enterococcus faecalis* (EF) was chosen as the competitor. These gram-positive bacteria have very similar size and shape as SA.

Measurements were repeated three times and resulting value is an average value of these three measurements. The obtain data are shown in Figure 3 B. From obtain data it is seen that on the surface of MPs-MIPs, prepared for selective detection of SA, 65% larger amount of SA than competitor (EF) was detected. By this experiment, the selectivity of developed MPs-MIPs was confirmed.

Figure 3 A) Quantification of template removal step (MIPs/NIPs were washed out by mixture of 5% HAc and 1% SDS in ration 1 : 1 three times and then once by 200 µl MilliQ water) B) Cross-adsorption of the magnetic imprinted nanoparticles (EF was used as a competitor of interaction)

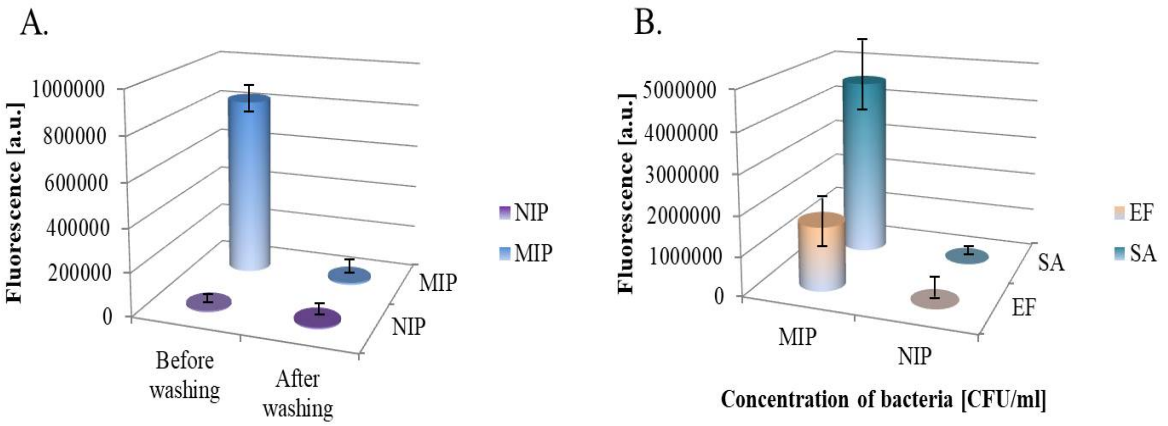

CONCLUSION

In this work, the MIPs selective for *Staphylococcus aureus* were prepared *via* a technique of non-covalent molecular imprinting. Dopamine was used as a functional monomer. Experiments focused on molecular recognition efficiency of created polymers were carried out. The resulting imprinted polymers demonstrated great binding properties and high selectivity under the optimal conditions. Moreover, this method is very simple, specific, low cost and eco-friendly. Future work will be focused on isolation of bacteria from real sample for example from milk. SA is the bacteria that causes range of serious infections and is a threat to public health. Therefore, the Legislation of EU has set limits that cannot be exceeded in commercially available foods. The presented technique enables fast and easy method could find potential in food industry.

ACKNOWLEDGEMENTS
The research was financially supported by Czech Science Foundation project No. 16-23647Y

REFERENCES

Chen, L.X. et al. 2016. Molecular imprinting: perspectives and applications. Chemical Society Reviews, 45(8): 2137–2211.

Hutarova, J. et al. 2017. Molecular imprinting technology for targeted analysis of proteins. In Proceedings of International Phd Students Conference MendelNet 2017. Brno, Czech Republic, 8–9 November, Brno: Mendel University in Brno, Faculty of AgriSciences, pp. 873–877.

Jiang, J.H. et al. 2011. Surface Characteristics of a Self-Polymerized Dopamine Coating Deposited on Hydrophobic Polymer Films. Langmuir, 27(23): 14180–14187.

Lazcka, O. et al. 2007. Pathogen detection: A perspective of traditional methods and biosensors. Biosensors & Bioelectronics, 22(7): 1205–1217.

Li, J.P. et al. 2012. Molecularly Imprinted Polymers as Recognition Elements in Sensors. Amsterdam: Elsevier Science Bv.

Mattiasson, B., Ye, L. 2015. Molecularly Imprinted Polymers in Biotechnology. In Molecularly Imprinted Polymers in Biotechnology. Cham, UK: Springer Int Publishing Ag, pp. 85–99.

Pan, J.M. et al. 2011. Magnetic molecularly imprinted polymers based on attapulgite/Fe3O4 particles for the selective recognition of 2,4-dichlorophenol. Chemical Engineering Journal, 174(1): 68–75.

Zhao, Y.Y. et al. 2018. Surface imprinted polymers based on amino-hyperbranched magnetic nanoparticles for selective extraction and detection of chlorogenic acid in Honeysuckle tea. Talanta, 181(3): 271–277.

Zhou, W.H. et al. 2010. Mussel-inspired molecularly imprinted polymer coating superparamagnetic nanoparticles for protein recognition. Journal of Materials Chemistry, 20(5): 880–883.

Effect of surfactants and polymers on stability of superparamagnetic nanoparticles and on immobilization and release of antitumor agents

Hana Buchtelova[1], Zuzana Skubalova[1], Jiri Kudr[1], Vladislav Strmiska[1,2], Vojtech Adam[1,2], Zbynek Heger[1,2]
[1]Department of Chemistry and Biochemistry
Mendel University in Brno
Zemedelska 1, 613 00 Brno
[2]Central European Institute of Technology
Brno University of Technology
Technicka 3058/10, 616 00 Brno
CZECH REPUBLIC

hanabuchtelova@gmail.com

Abstract: The current study demonstrates design, preparation and characterization of biocompatible superparamagnetic iron oxide nanoparticles (SPIONs) coated with three different polymers polyvinylpyrrolidone (PVP) polyoxyethylene stearate (POES) and chitosan (Chit). Such modified nanoparticles were loaded with doxorubicin, as model anticancer drug. Resulting complex has an exceptional stability in physiological conditions. The highest release of complexed Dox was in endosomal environment in case SPIONs with POES. The cytotoxic effects of the complex were tested using breast cancer/healthy epithelial cell lines. Use of SPIONs increased the cytotoxicity of doxorubicin when compared to free doxorubicin and decreased the cytotoxicity in healthy cells. The results demonstrate that modification of SPIONs could have a potential in nanomedicine as versatile nanoplatform to enhance efficiency of anticancer therapy.

Key Words: biocompatibility, SPION, nanomedicine, cytotoxicity

INTRODUCTION

Nanomedicine is a relatively new field of science and a term defines design and testing of functional nanounits in medicine (Boisseau and Loubaton 2011). Material scientists have performed exceptional accomplishments in the design of various types of materials that can be used in nanomedical therefore opens up a vast field of research and application (Linkov et al. 2008).

The frequent drawback of these materials is common systemic toxicity. Superparamagnetic iron oxide nanoparticles (SPIONs) have been used for many years as magnetic resonance imaging (MRI) contrast agents, tissue reparation, or for a drug delivery. Bare SPIONs are often insufficiently stable for a specific accumulation in target tissue (Singh et al. 2010).

Here, we present hybrid SPIONs coated with polyvinylpyrrolidone (PVP), polyoxyethylene stearate (POES) or chitosan (Chit) shell for delivery of conventional cytostatic agent doxorubicin (Dox). Due to unique physical and chemical properties, SPIONs have many usable properties in biomedicine, like tissue repair, magnetic resonance imaging (MRI), detoxification of biologic fluids, drug and gene delivery, biological sensing, and hyperthermia (Naqvi et al. 2010). Nevertheless, the biomedical applications of SPIONs arouse interest about their cytotoxicity (Liu et al. 2013).

We show that SPIONs exhibit good binding efficiency of Dox, exceptional stability in non–target plasma environment. SPIONs (stable in dispersion for more than 6 h) has the highest release in a slightly acidic environment adequate to the hypoxic or endosomal environment and tumor hypoxic tissue. Cytotoxicity was tested *in vitro* on two types of cells – normal breast and breast cancer. Surface coating and drug immobilization resulted in higher cytotoxicity, due to a synergistic interplay. SPIONs are pronouncedly biocompatible. Our results imply suitability of the use of SPIONs with surface modification for medical purposes.

MATERIAL AND METHODS

Synthesis of SPIONs

KNO_3, KOH and ddd water was added into a screwable vessel. After stirred was added Fe_SO_4 during magnetic stirring. Immediately transfer vessel to a preheated water bath (90 °C) for 2 h.

SPIONs coating with PVP, POES and Chit and noncovalent complexation of Dox

Equal volumes of SPIONs was modified *i*) 10 mg/ml of PVP were mixed and incubated (20 °C, 30 min). After that, the solution of SPIONs was mixed with Dox and incubated (20 °C, 30 min). *ii*) 5 mg/ml of POES were mixed and ultrasonicated. After that, the solution of SPIONs was mixed with Dox and ultrasonicated. *iii*) 2.5 mg/ml of Chit were mixed and ultrasonicated. After that, the solution of SPIONs was mixed with Dox and ultrasonicated. Finally, resulting nanoparticles was separated remove unbound Dox and resuspended in MilliQ water. Loading efficiency (LE) of Dox to SPIONs was analysed by UV–Vis spectroscope Infinite 200 PRO (Tecan, Männedorf, Switzerland) at λ 480 nm.

Scanning electron microscopy (SEM)

SEM analyses were performed using the MIRA 3 electron microscope (Tescan, Brno, Czech Republic) after drying the samples on the grid.

Evaluation of colloidal stability of SPIONs in physiological environments

To demonstrate their colloidal stability SPIONs dispersed in the Ringer´s solution were placed in the stationary rack and kept at 25 °C. The dispersion was photodocumented in annotated time intervals (up to 12 h).

In vitro cumulative drug release kinetic studies

1 ml of SPIONs was dispersed in solutions mimicking various conditions, including plasma (Ringer´s solution), neutral intracellular fluid and acidic environment of endosomes. The temperature was maintained at 37 °C. At fixed time intervals, SPIONs was separated by a magnet and 50 µl of medium was withdrawn and subsequently replaced with fresh medium to maintain the sink conditions. The amount of released Dox was determined by UV–Vis spectroscopy at λ 480 nm. The cumulative release of Dox was calculated as follows:

$$\text{Cumulative release (\%)} = (\text{Dox in the medium}) / (\text{Initial Dox}) \times 100$$

Cell lines and culture conditions

Two human cell lines were used: i) the HBL–100 normal human breast cell line, ii) the MDA–MB–231 –human breast cancer cell line. All cell lines were purchased from Health Protection Agency Culture Collections (Salisbury, UK).

HBL–100 and MDA–MB–231 were cultured in RPMI–1640 with 10% foetal bovine serum (FBS), UKF–NB–4 Iscove's modified Dulbecco medium (IMDM) with 10% FBS. Media were supplemented with penicillin and streptomycin, and the cells were maintained in a humidified incubator Galaxy® 170 R (Eppendorf, Hamburg, Germany). Prior all analyses, cells were counted using Countess II FL (Thermo Fisher Scientific, Waltham, MA, USA).

Estimation of cytotoxicity

The viability was assayed using MTT (3– (4,5–dimethylthiazol–2–yl) –2,5–diphenyltetrazolium bromide) assay. Cell was incubation for 24 h at 37 °C with 5% CO_2 to ensure cell growth. After treatment, 10 µl of MTT [5 mg/ml in phosphate buffered saline (PBS)] was added to the cells and incubated. After that, MTT–containing medium was replaced by 100 µl of dimethyl sulfoxide (DMSO) and, absorbance was determined at 570 nm using Infinite 200 PRO (Tecan, Männedorf, Switzerland).

Descriptive statistics

For the statistical evaluation of the results using paired *t*–test and ANOVA. Unless noted otherwise, the threshold for significance was $p < 0.05$. For analyses Software Statistica 12 (StatSoft, Tulsa, OK, USA) was employed.

RESULTS AND DISCUSSION

Physico–chemical characterization of SPIONs and complexation with Dox

SPIONs were tested for their LEs (loading efficiency) towards Dox. Table 1, 2 and 3 illustrates that the highest LE (red colour) was achieved for SPIONs coated with *i*) 10 mg/ml of PVP *ii*) 5 mg/ml of POES *iii*) 2.5 mg/ml of Chit.

Table 1 Analysis of Dox loading efficiency to SPIONs coated with various amount of PVP.

	Concentration of PVP (mg/ml)	2.5	5	10
Ultrasonication	10 °C	0	28	17
	20 °C	21	12	21
	40 °C	18	13	19
Incubation 30 min	10 °C	5	14	8
	20 °C	11	13	40
	40 °C	12	11	9

Table 2 Analysis of Dox loading efficiency to SPIONs coated with various amount of POES.

	Concentration of POES (mg/ml)	2.5	5	10
Ultrasonication	10 °C	29	36	21
	20 °C	24	11	18
	40 °C	14	21	17
Incubation 30 min	10 °C	6	15	10
	20 °C	0	13	11
	40 °C	11	8	14

Table 3 Analysis of Dox loading efficiency to SPIONs coated with various amount of Chit.

	Concentration of Chit (mg/ml)	2.5	5	10
Ultrasonication	10 °C		0	0
	20 °C	0	0	5
	40 °C	0	0	7
Incubation 30 min	10 °C	0	0	8
	20 °C	0	0	1
	40 °C	0	0	9

SEM micrographs showed that SPIONs demonstrated relatively uniform oval–to–spherical morphology and were well dispersed (Figure 1A). This was confirmed by incubating modified SPIONs for 12 h. They were found to disperse readily and remained stable in dispersion for more than 12 h (Figure 1B).

In vitro drug release studies

Drug release studies were conducted with various environments, which mimic low pH of endosomes (pH 5), intracellular neutral pH (pH 6.9) and environment of plasma (pH 7.4). Release profiles demonstrate pH–responsive behaviour of SPIONs PVP, SPIONs POES and SPIONs Chit, which the highest released was 58% of complexed Dox during 4 h incubation in endosomal environment in case SPIONs POES (Figure 3).

Figure 1 (A). SEM micrographs of SPIONs (B) Photodocumentation of colloidal stability of synthesized SPIONs, SPIONs PVP, SPIONs POES and SPIONs Chit at start–point (0 h), and 12 h.

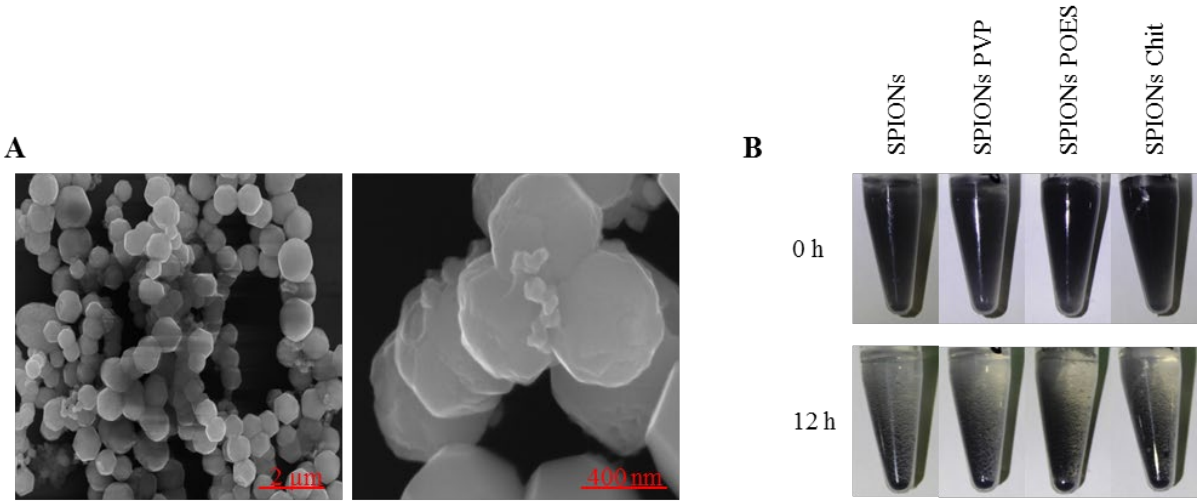

Figure 2 In vitro cumulative release profiles of Dox from SPIONs PVP determined in various physiological pH.

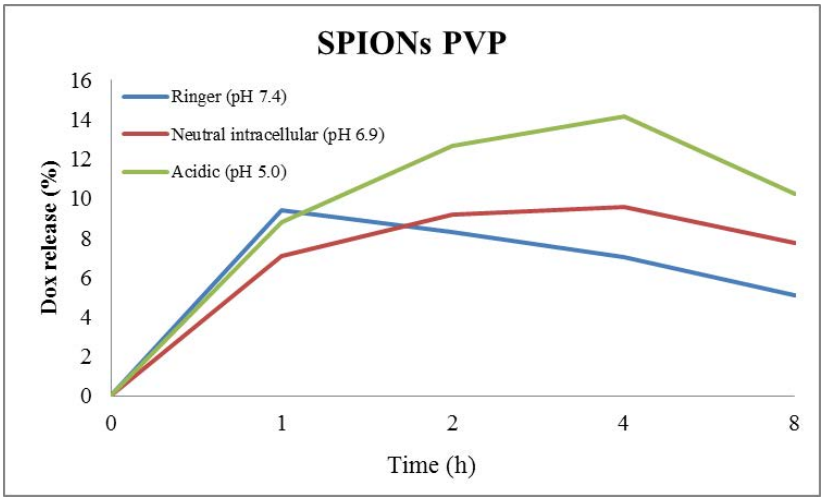

Figure 3 In vitro cumulative release profiles of Dox from SPIONs POES determined in various physiological pH.

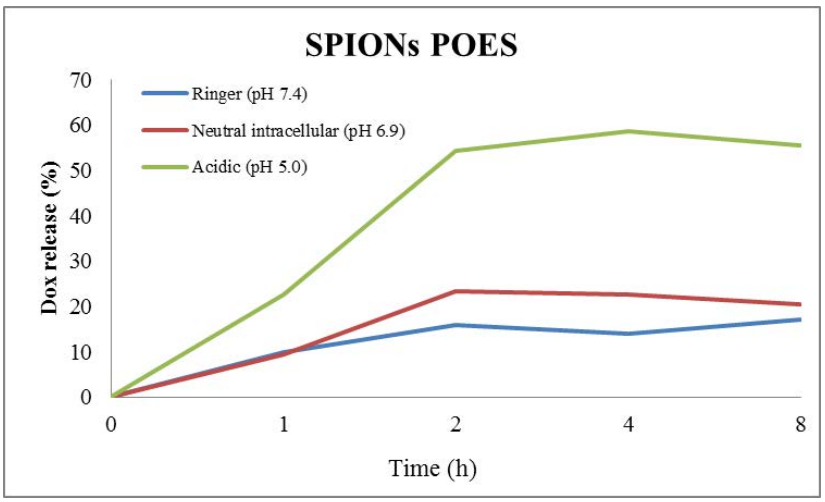

Figure 4 In vitro cumulative release profiles of Dox from SPIONs Chit determined in various physiological pH.

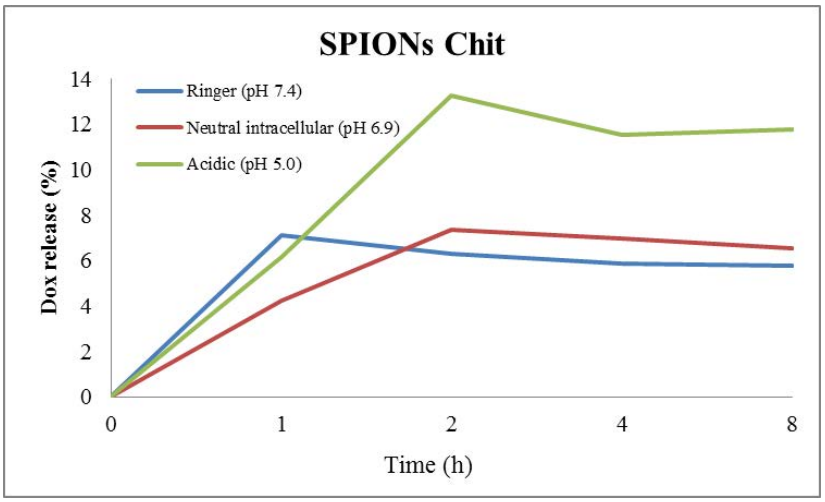

Synergistic cytotoxicity of Dox immobilized on SPIONs

Cytotoxic testing was performed on two different cell lines – breast cancer (MDA–MB–231) and normal breast (HBL–100). Immobilization of Dox resulted in a significant ($p < 0.01$) increase in cytotoxic effects in all tested cells (with the IC_{50} values are summarized in Table 4). Interestingly, non–modified SPIONs did not exerted cytotoxic action in both tested cell lines (n.d. – not detected).

Table 4 Summary of $24IC_{50}$ values obtained from MTT assay for tested cell lines after 24 h treatments. All values are presented as mean ± SD of six biological replicates

	MDA–MB–231	**HBL–100**
	$24IC_{50}$ (μM)	
SPIONs PVP	2	8
SPIONs POES	1	7.1
SPIONs Chit	0.5	1.8
Free Dox	125	89
SPIONs	n.d.	n.d.

CONCLUSION

We designed, prepared and tested cytotoxicity and biocompatibility of various modified SPIONs with exceptional nanomedicine platforms. We also showed that PVP and FDA–approved POES or Chit natural polymer such core–shell nanoparticles which significantly enhances the Dox performance. Our *in vitro* results are restricted and further *in vivo* tests must be carried out in the future, it is obvious that combination of SPIONs and polymers have exhibit potential for nanomedicine. Finally, based on available literature, SPIONs are promising magnetic resonance imaging contrast agents, tissue reparation, or for a drug delivery, hence their use will most likely enable for tracing and imaging.

ACKNOWLEDGEMENTS

Financial support from Czech Science Foundation (project GA CR 17–12816S), AF–IGA–IP–2018–007 and CEITEC 2020 (LQ1601) is highly acknowledged.

REFERENCES

Boisseau, P., Loubaton, B. 2011. Nanomedicine, nanotechnology in medicine. Comptes Rendus Physique, 12(7): 620–636.

Linkov, I. et al. 2008. Nanotoxicology and nanomedicine: making hard decisions. Nanomedicine: Nanotechnology, Biology and Medicine, 4(2): 167–171.

Liu, G. et al. 2013. Applications and potential toxicity of magnetic iron oxide nanoparticles. Small, 9(9–10): 1533–1545.

Naqvi, S. et al. 2010. Concentration–dependent toxicity of iron oxide nanoparticles mediated by increased oxidative stress. International Journal of Nanomedicine, 5: 983.

Singh, N. et al. 2010. Potential toxicity of superparamagnetic iron oxide nanoparticles (SPION). Nano Reviews, 1(1): 5358.

MALDI-TOF MSI method for determining spatial distribution of infection markers in pulmonary tissues of pigs

Tomas Do[1], Rea Jarosova[2], Lada Smidova[1], Roman Guran[1,3], Petra Ondrackova[4], Martin Faldyna[4], Zbysek Sladek[2], Ondrej Zitka[1,3]
[1]Department of Chemistry and Biochemistry
[2]Department of Morphology, Physiology and Animal Genetics
Mendel University in Brno
Zemedelska 1, 613 00 Brno
[3]Central European Institute of Technology
Brno University of Technology
Purkynova 123, 612 00 Brno
[4]Department of Immunology
Veterinary Research Institute
Hudcova 296/70, 621 00 Brno
CZECH REPUBLIC

xdo1@mendelu.cz

Abstract: In recent years the matrix-assisted laser desorption/ionization time-of-flight mass spectrometry imaging (MALDI-TOF MSI) is used for molecular mapping of diverse biomarkers such as proteins or peptides in animal/plant tissue sections. It takes full advantage of the benefits of MALDI-TOF technique which is the ability of rapid measurements of all mass spectra in a wide mass range and detection of analytes molecular weights. Interleukins, the group of mostly proinflammatory cytokines, are the proteins that are produced as immune response on bacterial infection *Actinobacillus pleuropneumonia*. The aim of this study was to develop a MALDI-TOF MSI method for quantitative visualization of spatial distribution of interleukins and other cell markers of lymphocytes, granulocytes and macrophages in porcine tissues of lymph nodes and lungs. The determination of the spatial distribution of produced proteins will bring further useful knowledge of the pathogenesis of this economically important disease of pigs, which can also contribute to reducing the consumption of antimicrobials.

Key Words: mass spectrometry imaging, cytokines, interleukins, infection, pig model

INTRODUCTION

Actinobacillus pleuropneumoniae (APP) belongs among the most important bacterial pulmonary pathogens in pigs of all ages and is found worldwide. APP is gram-negative bacteria from the family *Pasteurellaceae* that causes swine disease called porcine pleuropneumonia that is characterized as an exudative, fibrinous, hemorrhagic, and necrotizing pleuropneumonia (Zimmerman et al. 2012). This bacterial infection mainly affects the lung parenchymal tissue of the animal. The clinical course of disease can vary from per-acute to chronic depending on the serotype of infection, the immune status of the host, and the number of bacteria reaching the lung. Clinical signs during per-acute or acute disease include high fever, increased respiratory rate, coughing/sneezing, dyspnea, anorexia, ataxia, vomiting, diarrhoea, and severe respiratory distress with cyanosis. These symptoms of disease negatively affect the economy of the breeding itself (Bossé et al. 2002).

Virulence of APP is multifactorial as in most pathogenic bacteria. Virulence factors of APP include the capsular polysaccharides, lipopolysaccharides, membrane proteins, adhesion factors and exotoxins (Frey 1995). The immune response of organism is local production of the cytokines interleukin (IL)-1β, IL-8, IL-6 and tumor necrosis factor (TNF)-α in porcine lungs (Ondrackova et al. 2010, Hsu et al. 2016).

Holzlechner and co-workers showed that MALDI-MSI can be used as tool for the characterization and *in situ* localization of immune cell accumulations without using antibodies, which is based on

protein expression in these cells. They also detect *m/z* values allowing for identification and discrimination of lymphocytes, monocytes, and polarized macrophages by intact cell mass spectrometry (ICMS) (Holzlechner et al. 2017).

The matrix assisted laser desorption/ionization technique is routinely used for the analysis of peptides, proteins and identification of bacteria. One of the characteristics of MALDI is soft ionization of biomolecules that allows to generate mostly singly charged ions when short UV laser pulses are fired onto the surface with sample and matrix. Due to soft ionization of biomolecules, MALDI was found as useful tool for mass spectrometry imaging of a variety of samples providing us the information about the spatial distribution of molecules. MALDI MSI was first used for molecular mapping of protein expression in human and mice tissues of brain (Stoeckli et al. 2001). The typical procedure for MALDI MSI on tissues consists of collecting thin tissue section using a cryostat (Tucker et al. 2011), attaching section on a sample plate, and depositing of a matrix, either as a thin layer, or as a spot pattern. In this approach, for co-crystallization with analytes is usually used as a matrix a weak organic acid such as sinapinic acid or 2,5-dihydroxybenzoic acid. The sample plate with section of tissue is then introduced in the mass spectrometer and both the intensities of *m/z* values and their respective x/y positions within a sample are acquired. From a data set, numerous images representing the spatial distribution of the analytes of interest can be obtained. Usually, the molecular weight of analytes are determined using a time-of-flight (TOF) mass analyzer (Rohner et al. 2005). Currently, it is effort to develop MALDI MSI technique in different ways as time of analysis (Baker et al. 2017), spatial resolution (Baker et al. 2017, Huang et al. 2018) and the ionization efficiency and detection of different analytes (Hansen and Lee 2018). A schematic general workflow of the MALDI MSI is described in Figure 1.

Figure 1 Scheme of general workflow of MALDI mass spectrometry imaging.

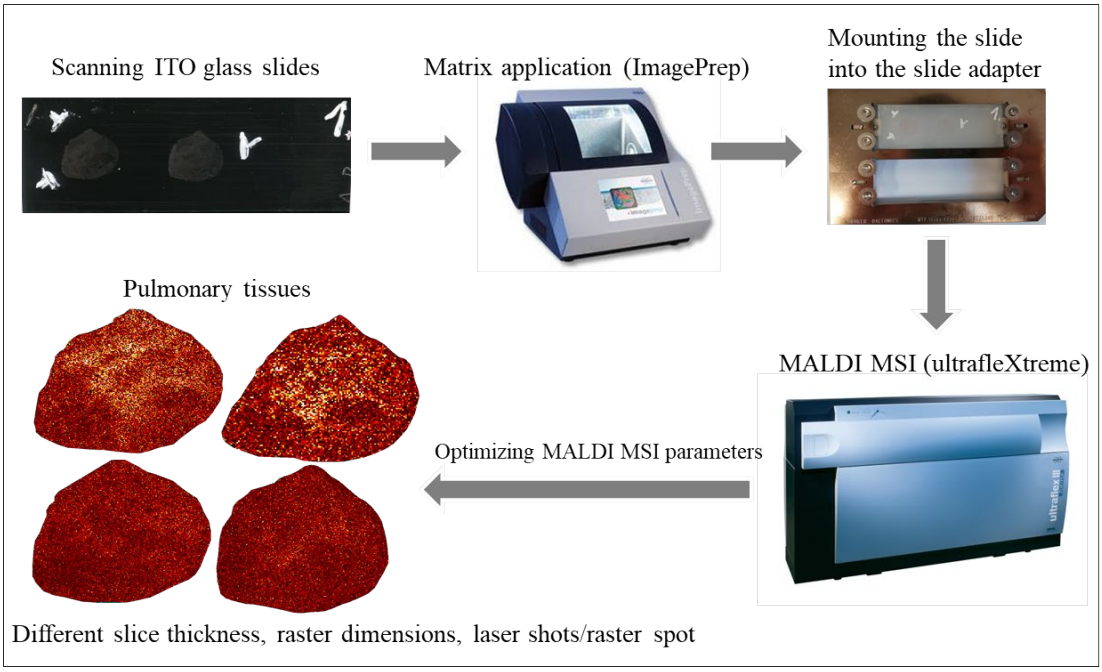

In the present study, we have focused on optimizing the MALDI-TOF mass spectrometry imaging of interleukins and other cell markers of lymphocytes, granulocytes and macrophages in porcine tissues of lymph nodes and lungs. The results from this study will help us in future experiments with cytokines in different tissues.

MATERIAL AND METHODS

Materials

Sinapinic acid (SA) and all solvents (HPLC grade) used were purchased from Sigma-Aldrich (MO, USA) if not otherwise stated. Conductive indium-tin oxide (ITO) one-side coated glass slides and protein calibration standards were purchased from Bruker Daltonik GmbH (Germany).

Collection and Processing of Lymphatic and Pulmonary Tissue

Pieces of lymphatic and pulmonary tissues were taken from infected pigs by APP. Pig breeding was carried out at accredited experimental stables of Veterinary Research Institute in Brno (authorization to use experimental animals, file no. 58809/2014-MZE-17214, valid until 21. 8. 2019). This accreditation also allows to experimentally infect animals under controlled conditions. The experiment was performed in compliance with the Act No. 246/1992 Coll. of the Czech National Council on the protection of animals against cruelty, and with the agreement of the Branch Commission for Animal Welfare of the Ministry of Agriculture of the Czech Republic (approval no. 31674/2018-MZE-17214).

The infection with APP (field-origin strain, biotype 1, serotype 9, KL2-2000) was performed intranasally during inhalation, and the infectious dose of $2x\ 10^9$ bacteria was administered to the second third of each nasal cavity as described previously (Ondrackova et al. 2013). After euthanasia of the animals, samples of tracheobronchial lymph nodes and affected lung tissue were taken for subsequent laboratory analyses.

Cryosections of pulmonary tissue were prepared according to the following protocol *preparing a cryostat section for MALDI imaging* from FlexImaging 3.0 User Manual. The samples were cut to a thickness of 5–10 µm by the cryostat (Leica Microsystems, CM 1900, GmbH, Wetzlar, Germany) at temperature -20 °C. Cryosections for MALDI MSI were mounted onto ITO glass slides and stored at -80 °C.

Prior to analysis, the slides were warmed by hand and desiccated under vacuum for 15 min. Then, the slides were washed in a Coplin jar with ethanol (twice in 70% ethanol for 2 min and once in 100% ethanol for 2 min). The matrix application samples were dried under vacuum for 15 min, and the positions of the tissue slices were marked with three guide marks using a white pencil corrector. Afterwards, the glass slides were scanned by an Epson Perfection V500 Office scanner (Epson Europe B.V., Netherlands) at a resolution of 3200 DPI.

MALDI matrix was sprayed onto ITO glass slides using ImagePrepTM standard programs (Bruker Daltonik GmbH, Germany). Sinapinic acid (Sigma-Aldrich, St. Louis, MO, USA) was used as MALDI matrix. SA was prepared in concentration of 10 mg/ml in 60% acetonitrile and 0.2% trifluoroacetic acid (TFA). MALDI matrix mixtures were thoroughly vortexed and ultrasonicated using Bandelin 152 Sonorex Digital 10P ultrasonic bath (Bandelin electronic GmbH, Berlin, Germany) for 2 minutes at 50% of intensity at room temperature. The samples were ready for analysis after drying.

MALDI MSI analysis

The mass spectrometry experiments were performed on a MALDI-TOF mass spectrometer Bruker ultrafleXtreme (Bruker Daltonik GmbH, Bremen, Germany) using a protocol according to (Guran et al. 2017). The total sample set consisted of 2 ITO glass slides containing 4 tissue sections. The scanned images of tissue slices were loaded into FlexImaging 3.0 software (Bruker Daltonik GmbH, Germany), and a MALDI adapter with two ITO glass slides was loaded into the mass spectrometer. The position of the MALDI adapter was adjusted according to the white guide marks on the ITO glass slides. The regions of acquisition were highlighted by the mouse pointer in FlexImaging, and 50 µm and 100 µm raster width were chosen. External calibration was performed using a protein standard mixture in an *m/z* range of 4–20 kDa. The intensity of each scan over the entire acquired mass range was mapped on the tissue section image to visualize the location of each *m/z* value detected. These images were generated and visualized using SCiLS Lab 2014b software (SCiLS–Bruker Daltonik GmbH, Germany). The laser power was set to 85% for the SA matrix. MALDI MSI of proteins was performed in linear positive mode in a *m/z* range of 4–20 kDa. A total of 1000 spectra were summed for each spot using a random walk raster pattern, with no evaluation criteria.

Spectral processing and statistics

The MSI data from FlexImaging were converted and uploaded into the SCiLS Lab software used for pipeline segmentation and statistical analysis (namely the Anderson-Darling normality test and the Kruskal-Wallis test).

RESULTS AND DISCUSSION

In the study (Holzlechner et al. 2017), they were able to visualize the localization of lymphocytes and macrophages in human colon tissue sections by MALDI MSI. Therefore, we decided to utilize and optimize the MALDI-TOF MSI method to obtain spatial (2D) distribution of interleukins and other cell markers of lymphocytes, granulocytes and macrophages in porcine tissues of lymph nodes and lungs for our future research. In the present work the tissue thickness and laser shots per raster spot were optimized. Sections of various thickness (from 7 to 10 µm), rasters of various dimensions (50×50, 100×100) and different numbers of laser shots per raster spot (300, 500, 1000 and 1200 laser shots per raster spot) were tested. For analysis were used cryo-sectioned frozen tissue samples because there are no other interferences for MALDI-TOF mass spectrometry. Also can be used formalin-fixed and paraffin-embedded (FFPE) sample, but preparation of FFPE sample is more complicated. Paraffin can suppress ionization and formaldehyde fixation causes dehydration, denaturation, crosslinking (methylene bridges), precipitation and protein agglutination, which prevents their detection (Guran et al. 2016). Prior to protein MSI analysis, the samples were processed using a solvent washing step. The MSI data were then imported into SCiLS Lab software for post-processing and generation of protein profiles and specific ion maps. A several peaks with notable signal intensity were generated. For an example, the peaks at *m/z* 10827.457 and 15117.282 Da, that should represent cell markers of lymphocytes or monocytes according study (Holzlechner et al. 2017), were found in each pulmonary tissues. These peaks were selected to generate MSI images (Figure 2) and intensity box plots (Figure 3) to view the differences among various raster spots and various thicknesses of tissue sections. The optimal size of a raster spot was 50×50 and the optimal number of laser shots per raster spots was determined to be at least 500.

*Figure 2 MALDI ion images of selected m/z values (10827.457 and 15117.282 Da) representing markers of monocytes and lymphocytes in pulmonary tissue with various (**A**) size of a raster spot (50×50, 100×100) and various (**B**) thicknesses of cryosections (10, 7, 8 µm).*

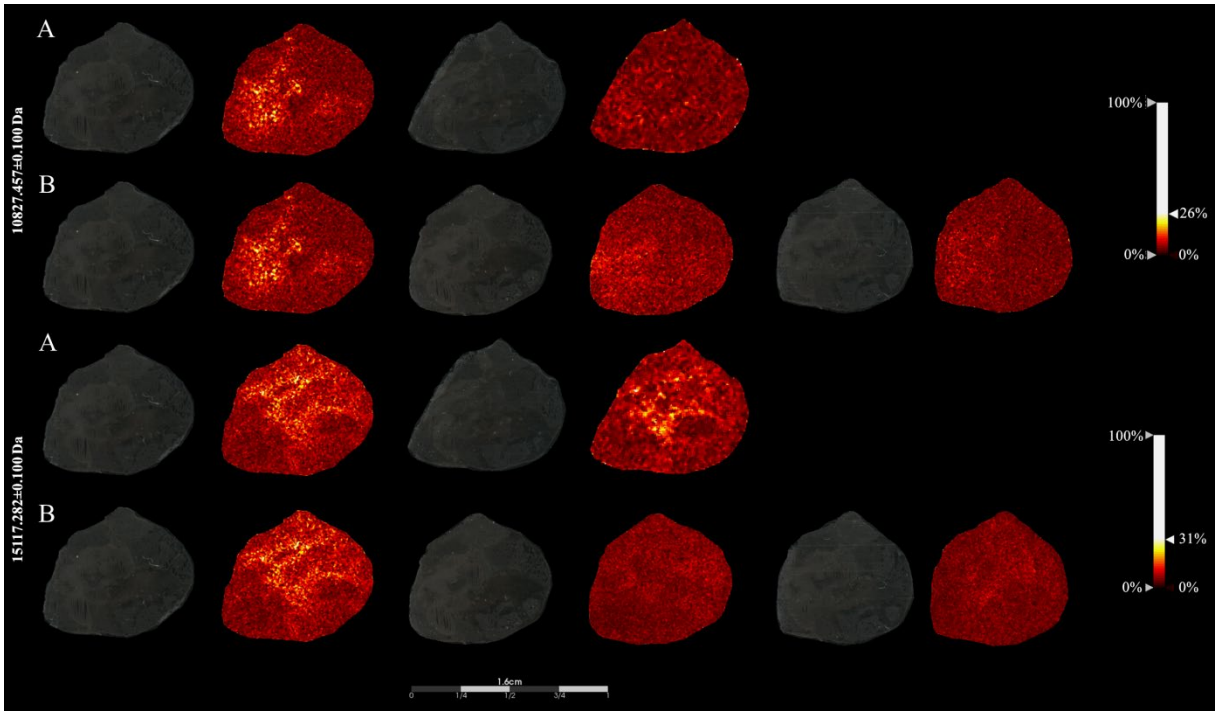

The MSI data were submitted to SCiLS Lab where were revealed significant ($p < 0.001$) differences among tissues by the Kruskal-Wallis test. The peak at *m/z* 15117.282 Da varied significantly ($p < 0.001$) among pulmonary tissue with various thickness sections. The peak at *m/z* 10827.457 Da varied significantly ($p < 0.001$) among sections unlike between sections with thickness 10 µm and 7 µm ($p \geq 0.05$, $r = 0.89$). Higher intensities of the peaks at m/z 10827.457 and 15117.282 Da were found in section with thickness 10 µm according the intensity box plots.

*Figure 3 Intensity box plots of 10827.457 Da (**A**) and 15117.282 Da (**B**) of pulmonary tissue with various thicknesses of cryosections.*

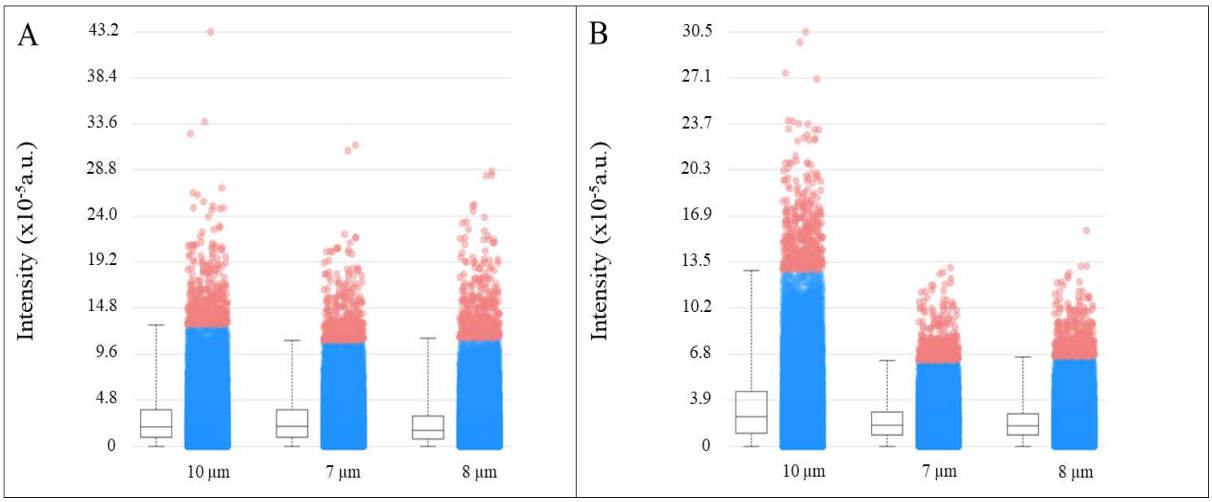

CONCLUSION

Interleukins are of special interest as they have been shown to be involved in disease called porcine pleuropneumonia. This study demonstrates that MALDI MSI method was optimized to successfully visualize the spatial distribution of a several peaks, for an example the peaks at m/z 10827.457 and 15117.282 Da, representing interleukins and other cell markers of lymphocytes, granulocytes and macrophages in porcine cryo-sectioned frozen tissues of lymph nodes and lungs. This result is promising for future research with cytokines in different tissues.

ACKNOWLEDGEMENT

This research was carried out with the support of the Ministry of Education, Youth and Sports of the Czech Republic under the project CEITEC 2020 (LQ1601). The research team has been supported by grant no. AF-IGA-2018-tym005.

REFERENCES

Baker, T.C. et al. 2017. Recent advancements in matrix-assisted laser desorption/ionization mass spectrometry imaging. Current Opinion in Biotechnology, 43: 62–69.

Bossé, J.T. et al. 2002. Actinobacillus pleuropneumoniae: pathobiology and pathogenesis of infection. Microbes and Infection, 4(2): 225–235.

Frey, J. 1995. Virulence in Actinobacillus pleuropneumoniae and RTX toxins. Trends in Microbiology, 3(7): 257–261.

Guran, R. et al. 2017. MALDI MSI of MeLiM melanoma: Searching for differences in protein profiles. PLOS ONE, 12(12): e0189305.

Guran, R. et al. 2016. MALDI zobrazovací hmotnostní spektrometrie pro studium fyziologických pochodů v nádorech. Chemické listy, 110(2): 106–111.

Hansen, R.L., Lee, Y.J. 2018. High-Spatial Resolution Mass Spectrometry Imaging: Toward Single Cell Metabolomics in Plant Tissues. Chemical Record, 18(1): 65–77.

Holzlechner, M. et al. 2017. *In Situ* Characterization of Tissue-Resident Immune Cells by MALDI Mass Spectrometry Imaging. Journal of Proteome Research, 16(1): 65–76.

Hsu, C.-W. et al. 2016. Involvement of NF-κB in regulation of Actinobacillus pleuropneumoniae exotoxin ApxI-induced proinflammatory cytokine production in porcine alveolar macrophages. Veterinary Microbiology, 195: 128–135.

Huang, X. et al. 2018. Utilizing a Mini-Humidifier to Deposit Matrix for MALDI Imaging. Analytical Chemistry, 90(14): 8309–8313.

Ondrackova, P. et al. 2010. Porcine mononuclear phagocyte subpopulations in the lung, blood and bone marrow: dynamics during inflammation induced by Actinobacillus pleuropneumoniae. Veterinary Research, 41(5): 64.

Ondrackova, P. et al. 2013. Distribution of porcine monocytes in different organs during experimental Actinobacillus pleuropneumoniae infection and the role of chemokines. Veterinary Research, 44(1): 98.

Rohner, T.C. et al. 2005. MALDI mass spectrometric imaging of biological tissue sections. Mechanisms of Ageing and Development, 126(1): 177–185.

Stoeckli, M. et al. 2001. Imaging mass spectrometry: A new technology for the analysis of protein expression in mammalian tissues. Nature Medicine, 7: 493.

Tucker, K.R. et al. 2011. The modified-bead stretched sample method: development and application to MALDI-MS imaging of protein localization in the spinal cord. Chemical Science (Royal Society of Chemistry: 2010), 2(4): 785–795.

Zimmerman, J.J. et al. 2002. Diseases of Swine. 10th ed., Ames, Iowa: Wiley-Blackwell.

Isolation of histamine using γ-Fe_2O_3 nanoparticles

Milica Gagic[1,2], Pavel Kopel[1,2], Vedran Milosavljevic[1,2], Natalia Cernei[1,2], Ondrej Zitka[1,2], Pavel Svec[1], Ewelina Jamroz[3], Vojtech Adam[1,2]
[1]Department of Chemistry and Biochemistry
Mendel University in Brno
Zemedelska 1, 613 00 Brno
[2]Central European Institute of Technology
Brno University of Technology
Purkynova 123, 612 00 Brno
CZECH REPUBLIC
[3]Institute of Chemistry
University of Agriculture, Cracow
Balicka str. 20, 30149
POLAND

gagic.milica@gmail.com

Abstract: Histamine, biologically active amine, is normally present in the body and it is involved in a local regulation of physiological processes. It occurs in food as a product of microbial decarboxylation of the amino acid histidine, and the ingestion of foods that contain high levels of histamine can lead to poisoning. Hence, the presence of this biogenic amine is considered as an indicator of food spoilage. Many different methods are available to detect the presence of histamine in food samples. The aim of this study was to design a fast and low-cost method for histamine identification employing magnetic isolation and subsequent reaction of desorbed histamine with ninhydrin for final ion exchange chromatography quantification.

Key Words: fish poisoning, biogenic amines, nanoparticles, food safety, rapid method

INTRODUCTION

Biogenic amines are non-volatile, heat stable, low molecular weight bases with biological activity and have aliphatic, aromatic or heterocyclic structure (Tapingkae et al. 2010). They can be formed and degraded as a result of normal metabolic activity in animals, plants, and humans and are usually produced by the decarboxylation of amino acids.

Histamine [2-(4-imidazolyl)-ethylamine] is short-acting biogenic amine synthesized from the amino acid histidine through the catalytic activity of enzyme histidine decarboxylase (Dy and Schneider 2004). It is synthesized and stored at high concentrations within granules in basophils and mast cells and effects of this biologically active chemical are usually seen when it is released in large amounts or ingested in unusually high quantity. Histamine exerts its effects through differential activation of four distinct subtypes of G-protein coupled receptors on cellular membranes (Lehane and Olley 2000).

Histamine in low concentrations is also produced during microbial decomposition of Scombroid fish flesh such as tuna and mackerel (Halasz et al. 1994). However, when fish is spoiled, the amount can increase to a toxic level (up to 50 mg per 100 g of the product), causing food poisoning. Histamine has been identified as a significant chemical hazard and formation of histamine can lead to adverse reactions, especially in allergic suffering consumers. To prevent potential risk caused by histamine its detection in foods is of great importance.

A plethora of techniques have been described to provide information about the levels of histamine in different sorts of food (Onal 2007). This study focuses on the design and optimization of the method based on the isolation of histamine using paramagnetic particles (PMPs) with consequent quantitative determination by ninhydrin colorimetric assay. Due to their unique physicochemical properties, PMPs (functionalized maghemite γ-Fe_2O_3 nanoparticles) have received considerable attention in the analysis

of residues in food samples. Application of magnetic particles for histamine analysis is a good alternative to traditional methods because histamine is typically present in very low concentration over a high concentration of background material. By using their magnetic properties particles are applied as adsorbents during isolation, separation, and preconcentration of the target analytes (Jimenez et al. 2016).

This study consists of the synthesis of particles with magnetic properties (maghemite Fe_2O_3) followed by a coating of the magnetic core with different organic compounds. The ability of synthesized particles to adsorb histamine on the surface was tested by employing ion-exchange liquid chromatography (IEC) with post-column ninhydrin derivatization together with visible light range (VIS) detection with an integrated two-channel photometer simultaneously working at 440 and 570 nm, respectively.

MATERIAL AND METHODS

Chemicals

The chemicals were purchased from Sigma-Aldrich (St. Louis, MO, USA) in ACS purity unless noted otherwise.

Synthesis of paramagnetic nanoparticles

Maghemite nanoparticles were prepared by sodium borohydride reduction of iron nitrate ($Fe(NO_3)_3 \cdot 9H_2O$) according to the already known procedure (Heger et al. 2015, Nejdl et al. 2014). 7.48g of $Fe(NO_3)_3 \cdot 9H_2O$ was dissolved in 400 mL of water. Under stirring 1g of $NaBH_4$ was added, which was previously dissolved in 50mL of 3.5% NH_3. The obtained solution was heated at boiling temperature for 2h. After cooling, the dark product was separated by external magnetic field and washed several times with water. The nanoparticles, prepared in this way were used as a core for surface modification.

Seven different functionalized PMPs will be applied separately in order to obtain specific histamine binding activity, for each of them. A versatile and inexpensive method for the introduction of functional groups on the surface of maghemite particles will be established based on the particles modification with each of seven different organic molecules, as follow: N-(3-trimethoxysilylpropyl) diethylenetriamine, 3-(Triethoxysilyl)propyl isocyanate, (3-glycidyloxypropyl)trimethoxysilane, (3-aminopropyl)triethoxysilane, 2,6-Pyridinedicarboxylic acid, titanium(IV) butoxide and for the last surface functionalization, combination of tetraethyl orthosilicate (TEOS) and titanium(IV) butoxide will be used.

Procedure for histamine isolation for subsequent analysis using IEC-VIS

Initially, the paramagnetic particles are ultrasonicated and washed thrice with PBS (3x250 µl; pH 7.4). Consequently, the binding buffer is added (250 µl) and mixed with standard histamine of known concentration. Subsequently, an external magnetic field is applied to isolate the adsorbent with the adsorbed histamine on the surface of the magnetic particles. The liquid phase is decanted and the particles are washed twice with washing buffer. In the next step, histamine is eluted by the dispersion of the magnetic particle with elution buffer. Finally, the solution is collected and analyzed by IEC (see Figure 1).

For determination of histamine, an IEC Model AAA – 400 (Ingos, Prague, Czech Republic) with post-column derivatization by ninhydrin and an absorbance detector in visible light range was used (Cernei et al. 2016). A glass column with an inner diameter of 3.7 mm and length of 350 mm was filled manually with strong cation exchanger Ostion LG ANB (Ingos, Prague, Czech Republic) in sodium cycle with ~12 µm particles and 8% porosity. The column was thermostated at 60 °C. Double channel VIS detector with an inner cell of 5 µl was set to two wavelengths: 440 and 570 nm. Prepared solution of ninhydrin was stored under a nitrogen atmosphere in the dark at 4 °C. Elution of histamine was carried out by a buffer containing 10.0 g of citric acid, 5.6 g of sodium citrate, and 8.4 g of sodium chloride per liter of solution (pH 2.7). The flow rate was 0.25 ml/min. The reactor temperature was set to 120 °C.

Figure 1 Experimental workflow

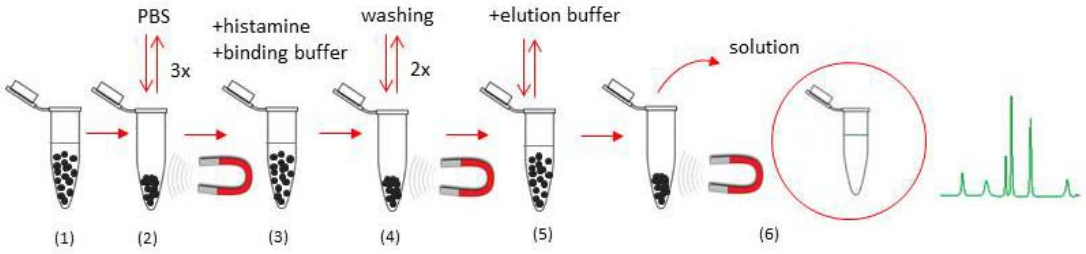

Legend: 1 – PMPs in storage solution, 2 – Washing of PMPs using PBS, 3 – Binding of histamine with PMPs and buffer, 4 – Washing of PMPs with bound histamine 5 – Elution of histamine 6 – IEC analysis of the obtained solution

Effect of pH

The interaction between the prepared PMPs and the histamine is significantly affected by the pH value of the buffers used in the experimental procedure. The pH value may alter the surface charge of particles and thus it may interact with the studied analyte. In order to determine the convenient pH value, the effect of pH on the adsorption and releasing of histamine was investigated.

Statistical analyses

The content of histamine was made using standard deviation from 3 determinations. The detection limits (3 signal/noise, S/N) were calculated according to Long and Winefordner (Long and Winefordner 1983).

Reusability of PMPs

We tested reusability of PMPs, to investigate whether PMPs could be totally released from the histamine and reused. Used PMPs were dissolved in hydrochloric acid (3 M). Particles were separated by using an external magnetic force field. Furthermore, the obtained solution was evaporated using a nitrogen evaporator Ultravap RC. The evaporated sample was resuspended in H_20 and the final product was quantified by IEC.

RESULTS AND DISCUSSION

The nanomaghemite synthesis was carried out by reduction of iron chloride and its subsequent modification. Seven different PMPs were prepared which differed from each other in their composition and functionalization procedure. To determine the binding specificity and effectiveness of the prepared PMPs toward histamine, IEC-Vis analysis was carried out. In the first step of the experiment, binding conditions were evaluated by mixing the histamine with Britton Robinson (BR) buffer at different pH values, eluting bound histamine with a high salt concentration buffer and analyzing fraction for the target analyte. According to the obtained results, BR pH 4 and 2M saturated BR pH 9 were selected for further experiments as binding and elution buffer, respectively. The protocol for the isolation and detection of histamine using functionalized PMPs is shown in Figure 1.

MAN_181 and MAN_183 were the most successful particles in the suggested assay. As shown in Table 1, high recovery percentages indicate that the aforementioned PMPs can be applied with high accuracy for the determination of the histamine. This was likely caused by the same surface coating of nanomaghemite core with titanium(IV) butoxide. To obtain further insight into beads morphology of these particles the SEM and XRF were employed. Due to the extremely low percentage recovery of the histamine, other particles were excluded from further characterization (Table 1).

Results of the reusability test showed that particles could be recycled easily. Histamine was not retained on PMPs surface after elution step, very low analyte recoveries were detected after quantification by IEC analysis (data not shown). Reusability is one of the important properties of these particles and the possibility of full recovery after elution makes these particles highly desirable.

Table 1 Overview of synthesized PMPs, their modifications and extraction recoveries

Label	Modification	Recovery (%)
MAN_175	N-(3-trimethoxysilylpropyl)diethylenetriamine	0.5
MAN_176	3-(Triethoxysilyl)propyl isocyanate	17.12
MAN_177	3-glycidyloxypropyl trimethoxysilane	0.52
MAN_178	(3-Aminopropyl)triethoxysilane	0.06
MAN_179	2,6-Pyridinedicarboxylic acid	0.34
MAN_181	Titanium(IV) butoxide	94.5
MAN_183	TEOS + Titanium(IV) butoxide	80.82

Data from electron microscopy (Figure 2a–b) indicate that the magnetic particles were non-uniform clustered (agglomerated) polycharged particles, but it didn't have an influence on their magnetic properties. As is shown in Figure 2, the size of PMPs for MAN_181 and MAN_183 ranged in µm. Additionally, XRF was employed to reveal the elemental composition of PMPs. In both cases, iron and titanium were determined as the most abundant elements and that is direct confirmation of the functional groups provided by surface functionalization with titanium(IV) butoxide, a compound which is used for coating of PMP_181 and PMP_183 (see Figure 2c–d).

Figure 2 Characterization of MAN_181 and MAN_183. Micrographs of the surface of PMPs were obtained using SEM. The XRF elemental composition of the particles is shown in the third and fourth panel for MAN_181 and MAN_183 respectively.

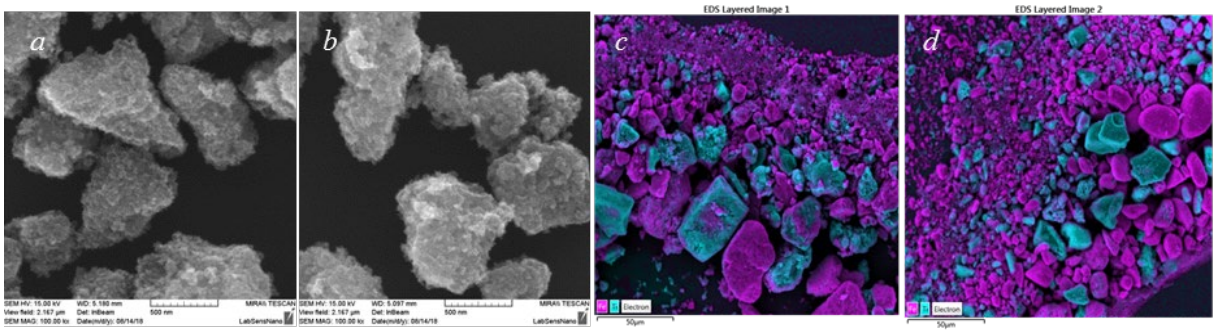

Legend: a – SEM photography of MAN_181, b – SEM photography of MAN_183, c – XRF of MAN_181, d – XRF of MAN_183. Violet color corresponds to iron, blue color corresponds to titanium.

CONCLUSION

A major part of this study was to test binding affinity of seven different functionalized paramagnetic particles against histamine. Methodology optimized in this study employed the application of an external magnetic field in the isolation of the magnetic particles in the separation of histamine without additional steps that could cause loss of analyzed analyte. Two types of seven tested PMPs showed a certain potential for improving of efficiency of separation of histamine from the solution. Besides, specificity of these PMPs in complex matrices and interference from other compounds, commonly found in food samples, need to be tested. In order to address these challenges, other biogenic amines (tyramine, spermine, spermidine, putrescine, cadaverine) will be analyzed in parallel with histamine. This project will aim to ascertain the histamine level in different products as it can serve as a food quality marker and more research will be undertaken in our laboratory.

ACKNOWLEDGMENTS

The research was financially supported by grant no. AF-IGA-IP-2018/076.

REFERENCES

Cernei, N. et al. 2016. Determination of Histamine in Silages Using Nanomaghemite Core (Fe2O3)-Titanium Dioxide Shell Nanoparticles Off-Line Coupled with Ion Exchange Chromatography. International Journal of Environmental Research and Public Health, 13(9): 904.

Dy, M. et al. 2004. Histamine-cytokine connection in immunity and hematopoiesis. Cytokine & Growth Factor Reviews, 15(5): 393–410.

Halasz, A. et al. 1994. Biogenic-amines and their production by microorganisms in food. Trends in Food Science & Technology, 5(2): 42–49.

Heger, Z. et al. 2015. 3D-printed biosensor with poly(dimethylsiloxane) reservoir for magnetic separation and quantum dots-based immunolabeling of metallothionein. Electrophoresis, 36(11–12): 1256–1264.

Jimenez, A.M.J. et al. 2016. Specific Magnetic Isolation of E6 HPV16 Modified Magnetizable Particles Coupled with PCR and Electrochemical Detection. International Journal of Molecular Sciences, 17(5).

Lehane, L. et al. 2000. Histamine fish poisoning revisited. International Journal of Food Microbiology, 58(1–2): 1–37.

Long, G.L. et al. 1983. Limit of Detection A Closer Look at the IUPAC Definition. Analytical Chemistry, 55(07): 712A–724A.

Nejdl, L. et al. 2014. Remote-controlled robotic platform ORPHEUS as a new tool for detection of bacteria in the environment. Electrophoresis, 35(16): 2333–2345.

Onal, A. 2007. A review: Current analytical methods for the determination of biogenic amines in foods. Food Chemistry, 103(4): 1475–1486.

Tapingkae, W. et al. 2010. Degradation of histamine by extremely halophilic archaea isolated from high salt-fermented fishery products. Enzyme and Microbial Technology, 46(2): 92–99.

Preparation of cryosections from frozen porcine pulmonary tissue for MALDI mass spectrometry imaging

Rea Jarosova[1], Vendula Smolikova[2,3], Marek Dvorak[2], Roman Guran[2,3], Tomas Do[2], Petra Ondrackova[4], Ondrej Zitka[2,3], Zbysek Sladek[1]
[1]Department of Morphology, Physiology and Animal Genetics
[2]Department of Chemistry and Biochemistry
Mendel University in Brno
Zemedelska 1, 613 00 Brno
[3]Central European Institute of Technology
Brno University of Technology
Purkynova 123, 612 00 Brno
[4]Department of Immunology
Veterinary Research Institute
Hudcova 296/70, 621 00 Brno
CZECH REPUBLIC
xjaroso3@node.mendelu.cz

Abstract: In last decades, a matrix-assisted laser desorption/ionization mass spectrometry imaging (MALDI MSI) was used for mapping the spatial distribution of different molecules, mainly peptides, proteins, lipids and metabolites, in different types of tissue. Cryosections are the best suited for getting as much information as possible because the preparation of samples for MALDI MSI does not include deparaffinization and antigen-retrieval steps which are needed in case of conventional formalin-fixed and paraffin-embedded (FFPE) tissue sections. To analyse infection markers like interleukins in the tissue sections of porcine lungs affected by *Actinobacillus pleuropneumoniae*, it was necessary to obtain very well prepared cryosections for MALDI MSI. Therefore, this work was focused on optimization of preparation of frozen porcine lungs and its cryosections with conserved morphological structure.

Key Words: cryosectioning, lungs, pig, pleuropneumonia, mass spectrometry imaging

INTRODUCTION

The *Actinobacillus pleuropneumoniae* (APP) bacterium causes pleuropneumonia in pigs, which, together with the porcine reproductive and respiratory syndrome (PPRS), is the most widespread disease in swine-breeding, where it causes significant breeding and economic losses (Zimmerman et al. 2012). This Gram-negative bacterium colonizes the cells of the lower respiratory tract (Baarsch et al. 2000), where it causes necrotic and hemorrhagic pneumonia (Zimmerman et al. 2012) and thus induces an inflammatory response in the lungs of pigs (Inzana 1991). APP infection is therefore a suitable model for the study of an inflammatory response.

Specific patterns of acute and chronic inflammation are seen during particular situations that arise in the body. Therefore, detection of pathological changes in tissues may indicate the stage of the inflammatory process. However, this method reveals only those processes that are visible. Beside this, cell-derived mediators, plasma-derived mediators, high systemic levels of acute-phase proteins and other agents are released during inflammation. It is therefore obvious that the use of analytical methods for the detection of inflammatory components provides essential data for understanding the pathogenesis. The use of new methods for detection of inflammation components is therefore highly relevant.

Matrix-assisted laser desorption/ionization mass spectrometry (MALDI MS) has been applied to the analysis of biomolecules (DNA, proteins, peptides and sugars) and large organic molecules. Therefore, MALDI is a diagnostic tool with much potential because it allows the rapid identification of proteins and changes to proteins without the cost or computing power of sequencing. MALDI is used for mass spectrometry imaging (MSI), providing the information about the spatial distribution of

molecules in various tissues (Stoeckli et al. 2001). General workflow of MALDI MSI includes collecting thin tissue sections using a cryostat (Tucker et al. 2011), attaching sections on a sample plate or ITO (indium-tin oxide) glass slide, and depositing of a matrix (Rohner et al. 2005). Besides cryo-sectioned frozen tissues, formalin-fixed and paraffin-embedded (FFPE) tissues may be used for MALDI MSI, but FFPE tissue demands more complicated preparation prior to MSI analysis because paraffin can have negative effect on ionization and formaldehyde fixation causes dehydration, denaturation, crosslinking (methylene bridges), precipitation and protein agglutination, which have negative influence on detection (Guráň et al. 2016).

The aim of this work was the optimization of sectioning of frozen porcine lungs to produce cryosections of the best quality for the MALDI MSI.

MATERIAL AND METHODS

Chemicals and material

All solvents (HPLC grade) and other chemicals were purchased from Sigma Aldrich (St. Louis, MO, USA), unless otherwise stated. Conductive indium-tin oxide (ITO) one-side coated glass slides and peptide/protein calibration standards were purchased from Bruker Daltonik GmbH (Bremen, Germany).

Animals and experimental infection

In this experiment were used 4 eight-week-old pigs (*Sus scrofa f. domestica*) from the herd without APP anomaly or vaccination. The pigs were kept in the accredited barrier-type animal facilities of the Veterinary Research Institute (VRI). The animal care protocol for this experiment followed the Czech guidelines for animal experimentation and was approved by the Branch Commission for Animal Welfare of the Ministry of Agriculture of the Czech Republic. The pigs were allowed to acclimatize in the animal facilities for one week, and then the experimental infection was performed.

An The infection with APP field strain (biotype 1, serotype 9, KL2–2000) from the fourth passage was performed intranasally during inhalation, and the infectious dose of 1 x 10^9, 1 x 10^8, 1 x 10^7, 1 x 10^6 bacteria for each individually pig was administered to the second third of each nasal cavity of pig. The total infective dose of 4 ml was administered 2 ml per nasal cavity. Infected pigs were euthanized 24 h after infection. The experimental materials - porcine lungs and tracheobronchial lymph node (TBLN) were collected by trained staff from authorized and registered slaughterhouse at VRI.

Preparing of frozen sections

Porcine necrotic lung tissue was filled over the bronchus by mixture of embedding medium Tissue Tek (O.C.T. compound, Sacura – Finnetek) with phosphate-buffered saline solution (PBS) (Bio Whittaker, Lonza) in rate 1 : 1 for preserving a morphological structure of lungs compared to physiology state. TBLN were inserted into the embedding medium Tissue Tek, and all samples were frozen by super-cooled n-heptane placed on the dry ice.

The tissue samples were cut to a thickness of 5–10 μm using the cryostat (Leica Microsystems, CM 1900, GmbH, Wetzlar, Germany) at temperature -20 °C (Figure 1). The cuts of tissue were placed on slides and fixed in pre-cooled acetone for 5 minutes and stained with Mayer haematoxylin. The histological slides were evaluated by using the light microscope (Olympus BH-2, Japan) and images were taken by camera (Canon EOS 1100D, Japan) using software (Quick Photo Micro 3.0, PROMICRA, Czech Republic).

Preparing of frozen sections for MALDI MSI

Porcine necrotic lung tissue was filled over the bronchus by mixture of embedding medium Tissue Tek (O.C.T. compound, Sacura-Finnetek) with phosphate-buffered saline solution (PBS) (Bio Whittaker, Lonza) in rate 1 : 1 for preserving a morphological structure of lungs compared to physiology state. TBLN were inserted into the embedding medium Tissue Tek, and all samples were frozen by super-cooled n-heptane placed on the dry ice.

The tissue samples were cut to a thickness of 7, 8 and 10 μm on the cryostat (Leica Microsystems, CM 1900, GmbH, Wetzlar, Germany) at temperature -20 °C. The cuts of tissue were placed on ITO slides and fixed in 70% ethanol for 90 sec, then 100% ethanol for 90 s, ten times soaked in ultra-distilled water and again fixed in 70% ethanol for 90 s, then 100% ethanol for 90 s. Slides were stored at -80 °C.

Figure 1 The Leica CM1900 Cryostat –this apparatus was used to section frozen tissue onto slides

MALDI MSI analysis

The MSI was performed on a MALDI-TOF mass spectrometer Bruker ultrafleXtreme (Bruker Daltonik GmbH, Bremen, Germany) using a protocol according to Guran and coworkers (Guran et al. 2017). The total sample set consisted of 2 ITO glass slides containing 4 tissue sections. MALDI matrix was sprayed onto ITO glass slides using ImagePrep^{TM} standard program (Bruker Daltonik GmbH, Bremen, Germany). Sinapinic acid (SA) was used as MALDI matrix. SA was prepared in a concentration of 10 mg/ml in 60% acetonitrile and 0.2% trifluoroacetic acid (TFA). The scanned images of tissue slices were loaded into FlexImaging 3.0 software (Bruker Daltonik GmbH, Germany), and a MALDI adapter with two ITO glass slides was loaded into the mass spectrometer. The position of the MALDI adapter was adjusted according to the white guide marks on the ITO glass slides. The regions of acquisition were highlighted by the mouse pointer in FlexImaging, and 50 µm width of raster spot was chosen. External calibration was performed using a protein standard mixture in an *m/z* range of 4–20 kDa. The MSI images were generated and visualized using SCiLS Lab 2014b software (SCiLS–Bruker Daltonik GmbH, Bremen, Germany). The laser power was set to 85%. MALDI MSI of proteins was performed in linear positive mode in a *m/z* range of 4–20 kDa. A total of 1000 spectra were summed for each spot.

RESULTS AND DISCUSSION

The data obtained from our histological sections showed, that the most suitable method of processing pulmonary tissue samples was filling the lungs by cryoprotective agent for preserving the morphological structure and freeze it in a super-cooled n-heptane. In comparison to the authors (Prince and Porter 1975), whose used a 1 : 2 mixture of an O.C.T. embedding compound (Tissue Tek) and phosphate-buffered saline (PBS) injected intratracheally into fresh lung tissue, we have filled lungs over the lung *bronchus* by a mixture 1 : 1 of an embedding compound Tissue Tek with PBS according to Yeh and coworkers (Yeh et al. 2015) for preserving the morphological structure of the lungs compared to the physiology state. This method was used to create standard frozen sections without significant artifacts as is presented in Figures 2A, 3 and 4. Figure 2B shows unpreserved structure.

In closer look onto Figures 2A, 3 and 4, it is apparent, that all tissue structures remained almost untouched. Only the section of pulmonary tissue, which was frozen without previous filling with mixture of Tissue Tek and PBS, showed some changes; the most visible are collapsed alveoli (Figure 2B, in the bottom right of the figure). Therefore, the use of filling before freezing was necessary to make cryosections for MALDI MSI in the best quality. In scanned images of pulmonary tissue cryosections (Figure 5, top row) there are not visible any significant defects of the tissue. It confirms, that the sections were prepared as well as in Figure 3.

Figure 2 A porcine lung tissue sample filled over the lung bronchus by a mixture of Tissue Tek with PBS (1 : 1) and frozen in n-heptane placed on a dry ice. (A) preserved alveolar structure. (B) pulmonary tissue without filling with mixture of Tissue Tek with PBS, collapsed alveoli, shot structure. It does not correspond to the structure of the lungs of the physiology state. Stained by Mayer haematoxylin. In magnification 100 x

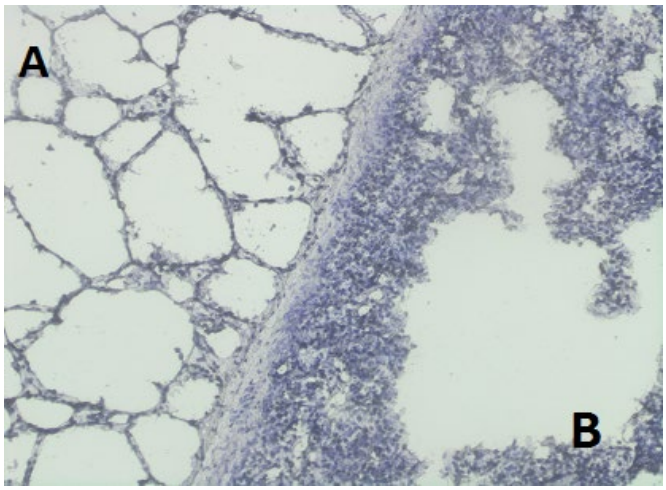

Figure 3 Porcine lung tissue frozen by n-heptane placed on a dry ice, tissue filled with mixture of Tissue Tek with PBS (1 : 1). Stained by Mayer haematoxylin. In magnification 100 x

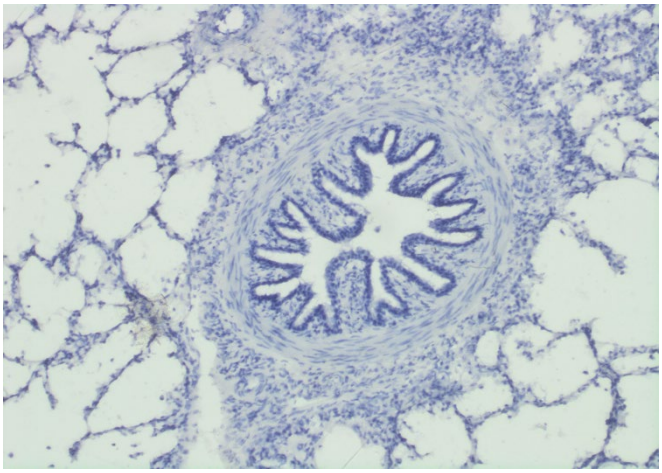

Figure 4 Porcine tracheobronchial lymph node frozen by n-heptane placed on a dry ice. Stained by Mayer haematoxylin. In magnification 100 x

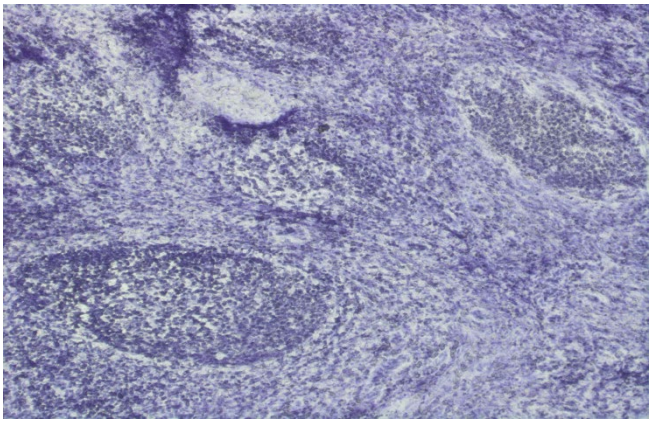

The MALDI MSI analysis of prepared cryosections showed good spatial distribution of a mass peak at *m/z* 10827.5 Da (Figure 5, bottom row). This peak probably corresponds to S100 calcium-binding protein A8 (S100A8) as was investigated by Wehder and co-workers (Wehder et al.

2010). S100A8 protein is involved, inter alia, in the regulation of cell proliferation and acute inflammation (Wehder et al. 2010). Regarding the tissue slice thickness, the data from MSI provided evidence, that the highest intensity of mass peak at *m/z* 10827.5 Da was achieved at slice with 10 µm thickness (Figure 5, the first MSI image from the left in the bottom row). This was probably caused by higher dilution and diffusion of analyte at lower slice thicknesses after application of matrix solution. Based on Figure 5 it is apparent, that the process of cryosectioning of frozen porcine lungs was well optimized and therefore can be used for future experiments aiming at the detection of spatial distribution of different infection markers in porcine lungs infected by *Actinobacillus pleuropneumoniae* (APP) bacterium.

Figure 5 MALDI MSI image of mass peak at m/z 10827.5 Da in porcine lung tissue slices with thickness 10, 8 and 7 µm.

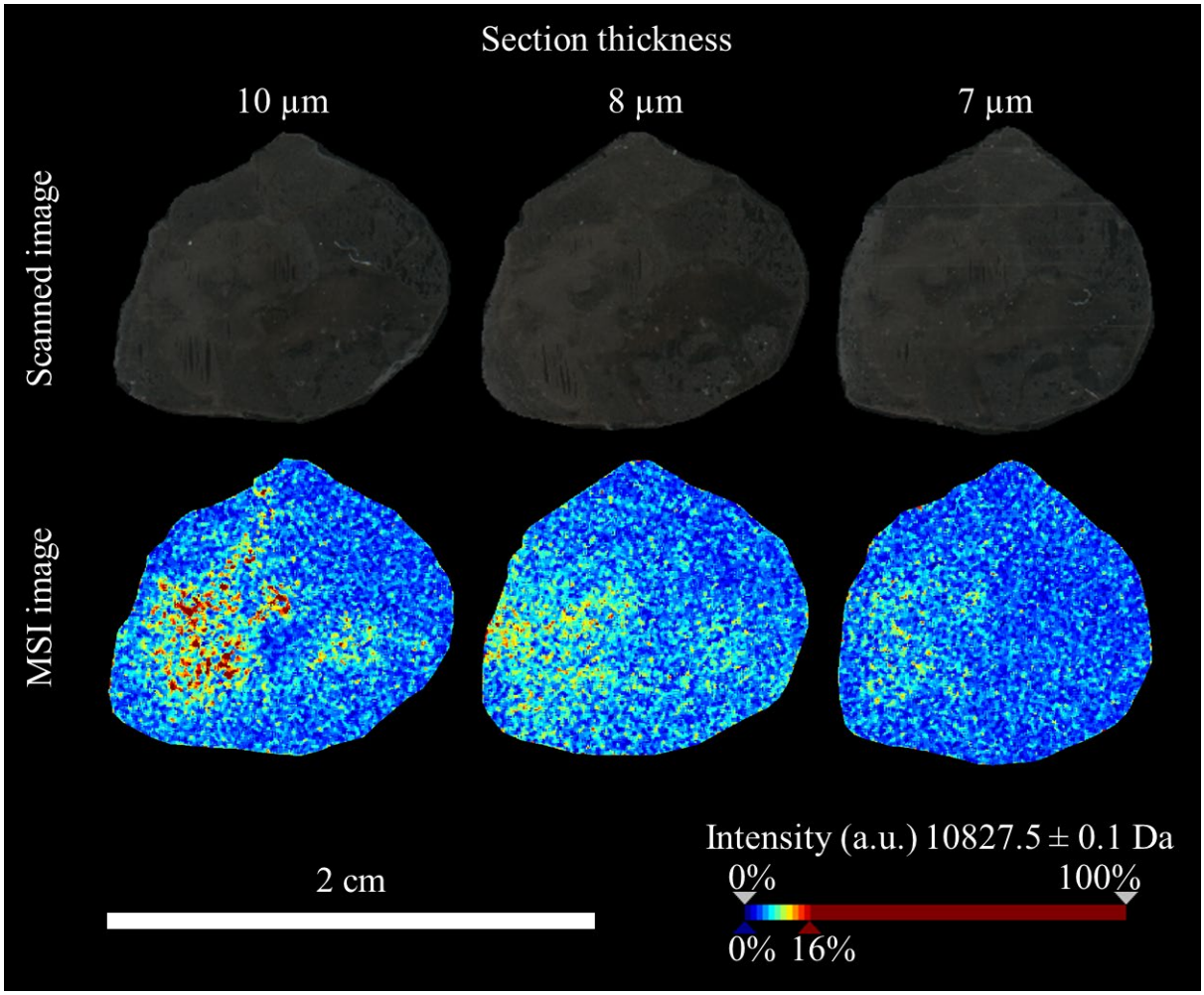

CONCLUSION

In this work, different ways of preparation of porcine lung tissue cryosections were tested. The way when lungs were filled over the lung *bronchus* by a mixture of Tissue Tek with PBS (1 : 1) and frozen in n-heptane placed on a dry ice was chosen as the most appropriate method for the subsequent evaluation by MALDI MSI.

ACKNOWLEDGEMENTS

The This research was carried out with the support of the Ministry of Education, Youth and Sports of the Czech Republic under the project CEITEC 2020 (LQ1601). The research team has been supported by grant no. AF-IGA-2018-tym005.

REFERENCES

Baarsch, M.J. et al. 2000. Pathophysiologic correlates of acute porcine pleuropneumonia. American Journal of Veterinary Research, 61(6): 684–90.

Guran, R. et al. 2017. MALDI MSI of MeLiM melanoma: Searching for differences in protein profiles. PLOS ONE, 12(12): e0189305.

Guráň, R. et al. 2016. MALDI zobrazovací hmotnostní spektrometrie pro studium fyziologických pochodů v nádorech. Chemické listy, 110(2): 106–111.

Inzana, T.J. 1991. Virulence properties of Actinobacillus pleuropneumoniae. Microbial Pathogenesis, 11(5): 305–16.

Prince, G.A., Porter, D.D. 1975. Cryostat Microtomy of Lung Tissue in an Expanded State. Stain Technology, 50(1): 43–45.

Rohner, T.C. et al. 2005. MALDI mass spectrometric imaging of biological tissue sections. Mechanisms of Ageing and Development, 126(1): 177–185.

Stoeckli, M. et al. 2001. Imaging mass spectrometry: A new technology for the analysis of protein expression in mammalian tissues. Nature Medicine, 7: 493.

Tucker, K.R. et al. 2011. The modified-bead stretched sample method: Development and application to MALDI-MS imaging of protein localization in the spinal cord. Chemical Science, 2(4): 785–795.

Wehder, L. et al. 2010. Depicting the Spatial Distribution of Proteins in Human Tumor Tissue Combining SELDI and MALDI Imaging and Immunohistochemistry. Journal of Histochemistry and Cytochemistry, 58(10): 929–937.

Yeh, Y.C. et al. 2015. Using frozen section to identify histological patterns in stage I lung adenocarcinoma of </= 3 cm: accuracy and interobserver agreement. Histopathology, 66(7): 922–38.

Zimmerman, J.J. et al. 2012. Diseases of Swine. 10th ed., Wiley-Blackwell.

Zinc phosphate nanoparticles as an antimicrobial agent and their impact on rats microbiota

Silvia Kociova[1], Zuzana Bytesnikova[1], Pavel Horky[2], Pavel Kopel[1,3], Vojtech Adam[1,3], Kristyna Smerkova[1,3]
[1]Department of Chemistry and Biochemistry
[2]Department of Animal Nutrition and Forage Production
Mendel University in Brno
Zemedelska 1, 613 00 Brno
[3]Central European Institute of Technology
Brno University of Technology
Purkynova 123, 612 00 Brno
CZECH REPUBLIC

xkociova@mendelu.cz

Abstract: Nano minerals, especially trace minerals, are widely used in different fields, but mostly in animal systems. They can improve overall immunity and also a digestive efficacy in livestock. In this case, nanometals as nano mineral substances were synthetized, particular the zinc phosphate-based nanoparticles (ZnNPs). The antibacterial activity against three bacterial strains – *E. coli, S. aureus* and methicillin-resistant *S. aureus* was determined using different methods. After promising *in vitro* testing, the impact of these zinc nanoparticles on rats after oral exposure during 30 days of treatment was investigated. The antibacterial effects on rats gut microbiota were monitored, with the aim to reduce the number of pathogenic bacteria.

Key Words: antimicrobial activity, nano minerals, zinc, rats

INTRODUCTION

Nano minerals are broadly used in various sectors including agriculture, animals and food systems and also in fields like biology, biotechnology, and physiology (Sindhura et al. 2014, Swain et al. 2015). The natural properties of nanometals are mainly determined by its size, shape, composition, morphology and crystalline structure (Dickson and Lyon 2000). The particle size is the main attribute, which heavily influences the functional activities of nano minerals (Lewis and Klibanov 2005, Rosi and Mirkin 2005). Nano zinc and nano zinc oxide (ZnO) are the third most globally produced metal nanoparticles (NPs), annually by volume, after nano SiO_2 and nano TiO_2 (Piccinno et al. 2012). This sudden rise in the demand is mostly attributed to their better antibacterial effects than the conventional ZnO (Padmavathy and Vijayaraghavan 2008). Zn-based nanoparticles, including ZnO NPs like the most studied representative of this type of nanoparticles, showed bactericidal effects on Gram-positive and Gram-negative bacteria as well as the spores, which are resistant to high temperature and high pressure (Azam et al. 2012). From these pathogenic bacteria, there are dominant bacterial causes of severe secretory diarrhoea, which can be still a significant reason of death. A few studies have already proved that the dose of ZnO NPs have influenced growth performance on livestock and also they can be used as antimicrobial and immune agent to reduce the diarrhoea rate in piglets (Hongfu 2008, Mishra et al. 2014).

In particular, ZnO inhibits the bacterial viability, but the precise mechanism of its antibacterial activity has not been well understood so far. One of the proposed possibility is the generation of hydrogen peroxide as the major factor of the antibacterial effect. It is also supposed that, due to electrostatic forces between the particles and the bacteria surface could be another mechanism of antimicrobial effect of ZnO NPs. In addition, generation of reactive oxygen species (ROS), zinc ion release, membrane dysfunction and nanoparticle internalization could be possible reasons of cell damage (Hajipour et al. 2012, Zhang et al. 2008).

The main purpose of this work was to synthesize zinc-based nanoparticles, specifically four types of zinc-phosphate nanoparticles, with the antimicrobial activity. These zinc-phosphate NPs were prepared by synthesis of zinc nitrate with hydrogen phosphate (ZnA and ZnB), diphosphate (ZnC) or triphosphate (ZnD). The antibacterial activity of ZnNPs were tested *in vitro* and then also *in vivo*. *In vitro* antibacterial effect was investigated on three bacterial strains – *E. coli*, *S. aureus* and methicillin-resistant *S. aureus*. Further, zinc nanoparticles were tested on rats, and the effect of ZnNPs on total aerobic bacteria and coliforms in their feces during 30 days of treatment was studied.

MATERIAL AND METHODS

Determination of antibacterial activity *in vitro*

The antimicrobial effect of ZnO and Zn-phosphate nanoparticles were evaluated using three strains of bacteria. Bacterial cultures (*Staphylococcus aureus* NCTC 8511, *Escherichia coli* NCTC 13216, methicillin-resistant *S. aureus* (MRSA) CCM 7110) were cultivated in Müeller-Hinton broth (MHB, Oxoid, Hampshire, UK) overnight at 37 °C and subsequently diluted to a concentration $\sim 1\times10^6$ CFU/ml, where the concentrations are determined by optical density at 600 nm (OD_{600}).

Growth curves: The 100 µl of diluted bacterial suspensions was added into a 96-well microplate and mixed with individual ZnO or Zn-phosphate NPs in ratio 1:1, with total volume 200 µl. The growth of bacteria suspension with Zn NPs, with maximal concentration 5 mM, was detected by Multiskan EX (Thermo Fisher Scientific). The optical density measurements (OD_{620}) were carried out at zero time-point, and then each half-hour for 24 h at 37 °C. An equal volume of sterile water instead of Zn NPs was used as a control, marked as 0 mM.

Spread-plate method: Bacterial cultures diluted at concentration $\sim 1\times10^8$ CFU/ml were further diluted in tenfold steps with MHB. The 900 µl of these bacterial suspensions were mixed with 100 µl of Zn-phosphate NPs or ZnO at concentration 5 mM. These mixtures were incubated for 2 hours at 37 °C. After incubation, 100 µl of inoculum from each sample was applied on MH agar plates by spreading and followed by incubation at 37 °C for 24 h.

Live/dead assay: The individual bacteria were incubated with ZnO and Zn-phosphate NPs and prepared and diluted as in the previous cases, then was the suspensions centrifuged and washed with 0.85% NaCl. The fluorescent dyes SYTO9 (Thermo Fisher Scientific, USA) and Propidium Iodid (PI; Sigma Aldrich, St. Louis, USA) were added into these prepared bacterial solutions. Further, 5 µl of each mixture was observed with an Olympus IX71 inverted fluorescence microscope (Olympus, Tokyo, Japan).

In vivo antibacterial testing

As a model animal for this experiment were selected male rats of the *Wistar albino* strain, which were divided into seven groups. The rats diet contained Zn NPs ZnO and also with commercial zinc nanoparticles ZnO-N, each of them in a dose of 2000 mg Zn/kg diet. Feed and water were available *ad libitum*. One group was served as a control (C) without zinc addition into the diet.

Total aerobic bacteria and coliforms counting: The samples of rat's feces were homogenized and diluted with sterile physiological solution 1:9 w/v. Then, the homogenate was furthermore diluted in tenfold steps. Further, 1 ml of each suspension was placed into empty Petri dishes, and then potting by Plate count agar (PCA) and MacConkey agar (MCA) in duplicate. After 24 h of incubation in 37 °C, total counts from PCA and counts of coliforms from MCA were determined.

RESULTS AND DISCUSSION

In vitro antibacterial activity characterization

First, we treated the bacteria with synthetized ZnNPs and also with ZnO and commercial ZnO-N. A substantial antibacterial activity trend was observed by measuring the optical density at 620 nm during 24 h. From growth curves, which are shown below, the minimal inhibition concentrations (MIC) were found out. The representative measurements with ZnA are shown in Figure 1A. In this case the MIC values ranged from 1.25 mM for *E. coli* and *S. aureus* to 2.5 mM for MRSA. In general, the substantial inhibition effect exhibited the Zn NPs against *S. aureus*. For instance, the 5 mM ZnC, as a maximal

concentration, had no effect on *E. coli* bacterial population. Lower efficacy can be seen on MRSA experiment, where in MRSA phenotype, different SCCmec genotypes confer different resistance characteristics and virulence factors present in this SCCmec cassette (Kaito et al. 2011) or a putative metal resistance gene was also found in various MRSA isolates (Cavaco et al. 2010).

Figure 1 Characterization of antibacterial activity by A) growth curves; B) spread-plate method

A)

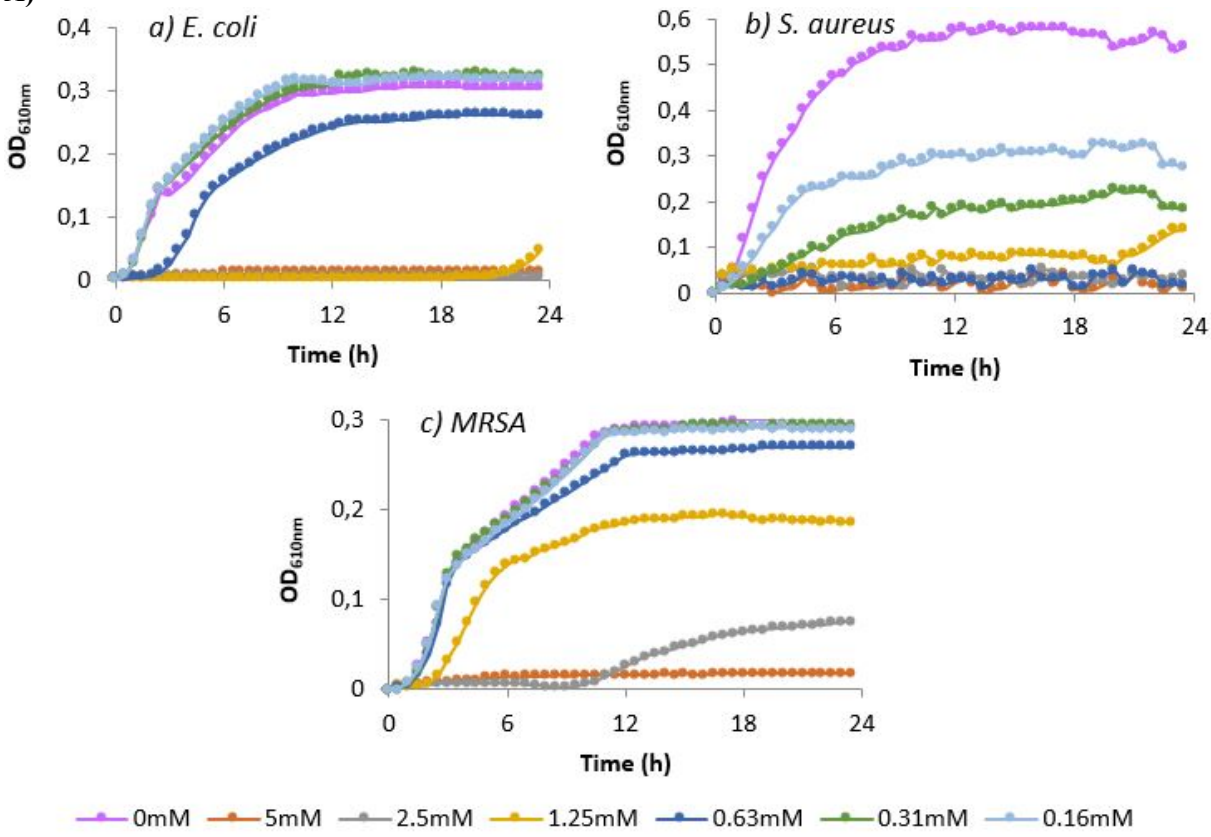

B)

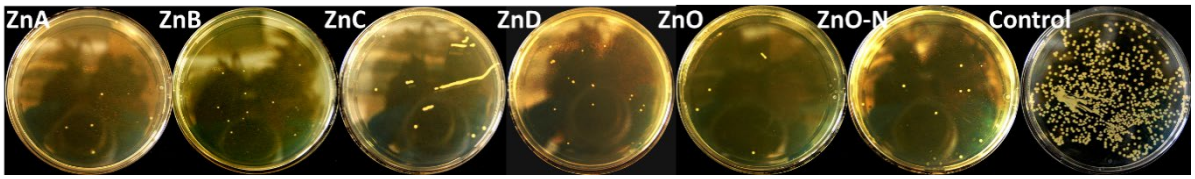

The amount of viable bacteria after treatment with 5 mM Zn was found out by spread-plate technique. In Figure 1B is obvious decrease of *S. aureus* bacterial colonies compared to control. Based on the Table 1, the growth was significantly reduced compared to control. Almost all types of zinc compounds caused above 90% inhibition of bacterial growth, except lower inhibition effect of ZnC (no inhibition) and ZnD against *E. coli*. Another inhibition effects lower than 90% were observed against MRSA with ZnC, ZnO and ZnO-N, these outcomes correspond with growth curves results.

Table 1 Overview of % inhibition effects of Zn NPs and ZnO on using Spread-plate method

	ZnA	ZnB	ZnC	ZnD	ZnO	ZnO-N
E. coli	99.57	100.00	0	71.75	98.54	96.61
S. aureus	98.03	99.31	98.61	99.50	98.49	97.63
MRSA	93.56	92.14	84.81	92.37	87.58	88.02

In order to verify previous results and test the viability of bacterial cells, Live/dead assay was performed. Using this method with a fluorescence microscope we could track the ratio of living cells to

the dead cells, if some populations were present. As examples there are pictures of MRSA after interaction with fluorescence dyes (Figure 2). The micrographs show that despite lower inhibitory effects in previous assays, in this case it can be seen that ZnNPs and ZnO have good inhibition effect, except ZnC and ZnD, although there is no significant reduction of bacterial growth, but the number of dead cells has increased markedly.

Figure 2 Fluorescent micrographs showing live and dead (SYTO9, green) and dead (PI, red) bacterial cells from Live/dead assay; the scale bar – 20μm

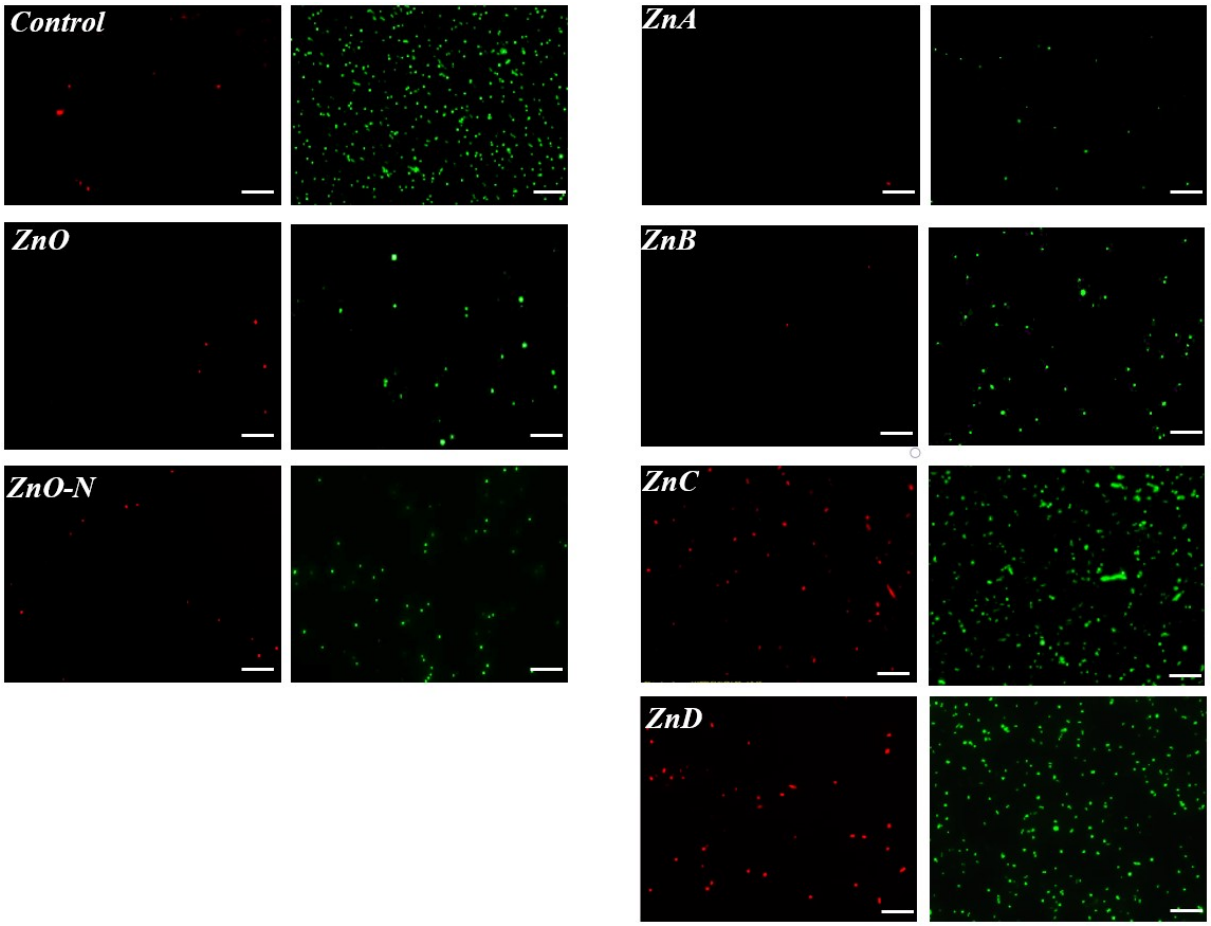

Impact of ZnNPs on rats – counts of bacteria in feces

The synthetized Zn NPs exhibited great antimicrobial properties against bacterial strains *in vitro*. Thus their activity was further tested in whole animal organism. The total number of bacteria and coliforms in rats feces decreased.The rats were treated with ZnNPs and ZnO during 30 days. After first 10 days, there were not significant changes in amount of bacteria against control group, whereas after 30 days there were considerable decrease of bacteria populations. Especially in the case of ZnA and ZnC were significant decrease of coliforms, which are mostly the main cause of digestive problems, immunity and overall performance.

CONCLUSIONS

This work dealt with different types of Zn phosphate-based nanoparticles and their antibacterial effects characterization. In the first part, the *in vitro* antimicrobial activity against bacterial strains using three techniques was investigated. ZnNPs have shown sufficient antimicrobial activity, so we tested them in whole animal organism, rats. They were orally treated by zinc for 30 days, when they had uncontrolled access to feed containing ZnNPs and also ZnO. After this time, we evaluated their effect on bacterial population in rats.

ACKNOWLEDGEMENTS
The study was financially supported by Ministry of Agriculture of the Czech Republic (QK1720349 "Nanoparticles zinc as an alternative to antibiotics in pigs"). Financial support from ERDF "Multidisciplinary research to increase application potential of nanomaterials in agricultural practice" (No. CZ.02.1.01/0.0/0.0/16_025/0007314) is gratefully acknowledged as well.

REFERENCES

Azam, A. et al. 2012. Antimicrobial activity of metal oxide nanoparticles against Gram-positive and Gram-negative bacteria: a comparative study. International Journal of Nanomedicine, 7: 6003–6009.

Cavaco, L.M. et al. 2010. Cloning and Occurrence of czrC, a Gene Conferring Cadmium and Zinc Resistance in Methicillin-Resistant Staphylococcus aureus CC398 Isolates. Antimicrobial Agents and Chemotherapy, 54(9): 3605–3608.

Dickson, R.M., Lyon, L.A. 2000. Unidirectional plasmon propagation in metallic nanowires. Journal of Physical Chemistry B, 104(26): 6095–6098.

Hajipour, M.J. et al. 2012. Antibacterial properties of nanoparticles. Trends in Biotechnology, 30(10): 499–511.

Hongfu, Y.B.Z. 2008. Effects of Nano-ZnO on growth performance and diarrhea rate in weaning piglets. China Feed, 1:08.

Kaito, C. et al. 2011. Transcription and Translation Products of the Cytolysin Gene psm-mec on the Mobile Genetic Element SCCmec Regulate Staphylococcus aureus Virulence. Plos Pathogens, 7(2): e1001267.

Lewis, K., Klibanov, A.M. 2005. Surpassing nature: rational design of sterile-surface materials. Trends in Biotechnology, 23(7): 343–348.

Mishra, A. et al. 2014. Growth performance and serum biochemical parameters as affected by nano zinc supplementation in layer chicks. Indian Journal of Animal Nutrition, 31: 384–388.

Padmavathy, N., Vijayaraghavan, R. 2008. Enhanced bioactivity of ZnO nanoparticles – an antimicrobial study. Science and Technology of Advanced Materials, 9(3): 035004.

Piccinno, F. et al. 2012. Industrial production quantities and uses of ten engineered nanomaterials in Europe and the world. Journal of Nanoparticle Research, 14(9): 1109.

Pláteník, J. 2009. Volné radikály, antioxidanty a stárnutí. Interní Medicína pro praxi, 11(1): 30–33.

Rosi, N.L., Mirkin, C.A. 2005. Nanostructures in biodiagnostics. Chemical Reviews, 105(4): 1547–1562.

Sindhura, K.S. et al. 2014. Synthesis, characterization and evaluation of effect of phytogenic zinc nanoparticles on soil exo-enzymes. Applied Nanoscience, 4(7): 819–827.

Swain, P.S. et al. 2015. Preparation and effects of nano mineral particle feeding in livestock: A review. Veterinary World, 8(7): 888–891.

Zhang, L.L. et al. 2008. ZnO nanofluids - A potential antibacterial agent. Progress in Natural Science-Materials International, 18(8): 939–944.

Fluorescence *in vivo* imaging in the monitoring of effect of nanoparticles on microalgae

Kristyna Pavelicova, Aneta Strejckova, Ivan Rankic, Tereza Vaneckova, Jaroslava Zelnickova, Dalibor Huska, Marketa Vaculovicova
Department of Chemistry and Biochemistry
Mendel University in Brno
Zemedelska 1, 613 00 Brno
CZECH REPUBLIC

xpavelic@node.mendelu.cz

Abstract: In this study, the fluorescence *in vivo* imaging was used to investigate the effect of selected nanoparticles – NPs (ZnO) on microalgae (*Scenedesmus quadricauda* and *Chlorella vulgaris*) growth. The intrinsic fluorescence was affected by application of nanoparticles into the growing medium (liquid and solid) due to a change in growth and metabolic activity of microalgae. Pigments, especially chlorophylls and carotenoids, are responsible for autofluorescence of microorganisms. Therefore, fluorescence can be used as a tool for rapid and easy evaluation of the expression of these compounds. These pigments minimize photooxidative cell damage. Pigments expression can be disturbed by other stress-related substances such as presence of NP that are likely to damage this protective mechanism i) indirectly (by formation of reactive oxygen species) and ii) directly (by disturbing biomembranes). Fluorescence imaging is an efficient and powerful technique, but its application to plants or algae is not very common. By fluorescence imaging and correlation with the total amount of chlorophylls and carotenoids, it was possible to evaluate the effect of NPs on individual microalgae specie by *in vivo* imaging.

Key Words: in vivo imaging, *Chlorella vulgaris*, *Scenedesmus quadricauda*, fluorescence, nanoparticles

INTRODUCTION

Algae are eukaryotic photosynthetic microorganisms with variety of species living in an extensive variety of ecological circumstances. About 50,000 species of algae are present, but only around 30,000 of them have been analysed. Algae are generally divided into macroalgae (algae that can be seen without the help of a microscope) and microalgae (free floating microscopic plants that are identified under microscope and usually measured in micrometers) (Singh and Patidar 2018). In microalgae, pigments with fluorescent activity (in particular, carotenoids and chlorophylls) have an important role in photosynthesis mainly thanks to their antioxidant activity and/or ability to defend against the formation of reactive oxygen species (ROS).

Fat-soluble chlorophylls are pigments with a porphyrin ring responsible for the conversion of solar energy into chemical energy. And carotenoids (β-carotene, lycopene, astaxanthin, zeaxanthin, vialoxanthin and lutein) light absorption in range of visible spectrum, where chlorophyll does not (400–530 nm) (Chen et al. 2018), (D'Alessandro et al. 2016).

During plant growth and development, plants are exposed to a variety of abiotic stresses including drought, freezing, low or high temperature, high and low light intensity, heavy metal toxicity and several others (Mohanta et al. 2017). To understand the mechanism of defence against these influences, it is necessary to investigate the metabolic pathways in plant. This can be accomplished by many methods such as mass spectrometry (Turemis et al. 2018), quantitative polymerase chain reaction (Gao et al. 2018) or liquid chromatography (Cerón-García et al. 2018). However, the use of imaging methods may provide numerous advantages, mainly financial and time-saving benefits. Optical imaging, particularly fluorescence imaging, is widely used in examination of cells (microscopy). The most commonly used imaging techniques include ultrasound, computed tomography and magnetic resonance. (Deborde et al. 2017, Zhao et al. 2018).

Although fluorescence is not very common in plant biology, it has many advantages including cost-effectiveness and variability compared to other methods. Fluorescence *in vivo* imaging has a good potential for a wide range of molecular diagnostic application. These methods are increasingly used for their quantitative sensitivity, natural biological safety and ease of use (Ghoroghchian et al. 2009).

MATERIAL AND METHODS

Preparation of nanoparticle solutions

Solutions of ZnO NPs were prepared by mixing a stock solution of the commercial NPs (Houston, USA) with distilled water at four different concentrations (0 mg/l, 10 mg/l, 50 mg/l a 100 mg/l). Solutions were sonicated for 10 minutes before use.

Preparation of Bold´s Basal Medium (BBM)

Bold´s Basal Medium (BBM) has been prepared according to published method (Demirel et al. 2018). The final solutions were prepared by mixing 2 ml solutions of NPs (0 mg/l, 10 mg/l, 50 mg/l a 100 mg/l). Volumes were adjusted with BBM medium to 150 ml. One of these solutions (0 mg/l) was used as a control. All solutions were autoclaved for 5 minutes and subsequently these media were added to Petri dishes.

SPOT test

At first, the stock solution of microalgae (*Scenedesmus quadricauda and Chlorella vulgaris*) was prepared at absorbance of 0.13 AU. Next, four samples were prepared by serial dilution in ratio 1:1 with BBM without NPs. Individual samples (5 µl) were spotted onto Petri dishes with NPs containing BBM (three spots per sample). In total, 4 Petri dishes containing 12 spots/each (4 microalgae dilutions, in triplicates) were prepared for the each microalgae specie *(Scenedesmus quadricauda and Chlorella vulgaris*).

In vivo fluorescence imaging

Monitoring of influence of nanoparticles on microalgae was performed using an In Vivo Xtreme Imaging System by Bruker (Massachusetts, USA). The parameters used for image acquisition were following: exposition time – 4 s, binning – 4x4 pixels, fStop – 1.1, field of view – 10x10 cm.

Monitoring of influence of nanoparticles on microalgae has been performed using excitation filter of 650 nm and emission filter of 700 nm. Individual samples were measured consecutively for 6 days. For image post processing and analysis Bruker Molecular Imaging Software (Bruker, Massachusetts, USA) was used.

RESULTS AND DISCUSSION

Convential method of toxicity assesment is the use of a spot test with visual semi-quantitative detection, however this approach is no suitable for every microalgae specie and also the quantification is imposible. For this reason, the option of use of fluorescence imaging was investigated in this study.

Figure 1A shows the photograph of common apperance of a spot test (*Chlamydomonas reinhardtii)*; however in Figure 1B is the test for *Chlorella vulgaris*, which cannot be visually evaluated. In such cases, the proposed method is applicable and the fluorescence image can be acquired (Figure 1C).

Figure 1 Spot test of microalgae Chlamydomonas reinhardtii (A) visible by naked eye, Chlorella vulgaris including 100 mg/l NPs (B) invisible to the naked eye and Chlorella vulgaris including 100 mg/l NPs by fluorescence imaging (C)

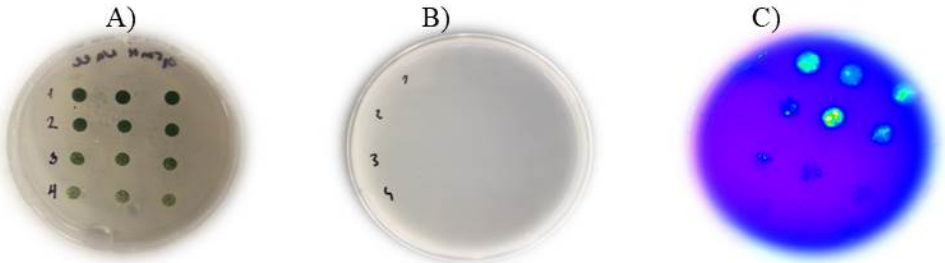

To test the suggsted method, the evaluation of potential effect of nanoparticles on microalgae was carried out by fluorescence imaging.

In this study, the samples of microalgae were monitored for 6 days and a change in fluorescence intensity was observed in pW/mm^2.

Figure 2 Microalgae Chlorella vulgaris including 100 mg/l NPs (bottom) and microalgae without NPs (above). Fluorescence images captured at time intervals as noted.

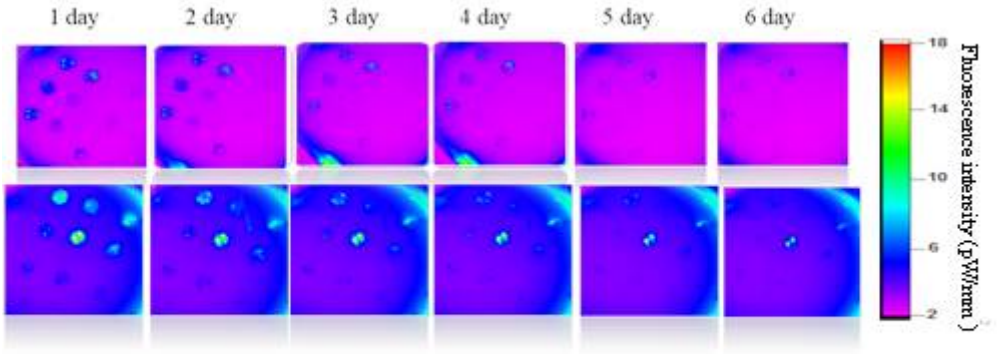

The fluorescence intensity was significantly higher in samples of microalgae exposed to nanoparticles (Figure 2bottom) than microalgae without NPs (Figure 2top). This could be due to the increased content of plant pigments, which could be explained by the effort to overcome the toxicity induced by NPs (Middepogu et al. 2018). But images show that fluorescence intensity was decreasing progressively. Which could be the fact that metal NPs and ions affecting metabolism in the form of excessive increasing levels of reactive oxygen species (ROS) within the microalgae (Moreno-Garrido et al. 2015).

Another advantage of the presented method is the option to obtain quantifiable data and therefore the effect of NPs on different microalgae species was evaluated as shown in Figure 3.

Figure 3 Fluorescence intensities of microalgae exposed to concentrations of NPs (100 mg/l – a, 50 mg/l – b, 10 mg/l – c) in Chlorella vulgaris (A) and Scenedesmus quadricauda (B). The fluorescence of controls was subtracted, spots of same area were integrated and the net fluorescence was plotted.

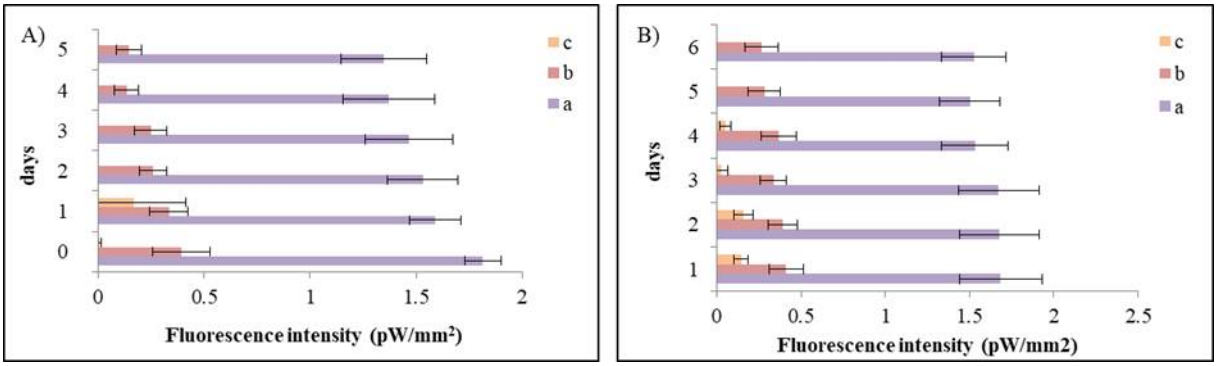

The results show that all concentrations of NPs had a noticeable impact on microalgae, therefore fluorescence intensity decreased in time gradually. The highest fluorescence intensity was detected at the highest concentration of NPs. It should be noted that the fluorescence signal of control, un-treated microalgae was decreasing as well, however the rate of decrease was lower in control experiment compared to the version exposed to the 100 mg/l NPs.

Based on our results, following hypothesis was formed. The highest concentration of nanoparticles (100 mg/l) affects probably the biosynthesis of plant pigments almost instantly.

It is important to note that the literature is not available for such assessment and further investigation is required.

For biological evaluation of the effect of NPs on microalgae, the growth rates were calculated (Figure 4). It can be concluded that in *Chlorella vulgaris* the smallest concentration (10 mg/l) increased the fluorescence intensity but concentrations of 50 mg/l and 100 mg/l reduced it. It may reflect the amount of biomass. The concentration of nanoparticles (10 mg/l) increased the amount of biomass, while concentration of nanoparticles reduced it. In contrary, in *Scenedesmus quadricauda* (Figure 4B), all NP concentrations lead to the same effect.

Figure 4 Growth rate of Chlorella vulgaris (A) and Scenedesmus quadricauda (B).

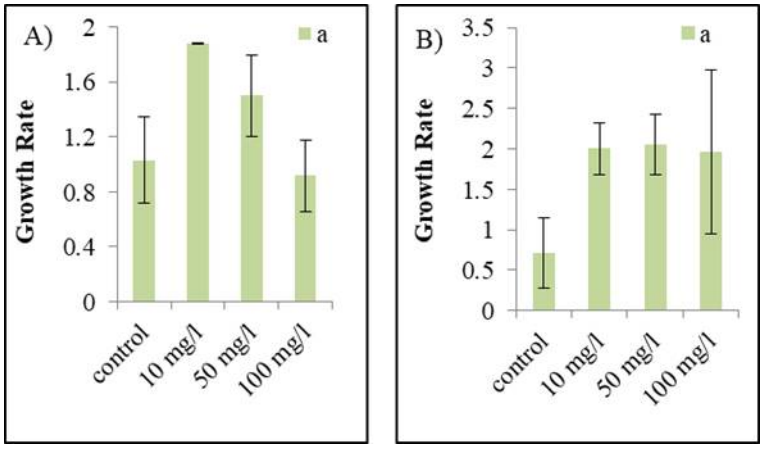

CONCLUSION

Currently, the *in vivo* imaging method is used primarily in animals, whereas in plants their use is not so common. Therefore, in this study, the fluorescence imaging method was suggested and optimized as an efficient tool for evaluation and quantification of common toxicity tests used in microalgae. From the methodological point of view, the proposed method is providing valuable data without causing any damage to the biological samples. The plant samples are exposed to the irradiation for short period of time (seconds) and the light flux as well as the wavelength of the irradiation is not at the toxic levels for the cells.

Microalgae are the first trophic level of the food chain, providing oxygen and biological energy for other organisms and playing very fundamental roles in keeping the balance of aquatic ecosystems. Nanoparticles are inevitably released into the aquatic environment for being widely used (Yu et al. 2018). During this study, the effect of NPs on *Scenedesmus quadricauda* and *Chlorella vulgaris* was studied. The NPs can be a stress factor and promote the emergence of ROS. Mentioned changes in growth of microalgae were observed using modern *in vivo* fluorescence imaging technology.

ACKNOWLEDGEMENTS

The research was financially supported by IGA grant, no. TP_1/2017.

REFERENCES

Cerón-García, M.C. et al. 2018. Maximizing carotenoid extraction from microalgae used as food additives and determined by liquid chromatography (HPLC). Food Chemistry, 257: 316–324.

Chen, C. et al. 2018. Effects of carotenoids on the absorption and fluorescence spectral properties and fluorescence quenching of Chlorophyll a. Spectrochimica Acta Part A: Molecular and Biomolecular Spectroscopy, 204: 440–445.

D'alessandro, E.B. et al. 2016. Concepts and studies on lipid and pigments of microalgae: A review. Renewable and Sustainable Energy Reviews, 58: 832–841.

Deborde, C. et al. 2017. Plant metabolism as studied by NMR spectroscopy. Progress in Nuclear Magnetic Resonance Spectroscopy, 102(103): 61–97.

Demirel, Z. et al. 2018. Influence of Media and Temperature on the Growth and the Biological Activities of Desmodesmus protuberans (FE Fritsch & MF Rich) E. Hegewald. Turkish Journal of Fisheries and Aquatic Sciences, 18(10): 1195–1203.

Gao, D. et al. 2018. Transcriptome-wide identification of optimal reference genes for expression analysis of Pyropia yezoensis responses to abiotic stress. Bmc Genomics, 19.

Ghoroghchian, P.P. et al. 2009. In vivo fluorescence imaging: a personal perspective. WIREs Nanomedicine and Nanobiotechnology, 1: 156–167.

Middepogu, A. et al. 2018. Effect and mechanism of TiO_2 nanoparticles on the photosynthesis of Chlorella pyrenoidosa. Ecotoxicology and Environmental Safety, 161: 497–506.

Mohanta, T.K. et al. 2017. Systems biology approach in plant abiotic stresses. Plant Physiology and Biochemistry, 121: 58–73.

Moreno-Garrido, I. et al. 2015. Toxicity of silver and gold nanoparticles on marine microalgae. Marine Environmental Research, 111: 60–73.

Singh, G., Patidar, S.K. 2018. Microalgae harvesting techniques: A review. Journal of Environmental Management, 217: 499–508.

Turemis, M. et al. 2018. Optical biosensor based on the microalga-paramecium symbiosis for improved marine monitoring. Sensors and Actuators B-Chemical, 270: 424–432.

Yu, Z. et al. 2018. Effects of TiO_2, SiO_2, Ag and CdTe/CdS quantum dots nanoparticles on toxicity of cadmium towards Chlamydomonas reinhardtii. Ecotoxicology and Environmental Safety, 156: 75–86.

Zhao, J. et al. 2018. Recent developments in multimodality fluorescence imaging probes. Acta Pharmaceutica Sinica B, 8(3): 320–338.

Evaluation of cytotoxicity of biphasic TiO_2 nanoparticles with organic surface coatings

Zuzana Skubalova[1], Hana Buchtelova[1], Vladislav Strmiska[1,2], Simona Dostalova[1,2], Petr Michalek[1,2], Sona Krizkova[1,2], Vojtech Adam[1,2], Zbynek Heger[1,2]
[1]Department of Chemistry and Biochemistry
Mendel university in Brno
Zemedelska 1, 613 00 Brno
[2]Central European Institute of Technology
Brno University of Technology
Technicka 3058/10, 615 00 Brno
CZECH REUBLIC

xskubal1@mendelu.cz

Abstract: Titanium dioxide nanoparticles (TiO_2 NPs) are used in lots of human applications because of their extraordinary nano scaled properties. Particularly, due to their photoprotective properties, they are used in topical dermatologic preparation and also as white pigment. Due to these properties their use in human life is more and more frequent. Despite the fact that nano dimension brings various beneficial properties, it could bring also bad features. Therefore, in this study, we evaluated a cytotoxicity of two types of biphasic TiO_2 NPs using distinct cells of epithelial origin. We found that TiO_2 NPs can induce cytotoxic stress resulting in fragmentation of DNA.

Key Words: nanotoxicology, TiO_2 nanoparticles, *in vitro* tests

INTRODUCTION

Nanotechnologies are developing very rapidly, and the production of different types of nanomaterials promises a wide range of uses, mainly thanks to the new acquired properties (Grumezescu 2016). But the living biological systems are more easily transduced due to nano dimension material, so the physiological effects of penetrated nanoparticles could have a greater impact on the whole organism (Hamblin et al. 2016).

TiO_2 nanoparticles (NPs) have been widely used in industry since 1990. One of the extensive branches of application is cosmetics industry (Johnson et al. 2011). TiO_2 NPs have photoprotective properties, they reflect and scatter UV radiation, but no visible light, thus they act as effective UV filters (Hamblin et al. 2016). TiO_2 NPs can exist in three crystalline forms: anatase, rutile and brookite (Horie et al. 2016). In our study we used two types of biphasic TiO_2 NPs containing brookite and anatase crystalline forms. The TiO_2 NPs were surface–capped with dichloroacetic acid (DCAA) and monochloracetic acid (MCAA) to increase their stability and enhance their photocatalytic activity. Overall, the study shows that upon administration to epithelial cells, both types of TiO_2 NPs can induce cytoxicity through DNA fragmentation.

MATERIALS AND METHODS

Cell cultures

The human prostatic cell lines used in this study were: i) the PNT1A established by immortalization of normal adult prostatic epithelial cells by transfection with a plasmid containing SV40 genome with a defective replication origin; ii) the A375 human melanoma cell line, originally established from a lymph node metastasis of a melanoma patient; and iii) SH–SY5Y human cell line established from a bone marrow metastasis of a 4–y–old female neuroblastoma patient. All cell lines were purchased from Health Protection Agency Culture Collections (Salisbury, UK). Cells were cultured in a RPMI–1640 medium with 10% FBS. Media were supplemented with penicillin (100 U/mL) and streptomycin (0.1 mg/mL), and the cells were maintained at 37 °C in a humidified incubator

(Eppendorf, Hamburg, Germany) with 5% CO_2. The treatment with sarcosine was initiated after cells reached 60–80% confluence.

Synthesis and characterization of TiO_2 NPs

TiO_2 NPs were prepared by using reductive colloidal synthesis and using the sintering at extreme conditions. TiO_2 NPs was capped by dichloroacetic acid (DCAA) and monochloroaceitc acid (MCAA). The morphology of NPs was investigated using transmission electron microscope (TEM) Tecnai F20 (FEI, Eindhoven, Netherlands). The crystallinity of TiO_2 NPs was examined by X–ray diffraction (XRD, Smart Lab diffractometer Rigaku, Rigaku, Tokyo, Japan) using the Cu lamp and the Bragg–Brentano geometry.

Investigation of internalization of TiO_2 NPs

TiO_2 NPs labeling was performed using recombinantly produced TdTomato that was cloned into BamHI and XhoI sites of pRSET–B plasmid (Thermo Fisher, Waltham, MA, USA) in frame with 6xHis, T7 and Xpress tag. The integrity of open reading frame confirmed with Sanger sequencing. The TdTomato was produced in BL21(DE3)pLysS *E. coli* and isolated and precipitated in ammonium sulphate. For labeling, 0.1 µL of TdTomato was mixed with 10 µL of TiO_2 NPs. Unbound TdTomato was removed by repeated centrifugation (10 000×g, 5 min). Internalization was investigated using EVOS FL Auto Cell Imaging System (Thermo Fisher) upon 3 h incubation of NPs with cells and washing with phosphate buffered saline (PBS, pH 7.4).

Screening of effect of biphasic TiO_2 NPs on cellular viability

Screening of cytotoxicity (MTT verified by trypan blue exclusion) was performed to identify antiproliferative and cytotoxic effects of TiO_2 NPs. Treatments were carried out for 24, 48 and 72 h. Then, 10 µL of MTT [5 mg/mL in phosphate buffered saline (PBS)] was added to the cells and the mixture was incubated for 4 h at 37 °C. After that, MTT–containing medium was replaced by 100 µL of 99.9% dimethyl sulfoxide (DMSO) and after 5 min incubation the absorbance of the samples was determined at 570 nm using Infinite 200 PRO (Tecan, Männedorf, Switzerland).

Single–cell gel electrophoresis for analysis of DNA fragmentation

The cells were plated at a density of 106 cells/well in six–well dishes and treated with TiO_2 NPs (100 µg/mL) for 24 h. As positive control, 150 µM H_2O_2 was employed. After harvesting, about 15 µL of the cell suspension was mixed with 75 µL of 0.5% low melting point agarose (CLP, San Diego, CA, USA) and layered on one end of a frosted plain glass slide. Then, it was covered with a layer of the low melting agarose (100 µL). After solidification of the gel, the slides were immersed in a lysing solution (2.5 M NaCl, 100 mM Na_2EDTA, 10 mM Tris, pH 10) containing 1% Triton X–100 and 10% DMSO), with an overnight incubation at 4 °C. A cold alkaline electrophoresis buffer was poured into the chamber and incubated for 20 min at 4 °C. The electrophoresis was carried at 4 °C, (1.25 V/cm, 300 mA) for 30 min. The slides were neutralized (0.4 M Tris, pH 7.5) and then stained with ethidium bromide (2 µg/mL). The cells were analysed under fluorescence microscope EVOS FL Auto Cell Imaging System (Thermo Fisher Scientific) and classified according to the shape of the fluorescence of the comet tail [0 (no visible tail) to 4 (significant DNA in tail)].

Descriptive statistics and applied bioinformatic tools

For the statistical evaluation of the results, the median was taken as the measurement of the main tendency, while the standard deviation was taken as the dispersion measurement. Differences between groups were analysed using a paired t–test. For analyses, Software Statistica 12 (StatSoft, Tulsa, OK, USA) was employed.

RESULTS AND DISCUSSION

Both types of synthesized TiO_2 NPs had oval–to–spherical morphology with diameter ranging between 15–20 nm (Figure 1A). Moreover, XRD analyses confirmed that both types of TiO_2 NPs had a biphasic crystallinity with anatase prevailing for DCAA–capped NPs and with an equal distribution of brookite and anatase for MCAA–capped NPs (Figure 1B). Overall, these analyses validated the suitability of TiO_2 NPs for further cellular testing of their potential cytotoxic effects.

Figure 1 (A) TEM micrographs of synthesized TiO_2 NPs, scale bar, 50 nm. (B) Distribution patters of anatase and brookite in prepared NPs

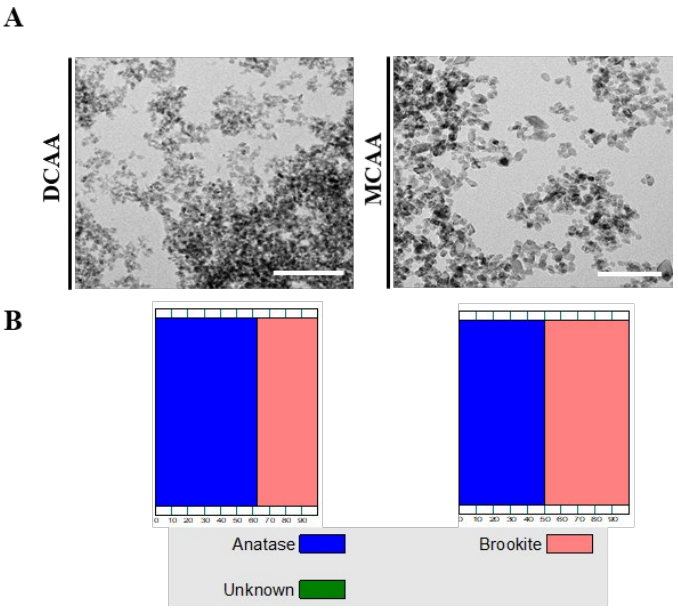

We further studied the effect of TiO_2 NPs on viability of three distinct cell lines of epithelial origin. Figure 2 depicts that within the tested cell lines, NPs exhibited significantly different IC_{50} values. The highest toxicity was found for neuroblastoma–derived cells SH–SY5Y, while the A375 cells (melanoma) were relatively tolerant to NPs presence. Overall, anatase–prevailing NPs DCAA were more toxic that MCAA NPs.

Figure 2 IC_{50} values obtained from MTT assay and trypan blue exclusion upon 24, 48 and 72 h incubation.

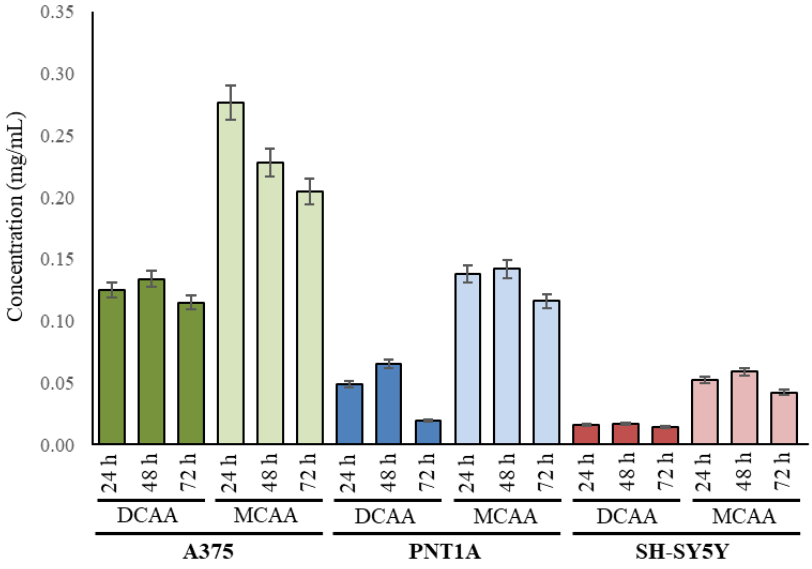

As it was shown in next experiment, both types of TiO_2 NPs were able to be cross the cellular membranes and internalize within intracellular space (Figure 3). Internalization is among the most important prerequisites for inducing further cytotoxic actions by dissolving the NPs in organelles or binding the intracellular metabolites or proteins for further use in signaling.

Figure 3 Fluorescence micrographs of TdTomato–labeled TiO_2 NPs.

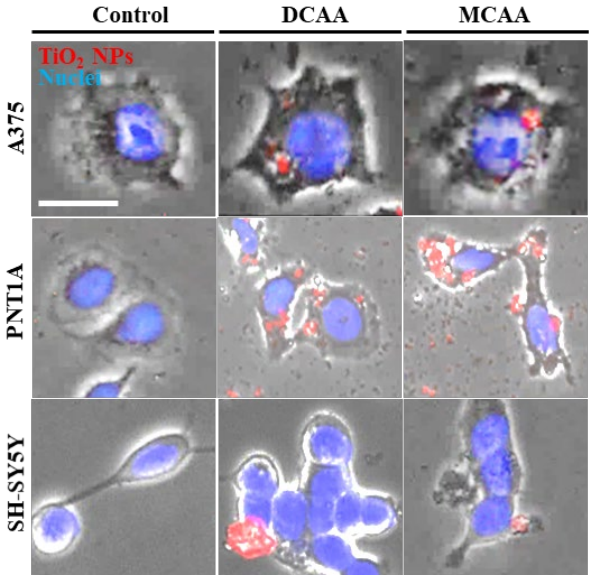

To elucidate a mechanism responsible for TiO_2 NPs cytotoxicity, we focused on analysing the DNA fragmentation in A375 cells. Figure 3 demonstrates that both types of NPs were able some extent induce the DNA fragmentation. The highest portion of uncoiled DNA was found for DCAA TiO_2 NPs, which is in line with their cytotoxicity and prevalence of anatase crystallinity.

Figure 3 Comet assay demonstrating the uncoiling of DNA in A375 cells due to the exposure to TiO_2 NPs. Scale bar, 30 µm. Bar graph shows quantitation of comet grades.

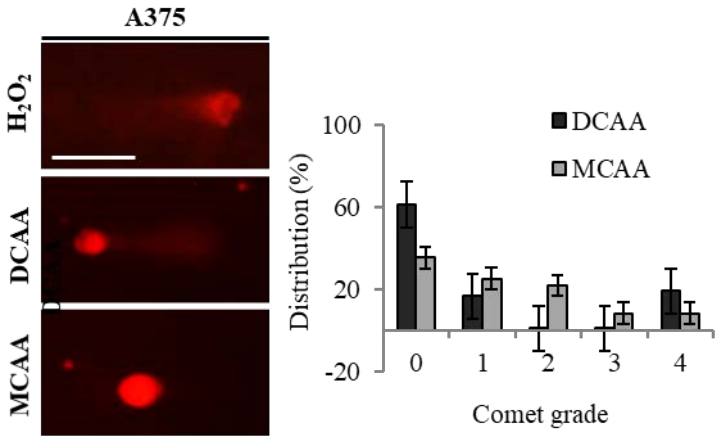

CONCLUSION

We successfully prepared two types of biphasic TiO_2 NPs. Using several approaches, we identified that despite both types of NPs are able to internalize to intracellular space, DCAA NPs with a prevailing anatase in their crystallinity planes exhibit higher cytotoxicity to all three types of tested epithelial cell lines. The results demonstrate that despite Ti–based nanomaterials are commonly used in dermatology and industry, during long–term exposures, they can possess a significant health risk. Future studies on a molecular mechanism of cytotoxicity are on the way.

ACKNOWLEDGEMENTS

The research was financially supported by grant no. AF–IGA–IP–2018/016.

REFERENCES

Grumezescu, A.M. 2016. Nanobiomaterials in Galenic formulations and cosmetics. Applications of Nanobiomaterials. 1st ed., Oxford UK: Elsevier.

Hamblin, M.R. et al. 2016. Nanoscience in Dermatology. 1st ed., London UK: Academic press.

Horie, M. et al. 2016. Does photocatalytic activity of TiO_2 nanoparticles correspond to photo–cytotoxicity? Cellular uptake of TiO_2 nanoparticles is important in their photo–cytotoxicity. Toxicology Mechanisms and Methods, 26(4): 284–294.

Johnson, A.C. et al. 2011. An assessment of the fate, behaviour and environmental risk associated with sunscreen TiO_2 nanoparticles in UK field scenarios. Science of the Total Environment, 409(13): 2503–2510.

Modification of electrothermal atomic absorption spectrometry for determination of arsenic in high salinity samples

Vendula Smolikova[1,2], Pavlina Pelcova[1], Josef Hedbavny[1], Lucie Zlamalova[1], Andrea Ridoskova[1,2]
[1]Department of Chemistry and Biochemistry
Mendel University in Brno
Zemedelska 1, 613 00 Brno
[2]Central European Institute of Technology
Brno University of Technology
Purkynova 123, 612 00 Brno
CZECH REPUBLIC

xsmoliko@mendelu.cz

Abstract: The electrothermal atomic absorption spectrometry (ET-AAS) method was optimized for determination of the arsenic content in high salinity samples. The combination of palladium (1 g/l) modifier, graphite furnace temperature program and graphite tube modified with tungsten carbide significantly reduced the matrix interference in the sample with NaCl concentration of 10 g/l. Optimized temperature program ensured the reduction of the background absorbance about 95–100%. The modification of graphite furnace surface by tungsten carbides ensured the shift of background absorbance prior to the absorbance of the analyte and considerable extension lifetime of graphite tubes.

Key Words: arsenic, palladium modifier, tungsten carbide, ET-AAS, background correction

INTRODUCTION

Arsenic with mutagenic and carcinogenic effects on humans belongs among the highly toxic substances in the environment. Inorganic arsenic forms, such as arsenate (As^{V}) and arsenite (As^{III}), have higher toxicities than organic arsenic species. Human populations worldwide are primarily exposed to inorganic arsenic through the consumption of contaminated water (Cubadda et al. 2017). Determination of total arsenic content in aqueous samples is usually performed by electrothermal atomic absorption spectrometry. Arsenic determination by ET-AAS may be complicated by losses of the analyte during the pyrolysis stage and interferences caused by matrix (e.g., sea water, mineralized water) (Bermejo-Barrera et al. 1996, Bozsai et al. 1990, Welz et al. 1988).

The most, palladium nitrate or palladium-magnesium nitrate modifiers are used for determination of arsenic content in high salinity samples (Bermejo-Barrera et al. 1996, Welz et al. 1988). This modifiers cause stabilization of volatile analytes, including arsenic, to higher pyrolysis temperatures, and ensure the separation of the arsenic from the matrix during the pyrolysis phase without the loss of analyte. Reducing the background absorption can also be achieved by inserting a pre-atomization cool-down step into the graphite furnace temperature program (Bozsai et al. 1990, Cabon 2000, Pszonicki and Dudek 1999) or surface-modified graphite tubes (Kulik et al. 2009, Volynsky 1998).

The aim of this study was to optimize the ET-AAS method for arsenic determination in high salinity samples. The combination of palladium modifier, graphite furnace temperature program and graphite tube modified with tungsten carbide was tested and optimized for sensitive and precise arsenic determination.

MATERIAL AND METHODS

Instrumentation

Measurements were performed using graphite furnace atomic absorption spectrometer 280Z AA (Agilent Technologies, Santa Clara, CA, USA) with Zeeman background correction. Determination of arsenic was carried out under the conditions recommended by the manufacturer for As (193.7 nm) with

a spectral bandwidth of 0.5 nm. Ultrasensitive hollow cathode lamp (Agilent Technologies, Santa Clara, CA, USA) was used as the radiation source of As (lamp current 10 mA). The ultrasonic bath Elmasonic P (Elma, Singen, Germany) was used for graphite furnace surface-modification.

Reagents

All solutions were prepared from analytical grade chemicals. Arsenic (III) standard solution with the concentration of 1000 ± 4 mg/l (Fluka, Czech Republic) was used for the preparation of calibration solutions (calibration range 0–100 µg/l). Palladium 10 g/l (Fluka, Czech Republic) was used for the preparation of 1% (v/v) Pd modifier and $Na_2WO_4 \cdot 2H_2O$ (Lachema, Czech Republic) was used for graphite furnace surface-modification. The 65% HNO_3 (Penta, Czech Republic) purified by sub-boiling distillation apparatus (Type BSB-939IR, Berghof, Eningen, Germany) and demineralized water produced by Millipore Milli Q system (Millipore, Bedford, MA, USA) were used for sample dilution.

Graphite furnace surface-modification

Pyrolytic graphite tubes were impregnated with aqueous solution Na_2WO_4 (50 g/l). Tubes were placed in the solution and soaked for 3 minutes in the ultrasonic bath under atmospheric pressure. Tubes were then carefully wiped and heated twice in the atomizer according to the graphite furnace temperature program (Table 2). The operation was repeated three times (Figure 1). Every day before the measurement starts, 10 µl of sodium tungsten solution (50 g/l) were dispensed onto the inner surface of the furnace and heated according to the graphite furnace temperature program (Table 2).

Figure 1 Scheme of graphite furnace surface-modification

Procedure

The standard arsenic solution (50 µg/l) in solution NaCl (10 g/l) was used for method optimization. The samples were acidified with 3% (v/v) HNO_3 before analysis. The palladium modifier (injection volume 10 µl) was pre-injected into graphite furnace before the sample injection (sampling volume 20 µl).

RESULTS AND DISCUSSION

Graphite furnace program optimization

Firstly, arsenic content in the sample with high concentration of NaCl (10 g/l) was measured under the graphite furnace temperature program recommended by the manufacturer of ET-AAS (Table 1). The palladium (1% v/v) was used as the modifier.

Table 1 Graphite furnace temperature program recommended by the manufacturer of ET-AAS

Step	1	2	3	4	5	6	7
Temperature, *°C*	85	95	120	1400	1400	2600	2800
Ramp time, *sec*	5	40	10	5		0.6	2
Hold time, *sec*				1	2	2	
Read						ON	
Argon flow, *l/min*	0.3	0.3	0.3	0.3	0	0	0.3

Legend: 1,2,3 – drying steps; 4,5 – pyrolysis steps; 6 – atomization step; 7 – cleaning step

High concentration of sodium chloride in the sample matrix generated high background absorbance which deformed the absorbance of analyte (Figure 2). When the temperature program recommended by the manufacturer was used for arsenic determination, the method recovery of arsenic in the sample with high salinity was only 50–70% with RSD = 17.8%. The limit of detection for As in solution NaCl (10 g/l) was 12.2 µg/l (sample volume 20 µl, 10 replicates).

Figure 2 The absorption signal of arsenic at temperature program stated in Table 1

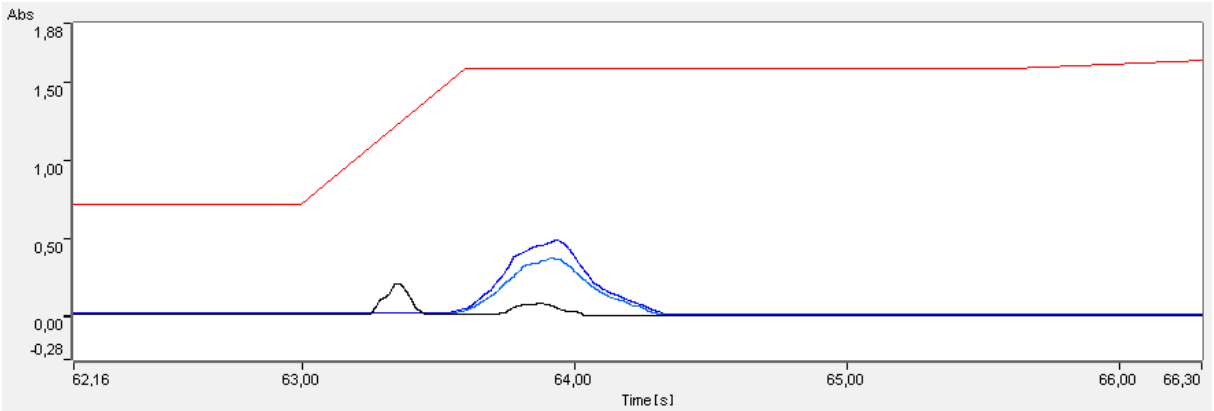

Legend: Red line – temperature program; blue line – analyte absorbance; black line – background absorbance

To reduce the background absorption a cool-down step before atomization was incorporated into the graphite furnace temperature program (Table 2). Longer duration of drying step prevented boiling of the sample in the graphite tube.

Table 2 Graphite furnace temperature program with pre-atomization cool-down step

Step	1	2	3	4	5	6	7
Temperature, *°C*	90	150	300	1300	130	2300	2650
Ramp time, *sec*	9	30	25	10	15	1	5
Hold time, *sec*		20		30	1	3	
Read						ON	
Argon flow, *l/min*	0.3	0.3	0.3	0.3	0.3	0	0.3

Legend: 1,2,3 – drying steps; 4 – pyrolysis step; 5 – cool-down step; 6 – atomization step; 7 – cleaning step

A cool-down step between the steps of pyrolysis and atomization ensured that the sample matrix effect was reduced, and the background absorption was lower about 95–100% (Figure 3). The RSD was decreased to less than 1%. The method recovery of arsenic with temperature program using cool-down step was 98–100%. Limit of detection for As in solution NaCl (10 g/l) was decreased to 1.1 µg/l (sample volume 20 µl, 10 replicates).

Figure 3 The absorption signal of arsenic at temperature program stated in Table 2 (with pre-atomization cool-down step)

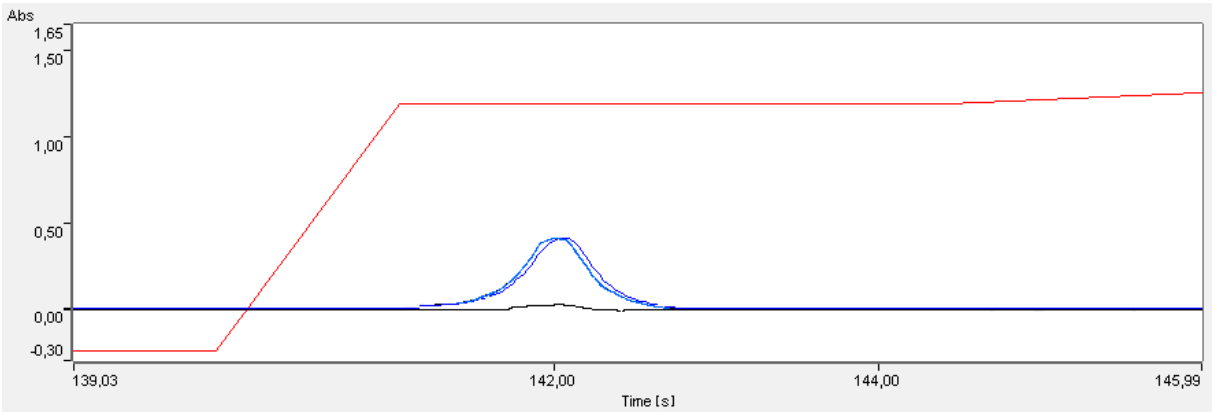

Legend: Red line – temperature program; blue line – analyte absorbance; black line – background absorbance

Bozsai et al. (1990) achieved similar results using palladium-magnesium nitrate modifier, pyrolysis temperature 1300 °C and the temperature drop after the pyrolysis step. It is assumed that high background absorbance is caused by Rayleigh scattering by larger salt particles in the cooler regions at the tube ends. When the pre-atomization cool-down step is incorporated into the graphite furnace temperature program, the tube is heated more uniformly and the effect of the cool tube ends is avoided almost completely (Bozsai et al. 1990).

Moreover, standard addition calibration method instead of matrix-free calibration was used to reduction matrix interferences. This step improved the performance of the methodology and made it independent of the knowledge of the NaCl concentration in the sample.

Graphite furnace surface-modification

Although we have achieved very good results of arsenic recovery through temperature program improvement, the lifetime of the graphite tube was reduced due to the aggressive composition of the sample matrix. The surface of the graphite tube was significantly damaged after about 50 firing cycles. For this reason, we have combined the cool-down step temperature program with the modification of graphite furnace surface by tungsten carbides.

Figure 4 The absorption signal of arsenic at temperature program stated in Table 2 (pre-atomization cool-down step) and at the modification of graphite furnace surface by tungsten carbides

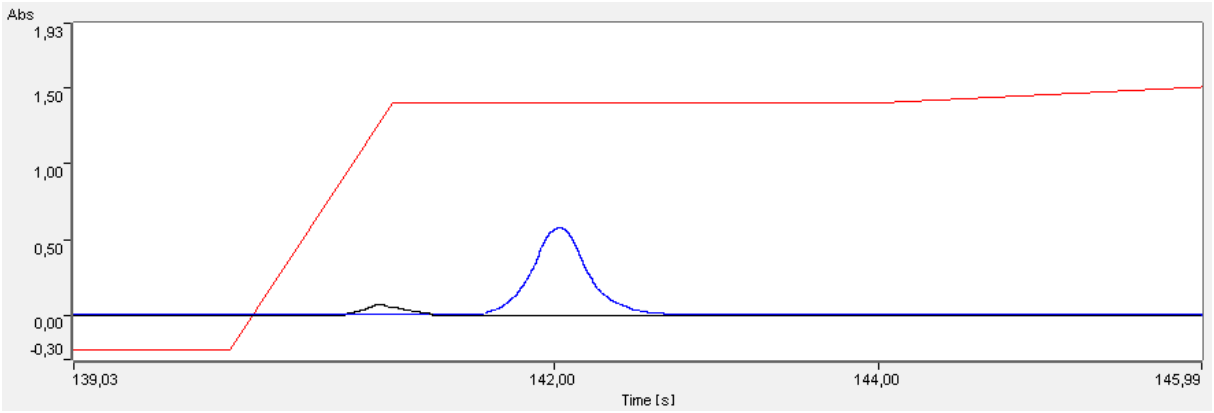

Legend: Red line – temperature program; blue line – analyte absorbance; black line – background absorbance

The modification of graphite furnace surface by tungsten carbides led to the shift of the total background absorbance prior to the actual absorbance of the analyte. This prevents the distortion of the analyte absorbance (Figure 4). The lifetime of the graphite tube was significantly increased to 250 firing cycles.

CONCLUSION

The sensitive and precise method has been proposed and optimized for arsenic determination in samples containing high concentrations of chlorides. The interference effect of the sample matrix was reduced by the combination of palladium (1 g/l) modifier, graphite furnace temperature program with the cool-down pre-atomization step and graphite tube modified with tungsten carbides. The background absorbance was reduced about 95–100%. The new methodology allowed the determination of arsenic in solution NaCl (10 g/l) with the recovery of 98–100%. Limit of detection was decreased 11.3 times. Moreover, the lifetime of the graphite tube was increased five times.

ACKNOWLEDGEMENTS

This research was carried out with the support of the Ministry of Education, Youth and Sports of the Czech Republic under the project CEITEC 2020 (LQ1601). The research has been supported by grant no. AF-IGA-2018-tym005.

REFERENCES

Bermejo-Barrera, P. et al. 1996. Comparison of different chemical modifiers for the direct determination of arsenic in sea water by electrothermal atomic absorption spectrometry. Fresenius Journal of Analytical Chemistry, 355: 174–179.

Bozsai, G. et al. 1990. Determination of arsenic, cadmium, lead and selenium in highly mineralized waters by graphite-furnace atomic-absorption spectrometry. Talanta, 37(6): 554–553.

Cabon, J.Y. 2000. Effects of various salts on the determination of arsenic by graphite furnace atomic absorption spectrometry. Direct determination in seawater. Fresenius Journal of Analytical Chemistry, 367: 714–721.

Cubadda, F. et al. 2017. Human exposure to dietary inorganic arsenic and other arsenic species: State of knowledge, gaps and uncertainties. Science of the Total Environment, 579: 1228–1239.

Kulik, A.N. et al. 2009. Tungsten-assisted modification of graphite furnaces for an atomic absorption spectrometer. Journal of Applied Spectroscopy, 76(4): 564–569.

Pszonicki, L., Dudek, J. 1999. Modifier effects in the determination of arsenic, antimony and bismuth by electrothermal atomic absorption spectrometry. Journal of Analytical Atomic Spectrometry, 14: 1755–1760.

Volynsky, A.B. 1998. Graphite atomizers modified with high-melting carbides for electrothermal atomic absorption spectrometry. II. Practical aspects. Spectrochimica Acta Part B: Atomic Spectroscopy, 53(12): 1607–1644.

Welz, B. et al. 1988. Palladium nitrate – magnesium nitrate modifier for graphite furnace atomic absorption spectrometry. Part 2. Determination of arsenic, cadmium, copper, manganese, lead, antimony, selenium and thallium in water. Journal of Analytical Atomic Spectrometry, 3: 695–701.

Investigating the interplay between sarcosine and Ca^{2+}-dependent signaling in prostate cells

Vladislav Strmiska[1,2], Hana Buchtelova[1], Petr Michalek[1,2], Sona Krizkova[1,2], Vojtech Adam[1,2], Zbynek Heger[1,2]
[1]Department of Chemistry and Biochemistry
Mendel University in Brno
Zemedelska 1, 613 00 Brno
[2]Central European Institute of Technology
University of Technology in Brno
Technicka 3058/10, 615 00 Brno
CZECH REPUBLIC

vladislav.strmiska@mendelu.cz

Abstract: It has been shown that sarcosine supplementation stimulates proliferation and invassivenes of prostate cells. Nevertheless, the exact molecular mechanism responsible for this phenomenon is not known. In the present study we demonstrate that sarcosine increases expression of calmodulin (CaM), an important intracellular signaling molecule. Through this, sarcosine activates calmodulin-dependent protein kinases signaling. Pathway of activation CaM-dependent protein kinases can activate regulation of mitosis, proliferation, cell death, gene transcription and phosphorylation/ dephosphorlation of proteins. This is done through CaM binding of four Ca^{2+} ions. Interestingly, in this study, we identified decrese in free Ca^{2+} correlating with sarcosine-induced up-regulation of CaM. The influence of CaM to cell cycle changes was further verified using post transcritrional gene silencing using CaM-siRNA complex. Co-treatment of prostate cells with CaM-siRNA and sarcosine showed decrease in CaM-dependent kinases and cell invasiveness compared to sarcosine treatment only.

Key Words: sarcosine, calmodulin, prostate, prostate cancer, human cells

INTRODUCTION

Sarcosine is an imino acid and a potential biomarker of prostate cancer (PCa). Concentration of sarcosine is substantially increased during PCa progression to its metastasis (Sreekumar et al. 2009).

Calmodulin (CaM) is a ubiquitous calcium-binding protein (Zayzafoon 2006). It is responsible for intracellular interactions connected with regulation of proliferation and malignity (Rasmussen and Means 1989). CaM acts primarily through CaM-dependent signalling pathways connected into regulatory system important for cellular pathophysiology (Zayzafoon 2006). CaM-dependent protein kinases are activated after presence of CaM in neighbouring subunits activated by Ca^{2+} ions (Rokhlin et al. 2007). If CaM is accumulated in sufficient amount, autophosphorylation occurs, leading to persistent activation of the enzyme (Wang et al. 2015). The major mediator system affecting cellular proliferation driven by Ca^{2+}/CaM is CaM-dependent protein kinase II (CaMKII). CaMKII phosphorylate over 40 different proteins, including enzymes, kinases and transcription factors (Erickson 2014).

Our results demonstrate a unique connection between sarcosine and CaM-dependent signaling through up-regulation of CaM-dependent kinases. We also show that sarcosine affects Ca^{2+} homeostasis. Moreover, functional siRNA analyses revealed an importance of CaM-sarcosine interplay in proliferation and clonogenicity of prostate cells.

MATERIAL AND METHODS

Prostatic cell lines

Three human prostatic cell lines were used for an experiment, representing benign and malignant cells: *i*) the PNT1A human cell line established by immortalization of normal adult prostatic

epithelial cells by transfection with a plasmid containing SV40 genome with a defective replication origin *ii*) LNCaP human cell line estabished from an androgen-sensitive metastasis located in the left supralavicular lymph node, *iii*) PC3 human prostate adenocarcionoma cell line established from a grade 4 prostatic adenocarcinoma. All cell lines used for experiments were purchased from Health Protection Agency Culture Collections (Salisbury, UK).

Culture conditions and treatment protocols

All cell lines were culture in RPMI-1640 medium with 10% fetal bovine serum and supplemented by penicillin (100 U/mL) and streptomycin (0.1 mg/mL). The cells were maintained at 37 °C in humidified incubator with 5% CO_2. The exogenous supplementation with sarcosine (10 μM) and siRNA (200 pM) was initiated after cells reached ~80% confluence. The cells were harvested after 24; 48 and 72 h for western blotting, after 24 h for immunofluorescence and FURA-2. All experiments were designed as five biological replicates (n = 5) measured three times at each time point.

2D-DIGE proteome alanysis

Total cellular protein were isolated form cells stimulated by sarcosine (10 μM) after 24 h and un-treated group as a control. Compared group of proteins were labeled with fluorescen dyes directly and each 50 μg of proteins were separate by isoelectric point (IPG: 7 cm, pH 3 to 10). After that for second dimension were used 12.5% SDS-PAGE. Evaluated were different spots of protein expression between sarcosine stimulated and un-stimulated group of cells by Azure c600imager (Azure Biosystems, Dublin, CA, USA).

Imunocytometry (ICC) of CaM

For ICC, the cells were seded into eight-well chamber slides and after 24 h of adherence were treated by sarcosine (10 μM). As a control were used cells without treating. Cells were fixated after 24 h incubation by 4% formaldehyde, permeabilizated by 0.25% Triton X-100, blocked in 5% bovine serum albumin in phosphate buffered saline (PBS) and imunostained with primary antibody overnight in 4 °C. Detection was accomplished using CruzFluor™ 645 (CFL 645) labeled secondary antibody. DNA staining by Hoechst were used for counter. ICC was evaulated by confocal laser scanning microscope (CLSM) Carl Zeiss LSM 880 (Carl Zeiss, Jena, Germany).

Western blot of CaM and CaM-dependent kinases

Total cellular proteins were extracted with 100 μL of thiourea (2 M) buffer containing protease inhibitor cocktail. After electrophoresis, the proteins were electrotransferred onto a polyvinylidene fluoride membrane, with the rest of membrane surface blocked in 5% (w/v) bovine serum albumin in PBS for 1 h at 37 °C to avert non-specific binding. Membranes were incubated with primary rabbit anti-CaM (dilution 1:1000), rabbit anti-CaMKII (dilution 1:1000), rabbit anti-CaMKIV (dilution 1:200), rabbit anti CaMKK (dilution 1:100), rabbit anti-CaMKK2 (dilution 1:1000) or mouse anti-GAPDH (dilution 1:700) antibodys, overnight at 4 °C. After washing, membranes were incubated with goat anti-rabbit or goat anti-mouse secondary antibodies HRP-linked (Cell Signalling, Leiden, Netherlands)for 1 h at 20 °C. The chemiluminiscence was indicated by Bio-Rad Immun-Star HRP Luminol/Enhancer and detecton by Azure c600imager (Azure Biosystems, Dublin, CA, USA).

Free cytosolic Ca^{2+}

Intracellular free Ca^{2+} ions were evaluated by high affinity fluorescent selective indicator. Cells were seded into six-well plate and treated by transfection medium with control-siRNA and CaMI-siRNA (200 pM), sarcosine (10 μM)for 24 h and un-treated cells as a control group. Cells were subsequently labeled with Fura 2 acetoxymethyl ester (10 μg/mL) (Fura-2 AM, Abcam). The ratio of the emission correlated to the free amount of intracellular Ca^{2+} concentration. DNA staining by elipticine were used for nuclei conterstaining. Imaging was performed using EVOS FL Auto Cell Imaging System (Thermo-Fisher, Waltham, MA, USA).

Wound-healing assay (Scratch test)

The cells were seeded into 6-well plate to reach confluence ~80%. After seeding a pin was used to a scratch and remove cells from a discrete area of the confluent monolayer to form a cell-free zone. After that, cells were treated with sarcosine (10 μM), transfection medium with control-siRNA, CaMI-siRNA and untreated group as a control. After 6; 12, 24 and 48 h, the micrographs of cells were taken

using EVOS FL Auto Cell Imaging System and compared with micrographs obtained in 0 h, using TScratch software.

Descriptive statistics

For the statistical evaluation of the results, the mean was taken as the measurement of the main tendency, while standard deviation was taken as the dispersion measurement. Differences between groups were analyzed using paired t-test. Unless noted otherwise, the threshold for significance was $p < 0.05$. For analyses Software Statistica 12 (StatSoft, Tulsa, OK, USA) was employed.

RESULTS AND DISCUSSION

First, we compared differentially expressed proteins sarcosine treated cells and control non-treated group. Figure 1 illustratse representative 2D-DIGE proteomic signature with a quantitation of expression of spots annotated as CaM (IP 3.9, M_w 17 kDa). It clearly follows from the data that sarcosine influences proteome of prostate cells and up-regulates CaM. CaM can be further used in cells as an signaling molecule for CaM-dependent pathways, which can be connected with cancer progression and invasiveness.

Figure 1 (A) Representative 2D-DIGE of PCa cells (LNCaP) proteome. Red arrow shows spot identified as CaM. (B) Densitometry of CaM spots from 2D-DIGE for tested cell lines in two times of treatment (24 and 48 h).

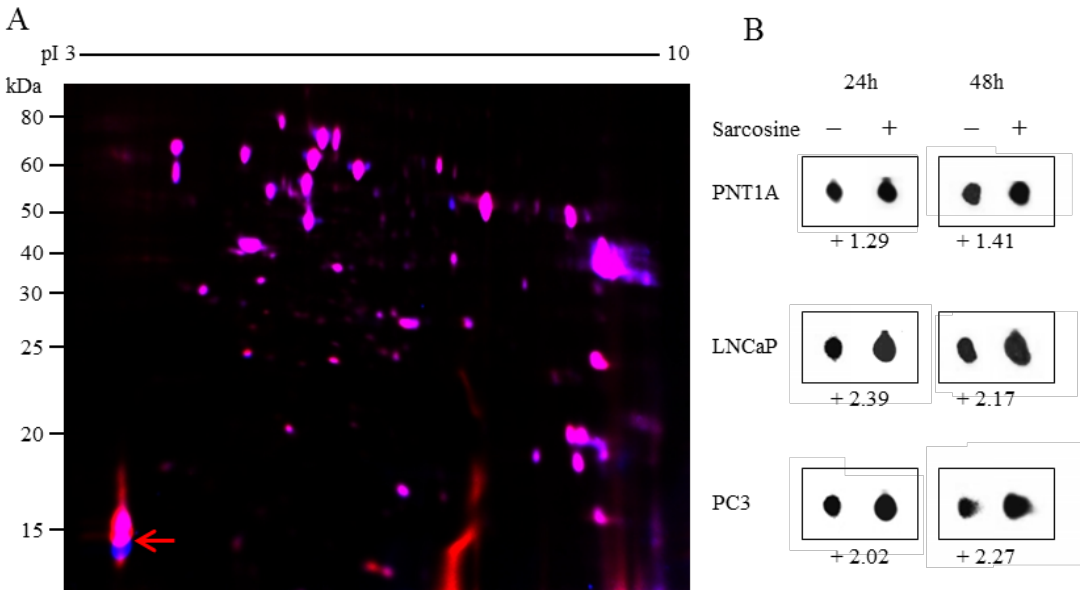

CaM expression was also evaluated by CLSM (Figure 2) that indicates intracellular localization of CaM and also a significant up-regulation due to sarcosine treatment. All three tested cell lines show increased expression of intracellular CaM after sarcosine supplementation.

We further investigated CaM expression upon 24 and 48 h of sarcosine stimulation compared control. Figure 3 depicts increased expression for CaM in time. Noteworthy, expression of CaM-dependent kinases decreased after siRNA-mediated knock-down of CaM. This fact demonstrates that sarcosine can plausibly affect cell cycle directly through the intracellular messenger CaM.

Intracellular Ca^{2+} activates CaM. This means that intracellular level of Ca^{2+} could be bound and homeostasis should be altered. Indeed, different intracellular concentration of Ca^{2+} (Figure 4) correlated with expression of CaM. Lower free Ca^{2+} concentration shows higher occurrence upon up-regulation of CaM by sarcosine. Upon silencing of CaM, increased pool of Ca^{2+} occurs. Upon CaM silencing combined with sarocisne exposure, free Ca^{2+} increases, confirming a direct effect of sarcosine to CaM.

Figure 2 Representative ICC of CaM in tested cells after 24 h treatment with sarcosine (10 μM) and control un-treated group.

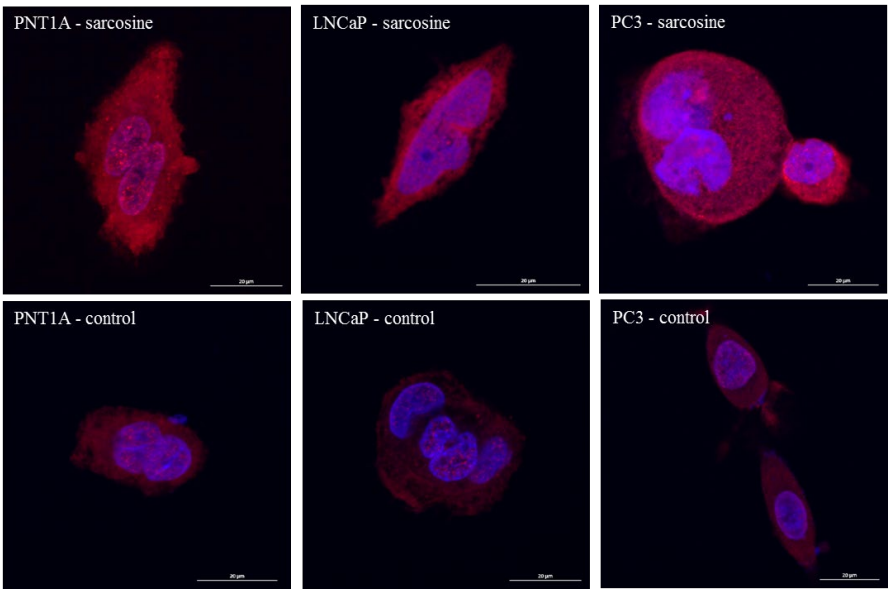

Figure 3 (A) Western blot validation of CaM expression. (B) Expression of CaM-dependent kinases upon CaM silencing and parallel administration to sarcosine.

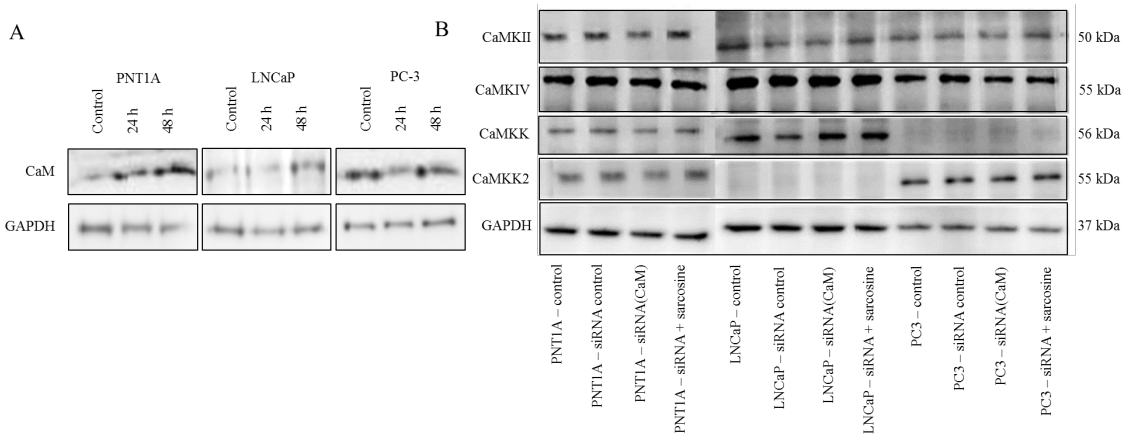

Figure 4 Concentraion of free intracellular Ca^{2+}in PCa cell after sarcosine treatment and CaM silencing. Ca^{2+} is shown in blue and nuclei in green. The scale bar is 100 μm.

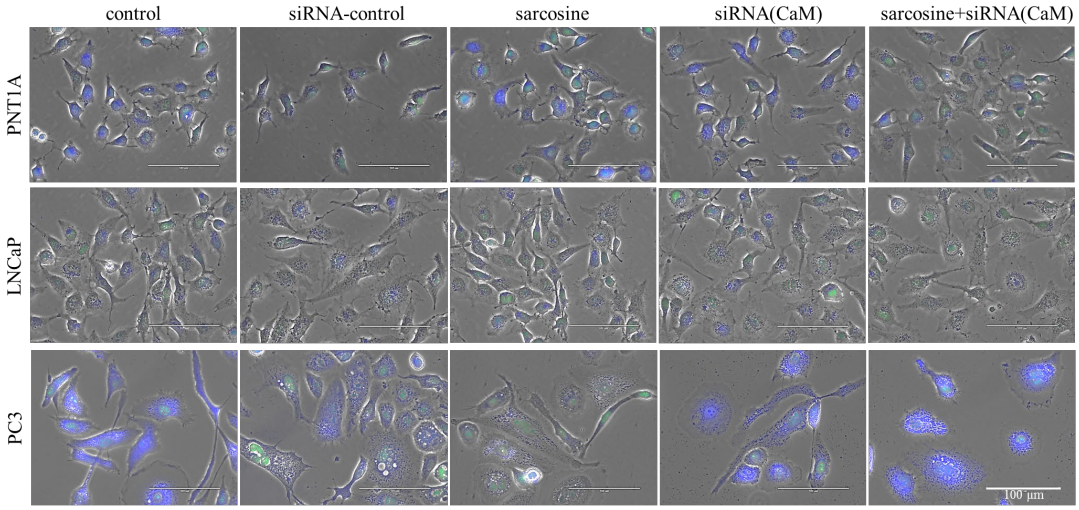

CONCLUSION

Sarcosine up-regulates CaM in prostate-derived cells, and therefore alters the Ca^{2+} homeostasis and pathways drived by CaM-dependend kinases. This signaling cascade can alter cell cycle and proliferation. The need of calcium in this processes has been demonstrated many times. Possibility of silencing CaM can be a new modality to decrease tumor progression, including frequently developing bone methastases.

ACKNOWLEDGEMENTS

The research was financially supported by the Czech Science Foundation (GA CR 16-18917S), League Against Cancer Prague, CEITEC 2020 (LQ1601) and Internal Grant Project AF-IGA-IP-2018/003.

REFERENCES

Erickson, J.R. 2014. Mechanisms of CaMKII activation in the heart. Frontiers in Pharmacology, 5: 59.

Rasmussen, C.D., Means A.R. 1989. Calmodulin, cell growth and gene expression. Trends in Neurosciences, 12(11): 433–438.

Rokhlin, O. et al. 2007. Calcium/calmodulin-dependent kinase II plays an important role in prostate cancer cell survival. Cancer Biology & Therapy, 6(5): 732–742.

Sreekumar, A. et al. 2009. Metabolomic profiles delineate potential role for sarcosine in prostate cancer progression. Nature, 457(7231): 910.

Wang, Y.-y. et al. 2015. The emerging role of CaMKII in cancer. Oncotarget, 6(14): 11725.

Zayzafoon, M. 2006. Calcium/calmodulin signaling controls osteoblast growth and differentiation. Journal of Cellular Biochemistry, 97(1): 56–70.

Perspectives of application of phototrophic sulfur bacteria in hydrogen sulfide utilization

Martin Struk, Ivan Kushkevych
Department of Experimental Biology
Masaryk University
Kamenice 5, 625 00 Brno
CZECH REPUBLIC

martin.struk@mail.muni.cz

Abstract: Sulfur is an essential chemical element for all living organisms. Microorganisms can utilize reduced and oxidized sulfur, preferably sulfate because it can be easily utilized in their biological processes. In this article, the most notable pathways: assimilatory sulfate reduction, dissimilatory sulfate- and sulfur reduction were described. The resulting compound from all three pathways is toxic hydrogen sulfide. It has a negative impact on human health, the environment and due to its corrosive properties also limits some industrial processes. The chemical methods of its removal are costly; therefore, the biological methods are researching as an alternative. The promising organisms are phototrophic green and purple sulfur bacteria. They oxidize hydrogen sulfide present in the environment, resulting in the creation of elemental sulfur.

Key Words: sulfur cycle, sulfates, hydrogen sulfide, phototrophic sulfur bacteria, sulfate-reducing bacteria

INTRODUCTION

Sulfur is one of the essential chemical elements needed for biochemical functioning and is an elemental macronutrient for all living organisms. Sulfur can be found in amino acids (cysteine, cystine, and methionine) and vitamins (biotin and thiamine). Moreover, sulfur is included in many cofactors such as glutathione, thioredoxin or iron-sulfur proteins. The relevant inorganic sulfur compounds are sulfate, sulfite, elemental sulfur, thiosulfate, (poly-)thionate, (poly-)sulfide and sulfide (Hell et al. 2008).

Many microbial groups are involved in sulfur transformation process in nature. This process can be in anaerobic as well as in aerobic conditions. The main pathways of the sulfur cycle are assimilatory sulfate reduction and mineralization, dissimilatory sulfate- and sulfur reduction, leading to the formation of hydrogen sulfide (Kushkevych et al. 2015a, b, c). Another pathway of sulfur transformation is oxidation of reduced sulfur form, including hydrogen sulfide, and elemental sulfur oxidation. The process is important because toxic hydrogen sulfide accumulated can be utilized by anaerobic phototrophic green and purple sulfur bacteria. Hydrogen sulfide is oxidized in the process of anoxygenic photosynthesis and elemental sulfur is accumulated in inside the cells (in purple sulfur bacteria, *Chromatiaceae* family) and on the outside cells (green sulfur bacteria, *Chlorobiaceae* family).

The aim of this work is to characterize the pathways of sulfur cycle and summarize the role of phototrophic sulfur bacteria in the process of hydrogen sulfide utilization and describe the perspectives for their potential application.

MATERIAL AND METHODS

The objects of this research were photosynthetic sulfur bacteria isolated from various sulfur-rich biotopes. Accumulated cultures of the bacteria were grown in modified Van Neil liquid medium with the following composition (g/l): ammonium chloride (1), magnesium chloride (0.5), potassium dihydrogen phosphate (1), sodium chloride (1), sodium bicarbonate (5), sodium sulfide nano-hydrate (1), distilled water (1 liter), and microelements. The medium was sterilized in an autoclave at 1 atm. Before inoculation of samples, 10% solution of sodium hydrogen carbonate and sodium sulfide nonahydrate were sterilized separately and introduced into the Van Niel medium. The pH of the medium was adjusted to 7.5 by 10% solution of phosphatic acid. After that, a solution of vitamin B_{12} (5 μg/l) was added in sterile conditions. To accumulate biomass of green and purple sulfur bacteria, the samples were cultivated in the medium for

over 10 days anaerobically. The temperature (+25 °C) and a source of light (lamp with a red filter) were constant during cultivation. Anaerobic conditions were achieved by filling the tubes fully with the medium.

RESULTS AND DISCUSSION

Assimilatory sulfate reduction and mineralization

Transformation of reduced and oxidized sulfur in nature can occur in both aerobic and anaerobic conditions. From all the sulfur forms in the environment, the sulfate is the most important because all the organisms can assimilate and utilize sulfate in their biological processes.

Sulfate is incorporated into organic matter – plants, animals and is utilized in their metabolism. In an organism, sulfate is reduced through the assimilatory reductive pathway. In this pathway, sulfate is activated and adenosine 5′-phosphosulfate (APS) is formed. Later the APS is directly or via 3′-phosphoadenosine 5′-phosphosulfate (PAPS) reduced to sulfite and later to hydrogen sulfide. Hydrogen sulfide is then incorporated into the molecule of amino acid. Thus, the final product may be cysteine and methionine. These amino acids are an essential part of metabolism in organisms. Multiple bacteria can also grow by oxidizing sulfite (SO_3^{2-}), for example, *Sulfitobacter*. The sulfur contained in amino acids, tissues etc. is released after the death of the organism in the process of mineralization and decomposition. Among the many compounds, hydrogen sulfide is created in these processes (Hell et al. 2008).

Dissimilatory sulfate reduction

Another way to reduce sulfate is in the process of dissimilatory sulfate reduction. This pathway is natural to sulfate-reducing bacteria (SRB) (Kushkevych et al. 2017a, b). This group of microorganisms is anaerobic and use sulfate as an electron acceptor. The first step is similar to the assimilation pathway – the sulfate is activated, and APS is created. Later parts include reduction of APS to sulfite and then its reduction to sulfide. Thiosulfate ($S_2O_3^{2-}$) is also used as a substrate in dissimilatory metabolism by the majority of sulfur-oxidizing and also many sulfide-producing bacteria. Complete reduction of thiosulfate to sulfide is a process associated with soluble enzymes which require type *c* cytochromes, quinone pool or thiols. It is suggested that this process is part of sulfite reduction and thus the dissimilatory sulfate reduction (Hell et al. 2008).

For sulfate reduction, SRB need exogenous electron donors, such as organic compounds and molecular hydrogen (Kováč and Kushkevych 2017). Most sulfate-reducing microorganisms can also reduce other oxidized inorganic sulfur compounds, such as sulfite (SO_3^{2-}) or thiosulfate ($S_2O_3^{2-}$). Compared to sulfate, thiosulfate, and sulfite are preferred as electron acceptors. The sulfide production rates in both cases were found to be considerably higher than those from sulfate (Hao et al. 1996).

Sulfate-reducing bacteria are an important group which takes part in the sulfur cycle in nature. These anaerobic microorganisms include following genera: *Desulfovibrio, Desulfomicrobium, Desulfobulbus, Desulfobacter, Desulfomonas,* and *Desulfotomaculum* (Kushkevych et al. 2018b). Genus *Desulfovibrio* is the most common of them and its species are often isolated from large intestines of humans and animals (Kováč and Kushkevych 2017, Kushkevych et al. 2018a, d, e). Sulfate-reducing bacteria have been also detected or isolated from marine and freshwater environments and from human engineered systems (Kushkevych et al. 2017b; 2018c). If the sulfate content is limited in these environments, SRB will compete with each other for the available sulfate. *Desulfovibrio* spp. has the highest affinity for sulfate followed by *Desulfobulbus* spp. and *Desulfobacter* spp. (Laanbroek et al. 1984).

Dissimilatory sulfur reduction

The third pathway which yields hydrogen sulfide is a dissimilatory reduction of elemental sulfur. The sulfur-reducers, such as genus *Desulfuromonas* and *Desulfonema* use reduced sulfur forms as the main electron acceptor for the respiration (oxidation) of organic compounds or H_2. Sulfide is the final product of sulfur reducing respiratory processes. These species are abundant and widespread in anoxic marine or brackish water sediments, but their occurrence in freshwater sediments is less frequent (Hell et al. 2008).

Thus, these three pathways including the process assimilatory sulfate reduction and dissimilatory sulfate- or sulfur reduction lead to hydrogen sulfide accumulation. Hydrogen sulfide is toxic compound and can be the main pollutant of the environment as well as its accumulation in the intestines of humans and animals lead to heterogeneous bowel diseases (Kushkevych et al. 2015; 2017a; 2018a, d, e).

Toxicity of hydrogen sulfide

Hydrogen sulfide is a colourless gas with a strong odour of rotten eggs. Naturally, hydrogen sulfide occurs in volcanic sites, mineral spring and natural gas (up to 90% of its composition). Its presence in various water bodies and soil is the result of sulfate-reducing bacteria activity, mainly in decaying organic matter, and has a negative impact on other organisms in the environment. High amounts and prolonged exposure can harm plants or cause adverse effects on marine ecology and coastal fisheries (Roth 2004). Hydrogen sulfide can poison several different systems in the human body and the most affected is the nervous system. It binds with iron in the mitochondrial cytochrome enzymes, thus preventing cellular respiration. It is also speculated that inflammatory bowel disease including ulcerative colitis or Crohn's disease is caused by the toxic molecule of hydrogen sulfide (Kováč et al. 2018, Kováč and Kushkevych 2017, Kushkevych 2017a).

Oxidation of hydrogen sulfide and elemental sulfur

Sulfur is essential for phototrophic organisms due to its redox properties. In photosynthetic carbon dioxide fixation in anoxygenic phototrophic sulfur bacteria, reduced sulfur is an electron donor. In nature, usually polluted areas, green and purple sulfur photosynthesizing bacteria are important groups in sulfur transformation. The main representatives of these microorganisms are two families, *Chlorobiaceae* (green sulfur bacteria) and *Chromatiaceae* (purple sulfur bacteria) (Hell et al. 2008).

The green sulfur bacteria (GSB) are anoxygenic phototrophic bacteria. Their light-harvesting complexes contain family specific bacteriochlorophyll *c*, *d*, or *e* and are located in special light-harvesting organelles (chlorosomes). The presence of these light-harvesting complexes allows them to grow under lower light intensity (25–80 lux) than purple sulfur bacteria. Other important cytological characteristics are the formation of sulfur globules outside of cell and presence of gas vesicles in some species. *Chlorobiaceae* are strictly anoxic and obligately phototrophic. Reduced sulfur compounds, sulfide and sulfur, are common photosynthetic electron donors in this group of bacteria. In addition, thiosulfate is used by several representatives. Species of this group have been found in various environments, such as freshwater lakes, fjords, oceans and ocean sediments (Overmann 2006).

The second important group is purple sulfur bacteria (PSB), which grow well under photoautotrophic conditions and use sulfide as a photosynthetic electron donor. Sulfide is oxidized to sulfate. Some of the species also oxidize thiosulfate and sulfite. The resulting elemental sulfur is accumulated as microscopically visible globules inside the cells. The important pigments are bacteriochlorophyll *a* or *b* and various carotenoids – spirilloxanthin, rhodopinal, spheroidene, and okenone (Hell et al. 2008).

Purple and green sulfur bacteria require light as an energy source and use reduced sulfur compounds as electron-donating substrates for photosynthetic CO_2 reduction. Sulfide present in the environment is oxidized and the resulting compound is elemental sulfur in the form of globules. There are two major pathways and also the *Sox* enzymatic system that utilizes H_2S.

In the first one, sulfide-quinone oxidoreductase pathway, electrons from sulfide are transferred to quinone pool in a cell by the enzyme. Sulfide-quinone oxidoreductase is a membrane-bound enzyme and its activity was proved in both purple and green sulfur bacteria. It presumably transfers electrons into the photosynthetic electron transfer chain via a complex of quinol-oxidizing Rieske iron-sulfur protein and cytochrome *b*. The second one is the flavocytochrome *c* pathway. During *in vitro* experiments, flavocytochrome *c* effectively catalyzed the transfer of electrons from sulfide through smaller cytochromes to the photosynthetic reaction centre. However, its significance *in vivo* is not as clear as it seems, due to the occurrence of several species successfully oxidizing sulfides without it. Another option is the *Sox* pathway. This pathway utilizes thiosulfate-oxidizing multi-enzyme complex. Sulfide binds to the enzyme *Sox*Y and remains bound to it until its final conversion to sulfate with the involvement of enzyme *Sox*CD (Hell et al. 2008).

The oxidation of elemental sulfur in most cases occurs aerobically. Bacteria *Acidithiobacillus ferrooxidans* and *Thiobacillus thioparus* can oxidize sulfur to sulfite by means of an iron-containing oxygenase enzyme, although it is suggested that an oxidase could play role in an energy saving mechanism. This oxygenase enzyme utilizes glutathione as a cofactor. The initial product of sulfur oxidation is sulfite rather than thiosulfate (Suzuki and Silver 1966). For the anaerobic oxidation of elemental sulfur, it is thought that the *Sox* pathway plays an important role. The mechanism of sulfur oxidation may be initially similar to oxidation of hydrogen sulfide with sulfate as a terminal product (Hell et al. 2008).

Biological methods of hydrogen sulfide utilization

Hydrogen sulfide has a negative impact not only on the human health and environment but also on some industrial processes, e.g. the production of biogas. If present in wastewater, sulfide can cause problems and its removal its on-going problem in many wastewater treatment plants and factories. In sewage water, sulfide is present as an equilibrium mixture of H_2S, HS^- and S^{2-}. The colourless gas H_2S tends to escape the wastewater and cause damage due to its potentially malodorous, toxic, and corrosive properties. Many current problems are also related to how efficiently remove hydrogen sulfide in biogas. In biogas reactors, sulfate-reducing bacteria can out-compete methanogens for substrates, e.g., H_2, CO_2, and acetate if a high amount of sulfate is present (Kushkevych et al. 2018b). The final product of SRB metabolism is toxic hydrogen sulfide. It can cause corrosion of metal parts of biogas reactors and inhibits the growth of methanogens (Kushkevych et. al 2017b). The chemical H_2S removal processes are expensive due to the high requirements of chemicals, energy and high disposal costs (Hell et al. 2008). For these reasons, biological treatment methods for hydrogen sulfide removal are desirable as an alternative to chemical treatment and the application of purple or green sulfur bacteria seems appropriate.

When attempting to utilize the abilities of GSB or PSB for sulfide removal in large-scale systems, there are few factors which are important to have in mind. Firstly, it is the selection of a suitable organism. It is suggested that, for several reasons, green sulfur bacteria are more suitable than purple sulfur bacteria for H_2S removal. GSB deposit elemental sulfur extracellularly, which enables recovery of the sulfur if needed. On the other hand, most PSB accumulates the elemental sulfur intracellularly. GSB oxidize more sulfide per light input than purple bacteria. Green sulfur bacteria have also higher tolerance and affinity for uptake sulfide. Lastly, when organic nutrients are available, sulfide uptake in purple bacteria is diminished. Another important factor influencing the phototrophic bacteria and their use is a source of light. The attention is turning to more cost-efficient alternatives, such as light-emitting diodes, from classical incandescent lamps. Conversion of electrical into photosynthetically active light happens with a higher efficiency than is possible with incandescent lamps; the heat management is easier and the sources of light are more compact (Hell et al. 2008).

Kobayashi et al. (1983) investigated the feasibility of photosynthetic bacteria to remove H_2S from anaerobic waste treatment effluent. Using submerged tube system containing fixed films of photosynthetic bacteria (mostly *Chlorobium*), they managed to obtain the final effluent completely devoid of H_2S. These types of reactors have one disadvantage and that is poor suitability to treat wastewaters containing solids. This could be improved by using tubes with a larger diameter or plane transparent panels with light-diffusing optical fibres. In the case of PSB, it was reported that presence of the purple sulfur bacteria, e.g. *Thiocapsa roseopersicina*, in the dairy wastewater lagoons led to a reduction of the odour and toxicity in these lagoons (Dungan and Leytem 2015).

CONCLUSION

Sulfate-reducing and phototrophic sulfur bacteria are a very important part of the sulfur cycle in nature, especially the latter one can utilize toxic hydrogen sulfide from the environment. This ability of families *Chlorobiacea* and *Chromatiaceae* could be used to reduce the content of hydrogen sulfide in wastewater or biogas purification although further research is still needed.

ACKNOWLEDGEMENTS

This study was supported by Grant Agency of the Masaryk University (MUNI/A/0906/2018).

REFERENCES

Dungan, R.S., Leytem, A.B. 2015. Detection of Purple Sulfur Bacteria in Purple and Non-purple Dairy Wastewaters. Journal of Environment Quality, 44(5): 1550–1555.

Hao, O.J. et al. 1996. Sulfate-reducing bacteria. Critical Reviews in Environmental Science and Technology, 26(2): 155–187.

Hell, R. et al. 2008. Sulfur metabolism in phototrophic organisms. 1st ed., Dordrecht: Springer.

Kobayashi, H.A. et al. 1983. Use of photosynthetic bacteria for hydrogen sulfide removal from anaerobic waste treatment effluent. Water Research, 17(5): 579–587.

Kováč, J., Kushkevych, I. 2017. New modification of cultivation medium for isolation and growth of intestinal sulfate-reducing bacteria. In Proceeding of International PhD Students Conference MendelNet 2017 [Online]. Brno, pp. 702–707. Available at: https://mendelnet.cz/pdfs/mnt/2017/01/52.pdf. [2018-09-09].

Kováč, J. et al. 2018. Metabolic activity of sulfate-reducing bacteria from rodents with colitis. Open Medicine [Online], 13(1): 344–349. Available at: http://www.degruyter.com/view/j/med.2018.13.issue-1/med-2018-0052/med-2018-0052.xml [2018-09-12].

Kushkevych, I. et al. 2015a. Activity of Na^+/K^+-activated Mg^{2+}-dependent ATP hydrolase in the cell-free extracts of the sulfate-reducing bacteria Desulfovibrio piger Vib-7 and Desulfomicrobium sp. Rod-9. Acta Veterinaria Brno, 84(1): 3–12.

Kushkevych, I. et al. 2015b. Activity of selected salicylamides against intestinal sulfate-reducing bacteria. Neuroendocrinology Letters, 36(1): 106–113.

Kushkevych, I.V. 2015c. Activity and kinetic properties of phosphotransacetylase from intestinal sulfate-reducing bacteria. Acta Biochemica Polonica, 62(1): 1037–108.

Kushkevych, I. et al. 2017a. Kinetic properties of growth of intestinal sulphate-reducing bacteria isolated from healthy mice and mice with ulcerative colitis. Acta Veterinaria Brno, 86(4): 405–411.

Kushkevych, I. et al. 2017b. Production of biogas: relationship between methanogenic and sulfate-reducing microorganisms. Open Life Sciences, 12(1): 82–91.

Kushkevych, I. et al. 2018a. Effect of selected 8-hydroxyquinoline-2-carboxanilides on viability and sulfate metabolism of Desulfovibrio piger. Journal of Applied Biomedicine, 16(3): 241–246.

Kushkevych, I. et al. 2018b. The diversity of sulfate-reducing bacteria in the seven bioreactors. Archives of Microbiology, 200(6): 945–950.

Kushkevych, I. et al. 2018c. A new combination of substrates: biogas production and diversity of the methanogenic microorganisms. Open Life Sciences, 13(1): 119–128.

Kushkevych, I. et al. 2018d. Activity of ring-substituted 8-hydroxyquinoline-2-carboxanilides against intestinal sulfate-reducing bacteria Desulfovibrio piger. Medicinal Chemistry Research, 27(1): 278–284.

Kushkevych, I. et al. 2018e. Cross-correlation analysis of the Desulfovibrio growth parameters of intestinal species isolated from people with colitis. Biologia, 73(10): 1–7.

Laanbroek, H.J. et al. 1984. Competition for Sulfate and Ethanol Among Desulfobacter, Desulfobulbus, and Desulfovibrio Species Isolated from Intertidal Sediments. Applied and Environmental Microbiology, 47(2): 329.

Overmann, J. 2006. The Family Chlorobiaceae. In The Prokaryotes. New York: Springer New York, pp. 359–378.

Roth, S.H. 2004. Toxicological and Environmental Impacts of Hydrogen Sulfide. In Signal Transduction and the Gasotransmitters. Totowa, NJ: Humana Press, pp. 293–313.

Suzuki, I., Silver, M. 1966. The initial product and properties of the sulfur-oxidizing enzyme of thiobacilli. Biochimica et Biophysica Acta (BBA) - Enzymology and Biological Oxidation, 122(1): 22–33.

Effect of apoferritin surface-biomacromolecular modification on cellular uptake and inhibition of protein corona

Barbora Tesarova[1,2,3], Simona Dostalova[1,2], Marketa Charousova[1,2,3], Zuzana Skubalova[1,2], Roman Guran[1,2], Tomas Do[1,2], Vojtech Adam[1,2], Zbynek Heger[1,2]
[1]Department of Chemistry and Biochemistry
Mendel University in Brno
Zemedelska 1, 613 00 Brno
[2]Central European Institute of Technology
Brno University of Technology
Purkynova 123, 612 00 Brno
CZECH REPUBLIC
[3]Brno Ph.D. Talent Scholarship Holder
Funded by the Brno City Municipality

tesarova.barca@seznam.cz

Abstract: The effects of surface modifications (PEGylation and PASylation) of natural nanocarriers based on apoferritin (FRT) were tested in this work. The main goals of performed PEGylation/PASylation were decreased protein corona formation leading to better internalization of drugs into diseased cells and therefore higher efficiency of treatment. The influence of created protein coronas on the amount of internalized experimental drug ellipticine (Elli) was evaluated *via* fluorescence microscopy. Various properties of these modified nanoparticles were studied, such as their cytotoxicity or release kinetics of Elli. According to performed experiments, PAS-10 modification appeared as the most appropriate surface modification.

Key Words: apoferritin, nanomedicine; PASylation, PEGylation, protein coronas

INTRODUCTION

One of the most limiting factors of a nanocarrier use in therapy is immediate binding of plasma proteins on their surface upon entering blood stream. This process is known as protein corona formation. Protein corona can be defined as a natural interface between nanomaterials and living matter in biological milieu (Monopoli et al. 2013). It is known that corona formation could affect endocytosis or functional properties of nanocarrier (Yan et al. 2013). The most important fact is that, according to Salvati et al., corona interferes with targeting moieties, which leads to inhibited receptor-mediated uptake of the nanocarriers (Salvati et al. 2013). Moreover, protein coronas, which were taken up by target cells, could alter cells functions (Bros et al. 2018).

To minimalize or completely inhibit binding of additional biomolecules leading to formation of protein corona it is possible to modify the surface of nanocarrier. In this contribution, we focused on two very promising surface modifications: PEGylation and PASylation. PEGylation is generally defined as modification of proteins, peptides or small organic molecules by covalent binding with one or more poly-ethylene glycol (PEG) chains (Eto et al. 2008). PEG is approved by Food and Drug Administration (FDA) for human oral, intravenous and dermal pharmaceutical use (Li et al. 2013). Despite this fact, the use of PEGylation has some drawbacks including potential immunogenic effects (Armstrong et al. 2007), non-biodegradability of PEG, possible cellular vacuolization or decreased biological activity of a drug after performed PEGylation (Yu et al. 2007). Therefore, we also focused on PASylation, which represents biological alternative to PEGylation. PAS sequences are hydrophilic, uncharged, comprising of small residues of amino acids proline, alanine and (Binder et al. 2017).

As a nanocarrier we chose FRT, which is a biocompatible ubiquitous protein naturally occurring in human body (Bulvik et al. 2012). The structure of FRT is pH dependent. In our Research group we took advantage of this fact and published a study, where we described easy-to-use encapsulation of cytostatic drug doxorubicin (Dox) into FRT (Dostalova et al. 2017). For the purpose of this study was

used experimental cytotoxic drug Elli. Elli has not been approved by FDA due to many side effects, such as its mutagenicity or hemotoxicity (Stiborova et al. 2011). Elli is classified as an alkaloid, which mechanism of action is presumably based on intercalation into DNA and inhibition of topoisomerase II (Tmejova et al. 2014).

By encapsulation of Elli into FRT we show that even experimental drugs can be used as cargoes for FRT-based delivery with pronounced cytotoxic effects. By modifying the surface of FRT with PEGylation or PASylation, we increased the internalization of Elli into cells and also decreased the formation of protein corona. Furthermore, we also evaluated cytotoxic effects *via* MTT assay and we also studied one of the possible mechanism of toxicity, which is formation of reactive oxygen species (ROS).

MATERIAL AND METHODS

Chemicals

All chemicals of ACS purity were obtained from Sigma-Aldrich (St. Louis, MO, USA).

Encapsulation of Elli into FRT

The stock solution of Elli with concentration of 1 mg/mL was prepared by dissolving Elli in 1 M HCl and deionized water in ratio 1 : 150. For each sample, 200 µL of 1 mg/mL Elli was added to 100 µL of deionized water and 20 µL of 50 mg/mL horse spleen FRT and gently mixed for 15 min. To reassemble the FRT structure disassembled by acidic Elli and encapsulate Elli in FRT cavity, 0.66 µL of 1 M sodium hydroxide solution was added and the samples were mixed for further 15 min. To filter out non-encapsulated Elli, solution exchange was performed 3× (centrifugation at 6,000 *g* for 15 min). The concentration of encapsulated Elli was evaluated by absorbance measurement at 420 nm using Tecan Infinite 200 PRO (Männedorf, Switzerland).

Surface modification with PEG

50 µL of 10 mM PEG maleimide in PBS (phosphate buffered saline, pH 7.4: 0.137 M NaCl + 0.0027 M KCl + 0.0014 M KH_2PO_4 + 0.0043 M Na_2HPO_4) and 629 µL of PBS was added to FRTElli and mixed for 1 h. To remove unbound PEG, the sample was 5× diafiltrated using Amicon® Ultra 0-5 mL 50K Merck Millipore (Billerica, MA, USA) at 6,000 *g* for 15 min.

Surface modification with PAS

25 µL of 1.3 nm gold nanoparticles was added to FRTElli and the samples were mixed for 14 h to allow adsorption of Au nanoparticles to the charged amino acid residues on the surface of FRTElli nanoparticles (creating FRTElli-Au). Solution exchange was performed 2× to remove unbound Au nanoparticles. 3 µL of 1.25 mg/mL PAS-10 (ASPAAPAPASC) and PAS-20 (ASPAAPAPASPAAPAPSAPAC) was added to FRTElli-Au and the samples were incubated for 1 h at 45 °C to allow binding of cysteine to gold. Then, solution exchange was performed to remove unbound molecules of PAS peptides.

Short-term cytotoxicity of PEGylated/PASylated FRTElli

The cell viability of breast cancer cell lines MDA-MB-231, MDA-MB-468, MCF-7, T-47D, ZR-75-1 and nonmalignant cell line HBL-100 was assayed using MTT (3-(4,5-dimethylthiazol-2-yl)-2,5-diphenyltetrazolium bromide) assay to determine 24IC_{50} values. The suspension of 5,000 cells in medium (50 µL) was added to each well of 96-well plates, followed by incubation for 24 h at 37 °C with 5%CO_2 to ensure cell growth. After 24 h treatment, MTT dye solution (10 µL, 5 mg/mL in PBS) was added to each well and the mixture was incubated for further 3 h at 37 °C. After that, medium containing MTT solution was replaced with 99.9% dimethyl sulfoxide (100 µL to each well), incubated for 5 min and the absorbance of the samples was determined using Tecan Infinite 200 PRO (λ=570 nm). The experiments were performed in three independent repetitions.

Release kinetics study

Release kinetics study was performed in order to test the stability of PEGylated and PASylated FRTElli. Prepared nanoparticles were incubated in Ringer's solution (0.65% NaCl, 0.042% KCl, 0.025% $CaCl_2$, 0.02% sodium bicarbonate) at 37 °C. The mixture was centrifuged at 6000 g and 4 °C

for 15 min at various time points (0, 1, 2, 4, 8 and 24 h). The pellets containing the nanocarrier were resuspended in Ringer's solution. The total amount of released Elli was measured by absorbance measurement at 420 nm using Tecan Infinite 200 PRO.

ROS formation

For ROS formation assay, a suspension of 10,000 MCF-7 or HBL-100 cells in medium was added to each well of a 24-well plate. After overnight incubation, the cells were treated with FRTElli with modified surface ($24IC_{50}$, 6 h). After treatment, the cells were rinsed with PBS and directly used for analysis of ROS using CellROX® Green Reagent (Thermo Fisher Scientific, Waltham, MA, USA) according to manufacturer's instructions. Hoechst 33342 was employed for nuclei counterstaining. Cells were visualized using the EVOS FL Auto Cell Imaging System (Thermo Fisher Scientific).

Fluorescently labeled protein coronas

To label FRT, 4 µL of fluorescent dye cyanine 3 (Lumiprobe, Hannover, Germany) and 100 µL of nanoparticle's solution were added to 896 µL of 0.05 M borate buffer (pH = 8.5) and mixed for 1 h. To label fetal bovine serum (FBS), FBS was centrifuged at 22,000 *g* and 4 °C for 30 min to remove aggregates, followed by incubation of 500 µL of FBS with 8 µL of fluorescent dye cyanine 5 (Lumiprobe) and 492 µL of 0.05 M borate buffer (pH = 8.5).To remove unbound cyanine dye molecules, the samples were 5× diafiltrated using Amicon® Ultra 0-5 mL 100K Merck Millipore at 6,000 *g* for 15 min. After diafiltration the samples were adjusted to 100 µL and 400 µL of 10× diluted labeled FBS was added to them. The samples containing a mixture of fluorescently labeled FBS and PEGylated/PASylated FRTElli nanoparticles were incubated at 600 rpm and 37 °C for 35 min. To remove unbound proteins from nanoparticles, the samples were 5× centrifuged at 6,000 *g* for 15 min. Then, a suspension of 10,000 MDA-MB-468 cells in medium were added wells of a 24-well plate. After overnight incubation, the cells were treated with FRTElli with modified surface ($24IC_{50}$, 6 h). After treatment, the cells were rinsed with PBS and directly used for fluorescence microscopy. Hoechst 33342 was employed for nuclei counterstaining. Cells were visualized using the EVOS FL Auto Cell Imaging System obtained from Thermo Fisher Scientific.

RESULTS AND DISCUSSION

MTT assay (Figure 1) was performed in order to determine value of $24IC_{50}$. The value of $24IC_{50}$ is crucial for cytotoxicity evaluation of performed surface modifications. $24IC_{50}$ was determined for five malignant breast cell lines (MDA-MB-468, MDA-MB-231, MCF-7, T-47D, ZR-75-1) and for one non-malignant breast cell line (HBL-100). The results from MTT assay showed that surface modification with PEG was more cytotoxic than PASylation for all cell lines and also that PAS-10 is more cytotoxic than PAS-20, except for the cell line T-47D and ZR-75-1.

Figure 1 MTT assay performed on FRT with modified or unmodified surface

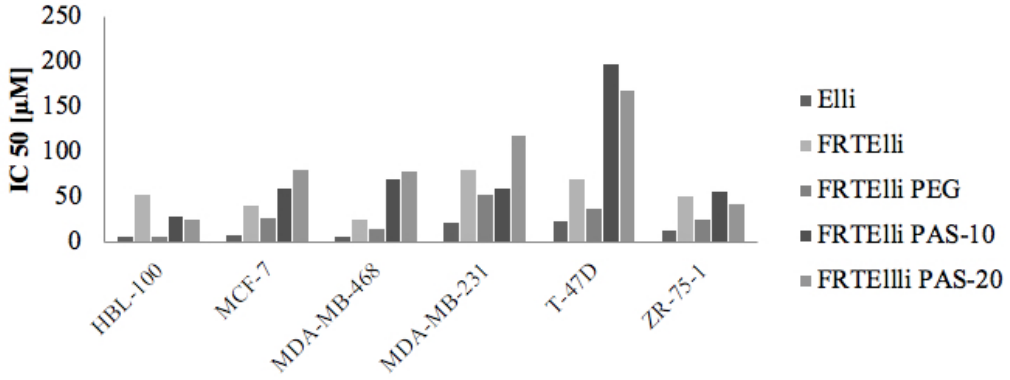

Figure 2 showed that neither PEGylation, nor PASylation caused any changes in the release kinetics in off-target plasma environment of Elli after 24 h study, showing exceptional stability of encapsulated Elli in plasma.

Figure 2 Release kinetics study on FRT with modified or unmodified surface.

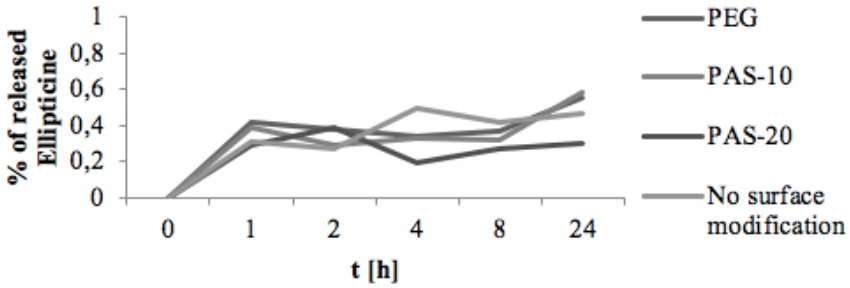

The internalization of Elli into FRT is showed in Figure 3 with ROS/nuclei co-staining and fluorescence microscopy analysis of tested cell lines. Green color represents fluorescence of Elli. Figure 3 shows successful internalization of Elli into nuclei, especially to malignant cell line MCF-7. The internalization of Elli into non-malignant HBL-100 cells was 84% lower than into malignant cell line MCF-7. It must be noted that only surface modification with PAS-10 increased the internalization of Elli (166±6% compared to 100±4% of Elli), in case of PEGylation the internalization was 52% lower than for Elli and in case of PAS-20 5% lower than for Elli. Figure 3 illustrates that all three performed surface modifications induced increased formation of ROS compared to unmodified FRTElli within both tested cell lines, but, overall, the highest ROS formation was found in PAS-10 modified FRTElli for non-malignant cell line HBL-100 (218±8% compared to 100±4% of Elli) and in PAS-20 modified FRTElli for malignant cell line MCF-7 (269±9% compared to 100±4% of Elli). The fact that internalization of Elli is decreased for non-malignant cell line HBL-100, while the ROS formation is increased compared to malignant cell line MCF-7 suggest, that HBL-100 cells are more sensitive to Elli.

Figure 3 Internalization of Elli into FRT, ROS/nuclei staining (the length of the scale bar is 25 μm)

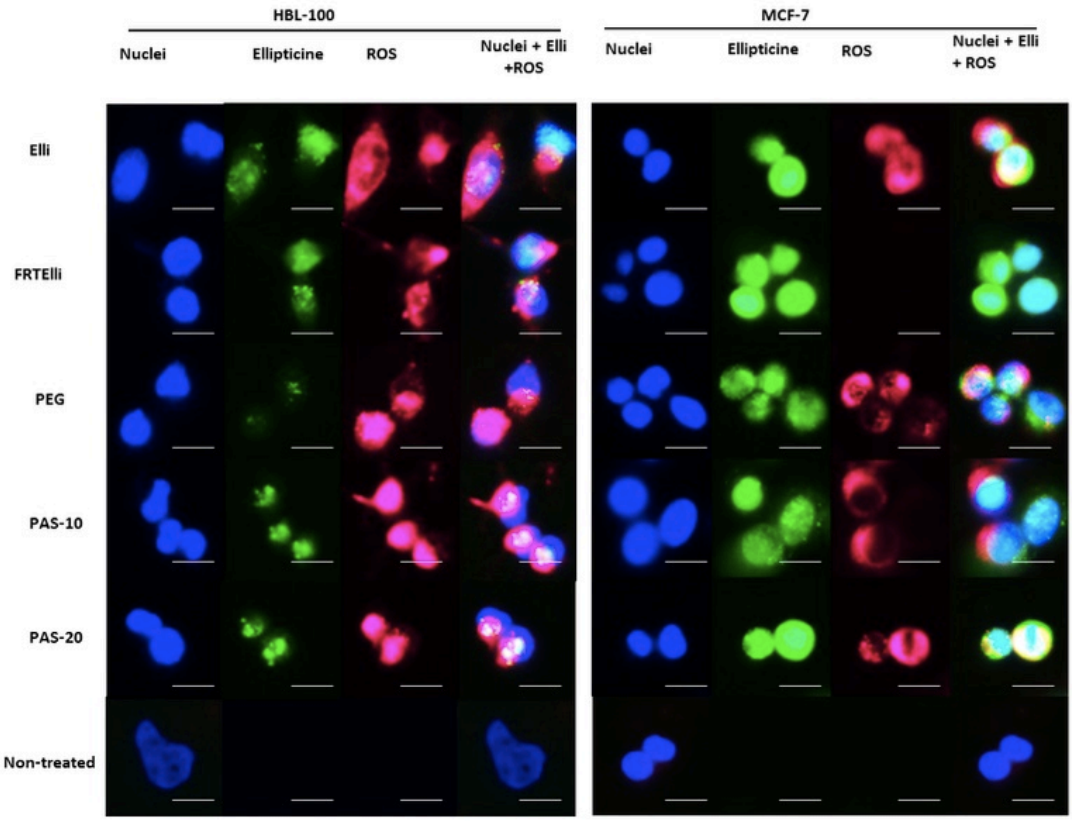

Before protein corona formation we fluorescently labeled FBS in order to further investigate the formation of protein coronas and then we performed fluorescence microscopy analysis of tested samples on MDA-MB-468 cell line. As it can be seen from Figure 4, red color represents proteins forming protein coronas, green color represents fluorescence of Elli and blue color represents stained nuclei. Figure 4

shows, that Elli internalized successfully also into nuclei of MDA-MB-468. It must be noted, that all three surface modification increased internalization of Elli compared to unmodified FRTElli. The highest internalization of Elli was noted on PAS-10 modified FRTElli, which was even higher than for non-encapsulated Elli (121±5% compared to 100±4% of Elli). PEGylated FRTElli had decreased internalization of Elli compared to PAS-10 or non-encapsulated Elli (82±3% compared to 100±4% of Elli). The lowest internalization was noticed for FRTElli with PAS-20 surface modification (48±2% compared to 100±4% of Elli). We also focused on evaluation of protein corona formation. As it can be seen, the highest protein corona formation was detected on FRTElli without any surface modification, which also corresponds to a fact, that there was observed the lowest degree of Elli internalization. On the other hand, almost no protein corona formation was observed on non-encapsulated Elli and FRTElli modified with PAS-10 (23±1% compared to 100±4% of FRTElli). PEGylation also caused significant decrease of protein corona (28±2% compared to 100±4% of FRTElli). Surface modification with PAS-20 appeared as the least useful due to insignificant decrease of protein corona (87±4% compared to 100±4% of FRTElli) and insufficient internalization of Elli.

Figure 4 Fluorescently labeled protein coronas on modified/unmodified surface of FRT (the length of scale bar is 25 μm)

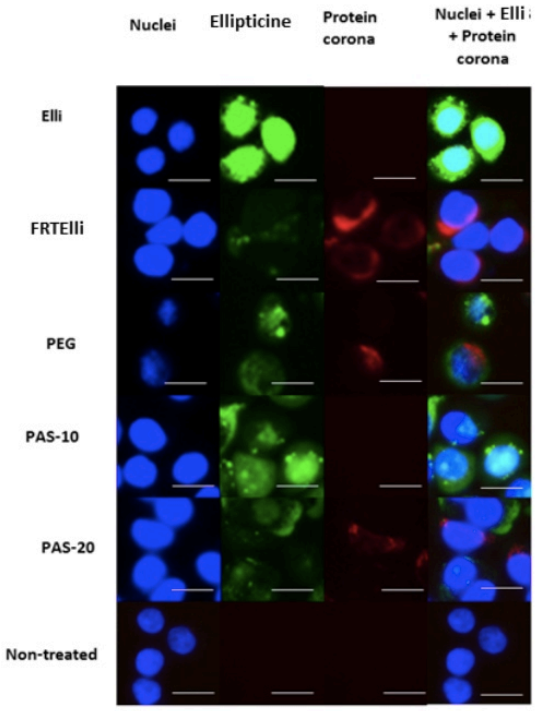

CONCLUSION

The experiment presented in this work served as suitable platform for the prediction of *in vivo* behavior of FRT nanocarrier, based on *in vitro* tests of protein corona formation. The surface of FRT was modified with polymer (PEG) and peptides (PAS) in order to decrease negative interactions with surrounding environment. Overall, the results showed that decreased protein corona formation led to increased internalization of Elli. All three tested modifications favorably influenced the internalization of Elli and also protein corona formation, while as the most beneficial appeared the modification with PAS-10. To further determine the identity of proteins composing protein coronas, 2-D fluorescence difference gel electrophoresis (DIGE) followed by mass spectrometry (MS) analysis will be performed.

ACKNOWLEDGEMENTS

The authors gratefully acknowledge financial support from the Grant Agency of the Czech Republic (GACR 17-12816S), by grant no. AF-IGA-IP-2018/019 and Brno Ph.D. Talent.

REFERENCES

Armstrong, J.K. et al. 2007. Antibody against poly(ethylene glycol) adversely affects PEG-asparaginase therapy in acute lymphoblastic leukemia patients. Cancer, 110(1): 103–111.

Binder, U. et al. 2017. PASylation®: A versatile technology to extend drug delivery. Current Opinion in Colloid & Interface Science, 31(1): 10–17.

Bros, M. et al. 2018. The Protein Corona as a Confounding Variable of Nanoparticle-Mediated Targeted Vaccine Delivery. Frontiers in Immunology, 9(1): 1–10.

Bulvik, B.E. et al. 2012. Cardiac protection by preconditioning is generated via an iron-signal created by proteasomal degradation of iron proteins. PloS one, 7(11): 1–9.

Dostalova, S. et al. 2017. Apoferritin as an ubiquitous nanocarrier with excellent shelf life. International Journal of Nanomedicine, 12(1): 2265–2278.

Eto, Y. et al. 2008. Development of PEGylated adenovirus vector with targeting ligand. International Journal of Pharmaceutics, 354(1): 3–8.

Li, W. et al. 2013. Current drug research on PEGylation with small molecular agents. Progress in Polymer Science, 38(1): 421–444.

Monopoli, M.P. et al. 2013. Formation and characterization of the nanoparticle-protein corona. Methods in Molecular Biology, 1025(1): 137–55.

Salvati, A. et al. 2013. Transferrin-functionalized nanoparticles lose their targeting capabilities when a biomolecule corona adsorbs on the surface. Nature Nanotechnology, 8(1): 137–143.

Stiborova, M. et al. 2011. Ellipticine cytotoxicity to cancer cell lines - a comparative study. Interdisciplinary Toxicology, 4(1): 98–105.

Tmejova, K. et al. 2014. Electrochemical Study of Ellipticine Interaction with Single and Double Stranded Oligonucleotides. Anti-Cancer Agents in Medicinal Chemistry, 14(2): 331–340.

Yan, Y. et al. 2013. Differential Roles of the Protein Corona in the Cellular Uptake of Nanoporous Polymer Particles by Monocyte and Macrophage Cell Lines. ACS Nano, 7(12): 10960–10970.

Yu, P. et al. 2007. Investigation on PEGylation strategy of recombinant human interleukin-1 receptor antagonist. Bioorganic & Medicinal Chemistry, 15(5): 396–405.

Utilization of antibody-nanoparticle conjugates as a tool for immunochemistry with ICP-MS detection

Marcela Vlcnovska[1, 2], Michaela Tvrdonova[3], Marketa Vaculovicova[1, 4], Tomas Vaculovic[3]
[1]Department of Chemistry and Biochemistry
Mendel University in Brno
Zemedelska 1, 613 00 Brno
[2]Department of Biochemistry
[3]Department of Chemistry
Masaryk University
Kamenice 753/5, 625 00 Brno-Bohunice
[4]Central European Institute of Technology
Brno University of Technology
Purkynova 123, 612 00 Brno
CZECH REPUBLIC

marcelavlcnovska@seznam.cz

Abstract: Immunoanalytical techniques are key methods of application in clinical diagnostics, genomics, proteomics and other biochemical and molecular biology disciplines. Most often, they are based on the ability of labeled antibodies to bind specific antigens. It is possible to use a large variety of nanomaterials that are designed, synthesized and adapted to allow highly sensitive detection of advanced immunoassays. Detection can be a highly efficient analytical method of laser ablation followed by inductively coupled plasma mass spectrometry (LA-ICP-MS), which allows the detection of elemental tags suitably conjugated to antibodies. The aim of this work was to conjugate model anti-mouse antibody on a surface of 10nm and 60nm gold nanoparticles and choose the better one for conjugation experimentally by using dot-blot immunobinding assay followed by LA-ICP-MS. It has been experimentally proven that 10nm gold nanoparticles are more suitable for conjugation with antibodies because of lower non-specific sorption on a membrane.

Key Words: Immunochemistry, dot-blot, gold nanoparticles, LA-ICP-MS

INTRODUCTION

A nanoparticle is an object with at least one of three dimensions smaller than 100 nm. The properties of nanoparticles allow their application not only in material engineering, chemical synthesis, semiconductor technologies, etc. but also in biochemistry, molecular biology, biomolecular engineering and biomedicine. They are used in *in vitro* and *in vivo* imaging, as well as in biochemical analyses (Filipponi and Sutherland 2013). Their properties and ability of biomolecules conjugation enable modifications of traditional immunoassays (Hu and Li 2011).

Immunoassays are bioanalytical techniques using antibodies for a specific detection and quantification/quantitation of target molecules by unique antigen-antibody reactions. These methods find abundant utilization especially in the laboratories of clinical chemistry and biochemistry. They are used to detect and quantify low amount of proteins, hormones, various metabolites and pathogens, drugs, and even nucleic acids in a sample. They are highly specific and sensitive and allow qualitative and quantitative detection of the analyte in a complex medium, such as urine, serum, whole blood or tissue, without necessary previous extraction (Wu 2017).

By conjugating of the antibodies on the surface of nanoparticles, it is possible to achieve better detection limits of immunochemical methods. In addition, a wide range of nanoparticle properties make it possible to use different analytical methods for detection: colorimetric, electrochemical, or optical (fluorescence, chemiluminescence). This often allows a user to select nanoparticles according to the laboratory equipment without the need to purchase new costly detection devices (Cardoso et al. 2012).

Indirect quantification of antigen by labelled antibody is increasingly used for laser ablation followed by inductively coupled plasma mass spectrometry (LA-ICP-MS). The most important advantage of mass spectrometry is the ability to simultaneously measure several elements in one measurement and its sensitivity makes it possible to detect the presence of the ultra-trace element in almost any matrix (Waentig et al. 2012).

MATERIAL AND METHODS

Materials

All chemicals were purchased from Sigma-Aldrich Chemical Co. (St. Louis, MO, USA) in ACS purity, unless otherwise indicated. All solutions were diluted using ultra-pure Mili-Q water prepared by a Milipore purification system (Bedford, MA, USA).

Mouse Immunoglobulin Natural Mouse IgG protein ab198772 (Abcam, Cambridge, United Kingdom) was used as the model antigen, and the anti-mouse IgG HbL Ab6708 mouse antibody (Abcam, Cambridge, UK) was used as the model antibody.

For the preparation of conjugates, the commercial kits of gold nanoparticles GOLD Conjugation Kit (10 nm, 20 OD) ab201808 (Abcam, Cambridge, UK) and GOLD Conjugation Kit (60 nm, 20OD) ab188216 (Abcam, Cambridge, UK) were used.

Preparation of conjugates

The conjugation was performed according to the manufacturer's instructions. Briefly, the diluted antibody by antibody diluent was mixed with the reaction buffer and subsequently lyophilized nanoparticles. A few minutes later (depends on a size of nanoparticles) a Quencher was added.

Dot-blot

Before use, the PVDF membrane (Bio-Rad, USA) needs to be activated by soaking in methanol and in blotting buffer (50% (v/v) 2x blotting buffer with 40% (v/v) H_2O and 10% (v/v) MetOH needs to be always newly prepared) (2x blotting buffer 25mM Trizma base, 150mM glycine, 10% (v/v) methanol) both for 30 s. Then the membrane was placed on a filter-paper wetted by blotting buffer to prevent drying. Further, immunoglobulin samples (0.5 µl) were applied and dried for 20-30 minutes at a laboratory temperature. All following steps were carried out at room temperature, 60 rpm using Multi RS-60 (Biosan, Latvia). Next step was blocking of the membrane by 10% skimmed milk in PBS (137mM NaCl, 2.7mM KCl, 1.8mM KaH_2PO_4, and 10mM Na_2HPO_4, pH 7.4) for 30 minutes. Subsequently, incubation with antibody in PBS with 1 mg/ml BSA was carried out for 1 hour and following by washing. After the three times repeated washing with PBS containing 0.05% (v/v) Tween-20 for 5 min, the membrane was analysed by LA-ICP-MS.

LA-ICP-MS

LA-ICP-MS analyses of the dot blots were performed as described in Tvrdonova et al. (2018). A laser ablation system UP213 (NewWave, USA) emitting laser radiation of 213 nm with a pulse width of 4.2 ns and a quadrupole ICP-MS spectrometer Agilent 7500ce (Agilent Technologies, Japan) was used. The imaging of the dot blots was performed using the following ablation parameters: a laser beam diameter of 110 µm, laser beam fluence of 2.5 J/cm^2, a repetition rate of 10 Hz, a scan speed rate of 150 µm/s, and a distance between individual lines of 115 µm. The whole spot was ablated and the Au signals were measured. The sum of intensities across the whole spot was then calculated. The images of the dot blots were created using lab-made software Laser Ablation Tool for processing of raw data and Excel for presenting the maps as surface plots with the intensity shown in a color-coded intensity scale.

RESULTS AND DISCUSSION

Preparing of conjugates

Two types of commercial nanoparticles were used to prepare conjugates. The nanoparticles were delivered as a lyophilized mixture and the conjugation reaction was initiated by the addition of the antibody and the reaction buffer that was part of the kit. Immobilization of antibodies to the functional

surface of nanoparticles was performed by covalent bonding through primary amines. In the case of antibodies, these are lysine residues.

Figure 1 Scheme of random spatial orientation of antibodies on the functionalized surface of NPs bound by lysine residues according to Richards et al. (2017)

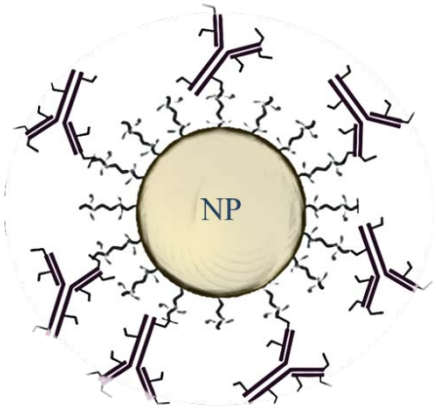

Covalent antibody binding to the modified surface of the gold nanoparticles traditionally occurs *via* the functional groups contained in the side chains of the amino acids forming the primary structure of the antibody. The resulting orientation of the bound antibodies to the particle is random (Figure 1). This is because the primary structure of the antibody always contains a greater number of binding amino acids and the interaction can occur with any one of them (Richards et al. 2017).

Analysis of dot-blot membranes by LA-ICP-MS

At first, the suspensions of nanoparticles were adjusted to the same optical density (OD). Absorbance spectra of conjugated nanoparticles were obtained by spectrophotometric analysis. The absorbance spectra are shown in Figure 2.

Figure 2 Absorbance spectra of 10nm and 60nm gold nanoparticles

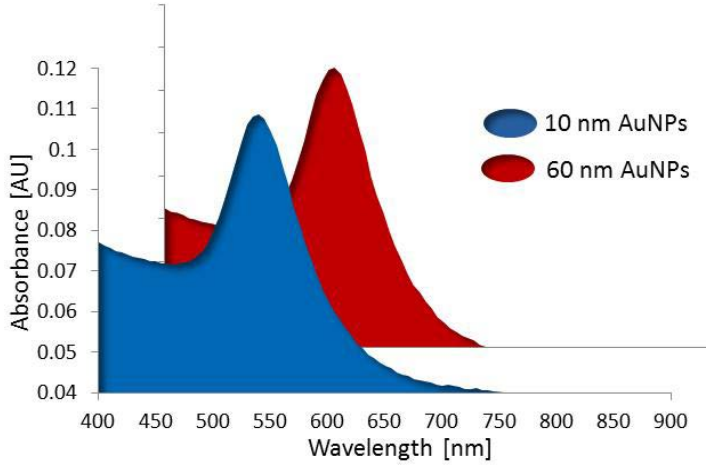

Nanoparticles of the same OD were diluted 100× and to the concentration of antibody of 6.7 ng/ml. 0.5 µl of these suspensions were applied on the activated PVDF membrane (without presence of antigen). In one case, the spot was analysed by LA-ICP-MS. In the second case, the membrane was washed before analysis to demonstrate the non-specific sorption on the membrane without the antigen. As seen from Figure 3, 60nm nanoparticles provided higher signal despite the same OD (in case of no washing). It is caused by higher number of atoms forming the 60nm nanoparticle and therefore, higher Au signal was observed. Negative side effect of 60nm nanoparticles was higher nonspecific sorption on the membrane (when the membrane was washed). As a result, 10nm particles were chosen as more suitable for conjugation.

Figure 3 Nonspecific sorption evaluations

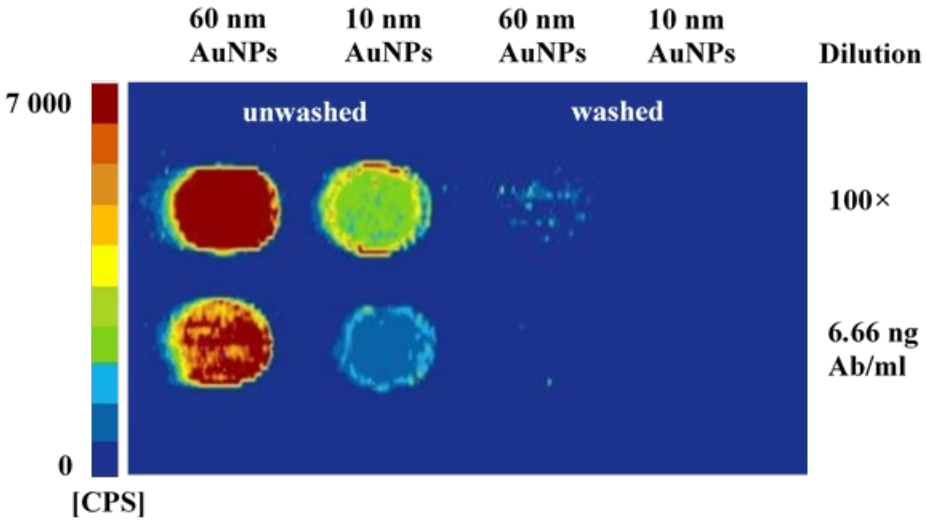

The ability of antibodies to bind the antigen was verified by dot-blot technique followed by LA-ICP-MS, (Figure 4). The intensity of Au signals was measured, as a dependence of mouse immunoglobulin applied to the blotting membrane. Labelled antibody (anti-mouse immunoglobulin) was applied in the total amount of 6.7 ng for each experiment. The applied amount of antigen was in the range of 0.1–0.5 ng.

Figure 4 Intensity of the Au signals depending on the amount of mouse immunoglobulin applied on the blotting membrane displayed in the colour-coded intensity scale

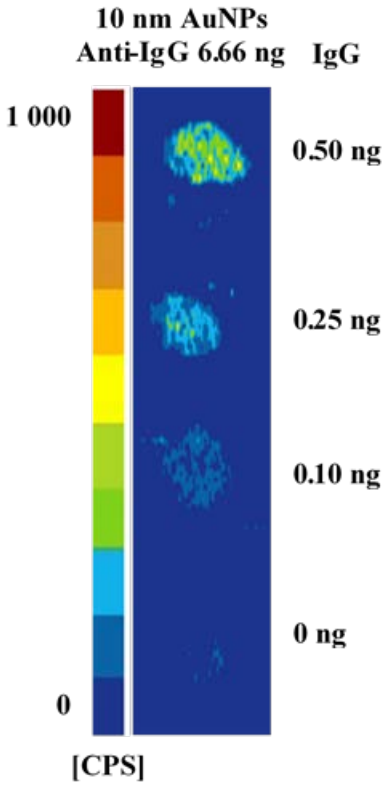

The Figure 4 shows not only that the ability of antibody to bind antigen was maintained, but also that the Au signal is proportionate to the amount of antigen present on the membrane.

CONCLUSION

Immunochemical methods are commonly used to analyse biological samples in both diagnostic and advanced research. They are able to specifically recognize the analyte in a complex matrix, such as a blood serum, or a histological section using a properly labelled antibody.

In this work, the immunoassay method is based on the preparation of the antibody bio-conjugate with suitable metal-based nanoparticles. The labelled antibodies are visualized with LA-ICP-MS after the immunoassay.

Experimentally, it has been demonstrated that by conjugating to 10nm nanoparticles the antibody does not lose its ability to bind the antigen. The method appears to be suitable for qualitative and quantitative analysis of low concentrations of analyte.

ACKNOWLEDGEMENTS

The research was financially supported by the Grant Agency of Czech Republic (GACR 17-12774S).

REFERENCES

Cardoso, M.M. et al. 2012. Antibody-Conjugated Nanoparticles for Therapeutic Applications. Current Medicinal Chemistry, 19(19): 3103–3127.

Filipponi, L., Sutherland, D. 2013. Nanotechnologies: Principles, Applications, Implications and Hands-on Activities. Luxembourg: Publications Office of the European Union.

Hu, W.H., Li, C.M. 2011. Nanomaterial-based advanced immunoassays. Wiley Interdisciplinary Reviews-Nanomedicine and Nanobiotechnology, 3(2): 119–133.

Richards, D.A. et al. 2017. Antibody fragments as nanoparticle targeting ligands: a step in the right direction. Chemical Science, 8(1): 63–77.

Tvrdonova, M. et al. 2018. Gold nanoparticles as labels for immunochemical analysis using laser ablation inductively coupled plasma mass spectrometry. Analytical and Bioanalytical Chemistry. In press. Available at: https://link.springer.com/article/10.1007/s00216-018-1300-7#citeas.

Waentig, L., et al. 2012. Comparison of different chelates for lanthanide labeling of antibodies and application in a Western blot immunoassay combined with detection by laser ablation (LA-)ICP-MS. Journal of Analytical Atomic Spectrometry, 28(8): 1311–1320.

Wu, A.H.B. 2017. Immunochemical Techniques. In Clinical Chemistry: Principles, Techniques and Correlations. 8th ed., Philadelphia: Lippincott Williams and Wilkins, pp. 159–176.

Combinations of capillary electrophoresis-UV/Vis and molecularly imprinted polymers for detection of phytoestrogens

Kristyna Zemankova, Jaroslava Bezdekova, Marcela Vlcnovska, Lucia Zibekova, Romana Bacova, Martina Kolackova, Marketa Vaculovicova
Department of Chemistry and Biochemistry
Mendel University in Brno
Zemedelska 1, 613 00 Brno
CZECH REPUBLIC

zemankova.kristyna@seznam.cz

Abstract: Phytoestrogens intake plays an important role in cancer treatment or prevention of tumor or heart disease, cardiovascular disease and others chronic diseases such as osteoporosis. Soy food is the most significant source of these phytoestrogens. The most commonly used methods for phytoestrogen determination include electrophoretic or chromatographic separation mechanics. In this study, the benefits of coupling molecularly imprinted polymers with capillary electrophoresis-UV/Vis for detection of phytoestrogens are shown. Polydopamine imprinted layer formed enables efficient isolation/extraction of target compounds (genistein and biochanin A) from milk sample and consecutive microcolumn separation with absorbance detection enables to distinguish nonspecifically bound interferents.

Key Words: molecularly imprinted polymers, phytoestrogens, capillary electrophoresis, genistein

INTRODUCTION

Phytoestrogens (PEs) and their derivatives have received special consideration due to their high quantity in food, especially in vegetables and soy products (Montes-Grajales et al. 2018). The available knowledge suggests that phytoestrogens can affect a number of physiological and pathological processes related to reproduction, bone remodeling, skin, cardiovascular, nervous, immune systems and metabolism (Sirotkin and Harrath 2014). Soy PEs intake may reduce the danger of cardiovascular and others chronic diseases, such as osteoporosis (Cepeda et al. 2017). Phytoestrogens comprise several groups of compounds: isoflavones, lignans, coumestans and prenyl flavonoids (Cassidy 2004).

Genistein and biochanin A, belong to the group isoflavonoids (Chrzanowska et al. 2015). The isoflavones, occur mostly in soya beans and a few other legumes (Cassidy 2004). Genistein and biochanin A are considered to be important constituents of human and animal food, as they have a serious influence on health (Chrzanowska et al. 2015). Genistein and biochanin A have anticancer, antioxidant and antiosteoporosis effects (Ma et al. 2013).

Molecularly imprinted polymers (MIPs) are synthetic materials with artificially generated recognition sites able to selectively interact with a target molecule in front to closely-related compounds. Recently, MIPs are attracting widespread attention due to their properties such as variability, flexibility, and/or relatively low cost (Samah et al. 2018). Moreover, also due to their high chemical, mechanical stability (Uzuriaga-Sanchez et al. 2016) and rapidity and simplicity in preparation (Samah et al. 2018). Thus, MIPs have promising applications to recognize protein and amino acid (Uzuriaga-Sanchez et al. 2016), pesticides (Vilela et al. 2007), drugs, food (Sureda et al. 2017), folic acid etc.

MATERIALS AND METHODS

Chemicals

Dopamine hydrochloride, Trizma base, Phytoestrogens (genistein and biochanin A), Sodium dodecyl sulfate and Acetic acid were obtained from Sigma-Aldrich (St. Louis, MO, USA) in ACS purity. Sodium tetraborate decahydrate and Dynabead MyOne Silane were purchased from Thermo

Fisher Scientific (Waltham, MA, USA). Ethanol and methyl alcohol were obtained from Penta (Prague, CZ).

Capillary Electrophoresis (CE)

Quantification of phytoestrogens, genistein and biochanin A, was performed by CE instrument 7100 (Agilent Technologies, Germany) with absorbance detection at wavelength of 254 nm. Fused silica capillary with an internal diameter of 75 µm, with the total length of 64.5 cm and an effective length of 56 cm was used. The sample was introduced hydrodynamically at 35 mbar for 3 s and a separation voltage of 12 kV was applied. A background electrolyte (BGE) was composed of 30 mM sodium borate buffer, 20 mM sodium dodecyl sulfate (SDS) containing 5% (v/v) ethanol at pH 9.6. Prior to the analysis, the capillary was washed for 60 seconds using BGE.

Genistein and biochanin A were solved in 80% ethanol. Solutions were prepared in different concentrations of 0.5, 0.25, 0.125, 0.6, 0.3, 0.015, 0.0075, 0.0039 and 0.00195 mg/ml.

Preparation of Molecularly imprinted polymers

Molecularly imprinted (MIPs) and non-imprinted polymers (NIPs) were prepared in microtitration plate. For preparation of MIP, 5 mg of dopamine were dissolved in 1 ml of solution of genistein (genistein was solved in 80% solvent of ethanol) and for preparation of NIP only in 80% ethanol. Then, 1 ml of 20 mM TRIS (pH 10.2) was added to MIP and NIP, respectively. The resulting solution was reacted for 24 h at 25 °C. During the reaction, the colorless and clear solution gradually changed to brown color. After polymerization reaction, the template (genistein) was removed by washing by 50 µl of 90% solution of methanol for 3 times. Prepared MIPs were used for isolation of genistein from sample.

RESULTS AND DISSCUSION

The aim of this study was to develop a method for isolation and quantification of phytoestrogens by capillary electrophoresis with UV/Vis detection in combination with sample preparation by MIP technology.

CE Optimization

Figure 1 CE separation of PEs as a dependence on separation voltage. Other CE parameters described in Experimental section

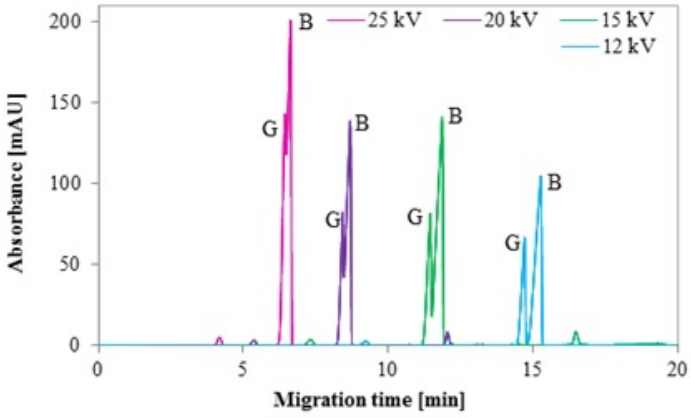

Legend: G – Genistein, B – Biochanin A

To enable the separation of neutral molecules of PEs, the micellar electrokinetic chromatography was used, employing SDS as the detergent ensuring the different electrophoretic mobilities. From the key parameters, separation voltage plays a crucial role. Therefore, the separation voltage was optimized (see Figure 1). Higher separation voltages increase the electrophoretic velocity of the analytes but also increase the current and Joule heating leading to the lowering the separation resolution. This heating may affect the stability of the complex by disrupting the non-covalent interactions. Heating effects can be mitigated by lowering the current (for example, by decreasing the separation voltage or lowering the ionic strength of the buffer) or by enhancing heat dissipation (for example, by decreasing the surface

area-to-volume ratio of the capillary or a capillary cooling system); however, these options can be detrimental to separation efficiency (11). The optimal separation was achieved at 12 kV and therefore this voltage was used in following experiments.

Quantification of genistein and biochanin A by CE

Using optimized CE analysis, calibration curves were constructed for both PEs (Figure 2). Linear dependence in genistein concentration was observed exhibiting the coefficient of determination $R^2 = 0.9999$ and in biochanin A was observed exhibiting the coefficient of determination $R^2 = 0.9999$.

Limits of detection were determined as 0.23 µg/ml and 0.64 µg/ml for genistein and biochanin A, respectively. Similarly, limits of quantification were calculated to be 0.69 µg/ml and 2.07 µg/ml for genistein and biochanin A, respectively.

Figure 2 Calibration curves of genistein and biochanin A obtained from integration of CE peak area. Separation conditions described in Experimental

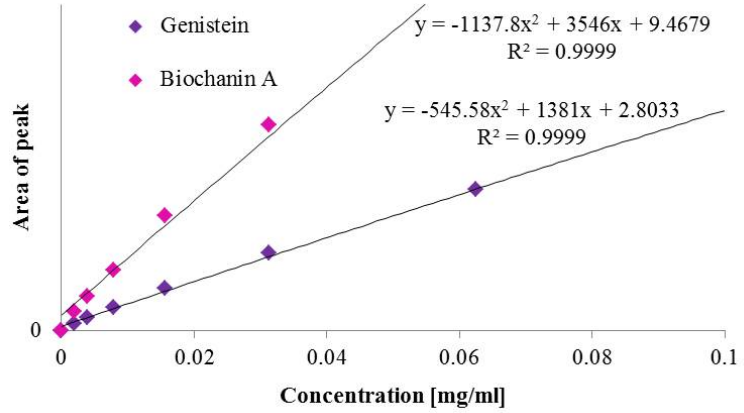

MIP

MIP technology is offering numerous benefits for sample preparation a analyte isolation such as flexibility and variability as well as low cost and effectivity, however, the system has to be carefully adjusted to minimize the background signal and lower the limit of detection.

One of the steps to be optimized is the temple removal before the sample solution is applied on the MIP surface.

In this study, the MIP for genistein (template) was prepared and template removal by 90% methanol (50 µl) was investigated. As can be seen from Figure 3, the surface has to be washed three times to decrease significantly the release of the template from MIP. The blue column represents the signal of standard solution of genistein (1 mg/ml) and after third washing of the surface, the peak area of the eluted genistein decreased to 2% of its original value.

Figure 3 Washing by 90% methanol (50 µl)

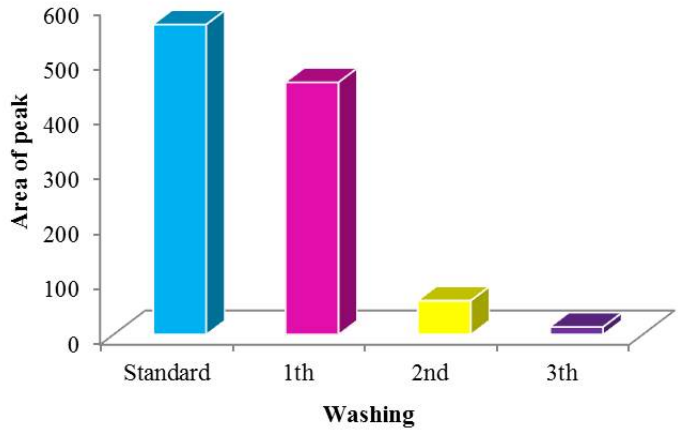

CONCLUSION

In this work, the CE analysis with UV/Vis detection was introduced for separation of two important PEs and subsequently, MIP technology using polydopamine polymer was employed for sample preparation. The surface washing process was optimized and in the next phase, utilization of the proposed method for detection of PEs in real biological samples is planned.

ACKNOWLEDGEMENTS

The research was financially supported by grant IGA no. TP 4/2017.

REFERENCES

Cassidy, A. 2004. Phytoestrogens and women's health. Women's Health Medicine, 1(1): 30–33.

Cepeda, S.B. et al. 2017. Beneficial role of the phytoestrogen genistein on vascular calcification. Journal of Nutritional Biochemistry, 50(6): 26–37.

Chrzanowska, A.M. et al. 2015. Surface molecularly imprinted silica for selective solid-phase extraction of biochanin A, daidzein and genistein from urine samples. Journal of Chromatography A, 1392(2): 1–9.

Ma, F.-Y. et al. 2013. Simple and efficient preparation of biochanin A and genistein from Dalbergia odorifera T. Chen leaves using macroporous resin followed by flash chromatography. Separation and Purification Technology, 120(3): 310–318.

Montes-Grajales, D. et al. 2018. Phytoestrogens and mycoestrogens interacting with breast cancer proteins. Steroids, 134(1): 9–15.

Samah, N.A. et al. 2018. Molecularly imprinted polymer for the removal of diclofenac from water: Synthesis and characterization. Science of The Total Environment, 631–632(2): 1534–1543.

Sirotkin, A.V., Harrath, A.H. 2014. Phytoestrogens and their effects. European Journal of Pharmacology, 741(1): 230–236.

Sureda, A. et al. 2017. Hypotensive effects of genistein: From chemistry to medicine. Chemico-Biological Interactions, 268(2): 37–46.

Uzuriaga-Sanchez, R. J. et al. 2016. Magnetically separable polymer (Mag-MIP) for selective analysis of biotin in food samples. Food Chemistry, 190(3): 460–467.

Vilela, M.L.B. et al. 2007. Endocrine Disruptors and Hypospadias: Role of Genistein and the Fungicide Vinclozolin. Urology, 70(3): 618–621.

AUTHORS INDEX

Name of publication:	MendelNet 2018 *Proceedings of 25th International PhD Students Conference*
Editors:	Assoc. Prof. Ing. Radim Cerkal, Ph.D. Ing. Natálie Březinová Belcredi, Ph.D. Ing. Lenka Prokešová
Publisher:	Mendel University in Brno Zemědělská 1665/1 613 00 Brno Czech Republic
Year of publication:	2018
Number of pages:	565
ISBN:	978-80-7509-597-8

Contributions are published in original version, without any language correction.